

INTRODUCTION TO

Autogyros, Helicopters,  
and Other  
V/STOL Aircraft

Volume II:  
**HELICOPTERS**



Franklin D. Harris

**Introduction to  
Autogyros, Helicopters, and Other  
V/STOL Aircraft**

Volume II: Helicopters

*Edited by*  
Catherine Dow, Dow Technical Services

*Cover Design by*  
Susan O

*Cover Photo*  
On June 26, 1936, Henrich Focke's F.61 astounded the world. This was the first truly practical helicopter. A year later, the F.61 had captured all of the helicopter world records.

NASA/SP-2012-215959 Vol II

**Introduction to  
Autogyros, Helicopters, and Other  
V/STOL Aircraft**

Volume II: Helicopters

**Franklin D. Harris**

Piedmont, Oklahoma



National Aeronautics and  
Space Administration

Ames Research Center  
Moffett Field, California 94035-1000

October 2012

Prepared for Monterey Technologies, Inc.  
under NASA Contract NNA07BB01C  
Subcontract 200703.NNA07BB01C  
Task Order 01C-53  
ISBN: 978-0-615-71562-9

Available from:

NASA Center for AeroSpace Information  
7115 Standard Drive  
Hanover, MD 21076-1320  
(301) 621-0390

National Technical Information Service  
5285 Port Royal Road  
Springfield, VA 22161  
(703) 487-4650

## DEDICATION

To two terrific offspring whom I am very proud of:

Leslie B. Harris Doyle—She chided me about my very first try at an opening sentence, “A helicopter is not an airplane.” And even laughed. Without knowing it, she encouraged me to respect the general wisdom of every reader. Just as important, she helped me transition from tennis in Arizona to horseback riding in Oklahoma. Now I own a horse and a saddle and bridle. She “boards” my horse on her property, includes me on trail rides, and has taught me how to barrel race so I can occasionally participate in our local rodeo along with her other students.

Glenn J. Harris III—He bought me my first computer in 1992, set it up, showed me how to use Microsoft® Word and Excel®, and is now my full-time IT guy. Based on this Volume II, he upgraded me to a solid state hard drive, Windows® 7, Office 2003, and threw in a color printer for good measure. When I visit NASA Ames Research Center, he puts me up for a night on his houseboat—at no charge!



**Grit and the author near the end of a trail ride.**



# TABLE OF CONTENTS

PREFACE.....	xi
ACKNOWLEDGMENTS.....	xiii
<b>1 PIONEERING EFFORTS.....</b>	<b>1</b>
1.1 EARLY HOVERING PERFORMANCE .....	5
1.2 STABILITY AND CONTROL.....	9
1.3 POWER-OFF LANDING .....	23
1.3.1 Power-Off Landing.....	23
1.3.2 Power Failure in and Near Hover.....	37
1.4 CLOSING REMARKS .....	43
<b>2 MODERN RESULTS.....</b>	<b>49</b>
2.1 ENGINES.....	53
2.1.1 Piston Engines .....	53
2.1.2 Turbine Engines.....	63
2.2 WEIGHT .....	87
2.2.1 A Helicopter Sizing Method.....	110
2.3 HOVER PERFORMANCE.....	119
2.3.1 Hover Power Margin .....	119
2.3.2 Hover Ceiling Versus Gross Weight.....	122
2.3.3 UTTAS and AAH Hover Performance .....	138
2.3.4 Tail Rotor Performance in Hover.....	141
2.3.5 Other Anti-torque Devices.....	146
2.3.6 Bell Model 222 and Aerospatiale Dauphin 2 Hover Performance.....	151
2.3.7 Blade Element Momentum Theory Revisited .....	152
2.3.8 Single Rotor Helicopter Summary .....	172
2.3.9 Twin-Rotor Helicopters .....	178
2.3.10 Ground Effect.....	198
2.3.11 Closing Remarks .....	200
2.4 FORWARD-FLIGHT PERFORMANCE.....	207
2.4.1 Airplane .....	211
2.4.2 Single Rotor Helicopter.....	230
2.4.3 Twin-Rotor Helicopter.....	238
2.4.4 Takeoff Following an Engine Failure.....	251
2.4.5 Closing Remarks .....	265
2.5 FUEL EFFICIENCY .....	267
2.5.1 Helicopter Lift-to-Drag Ratio (L/D).....	277
2.5.2 Equivalent Parasite Drag Flat Plate Area ( $f_e$ ).....	278
2.5.3 Rotor Hub Parasite Drag Area.....	295

2.5.4	The Doorhinge Rotor Hub.....	310
2.5.5	Closing Remarks .....	314
2.6	VIBRATION .....	315
2.6.1	Occupant Vibration, Humans Complain.....	319
2.6.2	Structural Fatigue, Parts Break.....	332
2.6.3	Hub Vibratory Loads, Aircraft Response .....	343
2.6.4	Blade Vibratory Response, Hub Vibratory Loads .....	396
2.6.5	Blade Airloads, Blade Vibratory Response .....	420
2.6.6	Closing Remarks .....	434
2.7	NOISE .....	437
2.7.1	Sound, Noise, and Human Hearing .....	437
2.7.2	Loudness Curves, Sound Pressure Level, and the Decibel .....	440
2.7.3	Weighted Loudness Curves .....	442
2.7.4	Propellers and Rotors at Zero Speed .....	444
2.7.5	Overall Sound Pressure Level (OSPL) in Hover.....	468
2.7.6	The Quiet Helicopter Program .....	498
2.7.7	Government Noise Regulations for Helicopters.....	509
2.7.8	Noise in Forward Flight.....	514
2.7.9	Closing Remarks .....	535
2.8	PURCHASE PRICE.....	539
2.8.1	Civil Marketplace .....	539
2.8.2	Military Procurement.....	550
2.8.3	Concluding Remarks .....	570
2.9	OPERATING COSTS.....	579
2.9.1	Airplanes.....	579
2.9.2	Helicopters.....	595
2.9.3	A Direct Operating Cost (DOC) Calculator .....	602
2.9.4	S-61 Direct Operating Costs in 2011.....	616
2.9.5	Fuel and Maintenance DOCs in 2011.....	617
2.9.6	Parts and Prices, Limited-Life Parts, and Scheduled Maintenance.....	637
2.9.7	Total Operating Cost (TOC).....	653
2.9.8	Concluding Remarks .....	660
2.10	ACCIDENT RECORD.....	663
2.10.1	History, Accident Rate, and Predictions.....	663
2.10.2	In All, 11,426 Accidents From 1964 Through 2011 .....	675
2.10.3	Detailed Accident Analysis.....	683
2.10.4	Concluding Remarks .....	696
<b>3</b>	<b>CONCLUDING REMARKS.....</b>	<b>699</b>
<b>4</b>	<b>REFERENCES .....</b>	<b>703</b>

APPENDIX A—Rotorcraft Stability and Control in Hover .....	741
APPENDIX B—Self-Induced Velocity Generated by a Lifting Line Wing or Rotor Blade .....	755
APPENDIX C—Ad Hoc Committee .....	815
APPENDIX D—Rotor Hubs .....	833
APPENDIX E—Fatigue Article.....	869
APPENDIX F—Dynamics of a Free-Free Uniform Beam .....	875
APPENDIX G—Project Hummingbird .....	889
AIRPLANES, ENGINES, AND HELICOPTERS.....	933
INDIVIDUALS .....	937
INDEX .....	941



## PREFACE

There are hundreds of histories and tens of thousands of technical works about helicopters; more than enough topics to fill many books bigger and heavier than the one you have in hand. From this storehouse of literature, I decided that subjects dealing with helicopter shortcomings would be of most value for this introduction to helicopters. In my mind, the short list only includes engines, weight, performance, vibration, noise, purchase price, operating costs, and safety record. Here, in a nutshell, is why I chose these eight topics.

**Engines**—Without knowing at least a smattering of how piston and turbine engines operate (and what their limitations are), you are placed at a severe disadvantage when talking to engine manufacturers. These manufacturers have, more often than not, saved a helicopter development program from the scrap pile. They have done this by upping the takeoff rating of the chosen engine to make up for an overweight, underperforming helicopter prototype.

**Weight**—The track record for meeting estimated weight empty and design takeoff gross weight is no better for helicopters than for fixed-wing aircraft. Where we get our eternal optimism, given our historical trend data and weight estimating methodology, is beyond me.

**Performance**—Hover performance cannot, even today, be predicted to within  $\pm 5$  percent, and it always seems to come out minus given flight test data. The helicopter's forward flight performance is severely limited by excessive profile and induced power, disproportionately high hub drag, and non-retractable landing gear. With these configuration burdens, it is no wonder that helicopter fuel efficiency is poor when compared to fixed-wing aircraft.

**Vibration**—Despite enormous theoretical progress that has identified many sources of vibration, no lightweight, low-cost invention to reduce helicopter vibration to airliner levels has been devised. Vibration suppressors and absorbers are the Band-Aid of choice, and these solutions are trotted out shortly after a prototype's first flight when the test pilot says he cannot read the instrument panel above 100 knots. It has, in fact, been the use of many different types of anti-vibration devices, added to the basic machine by each manufacturer, that has saved the day as the rotorcraft industry expanded.

**Noise**—High tip speeds, especially of tail rotors, and no engine exhaust mufflers lead to very noisy helicopters, which, in turn, continue to dampen community acceptance of these machines. The design choice to wring out every pound of airframe weight empty per installed engine horsepower has relegated lower-noise configurations to an undeserved place on the priority list. Noise research by a very small, but staunch, band of advocates has been shortchanged by the low priority on noise set by the rotorcraft industry. A design approach yielding high performance *and* low noise was demonstrated by Hughes with its OH-6. No manufacturer of note has applied the Hughes' technology and design approach that became available in the early 1970s.

Purchase Price—Helicopter fleet size continues to grow despite the 50 percent premium paid (over comparable fixed-wing aircraft) to have vertical and forward flight capability in one machine. The fact that the purchase price of a helicopter appears to depend about equally on weight empty and installed power may be an eye-opener, but this fact does not offer much insight into how to make the initial purchase price low enough to attract major airline companies that could best establish helicopter service on short-haul routes. Only recently has there been a helicopter airline service established that has stayed in business. If you get to Vancouver, British Columbia, go see Helijet's operation.

Operating Costs—To say that helicopter operating costs are excessive compared to fixed-wing standards is a real understatement. Of the 5,000 to 7,000 parts and/or components in a helicopter, about 50 to 75 have to be replaced for every 1,500 to 5,000 hours of flight time. And, as you probably guessed, these must-be-replaced components are the most expensive, which lays a foundation for unacceptably high maintenance costs. Throw in low miles per gallon of fuel used, and many potential buyers say, "No thanks."

Safety Record—The quite favorable trend of fewer and fewer helicopter accidents per year, even as the number of helicopters flying has increased over the past six decades, is a heartwarming story to relate. However, the industry did learn an expensive lesson when it introduced helicopters powered by single turbine engines, which caused a wide spike in accidents per year. This spike distorted the yearly trend in accidents per 100,000 flight hours. The current trend is to sell four helicopters and have an accident with one of them. Loss of engine power due to running out of gas is quite common, and the upward trend in loss-of-control accidents per year is very, very disturbing.

So there you have it.

This introduction to these yet-to-be-improved helicopter shortcomings will show you why they are so difficult to solve. I hope you will be a part of their solution, and I hope you will start with the efforts offered in the Concluding Remarks of this volume.

## ACKNOWLEDGMENTS

In the acknowledgments in the first volume of this three volume set, I expressed my gratitude to the many men and women who gave me their help when I really needed it. And each and every one has continued giving me their help as this second volume unfolded. In this second volume, I found that I needed even more expert assistance, particularly when confronted by several stone walls. For example:

In dealing with helicopter weights, I was able to rely on Mike Scully, who is, I believe, the world's authority on the subject. Mike also helped shape what you will read about engines.

The subject of performance is very dear to my heart, and I thought it would be a rather straightforward subject to address. But thanks to Tom Wood and Jack Gallagher (who was President of New York Helicopter Airways) you have much more information about power-off landings and about the FAA's requirement for Category A takeoffs and landings from heliports. Also, Jack told me he preferred tandem rotor machines to the single rotor configuration because they are much less sensitive to crosswinds during takeoff and landing.

The vibration chapter would have been considerably less useful to you if Tom Norman, Bob Kufeld, Ethan Romander, Carl Russell, Randy Peterson, Wayne Johnson, and several others from the NASA Ames Research Center Aeromechanics Branch, headed up by Bill Warmbrodt, hadn't jumped in when they did.

There is no question that writing in some depth about noise took me out of my technical comfort zone. Fortunately Wayne Johnson clarified more than a few key technical points that I had lost track of over the years. And then Ben Sim, Ken Brentner, Charlie Cox, and, of course, Fred Schmidt (who has been an acknowledged expert in the subject for decades) helped me expand the scope of this rather difficult subject.

Opening up the subject of helicopter purchase price, which Mike Scully and I had written a paper about, put me back in touch with Sharon Desfor, President of HeliValue\$, Inc. She and her staff publish *The Official Helicopter Blue Book*<sup>®</sup>. Sharon is one person who *really* keeps her ear to the ground about commercial helicopters. We were able to reminisce about several manufacturers, and their trials and tribulations in bringing new helicopters to the marketplace. You have much more history and authoritative selling price data about civil helicopters because of her. For the world of military helicopter procurement, I turned to Webb Joiner (past President of Bell Helicopter) for history about the Huey program. And for the Army's side of procurement, Bud Patnode (Colonel Clarence A. Patnode Jr., retired) and Bud Forster (Lieutenant General William H. Forster, retired) filled in several blanks in my memory. Webb and both retired U.S. Army officers allowed me to include some of their written thoughts about keeping a very tight rein on requirements and specifications, particularly during development, which is invaluable advice.

Newly minted helicopter engineers, and even many practicing engineers, have too little exposure to helicopter operating costs, which is very disappointing to me. With Bill de Decker's help, this chapter may fill in a serious educational gap. Bill and his cohort Alan Conklin (now departed) brought the firm of Conklin & de Decker into the world. They created an invaluable data bank of operating cost data (for both fixed-wing and rotary wing aircraft) with their software called Aircraft Cost Evaluator (ACE). ACE is acknowledged by the worldwide aviation community as the leading product of its type, and it is still expanding as new aircraft arrive on the scene. Bill gave me unbelievable access to their company's data bank, and this privilege put *realistic* operating cost data at your fingertips.

Reading about accidents with commercially manufactured helicopters and amateur-built autogyros in the cold light of day is always a sobering experience. Fortunately, I was able to turn to Eugene Kasper (Test and Evaluation Engineer, Flight Control and Cockpit Integration Division, U.S. Army Aeroflightyynamics Directorate at NASA Ames Research Center). Gene has maintained National Transportation Safety Board reports in his massive Microsoft® Word and Excel® files that we began in the late 1990s. His continued interest in rotorcraft safety, and his thoroughness in studying accident reports, provides you with an invaluable source.

I would be quite remiss if I did not again thank three marvelous women who have done so much to bring this Volume II to completion. Kathy Ponce at the NASA Ames Research Center library has not once failed to find some obscure reference that the world has forgotten, but is of immense value to you. Cathy Dow has edited this Volume II with superb professional skill, as she did in Volume I, while continuing to managed me with both timely suggestions and gentle persuasion. And, of course, I thank my wife, Sue, for her patience with me through the ups and downs during another year and a half of writing.

# 1 PIONEERING EFFORTS

There is a wealth of history documenting the origins of powered lift and the many inventors who struggled for over 250 years to give the helicopter a place in the world's transportation system. A fascinating glimpse of the struggle is provided by Gene Liberatore in *Helicopters Before Helicopters* [1]. Efforts to create a man-carrying, powered lift system began well before the airplane was conceived as Fig. 1-1 suggests. Despite over 40 powered lift attempts up to 1903, no promising results comparable to the achievement of the Wright brothers can be pinpointed. This state of affairs continued until the early 1920s.

The struggle to achieve a truly operational helicopter that rivaled the Cierva C.30 autogyro finally ended when Henrich Focke, Anton Flettner, and Igor Sikorsky were each able to begin production deliveries of their separate designs during the early part of World War II. Excellent accounts of this struggle are provided by Boulet [2] and Gablehouse [3]. The story is well summarized by Brooks [4] and Gibbs-Smith [5], and by Apostolo [6], with beautiful illustrations, one of which is of the Sikorsky R-4, Fig. 1-2.

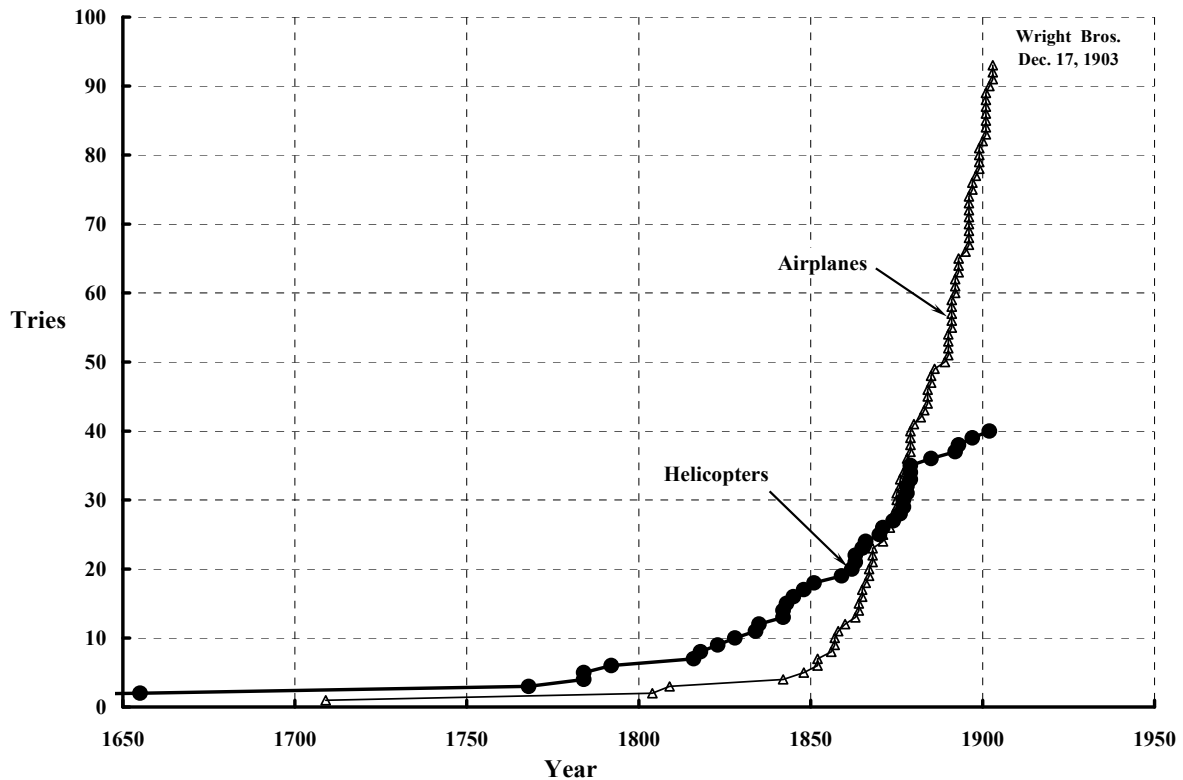


Fig. 1-1. Pursuing the helicopter was the real goal of early inventors.

## 1. PIONEERING EFFORTS



**Fig. 1-2. The Sikorsky R-4 was the first production helicopter in the U.S. [6].**

In reading these histories and many others, one must conclude that the practical helicopter was pursued with every bit as much energy (and money) as the airplane—at least up until the achievements of the Wright brothers really took root in Europe in 1909. Many inventive geniuses such as Bréguet and Sikorsky struggled unsuccessfully with the helicopter in the very early 1900s before turning their skill to evolving the airplane. Fortunately, many of these pioneers returned to help make rotorcraft what they are today.

Boulet's history [2], even as brief as it is, describes over 70 different helicopters that evolved prior to 1945. A common thread clearly exists for this long period that stretches back to at least 1784. In that year, Launoy and Bienvenue flew a simple, stick model, coaxial rotor system. What followed were, with one very notable exception, helicopters that used rotors of the same size, in pairs, to ensure equilibrium in applied torque. From Boulet, the configurations tried were distributed as shown in Fig. 1-3.

Of this group of pre-1945 helicopters (and a few models), only three types were produced in quantity. The first was the side-by-side configuration pioneered by Henrich Focke and designated as the FA 223. Out of 30 aircraft ordered by the German Government, 9 were completed by the end of World War II. The Focke-Achgelis FA 223 was based on the truly successful F. 61, which hovered in late June of 1936. By June of the following year, the F. 61 held the altitude record (2,100 meters) and easily flew 100 kilometers cross country.<sup>1</sup> The

---

<sup>1</sup> Boulet (page 61 of reference [2]) suggests that “the helicopter enthusiasts, in 1934, must have been rather discouraged. Ten years after the first flight in a closed circuit by Oehmichen, the official altitude world record was only 18 meters (+2 meters compared with the altitude reached by Oehmichen) and the straight line record barely reached over one kilometer. Nobody then suspected the progress which would be made during the ten following years.”

## 1. PIONEERING EFFORTS

second type to go into production was created by Anton Flettner and designated the FL 282. The two main rotors of his design were nearly coaxial but, in fact, were intermeshed like an eggbeater. This configuration is referred to technically as a synchropter. Out of a German Government order for 30, 24 were delivered. Flettner developed his configuration with the FL 265. Six of this very successful earlier model were ordered by the German Navy, and the first prototype flew in May of 1939. You can read a superb story of German helicopter development in *Helicopters of the Third Reich* written by Steve Coates [7].

The third type was produced in the United States. The single-main-rotor plus anti-torque tail rotor configuration was developed by Igor Sikorsky with his VS 300. The first flight of the VS 300 was in September of 1939, and by December 1941 Sikorsky had refined the design to what most laymen think of as the modern helicopter. The success of the VS 300 led to production orders from the U.S. Army Air Corps for 126 of the Sikorsky Model R-4s. The prototype, the XR-4, first flew in January of 1942, and the production order was filled in 18 months. The R-4 was quickly followed by the R-6. Four prototypes, and 416 out of 900 R-6s ordered by the U.S. Army Air Corps, were delivered by the end of World War II. The success of the R-4 also led to the R-5, whose prototype first flew in late August of 1943. By the end of World War II, 123 of this larger model had been delivered.

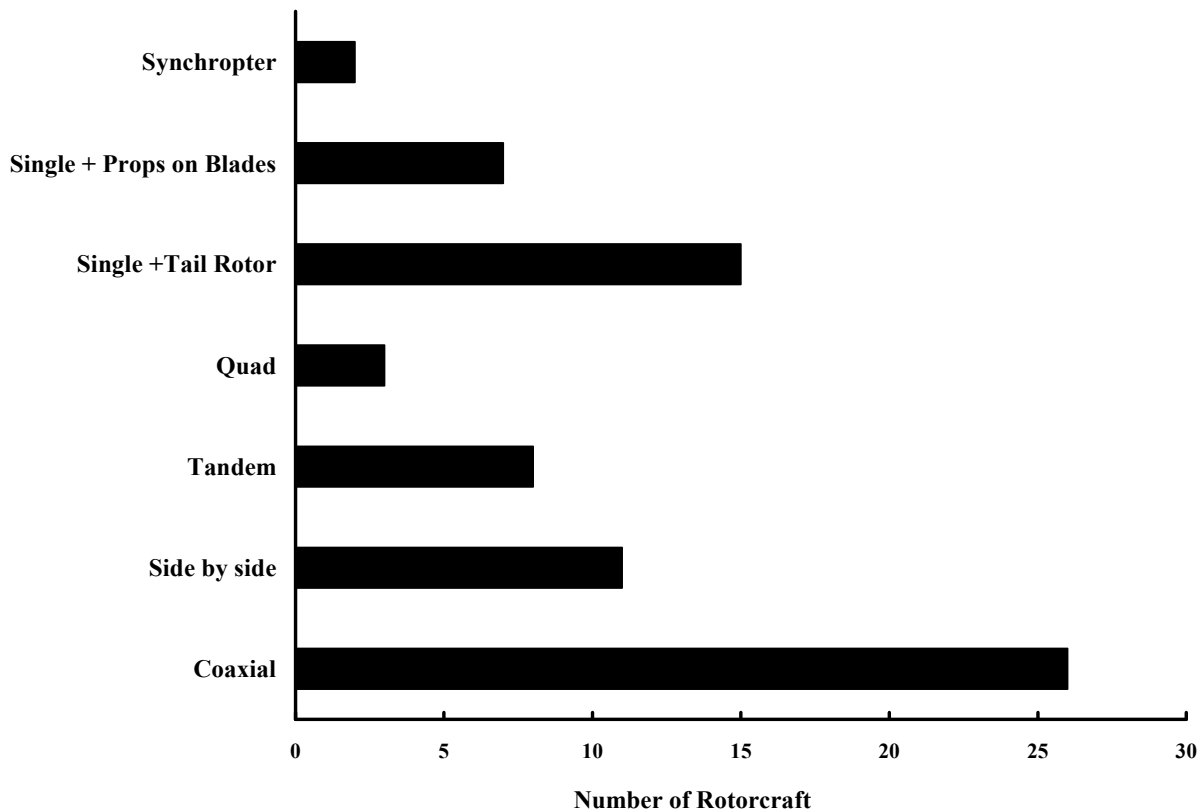


**Fig. 1-3. At least 72 different helicopters were built by 1945.**

## 1. PIONEERING EFFORTS

In many ways, World War II stimulated helicopter evolution and production just as World War I gave impetus to the airplane. Out of some 70-plus configurations, 3 basic types survived the weeding-out development process that started around 1784. And of the roughly 700 rotorcraft produced by 1945, about 665 (or over 95 percent) were the single-main-rotor plus anti-torque tail rotor configuration. In contrast to this 160-year rotorcraft development cycle, the first modern airplanes—albeit a model glider flown by Cayley in 1804 and, more comparably, a stable, rubber-band-powered model flown by Penaud in 1871—were developed in about 50 years.

There is another interesting parallel between airplane and rotorcraft development. While the Wright brothers were successful with a biplane having canard control surfaces, it was the mono-plane with control surfaces on the tail that became the production choice. Similarly, Boulet (page 44 of reference [2]) asks that “three men share the glory to be the first to fly and control a helicopter” and he suggests the following:

- Pescara with a coaxial helicopter. First controlled flight of about one minute. By January of 1922, the several times rebuilt and modified aircraft had demonstrated hover for approximately ten minutes.
- De Bothezat’s quad rotor helicopter. First flight of more than one minute in December of 1922.
- Oehmichen with a quad rotor helicopter. First kilometer flown in a closed circuit in May of 1924.

To this list one could add:

- Florine’s tandem rotor helicopter. Raised the airborne record to nearly 10 minutes and reached somewhat over 15-foot altitude in October of 1933.
- The Bréguet–Dorand coaxial design. By December of 1936 had demonstrated forward flight to about 500-foot altitude, endurance slightly over 1 hour, top speed of 108 km/hr, but with maximum hover time of 10 minutes.

History records that none of these configurations went into production during the first step in bringing the helicopter into practical use.

## 1.1 EARLY HOVERING PERFORMANCE

During the struggle to get the preproduction helicopters off the ground, finding a reliable engine, transmitting power to the pair (or pairs) of rotors, and getting control of the “machine” was an ever-recurring theme. With respect to installing enough power to hover, the pioneers appear to have taken a very reasonable approach. They had available, for example, at least one basic theory. This theory defined the ideal horsepower required to hover out of ground effect ( $HP_{ideal}$ ) in terms of the rotor thrust ( $T$ ) (somewhat in excess of takeoff weight), the rotor or rotors swept disc area ( $A$ ), and the density of air ( $\rho$ ). The theory gives the quite simple result that

$$(1.1) \quad HP_{ideal} = \frac{T}{550} \sqrt{\frac{T}{2\rho A}} \quad (\text{hover out of ground effect}).$$

Accounting correctly for rotor(s) area ( $A$ ) requires some care when using Eq. (1.1), because it was originally derived for one thrusting rotor disc. For example, the area is  $\pi R^2$  for a single main rotor having a blade radius ( $R$ ). With the coaxial configuration, the area is also  $\pi R^2$  even though there are two rotor discs. This is true for the coaxial rotor system because the same column of air that passes through the upper rotor passes through the lower rotor. In the case of two rotors not overlapped (i.e., the tandem or side-by-side arrangements), the applicable area would be  $2 \pi R^2$ . Obviously then, the area for the nonoverlapped quad-rotor would be  $4 \pi R^2$ .

When two rotors are overlapped as in the Flettner synchropter design, there is considerable mixing of the two columns of air, and the problem becomes rather difficult. But to a first approximation, the applicable area to use in Eq. (1.1) is given as

$$(1.2) \quad A = 2\pi R^2 \left[ 1 - \frac{1}{\pi} \left( \frac{\pi}{2} - \frac{d}{2R} \sqrt{1 - \left( \frac{d}{2R} \right)^2} - \sin^{-1} \left( \frac{d}{2R} \right) \right) \right].$$

The distance between the centerlines of the two rotor hubs is denoted by ( $d$ ) in Eq. (1.2), and the rotor discs are assumed to be in about the same horizontal plane.

This theory for hover power required, Eq. (1.1), was derived from basic fluid dynamic principles established by W. J. Macquorn Rankine, R. E. Froude, and W. Froude in the years from 1865 to 1889. It was subsequently improved by Albert Betz and Ludwig Prandtl in 1920.<sup>2</sup> The pioneers must have quickly become aware that this available theory had more than a few shortcomings because they generally installed about twice the power specified by Eq. (1.1). More precisely, they took the most readily available engine and then built helicopters with rotor diameters nearly twice that suggested by the simple theory. Because belt-drive transmissions were the most common means of reducing engine RPM to rotor RPM

---

<sup>2</sup> You will find that references [8], [9], [10], [11], and [12] provide an excellent window into some of the great aerodynamic, structures, dynamics, and mathematical work that formed such an important part of rotorcraft development.

## 1.1 EARLY HOVERING PERFORMANCE

in the early 1900s, as much as one-half of the engine power never reached the rotors. And even with the use of gears and shafts, Boulet's history also recounts several instances (for example, read the Bartram Kelley story, page 104 of reference [2]) when the engine did not deliver the power claimed by the manufacturer.

The relation between actual installed horsepower and the ideal horsepower to hover provides an interesting capsule view of what the early inventors were doing to demonstrate a feasible helicopter. Fig. 1-4 provides this view by using the historically available data. All but one pioneer (the Luyties large model of Dec. 1907) installed more power than required by the ideal theory given in Eq. (1.1) as Fig. 1-4 shows. One has to assume that each inventor fully expected his "machine" to hover out of ground effect (HOGE), that is, at altitudes many times the rotor diameter. However, about one-half of the inventors were, at best, in a marginal power—not to mention control—situation. If it had not been that the early efforts were to just get in the air so that stability and control could be demonstrated, progress would have been even slower. Boulet carefully points out the progressive improvement in hover altitude. By 1922, the record for hovering altitude was still only about 15 meters or 45 feet. This is a very important technical point because it raises the question of ground effect and its augmentation of lifting capability for a given design.

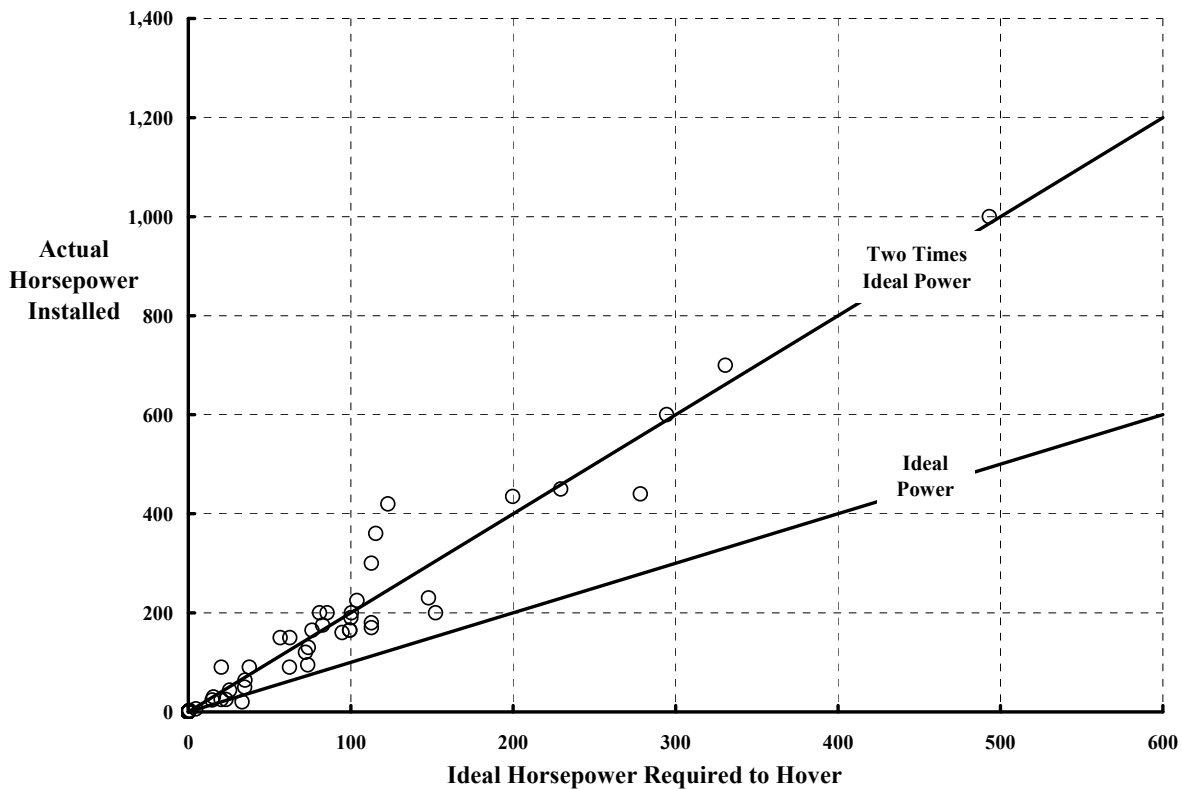


**Fig. 1-4. In the period from 1907 to 1922, some early inventors installed enough power to hover.**

## 1.1 EARLY HOVERING PERFORMANCE

The effect of the ground on reducing the power required to hover becomes progressively more pronounced as the distance from the rotor hub plane to the ground is decreased. A formal theory for hover performance in ground effect had to wait until 1937 when Betz [13] was able to provide an approximation that modified Eq. (1.1) to

$$(1.3) \quad HP_{\text{ideal}} = \left( \frac{T}{550} \sqrt{\frac{T}{2\rho A}} \right) \frac{2Z}{R} \quad (\text{hover in ground effect}).$$

The distance from the rotor hub plane to the ground is denoted by  $Z$  in Eq. (1.3), and the Betz approximation only applies when the helicopter is below an altitude where  $Z/R$  is on the order of one-fourth or less. This criteria was, in fact, the situation for most of the early inventors. It would seem that these several first attempts to hover encountered a situation where (1) the rotors themselves were about 50 percent efficient relative to the ideal power given by Eq. (1.1), (2) only half the installed power was transmitted to the rotors, and (3) the benefit of ground effect reduced power required by perhaps one-half.

Looking back with this technical perspective, you have to say that the early inventors (in the 1907 to 1922 period that Boulet singles out) were fighting a real uphill battle.

By the end of 1922, the helicopter was beginning to reflect both the hardware and theoretical progress that was improving fixed-wing aircraft. The Boulet photographs show, for example, that propeller shapes for rotors became more common. There was a progressive reduction in the number of blades per rotor, and the individual blades became quite a bit narrower in chord ( $c$ ) for any given radius ( $R$ ). Clearly the beneficial concept of higher blade-aspect ratio ( $AR$ , the ratio of blade radius to blade chord, or  $R/c$ ) was being applied. The blade cross section or airfoil shape changed from simple, flat slabs that were more characteristic of windmills into at least “modern” airfoils. These vintage airfoils were carefully curved on the upper surface, but the bottom surface was basically flat. This evolution of blades and airfoil shapes has been traced well back in time by Jan Drees [14] and is a fascinating story of its own.

Significant theoretical progress was also made in estimating the power required to hover. The subject in itself was not of major importance to fixed-wing propeller designers in this period because it was airplane cruise and maximum speed they sought. Static thrust for takeoff was simply a by-product of their designs. But, of course, to rotorcraft inventors just the reverse was true. Groundwork for this important theoretical advancement was first laid by W. Froude and S. Drzewiecki before 1900. It was brought to fruition by Betz in 1925 as Glauert summarizes in volume IV of reference [10]. Thus, the ideal power required to hover out of ground effect as provided by Eq. (1.1) was updated to include an additional term and a touch of empiricism to give the more practical result of

$$(1.4) \quad HP_{\text{HOGE}} = k_i \left( \frac{T}{550} \sqrt{\frac{T}{2\rho A}} \right) + \frac{\rho b c R V_t^3 C_{do}}{8 \times 550}.$$

The empiricism was introduced by the coefficient ( $k_i$ ) which designers increased from the ideal value of 1.00. Values of  $k_i$  from 1.10 to 1.25 were most often used.

## 1.1 EARLY HOVERING PERFORMANCE

The final term in Eq. (1.4) became known as the profile power ( $HP_o$ ) term. This addition acknowledged that it takes some power just to drag the blades around even if they are not lifting. This power is very dependent on the drag coefficient<sup>3</sup> of the airfoil ( $C_{do}$ ), on the tip speed cubed ( $V_t$ ), and on the total blade physical area ( $bcR$ ).

The power-required formula provided by Eq. (1.4) led to having two areas that described a rotor—one being the swept disc area ( $\pi R^2$ ) and the other being the physical total blade area ( $bcR$ ) for rectangular blades. These two areas were formed into a ratio referred to as solidity ( $\sigma$ ). This descriptive parameter remains in use to this day, so remember that

$$(1.5) \text{ Solidity} \equiv \sigma \equiv \frac{bcR}{\pi R^2} = \frac{bc}{\pi R} \text{ for rectangular blades.}$$

Equation (1.4) also suggested a number of nondimensional forms that were finally resolved to some extent by the N.A.C.A. [15]. Two key coefficients were adopted—one for thrust and one for power—and both were based on the swept disc area. For the thrust coefficient

$$(1.6) C_T = \frac{T}{\rho A V_t^2}$$

and for the power coefficient

$$(1.7) C_P = \frac{P}{\rho A V_t^3}.$$

With these coefficients in hand, the hover power required provided by Eq. (1.4) was made less cumbersome (in fact, disguised to some) and became

$$(1.8) \begin{aligned} C_{P_{HOGE}} &= C_{P_i} + C_{P_o} \\ &= k_i \frac{C_T^{3/2}}{\sqrt{2}} + \frac{\sigma C_{do}}{8}. \end{aligned}$$

From 1922 to mid-1936—when the truly successful helicopter, the F. 61, first hovered—you will see an apparent lack of progress made with helicopters. This period, which was the subject of Volume I, was discussed in detail by Brooks [4] and mentioned by Boulet [2] in passing, and was dominated by Cierva, Pitcairn, and Kellett and their development and production of the autogyro. Perhaps most importantly, the modern rotor system—having a few blades that are long and slender (i.e., high-aspect ratio)—was evolved during this period. It was also during this period that autogyros incorporated lead-lag dampers to preclude the destructive ground resonance phenomenon, and practical demonstrations of blade feathering through a washplate gave future helicopter pilots firm control. Thus, the 12 or so years that were spent in creating hubs, blades, and control systems, and solving many structural dynamic and aerodynamic problems, were clearly one of the most fruitful periods in rotorcraft, if not helicopter, development.

---

<sup>3</sup> The drag of airfoils, while clearly seen in experiments, was calculated as zero up until the early 1910s. With the work of Prandtl and his students, a realistic theory finally became available that showed that  $C_{do}$  was on the order of 0.01 to 0.015. This began to bridge the gap between test and theory. Improvements to the theory are still being made today.

## 1.2 STABILITY AND CONTROL

The period from mid-1936 to March 1946, when the Bell Model 47 received the first Civil Aviation Authority (the CAA, which preceded the FAA) certification for civilian use in the United States, must have been a very exciting 10 years for the pioneers. For example, Igor Sikorsky's triumph in evolving the VS-300, the prototype of modern, single-main-rotor plus anti-torque tail rotor helicopters, is just one of the fascinating stories found in Boulet's history. Threaded within this history is the underlying story of helicopter stability and control. The early helicopters, although helped by autogyro development, were not at all stable. The tale related by Frank Gregory<sup>4</sup> on first flying the Sikorsky VS-300 in 1940 when he was a U.S. Army captain, captures the essence of the stability and control problem.

Captain Gregory, after learning how to use the collective stick to get the aircraft off the ground, recounts that

“once in the air there was a slight disturbance and the nose of the aircraft seemed to come up too quickly, so I moved the [cyclic] stick forward. In so doing the nose went down all right, but to my complete surprise, the aircraft started moving forward and climbing. In all my experience with flying heretofore, when I pushed the stick forward the airplane had always gone down. I was halfway across the airport before I finally stopped the machine. After about eight minutes of flying, I finally got the craft back on the ground, much to the relief of Sikorsky, although, of the group which had been watching my flight, he was most enthusiastic in his congratulations.”

The inherent instability of all early helicopters was only overcome by the skill of the pilot when given an adequate control system. The Wright brothers, assisted by glider testing, solved most of their stability and control problems before the onset of their successful powered flying, as many historians have pointed out. In contrast, the early helicopter pioneers seemed to be tackling the power, stability, and control problems all at the same time.

Stability and control of the helicopter was formally studied by analysis at least as early as 1923 judging by the work of G. A. Crocco published by the N.A.C.A. in reference [17]. His work and that of Kurt Hohenemser [18] in 1939, plus Igor Sikorsky's personal, but perhaps too brief, ground instructions, may be all that Captain Gregory had at hand before his first flight. But, in retrospect, a simple understanding of the VS-300 control and inherent instability in hovering flight is relatively easy to recreate.

The simplified force and moment diagram for the situation Captain Gregory found himself in, once he added enough collective pitch to hover, is shown in Fig. 1-5. Based on advanced theory, the equations for all six components of motion can be reduced to (1) fore and aft or longitudinal motion at nearly constant height, and (2) helicopter pitching motion for the hovering helicopter. The two equations describing the motion of the aircraft center of gravity (cg) are

---

<sup>4</sup> Reference [2], page 95–96. The pioneering experiences of Colonel H. Franklin Gregory are more fully related in his own book titled *Anything A Horse Can Do* [16].

## 1.2 STABILITY AND CONTROL

$$(1.9) \quad \sum F_x = -W \times \theta_{cg} - H_s - \frac{W}{g} \frac{\partial^2 x_{cg}}{\partial t^2} = 0$$

and

$$(1.10) \quad \sum M_{cg} = h \times H_s + M_p - I_{cg} \frac{\partial^2 \theta_{cg}}{\partial t^2} = 0.$$

These two equations of motion assume that rotor thrust ( $T_s$ ) is equal to helicopter weight ( $W$ ) and that the body pitch angle ( $\theta_{cg}$ ) is a small angle. The rotor inplane force, called the rotor H-force ( $H_s$ ), acts in the rotor plane perpendicular to the rotor shaft. Thus, the H-force acts at the hub, which is a distance ( $h$ ) above the center of gravity. The rotor blades can introduce a hub pitching moment ( $M_p$ ) as discussed in detail in Volume I. This hub moment is approximated as

$$(1.11) \quad M_p = \frac{F_c r_\beta b}{2} a_{1s}$$

where the blade centrifugal force is ( $F_c$ ) in pounds, the flapping hinge offset is ( $r_\beta$ ) in feet, the number of blades is ( $b$ ), and the longitudinal flapping is ( $a_{1s}$ ) in radians.

Classically, engineers search for the stability of the system and then review the control aspects. But from Captain Gregory's point of view, one could say that he was in trouble from the onset—that is, at time equals zero (i.e.,  $t = 0$ ). He stated that “.... there was a slight disturbance and the nose of the aircraft seemed to come up too quickly, so I moved the [cyclic] stick forward.”

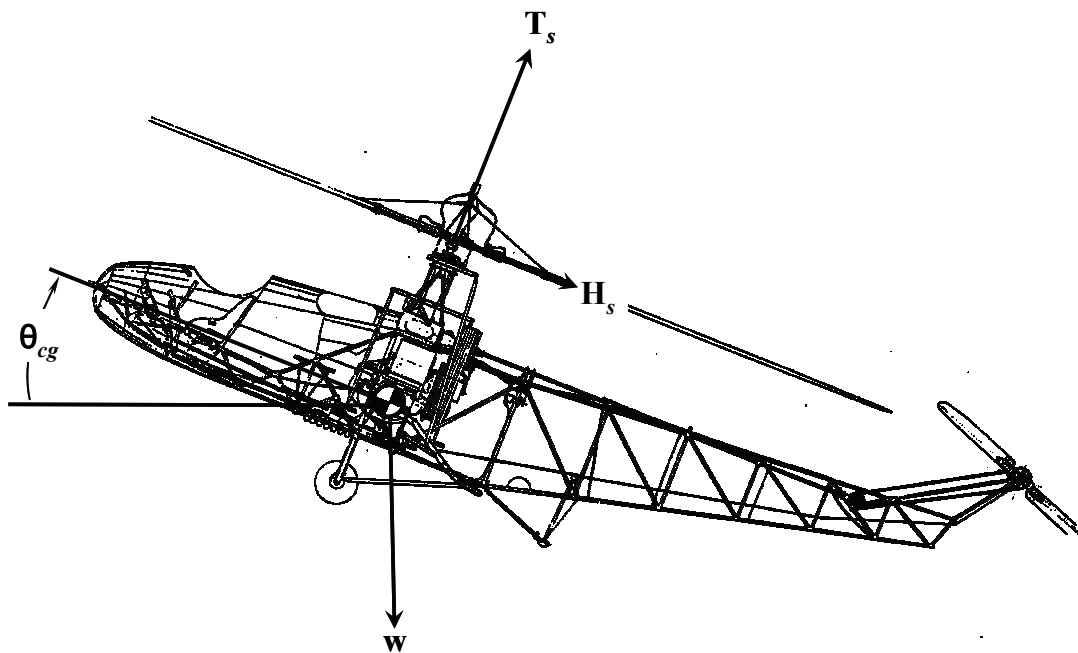


**Fig. 1-5. The primary forces and moments involved in longitudinal helicopter stability and control in hover.**

If you assume that the “slight disturbance” was a longitudinal gust of wind ( $V_{\text{gust}}$ ) while Captain Gregory held the longitudinal cyclic stick fixed, then the initial helicopter response is, from Eq. 15 in Appendix A, quite simply approximated as

$$(1.12) \quad \theta_{\text{cg}} = V_{\text{gust}} \times \left[ \frac{\partial M_p / \partial V + h \times \partial H_s / \partial V}{2I_{\text{cg}}} \right] \times t^2.$$

Both the hub moment ( $M_p$ ) and H-force speed derivatives introduced here depend on the longitudinal flapping. That is, because

$$(1.11) \quad M_p = \frac{F_c r_\beta b}{2} a_{1s}$$

and

$$(1.13) \quad H_s \approx W a_{1s},$$

it follows that

$$(1.14) \quad \frac{\partial M_p}{\partial V} = \left( \frac{F_c r_\beta b}{2} \right) \frac{\partial a_{1s}}{\partial V} \quad \text{and} \quad \frac{\partial H_s}{\partial V} \approx W \frac{\partial a_{1s}}{\partial V}.$$

Therefore, the initial helicopter response to a gust becomes

$$(1.15) \quad \theta_{\text{cg}} = V_{\text{gust}} \left[ \frac{F_c r_\beta b + 2 h W}{4I_{\text{cg}}} \right] \left( \frac{\partial a_{1s}}{\partial V} \right) t^2.$$

In Volume I, the longitudinal flapping was found to be very sensitive to speed, being on the order of

$$(1.16) \quad a_{1s} = 2\theta_0 V / V_t - B_{1c}.$$

Therefore, the partial derivative of longitudinal flapping ( $a_{1s}$ ) with respect to speed ( $V$ ) is

$$(1.17) \quad \frac{\partial a_{1s}}{\partial V} = \frac{2\theta_0}{V_t}.$$

With this last substitution, the initial helicopter response to a gust is approximated in the first few seconds of pitch motion by

$$(1.18) \quad \theta_{\text{cg}} = V_{\text{gust}} \left[ \frac{F_c r_\beta b + 2 h W}{4I_{\text{cg}}} \right] \left( \frac{2\theta_0}{V_t} \right) t^2.$$

## 1.2 STABILITY AND CONTROL

The VS-300 configuration Captain Gregory was flying that day in late 1940 is not absolutely recorded. However, the data<sup>5</sup> of primary interest suggests that, for a gust of 5 feet per second, he experienced an initial response, in degrees, of about

$$(1.19) \quad \begin{aligned} \theta_{cg} &\approx 1.15^\circ \times t^2 \text{ in degrees} \\ d\theta_{cg}/dt &\approx 2.3 \times t \text{ in deg/sec} \end{aligned}$$

Fig. 1-6 gives you some idea of what Captain Gregory experienced (and, in fact, what most student pilots first experience). Had he not “moved the stick forward,” the helicopter would have begun the unstable oscillation shown by the open circles in Fig. 1-6. The period of this oscillation (i.e., the time to complete one cycle) is on the order of 12 seconds. Furthermore, the amplitude doubles every 3.6 seconds! The fact that Captain Gregory just stayed above the ground for his first 8-minute flight would seem to be a major miracle.

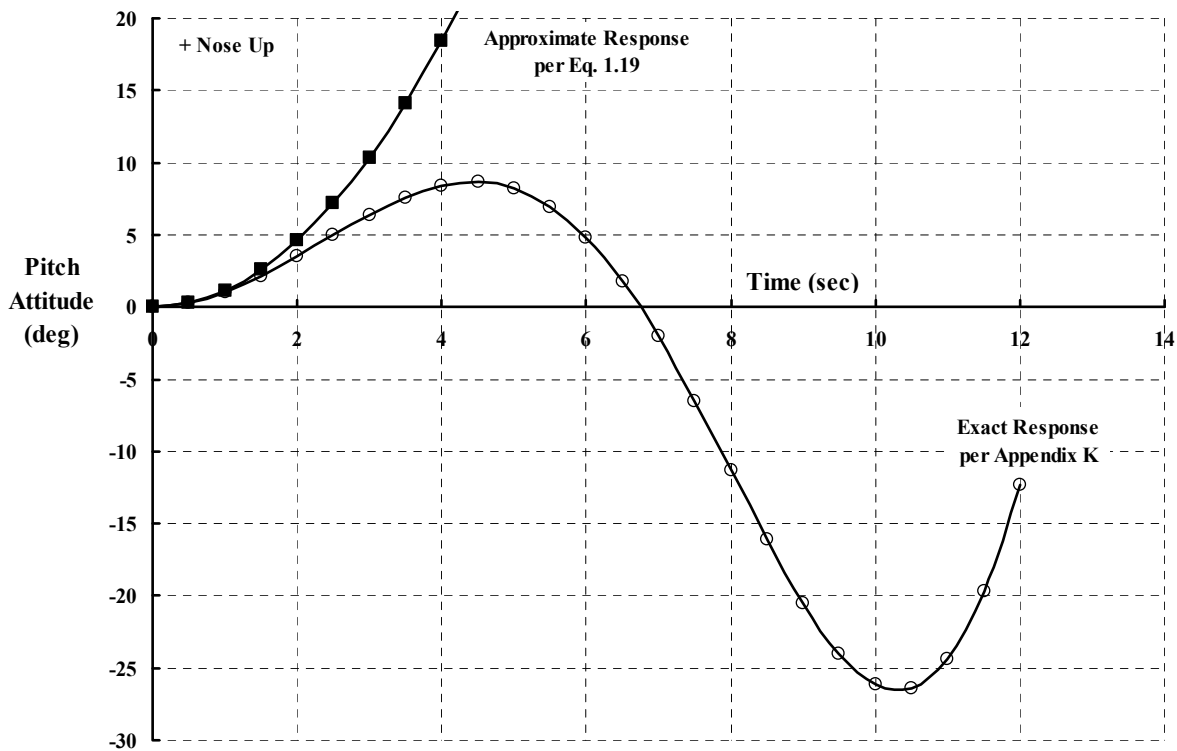


**Fig. 1-6. The Sikorsky VS-300 was a challenge to hover (response to a 5-ft/sec wind gust with controls fixed).**

<sup>5</sup> Technical information provided by Harold Ulisnik, Sikorsky Aircraft, allowed the following data on the VS-300 to be compiled:  $W = 1,290$  lb,  $I_{cg} = 1,000$  slug-ft<sup>2</sup>,  $h = 5$  ft,  $R = 15$  ft 1 in.,  $c = 12$  in.,  $b = 3$ ,  $\sigma = 0.0633$ ,  $V_t = 353$  ft/sec,  $\Omega = 23.4$  rad/sec,  $F_C = 3,892$  lb,  $r_B = 2.125$  in.,  $I_f = 81$  slug-ft<sup>2</sup>,  $\gamma = 9.27$ ,  $B_{1C} = \pm 10$  deg,  $\delta_{cyclic} = \pm 10$  in.,  $\rho = 0.002378$  slug/ft<sup>3</sup>,  $C_T = 0.00609$ , and  $\theta = 0.19$  rad.

What Captain Gregory learned quickly was to make smooth, but small, control movements roughly in proportion to the helicopter pitch rate, not pitch attitude. In effect, he first became a rate gyro. His control of the VS-300 went from the longitudinal cyclic stick ( $\delta_{\text{cyclic}}$ ) through the control linkage to the blade longitudinal feathering angle, ( $B_{1C}$ ), which then changed the longitudinal flapping angle ( $a_{1S}$ ). Stated in an engineering way

$$(1.20) \quad a_{1S} = 2\theta_0 V/V_t - B_{1C} = 2\theta_0 V/V_t - \frac{\partial B_{1C}}{\partial \delta_{\text{cyclic}}} \delta_{\text{cyclic}}.$$

The control ratio of the VS-300 was on the order of  $-1$  degree of  $B_{1C}$  per 1 inch of aft stick. Thus, aft stick produced rearward flapping and a nose-up moment about the helicopter center of gravity as Fig. 1-5 suggests. Acting with both a sense of pitch rate and, to a lesser extent, pitch attitude, Captain Gregory's control inputs can be described as

$$(1.21) \quad \delta_{\text{cyclic}} = \frac{\partial \delta_{\text{cyclic}}}{\partial \dot{\theta}_{\text{cg}}} \dot{\theta}_{\text{cg}} + \frac{\partial \delta_{\text{cyclic}}}{\partial \theta_{\text{cg}}} \theta_{\text{cg}},$$

and the control of rotor forces and moments through longitudinal flapping then becomes

$$(1.22) \quad a_{1S} = 2\theta_0 V/V_t - \frac{\partial B_{1C}}{\partial \delta_{\text{cyclic}}} \left[ \frac{\partial \delta_{\text{cyclic}}}{\partial \dot{\theta}_{\text{cg}}} \dot{\theta}_{\text{cg}} + \frac{\partial \delta_{\text{cyclic}}}{\partial \theta_{\text{cg}}} \theta_{\text{cg}} \right].$$

By reacting to pitch rate, the pilot introduces sufficient damping to control the inherently unstable helicopter. Additional control motions can then be made to precisely hover the rotorcraft over any given spot.

I have taken some license in the story of VS-300 stability and control development. A more factual account, based on the aircraft log, was provided by a letter<sup>5</sup> from Harold Ulisnick as follows:

“The VS-300 was first flown 14 September 1939 with full cyclic control on the main rotor. The aircraft was nearly uncontrollable not so much because of lack of skill on the part of the pilot, but due to the fact that the controls were rigged about  $60^\circ$  out of phase [a longitudinal stick input resulted in considerable lateral aircraft response, etc.]. Cyclic control was non-linear, and spongy. Additionally, aircraft vibratory levels were extremely high.

Following the crash on 9 December 1939, the VS-300 was rebuilt with main rotor collective control only, single tail rotor anti-torque/directional control, and twin horizontal tail rotors for longitudinal and lateral control. The first reference I have to Lieut. Gregory piloting the VS-300 is on 24 July 1940. Several very short duration flights were made. The aircraft was configured as above.

Following many changes to the geometry of the two horizontal tail rotor support structures [directed at improving control characteristics], Captain Gregory again flew the machine on 16 April 1941. Stability and control were adequate enough to permit Mr. Sikorsky on 6 May to set a world endurance record [in hover] for helicopters of 1 hr., 5 min., and 14.5 sec. Maj. Gregory again flew the aircraft on 7 May 1941. Forward flight stability was still poor due to main rotor downwash impinging on the two

## 1.2 STABILITY AND CONTROL

horizontal tail rotors. Lateral control was marginal. Also, there was a lateral ‘shuffle’ that continued to plague development.

Experiments were made with lateral cyclic in the main rotor, but twin horizontal tail rotors were retained for longitudinal control and for just-in-case. Confusion over control precession angle still remained.

Maj. Gregory next flew the VS-300 on 14 August 1941 by which time the two horizontal tail rotors had been removed to be replaced by one horizontal tail rotor for longitudinal control. The main rotor now had lateral/collective control. Lateral control was now satisfactory and control phase angle was finally understood. Note that, by this time, the mechanism for inputting control to the main rotor from stationary coordinates to rotating coordinates had been completely revised relative to the manner in which it had been accomplished in the aircraft as it was originally flown. In effect, the swashplate had now been partially invented.

Return to full cyclic control in the main rotor due to success experienced with main rotor lateral cyclic was made in late November 1941. On 8 December 1941 first flight was made with the new control system. Much work was done ‘refining’ the control system (stiffening, collective/throttle synchronization, fine tuning phase angle, etc.).

Lt. Col. Gregory next flew the machine on 20 November 1942 with a two bladed 29 foot diameter main rotor. Decision was made to return to a 3-bladed main rotor. A new 30 foot diameter main rotor was constructed. On 23 April 1943 Lt. Col. Gregory flew the machine in its final configuration. The basic overall geometry had now been established. The XR-4, (Sikorsky VS-316), contracted for back on 21 December 1942 quickly followed.”

The several configuration steps Sikorsky took in arriving at the prototype of the modern, single rotor helicopter today are illustrated with photographs in Boulet’s history [2].<sup>6</sup>

The next major step in helicopter development also improved helicopter stability and control. In January of 1943, Arthur Young successfully flew a unique helicopter having a single, two-bladed main rotor plus anti-torque tail rotor. His design incorporated a mechanical gyroscope rotating with, and partially controlling, the blade feathering motion. This “stabilizer bar” changed the helicopter from an inherently unstable “machine” into a more controllable aircraft. From model helicopter tests begun in early 1940, Art Young found that the stability augmentation in hover could be so complete that his model would simply drift with the wind. (Art Young describes his pioneering work with models in reference [21] and then again, more completely, in reference [22].) His accomplishment was greeted with enthusiasm by Lawrence Bell, president of Bell Aircraft Company and an aviation pioneer in his own right. The result of this collaboration, after three prototypes and several accidents, was the now-familiar Bell Model 47. This helicopter received the world’s first civil certification (from the then CAA) on March 8, 1946.<sup>7</sup>

---

<sup>6</sup> You will find more fascinating test pilot tales about the VS-300 in the book by Charles Morris, *Pioneering the Helicopter* [19]. He was hired by Sikorsky in early 1941 as the chief flight test pilot and, fortunately, Igor Sikorsky provided a history in his famous book, *Story of the Winged-S* [20].

<sup>7</sup> The Young rotor system was further discussed and explained by Klemin in the popular magazine *Aero Digest* [23]. The stability and control aspects of the invention were tried on the Sikorsky H-19 with great success [24]. Richard Tipton [25] recounts the early history of the trailblazing efforts of Larry Bell and Art Young. Art Young

The Bell rotor system (with the Young Stabilizer Bar) as it came to be known, is illustrated schematically in Fig. 1-7. The Bell Model 47 hardware is shown in Fig. 1-8. The inputs from the pilot through the swashplate are mixed with the stabilizer bar inputs before being passed on to the blade.

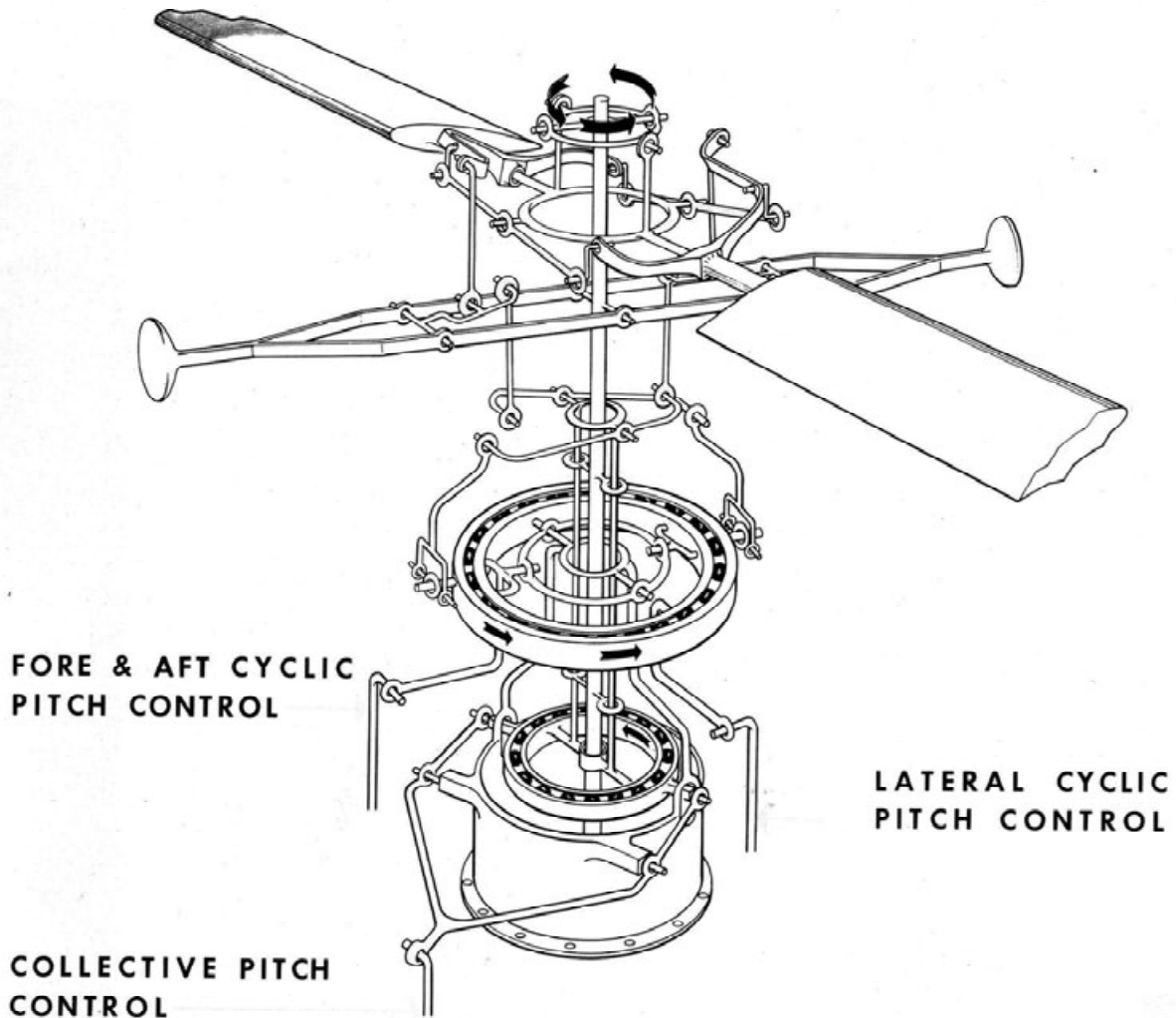
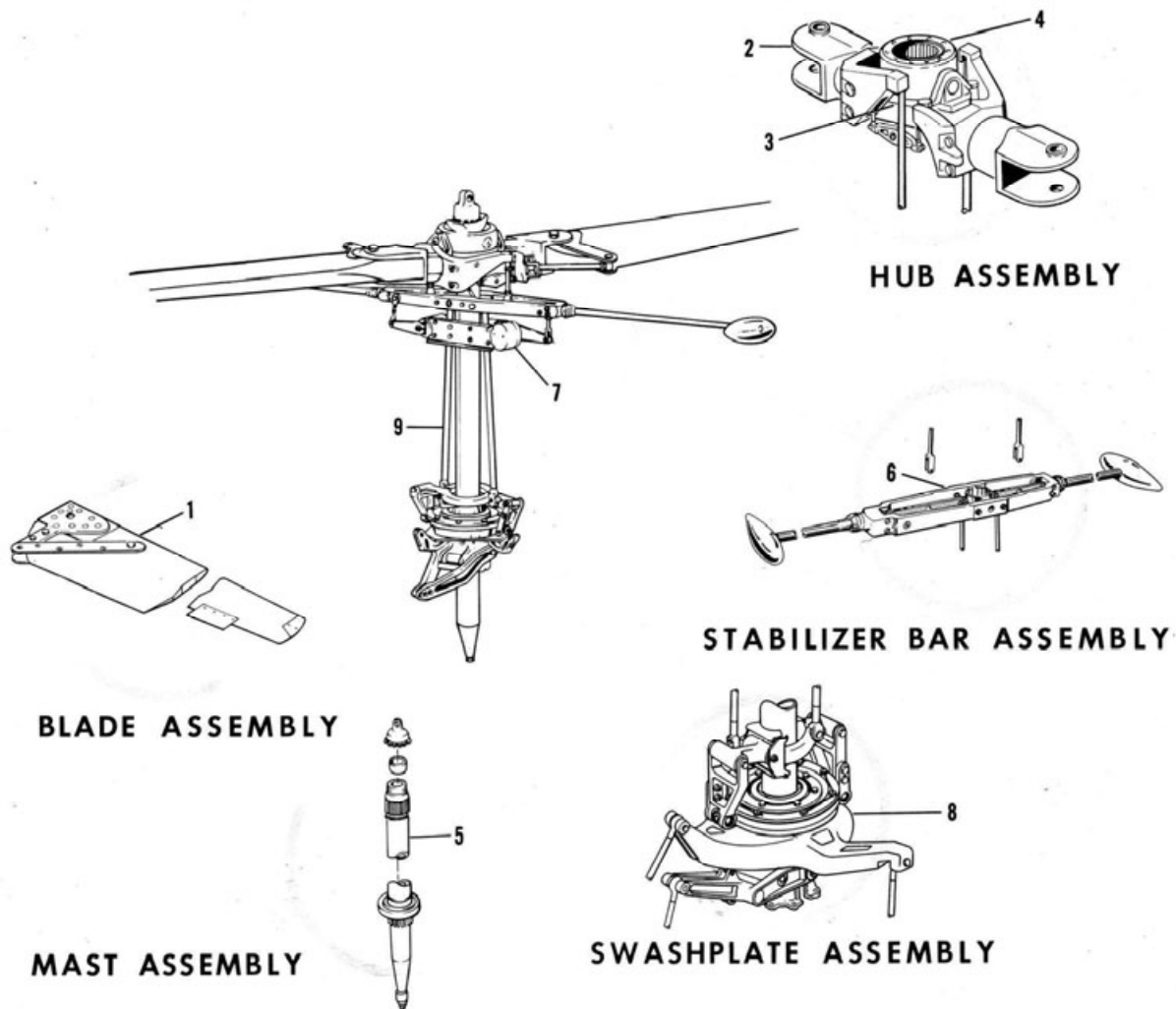


**Fig. 1-7. Arthur Young invented the stabilizer bar, which significantly improved helicopter stability and control [28].**

left what was to become Bell Helicopter in June of 1945. Bart Kelley, a lifelong friend to Young and himself a leader in the birth of this evolving technology [26, 27], became the technical director of the newly created helicopter company in 1946.

## 1.2 STABILITY AND CONTROL



The rotor blades (1) rotate and furnish lift. They are attached to the blade grips (2) by single retention bolts and stiff drag braces. The grips are attached to the yoke (3) through thrust and radial bearings in a manner similar to propeller blade retention. The yoke is underslung by pillow blocks from the gimbal ring (4) which is attached to the mast (5) by a splined trunnion.

The stabilizer bar assembly (6) consists of a center frame, two outer bars and streamlined weights. The assembly is mounted below the main rotor, with its axis at right angles to that of the main rotor. The motion of the bar about its pivot point on the mast is controlled by hydraulic dampers (7).

The mast control assembly consists of a swashplate (8) which encircles the mast near its base, push-pull tubes (9) which run alongside the mast, and mixing levers located in the frame of the stabilizer bar. The inner section of the swashplate does not rotate but is mounted on a support which permits it to be tilted in any direction. The outer section of the swashplate and control rods rotate with the rotor. The pilot actuates the cyclic control which tilts the swashplate, and in turn changes the cyclic blade pitch as the outer swashplate rotates.

**Fig. 1-8. The Young Stabilizer Bar and ground-resonance free, two-bladed rotor system put Bell Helicopter in business [28].**

What is too often missed in the discussion of the work by Art Young is the fact that his two-bladed rotor system completely solved the ground resonance problem (see Volume I) that had plagued rotorcraft nearly from the beginning. The lag hinge was removed, and the bladed attachment was made very strong in the inplane direction. It virtually uncoupled the lead-lag motion from the landing gear degree of freedom. In my view, this was the more rewarding benefit to the rotorcraft industry. More helicopters have been delivered with the two-bladed rotor system than any other type.

Stanley Hiller Jr., also working with a small group of very talented individuals, made the next major step to improved helicopter stability and control. Hiller's story is related by Jay Spenser in an excellent book, *Vertical Challenge, The Hiller Aircraft Story* [29]. Working somewhat in isolation on the west coast of the United States, Hiller initially began with a reasonably successful coaxial helicopter that evolved into the UH-4 Commuter. But it was with his UH-5, a conventional, single-main-rotor plus tail rotor design, that Joe Stuart III, Ed Bennett, and Hiller made a real breakthrough. The two-bladed rotor system they pioneered is shown in Fig. 1-9 and Fig. 1-10. The engineering fundamentals of this most successful mechanical stability and control invention were explained by Joe Stuart [30-32].

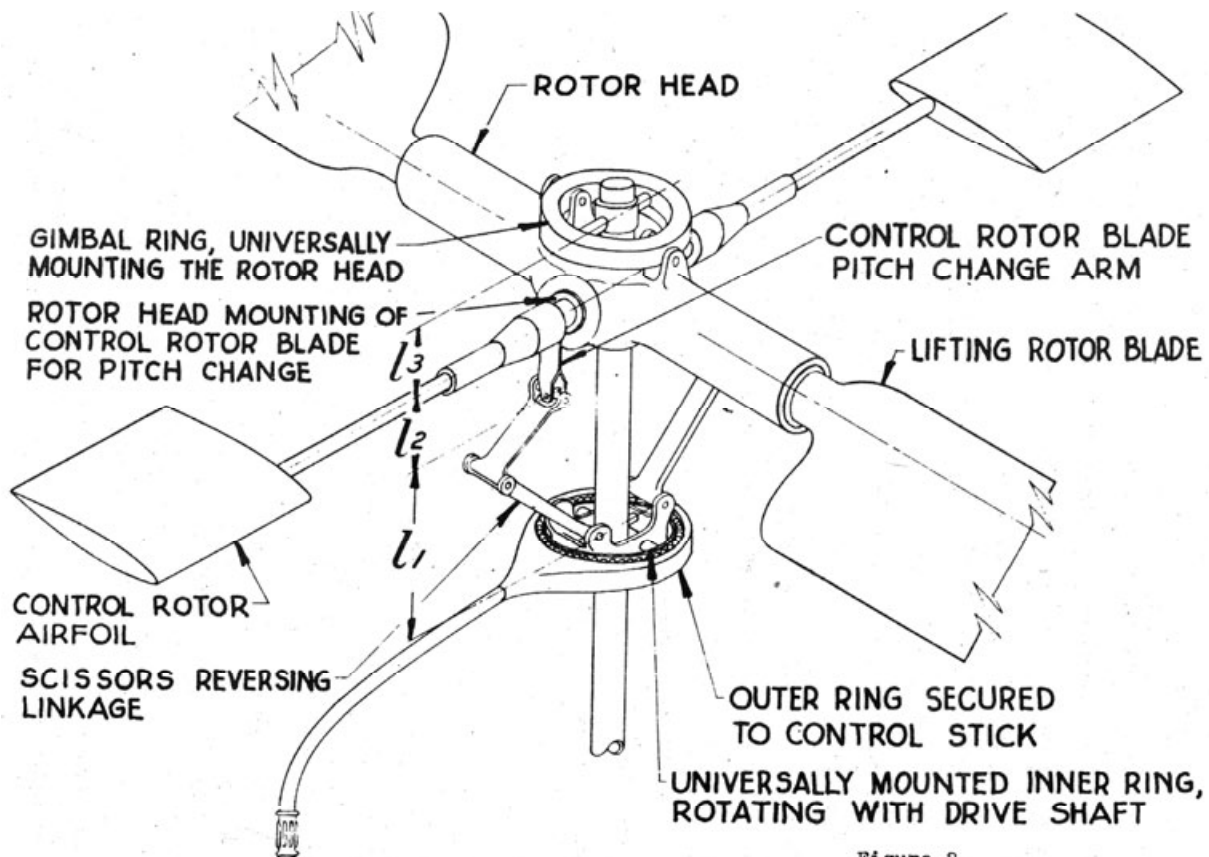


Figure 2.

p. 6-a.

Schematic Diagram, Hiller Simplified Control Rotor Linkage.

**Fig. 1-9. Joe Stuart III, Ed Bennett, and Stanley Hiller developed the servo paddle control system that solved the helicopter stability problem [30, 31].**

## 1.2 STABILITY AND CONTROL

The application of Stuart's theory to the Hiller UH-12 (i.e., the Model 360) was conveyed by Don Jacoby [33], and Klemin [34] wrote glowingly about the door that had been opened.

The pilot controlled the feathering of the servo paddles (the control rotor airfoil), and the servo paddles controlled blade feathering. The results were that pilot control loads were very, very low. This encouraged the direct control of longitudinal and lateral cyclic by a stick directly connected to the swashplate. The collective control was conventional. This combination of aerodynamic surfaces at the ends of a gyro bar provided the most stability in the early helicopters. For Hiller, it led to the very successful Model 360 product line that helped support some of the most innovative research and development the rotorcraft industry saw during the 1950s.

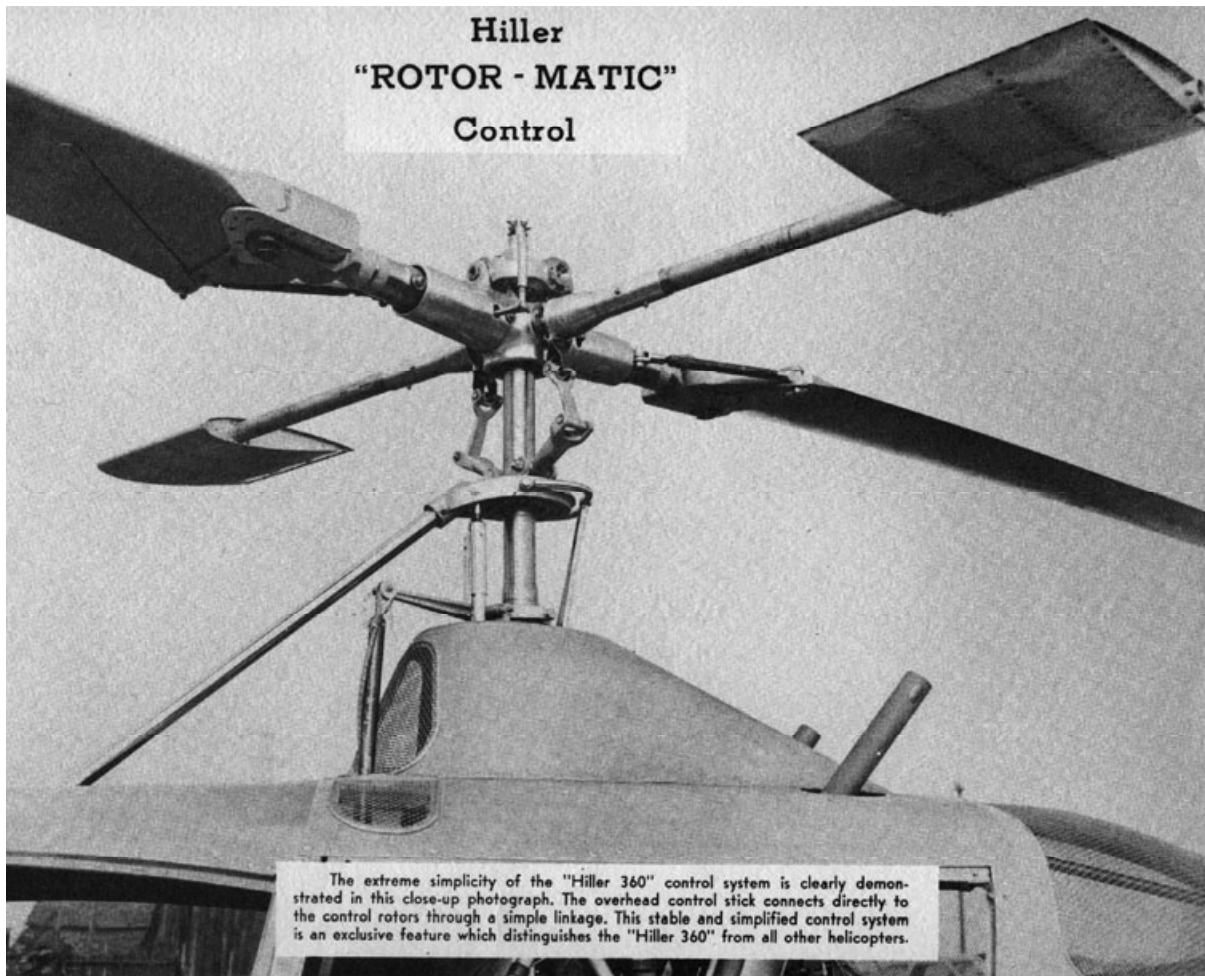


**Fig. 1-10. The Hiller Servo Paddle Control Bar and Bell two-bladed rotor system put Hiller in business (photo from author's collection).**

The Hiller rotor system, like Young's, was also two bladed with very stiff joining of the blades to the teetering hub. Both were free of the ground resonance "phenomena." (In my opinion, the Hiller system should be resurrected for use in the small, one- or two-place helicopters that frequently come to pass. The low-cost advantage of inherent stability with a simple aeromechanical system *plus* the cost of *only* two blades is just the place to start.)

The subject of helicopter stability and control was addressed in considerable detail by Rene Miller in his classic paper, *Helicopter Control and Stability in Hovering Flight* [35]. And the behavior of the three basic rotor systems available to future helicopter development was thoroughly summarized by Gerhard J. Sissingh [36, 37], starting with his work in Germany in 1939.<sup>8</sup> In the engineering terminology of this book, the longitudinal flapping for each rotor system can be uniquely described as follows:

For the "normal" rotor blade as Sissingh called it, that is, the three-bladed, articulated rotor system adapted by Focke, Sikorsky, and Piasecki

$$(1.23) \quad a_{1S} = 2\theta_0 V/V_t - \frac{\partial B_{1C}}{\partial \delta_{\text{cyclic}}} \delta_{\text{cyclic}} \quad \text{for articulated rotor system.}$$

For the Young, two-bladed, stabilizer bar rotor system, both the pilot's stick ( $\delta_{\text{cyclic}}$ ) and bar motion ( $\delta_{\text{stab. bar}}$ ) can make an input to blade feathering. Therefore,

$$(1.24) \quad a_{1S} = 2\theta_0 V/V_t - \frac{\partial B_{1C}}{\partial \delta_{\text{cyclic}}} \delta_{\text{cyclic}} + \frac{\partial B_{1C}}{\partial \delta_{\text{stab. bar}}} \delta_{\text{stab. bar}}$$

where the stabilizer bar input ( $\delta_{\text{stab. bar}}$ ) depends on both body pitch angle and body pitch rate according to

$$(1.25) \quad \delta_{\text{stab. bar}} = \frac{\partial \delta_{\text{stab. bar}}}{\partial \dot{\theta}_{\text{cg}}} \dot{\theta}_{\text{cg}} + \frac{\partial \delta_{\text{stab. bar}}}{\partial \theta_{\text{cg}}} \theta_{\text{cg}}.$$

For the Hiller, two-bladed, servo paddle rotor system, the pilot's cyclic stick motion ( $\delta_{\text{cyclic}}$ ) goes first to create the servo paddle motion ( $\delta_{\text{servo paddle}}$ ) so that

$$(1.26) \quad a_{1S} = 2\theta_0 V/V_t - \frac{\partial B_{1C}}{\partial \delta_{\text{servo paddle}}} \delta_{\text{servo paddle}}.$$

The servo paddle motion is then described as

$$(1.27) \quad \delta_{\text{servo paddle}} = \frac{\partial \delta_{\text{servo paddle}}}{\partial \delta_{\text{cyclic}}} \delta_{\text{cyclic}} + \frac{\partial \delta_{\text{servo paddle}}}{\partial \dot{\theta}_{\text{cg}}} \dot{\theta}_{\text{cg}} + \frac{\partial \delta_{\text{servo paddle}}}{\partial \theta_{\text{cg}}} \theta_{\text{cg}}.$$

---

<sup>8</sup> At the end of World War II, several members of the United States aircraft industry toured through Germany to gain insight into the many accomplishments made there. Dick Prewitt summed up rotary wing development [38]. A similar assessment was made by Liptrot in Britain [39]. Both Kurt Hohenemser and Gerhard Sissingh [40, 41] found their way to the U.S. and contributed enormously to the technology of rotorcraft, and both were members in good standing of the American Helicopter Society.

## 1.2 STABILITY AND CONTROL

Of course similar equations can be written for lateral control and stability, and the behavior of the helicopter about that axis system.

The work by Sissingh [37] shows the essence of these two, pioneering, mechanical stability augmentation systems. Several linkage ratios and key derivatives are given that will reduce the inherent instability of the helicopter as it evolves into a more manageable machine.

The advent of hydromechanical control systems was followed by powerful electronics and computers. The industry first saw the stability augmentation system [42, 43] on a Sikorsky H-19 late in the summer of 1950. This was followed with successful application on a Piasecki XHJP-1, the prototype of the HUP-1. Today, the industry thinks in terms of an automatic flight control system (AFCS).

This introduction to helicopter stability and control would not be complete without acknowledging the role that model helicopters have played. Spenser, on page 166 of reference [29], points out that

“another interesting use of the [Hiller Servo Paddle] Rotomatic system in more recent years would underscore its value: almost all radio-controlled gasoline-powered scale model helicopters—be they models of Sikorskys, Bells, Agustas, Bölkows, or whatever—require Hiller Rotomatic paddles for sufficient stability and control to fly. Without Hiller’s patented paddles, model helicopter flight would probably not have been able to evolve parallel to radio-controlled model airplanes as a hobby.”

This important point can be reinforced by the pioneering efforts of John Burkam,<sup>9</sup> a truly creative engineer. His very simple, small, and light, rubber-band-powered model helicopter is shown in Fig. 1-11. The plans for this model first appeared in the January 1970 issue of *American Aircraft Modeler* [44]. The lead-in to the construction details in the article reads:

### Penni Helicopter

World’s first, real, rubber powered copter is simple but a scientifically developed free-flight demonstrating all principles of rotor-wing operation. Build it from scrap!

As originally conceived, Burkam used a Young Stabilizer Bar with the 16-inch-diameter rotor. Later, in 1982, a scaled-up version of the “Penni,” called the “Nicki,” was developed. It had a 24-inch-diameter rotor. Among other modifications, John incorporated the Hiller Servo Paddle. He explained<sup>9</sup> that “the reason for that [change] was that with 9 degrees or so of positive [pitch] angle on the paddles, it would tend to pull the helicopter out of a shallow dive and restore it to level flight.”

---

<sup>9</sup> John spent his career at what is now the Boeing Helicopter Division and retired in 1987. In private letters and telephone discussions, John explained that he had delivered well over a 1,000 kits of the Penni, the larger sized Nicki, and also a tandem rotor model called the Tricky.

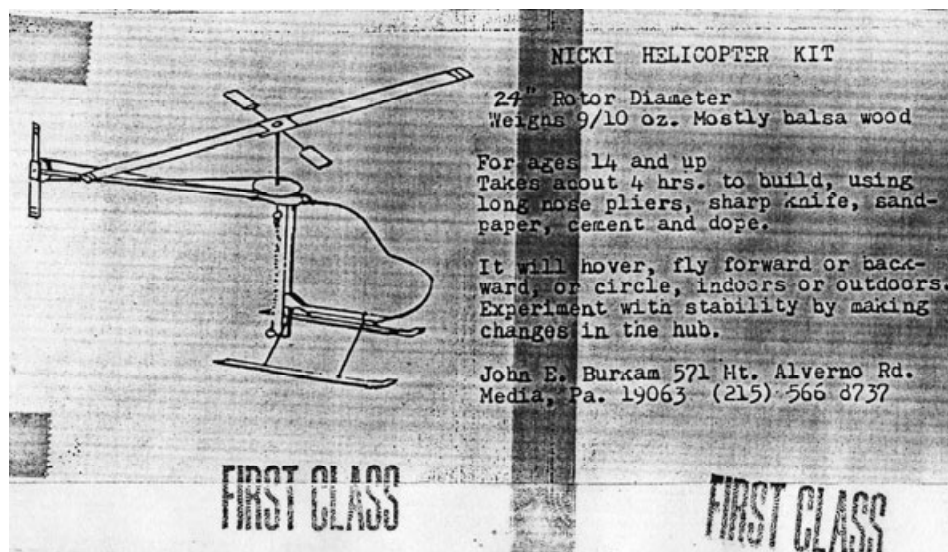


**Fig. 1-11.** The widely built “Penni” model helicopter was created in 1970 by John Burkam to demonstrate the stability of various hub types.



## 1.3 POWER-OFF LANDING

Power failures in a helicopter were not then, or are they today, as benign a situation as they were with an autogyro. The reasons for this statement are twofold. First, the helicopter inventors now had the possibility of power failure during hovering flight, and second, the powered rotor used in the helicopter required additional time, following the power failure, to transition into the autogyro mode. Two distinct critical regimes where power failure could be especially serious soon became clear. These two regimes were:

1. Power failure in forward flight while flying at low heights above the ground. Speeds from about 25 miles per hour up to maximum speed ( $V_{\max}$ ) where full-rated engine shaft horsepower ( $ESHP_{\text{rated}}$ ) was required. In fact, this regime could become critical whenever full  $ESHP_{\text{rated}}$  was used.
2. Power failure in hover at heights from 10 to 500 feet above the ground. This regime was quickly expanded to include flight at low speeds up to 25 miles per hour.

As more flight testing and operational experience was gained, a diagram of height versus airspeed was established for each model (Fig. 1-12). This H-V diagram, as it came to be known, conveyed the two flight regimes that the pilot should avoid. Later, the diagram became a standard chart found in the emergency procedures section of the pilot's flight manual. The diagram is occasionally referred to as the "deadman's curve."

Consider the low-altitude, forward-flight regime first and then later the hover and low-speed flight regime.

### 1.3.1 Power-Off Landing

You will recall from Volume I that Henrich Focke [45] set the number-one design requirement to provide for the "possibility of a forced landing in case of engine failure." Focke went on [46] to say that "on 10th May 1937 he [Rohlf, the test pilot] performed the very first auto-rotational landing, with engine off; a perfect 3-point, tail-down landing."

Sikorsky came to this same point of success in April of 1942 with the XR-4, the first production helicopter to follow the VS-300. The story is told by test pilot Charles Morris in Boulet's history.<sup>10</sup> Morris recounts a telephone call in late March of 1942 from Lieutenant

---

<sup>10</sup> See reference [2], pages 96–99. The Sikorsky VS-300 success led to an Army Air Corps contract for development of the XR-4, signed in December 1940. Ralph Alex, with a 16-member team, translated the 5-page technical specification into the first observation helicopter in 1 year. It flew first on January 14, 1942. The major acceptance demonstration was conducted April 20, 1942, and the helicopter was flown cross country to Wright Field (Ohio) arriving on May 17, 1942. The flight covered 760 miles in 16 flying hours over 5 days. By January 5, 1943, the XR-4 had successfully completed tests at Wright Field. The helicopter designation was changed from XR-4 to YR-4, and an initial order for 29 was placed. In all, 126 R-4s were built in 18 months. (Now *that* is a story of progress.)

### 1.3 POWER-OFF LANDING

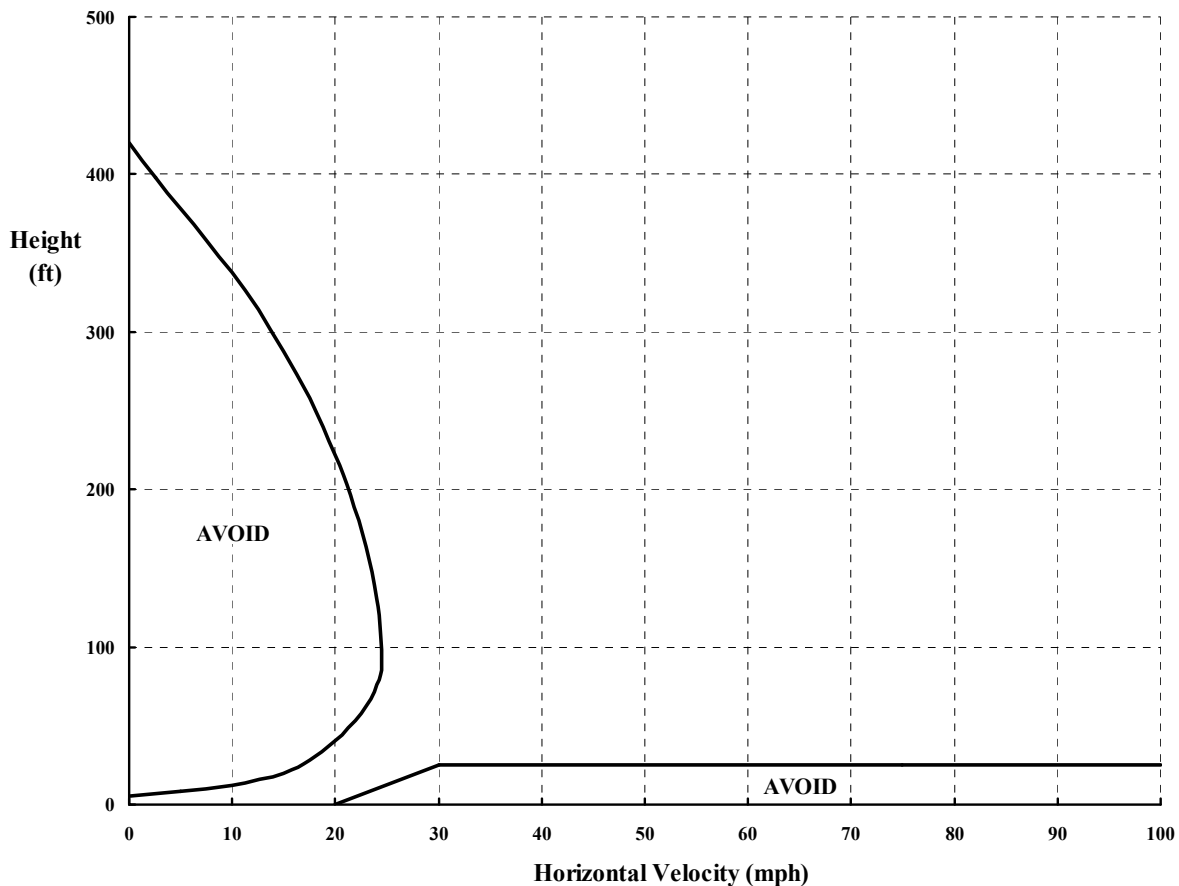


**Fig. 1-12. Typical flight regions to avoid when flying a helicopter.**

Colonel Frank Gregory (by then the Army chief of helicopters) requesting the demonstration of this first observation helicopter before an Army board as soon as possible. He described a full envelope of speed and altitude. Gregory concluded with the desire to “see it up to 500 or 1,000 feet anyway, but of course 5,000 feet would be excellent!”

Morris goes on to say, after gasping, “But we haven’t even found out yet how it handles in autorotation, when the engine quits. We have a lot of investigation still for forward speed. It seems too early to set a date.” Gregory’s response was, “Nonsense. Suppose we make it April 20. That will give you practically a full month to learn all you need to.” (The response of the Sikorsky team to this type of need is characteristic of the rotorcraft industry even today.) Morris recalls the ensuing effort as follows:

“We had no knowledge of the mysteries of high-speed flight, engine failure, and altitude. The last two were inseparable; it would be bordering on suicide to go even 100 feet off the ground without first investigating how the ship would handle without power. We knew, theoretically, that the rotor should keep right on turning, but theory and practice sometimes need a little coercing to get together. Nevertheless, we redoubled our efforts. On April 3rd, I flew the XR-4 to a nearby airfield. There, over the long paved runways, I would try to approach the power-off condition.

## 1.3 POWER-OFF LANDING

We decided that the safest procedure would be to fly forty to fifty miles an hour, about 100 feet high. Pitch [collective] would be reduced as rapidly as possible, and when the ship was within twenty feet of the ground, a so-called flare-out would be made by tilting rearward and slowing down the ship. We could tell when we had reached autorotation by watching the tachometers that showed engine and rotor speed.

These tests were the most difficult of any I have ever done. Active coordination of the throttle was required as pitch [collective] was quickly reduced. The rudder [tail rotor anti-torque thrust] had to be readjusted because of the changing power applied to the main rotor. I had to watch the airspeed indicator (to be sure I was not slowing down or speeding up), glance at the pitch indicator (to see how close it was to five degrees), keep an eye on the two tachometers (for signs of autorotation), and watch the ground, all this in a very short period of time!

Several attempts were made this first day, but the results were inconclusive. Their primary value was in the training I received, and I couldn't concentrate so hard for more than a few minutes at a time.

The second day of trials, I was able to secure actual autorotation by starting about 200 feet high. The glide, with the engine slightly throttled was quite pleasant, and it was obvious that the ship lost no part of its excellent control. We were greatly relieved, too, that the change from powered flight to autorotation and vice versa, was free from transitional vibrations. The completion of this test marked the casting aside of our last fetters—we could now feel free to fly at higher altitudes without fear of serious trouble if the engine should fail.

A few days later, Gregory (Lieutenant Colonel by now) dropped in to arrange final details of the official demonstration. I took him up for his first ride in the XR-4, and he spent more than twenty minutes flying it himself, handling the controls, getting the feel of it.

Finally I shouted, "I'll show you a power-off glide." He nodded his head and watched intently as I climbed to 300 feet above the airport, then lowered the pitch lever to three degrees, and throttled back. We glided down smoothly, and a broad grin lit his face as I banked slightly to one side and to the other. "I think I'll land her," I said, when we were about 100 feet high. I had never before actually landed a helicopter without power, but everything felt so right that it seemed quite natural to carry it through.

"Okay," he smiled. At about twenty feet I eased back slightly on the [longitudinal cyclic] control stick to sense its effectiveness, and at five feet from the ground, I moved the stick backward again. The glide decreased, the ship flared out as it tilted rearward, and we settled softly onto the runway. The tail wheel touched first, and the ship rocked forward onto the main landing gear, then rolled about ten feet to a stop. Our first power-off landing was a definite success."

From these two accounts of the importance of a power-off situation, you can appreciate more fully why it is such an important design consideration, and the detailed description provided by Morris emphasizes how pilot-sensitive the emergency procedures can be.

The engineering description of a landing following power failure in forward flight is relatively easy to set up and to understand. Broadly stated, this is a problem in energy management during four distinct phases as follows:

### 1.3 POWER-OFF LANDING

1. An awareness of the power failure,
2. A reaction to the failure with a rapid transition to gliding or autogyro flight,
3. A well-timed flaring out of the glide as the ground is approached, and
4. A judicious use of the last amount of stored energy in the rotor system.

The primary equation that governs the outcome starts with the power required from the engine. In this case where maneuvering is going to happen, the basic equation for engine shaft horsepower required (ESH<sub>P<sub>req'd</sub></sub>) is

$$(1.28) \quad \begin{aligned} 550\text{ESH}_{P_{\text{req'd}}} &= \text{Power Required in Steady Level Flight (550 HP)} \\ &+ \text{Power for Steady Climb (W dh/dt)} \\ &+ \text{Power for Accelerating Airspeed (W/g V dV/dt)} \\ &+ \text{Power for Accelerating Rotor Speed (I}_R \Omega \text{ d}\Omega/\text{dt)} \end{aligned}$$

A positive sign convention has been established in Eq. (1.28) for the three additional demands for engine power that are involved in the power-off maneuver.

It is not necessary for the moment to think about the details of how to estimate the horsepower required in steady, level flight (HP). Therefore, consider the first additional power required. This is the power required to change height above the ground. The term deals, of course, with the change in potential energy. This additional demand on the engine power depends on the weight (W) and the increase in height (h) above ground level with time (t). A positive rate of climb ( $V_{RC}$ ) means that dh/dt is positive. Conversely, in the power-off situation a negative change in height with time occurs. This leads to a rate of descent ( $V_{RD}$ ) and a negative value for dh/dt.

The second additional demand on the engine comes from a positive increase in airspeed (V) due to acceleration of dV/dt. Because, by definition

$$(1.29) \quad \begin{aligned} V &= \sqrt{(\text{Horizontal Speed})^2 + (\text{Rate of Climb or Descent})^2} \\ &= \sqrt{(V_H)^2 + (V_{RC} \text{ or } V_{RD})^2} \end{aligned}$$

it follows for the positive situation of climbing that

$$(1.30) \quad V \text{ d}V/\text{dt} = V_H \text{ d}V_H/\text{dt} + V_{RC} \text{ d}V_{RC}/\text{dt}.$$

In the power-off situation, it does not necessarily follow that the horizontal speed ( $V_H$ ) is always reducing or that some rate of climb might not briefly occur during the complete maneuver.

The third demand from the engine comes from an acceleration in rotor speed ( $\Omega$ ). This power depends on the polar moment of inertia ( $I_R$ ) of the rotor system, principally of the blades, plus many of the smaller rotating components that go along as rotor speed is

increased. Again, it is not a foregone conclusion that potential energy from height and kinetic energy from airspeed might not be used to accelerate rotor speed during the maneuver.

A very good engineering view of the time Charles Morris spent giving Lieutenant Colonel Gregory a complete power-off demonstration of the XR-4 in early April 1942 can be obtained from the previous three equations. Rather than amplifying the details, consider first the simple integration of the engine power, Eq. (1.28), with respect to time. Suppose at  $t = 0$ , the engine power is instantaneously reduced to zero. (A driveshaft failure would do this, for example, while simply throttling back quickly would not be a very close approximation.) Then, with zeroed engine shaft horsepower in Eq. (1.28), the power-required expression in integral form becomes

$$(1.31) \quad \int_0^{t=t_f} 550 \text{ HP } dt = -\int_{h_1}^{h_2} W \, dh - \int_{V_1}^{V_2} W/g \, V \, dV - \int_{\Omega_1}^{\Omega_2} I_R \, \Omega \, d\Omega \\ = -W(h_2 - h_1) - W/g \frac{1}{2}(V_2^2 - V_1^2) - I_R \frac{1}{2}(\Omega_2^2 - \Omega_1^2)$$

Now consider some physical data for the XR-4 and some estimates for the initial and final conditions. The XR-4 had a normal takeoff gross weight of about 2,000 pounds, and the early engine was rated at 165 horsepower. The three-bladed, 36-foot-diameter rotor turned at about 225 rpm giving  $\Omega = 23.5$  rad/sec and a tip speed of 420 ft/sec. The XR-4 rotor system polar moment of inertia ( $I_R$ ) was on the order of 450 slug-ft<sup>2</sup>.

With respect to the initial and final conditions, suppose you assume that Morris began the demonstration at 300 feet above the ground and at a cruise speed perhaps as high as 60 miles per hour or 88 ft/sec. This would put the advance ratio ( $\mu$ ) around 0.20. From references [47-50], the power required for steady, level flight would have been roughly 120 hp or about three-fourths of the rated engine power. The initial conditions, therefore, become

$$(1.32) \quad t = t_1 = 0, \quad h_1 = 300 \text{ ft}, \quad V_1 = 88 \text{ ft/sec}, \quad \Omega_1 = 23.5 \text{ rad/sec} \\ 550 \text{ HP}_1 = 66,000 \text{ ft-lb/sec} \quad \text{with } I_R = 450 \text{ slug-ft}^2$$

The final conditions are much easier to set, of course, because the XR-4 was stopped on the ground. Therefore,

$$(1.33) \quad t = t_f, \quad h_2 = 0, \quad V_2 = 0, \quad \Omega_2 = 0, \quad \text{HP}_2 = 0.$$

The horsepower required will vary with time, but for this simple illustration assume the power is constant over the complete demonstration at a value of  $\text{HP}_{\text{ref}}$ . Then the integral required by Eq. (1.31) has the first-order estimate of

$$(1.34) \quad \int_0^{t_f} 550 \text{ HP } dt = 550 \text{ HP}_{\text{ref}} t_f = 66,000 \times t_f \quad \text{for the XR-4 example.}$$

With this last rough approximation you see the relation between the three sources of energy as an expression in time of

### 1.3 POWER-OFF LANDING

$$t_f = \frac{Wh_1 + W/g \frac{1}{2} V_1^2 + I_R \frac{1}{2} \Omega_1^2}{550 \text{ HP}_{\text{ref}}}$$

(1.35) = + 9.1 seconds from the 300 feet initial height  
+ 3.6 seconds from the 60 mph initial airspeed  
+ 1.8 seconds from the 225 initial rpm

The power-off maneuver Morris demonstrated was, therefore, over in about 15 to 20 seconds.

Within this introductory framework you can now better appreciate the comments Morris made about the total concentration it took to develop the emergency procedure and to visually record data while he learned. Just as interesting is the speculation about Lieutenant Colonel Gregory's confidence. After all, Gregory, as an established autogyro pilot, had performed the full autorotation to a successful landing hundreds of times, but in this demonstration he was the passenger with a pilot who was doing it for the first time.

The introduction of Eq. (1.35) provides a step to defining a flight envelope in which an experienced pilot is likely to land successfully following a complete loss of power. This envelope has evolved into a chart of height versus airspeed that is normally placed in the flight manual as part of the Emergency Procedures section. A preliminary basis for this height-velocity diagram is to use time as a fixed parameter and find the line that relates height and velocity. From Eq. (1.35), this means solving for height (h) in terms of airspeed (V) for a given time (t<sub>f</sub>). Thus,

$$(1.36) \quad h = \frac{550 \text{ HP}_{\text{ref}} t_f}{W} - \frac{V^2}{2g} - \frac{I_R \Omega^2}{2W}$$

The results of applying Eq. (1.36) for the Sikorsky XR-4 example are shown in Fig. 1-13. The configuration data used for this example are a weight (W) of 2,000 pounds, a reference horsepower (HP<sub>ref</sub>) of 120 hp, an initial rotor speed (Ω) of 23.5 radians per second, and a rotor polar moment of inertia (I<sub>R</sub>) of 450 slug-feet<sup>2</sup>.

With Fig. 1-13 in hand, you can better appreciate the progressive increase in height that Morris selected as he developed the emergency procedures. He said that

1. "We decided that the safest procedure would be to fly forty to fifty miles per hour, about 100 feet high."....."Several attempts were made this first day, but the results were inconclusive."

2. "The second day of the trials, I was able to secure actual autorotation by starting about 200 feet high. The glide, with the engine slightly throttled [presumably at flight idle], was quite pleasant..."

3. A few days later, Morris demonstrated the XR-4 to Lt. Col. Gregory after climbing "to 300 feet above the airport [and probably at about 50 miles per hour], then lowered the [collective] pitch lever to three degrees, and throttled back."

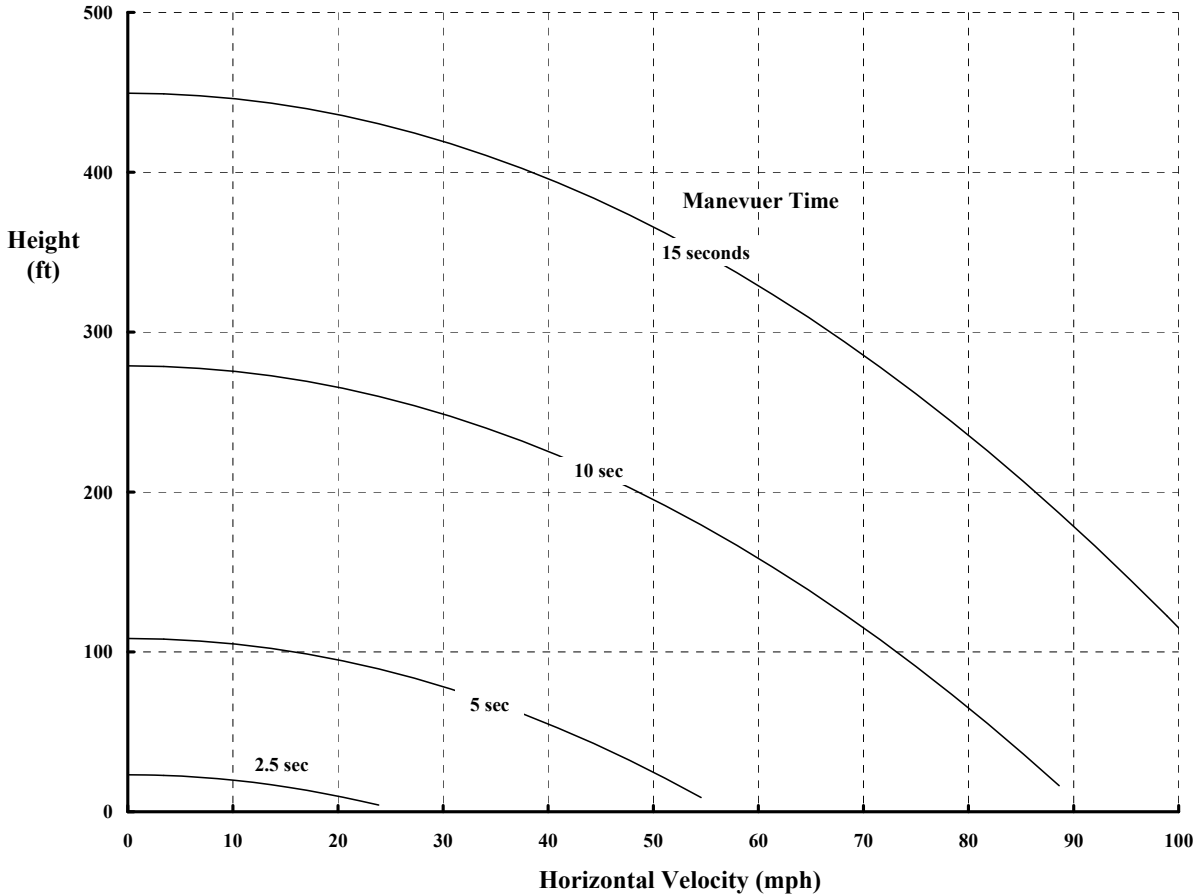


Fig. 1-13. The XR-4 power-off envelopes for four different maneuver times,  $t_r$ .

Morris, of course, was not dealing with a complete engine failure so the first second, or perhaps two, of becoming aware of the emergency was not demonstrated. This is the first of the four distinct phases outlined earlier and, in fact, he was only approximating the second phase in which the pilot must react rather quickly to make the transition to autogyro mode.

The first second or two following complete failure of power to the rotor system imposes a clear design constraint. You can see this from the rather simple analysis that follows. The important general characteristic is that the torque that reduces rotor speed goes down from the initial value in approximately a linear fashion. That is,

$$(1.37) \quad Q_{(t)} = Q_0 (1 - t/t_1).$$

The reasoning behind this rather fundamental behavior is simple physics. When the engine quits, the energy per second (i.e., the power) is supplied almost entirely by the kinetic energy from rotor inertia. The rotorcraft follows  $F = ma$  in the horizontal and vertical directions much slower. Thus, little kinetic energy becomes available until a second or two after the power failure. The full potential energy available from a loss in height follows even later. The deceleration in rotor speed reduces rotor thrust roughly in proportion to the square of rotor

### 1.3 POWER-OFF LANDING

speed, so the rotorcraft begins to fall first and slow down second. The rate of descent velocity ( $V_{RD}$ ), therefore, supplies the next source of energy to help offset the decaying rotor speed. The net result of this somewhat complex transient behavior is, perhaps surprisingly, the linear variation in rotor torque approximated by Eq. (1.37).

Even though the engine power goes instantaneously to zero at  $t = 0$ , the rotor winds down in a slower manner, and zero torque equilibrium is not reached until the time of  $t = t_1$ . Interestingly, the time to reach zero torque is on the order of  $t_1 = 2$  seconds (for no pilot input and from a straight and level flight condition). Accepting this first-order characteristic makes the problem easy. The rotor speed ( $\Omega$ ) is then determined by the simple equation

$$(1.38) \quad I_R \frac{d^2\psi}{dt^2} = I_R \frac{d\Omega}{dt} = -Q_{(t)} = -Q_0(1-t/t_1).$$

This rotor speed equation is integrated to give

$$(1.39) \quad I_R [\Omega_{(t)} - \Omega_0] = -Q_0(t - t^2/2t_1)$$

from which it follows that

$$(1.40) \quad \frac{\Omega_{(t)}}{\Omega_0} = 1 - \frac{Q_0}{I_R \Omega_0} (t - t^2/2t_1) = 1 - \frac{P_0}{I_R \Omega_0^2} (t - t^2/2t_1).$$

With the postulated linear variation in torque with time suggested by Eq. (1.37), the rotor speed decreases from  $t = 0$  to  $t = t_1$ . Then the rotor RPM begins to increase again. This droop in RPM reaches a minimum at  $t = t_1$  and has the value

$$(1.41) \quad \left[ \frac{\Omega_{(t)}}{\Omega_0} \right] = 1 - \frac{P_0}{2I_R \Omega_0^2} t_1.$$

For the XR-4 example, this becomes

$$(1.42) \quad \left[ \frac{\Omega_{(t)}}{\Omega_0} \right] = 1 - \frac{66,000}{2 \times 450 \times 23.5^2} \times 2 = 1 - 0.266 = 0.734.$$

There are several reasons, as you will see later, for not purposely allowing the rotor speed to drop below normal RPM by more than 20 to 30 percent. Charles Morris was demonstrating a helicopter that, in retrospect, was on pretty safe ground in this regard.

There is, of course, a loss in rotor thrust as the rotor speed decays in the first several seconds. This thrust variation is roughly in proportion to the square of rotor speed. Because thrust is approximately equal to weight at time zero, it follows that

$$(1.43) \quad \text{Thrust} \approx \left[ \frac{\Omega_{(t)}}{\Omega_0} \right]^2 (\text{Weight}) = \left[ 1 - \frac{P_0}{I_R \Omega_0^2} (t - t^2/2t_1) \right]^2 (\text{Weight}).$$

This loss in thrust leads immediately to the rotorcraft falling with an acceleration proportional to the difference between weight and thrust. A rate of descent velocity ( $V_{RD}$ ), therefore, builds up in accordance with the solution to  $F = ma$  of

$$(1.44) \quad V_{RD} = \int_0^t \frac{W-T}{W/g} dt = g \int_0^t (1-T/W) dt .$$

This equation is directly integrated because the ratio of thrust to weight is approximated from Eq. (1.43). The simple result is that

$$(1.45) \quad V_{RD} = g t^2 \left( \frac{P_0}{I_R \Omega_0^2} \right) \left[ 1 - \frac{t}{3t_1} - \left( \frac{P_0}{I_R \Omega_0^2} \right) \left( \frac{t^2}{3} - \frac{t^3}{4t_1} + \frac{t^4}{20t_1^2} \right) \right] .$$

The rate of descent when the torque is about zero (i.e.,  $t = t_1 \approx 2$  sec) then will be on the order of

$$(1.46) \quad V_{RD} = g \left( \frac{P_0}{I_R \Omega_0^2} \right) \left[ \frac{8}{3} - \frac{16}{15} \left( \frac{P_0}{I_R \Omega_0^2} \right) \right] \quad \text{at } t = t_1 = 2 \text{ sec}$$

= 20 ft/sec for the XR-4 example.

The rate of descent leads naturally to a loss in height, which, if the power failure happens near the ground, obviously becomes extremely important. This height lost is found by integrating Eq. (1.46) to find that

$$(1.47) \quad \Delta h = \frac{g t^3}{3} \left( \frac{P_0}{I_R \Omega_0^2} \right) \left[ 1 - \frac{t}{4t_1} - \left( \frac{P_0}{I_R \Omega_0^2} \right) \left( \frac{t}{4} - \frac{3t^2}{20t_1} + \frac{t^3}{40t_1^2} \right) \right] .$$

Assuming again the  $t = t_1 \approx 2$  sec situation means that the loss of height the pilot would have to deal with is about

$$(1.48) \quad \Delta h = 2g \left( \frac{P_0}{I_R \Omega_0^2} \right) \left[ 1 - \frac{1}{3} \left( \frac{P_0}{I_R \Omega_0^2} \right) \right] \quad \text{at } t = t_1 = 2 \text{ sec}$$

= 16 feet for the XR-4 example.

Now go back to the first and second distinct phases that follow an abrupt loss of power using the results obtained above. To repeat, these first two phases are:

1. An awareness of the power failure, and
2. A reaction to the failure with a rapid transition to gliding or autogyro flight.

These two phases could easily take 2 seconds. Furthermore, in that time the rotorcraft could well drop 15 to 20 feet and pick up a rate of descent velocity of 20 to 25 feet per second. And this situation could be expected at any horizontal airspeed from hover up to an airspeed where the full rated power of the engine was required. This rather simple overview illuminates,

### 1.3 POWER-OFF LANDING

therefore, a portion of the height-velocity diagram (begun with Fig. 1-13) that should be avoided.

The height-velocity diagram can show the area to be avoided. For example, continue the XR-4 illustration by replacing  $HP_{ref}$  of 120 hp with  $ESHP_{rated} = 165$  hp. Then Morris might have conservatively experienced an excessive droop in RPM down to 64 percent of normal RPM at the 2-second time. The rate of descent would then be about 27 ft/sec and the height loss more on the order of 21 feet. On this basis, Fig. 1-13 would be revised to show an AVOID area as illustrated in Fig. 1-14.

The AVOID area shown in Fig. 1-14 tapers down at low speed. This reflects a modern view that came with operational experience and theoretical work begun in the 1950s by I. C. Cheeseman in England [51] and pursued by Harry H. Heyson at NASA in the U.S.A. [52]. The low-speed region is somewhat more favorable because of ground effect that provides a beneficial cushioning and reduced power required.

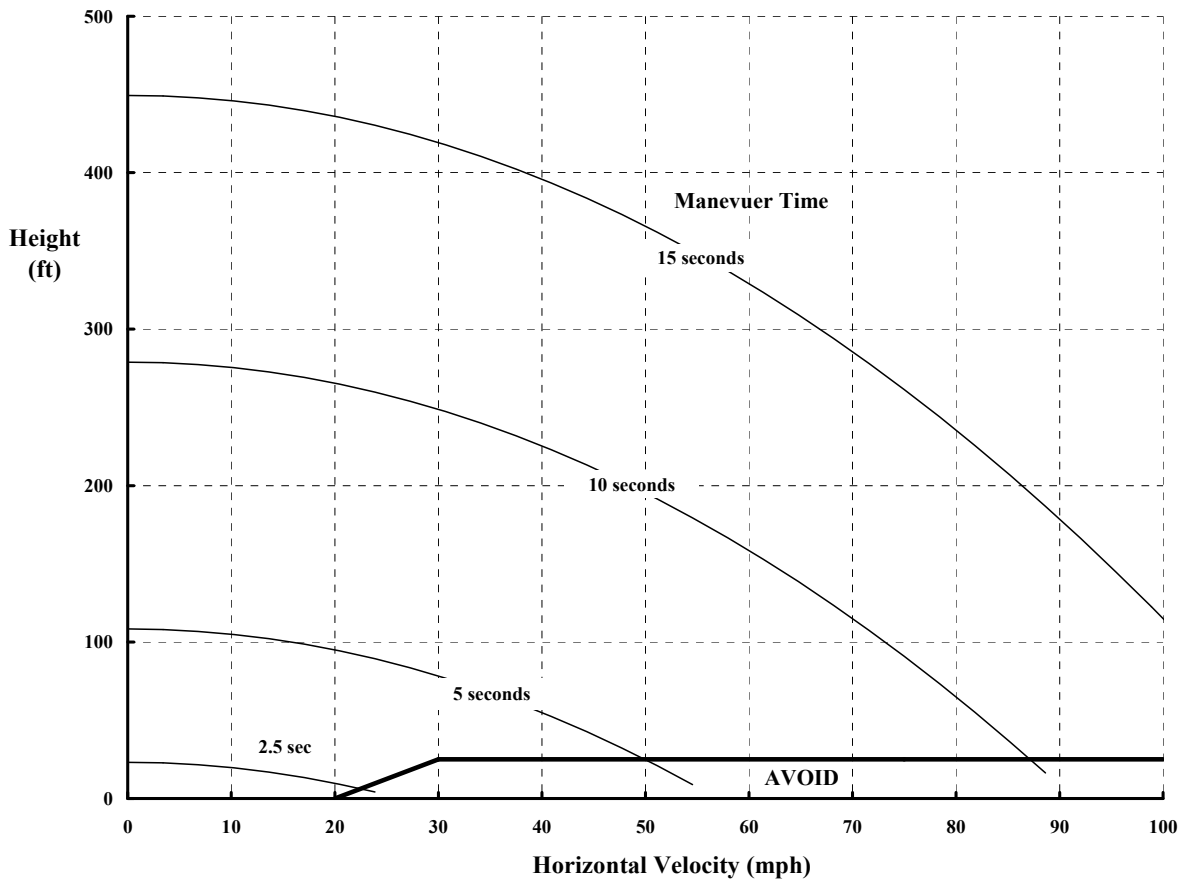


**Fig. 1-14. The XR-4 low-height AVOID region predicted with a simple theory.**

The second distinct phase of the power failure emergency deals with the reaction of the pilot after becoming aware of the situation. In the AVOID area, the reaction is likely to be rather instinctive upon seeing the loss in height. That is, the pilot would increase collective pitch to get thrust (even as the rotor speed is decaying). The simultaneous response must be to flare the rotorcraft nose up by moving the longitudinal cyclic stick aft. This control motion, if done quickly at high speed, can actually get the rotorcraft to climb and bring the rotor speed back to near normal RPM. After this 1- to 2-second period, the pilot has some opportunity to land safely.

The reaction—the second phase, *when the rotorcraft is well out of the AVOID area* of the height-velocity diagram—would be different. Generally, the procedure would be as Morris described. That is, a quick lowering of the collective pitch accompanied by some aft longitudinal cyclic to avoid an excessive droop in RPM as the transition to the autogyro gliding state is made.

The actual power-off glide, the third distinct phase, can be rather uneventful as autogyros demonstrated (and Morris records about his second day). The pilot has considerable latitude in glide speed. You can see this from data for the PCA-2 autogyro shown in Fig. 2-114 in Volume I. The glide can be stretched by gliding at an airspeed for the best lift-to-drag ratio just as is done with a fixed-wing aircraft. And as the ground is approached, a slight flare will reduce airspeed to the point where rate of descent is minimized. However, a major problem of this third distinct phase of the emergency can occur in this period. If the rotorcraft has an excessive minimum rate of descent (say upwards of 1,800 feet per minute or 30 feet per second), the skill and judgment of the pilot in the final 3 to 5 seconds become the deciding factor.

To this day, I am not aware of any simple theory (comparable to that developed for the AVOID area) that captures the period from flaring the glide to the final touchdown. Factors such as flaring nose-up reduces visibility and the pilot may lose reference to how close the tail is to the ground, or the few seconds of flight available from rotor inertia may be given up too soon in reducing rate of descent velocity. This last phase is entirely in the hands of the pilot.

You can read many technical articles about power-off landings. I doubt, however, that they will be as informative as what you can learn from an experienced pilot. To emphasize this point, consider a most recent book, *To Fly Like a Bird*, which tells many operational stories of the first Bell helicopters. In the last chapter, Joe Mashman<sup>11</sup> discusses autorotation. He highlights the efforts he and Floyd Carlson made to bring Larry Bell, Art Young, and Bart Kelley (with their pioneering Model 30) up to the point that Charles Morris and Sikorsky had reached earlier. Mashman relates that in late 1943:

---

<sup>11</sup> Joe Mashman, in reference [53], pages 170–172, provides another pioneering story that you can learn so much from. Joe switched over from flight testing Bell fixed-wing aircraft and was taught to fly helicopters by Floyd Carlson. Joe relates a great deal of the history of the Bell Model 47. The operational experiences he passes on are absolutely fascinating and provide key design considerations for a useful rotorcraft.

### 1.3 POWER-OFF LANDING

“We knew that if you lost your engine, you had to go to a low blade angle to keep the rotor turning. That’s what determined our minimum collective pitch setting in the helicopter, the setting that would keep the rotor blades turning at the optimal rpm due to the inflow of air up through the rotor. It wasn’t too hard to figure out, using what little aeronautical knowledge we already had.

What we didn’t know was how effective rotor inertia would be and how effective the flare would be. We did know how much inertia we’d get to a certain extent, because we could hover just above the ground and chop the throttle. As the aircraft began to settle, we would abruptly pull up the collective pitch lever and utilize the main rotor inertia to cushion the landing. That gave us an effective feel for the inertia and how much collective had to be pulled. But we didn’t have knowledge of the interaction between the flare and the collective pitch pull needed to make a safe power-off landing.

Sikorsky had already successfully demonstrated autorotation with their machines. But their helicopters had articulated rotor heads [on] which [the blades] were mounted with a slight [flapping hinge] offset. The articulated rotor follows the pitch of the fuselage as the tail hits the ground and then pitches forward. When the fuselage pitches forward, it carries the rotor forward. With the semi-rigid, seesaw-type Bell rotor, there’s no resistance to prevent teetering between the rotor and the mast. It’s just free to flap, so if you hit the tail and violently pitch forward, the rotor can’t follow fast enough, and that’s when it hits the tail boom, with what can be devastating results.”

With this background about the differences between the Sikorsky articulated rotor system with flapping hinge offset and the Young teetering rotor system, Mashman continues with:

“Early during the development program, Floyd Carlson had tried an autorotation in the original single-place Model 30, Ship 1. As he flared, his tail hit the ground and the main rotor sliced into the tail boom, cutting it right off. The helicopter was repaired [it became Model 30, Ship 1A], four wheels were put on, and the seat was widened so that another person could sit next to Floyd to read the instruments for him while he flew the aircraft. Now it was my turn to accompany him on the next autorotation attempts.

Floyd and I flew over to a little grass strip close to our Gardenville [New York] facility and began our flight test procedure. Starting in forward flight we reduced power by small increments and did a running touch-down landing preceded by a moderate flare. Floyd was doing the flying; there was only one set of controls. I’d call out the manifold pressure and the airspeed to him so he didn’t have to look down at the instrument panel. On the first one, we did a rolling touchdown, at about 60 percent power. Then we took off, went around again and cut the power back another inch or two of manifold pressure. We came in at the theoretically best autorotating speed, did a flare, and then touched down as we rolled off power. We just sort of gradually worked our way down in power settings until we achieved a complete power-off landing. It took about 45 minutes and involved about 15 takeoffs and landings....”

Mashman goes on to point out a key design philosophy that Bell Helicopter adopted for its future products. He says:

“To improve the helicopter’s autorotative capability, the engineers intentionally increased rotor inertia so that, in a steep flare, we could just slowly ease the nose forward while maintaining a decelerating attitude. With a low inertia rotor system, you can’t keep the helicopter in a flare very long. This is why the rotor systems of two-bladed Bell helicopters have high inertia, which provides outstanding power-off landing capability.”

Now, given what Morris and Mashman wrote, think again about the last phases of landing after power failure. These phases are:

3. A well-timed flaring out of the glide as the ground is approached, and
4. A judicious use of the last amount of stored energy in the rotor system.

The flaring portion of the maneuver is really a flaring of the tip path plane ( $\alpha_{\text{tip}}$ ) discussed earlier in relation to autogyros (see Fig. 2-28, Volume I). To arrest the rate of descent with a flare really means to increase  $\alpha_{\text{tip}}$  from about 10 degrees up to perhaps 20 to 30 degrees. During the glide, the tip path plane is flapped slightly aft relative to the hub plane, however, the rotorcraft fuselage attitude ( $\theta_{\text{cg}}$ ) relative to the ground is nearly zero (not terribly uncomfortable as Morris pointed out). Now to increase  $\alpha_{\text{tip}}$  in the final flare without increasing the fuselage attitude would require perhaps 15 to 20 degrees of longitudinal flapping ( $a_{1S}$ ). The Cierva-type hub, which has a flapping hinge offset ( $r_{\beta}$ ), would introduce a very large nose-up pitching moment to the body with this much flapping. Therefore, a combination of fuselage attitude and flapping (i.e.,  $\alpha_{\text{hp}} + a_{1S} = \alpha_{\text{tip}}$ ) that produced a reasonable flare had to be found by Morris. His configuration led to rather large nose-up body attitudes when the tail wheel touched down. In contrast, Carlson and Mashman, with the teetering rotor having zero flapping hinge offset, found they could introduce a great deal of flapping and much lower nose-up fuselage attitude to achieve the same  $\alpha_{\text{tip}}$ . The restraint for them was clearance between the rotor blades and the tail boom.

Mashman explained the final phase of the power failure procedure when he discussed not letting the helicopter slam down on its main gear after the tail wheel touched down. Without any horizontal velocity, and with zero rate of descent, the only energy left is from rotor inertia. As you saw from the XR-4 numerical example, rotor inertia provided less than 2 seconds in which to complete the final touchdown.

To completely analyze all four phases of the maneuver requires some form of simulation that has the pilot in the loop. In the pioneering days, that meant the pilots flew the prototype. Fortunately, today we can do much better. However, even a simple first-order simulation has a serious shortcoming that still exists today. The shortcoming is that thrust, and particularly power required at high  $\alpha_{\text{tip}}$ , is poorly predicted even with empirical modifications based on experiments.

### 1.3 POWER-OFF LANDING

Despite the complexity of the maneuver, some hint of test procedures was evolved. For example, the throttle chops done in a low hover that Mashman described helped succeeding pioneers approach evaluation of their configuration more safely. And from a design criteria point of view, the importance of rotor inertia and minimum rate of descent became clearer with each succeeding helicopter. In Fig. 1-15, I have created a *sweeping generality of a design criteria*. The figure reflects the success of (1) Cierva, Pitcairn, and Kellett with their autogyros, and (2) Focke, Flettner, Sikorsky, Young/Bell, Hiller, Piasecki, and Kaman with their helicopters.

Rotor energy, as used on the ordinate of Fig. 1-15, is expressed in units of horsepower. That is,

$$(1.49) \text{ Rotor Energy} \equiv \frac{I_R \Omega^2}{550 \text{ normal}} \text{ in horsepower.}$$

For the abscissa, I chose the installed rated shaft horsepower of the engine at sea level as an all encompassing measure of the configuration. Two lines, suggesting the importance of minimum rate of descent to the safe landing, are added to Fig. 1-15. This follows from the experiences of Mashman.

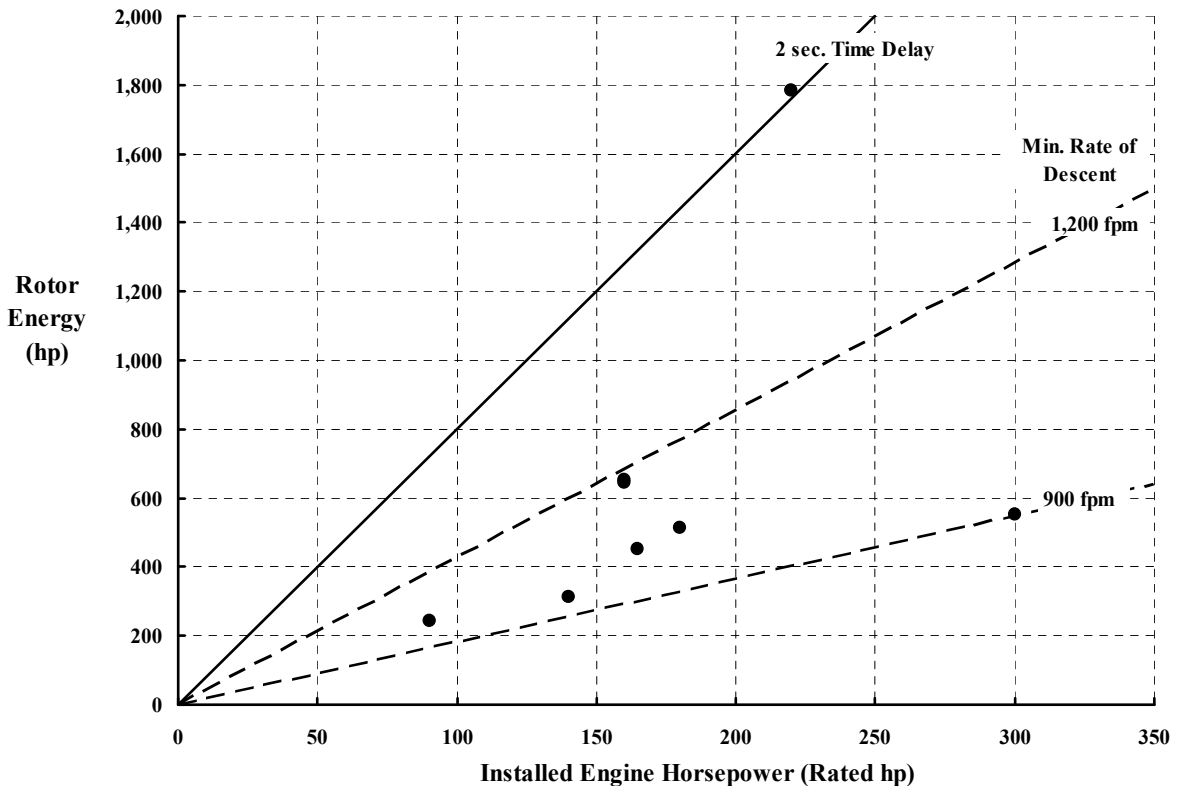


**Fig. 1-15. Both low, minimum rate of descent, and high rotor kinetic energy are important to a safe, power-off landing.**

In addition to minimum rate of descent, the drop in rotor speed immediately following an abrupt loss of power is reflected in Fig. 1-15. I suggest that a more conservative design criteria might have been chosen by the pioneers. Because any of their helicopters were capable of flying at the full rated shaft horsepower of the engine ( $ESHP_{rated}$ ), letting  $P_0$  equal 550 times  $ESHP_{rated}$  in Eq. (1.40) would better cover the power failure situation for the complete flight envelope.

Accept again that  $t_1$  is on the order of 2 seconds, and say the rotor-speed ratio should not go below 70 percent of normal RPM. Then the product of rotor inertia and rotor-speed squared should be selected so that

$$(1.50) \quad \frac{I_R \Omega_{normal}^2}{550} \geq \frac{ESHP_{rated}}{0.3} .$$

### 1.3.2 Power Failure in and Near Hover

The more serious side of the height-velocity diagram centers on a power failure when the rotorcraft is hovering. Performance in a vertical descent was hotly debated even for the autogyro as you found by reading the Glauert lecture of January 20, 1927 [54]. Early model rotor systems were tested in a wind tunnel and in free-flight drop tests [55-60]. More applicable data came from full-scale testing such as that provided by Wheatley [61]. The net result was that (1) early model tests were found not to be representative of full scale, and that (2) the bare essentials could only be empirically captured in crude theory. This left the problem of studying power-off vertical descent squarely in the laps of flight test and experimental test pilots.

What came from this early work was the conclusion that, in power-off vertical descent, the rotor had the performance of a parachute. Glauert advanced this finding at the end of his January 1927 lecture saying:

“Before concluding I wish to say just a few words about the possibility of the vertical descent of a gyroplane. The condition in which the windmill is then operating is unfortunately outside the scope of airscrew theory at present, and our conclusions must be based wholly on empirical results. In light of wind tunnel experiments and of dropping tests it appears that the velocity of steady vertical descent of a windmill is of the order of  $25 w$  [the paper has a typographical error and the correct expression is  $25 w^{1/2}$  ], where  $w$  is the loading per sq. ft. of disc area, and for a loading of 2 lbs. per sq. ft. this means a vertical velocity of 35 f.p.s. I see no reason for believing that the rate of descent of a full scale windmill can be appreciably less than this value, and so I do not believe that it would be safe for a gyroplane to descend vertically to the ground for any considerable height in still air. Of course, with the wind blowing and for a descent from low height, from which the full vertical velocity would not be attained, it might be possible to perform this manœuvre, but genuine steady vertical descent at a safe speed does not seem to be possible.”

### 1.3 POWER-OFF LANDING

The conclusion that Glauert advanced and that Wheatley confirmed with tests of the Pitcairn PCA-2 autogyro [see Volume I, Fig. 2-102, and Eq. 2.276] was simply

$$(1.51) \quad (R/D)^2 + (V_{\text{horizontal}})^2 = \frac{T_{\text{hp}}}{\frac{1}{2}\rho C_D (\pi R^2)}$$

and that

$$(1.52) \quad C_R = \frac{\sqrt{L^2 + D^2}}{q(A + S_w)} = \frac{D}{qA} = \frac{T}{\frac{1}{2}\rho V_{\text{RD}}^2 (\pi R^2)} \approx 1.2 \quad \text{for vertical descent}$$

from which it follows that the minimum *vertical* rate of descent velocity will be on the order of

$$(1.53) \quad \text{Min. } V_{\text{RD}} \approx \frac{1}{\sqrt{\frac{1}{2}\rho C_{R \text{ max}}}} \sqrt{T/\pi R^2} = 26.5\sqrt{T/\pi R^2} \quad \text{in ft/sec}$$

when the density of air is taken as 0.002378 slugs per cubic foot, and the maximum rotor drag coefficient is 1.2. Glauert's use of 25 rather than 26.5 reflects a modest impression that the maximum rotor drag coefficient was somewhat higher than the 1.20 I have used here.

What is so interesting about the discussion that followed Glauert's January 1927 lecture was that many in the audience were quite convinced that they had clearly witnessed the Cierva Autogyro perform vertical descents on landing. Others argued that even if it was not vertical descent, operationally controlled descent at 30-degree glide path angles was quite satisfactory.<sup>12</sup> More model experiments were requested and additional, more carefully conducted flight testing was demanded—all to be reported as soon as possible, of course.

The crux of the situation really centered around the rate of descent versus horizontal velocity performance at low speed. You can see this from typical flight data for the PCA-2 autogyro that was shown in Volume I, Fig. 2-102. The low-speed end of this data is presented here as Fig. 1-16.

From Fig. 1-16 you can see that landing into the wind would give the appearance of a much steeper glide angle while the rate of descent would still be rather low. This point was brought out by several members of the audience at Glauert's January 1927 lecture. In addition, the ground had the effect of increasing thrust to some extent which also softened the tail-down landing.

---

<sup>12</sup> The more important issue raised by the lecture was the position reiterated by Glauert that gyroplane high-speed performance and efficiency was not ever going to be comparable to fixed-wing aircraft. Cierva felt that Glauert was dismissing his Autogyro quite prematurely, and only on the basis of theory and some model tests that were currently in progress. Cierva stated that Glauert was wrong on all counts and was adamant about it in his letter that replaced his attendance at the lecture. Mr. Handley Page, a senior member of the aircraft industry, was in the audience. He expressed his opinion saying, "When the next paper comes I hope it will be a paper from Senor de la Cierva, but I suppose it will be replied to by letter from Mr. Glauert, who will be unable to be present. I do hope, however, that then we shall have the facts of the whole thing."

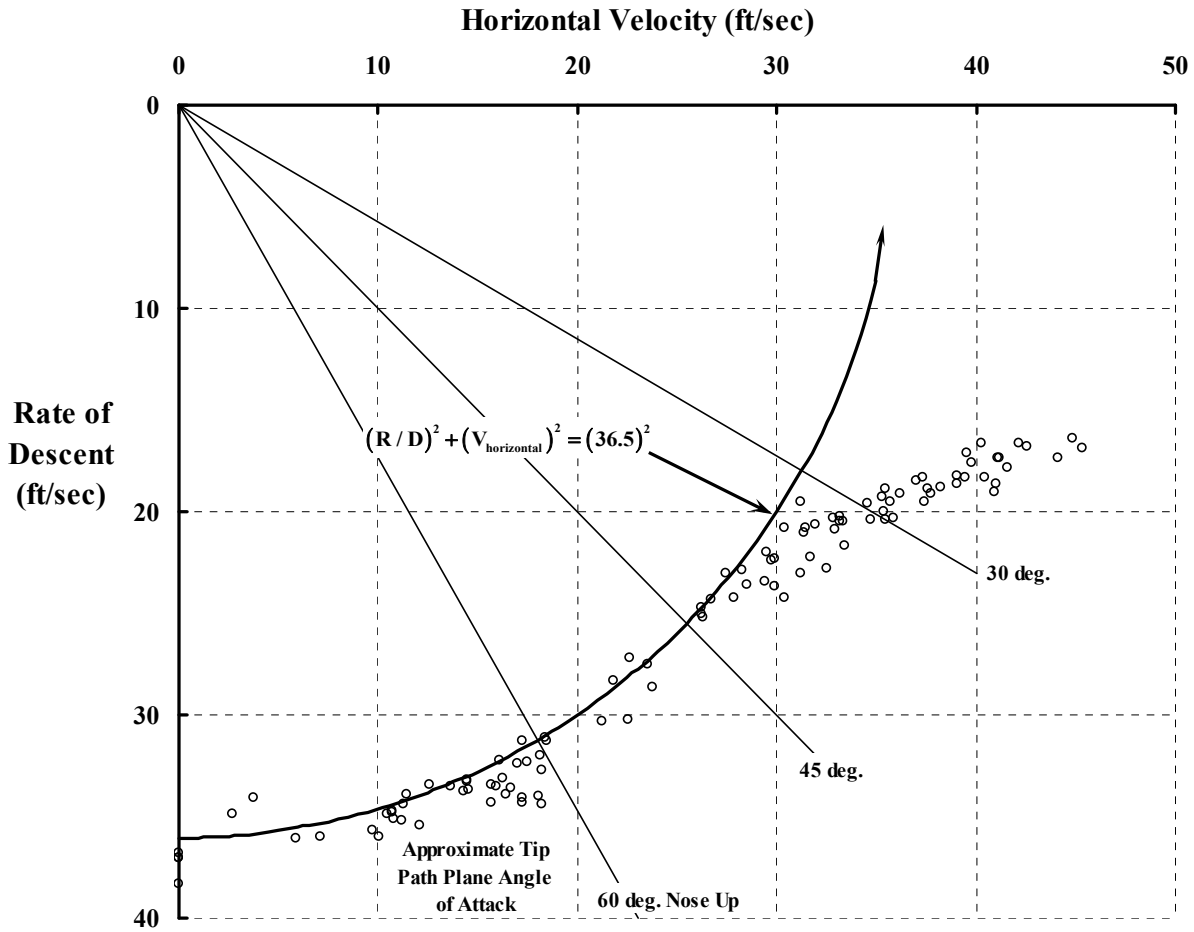


**Fig. 1-16. The PCA-2 low-speed gliding performance showed that the rotor had the drag of a parachute (power off, constant rotor speed, and hover out of ground effect).**

The solid line I have added to Fig. 1-16 provides a first extension from vertical descent of power-off performance. By assuming that

$$(1.54) \quad C_R = \frac{\sqrt{L^2 + D^2}}{q(A + S_w)} = \frac{W}{\frac{1}{2}\rho(V_{RD}^2 + V_H^2)(\pi R^2)} \approx 1.2 \text{ at low speed,}$$

it follows that the relation between vertical rate of descent velocity ( $V_{RD}$ ) and horizontal velocity ( $V_H$ ) will be graphically a circle described as

$$(1.55) \quad V_{RD}^2 + V_H^2 = \frac{W}{\frac{1}{2}1.2\rho(\pi R^2)} = \frac{W}{0.6\rho(\pi R^2)} \text{ at low speed.}$$

Thus, the early rotorcraft technology aspects of terminal velocity in vertical descent were laid for the helicopter pioneers.

### 1.3 POWER-OFF LANDING

What soon became apparent to the helicopter community was that this low-speed, high tip-path-plane angle-of-attack ( $\alpha_{tip}$ ) region had a number of very adverse operational characteristics. The primary up-flow through and about the rotor was very turbulent. This caused erratic control of vertical and near-vertical descent, and significantly increased overall helicopter vibration. In reality, rotorcraft did have a low-speed stall region using a definition based on highly turbulent flow. The region was bounded by  $\alpha_{tip}$  greater than 30 (or perhaps 45) degrees and combinations of  $V_{RD}$  and  $V_H$  near and within the circle given in Eq. (1.55).

Henrich Focke conveyed early exploration of power-off test results in figure 4 of his 1965 Cierva lecture [46]. He chose to make his point with power-off data from low speed. Pilot Rohlfs landed starting with a throttle chop in low-speed, level flight at about 4 meters per second (13 ft/sec) and at a height of roughly 160 meters (525 feet). The time history Focke included shows that Rohlfs chose to exchange altitude for horizontal velocity and avoid a vertical descent from such a height. The time history, in English units, becomes more informative by plotting height versus horizontal velocity as Fig. 1-17 shows.

The transition by pilot Rohlfs initially appears to be toward a vertical descent but, by 350 feet and about 5 seconds into the landing, he had already started to nose the F. 61 into a dive that took him well into forward flight. During this power-off landing, the vertical rate of descent reached a maximum of about 80 ft/sec at the 6-second point. After building up nearly 100 ft/sec of flight path airspeed, he pulled out of the dive and made the landing as if from a power failure in forward flight. Data from Focke suggests that Rohlfs nearly touched down at a very high speed, but apparently he simply glided parallel to the ground and let horizontal airspeed bleed off.

This interchange in  $V_{RD}$  and  $V_H$  for the Focke F. 61 helicopter is shown in Fig. 1-18. The first 3 seconds were spent well within the rotor turbulent flow region. The subsequent nose-down dive increased rate of descent and flight path airspeed, and took the helicopter out of the turbulent flow region. By 9 seconds the pull-up was well underway, and he was clearly back in control of the situation with still 150 feet of height available. Focke's time history, however, does show a rather hard landing.

As the pioneers gathered more experience in power-off landings from, and near, hover, a low-speed AVOID area was mapped out. It took the shape of a pear as illustrated in Fig. 1-19 for the XR-4 example. The character and design criteria related to both AVOID regions have received considerable attention [62-75].

The reliability of engines and drivetrain components rapidly improved as the pioneers gained and applied field experience. But to this day, Focke's number-one design requirement to provide for the "possibility of a forced landing in case of engine failure" has remained of paramount importance to the rotorcraft industry.

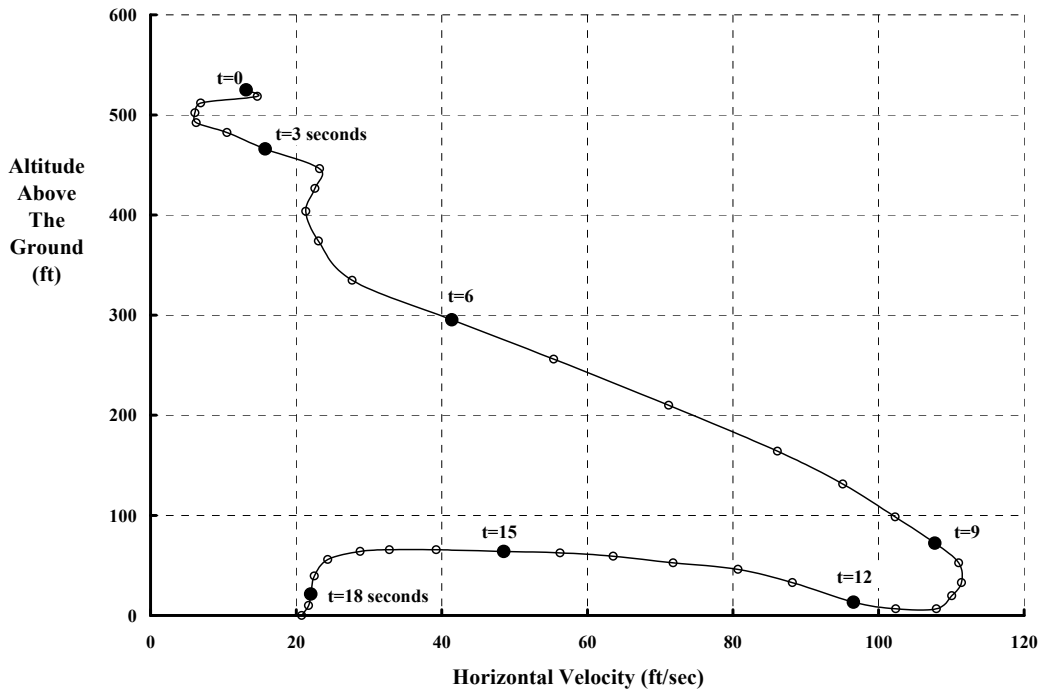


Fig. 1-17. Power-off vertical descents from high altitudes were avoided by pilots of early helicopters and still are today.

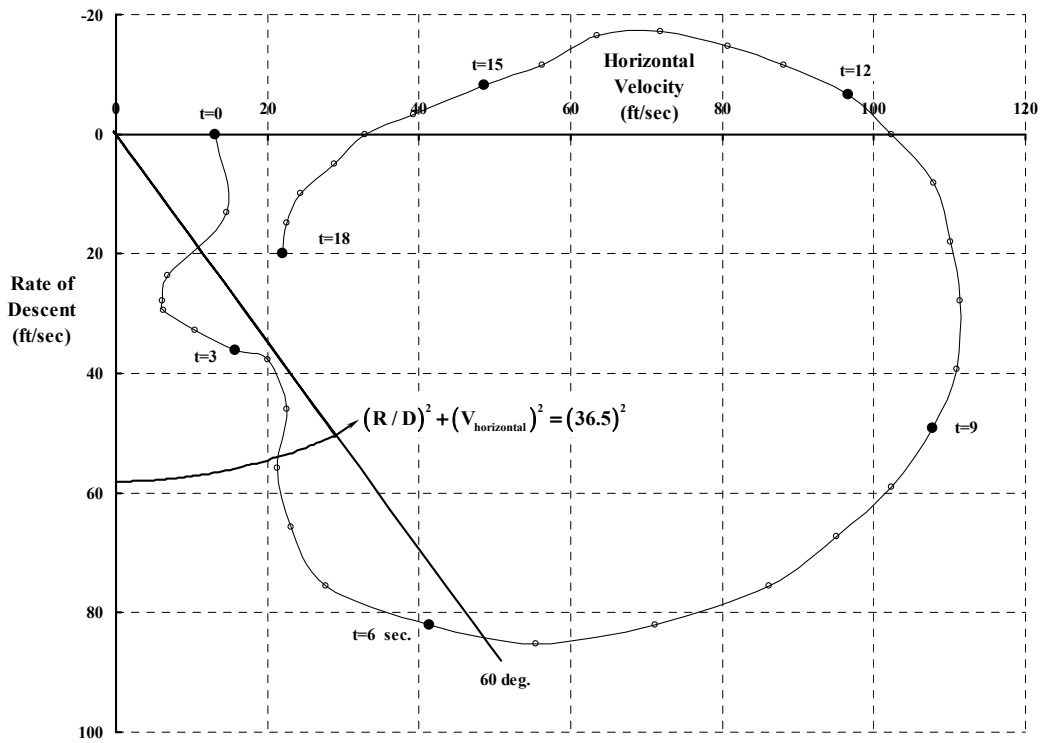
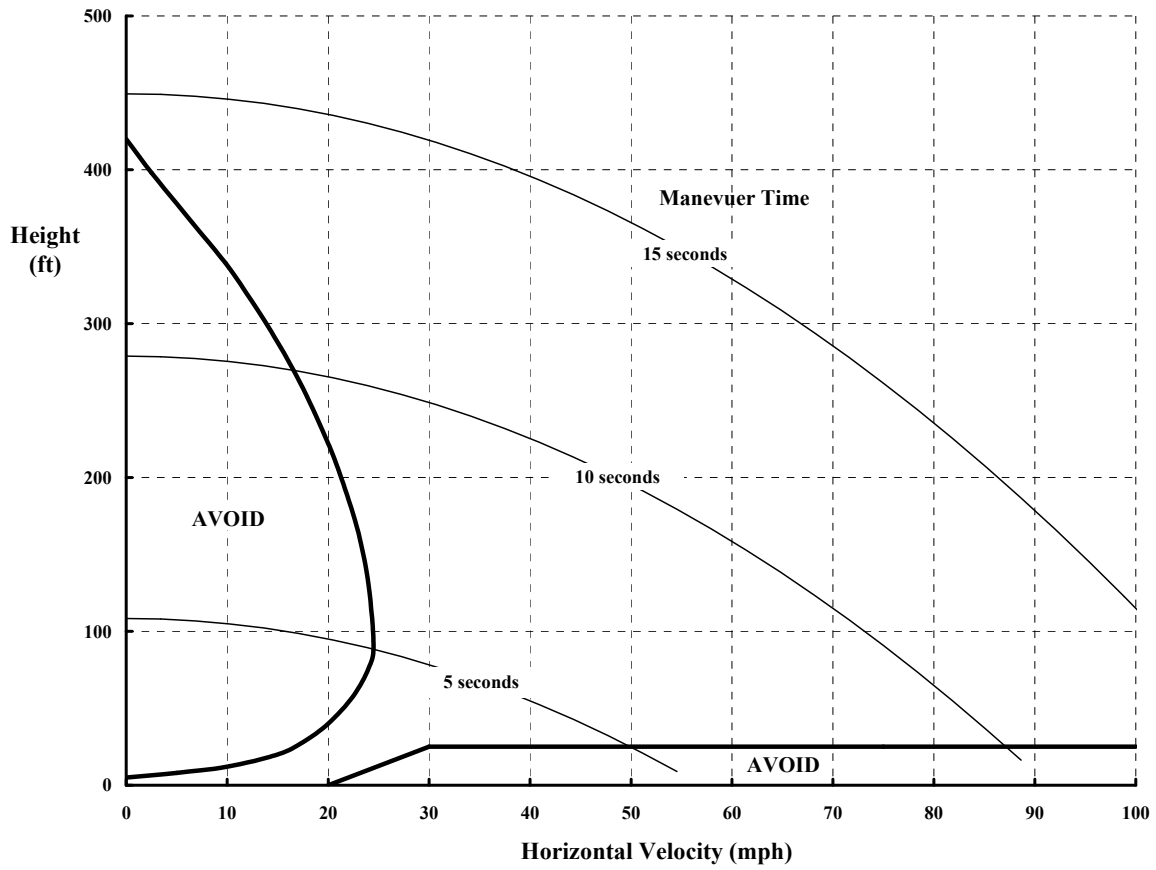


Fig. 1-18. Transition from vertical descent to descent in forward flight avoided the turbulence region of the rotor.

### 1.3 POWER-OFF LANDING



**Fig. 1-19. The XR-4 had two AVOID regions but only one could be predicted with a simple theory.**

## 1.4 CLOSING REMARKS

The rotorcraft industry completed the transition from autogyro to helicopter product line by the end of 1945. In Germany, the pre-World War II, 1936 experimental Focke F. 61 led to government war orders for the larger Focke Achgelis Fa-223. The German Government also placed war production orders for the Flettner Fl-282, which was based on the successful Flettner FL-265 experimental helicopter of 1939. Based on Focke's success, the Weir Company in England discontinued autogyro development and began its experimentation with the W.4 and W.5. And in the United States, the Army Air Corps led the transition when they selected the Sikorsky R-4 for production in 1942.

This transition from autogyro to helicopter product line is shown in Fig. 1-20. While the history may seem rather complex when presented graphically, it was, in fact, driven by two main factors. First, the commercial success of the autogyro did not carry over to enthusiastic military use. In fact, several evaluations of the autogyro versus the observation balloon were conducted by the U.S. Army Air Corps. Their conclusions, even before World War II began, were quite unfavorable with regard to the autogyro as Butler points out [76, 77]. Field evaluation was impeded by accidents with both the Kellett YG-1 and Pitcairn YG-2 direct control autogyros. Persistent occurrences of ground and air resonance complicated confidence in rotary wing technology by the decision makers of the day.

The second factor was, of course, Focke's success with the helicopter. This technology advancement, which gave a true rotorcraft hovering capability, was brought to the attention of Major General Oscar Westover (then Chief of Air Corps) by Lawrence LePage in early 1938. By the end of 1938, the U.S. Government had authorized \$2,000,000 for rotary wing and slow-speed, high-lift aircraft. The War Department was assigned as the lead agency. They issued a request for information (RFI) proposal in December 1939. The industry response led to the U.S. Air Corps Material Division at Wright Field issuing a request for proposal (RFP) to buy aircraft. From the several proposals submitted, the evaluation board selected two winners in June of 1940. They were:

- a. The Stinson Aircraft Company's C-105 fixed-wing, short-range, liaison aircraft, and
- b. The Platt-LePage Aircraft Corporation's larger variation of the Focke F. 61.

As Butler notes on page 10 of reference [77], neither the Pitcairn or Kellett autogyros, nor the Sikorsky helicopter designs were selected. The Platt-LePage helicopter was designated the XR-1, and the company was funded \$199,075 for one rotorcraft. Stinson received about \$3,000 each for immediate delivery of six off-the-shelf aircraft.

Despite best efforts by Haviland Platt and Laurence LePage, progress in developing their 440-horsepower, 5,200-pound-gross-weight helicopter was painfully slow. The XR-1 first hovered on May 18, 1941, but delivery dates kept being missed. An additional contract for \$144,662 led to a second, improved model designated the XR-1A. The U.S. Army finally took delivery of this helicopter in early August 1944. However, in April 1945, the U.S. Army terminated all contracts with the Platt-LePage Corporation.

## 1.4 CLOSING REMARKS

Technical difficulties experienced by Platt–LePage, from contract award well into late 1944, kept the door open for Sikorsky. His progress in solving the problems of the VS-300 and translating the configuration into the VS-300A laid the foundation for the Sikorsky XR-4. It was this helicopter, developed under the leadership of Ralph Alex, that gained the ultimate procurement support for the first successful incorporation of the helicopter into the Army Aviation force structure.

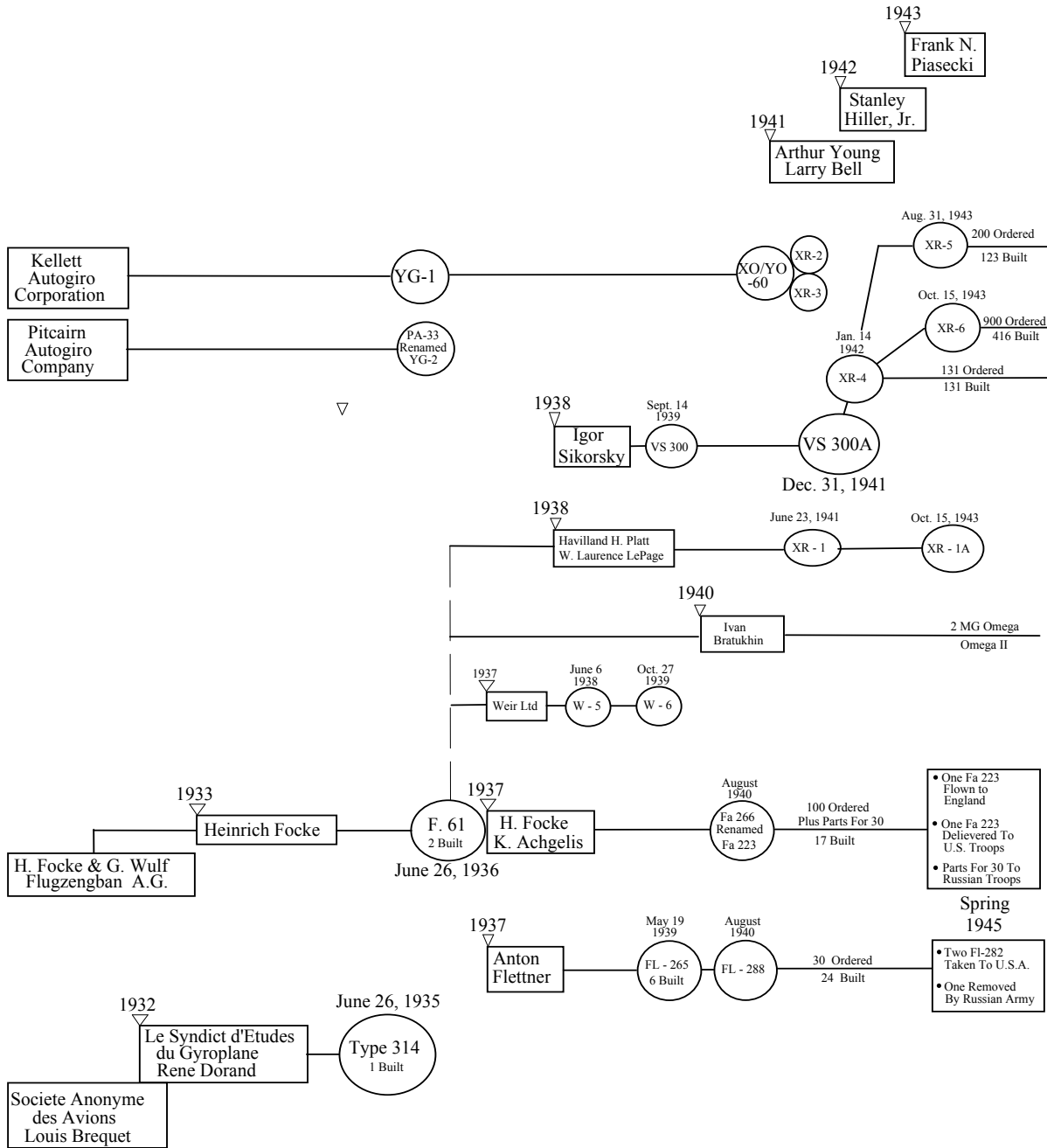


**Fig. 1-20. The rotorcraft industry made the transition from autogyros to helicopters before the end of World War II.**

The U.S. Air Corps had made good use of the autogyro before selecting the helicopter for its future and, in fact, this first rotorcraft gained significant support at the operational level. This support was strongly stated by First Lieutenant Erickson S. Nichols in a paper he presented at the Second Annual Rotating Wing Aircraft Meeting held on November 30 and December 1, 1939.<sup>13</sup> Lieutenant Nichols was introduced by session Chairman, Captain Franklin Gregory. Lieutenant Nichols noted in his introduction that

“Captain Gregory, at the meeting held here last year, gave a report on the history in the Army of the autogyro, and this year I have been asked to tell its tactical use for the Army and its military value and the tests which were made to determine the same.”

The points made by Lieutenant Nichols on Nov. 30, 1939, might simply be repeated today. He notes, for example, that

“the results of these tests, show that the autogyro could be used to great advantage for all types of reconnaissance, convoy duty, liaison, courier and command work. Also that due to its ability to hover over a particular spot [what an interesting choice of words!] it can provide almost constant observation of the terrain in the vicinity of a command either halted or on the march during daylight”. [A nighttime and all-weather capability was to come much later.]

These statements, plus a host of other important lessons, are invaluable reading and certainly justify Lieutenant Nichols’ closing remarks that

“being the only Air Corps Officer to be with the autogyro during all the tests described, from the results experienced I feel I have a right to be enthusiastic about the military and tactical value of autogyros, and as I am enthusiastic, it can readily be seen why I am known as the ‘Windmill Salesman’ among my friends in the Air Corps.”

You will find, not only in the histories related by Butler but in others as well, that the autogyro was not so favorably compared to conventional fixed-wing aircraft as Lieutenant Nichols was selling. For example, Cyrus W. Hardy [82]<sup>14</sup> points out that

“the [early] autogyro’s difficult flying characteristics and low pay load were undesirable. Their landing and takeoff distances were only a small advantage [and that even by late 1944] the autogyro still offered only minor advantages over the airplane and it was abandoned for the helicopter. The autogyro, however, left a wealth of technical information which provided a good foundation for future helicopter development.”

---

<sup>13</sup> Both the First Annual Meeting, October of 1938, and the second [79] were sponsored by the Philadelphia Chapter of the Institute of the Aeronautical Sciences. They were held at the Franklin Institute in Philadelphia, Pennsylvania. Proceedings of the two meetings were edited by Ralph McClarren, who was then the Assistant Associate Director in charge of aviation for the Franklin Institute. In corresponding with Mr. McClarren in March 1993, he sent me more details of these meetings plus the highlights of his career [80]. Dr. Alexander Klemin, a frequent contributor to *Aero Digest*, wrote a very positive summary article about the first meeting that appeared in the December 1938 issue of that popular magazine [81]. These meetings were the forerunner of the Annual Forum of the American Helicopter Society today and happened because of the vigorous efforts of E. Burke Wilford who was then Chairman of the Philadelphia Chapter.

<sup>14</sup> The first volume of the *Journal of the American Helicopter Society* was published in January of 1956. The then Technical Director of the Society, Alfred Gessow, became Editor. A subscription for one year was \$4.00, but the quarterly publication was included in AHS membership dues. This first journal, a premiere history and development issue, was devoted to the story of the birth and development of the helicopter industry. It makes for absolutely fascinating reading because of the articles from both military and commercial users. This historic volume was reprinted by the American Helicopter Society in May 2006.

## 1.4 CLOSING REMARKS

The autogyro also created a passionate group of rotary wing advocates within the military, and it established a fundamental, military operational use of rotorcraft that has been continually repeated over the last 50 years. Of course additional missions have been added through the years as rotorcraft capability expanded. You will also find the view of the Army in the mid-1950s expressed by Lieutenant Colonel Edgar C. Wood in the Journal of the American Helicopter Society (AHS), vol. 1, no. 1.

There were a number of Army leadership reasons for selecting the helicopter over the autogyro that Butler points out [76, 77]. There were just as many operational and technical reasons as well. For example, the helicopter could truly hover. Operationally, this capability, relative to the autogyro, does not appear as overwhelming as you might think. What hovering really allowed was looking over the landing spot before touching down. With the autogyro, the pilots were committed to land once they got close enough to the ground to see the terrain details. With the helicopter, even with wheels on what might appear as firm ground, the pilot could still “pull collective” if the situation warranted it and then search for a better spot. This was a very important point to the Army aviator.

The actual performance differences between one of the best autogyros available for evaluation, the Kellett YO-60 (Fig. 1-21) discussed earlier [84], and Sikorsky’s experimental XR-4, and then the YR-4B pre-production upgrade that followed [47-50], is quite illuminating as Table 1-1 and Fig. 1-22 show.

The differences in power required with airspeed shown in Fig. 1-22 are particularly interesting. The helicopter, with its high airframe drag and low installed engine horsepower, clearly would not compete at speeds above 75 miles per hour. The autogyro, with its loss in propeller efficiency at low speed (and despite its high installed power), would never compete at speeds below 75 miles per hour.



**Fig. 1-21. The 1943 Kellett YO-60 was the last autogyro the U.S. Army Air Force would purchase (photo from author’s collection).**

**Table 1-1. Autogyro vs. Helicopter in 1942**

<b>Configuration</b>	<b>Autogyro</b>	<b>Helicopter</b>
Manufacturer	Kellett	Sikorsky
Model	YO-60	YR-4B
Design Gross Weight	2800 lb	2450 lb
Operating Weight Empty	2180 lb	1980 lb
Normal Fuel	36 gal.	30 gal.
Parasite Drag Area at Cruise	13 sq ft	23 sq ft
<b>Performance</b>		
Cruise Speed	70 to 94 mph	65 mph
Maximum Speed	134 mph	85 mph
Minimum Speed	26 mph	0 mph
Maximum Range	210 statute miles	200 statute miles
Average Cruising Speed for Max Range	70 mph	65 mph
Maximum Endurance	2.2 hours	2.2 hours
Service Ceiling	13750 ft	8000 ft
<b>Dimensions</b>		
Main Rotor	3 blades	3 blades
Diameter	43.2 ft	38 ft
Chord at 70% Radius	12.92 in.	13.8 in.
Solidity	0.0476	0.0578
Airfoil (root)	23016 NACA	0012 NACA
Airfoil (tip)	23010 NACA	0012 NACA
Rotor Speed at Maximum Speed	241 rpm	241 rpm
Rotor Speed at Minimum Speed	189 rpm	241 rpm
Horizontal Tail	One	None
Span	10 ft	n/a
Chord	30 in.	n/a
Fuselage		
Number of Seats	2 (in tandem)	2 (side-by-side)
Overall Length	21 ft 5 in.	27 ft 11 in.
Propeller or Tail Rotor	2 blades	3 blades
Hamilton Standard, Constant Speed	2150 rpm	1275 rpm
Hub Model	2B20	Articulated
Blade Design	6135A-6	0012 NACA
Diameter	8.5 ft	7.92 ft
Solidity	n/a	0.0998
Engine	Jacobs I-6MB-8	Warner R-550-1
Maximum Rated Power	320 bhp	190 bhp
Operating Speed	2150 rpm	2250 rpm

## 1.4 CLOSING REMARKS

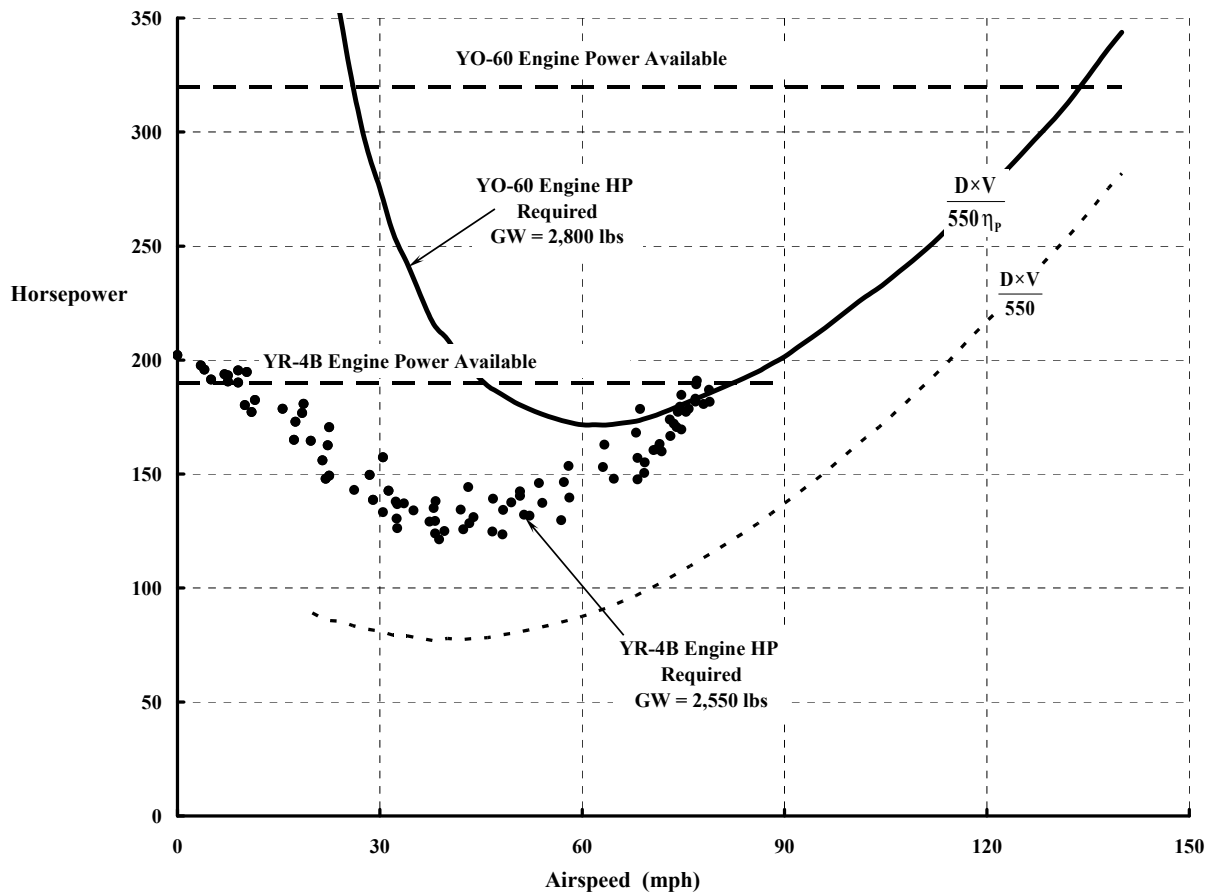


**Fig. 1-22. The U.S. Army had chosen the helicopter over the autogyro by the end of 1944.**

It took another 20 years before Army aviators got the best of both worlds, and more, in a Light Observation Helicopter powered with a gas turbine engine. You will encounter that story and others as you read about the modern results achieved with the helicopter in the next section.

## 2 MODERN RESULTS

In the November 1924 issue of *Mechanical Engineering* [85], Dr. Alexander Klemin, one of the most respected and enthusiastic spokesmen in the rotorcraft industry, published a technical article entitled *An Introduction to the Helicopter*. The third introductory paragraph he wrote reads as follows:

“To achieve utility, the helicopter must climb vertically with a moderate degree of useful load; attain a reasonable ceiling; achieve vertical descent with motors in action; achieve safe descent—if not vertically, then at least on a steep path with dead motor; have a reasonable speed in horizontal flight; be fairly stable and completely controllable; and have reasonable assurance of correct functioning of its mechanism. In these requirements we have the whole of the subject.”

It was in the period after World War II that the industry was able to meet “these requirements.”

In late 1961 the American Helicopter Society (AHS) devoted its October, November, and December issues of its NEWSLETTER magazine, now called *Vertiflite*, to updating technical data about as many helicopters and VTOLs as possible. The three-part summation, [86-88] was authored by Ralph Alex, the first and eighth president of the AHS. The articles were entitled *Helicopters From 'A to Z'*. (In my opinion these 3 issues are real collectibles, not just for the 135 configuration descriptions, but because the photographs were printed with superb clarity.) In his introduction, Alex included a number of statistics that quickly capture how the industry was doing. With some of my condensing, he noted that:

- The multitude of military uses has provided [the industry with] the basic support of the Armed Forces and has supplied most of the development motivation which has been responsible for the current state of the art. Military sales over the past 6 years were \$1,665,000,000. From 1941 through 1960, over 7,000 (1,200 Air Force, 1,800 Navy, 3,200 Army) helicopters were delivered to the Armed Forces.
- The vast commercial future predicted has progressed but not as rapidly as envisioned due to excessive manufacturing and operating cost. Commercial sales over the past 6 years were \$456,000,000. Over 1,500 helicopters for commercial use had been delivered since 1941. Orders for 182 helicopters had been placed for delivery in 1961.
- In 1960, the 235 commercial operators in the U.S. and Canada operated 882 helicopters, provided 56 flight schools and had annual sales gross of \$50 million.
- The scheduled airlines had 20 helicopters in service during 1960. They carried a total of 490,000 passengers and amassed 1,054,000,000 revenue ton miles including airmail and freight.
- The industry employed approximately 24,000 people directly and had a backlog of \$350,000,000 in unfilled orders. It exported 82 helicopters valued at 7.7 million dollars.

In addition to the articles by Alex and the often-referenced book, *Helicopters and Autogyros* by Gablehouse [3], you will find the period from 1945 on up to at least 1967 is

## 2. MODERN RESULTS

particularly well documented by Paul Lambermont and Anthony Pirie in their survey of *Helicopters and Autogyros of the World*, [89]. Their initial publication came out in 1958. A revised and enlarged book was published in 1970. The table of contents of the second edition lists over 500 rotorcraft (i.e., initial autogyros, helicopters, convertiplanes, and their product improvement models). An overview, including many photographs, is provided for each rotorcraft, and a brief historical introduction recaps the period from 1784 to 1903.

An excellent complement to the survey by Lambermont and Pirie is *The Illustrated Encyclopedia of Helicopters*, [6], by Giorgio Apostolo. His encyclopedia not only revisits the early history of rotorcraft, but it includes many superb artist renditions, three-dimensional views, and photographs. More recently, Jay Spenser has updated the early rotorcraft industry in *Whirlybirds: A History of the U.S. Helicopter Pioneers*, [90], which has many exceptional photographs. Taken together, these publications from Alex, Gablehouse, Lambermont and Pirie, Apostolo, and Spenser show that the rotorcraft industry has been steadily expanding as summarized earlier in Fig. 1-1.

In the United States, for example, Frank Piasecki succeeded in developing and then producing the tandem rotor helicopter starting with the XHRP-1 prototype that first flew in March of 1945. Arthur Young, assisted by Bartram Kelley and supported by the Lawrence Bell Corporation, significantly improved the inherent stability of the single-main-rotor helicopter with a prototype that first flew in free flight in early 1943. This prototype led to the Bell Model 30 and then to the very well-known Bell Model 47 that, in January of 1946, was the first helicopter to receive a civil certification. Charles Kaman started his company with the Flettner rotor system and had his prototype K-125 flying in January of 1947. By October of 1948, Stanley Hiller had decided against further development of the coaxial configuration and began deliveries of his Model 360, a single-main-rotor plus anti-torque tail rotor design that also improved the inherent stability of the helicopter. And, of course, Sikorsky's company grew by translating its early military helicopters into commercial models.

In Europe, consolidation of many diverse efforts also occurred. Great Britain saw Westland Aircraft Limited evolve from the groundwork of Cierva, A. V. Roe, Weir, Bristol, Fairey, and others. The cooperation between Sikorsky and Westland, begun in early 1947, led to a broad product line. In Italy, Augusta became the primary producer through a licensing agreement with the then Bell Aircraft Corporation. This led to the Bell Model 47 production in Italy starting early in 1955. The German and Austrian work of Focke, Flettner, Doblhoff, Dornier, Derschmidt, and others culminated in the formation of Bölkow and production of the first, practical, hingeless rotor system, which led to the BO-105 in the late 1960s.<sup>15</sup> Finally, in

---

<sup>15</sup> In May of 1993, while at an air show in California, I ran across a thin booklet by Heinz J. Nowarra [91]. It is packed with early photos and key history about German and Austrian helicopter activities from 1928 to 1945. I learned a great deal from this work and highly recommend it. In late 1994, while going through the Wayne Wiesner collection, I came across the U.S. Air Force test report of the Flettner-282 [92]. It was a fine helicopter and a tribute to its inventor, Anton Flettner. Certainly Focke and Flettner were the leaders in helicopter development until the disruption of World War II. In 1983, Gunter Reichert, a very good friend, gave me a marvelous book tracing the history of the Messerschmitt-Bölkow-Blohn (MBB) company up to the BO-105 (written in German with superb photos, although I cannot read German) [93]. Steve Coates' book [7] really rounds out the picture.

France, the pioneering work of Bréguet, Oemichen, Dorand, and others ultimately created Sud Aviation which led to Aerospatiale. More recently, Eurocopter has been established by combining the Bölkow and Aerospatiale teams. This has given the world a European rotorcraft product line that is quite comparable to what is available from the United States.

In Russia, a number of design teams formed to produce several rotorcraft types. This story of *Soviet Helicopters* was brought to light in 1983 by John Everett-Heath [94]. Heath traces progress from 1754 up to the modern efforts of Nikolai Kamov and Mikhail Mil [95, 96]. The influence of the Russian climate on design becomes rather clear when you read these books, and it explains why the very heaviest lifting helicopters have evolved in what is again Russia.

It is well known that helicopter development has been paced by military needs, and this has given the world some very powerful weapon systems [97]. However, the industry founders always saw their inventions helping mankind as Frank McGuire of Bell Helicopter carefully points out [98]. Progress throughout the decades since the 1940s confirms that the worldwide rotorcraft industry is in business to stay. Part of the industry has chosen product lines designed for larger transport and heavy-lift capability. Several 30-passenger configurations are available, and payloads of 25,000 kg (55,000 lb) can be lifted. The other side of the industry has proliferated the light- and medium-weight product lines. Cruise speeds of 150 miles per hour are common, and the speed record is over 400 km/h (249 mph or 216 knots). Ranges of 660 km (400 statute miles or 350 nautical miles) with internal fuel are the norm, and hover endurance is limited only by fuel capacity. Helicopters, regardless of manufacturer, have demonstrated their ability to perform a multitude of tasks and, from a user's point of view:

1. Engines have become more efficient and reliable.
2. Weight empty is more productively used.
3. Hover performance at high altitudes is routine.
4. Forward flight at higher speeds in comfort is possible.
5. Fuel efficiency has been significantly improved.
6. Costs, both initial and operational, are major factors in design and production.
7. Safety has steadily improved.

Modern results, from each of these preceding seven areas, will tell you just how mature the helicopter has become. The engineering explanations and analyses that follow are tied to the configuration evolution to help round out your appreciation of what has been accomplished in creating the rotorcraft industry. The second objective is to continue expanding your understanding of the (1) physical and mechanical aspects, (2) basic nomenclature, (3) engineering symbols, and (4) fundamental equations.



## 2.1 ENGINES

An engine is the heart of any aircraft propulsion system. This is not a simplistic or trite statement. The progress in aviation is so intertwined with what has been accomplished in this field that it too often is just taken for granted. Because of this intertwining, you will find some history about several helicopters in the engine discussion that follows.

For rotorcraft, the engine is, if it is possible, even more important than for fixed-wing aircraft. In fact, even conceptual rotorcraft design rarely proceeds without first having at least one proven engine in mind. Igor Sikorsky clearly understood this fact in 1908 before he had become 20 years old. You will find his recollections in Boulet's history very pointed (pages 24 through 30 of reference [2]). He traveled to Paris in January 1909, expressly "to make a correct decision on the type of motor to use." He finally selected one Anzani 25-horsepower engine to take home. It was a choice he described as, "Less bad than the rest." However, you may recall that it was this power plant that Louis Blériot used a few months later to make the first flight across the English Channel.

There are primarily two types of engines available to, and used by, the rotorcraft industry. One is the four stroke, spark ignition, internal combustion, reciprocating piston engine. The other is the gas turbine. You need to understand both of these power plants so consider the piston engine first.

### 2.1.1 Piston Engines

In 1862 Beau de Rochas, a Frenchman, proposed and patented a sequence of four operations, or strokes, that a spark ignition piston engine could have to produce power. Fig. 2-1 schematically illustrates these four strokes. Each stroke is 180 degrees of crankshaft rotation. This means that the crankshaft goes through two revolutions to produce one impulse of power. Referring to Fig. 2-1, Rochas proposed that:

1. There would first be an intake stroke to suck a fuel-air mixture through the open intake valve into a cylinder;
2. The second stroke would be a compression stroke with both valves closed to raise the temperature and pressure of the fuel-air mixture;
3. The third stroke, with both valves closed, would start with a spark to ignite the fuel-air mixture, which expands on combustion and forces the piston down; and finally
4. The fourth stroke would exhaust the cylinder free of the burned gases through the open exhaust valve.

The internal combustion engine that Rochas described came into being in Germany. In 1876 a German engineer, Nikolaus A. Otto, used these principles to create a 1-cylinder, 3-horsepower engine. The cylinder bore was 6.3 inches and the stroke was 11.8 inches. The

## 2.1 ENGINES

output shaft speed was 180 rpm. A countryman, Gottlieb Daimler,<sup>16</sup> followed with an 8-horsepower engine and then built a 16-horsepower engine nearly entirely of aluminum. The Daimler company, spurred on by a car racing enthusiast named Emil Jellinek, later created the Mercedes engine. (You might not know that Mercedes was the middle name of one of Jellinek's daughters.) These and other early engines were used to power dirigibles before the turn of the 20th century, and aviation had a power plant.

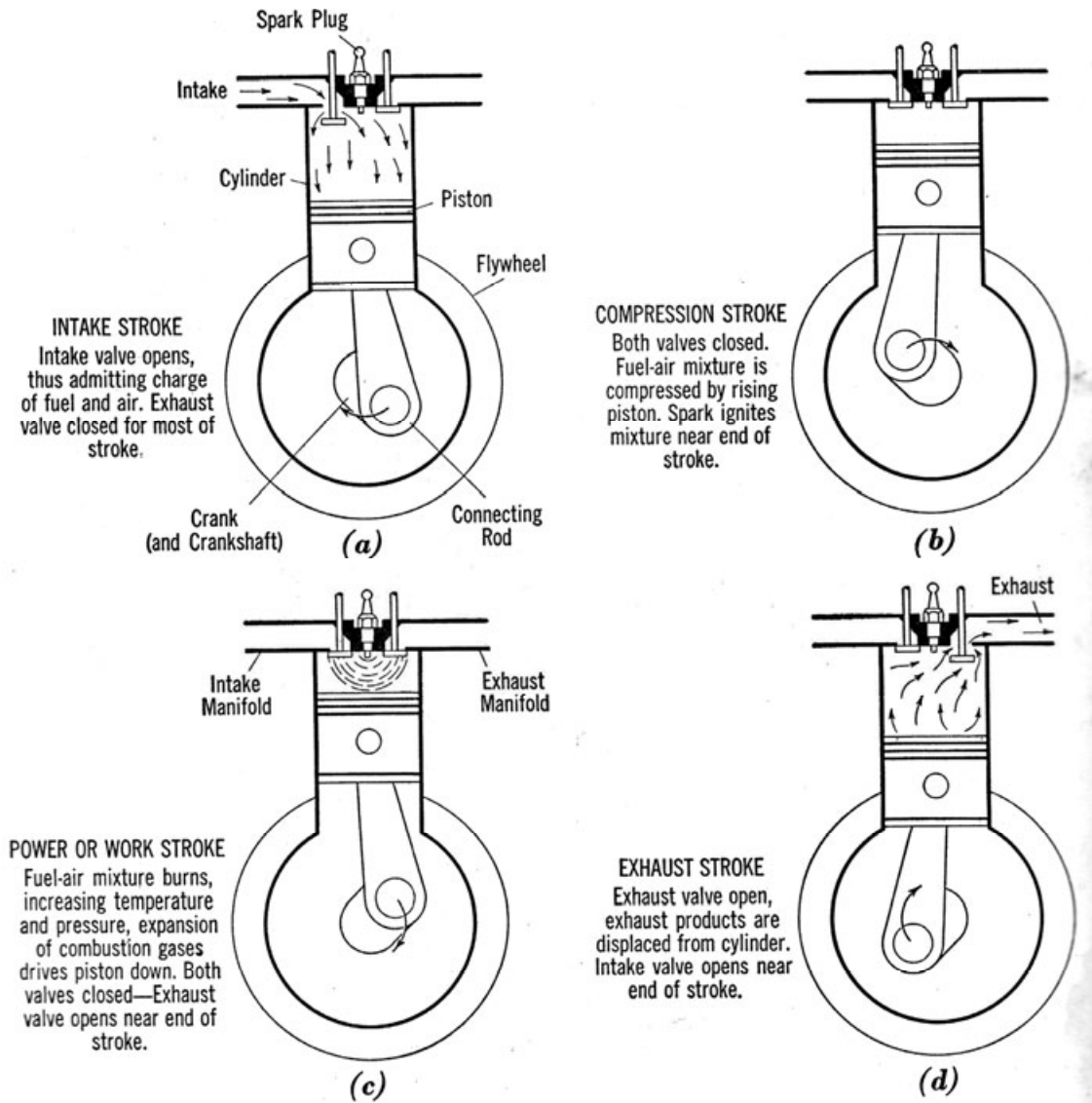


**Fig. 2-1. The internal combustion engine became a reality for aviation just before the turn of the 20th century.**

<sup>16</sup> You will find the Daimler–Mercedes-Benz story of car and engine development in references [99] and [100] very interesting. Both Benz and Daimler were rather poorly treated by business associates, and it was not until 1926 that the forerunner of today's company was in place. However, the push for higher touring-car speeds (and then racing cars) was a prime motivation for improving early gasoline engines.

Despite the progress made with automobile and motorcycle engines, early aviation pioneers found them quite heavy for the amount of power they produced. Both the Wright brothers and Samuel Langley found that they had to build their own engines to reach the goal of powered flight. The Wright engine barely did the job. Their engine dropped from 16 to about 12 horsepower at 1090 rpm after it warmed up. With four cylinders of 4-inch bore and 4-inch stroke, it weighed nearly 180 pounds. In contrast, the engine that Langley's assistant, Charles Manly, developed from a design started by Stephen Balzar, a New York City automobile builder, was a major step forward. Manly's engine produced 52 horsepower at 950 rpm with five cylinders. It had pistons of 5-inch bore and 5.5-inch stroke, and weighed 135 pounds. It was not until 1918 that another piston engine came along that outperformed the 0.385-horsepower-per-pound Manly engine. Most importantly, the Manly engine was very reliable. One can only wonder how much faster the Wright brothers and others would have progressed had they been able to use the Manly engine.

To understand the general trends in piston engine improvements, you need some background about the key parameters that govern piston engine performance. The brake horsepower (BHP) that a piston engine will produce is rather easy to calculate. The power stroke begins with an explosion. The explosion creates a very high initial pressure that moves the piston downward. During the power stroke, the top of the piston feels an average pressure that engine designers refer to as the indicated, mean, effective pressure (IMEP). This pressure, say in pounds per square inch, acts on the piston face of area (A) in square inches to produce a force in pounds. This force moves through a distance (L), say in feet, that is the length of a stroke. The piston force (P×A) times the stroke distance is the work done (in foot-pounds) by one cylinder during a power stroke. Thus,

$$(2.1) \text{ Work done} = (\text{Piston}_{\text{IMEP}})(A_{\text{piston}})(L_{\text{stroke}}).$$

Now think about the time it takes to do this work. In a four-cycle engine, the power stroke for each cylinder occurs only once every two revolutions of the crankshaft. Thus, the power stroke time (T) is the time it takes the crankshaft to turn 180 degrees or  $\pi$  radians. This relates to engine RPM as

$$(2.2) \text{ Work time} = T = \frac{t \text{ seconds}}{\pi \text{ radians}} = \frac{2 t \text{ seconds}}{2\pi \text{ radians}} = \frac{120}{\text{RPM}}.$$

The indicated horsepower, based on IMEP, is work done per unit of time by one cylinder (n = 1) or simply

$$(2.3) \text{ Indicated HP per piston} = \frac{\text{work done in foot-pounds}}{550 \text{ work time in seconds}} \\ = \frac{(\text{Piston}_{\text{IMEP}})(A_{\text{piston}})(L_{\text{stroke}})\text{RPM}}{550 \times 120}.$$

## 2.1 ENGINES

This indicated horsepower per cylinder is transmitted from each piston assembly along the crankshaft to an output shaft where it becomes useful power, which is called brake horsepower (BHP). BHP is somewhat less than indicated horsepower because of losses such as the friction drag of the pistons against the cylinder walls and internal pumping. In addition, some of the indicated power might be used to drive engine accessories like a supercharger, which I will discuss shortly. The key point here is that BHP depends on a piston pressure ( $P_{\text{pressure}}$ ), i.e., the brake, mean effective pressure; the piston face area ( $A_{\text{piston}}$ ) and stroke length ( $L_{\text{stroke}}$ ), which is a volume; the engine speed (RPM); and the number of cylinders ( $n$ ). Thus,

$$(2.4) \text{ BHP} = n \frac{(P_{\text{pressure}} \text{ in psi})(A_{\text{piston}} L_{\text{stroke}} \text{ in inches}^3) \text{ RPM}}{792,000}.$$

Despite the simplifications presented by Eq. (2.4), it does capture the fundamentals of piston engine performance. The vast majority of aviation engines run in a very narrow RPM range centered around 2700 rpm. There is also a finite pressure and temperature that a cylinder can withstand without an enormous weight penalty. Thus, the BHP is primarily a function of the number of cylinders and the size or displacement (i.e., the volume in cubic inches or liters) that each piston will create.

Fig. 2-2 illustrates the fundamental trend suggested by Eq. (2.4) for a number of aircraft piston engines available during the first half of the 20th century. The majority of data shown in this figure have come from the first six editions of Lionel S. Marks' *Mechanical Engineers' Handbook*, [101]. Perhaps the most authoritative stories of aircraft piston engine evolution, from an engineering viewpoint, are provided by Charles Fayette Taylor [102] and L. J. K. Setright [103].<sup>17</sup> These histories discuss the use of gearboxes to better optimize engine speed with propeller speed. They also point out the basic limitations to maximum piston speed.

The data in Fig. 2-2 reflects an increase in piston pressure as used in Eq. (2.4) from about 100 pounds per square inch with the early, small engines, up to about 300 pounds per square inch for the large engines of the mid-1950s. Thus, one could expect that new, small engines in the power range suited to small (i.e., one- to four-person) rotorcraft would perform above the historical trend line shown in the figure if advanced technology ensued.

It is not too unreasonable to think that a piston engine's weight would be in proportion to its size and the density of steel from which most engines were, and are, made. In turn, the size would be in proportion to the piston engine's total displacement. Fig. 2-3 basically confirms this reasoning. This weight trend can also be related to the rated BHP as shown in

---

<sup>17</sup> You will find a popular history of engines in the July 1953 issue of *Aero Digest* [104]. A more detailed engineering review is included in a terrific book called *The Lore of Flight* [105]. The illustrations are wonderful, and it is an invaluable guide for both laymen and experts. My friends at the Boeing Vertol V/STOL wind tunnel gave me a copy of this book when I left in 1974. It has been a continual source of enjoyment and knowledge ever since.

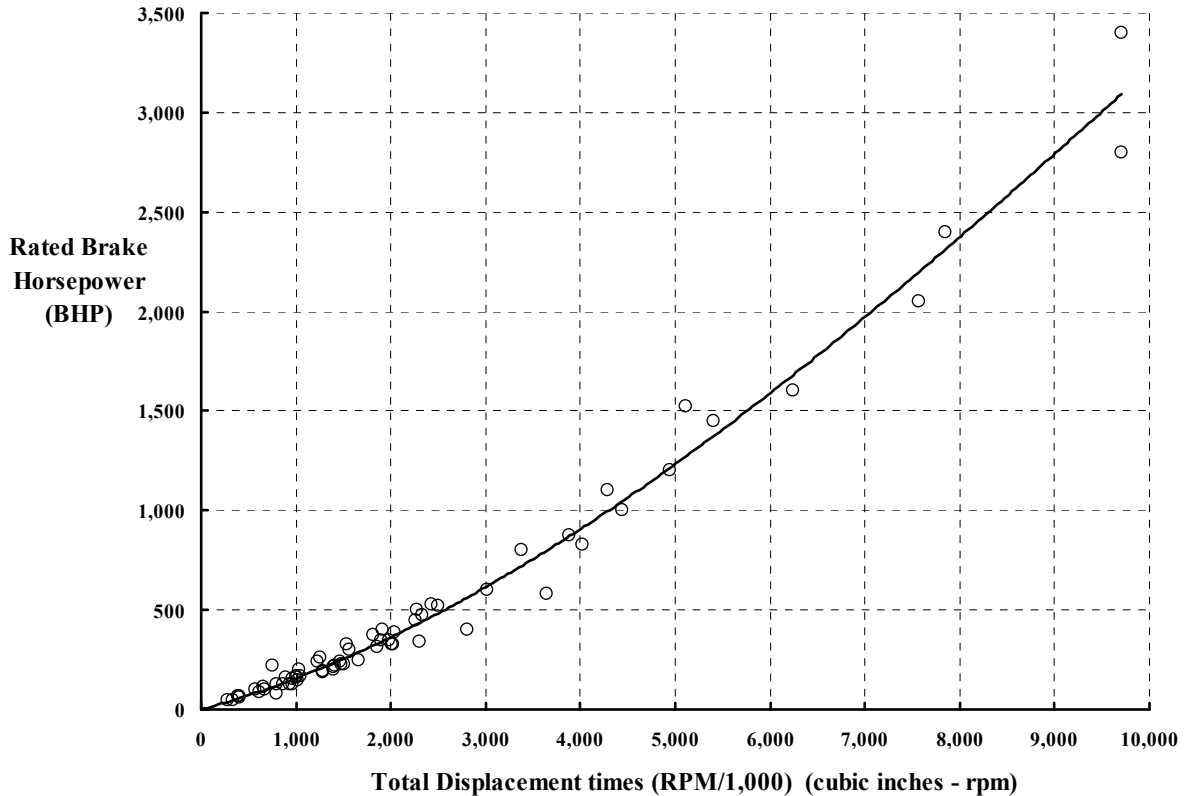


**Fig. 2-2. The piston engine provides power nearly in proportion to its cubic inches of displacement and to RPM.**

Fig. 2-4. The trend is not linear, however, because power improved with both size and increases in mean pressure as the technology evolved. This was suggested by Fig. 2-2.

A normal characteristic of the *un-supercharged* piston engine is to lose power output nearly in proportion to the density of air in which the engine is operating. Rated BHP is generally quoted by a manufacturer at standard sea-level conditions. Therefore, to extrapolate the power output of a piston engine, you can use an empirical, first approximation to the actual thermodynamic process given for an *un-supercharged* engine as

$$(2.5) \quad \text{BHP}_\sigma = \text{BHP}_{\text{S.L. rated}} \left( \frac{\text{Density Ratio} - 0.145}{0.845} \right).$$

You will remember that both ambient atmospheric pressure ( $P_{\text{am}}$ ) and temperature ( $T_{\text{am}}$ ) determine the density ( $\rho_{\text{am}}$ ). These properties of air are conventionally expressed in ratios. That is,

$$(2.6) \quad \delta = \frac{P_{\text{am}}}{P_0} = \left[ 1 - 0.00687558563 \left( \frac{H \text{ in feet}}{1,000} \right) \right]^{5.255876113}.$$

Similarly, an absolute-temperature ratio is commonly used in the form

## 2.1 ENGINES

$$(2.7) \quad \theta = \frac{T_{am}}{T_o} = \frac{T_{am} \text{ in } ^\circ\text{F} + 459.67}{518.67} = \frac{T_{am} \text{ in } ^\circ\text{C} + 273.15}{288.15}.$$

These properties of air are widely published [106]. In addition, a density ratio ( $\sigma$ ) equation that comes in very handy is

$$(2.8) \quad \sigma = \frac{\rho_{am}}{0.002378 \text{ slug/ft}^3} = \frac{\delta}{\theta} \approx \frac{518.67 \left[ 1 - 0.00687558563 \left( \frac{H \text{ in ft.}}{1,000} \right) \right]^{5.255876113}}{T_{am} \text{ in } ^\circ\text{F} + 459.67}$$

where H is pressure altitude expressed in feet. A standard day assumes that temperature decreases with altitude as

$$(2.9) \quad T_{am} \approx 59 ^\circ\text{F} - 3.566 \left( \frac{H}{1,000} \right)$$

so that density varies with pressure altitude in feet *on a standard day* approximately as

$$(2.10) \quad \sigma = \frac{\rho_{am}}{0.002378 \text{ slug/ft}^3} \approx \frac{518.67 \left[ 1 - 0.00687558563 \left( \frac{H \text{ in ft.}}{1,000} \right) \right]^{5.255876113}}{518.67 - 3.566 \left( \frac{H \text{ in ft.}}{1,000} \right)}.$$

The loss in power output with altitude has frequently been offset by adding a supercharger to the engine. This device compresses the intake air and makes the engine think (so to speak) and operate as if it were at sea level. However, running the engine at sea level with a supercharger on may require operation at partial throttle to avoid overheating the engine, or to avoid predetonation, which is called “knock.” With a supercharged engine, the pilot can draw the sea-level-rated power to altitudes of 10,000 feet or better. An engine manufacturer would state this feature by saying that its engine is “flat rated” from sea level up to some design altitude. A supercharged piston engine can be an ideal solution for rotorcraft operations such as hovering at high altitudes. For the supercharged engine, BHP empirically varies slightly differently with density above the design altitude. Thus Eq. (2.5) becomes, for the supercharged engine,

$$(2.11) \quad \text{BHP}_\sigma = \text{BHP}_{\text{Design Altitude}} \left( \frac{\sigma_{\text{Design Altitude}} - 0.1}{0.9} \right) \quad \text{for supercharged engine.}$$

Today the aviation piston engine has found itself powering light planes, small autogyros, and one- to four-place helicopters. The two major U.S. piston engine manufacturers are Lycoming and Continental whose products span the range from 100 to slightly over 400 rated horsepower. Output engine shaft speeds range from 2,400 to 3,400 rpm. Both companies offer four- and six-cylinder engines, and many are supercharged. This gives an extremely broad choice in horsepower for any design altitude. For example, in

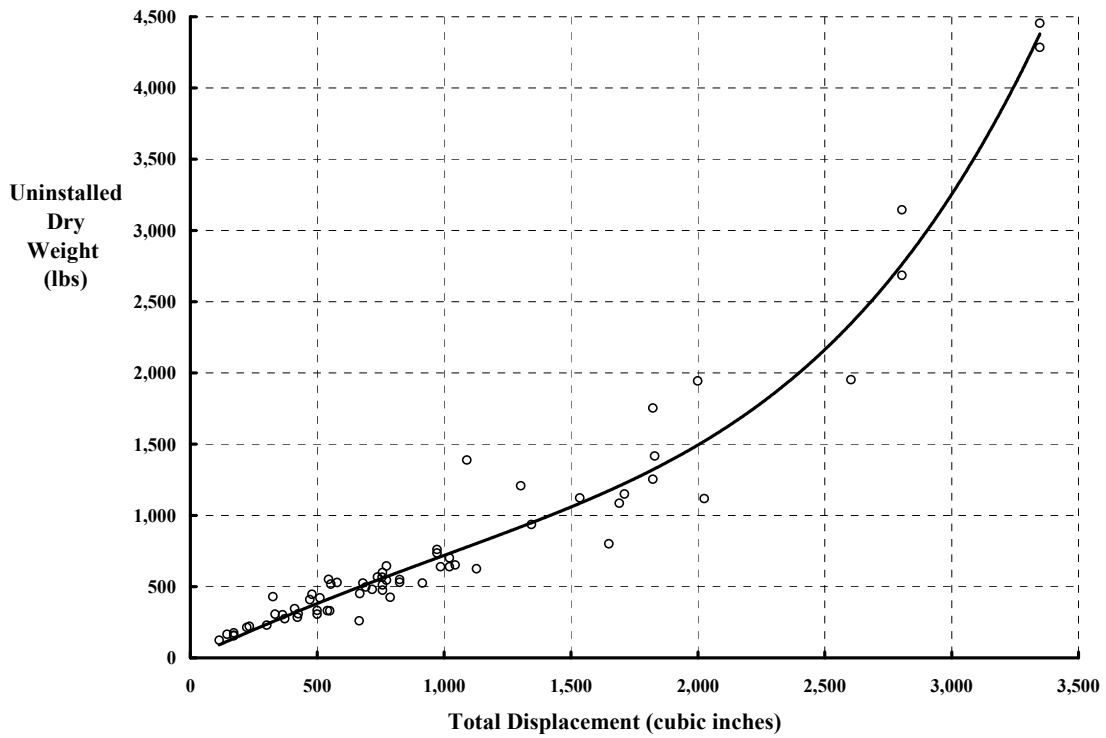


**Fig. 2-3. Smaller piston engines weigh about 0.75 pounds per cubic inch of total displacement.**

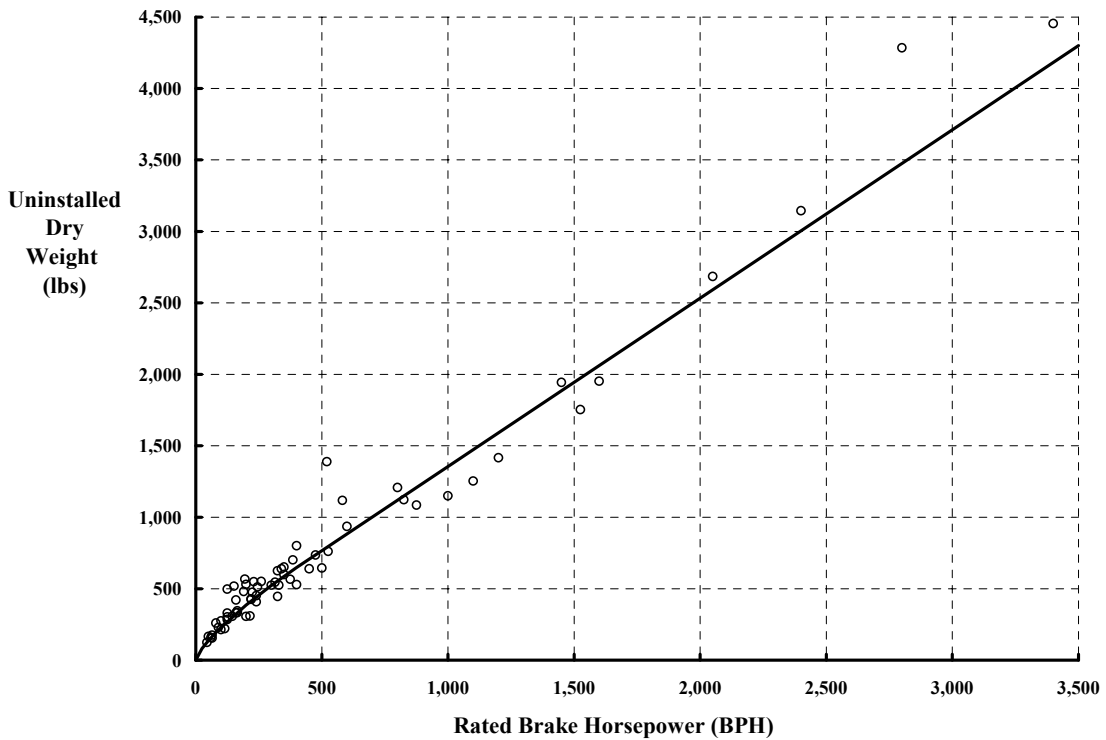


**Fig. 2-4. Piston engines would have improved if gas turbine engines had not become practical.**

## 2.1 ENGINES

Aviation Week & Space Technology [107] you will find a data list of U.S.-produced reciprocating engines that covers two pages (in small print). Data from this reference give the approximate bounds in available piston engine performance shown in Fig. 2-5.

A very important characteristic of piston engines is their fuel consumption. This characteristic is shown in Fig. 2-6, again using historical data [107]. The specific fuel consumption (SFC) at rated horsepower is a frequently quoted ratio for engines. SFC is simply the ratio of fuel flow in pounds per hour to rated BHP. This is the slope of the data as presented in Fig. 2-6. Historically, smaller piston engines are not as fuel efficient as larger engines, as the figure suggests. (It is worth remembering that one U.S. gallon of piston engine fuel weighs in the range of 5.9 to 6.1 pounds.)

Engine manufacturers obtain their engine's performance in a test cell using as close to an ideal setup as possible. This provides all potential users with a firm baseline. But when a given engine is installed in a rotorcraft (or any aircraft for that matter), its performance is compromised as you might expect. Getting air and fuel into the engine and getting exhaust overboard become very practical design issues that impact both maximum power available and fuel flow. Consider Fig. 2-7 and the data from three U.S. Army helicopters shown as an example.

The U.S. Army introduced two piston-powered cargo helicopters into service in the 1950s. One was the Piasecki H-21 that began life as the XHRP-X in 1945 and was developed under U.S. Navy contract. (The H-21 evolved into a turbine-powered commercial version, the Vertol Model 44, by the early 1960s). The 11,500-pound H-21 set the world speed record over a 3-kilometer course at 236 kilometers per hour (146 mph or 127 knots) in September 1953. The other helicopter was the 13,000-pound Sikorsky S-58 or H-34 that first flew in 1954. This helicopter was derived from the S-55 or H-19 that first flew in 1949 and was developed under U.S. Army contract. In July of 1956, an H-34 set world speed records over 100-, 500-, and 1,000-kilometer closed circuits. The highest speed was 219 kilometers per hour (136 mph or about 118 knots). The S-58 was re-engined with a gas turbine in 1971. Both of these 15- to 20-passenger helicopters used the Wright R-1820 reciprocating engine with supercharging.

Both the Piasecki H-21 and the Sikorsky H-34 were thoroughly evaluated by the Air Force for the Army at the Air Force Flight Test Center located at Edwards Air Force Base in California [108, 109]. The fuel flow versus BHP data recorded in these reports covers a range in engine RPM from 2300 to 2700 and altitudes from nearly sea level up to 15,000 feet.<sup>18</sup>

---

<sup>18</sup> The Air Force Flight Test Center at Edwards Air Force Base in California is not just the world's leading flight research center for airplanes. It has supported rotorcraft development of all types for several decades. Major General Peter Odgers traces the history of Edwards from a little-known lakebed at the turn of the century up to the first landing of the Space Shuttle *Columbia* in April 1981 [110]. Hundreds of detailed engineering flight test reports for military helicopters alone have been published. There is, in my opinion, no better source for rotorcraft data than the pilot-oriented results that come from this organization. The good, bad, and unacceptable features of a helicopter are clearly written up. In short, these reports are probably the best "design manuals" you could read. In October 1996, the Army moved their flight testing operation from Edwards to Fort Rucker, Alabama, and renamed it Army Aviation Technical Test Center. The library at the center contains a wealth of test reports.

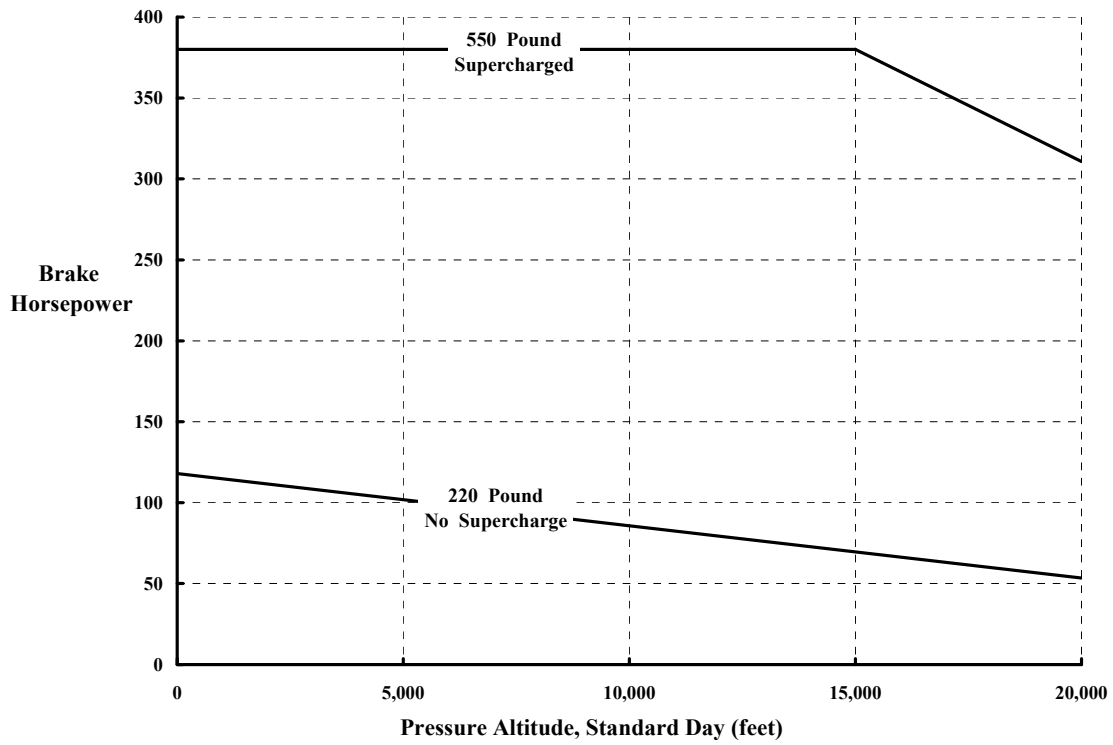


**Fig. 2-5. U.S.-produced piston engines provide a wide choice of options for light plane and rotorcraft manufacturers.**

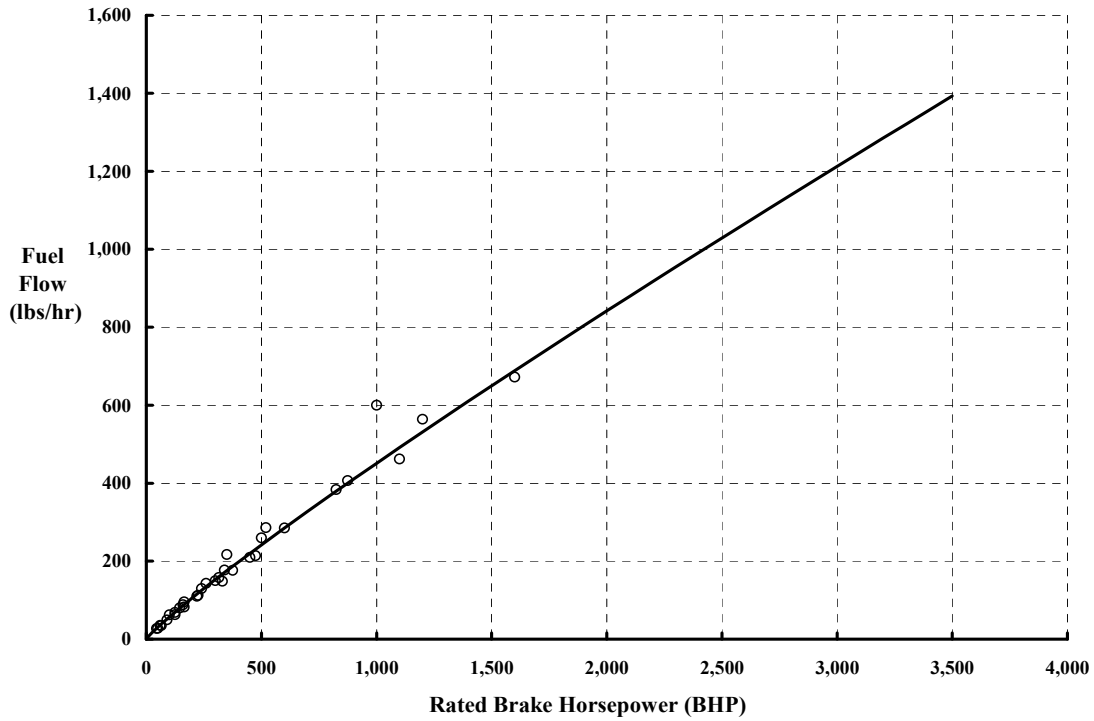


**Fig. 2-6. Piston engines burn fuel at a rate of about 0.5 pounds per hour for each rated horsepower delivered.**

## 2.1 ENGINES

This composite of engine performance is shown by the square, open symbols in Fig. 2-7. As you can see, fuel consumption does not vary linearly with the horsepower output of this engine. Furthermore, the optimum SFC is at partial power, not at rated power. The difference between uninstalled engine performance (as quoted by manufacturers and published in trade magazines) and performance when installed in a rotorcraft can be substantial. You can see this by comparing Fig. 2-6 with Fig. 2-7.

Fig. 2-7 also shows fuel consumption for an engine at the other end of the size spectrum. In the early 1960s, the Army bought a very small training helicopter that was developed by Hughes as its Model 269A. (The October 1961 advertisement [86] suggests that Hughes sold its 269A for \$22,500 and that it could be flown for just 13-cents-per-mile total direct operating costs. This product is offered today as the Schweizer Model 269A/A1.) This two-man, 1,550-pound helicopter used the Lycoming O-360-C2B, which was not supercharged. The helicopter was evaluated with the military designation of YHO-2HU [111]. Again, the installed engine performance was obtained over a range in RPM and altitudes. The fuel flow variation with BHP is not linear for this small engine either (although the data is rather compressed because of the scale).

The fuel flow at a given power setting with a piston engine depends on a raft of variables, not the least of which are density and RPM. More fundamentals of reciprocating engine design and operation is beyond the rudiments discussed previously and requires a book in itself.

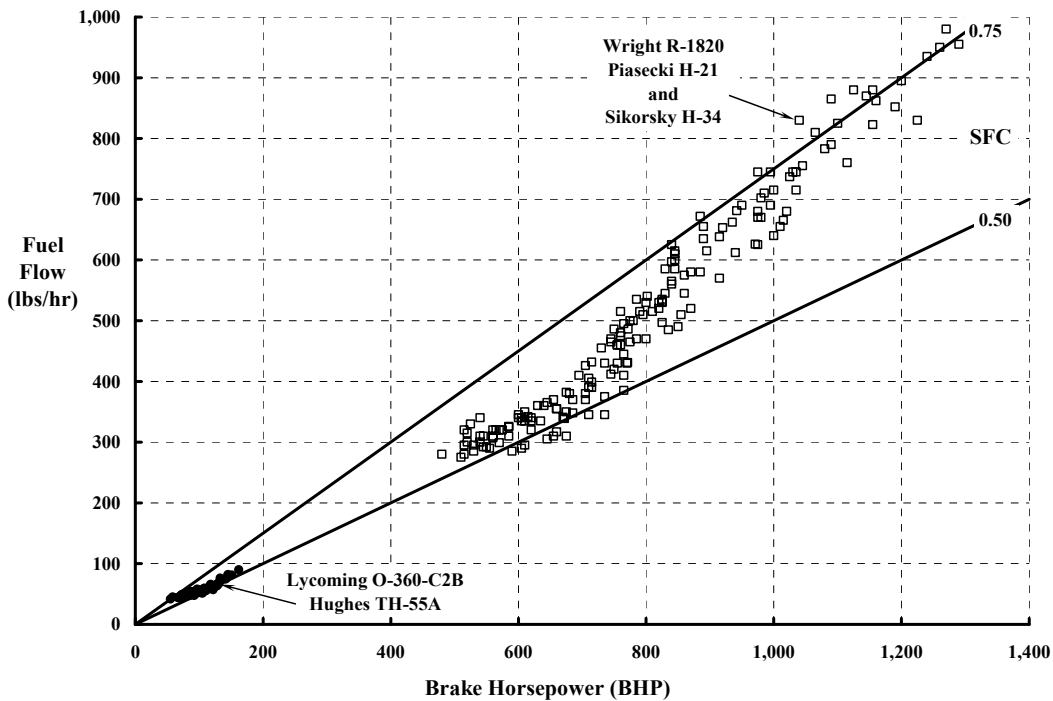


**Fig. 2-7. SFC improves when a piston engine is operated at partial power.**

### 2.1.2 Turbine Engines

Now turn your attention to turboshaft gas turbine engines. This power plant evolved after practical, pure jet propulsion became a reality just before World War II.<sup>19</sup> The shaft turbine that followed was a leap forward in simplicity as Fig. 2-8 suggests. Air enters the engine inlet and encounters a large capacity compressor, identical in principle to a piston engine supercharger. The compressed air flows into the combustion chamber where fuel is injected and the mixture is burned. This converts the fuel-air mixture into a supply of hot gas of greatly increased energy. The high-energy gas expands through the turbine wheels and then out the exhaust. The first turbine direct drives the compressor. The second turbine, called the power turbine, drives the output shaft.

The arrangement shown in Fig. 2-8 is generally referred to as a free turbine because the compressor/turbine assembly can turn separately from the output shaft/power turbine assembly. There are many fixed-shaft turbine engines however. With fixed turbine engines, the output shaft, compressor, and power turbine are all hard-mounted to one shaft. About 65 percent of the available power created in the thermodynamic process is used to turn the compressor. Another 30 to 35 percent of the power turns the output shaft. The remaining power is exhausted at high velocity out the tail pipe in the form of very hot jet thrust.

The shaft turbine engine turns in the range of 20,000 to 40,000 rpm with very small engines operating at over 60,000 rpm. These speeds are far in excess of what normal propellers use (i.e., about 1,000 rpm) or helicopter and other rotorcraft need (i.e., 250 to 350 rpm) and so some gear reduction is required. Tabulated engine characteristics such as those periodically provided by trade magazines [107] rarely include this key data. Instead the type of engine is more often classified as to (a) its compressor type—axial and/or centrifugal, and (b) its output—shaft, prop, fan, or pure jet. The implication of output type infers that the manufacturer may include a mechanical gearbox to bring down the output speed to something more useful to the airframe manufacturer.

A standard designation of stages or partitions of the gas turbine engine along with nomenclature was established by the military with MIL-E-5007 in 1949 [112]. The system description has been further detailed by the Society of Automotive Engineering in its publication ARP-681B [113]. These numbered stations or points along the engine are shown in Fig. 2-8 and Fig. 2-9. The nomenclature is in common use and is well worth remembering.

---

<sup>19</sup> You will recall that the first World War was called The Great War or The War to End All Wars. Apparently these were just working titles until we could number them. But, technology leaps do get made during these terrible periods. In January 1930 Commodore Frank Whittle patented the jet engine in England at his own expense. He found little interest in his practical ideas, but with capital from private friends, he successfully ran the first turbojet engine on April 12, 1937. A specially built Gloster E. 28/39 fighter, using a Whittle modified engine, first flew on May 15, 1941. Although Germany started later, the Pabst von Ohain turbojet ran in September of 1937. It was quickly developed into the He S3B and flown in the Heinkel He 178 on August 27, 1939, and the world was introduced to jet propulsion.

## 2.1 ENGINES

For example:

- $P_{am}$  – Ambient pressure far ahead or far behind the engine.
- $P_{S2}$  – Static pressure at the compressor inlet.
- $P_{T3}$  – Total pressure at the compressor outlet.
- $T_4$  – Temperature at the turbine inlet, written as TIT.
- $T_5$  – Temperature at the turbine outlet, written as TOT.
- $N_1$  – Compressor rotational speed, sometimes written as  $N_g$ .
- $N_2$  – Power turbine rotational speed, written as  $N_f$ .

In general, the subscript “s” means static and “T” means total. If no subscript to pressure is used, it probably means a static pressure.

The calculation of power from a gas turbine is not quite as straightforward as it is for a piston engine. However, it is worth your time to understand this power plant because it is the current engine of choice for most rotorcraft. A gas turbine in its most basic form operates schematically as shown in Fig. 2-9. The available energy level at any station in the cycle is derived from basic thermodynamic gas laws.

The general thermodynamic energy equation, found in any number of propulsion books, is the basic starting point for any propulsion system.<sup>20</sup> As a reminder, this fundamental is reproduced here, simply stated in differential equation form, as follows:

$$(2.12) \quad dL + dQ = C_v dT + \frac{vdP}{J} + \frac{Pdv}{J} + \frac{VdV}{gJ} + \frac{dh}{J}$$

where  $dL$  = Mechanical work input,  $dQ$  = Heat energy input,  $C_v dT$  = Internal energy,

$\frac{vdP}{J}$  and  $\frac{Pdv}{J}$  = Flow work,  $\frac{VdV}{gJ}$  = Kinetic energy, and  $\frac{dh}{J}$  = Potential energy.

---

<sup>20</sup> You will recall that the perfect gas equations are normally summarized as:

$$Pv = RT, \quad C_p - C_v = \frac{R}{J}, \quad \gamma = \frac{C_p}{C_v}, \quad JC_p = R \frac{\gamma}{\gamma - 1}$$

The several gas constants, in the English system, are:  $R = 53.3524117$  ft-lb/lb-°R,  $J = 778.02922$  ft-lb/BTU,  $C_p = 0.24$  BTU/lb-°R at sea level standard temperature of  $T_{am} = 59$  °F = (459.67 + 59 °F) degrees Rankine = 518.67 °R. Remember that thermodynamic equations always use temperature in the absolute Rankine degrees system where absolute zero is 0 °R or minus 459.67 °F. The ratio of specific heats for air is  $\gamma = 1.4$  at nominal temperatures.

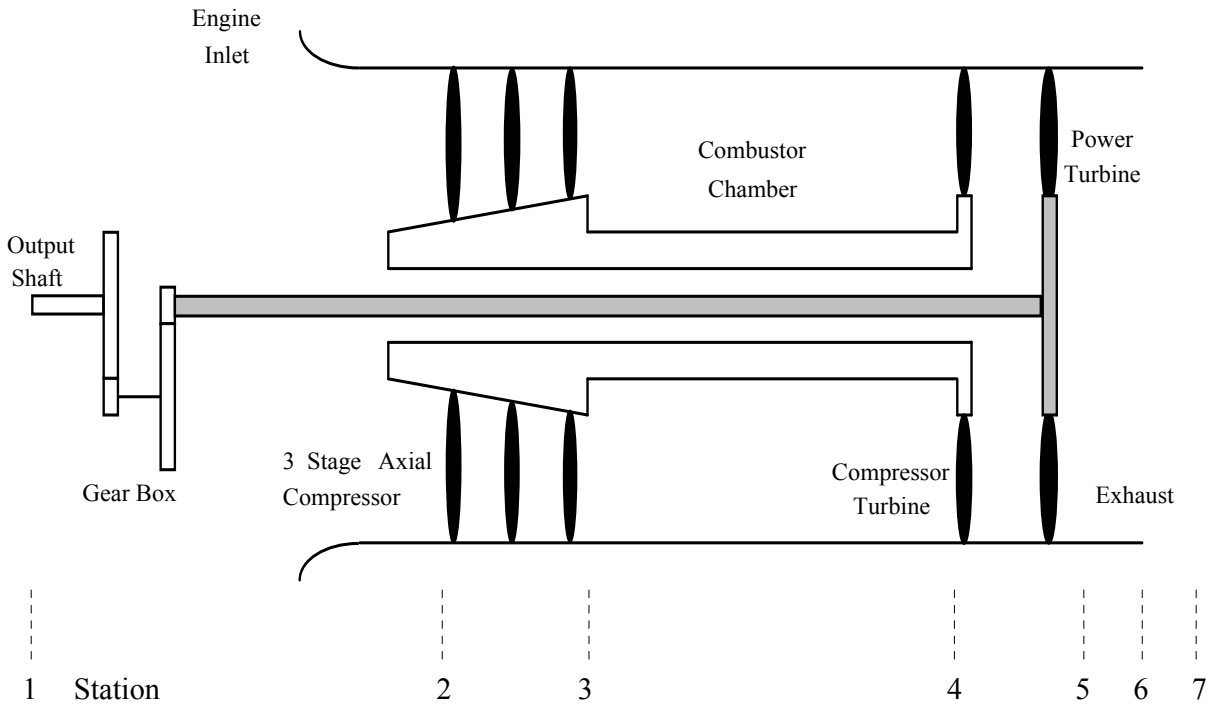


**Fig. 2-8. A free-shaft turbine has one turbine “wheel” driving the output shaft and a separate turbine “wheel” driving the compressor.**

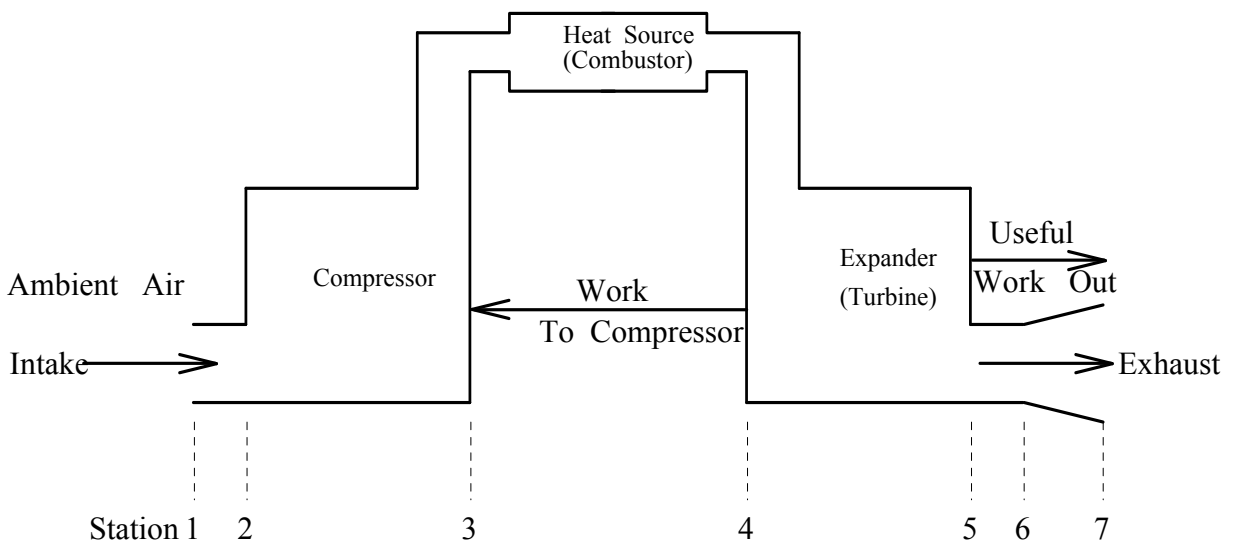


**Fig. 2-9. All thermal power plants can be schematically approximated as shown here.**

## 2.1 ENGINES

You can analyze the cycle characteristic of a gas turbine engine using this fundamental thermodynamic concept. That is, you can progress from the outside ambient air conditions to the engine inlet, through the engine, and out the exhaust. Thinking in terms of Eq. (2.12), you can also calculate the horsepower, temperature, and pressure situation at each station. Consider the following very simple example.<sup>21</sup> Suppose the rotorcraft is hovering at some altitude where the total pressure and temperature are just the outside, ambient conditions, say at 4,000-foot pressure altitude on a hot day when the temperature is 95 °F. Then,

$$P_{\text{am}} = 25.84 \text{ inches of Hg} \quad \text{and} \quad T_{\text{am}} = (95 \text{ °F} + 459.67) = 554.67 \text{ °R}.$$

As the air comes in, it is gathered up by the inlet, sent on to the compressor face, and then compressed. The compressor raises the gas (air in this case) temperature and pressure, and this takes horsepower that is supplied by its power turbine. The temperature rise depends on what compression you need. This compression is generally expressed as a pressure ratio. So to continue the example, suppose the air gets all the way from the outside to the compressor face with no losses. Then  $P_{T2} = P_{\text{am}}$  and  $T_{T2} = T_{\text{am}}$ . (Admittedly, this is rather ideal because getting air into the engine is a joint job for the rotorcraft designer and engine manufacturer. Both a pressure loss and a temperature rise generally occur in practice.) Now assume you have an engine whose compressor increases the pressure by a factor of 5.2. Then,

$$\frac{\text{Total pressure behind compressor}}{\text{Total pressure ahead of compressor}} = \frac{P_{T3}}{P_{T2}} = \text{PR} = 5.2.$$

The horsepower that the compressor needs to do this work becomes, with constants added to provide a numerical example, simply

$$\begin{aligned} \frac{\text{HP}_{\text{compressor}}}{\text{Airflow lbs/sec}} &= \frac{J C_p}{550 \eta_c} \times T_{T2} \times \left[ \left( \frac{P_{T3}}{P_{T2}} \right)^{\frac{\gamma-1}{\gamma}} - 1 \right] \\ (2.13) \quad &\approx \frac{0.33949}{\eta_c} (459.67 + T_{T2} \text{ in } \text{°F}) (\text{PR}^{0.2857} - 1). \\ &\approx 0.4 (459.67 + 95 \text{ °F}) (5.2^{0.2857} - 1) \\ &= 133.3 \text{ hp / (lbs/sec of airflow)} \end{aligned}$$

---

<sup>21</sup> During the mid-1950s, the engineers at Hiller were very active in teaching a rotary wing course at Stanford University in Palo Alto, California. Course notes were prepared and, thanks to Wayne Wiesner, the AHS Library and I have a copy. John B. Nichols gave the lecture on helicopter propulsion. His notes, dated May 5, 1954, contain the most concise, understandable transformation of thermodynamic laws into useful, simple engineering theory for any type of “engine” that I have ever seen. He never once uses words like adiabatic, reversible, isentropic, enthalpy, or entropy! The gas turbine example you are about to read is my condensation of Nichols’ 37-page, superbly lucid lecture. The information is too important to relegate to an appendix. Understanding the gas turbine engine is vital to rotorcraft engineering.

John Nichols passed away in mid-June of 1993. The AHS recognized his career on page 58 of the September/October 1993 issue of *Vertiflite* [114]. On the same page, the AHS noted the addition to its technical library of the lecture notes given by Wayne Wiesner. I missed the chance to ask John for permission to include his lecture notes in this book. However, I did get “permission” from Wayne who organized the Stanford course.

(This step assumes that compression begins at a relatively low temperature where  $C_p \approx 0.24$  and  $\gamma \approx 1.4$ . An average of the gas constants over the compression would be more correct. The compressor is assumed to be only 0.85 efficient in this example.)

The temperature rises through the compressor due to the compression of the air. When the air comes out from behind the compressor, it is at a higher total temperature of  $T_{T3}$  given approximately by

$$(2.14) \quad \frac{T_{T3}}{T_{T2}} = 1 + \frac{1}{\eta_c} \left[ \left( \frac{P_{T3}}{P_{T2}} \right)^{\frac{\gamma-1}{\gamma}} - 1 \right] = 1 + \frac{1}{0.85} [5.2^{0.2857} - 1] = 1 + .7078 \approx 1.71.$$

Because the air went into the compressor at

$$T_{T2} \approx T_{am} = 459.67 + 95 \text{ }^\circ\text{F} = 554.67 \text{ }^\circ\text{R}$$

it comes out at

$$T_{T3} = \frac{T_{T3}}{T_{T2}} T_{T2} = 1.71 \times 554.67 \text{ }^\circ\text{R} = 947.67 \text{ }^\circ\text{R} = 488 \text{ }^\circ\text{F} .$$

The air pressure will have been increased so that behind the compressor (station 3)

$$(2.15) \quad \begin{aligned} P_{T3} &= P_{T2} \times \text{Compressor Pressure Ratio} = P_{T2} \times PR \\ &= 25.84 \times 5.2 = 134.4 \text{ inches of Hg} \\ &= 12.7 \times 5.2 = 66 \text{ pounds per square inch} \end{aligned}$$

Now the airflow through the compressor, for a medium-sized turbine engine, could be on the order of 10 pounds per second. Using this illustrative value and the results from Eq. (2.13), this example compressor would “steal” some 1,333 horsepower from the following combustor and power turbine stages where the real power is produced.

Next, go from behind the compressor, through the combustor, to the front of the first turbine “wheel” that powers the compressor. Injecting fuel and igniting the mixture in the combustor raises the gas temperature to very high values as you will quickly understand. As this very hot fuel-air gas mixture comes out of the combustor, it moves to the turbine stage. The inlet or entrance to the power turbine stage sees temperatures on the order of

$$(2.16) \quad T_{T4} = T_{T3} + \frac{(\text{Fuel Flow lbs / sec})(\text{Fuel Heating Value BTU / lb})}{C_p \times (\text{Air Flow in lbs / sec})} .$$

Continuing the example, again assume the air flow is 10 pounds per second for this medium-sized gas turbine engine. This type of engine uses aviation fuel which has a heating value of approximately 18,500 BTU/pound. The fuel flow could easily be on the order of 1/80 of the airflow. This gives roughly 0.125 pounds per second or about 450 pounds per hour for the rate of fuel consumption. With this fuel flow, the temperature at the turbine inlet stage has become very hot, being on the order of

## 2.1 ENGINES

$$T_{T4} = T_{T3} + \frac{(0.125 \text{ lbs/sec})(18,500 \text{ BTU/lb})}{0.2474(10 \text{ lbs/sec})}$$

$$= 947.67 \text{ }^\circ\text{R} + 934.00 \text{ }^\circ\text{R} = 1882.67 \text{ }^\circ\text{R} = 1423 \text{ }^\circ\text{F}$$

With no pressure losses in the combustor, the fuel-air gas mixture will have the same pressure leaving the combustor as it did going in. Using this ideal assumption again, it follows that the total pressure at the turbine inlet will be

$$P_{T4} \approx P_{T3} = 134.4 \text{ inches of Hg}$$

$$= 66 \text{ pounds per square inch}$$

The engine manufacturer is clearly dealing with very high temperatures and pressures. The environment that the turbine has to perform in is harsh to say the very least.

Now consider the turbine stage. This stage takes energy out in the same sense as a windmill. It behaves as a compressor in reverse. Therefore, the shaft horsepower (SHP) that the turbine stage can produce depends on the pressure drop across the stage. Suppose, in the extreme, that the engine design allows the pressure to drop all the way down to the ambient pressure as it goes through the several turbine “wheels.” That is, assume  $P_{T5} = 25.84$  inches of Hg. This is an extreme assumption because then there would be no pressure to force the burned fuel-air residues out the exhaust nozzle. Still, this gives you a high-side feeling of the potential turbine power. Because the pressure at the turbine inlet was found to be  $P_{T4} \approx P_{T3} = 134.4$  inches of Hg, it follows that the pressure ratio across the turbine stage is

$$\frac{P_{T5}}{P_{T4}} = \frac{25.84 \text{ inch Hg}}{134.4 \text{ inch Hg}} = 0.1923$$

In addition, the temperature at the entrance to the turbine stage was found with Eq. (2.16) to be  $T_{T4} = 1423 \text{ }^\circ\text{F}$ . Thus, the turbine horsepower per lb/sec of gas mixture flow becomes

$$\frac{\text{HP}_{\text{turbine}}}{\text{Flow}} = \frac{J C_p \eta_T}{550} \times T_{T4} \times \left[ 1 - \left( \frac{P_{T5}}{P_{T4}} \right)^{\frac{\gamma-1}{\gamma}} \right]$$

$$(2.17) \quad \approx 0.389 \times \eta_T \times (459.67 + T_{T4} \text{ in } ^\circ\text{F}) \times \left[ 1 - \left( \frac{P_{T5}}{P_{T4}} \right)^{\frac{\gamma-1}{\gamma}} \right]$$

$$\approx 0.389 \times 0.85 \times (459.67 + 1423 \text{ }^\circ\text{F}) (1 - 0.1923^{0.2497})$$

$$= 209.7 \text{ hp / (lbs / sec of gas mixture flow)}$$

(Because the temperature is so high in this turbine stage, the gas constants have changed to  $C_p \approx 0.2746$  and  $\gamma \approx 1.3328$ . The turbine is assumed to be only 0.85 efficient in this example.)

The gas mixture flow in the turbine stage is actually slightly greater than the airflow alone because of the fuel that is added. The difference is, however, only by the fuel-air ratio of 1/80 or about 1 percent. Therefore, to a first approximation the SHP that the turbine can provide, using the 10-pounds-per-second airflow I assumed, is

$$\text{SHP}_{\text{turbine}} = 2097 \text{ hp.}$$

But of this available SHP from, say, two turbine “wheels,” the turbine that drives the compressor takes 1,333 horsepower. *That leaves only 764 horsepower for the turbine that drives the output gearbox.* This may startle you, however it is a rather typical result. To reinforce this point, the example is not complete without

$$(2.18) \quad \begin{aligned} \text{Useable Shaft Horsepower} &= \text{SHP}_{\text{turbine}} - \text{SHP}_{\text{compressor}} \\ &= 2097 - 1333 = 764 \text{ shp} \end{aligned}$$

Keep in mind that I chose a situation where the rotorcraft was hovering at 4,000-foot pressure altitude and the outside air temperature was assumed to be 95 °F. The performance of the turbine engine can be found at any other pressure altitude and temperature quite simply. Suppose you want to know what power a given engine will produce at sea level on a standard day. Because the engine performance is so tied to pressure and temperature ratios, the basic first-order parameters that allow converting from one altitude and temperature to another ambient condition are

$$(2.19) \quad \frac{\text{Useable SHP}}{\delta\sqrt{\theta}} \text{ or just } \frac{\text{SHP}}{\delta\sqrt{\theta}} \text{ and } \frac{\text{Fuel Flow}}{\delta\sqrt{\theta}} .$$

These ratios are called the referred power and referred fuel flow. Now, from Eq. (2.6) and Eq. (2.7), you will calculate for 4,000-foot pressure altitude and 95 °F outside air temperature that

$$\delta = \frac{25.84}{29.92} = 0.8636 \quad \theta = \frac{95 \text{ °F} + 459.67}{518.67} = 1.0694 \quad \delta\sqrt{\theta} = 0.8931 .$$

Therefore, the referred performance of this example engine becomes

$$\frac{\text{SHP}}{\delta\sqrt{\theta}} = \frac{764}{0.893} \approx 850 \text{ referred shaft horsepower} .$$

Then, the power at any other operating condition is simply

$$(2.20) \quad \text{SHP}_1 = \frac{\text{SHP}}{\delta\sqrt{\theta}} \times \delta_1 \sqrt{\theta_1} .$$

Thus, the usable SHP at sea level and 59 °F, where  $\delta_1$  and  $\theta_1$  are 1.0, is about 850 horsepower. In a like manner, the fuel flow can be referred as

$$\frac{W_{\text{ff}}}{\delta\sqrt{\theta}} = \frac{450}{0.893} \approx 500 \text{ referred fuel flow in lbs/hr} .$$

## 2.1 ENGINES

Then this referred fuel flow can be used to find the fuel flow at sea level and 59 °F as follows

$$(2.21) \quad W_{fr_1} = \frac{W_{fr}}{\delta\sqrt{\theta}} \times \delta_1\sqrt{\theta_1}.$$

Thus, the rate of fuel consumption is roughly 500 pounds per hour at sea level and 59 °F where  $\delta_1$  and  $\theta_1$  are 1.0.

The SFC is, of course, simply

$$(2.22) \quad \text{SFC} = \frac{\text{SHP}/\delta\sqrt{\theta}}{W_{fr}/\delta\sqrt{\theta}} \approx \frac{500}{850} = 0.592 \text{ lbs/hr per horsepower}.$$

To produce this power at sea level on a standard day where  $T_{am} = 59$  °F, the compressor ratio (PR) and turbine inlet temperature ( $T_4$ , or quite commonly TIT) will also adjust in a referred manner so that

$$\frac{\text{PR}}{\delta} = \frac{5.2}{0.8636} = 6.0213 = \text{referred compressor ratio}$$

and

$$\frac{T_{T5}}{\theta} = \frac{1882.67 \text{ °R}}{1.0694} = 1760.49 \text{ °R} = \text{referred TIT}.$$

The preceding elementary discussion of turboshaft engine performance can be very helpful to the rotorcraft designer in at least two ways. First of all, you get a much better feel for the constraints on an engine manufacturer recommending an engine to fill a need. Second, it lets you see what the engine manufacturer might do to increase power available when the rotorcraft requires more power than originally estimated! This second situation is, unfortunately, all too common.

Consider first the preliminary design task for the engine manufacturer to fill a new rotorcraft need. Thinking in terms of preliminary sizing, the number-one parameter that governs how much power the gas turbine will produce is the airflow that the engine will be designed to handle. This is because the fundamental thermodynamic equations such as Eq. (2.13) and (2.17) yield performance on a per pound/second of airflow or gas mixture flow, respectively. Current technology defines compressor pressure ratios, mechanical efficiencies, and the very important TIT.

You should understand that the TIT is perhaps the most important design and operating constraint to the engine manufacturer. Considerable progress has, of course, been made in raising this limiting temperature as the gas turbine has been refined. Early TIT limits of about 1,000 °F or 1,459.67 °R have been increased to 2,000 °F or 2,459.67 °R. Today, advanced materials and actual internal cooling of individual turbine blades are raising the TIT limits another 500 °F. As this key temperature limit has risen, there has been a corresponding increase in the compressor pressure ratio.

The very simple gas turbine equations just discussed illustrate the basic preliminary design trends that underlay this engine and the reasons engine manufacturers see things the way they do. Consider the situation where the turbine inlet temperature (TIT) is fixed (by technology) at some value, and the compressor pressure ratio is varied. The usable SHP per pound of airflow will then peak at a corresponding pressure ratio as shown in Fig. 2-10. The trend of increased power as TIT is increased is quite spectacular as Fig. 2-10 also shows. In essence, a whole family of gas turbine engines is presented in Fig. 2-10.

Now look at the lowest curve on Fig. 2-10 where  $TIT = 1,500\text{ }^{\circ}R$ . In the first place, if the compressor ratio is 1.0, there will be no flow through the engine. Fuel burned in the combustor will just turn the engine into a furnace. The turbine wheels will not turn, and the pilot will get no usable SHP. That is why the curves all start at zero power when the pressure ratio is 1.0. The importance of this point is not just academic as you might think. When the pilot starts the engine, he must be rather careful to get the compressor turning with the starter motor before he adds the fuel, otherwise the engine can get a “hot start” and damage the turbine. Automation of the starting process has significantly helped to make this problem a thing of the past.

By following the  $TIT = 1,500\text{ }^{\circ}R$  curve over the maximum power region to the point where  $PR = 11.5$  in Fig. 2-10, you will see that the SHP is again zero. At this point the temperature rise is so great in the compressor stage of the cycle that the only fuel that can be burned in the combustor gets used to turn the compressor turbine. No additional thermodynamic energy (i.e., additional fuel flow) can be introduced to get usable shaft turbine without going over the TIT limit of  $1,500\text{ }^{\circ}R$  used as an example level.

Fig. 2-10 shows just how much the engine usable SHP per pound/second of airflow can be increased given the technology to operate the turbine stage at very high temperatures. You should note that as the allowable TIT is increased, the preliminary design engine trend will “optimize” at successively higher compressor pressure ratios. However, the maximum power is achieved over a greater range in pressure ratio as higher TITs are allowed.

The companion curves to usable SHP are SFC curves. The preliminary design trends for this key engine performance characteristic are shown in Fig. 2-11; you can see that the rate of fuel consumption does not continually benefit from increasing TIT limits. This is in contrast to the trend in SHP shown in Fig. 2-10.

You will notice that Fig. 2-11 gives the distinct impression that there is an asymptotic lower limit to SFC; perhaps about 0.3 pounds per hour per horsepower. In fact, there is an absolute minimum to SFC on the order of 0.138 pounds per hour per horsepower assuming gas turbine jet fuel currently in use.<sup>22</sup> The logic is as follows:

---

<sup>22</sup> In discussing this rather simple result with Mike Scully in September of 2009, he refined my numbers somewhat and added that “there are many definitions for BTU. The ISO BTU definition (exactly 1,055.056 Joules per BTU) is also the official U.S. value (see NIST SP-1038). The ISO BTU quotes the lower heating values (LHV) for aviation fuels from MIL-STD-3013. The fuel density (lb/gal.) values in system specs are often higher than the minimums in MIL-STD-3013. DoD uses JP-8 on land and JP-5 on ships. JP-4 is only used for

## 2.1 ENGINES

1. JP-8 jet fuel weights approximately 6.7 pounds per U.S. gallon.
2. The heat content of JP-8 is about 18,400 BTUs per pound.
3. One horsepower is equivalent to 42.44 BTUs per minute or 2,546 BTUs per hour.
4. Thus, one hp = 2,546/18,400 pounds per hour or 0.138 lb/hr.
5. The lowest possible SFC is 0.1376 lb/hr/hp assuming JP-8.

Keep in mind that actual SFC must be higher than ideal because a significant amount of fuel is used to power the compressor as Eq. (2.18) shows.

The SFC and SHP preliminary design trends shown in Fig. 2-10 and Fig. 2-11 can be combined into one very informative data set as shown in Fig. 2-12. The primary variable is the four TIT limits used in this example. Both compressor pressure ratio and fuel-air ratio are adjusted, for a constant TIT, to move along any given line. The preliminary designs presented in this form help pinpoint the “optimum” performance at each TIT.

Given this background in preliminary design performance of the gas turbine, consider the actual engine performance currently available from engine manufacturers. The tabulated data [107], for example, provide trends in fuel flow at rated power with engine size for about 200 turboshaft and turboprop gas turbine engines. This important engine performance characteristic is shown in Fig. 2-13. Data for both turboshaft and turboprop engines are included in this survey. Note that this uninstalled engine performance is presented at sea level on a standard day where the outside air temperature is 59 °F. This is in contrast to the preliminary design example where I used 4,000-foot pressure altitude and an outside air temperature of 95 °F.

Based on the SFC of 0.60 upper boundary shown in Fig. 2-13, the smaller (and earlier) gas turbine engines have yet to benefit from technology that allows higher turbine inlet temperatures. The SFC line of 0.50 shows that engine manufacturers have made great progress in raising turbine inlet temperature limits in the medium-sized engines that mark a second generation. The fact that some engines are now beginning to operate at SFCs below 0.45 shows that a point of diminishing returns is near for SFC. This is not to suggest, however, that work has been discontinued on improving future turbine engines.

Finally, consider the issue of engine weight. The trends in gas turbine weight with rated SHP using tabulated data [107] are shown in Fig. 2-14. There is a distinction between turboshaft and turboprop made in this figure. However, the line is blurred between the two types because of the weight of the gearbox. Tabulated data give no details about a gearbox. In general, a turboshaft engine does not have a gearbox while the designation turboprop suggests the weight of a gearbox is included. This is particularly evident in the high-power region of the graph where the gearbox weight appears to be of the same magnitude as the turbine engine itself.

---

operations at very low temperature (e.g., Alaska in winter) because it is almost as dangerous as gasoline. Commercial jets use Jet A-1, which is very similar to JP-8. The use of these fuels is not driven by BTU/lb because the world will not pay a high price in \$ and operational limitations for modest performance gains.”

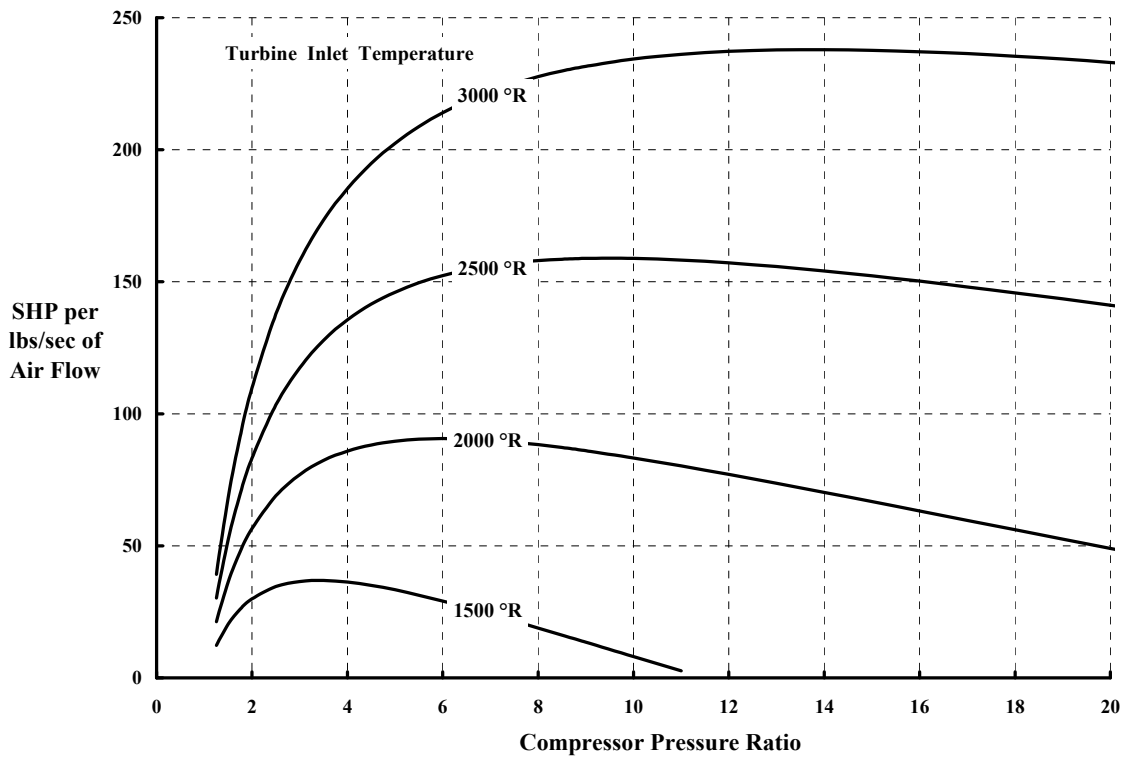


Fig. 2-10. Dramatic engine performance increases are obtained by raising TIT limits.

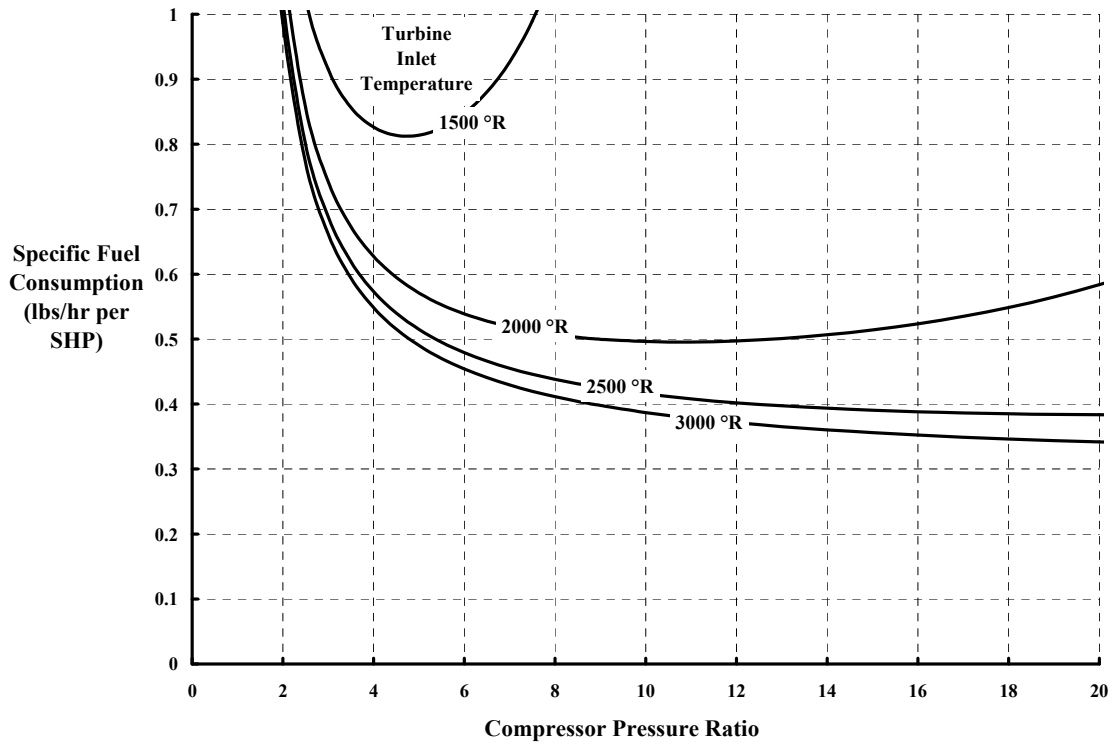


Fig. 2-11. There is a diminishing return to reducing fuel consumption as TIT limits are increased.

## 2.1 ENGINES

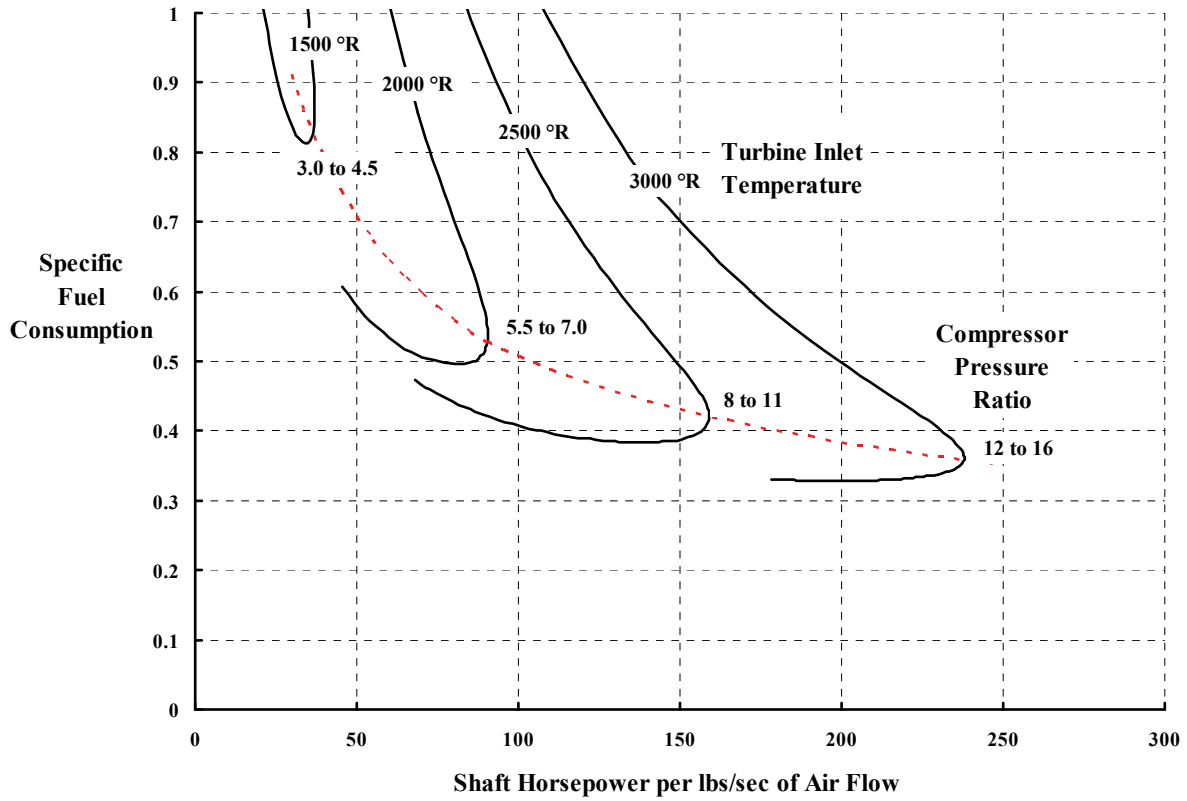


Fig. 2-12. Airflow and TIT are the key parameters of the gas turbine engine.

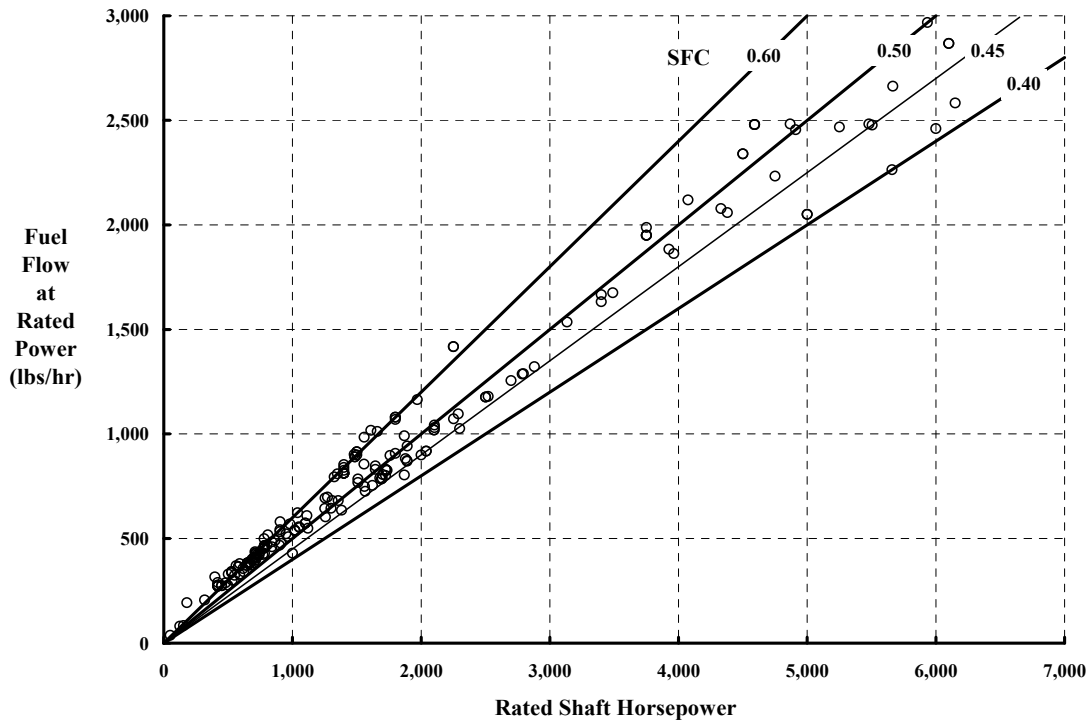
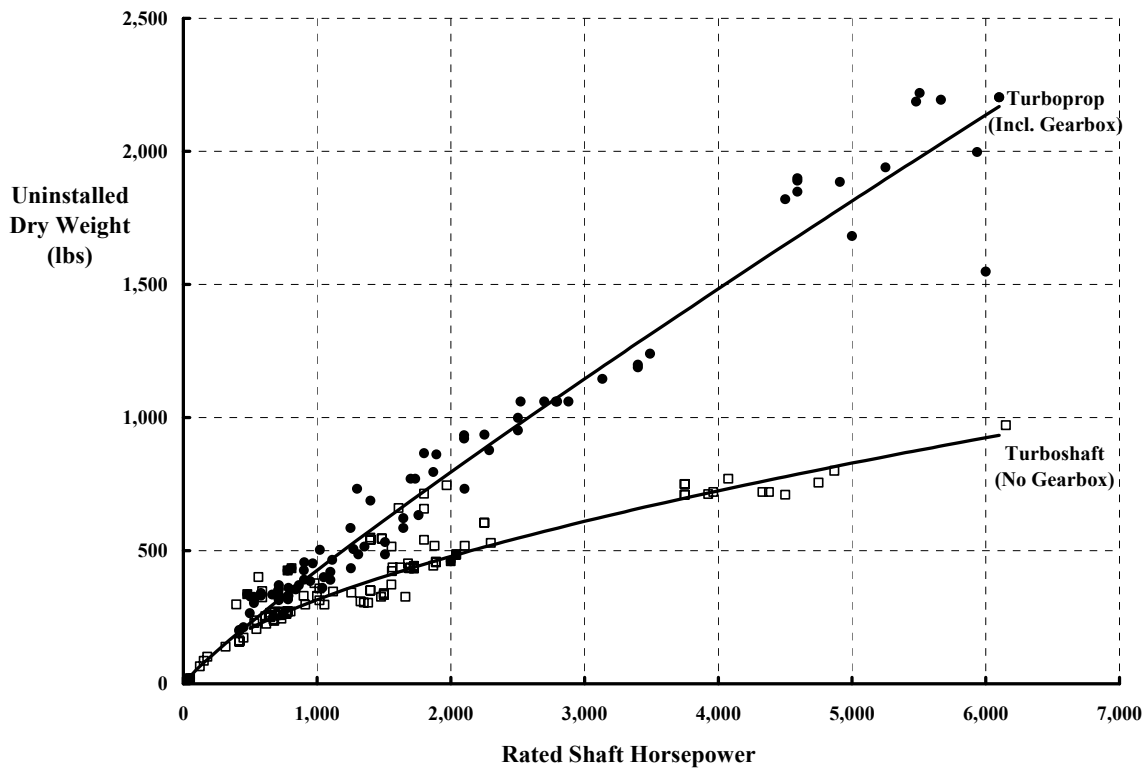


Fig. 2-13. Gas turbine engines burn fuel at a rate of approximately 0.45 pounds per hour for each rated SHP delivered.



**Fig. 2-14. Turboshaft engines without a gearbox are lighter than turboprop engines with a gearbox.**

This issue of who is furnishing the gearbox is a rather important distinction to the rotorcraft industry. Helicopters, for example, use large rotors that turn in the range of 250 to 350 rpm. This means a speed reduction from a power turbine speed on the order of 20,000 rpm. Most helicopter manufacturers have the technology, created from the piston engine era, to design a 10-to-1 speed-reducing gearbox. However, a 100-to-1 gearbox definitely requires a joint effort on the part of rotorcraft and engine manufacturers.

With the preceding background, let me now discuss turbine engines as they have come into use—and how they perform—when installed in rotorcraft. The turboshaft gas turbine found its way more slowly into the rotorcraft industry than it did in the fixed-wing field. In 1951, Charles Kaman experimented with two 175-horsepower Boeing 505 industrial gas turbines installed in his Navy HTK, the forerunner of his H-43 synchropter. In France, the Turbomeca engine company produced the Artouste II turboshaft engine. This was the first gas turbine specifically designed for a helicopter. It was installed in the then Sud-Aviation Company helicopter that became the Alouette II and made its maiden flight December 3, 1955. (You will find the fascinating story of the French rotorcraft industry in Boulet's history [2]. The combination of Turbomeca engines and Sud-Aviation, soon to become Aérospatiale, helicopters quickly made France a world leader in the industry.) Other members of the industry shortly followed suit proving that the high power-to-weight ratio offered by the turboshaft was here to stay.

## 2.1 ENGINES

In the late 1950s, the Department of the Army (through the Air Force) awarded the Bell Helicopter Corporation a contract for what became the first in the long line of Hueys. The experimental XH-40, powered by a Lycoming YT-53-L-1, was flight tested at Edwards Air Force Base in May and June of 1957. The test report [115] was delayed for nearly a year because of a 50-horsepower discrepancy (over the 300- to 700-hp range) between Lycoming test stand calibration of the engine and power available as measured with the engine installed in the XH-40.<sup>23</sup> The helicopter's performance was finally evaluated and published assuming the installed power measured at Edwards was representative [116].

The fuel flow for the installed Lycoming YT-53-L-1 free-shaft turbine engine is shown as a function of SHP delivered in Fig. 2-15. The two parameters are used in the referred sense that allows one curve to describe the effects of altitude and temperature. That is, the engine performance parameters include the  $\delta\sqrt{\theta}$  term discussed earlier.

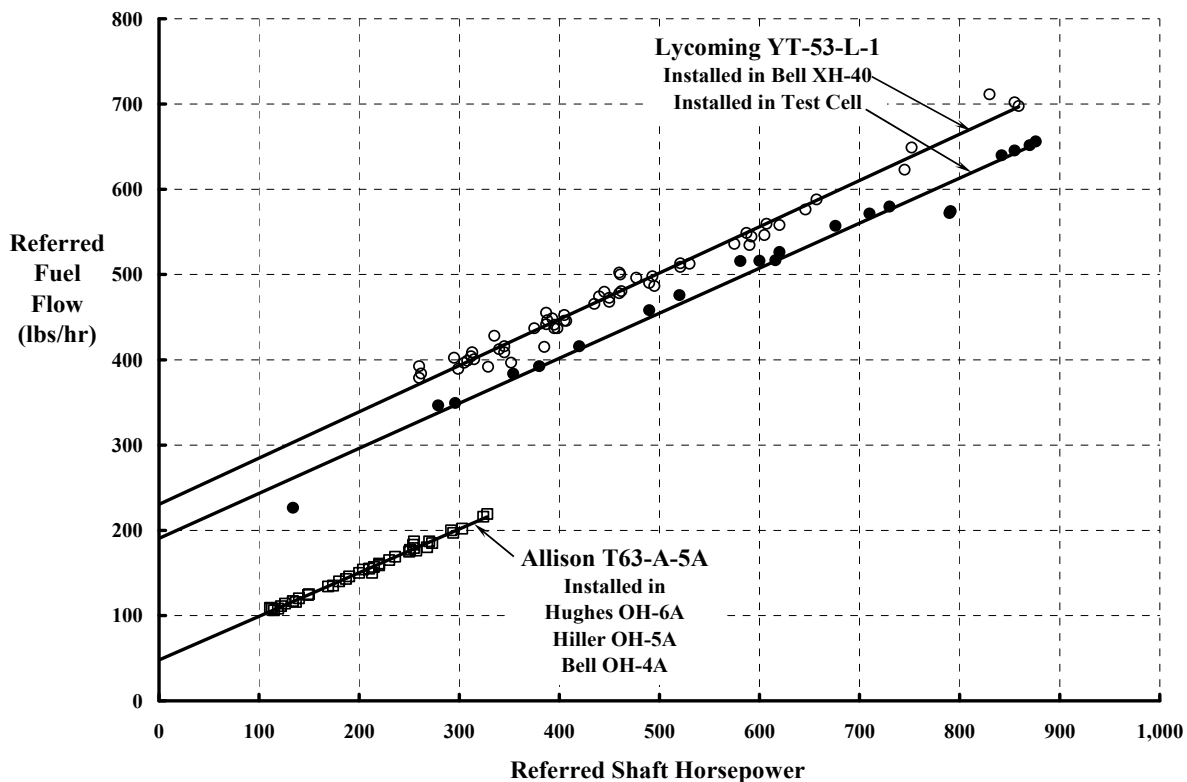


**Fig. 2-15. Gas turbine engines burn fuel at zero SHP to power their compressor.**

<sup>23</sup> The engine was returned to Bell for installation and flight test in the other two XH-40 helicopters. In one helicopter, the engine performed nearly identically in accordance with the test stand calibration. In the third helicopter, "the engine appeared to produce more power for a given gas producer speed than was determined during test stand calibration." The problem finally went into "the too hard file" with the conclusion that "these discrepancies will probably be determined as service experience is gained on the H-40." As it turned out, the first three XH-40s grew to a fleet of over 10,000 UH-1s or, more popularly, the Huey helicopter. Service experience from nearly two million flight hours has been gathered. The Huey helicopter is considered a success.

You will note in Fig. 2-15 that fuel flow varies nearly linearly with SHP. However, there is an apparent zero shift so that fuel needs to be burned even when no usable SHP is provided. This is a measure of how much thermodynamic energy is used by the compressor just to make the engine even run. You can also see from the figure that the slopes for both the larger Lycoming YT-53 engine and the smaller Allison T-63 engine (which I will discuss next) are about the same. This measure suggests that both engines were of the same technology level.

Gas turbine engines operate in such a way that, to the first approximation, fuel flow and power are related simply as

$$(2.23) \quad \frac{W_{fr}}{\delta\sqrt{\theta}} = a + b \left( \frac{\text{SHP}}{\delta\sqrt{\theta}} \right).$$

This handy approximation is quite useful for estimating mission fuel weight in rotorcraft preliminary design. The constant (a) in Eq. (2.23) reflects primarily the compressor and the turbine “wheel” that drives it. For the early T-63, which was nominally rated at 270 SHP, this constant is a referred fuel flow of 40 pounds per hour. The larger T-53, rated at 850 SHP, intercepts at 230 pounds per hour. The slope [for these two engines (b) is 0.545 lbs/hr per SHP] in the equation represents the useful energy that the fuel is providing. Virtually all gas turbine engines behave in the nearly linear fashion suggested by Fig. 2-15.

The smaller Allison T-63 engine shown in Fig. 2-15 was the power plant selected by the Army when they began a competition for a new Light Observation Helicopter in the early 1960s. The objective was to replace the piston-powered fleet of Hiller H-23s and Bell H-13s. This time the Department of the Army, rather than the Air Force, was the procurement agency. The “fly-off” competition began in January/February 1964 with the Hughes OH-6A, the Hiller OH-5A, and the Bell OH-4A. The development costs of about \$20 million for the three manufacturers and \$7 million for engines was paid by the Army. The helicopters were built to Federal Aviation Agency (FAA) civil regulations with only minor military requirements superimposed. The Army was buying “off-the-shelf products.” These helicopters were evaluated and results published in references [117], [118], and [119], respectively. (By this time the Air Force had turned over rotorcraft testing at Edwards Air Force Base to the Army, and this created the U.S. Army Aviation Systems Test Activity.)

The competition was, to say the very least, hard fought not only from the technical side but from the business side. The Hiller OH-5A and Hughes OH-6A appeared to receive the better product evaluation compared to the Bell OH-4A in the test reports. As it turned out, the Hughes OH-6A was the first-round winner (May 26, 1965), and the Army bought some 1,000 helicopters at just under \$20,000 a piece. However, both Bell and Hiller proceeded to quickly turn their helicopters into commercial products. Hiller came out with its FH-1100 and Bell began the very successful Model 206 line. Hughes soon followed with its Model 500. This onset of three, turbine-powered, “advanced technology” commercial products was highlighted in the 14th Annual Helicopter Edition of Flight Magazine [120].

## 2.1 ENGINES

When the Vietnam War started, the Army decided to buy another batch of 121 OH-6A light observation helicopters. However, they ended up buying the Bell commercial Model 206B (a great improvement over its original OH-4A), and it was designated as the Army's OH-58A. The flight evaluation of this helicopter was reported [121]. Despite the rough start<sup>24</sup> the world now had three exceptional, light helicopters, and they were each powered with the Allison 250-series shaft turbine.

This competition story of the 1960s was repeated again in the late 1970s in a somewhat different form. In this period the General Electric YT-700-GE-700 engine became available (through an Army-led competition) for consideration by the U.S. Army. The Army also found the need to update both its attack helicopter and utility helicopter fleets during this period. (At this time, Bell Helicopter Textron had a virtual monopoly on nearly every helicopter the U.S. Army was flying. The Bell OH-58As through Cs were being used for light observation, the Bell Huey UH-1Bs through Ds served for utility, and the Bell Cobra AH-1, prototyped in 9 months, provided the attack capability. In the Vietnam conflict, these rotorcraft demonstrated beyond any doubt just how valuable helicopters had become.)

Using the General Electric YT-700-GE-700 engine, the mid-1970s saw a “fly off” between helicopters prototyped by each of the four major United States rotorcraft manufacturers. The Army's new utility helicopter was to be either the Sikorsky YUH-60A or the Boeing Vertol YUH-61A. The attack helicopter competition was between the Bell YAH-63 and the Hughes YAH-64. Each helicopter was tested by the Army at Edwards Air Force Base, and results were published at the end of 1976 in references [123-126], respectively. This competition really tested the industry's capability in every aspect of modern rotorcraft engineering and manufacturing, as well as business management. The results of the competition, with respect to installed engine performance, were quite extraordinary.

Two YT-700-GE-700 engines were installed in each of the four prototype helicopters that were delivered for Army flight evaluation at Edwards in 1975. The evaluation of engine power available—uninstalled versus installed—for hovering at 4,000-foot pressure altitude with an ambient temperature of 95 °F is summarized in Table 2-1. Each evaluation concluded

---

<sup>24</sup> On July 24, 1968, the San Francisco Chronicle carried a United Press article from Washington that summed up a Congressional, House Armed Services Committee investigation into both the original award and the supplementary buy. It read in part: “The [original] contract award was marked by allegations including misconduct, prejudice, information leaks, influence peddling and industrial espionage. The report accused Hughes of building 1,000 light observation helicopters for the Army at the bargain basement rate of \$19,860 each, then quoting a price of \$55,000 each for 121 additional machines needed for Vietnam. Rather than pay the higher price, the Army canceled its supplementary order and met war needs with other existing models. The subcommittee said Hughes won the [original] contract over Hiller Aircraft Corp. by buying in or making a below cost bid in the hope of recovering an estimated \$10 million loss by pricing the same machine much higher for commercial buyers. Hiller's price was \$24,000 per helicopter. The Army had estimated each would cost \$30,000 to \$40,000. The subcommittee's 10-month-long investigation began when the Army asked Hughes to build the extra helicopters. The company, headed by Howard Hughes, denied that the loss would be recovered in prices of follow up Army contracts. The House investigators reprimanded the Army and urged that the Air Force and Navy take over its procurement of aircraft.” The subcommittee's findings became a matter of Congressional record [122].

that roughly 3½ percent of the engine's power was lost on installation. Further, the test conclusion comparison showed that the installed SHP only varied 15 horsepower between the four designs which, in itself, is quite remarkable. This represents a difference between the four helicopters of less than three-quarters of 1 percent (of the 2,365 hp) uninstalled power available.

The evaluation of the YT-700-GE-700 engine fuel flow as a function of SHP when installed in these four helicopters is examined in Fig. 2-16 and Fig. 2-17. The data is shown in the referred coordinates applicable to gas turbine engines. The YUH-60A engine performance data shown in Fig. 2-16 indicates that minimum SFC of 0.48 was obtained at high power in the range of 1,300 to 1,500 referred SHP. The scatter in the data is rather typical of flight measurements. This scatter, when both engines are included, amounts to ±35 pounds per hour in fuel flow at 1,400 SHP or about ±5 percent. At constant fuel flow of 700 pounds per hour, the scatter in power is ±70 horsepower or about ±5 percent. The engine prime item development specification (commonly called a PIDS) reflects the performance that the manufacture had to meet, or exceed, in nearly ideal test cell conditions. In this particular example, both right and left engines met "spec" in the test cell. The engine performance degraded when installed in the helicopter, although the right engine appears to have had better installed performance than the left engine.

I have scrutinized all the engines tested in the four development helicopters in Fig. 2-17 by just looking at the upper end of engine performance where the scatter in data has expanded considerably. The uncertainties in both power and fuel flow have increased to slightly over ±7 percent. The importance of, and confidence in, a company's product performance claims are rather compromised when these facts are introduced into published data. The only satisfactory recourse I have found is to turn to the pilot's flight handbook.

**Table 2-1. Installing Engines in Rotorcraft With a Minimum of Losses and a Maximum of Confidence Was Finally Proven in the 1970s**

Parameter	Utility		Attack	
	YUH-60A	YUH-61A	YAH-63	YAH-64
Model	YUH-60A	YUH-61A	YAH-63	YAH-64
Mission Weight, lb	16,853	16,411	16,054	14,242
Weight Empty, lb	12,113	11,704	13,338	11,556
Main Rotor Diameter, ft	53.67	49.00	51.50	48.00
Tail Rotor Diameter, ft	11.00	10.17	9.50	8.33
<i>Uninstalled</i> Shaft Horsepower Available at 4,000 ft/95 °F	2 × 1,178 or 2,356			
<i>Installed</i> Shaft Horsepower Available at 4,000 ft/95 °F	2,285	2,275	2,275	2,290
Installation Loss, Δ SHP	71	81	81	66

## 2.1 ENGINES

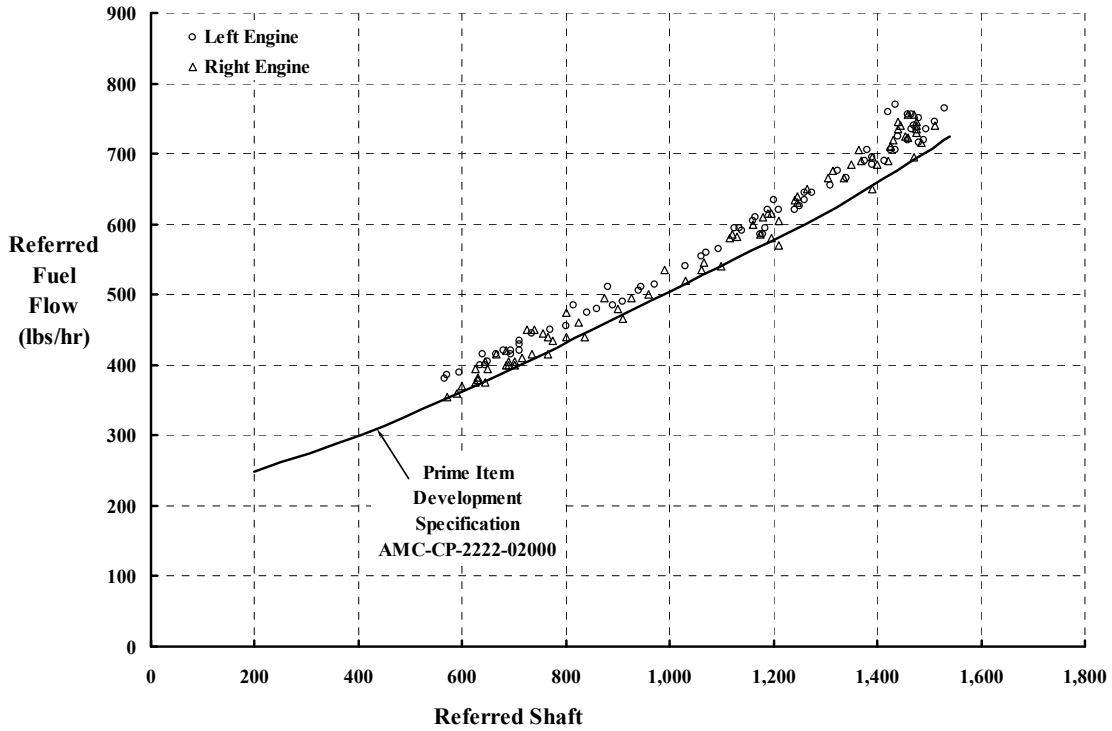


**Fig. 2-16.** In 1974, two General Electric YT700-GE-700 engines installed in the Sikorsky YUH-60A gave an SFC of 0.48 lbs/hr fuel flow per SHP.

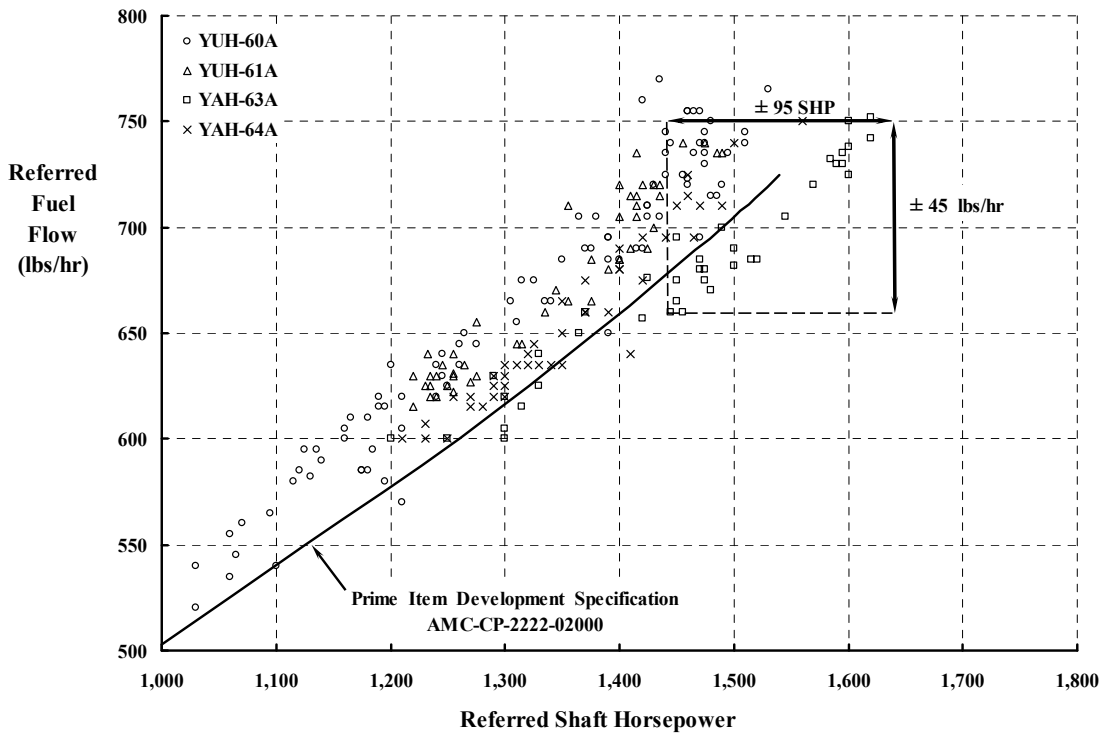


**Fig. 2-17.** There is about a 7 percent performance uncertainty when engines are installed in rotorcraft.

The U.S. Army invested heavily again in engines and rotorcraft in the mid- to late 1980s. The first step was funding of an Advanced Technology Demonstrator Engine (ATDE) program that would improve upon the Lycoming T-53 turboshaft gas turbine. The objective was an even more maintainable, lighter weight engine, still within the 750 to 1,000 SHP range. The farsighted ATDE program provided the technology for the Light Turbine Helicopter Engine Company T-800 engine. This engine is produced by the team of Allison Gas Turbine Corporation and the Garret Division of the Allied-Signal Aerospace Company (they go by the shorter name of LHTEC.) The LHTEC T-800 was selected as the Government Furnished Equipment (GFE) for the Army-funded development of a modern Light Helicopter, the Boeing-Sikorsky RAH-66 Comanche.

The RAH-66 came into being after a hard-fought competition managed by the U.S. Army. Two teams of major companies, Boeing/Sikorsky and McDonnell Douglas/Bell Helicopter, submitted massive proposals with their “paper” designs. There was no competitive “fly-off”—a marked departure from previous Army procurements. The Boeing/Sikorsky design and program was selected on April 5, 1991, and a final contract for \$2.8 billion was signed on April 12th. The May 1991 issue of *Rotor & Wing* magazine, page 10 of reference [127], provided a one-page summary of key factors in the competition and included the major specifications to be met by Boeing/Sikorsky. These were:

- 52-month development program with four prototypes
- Initial operating capability (IOC) in December of 1998
- 1,292 helicopters produced at the rate of 10 aircraft per month
- \$8.505 million per helicopter in 1988 dollars
- Unit and depot parts and labor (including the GFE T-800) costing \$492 per flight hour
- Total operating cost per flight hour under \$1,000
- Mission weight [empty] of 7,500 pounds
- Top speed of 190 knots

While the design emphasized reliability, maintainability, and overall user friendliness, the most advanced stealth and sensor technology was incorporated. Other, more classical technical features such as basic airframe, drivetrain, and rotor configuration were considered secondary to the costs and mission weight-empty specification requirements. This was a measure of how mature helicopter technology was thought to be in the late 1980s.<sup>25</sup>

---

<sup>25</sup> Many of the highly classified aspects of the design have yet to reach the public domain. I was the “Chief Engineer” for the McDonnell/Bell Super Team which lost to the Boeing/Sikorsky First Team. It was one of the most fascinating experiences of my career. The RAH-66 program began, rather early in its history, to run into budget problems [128]. The program was cancelled on Monday, February 23, 2004 [129]. One lesson the program taught was that development problems bring “help” from Congress.

## 2.1 ENGINES

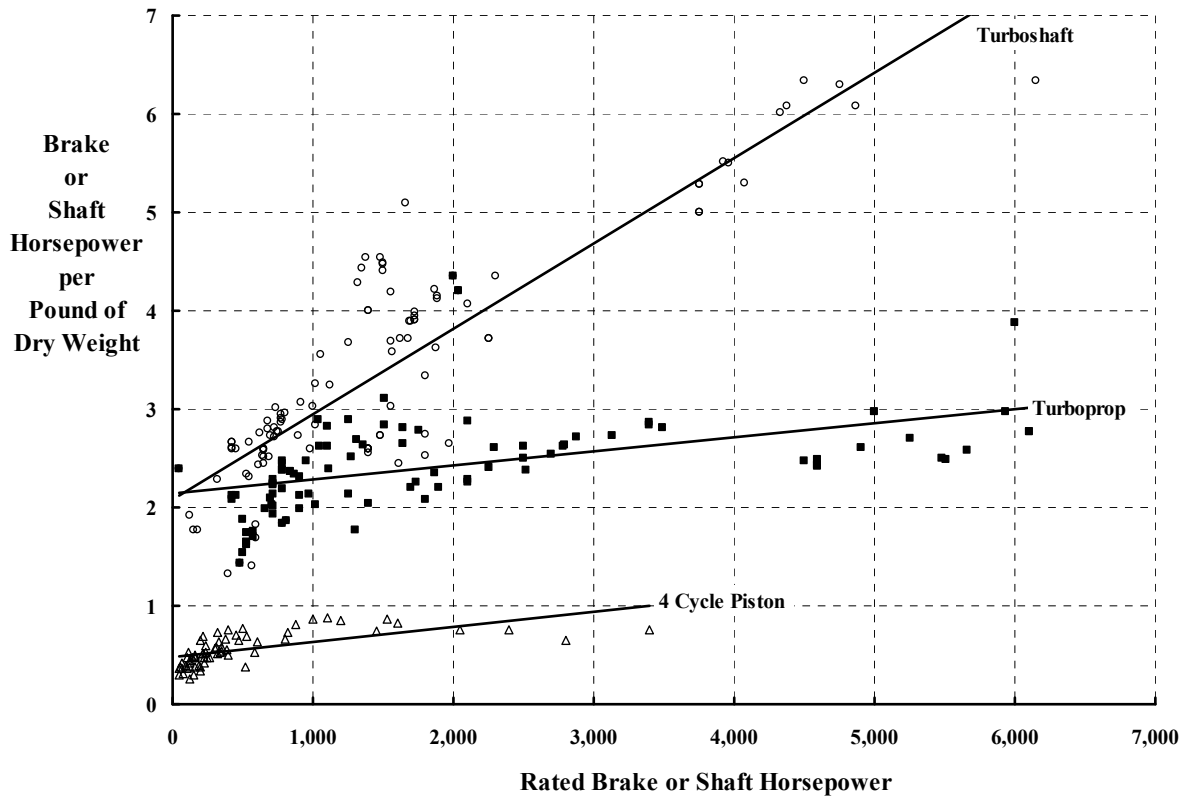


**Fig. 2-18. The gas turbine engine enjoys an enormous weight advantage over the piston engine.**

This introduction to engines would not be complete without contrasting piston and shaft turbine engines. For example, consider the comparisons in rated horsepower available at sea level per pound of dry weight shown in Fig. 2-18. Piston engines now are capable of about 0.75 BHP per pound in their mature, high-powered form. Turboprop turbines that include a gear box appear limited to about 2.5 to 3.0 SHP per pound in their mature, high-powered form. Turboshaft gas turbines—without a gearbox—show no obvious limit with size. Of course this leaves the burden of a 100-to-1 speed-reducing gearbox to the turboshaft engine user.

The modern turbine engine offers a very significant weight advantage compared to the four-cycle piston engine. It did not initially offer a comparable fuel-flow advantage as Fig. 2-19 shows. The small, Lycoming O-360 piston engine burns fuel at about one-half the rate of the nearly comparable Allison T-63, a vintage, 1960s, small gas turbine with a gearbox. In the larger engine category, the supercharged Wright R-1820 has a fuel flow again about one-half of the late 1950s Lycoming YT-53. But with two decades of development to draw on, both the General Electric YT-700 and LHTEC T-800 gas turbine engines have demonstrated fuel efficiency quite comparable to the piston engine at the end of its era.

What has happened, of course, is that only minor product performance improvements have been made to piston engines since the late 1950s. The industry has, instead, concentrated its resources on maturing the gas turbine, and they have been very successful. This does not mean, however, that the rotorcraft industry has forsaken the piston engine, as a quick review of any number of trade magazines and manufacturers' brochures will show. The number of new piston engines available for sport and experimental aircraft [130] is quite amazing. A large market still exists for used Bell Model 47s powered with the Lycoming VO-435 piston engine that is now rated at 260 BHP. The Hughes two-place Model 269A (i.e., the Army T-55 trainer) is still in production by the Schweizer Company and uses the Lycoming O-360-C2D piston engine. The Enstrom Company delivers its three-place, F-28 series with Lycoming HIO-360-C1A to F1AD engines. And, most encouragingly, Frank Robinson—beginning in the early 1979 with his R-22—has completely captured the small, two-place, light helicopter market. (In 1979, Robinson delivered 10 R-22s; in 1980, 78; and in 1981, 156, and he had captured 57 percent of the market.) The R-22 is powered by the Lycoming O-320-A2C rated at 150 horsepower for takeoff and 124 horsepower for continuous operation. The natural next step, a four-place, piston-engine-powered helicopter has followed with the R-44. This helicopter is delivered with a Lycoming VO-435 rated at 265 horsepower for takeoff. The spirited and innovative efforts demonstrated by Robinson and his company are reminiscent of the best efforts given by our rotorcraft pioneers.

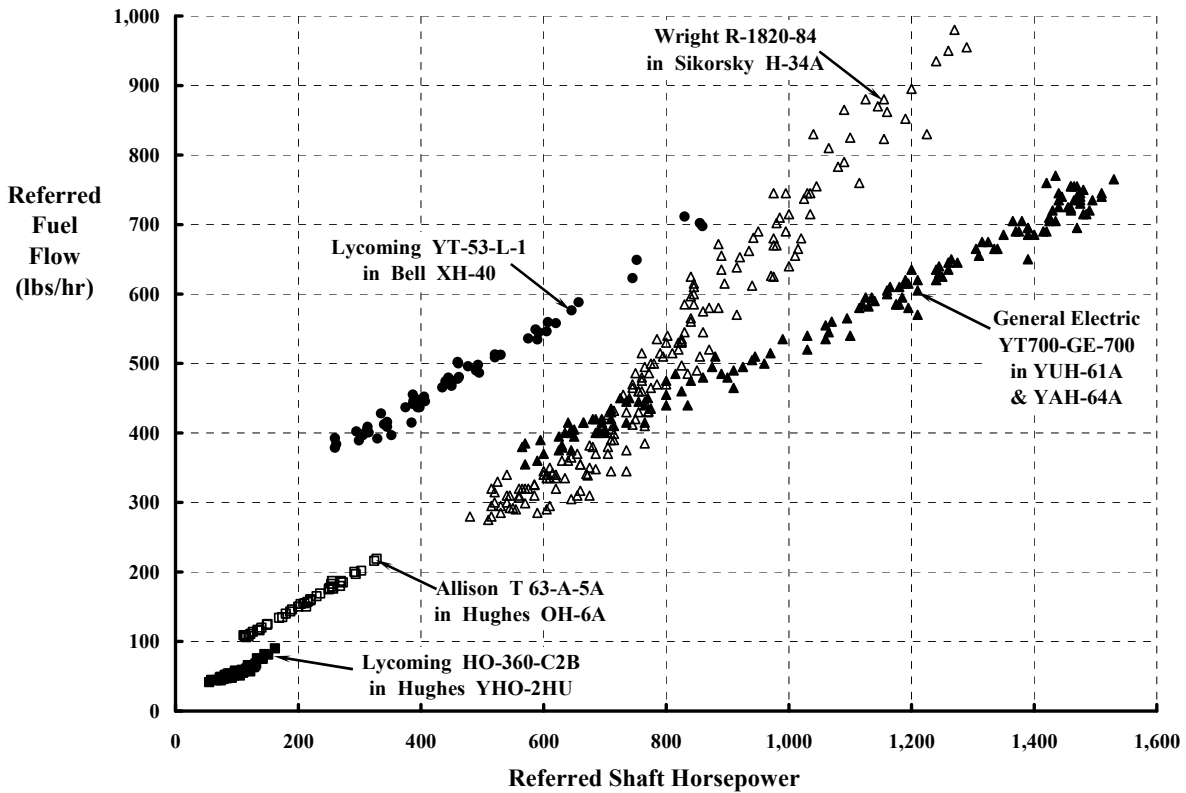


**Fig. 2-19. The piston engine enjoyed a fuel flow advantage over the turboshaft engine until the mid-1970s.**

## 2.1 ENGINES

You should also be aware that small helicopters fitting into the FAA Part 103 certification category for ultra-light aircraft are frequently created. This FAA category is designated for recreation and sport aircraft uses only. In late 1993 for example, Harry Parkinson (President of Advanced Technologies Inc.) announced the Ultrasport 254 in the October 1993 issue of *Rotor & Wing*. This one-place helicopter is sold for around \$30,000. It has a single, two-bladed main rotor and a weight empty of slightly less than 254 pounds, which is the upper limit restriction for FAA Part 103 aircraft. The takeoff gross weight of 482 pounds includes the 200-pound pilot and 30 pounds of fuel. The test helicopter was initially powered with a Rotax 503, two-cycle, piston engine. This two-cylinder engine has pistons of 2.834-inch bore and 2.40-inch stroke. It produces a maximum 50 BHP at 6,600 rpm and weighs 82 pounds with carburetors and exhaust system. The fuel flow at 50 horsepower is 6.8 U.S. gallons per hour (about 41 pounds per hour, which gives an SFC of 0.816. A Hirth 2703 engine is used in the production Ultrasport 254. This two-cylinder engine has pistons of 2.755-inch bore and 2.52-inch stroke. It produces 55 BHP at 6200 rpm and weighs 70.5 pounds. The fuel flow at 55 horsepower is 6.2 U.S. gallons per hour (about 37.2 pounds per hour) which gives an SFC of 0.676.

Finally, the small autogyro still has a very strong following. A noteworthy example of this rotorcraft class was offered by the Farrington Aircraft Corporation as the Model 18-A Gyroplane. This two-seats-in-tandem rotorcraft was originally developed by the Umbaugh Aircraft Corporation in the late 1950s and early 1960s. Production began again in April of 1991 when the very much improved Model 18-A was fully recertified by the FAA. The 1800-pound-gross-weight autogyro is powered with a Lycoming O-360-A1D and can be thought of as a direct competitor to the Robinson R-22. A more recent autogyro example is the Groen Brothers' Hawk.

The progress made by the propulsion industry can be summarized in several ways. For example, in February 1992 Dr. Richard Carlson was invited to address the National Academy of Engineering, which was honoring Dr. Alexander H. Flax. Dr. Carlson spoke about the future of rotary wing aircraft [131]. He used a particularly illuminating comparison between engines in the 1000-horsepower range that I have embellished here in Fig. 2-20. Another technical comparison is shown in Fig. 2-21 where SFC and shaft (or brake) horsepower per pound are summarized for both piston and gas turbine engines. This figure captures some of the historical trends and emphasizes how different the two engine classes are. Historically, the older engines fall towards the higher SFC and lower horsepower-per-pound range.

The contrast between piston and turboshaft engines is exemplified by their relative costs. In general, pricing information is rather difficult to come by. Yet, it is just this competitively sensitive data that engineers, in particular, need in order to balance their preoccupation with rotorcraft technology. Data from reference [132]<sup>26</sup> shows that, at equal

---

<sup>26</sup> An absolutely mandatory reference for rotorcraft study is published by HeliValue\$, Inc. [132]. Their *Official Helicopter Blue Book*<sup>®</sup> provides an enormous amount of configuration and pricing data that has been heavily relied on by the commercial marketplace for nearly two decades. I think the value of this reference to understanding helicopter technology, and seeing where engineers, in particular, can make very significant contributions to reduce product costs, is not realized by the technical community.

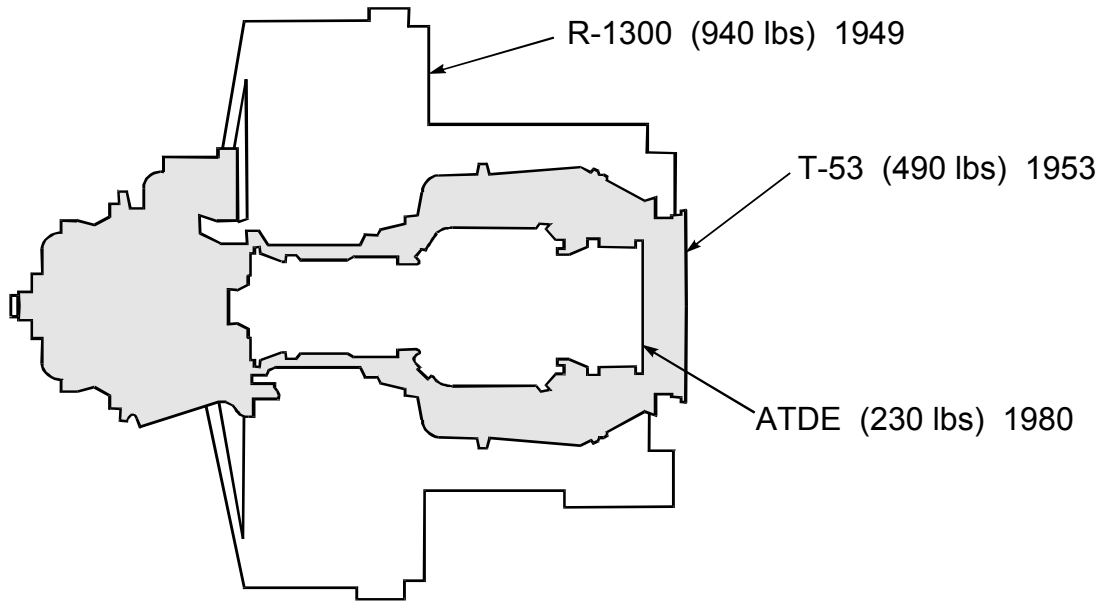


Fig. 2-20. Progress in the engine industry has been impressive [131].

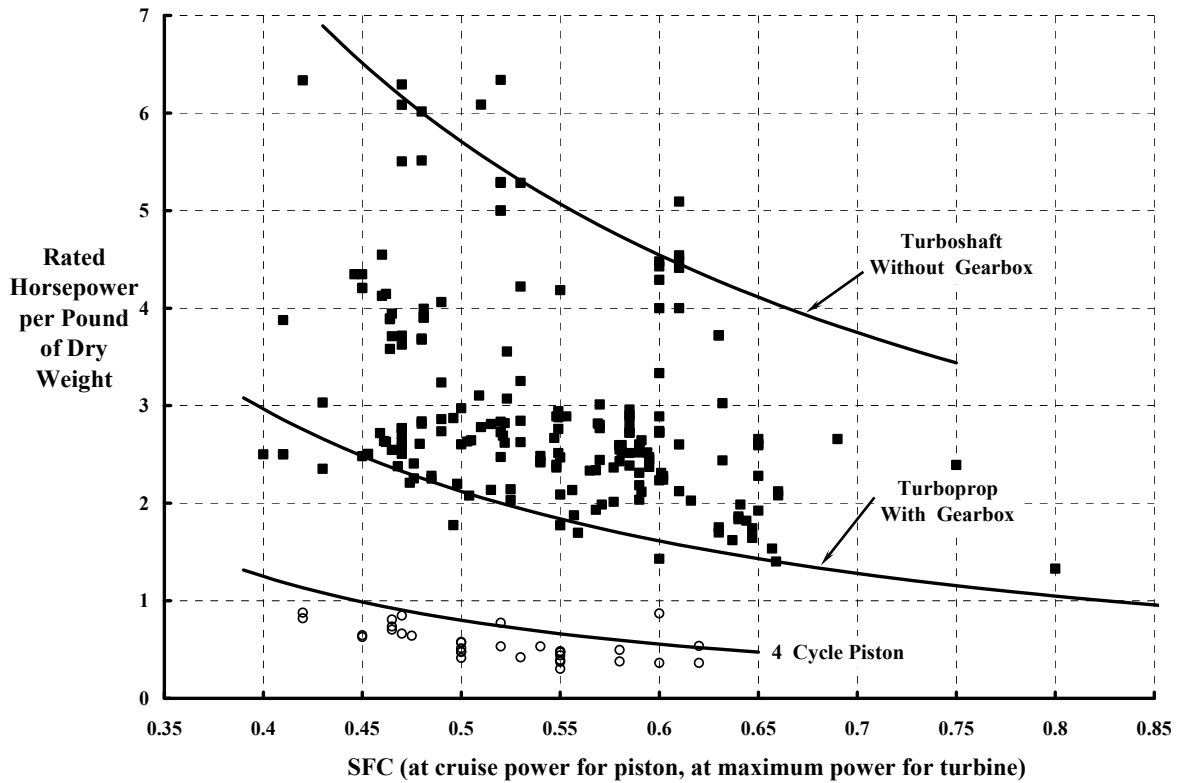


Fig. 2-21. Gas turbine engines have given the helicopter its most significant step forward.

## 2.1 ENGINES

power, the piston engine price is about one-third of the turbine engine price. The compilation shown in Fig. 2-22 emphasizes this difference.

The corner of a black square data symbol (for turbines) immersed in the open circle piston engine data is just visible on Fig. 2-22. This was the first suggestion of offering the turboprop engine at piston engine prices. The suggestion was made by the Allison Engine Company in the early 1990s with its very well proven, Model 250-series engine. You will recall that this gas turbine engine with a gearbox giving about 6600 rpm output started the Hughes Model 500, Hiller FH-1100, and Bell Model 206B product lines. The engine started as the Model 250-C18B, which later grew into the 250-C20. Allison has derated the growth engine back down to the original level of about 320 SHP at sea level on a standard day. The full influence (of what might be a very competitive move by Allison) on both Lycoming and Continental piston engine product lines has yet to be seen.

You may conclude from this introduction to engines that, at equal power:

1. Piston engines weigh at least three times what comparable turboshaft engines weigh.
2. Early turboshaft engines burned twice as much fuel as advanced piston engines.
3. Improvements in gas turbine engine performance have come by increasing turbine inlet temperatures.
4. Engine manufacturers can change a turboshaft to a turboprop by adding a gearbox.
5. Turboshaft engines presently cost three times what piston engines cost (but they have become much more reliable).

You should also appreciate that the single, most important factor that has improved rotorcraft is progress in engine technology.

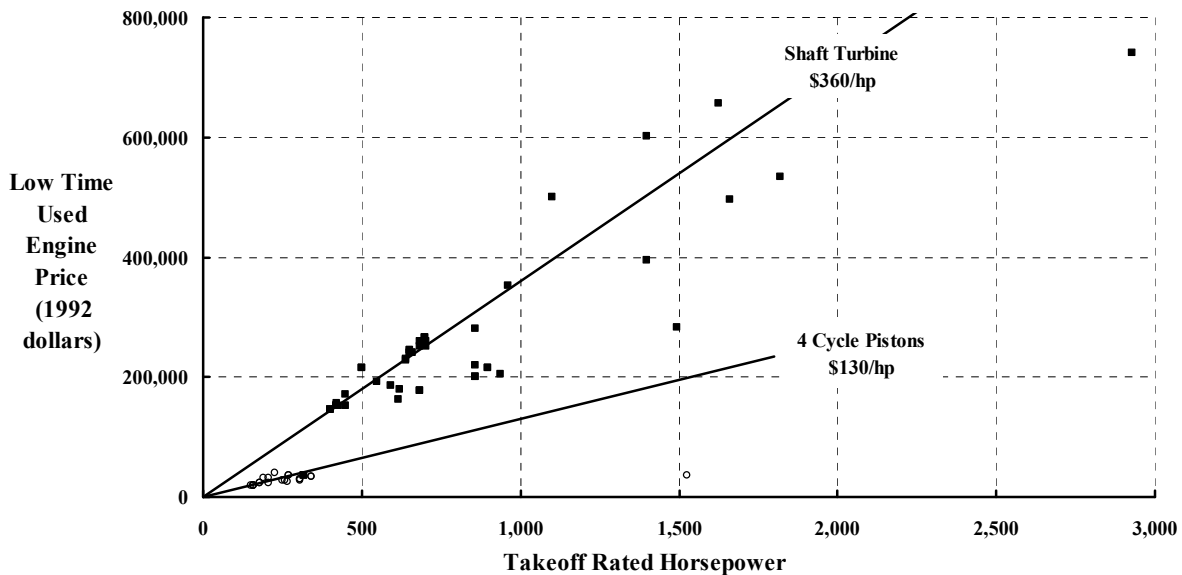


**Fig. 2-22. Turboshaft engines are priced about three times higher than four-cycle piston engines.**

## 2.2 WEIGHT

Rotorcraft weight is perhaps the clearest measure the industry has of its technological progress. This is because all facets of design and manufacturing finally come to light when you study modern helicopter weight results in some detail.

To understand and appreciate the progress made by the rotorcraft industry in reducing helicopter weight and obtaining a more efficient “machine,” you need to:

- a. Start with a framework for the discussion,
- b. Understand the terminology used,
- c. See two general trends that have appeared over five decades,
- d. Review detailed results for one specific helicopter class, and then
- e. Apply this background understanding to a broad range of products that the industry has created.

After absorbing these five points you will see a simple method of conceptually sizing and weighing a new, modern helicopter. This chapter on weights will then conclude with a short discussion of helicopter productivity. Let me start with a framework for the discussion.

A framework in which to discuss, examine, and evaluate modern helicopter weights is shown in Fig. 2-23. All manner of manufacturers’ brochures, specifications, and handbooks, as well as a similar array of trade magazines and military reports, can provide modern helicopter weights, performance, and configuration data relative to Fig. 2-23. Fortunately, these sources have become relatively consistent in using terms such as takeoff gross weight, useful load, and empty weight (or weight empty as used by the U.S. military). Unfortunately, the actual components and equipment that are included within the weight terms of Fig. 2-23 are far from consistent.

You might think that design weight enjoys special attention because of its placement in the top box on Fig. 2-23. In practice, this is generally not the case. A design weight is frequently first established as a configuration emerges from conceptual and preliminary design. Its specific weight value is influenced not only by customer needs but by engineering facts and regulatory requirements. In some cases, upper management may simply legislate a design weight value and even associate a “design-to-cost” or selling price for the product as well. From an engineering point of view, the design weight is a needed reference “number” by many individual contributors as the detail design progresses.

The design weight will generally be the highest reference weight during preliminary and detail design. It does not stand alone however. Associated with the design weight are a minimum of two limit load factors as suggested by Fig. 2-23. Positive and negative load factors on the order of +3.0 g and –0.5 g have been common practice in the rotorcraft industry for some time. These load factors and design weight combine to give one set of primary design loads. To understand this point a little better, consider a simple example.

## 2.2 WEIGHT

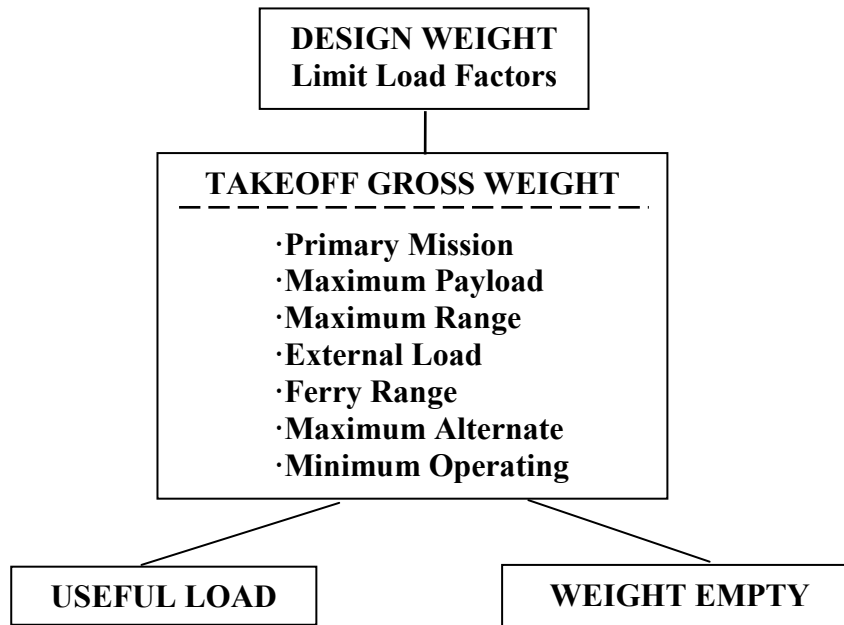


**Fig. 2-23. Takeoff gross weight is the sum of weight empty and useful load.**

The Bell Helicopter XH-40, the beginning of the Huey series, had a design gross weight of 5,400 pounds with limit flight load factors of +3.0 g and -0.5 g. This implies that a steep bank, sharp pull-up, or other maneuver will increase the rotor thrust from about 5,400 pounds to somewhat over 16,200 pounds. A primary component such as the main rotor shaft would have to be designed for the 16,200-pound tensile load. (The rotor shaft would also have to be strong enough for a negative or compressive load of -2,700 pounds.) Thus, a primary load for many components could be defined as

$$\begin{aligned} \text{Design Load} &= \text{Design Weight} \times \text{Limit Load Factor} \\ (2.24) \quad &= 5,400 \text{ lbs} \times 3.0 \text{ g for Bell XH-40 rotor shaft} \\ &= +16,200 \text{ lbs} \end{aligned}$$

Of course the complete set of design loads for all components does not remain constant as the rotorcraft completes the several design phases. In fact, it is not until the rotorcraft has completed its comprehensive military qualification or civil certification that the multitude of design loads settle down.

The takeoff gross weight depends on the design loads. It may surprise you to learn that the takeoff gross weight can frequently exceed the design weight. Fig. 2-23 suggests this by listing a number of different military missions or civilian applications. The reason for this apparent inconsistency is that a restricted flight load factor can be defined for the pilot in his flight manual so that the design load is not exceeded. In an engineering sense then, the definition of takeoff gross weight that I prefer is

$$(2.25) \quad \text{Takeoff Gross Weight} = \frac{\text{Primary Design Load}}{\text{Allowable or Restricted Load Factor}} \\ = \frac{\text{Design Weight} \times \text{Design Limit Load Factor}}{\text{Allowable Load Factor}}$$

An example of Eq. (2.25) at work can be found in any experimental flight test program. For instance, during flight testing of the XH-40 [115], the experimental helicopter was flown at takeoff gross weights as high as 5,720 pounds. This was 320 pounds greater than its design weight of 5,400 pounds. Care was taken, therefore, to not maneuver the helicopter up to the +3.0 g limit. Rather, the pilot restricted maneuvers to below +2.83 g as determined by

$$5,720 = \frac{5,400 \times 3.0}{2.83}.$$

The testing of the experimental XH-40 at flight weights higher than design weight followed a classical process of envelope expansion. In this case, the XH-40 became the H-40 and was the first production helicopter in the Huey series.<sup>27</sup> The design weight of the H-40 or HU-1A was increased to 5,725 pounds. Testing [116] was conducted with flight weights as high as 6,400 pounds. Again, care was taken not to exceed reduced maneuvering load factors so that primary design loads (i.e., maximum rotor-shaft tensile load) would not be violated.

By late 1964 the XH-40 had progressed through the UH-1A and reached the UH-1D model stage. The design weight was then 6,600 pounds while the positive limit load factor had been maintained at +3.0 g. The negative load factor had gone from -0.5 g to +0.5 g.<sup>28</sup> An ultimate load factor of +4.5 g had been introduced.<sup>29</sup> To accomplish these successive growth steps, the rotor blade chord was increased from 15 inches to 21 inches. The preproduction model of the UH-1D, the YUH-1D, was tested [133] at flight weights as high as 8,800 pounds. During testing at flight weight above the design weight of 6,600 pounds, the limit load factor was restricted to +2.2 g. The pilot was careful to fly the helicopter more gently in maneuvers.

Perhaps a pattern is now becoming clear to you. Modern helicopters, and most aircraft for that matter, are designed for loads well in excess of those that come with just straight and level flying. Flight can be attempted, and has been accomplished, at well beyond the design weight with almost all helicopters. Because all components have been designed including

---

<sup>27</sup> The U.S. Army designated this model as the HU-1 and later reversed the helicopter (H) and utility (U) nomenclature while adding a reference letter (A) to indicated that this would be the "A" model. This created the UH-1A designation.

<sup>28</sup> The ability of the teetering rotor system, regardless of the number of blades, to safely perform negative g maneuvers that come with, say, an aggressive push-over, began to be questioned. The flapping motion could become erratic and cause the hub to hit the rotor mast. This motion could cause extremely high loads and potentially severe damage to flight-critical components. Later, Bell two-bladed, teetering rotor systems incorporated modifications to reduce this problem.

<sup>29</sup> You may recall that a part that is loaded up to its limit load can be unloaded, and little or no damage to the part will have occurred. A part loaded to its ultimate load is expected to break.

## 2.2 WEIGHT

limit load factors, there is a “factor of safety” inherent in the reference number associated with the design weight.

There are, as you might now also suspect, many other safety factors that come into play for each individual part that is designed and built. Thus, the weight of any given part, and its cost, is very influenced by its detail design loads. When the helicopter is flown, the measured loads for a multitude of flight conditions can frequently show that the established design loads were too high. Of course flight test measurements can, and often do, show that the part is under designed. Rather than restrict the flight envelope of the helicopter, the under-designed part is generally redesigned. On the other hand, it is quite rare that an over-designed part will be resized to a lighter version. This is because “re-qualification of the part is more expensive than living with what we have” as upper management often says.

With the framework of Fig. 2-23 and the introduction to design weight, limit load factors, and design loads in hand, let me proceed to discuss takeoff gross weight.

The helicopter is the most utilitarian aircraft mankind currently has flying. Several roles or missions that can lead to a variety of takeoff gross weights are listed below the dashed line in the box in Fig. 2-23 to reflect this inherent, utilitarian characteristic. The highest takeoff gross weight likely occurs with a ferry range mission or a job where an external load is carried at the end of a sling. At the other end of the spectrum lies the minimum operating takeoff gross weight. This weight would only include a pilot, virtually no fuel and, of course, zero payload.

The takeoff gross weight for the overwhelming majority of helicopters introduced during the last 50 years is well below 50,000 pounds. However, this does not mean that there is an inherent limitation to helicopter size. These two points are emphasized in Fig. 2-24. The over 600 data points shown in Fig. 2-24 were collected over 45 years; they come from too many sources for me to reference. A reasonably representative summary starts with references [86-89, 94]. As you can see from Fig. 2-24, large helicopters capable of takeoff gross weights well above 50,000 pounds have already been built by the Mil and Kamov design bureaus in Russia. The Mil Mi-6 and Mi-10 are single rotor configurations with a main rotor diameter of just under 115 feet. The Mil Mi-12 was a side-by-side configuration that used components from the Mil Mi-6/-10. The Mi-12 had a cabin about 95 feet long and 14 feet wide, which is comparable to medium-sized commercial jet transports. The Mil Mi-26 is currently in service with Aeroflot and has a 70- to 100-passenger cabin. The Kamov Ka-22 was an experimental transport that could carry 100 passengers. The Ka-22 was a side-by-side “compound” helicopter having a fixed wing and two forward thrusting propellers, as well as two 65-foot, 7-inch-diameter main rotors. It set the rotorcraft world speed record in October of 1961 at 227 miles per hour or nearly 200 knots.

In the United States, the Boeing Helicopter Division had virtually completed, but not fully assembled, the YCH-62A, a tandem helicopter designed for external load, “sky crane” missions. The YCH-62A was to have a 148,000-pound takeoff gross weight and a rotor

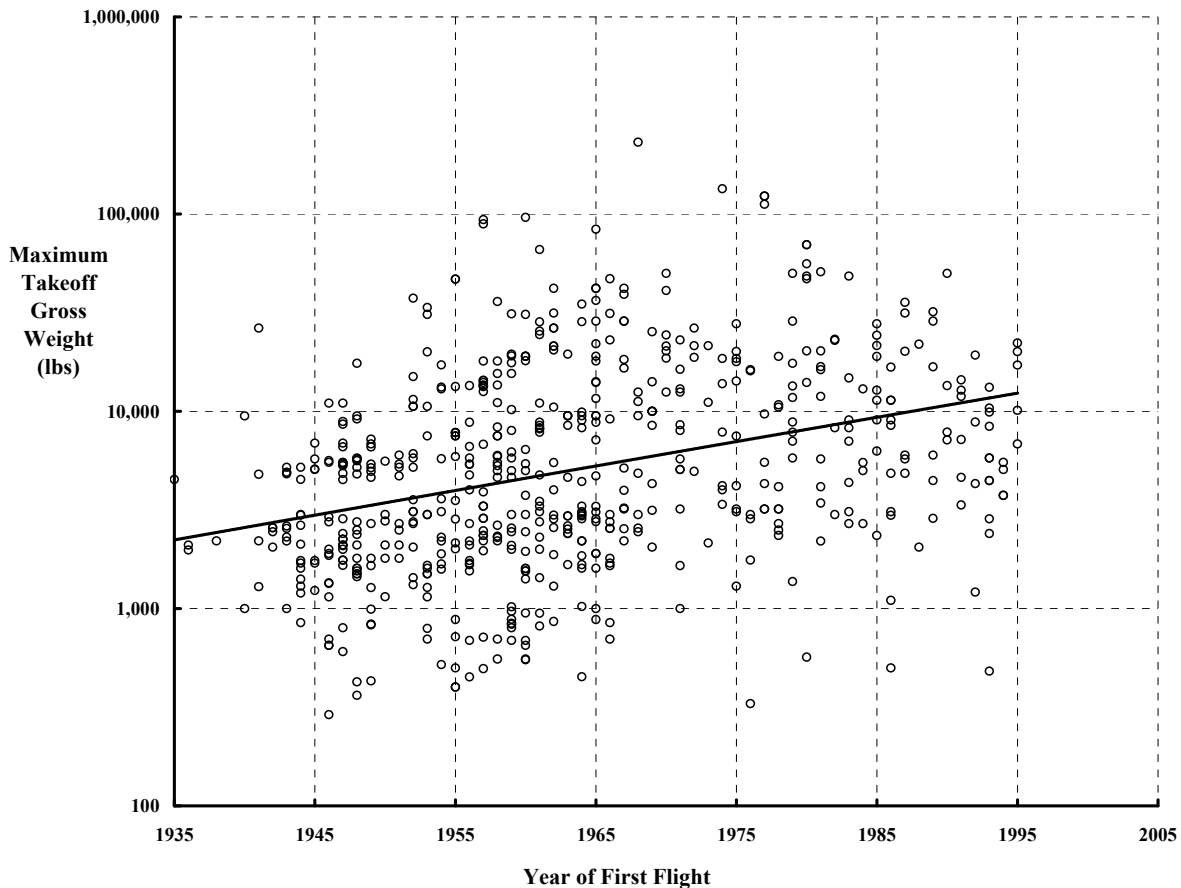


**Fig. 2-24. There is no inherent limitation to helicopter size.**

diameter of 92 feet. The Sikorsky CH-53E (at about 70,000-pounds takeoff gross weight) grew over 15 years from the lighter CH-53A model of just under 40,000-pounds takeoff gross weight when it went into service in 1965.<sup>30</sup>

Finally, you should be aware that Henrich Focke had a scaled-up version of his Fa-223 on the drawing board in 1941. This side-by-side helicopter, the Fa-284, was to have a takeoff gross weight of about 26,000 pounds. One can only marvel at the giant strides Focke was taking after his F. 61 demonstrated a path to true rotary wing flight.

The historical trend of takeoff gross weights shown in Fig. 2-24 immediately raises a question. Just how well has the rotorcraft industry done in producing helicopters that do useful work? To explore one facet of this question requires definitions of useful load and empty weight.

<sup>30</sup> The rotorcraft industry has excelled in growing the capability of an initial product. The CH-53 series is just one outstanding example. Another is the Boeing CH-47 series. This heavy-lift, tandem rotor, cargo helicopter began as the YHC-1B with a gross weight of 25,000 pounds in 1959. This preproduction helicopter grew slightly and entered service in 1962 as the CH-47A at 33,000 pounds. By 1985, the CH-47D had arrived and was capable of taking off at 50,000 pounds.

## 2.2 WEIGHT

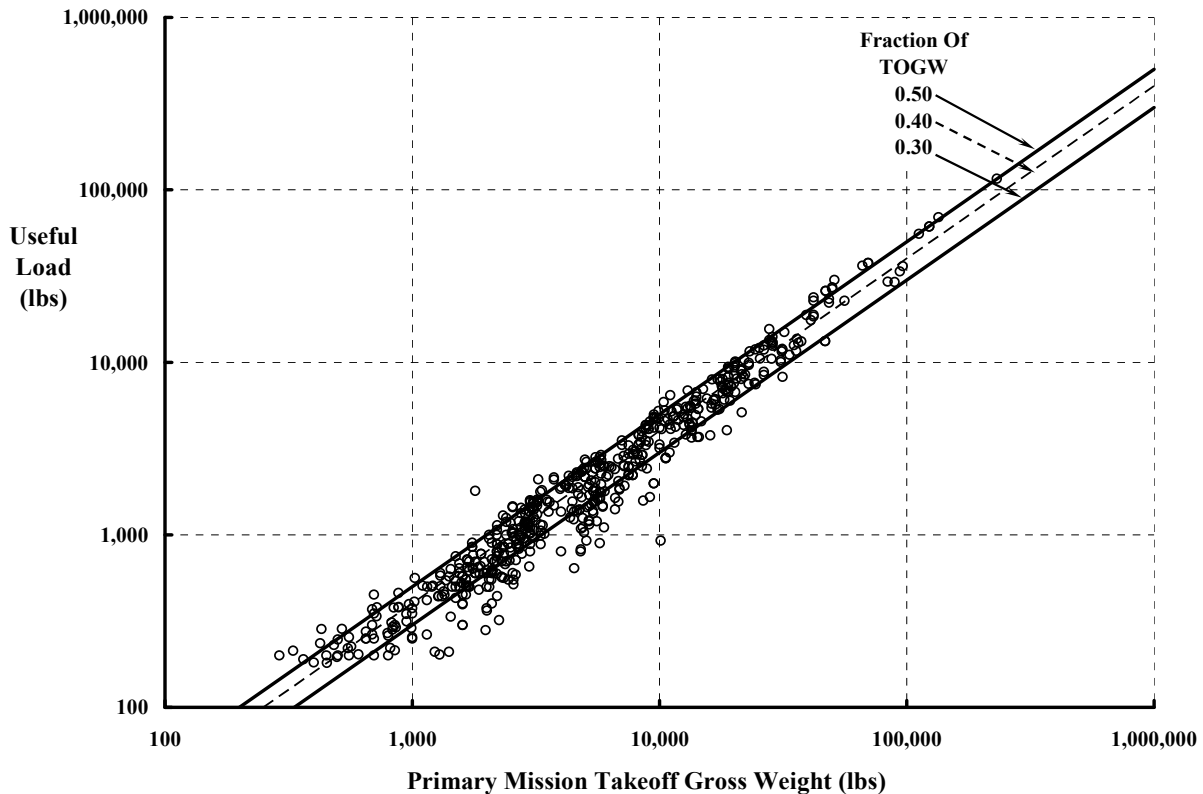


**Fig. 2-25. On average, the rotorcraft industry can obtain 40 percent useful load from takeoff gross weight.**

Consider the following definitions for weight empty and useful load. These categories, shown in boxes on Fig. 2-23, break down takeoff gross weight into two main elements. An introductory definition of weight empty is that (1) it accounts for all components that are not intended to be removed from the helicopter, and (2) *it does not account* for items loaded and/or unloaded (nor for materials that are consumed) during a flight. It follows then that useful load includes whatever is not in weight empty.

These rudimentary definitions of takeoff gross weight and its two subgroups are sufficient, for the moment, to understand the data presented in Fig. 2-25. This trend of useful load as a function of takeoff gross weight shows how well the rotorcraft industry has done over the last 50 years.

The takeoff gross weight I have chosen as the abscissa in Fig. 2-25 is for the primary mission.<sup>31</sup> However, it is by no means a certainty that the values I used are truly correct for anything more than a majority of the helicopters. Still, the message is clear. The industry is

<sup>31</sup> As I suggested earlier, the takeoff gross weight can vary considerably for any given helicopter depending on the allowable load factors given in the pilot's flight handbook. However, the empty weight does not vary appreciably for obvious, practical reasons. Therefore, there can be a variety of useful loads quoted for a given helicopter. Many sources are inconsistent in their tabulated weight data and few rarely define associated load factors.

capable, on average, of producing helicopters that give about 40 percent of takeoff gross weight to useful load.

Historically, there appears to be an upper bound to the percentage of takeoff gross weight available for useful load. For helicopters with a shaft-driven rotor system, Fig. 2-25 suggests a value of approximately 50 percent. You may be aware that there have been a few small helicopters built that had rotor-blade-tip jet propulsion. This class has yielded a useful load percentage well above the 50 percent level. Unfortunately, fuel consumption has been so high for non-shaft-driven rotor systems that little useful load has been left over for more than the pilot.

The list of items that might be included in useful load is really not too long. The reference for the most authoritative list today (at least for U.S. helicopters) would be Military Standard (MIL-STD) 1374A. This guiding document [134] provides a one-sheet format to itemize no more than 54 lines of weight and other information. The MIL-STD set of forms is used in conjunction with a set of weight definitions given in MIL-W-25140 [135]. In Table 2-2, I have taken some poetic license to show the most common items MIL-STD-1374A and MIL-W-25140 suggest be included in useful load.

**Table 2-2. Useful Load as Suggested by MIL-STD-1374A**

Load Condition				
Crew (no.)				
Passengers (no.)				
Fuel				
Unusable				
Internal (type/gals.)				
External (type/gals.)				
Oil				
Trapped				
Engine				
Auxiliary Fuel Tanks				
Baggage				
Cargo				
Internal				
External				
Gun Installations				
Guns				
Ammo				
Weapons Installed				
Fixed Devices				
Expendables				
Other Equipment				
Survival Kits				
Armor (removable)				
Etc.				
Total Useful Load				
Weight Empty				
Gross Weight				

## 2.2 WEIGHT

You can see from Table 2-2 that the useful load definition always starts with a load condition. After that comes the item and some room to add information about the item. All this goes in the first column. The following columns are used to fill in the weight for any other defined load condition. Generally, the first load condition is associated with the primary mission. The last three lines are used to total the useful load from the lines above, record the weight empty as enumerated on other sheets, and then add the two together to get the takeoff gross weight.

The discussion so far has given you a framework, some terminology, and two general trends to introduce you to the world of helicopter weight. Unfortunately, I may have left you with a somewhat misleading impression that is suggested by Fig. 2-25. There is, in fact, a widely held perception that a high ratio of useful load to gross weight or, alternately, a low ratio of weight empty to gross weight is a measure of “goodness.” However, as you will see, these ratios have varied considerably, both upwards and downwards, over the last several decades of modern helicopter development. What has happened is that more and more useful features and equipment have been added to the helicopter over this period. This has been made possible because of the gas turbine engine, improvements in materials, and innovative structural design that has reduced the weight of mandatory components needed to just fly. Therefore, to qualify this impression I may have given you, consider the evolution of light rotorcraft used by the U.S. Army for observation and scouting.

You will recall that the predecessor to the U.S. Army Air Corps, the Air Service of World War I, funded George DeBothezat’s development of a quadrotor in June of 1921. By May of 1923, despite having demonstrated a “flyable machine,” the results were less than encouraging, and DeBothezat left McCook Field with apparently poor feelings on both sides. Army interest in rotorcraft was not revived until the autogyro burst on the scene, although it did not perform well in the Army’s observation and scouting missions. The transition from autogyros to helicopters began in the early 1940s when Haviland Platt and Lawrence Le Page convinced the Air Corps to fund development of their version of Henrich Focke’s F. 61. Ultimately, the transition pitted the older Kellett YG-1B and newer YO-60 autogyros (and corresponding Pitcairn autogyro models) against the Platt–Le Page XR-1 side-by-side helicopter and the Sikorsky XR-4 single-main-rotor helicopter. The Sikorsky XR-4 ultimately won the Army’s confidence when it was accepted by Colonel H. Franklin Gregory on May 12, 1942.

One interesting aspect of this early period was the evolving definition of the military helicopter’s tactical mission and the meaning of the words “light observation/scout helicopter.”<sup>32</sup> The February 1941 specification for the Kellett XR-2/XR-3 autogyro [136, 137] (the prototype of the Kellett XO-60/YO-60) contains a paragraph that states:

---

<sup>32</sup> I am deeply indebted to Bernie Lindenbaum for copies of the autogyro and helicopter specifications [136-144]. These documents provided much more accurate technical insight into our rotorcraft history. Bernie was one of the earliest members of the American Helicopter Society. He was also the staunchest supporter of VTOL within the U.S. Air Force.

“B-4.0. The tactical mission of this [autogyro] aircraft is for experimentation and investigation into new and novel features which will improve the performance of this type of aircraft, and will increase its value as a reconnaissance and observation type of craft for work with ground troops.”

Similarly, the specification for the Sikorsky XR-4 dated January 1, 1942, [138] also has a paragraph B-4.0 that reads (with my italics):

“B-4.0. *The tactical mission of this [helicopter] aircraft is as yet undetermined*, due to its completely novel characteristics. It is presumed, however, to have excellent values in observation, liaison, communication, reconnaissance, gun-fire control, convoy and defense of ground objects, smoke screen, tree transport, life-saving, short-range light bombing and attack.”

Even in the May 4, 1942, specification for the YR-4A/YR-4B [139], the October 20, 1942, specification for the Sikorsky XR-6 [140], and still in the March 1945 specifications for the Sikorsky R-4A/-4B [141] (the very much improved production version of the preproduction YR-4A/-4B, which grew from the XR-4) there is still a note of skepticism. Paragraph B-4.0 reads:

“B-4.0. The tactical mission of this [helicopter] aircraft shall be short range liaison, observation, performance of courier mission, adjustment of artillery fire and general cooperation with the ground forces, and for general investigation of utilities of this type of *completely new and novel aircraft*.”

When the specification for the Sikorsky XR-5 [142] was submitted (dated June 1, 1942) and followed with the production for the R-5A [143] dated February 1, 1944, things were sounding more positive because the word “completely” had been dropped. Paragraph B-4.0 reads:

“B-4.0. The tactical mission of this aircraft shall be observation liaison, general cooperation with the various Ground Arms assisting the Artillery by locating suitable objectives and adjusting fire and for general investigation of the utility of this type of *new and novel type of aircraft*.”

The B-4.0 paragraph included with the January 17, 1944, specification for the Platt–Le Page YR-1A [144] was much more encouraging. It reads as follows:

“B-4.0. The tactical mission of this helicopter includes reconnaissance missions for surface forces for the purpose of observing and reporting on the disposition and activities of hostile ground, air and naval forces. In addition, it assists the artillery by locating suitable objectives and adjusting fire, and is a liaison agency for the use of ground commanders. It is also capable of operating off the decks of freighters, etc., to serve in convoy duty as an aerial spotter of enemy submarines and raiders.”

At least in this specification the word “aircraft” had been replaced with “helicopter” and words like “completely new and novel” had been deleted. You get the feeling that perhaps the new U.S. Army Air Forces felt that a helicopter rather than an autogyro was the “machine” to fill their requirement.

## 2.2 WEIGHT

This specific example you are reading about does not stop here, of course. Sikorsky quickly followed the R-4 series with a much improved derivative, the R-6. These rotorcraft, along with the R-5,<sup>33</sup> comprised the Army Air Corps helicopter fleet until the late 1940s. During the next decade, which included the Korean War, the Army replaced its first-generation Sikorsky helicopters with militarized Bell Model 47s (the H-13 series) and Hiller Model 360s (the H-23 series). The 1960s produced the Vietnam War, and the Army moved to gas-turbine-powered helicopters (see footnote 24, page 78). You will recall that the Army conducted a “fly off” competition between the Bell OH-4A, Hiller OH-5A, and Hughes OH-6A. The Hughes OH-6A and, later, the Bell OH-58A were chosen for this modernization step. In the late 1970s, after a modest upgrade that produced the OH-58C, the Army initiated a further helicopter improvement program leading to the Bell OH-58D, which entered operational service in the mid-1980s.

These five generations of early rotorcraft performed basically the same primary tactical mission for the Army that was defined in the midst of World War II.<sup>34</sup> This role was, and continues to be, a scouting mission that calls for aerial observation. As the helicopter proved itself and the turbine engine improved the product, mini guns were added for some missions. Aeroscouts could then locate *and* suppress enemy forces. The added feature of the 1960’s OH-6As and OH-58As was a passenger compartment that could hold two to four soldiers. The 1980’s OH-58D introduced a very sophisticated mission equipment package (MEP) to replace the voice radio, maps, and binoculars that earlier scout crews used [145, 146].

These five generations of rotorcraft are quite comparable and serve as a specific measure of progress over nearly 50 years, at least within this narrow size and aeroscouting category. The five decades of progress is summarized in Table 2-3. The primary scouting mission outlined in Table 2-3 is for aerial reconnaissance with an endurance on the order of 2.5 to 3 hours.

The historical data provided in Table 2-3 is not quite as informative as you might think, however. For one thing, it is not clear what the trend in useful load as a percent of primary-mission takeoff gross weight means. This trend, shown in Fig. 2-26, does suggest that in the early helicopter years the ratio was “improving,” but then, in the modernization, the industry produced a less efficient product!

---

<sup>33</sup> Almost in parallel with the R-4 and R-6 light helicopters, Sikorsky developed the larger R-5 that grew into his first commercial product, the S-51.

<sup>34</sup> During World War II, about 5,700 L-4 Piper Cub airplanes were bought for the scouting mission. The L-4 scout crew consisted of a pilot and observer, and their MEP consisted of voice radio, maps, and binoculars. The use of airplanes was a marked success. Counting the L-4s, L-5s, L-16s, and L-19s, the Army used a total of about 10,800 light airplanes before turning to the helicopter. About 100 early models of the H-13 were on hand when the Korean War began, and nearly 1,000 were produced during the war years (1950–1953). Another 600 H-13s were produced for operational use through 1965. Additional requirements for 400 TH-13 trainers continued production through 1970. Nearly 400 Hiller H-23s were produced during the Korean War with another 400 bought in the period from 1954 through 1958. During the nearly 7 years between September 1966 and July 1973 the Army received a total of 3,600 Light Observation Helicopters. About 1,400 were OH-6As and 2,200 were OH-58As. The seeds of true aeroscouting were sown by these early helicopters even though the crews had minimal mission equipment. The OH-58D updated the MEP.

One fact suggested by both Table 2-3 and Fig. 2-26 is that, for its engine power, the Hughes OH-6A was one of the most (if not *the* most) structurally efficient rotorcraft ever produced in quantity.

This specific example should now have you alert to the possibility that the ratio of useful load to takeoff gross weight is not necessarily a measure of “goodness” or industry success. In many cases, such as special purpose helicopters used by the military, the ratio is quite misleading.

The real insight into the world of rotorcraft weights comes from a careful and thorough review of empty weight.<sup>35</sup> The majority of the industry’s progress can best be seen by comparing the detailed group weight-empty statements available in MIL-STD-1374A format. In Part I, this MIL-STD provides a summary of the weight empty in several groups. This portion of the MIL-STD is rarely more than three pages long. A detailed accounting supporting the Part I summary is provided in a longer Part II.

Weight empty by groups can be broken down into three subheadings as shown in Fig. 2-27. Again, I have taken some liberty in rearranging the format of MIL-STD-1374A, Part I. In this case I have chosen the three subheadings so that weight empty is partitioned into approximately three equal groups by weight. The first subheading of Structural Groups gathers up 7 MIL-STD subgroups. The second subheading contains just the single Propulsion Group with its 11 subsystems and/or installations. The third subheading accounts for the remaining 12 other groups listed by MIL-STD-1374A, Part I. In practice, even the summary weight-empty statement required by the MIL-STD is going to be several pages long. This is

**Table 2-3. Evolution of U.S. Army Scout Rotorcraft**

<b>Model</b>	<b>YG-1B</b>	<b>YO-60</b>	<b>R-4B</b>	<b>R-6</b>	<b>OH-13S</b>	<b>OH-23G</b>	<b>OH-6A</b>	<b>OH-58C</b>	<b>OH-58D</b>
Crew (no. 2)	400	400	400	400	400	400	400	400	470
Passengers	0	0	0	0	0	0	0	0	0
Fuel	188	216	86	127	257	284	402	466	654
Oil	25	34	31	53	32	29	7	16	18
Cargo	0	0	0	0	220	0	139	178	0
Weapons Install.	0	0	0	0	0	0	0	0	114
Other Equip.	0	0	0	8	0	0	0	0	4
Useful Load	613	650	517	588	909	713	948	1060	1260
Weight Empty	1619	2180	2020	2034	1941	1914	1212	1885	3093
Gross Weight	2232	2830	2537	2622	2850	2627	2160	2945	4353

<sup>35</sup> Most authors, when discussing rotorcraft weight information and data, are very careful to point out that they have misgivings about the numbers they are quoting. The reasons for the misgivings are really too numerous to list. I have the most faith in data from helicopters that I was directly involved with. After that, I consider contractual data provided in U.S. Military documents as most authoritative. This restriction means that less than 100 helicopters, out of over 500 rotorcraft that can be identified, are well documented. And after that, weight data does become quite “iffy” in my mind; I then share the misgivings of all authors who have the courage to tackle the subject in some depth.

## 2.2 WEIGHT

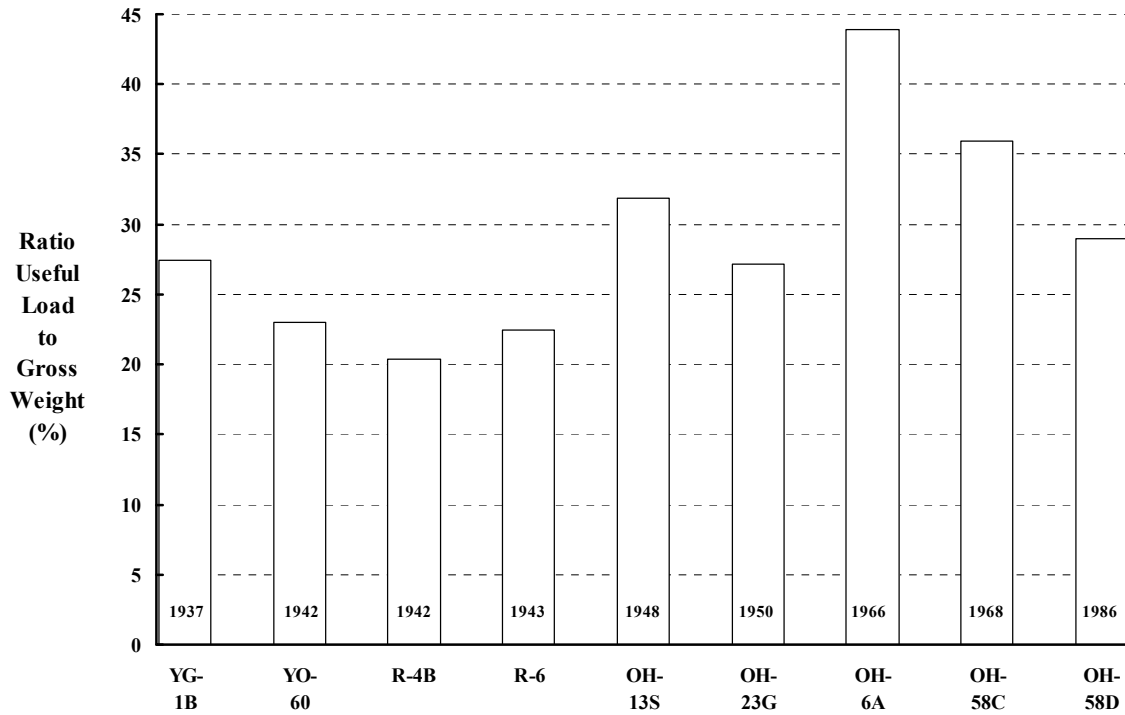


**Fig. 2-26. The ratio of useful load to takeoff gross weight is not necessarily a measure of “goodness.”**

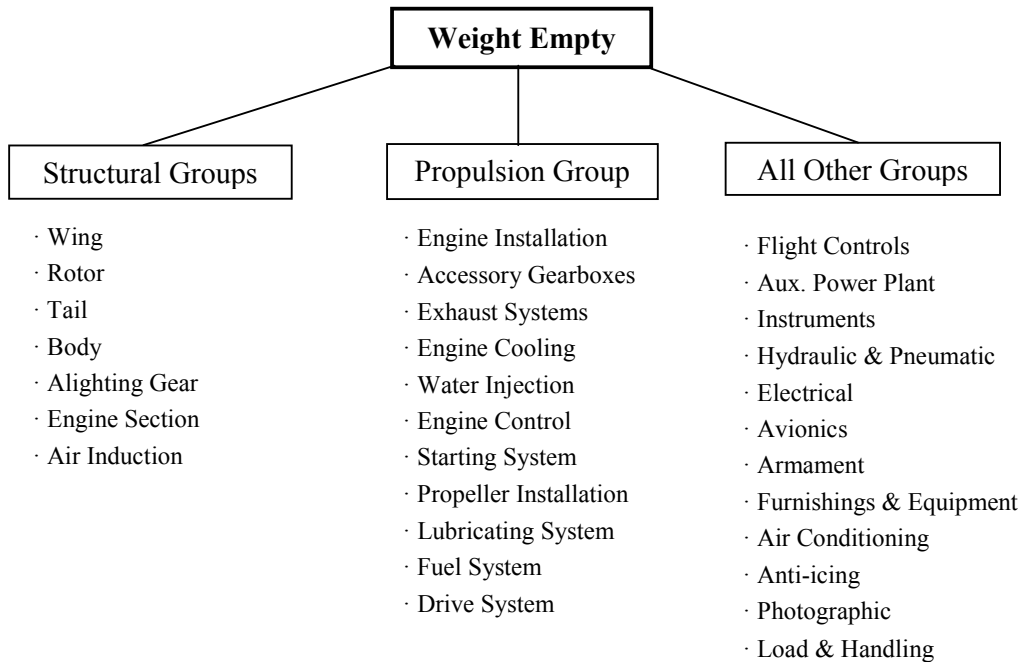


**Fig. 2-27. The summary weight-empty statement in U.S. MIL-STD-1374A, Part I format, starts with 30 line items.**

because most of the 30 major line items shown in Fig. 2-27 have from two to five subitems—and that is just for the Part I summary. A complete report satisfying MIL-STD-1374A requirements for a modern military rotorcraft will include the detailed weight statement in Part II. The Part II section of MIL-STD-1374A can be several hundred pages long.

This specific example of U.S. Army aeroscout evolution from the autogyro to the most modern scout helicopter can now be continued in more depth using data from the Military Standards. Consider a first step that takes you to the subheading level of Fig. 2-27. A summary of this historical data is shown in Table 2-4. Additional dimensional data is provided in Table 2-5.

As you review these two data tables, you may first notice that the OH-6A has the lowest Structural Groups and Propulsion Group weights. The OH-6A is also the smallest of the nine rotorcraft under study. Secondly, you should note that the OH-58D doubled the engine rated horsepower, and its weight for the All Other Groups is many times that of any of the other rotorcraft.

Now let me use the data from these tables to illustrate several modern results that the rotorcraft industry has achieved. The first and clearest point is the effect that the arrival of the turbine engine had on Propulsion Group weight. As shown in Fig. 2-28, the reduction in Propulsion Group weight from about 2.8 to nearly 1.1 pounds per horsepower is dramatic. This was probably a bigger step forward for the rotary wing industry than for the fixed-wing industry.

An equally interesting fact is that the piston-powered autogyros and helicopters needed about the same Propulsion Group weight. The reason for this is that autogyros used a heavy, metal propeller but had no main-rotor drive system to speak of. For example, the YG-1B propeller installation weighed about 80 pounds, and the YO-60 propeller installation was just over 110 pounds. These propeller installation weights are quite comparable to the early helicopter's main rotor transmission weight for the same engine power rating.

**Table 2-4. Evolution of U.S. Army Scout Rotorcraft**

<b>Model</b>	<b>Structural Groups</b>	<b>Propulsion Group</b>	<b>All Other Groups</b>	<b>Weight Empty</b>	<b>Useful Load</b>	<b>Gross Weight</b>
YG-1B	756	654	209	1619	613	2232
YO-60	944	905	331	2180	650	2830
R-4B	900	970	200	2019	517	2537
R-6	966	769	299	2034	588	2622
OH-13S	630	795	515	1940	910	2850
OH-23G	769	765	380	1914	713	2627
OH-6A	529	327	357	1212	948	2160
OH-58C	725	382	431	1885	1060	2945
OH-58D	1020	714	1359	3093	1260	4353

## 2.2 WEIGHT

A final point is illustrated in Fig. 2-29. Historical data shows that the rotorcraft industry has successfully reduced the weight of drive-system components accounted for in the Propulsion Group. Thus, the use of the gas turbine engine *plus* the reduction in drive-system weight accomplished over five decades was a major step in arriving at the modern helicopter.

**Table 2-5. U.S. Army Scout Rotorcraft Dimensions**

Model	Engine Type	Engine Model	Rated Power (hp)	Rotor Dia (ft)	Fuselage Length (ft)	Gross Weight (lb)
YG-1B	Piston	Jacobs R-755-A3	245	40.00	26.00	2,232
YO-60	Piston	Jacobs R-915-A1	325	42.00	21.42	2,830
R-4B	Piston	Warner R-550-3	200	38.00	35.50	2,537
R-6	Piston	Franklin O-405-9	235	38.00	34.60	2,622
OH-13S	Piston	Lycoming VO-435	260	37.17	32.67	2,850
OH-23G	Piston	Lycoming VO-540	305	35.42	27.67	2,627
OH-6A	Turbine	Allison T63-A-5A	317	26.33	22.79	2,160
OH-58C	Turbine	Allison 250-C20	400	33.33	29.60	2,945
OH-58D	Turbine	Allison T703-AD	650	35.00	30.20	4,353

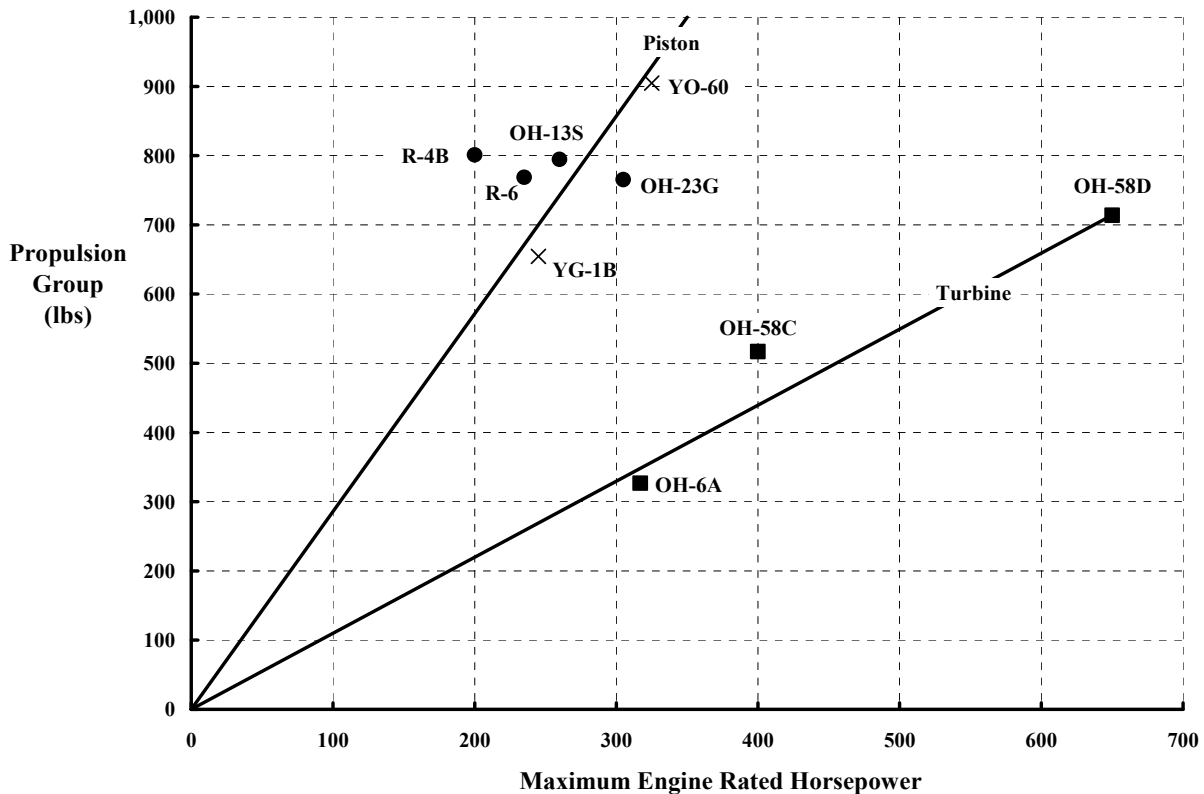


**Fig. 2-28. Turbine engines helped cut Propulsion Group weight by nearly 60 percent.**

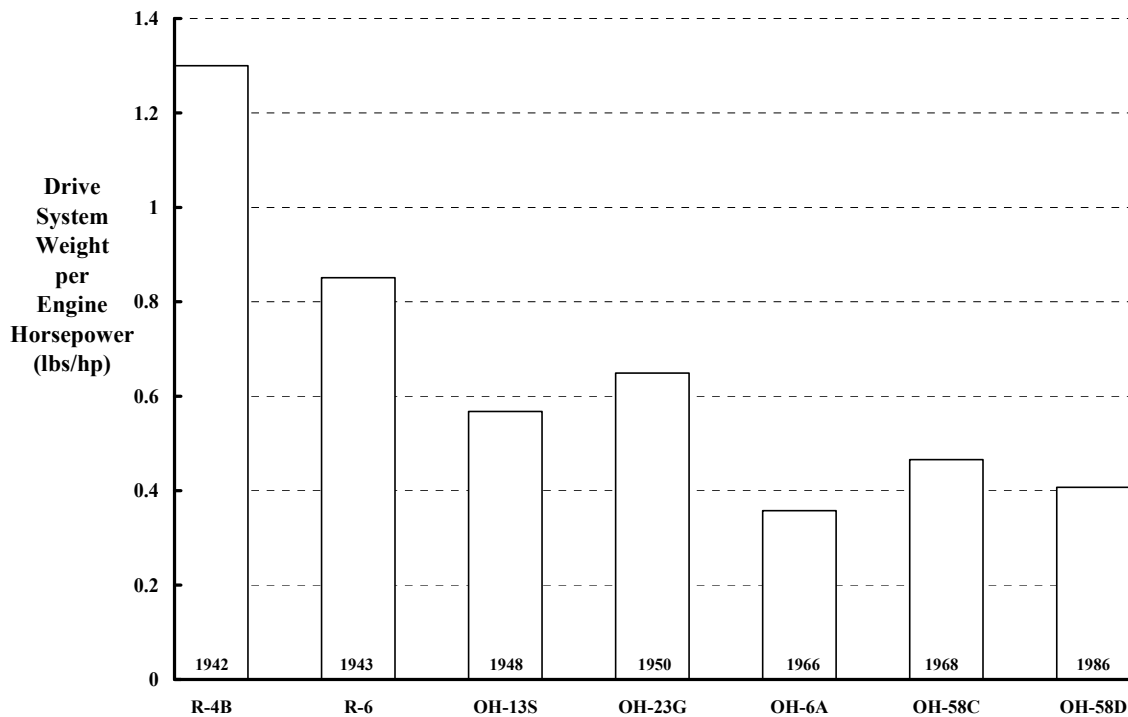


**Fig. 2-29. The reduction in helicopter drive-system weight over 50-plus years has been impressive.**

One industry accomplishment not captured by the drive-system weight data in Fig. 2-29 is the improvement in reliability and reduction in maintenance costs of this major system. The first step was made by Sikorsky in going from the R-4 series to the R-6 series. You can appreciate this dramatic first improvement when you read the last 60 pages of *Pioneering the Helicopter* [19] by Charles Morris. Morris first recounts the XR-4 flight from Bridgeport, Connecticut, to Dayton, Ohio, and delivery of the first, truly successful, single rotor helicopter to the U.S. Army Air Corps on May 17, 1942. The 16-hour-and-10-minute flight, spread over 5 days, was performed with a continuous eye on the main transmission oil temperature gauge. The transmission, it seems, was continually on the verge of overheating. The demonstrations, given the day after arriving, were done with the Sikorsky team (particularly Ralph Alex) having “fingers crossed.” Three days later, a major overhaul of the XR-4 was completed; it showed that the main transmission had been slowly “chewing itself to pieces.” It was replaced, and Morris went on—with 100 more flight hours—to train five Air Force officers. The XR-4 successfully completed its Wright Field testing on January 5, 1943.

Drive system and other improvements came with the R-6. Morris notes [19] that the R-6 was “conceived as a cleaned-up version of the R-4 type, with a 250-horsepower Franklin engine supplying a good margin of power. As it took shape, however, the effort to save weight and to smooth out the box-like contours of her predecessor resulted in a brand new machine.” Morris took the XR-6 for its first flight on October 15, 1943. He credits several months of development work for the unofficial record, long-distance flight that Colonel Frank Gregory

## 2.2 WEIGHT

and Ralph Alex made on March 2, 1944.<sup>36</sup> On that day, Gregory and Alex [the “aeroscout crew”] flew nonstop from Washington, D. C., to Dayton, Ohio, (387 miles) in 4 hours and 55 minutes. Transmission overheating was not reported; the 260-pound, XR-4 drive system that handled an inadequate 185-horsepower engine was advanced to the lighter, R-6, 200-pound drive system that could absorb 250 horsepower.

The rotorcraft industry did not, and has not, stopped its drive-system development work. You only need to read about the OH-6A world record program [147] to appreciate a real success story. Using one preproduction YOH-6A helicopter, a Hughes Tool Company/Army team captured 23 world helicopter records between March 12 and April 7 of 1966. I believe the nonstop, long-distance record was a real milestone. Robert Ferry started with a normal hover liftoff on April 6 at 2:20 p.m. (PST) from Culver City, California. He landed, 2,277 statute miles away, on the sand at Ormond Beach, Florida, on April 7 at 8:28 a.m. (EST). The record was set at 2,213 miles in 15 hours and 8 minutes for an average speed of 150 miles per hour. At that time, the YOH-6A was FAA certified (for the U.S. Army Light Helicopter competition) at a takeoff weight of 2,100 pounds. On the record-breaking flight, Ferry lifted off at 3,235 pounds, which was more than three times the basic weight empty of the helicopter. About 1,860 pounds of JP-5 fuel, contained mostly in auxiliary fuel tanks placed in the passenger compartment, were onboard. Ferry used all but 10 pounds of this fuel. Thus, the average fuel consumption was on the order of 1-1/4 statute miles per pound of fuel or about 8.5 statute miles per gallon. And the transmission did not overheat.

Today the rotorcraft industry expects propulsion and drive-system components to run 2,000 trouble-free hours between overhauls. The time between overhaul (TBO) on most components of the Allison 250-series gas turbines is at least 1,500 hours. The more expensive parts are already at or above 3,500 hours between overhaul. The rest of the Propulsion Group systems have TBOs well above 2,000 hours, and improvements are still being made. As you will see later in this introduction to weights, the industry has already demonstrated it can produce excellent propulsion systems with multi-engines totaling at least 25,000 horsepower.

Now let me proceed to the Structural Groups subheading in Fig. 2-27. The innovation in engineering design approaches, the advancements in materials, and the improvements in safety as well as many other factors come to the forefront here. However, they are so intertwined that it is more difficult to fully appreciate the progress of the rotorcraft industry in this area. But, for a starting point, consider Fig. 2-30. I have used primary mission takeoff gross weight as the abscissa on this figure. This is a direct, but rather crude, first approximation to a much more complex set of parameters.

---

<sup>36</sup> Colonel Gregory, in his book *Anything A Horse Can Do* [16], relates a number of improvements achieved with the R-6 including an early use of composites and successful sound proofing. He also discusses a rather typical array of development problems that were overcome.

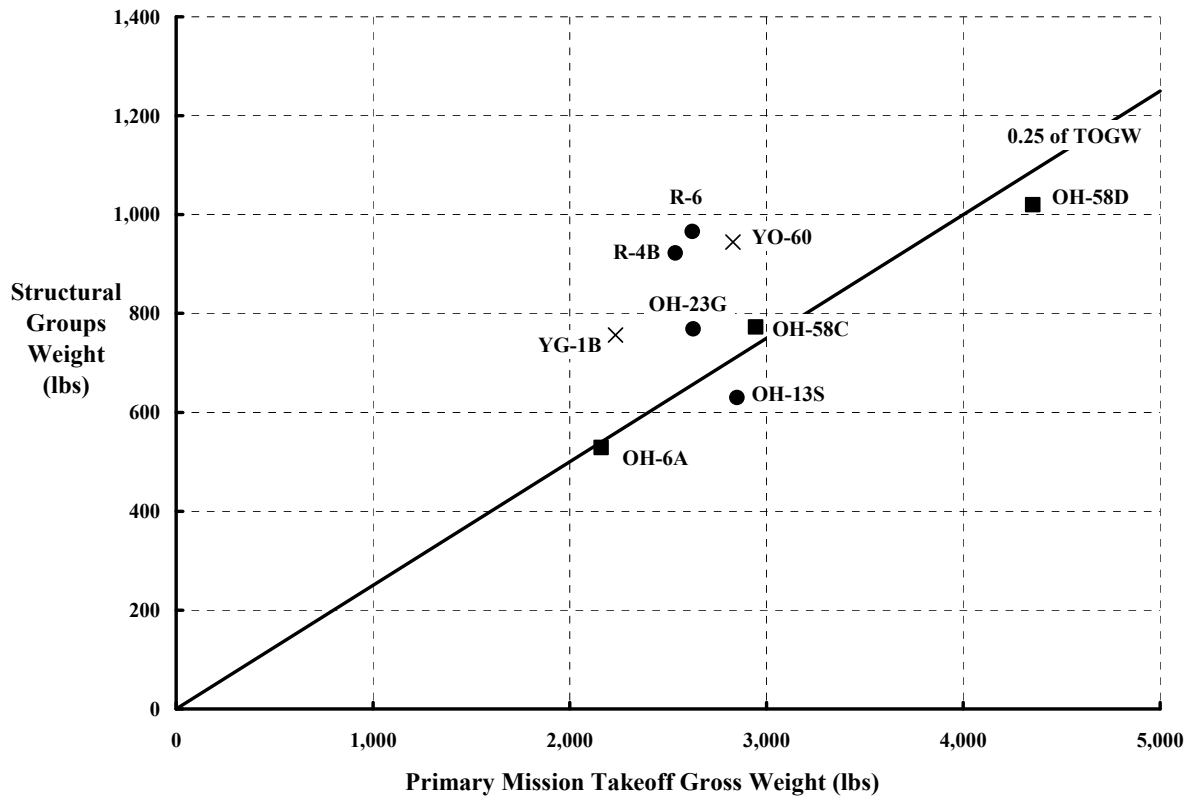


**Fig. 2-30. The Structural Groups amount to about 25 percent of primary mission takeoff gross weight.**

On the surface it would appear from Fig. 2-30 that little, if any, progress has been made by the rotorcraft industry over the past six decades. This, of course, is not the case. The industry has slowly but surely redistributed the structural weight between the six groups listed in Fig. 2-27. (I say six for this specific case because no wing group is involved with the scout rotorcraft under study here.) The magnitude of this redistribution is summarized in Fig. 2-31.

The improvements made to the body group have increased the crash worthiness of the basic structure, allowed for higher landing speeds without damage, increased visibility, provided more internal volume, and made getting in and out easier with additional, larger doors. These improvements were paid for by a somewhat reduced autorotational capability that came with less rotor inertia. The alighting gear weight reduction came by changing to a skid tube rather than the wheeled landing gear that autogyros and the first Sikorsky helicopters used.

Now let me discuss the All Other Groups weight-empty category that is shown in Fig. 2-27. It is here that lightweight, aeroscout helicopters have seen the most increase in usable features. In five decades, the percentage of weight empty devoted to All Other Groups has nearly tripled as Fig. 2-32 clearly shows.

## 2.2 WEIGHT

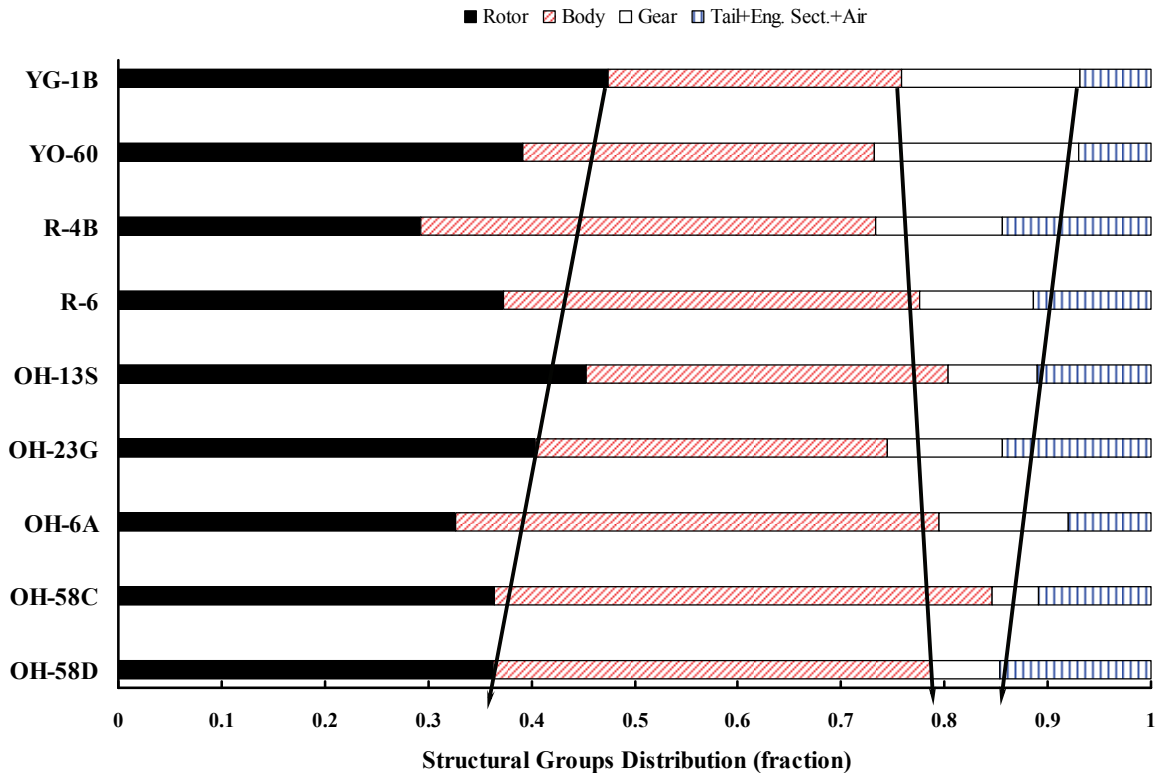


**Fig. 2-31. Over six decades, the industry has shifted weight from the rotor and alighting gear groups to improve the body group.**

The major elements of the All Other Groups for aeroscout rotorcraft are summarized in Fig. 2-33. The initial growth element was the addition of an hydraulic system that gave the scout crew “power steering.” This, in turn, allowed installation of an autopilot. The number and quality of flight instruments also grew over the decades. Some improvement in the furnishing and interior equipment, along with heating and cooling systems, was also forthcoming. (I would say that comfortable seats have yet to be installed though!) The major step forward in added features came from evolutions in the electronic world. These electronic items fall in the subheading of avionics as Fig. 2-27 shows.

The increase of avionics on the OH-58D was dramatic as references [145, 146] point out in considerable detail. These avionics gave the modern scout crew the most up-to-date “eyeballs” to replace their binoculars, an electronic navigation system to replace their paper maps, and the most all-encompassing communication system possible at the time. Finally, the OH-58D was equipped with a real, offensive, air-to-ground missile weapons system.<sup>37</sup>

<sup>37</sup> I was honored to receive the AHS 1986 Grover E. Bell Award for my “direction and leadership in the design and fielding of the United States Army Helicopter Improvement Program (OH-58D).” But, with no false modesty, I felt that it was one of the most splendid total team efforts the industry had seen for quite a while. It was for that team effort that I felt the award was appropriate, and I tried to say so in my acceptance remarks. I wrote the paper [145] to recognize the effort and spirit that went into the OH-58D program. My personal “high” came when I got to fly the OH-58D for an hour. A person is lucky to be a part of such an adventure even once in a lifetime.

Fig. 2-33 shows that the historically “normal trend” would have about doubled the All Other Groups’ weight by the time the OH-58D came along. Instead, the rotorcraft industry was able to incorporate electronic and computer technology as fast, and sometimes faster, than the fixed-wing industry.

By the 1980s, the light aeroscout helicopter was thought of more as a “mission platform.” This thinking carried forward to the Army’s development of its most modern, armed, aeroscout helicopter in the 1990s—the RAH-66 Comanche. Again, every improvement in avionics, flight control technology, and attack armament (including stealth shaping) was sought. You would be quite misled about the capabilities of the RAH-66 if you looked at it from only a historical weight trend view.

I have used the preceding material about aeroscout rotorcraft as a specific example to introduce you to the world of weights. However, in many ways the military light helicopter—and its larger, military, attack helicopter companion—do not represent the more commonly available utility and transport helicopters the industry offers. It is true that few modern helicopters have been developed solely to fulfill commercial marketplace needs. In fact, most commercial helicopters today are product derivatives using components developed for the military. With this thought in mind then, let me now broaden your view of modern helicopters to include a much wider range in takeoff gross weight and installed engine horsepower.

You have already seen from Fig. 2-24 that the overwhelming majority of modern helicopters fall well below a 50,000-pound takeoff gross weight. Fig. 2-25 showed you that, on average, the industry can obtain at least 40 percent useful load from takeoff gross weight. So now consider the distribution of weight empty between the three subheadings I selected in Fig. 2-27. As I mentioned in footnote 35, page 97, I prefer to illustrate modern weight results using data primarily from U.S. MIL-STD-1374A reports. This limits the number of post-1940 helicopters that can be studied. However, as Table 2-6 shows, the distribution of types is representative of the industry’s products.

**Table 2-6. A Sample of 92 Post-1940 Helicopters**

<b>Weight</b>	<b>Commercial and/or Military Use</b>	<b>Military Use Primarily</b>	
	<b>Passengers/Cargo</b>	<b>Scout</b>	<b>Attack</b>
Very Light	4 Pistons	None	None
Light	10 Pistons	8 Pistons	None
	11 Turbines	7 Turbines	
Medium	5 Pistons	None	7 Turbines
	26 Turbines		
Heavy	2 Pistons	None	None
	11 Turbines		
Very Heavy	3 Turbine	None	None

## 2.2 WEIGHT

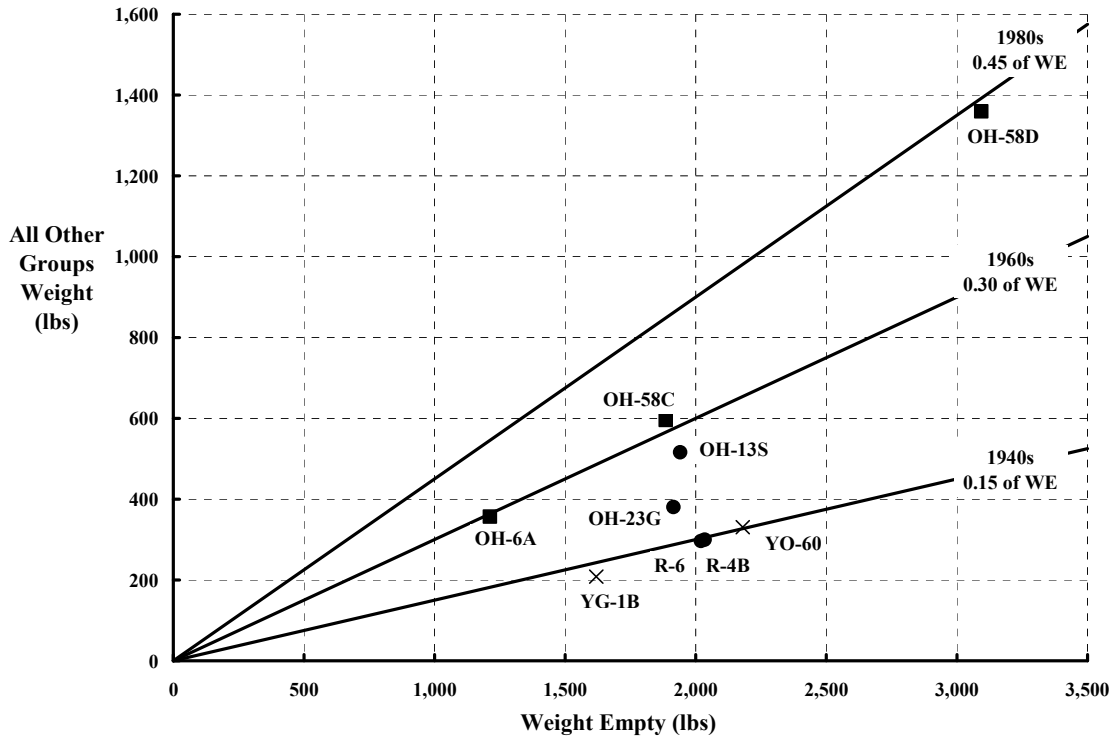


Fig. 2-32. The industry has increased the weight of All Other Groups to add aeroscout helicopter features.

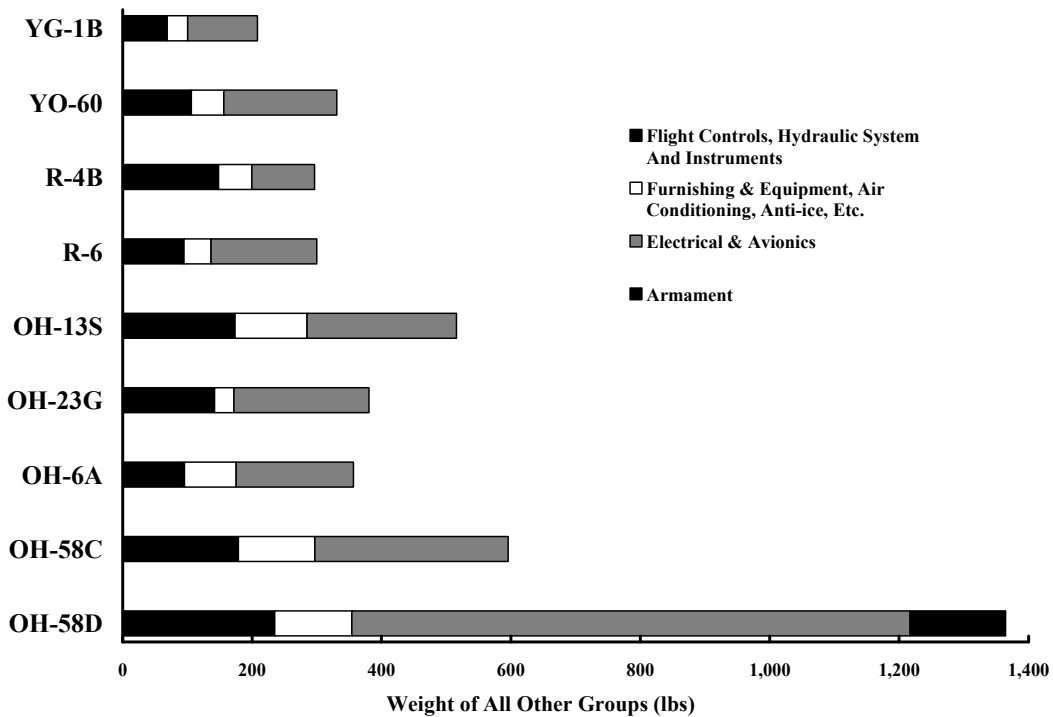


Fig. 2-33. The industry dramatically increased electrical and avionics features in the 1980's aeroscout helicopter.

Taken as a group, the 92 post-1940 (i.e., modern) helicopters show you that the rotorcraft industry has made considerable progress in maturing its current rotary wing products. The progress is most dramatic in the Propulsion Group as you learned from the specific aeroscout helicopters example. Fig. 2-34 emphasizes this view with a larger, more representative group of helicopters and uses a log-log axis system.

The reduction in Propulsion Group weight over five decades can be overstated somewhat (as I have in Fig. 2-34) by going from “top of scatter” of piston-powered, early helicopters to “bottom of scatter” for turbine-powered helicopters. The industry, on this overstated basis, has achieved a weight reduction on the order of 1.8/6.5 or nearly 75 percent. That is, Propulsion Group weight is approximated as

$$(2.26) \text{ Pistons at } 6.5 (\text{HP})^{0.9} \Rightarrow \text{Turbines at } 1.8 (\text{HP})^{0.9}.$$

Industry progress in reducing the Structural Groups portion of empty weight is appreciable when the broader range of helicopters from Table 2-6 is considered. This is confirmed in Fig. 2-35. Not only has the industry redistributed the several group weights within the Structural Groups, it has also succeeded in reducing weight. This weight reduction of about 30 percent has been accomplished with very innovative design and the application of advanced materials, and has not come at the expense of foregoing key features. Just the opposite trend has occurred. The industry has created a more crashworthy and reliable structure with modern interiors and improved accessibility.

$$(2.27) \text{ Pistons at } 0.36 (\text{TOGW}) \Rightarrow \text{Turbines at } 0.24 (\text{TOGW}).$$

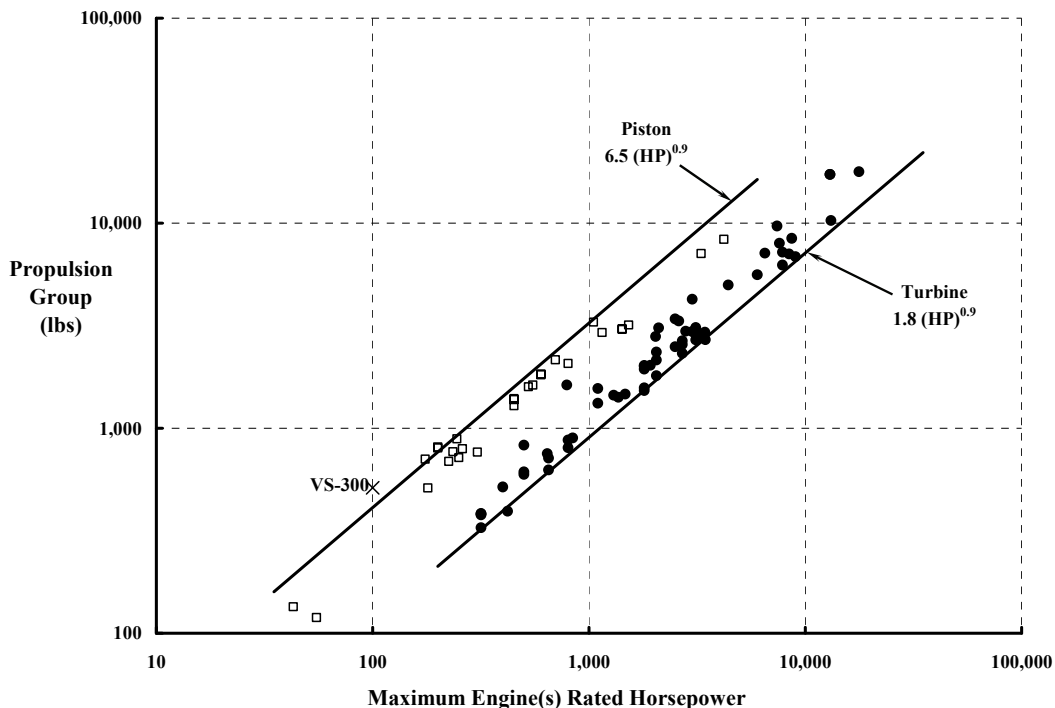


**Fig. 2-34. The gas turbine engine allowed the industry to reduce Propulsion Group weight dramatically.**

## 2.2 WEIGHT

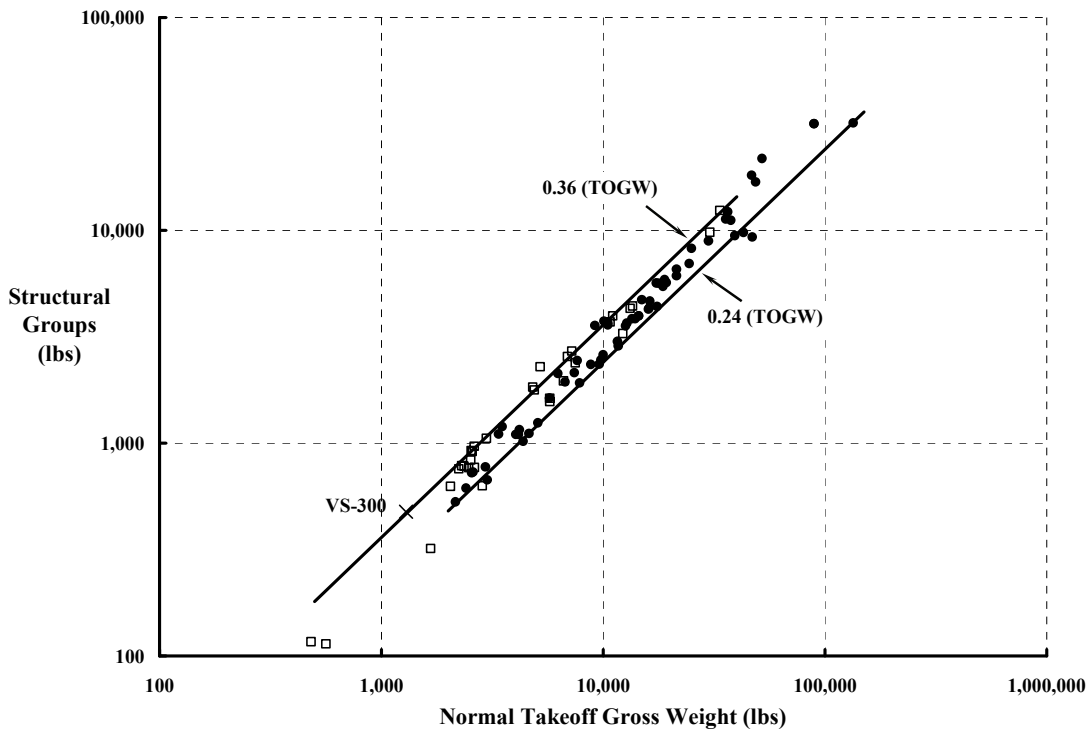


**Fig. 2-35. Innovative designs with advanced materials have reduced the weight of the Structural Group.**

The weight reductions achieved in the Structural Groups and the Propulsion Group have permitted the rotorcraft industry to increase the weight allocated to All Other Groups. The hydraulic-powered flight control system, which allowed an autopilot, was just the first of many added features to enhance the helicopter. Improvements in electronics have led to more automated flight instruments. Auxiliary power plants have been added to the larger helicopters, anti-icing is more frequently incorporated, and air conditioning is a quite commonly offered accessory. Fig. 2-36 shows that the industry has more than doubled the weight allocated to All Other Groups.

(2.28) Pistons at 0.13 (WE)  $\Rightarrow$  Turbines at 0.30 (WE).

As you can now appreciate, the rotorcraft industry has made considerable progress in the important area of helicopter weights since (1) Focke astounded the world with his F. 61 side-by-side and produced his Fa 223, (2) Flettner produced his Fl 282 synchropter, and (3) Sikorsky developed his VS-300 single rotor and delivered his R-4 series to the U.S. Army Air Corps. You have seen that the weights<sup>38</sup> of the Propulsion Group and Structural Groups have

<sup>38</sup> You will have noted in Fig. 2-34, Fig. 2-35, and Fig. 2-36 that I included data for the Sikorsky VS-300. The industry is (and most certainly I am) indebted to Harold Ullisnik for recapturing information about such a historically significant rotorcraft. Harold sent me a letter [148] that contained the VS-300 weight breakdown in MIL-STD-1374A. He obtained the actual weight data when he refurbished the VS-300 for its place in the Smithsonian Institute. This contribution, after retiring from Sikorsky Aircraft, is worth its weight in gold.

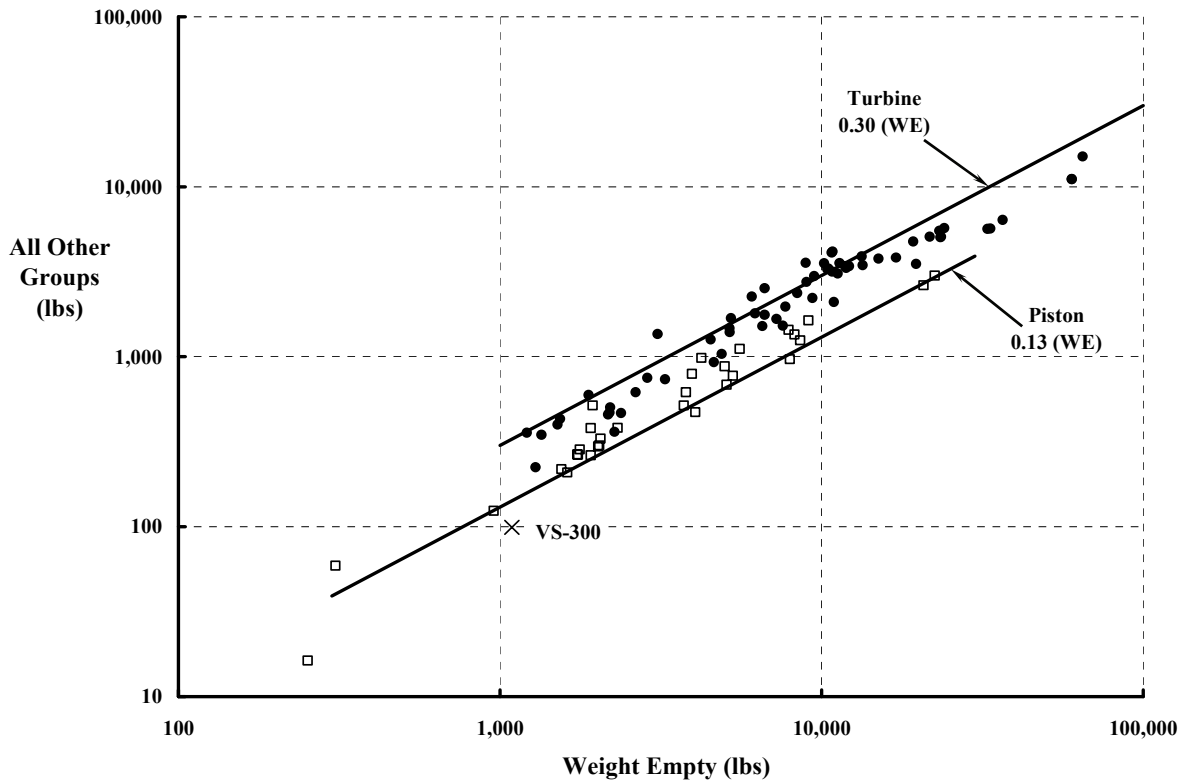


**Fig. 2-36. The industry has more than doubled the weight allocated to All Other Groups.**

been reduced to provide additional weight for more and better features in the All Other Groups. And along the way you have:

1. Seen a framework for the discussion as shown in Fig. 2-23,
2. Added weight terminology to your vocabulary,
3. Reviewed two general trends that have appeared over five decades; namely that
  - (a) There is no inherent limitation to helicopter size and
  - (b) The industry can obtain 40 percent useful load from takeoff gross weight,
4. Reviewed detailed results for the military aeroscout helicopters, and then
5. Seen this understanding applied to a broad range of products that the industry has created.

## 2.2 WEIGHT

### 2.2.1 A Helicopter Sizing Method

Let me now introduce you to a very abbreviated, helicopter sizing method by way of an example. The method itself is patterned after two very comprehensive and detailed methods that are widely used in the rotorcraft industry today. The sizing method you will see here is simply a very scaled down version of references [149-151] and is typical of an engineering problem. First, a group of known and, if necessary, assumed facts are given as input. Second, a sequence of equations that will lead to the problem's solution are constructed. Then third, the calculations with real numbers are completed giving an answer.

To begin the sizing method, suppose you tell me the design requirements are as follows:

You want a helicopter that transports eight passengers and their baggage, in safety and comfort, on a 2-hour flight at top cruise speed. Civil regulations require a pilot and a copilot.

The conceptual design method I will use to “rough out” a helicopter that meets your requirement is guided by Table 2-7 on page 111. The process starts by translating your design requirements into the Useful Load items outlined in Table 2-2. (In your design problem, only a few of the Useful Load items have been defined, so I have made assumptions about what you did not tell me.)

Frequently, a few items of Useful Load are “holy” (i.e., are held constant or fixed) during the conceptual sizing process. This is the case for your design problem. I have assumed that each crew member and passenger weighs 200 pounds. Ten bags at 20 pounds apiece seems reasonable. These fixed items are listed as the first set of inputs to the design problem and are shown at the top of Table 2-7.

For the moment, the unknown portion of Useful Load will be how much fuel and oil will be used during the 2-hour flight. Prudence says that some fuel reserve for flight beyond 2 hours should be included in the design. Therefore, I have added a half hour of fuel reserve to your design requirement. What this total, possible flight time of 2.5 hours means in pounds of fuel is yet to be determined, but it will be accounted for shortly.

At this point in the conceptual design process the oil is a very minor weight, and I will assume that 20 pounds of oil will be enough. No additional cargo is carried. Because this is a civil helicopter, there are no guns, weapons, or other equipment.

The Useful Load is, therefore, set at 2,220 pounds plus fuel weight when it is determined.

Now consider the second item of input to the design method outlined in Table 2-7 under Design Parameters. Because you stated no preference for your helicopter's configuration, I will select a single main rotor with a tail rotor. (We could just as easily be

**Table 2-7. A Simple Conceptual Design Example**

<b>DESIGN INPUT DATA</b>		
<b>Useful Load</b>		
Crew	400 lb	
Passengers	1600	
Fuel	2.5 hrs (lb TBD)	
Oil	20	
Baggage	200	
Cargo	0	
Guns/Weapons	0	
Other Equipment	0	
<b>Total Useful Load</b>	<b>2,220 lb + fuel</b>	
<b>Design Parameters</b>		
Configuration	Single Rotor	
Disc Loading	8 lb/sq ft	
Engine	Twin Turbines	
Engine SFC	0.40 lb/hr per hp	
Lift-Drag Ratio	3.19 at $V_{cruise}$	
<b>Weight Factors</b>		
Propulsion Group	1.80	
Structural Groups	0.24	
All Other Groups	0.30	
Installed Power	2.70	
<b>CALCULATION STEPS</b>	<b>RESULTS</b>	<b>NOTES</b>
Iteration Number	1,2,3 ... final	Converges Quickly
1. Start Gross Weight	10,341 lb	Started with 9,000 lb
2. Rated Horsepower	2,082 hp	= Eq. 1-131
3. Fuel for 2.5 Hours	2,082 lb	= SFC $\times$ ESHP $\times$ Flt Time
4. Propulsion Group	1,745 lb	= Eq. 1-129
5. Structural Groups	2,482 lb	= Eq. 1-129
6. All Other Groups	1,812 lb	= Eq. 1-130
7. Weight Empty	6,039 lb	= Steps 4 + 5 + 6
8. Useful Load	4,302 lb	= 2,220 + Step 3
9. End Gross Weight	10,341 lb	= Steps 7 + 8
10. Iteration Difference	0 lb	= Step 9 minus Step 1
11. Rotor Diameter	40.57 ft	= $\sqrt{4 GW/\pi DL}$
12. Continuous Cruise Speed	178 kts	From Eq. 1-132

discussing a tandem, coaxial, or synchropter configuration for this illustration.) You also did not specify a disc loading, so I will choose a representative value for you.<sup>39</sup> The disc loading of modern helicopters ranges from 6 to 12 pounds per square foot of main rotor(s) area. I will assume a disc loading of 8 pounds per square foot to start with. (Before closing this design illustration, results obtained by assuming disc loading values from 1 to 12 pounds per square foot will show you a rather interesting trend that has influenced the industry for five decades.)

<sup>39</sup> You will recall that disc loading is the ratio of helicopter gross weight to the area of the rotor or rotors, depending on the helicopter configuration. This was discussed in the section titled *Early Hovering Performance* on page 5.

## 2.2 WEIGHT

It seems reasonable to select a pair of gas turbine engines to power your helicopter. They will be more expensive than piston engines as you will recall. However, I have in mind a new engine model that is very fuel efficient. It has a specific fuel consumption (SFC) of only 0.40 pounds per hour per horsepower as suggested by Fig. 2-13.

The third part of input to the design process is the four items listed as weight factors. Some rational calculation of the three, major elements of weight empty shown in Fig. 2-27 must be made. To do this I will assume that the historical trends shown in Fig. 2-34, Fig. 2-35, and Fig. 2-36 are an adequate starting point. This means that I intend to assume a very modern design and calculate the three elements of weight empty from the three equations of

$$\begin{aligned} \text{Propulsion Group Wgt.} &\equiv \text{PG} = \text{Wgt. Factor} \times \text{HP}^{0.9} = 1.8 \text{HP}^{0.9} \\ (2.29) \text{ Structural Groups Wgt.} &\equiv \text{SGs} = \text{Wgt. Factor} \times \text{GW} = 0.24 \text{GW} \\ \text{All Other Groups Wgt.} &\equiv \text{AOGs} = \text{Wgt. Factor} \times \text{WE} = 0.30 \text{WE} \end{aligned}$$

There is a little algebra required here because I want the weight of All Other Groups directly, not in terms of weight empty as given by Eq. (2.29). Therefore, because

$$(2.30) \text{ WE} = (\text{PG} + \text{SGs}) + \text{AOGs} \text{ and } \text{AOGs} = \text{Wgt. Factor} \times \text{WE},$$

solving these two equations in two unknowns gives

$$(2.31) \text{ AOGs} = \frac{\text{Wgt. Factor}(\text{PG} + \text{SGs})}{1 - \text{Wgt. Factor}}.$$

On this basis, I will choose the weight factors for Propulsion Group, Structural Groups, and All Other Groups as 1.8, 0.24, and 0.30, respectively, as shown in Table 2-7.<sup>40</sup>

There is now only one last item to include in the input. Some estimate of horsepower needs to be made so that Propulsion Group weight can be calculated with Eq. (2.29). You will recall from Fig. 1-4 that some early inventors did not install enough engine horsepower to hover. In the chapters about modern hover and forward-flight performance that follow this discussion about modern helicopter weights, you will read that modern designs install maximum engine rated horsepower at sea level on a standard day approximately as

$$(2.32) \text{ ESHP}_{\text{Max. SLS}} = \frac{\text{Installed Power Factor}(\text{GW})}{550} (14.7) \sqrt{\frac{\text{GW}}{\text{A}}}.$$

The earlier inventors sometimes ended up with an installed power factor of 1.0 in Eq. (2.32). Their “machines” could just barely hover, in ground effect, at sea level on a standard day. Modern designers have used a factor of 1.7 to as high as 2.7 for helicopters that have high altitude hover and fast cruise performance.

---

<sup>40</sup> You should be aware that the industry has, over the decades, developed a detailed set of semiempirical weight trend equations that parallel Eq. (2.29). These detailed equations estimate the weight of every line item listed in Fig. 2-27. References [152-156] are just a fraction of what has been published. Furthermore, each major manufacturer has a Weights Department that closely guards a proprietary set of historical weight trend data.

I should mention that if you had stated a cruise speed requirement for your helicopter, I would have calculated the installed engine horsepower simply as

$$(2.33) \text{ ESHP}_{\text{Max. SLS}} = \frac{\text{Gross Weight}}{0.85 \times 550 \times (L/D)_{\text{Hel}}} \times (\text{Speed in ft/sec}).$$

Without any more information I would have guessed the lift-drag ratio of your helicopter at about 3.0 to 4.0, depending on speed. This would be based on the forward-flight portion of the performance chapter that follows this discussion of weights. The 0.85 factor in the denominator of Eq. (2.33) says that top cruise speed will be set with the engine designed to operate continuously at 85 percent of maximum turbine inlet temperature. This is a “wear and tear” or time between overhaul issue.

The simple form of estimating engine horsepower, Eq. (2.32), is suitable for this helicopter sizing illustration. I need only to choose a disc loading (i.e., GW/A) and an installed power factor. Table 2-7 shows that a disc loading of 8 and an installed power factor of 2.7 seem reasonable. (An alternate approach might be for you to specify what engines to use; then rotor diameter would have to be found using Eq. (2.32) and speed determined from Eq. (2.33)). Fuel quantity will be estimated as given at calculation step 3 in Table 2-7.

With all the input defined, it now becomes a simple matter to “turn the crank” and calculate some numbers that show what your helicopter will look like. The actual calculation proceeds in 3 or 4 iterations of 11 steps each, as described in the lower portion of Table 2-7. The reason for needing some iteration is because the Structural Groups’ weight depends on gross weight, but gross weight has yet to be determined.<sup>41</sup>

The calculation part of the design method starts by guessing a gross weight at iteration 1, step 1. My tendency is to guess low and hope for a light design that will be less costly. I chose 9,000 pounds, and after three iterations the process converges to a takeoff gross weight of just over 10,300 pounds.

Based on the design requirements you gave me a few pages back (plus a few assumptions on my part), your helicopter will

- a. Be a single rotor configuration,
- b. Have two turbine engines with a maximum rated horsepower of 1,040 hp each,
- c. Need a fuel tank that holds 2,040 pounds or about 315 gals,
- d. Have a 40.6-foot rotor diameter, and
- e. Enjoy a continuous cruise speed of 175-plus knots at 85 percent of maximum engine rated horsepower.

---

<sup>41</sup> In doing this simple engineering problem, I “programmed” Table 2-7 on the spreadsheet software called Microsoft® Excel®. Excel includes a Goal Seek routine under the Tools menu that performs the iteration in short order.

## 2.2 WEIGHT

You can expect a quiet, climate controlled, modern interior and a “jet smooth ride” for your passengers, the latest flight instruments and autopilot for the crew, and high reliability and low maintenance. As to the purchase price, well, that is another subject.

There is one classical helicopter design trend that you should be aware of. The trend deals with the influence of disc loading on the overall results. In the previous design study illustration, a disc loading of 8 pounds per square foot was assumed. What is interesting, as Fig. 2-37 shows, is that varying disc loading significantly affects gross weight and the required engine horsepower, but only begins to significantly affect the rotor diameter below a disc loading of 6.0. What this says is that the smallest helicopter falls in the disc loading range around 8. Very low disc loading drives the diameter up, while higher disc loading drives up the engine power and Propulsion Group weight. This increases the weight empty and gross weight. The increasing gross weight increases the Structural Groups and the weight empty, and the cycle continues.

The early pioneers had a narrow choice from a comparatively short list of relatively low-powered piston engines. As a consequence, their helicopters were low-disc-loading “machines.” The modern industry has a wide range of gas turbine engines to use and, accepting the cost, could even offer higher-disc-loading products with greater installed horsepower. The benefit, however, seems to be only 5- to 15-knots greater cruise speeds. The issue of helicopter maximum efficient cruise speed has been with the industry ever since Glauert raised the issue, and argued with Cierva about it, in the mid-1920s.

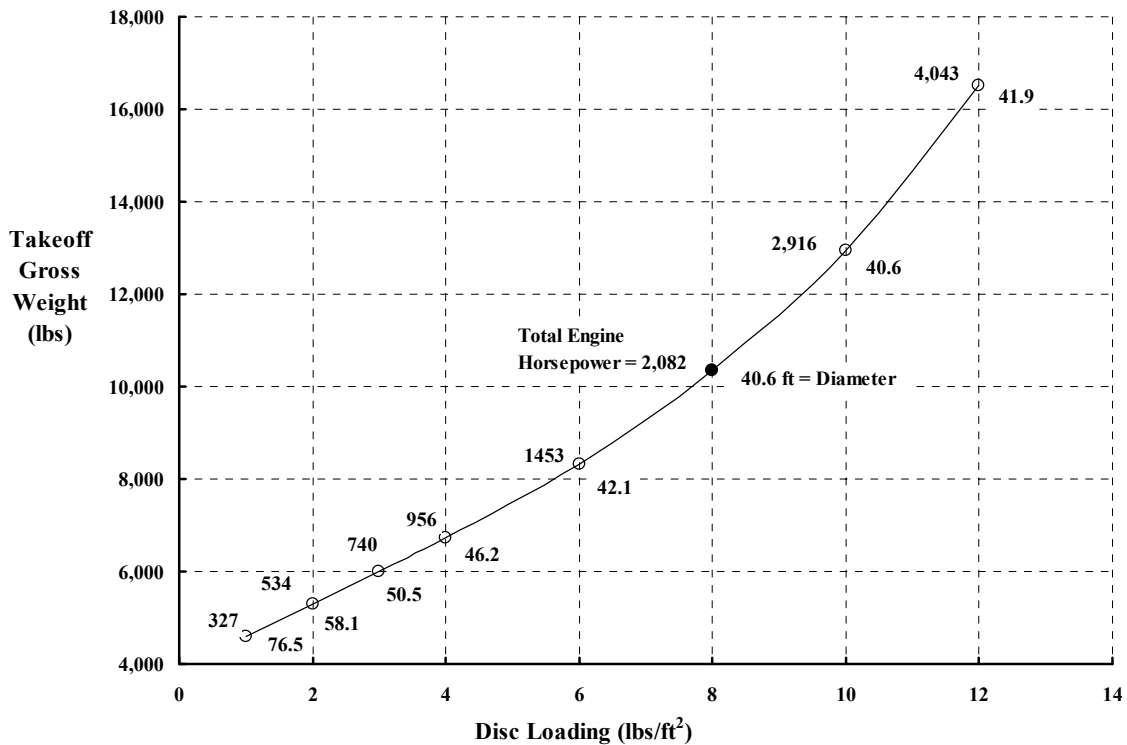


**Fig. 2-37. The industry avoids high-disc-loading helicopters. Example for a constant, fixed useful load of 2,220 pounds per Table 2-7.**

The rotorcraft industry has, over six decades, nearly doubled the level flight speed record. Today, that record stands at just over 216 knots. Unfortunately, the record was achieved by brute power because the record-setting helicopter had a lift-to-drag ratio of less than 2.6. This is not impressive at all from an aerodynamic efficiency point of view, as Glauert would be quick to point out. You can see the issue and the problem easily from the trend shown in Fig. 2-38 and the parameters of Eq. (2.33).

Now let me proceed to a final point—helicopter productivity—in this introduction to modern helicopter weights. A frequently used definition of productivity is work per unit of time. Work has the English units of pound-feet and time has the unit of seconds. The pound in question here is generally taken as payload in the transportation industry. Payload is the part of Useful Load that the user perceives as useful. For “your commercial helicopter” this would be the eight, paying passengers and I suppose their baggage, which together total 1,800 pounds. This leaves the feet and seconds to account for; but this is just velocity or, in the world of productivity, speed. Thus,

$$(2.34) \text{ Productivity} \equiv \frac{\text{Work}}{\text{Time}} = \text{Payload} \times \text{Speed} = PV.$$

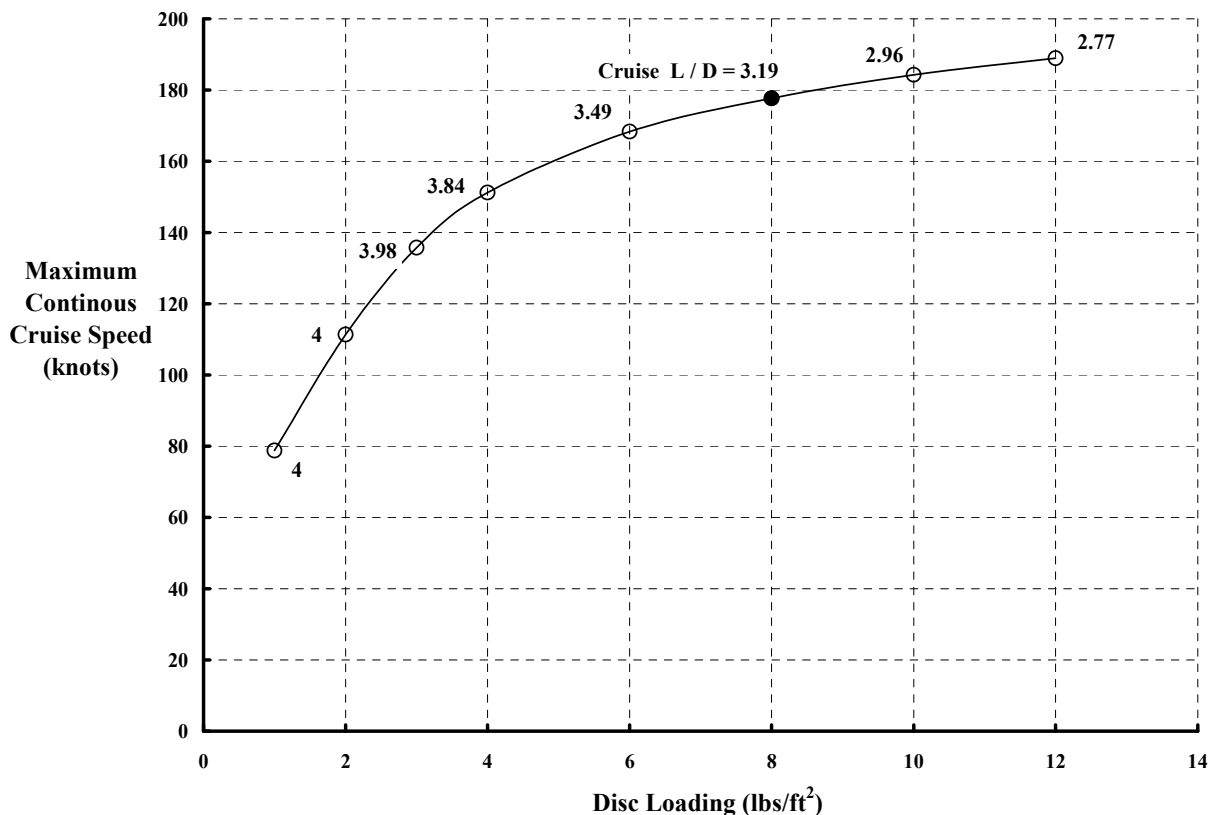


**Fig. 2-38.** The lift-to-drag ratio of current helicopters drops rapidly at speeds above 150 knots. Example for a constant, fixed useful load of 2,220 pounds per Table 2-7.

## 2.2 WEIGHT

So far the rotorcraft industry, unlike the fixed-wing industry, has been unable to significantly increase helicopter productivity by increases in speed. The brief discussion about disc loading, the current world speed record, and Fig. 2-38 give you a hint of what the industry has apparently come to accept as a serious limitation inherent in the helicopter. But if increasing helicopter productivity by doubling or tripling cruise speed is not practical, there appears to be no such limitation to increasing productivity by raising payload. Raising the payload of “your commercial helicopter” by a factor of 10 or 20 to provide 100- or even 200-passenger helicopters is well within the industry’s capability. Of course the question just behind this open door is one of user cost, and this means that the more appropriate measure would be productivity per unit of money. In United States units that means

$$(2.35) \text{ Productivity Per Dollar} = \frac{\text{Payload} \times \text{Speed}}{\text{User Dollars}} = \frac{\text{PV}}{\$}.$$

The subject of helicopter cost and price is addressed later. However, there is one bridge to costs that you may see used in published studies of helicopter productivity. The bridge is to imagine that (1) helicopter manufacturing costs, (2) the purchase price, (3) the user or operator’s costs, and (4) the end-benefactor cost (say a passenger’s ticket price) *ALL* are proportional to the helicopter’s weight empty.<sup>42</sup> This presumption leads to

$$(2.36) \text{ Productivity Per Dollar} \propto \frac{\text{Payload} \times \text{Speed}}{\text{Weight Empty}} = \frac{\text{PV}}{\text{WE}}.$$

If this proportionality as stated by Eq. (2.36) was followed, then Fig. 2-37 suggests that disc loadings approaching 1.0 would have the lowest weight empty. One would blindly ignore the fact that the rotor diameter had become quite large. Using the design method in Table 2-7, even with all its simplicity, gives you the trend of the parameter PV/WE with disc loading shown in Fig. 2-39. On this basis, “your optimum helicopter” should be designed with a disc loading of 3, a rotor diameter of 50.5 feet, and a cruise speed of around 136 knots. I believe you would say this conceptual design was too slow and too big to be called a modern, low-drag, twin-turbine helicopter.

The other end of the conceptual design spectrum emphasizes low aerodynamic drag, high speed, and the installation of higher-powered engines to get that speed. The disc loading becomes higher, the helicopter stays small, but the parameter PV/WE is significantly reduced. This trend, shown in Fig. 2-40, uses the previous data but graphed with cruise speed as the abscissa. Again, the low productivity per dollar, measured by PV/WE, at high disc loading comes about because the industry has not succeeded in raising the helicopter lift-to-drag ratio much above 4.0. At the high speeds potentially possible with disc loadings approaching 12, the lift-drag ratio is falling from 4.0 to something on the order of 2.5. This aerodynamic performance problem has deprived the rotorcraft industry of a development path enjoyed by the fixed-wing industry.

---

<sup>42</sup> To say that I am not in favor of these assumptions would be an understatement! On more than one occasion I have seen the focus placed solely on reducing weight empty regardless of the manufacturing or material costs; ignoring the issue of rotorcraft costs is not something I recommend.

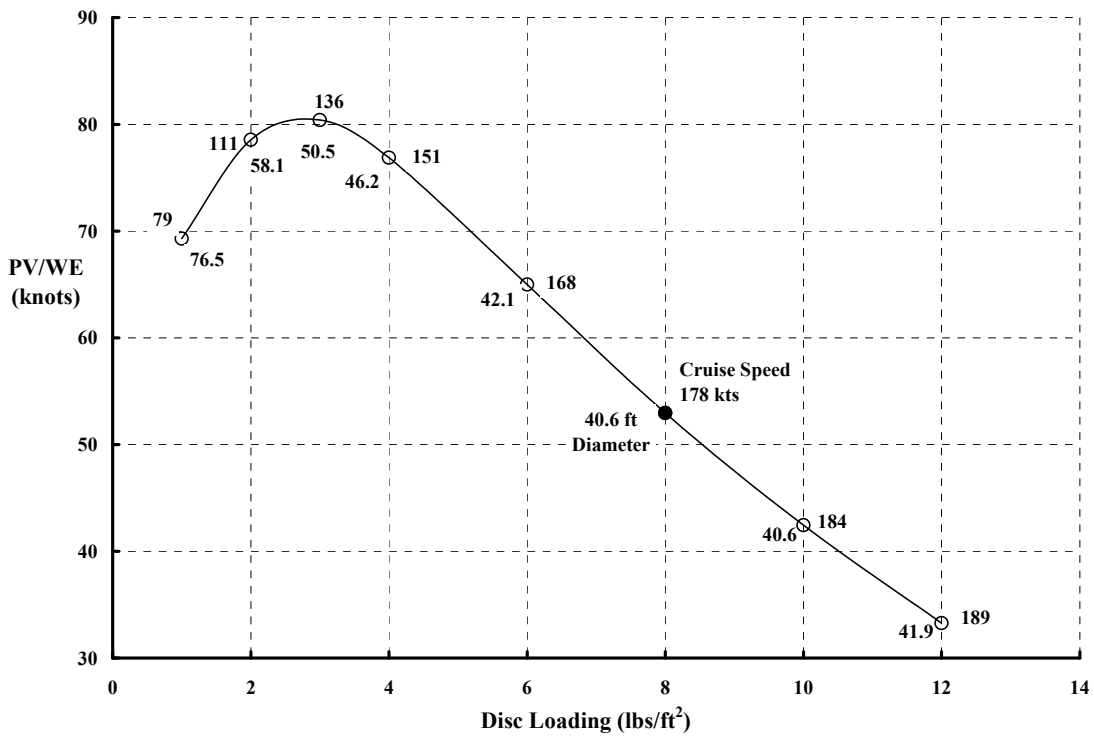


**Fig. 2-39. The industry avoids low-disc-loading helicopters because they are too big and too slow. Example for a constant, fixed useful load of 2,220 pounds per Table 2-7.**

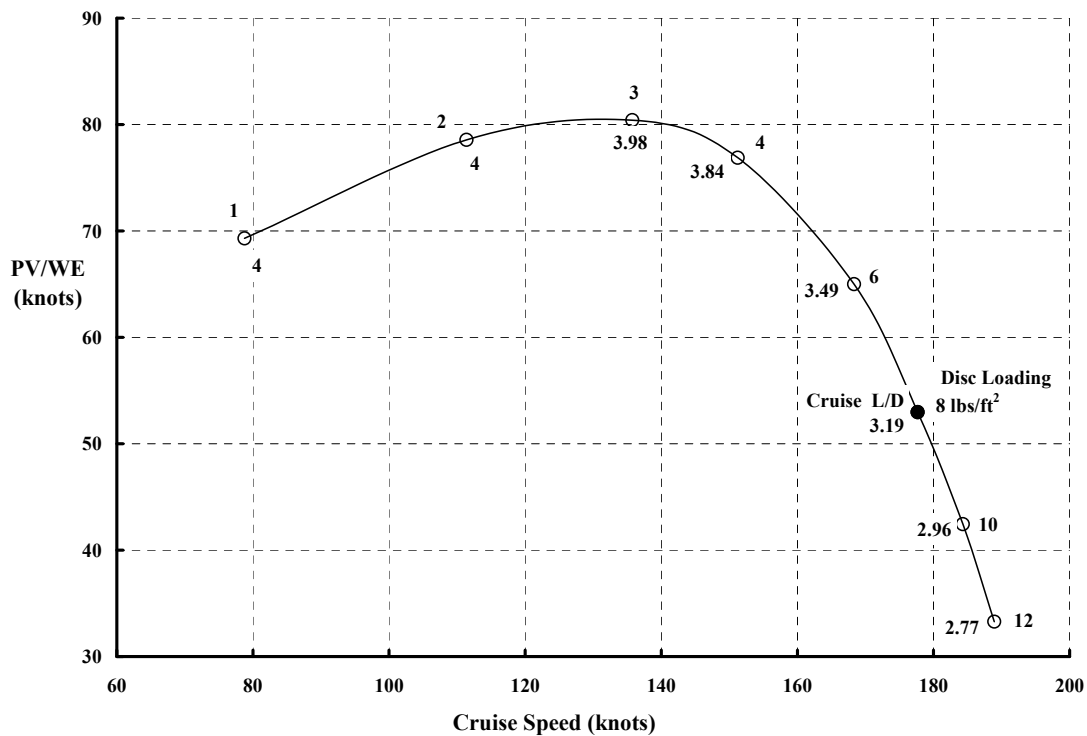


**Fig. 2-40. The industry avoids high-disc-loading helicopters because of excessive costs to get speed. Example for a constant, fixed useful load of 2,220 pounds per Table 2-7.**

## 2.2 WEIGHT

This introduction to modern helicopter weights has given you a framework and associated terminology to discuss the industry's progress in a very vital area. You have seen that:

1. There is no limitation to helicopter size,
2. The overwhelming number of helicopters have takeoff gross weights well below 50,000 pounds,
3. The modern helicopter grew from the small "machines" that replaced the autogyro, and these early helicopters gave the military a true aerial scout capability,
4. The ratio of useful load to gross weight is not always a measure of "goodness," particularly for special-purpose helicopters that the military use,
5. The application of the turbine engine was a major step,
6. Weight reduction in Propulsion Group and Structural Groups was used to add features in the All Other Groups,
7. Simple methods can be used to roughly size a helicopter,
8. Helicopter productivity depends on payload and speed, and
9. Efficient helicopter aerodynamic performance at high speed has yet to be achieved, and this has impeded the industry.

In closing this discussion about weight, it is probable that further weight-empty reductions will be made as the modern helicopter continues to mature. It would be my hope that these reductions in weight will be accompanied by reductions in costs and improvements in performance. However, it is well to keep in mind Lieutenant Alexander Klemin's statement opening Chapter III of his book, *Aeronautical Engineering and Airplane Design* [157]. In 1918, Lieutenant Klemin<sup>43</sup> wrote:

"Hardly any branch of practical airplane design offers such difficulties as the estimates of weight. A manufacturer – who has built a number of machines and has kept careful weight schedules has valuable data in his possession, but is, as a rule, chary of making such data public. Even an experienced manufacturer, however, may be at a loss when building an entirely new type, particularly if the new type is of a very different size from that to which he has been accustomed.

Theoretical considerations apply only to a limited extent. Empirical formulas have been suggested by several authorities, but are only partly satisfactory. The authors' thanks are due to manufacturers and others for such data as they have permission to publish."

---

<sup>43</sup> Dr. Alexander Klemin became a staunch supporter of rotorcraft. He was born in London on May 15th, 1888, and died unexpectedly on March 14th, 1950. An obituary by Group Captain R. N Liptrot was published in the *Journal of the Helicopter Association of Great Britain*, vol. 4, no. 1. Each year the American Helicopter Society gives an award—the Klemin Award—to a very deserving society member.

## 2.3 HOVER PERFORMANCE

The improvements in rotorcraft performance over the past five decades have been nothing short of astounding. Cruise speeds, under 75 miles per hour in the early 1940s, have doubled to modern speeds ranging from 150 to 170 miles per hour (130 to 150 knots). Many helicopters are available that can do useful work at altitudes from 10,000 to 20,000 feet thanks to the turbocharged piston engine and the transition to gas turbine engines. Payloads of 20,000 pounds can easily be moved well over 100 nautical miles. Extended range beyond 600 nautical miles is common place, and aerial refueling permits comfortable, long-distance, over-water flights such as California to Hawaii (2,100 nautical miles). Helicopters have flown around the world. In short, over 50 years the helicopter has matured in the category of performance.

To appreciate the progress made by the rotorcraft industry in reaching this mature level of performance, it helps to understand helicopter performance in the three major areas of:

1. Hovering, including takeoff,
2. Forward flight and landing, and
3. Fuel efficiency.

These topics, combined with the previous background about engines and weights, form at least a minimum basis to see the modern progress made with the helicopter. Consider hover performance first.

### 2.3.1 Hover Power Margin

The takeoff and hovering performance of modern helicopters has established the unique character of these “machines.” When you see a hovering helicopter rescue a mountain climber stranded at 10,000 feet, you quickly appreciate the progress made since the early pioneering efforts to just get off the ground. The “performance secret” to these humanitarian successes lies in (a) installing an engine or engines with enough power, (b) minimizing the power required to takeoff and hover, (c) selecting the design horsepower and gear reduction for the transmission, and (d) achieving a structurally efficient helicopter. You already have some insight into engine performance from the earlier discussion, and from your introduction to modern helicopter weights you should be convinced that structurally efficient helicopters have been achieved. So consider the progress that has been made in ensuring an ample power margin between power available and power required for useful flight.

Let me first use some history as a broad introduction to power margin. The early pioneers, as you will recall from Fig. 1-4, had begun to appreciate just how much horsepower the helicopter would need to achieve a bare minimum of hovering performance. However, the transition to the modern era of consistently installing enough power to hover did not begin until the mid-1930s. The beginning of the modern era came when Maurice Claisse demonstrated a coaxial “gyroplane” designed by René Dorand, but guided by Louis Bréguet

## 2.3 HOVER PERFORMANCE

himself. These two French pioneers worked at Louis Bréguet's Société des Avions. Their efforts to develop the Bréguet Type 314 in the mid-1930s are recounted by Claisse in Jean Boulet's history [2]. The initial, inadequate ground runs with the Type 314 were followed by a disastrous, first hovering attempt on a Sunday in late November of 1933. During this initial, unsuccessful period, Claisse noted that they "found an engine made at Bréguet's for the Leviathan, called the Bréguet-Bugatti. It was a 500 HP engine. We cut it in two sections and we had an engine of 250 HP which seemed to fit our needs." The "machine" was rebuilt, more thorough ground testing was completed, and in June of 1935 flight testing began again. The 4,500-pound-gross-weight helicopter with 52.5-foot-diameter, two-bladed, coaxial rotors was readied in August of 1935 for a serious demonstration. Unfortunately, the 250-horsepower piston engine threw a connecting rod. Claisse went on to say that "fortunately, there was in Bréguet's hanger a Wright 90 engine, which was an excellent engine. It had a little too much power (420 HP), and the speed [RPM] was not exactly right. But we adjusted it, and then we had more power than necessary." Between December 1935 and December 22, 1936, Claisse went on to capture all the helicopter world records. These demonstrations earned the Bréguet airplane company a 3.2-million-Franc subsidy from the French Government for follow-on development. The Type 314 was damaged during subsequent autorotation testing, and with the coming of World War II Bréguet and his company had to concentrate on airplane deliveries. Claisse concluded his personal history with:

"We were not able to do it all. We gave up."

Fortunately, Focke, Flettner, Platt and Le Page, Sikorsky, and several others picked up the pioneers' legacy and development continued. After World War II, Bréguet and Dorand began anew. Bréguet continued with the coaxial configuration. His G-11E, a 28-foot-diameter, 2,915-pound-takeoff-gross-weight helicopter was powered with a 240-horsepower engine. It flew in early December of 1948. The G-11E was uprated to the Type III having a 31.5-foot-diameter, 450-horsepower engine, and a 4,630-pound, fully loaded flying weight. The Type III was the last helicopter for Bréguet. This great French aviation pioneer died in 1956.

Dorand became the head of the SNCAC, one of several French nationalized aircraft organizations. He favored Flettner's synchropter approach and launched his less-than-successful NC-2001. One of three prototypes briefly hovered in ground effect in June of 1948. The SNCAC was subsequently shut down, and Dorand formed his own company and began experimenting with single rotors turned by tip jet propulsion.

It is worth taking a moment to get a rough idea of the power margin of the Bréguet–Dorand Type 314. A first-order index of power margin comes from the power available and the ideal horsepower required to hover out of ground effect as discussed earlier in relation to the pioneering efforts. Applying Eq. (1.1) on page 5, but now using the Bréguet–Dorand Type 314 as the example, shows that

$$\begin{aligned}
 \text{HP}_{\text{ideal}} &= \frac{T}{550} \sqrt{\frac{T}{2\rho A}} && \text{Hover out of ground effect} \\
 (2.37) \quad &= \frac{4500}{550} \sqrt{\frac{4500}{2 \times 0.002378 \times 2140}} = 172 \text{ hp}
 \end{aligned}$$

Imagine now that Claisse and Dorand had proceeded with the original, 250-horsepower engine. The ratio of installed engine power to ideal would have been a miserly 1.45. I believe that the smaller engine did these French pioneers a favor when it threw a connecting rod. By turning to the 420-horsepower Wright 90 engine, Bréguet and Dorand gave Claisse a ratio of installed to ideal power of 2.44, and *then* they “had more power than necessary.” Considering that the Type 314 (*vintage 1935*) had a mechanical hydraulic-powered control system, and the controls were phased so that longitudinal stick motion gave equal roll and pitch response, Maurice Claisse certainly did not need the complication of an underpowered “machine.”

Before “giving up” as Claisse concludes, Bréguet presented a paper in November of 1936 [158] that summarized his work. This work really began in the very early 1900s. Interestingly, he provides only two photos of his Type 314 and devotes less than 2 pages out of 35 to what he refers to as “only a laboratory gyroplane.” Instead he indirectly comments that concepts of flapping, lead-lagging, and feathering were established well before Cierva began. Then he proceeds to outline his aerodynamic performance theory for the “gyroplane” in considerable detail. This lays the groundwork for his next design.

Bréguet proposes [158] “the gyroplane of the future.” His conceptual design envisions a coaxial, 25-meter-diameter (82.02-foot) rotor system to be used with a 12-passenger, airline-type fuselage. The design includes a retractable landing gear. An alternate fuselage appears to be a seaplane fuselage similar to the Boeing Clipper. He estimated the takeoff gross weight at 15 to 17 [metric] tons but used 15 tons or 33,069 pounds in all his figures. Four engines giving a combined output of 3,600 horsepower at an altitude of 3,000 meters (9,843-foot pressure altitude on a standard day) were to be “housed in one compartment of the aircraft.” Each of these *piston* engines (remember Bréguet presented this paper in November of 1936 before the gas turbine engine became an option) would have to be rated at about 1,300 horsepower at sea level to give the power he wanted at altitude. Based on his aerodynamic theory, Bréguet believed that the power required to hover at 3,000 meters would be 2,650 horsepower and that at a high-speed cruise power of 2,400 horsepower, his gyroplane would cruise at 400 kilometers per hour or 248 miles per hour (about 216 knots). There can be little doubt, however, that Bréguet intended to install enough engine horsepower. At sea level the ideal horsepower to hover for his design is 2,181 horsepower. He was, therefore, proposing a ratio of installed to ideal power of  $4 \times 1,300 / 2,181$  or around 2.38.<sup>44</sup>

---

<sup>44</sup> I found Bréguet’s paper fascinating although the definition of symbols was hard to follow, and the mixture of metric and English units complicated my understanding of his results. The ideal power to hover out of ground effect at 3,000 meters is 2,181 horsepower given the weight and diameter he proposed. This would suggest a hover efficiency of  $2,181 \div 2,650$  or about 82 percent, which modern helicopters have yet to achieve. Bréguet’s theory led to a 216-knot cruise speed that I can only imagine Glauert would have scoffed at. I suspect that Cierva would have seriously disagreed with Bréguet’s theory but liked the answer.

## 2.3 HOVER PERFORMANCE

**Table 2-8. The Rotorcraft Industry Has Flown Over 550 Separate Models as the Helicopter Matured**

<b>Configurations</b>	<b>Piston</b>	<b>Turbine</b>	<b>Row Totals</b>
Single Rotor	197	217	414
Tandem Rotors	31	22	53
Coaxial Rotors	37	10	47
Synchropter	11	9	20
Side-by-Side	16	2	18
Tri-Rotor	1	0	1
Quad-Rotor	1	0	1
Column Totals	294	260	554

I have compiled a survey of about 600 helicopters known to have flown since Bréguet and Dorand began what I believe to be the modern era of helicopter development. The shaft-driven configurations, numbering slightly over 550, are distributed as shown in Table 2-8. Modern results illustrating a simple view of power margin are summarized in Fig. 2-41. The results of this survey confirm Bréguet's accuracy in 1936.

The trend that this survey of over 550 shaft-driven helicopters suggests is an average installed-to-ideal-power ratio of 2.25. Designers who started out at a lower ratio generally uprated the engine before serious production was begun. Very few configurations were attempted below a ratio of 1.50, and none of these helicopters went beyond Bréguet's "laboratory model" stage. The rotorcraft industry learned the value of power margin, and each generation of helicopter model improved as Fig. 2-41 suggests.

A more definitive power margin criteria for U.S. Army helicopters became available in April 1974 [159]. This Army design requirement called for a 500-foot-per-minute vertical rate of climb at 4,000-foot pressure altitude with an outside air temperature of 95 °F using military rated power. The presumption was that future Army helicopters would at least be able to hover at this high/hot condition, hopefully with enough spare power to maneuver.

### 2.3.2 Hover Ceiling Versus Gross Weight

Although historically very informative, the surveys shown in Fig. 2-41 and Fig. 2-42 do not display hover performance in the way you are most likely to see it. Nor do they convey the fundamental physics behind these modern helicopter trends. Hover performance for a given helicopter is most often shown graphically as in Fig. 2-43. The envelope of the highest altitude that the helicopter can takeoff and hover out of ground effect (HOGE) is defined for a practical range in takeoff gross weight (TOGW). In general, the available engine horsepower decreases from its sea-level rating as altitude increases. Naturally, this limits takeoff from high-altitude heliports at heavy weight. The transmission may limit the TOGW at low altitude as Fig. 2-43 suggests. Finally, in combination with a minimal weight statement, you can quickly establish what the gross weight means in terms of useful load.

## 2.3 HOVER PERFORMANCE

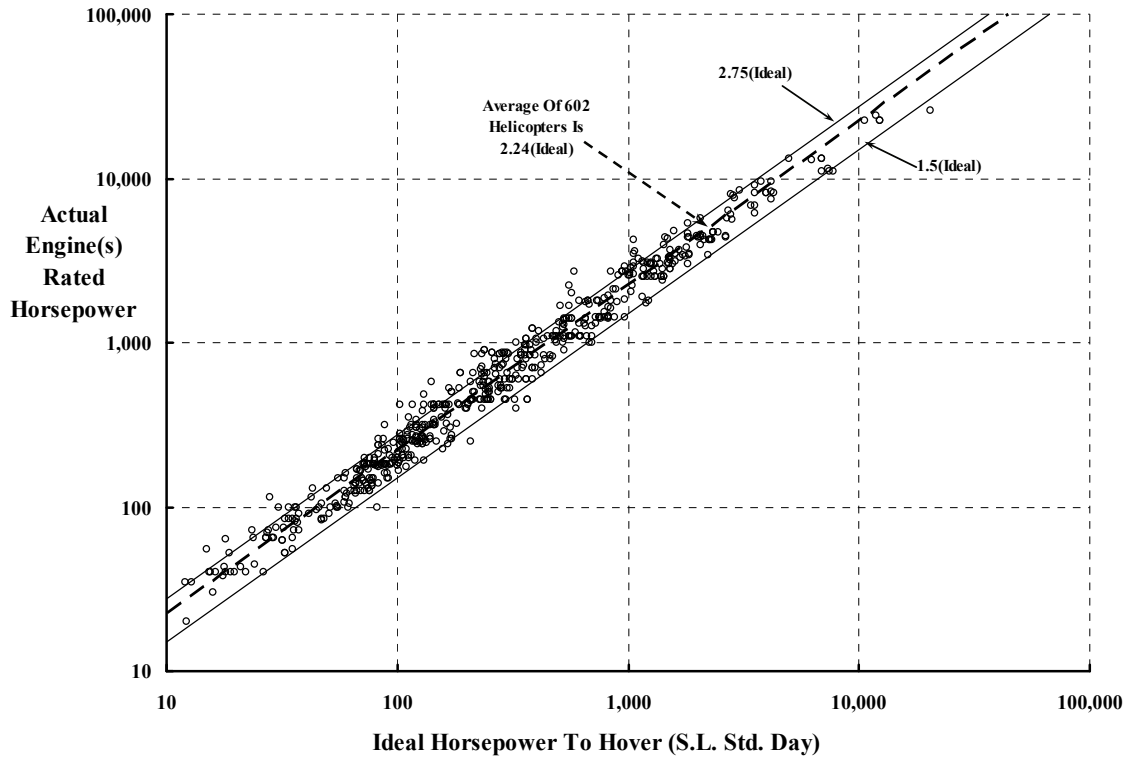


**Fig. 2-41. Rotorcraft always benefit from a healthy margin between engine power available and power required.**

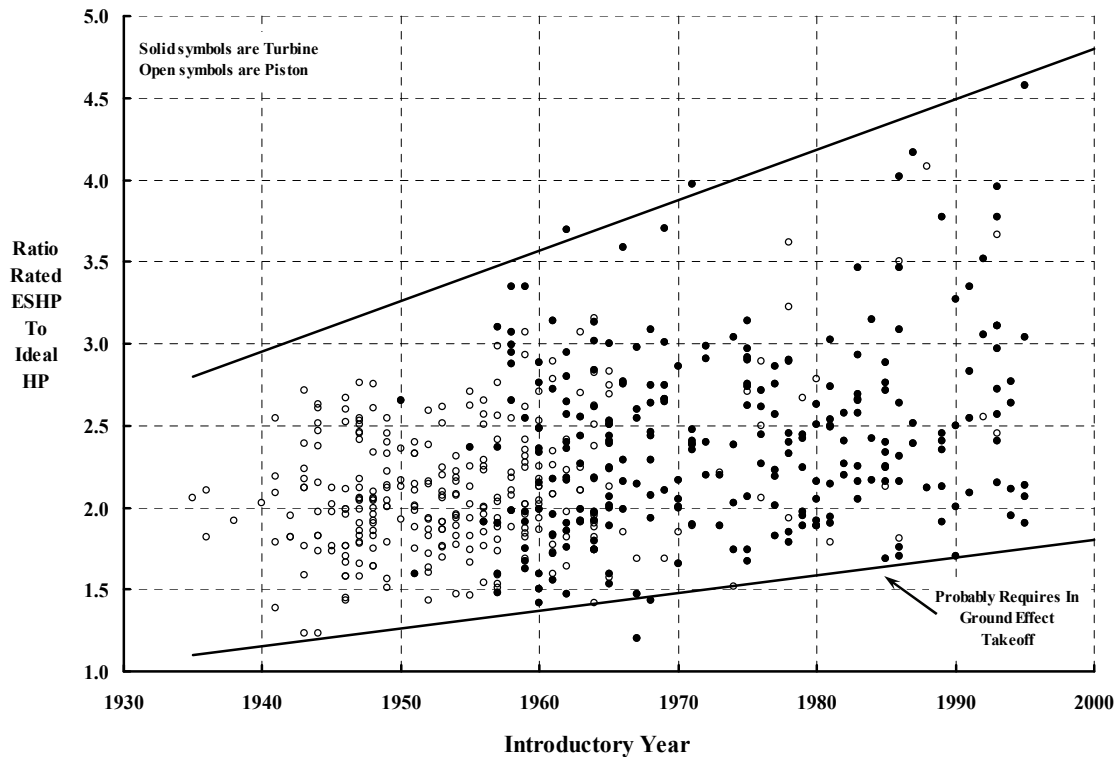


**Fig. 2-42. Power margin has continually increased.**

## 2.3 HOVER PERFORMANCE

Fig. 2-43 does a fair job of summarizing the characteristic trend of rotorcraft hovering performance, particularly if you are comparing one product to another.<sup>45</sup> However, it only begins to suggest what key factors and fundamental physics influence helicopter hovering performance. It will be a real help to your introduction to rotorcraft if you understand the details behind the typical summary presented in Fig. 2-43. After you see these details, I will come back to the format of Fig. 2-43 and then add a bit more.

The physics behind and leading to Fig. 2-43 are, fortunately, really quite easy to understand although it does take several pages to convey. The most important hover performance fundamentals are:

- a. The variation, with altitude and temperature, of power required to hover,
- b. The variation, with altitude and temperature, of engine power available, and
- c. The power that the transmission system is designed for.

Because the majority of the 600 helicopters surveyed are single rotor helicopters with a tail rotor for anti-torque, I will use this configuration to illustrate these 3 hover performance fundamentals.

Within the single-rotor group, the Sikorsky UH-60A, designated by the U.S. Army as the Black Hawk, has a great deal of information available in the public domain. This utility, tactical, transport helicopter emerged as the winner in the competition for a modern helicopter to replace the Bell UH-1 “Huey” series. The Army UH-60A is a measure of early 1970’s technology. The preproduction model, the YUH-60A, was flight evaluated [160] by the U.S. Army Aviation Engineering Flight Activity at Edwards Air Force Base from April 7 to September 17 of 1976. The production configuration, the UH-60A, was qualified [161] from October 27, 1979, to October 9, 1980. The final report was published in September of 1981 and contained the statement that the UH-60A had “undergone the most extensive qualification program of any helicopter in the history of the industry.” It would be hard to argue with the Army’s statement.

In my opinion, there is only one book worth reading about the complete history of the Sikorsky UH-60. Ray Leoni wrote it. He titled the saga *Black Hawk: The Story of a World Class Helicopter* [162], and it was published by the American Institute of Aeronautics and Astronautics (A.I.A.A.) in 2007. Ray was the leading figure behind Sikorsky’s helicopter

---

<sup>45</sup> Perhaps a word of caution is needed here. You will frequently see tables comparing helicopter characteristics published in trade magazines. These tables, until recently, could be most misleading. Very often the collection of numbers I have seen presented is an “apples-to-oranges” comparison. For example, under the weight columns, the maximum takeoff gross weight might well be quoted. Then, in the performance columns, the hover altitude might be quoted—but for the normal gross weight. If you look at Fig. 2-43, you can see that the maximum takeoff gross weight at which this helicopter can HOGE is just under 22,000 pounds. This corresponds to a sea level takeoff. But the comparative table may well quote the hover ceiling as 8,000 feet. Fig. 2-43 says this hover ceiling is associated with a “normal” gross weight of 18,500 pounds. The next helicopter product listed on the table could mix and match numbers from its hover ceiling chart and include in ground effect (HIGE) takeoff hover ceiling performance. The second product may appear to be superior, but you would be deceived.

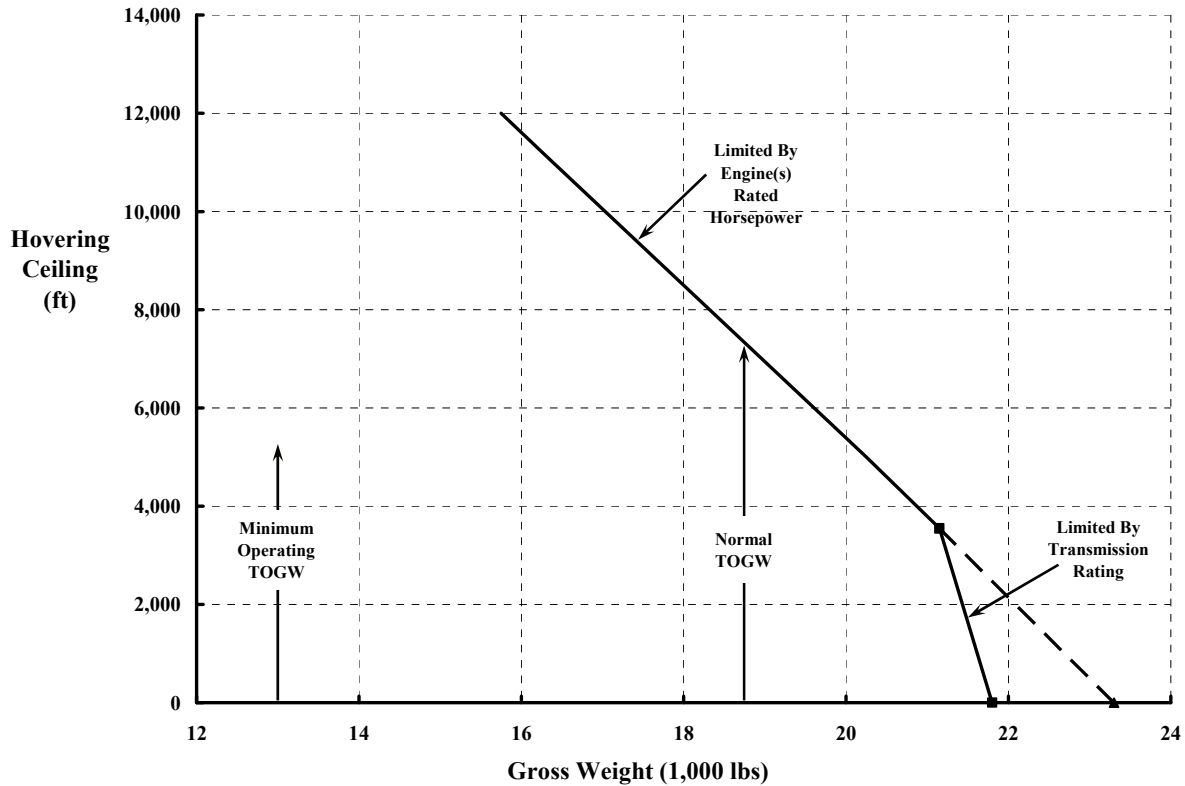


**Fig. 2-43. The most common display of hovering performance defines hover ceiling vs. takeoff gross weight.**

development—from conceptual design, to winning the U.S. Army competition with the entrée from the now Boeing Helicopter Division, to worldwide use of the UH-60 today. The insight about engineering details, company strategy, working with the U.S. Army, trials and tribulations—it is all there. The Foreword to Ray’s book was written by Sergei Sikorsky (Igor’s son), and the Preface was contributed by Charlie Crawford, who was Ray’s counterpart on the Army’s side. Charlie ate, slept, and breathed the Black Hawk program along with Ray. As Charlie wrote, “If you want to understand rotorcraft development, this is a must read book.”

After winning the fly-off competition against the Boeing-Vertol YUH-61A, the preproduction YUH-60A was considerably improved before entering into production. Table 2-9 shows that the combined efforts of the Sikorsky Aircraft Division and the General Electric Aircraft Engines Division gave the U.S. Army a superior helicopter.<sup>46</sup> Most importantly, the UH-60A has performed well in the field.<sup>47</sup>

<sup>46</sup> Preparing Table 2-9 required careful review of both the flight qualification reports [160, 161] and weight reports [163, 164].

<sup>47</sup> Further flight research of a production UH-60A to evaluate the rotor system in more detail was accomplished in the first half of 1987. This effort [165] in 1988 provided extensive data for performance, loads, and stability and control, as well as vibration levels throughout the airframe. More recently, NASA and the U.S. Army teamed up to provide the industry with the most comprehensive set of blade airloads data imaginable [166, 167].

### 2.3 HOVER PERFORMANCE

With this background about a representative single rotor helicopter, the UH-60 series, in hand, let me discuss hovering performance from the power-required perspective.

The power required to HOGE was obtained with the YUH-60A/UH-60A wheels about 100 feet above the ground. The distance from the bottom of the wheels to the main-rotor hub adds another 12 feet. This gives a height-to-diameter ratio over 2.0, which is representative of HOGE testing. While the final Army evaluation was based on the UH-60A results, I have chosen to include data from the YUH-60A evaluation as well to give you an appreciation of experimental “data scatter.” The results shown in Fig. 2-44 provide the power required versus altitude on a standard day for two gross weights. The lower weight is the primary mission gross weight of 16,260 pounds while the alternate gross weight of 20,250 pounds is near the maximum weight for the “A model” of the UH-60 series.

The fundamental trend is for hover power required to increase with altitude, and the UH-60A design is no exception. You saw earlier [from Eq. (1.4), repeated here for convenience] that a simple engineering approximation to the physics involved is given by

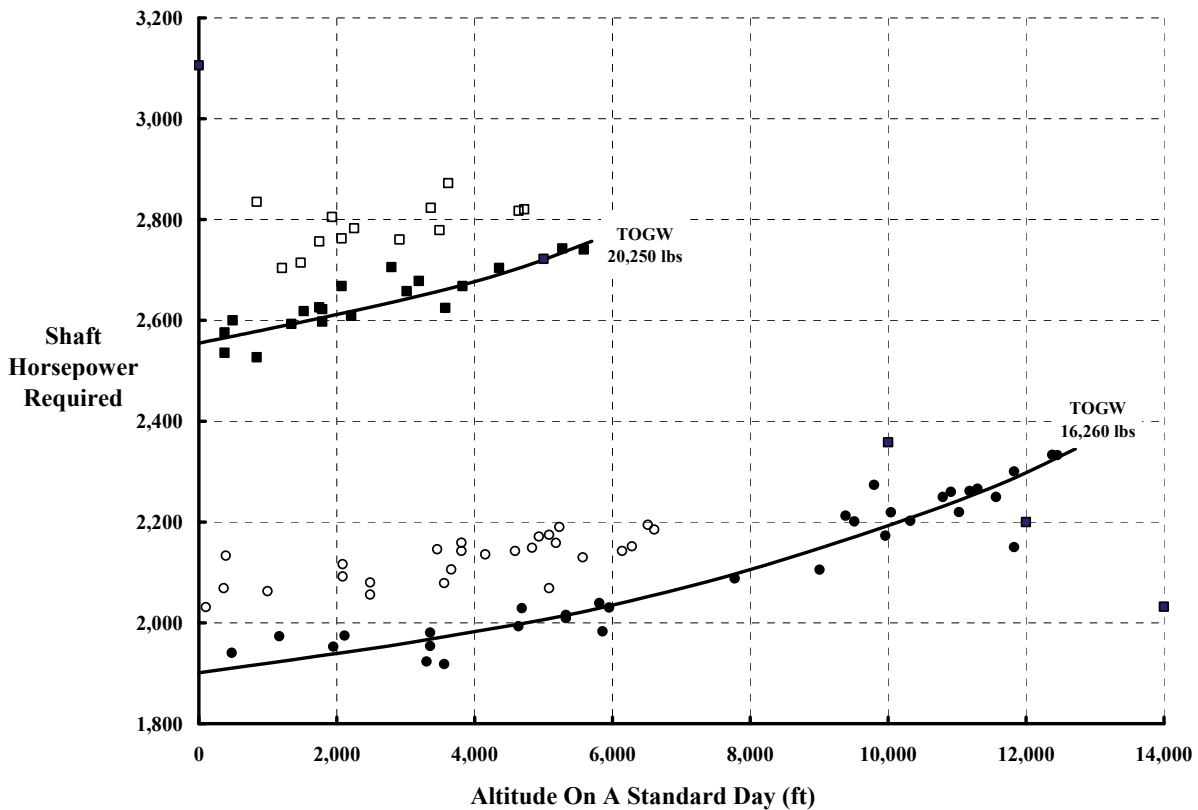


**Fig. 2-44. UH-60 power required to hover out of ground effect increases with altitude. (Open symbols for the YUH-60A; solid symbols for the UH-60A.)**

The combination of thorough reporting of the flight qualification coupled with subsequent flight research really benchmarked helicopter technical progress as it had evolved by the mid-1970s.

**Table 2-9. The UH-60A Improved Upon the YUH-60A**

<b>Basic Aircraft Information</b>	<b>YUH-60A</b>	<b>UH-60A</b>
<b>Power Installed</b>		
Twin Engines	YT700-GE-700	T700-GE-700
30 Min Rating SL, Std (installed)	1516 hp	1553 hp
100% RPM	20,000 rpm	20,900 rpm
Main Transmission Continuous Limit	2,791 hp	2,828 hp
Tail Transmission Continuous Limit	420 hp	Not quoted
<b>Weights</b>		
Weight Empty	11,182 lb	10,495 lb
Trapped Fluids	42 lb	50 lb
Crew (pilot, copilot, and gunner)	725 lb	725 lb
Weapons and Ammunition	164 lb	159 lb
Operating Empty Weight	12,113 lb	11,429 lb
Payload (11 combat-equipped troops)	2,640 lb	2,640 lb
Fuel (troop assault mission/includes a reserve)	2,100 lb	2,065 lb
Primary Mission Gross Weight (PEG)	16,853 lb	16,134 to 16,260 lb
Alternate Gross Weight (AGE)	19,930 lb	20,250 lb
Fuel Capacity/Weight	350 gal./2,275 lb	364 gal./2,366 lb
Test A/C EW With Inst, Full Oil, Fuel Drained	13,121 lb	11,820 lb
<b>Dimensions</b>		
<b>Main Rotor</b>		
Diameter	53 ft, 8 in.	Same
Blade Number	4	Same
Blade Chord	1.73 ft	1.73/1.75 ft
Solidity	0.0821	0.0826
100% RPM	263 rpm	257.9 rpm
100% Tip Speed	739.1 ft/sec	724.7 ft/sec
<b>Tail Rotor</b>		
Diameter	11 ft	Same
Blade Number	4	Same
Blade Chord	0.81 ft	Same
Solidity	0.1875	Same
100% RPM	1,214 rpm	1,189.8 rpm
100% Tip Speed	699.2 ft/sec	685.3 ft/sec
<b>Airframe</b>		
Nose-to-Tail Length	Not Avail	50 ft, 0.75 in.
Hub-to-Hub Distance	Not Avail	32.567 ft
Main/Tail Rotor(s) Clearance	Not Avail	2.8 in.
Vertical Tail Span	8 ft, 2 in.	Same
Vertical Tail Area	32.3 sq ft	Same
Horizontal Stabilator Span	172 in.	Same
Horizontal Stabilator Area	45 sq ft	Same
<b>Performance</b>		
<b>PMGW (equal payload of 2,640 lb)</b>		
Standard Day HOGE	8,800 ft	11,200 ft
Hot Day (35 °C at all pressure alts) HOGE	4,000 ft	5,900 ft
Cruise Speed (4,000 ft, 35 °C at eng MCP)	138 kts	147 kts
Economical Cruise Speed (4,000 ft, 35 °C)	130 kts	133 kts
<b>AGW</b>		
Standard Day HOGE	3,650 ft	5,000 ft
Hot Day (35 °C at all pressure alts) HOGE	Unable to HOGE	700 ft

### 2.3 HOVER PERFORMANCE

$$(2.38) \quad \text{HP}_{\text{HOGE}} = k_i \left( \frac{T}{550} \sqrt{\frac{T}{2\rho A}} \right) + \frac{\rho b c R V_t^3 C_{do}}{8 \times 550}.$$

The induced-power term is the first part of Eq. (2.38). It accounts for the power required by, say, the main rotor to support the helicopter weighing  $W$  pounds with a thrust of  $T$  pounds. The second term makes sure that the power to drag the main rotor blades around is included. The same equation can be used to approximate the power needed by the tail rotor to account for its anti-torque thrust. Because the engine generally provides power for accessories such as generators, hydraulic pumps, and cabin cooling or heating, an additional accessory power (that does not vary much with altitude) is frequently added.

A usable but very empirical “curve fit” to the UH-60A test results was created by Nagata [161]. It took the dimensional form

$$(2.39) \quad \text{ESHP}_{\text{Reqd.}} = 1.4572 \left( \frac{W}{550} \sqrt{\frac{W}{2\rho A}} \right) + 0.005897 \times \frac{\rho b c R V_t^3}{8 \times 550}.$$

This curve-fit equation was used by Nagata primarily to interpolate among the hover test data acquired out of ground effect at density altitudes below 2,160 feet. It failed to capture the measured results at density altitudes between 4,000 and 11,000 feet. An auxiliary graph was included in the report [161] to add a power increment reflecting this surprising and unexplained altitude effect.<sup>48</sup>

The effect of altitude on hover power required is clear enough when you study Eq. (2.38) for a moment. As you know, the density of air ( $\rho$ ) diminishes with increasing altitude. Therefore, the induced power will go up nearly as  $1/\sqrt{\rho}$ . The lesser power, used primarily to turn the blades, varies directly with density and, therefore, decreases with altitude. The proportions of the two, power-required elements, when calculated with UH-60A dimensions from Table 2-9 and with Eq. (2.39), for the primary mission gross weight of 16,260 pounds are

$$\text{ESHP}_{\text{Reqd.}} = 1,675 + 226 = 1,900 \text{ hp} \quad (\text{for Sea Level, Std Day})$$

$$\text{ESHP}_{\text{Reqd.}} = 1,804 + 195 = 2,000 \text{ hp} \quad (\text{for 5,000 ft, Std Day})$$

Thus, the helicopter’s hovering power required is dominated by the induced-power term. Based on the UH-60A flight test results, the crudest, first approximation that captures the physics would simply be

---

<sup>48</sup> During early flight testing of the OH-58D [145], I learned not to use the word “phenomena” for such initially unexplainable results. Teddy Hoffman (our OH-58D program leader whom I revere) told me—in the most humorous way—that upper management and other laymen absolutely quake in their shoes when the chief engineer calmly says, “the pilot won’t go above 60 knots because the tail wag vibration is so bad. Must be some phenomena.” Up until then I thought everyone had the problem-solving confidence that engineers have. Teddy also recommended keeping an active “too hard file.” He also defined and quantified the word “features” for me in a way I will never forget.

$$(2.40) \text{ ESHP}_{\text{Reqd.}} = 1.6 \left( \frac{W}{550} \sqrt{\frac{W}{2\rho A}} \right) = \frac{\text{Ideal Horsepower}}{0.625}$$

No doubt you are aware that experimental data virtually always contains some “scatter.” Rotorcraft flight testing offers no exception to this engineering fact. The results presented in Fig. 2-44 are for the most part quite representative of what the modern rotorcraft industry deals with on an everyday basis. The power-required differences between two virtually identical helicopters is frequently as large as Fig. 2-44 suggests. Engineering analysis just as frequently fails to pinpoint all the reasons. The data scatter during a given test period for one helicopter frequently is as large as Fig. 2-44 shows. Efforts by everyone to reduce or explain the scatter just as frequently fail to improve the situation. I have brought this fact of life to your attention using engine performance as an example in Fig. 2-45. Here you see an expanded ordinate (i.e., the referred shaft horsepower axis) and not starting from zero power. In short, I have “blown up” the data presentation in Fig. 2-45. This scale makes an error band of ±100 horsepower or roughly ±5 percent appear quite large. However, this is a realistic situation because even the most modern theories and experimental instrumentation rarely can reduce the uncertainty in how much power it takes to hover.

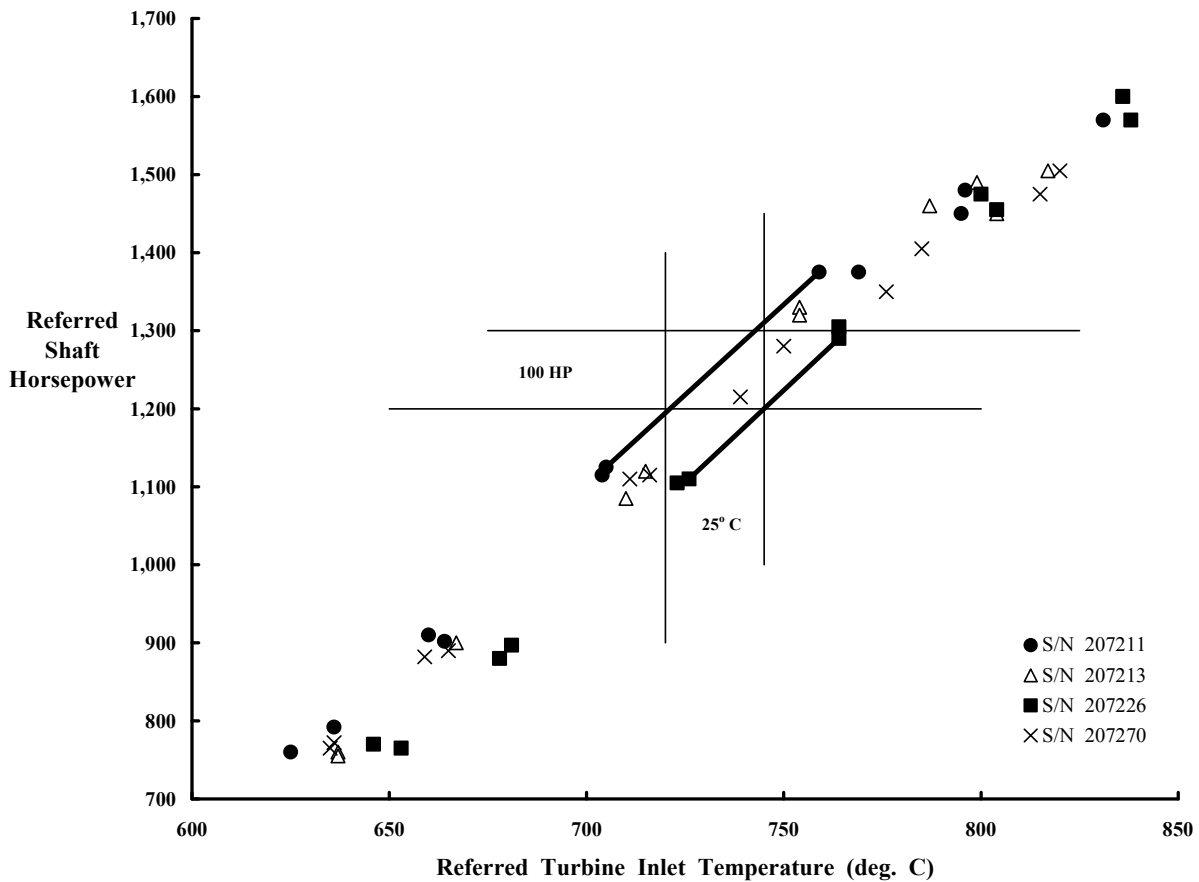


Fig. 2-45. “Identical” engines vary in performance.

## 2.3 HOVER PERFORMANCE

The real-life uncertainty of  $\pm 100$  horsepower at the primary mission gross weight of 16,260 pounds is hardly comforting to those who produce or use helicopters today. When viewed as if the power required were accurately known, the uncertainty translates to not knowing what weight can be lifted. Consider this view. The UH-60 requires roughly 2,000 horsepower to hover at low altitudes. This translates to about 8 pounds of lifted weight per horsepower. The uncertainty of  $\pm 100$  horsepower, therefore, equates to about  $\pm 800$  pounds in gross weight. But this  $\pm 800$ -pound uncertainty strikes at the useful load that contains the payload (2,640 pounds) and fuel (2,065 pounds). Plus or minus 800 pounds out of 4,705 pounds, therefore, is an uncertainty of  $\pm 17$  percent!

With this understanding of hover power required, let me proceed to examine engine power available in some detail. Two T700-GE-700 engines are installed in the UH-60A. Each engine is nominally rated at 1,553 *installed* horsepower at the sea level, standard day condition. The rating is called an intermediate rated power (good for no longer than 30 minutes at a time) or IRP by the U.S. Army. The total of 3,106 installed horsepower at sea level decreases with altitude as you learned earlier from the discussion about engines. Fig. 2-46 adds the final power-available line, *but not its data scatter*, to the power-required graph of Fig. 2-44. (I have removed the YUH-60A power-required data and put them in the “too hard file.”)

The power margin, as noted in Fig. 2-46, is the difference between engine power available and helicopter power required. At the point where this difference shrinks to zero, the helicopter has reached the altitude where it can just hover out of ground effect. This altitude is referred to as the hover ceiling. You might note in passing that the power margin index that I used in the broad survey of 550 shaft-driven helicopters can now be related to the practical power margin in Fig. 2-46. For example, at a gross weight of 16,260 pounds the ideal HOGE horsepower required for the UH-60A is

$$HP_{\text{ideal}} = \frac{16,260}{550} \sqrt{\frac{16,260}{2 \times 0.0023769 \times 2,262}} = 1,150 \text{ hp}.$$

The simple power-margin index becomes  $3,106/1,150 = 2.7$ . At 20,250 pounds the index (about 1.94) is still favorable, although I have never talked to a pilot who said he ever had enough power margin.

As it turned out, the Sikorsky/General Electric team made some reasonable and cost effective changes in going from the YUH-60A to the UH-60A. For example, the engine speed was increased and the rotor system was slowed down as Table 2-9 notes. This increased the practical power margin in production by about 40-plus horsepower.

While the data scatter in *power available* is not shown in Fig. 2-46, that does not mean it does not exist. The flight qualification test report for the YUH-60A provided a very clear data-scatter example as you saw in Fig. 2-17, page 80. In addition, Fig. 2-45 shows how four preproduction engines performed in General Electric’s test cell before delivery. The variation

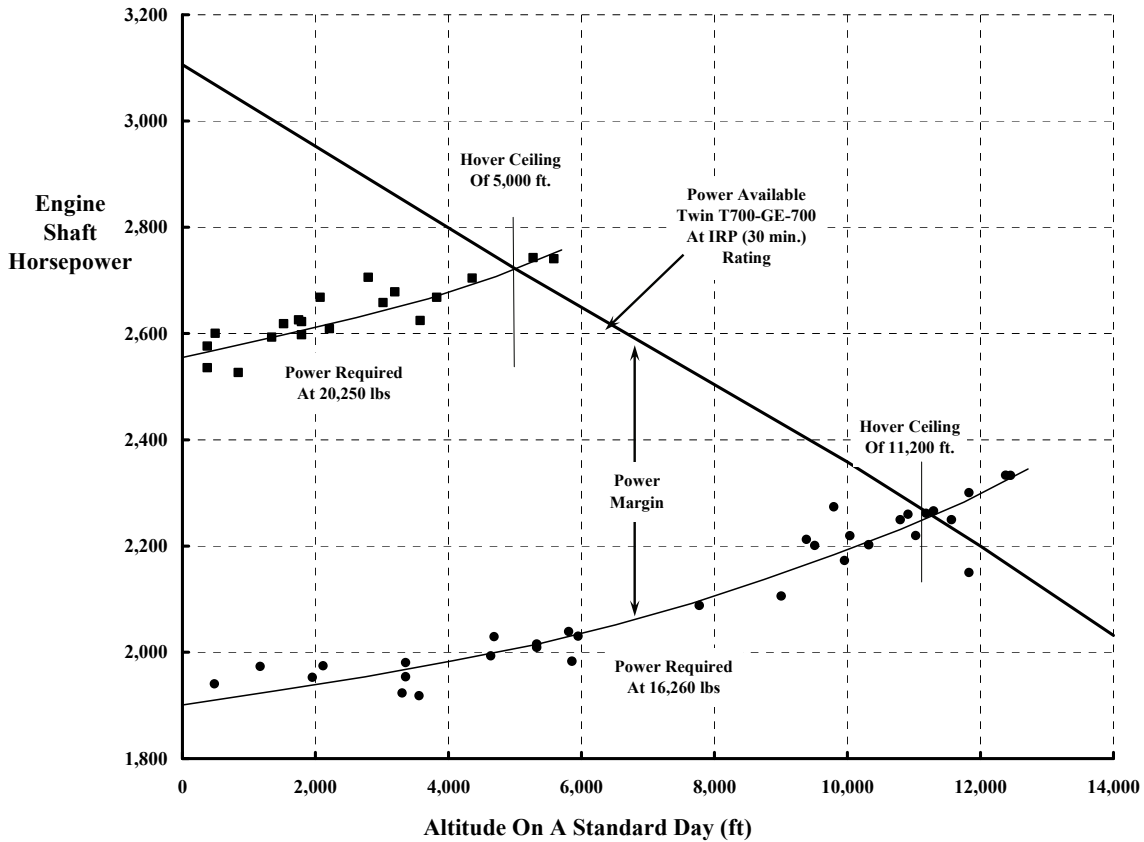


**Fig. 2-46. Power margin of the UH-60A decreases with altitude. (Solid symbols for the UH-60A; open symbols for the YUH-60A removed for clarity.)**

in turbine inlet temperature required to produce 1,250 horsepower is about 25 °C. This illustrates a representative difference that can be expected in production. Although I have not differentiated it, each engine was tested at turbine speeds from 19,000 to 21,000 rpm.

Before introducing transmission-limited power, let me use the power-available data from Fig. 2-45 to raise a very important point. The question posed by the figure is this: If you were the engine manufacturer, what turbine inlet temperature would you pick to ensure consistent delivery of engines rated at 1,250 horsepower? Apparently, as you can see from the figure, all four prototype engines could be delivered if you chose a temperature of 755 °C. A helicopter producer would, quite naturally—in view of the power required to hover *and* his uncertainties—strongly suggest that he get delivery of engines with an extra 100 horsepower (i.e., the 1,350 horsepower at 755 °C capability achieved by the YT700-GE-700, Serial Number 207211 engine). Then his helicopter might have the more competitive hover performance. But you, as the engine manufacturer, probably could deliver only 10 out of 1000 production engines to this helicopter producer. This important point does not stop here.

## 2.3 HOVER PERFORMANCE

You, as the helicopter manufacturer, must assure the certifying agency *and* the user/pilot that the flight handbook performance will be achievable for a reasonable period after delivery. Keep in mind that the engine will deteriorate over 1,000 hours of operating time. While more than 1,250 horsepower will be available at 755 °C when your helicopter is delivered, the pilot, after a year or two of operation, will quite likely see 755 °C plus another 15 °C (or 770 °C) on his turbine temperature gauge just to lift off at the same conditions. This means that both manufacturers must keep the user in mind by including a field degradation allowance before settling on engine performance used to create the pilot's handbook.

The engine manufacturer needs to profitably deliver virtually all engines he makes, the helicopter producer needs to be profitably competitive, and the user needs to have economical performance over the long haul. All these needs are influenced by the data presented in Fig. 2-45 and Fig. 2-46. A compromise might easily be a 1,200-horsepower engine that operates at or below 740 °C when delivered. The pilot would be informed (in the flight handbook) that when the turbine temperature starts reading close to 755 °C, a check liftoff should be performed, and an engine overhaul is imminent.

Now on to the part that transmissions play in hover performance.

The third key factor involved in the physics of hover performance is the rating of the transmission. The limit is frequently expressed in terms of the engine shaft horsepower. However, it is primarily a limit torque in some particular gear that defines the limit. This torque and an associated rotational speed are really closer to the heart of a transmission limit. The main-rotor-transmission output torque is displayed to the pilot, usually on a percent gauge. The pilot, therefore, monitors both a turbine gas temperature gauge for thermodynamic limits and a torque meter gauge for mechanical limits.

The YUH-60A main rotor transmission was uprated from 2,791 engine shaft horsepower (ESHP) at 263 main rotor rpm to 2,828 ESHP at 257.9 rpm for the production UH-60A. Fig. 2-47 shows this higher rating added (as the horizontal dashed line) to the power-required and power-available example you have seen developing. For this modern helicopter the transmission was designed and qualified to allow for growth in takeoff gross weight. The margin between power required at the UH-60A alternate gross weight of 20,250 pounds and the transmission-limited ESHP of 2,828 horsepower is sufficient for a sea-level takeoff at a higher weight of 21,800 pounds. More practically, this margin allows for reasonable flying and maneuvering in turbulent air at the alternate, 20,250-pound gross weight.

Over the decades, mechanical drive system technology—both engineering and manufacturing—has been impressive. It is quite rare to have a transmission not perform in the field as advertised. When failures have occurred, they have generally been traced to a minor detail that did not quite fit all previous experience. The design is repaired, and the new experience is incorporated in the “don't ever forget file.” This experience has, in a large measure, accounted for the very much improved safety record of helicopters.

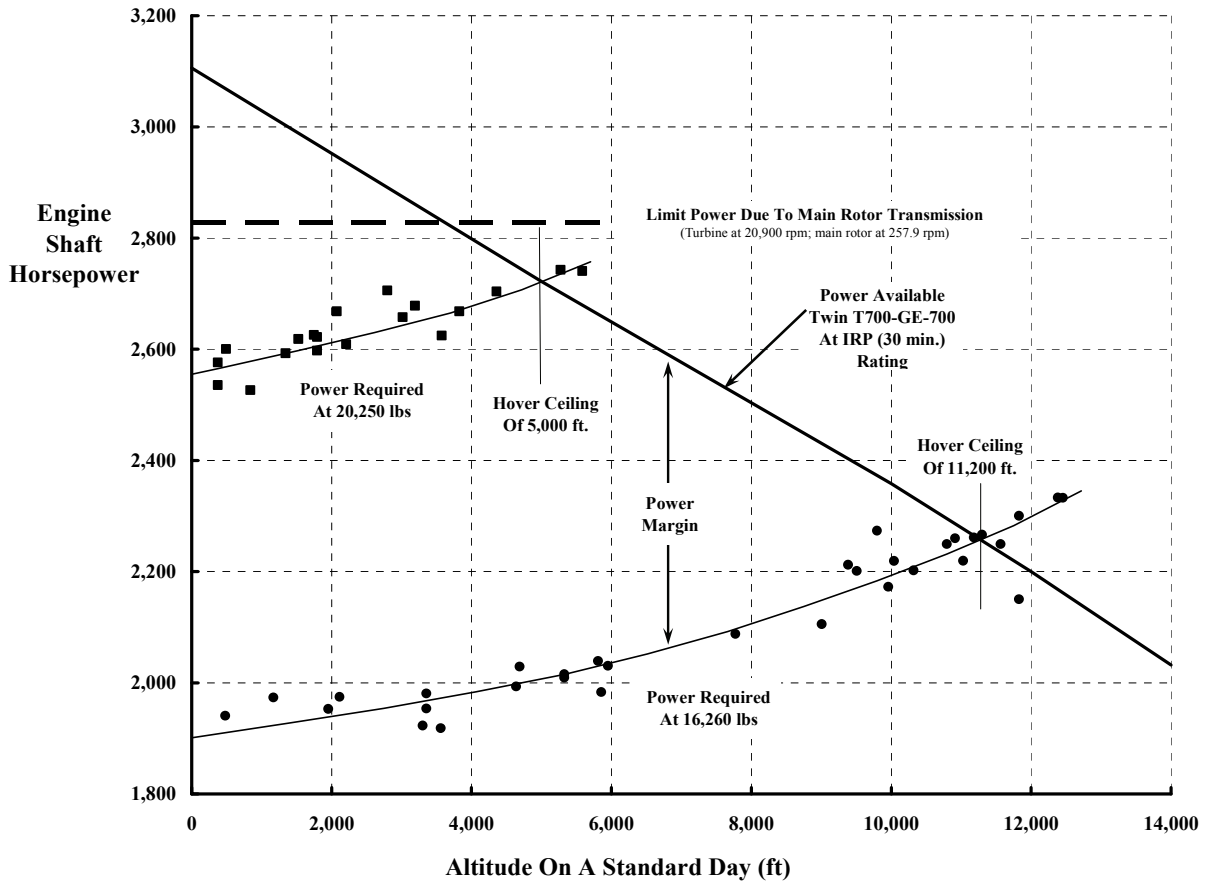


**Fig. 2-47. The transmission limit can put a cap on rotorcraft hovering performance as the dashed line shows for the UH-60A.**<sup>49</sup>

The final display of modern helicopter hovering performance is not in the engineering form of Fig. 2-47. The more useful final graph is hovering ceiling (i.e., pressure altitude in feet) versus gross weight. For example, UH-60A test data provided in appendix E of reference [161] displays the hover capability in the more common form you saw in Fig. 2-43, which opened this hover performance discussion several pages ago. This summary for the UH-60A is shown in Fig. 2-48 for both a standard day and an Army-defined hot day (where the outside air temperature is 35 °C at all pressure altitudes). I have added the YUH-60A hot-day results from reference [160] to complete this example.

<sup>49</sup> In setting the torque limits, transmission designers are most concerned with the loads acting on each tooth of each gear. These loads act to both bend and shear a gear tooth from its “hub.” Tooth-bending stresses are high, and there can be a great deal of scrubbing involved. Long, maximum-power runs “on the bench” using several transmissions are generally made before a transmission is installed in the first helicopter. I doubt you can find any other transmission that converts as much torque per pound of weight empty. In my opinion, these designers stand head and shoulders above those who design transmissions for lesser applications.

## 2.3 HOVER PERFORMANCE

Fig. 2-48 clearly shows that the UH-60A hover ceiling was an improvement over the preproduction YUH-60A. There is, however, an even better way to see successive product improvements. This more informative picture comes by showing hover ceiling as a function of useful load (*not gross weight* as in Fig. 2-48). Then the comparative results between the two UH-60A-series helicopters used in this illustration are much more impressive as you can appreciate from Fig. 2-49.

Let me complete this portion of your introduction to modern helicopter hovering performance with another survey result. The background you have just finished reading should let you quickly understand and then appreciate Fig. 2-50. The 150-plus different helicopter models (out of 550) form an envelope of product capability offered by the rotorcraft industry up to 1995. This envelope has continually expanded over the last five decades. Turbocharged piston engines gave early helicopters high-altitude performance with a very useful load. Turbine engines quickly led to larger helicopters that increased useful load tenfold, and then tenfold again.

The modern results achieved by the rotorcraft industry shown in Fig. 2-50 have come, in part, by investing heavily in aerodynamic research. Perhaps a disproportionate share of this aerodynamic research money has gone to reducing hover power required. Two facts have, however, clearly emerged from this long effort to mature the helicopter. They are:

1. A reduction in the uncertainty of initial power-required estimates has been achieved over five decades.
2. When power required is viewed in a nondimensional form,<sup>50</sup> it is not at all obvious that substantial progress in hovering efficiency has been achieved.

In May 1980, a measure of rotorcraft aerodynamic theory versus experimental results was provided by the aerodynamic staff at Bell [168]. The uncertainty in predicting a hover ceiling/gross weight result such as Fig. 2-48 was shown to be about  $\pm 3$  percent. The power available was assumed to be known exactly in this study of 17 helicopters. Therefore, the uncertainty lay in predicting power required to hover. Considering the complexities of this engineering problem, you may well think that  $\pm 3$  percent is rather good. However, the Bell analysis [168] notes that this uncertainty amplifies to  $\pm 18$  percent of fuel load,  $\pm 6.7$  percent of useful load, or  $\pm 10.5$  percent of payload when applied to a Bell Model 206A.

---

<sup>50</sup> You will remember this nondimensional form from Eqs. (1.6), (1.7), and (1.8) on page 8. Two coefficients were defined that remove—to a first-order approximation—effects of wide ranges in helicopter size and configuration. The nondimensional, coefficient forms for rotor thrust, Eq. (1.6), and power, Eq. (1.7), can be used for a complete helicopter by simply changing the subscripts. That is,

$$C_T = \frac{T}{\rho AV_t^2} \rightarrow C_w = \frac{W}{\rho AV_t^2} \quad \text{and} \quad C_P = \frac{P}{\rho AV_t^3} \rightarrow C_{P_{\text{Reqd.}}} = \frac{550 \times \text{ESHP}_{\text{Reqd.}}}{\rho AV_t^2}$$

## 2.3 HOVER PERFORMANCE

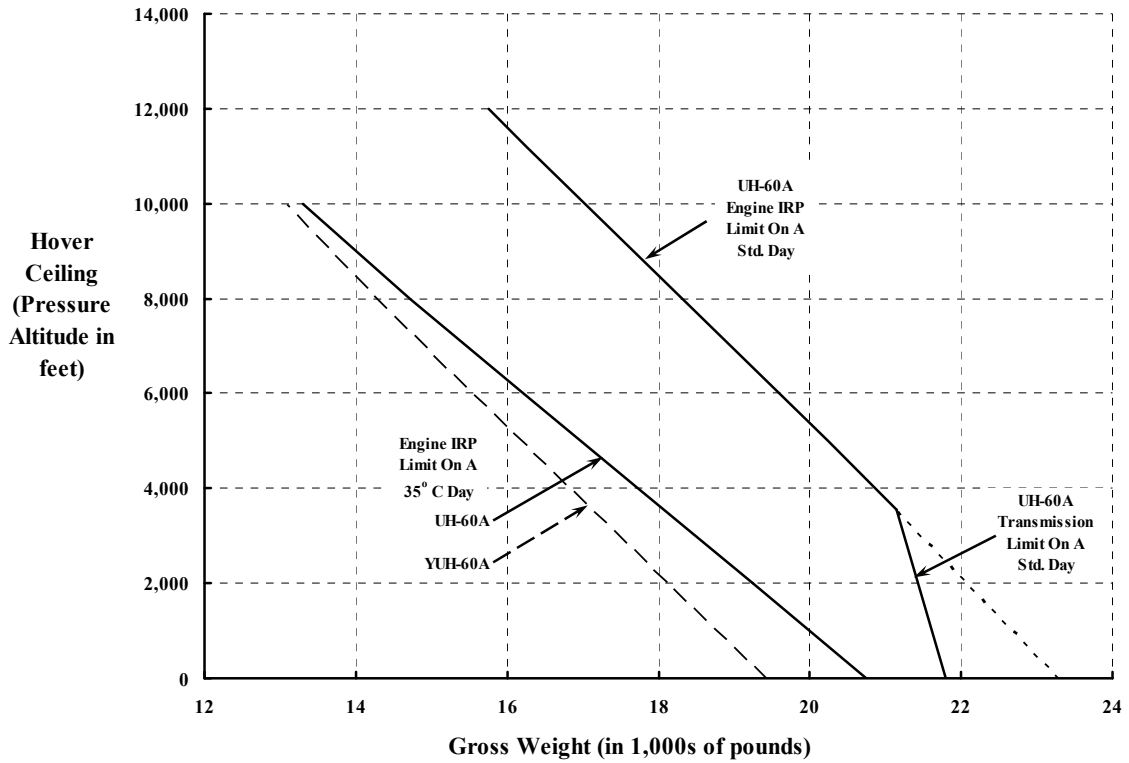


Fig. 2-48. The final output of the engineering analysis of Fig. 2-47 is found in this more common format.

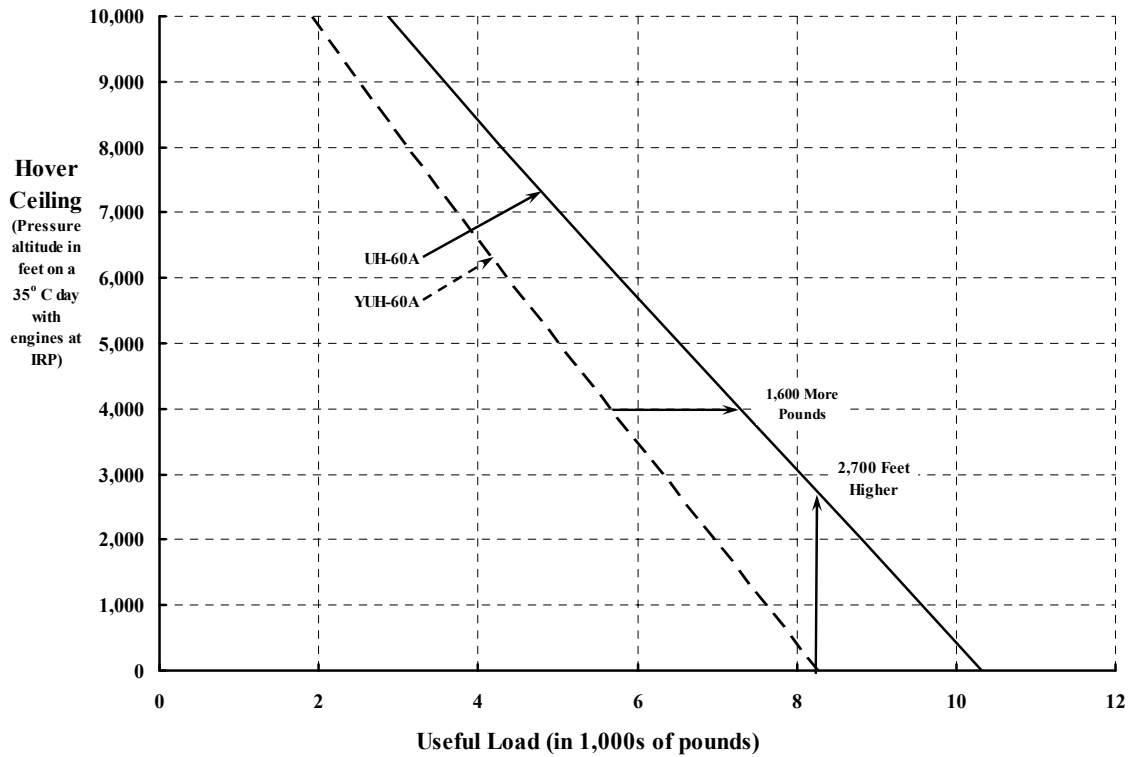
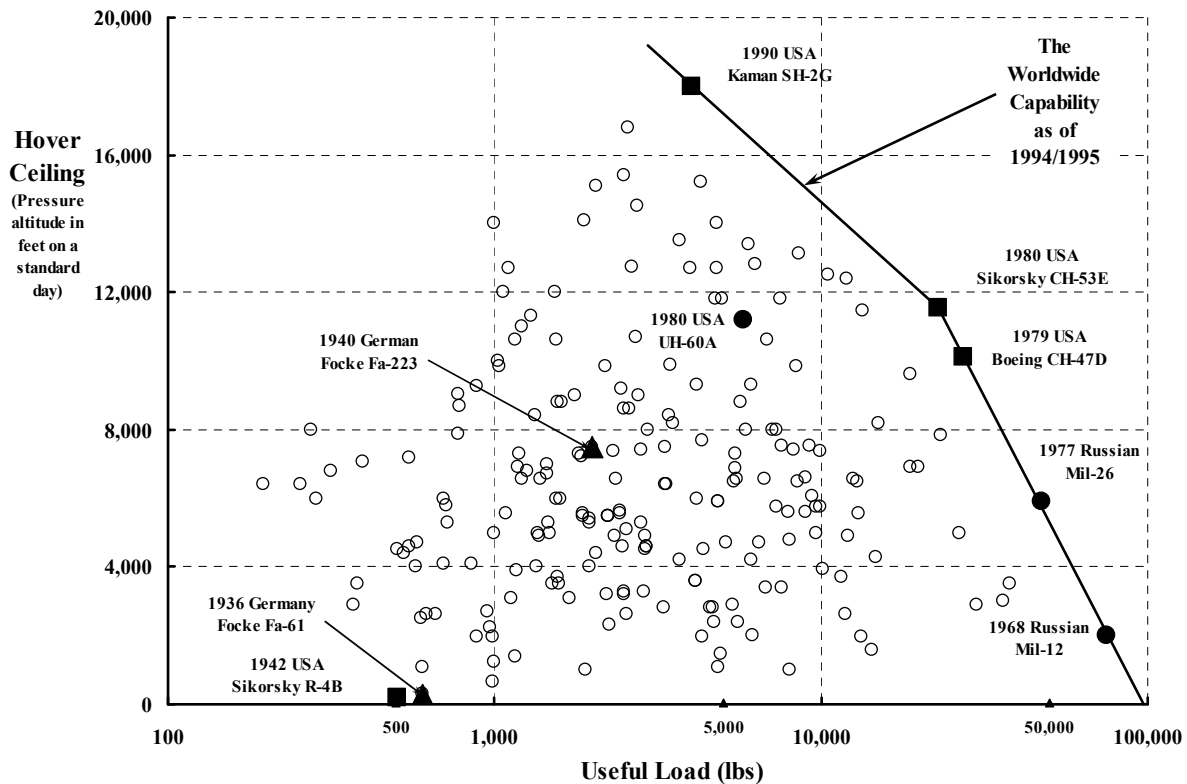


Fig. 2-49. The UH-60A was a major improvement on the YUH-60A when compared on a useful-load basis.

## 2.3 HOVER PERFORMANCE



**Fig. 2-50. The industry has continually expanded the hover ceiling and useful load capabilities of helicopters. (Note: UH-60A at 11,200 feet with PMGW = 16,260 and WE = 10,465.)**

The question of how much helicopter performance has improved is continually asked. In overall product terms, I believe you should be impressed, but an assessment of Army helicopter performance trends [169] gave a somewhat mixed opinion. Richard Lewis,<sup>51</sup> the author of this April 1972 review, concluded that

“...the nondimensional performance of Army rotorcraft is essentially independent of aircraft configuration. This is not meant to imply that progress is lacking. It should be kept in mind that the data represent only the current generation of Army rotorcraft and they are close contemporaries. It does suggest that drastic variations in demonstrated performance levels are not easily achieved and warrant examination.

It is hoped that the data presented herein will be of use to rotorcraft designers and evaluators. The understanding that performance trends are closely grouped will permit attention to be focused toward important technical areas such as noise, directional control and vibration, where breakthroughs in rotorcraft design are both necessary and desirable.”

<sup>51</sup> Dick was then Deputy Director of Flight Test for the U. S. Army Aviation Systems Test Activity at Edwards Air Force Base in California. When he wrote his paper, he and his group had a wealth of flight test data from every helicopter that had passed through. He was able to support his conclusions using data from just six helicopters.

Fig. 2-51 provides a somewhat different conclusion 20 years later. This hover-engine-horsepower-required versus takeoff-weight survey (but in the classical  $C_p$  versus  $C_w$  coefficient form) includes 54 different flight tests [108, 109, 115, 116, 118, 121, 124, 125, 133, 170-188, 190-206] and [207-210]. Every  $C_p - C_w$  data point for each test is included in Fig. 2-51. Thus, “data scatter” in both configuration and experiment is apparent. A  $\pm 12$  percent spread from the semiempirical result of

$$(2.41) \quad C_{P_{\text{Reqd.}}} = 0.0157 C_w + 1.045 C_w^{3/2}$$

captures hover-power-required technology for today’s helicopter types.

Equation (2.41) is handy and rather easy to derive when you start with the nondimensional form of the basics. Equation (2.38), in nondimensional form, becomes

$$(2.42) \quad C_p = \frac{k_i}{\sqrt{2}} C_T^{3/2} + \frac{\sigma C_{\text{do}}}{8}.$$

Suppose now that the airfoil drag coefficient ( $C_{\text{do}}$ ) is calculated as

$$(2.43) \quad C_{\text{do}} = \frac{C_{\text{do}}}{C_\ell} C_\ell \quad \text{where} \quad C_\ell = \frac{6C_T}{\sigma} \quad \text{so that} \quad C_{\text{do}} = \frac{C_{\text{do}}}{C_\ell} \frac{6C_T}{\sigma} = \frac{6}{(L/D)_{\text{Airfoil}}} \frac{C_T}{\sigma}.$$

Then it follows that

$$(2.44) \quad C_p = \frac{k_i}{\sqrt{2}} C_T^{3/2} + \frac{\sigma C_{\text{do}}}{8} = \frac{k_i}{\sqrt{2}} C_T^{3/2} + \frac{\sigma}{8} \frac{6}{(L/D)_{\text{Airfoil}}} \frac{C_T}{\sigma} = \left[ \frac{6}{8(L/D)_{\text{Airfoil}}} \right] C_T + \frac{k_i}{\sqrt{2}} C_T^{3/2}.$$

A rational value for the airfoil lift-to-drag ratio of around 50, and a just as rational value for the induced-power correction factor ( $k_i$ ) of 1.48, leads to Eq. (2.41). Using engine power and weight for the coefficients completes the insight. The implication of this result is that the equation describes an envelope of best performance for any typical modern helicopter. In the ideal case,  $k_i = 1.0$ , which shows that improvement is possible!

There is another way to compare optimum performance of several helicopters. This frequently employed view is shown in Fig. 2-52 and uses the system aircraft hover Figure of Merit (FM) as the measure of optimum. You will recall that this parameter is defined as the ratio of ideal power to actual power. In aircraft terms, this amounts to

$$(2.45) \quad \text{A/C Hover Figure of Merit} = \frac{\frac{1}{\sqrt{2}} C_w^{3/2}}{\text{Actual } C_{\text{SHP}}}.$$

The conventional approach to displaying aircraft FM is versus the weight coefficient ( $C_w$ ). This choice for the abscissa is not used in Fig. 2-52 because the many helicopters shown all have a considerable difference in solidity ( $\sigma$ ). The basis for using  $C_w^{3/2}$  divided by solidity is arrived at as follows:

## 2.3 HOVER PERFORMANCE

$$(2.46) \text{ A/C Hover Figure of Merit} = \frac{\frac{1}{\sqrt{2}} C_w^{3/2}}{\text{Actual } C_{SHP}} = \frac{\frac{1}{\sqrt{2}} C_w^{3/2}}{\frac{\sigma C_{do}}{8} + \frac{k_i}{\sqrt{2}} C_w^{3/2}} = \frac{1}{\frac{\sqrt{2} C_{do}}{8} \left[ \frac{\sigma}{C_w^{3/2}} \right] + k_i}.$$

Because the group of helicopters use nominally the same airfoil for the main rotor blades (i.e.,  $C_{do}$  is about 0.01), the primary variable is  $C_w^{3/2}/\sigma$ . This keeps all helicopters in the same range on the abscissa. Furthermore, Fig. 2-52 shows that  $C_w^{3/2}/\sigma$  must approach 0.01 to maximize FM. The limit is, of course, that  $C_w/\sigma$  must not be too high or the airfoil average lift coefficient [per Eq. (2.43)] giving maximum airfoil lift-to-drag ratio will be exceeded. Equation (2.46) obviously says the maximum FM cannot exceed  $1/k_i$ , which occurs if it were possible to have a zero airfoil drag coefficient. The heavy, solid line on Fig. 2-52 using Eq. (2.46) was computed with  $C_{do} = 0.01$  and  $k_i = 1.48$ , which places the line in the semiempirical category. Clearly, a much more detailed engineering calculation is required to explain the spread in FM for the 54 examples.

A more detailed engineering estimate of engine horsepower required to hover takes the form

$$(2.47) \text{ ESHP} = \frac{\text{RHP}_{\text{Main Rotor(s)}}}{\eta_{\text{Main Rotor(s)}}} + \frac{\text{RHP}_{\text{Tail Rotor(s)}}}{\eta_{\text{Tail Rotor(s)}}} + \text{SHP}_{\text{Accessory}}.$$

In this approach, the engine delivers power to the main rotor ( $\text{RHP}_{mr}$ ) but a transmission efficiency ( $\eta$ ), on the order of 0.97, is charged. This is true if the helicopter has a tail rotor as well. Of course the engine also delivers power to run accessories such as the electrical and hydraulic subsystems as well. All computations are made for the helicopter at a given weight, which means that rotor thrust is greater than the weight. This helps to account for rotor downwash on the helicopter fuselage and appendages. With Eq. (2.47) in mind, consider the amount of engine power required by the total helicopter and then by the tail rotor in the single rotor configuration for four helicopters evaluated in 1976.

### 2.3.3 UTTAS and AAH Hover Performance

Perhaps the most extraordinary hover performance experimental results I ever encountered came when the competitive flight test data for the utility tactical transport aircraft system (UTTAS) and advanced attack helicopter (AAH) became available. The Sikorsky YUH-60A [123] competed with the Boeing-Vertol YUH-61[124] for the utility helicopter, and the Bell YAH-63A [125] competed with the Hughes YAH-64A [126]. The experimental engine power required to hover as a function of weight for the four configurations is shown in Fig. 2-53. The data, in aircraft coefficient form, shows that the two utility helicopters are nearly indistinguishable from Eq. (2.41) in nondimensional performance. What deviates are the two attack helicopters; the YAH-63A being on the low side of Eq. (2.41) by about -5 percent and the YAH-64A being on the high side by +5 percent.

## 2.3 HOVER PERFORMANCE

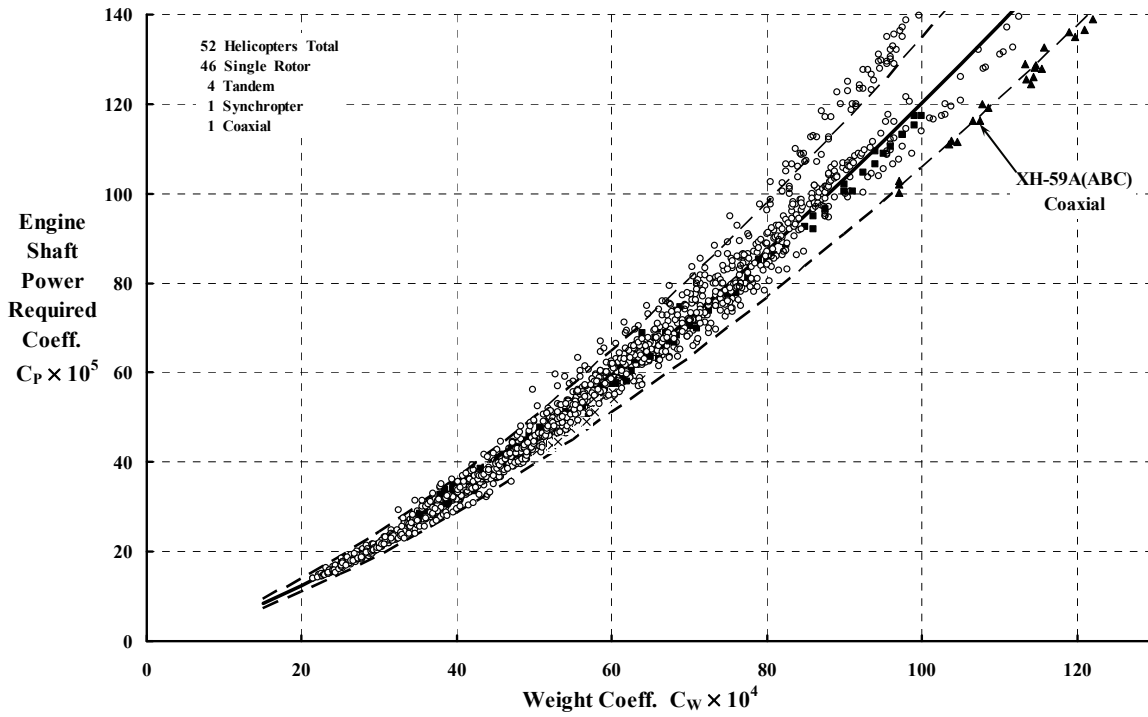


Fig. 2-51. The industry has established conventional helicopter hover power required to within  $\pm 12$  percent (single rotors are open circles; tandems are black squares).

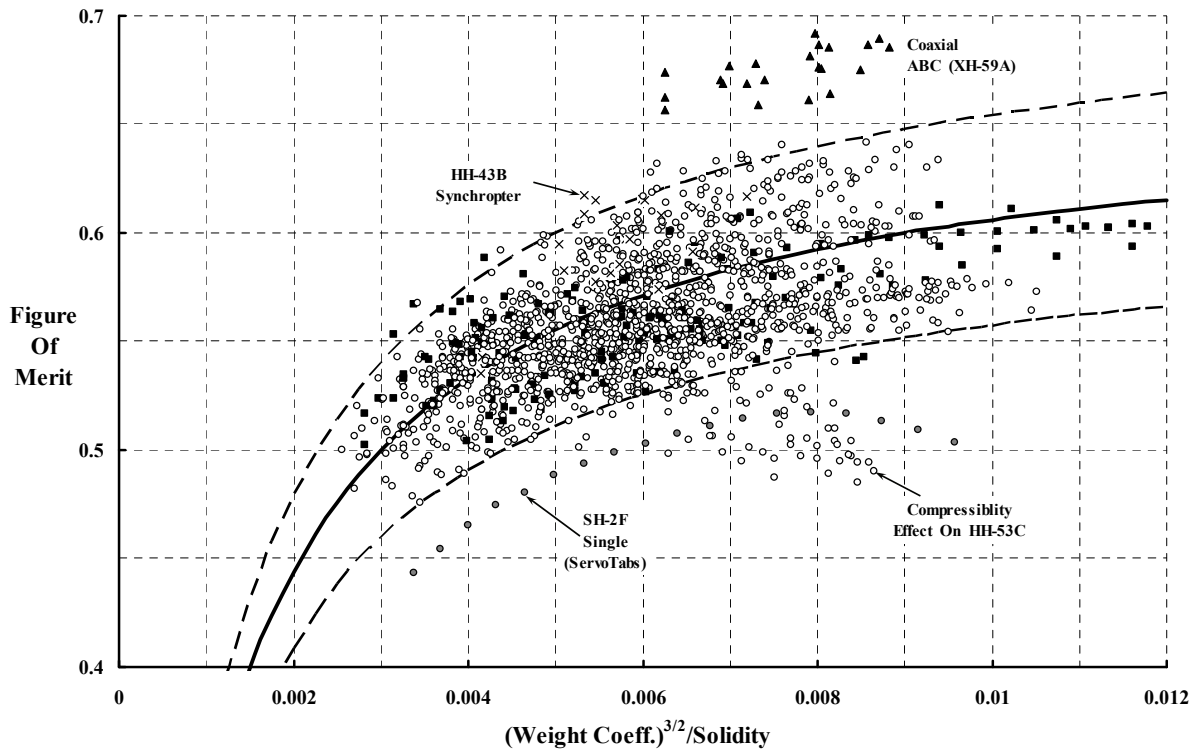


Fig. 2-52. Modern helicopter aircraft FM is far from ideal.

### 2.3 HOVER PERFORMANCE

The primary differences between the four configurations are due to tail rotor horsepower required and the secondary differences are in main rotor solidity. The test reports for the four helicopters included tail rotor power measurements. Thus, measured tail rotor power can be subtracted from the measured total power illustrated by Fig. 2-53, and this leads to Fig. 2-54, which was observed in 1987[211].

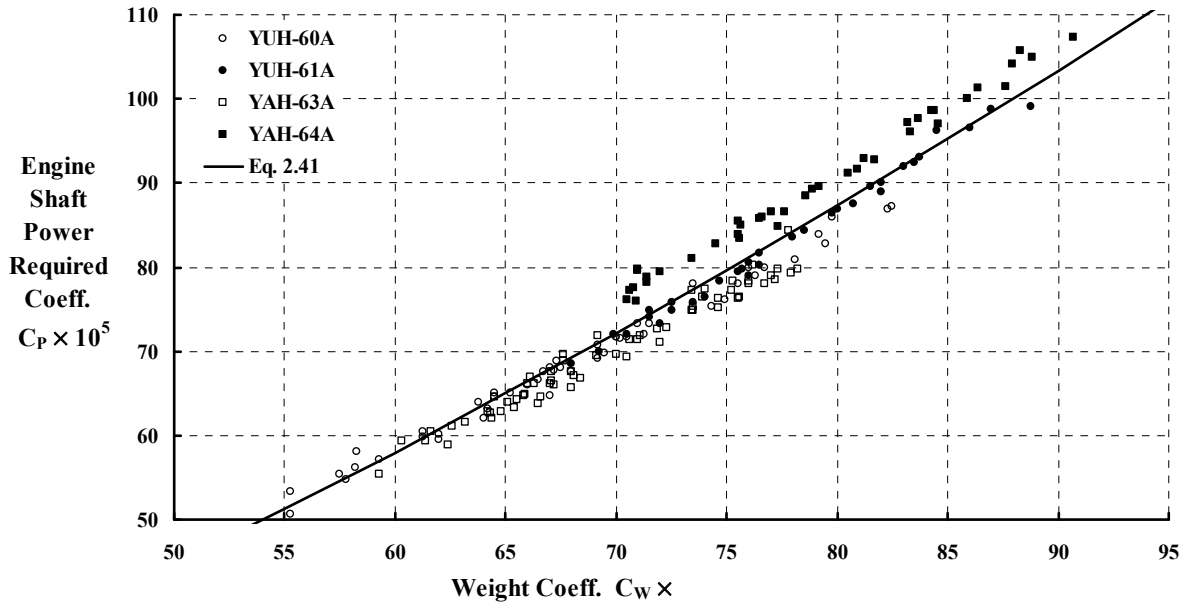


Fig. 2-53. All four helicopter hover performance results were extraordinarily close.

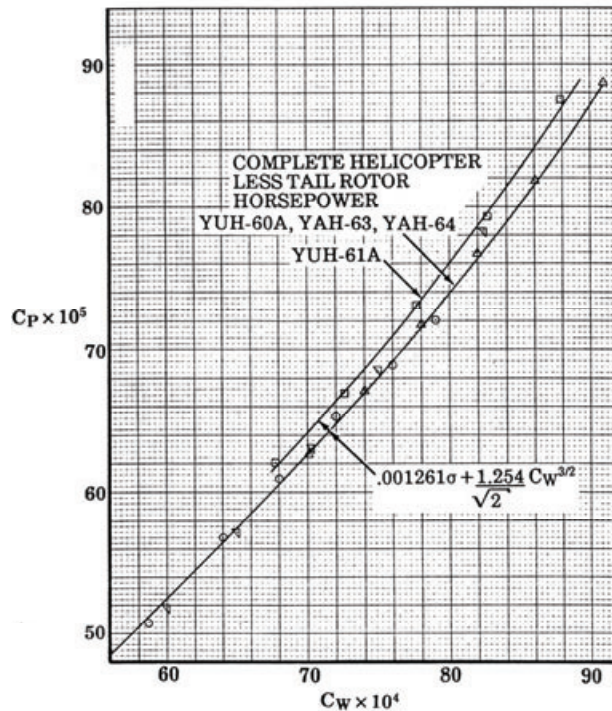


Fig. 2-54. Without tail rotor power, all four helicopters had the same  $C_P$ - $C_W$  performance when solidity differences were accounted for [211].

I find it quite amazing that both UTTAS and AAH helicopters could have their HOGE performance results estimated from such a simple engineering approximation as

$$(2.48) \quad C_p = 0.001261\sigma + \frac{1.254}{\sqrt{2}} C_w^{3/2}.$$

The comparative tail rotor performance for these four helicopters is also interesting.

### 2.3.4 Tail Rotor Performance in Hover

As a reminder, the evolution of the helicopter up until Igor Sikorsky's breakthrough in the early 1940s was dominated by inventors who used large main rotors in pairs. These early twin-rotor helicopters arranged the rotors in coaxial, side-by-side, tandem, and quadrotor configurations. The early inventors sought to achieve equilibrium with the engine input power and torque with both rotors lifting—in the belief that this was the most efficient helicopter that could be achieved. In fact, the side-by-side arrangement was used by Henrich Focke when he stunned the world in 1936 with the first truly successful helicopter, his F. 61. Focke went into production with his FA 223. A countryman, Anton Flettner, followed shortly with his equally successful FL 282. Flettner's design intermeshed the two main rotors in the fashion of an eggbeater, and this became the synchropter configuration.

It was in defense of this progress made in Germany at the start of World War II that Sikorsky developed his now famous VS-300. He used a large, single main rotor for lifting and a much smaller rotor to produce an anti-torque force. The tail rotor, as originally developed, contributed little lift; it served only to provide a basic anti-torque force and a measure of directional control. This comparatively small rotor was placed at the end of a tail boom, and its thrust was directed to the side as Fig. 2-55 shows.

Surprisingly, in the configuration Sikorsky pioneered, the distance aft ( $l_{tr}$ )—measured from the main rotor shaft—at which the tail rotor thrust (i.e.,  $T_{tr}$  or the anti-torque force) acts is not a major factor in the tail rotor power required to hover. This is because the moment arm is conventionally about equal to the main rotor radius ( $R$ ). That is,  $l_{tr}$  is approximately equal to  $R$ . With this rough approximation, the simplest aerodynamic theory shows that

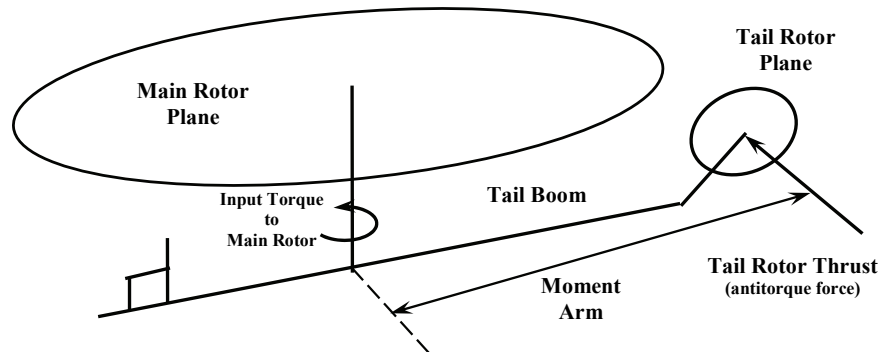


Fig. 2-55. Single rotor helicopter torque equilibrium.

## 2.3 HOVER PERFORMANCE

$$\begin{aligned}
 Q_{mr} &= \frac{P_{mr}}{\Omega_{mr}} = \text{main-rotor torque} \\
 (2.49) \quad T_{tr} &= \frac{Q_{mr}}{l_{tr}} \approx \frac{Q_{mr}}{R} = \frac{P_{mr}}{R\Omega_{mr}} = \frac{P_{mr}}{V_t} = \frac{550HP_{mr}}{V_t} = \text{tail-rotor thrust} \\
 HP_{tr} &\approx \frac{T_{tr}^{3/2}}{550\sqrt{2\rho A_{tr}}} = \frac{1}{550\sqrt{2\rho A_{tr}}} \left[ \frac{550HP_{mr}}{V_t} \right]^{3/2} = \text{tail-rotor horsepower}
 \end{aligned}$$

Thus, the tail rotor horsepower ( $HP_{tr}$ ) is more influenced by its own size ( $A_{tr}$ ), the main rotor horsepower ( $HP_{mr}$ ), and the main rotor tip speed ( $V_t$ ).

Completing the comparison of the four UTTAS/AAH configurations is quite informative. Consider the hover out of ground effect (HOGE) situation at the U.S. Army hot-day design condition where the pressure altitude is 4,000 feet and the outside air temperature is 95° F. At this ambient air condition, the density is 0.00192 slugs per cubic foot. Suppose you accept that the main rotor horsepower can be calculated from Eq. (2.48). Ignore transmission efficiency and accessory power for this example. Then, with the data from Table 2-10, a new table of results, Table 2-11, can be constructed. The Army's test reports [123-126] each give the gross weight that can be hovered out of ground effect on this hot-day condition. These weights are tabulated across the first row of Table 2-11. Using these weights, the main rotor "thrust" coefficient is calculated, based on gross weight from

$$(2.50) \quad C_w = \frac{GW}{\rho A_{mr} V_{t-mr}^2}$$

where ( $\rho$ ) is the air density, ( $A_{mr} = \pi R^2$ ) is the main rotor disc area, and ( $R$ ) is the main rotor radius. The main rotor tip speed ( $V_t$ ) is the reference velocity. You should be aware that the true main rotor thrust is generally 2 to 5 percent greater than the gross weight because the rotor downwash creates an airframe vertical drag.

Given the weight coefficient, I have obtained the total engine power coefficient ( $C_{P_{eng}}$ ) for each configuration from the flight test data given in each report. Then, for the sake of completeness, the engine horsepower required to hover is calculated with

$$(2.51) \quad SHP = \frac{\rho A_{mr} V_{t-mr}^3}{550} C_{P_{eng}}$$

The main rotor power coefficient ( $C_{P_{mr}}$ ) has been calculated in accordance with Eq. (2.48) and recorded on line 5 of Table 2-11. This leads to the main rotor horsepower ( $HP_{mr}$ ) and the main rotor torque—which the tail rotor thrust ( $T_{tr}$ ), acting at the moment arm ( $l_{tr}$ ), must counterbalance—being calculated by

$$(2.52) \quad HP_{mr} = \frac{\rho A_{mr} V_{t-mr}^3}{550} C_{P_{mr}} \quad \text{and therefore} \quad Q_{mr} = \frac{550HP_{mr}}{V_{t-mr}/R_{mr}} = T_{tr} l_{tr}$$

**Table 2-10. UTTAS and AAH Parameters**

Parameter	YUH-60A	YUH-61A	YAH-63A	YAH-64A
<b>Primary Mission GW (lb)</b>	<b>16,853</b>	<b>16,410</b>	<b>16,054</b>	<b>14,242</b>
<b>Main Rotor</b>				
Diameter (ft)	53.67	49	51.5	48
Design RPM	263	286	276	289
Tip Speed (fps)	739	734	744	726
Blade No.	4	4	2	4
Chord (ft)	1.73	1.917	3.55	1.75
Solidity	0.0821	0.0996	0.0878	0.092
Disc Area (ft <sup>2</sup> )	2,262.3	1,885.7	2,083.1	1,809.6
<b>Tail Rotor</b>				
Diameter (ft)	11	10.167	9.5	8.33
Design RPM	1,214	1,297	1,446	1,411
Tip Speed (fps)	699.2	688	719	615
Blade No.	4	4	2	4
Chord at 0.75 R (ft)	0.81	0.7326	1.4167	0.8333
Taper Ratio	1.0	0.6966	1.0	1.0
Solidity	0.188	0.1832	0.1899	0.2475
Disc Area (ft <sup>2</sup> )	95.03	81.18	70.88	54.50
Moment Arm (ft)	32.567	29.917	30.82	28.49

This gives the tail rotor thrust ( $T_{tr} = Q_{mr}/l_{tr}$ ) and, therefore, the tail rotor thrust coefficient ( $C_{Ttr}$ ) simply as

$$(2.53) \quad C_{Ttr} = \frac{T_{tr}}{\rho A_{tr} V_{t-tr}^2}.$$

Of course I have taken liberty in calling the anti-torque force the tail rotor thrust. In the single rotor configuration, the interference between the tail rotor and the airframe's vertical fin, body, and other appendages can be rather large [212]. This means that the actual tail rotor thrust could easily be 10 to 15 percent higher than the required anti-torque force.

The tail rotor power coefficient ( $C_{Ptr}$ ), given the tail rotor thrust coefficient, has been obtained from the flight test data for each configuration. This power coefficient is recorded on line 10, Table 2-11. This gives the tail rotor horsepower ( $HP_{tr}$ ) calculated from

$$(2.54) \quad HP_{tr} = \frac{\rho A_{tr} V_{t-tr}^3}{550} C_{Ptr}.$$

The next to the last line on Table 2-11, the ratio of tail rotor horsepower to main rotor horsepower, shows the wide variation that can occur between design approaches. The last line of Table 2-11 shows the simple sum of main- and tail-rotor horsepower, which is less than the total engine shaft horsepower. This indicates that transmission efficiencies and accessory power have not been accounted for. However, I must warn you that, because of experimental accuracy and data scatter, the end results might easily have gone 100 horsepower the other way [213].

## 2.3 HOVER PERFORMANCE

**Table 2-11. UTTAS and AAH Comparison**

Parameter	YUH-60A	YUH-61A	YAH-63A	YAH-64A
GW hovered at 4,000 ft, 95 °F	16,193	15,130	16,500	15,000
$C_W$	0.006825	0.007755	0.007451	0.008189
$C_{Peng}$ from test report	0.000686	0.000828	0.000761	0.000941
Total SHP	2,187	2,156	2,280	2,275
$C_{Pmr}$	0.000603	0.000731	0.000681	0.000773
$HP_{mr}$	1,924	1,904	2,040	1,869
$Q_{mr}$	38,423	34,948	38,833	33,987
$T_{tr}$	1,180	1,168	1,260	1,193
$C_{Ttr}$	0.01322	0.01583	0.01672	0.03013
$C_{Ptr}$ from test report	0.00196	0.00225	0.00177	0.00226
$HP_{tr}$	222	208	180	100
$HP_{tr}/HP_{mr}$	0.116	0.109	0.088	0.054
$HP_{mr} + HP_{tr}$	2,146	2,112	2,220	1,969

A tail rotor has its own  $C_P$  versus  $C_T$  behavior in hover. This data, for the UTTAS and AAH examples under discussion, is shown in Fig. 2-56. This performance data is for HOGE (specifically at 100-feet wheels-to-ground distance). Tail rotor performance when the aircraft is hovering in ground effect (HIGE) varies somewhat from performance in HOGE. The line shown on this figure is given by

$$(2.55) \quad C_{Ptr} = 0.001261\sigma + \frac{1.49}{\sqrt{2}} C_{Ttr}^{3/2}.$$

As the single main rotor plus tail rotor became the dominant configuration for most applications, more important issues of tail rotor placement and design became clearer. For example, roll angle trim of the helicopter was now tied to the tail rotor thrust. The main rotor thrust was tilted in the opposite lateral direction to keep the helicopter from drifting sideways. Even so, many early, small, single rotor helicopters hovered with “one wing low.” Tail rotor placement higher up above the boom lessened this adverse roll-trim characteristic because the anti-torque thrust acted closer to the main rotor plane. This placement added another gearbox in the tail rotor drivetrain of most single rotor helicopters.

A most important factor in the design and operation of tail rotors for the single-main-rotor helicopter has been safety. Unfortunately, the tail rotor, particularly on smaller helicopters operating on or near the ground, is quite accessible. People have inadvertently walked into it. Fortunately, special illuminating blade paint schemes, guard rings, flight and ground crew alertness, and educated awareness by passengers has significantly reduced injuries to people from tail rotors.

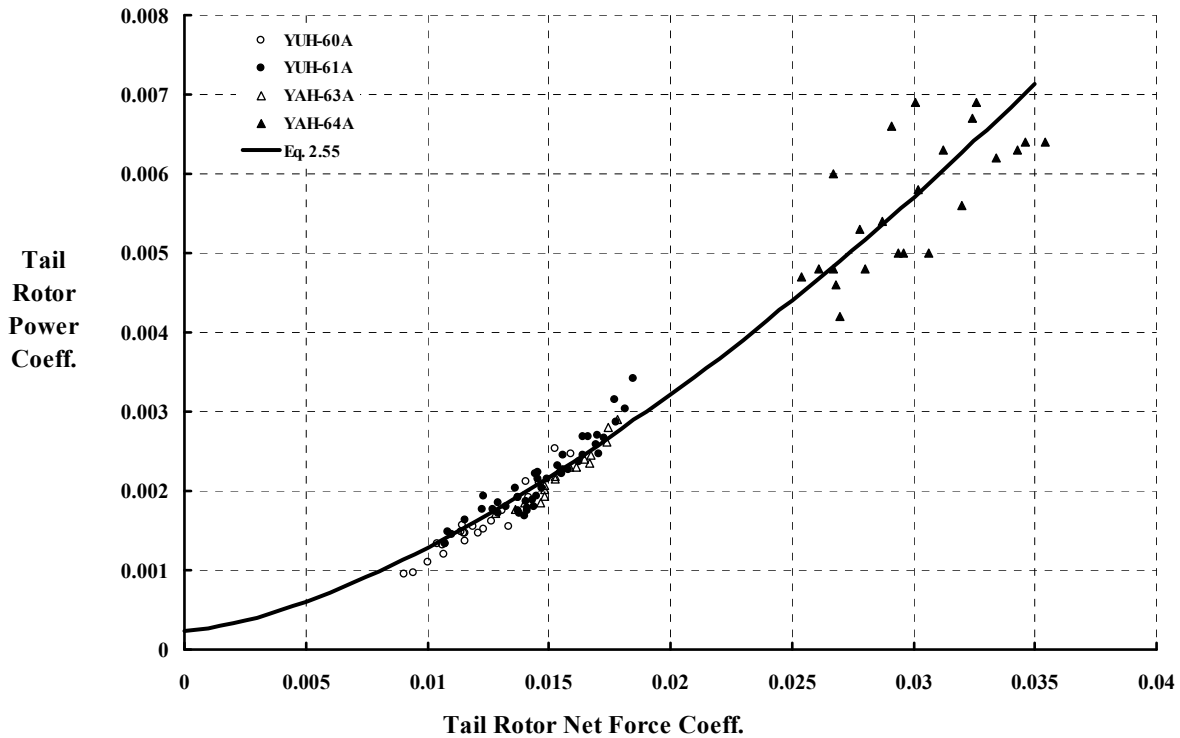


**Fig. 2-56. UTTAS and AAH tail rotor performance in HOGE.**

Pioneering study of tail rotors came with the analytical work of Ken Amer and Al Gessow in 1953 [214]. Toward the end of the 1960s, enough field experience had been gained with the single rotor helicopter to appreciate the very complex aerodynamic environment in which the tail rotor operates. Downwash from the main rotor, turbulent flow from the upstream fuselage, and flying in quartering winds all took on special importance to the designer and operator. The decades of the 1970s and 1980s saw intense engineering theoretical analysis, wind tunnel experiments, and flight testing [212, 214-232]. This research was rewarding. It uncovered (a) recommendations for tail rotor rotational direction, (b) advantages of the pulling tail rotor over the pushing placement, (c) adverse effects of the vertical fin, (d) ground effects, (e) losses in tail rotor effectiveness due to vortex ring flight conditions, and (f) regions of flight where complete loss of directional control could, and did, occur. This accumulating knowledge led to “over designing” newer tail rotors in relation to earlier design standards.

The last decade has seen the introduction of bearingless tail rotors through the use of composite materials [225]. These most modern tail rotors have helped to hold down manufacturing costs and are virtually maintenance free. The propeller-like noise of older-type tail rotors can now be significantly reduced by a combination of more blades and lower rotational speeds. Coupled with advanced flight control systems, the modern tail rotor reduces pilot workload in all but the most demanding flight conditions. Finally, canting the thrust axis of the tail rotor slightly upwards lets this primary anti-torque device add lift equal to its own weight.

## 2.3 HOVER PERFORMANCE

### 2.3.5 Other Anti-torque Devices

The propeller-like tail rotor is not the only way that modern, single rotor helicopters achieve yawing moment equilibrium in hover. Aerospatiale (the French helicopter manufacturer that merged with Germany's Messerschmitt-Bölkow-Blohm (MBB) in January 1992 to form Eurocopter) uses a ducted propeller or ducted fan called a Fenestron (Fig. 2-57) on several of its smaller helicopters. McDonnell Douglas, before merging with Boeing in the U.S. in August 1997, developed a nozzle exhaust called NOTAR (Fig. 2-58). The jet velocity of the NOTAR is created by a ducted fan located near the engine compartment. The fan air is ducted through the tail boom to the swiveling nozzle. A relatively small portion of the ducted-fan flow is used for boundary layer control (BLC) along the tail boom. In conjunction with the main rotor downwash over the tail boom, the BLC forces the tail boom to develop a lateral side force, which becomes added anti-torque.

It is worth noting that the NOTAR concept is not new. The concept was first tested on the Nord 1700 under the direction of André Bruel, with first flight in September 1948 [233]. A private company, Société Nationale de Constructions Aéronautiques du Nord, was established to develop the Nord 1700. Bruel patented the anti-torque by nozzle concept.



**Fig. 2-57. The SA 365 N-1 Dauphin 2 uses a Fenestron ducted-fan anti-torque device (photo from author's collection).**

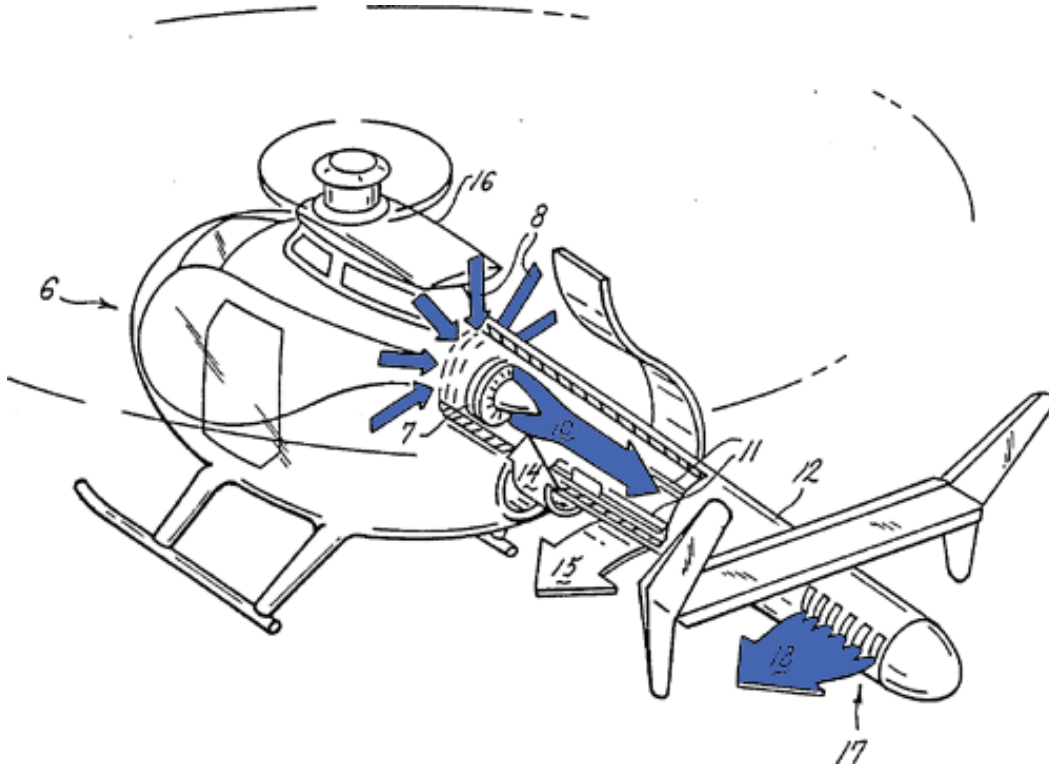


**Fig. 2-58. The MD Explorer uses a NOTAR nozzle anti-torque device (drawing from author's collection).**

The relationship between anti-torque force and the horsepower required to obtain this force is quite simple. The ideal horsepower (ideal HP) depends on the thrust ( $T$ ) desired, the ambient air density, and the area of the jet exhaust. From simple momentum theory, the system thrust and ideal horsepower required are given by

$$(2.56) \quad T = \rho A_{\text{exit}} V_{\text{exit}}^2 \quad \text{and} \quad \text{ideal HP} = \frac{\rho A_{\text{exit}} V_{\text{exit}}^3}{2 \times 550}$$

and, therefore, the fundamental relationship for each device is that

$$(2.57) \quad \text{ideal HP} = \frac{T^{3/2}}{550 \sqrt{4\rho A_{\text{exit}}}}$$

Now consider the three ways (so far) that an anti-torque force is produced with modern helicopters (see Fig. 2-59). For a tail rotor configured as an unducted fan, the air passing through the rotor quickly contracts to a column of air having an area equal to one-half of the rotor area. That is,  $A_{\text{exit}} = \frac{1}{2} A_{\text{tr}}$ . For a well-designed ducted fan, which the Fenestron closely approximates, the air passing through the fan does not contract downstream. Thus, for the Fenestron ducted fan, the exit area and the fan area are equal ( $A_{\text{exit}} = A_{\text{fan}}$ ). The total thrust is the sum of the fan's thrust and the duct's lift, which comes primarily from the lip of the duct. In the ideal ducted-fan system, one-half of the total thrust comes from the fan and one-half comes from the duct. For the NOTAR anti-torque device, behaving as a nozzle, the exit area can be as large as the designer can achieve, given the configuration constraints. At

### 2.3 HOVER PERFORMANCE

present, the NOTAR exit area is less than the fan area. That is, the ratio of nozzle area to fan area is less than one ( $A_n < A_{fan}$ ). These three anti-torque devices each have a different ideal horsepower equation. Following Eq. (2.57), you immediately have

$$(2.58) \text{ ideal HP}_{tr} = \frac{T^{3/2}}{550\sqrt{2\rho A_{tr}}} \quad \text{for the unducted tail rotor,}$$

$$(2.59) \text{ ideal HP}_{df} = \frac{T^{3/2}}{550\sqrt{4\rho A_f}} \quad \text{for the ducted tail rotor, and}$$

$$(2.60) \text{ ideal HP}_n = \frac{T^{3/2}}{550\sqrt{4\rho A_n}} \quad \text{for the nozzle .}$$

The primary advantage of the Fenestron and the NOTAR is, in my opinion, safety. Walking into either and getting hurt is a remote possibility. A person is met with just a blast of air with the NOTAR. Both configurations offer considerable protection should the pilot inadvertently swing the tail into a post or other grounded object. However, there is a perceivable performance difference between the three anti-torque devices. To begin with, ducting a free tail rotor (a shrouded tail rotor, if you prefer) can offer a diameter reduction. Suppose a comparison is made at equal anti-torque force (i.e., thrust). Then thrust from Eq. (2.58) can be substituted into Eq. (2.59), and a little arithmetic gives

$$(2.61) \text{ ideal HP}_{df} = \frac{D_{tr}}{2D_f} (\text{ideal HP}_{tr}) .$$

The diameter of the ducted fan ( $D_f$ ) can be one-half of the diameter of the tail rotor ( $D_{tr}$ ) and have equal ideal horsepower at equal thrust.

The static performance comparison between two tail rotors and an advanced Fenestron with stators is quite interesting and illustrates the effect of both diameter and solidity differences. Note from Table 2-12 that I have selected a comparison where the Fenestron diameter is about one-half of the diameter of the two tail rotors.

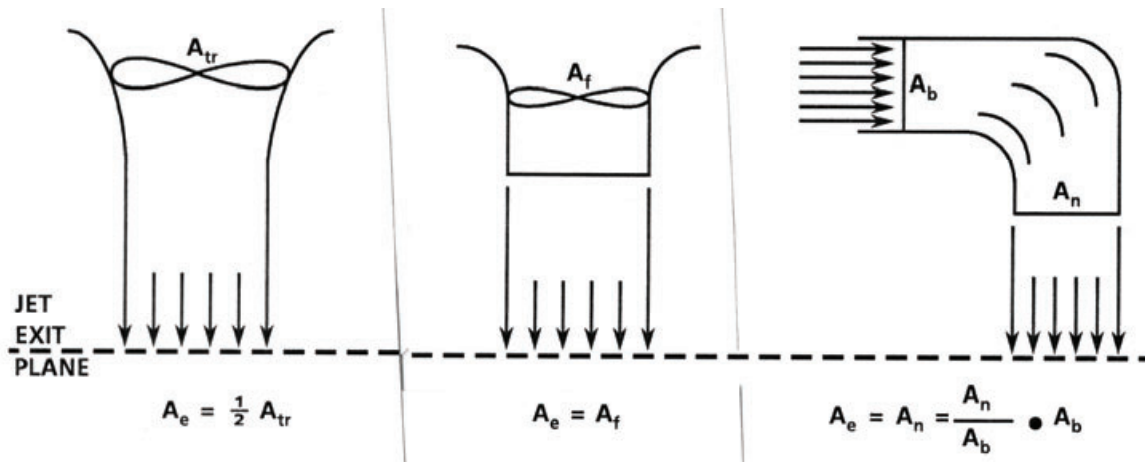


**Fig. 2-59. Three ways of producing an anti-torque force.**

The power coefficient ( $C_p$ ) versus thrust coefficient ( $C_T$ ) for the two tail rotors is displayed in Fig. 2-60. The Fenestron's performance is shown separately in Fig. 2-61 because of the large-scale difference. Keep in mind that identical power and thrust coefficients are used for the three anti-torque devices. That is,

$$(2.62) \quad C_T = \frac{T}{\rho(\pi R^2)V_t^2} \quad \text{and} \quad C_p = \frac{550 \text{ SHP}}{\rho(\pi R^2)V_t^3}$$

**Table 2-12. Anti-torque Device Comparison**

Parameter	Bell	Westland	Aerospatiale
Helicopter	Early Model 222	Early Lynx	SA 365N-1
Reference	[168]	[226]	[227]
Diameter (ft)	6.5	6.89	3.58
Blades	2	4	11
Chord (ft)	0.8333	0.5906	0.2525
Reference Solidity ( $bc/\pi R$ )	0.1632	0.2183	0.4939
Stators	No	No	Yes
Root Cutout ( $r/R$ )	0.1	0.384	0.333
RPM	1,881	1,824	4,009
Tip Speed (fps)	640	658	751
Reference Disc Area (ft <sup>2</sup> )	33.183	37.282	10.660

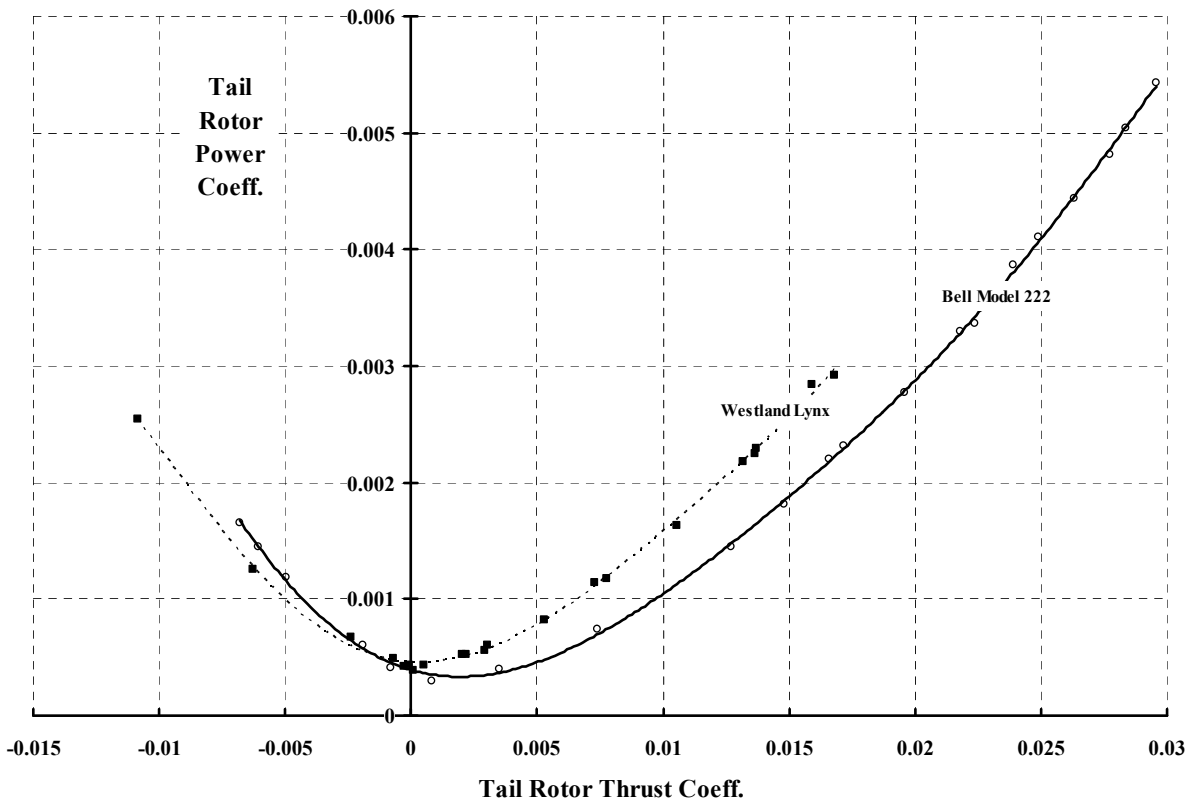


**Fig. 2-60. Isolated performance of two tail rotors.**

### 2.3 HOVER PERFORMANCE

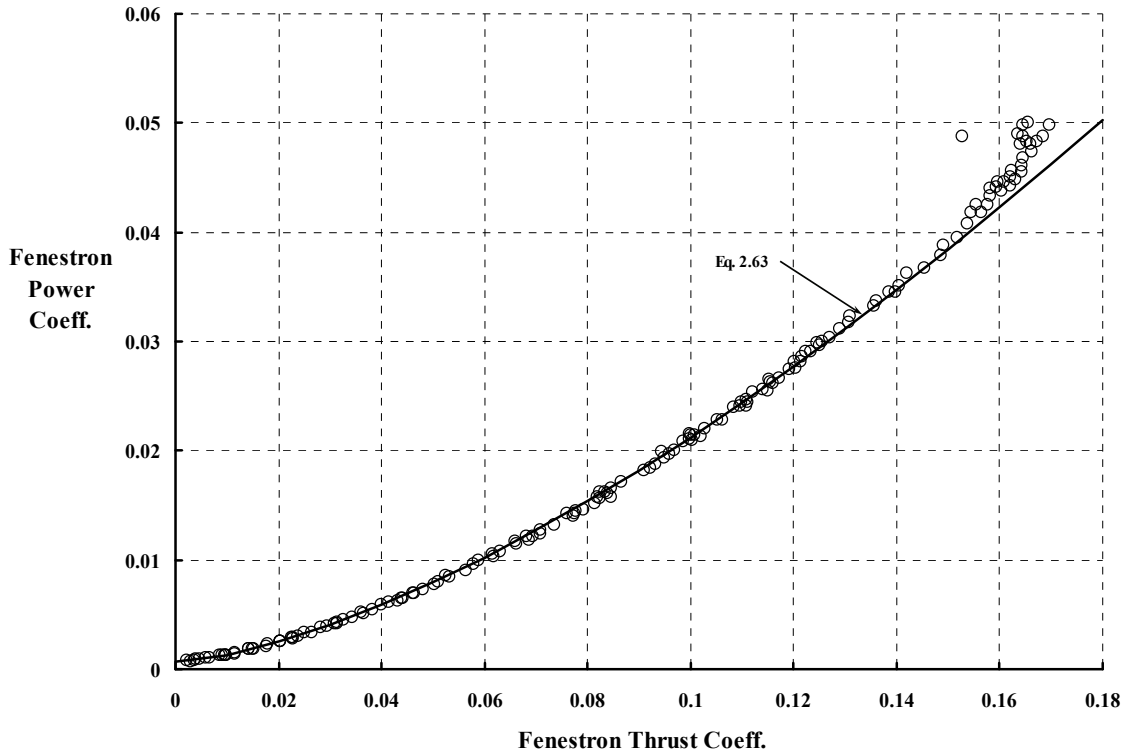


**Fig. 2-61. Isolated Fenestron performance.**

where the thrust ( $T$ ) is the system total thrust, which, for the Fenestron, includes both the fan thrust and the duct lift. The shaft horsepower (SHP) is, of course, the power required by the device, whether tail rotor or Fenestron.

The isolated Fenestron performance shown in Fig. 2-61 is accompanied by a semiempirical curve-fit equation given by

$$(2.63) \quad C_p = \frac{550 \text{ SHP}}{\rho (\pi R^2) V_t^3} = 0.001375 \sigma + 1.31 C_T^{3/2} .$$

The Westland Lynx isolated tail rotor performance, Fig. 2-60, in the working thrust range is approximated by

$$(2.64) \quad C_p = \frac{550 \text{ SHP}}{\rho (\pi R^2) V_t^3} = 0.001875 \sigma + 1.60 C_T^{3/2} .$$

The Bell 222 isolated tail rotor performance, Fig. 2-60, in the working thrust range is approximated by

$$(2.65) \quad C_p = \frac{550 \text{ SHP}}{\rho (\pi R^2) V_t^3} = 0.001 \sigma + 1.45 C_T^{3/2} .$$

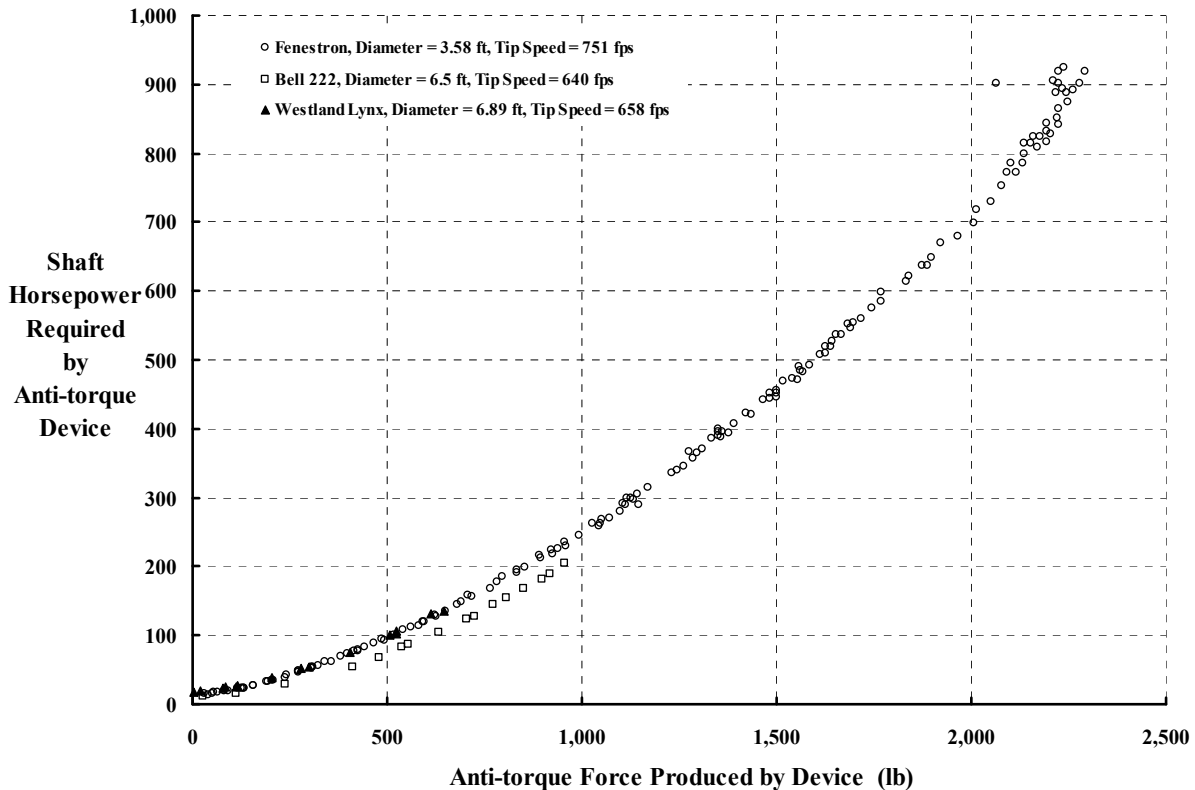


**Fig. 2-62. Isolated anti-torque device performance at sea level, standard day.**

The preceding three approximate equations really do little to compare the three configurations. A more direct view is simply horsepower versus thrust as shown in Fig. 2-62.

In the NOTAR case, the logic is the same as for a ducted fan. The ducted fan producing the nozzle flow is small compared to an unducted tail rotor. The small size allows the fan to be installed before the tail boom, but aft of the engine compartment, as shown schematically in Fig. 2-58.

### 2.3.6 Bell Model 222 and Aerospatiale Dauphin 2 Hover Performance

Having compared the Aerospatiale Fenestron ducted fan and the Bell Model 222 tail rotor, it is worth a moment to compare the complete helicopter performance of the two aircraft [168, 170]. First, some background. In 1979 the U.S. Coast Guard completed a competition for a new search and rescue helicopter. They selected the Aerospatiale SA 365 N-1 Dauphin 2 over the Bell Model 222. The contract called for delivery of 90 Dauphins. After some relatively minor setbacks caused primarily by trouble with the Lycoming LTS 101 engines, which caused a switch to Turbomecca ARRIEL 1C1 engines, the Dauphin performed well in the field. Bell continued offering its Model 222 (with the Lycoming LTS 101 engines) commercially, but the engine troubles persisted and initial customers were discouraged.

## 2.3 HOVER PERFORMANCE

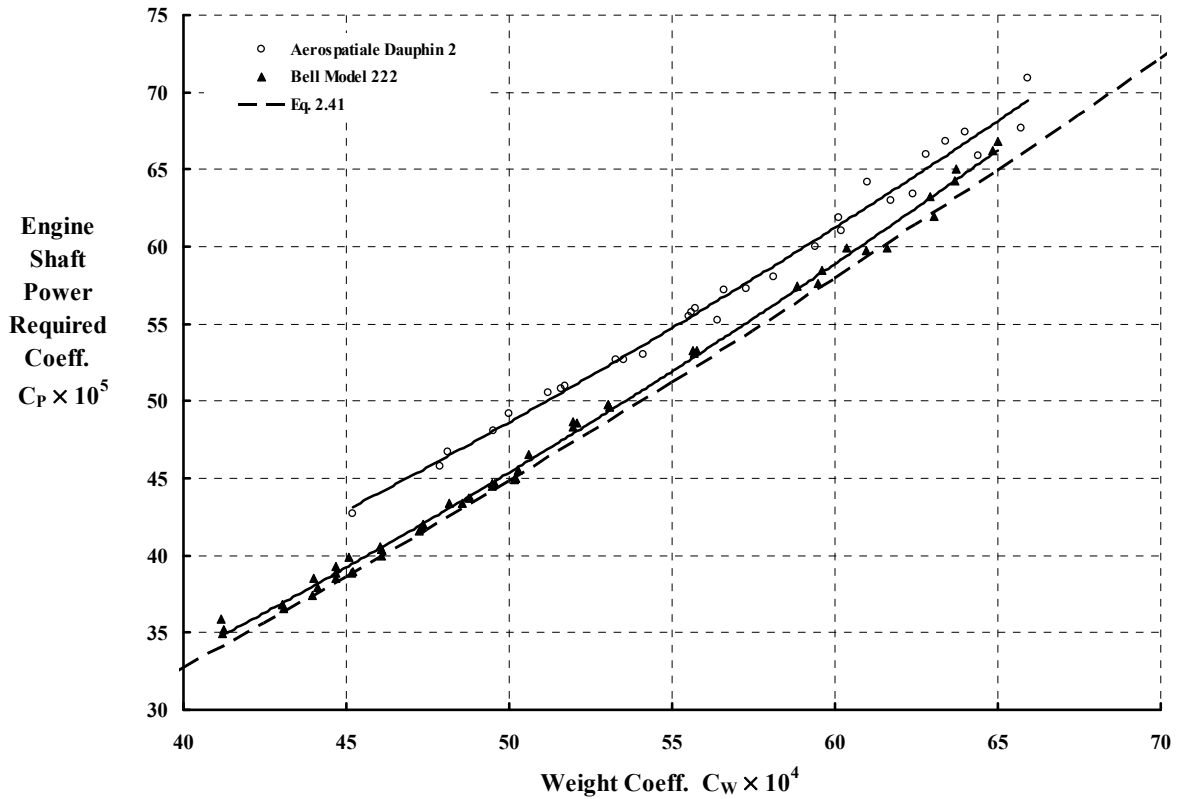


Fig. 2-63. Performance difference primarily due to anti-torque device.

Regarding comparative hover performance, the nondimensional performance in coefficient form is shown in Fig. 2-63. The difference between the two machines is due almost entirely to the anti-torque horsepower difference given in Fig. 2-62. That is, the roughly 40-horsepower difference between the Fenestron and the Bell Model 222 tail rotors shown in Fig. 2-62 equates to a 0.0025 increment in the Dauphin  $C_P$  shown in Fig. 2-63.

### 2.3.7 Blade Element Momentum Theory Revisited

The rotorcraft industry has used blade element momentum theory to predict power required by hovering helicopter rotors for nearly a century. Despite its shortcomings, the theory has served the industry quite well. Recent decades have seen an increase in the use of powerful computers to obtain greater accuracy in predicting airflow through and about the rotor (or rotors). This improved flow-field calculation, particularly of induced velocity, has led to more accurate prediction of power required to produce a given thrust. However, the knowledge to be gained from blade element momentum theory and applied to these advancing methods is not yet exhausted.

One very specific use of blade element momentum theory is identification of similarity parameters for thrust, power, and collective pitch for both single and multirotor configurations. The theory has, of course, been most frequently used to predict performance of a specific configuration, but in December 1937 rotary wing aerodynamicists were reminded of just how helpful the theory could be in its more nondimensional form. The purpose of this portion of Volume II is to bring attention to that fact again.

The derivation and use of blade element momentum theory are described in many well-known books [85, 234-242]. These works do not, however, emphasize a nondimensional form of the theory that Montgomery Knight and Ralph Hefner used with considerable success in 1937. Knight and Hefner's work was published in NACA TN No. 626 and entitled *Static Thrust Analysis of the Lifting Airscrew* [243]. In this report they used their form of the blade element momentum theory to eliminate solidity as an independent parameter. Experimental results supported their view. They continued to apply their understanding to the in-ground-effect performance problem and published NACA TN No. 835 in December of 1941 [244]. This later report, entitled *Analysis of Ground Effect on the Lifting Airscrew*, further substantiated their interpretation and use of blade element momentum theory. Today, the nearly complete development of free-wake hover performance theory provides an opportunity to reaffirm Knight and Hefner's approach, and extend their results beyond rotor performance characteristics to the spanwise distribution of key aerodynamic parameters [245].

The basis of blade element momentum theory (see chapter 4 of reference [234] for example) is formed by equating an element of thrust ( $dT$ ) calculated by momentum theory to the same element of thrust obtained by blade element theory. In hover, this amounts to

$$(2.66) \quad dT = 4\pi\rho v_{(r)}^2 r dr = \frac{1}{2} \rho b c_{(r)} \Omega^2 r^2 C_{l(r)} dr.$$

This fundamental assumption immediately simplifies to

$$(2.67) \quad C_{l(r)} = \frac{8\pi v_{(r)}^2}{b c_{(r)} r \Omega^2}.$$

When (a) the spanwise blade station is nondimensionalized using  $r = R x$ ; (b) a local blade element solidity is defined as  $\sigma_{(x)} = b c_{(x)} R / \pi R^2$ ; and (c) the tip speed,  $V_t = \Omega R$ , is taken as a reference velocity, the concise form of blade element momentum theory becomes

$$(2.68) \quad C_{l(x)} = \frac{8}{\sigma_{(x)}} \left[ \frac{v_{(x)}}{V_t} \right]^2 \left( \frac{1}{x} \right) \quad \text{where} \quad \sigma_{(x)} = \frac{b c_{(x)} R}{\pi R^2}.$$

To obtain an explicit expression for spanwise induced velocity scaled to tip speed, the classical assumption that

$$(2.69) \quad C_{l(x)} = a_{(x)} \alpha_{(x)} \approx a \left[ \theta_{(x)} - \phi_{(x)} \right] \approx a \left[ \theta_{(x)} - \frac{v_{(x)}}{x V_t} \right]$$

is used. Then the resulting quadratic from equating Eqs. (2.68) and (2.69) is solved to give

### 2.3 HOVER PERFORMANCE

$$(2.70) \quad \frac{v_{(x)}}{V_t} = \frac{a\sigma_{(x)}}{16} \left[ \sqrt{1 + 2 \left[ \frac{16\theta_{(x)}}{a\sigma_{(x)}} \right]} - 1 \right].$$

The beginnings of Knight and Hefner's view of blade element momentum theory are apparent in Eq. (2.70). The key is to see the appearance of  $a\sigma_{(x)}/16$ , its reciprocal, or this parameter, raised to some power. Therefore, the foundation for defining several useful similarity parameters is established by rewriting the induced velocity of Eq. (2.70) as

$$(2.71) \quad \frac{16}{a\sigma_{(x)}} \frac{v_{(x)}}{V_t} = \left[ \sqrt{1 + 2x \left[ \frac{16\theta_{(x)}}{a\sigma_{(x)}} \right]} - 1 \right].$$

The first similarity parameter to emerge from Eq. (2.71) is scaling of the blade element pitch angle by airfoil lift-curve slope and local solidity. That is,

$$(2.72) \quad \Theta_{(x)} \equiv \frac{16\theta_{(x)}}{a\sigma_{(x)}}.$$

Both Eqs. (2.71) and (2.72), when introduced into Eq. (2.69), redefine the blade element angle of attack and then the blade element lift coefficient, so that the second key similarity parameter is

$$(2.73) \quad \frac{16C_{l(x)}}{a^2\sigma_{(x)}} = \Theta_{(x)} + \frac{1}{x} - \frac{1}{x} \sqrt{1 + 2x\Theta_{(x)}}.$$

This equation forms the basis of Knight and Hefner's approach, and their view of rotor performance similarity parameters to both thrust and power coefficients. They chose constant chord, untwisted blades to show how solidity could be removed as an independent parameter from both performance coefficients.

Knight and Hefner approached the thrust problem first by reformatting blade element thrust so that Eq. (2.73) could be used. In modern notation, they preceded as follows:

$$(2.74) \quad dT = \frac{1}{2}\rho(\Omega r)^2 (bc dr) C_l = \frac{\sigma a^2}{16} \left[ \frac{1}{2}\rho(xV_t)^2 (bcR dx) \left( \frac{16C_l}{\sigma a^2} \right) \right].$$

Because  $bcR = \pi R^2 \sigma$  for a constant-chord blade, they could factor out solidity and disc area prior to spanwise integration so that

$$(2.75) \quad T = \frac{\sigma^2 a^2}{16} \left( \frac{1}{2}\rho V_t^2 \right) (\pi R^2) \int_{x_c}^B \left( \frac{16C_l}{\sigma a^2} \right) x^2 dx.$$

From this point they saw that the thrust problem, using Eq. (2.73), would lead to

$$(2.76) \quad \frac{32C_T}{\sigma^2 a^2} = \int_{x_c}^B \left( \frac{16C_l}{\sigma a^2} \right) x^2 dx = \int_{x_c}^B \left( \Theta x^2 + x - x \sqrt{1 + 2x\Theta} \right) dx.$$

Knight and Hefner<sup>52</sup> did not use a tip loss factor (i.e.,  $B = 1$ ) and also ignored loss of lift at the blade root (i.e.,  $x_c = 0$ ). Another possible conclusion can be drawn, however. For example, Gessow and Myers [234] note that Sissingh (who referenced Prandtl) suggested that the tip loss factor should vary with thrust coefficient as

$$(2.77) \quad B = 1 - \frac{\sqrt{2C_T}}{b} = 1 - \frac{\sqrt{2}}{\pi AR} \left( \frac{C_T}{\sigma^2} \right)^{1/2}.$$

There have been many discussions, some quite heated, as to what semiempirical factors such as tip loss, root cutout, and airfoil aerodynamic properties are most generally applicable when using blade element momentum theory to predict performance of a new helicopter product. So far, the rotary wing aerodynamic community has never guessed the right answer. One thing does seem clear, however. The tip loss factor depends on  $C_T/\sigma^2$ , which favors Knight and Hefner's similarity parameters, *but* the tip loss factor also depends on the blade-aspect ratio (AR). In their work, Knight and Hefner only varied the number of blades at equal blade-aspect ratio. While the influence of blade-aspect ratio is not large, some experimental data and a modern theory [245] will show that two wide-chord blades have slightly worse performance than four narrow-chord blades—at equal solidity.

To proceed then, the integrated result for untapered, untwisted blades is

$$(2.78) \quad \frac{32C_T}{\sigma^2 a^2} = \frac{(B^2 - x_c^2)}{2} + \frac{(B^3 - x_c^3)\Theta}{3} - \frac{(F^5 - H^5)}{10\Theta^2} + \frac{(F^3 - H^3)}{6\Theta^2}$$

where,  $F \equiv \sqrt{1 + 2B\Theta}$  and  $H \equiv \sqrt{1 + 2x_c\Theta}$  and, as a reminder,  $\Theta = \frac{16\theta}{\sigma a}$ .

Knight and Hefner, rather than see thrust versus collective pitch as  $C_T = f(\theta, \sigma)$ , sought confirmation that  $C_T/\sigma^2 = f(\theta/\sigma)$  through experiment. They tested two-, three-, four-, and five-bladed rotor configurations. All blades were manufactured as identically as possible. Each

---

<sup>52</sup> The view suggested by Knight and Hefner can also be arrived at another way. From Gessow and Myers' well-known textbook [234] (chapter 8, eq. 21), the simplest calculation of thrust coefficient at any advance ratio starts with

$$C_T = \frac{1}{2} \sigma a \left[ \frac{1}{3} \theta + \frac{1}{2} \mu^2 \theta + \frac{1}{2} \lambda \right] \quad \text{or} \quad \frac{C_T}{\sigma} = a \left[ \frac{1}{6} \theta + \frac{1}{4} \mu^2 \theta + \frac{1}{4} \lambda \right].$$

In hover, advance ratio ( $\mu$ ) is zero, and inflow ratio ( $\lambda$ ) is frequently set to its ideal, uniform, downwash value of  $\lambda = -(\frac{1}{2} C_T)^{1/2}$ . Thus, for hover

$$\frac{C_T}{\sigma} = a \left[ \frac{1}{6} \theta - \frac{1}{4} \sqrt{\frac{1}{2} C_T} \right].$$

This classical result says that comparing different solidity rotors with  $C_T/\sigma$  versus  $\theta$  will not remove the solidity parameter. However, by dividing through by solidity, the thrust and collective pitch similarity parameters are revealed because

$$\frac{C_T}{\sigma^2} = a \left[ \frac{1}{6} \left( \frac{\theta}{\sigma} \right) - \frac{1}{4\sigma} \sqrt{\frac{1}{2} C_T} \right] \quad \text{or} \quad \frac{C_T}{\sigma^2} = a \left[ \frac{1}{6} \left( \frac{\theta}{\sigma} \right) - \frac{1}{4} \sqrt{\frac{1}{2} \left( \frac{C_T}{\sigma^2} \right)} \right].$$

### 2.3 HOVER PERFORMANCE

blade had a 30-inch radius, no twist, a NACA 0015 airfoil, and a 2-inch constant chord from the 5-inch radius station to the tip. The tests were conducted at 960 rpm, which is a tip speed of about 250 feet per second. Their report includes an appendix with tabulations of all measurements.

Knight and Hefner illustrated their transformation by first plotting  $C_T$  versus  $\theta$  for each rotor set. This commonly obtained result is reproduced in Fig. 2-64. They did not include a comparison of their data in the coordinates of  $C_T/\sigma$  versus  $\theta$  as suggested by footnote 52. This comparison is shown in Fig. 2-65. This  $C_T/\sigma$  view can be of interest when blade stall is suspected. Knight and Hefner thoroughly discussed how blade stall was apparent in their data. They (and other investigators) refer to a loud, buzzing noise from the model at high thrust as an audible indication of blade stall. A quantitative barometric parameter of blade stall is average blade element lift coefficient. This blade-stall indicator is frequently defined as

$$(2.79) \quad C_L = (6 \text{ to } 7) \frac{C_T}{\sigma}.$$

When  $C_L$  approaches 1 for full-scale rotors, or is perhaps as low as 0.7 for many model rotors, signs of aerodynamic nonlinearity are frequently seen in test data. Fig. 2-65 shows that the two-bladed rotor has a departure from the general trend at its highest thrust point and perhaps at the prior point. At the lower point,  $C_L$  is on the order of 0.6 to 0.7 indicating the onset of separated flow along the blade span. For the untapered, untwisted blade, separated flow begins closer to the tip.

Using the test data shown in Fig. 2-66, Knight and Hefner were satisfied that their similarity parameters for thrust and collective pitch were correct. What appears in Fig. 2-64 as a configuration-oriented result where solidity, planform, and twist may all be factors, is now less complicated because solidity is removed as Fig. 2-66 demonstrates. (The inclusion of separated flow effects in the airfoil  $C_l$  versus  $\alpha$  assumption, rather than using the linear  $C_l = a\alpha$  assumption, has allowed prediction of the high-thrust blade-stall-affected behavior seen by the two- and three-bladed data in Fig. 2-66.)

The question might be raised as to whether Knight and Hefner's data (vintage 1937) is representative today considering the overall complexity of hover testing procedures and theoretical aerodynamics. To allay possible suspicions, consider Fig. 2-67. I have added experimental data contributed by Landgrebe [246],<sup>53</sup> Stepniewski [247], and Signor [226] to Knight and Hefner's result. This data bank, when included in the substantiation of similarity parameters for thrust and collective pitch, simply reinforces Knight and Hefner's suggestions as Fig. 2-67 shows. Their (perhaps antiquated) blade-element-momentum theoretical result is given by Eq. (2.78). Fig. 2-67 includes their result assuming a tip loss factor of  $B = 0.985$  (I did not vary the tip loss factor with  $C_T/\sigma^2$  or blade-aspect ratio), a representative root cutout of  $x_c = 0.17$ , and an airfoil lift-curve slope of  $a = 5.73$  per radian.

---

<sup>53</sup> Jack Landgrebe was kind enough to dig out the original tabulated data and send it to me. Now *that's* a friend.

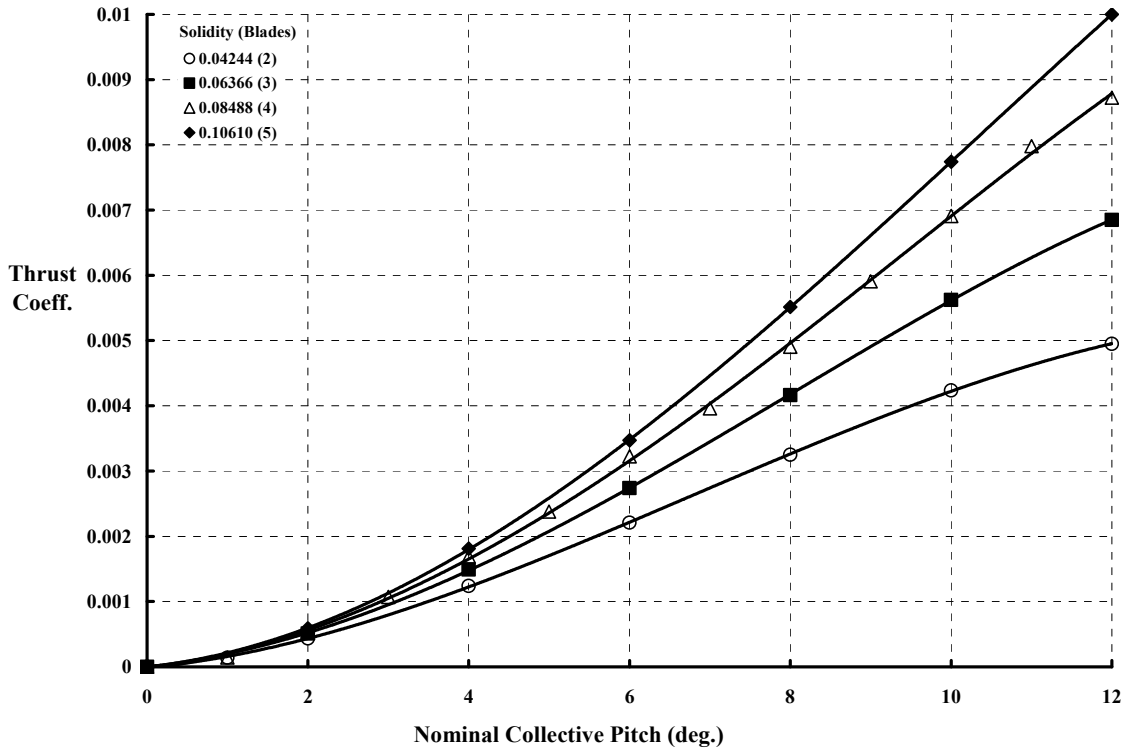


Fig. 2-64. Knight and Hefner's basic thrust data in 1937.

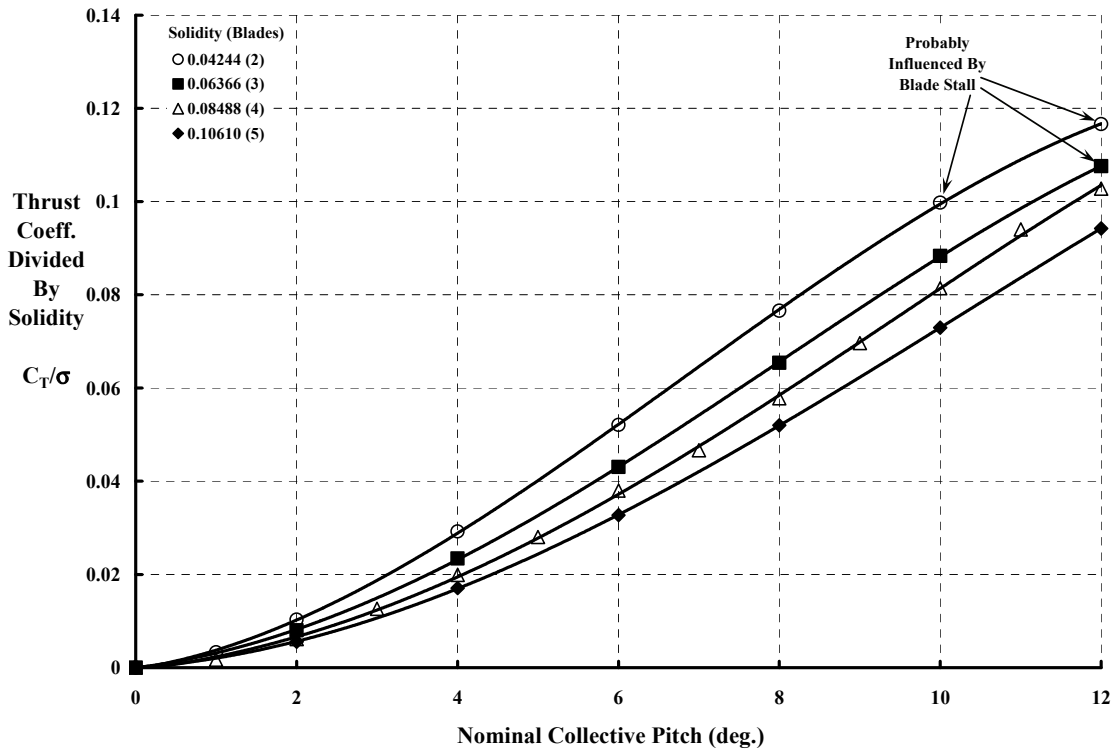
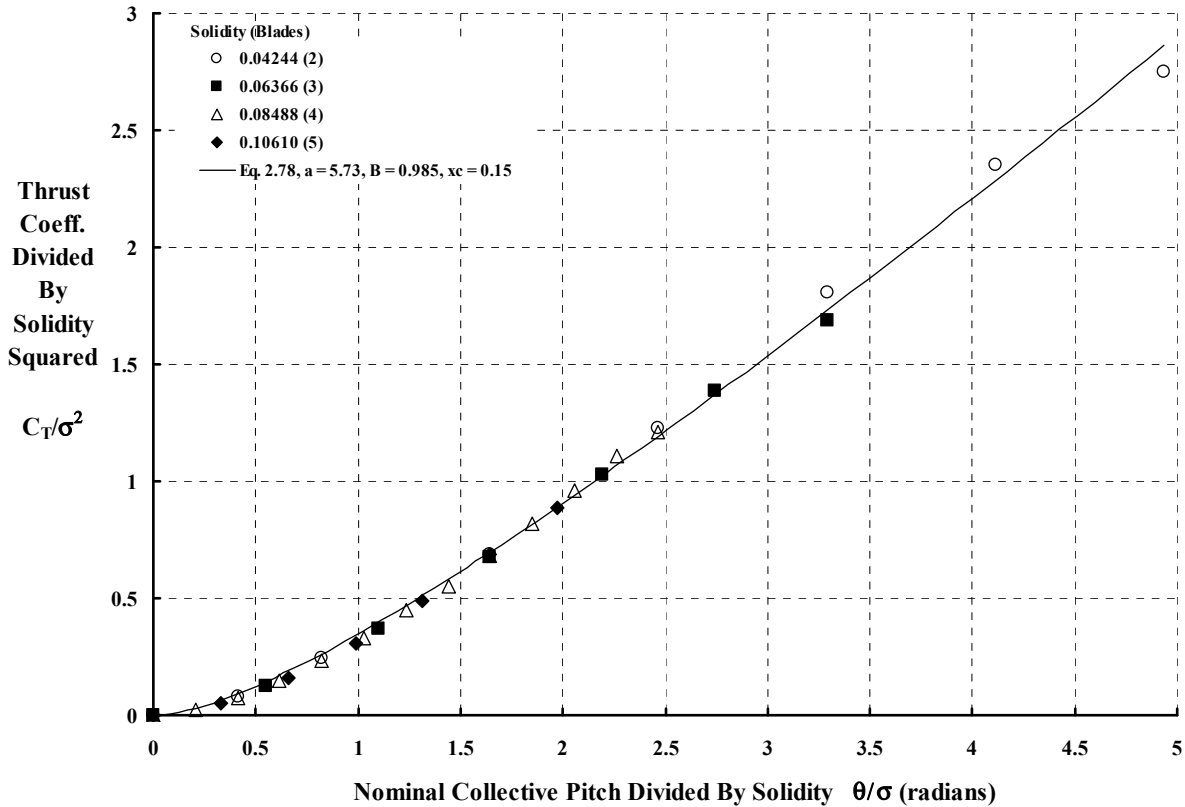


Fig. 2-65.  $C_T/\sigma$  is a blade-loading parameter that reflects airfoil lift coefficient and proximity to blade stall.

## 2.3 HOVER PERFORMANCE



**Fig. 2-66.  $C_T/\sigma^2$  and  $\theta/\sigma$  are similarity parameters that can remove solidity as a variable from the hover performance problem.**

Before turning to the subject of power required by a single, isolated rotor to produce thrust, two additional points can be made. The first point deals with the lifting-surface theories that are evolving. Many of these codes only solve the potential flow problem. This generally gives a blade element airfoil the lift-curve slope of  $a = 2\pi$  per radian in the incompressible case. To better estimate actual rotors (which experimentally appear to behave as if  $a \approx 5.73$  per radian), final data of thrust coefficient at a given collective pitch can be scaled using the more complete similarity parameters. If, for a given  $\theta$ , the rotor  $C_T$  is obtained with a theory that basically assumes  $a = 2\pi$ , then the corrections would be

$$(2.80) \quad C_{T(a=5.73)} = \left(\frac{5.73}{2\pi}\right)^2 C_{T(a=2\pi)} \quad \text{and} \quad \theta_{(a=5.73)} = \left(\frac{5.73}{2\pi}\right) \theta_{(a=2\pi)} .$$

The second point deals with the elastic twist deformation which occurs even with perfectly balanced aerodynamic torsional moments. Simple torsion theory must still include the “tennis racket” term, as it is commonly called. Therefore, even for a uniformly structured blade

$$(2.81) \quad GJ \frac{d\theta_e}{dr} = \int_r^R \left[ (I_\theta \Omega^2) (\theta + \theta_e) \right] dr .$$

This elementary differential equation can, of course, be solved exactly with hyperbolic functions. However, a useful engineering result is simply that

$$(2.82) \quad \frac{\theta_c}{\theta} \approx -\frac{\left(\frac{I_\theta V_t^2}{GJ}\right)}{1 + \frac{1}{2}\left(\frac{I_\theta V_t^2}{GJ}\right)} \left(x - \frac{1}{2}x^2\right).$$

Both tip speed and blade torsional, structural properties play a part in the nondimensional parameter  $I_\theta V_t^2 / GJ$ . However, values of this parameter ranging from 0.05 for a torsionally “stiff” blade to 0.35 for a relatively “soft” blade are frequently representative of both model and full-scale rotor blades. The elastic twist is, therefore, a factor in theory versus test comparisons such as shown in Fig. 2-67. Suppose, for example, that a blade root was preset to 10-degrees root collective pitch angle prior to startup. For an untwisted blade, the pitch angle at the 0.75 R station would also be 10 degrees. At operating speed, the blade tries to twist nose-down because of the torsional load created by the “tennis racket” term. The elastic twist between the root and the 0.75 R station could amount to a  $\theta_c/\theta$  ratio on the order of  $-0.025$  for a torsionally stiff blade to as large as  $-0.14$  for a soft blade. With a preset

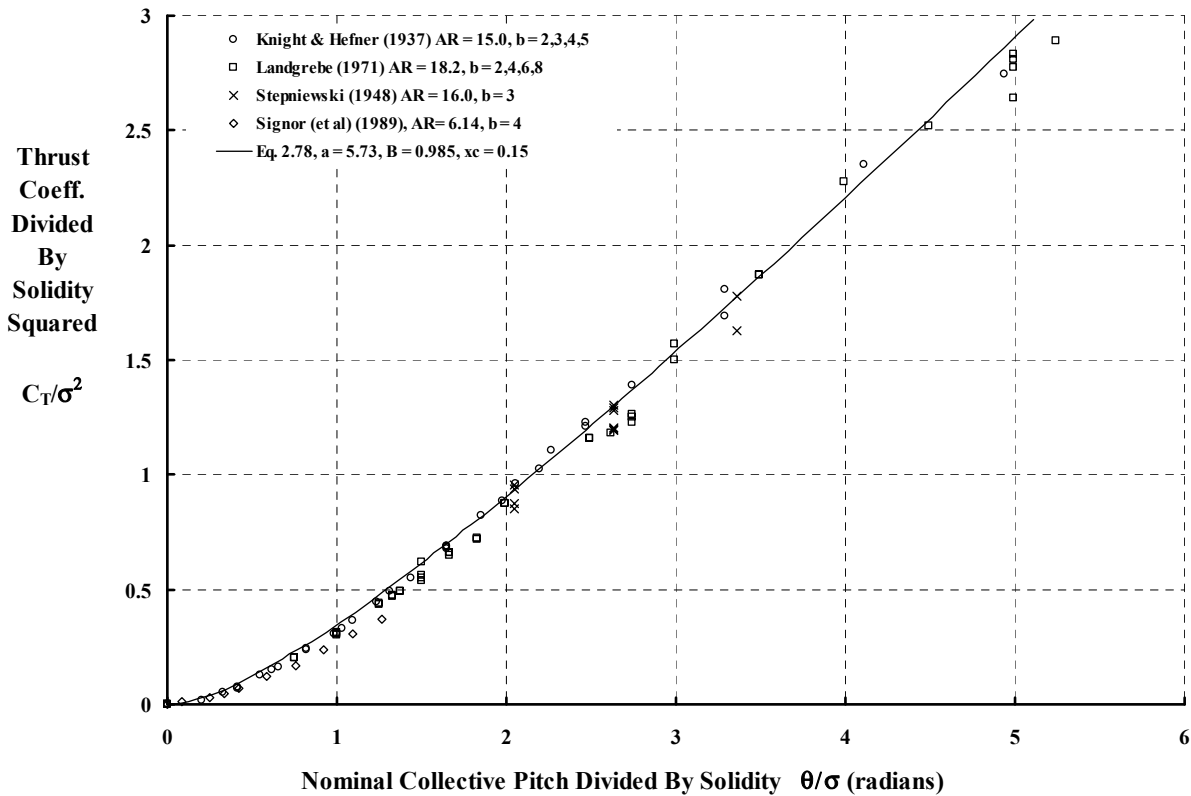


**Fig. 2-67. Knight and Hefner’s similarity parameters are quite useful when different rotors are compared.**

## 2.3 HOVER PERFORMANCE

10-degree blade angle, the 0.75 R station may, therefore, only be at 9.75 degrees and could, perhaps in the extreme, only be at 8.6 degrees. The agreement between blade element momentum theory and tests shown in Fig. 2-67 could be considerably altered if elastic twist were accounted for in blade element momentum theory, or any theory for that matter.

As more accurate lifting surface and free-wake theory is compared to experimental results, it seems advisable not to skip careful and detailed analysis of how thrust varies with blade pitch angle.

Knight and Hefner satisfied themselves that solidity could be removed as an independent parameter using the coordinates  $32C_T/a^2\sigma^2$  and  $16\theta/a\sigma$ . They then turned to investigating the power required to produce thrust. They found that the similarity parameters were quite appropriate provided *only the power increment above flat-pitch power* was dealt with. The need to handle *a power increment* rather than the total power can be seen very easily. For example, one well-known classical-engineering approximation that estimates total hover power required is

$$(2.83) \quad C_P \approx C_{P_0} + k_i \frac{C_T^{3/2}}{\sqrt{2}} \approx \frac{\sigma C_{d_0}}{8} + k_i \frac{C_T^{3/2}}{\sqrt{2}}.$$

Multiplying both sides of this equation by  $(32/a^2\sigma^2)^{3/2}$  produces the thrust similarity parameter. That is,

$$(2.84) \quad \left(\frac{32}{a^2\sigma^2}\right)^{3/2} C_P \approx \left(\frac{32}{a^2\sigma^2}\right)^{3/2} \frac{\sigma C_{d_0}}{8} + k_i \left(\frac{32}{a^2\sigma^2}\right)^{3/2} \frac{C_T^{3/2}}{\sqrt{2}},$$

which, on simplification, becomes

$$(2.85) \quad \frac{128\sqrt{2}}{a^3\sigma^3} C_P \approx \frac{16\sqrt{2}}{a^3\sigma^2} C_{d_0} + \frac{k_i}{\sqrt{2}} \left(\frac{32C_T}{a^2\sigma^2}\right)^{3/2}.$$

Multiplying Eq. (2.85) through by  $\sqrt{2}$  clears things a little more so that

$$(2.86) \quad \frac{256}{a^3\sigma^3} C_P \approx \frac{32}{a^3\sigma^2} C_{d_0} + K_i \left(\frac{32C_T}{a^2\sigma^2}\right)^{3/2}.$$

The preceding four equations make two points. First, power divided by solidity cubed is dependent on thrust divided by solidity squared. Second, perhaps a much-too-unique nondimensional form for the power at flat pitch (i.e., zero thrust) is being introduced. After all, minimum profile power in the form  $\sigma C_{d_0}/8$  is much easier to remember than  $32C_{d_0}/a^3\sigma^2$ . Knight and Hefner decided to subtract  $C_{P_0}$  at the onset. That is, they restated the problem as

$$\frac{C_P - \text{Min. } C_{P_0}}{a^3\sigma^3} = g \left[ \frac{16\theta}{a\sigma} \right] \quad \text{or} \quad \frac{C_P - \text{Min. } C_{P_0}}{\sigma^3} = f \left[ \frac{C_T}{\sigma^2} \right].$$

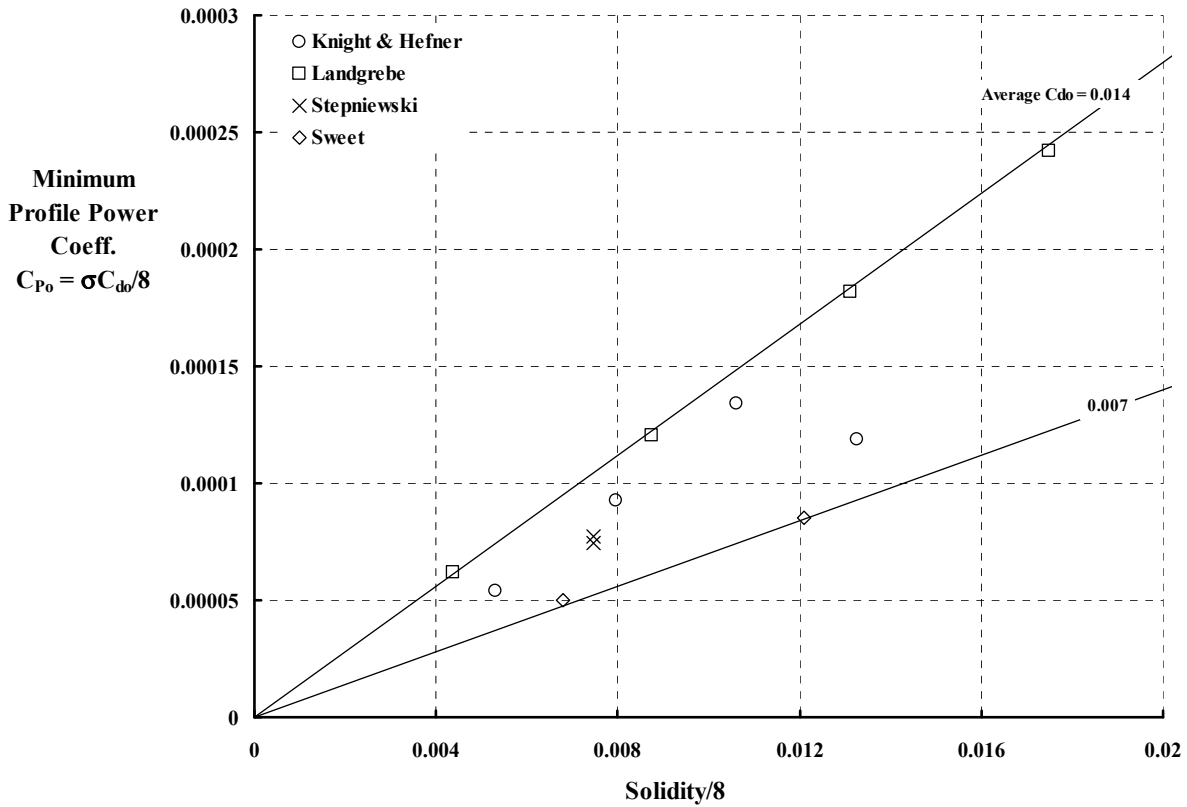


Fig. 2-68. Average airfoil drag coefficient varies considerably.

To effectively use Knight and Hefner's suggested form, the power at flat pitch (i.e., minimum  $C_{p0}$ ) must be accurately measured and/or calculated. Even a cursory search of test data shows that minimum  $C_{p0}$  as a function of  $\sigma/8$  yields a large difference in an airfoil's minimum drag coefficient. Variations in blade average airfoil and minimum drag coefficients ( $C_{d0}$ ) between 0.007 and 0.014 are quite common as Fig. 2-68 shows. However, Knight and Hefner's scatter about a  $C_{d0} = 0.0115$  is not so common.

Knight and Hefner's test results for their four rotor configurations are shown in the most fundamental form in Fig. 2-69. They did not include this graph of total power ( $C_p$ ) versus collective pitch ( $\theta$ ) in their report. Fig. 2-69 shows, however, that the trend established by the two-, three-, and four-bladed configurations is interrupted by the five-bladed rotor set. It appears to me that some constant abnormality exists in the measured power required for the five-bladed configuration. An arbitrary power shift upwards, consistent with the minimum  $C_{p0}$  scatter shown in Fig. 2-68, appears appropriate. This would be an increment of about  $\Delta C_{p0} \approx +0.000034$ . Without this increment, you might mistakenly conclude from Fig. 2-69 that there is little performance difference between four- and five-bladed rotors. Knight and Hefner did not comment on this point, presumably because they were looking closely at  $C_p$  minus  $C_{p0}$ .

### 2.3 HOVER PERFORMANCE

Knight and Hefner convinced themselves that they were on the right path by first plotting  $C_p$  minus minimum  $C_{p_0}$ , versus collective pitch,  $\theta$ . Their results are reproduced here in Fig. 2-70. They used the measured  $C_p$  minus the test minimum  $C_{p_0}$  for each rotor configuration to obtain  $C_p - C_{p_0}$ . As Fig. 2-70 shows, there is a clearly defined progression with blade number, which is in contrast to Fig. 2-69. They presumably concluded that, despite some inconsistency in the power at zero thrust (i.e., minimum  $C_{p_0}$ ), the additional power due to thrust was measured accurately enough for their purposes. (By making this presumption, I suggest that some mechanical or aerodynamic zero shifting in the torque balance may have occurred with the five-bladed configuration.)

Knight and Hefner used blade element momentum theory to define equations for both induced and profile power contributions to the test ( $C_p$  minus minimum  $C_{p_0}$ ) trends exhibited in Fig. 2-70. In modern notation, their derivations leading to their suggested similarity parameters can be conveyed fairly easily. For induced power, they transformed

$$(2.87) \quad P_i = \int_0^R v_{(r)} dT_{(r)} = \frac{1}{2} \rho b c R V_t^3 \left\{ \int_0^1 x^3 C_{l(x)} \left[ v_{(x)} / x V_t \right] dx \right\}$$

to

$$(2.88) \quad P_i = \frac{1}{2} \rho b c R V_t^3 \left( \frac{\sigma a^2}{16} \right) \left( \frac{\sigma a}{16} \right) \left\{ \int_0^1 \left( \frac{16 C_{l(x)}}{\sigma a^2} \right) \left( \frac{16 v_{(x)}}{\sigma a V_t} \right) x^2 dx \right\}$$

by assuming constant chord, untwisted blades, and constant airfoil lift-curve slope. Then, using Eqs. (2.88), (2.73), and (2.71), they addressed the resulting induced-power integral of

$$(2.89) \quad \frac{512 C_{P_i}}{\sigma^3 a^3} = \int_{x_c}^B \left( \Theta x^2 + x - x \sqrt{1 + 2x\Theta} \right) \left( \sqrt{1 + 2x\Theta} - 1 \right) dx .$$

Although Knight and Hefner chose the tip loss factor as  $B = 1$  and  $x_c = 0$ , the integrated result, including these two potential variables, is

$$(2.90) \quad \frac{512 C_{P_i}}{\sigma^3 a^3} = \frac{(F^7 - H^7)}{28\Theta^2} + \frac{(F^5 - H^5)}{10\Theta^2} - \frac{(F^3 - H^3)}{4\Theta^2} - (B^2 - x_c^2) - (B^3 - x_c^3)\Theta$$

where, again,  $\Theta = \frac{16\theta}{\sigma a}$  and  $F \equiv \sqrt{1 + 2B\Theta}$  and  $H \equiv \sqrt{1 + 2x_c\Theta}$ .

Knight and Hefner approached the profile power due to lift by assuming a parabolic airfoil drag polar. They tested a rectangular wing of aspect ratio 12 in an open-throat wind tunnel having a jet diameter of 9 feet. Correcting this data to infinite-aspect ratio gave them NACA 0015 properties at a Reynolds number of 242,000, which corresponded to their model rotor blade-tip conditions. They concluded that, for their model rotor tests, the blade element airfoil drag coefficient should be on the order of

$$(2.91) \quad C_d \approx C_{d_0} + \epsilon \alpha^2 \approx 0.0115 + 0.75\alpha^2 \quad \text{or} \quad C_d \approx C_{d_0} + kC_1^2 \approx 0.0115 + 0.0228C_1^2 .$$

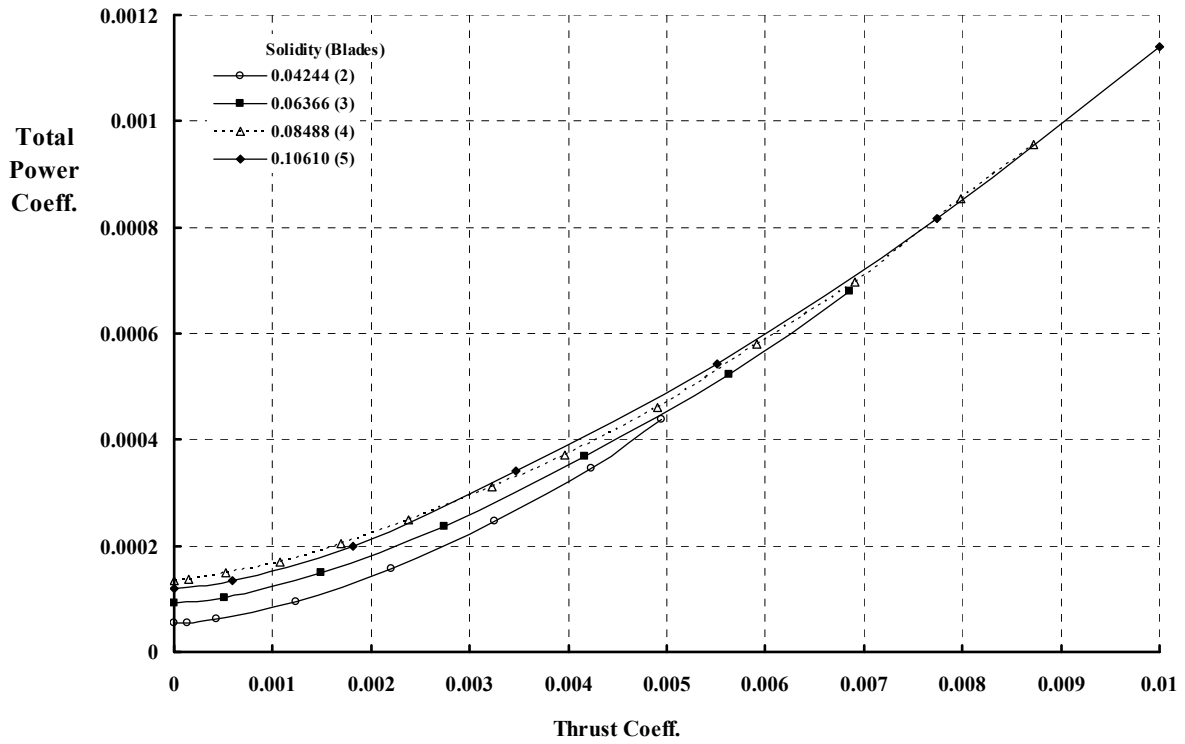


Fig. 2-69. Five-bladed model does not follow trend. Measurement tare at zero thrust presumed in error.

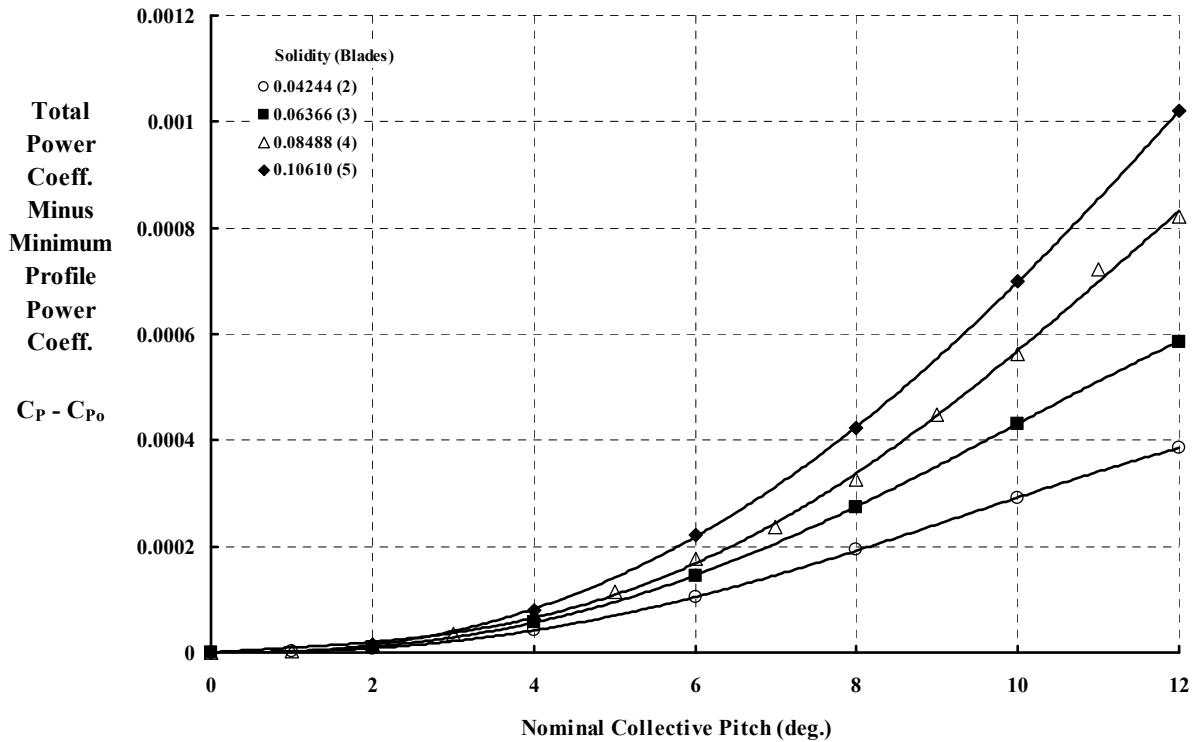


Fig. 2-70. Knight and Hefner used delta power as the basis for their similarity parameter.

### 2.3 HOVER PERFORMANCE

They averaged the minimum profile power measured from their two-, three-, four-, and five-bladed runs and arrived at  $C_{do} = 0.0115$ , which they stated was in agreement with their wing test. The four configurations did have some scatter as Fig. 2-68 shows. For the incremental profile power due to thrust, they transformed

$$(2.92) \quad \Delta P_o = b \int (\Omega r) d(\Delta D_o) = b \int_{r_c}^{BR} (\Omega r) \left[ \frac{1}{2} \rho (\Omega r)^2 c dr \right] (k C_l^2)$$

to

$$(2.93) \quad \Delta P_o = \frac{1}{2} \rho b c R V_t^3 k \left( \frac{\sigma a^2}{16} \right)^2 \int_{x_c}^B \left( \frac{16 C_l}{\sigma a^2} \right)^2 x^3 dx,$$

again by assuming constant chord and constant airfoil lift-curve slope. Using Eq. (2.73), they obtained the incremental profile power due to blade pitch angle in the integral form of

$$(2.94) \quad \frac{512 \Delta C_{P_o}}{\sigma^3 a^3 (k a)} = \int_{x_c}^B (\Theta x + 1 - \sqrt{1 + 2x\Theta})^2 x dx.$$

Knight and Hefner also chose  $B = 1$  and  $x_c = 0$  for this profile power integral. The result, including these two potential variables, is

$$(2.95) \quad \frac{512 \Delta C_{P_o}}{\sigma^3 a^3 (ka)} = (B^2 - x_c^2) + \frac{4(B^3 - x_c^3)\Theta}{3} + \frac{(B^4 - x_c^4)\Theta^2}{4} - \frac{(F^7 - H^7)}{14\Theta^2} + \frac{(F^3 - H^3)}{6\Theta^2}$$

where, again,  $\Theta = \frac{16\theta}{\sigma a}$  and  $F \equiv \sqrt{1 + 2B\Theta}$  and  $H \equiv \sqrt{1 + 2x_c\Theta}$ .

With both induced and incremental profile power coefficients theoretically expressed as similarity parameters, Knight and Hefner immediately were able to reach the conclusion shown in Fig. 2-71. They made their primary theory to test comparison [dismissing the integer 512 and  $a^3$  in both Equations (2.90) and (2.95)] simply as

$$\text{Exp.} \frac{(C_p - \text{Min. } C_{p_o})}{\sigma^3} \text{ versus } \frac{\theta_{\text{Test}}}{\sigma}.$$

Knight and Hefner's theory-versus-test comparison is included here as Fig. 2-71. They found that they had underpredicted the test result as Fig. 2-71 shows. This first comparison assumed an airfoil lift-curve slope of  $a = 5.73$  per radian, integration limits of  $B = 1$  and  $x_c = 0$ , and an airfoil drag rise with an  $\alpha^2$  of  $\epsilon = 0.75$  or with a  $C_l^2$  of  $k = 0.0228$ . They concluded that simply raising  $\epsilon$  from 0.75 to 1.25, or  $k$  from 0.02284 to 0.03807, brought theory into agreement with test, and this result is also shown in Fig. 2-71. Most importantly, they had convincing evidence that solidity could be removed as an independent parameter from the power coefficient as well as from the thrust coefficient.

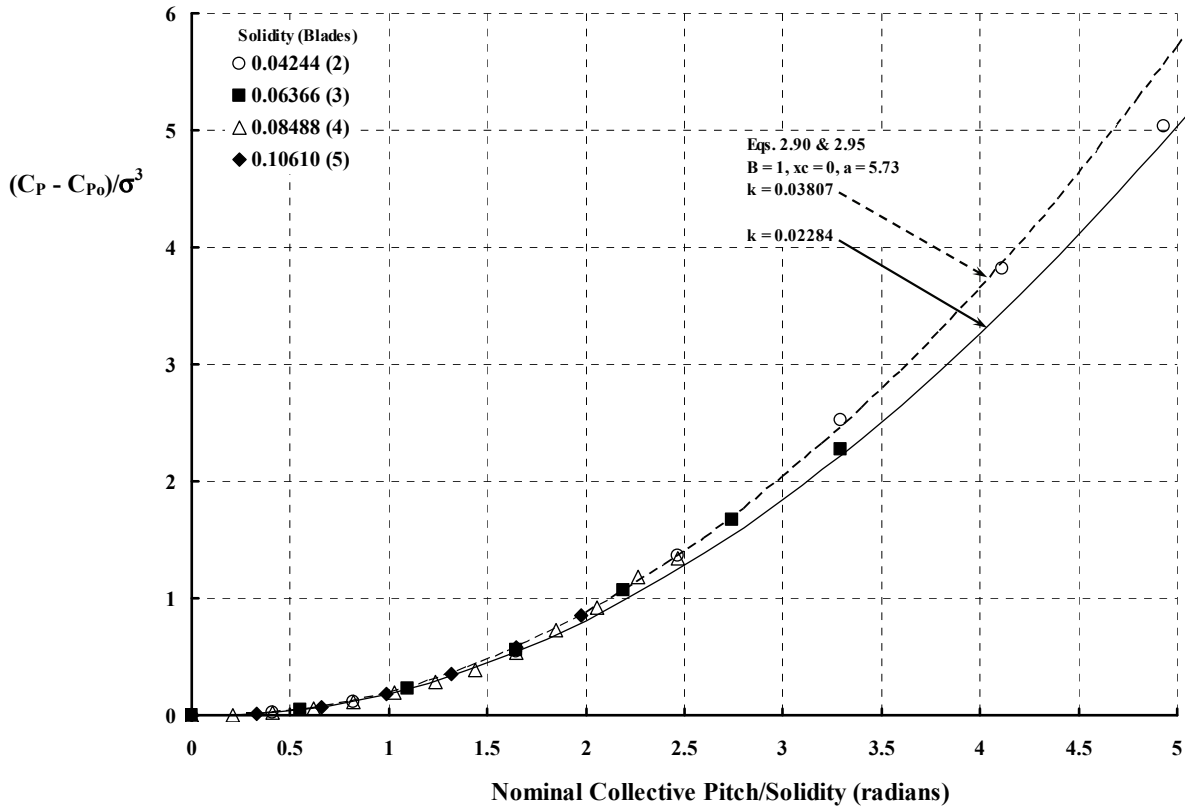


**Fig. 2-71. Knight and Hefner’s delta power similarity parameter removes solidity as an independent variable.**

Predicting power is a challenge given just a nominal blade angle recorded during test. Very few investigators care to take on this challenge today. Even fewer widely publish such a fundamental comparison. Today, blade angle is not generally set to the  $\pm 0.05$ -degree accuracy that Knight and Hefner demanded in their experiment. Furthermore, elastic twist is known to be excessive, and airfoil lift and drag coefficients, over the wide range of Reynolds and Mach numbers required, are rarely available. Nearly 60 years later, rotary wing aerodynamicists do the best they can with airfoil data, ignore elastic twist, and then adjust the theoretical collective pitch angle until the experimental thrust is matched. The published comparison is power versus thrust in some form.

One key conclusion to be drawn from Knight and Hefner’s application of blade element momentum theory to calculate induced and incremental profile power (at least up to blade-stall onset) is that

$$\text{Exp.} \left\{ \frac{512(C_p - \text{Min. } C_{p0})}{\sigma^3 a^3} \right\} \quad \text{should equal} \quad \text{Theory} \left\{ \frac{512 C_{pi}}{\sigma^3 a^3} + (ka) \left[ \frac{512 \Delta C_{p0}}{\sigma^3 a^3 (ka)} \right] \right\}.$$

Therefore, because induced power, profile power, and thrust depend on the collective pitch similarity parameter  $\Theta = 16\theta/\sigma a$ , they continued their analysis with a graph of

### 2.3 HOVER PERFORMANCE

$$\text{Exp.} \frac{(C_p - \text{Min. } C_{p0})}{\sigma^3} \quad \text{versus} \quad \text{Exp.} \frac{C_T}{\sigma^2}.$$

Their comparison is reproduced here as Fig. 2-72.

Because Knight and Hefner did not use a tip loss factor (i.e.,  $B = 1$ ) and also ignored loss of lift at the blade root (i.e.,  $x_c = 0$ ), they could only conclude that their airfoil drag polar was in error. Fig. 2-71 showed their theoretical results with  $k = 0.02284$  and with  $k = 0.03807$ . Another possible conclusion can be drawn, however. For example, Gessow and Myers [234] suggested that the tip loss factor should vary with thrust coefficient as shown with Eq. (2.77), which is repeated here for convenience:

$$B = 1 - \frac{\sqrt{2C_T}}{b} = 1 - \frac{\sqrt{2}}{\pi AR} \left( \frac{C_T}{\sigma^2} \right)^{1/2}.$$

Other investigators, including Prandtl and Goldstein, had suggested other semiempirical ways of treating blade-element lift and drag loading over the outboard region of the blade such as increasing the  $\sqrt{2}$  to 3.25 so that

$$(2.96) \quad B = 1 - \frac{3.25}{\pi AR} \left( \frac{C_T}{\sigma^2} \right)^{1/2}.$$

Knight and Hefner might have assumed that their airfoil drag polar was accurate. Then the difference between test and theory could be charged empirically to the tip loss factor. Fig. 2-72 shows that if the tip loss factor given by Eq. (2.96) is assumed, then correlation between test and theory is excellent with the airfoil drag polar described by  $k = 0.02284$ —as Knight and Hefner measured with their high-aspect-ratio wing test—and provided that the tip loss factor is increased to that given by Eq. (2.96).

Knight and Hefner showed that solidity could be removed as a parameter when comparing delta power versus thrust performance data from different rotor configurations. Additional data supporting their conclusion is seen in Fig. 2-73. The data summarized in Fig. 2-73 encompasses a wide range in blade geometry and aerodynamic parameters, however, all blades were untapered and untwisted.

The major contribution that Knight and Hefner made was showing how to remove solidity as an independent parameter when dealing with hovering rotor test data. Their suggestions appear just as valid today as they did in 1937. Their approach did not, however, alleviate the need to accurately predict and measure minimum profile power. Nor did it resolve the semiempirical trade between tip loss factor and airfoil drag polar. This trade has been used for decades “to make the answer come out right.”

There have been many discussions, some quite heated, as to what semiempirical factors (such as tip loss, root cutout, and airfoil aerodynamic properties) are most generally applicable when using blade element momentum theory to predict performance of a new helicopter product. So far, the rotary wing aerodynamic community has never guessed the right answer prior to flight test.

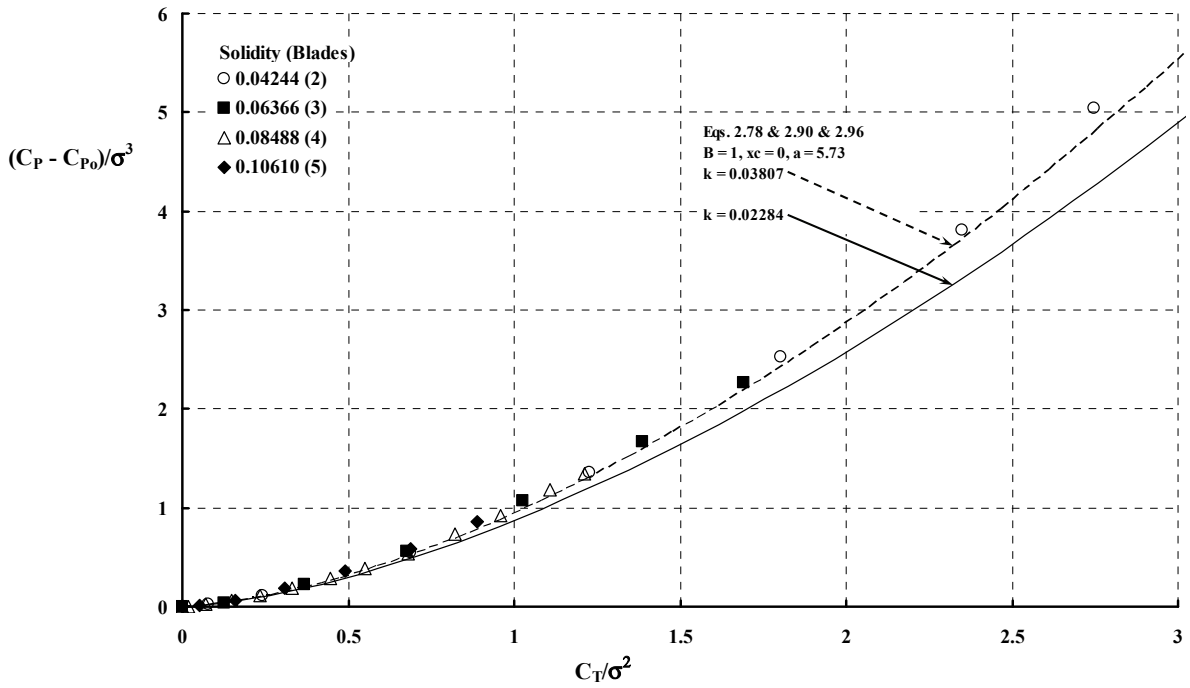


Fig. 2-72. Blade element momentum theory requires large tip loss factors to correlate with experiments when realistic airfoil data is used.

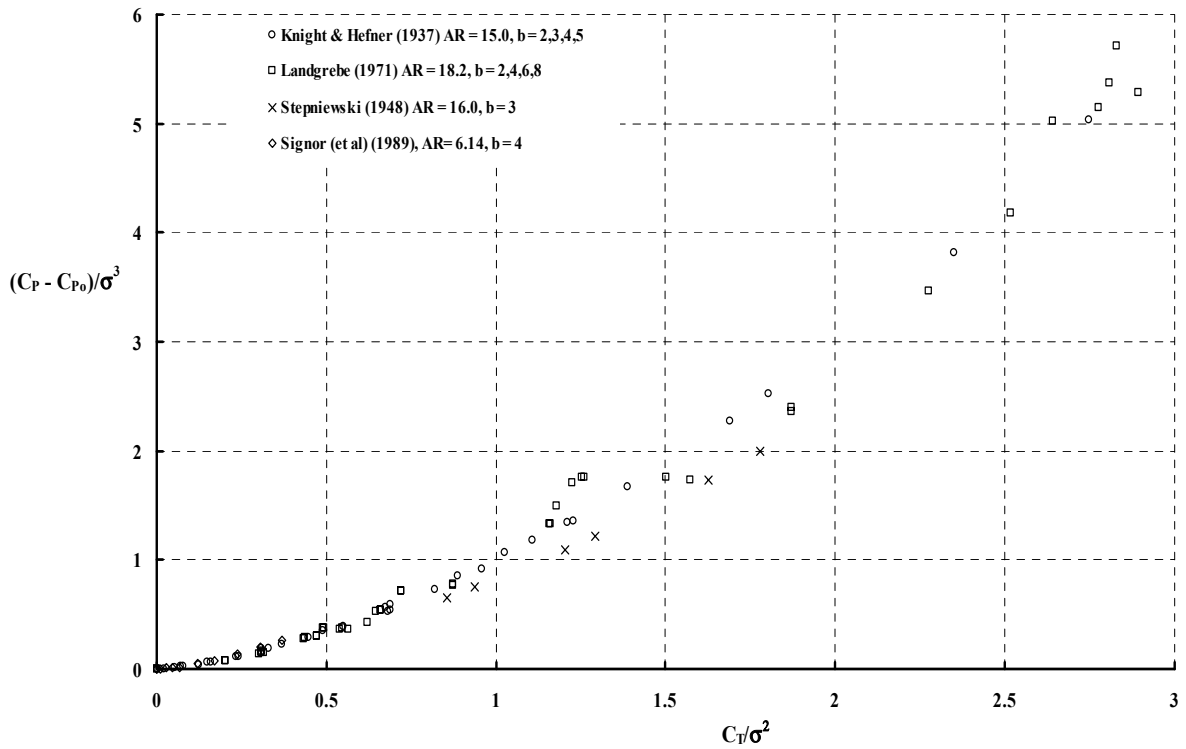


Fig. 2-73. Knight and Hefner's similarity parameter removes solidity as a variable so performance differences between rotors are clearer.

### 2.3 HOVER PERFORMANCE

You should be aware that blade element momentum theory is not able to resolve whether, for a given solidity, a few wide-chord blades are better or worse performing than many narrow-chord blades. The most definitive answer to date has come from test. Landgrebe [246] concludes from figure 21 of his report that six aspect-ratio-13.6 blades performed as well as eight aspect-ratio-18.2 blades. The constant solidity of the 0.14 test was performed at 525 and 700 feet per second, which tends to remove both Reynolds and Mach number considerations. A comparison of two narrow-chord versus two wide-chord blades was experimentally made by Sweet [248]. His results also support the conclusion that solidity is the primary variable as Fig. 2-73 shows.

Blade element momentum theory can suggest at least two twist distributions for an untapered blade that will minimize induced power. The more familiar of the two twist distributions comes from simple, axial momentum theory. According to simple axial momentum theory, the induced power will be a minimum when the axial-induced velocity is constant over the complete actuator disc. (This conclusion has never been proven, but has been used ever since W. J. M. Rankine initiated momentum theory for marine propeller design in 1865.) When only axial-induced velocity is considered (i.e., swirl-induced velocity is neglected), the blade element momentum theory suggestion comes from Eq. (2.71), which is repeated here for a constant chord blade as

$$(2.71) \quad \frac{16}{a\sigma} \frac{v_{(x)}}{V_t} = \left[ \sqrt{1 + 2x \left[ \frac{16\theta_{(x)}}{a\sigma} \right]} - 1 \right].$$

When the objective is uniform, axial-induced velocity, then Eq. (2.71) says that the product,  $x \theta_{(x)}$ , of the untapered blade should be a constant. The constant is classically defined as  $\theta_{tip}$ , and the twist distribution should be  $\theta_{tip}/x$ . In Knight and Hefner's similarity form, this twist distribution means that

$$(2.97) \quad \frac{16}{a\sigma} \frac{v}{V_t} = \left[ \sqrt{1 + 2x \left[ \frac{\Theta_{tip}}{x} \right]} - 1 \right] = \sqrt{1 + 2\Theta_{tip}} - 1 \quad \text{where} \quad \Theta_{tip} = \frac{16\theta_{tip}}{a\sigma}.$$

Then the blade element lift coefficient, given generally by Eq. (2.73), becomes simply

$$(2.98) \quad \frac{16C_l}{a^2\sigma} = \frac{\Theta_{tip}}{x} + \frac{1}{x} - \frac{1}{x} \sqrt{1 + 2x \left[ \frac{\Theta_{tip}}{x} \right]} = \frac{\Theta_{tip} + 1 - \sqrt{1 + 2\Theta_{tip}}}{x}.$$

The single rotor total thrust, induced power, and delta profile power due to airfoil lift follow directly from radial integration as was shown earlier for the untwisted blade starting with Eqs. (2.75), (2.88), and (2.93), respectively. The result for rotor thrust is

$$\begin{aligned}
(2.99) \quad \frac{32C_T}{\sigma^2 a^2} &= \int_{x_c}^B \left( \frac{16C_l}{\sigma a^2} \right) x^2 dx = \int_{x_c}^B \left( \Theta_{tip} + 1 - \sqrt{1 + 2\Theta_{tip}} \right) x dx \\
&= \left( \Theta_{tip} + 1 - \sqrt{1 + 2\Theta_{tip}} \right) \left( \frac{B^2 - x_c^2}{2} \right)
\end{aligned}$$

The result for induced power is

$$\begin{aligned}
(2.100) \quad \frac{512C_{P_i}}{\sigma^3 a^3} &= \int_{x_c}^B \left( \frac{16C_{l(x)}}{\sigma a^2} \right) \left( \frac{16v_{(x)}}{\sigma a V_t} \right) x^2 dx \\
&= \int_{x_c}^B \left( \Theta_{tip} + 1 - \sqrt{1 + 2\Theta_{tip}} \right) \left( \sqrt{1 + 2\Theta_{tip}} - 1 \right) x dx \\
&= \left( \Theta_{tip} + 1 - \sqrt{1 + 2\Theta_{tip}} \right) \left( \sqrt{1 + 2\Theta_{tip}} - 1 \right) \left( \frac{B^2 - x_c^2}{2} \right)
\end{aligned}$$

The result for profile power due to airfoil lift is

$$\begin{aligned}
(2.101) \quad \frac{512 \Delta C_{P_o}}{\sigma^3 a^3 (k a)} &= \int_{x_c}^B \left( \frac{16C_l}{\sigma a^2} \right)^2 x^3 dx = \int_{x_c}^B \left( \Theta_{tip} + 1 - \sqrt{1 + 2\Theta_{tip}} \right)^2 x dx \\
&= \left( \Theta_{tip} + 1 - \sqrt{1 + 2\Theta_{tip}} \right)^2 \left( \frac{B^2 - x_c^2}{2} \right)
\end{aligned}$$

The simplicity of these rotor thrust, induced power, and delta profile power expressions easily permits power to be expressed in terms of thrust. This removes collective pitch from the performance problem. Thus, by inspection, the delta profile power due to airfoil lift becomes

$$(2.102) \quad \frac{512 \Delta C_{P_o}}{\sigma^3 a^3 (k a)} = \left( \frac{2}{B^2 - x_c^2} \right) \left[ \frac{32C_T}{\sigma^2 a^2} \right]^2$$

The induced power is reduced to<sup>54</sup>

$$(2.103) \quad \frac{512 C_{P_i}}{\sigma^3 a^3} = \left( \frac{2}{\sqrt{B^2 - x_c^2}} \right) \left[ \frac{32C_T}{\sigma^2 a^2} \right]^{3/2}$$

The two rotor powers given by Eqs. (2.102) and (2.103) can be added together, and the several integers, as well as airfoil lift curve, collected. Thus, the performance of a single, isolated rotor with untapered blades having a  $\theta_{(x)} = \theta_{tip} / x$  twist distribution is

<sup>54</sup> The induced power squared divided by thrust cubed leads to

$$\frac{\left[ \left( \Theta_{tip} + 1 - \sqrt{1 + 2\Theta_{tip}} \right) \left( \sqrt{1 + 2\Theta_{tip}} - 1 \right) \right]^2}{\left( \Theta_{tip} + 1 - \sqrt{1 + 2\Theta_{tip}} \right)^3} = \frac{\left( \sqrt{1 + 2\Theta_{tip}} - 1 \right)^2}{\left( \Theta_{tip} + 1 - \sqrt{1 + 2\Theta_{tip}} \right)} = 2$$

### 2.3 HOVER PERFORMANCE

$$(2.104) \quad \frac{C_{P_i} + \Delta C_{P_o}}{\sigma^3} = \left( \frac{4k}{B^2 - x_c^2} \right) \left[ \frac{C_T}{\sigma^2} \right]^2 + \left( \frac{1}{\sqrt{2}\sqrt{B^2 - x_c^2}} \right) \left[ \frac{C_T}{\sigma^2} \right]^{3/2}.$$

This result is frequently presented without using Knight and Hefner's solidity-removing form so that

$$(2.105) \quad C_{P_i} + \Delta C_{P_o} = C_T \sqrt{\frac{C_T}{2(B^2 - x_c^2)}} + \left( \frac{4k\sigma}{B^2 - x_c^2} \right) \left[ \frac{C_T}{\sigma} \right]^2.$$

The hover performance of a single, isolated rotor having untapered blades twisted as  $\theta_{(x)} = \theta_{tip}/x$  is occasionally advanced as an ideal rotor (expressed in coefficient form). This is not correct for two reasons that become clear when the previous Eq. (2.105) is expanded to dimensional form. In practice, minimum profile power must, at the very least, be included so that the total power becomes

$$(2.106) \quad \begin{aligned} 550 \text{ HP} &= \text{Min. } P_o + \Delta P_o + P_i \\ &= \frac{(\rho bcR V_t^3)}{8} C_{d_o} + \frac{4k}{\rho bcR V_t (B^2 - x_c^2)} T^2 + \frac{T^{3/2}}{\sqrt{2\rho(\pi R^2)(B^2 - x_c^2)}}. \end{aligned}$$

Many investigators have examined the obvious question presented by Eq. (2.106), which is, "What configuration minimizes horsepower for a given thrust?" The minimum profile power term in Eq. (2.106) says, for example, that the blade area ( $bcR$ ) should be zero and/or the rotor should not turn (i.e.,  $V_t = 0$ ). The delta profile power term (the second term) says that the blade area should be infinitely large and/or the tip speed should be infinitely large. The induced-power term says that the blade radius should be infinitely large. Because, in practice, the induced power is two to three times the sum of the two profile terms, the least power for a given thrust is approached with the largest diameter rotor that the overall rotorcraft can accept.<sup>55</sup> Then the profile power must be minimized.

There is a more practical way to examine this optimization problem. If the induced power obtained with uniform, induced velocity is accepted as a minimum, then the minimum total profile power can be dealt with in terms of the airfoil lift-to-drag ratio. That is, let the search begin with total profile power expressed in the form

$$(2.107) \quad P_o = b \int_0^R (\Omega r) dD_o = b \int_0^R (\Omega r) \left[ \frac{1}{2} \rho (\Omega r)^2 (c_{(r)} C_{d(r)}) \right] dr,$$

and calculate the blade-element airfoil drag coefficient from its lift-to-drag ratio as

$$(2.108) \quad C_{d(r)} \equiv \frac{C_{l(r)}}{C_{l(r)}/C_{d(r)}} = \frac{C_{l(r)}}{(C_l/C_d)_{\max}}.$$

---

<sup>55</sup> The more practical design problem is how to maximize productivity per "buck."

If every blade element is operated at its maximum lift-to-drag ratio *and* this ratio is independent of the radius station, then Eq. (2.108) can be substituted into Eq. (2.107), which gives, with some rearrangement in advance,

$$(2.109) \quad P_o = \frac{\frac{1}{2}\rho\Omega}{(C_l/C_d)_{\max.}} \int_0^R \left[ b c_{(r)} C_{l(r)} (r\Omega^2) \right] r^2 dr.$$

Profile power, as collected in Eq. (2.109), highlights a bracketed term within the integral that is proportional to total thrust. That is, rewriting Eq. (2.67) shows that

$$(2.110) \quad b c_{(r)} r\Omega^2 C_{l(r)} = 8\pi v_{(r)}^2 = 8\pi v^2 = 8\pi \left( \frac{T}{2\rho\pi R^2} \right) = \frac{4T}{\rho R^2}.$$

This grouping of Eq. (2.67) to give Eq. (2.110), and then substituting the result into Eq. (2.109), reduces the total profile power to

$$(2.111) \quad P_o = \frac{\frac{1}{2}\rho\Omega}{(C_l/C_d)_{\max.}} \left( \frac{4T}{\rho R^2} \right) \int_0^R r^2 dr = \frac{\frac{2}{3}\Omega R}{(C_l/C_d)_{\max.}} T.$$

The induced power remains at its minimum so that the total power required to produce a given thrust is simply

$$(2.112) \quad 550 \text{ HP} = \text{Min. } P_o + \text{Min. } P_i = \frac{\frac{2}{3}\Omega R}{(C_l/C_d)_{\max.}} T + \frac{T^{3/2}}{\sqrt{2\rho(\pi R^2)}}.$$

Because the objective is the least horsepower for a given thrust (or conversely, the most thrust for a given horsepower), dividing Eq. (2.112) through by thrust reduces the optimization problem to

$$(2.113) \quad \frac{550 \text{ HP}}{T} = \frac{\frac{2}{3} V_t}{(C_l/C_d)_{\max.}} + \frac{T^{1/2}}{\sqrt{2\rho(\pi R^2)}} = \frac{\frac{2}{3} V_t}{(C_l/C_d)_{\max.}} + \sqrt{\frac{T}{2\rho(\pi R^2)}}.$$

Quite clearly, the “optimum” rotor is now seen as (1) carrying the thrust on the largest possible swept disc area, (2) turning with the lowest practical tip speed, and (3) using airfoils with the highest achievable lift-to-drag ratio. The blade planform geometry and twist distribution that provide this minimum power solution are given by

$$(2.114) \quad c_{(r)r} = \frac{4T}{b\rho V_t^2 (\text{Design } C_l)} \quad \text{and} \quad \theta_{(x)} = \frac{\text{Design } C_l}{a} + \frac{\sqrt{C_T/2}}{x}.$$

This blade geometry is actually a relatively poor description because it is based solely on simple, axial momentum theory that ignores the swirl- or inplane-induced velocity. Furthermore, because the theory assumes an infinite number of blades, the actual loading is poorly described near both the blade’s tip and root. Despite these and other shortcomings, Eq. (2.113) does provide a first-order estimate of the least power required to produce a given design thrust. Of course Eq. (2.113) is not applicable to off-design conditions; rather, it is an envelope to the best performance of all rotors at their individual design points.

## 2.3 HOVER PERFORMANCE

The preceding, somewhat lengthy discussion of blade element momentum theory gives you some background about the industry's tool used to calculate hover power required. This tool, or some variation, has been in use for over six decades. With the advent of digital computers, more sophisticated theoretical versions were programmed. In the last decade or so, the field of computational fluid dynamics (CFD) blossomed. CFD gave aerodynamicists the ability to calculate both the air flow through and about a rotor. It also allowed the prediction of airfoil lift, drag, and pitching moment, and tables of airfoil properties could be dispensed with. The insight obtained with CFD during the development of this very powerful predictive tool has been impressive, however the CFD rotary wing community has yet to predict complete helicopter hover performance, and display correlation of theory with test, in a comprehensive scope comparable to Kocurek [168].

### 2.3.8 Single Rotor Helicopter Summary

This detailed discussion about power required to hover began with Fig. 2-51 on page 139. The engine-power-required coefficient ( $C_{P_{eng}}$ ) versus helicopter weight coefficient ( $C_W$ ) is shown for a number of machines. While there is a range of  $\pm 12$  percent about a trend given previously by

$$(2.41) \quad C_{P_{Reqd.}} = 0.0157C_W + 1.045C_W^{3/2},$$

the accumulated flight test data makes it possible to get a composite picture of hover power required by single rotor helicopter. In the following discussion, blade element momentum theory plays a key role in seeing just what the industry's modern results are.

Consider Eq. (2.47), repeated here for convenience, as the starting point for any single rotor helicopter:

$$(2.47) \quad ESHP_{req} = \frac{RHP_{Main\ Rotor}}{\eta_{Main\ Rotor}} + \frac{RHP_{Tail\ Rotor}}{\eta_{Tail\ Rotor}} + SHP_{Accessory}.$$

The main rotor power required ( $RHP_{mr}$ ) and tail rotor power required ( $RHP_{tr}$ ), along with the accessory horsepower ( $SHP_{acc}$ ), are the three components of the problem. Because the industry has tried to develop the main rotor system as close to ideal as practical, calculate the main rotor power required by Eq. (2.106) with an empirical, induced-power "correction" factor ( $k_i$ ) (used to make the answer come out right). Thus,

$$(2.115) \quad \begin{aligned} 550 RHP &= \text{Min. } P_o + \Delta P_o + P_i \\ RHP_{mr} &= \frac{1}{550} \left\{ \frac{(\rho b c R V_t^3)}{8} C_{do} + \frac{4k}{\rho b c R V_t (B^2 - x_c^2)} W^2 + \frac{k_i (W^{3/2})}{\sqrt{2\rho(\pi R^2)(B^2 - x_c^2)}} \right\} \end{aligned}$$

where the tip loss factor ( $B$ ) I subscribe to is

$$(2.116) \quad B = 1 - \frac{3.25}{\pi AR} \left( \frac{C_w}{\sigma^2} \right)^{1/2} \quad \text{and} \quad B_{tr} = 1 - \frac{3.25}{\pi AR_{tr}} \left( \frac{C_{r-tr}}{\sigma_{tr}^2} \right)^{1/2},$$

and the blade proper does not begin until the inboard radius station ( $x_c$ ). As a reminder, ( $\rho$ ) is the air density, ( $b$ ) is the blade number, ( $c$ ) is blade chord, ( $R$ ) is blade radius, ( $V_t$ ) is tip speed, ( $C_{do}$ ) is the airfoil minimum drag coefficient, and ( $k$ ) is the airfoil drag rise with the square of the airfoil lift coefficient.

You will note that in constructing Eq. (2.115) from Eq. (2.106), I have simply replaced hover thrust ( $T$ ) with aircraft weight ( $W$ ). I have done this despite the fact that every single-rotor helicopter hovers with the main rotor thrust some 2 to 5 percent greater than the aircraft's weight (because of download). Neglecting this download factor ( $T/W$ ) of 1.02 to 1.05 means that the induced power "correction" factor ( $k_i$ ) will be artificially raised a few percent points as will the apparent airfoil drag rise with airfoil lift coefficient ( $k$ ). Keep in mind that the addition of a wing adds extra download that must be accounted for.

To avoid excessive subscripting, let me use the subscript ( $tr$ ) for the tail rotor and only use the subscript ( $mr$ ) for the main rotor where required.

The tail rotor thrust required to maintain yaw equilibrium follows from the discussion surrounding Eq. (2.49), starting on page 142. Thus,

$$(2.117) \quad T_{tr} = \frac{550 \text{ RHP}_{mr}}{(R + R_{tr}) \Omega_{mr}} = \frac{550 \text{ RHP}_{mr}}{(1 + R_{tr}/R) V_{t-mr}}.$$

Note here that the tail rotor moment arm ( $l_t$ ) has been replaced by the sum of the main rotor radius ( $R_{mr}$ ) and the tail rotor radius ( $R_{tr}$ ), which is geometrically closer to the single rotor helicopters under discussion.

A first-order approximation of the tail rotor horsepower is sufficient for this discussion, so assume that

$$(2.118) \quad 550 \text{ RHP}_{tr} = \text{Min. } P_{o-tr} + \Delta P_{o-tr} + P_{i-tr} \approx \text{Min. } P_{o-tr} + k_{tr} P_{i-tr}$$

and, therefore,

$$(2.119) \quad \begin{aligned} \text{RHP}_{tr} &\approx \frac{1}{550} \left\{ \frac{(\rho b_{tr} c_{tr} R_{tr} V_{t-tr}^3)}{8} C_{do-tr} + \frac{k_{tr} (T_{tr}^{3/2})}{\sqrt{4\rho A_{\text{exit}} (B_{tr}^2 - x_{c-tr}^2)}} \right\} \\ &= \frac{1}{550} \left\{ \frac{(\rho b_{tr} c_{tr} R_{tr} V_{t-tr}^3)}{8} C_{do-tr} + \frac{k_{tr}}{\sqrt{4\rho A_{\text{exit}} (B_{tr}^2 - x_{c-tr}^2)}} \left[ \frac{550 \text{ RHP}_{mr}}{(1 + R_{tr}/R) V_{t-mr}} \right]^{3/2} \right\}. \end{aligned}$$

You will recall from the anti-torque discussion that for an unshrouded tail rotor,  $A_{\text{exit}}$  equals  $\frac{1}{2} \pi R_{tr}^2$ , but if the anti-torque device is a ducted fan, then  $A_{\text{exit}} = \pi R_{fan}^2$ . My assumption for ducted fans is that the tip loss factor, Eq. (2.116), is always 1.0 but that the momentum area reflects the large root cutout ( $x_c$ ) characteristic of most ducted fans.

### 2.3 HOVER PERFORMANCE

Let me stop here for a moment to examine flight test data against the nondimensional form suggested by Knight and Hefner. From previous discussion, these early pioneers showed that displaying results as

$$\text{Exp.} \frac{(C_p - \text{Min. } C_{p0})}{\sigma^3} \quad \text{versus} \quad \text{Exp.} \frac{C_T}{\sigma^2}$$

should remove solidity ( $\sigma$ ) as a primary variable. Applying their view to flight test data from many single rotor helicopters requires a little reformatting as follows:

$$(2.120) \quad \frac{550}{\sigma^3} \left\{ \frac{\text{Exp. ESHP} - \frac{\text{Min. RHP}_{\text{mr}}}{\eta_{\text{mr}}} - \frac{\text{Min. RHP}_{\text{tr}}}{\eta_{\text{tr}}} - \text{SHP}_{\text{acc}} \pm \text{Error}}{\rho \pi R^2 V_t^3} \right\} \quad \text{vs} \quad \left\{ \frac{\text{Exp. } C_w}{\sigma^2} \right\}.$$

The minimum main rotor horsepower is simply

$$(2.121) \quad \text{Min. RHP}_{\text{mr}} = \frac{1}{550} \left\{ \frac{(\rho b c R V_t^3)}{8} C_{\text{do}} \right\}.$$

In like manner, the minimum tail rotor horsepower is

$$(2.122) \quad \text{Min. RHP}_{\text{tr}} \approx \frac{1}{550} \left\{ \frac{(\rho b_{\text{tr}} c_{\text{tr}} R_{\text{tr}} V_{\text{t-tr}}^3)}{8} C_{\text{do-tr}} + \frac{k_{\text{tr}}}{\sqrt{2\rho \pi R_{\text{tr}}^2 (B_{\text{tr}}^2 - x_{\text{c-tr}}^2)}} \left[ \frac{550 \text{ Min. RHP}_{\text{mr}}}{(1 + R_{\text{tr}}/R) V_{\text{t-mr}}} \right]^{3/2} \right\}.$$

The second term in the tail rotor power is induced power associated with tail rotor thrust. Keep in mind that when the helicopter is on the ground, friction between the landing gear and the ground provides anti-torque to react the main rotor's minimum horsepower; so the tail rotor can be at any reasonable thrust including zero. But, off the ground (or supported by a frictionless bearing so that the main rotor thrust is zero), some tail rotor thrust is required for yaw equilibrium to balance the torque of the main rotor at minimum power.

Equation (2.120) includes the fact that the flight test data being examined has errors. The error here is that (with reasonable estimates of minimum main- and tail-rotor powers) when the weight coefficient is zero, the sum of all powers in Eq. (2.120) should be zero. This point is illustrated in Fig. 2-73. One test procedure that minimizes this error is to run the aircraft on the ground at zero main- and tail-rotor thrusts. Data is recorded at several engine RPMs. The measured main rotor and tail rotor shaft torques (not powers), when plotted versus their respective rotor speeds squared, should show zero torque at zero rotor speed. If they do not, serious questions are raised. The engine torque versus engine RPM squared will not show zero because of the power required by accessories. Plotting engine horsepower versus RPM cubed should project to a power approximating the accessory power.

The results of applying Eq. (2.120) are shown in Fig. 2-74. This figure reflects modern results based on hover engine power required (out of ground effect) obtained with 40 single rotor helicopters. This group does not include results where compressibility was an obvious factor, such as those reported by Ritter [207]. A little statistical analysis plus educated guessing shows that the average constants for the 40 helicopters are:

- Main rotor minimum airfoil drag coefficient ( $C_{d0}$ ) = 0.008
- Tail rotor minimum airfoil drag coefficient ( $C_{d0-tr}$ ) = 0.016
- Tail rotor induced-power correction factor ( $k_{tr}$ ) = 1.35
- Main rotor transmission efficiency ( $\eta_{mr}$ ) = 0.96
- Tail rotor transmission efficiency ( $\eta_{tr}$ ) = 0.95

Because the flight test reports give little or no information about accessory power, I lumped  $\text{SHP}_{acc}$  and error into one constant horsepower for each individual helicopter. This lumped sum yielded 28 results with less than 5 percent error, 10 results with between 5 and 10 percent error, and 2 results with between 10 and 15 percent error when the blade element results are compared to experiment. These are percentages of the lowest-recorded engine shaft horsepower of the respective helicopter.

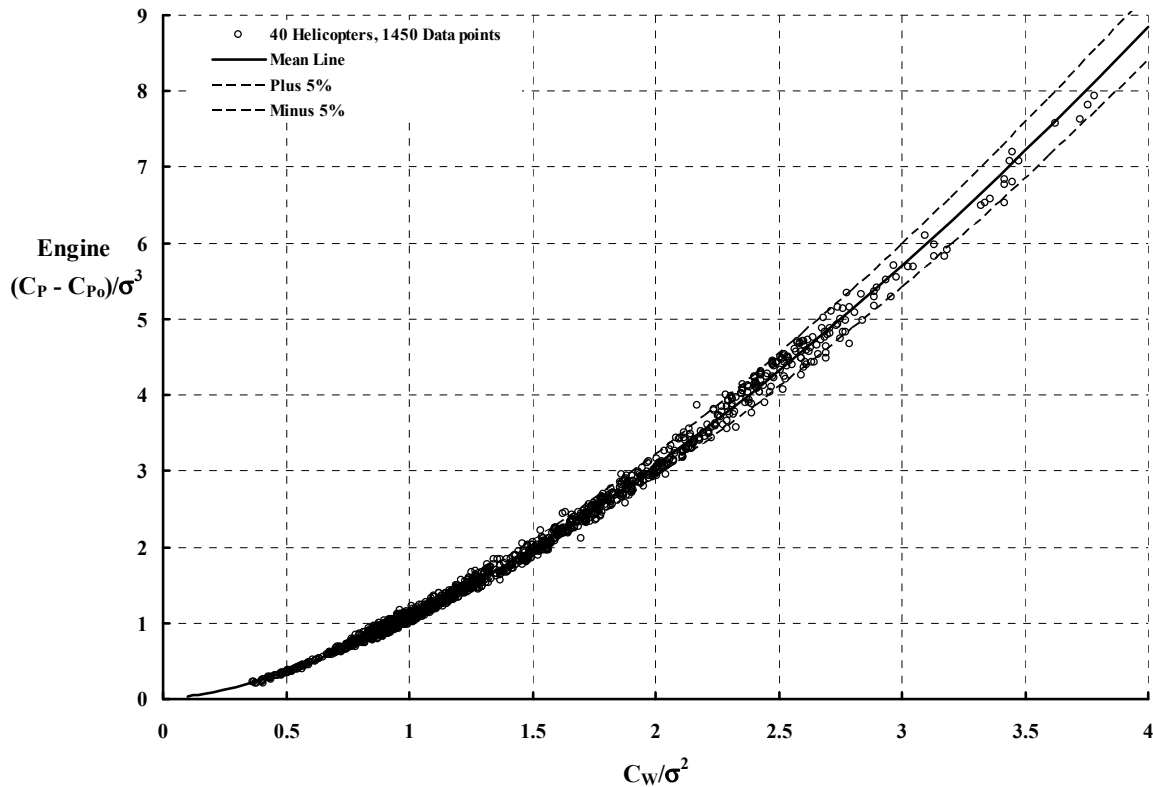


**Fig. 2-74.** Flight test data from 40 single rotor helicopters show that Knight and Hefner's similarity parameters remove solidity as a variable for engineering purposes.

### 2.3 HOVER PERFORMANCE

The 40 helicopters have a wide range in solidity and blade-aspect ratio as Fig. 2-75 shows. The main rotor blade count varies from two, for several Bell Helicopter products, up to seven for the largest Sikorsky helicopter. The two helicopters with high-solidity, ducted-fan, anti-torque devices (11 and 13 blades) are not shown in Fig. 2-75.

These very encouraging results are shown in Fig. 2-74. In 1939, Knight and Hefner provided a very unique, nondimensional form of blade element momentum theory. Their work has received far too little attention by the rotorcraft aerodynamic community.

The real question is, of course, how well does the semiempirically modified, blade element momentum theory convey the modern results of single-rotor-helicopter power required in hovering out of ground effect. The favorable answer is shown for the 40 helicopters discussed in Fig. 2-76. Equations (2.47), (2.115), (2.116), and (2.119) are used with the main rotor airfoil drag rise with lift coefficient squared ( $k$ ), and the induced-power “correction” factor ( $k_i$ ) defined. That is, along with

- Main rotor minimum airfoil drag coefficient ( $C_{do}$ ) = 0.008,
- Tail rotor minimum airfoil drag coefficient ( $C_{do-tr}$ ) = 0.016,
- Tail rotor induced-power correction factor ( $k_{tr}$ ) = 1.35,
- Main rotor transmission efficiency ( $\eta_{mr}$ ) = 0.96, and
- Tail rotor transmission efficiency ( $\eta_{tr}$ ) = 0.95,

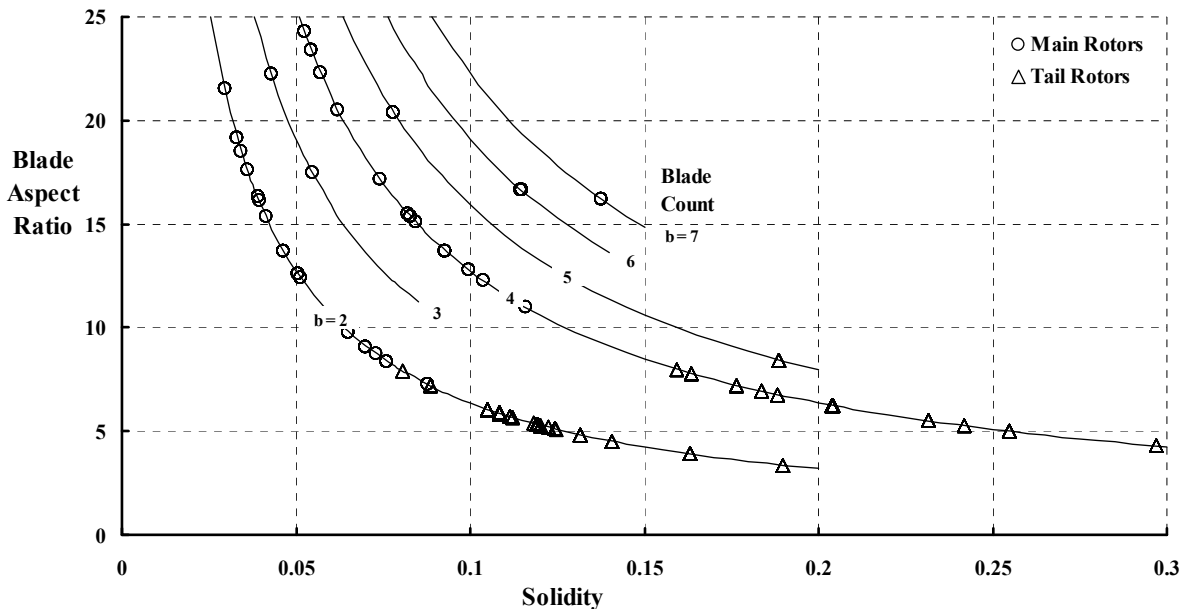


**Fig. 2-75. Flight test data from 40 single rotor helicopters covers a wide range in solidity, blade number, and blade-aspect ratio.**

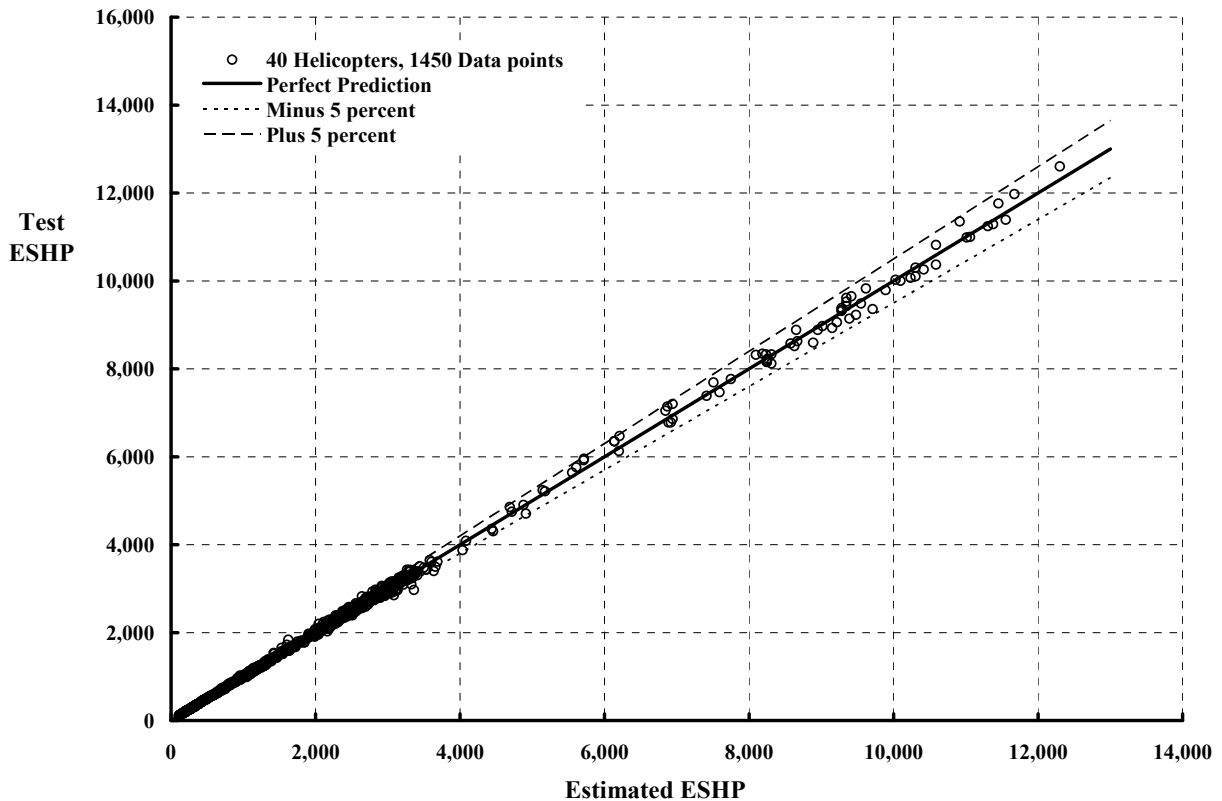


**Fig. 2-76. Hover engine horsepower required by 40 single rotor helicopters is estimated by blade element moment theory—given reasonable empirical constants.**

modern results also suggest that

- Main rotor airfoil drag coefficient rise with  $C_1^2$  is  $(k) = 0.008$ , and
- Main rotor induced power correction factor  $(k_i) = 1.12$ .

Fig. 2-77 provides two examples of the semiempirical use of blade element momentum theory as summarized in the preceding paragraphs. Basically, the theory predicts very reliable increments in power with weight increases. The primary problem in using the theory is accurately setting the estimated engine horsepower at “zero” weight, which only requires a very educated guess as to the input constants. Still, well over 40 successful helicopters have been developed by several companies using no better theory than what I have just described.

In 30 out of the 40 examples, the comparisons such as those shown in Fig. 2-77 required reducing the estimated power at zero weight coefficient so that the curve passes through the experimental data. In that sense, I hope that the engineering equations offered in this summary are conservative. The reason I have chosen a measure of conservatism is that marketing brochures and proposals to the military have, over six decades, promised more than was delivered [249].

## 2.3 HOVER PERFORMANCE

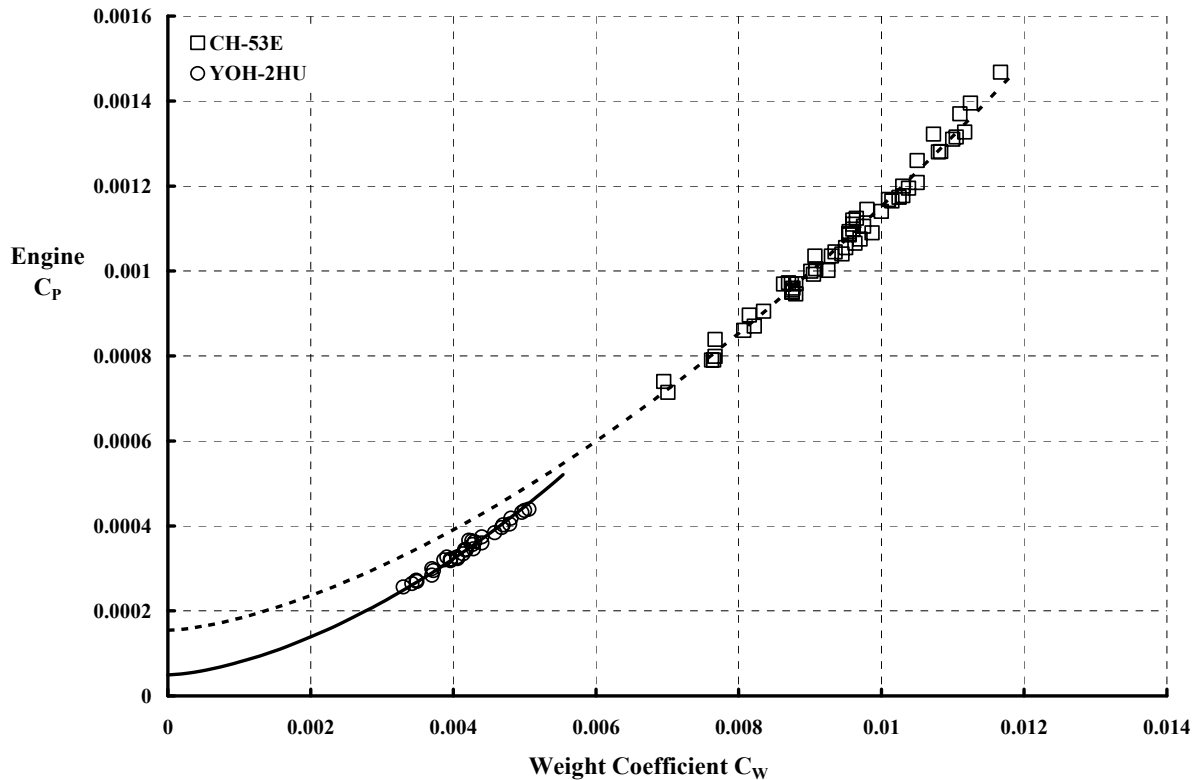


**Fig. 2-77. Hover power required of the smallest and largest single rotor helicopters in the 40 examples under discussion.**

### 2.3.9 Twin-Rotor Helicopters

There is no question that the single rotor plus tail rotor configuration dominates the helicopter world. However, experimental, prototype, and production versions of helicopters using multiple main rotors are more in evidence than you might think. The culling process (helped by World War II) quickly discarded tri-rotors and quad-rotors, and Focke's side-by-side pioneering effort. Experimental flight of at least 40 twin-rotor machines further reduced the field to 3 major manufacturers. Even a quick scan of industry efforts leads to the partial summary of production, twin-rotor helicopters provided in Table 2-13. Within this group, Frank Piasecki developed the tandem configuration starting with the HRP, which grew to the H-21 series, and then the HUP for the U.S. Navy, and its spin-off, the H-25, for the U.S. Army. Charlie Kaman developed the synchropter, the H-43 series, for the U.S. Air Force. And Nikolai Kamov developed and produced the coaxial configuration for the then Soviet military.

Modern results of twin-rotor hovering performance are shown in Fig. 2-51 and Fig. 2-52. The trouble is you cannot see the data points because the single rotor helicopter points are so dominant. The two figures, with single rotor helicopter data points removed, are

## 2.3 HOVER PERFORMANCE

repeated here as Fig. 2-78 and Fig. 2-79. The hover performance, expressed in engine  $C_P$  versus  $C_W$  coefficient form, is illustrated in Fig. 2-78. The solid line on this figure was obtained from Eq. (2.41), which is repeated here for convenience:

$$(2.41) C_{P_{\text{Reqd.}}} = 0.0157C_W + 1.045C_W^{3/2}.$$

**Table 2-13. Twin-Rotor Helicopters**

Manufacturer	Type	Power Plant	Model	Year	Max TOGW (lb)	Diameter (ft)	Total Engine(s) (SHP)
Piasecki	tandem	piston	HUP/H-25 Series	1948	6,005	35.00	525
Piasecki	tandem	piston	H-21 Series	1954	13,233	44.00	1,425
Boeing Vertol	tandem	turbine	CH-46 Series	1960	21,385	50.00	2,100
Boeing Vertol	tandem	turbine	Model 107	1962	19,000	50.00	2,800
Boeing Vertol	tandem	turbine	CH-47 Series	1967	29,850	60.00	5,700
Boeing Vertol	tandem	turbine	Model 234 Series	1981	51,000	60.00	8,150
Bristol	tandem	turbine	B-173 Series	1951	14,500	48.56	1,700
Bristol/Westland	tandem	turbine	B-192	1958	19,995	48.67	3,300
Yakovlev	tandem	piston	Yak-24 Series	1957	37,479	68.92	3,400
Kaman	synchropter	turbine	H-43 Series	1966	9,150	47.00	1,100
Kaman	synchropter	turbine	K-Max	1993	10,394	42.17	1,800
Flettner	synchropter	piston	FL-282	1941	2,205	39.38	140
Kamov	coaxial	piston	Ka-15	1952	3,100	32.71	225
Kamov	coaxial	piston	Ka-18	1957	3,310	32.71	275
Kamov	coaxial	turbine	Ka-25BSh	1967	16,535	51.65	1,800
Kamov	coaxial	turbine	Ka-32	1982	23,148	52.17	4,410
Kamov	coaxial	turbine	Ka-26	1965	7,165	42.65	650
Kamov	coaxial	turbine	Ka-27	1974	18,500	52.17	2,500
Kamov	coaxial	turbine	Ka-28	1975	18,500	52.17	2,500
Kamov	coaxial	turbine	Ka-29	1985	27,775	52.17	4,450
Kamov	coaxial	turbine	Ka-32	1975	27,775	52.17	4,410
Kamov	coaxial	turbine	Ka-50	1985	21,550	47.58	4,450
Kamov	coaxial	turbine	Ka-126	1990	7,165	42.65	720
Kamov	coaxial	turbine	Ka-226	1995	6,835	42.67	840
Focke	side-by-side	piston	FA-223	1940	9,480	39.38	1,000

## 2.3 HOVER PERFORMANCE

At the present time, to the best of my knowledge, Kamov has not made detailed flight test performance data available to the public for any of its coaxial helicopters. As a stand-in, I have used published data from the Sikorsky XH-59A, their Advancing Blade Concept helicopter [210, 250].

Twin-rotor helicopter performance in Figure of Merit form is shown in Fig. 2-79. Based on limited data, one would have to say that the coaxial helicopter enjoys a significant hover performance advantage.

There has been, on many occasions, rather heated technical (and marketing) discussions about how twin-rotor performance should be calculated and presented. For example, one question is, "In the calculation of total thrust, or weight, or power coefficients, what is the reference rotor area?" Another question is, "If Figure of Merit is the ratio of ideal power to actual power, what is the ideal power for twin rotors that are partially overlapped?" In general, the answers are quite straightforward for the coaxial helicopter because, with equal rotor diameter and equal blade number for the upper and lower rotors, simple momentum theory treats the system as one single rotor having twice the number of blades. Flight test reports for the Sikorsky XH-59A [210, 250] use the reference rotor area as simply  $\pi R^2$  where (R) is the radius of one blade. The reference area for the H-43 synchropter [193] has also been taken as  $\pi R^2$  even though there is a slight distance between the two rotor hubs. All flight test data for tandems has been reduced to coefficient form with a  $2 \pi R^2$  reference area.

The coaxial arrangement of twin rotors has received some theoretical and experimental study [251-253], but nowhere near as much effort as has gone into the single rotor configuration. Coleman's survey [253], performed in 1997, did uncover the salient features of what has been done. If you want to pursue the configuration further, I would recommend direct discussion with the Kamov Company.

It is primarily with the tandem rotor helicopter, developed by Frank Piasecki [90], that things get a little complicated. You might not know that Frank Piasecki's first venture was a small, single rotor machine, the PV-2, which was very successful. His first tandem helicopter, the XHRP-X, grew to become the H-21. This series had two rotors, but they were not overlapping. But then, in the mid-1940s, the U.S. Navy initiated a competition for a small helicopter to be used for airplane guard duty aboard its carriers. This helicopter was to fly alongside the carrier when airplanes were landing and taking off. The objective was to rescue pilots who went into the water. To meet the size constraints, Piasecki selected a very small, very overlapped, tandem rotor configuration (the XHJP-1, later to become the HUP) to compete against the Sikorsky conventional single rotor XHJS-1, a slightly enlarged R-5 or S-51. Piasecki's HUP won the fly-off competition and entered Navy service in January 1951.

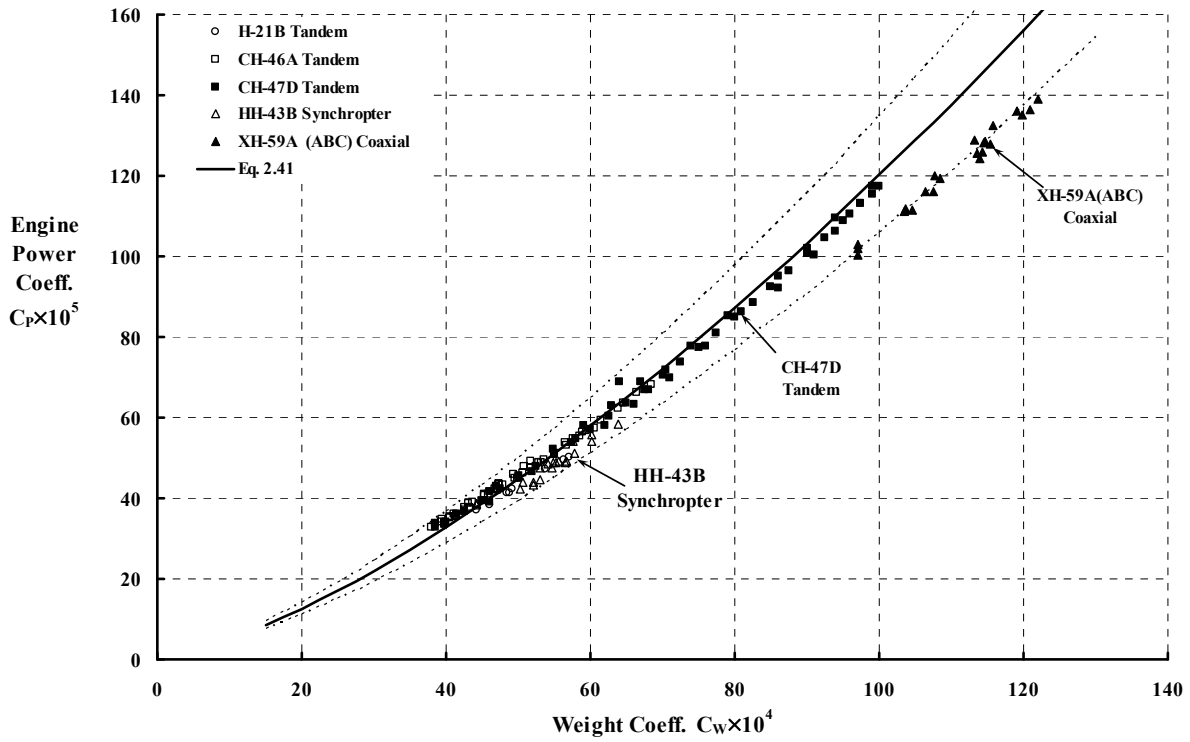


Fig. 2-78. Twin-rotor helicopter performance.

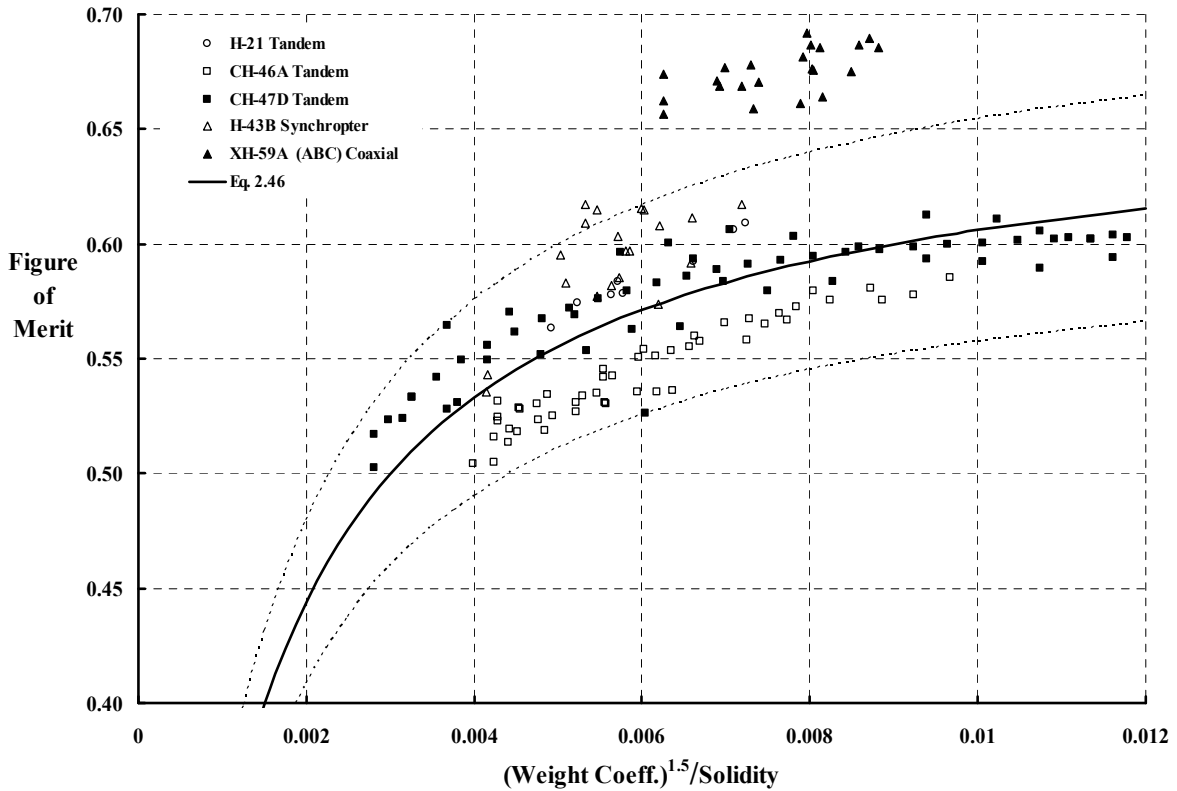


Fig. 2-79. Coaxial helicopters appear to have the highest Figure of Merit.

### 2.3 HOVER PERFORMANCE

There is some fundamental size logic and hover performance logic for the twin-rotor helicopter. To illustrate this logic, consider the following contrasting views that Piasecki (with his XHJP-1) and Sikorsky (with his XHJS-1) must have seen. The engine of choice at that time was the Continental R-975-34, rated at 500 horsepower. Both helicopters, fully loaded, weighed about 5,300 pounds [89]. For discussion purposes, say that 250 of the 500 horsepower was spent on ideal induced power at sea level on a standard day, where the air density was 0.002378 slugs per cubic foot. This would be a Figure of Merit of 0.5 and would ensure a power margin. For the single rotor machine, this would mean the rotor diameter would be 45.9 feet. That is,

$$(2.123) \quad \text{HP}_{\text{ideal}} = \frac{W}{550} \sqrt{\frac{W}{2\rho\left(\frac{\pi}{4}D^2\right)}} = \frac{5,300}{550} \sqrt{\frac{5,300}{2(0.002378)\left(\frac{\pi}{4}45.9^2\right)}} = 250 \text{ hp}.$$

The overall length of the single rotor, with both main rotor and tail rotor blades folded or removed, would be about 0.8 of the main rotor diameter, or about 37 feet.

Now think of splitting the 5,300 pounds gross weight onto two isolated rotors where the hubs are separated by slightly more than a diameter. This means two rotors, each having a diameter of 32.5 feet. That is,

$$(2.124) \quad \text{HP}_{\text{ideal}} = \frac{W/2}{550} \sqrt{\frac{W/2}{2\rho\left(\frac{\pi}{4}D^2\right)}} + \frac{W/2}{550} \sqrt{\frac{W/2}{2\rho\left(\frac{\pi}{4}D^2\right)}} = \frac{W}{550} \sqrt{\frac{W/2}{2\rho\left(\frac{\pi}{4}D^2\right)}} = 250 \text{ hp}.$$

The overall length of this nonoverlapped (i.e., not intermeshed) tandem rotor helicopter with all blades removed or folded would be about 42 feet.

On this basis, the single rotor and tandem rotor size competition would favor the single rotor configuration because it is some 5 feet shorter, however, the tandem configuration would provide more fuselage length for cargo. But the U.S. Navy competition was not for cargo space. The competition was for a small-sized machine that would not occupy much carrier space. (Apparently, a coaxial helicopter was not in consideration—perhaps because of height restrictions—and blade folding must have been a given.)

Piasecki's solution was to overlap the XHJP-1 rotors, which reduced the length to 32 feet with folded blades. With refinement that included a Sperry automatic pilot, the Navy had the HUP-2 shown in Fig. 2-80.

In 1947, to support the design decision to overlap the rotors, Mr. Wieslaw Z. Stepniewski and a small team of enthusiasts working at Piasecki Helicopter Corporation, conducted a fundamental tandem-rotor hover performance test. The experiment measured thrust and power required by two, three-bladed, 4-foot-diameter rotors. Hover-out-of-ground-effect performance was obtained at four overlapped co-planar positions. Funding for this test came as part of the U.S. Navy program to develop the HUP series when this nearly 6,000-pound-gross-weight tandem helicopter went into production. The model thrust and power



**Fig. 2-80. The Piasecki HUP was the world’s first overlapped tandem helicopter. Note that the rear rotor is considerably above the forward rotor (photo from author’s collection).**

data, though published [247, 254], received very limited distribution.<sup>56</sup> Fortunately, the key thrust and power tabulated data from this landmark test—the only one I know of—was recovered along with significant background [255] and is reproduced here as Fig. 2-81.

The procedure Mr. Stepniewski used during his co-planar, tandem rotor overlap experiment was quite straightforward. The fore and aft, 4-foot-diameter rotors were first individually tested to baseline isolated rotor performance. Then both rotors were set to a nominally equal collective pitch angle. Finally, the two rotors were “slid together” starting from a nonoverlapped position of  $d/D = 1.0365$ , where ( $d$ ) is the distance between rotor hubs and ( $D$ ) is rotor diameter. Repositioning for each overlap required stopping the model and hand adjusting the movable rear rotor towards the front rotor. Data was recorded at successive overlaps of  $d/D = 1.0365$ , 0.8802, 0.7604, and 0.6250. This overlap sweep was repeated six times. The lowest collective pitch of 7 degrees was tested at 1570 and 1780 rpm, and the mid-collective of 9 degrees at 1570, 1780, and 2015 rpm. The highest collective pitch, 11.5 degrees, was tested only at 1570 rpm. The RPM range gives tip speeds of 330, 383, and 422 feet per second. The tip Reynolds number ranges from 264,000 to 337,000.

<sup>56</sup> Mr. Wieslaw Z. Stepniewski participated in every tandem rotor helicopter developed by the now Boeing Helicopters Division. Mr. Stepniewski, better known worldwide as just “Steppy,” sent me an original of this very valuable report in 1995. I made a copy (returned the original) and put the raw data into a Microsoft® Excel® spreadsheet. Steppy answered all my questions about the data acquisition and reduction steps. I was able to reaffirm the results with only minor differences. With Steppy’s encouragement and consent, the thrust and power data were published in tabulated and graphical form [255]. This data, which lies behind the  $K_{OV}$  factor, should be of considerable value to current and future investigators.

## 2.3 HOVER PERFORMANCE

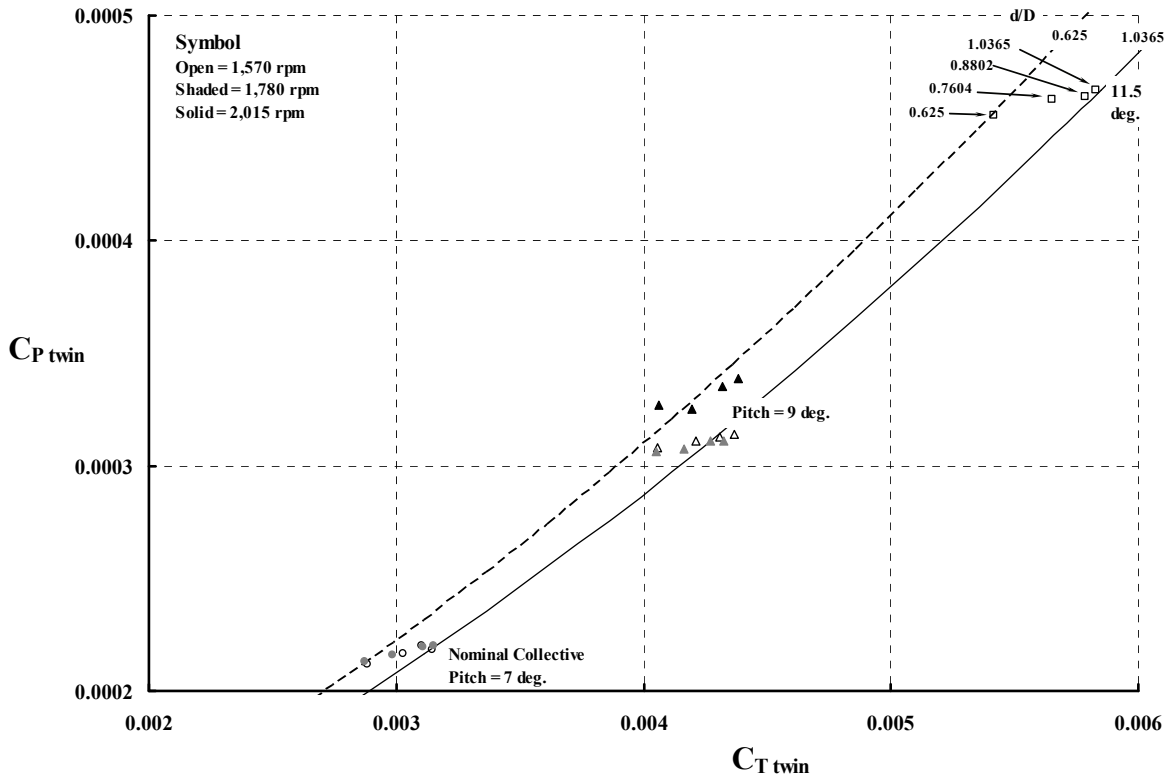


**Fig. 2-81. Stepniewski's 1947 co-planar, twin-rotor hover experimental results with varying overlap.**

This model twin-rotor hover performance, in practical engineering coordinates of  $C_{P \text{ twin}}$  versus  $C_{T \text{ twin}}$ , is shown in Fig. 2-81. The secondary variable is overlap expressed as a ratio of distance between the hubs ( $d$ ) to the rotor diameter ( $D$ ). The two coefficients are defined as

$$(2.125) \quad C_{P \text{ twin}} = \frac{P_1 + P_2}{\rho(2\pi R^2)V_t^3} \quad \text{and} \quad C_{T \text{ twin}} = \frac{T_1 + T_2}{\rho(2\pi R^2)V_t^2}.$$

The test results form visible trends in rotor system hover performance with increasing overlap *at constant collective pitch*. Approximate fairings through the data at  $d/D$  of 1.0365 and 0.6250 are shown in Fig. 2-81. (Note that the data set at 2015 rpm and 9-degree collective pitch appears out of line with the lower RPM results, however, the trend with overlap is quite consistent.) Fig. 2-81 clearly shows that overlapping *at constant collective pitch* reduces thrust much more than it reduces power.

The beauty of the twin-rotor experiment Mr. Stepniewski performed lies in *testing for the increment in performance* by sliding the two rotors together while holding all other variables constant. This approach illuminated the 8 to 12 percent overlap influences on performance even though the absolute data is, perhaps, no better than  $\pm 3$  percent in either

$C_{P \text{ twin}}$  or  $C_{T \text{ twin}}$ . There is, of course, some experimental data scatter even with this most fundamental testing approach. However, Fig. 2-81 shows experimental scatter was substantially reduced. Mr. Stepniewski and his small group obtained the major answers to how overlapping affects twin-rotor hover performance with just 36 thrust-power data points!

As a more complete historical footnote, the first application and extrapolation of this meager (some might say) amount of data was on the Piasecki PV-14 tandem rotor helicopter. This helicopter was initially designated by the U.S. Navy as the XHJP-1, and later became the HUP series in production. The HUP was the first tandem rotor helicopter intermeshed (i.e., overlapped) to a  $d/D$  on the order of 0.62. This small, 6,000-pound-gross-weight, piston-powered machine was followed by the CH-46 at 20,000 pounds, and then by the CH-47 with a gross weight approaching 50,000 pounds. The two, larger, very successful tandem rotor helicopters had slightly less overlapping (i.e.,  $d/D = 0.65$ ).

In Mr. Stepniewski's original report [247], analysis of each data set was presented. The basic experimental trends of thrust (in pounds) and power (in horsepower) versus rotor overlap ( $1-d/D$  in percent) were compared to the theory that Mr. Stepniewski included in an appendix to the report submitted to the U.S. Navy. The conclusions of that report [247] noted that the theory and model test results were in agreement and that "furthermore, in flight tests of the XHJP-1 helicopter, good correlation was found between the predicted and measured performance in hovering and vertical flight." In fact, the model test data was considered "slightly more conservative" than the theory, and the theory was "recommended for practical design."

Mr. Stepniewski and his team semiempirically reduced the thrust and power data to a simple overlap correction factor that was designated  $K_{ov}$ . This factor accounted for increasing power when two rotors are overlapped *while holding total thrust constant*. In its original form [247], the correction factor applied to the total power. Later, by subtracting a roughly approximated profile power from the total power, the  $K_{ov}$  factor became a correction to just induced power. This semiempirical step was described in detail [237]. Steppy and Chuck Keys later provided a modern source that discussed this  $K_{ov}$  factor, as well as thrust and power of intermeshing and overlapping rotors [238].

Considerable insight about overlapped (i.e., some say intermeshed) twin-rotor power required can be obtained using simple blade element momentum theory discussed earlier in paragraph 2.3.7. The hover performance of equal solidity, twin-rotor systems (having blades that are untapered with a  $\theta_{(x)} = \theta_{tip}/x$  pitch angle distribution along the blade, which is the basis of ideal rotor hover performance) is summarized in just a few equations, given some fundamental background. The amount of co-planar overlap is defined by the ratio of hub separation distance ( $d$ ) to rotor diameter ( $D$ ). This ratio ( $d/D$ ) dictates the portions of geometric planform area that are either nonoverlapped (nov) or overlapped (ov). The simple geometry of this problem is seen in Fig. 2-82, which outlines the planform view of twin, equal diameter, and overlapped rotors.

### 2.3 HOVER PERFORMANCE

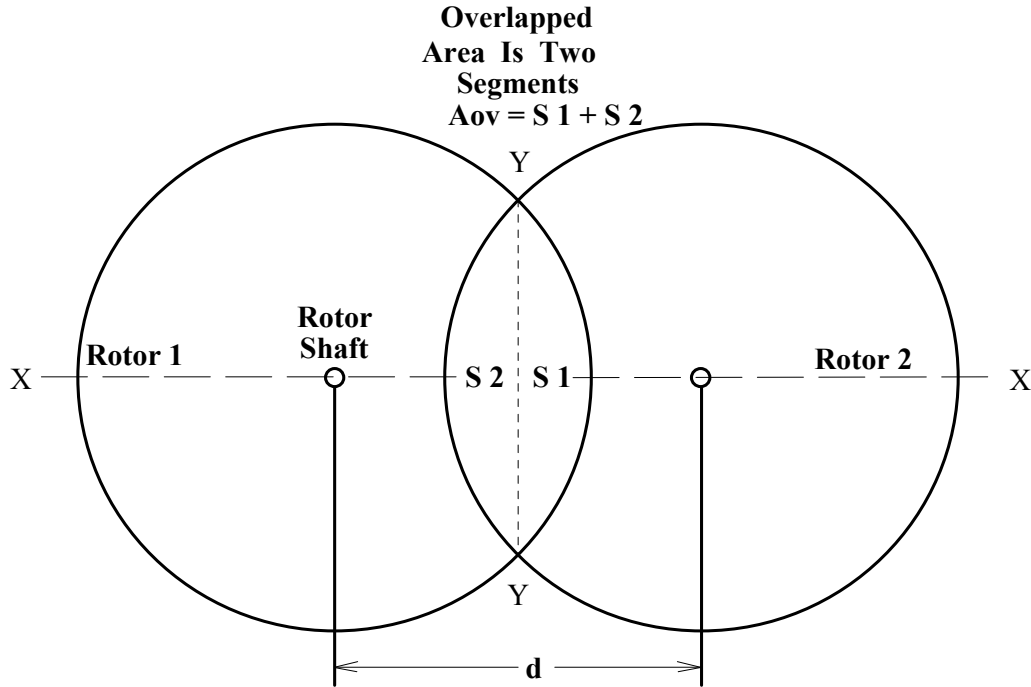


**Fig. 2-82. Twin-rotor geometry involves the area of overlapping circles and the basic geometry of segments.**

The area of one segment, or its mirror image as Fig. 2-82 shows, can be found in elementary science handbooks. For twin-rotor purposes, this area is defined by  $d/D$  as

$$(2.126) \text{ Area Segment 1} = \text{Area Segment 2} = R^2 \left[ \cos^{-1} \left( \frac{d}{D} \right) - \left( \frac{d}{D} \right) \sqrt{1 - \left( \frac{d}{D} \right)^2} \right].$$

Johnson (page 121 of reference [235]) defines a segment area parameter ( $m$ ) as

$$(2.127) \quad m \equiv \frac{2}{\pi} \left[ \cos^{-1} \left( \frac{d}{D} \right) - \left( \frac{d}{D} \right) \sqrt{1 - \left( \frac{d}{D} \right)^2} \right]$$

and thus, the *total nonoverlapped*, planform projected, geometric area ( $A_{\text{nov}}$ ) of *both* rotors is

$$(2.128) \quad \text{Twin } A_{\text{nov}} = \text{Rotor 1 } A_{\text{nov}} + \text{Rotor 2 } A_{\text{nov}} = 2\pi R^2 (1 - m).$$

Following similar logic, the *total overlapped*, planform projected, geometric area ( $A_{\text{ov}}$ ), is

$$(2.129) \quad \text{Twin } A_{\text{ov}} = \text{Area Segment 1} + \text{Area Segment 2} = 2\pi R^2 \left( \frac{m}{2} \right).$$

The planform projected, geometric area of a twin-rotor configuration accounting for any amount of overlap defined by  $d/D$  (or  $m$ ) is, of course, simply

$$(2.130) \quad \text{Twin Geometric Area} \equiv A_{\text{geo}} = \text{Twin } A_{\text{nov}} + \text{Twin } A_{\text{ov}} = 2\pi R^2 \left(1 - \frac{m}{2}\right).$$

Note that when the two rotor discs are just touching at their perimeters,  $d/D = 1$  and  $m = 0$  from Eq. (2.130). Therefore,  $A_{\text{geo}} = 2\pi R^2$ . At the most overlapped condition of a coaxial, twin-rotor system,  $d/D = 0$  and  $m = 1$  so that  $A_{\text{geo}} = \pi R^2$ .

Hover thrust and power for co-planar, overlapped configurations, expressed in terms of tip collective pitch ( $\theta_{\text{tip}}$ ), are easily derived. Because the blades are untapered, solidity (*using the blade number of one rotor*) can be used to scale the tip collective pitch as Knight and Hefner showed [243]. Therefore, let

$$(2.131) \quad \Theta_{\text{tip}} \equiv \frac{16}{a} \left( \frac{\theta_{\text{tip}}}{\sigma} \right) \quad \text{and} \quad \sigma = \frac{bcR}{\pi R^2} \quad \text{with both rotors of equal geometry.}$$

Simplistic airfoil lift and drag aerodynamics for all blade elements are assumed as

$$(2.132) \quad C_\ell = a\alpha \quad \text{and} \quad C_d = C_{d0} + kC_\ell^2.$$

Finally, the induced velocity in the *nonoverlapped region* is identical to the induced velocity of the single, isolated rotor according to blade element momentum theory. That is, *assuming both rotors have identical geometry*,

$$(2.133) \quad \frac{16}{a\sigma} \frac{v_{\text{nov}}}{V_t} = \left[ \sqrt{1 + 2x \left[ \frac{16\theta_{\text{tip}}}{a\sigma x} \right]} - 1 \right] = \sqrt{1 + 2\Theta_{\text{tip}}} - 1.$$

The induced velocity in the overlapped region was derived by Mr. Stepniewski who first published his work in 1948 [254]. Today, the somewhat revised discussion and derivation is contained in reference [238], starting at page 112. Following this approach, uniform induced velocity will also occur in the overlapped region with constant chord blades having a  $\theta_{(x)} = \theta_{\text{tip}}/x$  twist distribution, where  $x$  is radius station ( $r$ ) divided by rotor radius ( $R$ ). When rotor 1 and rotor 2 have equal geometry, it follows that the magnitude of this uniform induced velocity in the *overlapped region* will be

$$(2.134) \quad \frac{8}{a\sigma} \frac{v_{\text{ov}}}{V_t} = \sqrt{1 + \frac{1}{2} [\Theta_{\text{tipR1}} + \Theta_{\text{tipR2}}]} - 1 = \sqrt{1 + \Theta_{\text{tip}}} - 1.$$

With the preceding fundamentals in hand, integration of the blade element momentum

equation yields the twin-rotor thrust coefficient,  $C_{T \text{ twin}} \equiv \frac{T_1 + T_2}{\rho (2\pi R^2) V_t^2}$ , as

$$(2.135) \quad C_{T \text{ twin}} \equiv \frac{a^2 \sigma^2}{32} \left\{ \frac{1}{4} \left( \sqrt{1 + 2\Theta_{\text{tip}}} - 1 \right)^2 (1 - m) + \frac{1}{2} \left( \sqrt{1 + \Theta_{\text{tip}}} - 1 \right)^2 (m) \right\}.$$

### 2.3 HOVER PERFORMANCE

The twin-rotor power coefficient is defined as  $C_{P \text{ twin}} \equiv \frac{P_1 + P_2}{\rho (2\pi R^2) V_t^3}$ . The total rotor

power required equals the sum of (a) induced power due to collective pitch, (b) minimum profile power, and (c) delta profile power due to collective pitch. The three elements, found by integrating blade element momentum equations, are

$$(2.136) \text{ (a) } C_{P_i \text{ twin}} = \frac{a^3 \sigma^3}{512} \left\{ \frac{1}{4} \left( \sqrt{1+2\Theta_{\text{tip}}} - 1 \right)^3 (1-m) + \left( \sqrt{1+\Theta_{\text{tip}}} - 1 \right)^3 (m) \right\},$$

$$(2.137) \text{ (b) } \text{Min. } C_{P_o \text{ twin}} = \frac{\sigma C_{do}}{8}, \text{ and}$$

$$(2.138) \text{ (c) } \Delta C_{P_o \text{ twin}} = \frac{a^3 \sigma^3 (ka)}{512} \left\{ \left( \Theta_{\text{tip}} + 1 - \sqrt{1+2\Theta_{\text{tip}}} \right)^2 (1-m) + \left( \Theta_{\text{tip}} + 2 - 2\sqrt{1+\Theta_{\text{tip}}} \right)^2 \left( \frac{m}{2} \right) \right\}.$$

Twin-rotor hovering performance for rotors using untapered blades having a  $\theta_{(x)} = \theta_{\text{tip}}/x$  twist distribution can be summarized in practical engineering,  $C_{P \text{ twin}}$  versus  $C_{T \text{ twin}}$ , form. A useful, first-order approximation [255] for twin rotors where  $C_{T \text{ twin}}/\sigma^2$  lies between 1 and 2, and  $d/D$  lies between 0 and 1, is

$$(2.139) C_{P \text{ twin}} \equiv \frac{\sigma C_{do}}{8} + \frac{4k}{\sigma} C_{T \text{ twin}}^2 + k_i \left\{ \left[ \sqrt{2} - \frac{\sqrt{2}}{2} \left( \frac{d}{D} \right) + \left( 1 - \frac{\sqrt{2}}{2} \right) \left( \frac{d}{D} \right)^2 \right] \frac{C_{T \text{ twin}}^{3/2}}{\sqrt{2}} \right\}.$$

Keep in mind that solidity is calculated *using the blade number of one rotor* and the reference area is  $2\pi R^2$ .

The preceding simple theory confirms the experimental trends that Mr. Stepniewski observed in his 1947 model test, as Fig. 2-83 shows. The variation of rotor system thrust and power when twin rotors are overlapped is quite dependent on whether collective pitch is held constant, or total thrust is held constant, or total power is held constant.

The third term in Eq. (2.139) is the minimum induced power of hovering twin rotors having the assumed blade geometry. This power is multiplied by the induced power correction factor ( $k_i$ ) as you saw with single rotor configuration. If the two rotors are not overlapped, then  $d/D \geq 1$  and the bracketed term is 1.0, in which case the twin-rotor induced power reduces to the ideal power of two, isolated, single rotors.

The fully overlapped configuration, a co-planar coaxial arrangement, has  $d/D = 0$ , and the bracketed term is  $\sqrt{2}$ . There is considerable confusion about this result in both technical and marketing literature. Because part of this confusion is caused by nomenclature, it is worth a moment to express the result without using coefficients. To begin with,

$$(2.140) \text{ Ideal induced } C_{P \text{ twin}} \equiv \frac{P_1 + P_2}{\rho (2\pi R^2) V_t^3} = \sqrt{2} \left( \frac{C_{T \text{ twin}}^{3/2}}{\sqrt{2}} \right) = C_{T \text{ twin}}^{3/2} \quad \text{when } d/D = 0.$$

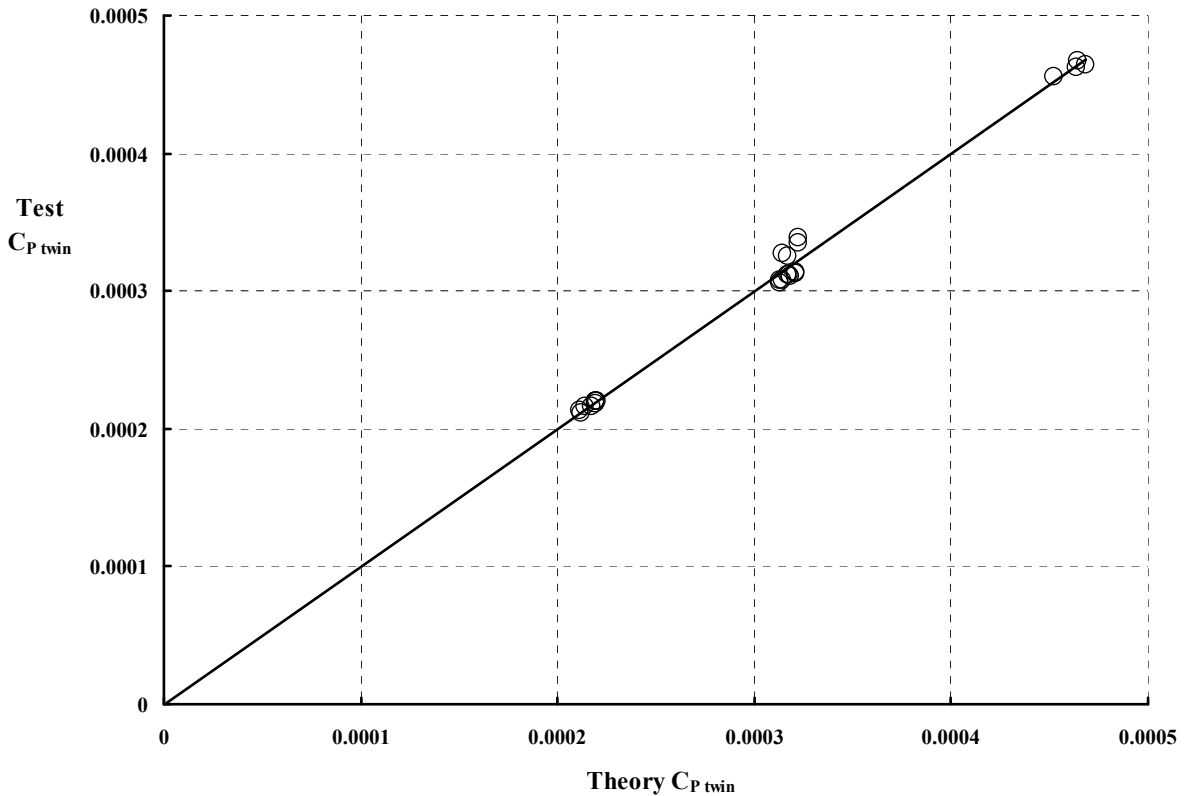


**Fig. 2-83. Stepniewski’s twin-rotor performance shown in Fig. 2-81 is predicted using Eq. (2.139) with  $C_{do} = 0.008424$ ,  $k = 0.0108$ , and  $k_i = 1.2023$ .**

Then,

$$(2.141) \quad \text{Ideal induced power} = P_1 + P_2 = \rho (2\pi R^2) V_t^3 \left[ \frac{T_1 + T_2}{\rho (2\pi R^2) V_t^2} \right]^{3/2} \quad \text{when } d/D = 0.$$

A little bit of algebra sorts things out so that

$$(2.142) \quad (P_1 + P_2)_{\text{ideal}} = \frac{(T_1 + T_2)^{3/2}}{\sqrt{\rho (2\pi R^2)}} = (T_1 + T_2) \sqrt{\frac{T_1 + T_2}{2\rho (\pi R^2)}} \quad \text{when } d/D = 0,$$

which is exactly the momentum theory for a single rotor carrying a thrust of  $T_1 + T_2$  on one rotor having an area of  $\pi R^2$ .

As a concluding example, suppose an 8,250-pound helicopter is supported by twin rotors, each having a diameter of 47 feet. Each rotor has a swept disc area ( $\pi R^2$ ) of 1,735 square feet, a solidity of 0.03542, and a tip speed of 640 feet per second. The helicopter is hovering out of ground effect at sea level on a standard day where the air density is 0.002378 slugs per cubic feet. On this basis, the twin-rotor weight coefficient would be

### 2.3 HOVER PERFORMANCE

$$(2.143) \quad C_{w \text{ twin}} = \frac{T_1 + T_2}{\rho(2\pi R^2)V_t^2} = \frac{8,250}{0.002378(2 \times 1,735)640^2} = 0.002441.$$

Now assume each rotors' performance constants are  $C_{do} = 0.010$ ,  $k = 0.010$ , and  $k_i = 1.20$  and then, using Eq. (2.139), compute the total rotor horsepower (RHP) required by both rotors as the twin rotors move from a nonoverlapped arrangement ( $d/D = 1$ ) to a co-planar coaxial position ( $d/D = 0$ ). The results are presented in Fig. 2-84.

The lowest line (the short, dashed line) on Fig. 2-84 is the ideal, induced *rotor* horsepower. (Because I have not addressed transmission efficiency and accessory power yet, the powers under discussion are just rotor powers.) Notice that at  $d/D = 1.0$ , the total RHP is about 333 horsepower. In contrast, when  $d/D = 0$ , the ideal induced power has increased to  $RHP = 475$ . The ratio of these two RHPs is exactly  $\sqrt{2}$ .

The middle line on Fig. 2-84 is the ideal, induced rotor horsepower increased by the empirical factor,  $k_i = 1.2$ . The top line on Fig. 2-84 is the total rotor horsepower, which includes the profile power.

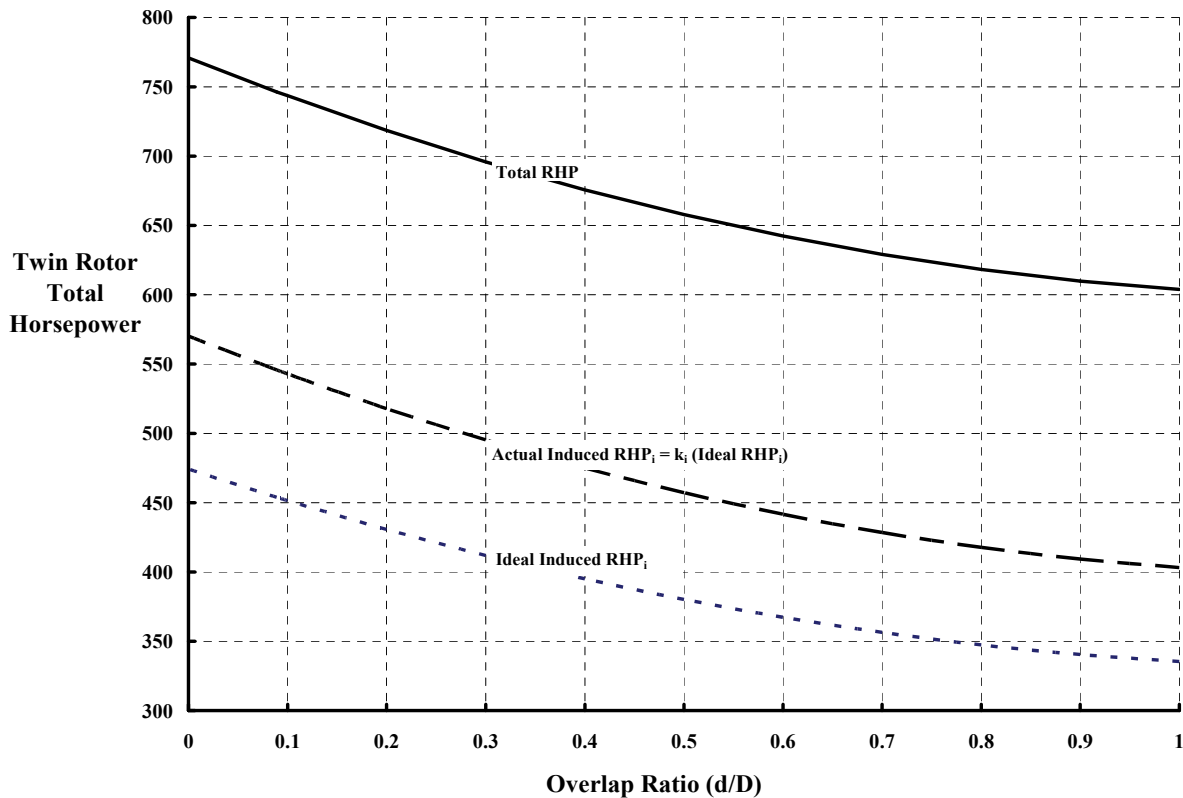


**Fig. 2-84.** An example of the effect of overlapping twin rotors at constant total thrust using Eq. (2.139) with  $C_{do} = 0.010$ ,  $k = 0.010$ , and  $k_i = 1.20$ .

## 2.3 HOVER PERFORMANCE

Of course a co-planar, coaxial, twin rotor cannot be physically constructed if the rotors are rotating in opposite directions, however the synchropter does come very close. The Kaman H-43 synchropter (Fig. 2-85) has two hubs separated by 4 feet, 2.25 inches. Its rotor diameter is 47 feet. Therefore,  $d/D = 0.0891$  [193]. Note that to obtain this compactness, the two rotor shafts are laterally inclined so that the included angle between the two shafts is 13.0 degrees. This means that the actual rotor thrust must exceed the gross weight by a little more than 0.5 percent. Keep in mind that this 0.5 percent of gross weight amounts to about 50 pounds, which could be baggage for one or two people.

The preceding numerical example was, in fact, a calculation of the Kaman H-43 power required to hover at 8,250 pounds at sea level on a standard day with 260 rpm rotor speed. From the flight test report [193], the engine shaft horsepower (ESHP) required is 820 hp. From Fig. 2-84, the rotor horsepower (RHP) required for  $d/D = 0.0891$  is 746 hp. With a

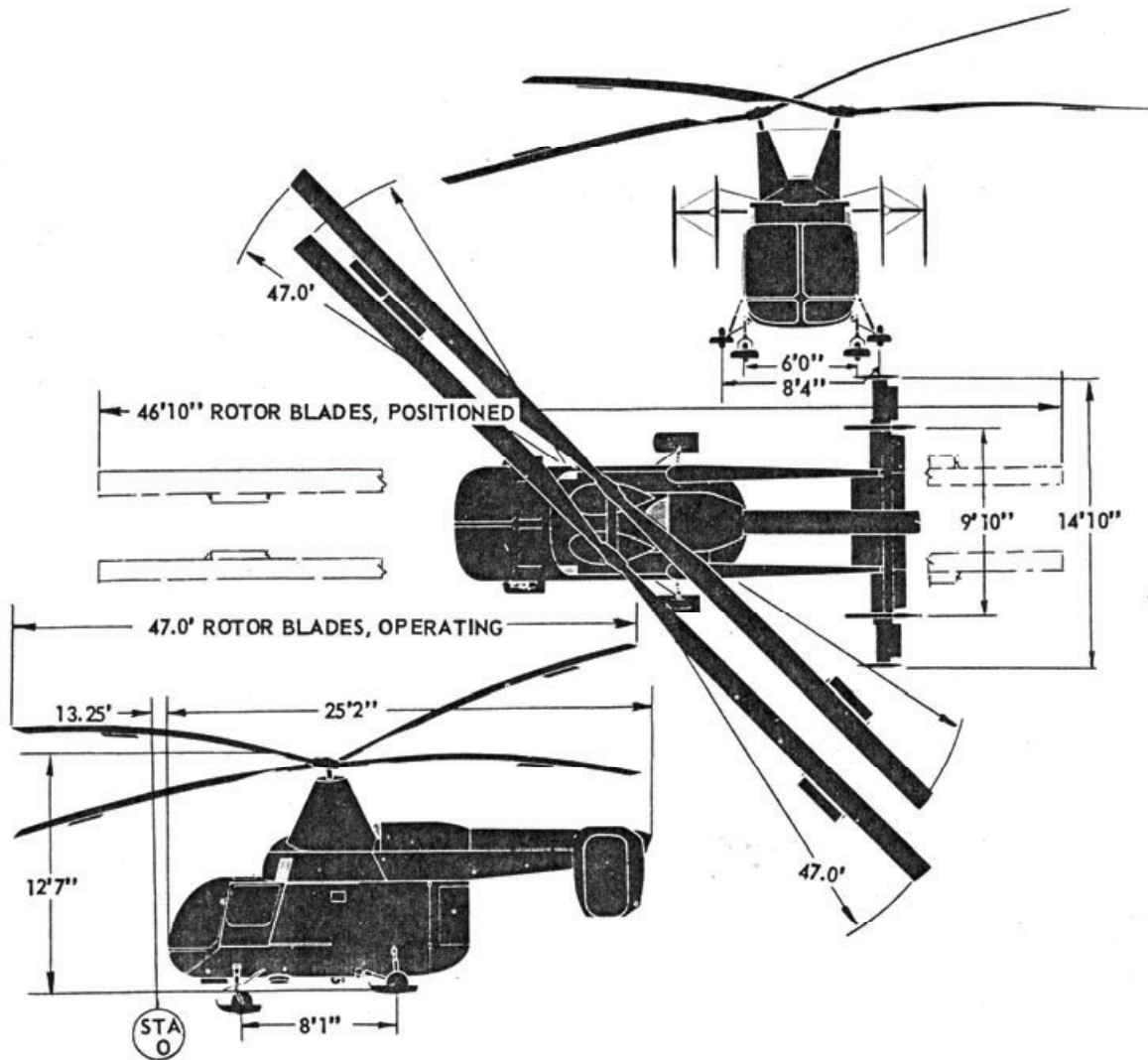


**Fig. 2-85. The Kaman H-43 Huskie has extremely overlapped twin rotors (drawing from author's collection).**

## 2.3 HOVER PERFORMANCE

transmission efficiency of 0.95 (a little low, I suspect) and 35 horsepower for accessories, you have

$$(2.144) \quad \text{ESHP} = \frac{\text{RHP}_{\text{Main Rotors}}}{\eta_{\text{Main Rotors}}} + \text{SHP}_{\text{Accessory}} = \frac{746}{0.95} + 35 = 820 \text{ hp} .$$

This H-43 calculated result, built on Mr. Stepniewski's 1947 model rotor experiment, is rather satisfying in my opinion.

It should not come as a surprise that the former N.A.C.A. (renamed and refocused to NASA in 1958) continued its rotorcraft research, albeit with ever-decreasing emphasis. In November 1960 George Sweet reported hovering measurements for twin rotors with and without overlap [248]. Sweet used an improved rotor test stand used in earlier tests by Dingeldein [256] and others at N.A.C.A. Langley. Sweet, in his introduction, stated that

“until recently there has been some question as to the accuracy of test results from twin-rotor helicopters, either because of scale effects or because of insufficiently accurate instrumentation. For example, the results of the twin-rotor tests of reference 1 [256]<sup>57</sup> indicate a large increase in hovering performance, whereas the data of reference 2,<sup>58</sup> for essentially the same configuration, show no increase in performance.”

In the same introduction, Sweet said that “the present instrumentation is greatly improved over that used in the tests of reference 1, inasmuch as the performance of each rotor was measured individually.” It is important to note that Sweet measured the thrust and torque of each rotor, whether in tandem, or as the forward rotor alone, or the aft rotor alone. Sweet, therefore, chose to define thrust and power coefficients of each rotor individually based on the area of one rotor ( $A = \pi R^2$ ).

Sweet was very thorough in his experiment and use of the tandem-rotor test stand. He had low solidity (0.0543), two-bladed rotors, and a set of higher solidity (0.0968) blades available to him. Before adjusting the twin rotors to the overlap separation of  $d/D = 0.615$ , he tested each rotor as a single rotor and then went on to test twin rotors at a separation of  $d/D = 1.015$ . The result of this confidence-building initial testing is shown here in Fig. 2-86 (in Knight and Hefner's format). Sweet could discern little  $C_P$  versus  $C_T$  difference between a rotor tested on the forward hub and a rotor tested on the aft hub of the tandem-rotor test stand, and there was little  $C_P$  versus  $C_T$  difference when the twin-rotor hubs were separated by slightly more than a diameter.

The prediction line (the solid line shown in Fig. 2-86) was computed using Knight and Hefner's extended equations, (2.90) and (2.95), as discussed in section 2.3.7, Blade Element Momentum Theory Revisited. I used an airfoil lift-curve slope ( $a$ ) of 5.73 per radian, an airfoil drag coefficient rise with airfoil lift coefficient ( $k = dC_d/dC_l^2$ ) of 0.007, and a blade-root cutout ( $x_c$ ) of 0.15, and calculated the tip loss factor ( $B$ ) with Eq. (2.96). The minimum

---

<sup>57</sup> Sweet makes it very clear that Dingeldein's test and conclusion [256] are suspect.

<sup>58</sup> Sweet refers to Stepniewski's 1949 overlap test and the data shown in Fig. 2-83.

power coefficient at zero thrust ( $C_{P0} = \sigma C_{d0}/8$ ) was calculated with a minimum airfoil drag coefficient ( $C_{d0}$ ) of 0.007.

The experimental results that Sweet obtained can be “predicted” with a simpler application of twin-rotor blade element momentum theory by modifying Eq. (2.139) to read as

$$(2.145) \quad C_{P \text{ twin}} \cong \frac{\sigma C_{d0}}{8} + FF \left\{ \frac{4k}{\sigma(B^2 - x_c^2)} C_{T \text{ twin}}^2 + \frac{1}{\sqrt{B^2 - x_c^2}} \left[ \sqrt{2} - \frac{\sqrt{2}}{2} \left( \frac{d}{D} \right) + \left( 1 - \frac{\sqrt{2}}{2} \right) \left( \frac{d}{D} \right)^2 \right] \frac{C_{T \text{ twin}}^{3/2}}{\sqrt{2}} \right\}.$$

Here the induced-power correction factor ( $k_i$ ) is set equal to  $1/\sqrt{B^2 - x_c^2}$ , and the tip loss

factor ( $B$ ) is given by  $B = 1 - \frac{3.25}{\pi AR} \left( \frac{C_{T \text{ twin}}}{\sigma^2} \right)^{1/2}$ . I have introduced a fudge factor ( $FF$ ) which is

used to make the basic curve shape pass through the experimental data. When the two rotors are not overlapped,  $d/D = 1$ . As a reminder, the solidity ( $\sigma$ ) is for just one rotor. My comparison to Sweet’s data using Eq. (2.145) is shown with the solid line in Fig. 2-86. The calculation was made with an airfoil drag coefficient rise with airfoil lift coefficient ( $k = dC_d/dC_l^2$ ) of 0.007, and the minimum power coefficient at zero thrust ( $C_{P0} = \sigma C_{d0}/8$ ) was calculated with a minimum airfoil drag coefficient ( $C_{d0}$ ) of 0.007. To make the approximation that Eq. (2.145) offers come out “close enough,” I chose  $FF = 1.0$ .

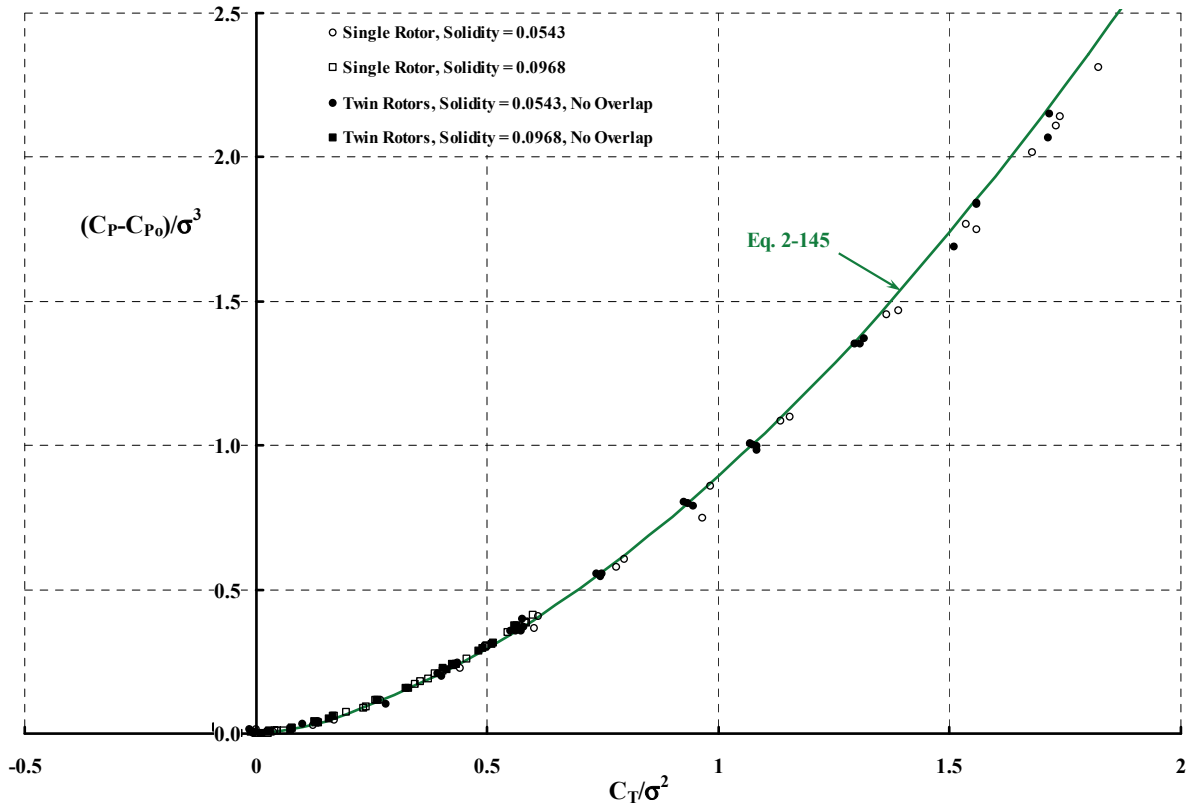


Fig. 2-86. Sweet reaffirmed Knight and Hefner’s accounting for solidity.

## 2.3 HOVER PERFORMANCE

Sweet makes it very clear that blade element momentum theory provides a quite satisfactory comparison to his single-rotor and nonoverlapped twin-rotor experimental results. His data provides convincing evidence that nonoverlapped twin rotors are, to the first approximation, nothing more than two, isolated, single rotors. He then proceeds to the overlapped case.

For the overlapped twin rotors, Sweet chose a pair of the higher solidity blades ( $\sigma = 0.0968$ ) having a diameter of 15.25 feet. The twin-rotor test stand was reconfigured to a hub separation of  $d/D = 0.615$ . He then ran the two rotors over the complete  $C_P$  versus  $C_T$  range. His twin-rotor experimental results, which I have converted to dimensional thrust and horsepower at sea level on a standard day, and at a tip speed ( $V_t$ ) of 500 feet per second, are shown in Fig. 2-87. My interpretation (Fig. 2-87) of Sweet's experimental results uses Eq. (2.145) with a fudge factor to construct the three lines shown. The fudge factor is 1.03 for the high-solidity rotor in both the single-rotor and the twin-rotor, nonoverlapped configurations. However, for the overlapped configuration, the fudge factor is 1.07.<sup>59</sup>

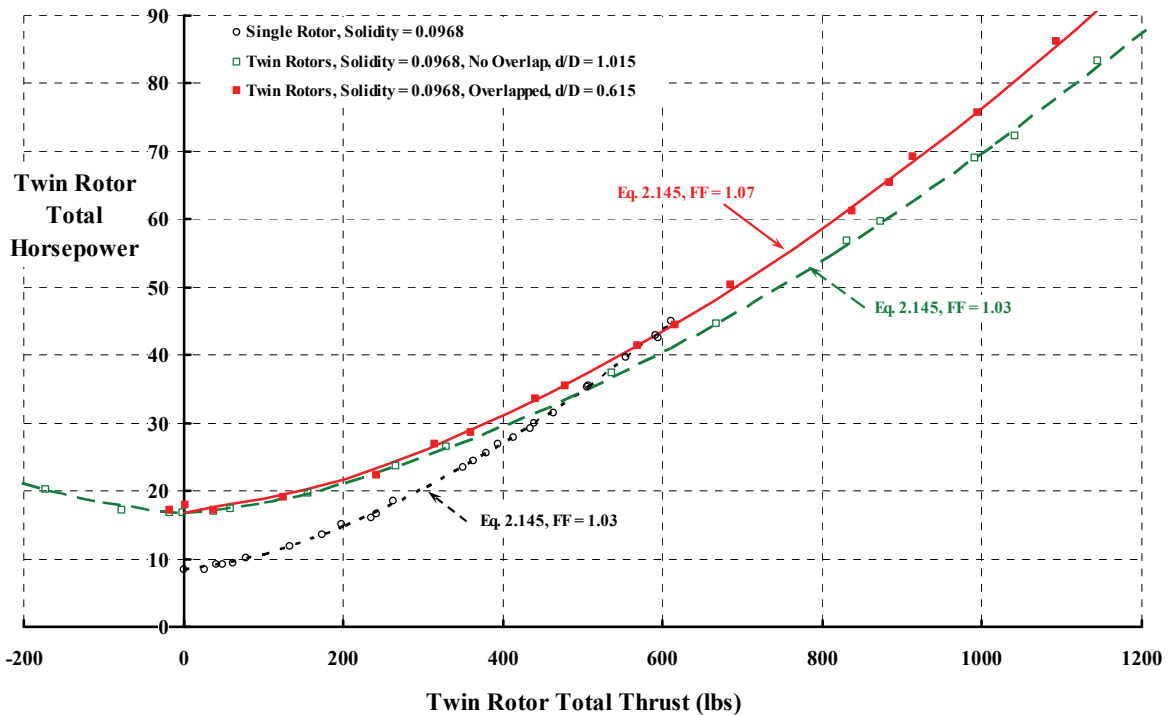


Fig. 2-87. Sweet's twin-rotor results for two overlapped separations.

<sup>59</sup> As of November 2006 there are no published results from other, more powerful theories that have tried to predict Sweet's test results. The industry's reliance on simple blade element theory shows a lack of maturity that is difficult to convey to upper management.



**Fig. 2-88. The Sikorsky XH-59A has a closely spaced, coaxial rotor system because the nearly rigid blades do not flap. The canister between the rotors is test instrumentation. The helicopter is in its high-speed, auxiliary jet propulsion configuration (photo from author's collection).**

With this understanding of tandem and synchropter hovering performance, turn your attention to twin rotors arranged one above the other, which is commonly called a coaxial helicopter. Because the practical, coaxial helicopter cannot have co-planar, totally overlapped, twin rotors, the vertical gap between the upper and lower rotors must be accounted for. Unfortunately, within the constraint that each rotor must have equal—but opposite—torques to ensure yaw moment equilibrium, there is little experimental evidence that vertical spacing between the rotors makes a bit of difference within practical configurations [253]. By practical configurations, I mean those in production, and that means the products of the Kamov Company in Russia. The vertical spacing ( $h$ ) ratioed to the diameter ( $D$ ) lies in the narrow range of 0.088 to 0.095 for their coaxial configurations. The Kamov rotor systems are articulated, and careful attention is paid to rotor blade interference. Of course if the blades are more like propellers, the spacing can be reduced. This is the case with the Sikorsky XH-59A (Fig. 2-88), perhaps better known as the Sikorsky ABC™, where  $h = 2.5$  feet,  $D = 40$  feet, and  $h/D = 0.0625$  [257].

The Sikorsky ABC helicopter finished up its concept development program in the early 1980s. In 2004, Burgess wrote an excellent program overview [258]. He points out that this program included model testing [259] and full-scale helicopter wind tunnel testing [260, 261], as well as flight testing [210]. An assessment of the aircraft's hovering performance was published in 1977 [250].

The literature as summarized by Coleman [253] indicates that the coaxial, twin-rotor system acts, in hover, as a single rotor, and that the reference area for the thrust and power coefficients is based on  $\pi R^2$ , not  $2\pi R^2$ . To accommodate this approach, Eq. (2.139) with  $d/D = 0$  can be converted to  $C_{P \text{ coaxial}}$  and  $C_{T \text{ coaxial}}$  form as follows. The first step is

$$(2.146) \quad C_{P \text{ coaxial}} = \frac{P_1 + P_2}{\rho(\pi R^2)V_t^3} \cong 2 \left\{ \frac{\sigma C_{do}}{8} + \frac{4k}{\sigma} C_{T \text{ twin}}^2 + k_i \left[ \sqrt{2} \right] \frac{C_{T \text{ twin}}^{3/2}}{\sqrt{2}} \right\}.$$

### 2.3 HOVER PERFORMANCE

$$\text{Now, } C_{T \text{coaxial}} = \frac{T_1 + T_2}{\rho(\pi R^2) V_t^2} = 2C_{T \text{twin}},$$

and, therefore,

$$(2.147) \quad C_{P \text{coaxial}} \cong 2 \left\{ \frac{\sigma C_{do}}{8} + \frac{4k}{\sigma} \left( \frac{C_{T \text{coaxial}}}{2} \right)^2 + k_i \left( \frac{C_{T \text{coaxial}}}{2} \right)^{3/2} \right\},$$

which reduces to

$$(2.148) \quad C_{P \text{coaxial}} \cong \frac{\sigma C_{do}}{4} + \frac{2k}{\sigma} (C_{T \text{coaxial}})^2 + k_i \frac{(C_{T \text{coaxial}})^{3/2}}{\sqrt{2}}.$$

Remember for this special case of twin rotors (i.e., the coaxial configuration), the thrust and power coefficients are based on  $\pi R^2$ , but the *solidity* ( $\sigma$ ) is still based on just one rotor. The solidity can be converted to the total number of blades for the two rotors by saying  $\sigma = \frac{1}{2} \sigma_{\text{coaxial}}$ . Then the “standard”  $C_{P \text{coaxial}}$  and  $C_{T \text{coaxial}}$  form becomes

$$(2.149) \quad C_{P \text{coaxial}} \cong \frac{\sigma_{\text{coaxial}} C_{do}}{8} + \frac{4k}{\sigma_{\text{coaxial}}} (C_{T \text{coaxial}})^2 + k_i \frac{(C_{T \text{coaxial}})^{3/2}}{\sqrt{2}}.$$

The Sikorsky XH-59A flight test data provides the only readily available and published, full-scale, coaxial helicopter hovering data with which to test the first-order approximation of Eq. (2.149). Therefore, following the Kaman H-43 example, assume  $k = 0.010$  and  $k_i = 1.20$ . However, assume the minimum airfoil drag coefficient of the XH-59A blade is lower than that of the H-43 (say  $C_{do} = 0.008$  instead of 0.010) because of modern blade construction and surface condition. Because Eq. (2.149) returns just rotor horsepower (RHP), assume the H-43 transmission efficiency of 0.95 and accessory horsepower of 30 hp.

$$(2.150) \quad \text{Engine } C_{P \text{coaxial}} \cong \frac{\text{Rotor } C_{P \text{coaxial}} \text{ per Eq.(3.203)}}{0.95} + \frac{550 \times 30}{\rho(\pi R^2) V_t^3}.$$

Note that my assumption here is that accessory power is constant regardless of the air density and engine RPM.

Now for some results. The XH-59A rotor diameter is 36 feet, the coaxial solidity with 6 blades (2 rotors  $\times$  3 blades per rotor) is 0.127, and the tip speed at 100 percent rotor RPM is 650 feet per second [250]. Continuing with the assumption that rotor thrust equals aircraft weight, you have the comparison shown in Fig. 2-89.<sup>60</sup>

---

<sup>60</sup> My first try at “correlation” was with  $C_{do} = 0.01$  and resulted in the answer being wrong. The line was parallel to the flight test results, but too high. So I adjusted the  $C_{do}$  to 0.008 and got the right answer. Given the five constants to be selected, you can get “correlation” with any flight test data. Of course it is very helpful to have the test results first.

A most illuminating result about twin rotors is that the induced-power correction factor ( $k_i$ ) is on the order of 1.2, which comes from Mr. Stepniewski's 1947 model rotor overlap experiment. You saw from the single rotor discussion that this factor was more on the order of 1.4. That is, Eq. (2.42) for the single rotor semiempirically follows

$$(2.151) \text{ Engine } C_p = \frac{\sigma C_{do}}{8} + \frac{k_i}{\sqrt{2}} C_W^{3/2},$$

where transmission efficiency is buried in  $k_i$  (equals 1.4), accessory power appears as a higher  $C_{do}$  (say 0.01), and the tail rotor is folded into both terms.

In contrast, a twin-rotor helicopter semiempirically follows the slightly refined Eqs. (2.149) and (2.150),

$$(2.152) C_{p \text{ twin}} \cong \frac{\sigma C_{do}}{8} + \frac{4k}{\sigma} C_{T \text{ twin}}^2 + k_i \left\{ \left[ \sqrt{2} - \frac{\sqrt{2}}{2} \left( \frac{d}{D} \right) + \left( 1 - \frac{\sqrt{2}}{2} \right) \left( \frac{d}{D} \right)^2 \right] \frac{C_{T \text{ twin}}^{3/2}}{\sqrt{2}} \right\}$$

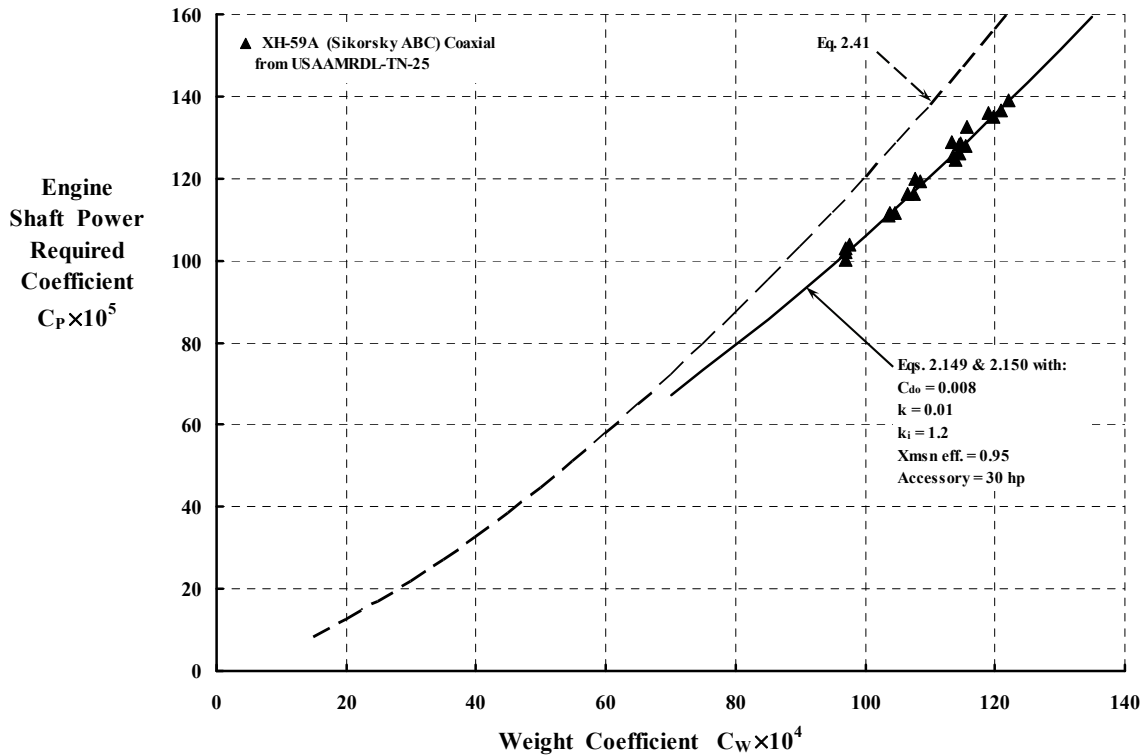


Fig. 2-89. Sikorsky's XH-59A hover power required.

## 2.3 HOVER PERFORMANCE

from which it follows that

$$(2.153) \quad \text{Engine } C_{P \text{ twin}} \cong \frac{\frac{\sigma C_{do}}{8} + \frac{4k}{\sigma} C_{W \text{ twin}}^2 + k_i \left\{ \left[ \sqrt{2} - \frac{\sqrt{2}}{2} \left( \frac{d}{D} \right) + \left( 1 - \frac{\sqrt{2}}{2} \right) \left( \frac{d}{D} \right)^2 \right] \frac{C_{W \text{ twin}}^{3/2}}{\sqrt{2}} \right\}}{\eta_{\text{xmsn}}} + \frac{550 \text{SHP}_{\text{accessory}}}{\rho (\pi R^2) V_t^3}$$

where  $k_i = 1.2$ . Of course a fudge factor may be used to improve the correlation after some real test data has arrived.

This result for twin-rotor helicopters versus single rotor helicopters helps quantify the fact that a coaxial helicopter is, in fact, capable of a 10 to maybe 15 percent hover engine power required improvement in *nondimensional* coefficient form. The configuration continues to receive engineering attention [262-264].

### 2.3.10 Ground Effect

Ground effect is the one factor that can, without question, improve hover performance. The favorable effect becomes increasingly influential as the distance of the main rotor plane to the ground ( $Z$ ) becomes less than twice the main rotor diameter ( $D$ ). Thus, hovering out of ground effect (HOGE) means that  $Z > 2D$ . The distance  $Z$  is frequently measured from the ground to the helicopter's wheels or skids, *plus* the distance from the landing gear up to the main rotor hub. Therefore, even when the helicopter is on the ground, the rotor hub or plane is some 6 to 8 feet above the ground—at least with prudent designs that have concern for people walking about the aircraft when the main rotor is turning. Very few conventional helicopters can physically have the ratio of  $Z$  to  $D$  much less than 0.3.

There have, of course, been several experiments and many (actually too many to reference) theoretical studies of the behavior of an isolated model's main rotor when in ground effect [13, 244, 265-268]. However, in 1976 it was Jim Hayden who finally conducted a semiempirical study of full-scale helicopters that provided usable results for the working engineer [268]. Hayden used the simplest performance approximation to build his ground effect calculation method. He started with Eq. (1.4), repeated here for convenience:

$$(1.4) \quad \text{HP}_{\text{HOGE}} = k_i \left( \frac{T}{550} \sqrt{\frac{T}{2\rho A}} \right) + \frac{\rho b c R V_t^3 C_{do}}{8 \times 550}.$$

He assumed that this fundamental equation would represent any of the 17 U.S. Army-evaluated configurations under study, whether hovering in ground effect (HIGE) or out of ground effect (HOGE). He replaced thrust ( $T$ ) with gross weight ( $W$ ) and used engine shaft horsepower to calculate the power coefficient ( $C_P$ ). Hayden approached the aircraft performance data analysis with Eq. (1.4) in coefficient form and added an in-ground-effect variable ( $K_{ge}$ ) so that

$$(2.154) \quad C_p = K_{ge} (C_{p_i})_{HOGE} + (C_{p_o})_{HOGE} = K_{ge} \left[ k_i \frac{C_w^{3/2}}{\sqrt{2}} \right]_{HOGE} + \left[ \frac{\sigma C_{do}}{8} \right]_{HOGE}$$

where, as a reminder,

$$(2.155) \quad C_w = \frac{W}{\rho A V_t^2} \quad \text{and} \quad C_p = \frac{550 \text{SHP}_{\text{engine}}}{\rho A V_t^3}.$$

After careful linear regression analysis of  $C_p$  versus  $C_w^{3/2}$  curves from 73 examples obtained with the 17 aircraft, Hayden proposed that

$$(2.156) \quad K_{ge} = \frac{1}{0.9926 + 0.03795 \left( \frac{1}{Z/D} \right)^2}$$

and supported this engineering approximation with Fig. 2-90. (I have reversed the axes from Hayden's original work and added a set of dashed lines to band the data.) I created the dashed lines in Fig. 2-90 simply with

$$(2.157) \quad K_{ge} = \frac{1}{0.9926 + 0.03795 \left( \frac{1}{Z/D \pm 0.05} \right)^2}.$$

The data in Fig. 2-90 does produce one of those occasional trends that are undesirable. As the ground is approached (i.e.,  $Z/D$  gets small), the curve becomes very steep. Very small changes in vertical height will cause large changes in power at constant gross weight. The flight test data was obtained by tethering the aircraft at each fixed height which helps. Getting accurate data without tethering is quite difficult and time consuming. However, incorrect tethering can lead to the pilot's loss of control.

You will notice the one YUH-60A data point in Fig. 2-90, which comes from the analysis presented in Fig. 2-91. This point, from reference [123], shows power required while the helicopter hovered at 100-foot wheel height. The solid line through the open circles is given for this HOGE condition by

$$(2.158) \quad C_p = 1.0 \left[ 1.47335 \frac{C_w^{3/2}}{\sqrt{2}} \right]_{HOGE} + \left[ \frac{(0.08204)(0.009705)}{8} \right]_{HOGE}.$$

The solid line through the solid squares is obtained by replacing  $K_{ge} = 1.0$  in Eq. (2.158) with  $K_{ge} = 0.8$ . This approximates the 5-foot wheel height ( $Z/D = 0.317$ ) HIGE data obtained with the YUH-60A. The dashed line in Fig. 2-91 represents the result from Hayden's Eq. (2.156), which gives  $K_{ge} = 0.7295$ .

## 2.3 HOVER PERFORMANCE

You might think that this example of modern results shows an excessive (if not appalling) amount of empiricism with which to predict in-ground-effect performance. Unfortunately, this situation from 1976 still exists today. The hover performance prediction problem (for either HOGE or HIGE) for a complete rotorcraft has yet to be solved. In general, the industry always predicts an optimistic hover performance result with each new rotorcraft and, so far, has always been soundly disappointed.

### 2.3.11 Closing Remarks

This introduction to modern helicopter hover performance has shown you that the “bottom line” of hover performance is a decision-making chart of hover ceiling versus useful load (recall Fig. 2-49). To arrive at this chart, you need accurate engine horsepower available (from paragraph 2.1), careful bookkeeping of helicopter weight (discussed in paragraph 2.2), and accurate engine horsepower required as reviewed in the preceding several pages. The engine horsepower required to hover out of ground effect relies—initially for a new configuration—on prediction of a  $C_P$ - $C_W$  curve where power is engine shaft horsepower. Today, each manufacturer has a wealth of background and prediction technology to obtain a  $C_P$ - $C_W$  curve, and considerable progress has been made since the early pioneering days to ensure that a sufficient power margin is inherent in a new design. However, even as late as the mid-1970s, progress fell far short of customer expectations. This deficiency was made quite clear in the UTTAS and AAH competition. You will find the position of the U.S. Army pointedly stated [123-126] as follows:

Reference [123] – Para. 185. Within the scope of these tests, the YUH-60A helicopter failed to meet the following commitments of the Prime Item Development Specification:

- a) The helicopter could not hover out-of-ground-effect at the primary mission gross weight, 4,000 feet pressure altitude, 35° C and 95 percent intermediate rated power.
- b) The aircraft could not climb vertically 550 ft/min at a pressure altitude of 4,000 feet, 35° C, 95 percent intermediate rated power and primary mission gross weight.

Reference [124] – Para. 195. Within the scope of these tests, the YUH-61A helicopter failed to meet the requirements of the following paragraphs of the Prime Item Development Specification:

- a) The helicopter could not hover out-of-ground-effect, nor could it climb vertically 603 ft/min using 95 percent intermediate rated power, at primary mission gross weight at 4,000 feet pressure altitude, 35° C.

Reference [125] – Para. 145. Within the space of these tests, the YAH-63 failed to meet the following requirements of the System Specification:

- a) The aircraft could not hover at specified conditions and, therefore, failed to meet the 450 ft/min vertical rate of climb requirement.

Reference [126] – Para. 150. The YAH-64 was found to be not in compliance with the following paragraphs of the Army System Specification against which it was evaluated. Additional specification non-compliances beyond the scope of this evaluation may exist.

- a) The computed vertical climb rate was 184 ft/min, 266 ft/min less than specification.

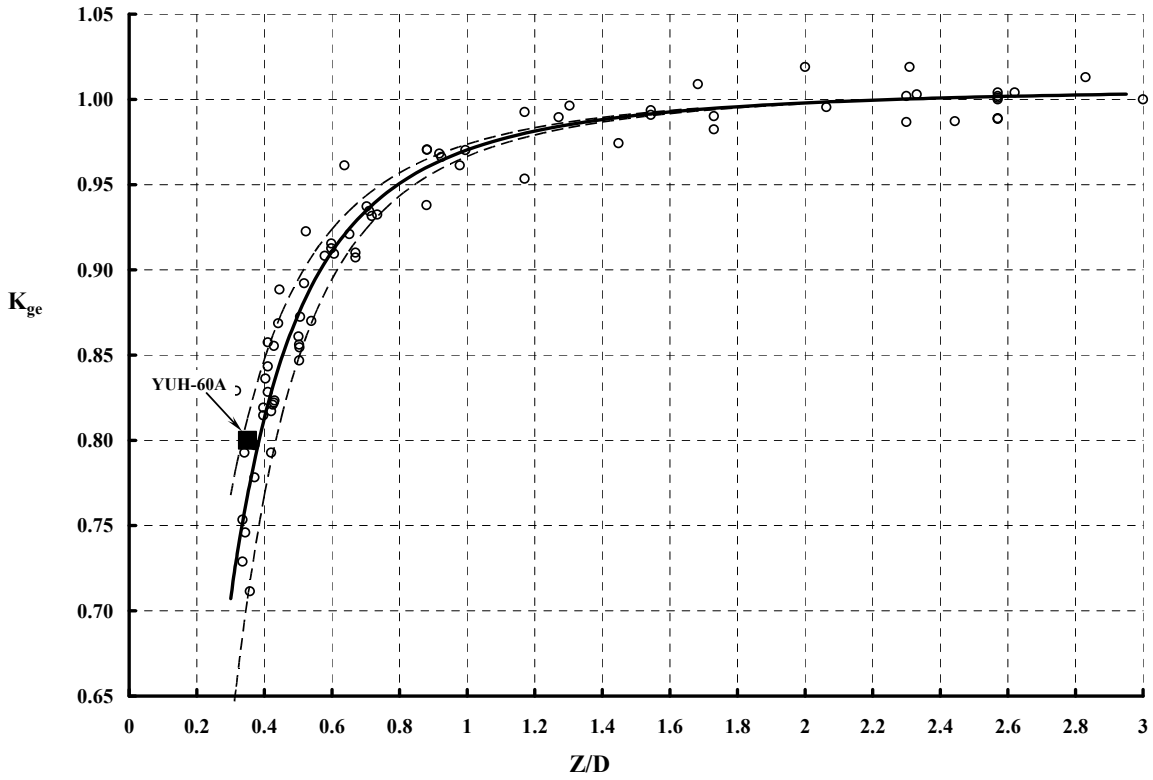


Fig. 2-90. The Hayden ground effect variable.

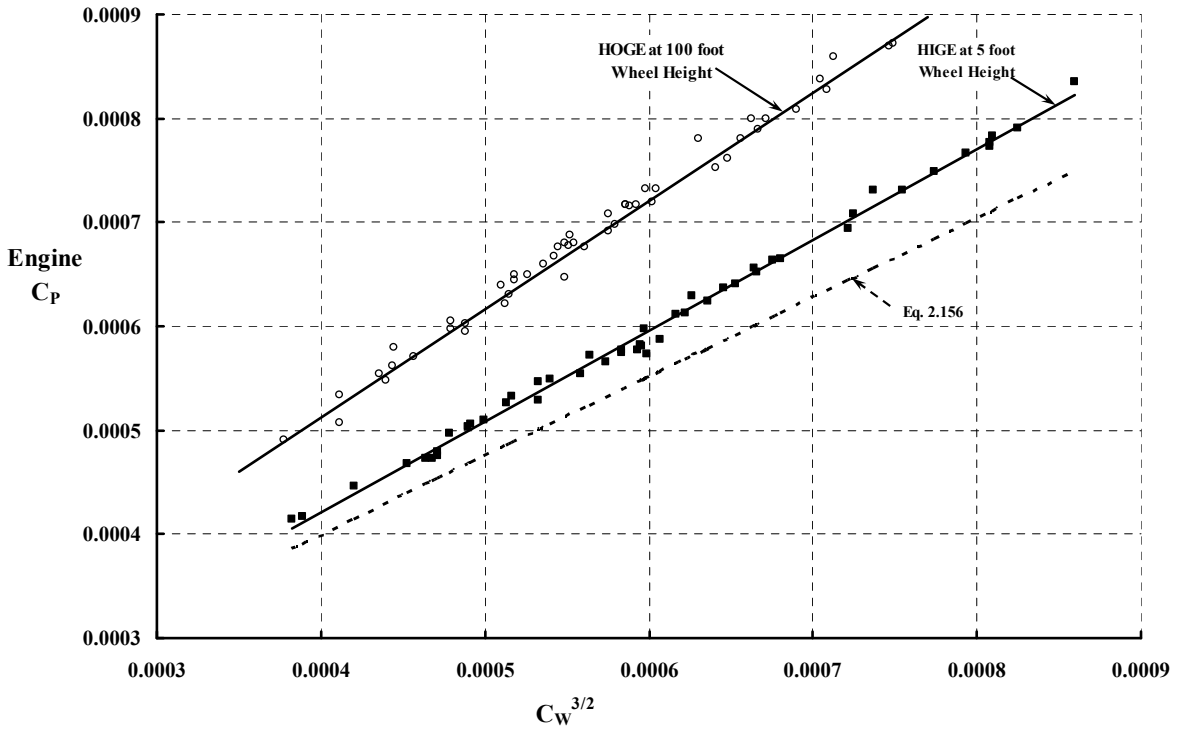


Fig. 2-91. YUH-60A hover performance HOGE and HIGE at 5-foot wheel height.

## 2.3 HOVER PERFORMANCE

I have *not* included these four evaluations to discourage you. Rather, the U.S. Army evaluations point out how difficult the hover performance prediction and measuring problem has been—and continues to be. The industry has spent millions of dollars on improvement so that marketing brochures and proposals to the government are credible. However, (1) a slight shortfall in installed engine horsepower, (2) creeping up weight empty, and (3) a small error in estimated power required to hover each contribute to missed expectations. Despite the shortfalls in technology, once the helicopter is in flight test and the situation is clearer, engine manufacturers frequently can obtain a little more power, at a reasonable price, to ensure ultimate success [145].

The most penetrating review of modern industry's capability that I have ever read was provided by Charlie Crawford, a longtime friend,<sup>61</sup> in May of 1989. He presented the 9th Nikolsky Lecture at the 45th Annual Forum of the American Helicopter Society (AHS). His Lecture was published later in the AHS Journal [249]. Charlie took the UTTAS and AAH competitions apart with comparisons of predictions versus results, with particular emphasis on optimistic weight empty and aerodynamic predictions. This paper is a must-read to gain an appreciation of modern helicopter development.

Despite the industry's shortfalls, Charlie points out that persistency paid off, and today the UH-60 and AH-64 perform admirably in the field, demonstrating the success of modern industry. The same can be said about the many civil helicopters operating around the world.

These paragraphs about hover performance would be incomplete without comparing some measure of pioneering efforts against modern results—including my interpretation. Fortunately, Fred Gustafson and Al Gessow at the N.A.C.A. obtained and published [47, 48] flight test data (including nondimensional engine  $C_P$  versus  $C_W$ ) for the Army YR-4B (the Navy's HNS-1) in hover [48]. Their results are shown in Fig. 2-92 with large symbols superimposed on an enlargement of Fig. 2-51. The large, black triangle is the one test point obtained out of ground effect with the "original" (i.e., production) blades. The several, large, black circles show the performance improvement with the "alternate" blades. The two blade configurations are shown in planform view in Fig. 2-93. Gustafson and Gessow, in their first conclusion, wrote that

"1. An increase in thrust available for hovering at altitude [sea level, but HOG] of more than 300 pounds has been obtained by replacing the original set of main-rotor blades by one of different aerodynamic design and surface condition."

The two blade configurations were significantly more different than the planform view suggests. The production blades (i.e., the "original" blades) were fabric covered and untwisted with a thrust-weighted solidity of 0.060. The airfoil was a NACA 0012 at the ribs, but left much to be desired aft of the 35 percent chord where the spruce leading edge "fairing" stopped. The trailing edge was wire. The "alternate" blades had a thrust-weighted solidity of 0.042, were plywood covered, and had "an 8-degree twist, the pitch decreasing linearly from root to tip." The alternate blade airfoil was a modified NACA 23012. Gustafson and Gessow

---

<sup>61</sup> Charles Crawford died in mid-August 2012, and we lost a driving force in the industry. And I lost a good friend.

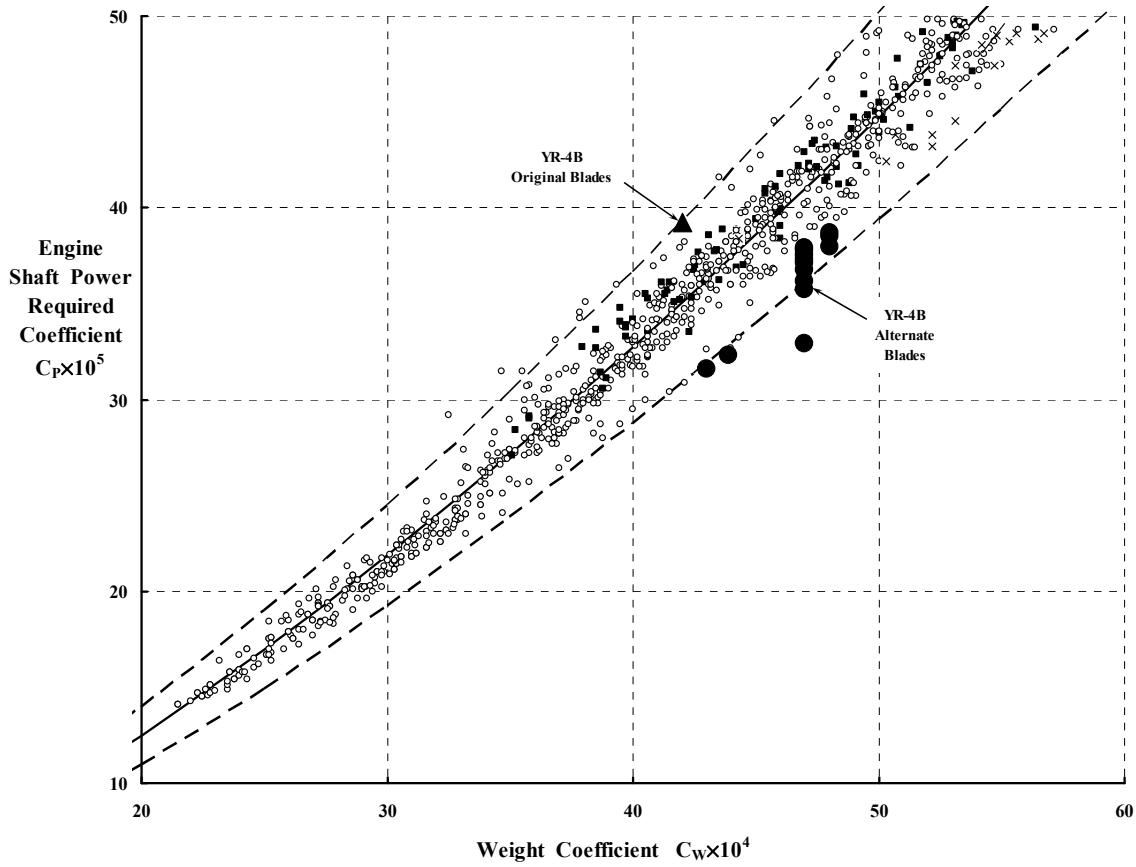


Fig. 2-92. Sikorsky YR-4B hover performance reported in 1945 suggests that modern results are a step backward. I do not agree with that suggestion.

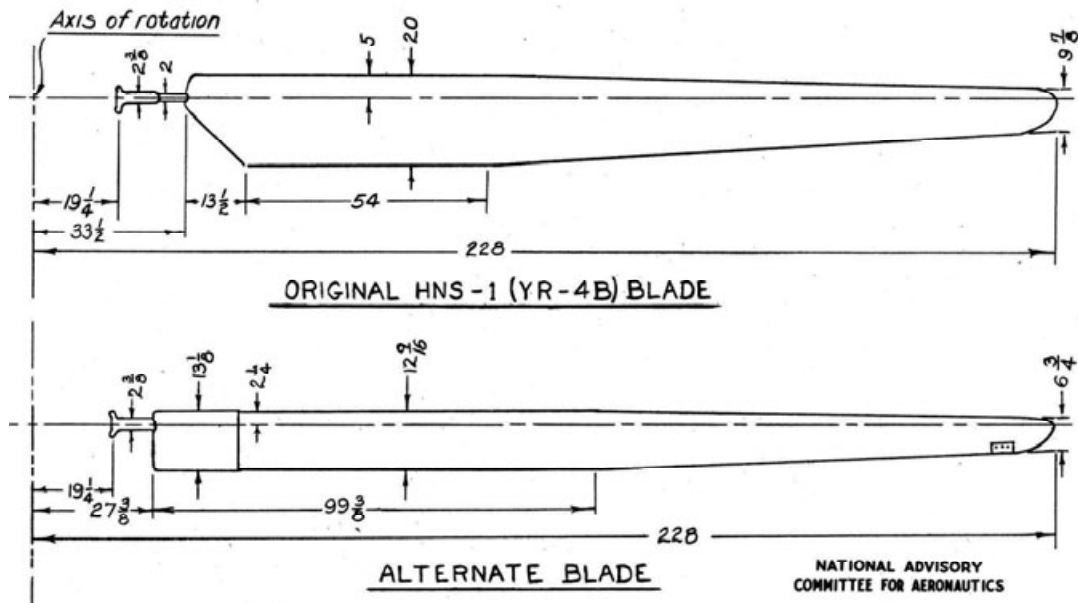


Fig. 2-93. Sikorsky YR-4B hover performance measured in 1945 with two different blade configurations.

## 2.3 HOVER PERFORMANCE

refer to airfoil tests performed on 10 practical-construction sections by Tetervin [269]. They also reference the static thrust tests of six rotor blade designs on the YR-4B conducted by Dick Dingeldein and Ray Schaefer in the Langley full-scale tunnel [270]. Dingeldein and Schaefer continued tunnel testing of the full-scale YR-4B in forward flight, and this work was reported in 1947 [271]. The alternate blade set was studied in more detail by Gustafson and Gessow [272], and Gessow was able to understand the effect of blade twist and tell everyone in the fall of 1948.

These seven reports [47, 48, 269-273] written by the early helicopter pioneers at the N.A.C.A. are, in my estimation, worth their weight in gold. They are an absolute foundation to the study of early helicopter hovering performance.<sup>62</sup>

The concentration of the early N.A.C.A. pioneers on main rotor performance (in  $C_{Pmr}$  versus  $C_W$  or  $C_{Tmr}$  form) skipped over one facet of the hovering helicopter problem that is quite important, particularly to the pilot. This facet is that hover performance ultimately depends on the *engine* horsepower required to hover. To make this point, reconsider Eq. (2.47) repeated here for convenience:

$$(2.47) \quad \text{ESHP} = \frac{\text{RHP}_{\text{Main Rotor(s)}}}{\eta_{\text{Main Rotor(s)}}} + \frac{\text{RHP}_{\text{Tail Rotor(s)}}}{\eta_{\text{Tail Rotor(s)}}} + \text{SHP}_{\text{Accessory}}$$

Enough flight test data is provided by Gustafson and Gessow [47, 48] to show how well the equality matches up. Using tabulated data from these two reports, Fig. 2-94 shows that a linear regression analysis quantifies Eq. (2.47) for the YR-4B to

$$(2.159) \quad \text{Engine BHP} = \frac{\text{RHP}_{mr}}{0.955} + \frac{\text{RHP}_{tr}}{1.0} + 12.5.$$

This result says the main rotor transmission efficiency ( $\eta_{mr}$ ) is about 0.95, the tail rotor drive-train efficiency ( $\eta_{tr}$ ) is *ideal* being 1.0 (which I will explain shortly), and 12.5 horsepower is used to drive accessories. The main rotor horsepower ( $\text{RHP}_{mr}$ ) and tail rotor horsepower ( $\text{RHP}_{tr}$ ) were obtained “by means of strain-gauge torque meters. The strain-sensitive elements for the main rotor were mounted on the drive shaft between the gear box and the pylon thrust bearing. Those for the tail rotor were mounted between the tail rotor gear box and the rearmost shaft bearing.” This latter statement says the tail rotor torque meter measured both the power absorbed by the transmission as well as the tail rotor, which explains why  $\eta_{tr} = 1.0$ . Additionally, “the engine manifold pressure, intake-air temperature, and rpm values were used to calculate engine brake horsepower (BHP) by use of the calibration curve given in Technical Order AN-01-10 DA-1.” The main rotor efficiency is quite reasonable. The tail rotor efficiency should be basically 1.0 because the measurement includes the tail rotor

---

<sup>62</sup> The outpouring of efforts from the N.A.C.A. that followed these seven reports is phenomenal, as any literature search will quickly uncover. By 1951, Al Gessow and Garry Myers were able to publish their classic book [234], which is a true treasure. You can track down nearly all of the pre-1950 N.A.C.A. work just from the references provided in appendix IIA of their book. And contributions from the N.A.C.A. did not stop, as you will read in the 6th Nikolsky Lecture given by John Ward in 1986 at the 42nd Annual National Forum of the American Helicopter Society [274].

gear box. Whether the engine was really performing up to spec is a matter for speculation. I would take issue with the accessory power.

While you may express some dissatisfaction with this mid-1944 YR-4B result, Bill Bousman at NASA Ames Research Center [213], in analyzing UH-60A flight test data some 55 years after Gustafson and Gessow’s efforts, experienced the same dissatisfaction.

I have included this simple example to draw your attention to the accessory power. I very much doubt that the YR-4B had 12.5 horsepower used for accessories—maybe 3 or 4 horsepower, but hardly 12.5 horsepower. A starter-generator and a battery and an oil cooler blower maybe, but no hydraulic system and minimal gearbox cooling. A slipping clutch would result in a power loss, of course, and surely heating would be a factor then.

What I believe is that the gains made over six decades to improve main rotor(s) and tail rotor performance with blade geometry—and all of the gains made to improve transmissions—have gone to accessory power. Modern helicopters have oil pumps, oil cooler blowers, power steering (i.e., hydraulic systems), interior climate control (air conditioning and heating), deicing for blades and other components, heavy electrical loads for computers, fly-by wire, and search and rescue equipment. Accessory power loss for Bell Helicopter products used to support Kocurek’s paper [168] ranged from 14 horsepower for a Bell Model 206 to over 60 horsepower for a well-furnished Bell Model 214ST. This is just one example of accessory power benefiting from improved rotors and transmissions.

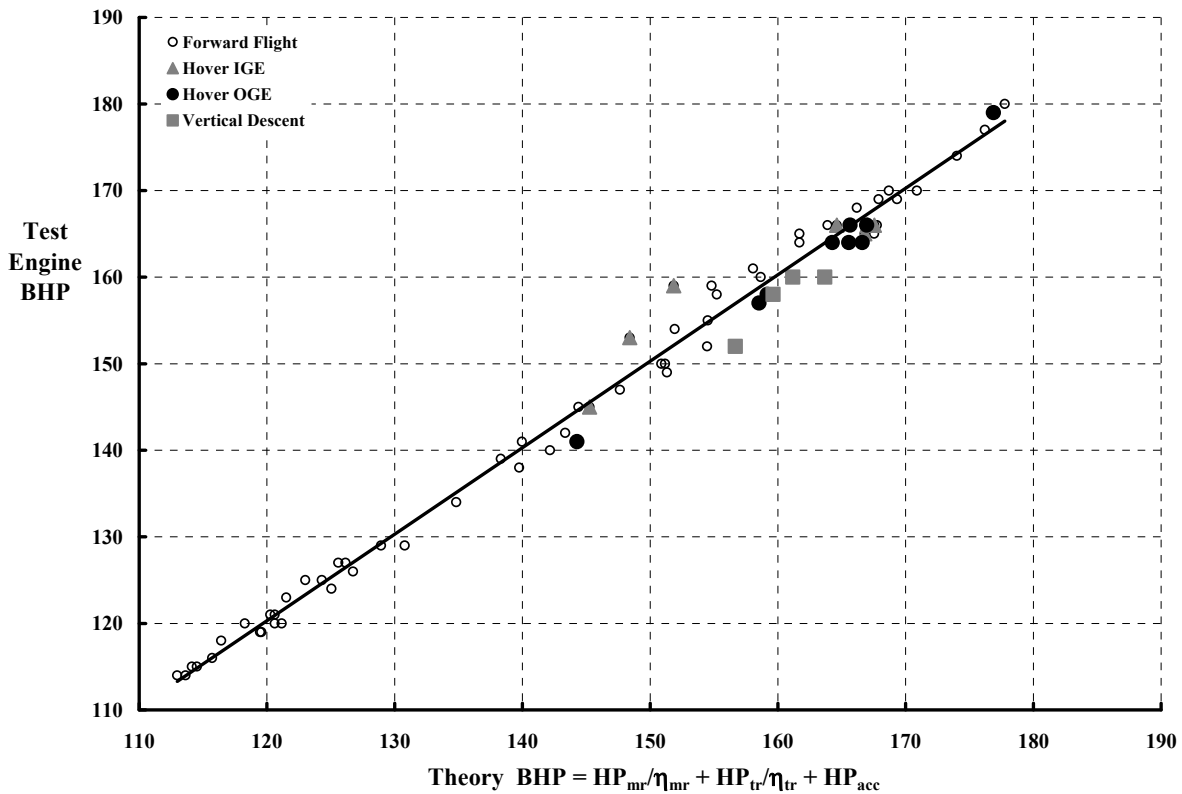


Fig. 2-94. Power equality with the YR-4B in 1944 per Eq. (2.159).



## 2.4 FORWARD-FLIGHT PERFORMANCE

The subject of helicopter forward-flight performance is so tied to the growth of U.S. Army Aviation that some historical background is a prerequisite. Army Aviation, despite evaluation of the autogyro, really began with very light, fixed-wing aircraft. In fact, it was the Piper Cub—the popular J-3 model—which began it all [275].

There are many who will disagree with this opening statement about Army Aviation, with good reason. The U.S. Army's air force can easily be traced back to the American Civil War when telegraph-equipped, tethered balloons were first used as vantage points to observe terrain and disposition of opposing forces, and adjust artillery fire. Essentially the same techniques were used in the Spanish American War and, more extensively, in World War I when the telephone replaced the telegraph, adding voice communication capability. However, World War I also saw the introduction of photo reconnaissance by airplane and a new air observation mission, a "scouting mission," was born.

A more recent point of view [276] was published by Dr. John Kitchens,<sup>63</sup> who wrote:

"On 6 June 1942, the secretary of war ordered the establishment of organic air observation for Field Artillery. Through companion memoranda sent to the commanding generals of the Army Air Forces (AAF) and the Army Ground Forces (AGF) the War Department issued specific instructions for organizing organic air observation. It also provided guidelines for relations between the AAF and this new air arm of the AGF."

With this directive from the top, the United States Army placed light airplanes under the command of field artillery battalions. The "scouts" functioned as aerial observation posts (Air OPs) for target acquisition and fire adjustment, and became an integral part of the fire direction system. During World War II about 5,700 L-4 Piper Cub airplanes were procured for this purpose. These two-place, tandem-seating, 1,220-pound-gross-weight monoplanes were powered by 65-horsepower reciprocating engines. The troops in Europe referred to these rugged and reliable airplanes as a "Maytag Messerschmitts." The L-4 "scout" crew consisted of a pilot and observer, and their "mission equipment package" consisted of voice radio, maps, and binoculars. The application was a marked success. Artillery fire could be more accurately and rapidly adjusted over a wider battlefield at longer ranges. The L-4s could operate from unimproved airstrips, which were generally plentiful. Being simple aircraft, L-4s proved highly reliable and easy to maintain, even in their most forward areas. The only significant threat to crew survival, enemy ground fire, was largely suppressed by the highly responsive artillery firepower, which the crew could direct.

After World War II the Army's concept of aviation broadened beyond field artillery, and light airplanes were placed in other service branches such as Infantry, Armor, Engineers, and Signal. The principal postwar airplane was the Stinson L-5, which had been used mainly by the Army Air Corps during World War II for liaison missions. About 900 of these Stinsons were made available to the Army ground forces by the then newly formed United States Air

---

<sup>63</sup> Dr. Kitchens is the Aviation Branch Command Historian at the U.S. Army Aviation Center located at Fort Rucker, Alabama. You can find the complete article on the Army Aviation Museum website.

## 2.4 FORWARD-FLIGHT PERFORMANCE

Force. The L-5 was a two-place, tandem-seating, 2000-pound-gross-weight airplane powered by a 185-horsepower reciprocating engine. The Army's L-5 inventory was supplemented in 1948 by a new procurement of about 800 Aeronca L-16 airplanes. The 1,300-pound-gross-weight, two-place, tandem-seating L-16, together with its 95-horsepower engine was, in many respects, a return to the L-4-sized aircraft of World War II.

The L-5 and L-16 were the core of the Army's fleet for artillery observation, reconnaissance, and liaison when the Korean War began. Between December 1950 and October 1954, however, these airplanes were rapidly replaced by the delivery of about 2,400 Cessna L-19 Bird Dogs. The L-19 was a two-place, tandem-seating, 2400-pound-gross-weight airplane powered by a 213-horsepower reciprocating engine. The new feature offered by the L-19 was an all-metal construction in contrast to the fabric-covered wood and metal structures of the L-4, L-5, and L-16. The pilot and observer's mission equipment, however, continued to be voice radio, maps, and binoculars. A total of 3,400 L-19s were ultimately procured as production extended to 1964, and of these, about 800 were used as trainers (designated TL-19Ds). The L-19, redesignated the O-1 in 1962, was the last tactical light airplane procured by the Army for field artillery fire direction, aerial observation, reconnaissance, and liaison.

The Army began procuring light, two-place, side-by-side-seating helicopters in small lots in 1948. Significant quantities of both Bell H-13s and Hiller H-23s were procured during FY51, the first fiscal year of the Korean War. Those helicopters that were delivered in time were used principally in medical evacuation [277] and administrative roles (staff liaison and communication) rather than tactical missions. The Korean War did, however, demonstrate the feasibility of large-scale use of light helicopters, and these rotary wing aircraft proved more reliable and easier to maintain in the field than had been anticipated. While less reliable and less maintainable than airplanes such as the L-19, the light helicopter more than offset this disadvantage with its ability to hover, land virtually anywhere, and operate safely near the ground at low speed.

The Bell H-13 had a gross weight of 2,450 pounds and was powered by a 200-horsepower reciprocating engine. The Army had about 100 early models of the H-13 when the Korean War began, and nearly 1,000 were produced during the war years (1950–1953). Another 600 H-13s were produced for operational use through 1965. Production continued through 1970 with additional requirements for 400 TH-13 trainers. The Hiller H-23 had a gross weight of 2,700 pounds and was powered by a 250-horsepower reciprocating engine. Nearly 400 were produced during the Korean War with another 400 procured in the period from 1954 through 1958.

This brief, introductory bit of history shows how the U.S. Army made the transition from light airplanes to light helicopters during the Korean War.<sup>64</sup>

---

<sup>64</sup> In putting together the OH-58D story [145], I was very lucky to have Perry Craddock at Bell write the historical introduction. Perry was an original Maytag Messerschmitt pilot. What you have just read is a portion of his very authoritative history about U.S. Army scout helicopter evolution.



**Fig. 2-95. The Cessna L-19 Bird Dog was the last tactical light airplane procured by the Army (photo from author's collection).**



**Fig. 2-96. The Bell H-13 (and the Hiller H-23) replaced the L-19 during the Korean War. Large numbers were bought beginning in fiscal year 1951 (photo from author's collection).**

The comparison between the two aircraft types is a good starting point for a discussion about helicopter forward-flight performance. A very interesting comparison of the Piper L-4A and the Cessna L-19A Bird Dog (Fig. 2-95) to the Bell H-13H (Fig. 2-96) and Hiller UH-23E is presented in Table 2-14.

## 2.4 FORWARD-FLIGHT PERFORMANCE

**Table 2-14. Early U.S. Army Aviation Aircraft**

<b>Basic Aircraft Information</b>	<b>Piper L-4A</b>	<b>Cessna L-19A</b>	<b>Bell H-13H</b>	<b>Hiller UH-12E</b>
<b>References</b>	[278, 279]	[280-282]	[171]	[192]
<b>Power Installed</b>	Continental	Continental	Lycoming	Lycoming
Engine Model	A65-8	0-470-11-C1	0-435-23	VO-540-C1A
Takeoff Rating at Sea Level (hp)	65	213	255	338
RPM for Rated Horsepower	2,300	2,600	3,400	3,200
Cruise Rating (hp)	60	190	200	305
RPM for Cruise	2,150	2,300	3,100	2,900
<b>Weights</b>				
Empty (full oil, trapped fuel) (lb)	750	1,686	1,789	1,717
Fuel Full (lb)	70	243	258	276
Two Crew (lb at 170 lb/man)	340	340	340	340
Two Parachutes (lb at 30 lb/man)	None	70	None	None
Baggage	10	30	60	60
Takeoff Weight (lb)	1,170	2,369	2,447	2,393
Overload Weight (lb)	1,220	n/a	2,550	2,750
<b>Dimensions</b>				
<b>Wing or Main Rotor</b>				
Span or Diameter (ft)	35.21	36.00	35.125	35.333
Wing or Disc Area (ft <sup>2</sup> )	188.5	174.0	968.5	982.0
Wing or Blade Chord (ft)	5.33	4.94	0.917	0.953
Number of Blades	n/a	n/a	2	2
Solidity	n/a	n/a	0.03323	0.03428
<b>Propeller or Tail Rotor</b>				
Manufacturer	Sensenich	McCauley	Bell	Hiller
Model	n/a	1A200/FM9047	n/a	n/a
Diameter (in.)	72	90	68	66
Blade Number	2	2	2	2
Blade Chord	0.81 ft	n/a	0.377 ft	0.51 ft
Solidity	0.1875	n/a	0.0845	0.118
Pitch Change	No	No	Yes	Yes
Airfoil	RAF 6	RAF 6	NACA 230xx	NACA 0012
<b>Airframe</b>				
Nose-to-Tail Length (ft)	22.375	25.8	27.333	29.8
Height (ft)	6.67	7.50	9.28	10.125
Vertical Stabilizer Area (ft <sup>2</sup> )	10.57	19.23	n/a	n/a
Horizontal Stabilizer Area (ft <sup>2</sup> )	25.3	15.95	None	None

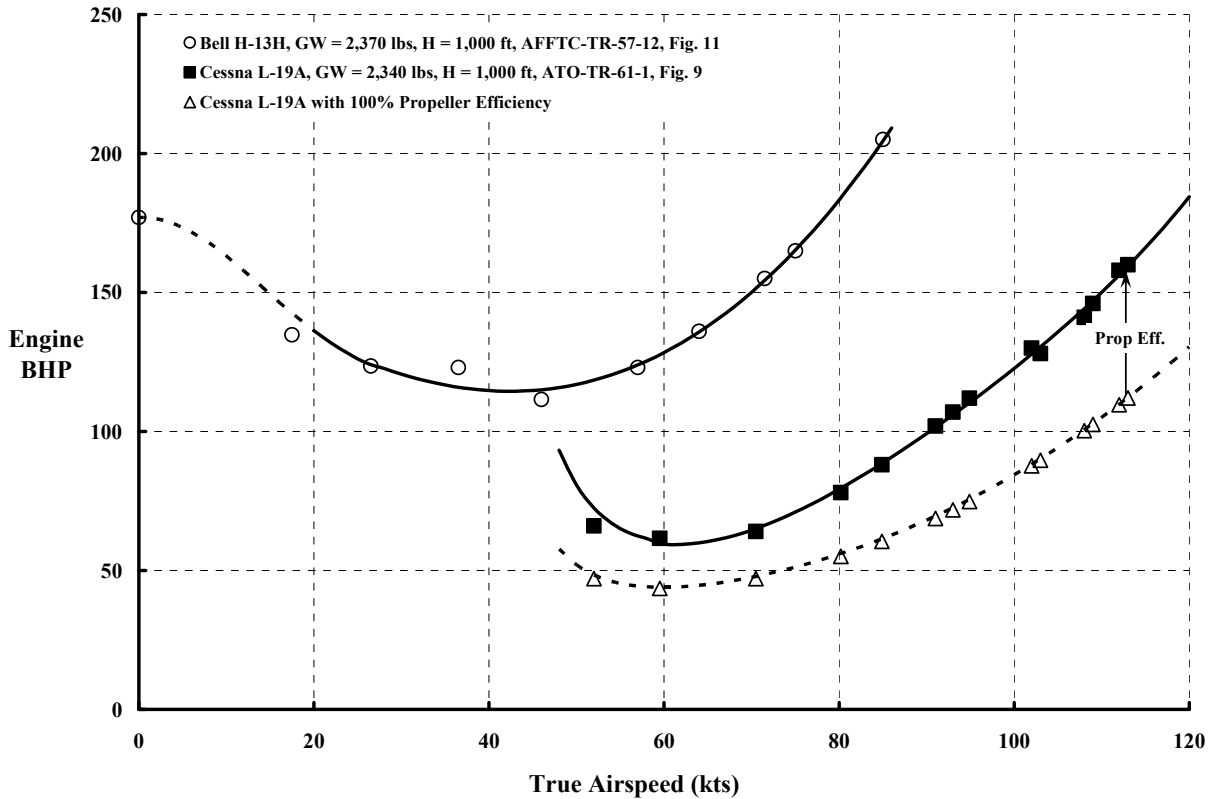


Fig. 2-97. Comparison of early U.S. Army aircraft performance.

You will recall from Volume I that Cierva compared his autogyro to the airplane and tried to make a convincing story that the two aircraft were nearly equal in performance. My more detailed comparison of the Pitcairn PA-8 Mailplane to the Pitcairn PCA-2 Autogyro did not support Cierva's outlook. In this volume, Table 2-14 provides another comparison of the helicopter to the airplane. As a first step toward understanding helicopter forward-flight performance, consider the contrasting power required versus speed curves provided in Fig. 2-97. I have chosen to contrast the Army's L-19A (fixed-wing airplane) [281] with the Army's H-13H (rotary wing helicopter) [171]. Both aircraft were tested at nearly equal weights, at an altitude of 1,000 feet. From a configuration point of view, the two aircraft have virtually equal "wing" spans as Table 2-14 shows.

### 2.4.1 Airplane

First let me discuss the power required versus speed data of the L-19A. This discussion will serve as a reminder of fixed-wing aerodynamics and provide a jumping-off point to helicopter forward-flight performance. As you are no doubt aware, the engine power required is determined by the aircraft's propeller thrust ( $T_p$ ) in pounds at a given true airspeed

## 2.4 FORWARD-FLIGHT PERFORMANCE

(V)<sup>65</sup> in feet per second, and the propeller efficiency ( $\eta_p$ ), which generally varies with airspeed. That is,

$$(2.160) \quad \text{Engine BHP} = \frac{T_p V}{550\eta_p}.$$

In steady, level flight, propeller thrust is frequently taken as equal to aircraft drag (D) in pounds. This follows because of a small angle-of-attack assumption in Eqs. (2.161) and (2.162), which are simple trim equations for an airplane. (In fact, at low speeds when the airplane is approaching stall and the aircraft angle of attack is not small, the propeller thrust can contribute an appreciable amount of lift.) Thus, in steady, level flight, it is common to begin with the fundamental statements that

Parallel to the flight path velocity (positive is forward)

$$(2.161) \quad \begin{aligned} \sum F_x = 0 = & W \sin \gamma + T_{\text{prop}} \cos(\alpha_{AC} + i_{\text{prop}}) - H_{\text{prop}} \sin(\alpha_{AC} + i_{\text{prop}}) - D_{\text{fuselage}} \\ & - D_{\text{wing}} - L_{\text{tail}} \sin(\alpha_{AC} + i_{\text{tail}} - \alpha_{\text{interference}}) \\ & - D_{\text{tail}} \cos(\alpha_{AC} + i_{\text{tail}} - \alpha_{\text{interference}}) \end{aligned},$$

Perpendicular to the flight path velocity (positive is down)

$$(2.162) \quad \begin{aligned} \sum F_z = 0 = & W \cos \gamma - T_{\text{prop}} \sin(\alpha_{AC} + i_{\text{prop}}) - H_{\text{prop}} \cos(\alpha_{AC} + i_{\text{prop}}) - L_{\text{fuselage}} \\ & - L_{\text{wing}} - L_{\text{tail}} \cos(\alpha_{AC} + i_{\text{tail}} - \alpha_{\text{interference}}) \\ & - D_{\text{tail}} \sin(\alpha_{AC} + i_{\text{tail}} - \alpha_{\text{interference}}) \end{aligned}, \text{ and}$$

$$(2.163) \quad \text{Engine BHP}_{\text{req'd.}} = \frac{\sum F_x V}{550\eta_p}.$$

The basis of airplane drag is the aircraft lift-drag polar, which, following Oswald's 1931 fundamental report [283], is seen in coefficient form [284] as

$$(2.164) \quad C_D = \frac{D}{qS} = C_{Df} + \frac{C_L^2}{\pi AR e}$$

where ( $C_{Df}$ ) is the drag coefficient at zero lift, ( $C_L$ ) is the lift coefficient equal to  $L/qS$ , ( $S$ ) is the reference area normally taken as the wing area, ( $AR$ ) is the wing-aspect ratio equal to wing span ( $b$ ) squared divided by wing area ( $S$ ), and ( $e$ ) is the "airplane efficiency factor" as

---

<sup>65</sup> Considerable care is taken when referring to airspeed. Airspeed indicators are not all that accurate, particularly at low speed and/or high angle of attack. The indicator itself can have calibration errors, and nonlinear behavior is not uncommon. Because the indicator depends on a pitot-static probe, there can be indicated airspeed errors due to the location of the probe on the aircraft. In flight tests, the indicated airspeed is carefully calibrated with an absolutely believed airspeed, which allows conversion from  $V_{\text{indicated}}$  to  $V_{\text{true}}$ . Most flight test reports only present data in terms of true airspeed. *True airspeed equals indicated airspeed divided by the square root of the density ratio.* Think of true airspeed as the speed at which the aircraft follows a car on the ground, regardless of the altitude that the aircraft is flying at—assuming there is no wind. In that sense, true airspeed might better be called true ground speed.

Oswald referred to it. (As time went on, aerodynamic performance engineers came to call (e) the Oswald efficiency factor.)

Fig. 2-97 shows the Cessna L-19A power-required curve at a gross weight of 2,340 pounds and at 1,000-foot pressure altitude on a standard day, assuming the propeller is 100 percent efficient. This curve is based on the lift-drag polar of the L-19A being<sup>66</sup>

$$(2.165) \quad C_D = \frac{D}{qS} = 0.04 + \frac{C_L^2}{\pi(7.448)(0.7064)} = 0.04 + 0.0605 C_L^2.$$

Practicing aerodynamic performance engineers will immediately recognize that if  $C_{Df}$  is 0.04, then the commonly used equivalent flat plate area ( $f$  being Oswald's notation, or to others,  $f_e$ ) is  $f_e = C_{Df} S = D_f / q = 0.04 (174) = 7$  square feet. Notice that the fixed-pitch metal propeller, with relatively poor propeller efficiency, costs the L-19A about 20 knots in top speed.

There is a very interesting aspect of fixed-wing flight testing and the power required versus airspeed data obtained. The aspect is how to collapse data obtained at several altitudes (but just one weight) to a single, generalized, power-required curve. In 1928, Walter S. Diehl published a NACA report [285] about the reduction of observed airplane performance to standard conditions. His introduction and historical review are well worth reading. Diehl's work was followed by Oswald's very broad study about airplane performance [283]. By mid-1951, the Air Force had generated a very comprehensive flight test engineering handbook [286].<sup>67</sup> This manual was the "bible" when the U.S. Army Aviation Test Office (ATO) took up residence at Edwards Air Force Base in California. Keith Putnam was the Chief of the ATO at its inception. The first formal flight testing that the ATO did was with the L-19A, with results reported in ATO-TR-61-1 [281].

Airplane power-required data, obtained at any pressure altitude and outside air temperature, collapses to a single curve if the power and airspeed are each multiplied by the square root of the air density ratio ( $\rho/\rho_0 = \sigma$ ). That is, the coordinate system is

$$\text{BHP}_{\text{req'd.}} \sqrt{\sigma} \quad \text{versus} \quad V \sqrt{\sigma}.$$

It is rather easy to see this with the airplane's lift-drag polar in dimensional form. From Eq. (2.164),  $C_{Df} S$  is replaced by ( $f_e$ )—the equivalent flat plate area in square feet—and lift ( $L$ ) is set equal to the aircraft weight ( $W$ ) in pounds, which gives

$$(2.166) \quad D = \frac{1}{2} f_e \rho V^2 + \frac{2}{\pi e} \frac{1}{\rho V^2} \left( \frac{W}{b} \right)^2.$$

Then the engine brake horsepower required, following Eq. (2.163), becomes

<sup>66</sup> I backed this result out from TL-19D flight test data using propeller efficiency data provide by Hal Bohemen of the McCauley Propeller Company.

<sup>67</sup> This handbook was corrected and revised in January 1966.

## 2.4 FORWARD-FLIGHT PERFORMANCE

$$(2.167) \text{ Engine BHP}_{\text{req'd.}} = \frac{DV}{550\eta_p} = \frac{1}{550\eta_p} \left( \frac{1}{2} f_e \rho V^3 + \frac{2}{\pi e} \frac{1}{\rho V} \left( \frac{W}{b} \right)^2 \right).$$

Multiplying both sides of Eq. (2.167) by  $\sqrt{\sigma} = \sqrt{\rho/\rho_o}$  leads, with a little algebra, to

$$(2.168) (\text{Eng. BHP}_{\text{req'd.}})\sqrt{\sigma} = \frac{DV\sqrt{\sigma}}{550\eta_p} = \frac{1}{550\eta_p} \left[ \frac{\rho_o}{2} f_e (V\sqrt{\sigma})^3 + \frac{2}{\pi\rho_o e} \left( \frac{W}{b} \right)^2 \left( \frac{1}{V\sqrt{\sigma}} \right) \right].$$

Now the power-required curve depends on the constants  $\frac{\rho_o}{2} f_e$  and  $\frac{2}{\pi\rho_o e} \left( \frac{W}{b} \right)^2$ .

Using the L-19A flight test data [281], you can see from Fig. 2-98 that density altitude has a substantial effect on power required, but by following Eq. (2.168) the data is reduced to one line as Fig. 2-99 shows.

As you saw from Fig. 2-97, propeller efficiency ( $\eta_p$ ) might be better called propeller inefficiency. To illustrate this point, consider Fig. 2-100. The L-19A was tested in 1957 in a training configuration with a metal constant-speed propeller (i.e., a variable-pitch propeller) [282]. This configuration was designated as the TL-19D. The power-required comparison of the L-19A to the TL-19D, shown in Fig. 2-100, is really just a comparison of the fixed-pitch propeller versus the variable-pitch propeller, and the performance improvement is easily worth 10 knots. As Miller and Sawers relate [287], “The variable-pitch propeller was first used [commercially] in 1933 on the Boeing 247 and the Douglas DC-1 to improve the takeoff performance of airplanes which would otherwise have had their payload limited.” A much more technically oriented discussion of the evolution of the variable-pitch propeller is provided by George Rosen in his superb book, *Thrusting Forward: A History of the Propeller* [288].<sup>68</sup>

The reason I have brought your attention to the propeller is twofold. First, the fixed-wing branch of aerodynamics has created a wealth of experimental and theoretical work that rotorcraft engineers can use. Second, Volume III, which deals with other V/STOL aircraft, shows that aircraft such as the tiltrotor and tiltwing, and several other configurations, depend on propeller performance. Therefore, let me (1) provide some information about early NACA research into propeller performance, then (2) show how the rotorcraft engineer can look at propeller performance, and finally (3) show how airplane performance can be calculated in the rotorcraft reference frame.

Shortly after its inception, the N.A.C.A. initiated a very comprehensive propeller research program. This program included model and full-scale wind tunnel tests in comparison to flight tests of the VE-7 airplane (Fig. 2-101). The VE-7 was designed as an

---

<sup>68</sup> George Rosen’s book was published by Hamilton Standard and the British Aerospace Dynamics Group to commemorate the 50th anniversary of the joint efforts of these two companies. In May 1988 I gave a local AHS Chapter speech about propellers. The Chapter gave me a copy of Rosen’s book, which I have kept in my highly cherished file.

## 2.4 FORWARD-FLIGHT PERFORMANCE

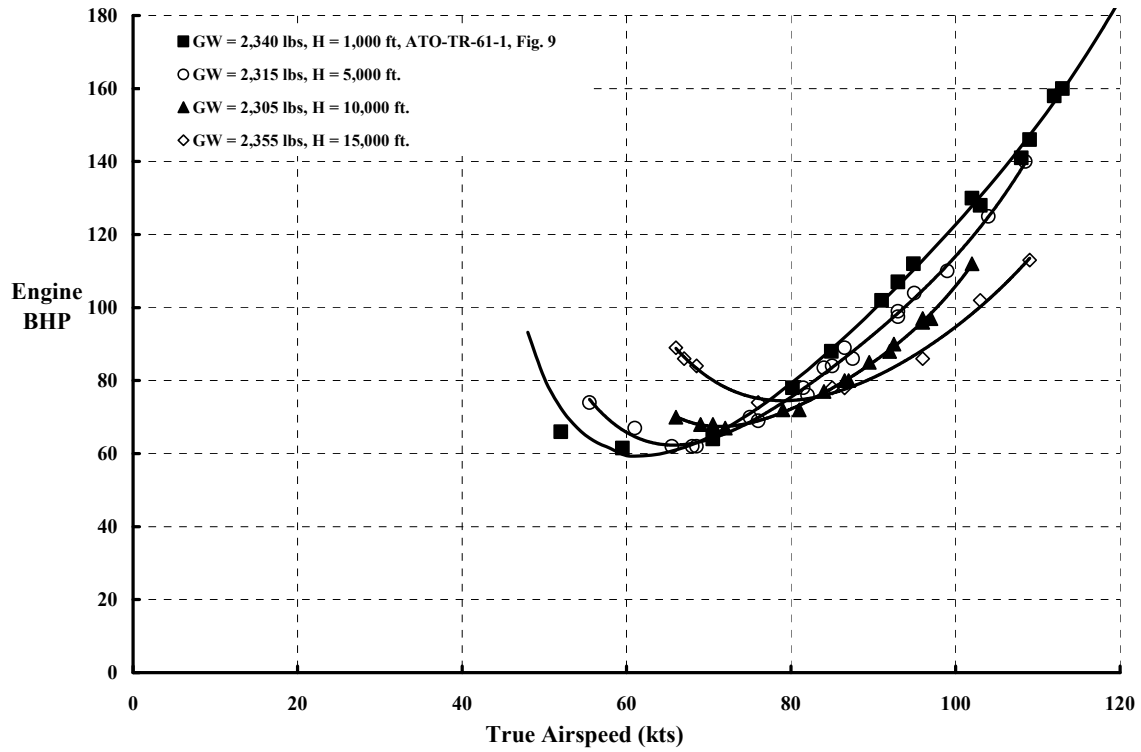


Fig. 2-98. Cessna L-19A flight test data at several altitudes [281].

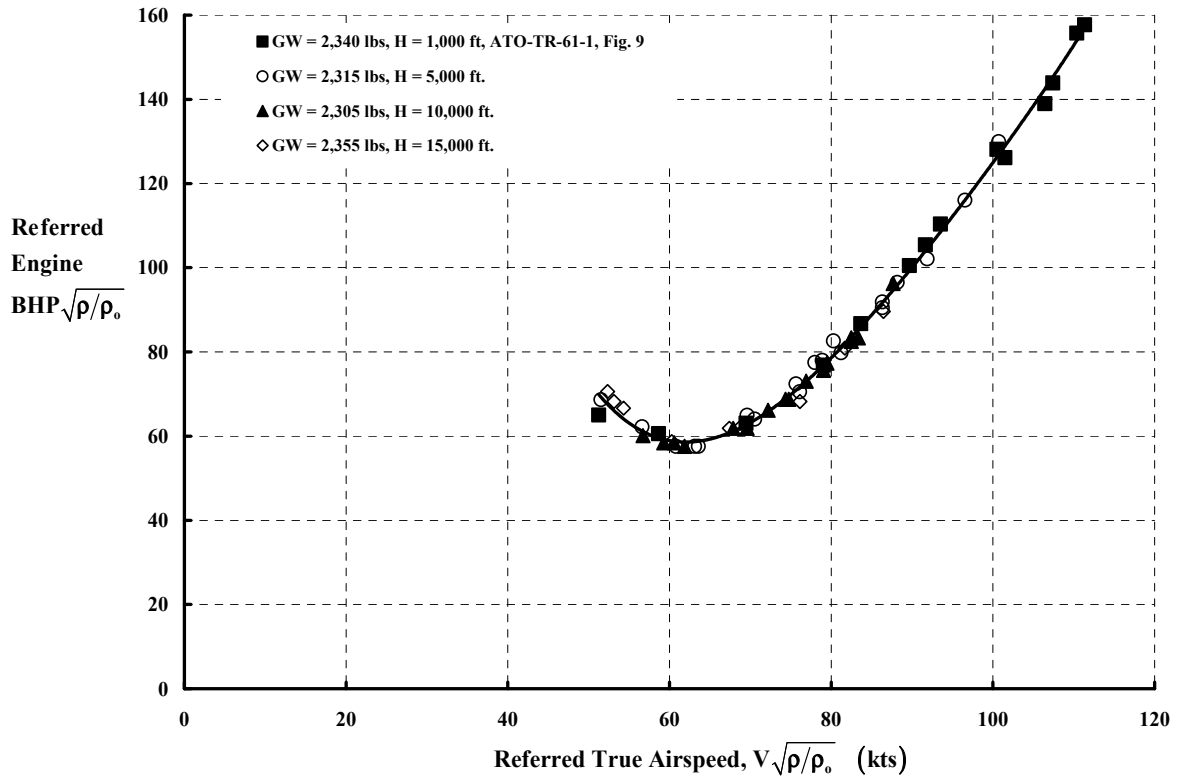
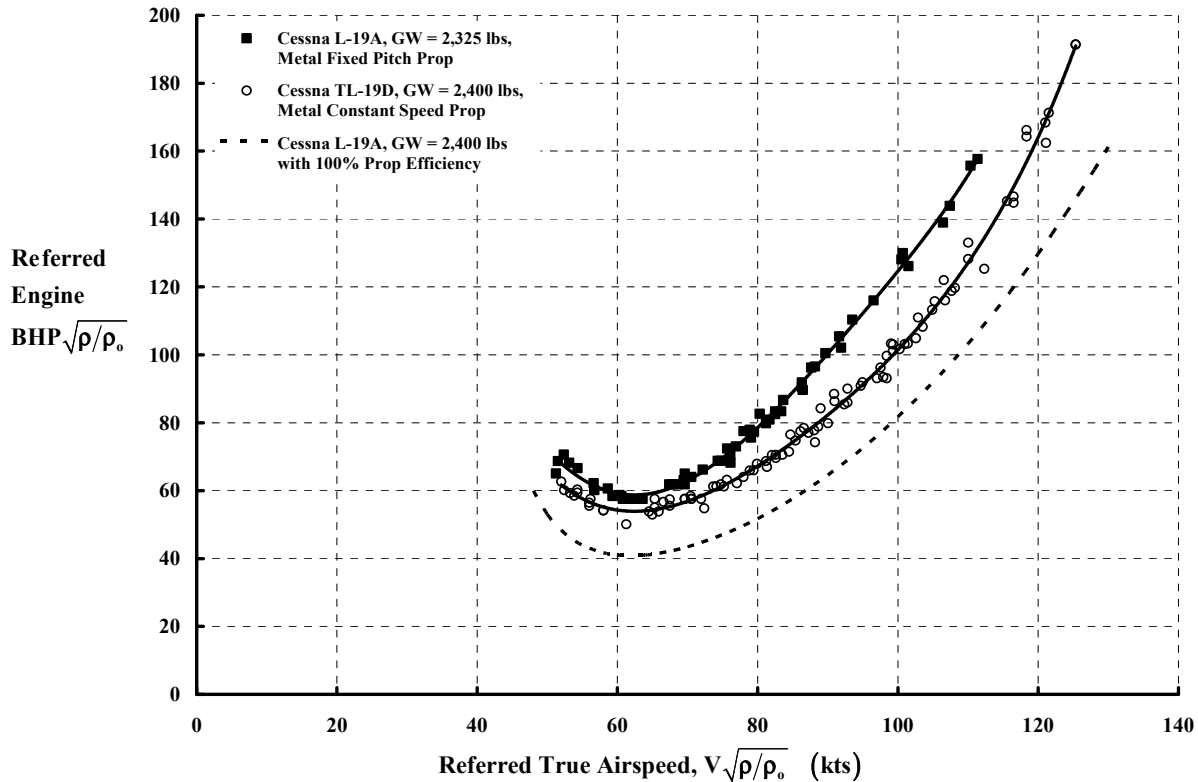


Fig. 2-99. Cessna L-19A flight test data in referred power and airspeed [281].

## 2.4 FORWARD-FLIGHT PERFORMANCE



**Fig. 2-100. Cessna L-19A flight test data shows improved performance with variable-pitch (i.e., constant speed) propellers.**

advanced trainer for the U.S. Army by Birdseye B. Lewis and Chance M. Vought (they became the Chance Vought Corp. in May 1922). The airplane was evaluated by the Army at McCook Field in Dayton, Ohio, in 1918. Lieutenant Alexander Klemin contributed to the static and flight test reports. The U.S. Navy adopted the VE-7 for training and carrier-landing trials. Some 129 VE-7s were built in several versions [289]; one VE-7 went to the N.A.C.A. Langley Memorial Aeronautical Laboratory.

Initial N.A.C.A. propeller research program results were authored by Durand and Lesley [290]. They compared model propeller performance (obtained by Durand at the aerodynamic laboratory of Stanford University) to flight test data. Lesley contributed VE-7 flight test data with five propellers, which was acquired at the Langley Memorial Aeronautical Laboratory. Their conclusion was that “efficiencies realized in flight are close to those derived from model tests,” but that “both thrust developed and power absorbed in flight are from 6 to 10 percent greater than would be expected from the results of model tests.” There was, apparently, considerable concern about the flight test results reported by Lesley, which led to further flight testing of the VE-7 with five propellers [291]. At issue were the results in power-off glide tests that differed from Lesley’s findings. The situation was complicated by no direct measurement of either thrust or power. Around this time the 20-foot, open-throat wind tunnel came online at N.A.C.A. Langley [292]. Weick reported results of the “first complete propeller test made in the Propeller Research Tunnel” [293]. He concluded that

## 2.4 FORWARD-FLIGHT PERFORMANCE

- “1. The results obtained agree as well as can be expected with both flight tests and model wind tunnel tests.
2. The accuracy of the observations in the Propeller Research Tunnel tests, which are made under full-scale conditions, is apparently of about the same order as that of model propeller tests.
3. From comparison of these tests with flight tests, it seems likely that the engines used in the flight tests delivered somewhat less power in flight than would have been expected from dynamometer tests.
4. The effect of the tail surfaces on the propeller characteristics is negligible.
5. The effect of the wings on propulsive efficiency is important and deserves further investigation.”

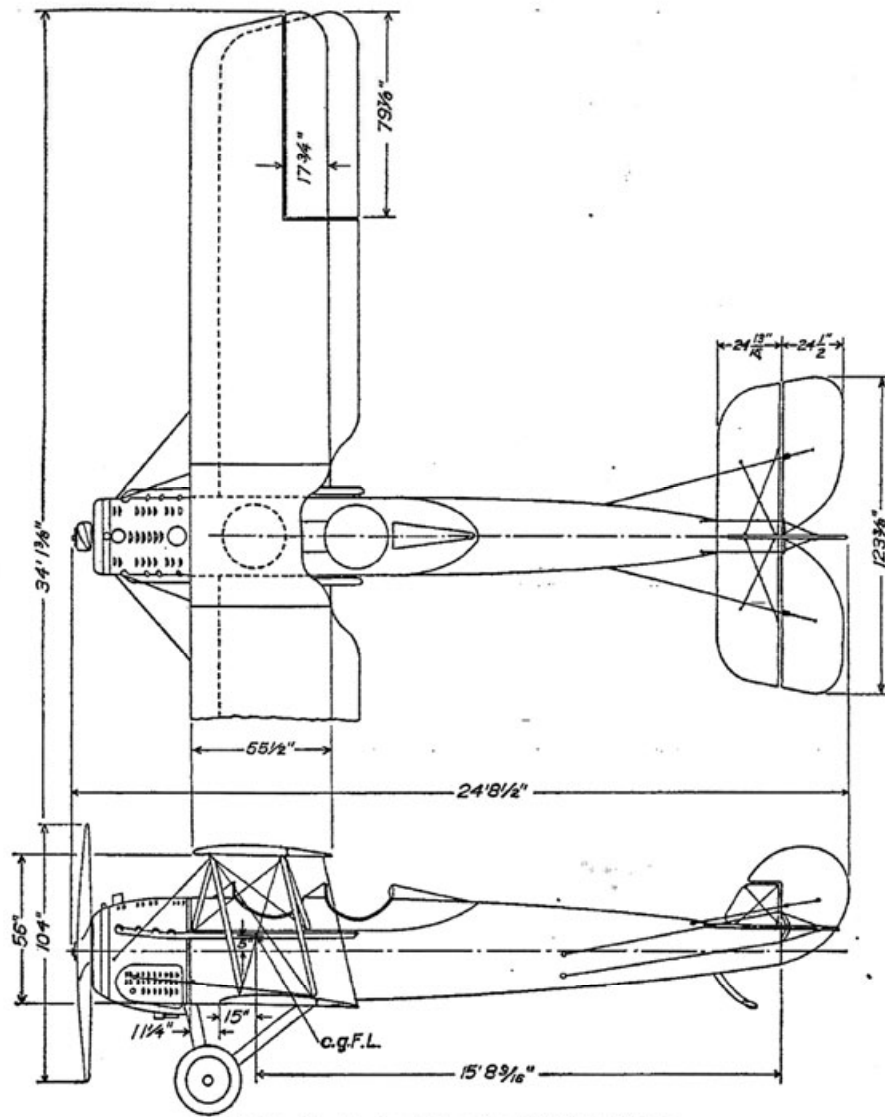


FIG. 2.—Elevational and plan views of the VE-7 a/r plane

**Fig. 2-101. The VE-7 test bed for early N.A.C.A. propeller research.**

## 2.4 FORWARD-FLIGHT PERFORMANCE

The third conclusion Weick related was, and in my opinion still is, a serious problem in flight tests. The engine performance was based on the engine manufacturer's measurement of the output of a new engine. The performance was described with charts relating air conditions and engine RPM to output power. In flight testing, these charts were used to obtain engine power from the pilot's notes. Weick, on the other hand, measured engine torque and propeller thrust directly during his wind tunnel research. Crowley and Mixson [291] carefully calibrated the VE-7 engine (a Wright E-2) before and after their flight testing and found deterioration amounting to 3 percent.

Weick, having evaluated the wooden fixed-pitch propeller [293], immediately tested a metal variable-pitch propeller [294]. The blades of the two-bladed propeller (Fig. 2-102) were rather standard for this between-World-Wars era, and the pitch was only ground adjustable. The title of Weick's report is a little misleading today. He suggests that "a series of metal propellers" were tested. In fact, he tested "the 9-foot-diameter propeller" (actually 8 feet, 11 inches in diameter) at five different pitch settings measured at the 42-inch-radius station ( $x = r/R = 42/54 = 0.778$ ). The pitch settings were 11, 15, 19, 23, and 27 degrees. The pitch setting was made by inclinometer against the bottom surface of the airfoil, which, as Fig. 2-102 suggests, was flat. He notes that

"since each blade as a whole was rotated in the hub to the desired setting, all of the angles along the blade varied the same amount, so that the pitch did not change uniformly. It is, however, common practice to design detachable blade metal propellers with a certain distribution of blade angles and then turn the blades to any pitch required for a particular airplane, thus facilitating production."

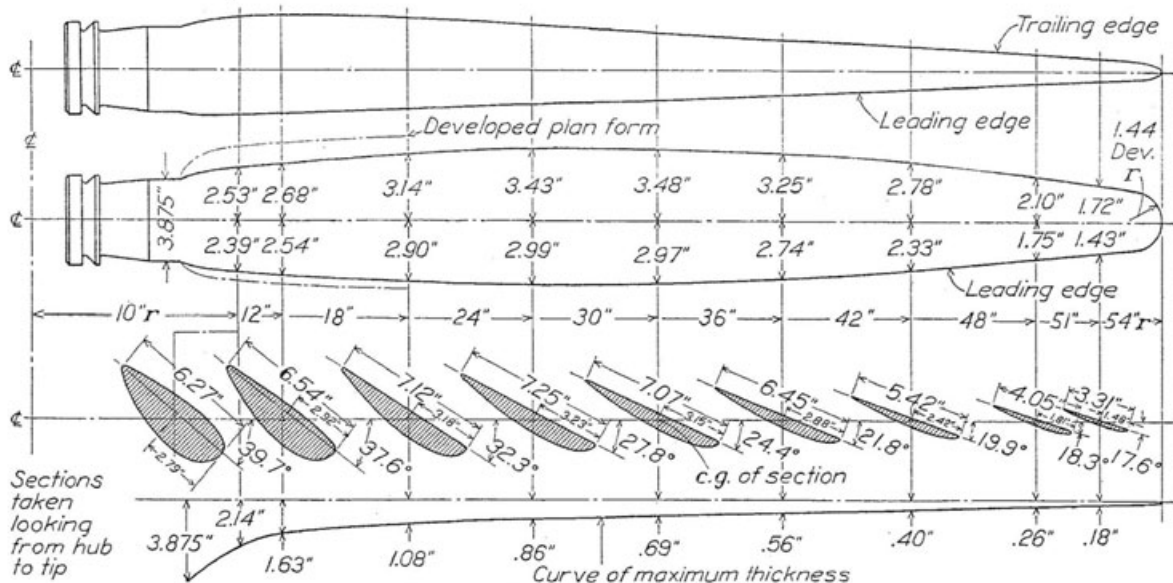


FIG 1.—Metal blade for 9 ft. diameter propeller. Right hand. No. 4412

**Fig. 2-102. The first variable-pitch propeller tested in Langley's 20-foot, open-throat propeller research tunnel. The propeller Activity Factor was 135.**

Propeller designers frequently refer to a propeller's geometry by its Activity Factor (AF), a measure of the integrated capacity of the blade elements to absorb power. As discussed by Perkins and Hage [284] for example, propeller AF is generally calculated as

$$(2.169) \text{ Activity Factor} = \text{AF} = (\text{Blade No.}) \left( \frac{100,000}{16} \right) \int_{\text{root}}^{\text{tip}} (r/R)^3 (b/D) d(r/R)$$

where propeller engineers use (b) as the blade chord. The helicopter designer, using Gessow and Myers' book, *Aerodynamics of the Helicopter* [234], will recognize this AF as a form of power-weighted solidity because of the  $(r/R)^3$  term multiplying the chord-to-diameter ratio (b/D) before integration. A power-weighted chord in the helicopter world is generally calculated as

$$(2.170) \text{ Power-Weighted Chord} = c_e = \frac{\int_0^1 c x^3 dx}{\int_0^1 x^3 dx} = 4 \int_0^1 c x^3 dx.$$

These two views of prop-rotor geometry are related simply as

$$(2.171) \text{ Rotor-Power-Weighted Solidity} \equiv \sigma_e = \frac{b c_e}{\pi R} = \frac{128 \text{ AF}}{100,000 \pi}$$

where rotorcraft engineers use (b) as the number of blades and (c) as the chord. Both power-weighted solidity and AF are definitions that, strictly speaking, apply only to the hover or static thrusting regime. This is because the chord is weighted only by the cube of local velocity due to rotation. At the other extreme, when the prop-rotor is in forward flight but not rotating, the actual blade area would be numerically correct. This would be the case, for example, in calculating the drag of a feathered propeller during engine-out flight. Weick's propeller had an AF of 135, which gives a rotor-power-weighted solidity of 0.055.

The output of Weick's variable-pitch propeller test was propeller-efficiency versus propeller-advance ratio [294]. The raw data (provided in tabulated form) was plotted, and Weick created faired lines for each pitch angle, which yielded Fig. 2-103.

Propeller efficiency is simply the ratio of ideal power required to produce thrust [ $T_p V$  or  $DV$  following (2.172)] to the actual power required. In equation form,

$$(2.173) \eta_p = \frac{T_p V}{T_p V + (P_o + P_i)_{\text{Propeller}}}$$

where  $(P_o)$  is the propeller's profile power and  $(P_i)$  is the propeller's induced power. Both of these propeller powers, which detract from propeller performance and lower efficiency, will be discussed shortly. Propeller advance ratio ( $J = V/nD$ ) uses airspeed ( $V$ ) in feet per second, divided by propeller rotational speed ( $n$ ) in revolutions per second and propeller diameter ( $D$ ) in feet.

You can immediately see from Fig. 2-103 why adjusting propeller pitch in flight was a major step forward in the fixed-wing world. For takeoff, the pilot could run the engine up to maximum RPM and put the propeller at a relatively low pitch. This would get the aircraft quickly up to speed. With increasing speed, the advance ratio would increase and the engine

## 2.4 FORWARD-FLIGHT PERFORMANCE

could be set to a constant RPM, and the propeller pitch could be adjusted so that the propeller operated along the heavy dashed line shown in Fig. 2-103. In climb to altitude, the pilot could select a different pitch. Then, in cruise, another pitch could be selected. Rosen [288] referred to this variable-pitch feature as “giving the pilot a gear shift.”

The rotorcraft engineer sees propeller performance data such as those shown in Fig. 2-103 in a different coordinate system. The coordinate system is actual power graphed versus ideal power. That is,

$$T_p V + (P_o + P_i)_{\text{Propeller}} \text{ versus } T_p V.$$

Rather than use propeller coefficient nomenclature, which nondimensionalizes power by  $\rho n^3 D^5$ , let me use the rotor term of  $\rho(\pi R^2) V_t^3$ . Then you have

$$(2.174) \text{ Actual Power} \equiv C_{P_{\text{actual}}} = \frac{T_p V + (P_o + P_i)_{\text{Propeller}}}{\rho(\pi R^2) V_t^3} = C_T \left( \frac{V}{V_t} \right) + C_{P_o} + C_{P_i}.$$

Notice in Eq. (2.174) that where you might expect to see a propeller-advance ratio ( $J = V/nD$ ) term, you now see a rotor-inflow ratio (i.e.,  $V/V_t$ ). To the rotorcraft engineer, the propeller is a rotor with tip path plane perpendicular to the free-stream velocity and, therefore,

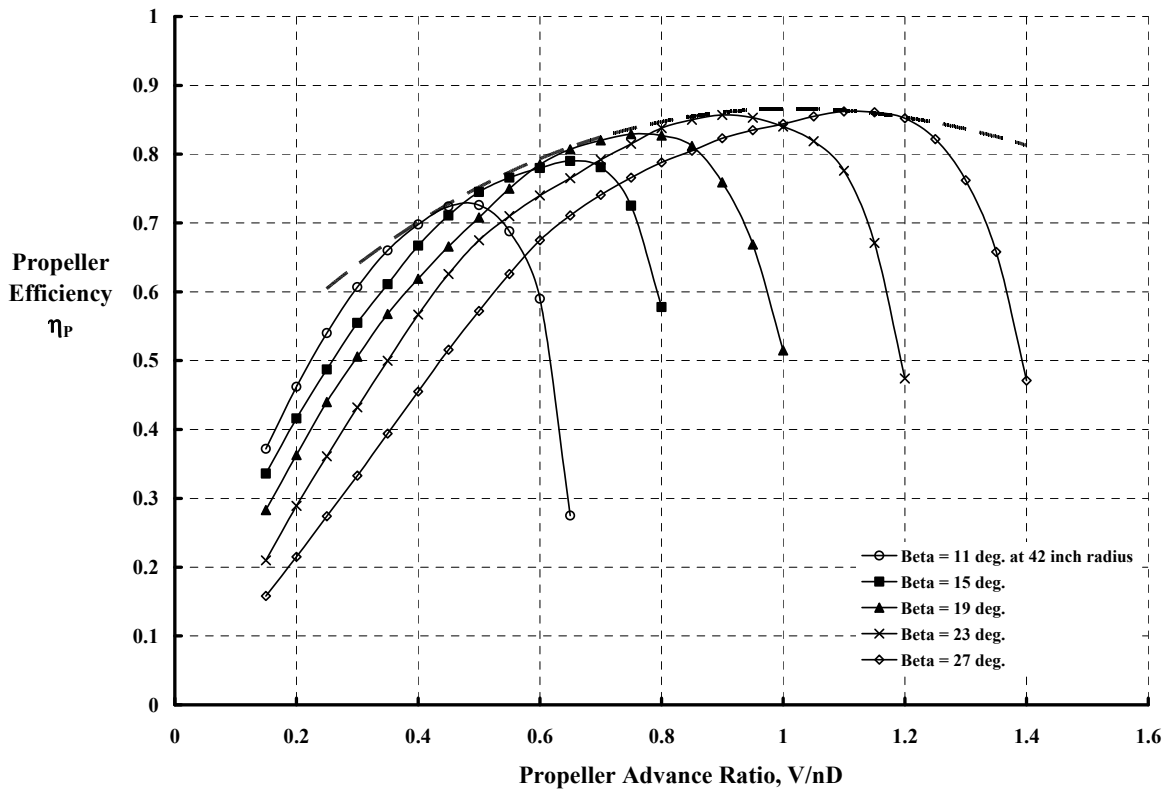


Fig. 2-103. The first variable-pitch propeller tested in the Langley 20-foot, open-throat wind tunnel achieved very respectable efficiencies.

$\alpha_{\text{tip}} = -90$  degrees following Fig. 2-28 on page 63 of Volume I. Thus, from a rotorcraft point of view,  $\mu = 0$  and  $-\lambda_0 = J/\pi$ .<sup>69</sup>

Actual power versus ideal power in rotorcraft nomenclature is shown in Fig. 2-104 using Weick's data [294]. The long, dashed line in this figure represents the simple case where actual power exactly equals ideal power. The various blade-pitch angles ( $\beta$ ) that Weick evaluated are each now seen breaking away from an envelope line. Fig. 2-104 shows that performance at a given pitch angle reaches some sort of maximum capability and then reverses itself. You might think that this apex and reversal is a manifestation of propeller stall. In general, it is not, and Fig. 2-105 shows why. Consider the lowest-pitch-setting data in Fig. 2-105. The propeller thrust varies nearly linearly with inflow ratio. In fact, with a slight

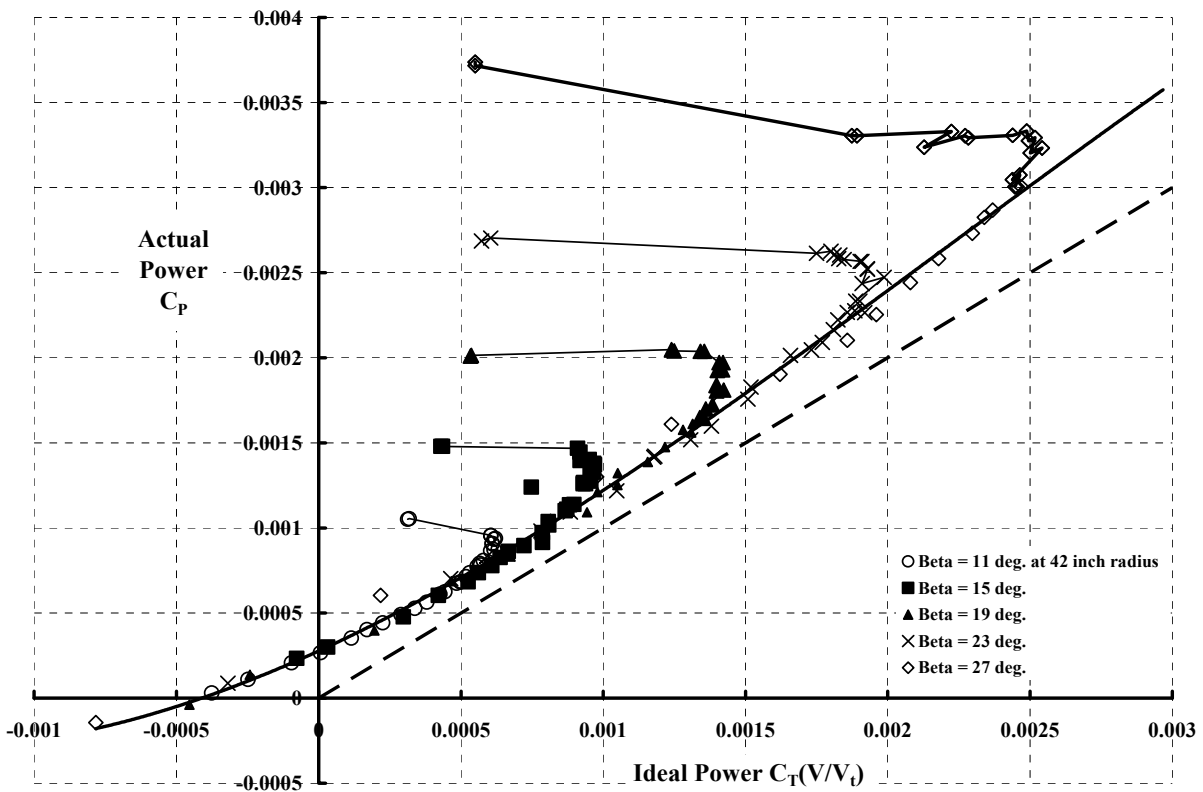


Fig. 2-104. Propeller performance in a rotorcraft format.

<sup>69</sup> Thrust refers to the axial force in the shaft. Rotor and propeller thrust coefficients are related as

$$\text{Rotor } C_T = \frac{T}{\rho(\pi R^2)V_t^2} = \frac{4}{\pi^3} \frac{T_p}{\rho(\pi D^2/4)n^2 D^4} = \frac{4}{\pi^3} \text{Propeller } C_T.$$

Power implies torque times shaft rotational speed for both rotor and propeller. The power coefficients are related as

$$\text{Rotor } C_p = \frac{P}{\rho(\pi R^2)V_t^3} = \frac{4}{\pi^4} \frac{P}{\rho(\pi D^2/4)n^3 D^5} = \frac{4}{\pi^4} \text{Propeller } C_p.$$

## 2.4 FORWARD-FLIGHT PERFORMANCE

extrapolation, the propeller at this low blade-pitch angle could easily produce a rotor thrust coefficient ( $C_T$ ) of 0.01 at zero-inflow ratio (a takeoff condition). But with a  $C_T$  of 0.01 and  $V/V_t = 0$ , the ideal power ( $C_T V/V_t$ ) must be zero. At the other extreme, where the thrust coefficient is zero (because inflow has overcome blade pitch), the ideal power must be zero again. Therefore, in between  $V/V_t = 0$  and the  $V/V_t$  where  $C_T$  goes to zero, the ideal power must reach a maximum. In the case where the pitch is at 11 degrees, this maximum occurs around  $V/V_t = 0.1$ . At the maximum pitch that Weick tested ( $\beta = 27$  degrees), the maximum situation for ideal power occurs at  $V/V_t$  about equal to 0.25. There is, however, evidence of propeller stall at this higher blade-pitch angle, which is measured in rotorcraft terms by the parameter ( $C_T/\sigma$ ) as Eq. 2.293 (page 234 in Volume I) showed. The propeller Weick tested had an Activity Factor of about 135 or a rotor solidity of about 0.055. Fig. 2-105 shows that the 27-degree pitch angle could not produce a  $C_T$  much more than 0.012. This gives a maximum  $C_T/\sigma$  on the order of 0.22 and suggests that the average airfoil was operating at a lift coefficient of 1.3.

With this introduction to experimental trends of propeller performance, turn your attention to calculating propeller profile and induced powers as required by Eq. (2.174), which is repeated on the next page for convenience:

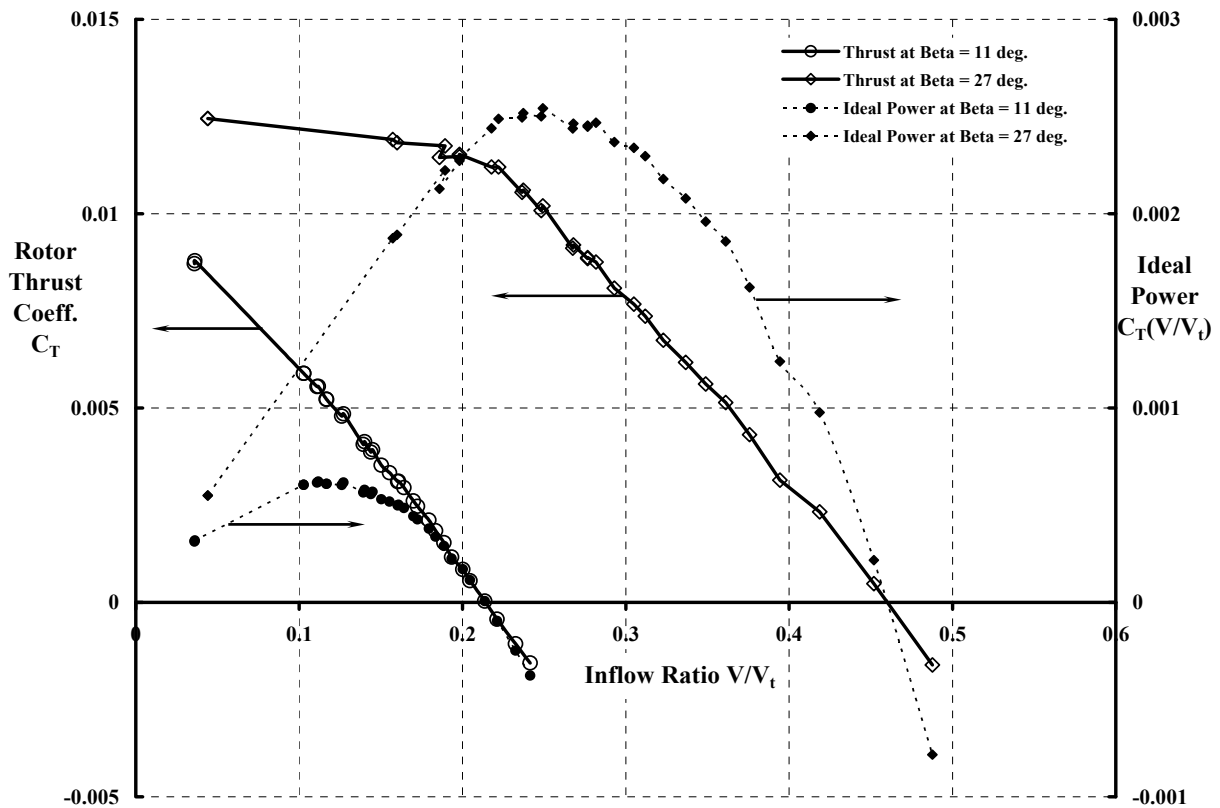


**Fig. 2-105. Ideal power reaches a peak and falls, but not because the propeller stopped producing thrust. The ideal power must go to zero when  $V/V_t = 0$ .**

$$(2.174) \text{ Actual Power} \equiv C_{P_{\text{actual}}} = \frac{T_p V + (P_o + P_i)_{\text{Propeller}}}{\rho(\pi R^2) V_t^3} = C_T \left( \frac{V}{V_t} \right) + C_{P_o} + C_{P_i} .$$

Profile power was introduced with Eq. 2.277 (page 227 in Volume I) discussing autogyro performance. From this introduction, the profile power is

$$(2.175) P_o = \frac{\rho b}{2} \int_0^R V_r dD = \frac{\rho b}{2} \int_0^R c_r (V_r)^3 C_d dr$$

where ( $\rho$ ) is the air density in slugs per cubic feet, ( $b$ ) is the number of blades, and ( $c_r$ ) is the blade chord at radius ( $r$ ). The velocity at a blade element ( $V_r$ ) is, to the first approximation, the resultant of rotational speed ( $\Omega r$ ) and airspeed ( $V$ ), both in feet per second. Following Fig. 2-106 and neglecting the induced velocity ( $v_i$ ), the resultant velocity at a blade element is

$$(2.176) V_r = \sqrt{(\Omega r)^2 + V^2} .$$

In coefficient form, the profile power integration then appears as

$$(2.177) C_{P_o} = \frac{b}{2} \frac{1}{\pi R} \int_0^1 c_r \left( \sqrt{x^2 + \left( \frac{V}{V_t} \right)^2} \right)^3 C_d dx .$$

Suppose now, for the sake of simplicity, that the power-weighted chord defined by Eq. (2.170) is used so that the local blade chord ( $c_r$ ) can be taken outside the integral. Suppose also that the airfoil drag coefficient ( $C_d$ ) is taken as a constant, at some average value, which reduces the integration to

$$(2.178) C_{P_o} = \frac{\sigma_e C_{d_{\text{avg}}}}{2} \int_0^1 \left( \sqrt{x^2 + \left( \frac{V}{V_t} \right)^2} \right)^3 dx$$

with the result that profile power is approximately

$$(2.179) \begin{aligned} C_{P_o} &= \frac{\sigma_e C_{d_{\text{avg}}}}{2} \int_0^1 \left( \sqrt{x^2 + \left( \frac{V}{V_t} \right)^2} \right)^3 dx \\ &\approx \frac{\sigma_e C_{d_{\text{avg}}}}{8} \left\{ 1 + 3 \left( \frac{V}{V_t} \right)^2 + \left[ \frac{9}{8} + \frac{3}{2} \ln(2) - \frac{3}{2} \ln \left( \frac{V}{V_t} \right) \right] \left( \frac{V}{V_t} \right)^4 \right\} . \end{aligned}$$

The average airfoil drag coefficient ( $C_{d_{\text{avg}}}$ ) can be approximated as

$$(2.180) C_{d_{\text{avg}}} = C_{d_o} + \epsilon C_l^2 = C_{d_o} + \delta \left( 6 \frac{C_T}{\sigma} \right)^2$$

## 2.4 FORWARD-FLIGHT PERFORMANCE

where ( $C_{do}$ ) is the airfoil minimum drag coefficient and ( $\delta$ ) is the airfoil drag rise with lift coefficient squared. I have found that a reasonable value of ( $\delta$ ) is ( $C_{do}$ ) so that at  $C_l = 1$ , the average drag coefficient is  $2C_{do}$ .

Now consider the propeller's induced power. From simple momentum theory you have

$$(2.181) \quad P_i = \int_0^R v_i dT.$$

By assuming the induced velocity constant, the integration yields the result that  $P_i = Tv_i$ , and again, from momentum theory, the induced velocity is

$$(2.182) \quad v_i = \sqrt{\left(\frac{V}{2}\right)^2 + \frac{T}{2\rho A}} - \frac{V}{2}.$$

Therefore, the propeller's induced power is, to the first order,

$$(2.183) \quad P_i = T \left( \sqrt{\left(\frac{V}{2}\right)^2 + \frac{T}{2\rho(\pi R^2)}} - \frac{V}{2} \right).$$

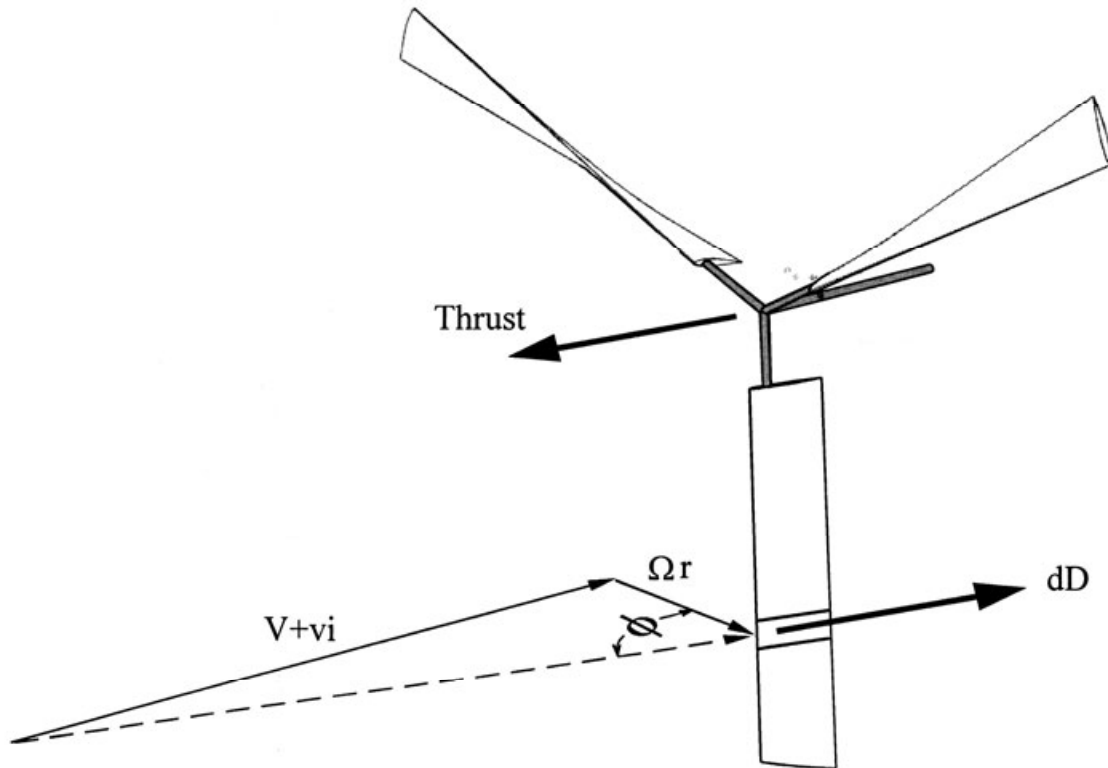


**Fig. 2-106. Propeller blade element geometry.**

Dividing Eq. (2.183) through by  $\rho(\pi R^2)V_t^3$  puts the dimensional result into rotor power coefficient form. The result is

$$(2.184) \quad C_{P_i} = C_T \left( \sqrt{\left(\frac{V}{2V_t}\right)^2 + \frac{C_T}{2}} - \frac{V}{2V_t} \right).$$

Weick's test results for the variable-pitch propeller can be estimated with relatively simple theory. The results of test versus simple theory are shown in Fig. 2-107. The simple theory is

$$(2.185) \quad \text{Rotor } C_P = C_T \left(\frac{V}{V_t}\right) + \frac{\sigma_e \left[ C_{d_0} + \epsilon \left(6 \frac{C_T}{\sigma}\right)^2 \right]}{8} \left\{ 1 + 3 \left(\frac{V}{V_t}\right)^2 + \left[ \frac{9}{8} + \frac{3}{2} \ln \left(\frac{2}{V/V_t}\right) \right] \left(\frac{V}{V_t}\right)^4 \right\} + C_T \left( \sqrt{\left(\frac{V}{2V_t}\right)^2 + \frac{C_T}{2}} - \frac{V}{2V_t} \right)$$

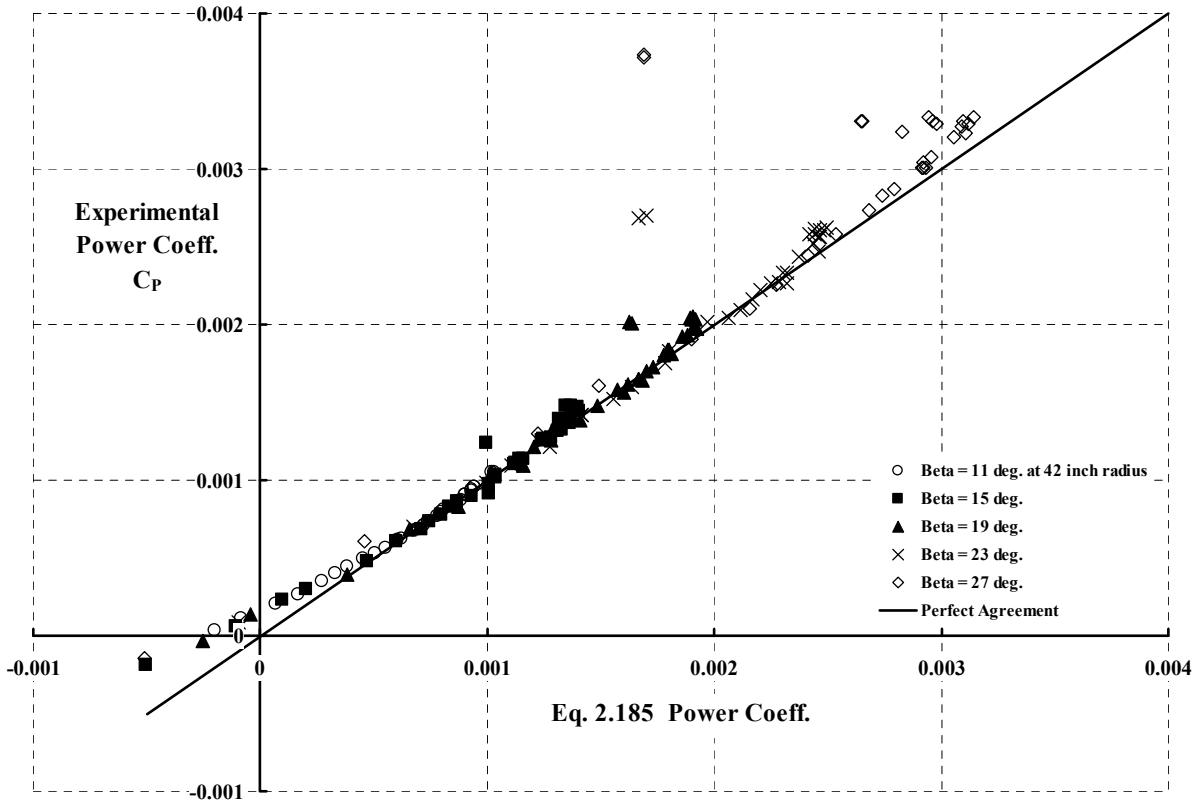


Fig. 2-107. Propeller performance about the optimum design point can be predicted with relatively simple theory.

## 2.4 FORWARD-FLIGHT PERFORMANCE

For the comparison in Fig. 2-107, I used  $C_{do} = 0.02$ ,  $\delta = 0.02$ , and  $\sigma = 0.055$ . Because Weick tabulated his raw data [294], each pitch angle had data for the wind tunnel velocity, propeller RPM, and experimental thrust, along with the experimental engine torque. This gives a known inflow ratio ( $V/V_t$ ) and rotor thrust coefficient ( $C_T$ ) required by Eq. (2.185).

As a final note to this propeller discussion, a more complete study of propeller performance as seen from a rotorcraft perspective is available in NASA Contractor Report 196702 [295].

With this background, let me return to prediction of the Cessna TL-19D power-required curve first seen in Fig. 2-100. The basic lift-drag polar of the TL-19D was given by Eq. (2.165) as

$$(2.165) \quad C_D = \frac{D}{qS} = 0.04 + \frac{C_L^2}{\pi(7.448)(0.07064)} = 0.04 + 0.0605 C_L^2$$

and, therefore, the drag—following Eq. (2.166) and with  $f_e = C_{Df} S = 0.04(174) = 7$  square feet—becomes

$$(2.186) \quad D = 7.0 \left( \frac{\rho V^2}{2} \right) + \frac{0.0605}{174(\rho V^2/2)} L^2.$$

For this example, flight test data from steady, level flight will be used, so propeller thrust ( $T_p$ ) equals aircraft drag ( $D$ ), and wing lift ( $L$ ) equals weight ( $W$ ). The propeller thrust coefficient in rotorcraft terms—so that Eq. (2.185) can be used—is simply

$$(2.187) \quad C_T = \frac{D}{\rho(\pi R^2)V_t^2},$$

and the propeller diameter of the TL-19D is 90 inches, which means that  $R = 3.75$  feet and the propeller area is  $\pi R^2 = 44.18$  square feet. According to the McCauley Propeller Company, its propeller number 2A36CI-U/90M-0 has an Activity Factor of 82.3, which makes the power-weighted solidity equal to 0.025.

This is all the geometric data needed to calculate the power required versus true airspeed of the TL-19D. Only a weight, an altitude, the propeller RPM, and a range of airspeeds are now required. The comparison of test to simple theory is shown in Fig. 2-108. Test results from figure 3 of reference [282] are given for the TL-19D at a weight of 2,400 pounds and a density altitude of 1,500 feet. The pilot flew the test points with a constant engine/propeller speed of 1,900 rpm up to about 110 knots. Beyond 110 knots, he had to steadily increase RPM to get more power out of the engine. At the maximum rated engine speed, 2,600 rpm, he was able to record 131 knots. At this maximum speed point, the propeller tip was approaching the speed of sound. That is, the propeller helical tip Mach number of the TL-19D was

$$(2.188) \quad \text{Helical Tip Mach No.} = \frac{\sqrt{V_t^2 + V^2}}{a_s} = \frac{\sqrt{1,021^2 + (1.69 \times 131)^2}}{1,110} = 0.941.$$

Fortunately, this metal propeller, much like Weick’s propeller shown in Fig. 2-102, had very thin airfoils over the outer radius stations of the blade. This geometry minimizes propeller profile power rise with helical tip Mach number.

Fig. 2-108 shows the power components that lead to the total predicted engine brake horsepower versus airspeed, which is the heavy solid line on the figure. The first component is the basic airframe induced power, which is the power required to produce airframe lift. This power is calculated from Eq. (2.186) as

$$(2.189) \text{ Airframe BHP}_{\text{induced}} = \frac{D_i V}{550} = \left[ \frac{dC_d/dC_l^2}{S(\rho V^2/2)} W^2 \right] \frac{V}{550}$$

where, for the TL-19D,  $dC_d/dC_l^2 = 0.0605$ , and wing area (S) is 174 square feet.

The airframe has a parasite drag that must be overcome by the propeller. The brake horsepower delivered to the propeller to overcome this drag is

$$(2.190) \text{ Airframe BHP}_{\text{parasite}} = \frac{D_{\text{para}} V}{550} = f_c \left( \frac{\rho V^2}{2} \right) \frac{V}{550}$$

where the equivalent parasite drag area ( $f_c$ ) for the TL-19D is 7 square feet.

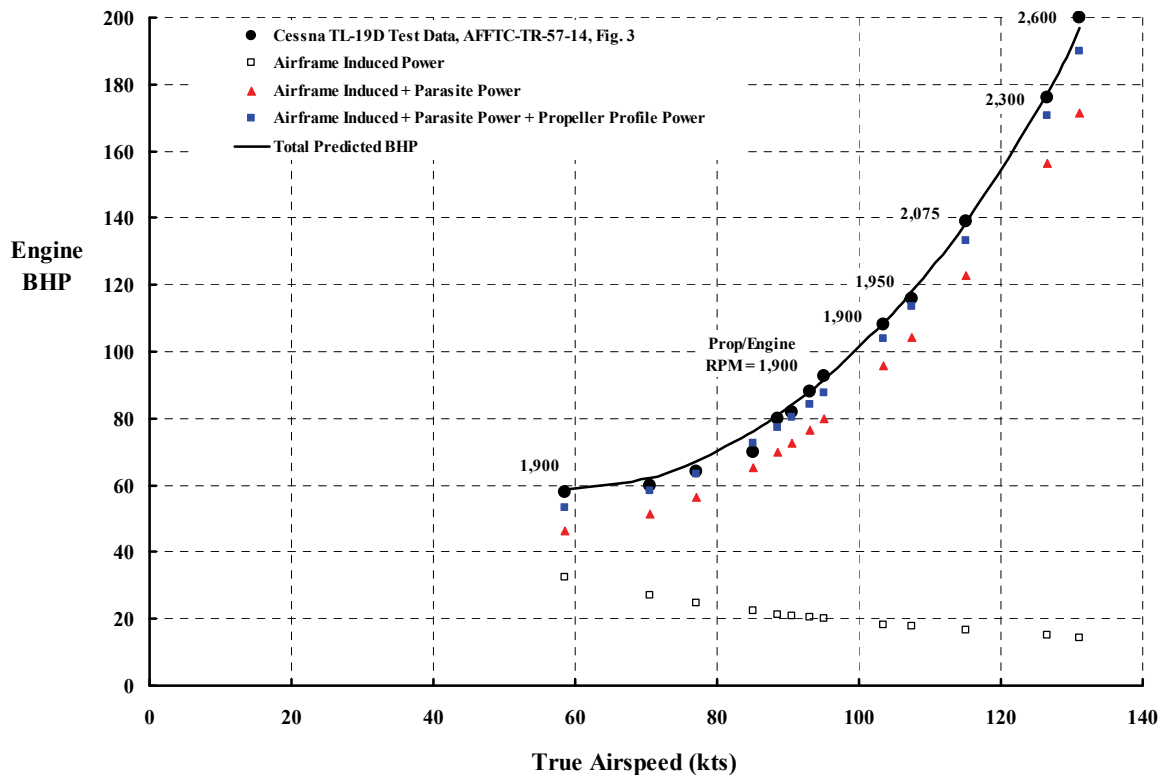


Fig. 2-108. Measured Cessna TL-19D flight test power required can be predicted with rotorcraft methodology (weight = 2,400 pounds and altitude = 1,500 feet).

## 2.4 FORWARD-FLIGHT PERFORMANCE

The sum of airframe-related brake horsepower [Eqs. (2.189) and (2.190)] is shown in Fig. 2-108 with the solid triangle symbols.

The propeller itself requires engine power to overcome its profile drag, and this power is calculated as

$$(2.191) \text{ Prop BHP}_{\text{profile}} = \left( \frac{\rho A V_t^3}{550} \right) \left( \frac{\sigma_e}{8} \right) \left[ C_{\text{do}} + \delta \left( 6 \frac{C_T}{\sigma} \right)^2 \right] F \left( \frac{V}{V_t} \right)$$

where

$$(2.192) F \left( \frac{V}{V_t} \right) = \left\{ 1 + 3 \left( \frac{V}{V_t} \right)^2 + \left[ \frac{9}{8} + \frac{3}{2} \ln \left( \frac{2}{V/V_t} \right) \right] \left( \frac{V}{V_t} \right)^4 \right\}$$

with TL-19D propeller parameters of  $A = 44.18$  square feet, solidity  $\sigma_e = \sigma = 0.025$ ,  $C_{\text{do}} = 0.024$ , and  $\delta = 0.024$ . The propeller thrust coefficient is calculated from the sum of airframe parasite and induced drags.

To produce thrust, the propeller creates an induced velocity that leads to the fourth component of power, the propeller-induced power, calculated as

$$(2.193) \text{ Prop BHP}_{\text{induced}} = \left( \frac{\rho A V_t^3}{550} \right) (C_T) \left( \sqrt{\left( \frac{V}{2V_t} \right)^2 + \frac{C_T}{2}} - \frac{V}{2V_t} \right)$$

where the propeller thrust coefficient is calculated from the sum of airframe parasite and induced drags.

So that you will not think that the proceeding simple theory is of limited use, the prediction of all TL-19D flight test power-required data is shown in Fig. 2-109. The success of such a simple theory depends on the absence of stall and compressibility effects. And the prediction depends on a variable-pitch propeller, although adequate results can often be obtained even with a fixed-pitch propeller.

This brief discussion about airplane forward-flight performance does not include many other facets such as climb and descent performance, takeoff and landing calculation methods, and performance during maneuvers. There are many textbooks and handbooks available that delve into these details. I grew up with Perkins and Hage [284], but you will, of course, have your favorite.

Finally, as a prelude to helicopter forward-flight performance, Table 2-15 provides a translation of propeller and rotor notations that I have found handy.

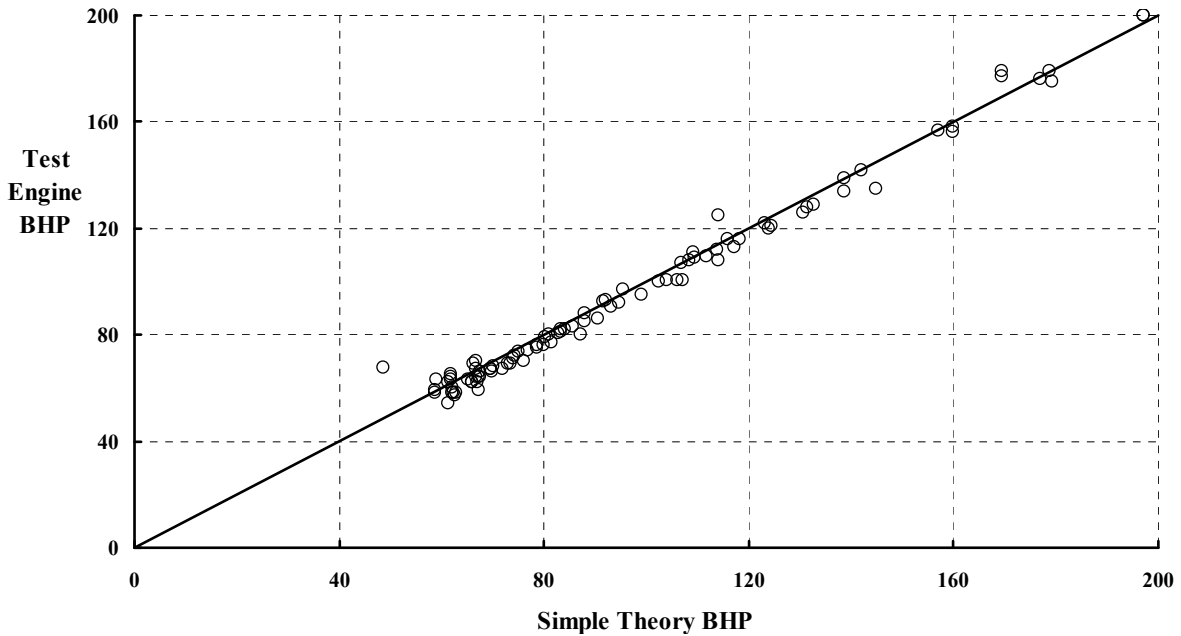


**Fig. 2-109. Measured Cessna TL-19D flight test power required can be predicted with rotorcraft methodology (weight = 2,400 pounds and density altitudes range from 1,500 to 10,000 feet).**

**Table 2-15. Propeller and Rotor Nomenclature**

Parameter	Helicopter Rotor	Airplane Propeller
Prop-Rotor Diameter (ft)	D	D
Blade Radius (ft)	R	R
Shaft Rotational Speed	$\Omega$ (radians/sec)	n (revolutions/sec)
Tip Speed (ft/sec)	$V_t = \Omega R$	$V_t = \pi n D$
Disc Area (sq ft)	$A = \pi R^2$	$A = \pi D^2 / 4$
Air Density (slug/ft <sup>3</sup> )	$\rho$	$\rho$
Flight Speed (ft/sec)	V	V
Thrust (lb)	T	T
Thrust Coefficient	$C_T = T / \rho A V_t^2$	$C_T = T / \rho n^2 D^4$
Power (ft-lb/sec)	P	P
Power Coefficient	$C_P = P / \rho A V_t^3$	$C_P = P / \rho n^3 D^5$
Tip-Path-Plane Angle of Attack (radian)	$\alpha_{tpp}$ measured from rotor disc parallel to wind	$\alpha$ measured from shaft horizontal
Advance Ratio	$\mu = V \cos \alpha_{tpp} / V_t$	$J = V / nD$
Inflow Ratio	$\lambda_o = V \sin \alpha_{tpp} / V_t$	See Advance Ratio
Induced Velocity (ft/sec)	$v_i$	u or w
Induced-Inflow Ratio	$\lambda_i = v_i / V_t$	Rarely used
Propulsive Efficiency	$\eta_P = C_T \lambda_o / \text{measured } C_P$	$\eta_P = C_T J / \text{measured } C_P$

## 2.4 FORWARD-FLIGHT PERFORMANCE

### 2.4.2 Single Rotor Helicopter

You saw the contrast between an early U.S. Army helicopter (the H-13) and an airplane (the L-19A) engine brake horsepower required versus airspeed trends in Fig. 2-97. The contrast is, admittedly, rather startling, particularly to a fixed-wing engineer. After all, the airplane engineer sees that at 150 horsepower the L-19A goes 40 knots faster. Not only that, but at 150 horsepower, the engine is burning about 65 pounds of fuel per hour. Because Table 2-14 shows that both the Bell H-13H and the Cessna L-19A have about 250 pounds of fuel to burn, both aircraft can fly for 3.75 hours, but in that time the L-19A will cover some 400 nautical miles at 110 knots, while the H-13H will only cover about 250 nautical miles at 70 knots. To top it off, today's fixed-wing engineer probably does not think that the 1950's L-19A was a particularly great performing airplane, primarily because its maximum lift-to-drag ratio, based on engine brake horsepower and 2,400 pounds weight, was on the order of

$$(2.194) \text{ Aircraft } \frac{L}{D} = \frac{W}{550\text{BHP}/1.69V} = \frac{2,400}{550 \times 150 / 1.69 \times 110 \text{ knots}} = 5.4,$$

and the H-13 helicopter was even worse at 3.4, some 2 points lower.

A simple photo of the H-13 (Fig. 2-110) would cause the fixed-wing engineer to make a long list of aerodynamic deficiencies. The list would surely include:

1. The thing is built of tubes; all very high-drag components.
2. Even World War I airplanes had their fuselage covered with doped canvas.
3. Why isn't the landing gear retractable?
4. Does it at least have doors to cover the large cockpit openings?
5. All that poorly shaped blade retention hardware must have high drag.
6. Are all those bars, linkages, and pipes between the rotor hub and fuselage streamlined?
7. Let's put the fuel tanks inside.
8. It reminds me of Bleriot's Model XII that got across the English Channel in 1909.
9. Propellers—okay rotors—are not suppose to go through the air edgewise.
10. You're lucky it can get to 80 knots.
11. Well, it can at least hover and takeoff and land vertically. That's something.
12. How do you calculate the power-required curve for this helicopter anyway? What's the equivalent flat-plate drag area? What's Oswald's efficiency factor for an edgewise flying rotor?

Of course this gives the helicopter aerodynamic performance engineer an opportunity to offer an explanation and some insight.



**Fig. 2-110. The H-13 lacked aerodynamic refinements (photo from author’s collection).**

The H-13 began life as the Bell Model 47 and was certificated by the CAA (now the FAA) on March 8, 1946. It was designed to at least hover with the then available engine. The rotor diameter was large to ensure a reasonable power margin at that time. Every weight-empty savings that could be obtained was obtained. Hence, an uncovered fuselage, removable doors, and the bare necessities for a landing gear. The engine, main rotor transmission, and fuel tanks were placed directly under the rotor shaft. The large, bulbous “windshield” was selected for maximum crew visibility. The blade attachment was designed with a high margin of safety and very low fatigue stresses. The attachment hardware was a high-drag item as were the rotor shaft and control linkage. Because the Bell Model 47 was designed to use the installed power most efficiently in hover, the high-speed performance was simply a fallout.

There are a number of very aerodynamically “clean” helicopters in production today. One good example is the Sikorsky twin-turbine-engine Model S-76 shown in Fig. 2-111, which first flew in January 1975. From *Jane’s All the World’s Aircraft* [296], some 510 increasingly improved models of the S-76 have been delivered since early 1979. This medium-sized helicopter has a crew of 2 and room for as many as 12 to 14 passengers. The aircraft meets Federal Aviation Regulations (FAR), Part 29 with Category A Instrument Flight Rules (IFR) and sold for about \$6 million in 2002. Drag reduction is evident in the retractable, wheeled landing gear and airplane-shaped fuselage. However, the main rotor blade attachment hardware, the hub, is still a high-drag item. Evan Fradenburgh (a close friend and top-notch engineer) went to considerable effort to make the S-76 a low-drag helicopter [297].

## 2.4 FORWARD-FLIGHT PERFORMANCE



**Fig. 2-111. The Sikorsky S-76 is one example of an aerodynamically “clean” helicopter (photo from author’s collection).**

Now let me discuss the power-required curve of the H-13H shown in Fig. 2-97. This primary performance curve can be estimated with a simple theory that is no more complicated than that for the L-19A series. You learned the basics in Volume I; let me apply those basics to the helicopter.

As a starting point use Eq. (2.47), repeated here for convenience, with the notation change for calculating brake horsepower required:

$$\text{Eq. (2.47) } \text{BHP}_{\text{req'd.}} = \frac{\text{RHP}_{\text{mr}}}{\eta_{\text{mr}}} + \frac{\text{RHP}_{\text{tr}}}{\eta_{\text{tr}}} + \text{BHP}_{\text{Accessory}}$$

Consider the main rotor horsepower ( $\text{RHP}_{\text{mr}}$ ) first. As with the L-19A, the main rotor requires power to overcome helicopter drag (i.e., the power associated with the equivalent flat plate area), the profile power (i.e., the power associated with turning the rotor against its own drag created by  $C_{\text{do}}$ ), and the induced power (i.e., the power associated with thrust and induced velocity).

The helicopter’s main rotor provides both a lift force ( $F_z$ ) and a propulsive force ( $F_x$ ), which correspond to an airplane’s propeller thrust. In steady, level flight, the resultant force  $\sqrt{F_z^2 + F_x^2}$  is adequately approximated for this example by the helicopter’s weight ( $W$ ). The propulsive force comes by tilting the tip path plane ( $\alpha_{\text{tp}}$ ) nose down, which is in the negative direction. Thus,

$$(2.195) \quad F_x = -W\alpha_{\text{tp}} = D = f_e \left( \frac{1}{2} \rho V^2 \right)$$

where ( $f_c$ ) is the equivalent flat plate area in square feet, ( $\rho$ ) is the air density in slugs per cubic foot, and ( $V$ ) is the helicopter's true airspeed in feet per second. Then, following the L-19A example [Eq. (2.190)], the main rotor horsepower required for the H-13H to overcome parasite drag is

$$(2.196) \text{ Parasite RHP}_{\text{mr}} = \frac{D_{\text{para}} V}{550} = f_c \left( \frac{\rho V^2}{2} \right) \frac{V}{550}.$$

In like manner, the main rotor requires horsepower to produce thrust, which is calculated as

$$(2.197) \text{ Induced RHP}_{\text{mr}} = \frac{W v_i}{550}$$

where the rotor induced velocity ( $v_i$ ) is obtained for steady, level flight (when the tip-path-plane angle is small) approximately as

$$(2.198) v_i = \left[ \sqrt{\frac{V^4}{4} + \left( \frac{W}{2\rho\pi R^2} \right)^2} - \frac{V^2}{2} \right]^{\frac{1}{2}}$$

so that induced power is

$$(2.199) \text{ Induced RHP}_{\text{mr}} = \frac{W v_i}{550} = k_i \frac{W}{550} \left[ \sqrt{\frac{V^4}{4} + \left( \frac{W}{2\rho\pi R^2} \right)^2} - \frac{V^2}{2} \right]^{\frac{1}{2}}.$$

The inclusion of an induced power correction factor ( $k_i$ ) is the rotorcraft equivalent of the airplane's Oswald efficiency factor, but in the numerator. Ray Prouty, on pages 125 through 129 of his excellent and practical helicopter engineering book, *Helicopter Performance, Stability, and Control* [242], calculates that a rotor's Oswald efficiency factor can vary between 0.5 and 0.8.<sup>70</sup> A useful (but crude) approximation I use [211] is that

$$(2.200) k_i = 1.075 \cosh(7.5\mu^2)$$

where ( $\mu$ ) is the main rotor's advance ratio ( $V/V_t$ ).

The main rotor's profile power calculation is much like that for a propeller. That is,

$$(2.201) \text{ Profile RHP}_{\text{mr}} = \left( \frac{\rho A V_t^3}{550} \right) \left( \frac{\sigma_e}{8} \right) [C_{\text{do}} + \delta C_{\text{1avg.}}] [F_{\text{mr}}(\mu)]$$

<sup>70</sup> Ray Prouty's complete paper [298] about the adverse induced drag behavior of the lifting rotor was published in July 1976. He originally presented the paper at the American Helicopter Society Symposium on Helicopter Aerodynamic Efficiency held in Connecticut in March 1975. His paper came from his thesis for a Master's Degree from the California Institute of Technology in 1958. I have always thought that Ray did his best to alert the industry about a serious deficiency in rotor aerodynamic theory—but very few of us paid attention.

## 2.4 FORWARD-FLIGHT PERFORMANCE

where the advance ratio function ( $F_{mr}$ ) for the main rotor is, from Eq. 2.295 on page 236 in Volume I,

$$(2.202) \quad F_{mr}(\mu) = 1 + 4.65\mu^2 + 4.15\mu^4 - \mu^6.$$

Because the rotor remains in roll equilibrium while in edgewise flight, the average airfoil lift coefficient ( $C_{l_{avg}}$ ) needed by Eq. (2.201) is calculated as

$$(2.203) \quad C_{l_{avg}} = \left(6 \frac{C_w}{\sigma}\right) \left(\frac{1 + 3\mu^2/2}{1 - \mu^2 + 9\mu^4/4}\right).$$

This equation for the average airfoil lift coefficient was developed on page 44 of reference [211].

Now consider the power required by the tail rotor. Without doing a thorough trim analysis that includes roll and yaw as well as pitch, some assumption about the tail rotor tip-path-plane angle and thrust must be made. For this example, I will assume that the pilot has trimmed the aircraft so that the tail rotor is not producing any propulsive force (i.e.,  $F_x = 0$ ). Then only an estimate of tail rotor thrust is required to begin the calculation.

The tail rotor thrust (i.e., the anti-torque force) is calculated just as it was in hover. That is,

$$(2.204) \quad T_{tr} = \frac{550 \text{RHP}_{mr}}{(R + R_{tr}) \Omega_{mr}} = \frac{550 \text{RHP}_{mr}}{(1 + R_{tr}/R) V_{t-mr}},$$

and then the induced power is simply a repeat of the main rotor's computation, but with thrust substituted for weight and subscripted with (tr) to indicated tail rotor. Thus,

$$(2.205) \quad \text{Induced RHP}_{tr} = \frac{T_{tr} v_i}{550} = k_i \frac{T_{tr}}{550} \left[ \sqrt{\frac{V^4}{4} + \left(\frac{T_{tr}}{2\rho\pi R_{tr}^2}\right)^2} - \frac{V^2}{2} \right]^{\frac{1}{2}}.$$

Of course the induced power correction factor ( $k_i$ ) must be based on the tail rotor advance ratio, which means that

$$(2.206) \quad \text{Tail rotor } k_i = 1.075 \cosh(7.5\mu_{tr}^2).$$

The tail rotor profile power calculation is much like that for a propeller. That is,

$$(2.207) \quad \text{Profile RHP}_{tr} = \left(\frac{\rho A_{tr} V_{t-tr}^3}{550}\right) \left(\frac{\sigma_{e-tr}}{8}\right) [C_{do} + \delta C_{l_{avg}}^2]_{tr} [F_{tr}(\mu_{tr})]$$

where the tail rotor advance ratio function ( $F_{tr}$ ) is the same as the main rotor function, although the tail rotor advance ratio must be used:

$$(2.208) \quad F_{tr}(\mu_{tr}) = 1 + 4.65\mu_{tr}^2 + 4.15\mu_{tr}^4 - \mu_{tr}^6.$$

Because the tail rotor also remains in roll equilibrium while in edgewise flight, the average airfoil lift coefficient ( $C_{l_{avg}}$ ) is now based on the tail rotor thrust-coefficient-to-solidity ratio ( $C_T/\sigma$ ):

$$(2.209) \text{ Tail rotor } C_{l_{avg}} = \left(6 \frac{C_T}{\sigma}\right)_{tr} \left(\frac{1 + 3\mu_{tr}^2/2}{1 - \mu_{tr}^2 + 9\mu_{tr}^4/4}\right).$$

The results of applying these simple equations to the Bell H-13H are shown in Fig. 2-112. (The computations summarized in Table 2-17 used input from Table 2-16.) As the figure shows, the main-rotor brake horsepower required dominates the answer. The sharp reduction in induced power is simply replaced by power required to overcome the parasite drag, which is calculated assuming an equivalent flat plate drag area ( $f_e$ ) of 15 square feet. The profile power of the main rotor increases slightly with speed, which can be better appreciated with Table 2-17. I assigned the average airfoil a minimum drag coefficient ( $C_{do}$ ) of 0.01 and set ( $\delta$ ), the drag rise with average airfoil lift coefficient squared, equal to 0.012. Lacking any data, a main rotor transmission efficiency of 0.97 was assumed.

The difference between the main-rotor total brake horsepower required (the  $\times$ 's in Fig. 2-112) and the heavy, solid line without symbols accounts for the tail rotor and 3 horsepower of accessories. The brake horsepower required by the tail rotor drops rapidly with speed, from 14.2 at hover to below 10 at 80 knots, as Table 2-17 shows.

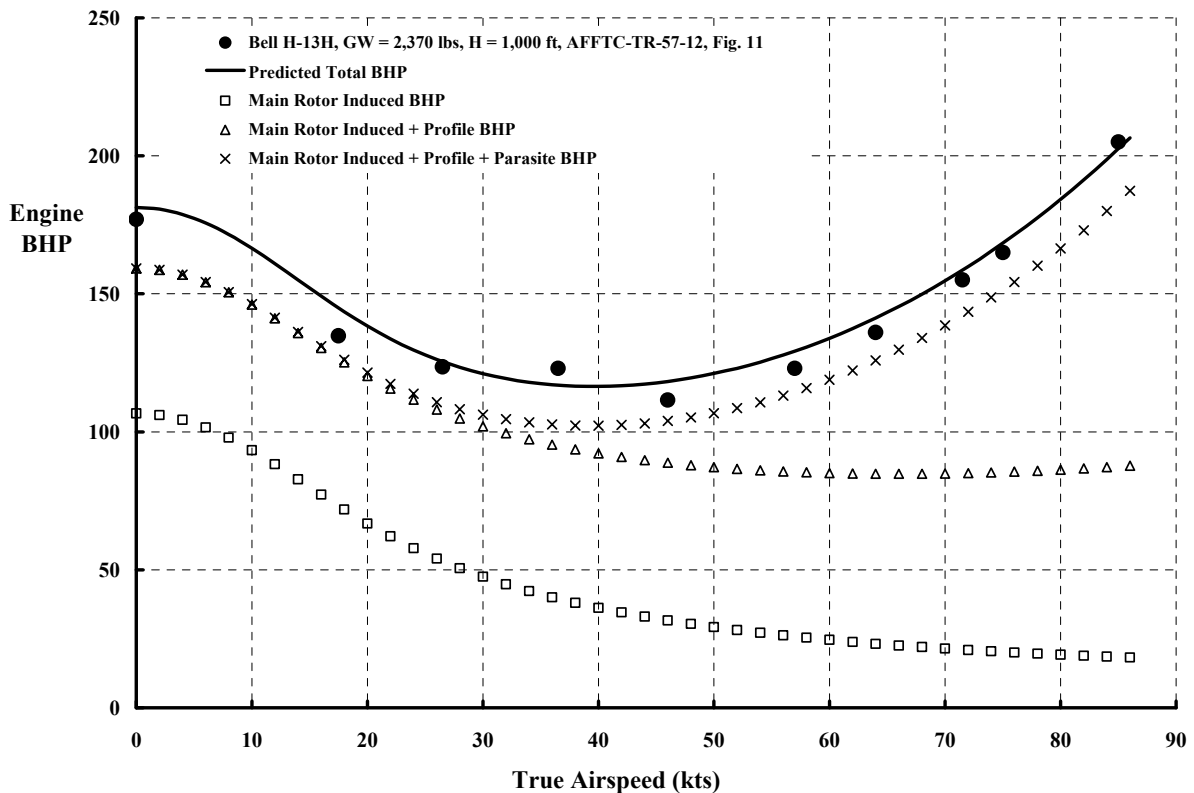


**Fig. 2-112. Bell H-13H flight test power required can be closely estimated with simple methodology (computations in Table 2-17 using input from Table 2-16).**

## 2.4 FORWARD-FLIGHT PERFORMANCE

**Table 2-16. H-13H Inputs to Sample Power-Required Calculation**

Parameter	Main Rotor	Tail Rotor
Density	0.002309	0.002309
Radius	17.5625	2.8385
Tip Speed	632.67	767.59
Solidity	0.03325	0.08465
Airfoil C <sub>do</sub>	0.010	0.012
Airfoil $\delta$	0.010	0.012
Transmission Efficiency	0.97	0.98
H-13 Flat Plate Area	15	n/a

**Table 2-17. H-13H Sample Power-Required Calculation**

Forward Speed (kts)	0	16	32	48	64	80
<b>Parameter</b>						
<b>Main Rotor</b>						
Advance Ratio	0.000	0.043	0.085	0.128	0.171	0.214
Induced Velocity	23.02	16.68	9.65	6.51	4.89	3.92
k <sub>i</sub>	1.075	1.075	1.077	1.083	1.101	1.139
Induced RHP	106.6	77.3	44.8	30.4	23.2	19.2
Average C <sub>l</sub>	0.478	0.480	0.487	0.497	0.513	0.532
Average C <sub>do</sub>	0.0123	0.0123	0.0124	0.0125	0.0126	0.0128
F( $\mu$ )	1.000	1.009	1.034	1.078	1.139	1.221
Profile RHP	52.6	53.1	54.7	57.5	61.6	67.1
Parasite RHP	0.0	0.6	5.1	17.3	41.0	80.1
Total RHP	159.2	131.0	104.6	105.2	125.8	166.4
<b>Total MR BHP</b>	<b>164.1</b>	<b>135.1</b>	<b>107.8</b>	<b>108.5</b>	<b>129.7</b>	<b>171.6</b>
<b>Tail Rotor</b>						
Advance Ratio	0.000	0.035	0.070	0.106	0.141	0.176
Main Rotor Torque	2431	2000	1597	1607	1921	2541
Thrust	119.1	98.0	78.3	78.7	94.2	124.5
Induced Velocity	31.92	23.44	12.09	8.26	7.43	7.87
k <sub>i</sub>	1.075	1.075	1.076	1.079	1.087	1.104
Induced RHP	7.4	4.5	1.9	1.3	1.4	2.0
Average C <sub>l</sub>	0.245	0.202	0.163	0.167	0.203	0.276
Average C <sub>do</sub>	0.0127	0.0125	0.0123	0.0123	0.0125	0.0129
F <sub>tr</sub> ( $\mu$ )	1.000	1.006	1.023	1.052	1.094	1.148
Profile RHP	6.5	6.4	6.4	6.6	7.0	7.5
Total RHP	13.9	10.9	8.3	7.9	8.3	9.5
<b>Total Tail Rotor BHP</b>	<b>14.2</b>	<b>11.1</b>	<b>8.4</b>	<b>8.0</b>	<b>8.5</b>	<b>9.7</b>
Accessory BHP	3.0	3.0	3.0	3.0	3.0	3.0
<b>H-13 Total BHP</b>	<b>181.3</b>	<b>149.2</b>	<b>119.3</b>	<b>119.5</b>	<b>141.2</b>	<b>184.3</b>

The preceding numerical example shows what a simple theory, a slide rule, some elbow grease, and paper and pencil could do before the digital computer came along. While these tools were sufficient for development of early, low-speed helicopters, performance parameters that far exceeded the capability of a slide rule accompanied the onset of turbine-powered helicopters. Comprehensive computer codes today account for the forces and moments of the complete helicopter, model the airflow through and about the main and tail rotors and, most importantly, include nonlinear aerodynamics. The next generation of comprehensive codes use computational fluid dynamics (CFD), which can compute the lift, drag, and pitching moment of any rotor blade element. This replaces approximation of average airfoil lift and drag by  $C_d = C_{d_0} + \delta C_l^2$  or more complicated means.

This discussion of single rotor helicopter performance would be incomplete without three comments about the L-19A airplane versus the H-13H helicopter. The first comment is self evident. The equivalent parasite drag area of the H-13H is  $f_e = 15$  square feet versus 7 square feet for the L-19A. Thus, the helicopter's engine horsepower required to overcome just airframe drag is more than twice that of the comparable airplane. The second comment is not so evident. The engine horsepower required to overcome induced drag is, following simple theory, nearly equal between helicopter and airplane if the wing spans are equally loaded. To see this point, first consider the induced drag for an airplane, which is calculated as

$$\begin{aligned}
 \text{Airplane Induced Drag} &= qSC_{Di} = qS \left[ \frac{C_L^2}{\pi AR} \right] (1 + \delta) \\
 (2.210) \qquad \qquad \qquad &= qS \left[ \frac{L^2}{q^2 S^2 \pi (b_w^2 / S)} \right] (1 + \delta) = \frac{1}{\pi q} \left[ \frac{L}{b_w} \right]^2 (1 + \delta)
 \end{aligned}$$

where ( $q$ ) is the dynamic pressure ( $1/2 \rho V^2$ ), ( $L$ ) is airplane weight (in steady, level flight), ( $b_w$ ) is wing span, and ( $\delta$ ) is the correction for nonelliptical bound circulation distribution over the wing span. Even with a wing of poor planform shape (rectangular) and adverse twist, the increase of induced drag above ideal (i.e.,  $\delta = 0$ ) is rarely greater than  $\delta = 0.07$ .

Now for the helicopter rotor induced drag. The induced power ( $P_i$ ) is simply equal to lift ( $L$ ) times induced velocity ( $v_i$ ). Because drag is power divided by velocity ( $V$ ), it follows that

$$(2.211) \quad \text{Helicopter Induced Drag} = k_i \frac{P_i}{V} = k_i L \left( \frac{v_i}{V} \right).$$

Glauert gave the classical approximation for induced velocity as

$$(2.212) \quad v_i = \frac{T_{hp}}{2\rho(\pi R^2) \sqrt{(V_{FP} \sin \alpha_{hp} - v_i)^2 + (V_{FP} \cos \alpha_{hp})^2}}.$$

Suppose now that the hub-plane angle of attack ( $\alpha_{hp}$ ) is virtually zero in steady, level flight and that the flight path velocity ( $V_{FP}$ ) is true airspeed ( $V$ ) in steady, level flight. Assume that the rotor thrust ( $T_{hp}$ ) equals rotor lift. Then it follows that

## 2.4 FORWARD-FLIGHT PERFORMANCE

$$(2.213) \text{ Helicopter Induced Drag} = k_i L \left[ \frac{L}{2\rho(\pi R^2) V \sqrt{v_i^2 + V^2}} \right] = k_i \frac{L^2}{2\rho(\pi R^2) V^2 \sqrt{1 + (v_i/V)^2}}.$$

Because rotor diameter (D) is twice rotor radius (R), and dynamic pressure (q) is  $(1/2 \rho V^2)$ , you have

$$(2.214) \text{ Helicopter Induced Drag} = k_i \frac{1}{\pi q} \left[ \frac{L}{D} \right]^2 \left( \frac{1}{\sqrt{1 + (v_i/V)^2}} \right) \approx k_i \frac{1}{\pi q} \left[ \frac{L}{D} \right]^2 \text{ when } \frac{v_i}{V} \text{ is small.}$$

You can see from Eq. (2.214) that by 32 knots  $(v_i/V)^2$  is about 0.032, so that induced drag for the two lifting devices depends on span loading and dynamic pressure. But note particularly that the correction for a non-ideal span loading ( $k_i$ ) has reached 1.139 by an advance ratio of 0.214, according to Eq. (2.200). This adverse trend deserves a little more discussion (because it is not widely acknowledged), which you will learn later in this volume.

The third comment regarding the H-13H versus the TL-19D is evident by looking very closely at Fig. 2-108 and Fig. 2-112. While the induced power is on the same order, approximately 30 horsepower at 60 knots, profile power is significantly greater for the helicopter, about 60 horsepower at 60 knots. The difference in parasite power at 60 knots (i.e., 36 horsepower for the H-13H with  $f_e = 15$  square feet and 17 horsepower for the L-19A with  $f_e = 7$  square feet) is relatively insignificant. Of course at high speed the story changes.

This leads me to the conclusion that early helicopters suffered from excessive parasite power *and* excessive profile power when compared to propeller-driven airplanes.

### 2.4.3 Twin-Rotor Helicopter

The competition between twin-rotor and single rotor helicopters really heated up in the 1950s. In that decade, Kaman came forward with his H-43B synchropter, Piasecki perfected his H-21 nonoverlapped tandem, and Sikorsky offered the single rotor H-34, a militarized version of his commercial S-58. A great deal can be learned about twin-rotor helicopter performance from a comparison of these three helicopters [299]. But first a little history about each machine.

In 1951, Charles Kaman<sup>71</sup> experimented with two 175-horsepower Boeing 505 industrial gas turbines installed in his Navy HTK, the forerunner of his H-43 synchropter. With U.S. Air Force support, Kaman upgraded his synchropter with the Lycoming T-53-L-1 engine. This turbine-powered helicopter was specially designed as a crash rescue and fire fighter, and was designated as the H-43B. It was found at many airfields. When an Air Force

---

<sup>71</sup> Kaman's early history is well described in the book *Vertical Flight—The Age of the Helicopter* edited by Walter Boyne and Donald Lopez [300]. The forward to this book was written by Joe Mallen, then Chairman of the American Helicopter Society. Joe was my first boss at Vertol when I was placed in the Preliminary Design group after graduating from Rensselaer Polytechnic Institute in June 1956. Joe has remained a mentor and close friend throughout my career.

airplane crashed, the H-43B would scramble and fly to the downed airplane, and the pilot would use the helicopter's downwash to blow the flames away from the airplane. This rescue mission directly parallels the Navy's use of the Piasecki small HUP for plane guard duty alongside aircraft carriers.

Frank Piasecki's H-21 was selected the winner (over the Sikorsky S-58 and other submittals) in a U.S. Air Force competition for an arctic search and rescue helicopter. The H-21B served the Air Force as an assault version, while the H-21C model served the U.S. Army as a troop transport. The H-21 series followed the development of the XHRP-X (the dogship) and the HRP-1, which the U.S. Navy funded. The early nickname was the Flying Banana, and initial operational use was as a troop carrier.

Igor Sikorsky's follow-on to the S-55 was the S-58, which was developed for the commercial market. As the Korean War came to an end, military requirements became clearer, and the Army, Marine Corp, Navy, and Coast Guard all bought militarized S-58 versions basically designated as the H-34.

The Sikorsky H-34A and Piasecki H-21B/C played key roles as the services saw the need for bigger helicopters that could carry at least a fully armed squad of soldiers. Both troop-carrying helicopters and the rescue helicopter, Kaman's H-43B, were thoroughly evaluated by the Air Force at Edwards Air Force Base in California. Of the three, the H-21B had the poorest flying qualities and the H-34A had had the best handling characteristics. The H-43 was evaluated as having "poor directional and lateral controllability during the approach and landing, often resulting in considerable pilot concern."

The engine-horsepower-required variation with true airspeed for these three helicopters (Table 2-18) is illustrated in Fig. 2-113. This flight test data was acquired at 1,000-foot density altitude with each helicopter operating at a disc loading (DL =  $W/A$ ) of

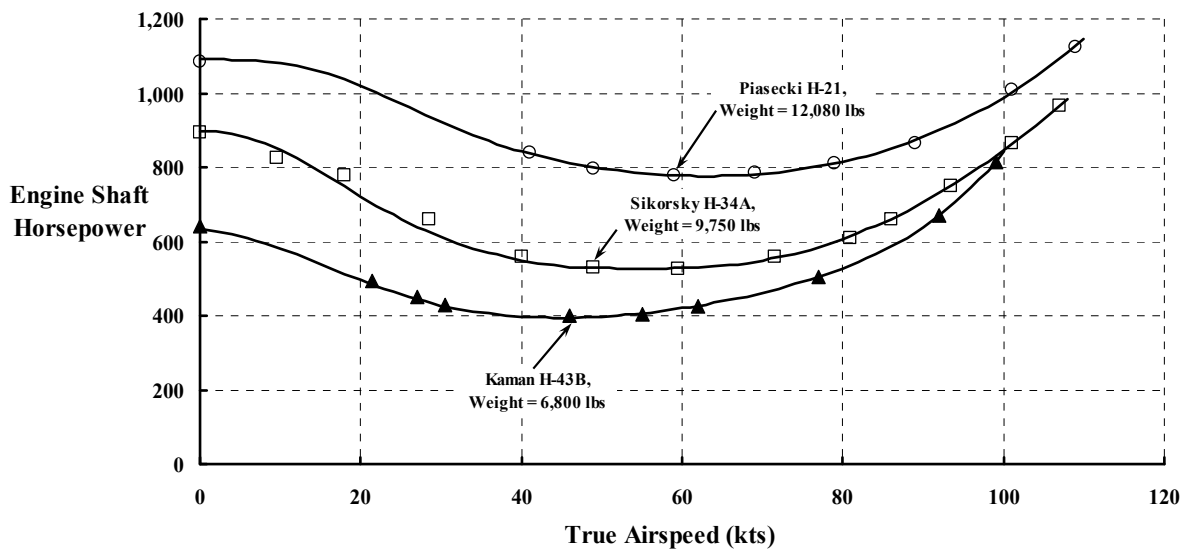


Fig. 2-113. Two twin-rotor helicopters and one single rotor helicopter.

## 2.4 FORWARD-FLIGHT PERFORMANCE

**Table 2-18. The Second Generation of Helicopters**

<b>Basic Aircraft Information</b>	<b>Kaman H-43B</b>	<b>Piasecki H-21B/C</b>	<b>Sikorsky H-34A</b>
<b>References</b>	[193]	[109]	[108]
<b>Power Installed</b>			
Engine Model	Lycoming T-53-L-1B	Wright R-1820-103	Wright R-1820-84
Takeoff Rating at Sea Level (hp)		1,425 at 2,800 rpm	1,425 at 2,800 rpm
Military Rating (30 min) (hp)	860 at 6,680 rpm	1,400 at 2,700 rpm	1,400 at 2,700 rpm
Normal (Continuous) Rating (hp)	680 at 6,320 rpm	1,275 at 2,500 rpm	1,275 at 2,500 rpm
<b>Power Limits</b>			
Transmission (30 min) (hp)	825 at 260 rpm		
<b>Weights</b>			
Empty (full oil, trapped fuel) (lb)	4,444	8,785	7,404
Extra Equipment (lb)	0	442	345
Two Crew (lb at 200 lb/man)	400	400	400
Minimum Operating (lb)	4,844	9,500	8,149
Fuel Full at 6 lb/gal (lb)	1,200	1,740	1,560
Design Gross Weight (lb)	6,044	13,300	11,867
Maximum Takeoff Weight (lb)	8,250	15,100	13,300
<b>Dimensions</b>			
<b>Main Rotor(s)</b>	<b>Two</b>	<b>Two</b>	<b>One</b>
Diameter (ft)	47.0 each rotor	44.0 each rotor	56.0
Disc Area (ft <sup>2</sup> )	1,735 each rotor	1,520 each rotor	2,460
Blade Chord (in.)	15.69	16.5	16.4
Number of Blades	2 each rotor	3 each rotor	4
Solidity	0.071 each rotor	0.06	0.06215
Airfoil	NACA 23012	NACA 0012	NACA 0012
Projected Disc Area (ft <sup>2</sup> )	1,931	3,040	n/a
Distance Between Hubs (ft)	4.1875	41.74	
<b>Tail Rotor</b>	<b>None</b>	<b>None</b>	<b>One</b>
Diameter (in.)			112
Blade Number			4
Blade Chord (in.)			7.0
Solidity			0.1592
Airfoil			NACA 0012
<b>Airframe</b>			
Nose-to-Tail Length (ft)	25.17	52.9	44.17
Height (ft)	12.58	15.90	15.83
Vertical Stabilizer Area (ft <sup>2</sup> )			
Horizontal Stabilizer Area (ft <sup>2</sup> )			
<b>Center of Gravity Limits</b>			
Forward (in.)	3.0 rotor hub	41.0 CL between rotor	6.3 rotor hub
Aft (in.)	2.5 rotor hub	6.5 CL between rotor	10.4 rotor hub

## 2.4 FORWARD-FLIGHT PERFORMANCE

4 pounds per square foot. The H-21B, at a gross weight of 12,080 pounds supported on two, nearly nonoverlapped, 44-foot-diameter rotors, has a disc loading of just under 4.0. Similarly, the H-34A, at 9,750-pounds gross weight supported on one 56-foot-diameter rotor, has a disc loading just under 4.0. And the H-43B, at 6,800 pounds with *nearly* coaxial 47-foot-diameter rotors is hovering at a disc loading of 4.0.

In and of themselves, the power-required trends shown in Fig. 2-113 are not startling. However, when rescaled to engine shaft horsepower per ton of gross weight, a very important facet about twin-rotor performance in level flight jumps right out at you as Fig. 2-114 shows. This figure shows that the tandem rotor H-21 power required does not experience as favorable a decrease with airspeed as its H-34 counterpart. In contrast, the H-43 with *nearly* a coaxial rotor arrangement (perhaps a very overlapped side-by-side rotor system would be more descriptive) behaves at low speed much like the H-34 single rotor.

Fig. 2-114 leads me to the major point about twin-rotor performance in steady, level flight. The point is that the tandem rotor machine has a significant power-required increase due to rotor flow field interference, particularly at low speed. The study of mutual tandem rotor flow interference in forward flight began with Stepniewski's work in the early 1950s, which you will find in the modern literature [238]. His efforts provided initial power-required estimates for all tandem rotor helicopters developed by Piasecki, then Vertol, then Boeing Vertol, and now the Boeing Helicopter Division. *Stepniewski's approach used momentum theory.*

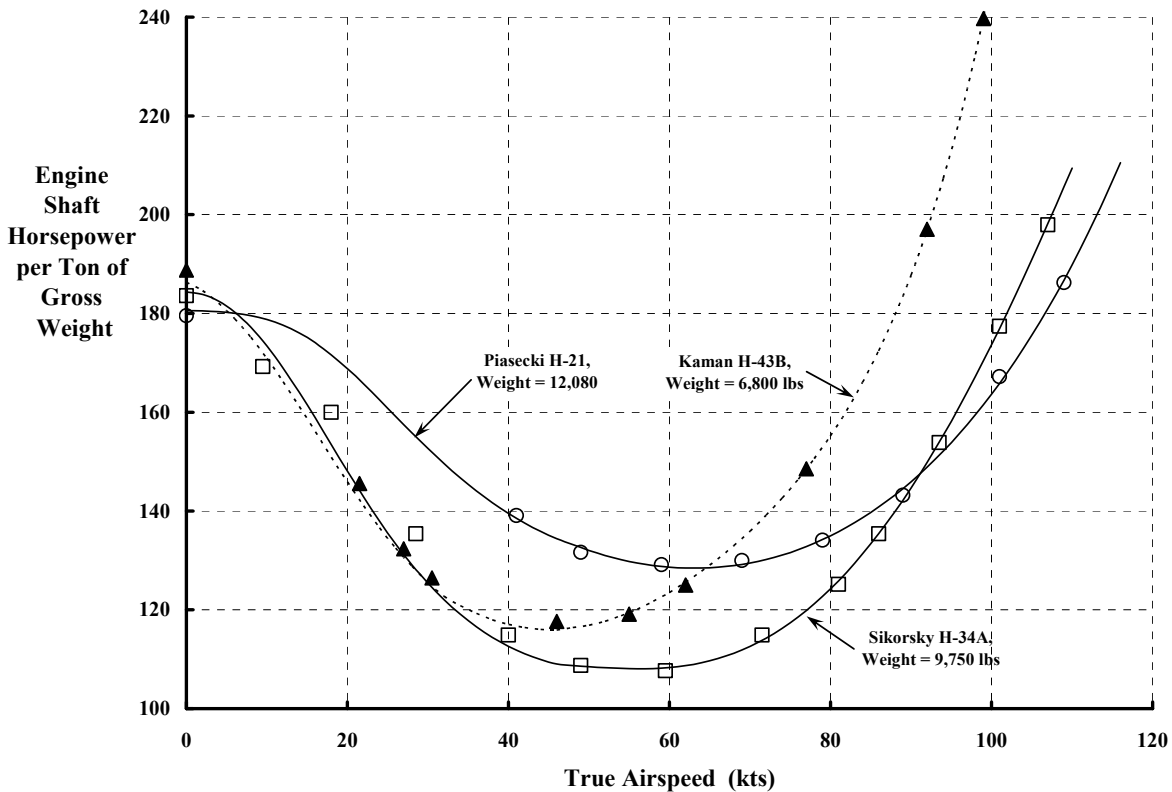


**Fig. 2-114. The nearly nonoverlapped H-21 tandem rotor configuration does not behave as two isolated rotors in forward flight.**

## 2.4 FORWARD-FLIGHT PERFORMANCE

The next evolutionary step beyond momentum theory to calculate induced velocity was made at N.A.C.A. Langley. The analytical approach, begun in 1945 by Coleman, Feingold, and Stempin [301], was accelerated in 1952 by Castles and De Leeuw at Georgia Institute of Technology (funded by the N.A.C.A.) [302] and then was refined in the early 1960s by Harry Heyson.<sup>72</sup> Over his career, Heyson authored some 50 NACA and NASA reports, most dealing with induced velocity through and about single- and twin-rotor systems. In June of 1978, he published a brief survey of rotary wing induced velocity theory [303], which is a must-read report. In this survey Heyson states that “Glauert’s formulation [ref. [304] and Eq. (2.198)] of the induced velocity of a rotor was merely a plausible guess.” And then Heyson turns right around and shows that a simple vortex theory gives Glauert’s formulation.

The “simple vortex theory” that Heyson (and his predecessors) used (Fig. 2-115) replaces the spiral wake trailed from a rotor blade with the mathematically tractable set of vortex rings bounded by a cylindrical wake. With considerable applied mathematical skill, Heyson solved for the velocity flow field and provided the industry with immensely valuable tables and charts of induced velocity. One example, figure 7 from Heyson’s NACA Report 1319 [305], is shown here in Fig. 2-116.

Heyson found that a fundamental variable inherent to his “simple vortex theory” was the wake skew angle, the geometry being illustrated in Fig. 2-117. This fundamental angle, shown as 45 degrees in Fig. 2-117, is calculated simply as

$$(2.215) \quad \tan \chi = \frac{V \cos \alpha_{\text{tip}}}{v - V \sin \alpha_{\text{tip}}}$$

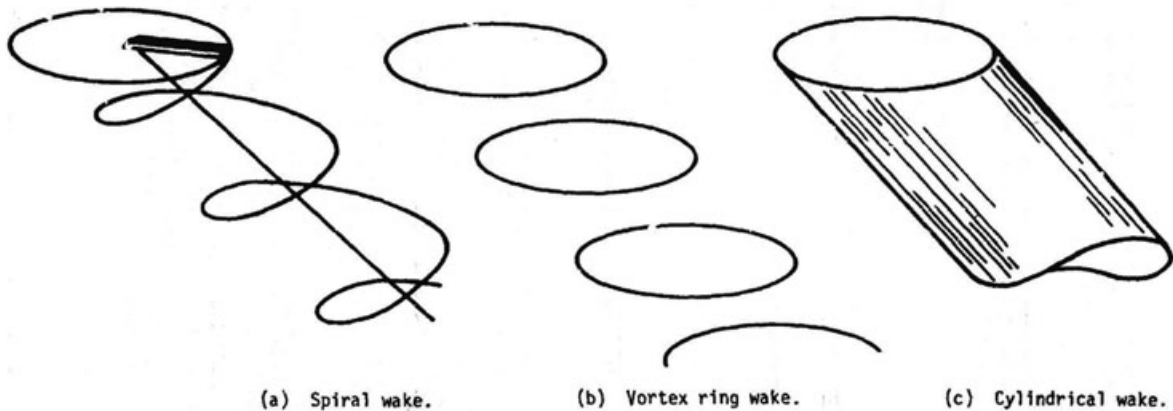


Figure 1. - Assumed wake of rotor.

**Fig. 2-115. Heyson’s approximation of the vortex system created by a rotor blade.**

<sup>72</sup> In my opinion, Harry Heyson, over a two-decade period, single handily carried the rotorcraft industry forward in its efforts to understand and calculate induced velocity. His contributions extended to understanding and calculating wind tunnel wall corrections used in V/STOL testing.

where ( $V$ ) is flight path velocity, ( $\alpha_{\text{tpp}}$ ) is the tip-path-plane angle of attack, and ( $v$ ) is the mean induced velocity as calculated with Glauert's "formulation." (Heyson used the notation of  $v_0$  for the mean induced velocity, whereas I have dropped the subscript.) Note that the wake skew angle, Eq. (2.215), is zero in hover and approaches the cotangent of the tip-path-plane angle of attack at very high speed.

Heyson's work alone carried the industry until the digital computer came along. With that slide rule replacement, Ray Piziali and Frank DuWaldt at Cornell Aero Labs set about modeling a rotor blade and its vortex system with a true parallel to the fixed-wing trailed vortex system [306]. Their vintage 1962 vortex theory was built on visualizing the wake structure shown in Fig. 2-118.

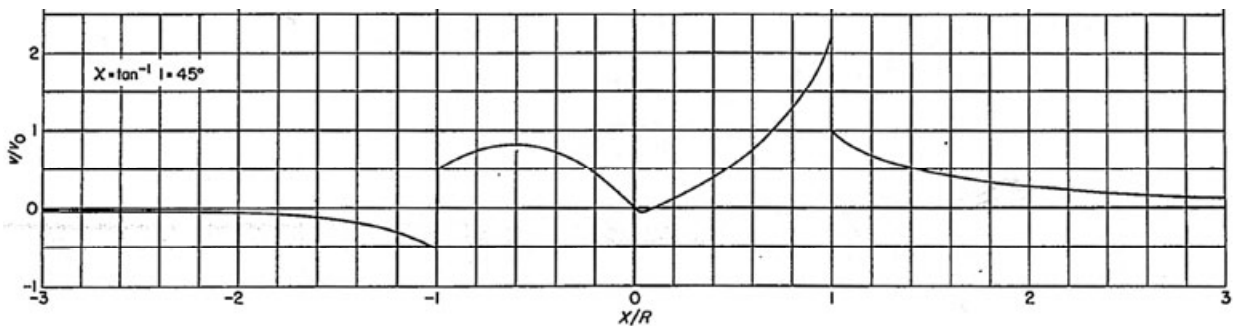


Fig. 2-116. Heyson's induced velocity distribution along the X-axis of a rotor with triangular disc loading [305].

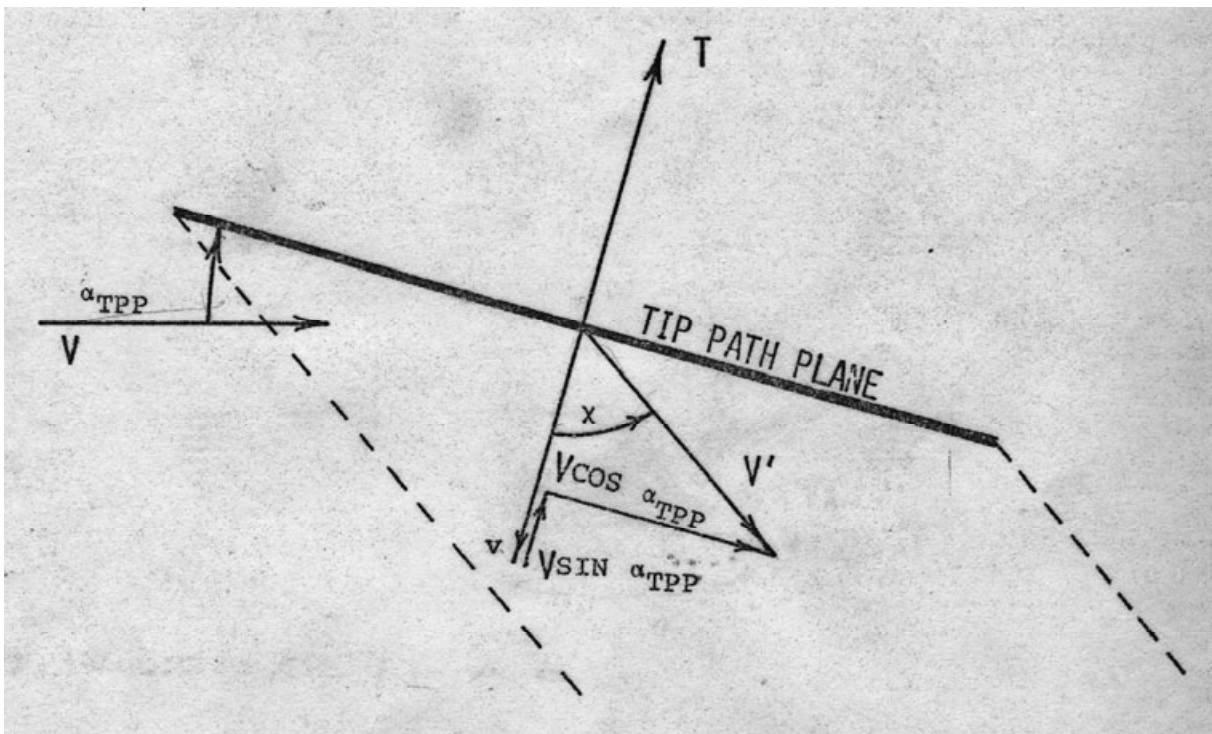
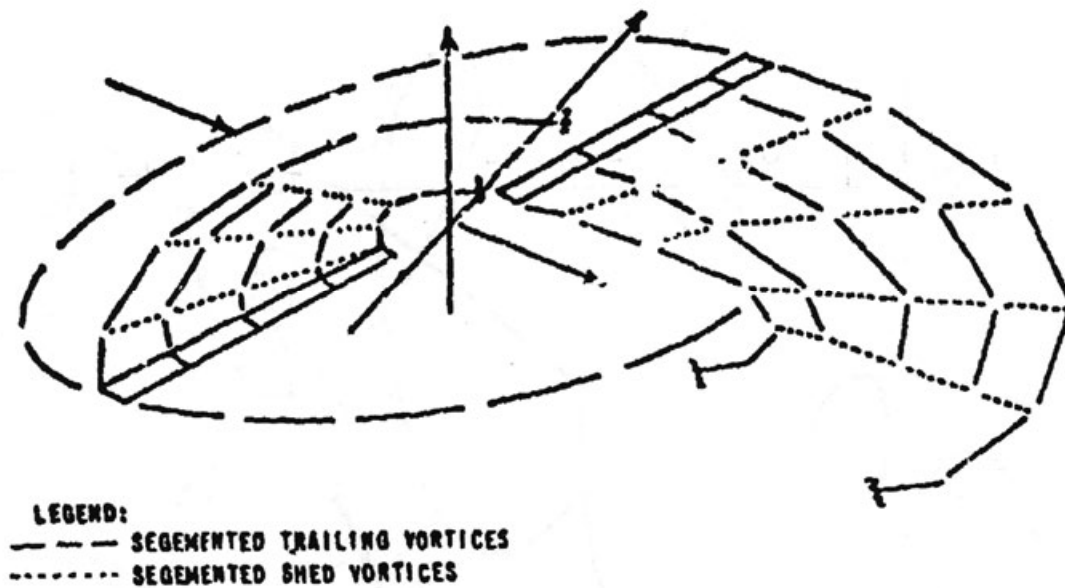


Fig. 2-117. The wake skew angle,  $\chi$ , is a fundamental parameter.

## 2.4 FORWARD-FLIGHT PERFORMANCE



**Fig. 2-118.** Piziali and DuWaldt modeled the vortex system trailed from rotor blades with straight line segments carefully placed in space. This was the beginning of the “prescribed wake model” [306].

The encore to Piziali and DuWaldt’s digital-computer-assisted breakthrough came when Peter Crimi, then at Cornell Labs, freed the wake segments to find their own equilibrium position in space [307]. The results (Fig. 2-119) showed the rotor wake to be highly distorted, so much so that even today computer graphics can barely display the complexity. Crimi’s quantitative comparison of calculated induced velocity distributions to measurements that Heyson obtained [305] were impressive. In short, a foundation for the long-sought capability to predict induced velocity through and about rotor systems became fact by the mid-1960s.

To say that this long-sought technology advancement spread like wildfire would be an exaggeration. Johnson, in Chapter 13 of his invaluable book, *Helicopter Theory* [235], relates a realistic and detailed view of progress. In fact, each decade since the 1960s has seen engineers at universities and in industry make steady refinements. Many of the refinements solved mathematical instabilities, a more complete model for the complete helicopter grew, and now computational fluid dynamics tools are solving the problem. As I write these words, I am convinced that it is only the capacity and speed of the digital computer that are impeding the day-to-day use of a very important design tool for practicing helicopter performance engineers. You will find an excellent review of rotor wakes by Jim McCroskey particularly interesting [308]. A further discussion about calculating induced velocity and rotor-induced power is included in Appendix B.

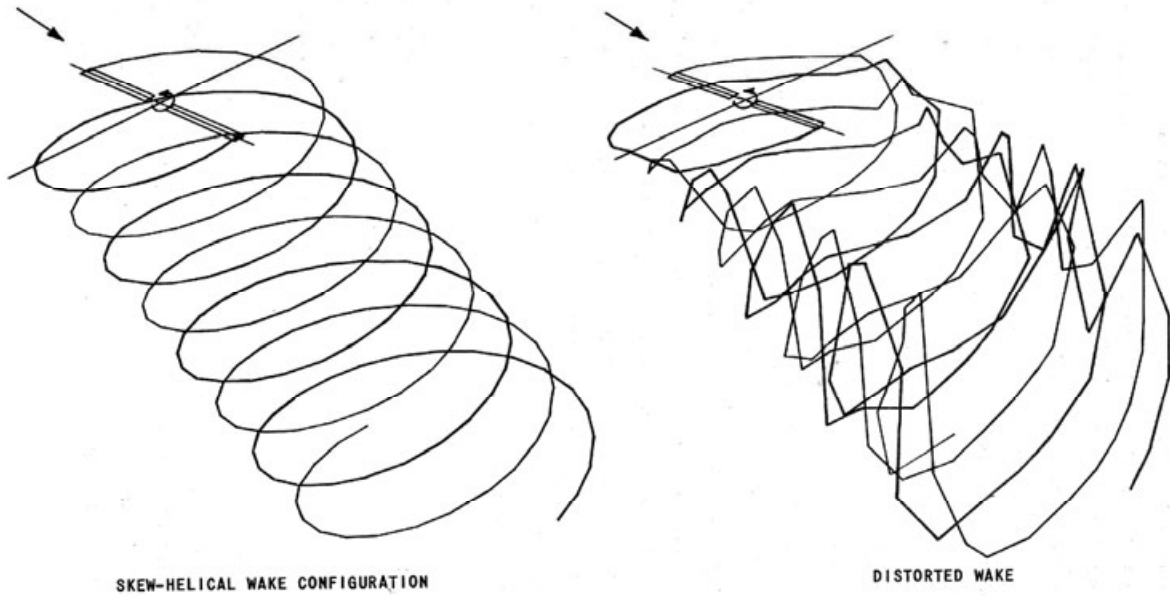


**Fig. 2-119. Crimi removed the skewed helical prescribed-wake constraint and produced the highly distorted, free-wake model in late 1965 [307].**

Now let me return to the specific problem of calculating power required for the H-21 example shown in Fig. 2-113 and Fig. 2-114. At the time that this aircraft was developed, only Stepniewski's semiempirical method [237, 238] was available. For the following discussion, however, I want you to see how valuable Heyson's work was when coupled with simple blade element momentum theory. The tandem-rotor-helicopter power required is written as

$$(2.216) \quad \text{Engine SHP} = \frac{\text{RHP}_{\text{front}}}{\eta_{\text{front}}} + \frac{\text{RHP}_{\text{rear}}}{\eta_{\text{rear}}} + \text{SHP}_{\text{acc}}.$$

To save space, I will use the subscripts (f) and (r) to mean front and rear. The two rotor horsepowers are calculated, with simple theory, as

$$(2.217) \quad \text{RHP}_f = k_i \frac{T_f (v + \Delta v)_f}{550} + \left( \frac{\rho A V_t^3}{550} \right) \left( \frac{\sigma_e}{8} \right) [C_{\text{do}} + \delta C_{1\text{avg.}}]_f [F(\mu)] + \left( \frac{F_X V}{550} \right)_f$$

and

$$(2.218) \quad \text{RHP}_r = k_i \frac{T_r (v + \Delta v)_r}{550} + \left( \frac{\rho A V_t^3}{550} \right) \left( \frac{\sigma_e}{8} \right) [C_{\text{do}} + \delta C_{1\text{avg.}}]_r [F(\mu)] + \left( \frac{F_X V}{550} \right)_r.$$

A detailed trim analysis would show that in steady, level flight the propulsive force ( $F_X$ ) would not, in general, be equal for the two rotors, but the sum of the two propulsive forces would equal the airframe parasite drag. That is,  $F_{Xf} + F_{Xr} = f_{eq}$  following Eq. (2.195) for a single rotor machine. A trim analysis would also show that the rotor thrusts ( $T_f$  and  $T_r$ ) *could* differ significantly, if for no other reason than the wide range in center of gravity allowed by the tandem rotor helicopter. Of course the airframe does introduce, in itself, lift, drag, and

## 2.4 FORWARD-FLIGHT PERFORMANCE

pitching moments that could add differential thrusts to both rotors. To the first approximation, however, the sum of the two thrusts must be the helicopter's weight (i.e.,  $T_f + T_r = W$ ).

Let me assume for this H-21 performance calculation that the two rotors are equally loaded. This means that each rotor carries one-half of the gross weight and each rotor overcomes one-half of the airframe drag. Make the practical assumption that the transmission efficiencies ( $\eta_f$  and  $\eta_r$ ) are the same for both rotors. These simplifications allow the total rotor horsepower to be approximated as

$$(2.219) \quad \text{RHP}_f + \text{RHP}_r = k_i \frac{(W/2)(v + \Delta v)_f}{550} + k_i \frac{(W/2)(v + \Delta v)_r}{550} + 2 \left\{ \left( \frac{\rho A V_t^3}{550} \right) \left( \frac{\sigma_e}{8} \right) [C_{do} + \delta C_{1\text{avg}}] [F(\mu)] \right\} + f \left( \frac{\rho V^2}{2} \right) \frac{V}{550}$$

The profile power of each rotor will be equal, so calculating this power for just one rotor and then multiplying by two will be adequate for this example. Just so there is no misunderstanding, the profile power of one rotor uses the solidity ( $\sigma$ ) of just one rotor, and the average airfoil lift coefficient ( $C_{1\text{avg}}$ ) for this one rotor is

$$(2.220) \quad C_{1\text{avg}} = \left( 6 \frac{C_T}{\sigma} \right) \left( \frac{1 + 3\mu^2/2}{1 - \mu^2 + 9\mu^4/4} \right) \quad \text{and} \quad C_T = \frac{W/2}{\rho(\pi R^2) V_t^2}$$

The tandem-rotor performance problem is now reduced to finding the total induced velocity ( $v + \Delta v$ ) for both the front and the rear rotors as shown in Fig. 2-120. In this regard, I believe that the work of Bob Huston and Harry Heyson in the late 1950s and early 1960s offers a clear and simple method for calculating ( $\Delta v_f$ ) and ( $\Delta v_r$ ), which are the crux of the problem. In my mind, their work superseded Stepniewski's original efforts and predates the many methods that allow the free wakes of both rotors to intermingle in what is seen today as a visual mess—as you can well imagine from Fig. 2-119.

Fig. 2-120 shows a sketch of the H-21 tandem rotor system at a negative tip-path-plane angle of attack that goes with propelling in forward flight. The subscript notation I will use is that ( $\Delta v_r$ ) is the increment of velocity *induced on the rear rotor by the front rotor*, and ( $\Delta v_f$ ) is the increment of velocity *induced on the front rotor by the rear rotor*. Huston found that the interference velocity ( $\Delta v_f$ ) acting on the front rotor due to the rear rotor was an upwash, but relatively small. In contrast, the front rotor induces a very large downwash ( $\Delta v_r$ ) on the rear rotor.

In 1958, Huston [309] tackled the tandem-rotor power required problem drawing heavily on Heyson's induced velocity distribution charts [310].<sup>73</sup> At that time, Huston and Heyson had access to preliminary tandem-rotor wind tunnel test results that Huston finally

---

<sup>73</sup> Bob Huston's work earned him a Master of Science Degree from the University of Kansas. Harry Heyson suggested the thesis topic. Bob went on to N.A.C.A./NASA Langley and remains, in retirement, a strong rotorcraft advocate.

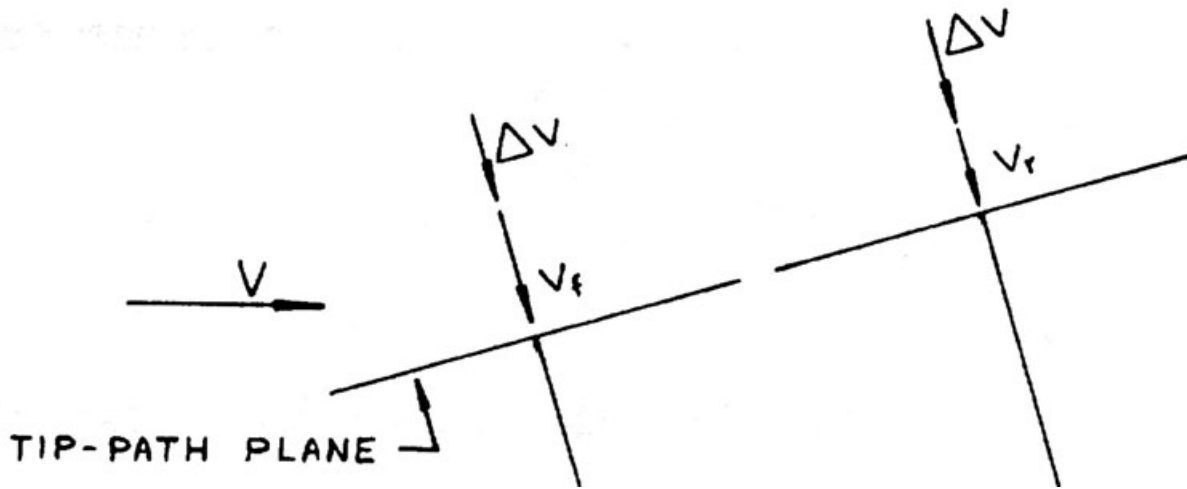


Fig. 2-120. H-21B tandem-rotor induced velocity interference diagram.

published some 5 years later [311].<sup>74</sup> Following Huston's approach, I have used Heyson's charts [305] to obtain the interference velocities (divided by the induced velocity of the rotor that created the interference) as a function of the wake skew angle. These estimates are shown in Fig. 2-121. Each data point shown in Fig. 2-121 was read from enlargement of charts such as the one shown in Fig. 2-116. The distance between the H-21 hubs is 41.875 feet, and the blade radius is 22 feet. This gives, in Heyson's coordinate system,  $x = 41.875/22 = 1.89$ . From Fig. 2-116, for a wake skew angle of 45 degrees, the interference-velocity ratio is about 0.32. The interference-velocity ratio of  $-0.06$  for the rear rotor's interference on the front rotor is read at Heyson's  $x = -1.89$ . A curve fit to the six Heyson chart values [305] gives

$$(2.221) \quad \frac{\Delta v_{\text{rear on front}}}{v_r} = -0.1513 \left( \frac{\chi_r}{90} \right) + 0.0561 \left( \frac{\chi_r}{90} \right)^2$$

$$\frac{\Delta v_{\text{front on rear}}}{v_f} = 0.0165 \left( \frac{\chi_f}{90} \right) + 1.2318 \left( \frac{\chi_f}{90} \right)^2$$

<sup>74</sup> Huston's 1963 wind tunnel test report provides the most fundamental tandem rotor results I am aware of. Individual rotor power data at equal thrust for two different rotor separations are shown. In 1967, Pruyne and a select group conducted a detailed flight test program with the Boeing CH-47 [312, 313]. The test parameters were so comprehensive that five volumes were required to report the results. Nothing comparable to Pruyne's work was attempted until Bousman at NASA Ames Research Center led a dedicated group who, with a heavily instrumented Sikorsky UH-60A, conducted flight tests over a broad range in the flight envelop. This U.S. Army/NASA Airloads Program, with testing conducted in the mid-1990s, provided a monumental data base for a single rotor helicopter. And, because of Bousman's dedication, the test results reside in a computer, which allows nearly instantaneous access to any data channel at any test point.

## 2.4 FORWARD-FLIGHT PERFORMANCE

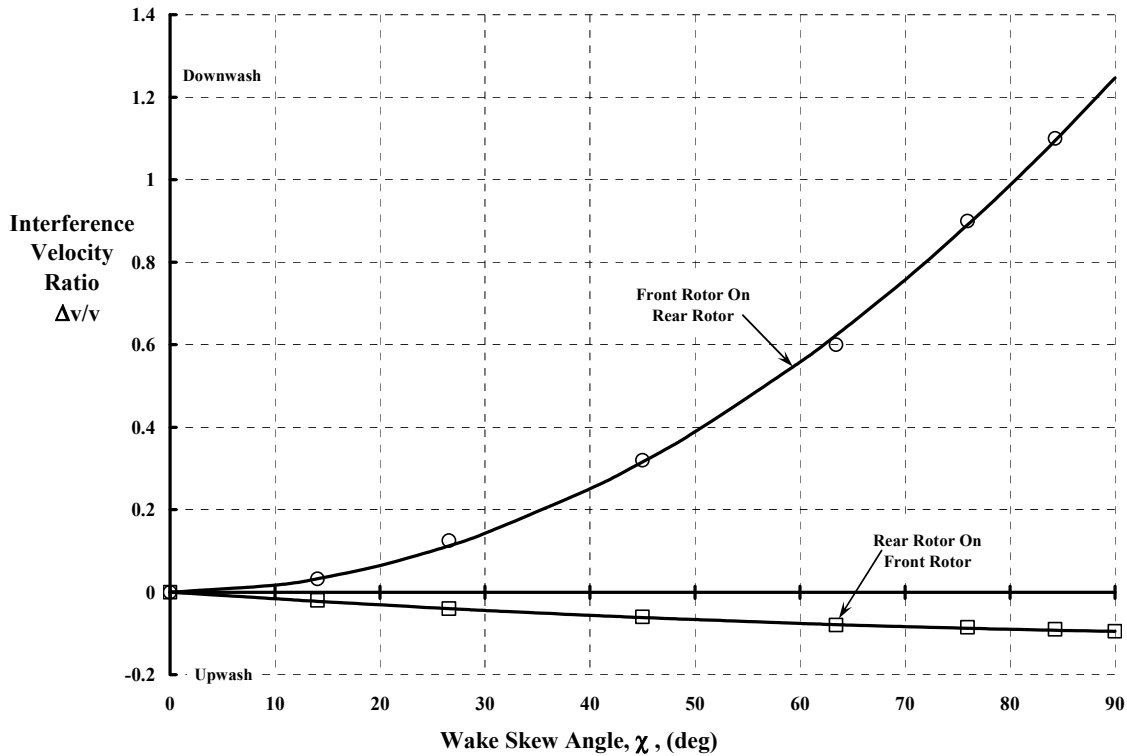


**Fig. 2-121. Heyson's interference velocities for an H-21 with coplanar hubs separated by 1.89 R.**

The immediate next step is to calculate the wake skew angle for both rotors. This angle will not be the same for front and rear rotors because of the very different interference velocities. For the front rotor you have

$$(2.222) \quad \tan \chi_f = \frac{V \cos \alpha_{tpp}}{v_f + \Delta v_{\text{rear on front}} - V \sin \alpha_{tpp}},$$

and for the rear rotor you have

$$(2.223) \quad \tan \chi_r = \frac{V \cos \alpha_{tpp}}{v_r + \Delta v_{\text{front on rear}} - V \sin \alpha_{tpp}}.$$

Note in these two preceding equations that the front-rotor wake skew angle ( $\chi_f$ ) depends on the velocity induced on the front rotor by the rear rotor. The converse is true for the rear rotor. This means that the two equations are dependent on each other, which is dealt with most easily by iteration. For this example of equally loaded H-21 rotors in steady, level flight, the primary induced velocity called for in Eqs. (2.222) and (2.223) is adequately estimated by

$$(2.224) \quad v_f = v_r = v = \frac{W/2}{550} \left[ \sqrt{\frac{V^4}{4} + \left( \frac{W/2}{2\rho\pi R^2} \right)^2} - \frac{V^2}{2} \right]^{\frac{1}{2}},$$

and the forward tilting tip-path-plane angle ( $\alpha_{\text{tip}}$ ) of the equally loaded rotors is approximately

$$(2.225) \alpha_{\text{tip}} \approx -\frac{\text{Propulsive Force}}{\text{Thrust}} = -\left(\frac{1}{2}\rho V^2\right) \frac{f_c}{W}$$

The H-21B power required as measured in flight test [109] and calculated with the 1960's technology just outlined (see Table 2-19 and Table 2-20) are compared in Fig. 2-122. Clearly, the rear rotor has excessive induced power due to the interference velocity of the front rotor. This rotor-rotor interference keeps the H-21 power required from decreasing rapidly from hover, and is a key difference when compared to the H-34 single rotor helicopter.

**Table 2-19. H-21 Inputs to Sample Power-Required Calculation**

Parameter	Main Rotor
Gross Weight	12,080
Density	0.002309
Radius	22.0
Tip Speed	569
Solidity	0.0597
Airfoil C <sub>do</sub>	0.0085
Airfoil $\delta$	0.0085
Transmission Efficiency	0.96
H-21 Flat Plate Area	28

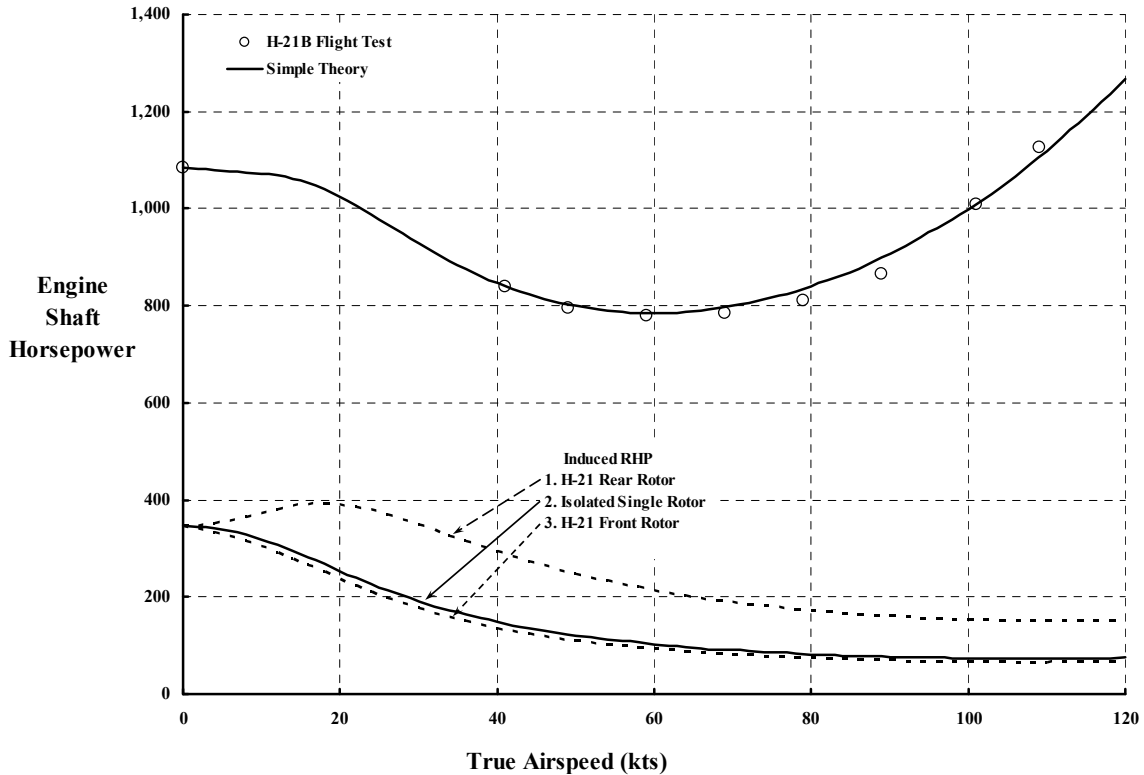


**Fig. 2-122. H-21 performance calculated with 1960's simple theory.**

## 2.4 FORWARD-FLIGHT PERFORMANCE

**Table 2-20. H-21 Sample Power-Required Calculation**

<b>Forward Speed (kts)</b>	<b>0</b>	<b>20</b>	<b>40</b>	<b>60</b>	<b>80</b>	<b>100</b>	<b>120</b>
<b>Either Rotor</b>							
Thrust (lb)	6,040	6,040	6,040	6,040	6,040	6,040	6,040
Propulsive Force (lb)	0	19	76	171	304	475	685
Rotor $k_i$	1.075	1.075	1.081	1.106	1.173	1.319	1.601
Tip Path Plane (deg)	0.00	-0.18	-0.72	-1.62	-2.89	-4.51	-6.49
Induced Velocity (fps)	29.33	21.48	12.51	8.45	6.36	5.09	4.24
Average $C_l$	0.3	0.269	0.28	0.288	0.3	0.325	0.350
Average $C_{do}$	0.00911	0.00912	0.00915	0.00921	0.00929	0.00940	0.00954
F( $\mu$ )	1.000	1.011	1.042	1.095	1.169	1.265	1.381
Rotor Profile RHP	159.8	161.7	167.4	177.0	190.6	208.6	231.2
<b>Front Rotor</b>							
$\Delta v$ on Front Rotor (fps)	0.00	-1.33	-1.04	-0.75	-0.58	-0.46	-0.38
Net Induced Velocity (fps)	29.33	20.14	11.47	7.70	5.78	4.62	3.86
Wake Skew Angle (deg)	0.0	59.1	79.7	84.0	84.7	83.9	82.4
Induced RHP	346.2	237.9	136.2	93.5	74.4	67.0	67.8
<b>Rear Rotor</b>							
$\Delta v$ on Rear Rotor (fps)	0.00	11.63	12.26	9.21	7.03	5.53	4.45
Net Induced Velocity (fps)	29.3	33.1	24.8	17.7	13.4	10.6	8.7
Wake Skew Angle (deg)	0.0	45.5	69.2	78.5	81.5	81.9	81.1
Induced RHP	346.2	391.0	294.1	214.5	172.4	153.8	152.7
<b>Total Helicopter</b>							
Parasite RHP	0.0	2.3	18.7	63.1	149.6	292.2	504.9
Total RHP	1,012	955	784	725	778	930	1,188
Accessory BHP	30	30	30	30	30	30	30
<b>H-21B Total BHP</b>	<b>1,084</b>	<b>1,024</b>	<b>846</b>	<b>785</b>	<b>840</b>	<b>999</b>	<b>1,267</b>

There is an additional facet of the tandem rotor helicopter that Fig. 2-122 shows and that you should know. The rotor-rotor interference mismatches the front and rear rotor horsepowers. Because both rotors operate at the same rotor speed, there is a net difference in rotor torques. The mismatched torques introduce a yawing moment about the helicopter center of gravity. The pilot must counter this yawing moment with a pedal input. On the H-21 tandem helicopter, the pilot's right pedal input puts in lateral cyclic differentially, which causes the front rotor to tilt to starboard and the rear rotor to tilt to port. Thus, the 150-horsepower difference between the front and rear rotors (shown in Fig. 2-122) means that the pilot is dealing with a substantial directional trim problem when speed and power changes are made. Fortunately computer-assisted piloting, added to the CH-46 and CH-47 tandem helicopters that came after the H-21, has significantly lowered pilot workload.

#### 2.4.4 Takeoff Following an Engine Failure

The preceding comparison of the H-34 and H-21 helicopters brings to light a very important fact about power required versus forward speed. This fact is illustrated in Fig. 2-114 and deals with the ability of a hovering twin-engine helicopter to reach steady, level flight following the loss of one engine. When you look closely at Fig. 2-114 you can see that minimum power required in all three examples is greater than one-half of the hover power required. To emphasize the point, suppose that each helicopter was powered by two engines, not one. And suppose each helicopter was hovering at an altitude and gross weight where maximum takeoff power of each engine was required. If an engine goes off-line, the best the pilot can hope for is a partial power glide, hopefully to a reasonable landing site. When safety is the primary concern—particularly in the passenger-carrying commercial world—the solution is, of course, to never take off using maximum power. More precisely, the helicopter should take off at a gross weight some 10 to 15 percent less than the machine's maximum capability. But this may mean a reduced number of passengers, or less fuel, or a decrease in both. Of course there is an alternate. The pilot could simply burn up the remaining engine by exceeding specification fuel flow and operating temperature.

This performance problem is not unique to helicopters. It was a primary concern with passenger-carrying airplane design, particularly between the two world wars. A perfect example occurred during the development of the Donald Douglas DC-1 [314]. On March 31, 1930, a Transcontinental & Western Air Inc. (later TWA) Fokker tri-motor crashed in a field near Bazaar, Kansas. Knut Rockne (the famous football coach at Notre Dame) was one of the eight people killed. The public outcry about commercial aviation safety—and tri-motor-powered airplanes in particular, including the Ford Tri-motor—was far reaching. All of the airlines wanted the new (vintage 1933) Boeing Model 247 powered by twin Pratt & Whitney Wasp piston engines turning fixed-pitch propellers. United Air Lines, Inc., with close business ties to Boeing, moved first and bought up every Model 247 Boeing could produce. TWA's response was to solicit the manufacturing side of the business for an airliner that had better performance than the Boeing Model 247. The TWA specification called for three engines and demanded that the airplane “fully loaded, must make satisfactory takeoffs under good control at any TWA airport on any combination of two engines.” Charles Lindbergh was a stock holder and technical advisor to TWA at that time, and it is frequently said that he championed this requirement. Albuquerque New Mexico (at 5,000 feet and with temperatures above 90° F on a hot summer day) was one of the airports TWA served. Donald Douglas responded to TWA's request with the *twin-engine* DC-1. Douglas bet that (1) the new, high-powered, supercharged engines being developed by both Pratt & Whitney and Wright Aeronautical, along with (2) the evolving NACA cowling, and (3) constant speed (i.e., variable pitch) propellers would satisfy the TWA requirement. On September 4, 1933, the DC-1 took off from Winslow, Arizona, with one engine off, and flew with one engine out to Albuquerque. The next day, the pilot shut down an engine during the takeoff run, continued the takeoff, climbed to 8,000 feet, and returned to Winslow. You know the story after that; Douglas quickly evolved the DC-1 into a few DC-2s, and the DC-3 went into full production. With the DC-3, airlines started making a profit.

## 2.4 FORWARD-FLIGHT PERFORMANCE

Given that short story as background, let me return to multi-engined helicopters and their takeoff performance following an engine failure. The common phrase for this situation is one engine inoperative (OEI).

With the success of the H-34 and H-21 during the Korean War, the U.S. Army and the Marines acquired an apparently insatiable need for more useful load (fuel plus payload) capability. This capability was not achievable with even the most powerful piston engines developed during World War II.<sup>75</sup> The turbine engine was the solution—and not just one turbine engine that powered the small Army scout helicopters, but two large turbine engines. In fact, Sikorsky's latest version of the CH-53, the early 1980's E model, uses three General Electric T-64-GE-416 turbine engines. This engine is rated at 4,380 shaft horsepower for 10 minutes at sea level on a standard day. That is 13,140 installed engine shaft horsepower lifting 69,750 pounds, which is 375 horsepower per ton of gross weight. The world's largest helicopter, the Mil M-26 [95], uses two 11,400-horsepower shaft turbines to lift 123,480 pounds gross weight, which is 370 horsepower per ton. Most recently, Augusta/Westland, a subsidiary of EH Industries, Limited, flew its first production EH 101 in December 1999. The EH 101 has three Rolls Royce Turbomeca RTM 322-01/8 turboshaft engines with a takeoff rating of 2,100 shaft horsepower (but a transmission limited to 5,580 horsepower). The maximum takeoff gross weight is 34,400 pounds giving some 325 horsepower per ton. In direct contrast, Sikorsky's 1942 R-4B, the U.S. Army's first helicopter, barely lifted 2,450 pounds with 190 installed horsepower, which is 155 horsepower per ton of gross weight. The Bell H-13H, a follow-on to the R-4B, used 255 horsepower to lift 2,850 pounds (or nearly 180 horsepower per ton of gross weight) but was still underpowered.

Of course tri-motor-powered helicopters have less trouble meeting a stringent TWA-worded takeoff specification. However, the fundamental OEI performance of twin-engine-powered helicopters has been a thorn in the industry's side. To examine this design and operating issue in more depth, let me continue using the H-34 and H-21 helicopters as an example. Furthermore, I will revert to rotor performance in coefficient form to generalize the situation. That is, power and weight coefficients will be

$$(2.226) \quad \text{Engine } C_p = \frac{550 \text{ BHP}}{\rho A V_t^3} \quad \text{and} \quad C_w = \frac{W}{\rho A V_t^2}.$$

For the H-34 the reference rotor area ( $A$ ) will be  $\pi(28)^2$ , and for the H-21 the area will be  $2\pi(22)^2$  following Table 2-18. The difference between the coefficients in hover and at the speed (I will use advance ratio) for minimum power required is what I want you to see.

Flight test data for the H-34A [108] and the H-21B [109] is the basis for this discussion. In each report, the data acquired at various weights, rotor speeds, and altitudes was reduced to coefficient form. Useable power coefficient versus weight coefficient graphs

---

<sup>75</sup> Two notable exceptions are the Sikorsky S-56 (designated as the CH-37 by the U.S. Army), and the S-60 crane, which evolved into the twin-turbine-powered S-64 (the CH-54 Skycrane) and, in turn, led to the U.S. Marine Corps CH-53 series.

at several advance ratios, as well as hover, are included in each report. It is from the several power/weight coefficient graphs that I created Fig. 2-123.

You can quantify the OEI problem using the H-34 data in Fig. 2-123. Imagine the H-34 as a twin-engine helicopter operating in hover at a power coefficient of  $C_P \times 10^5 = 45$ . Assume that this is the takeoff power rating provided by two engines. According to Fig. 2-123, a gross weight equal to  $C_T \times 10^4 = 51$  could be hovered out of ground effect at this power. Now suppose that one engine failed, and the power available dropped by one-half to  $C_P \times 10^5 = 22.5$ . The pilot, given some altitude, could transition into forward flight to the speed for minimum power required. For the H-34, this would be an advance ratio of  $\mu = 0.14$ . At the reduced power of  $C_P \times 10^5 = 22.5$ , Fig. 2-123 shows that the pilot could maintain level flight at a weight corresponding to  $C_T \times 10^4 = 47.5$ . This means that the pilot *should not* have taken off (i.e., hovered) at a gross weight greater than that corresponding to  $C_T \times 10^4 = 47.5$ . The helicopter would be, in effect, overloaded by about 7.4 percent. That is, the ratio of weight coefficients is  $51/47.5 = 1.074$ . For takeoff, the pilot should, for safety's sake, off-load useful load before takeoff. In a commercial operation, this would mean reducing the number of passengers—a serious revenue loss. Of course if a contingency rating for OEI was provided by the engine manufacturer, say of about 11 percent (i.e.,  $25/22.5 = 1.11$ ) then the pilot could take off at the maximum helicopter capability. The H-34 could continue level flight at an advance ratio of 0.14 at a gross weight corresponding to  $C_T \times 10^4 = 51$  if one engine was qualified to an emergency rating of  $C_P \times 10^5 = 25$ . Of course in twin-engine operation both engines *could* give a  $C_P \times 10^5 = 50$ , but the pilot's operating manual would have to be very

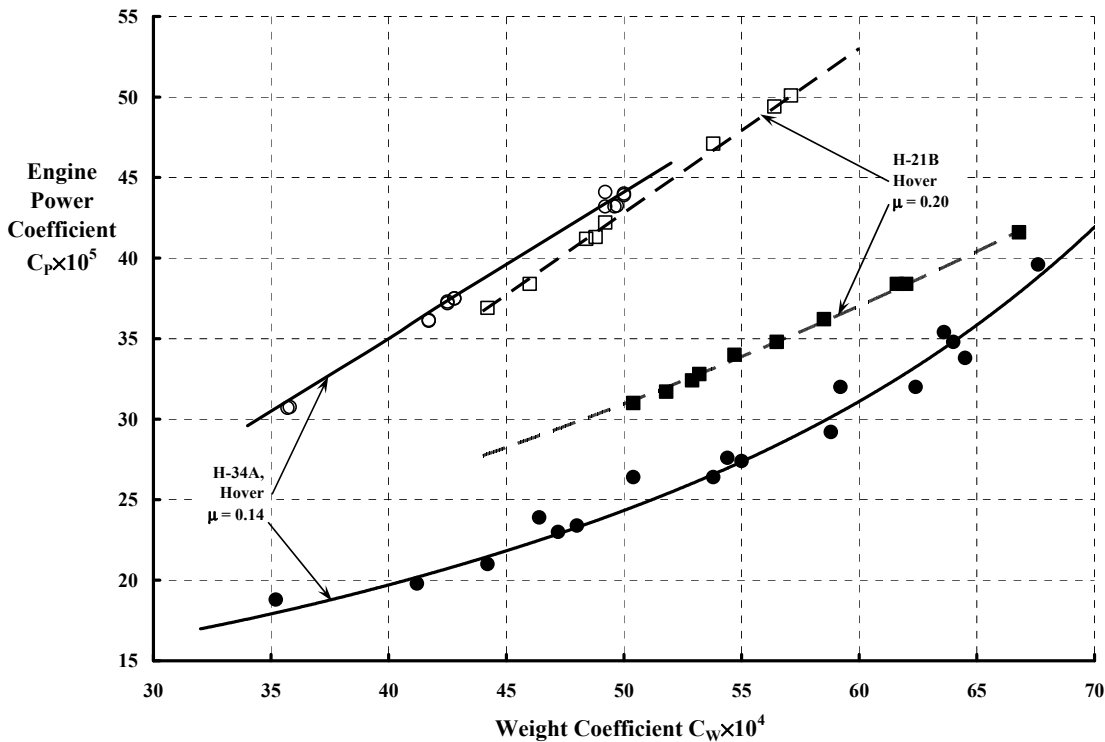


**Fig. 2-123. H-34 and H-21 performance in hover and at speed for minimum power required.**

## 2.4 FORWARD-FLIGHT PERFORMANCE

clear that the pilot had, in effect, taken extraordinary advantage of the emergency power concept. An example of this extraordinary situation comes immediately to mind. The situation I remember is the TV images of the last helicopter lifting off from the U.S. Embassy roof in Saigon at the bitter end of the Vietnam War.

The passenger-carrying commercial business is perhaps the best example of the helicopter's design problem in matching takeoff performance with OEI performance. To understand the performance issue, you need to review the progress that the industry has made in introducing helicopters into the "airline" business. Vertical takeoff and landing (VTOL) rotorcraft champions have never lost the belief that their aircraft can solve traveling congestion problems. Intercity travel could be improved with rooftop heliports. Even growing airport congestion would benefit because short runways, rather than building more 10,000-foot concrete strips, would improve travel immensely. In fact, the rotorcraft industry got the chance to prove its point starting in the early 1950s.

In the early 1950s, the FAA supported certificated helicopter mail and cargo delivery, and passenger-carrying service. Three "airlines" were subsidized by the U.S. Government through the FAA in "Project Hummingbird." They were New York Airways, Chicago Helicopter Airways, and Los Angeles Airways. The FAA considered the adventure an "experiment in the use of helicopters and evolving V/STOL aircraft in commercial transport service" [315]. On April 11, 1965, the FAA-subsidized experiment was over, primarily because no end to government subsidy requirements [316] appeared in sight.

A great deal was learned from the FAA's Project Hummingbird "experiment" however. The economic report published in November 1960 by the Economics Branch of the FAA Office of Plans [315] is an invaluable source for this early history.<sup>76</sup> For example, Table 2-21 shows key dates for the three airlines. Table 2-22 shows many operating parameters including revenue and subsidy growth over the first 7 years as the FAA summarized the combined operations of the three airlines.

**Table 2-21. The First Helicopter Airlines [315, 316]**

<b>Dates</b>	<b>Los Angeles Airways</b>	<b>Chicago Helicopter Airways</b>	<b>New York Airways</b>
<b>Certificated for:</b>			
Mail and Property	October 1947	July 1949	March 1952
Passengers	October 1951	August 1956	March 1952
<b>Service Began for:</b>			
Mail and Property	October 1947	September 1949	October 1952
Passengers	November 1954	November 1956	July 1953
<b>Subsidy Cancelled</b>	April 11, 1965	April 11, 1965	April 11, 1965

<sup>76</sup> The title of this report is *The Helicopter and Other V/STOL Aircraft in Commercial Service*. There is a secondary volume available [317] that was published in April 1961 titled *A Technical Summary and Compilation of Characteristics and Specifications on Steep-Gradient Aircraft*. This aircraft data source was prepared by the FAA Aircraft Branch, Air Commerce Division of the Office of Plans. The snapshot of V/STOL (i.e., steep-gradient aircraft) is as valuable a resource as the economic report.

**Table 2-22. Economic and Operational Progress [315]**

Parameter	1953	1954	1955	1956	1957	1958	1959
Revenue Passengers (000)	1	8	28	63	153	229	366
Revenue Passenger Miles (000)	26	183	628	1,585	3,275	4,885	7,477
Mail Ton Miles (000)	123	115	97	90	92	83	87
Freight and Express Ton Miles (000)	1	16	36	42	40	38	48
Total Revenue Ton Miles (000)	n/a	150	194	282	449	594	857
Revenue Aircraft Miles Flown (000)	1,006	1,071	1,152	1,317	1,603	1,675	1,899
Aircraft Departures (000)	90	90	94	104	126	127	138
Average Flight Stage (miles)	11.2	12.0	12.3	12.7	12.7	13.3	13.7
Passenger Revenues (000)	n/a	n/a	\$208	\$438	\$968	\$1,459	\$2,309
Federal Subsidy (000)	n/a	n/a	\$2,710	\$2,834	\$4,173	\$4,616	\$4,914
Total Operating Revenues (000)	n/a	n/a	\$3,355	\$3,711	\$5,032	\$6,289	\$7,760
Operating Costs Per Available Ton Mile							
Direct	n/a	n/a	\$3.62	\$3.22	\$2.93	\$2.47	\$2.54
Indirect	n/a	n/a	\$3.13	\$3.15	\$1.89	\$1.51	\$1.51
Total	n/a	n/a	\$6.75	\$6.37	\$4.82	\$3.98	\$4.05
Operating Costs Per Revenue Ton Mile							
Direct	n/a	n/a	\$8.16	\$6.55	\$6.99	\$6.22	\$5.20
Indirect	n/a	n/a	\$7.06	\$6.41	\$4.51	\$3.82	\$3.09
Total	n/a	n/a	\$12.22	\$12.96	\$11.50	\$10.04	\$8.29

The 3 helicopter airlines operated 7 Bell Model 47s, 10 Sikorsky S-55s, and 2 Sikorsky S-51s in 1955. At the end of 1959 the fleet had grown to 24 aircraft and included 6 Sikorsky S-58s (H-34s) and 5 Vertol V-44Bs (H-21B). In summarizing the “experiment’s” progress through 1959, the FAA report expressed three important views:

- “1. The helicopter has achieved its greatest success in commercial transport services as a special purpose vehicle transferring fixed-wing air passengers between airports in the Chicago and New York metropolitan areas.
2. Despite the achievement of a sizable growth in passenger traffic and improved operating efficiency, the three helicopter airlines have been unable to reduce their aggregate subsidy requirements with the single-engine, piston-powered helicopters which have been available.
3. The inability of the helicopter airlines to achieve any significant progress toward economic self-sufficiency utilizing their relatively small, high unit cost helicopters has not been entirely unexpected. The Civil Aeronautics Board has indicated several times in certificate renewal and mail rate decisions that no final judgment of the helicopter experiment would be made until larger aircraft become available and had been placed in service.”

The “larger aircraft” that the budding helicopter airline industry wanted were the Sikorsky S-61 (a derivative of the Navy HSS-2, later to become the CH-3) and the Boeing Vertol Model 107 (a derivative of the Army YHC-1A, later to become the Marine CH-46). Basic data for both aircraft are provided in Table 2-23, which you can compare to Table 2-18.

## 2.4 FORWARD-FLIGHT PERFORMANCE

I have included the Sikorsky S-62 in Table 2-23 because this single-turbine-powered helicopter went into service with Los Angeles Airways in late December 1960. The aircraft was so successful that a San Francisco bay area helicopter airline sprang up. The San Francisco & Oakland Helicopter Airlines (SFO) began operating June 1, 1961. *And SFO was not subsidized.* Because of this positive factor, the Civil Aviation Board gave SFO the first permanent operating certificate in November 1963 [316].

The two Sikorsky machines had boat hulls. The S-62 was the first amphibious helicopter; wheels were mounted under the floats for land operations. The S-61, used by New York Airways, had the floats and retractable gear replaced with fixed gear. The Boeing-Vertol Model 107-II had a fixed gear, but was fully qualified for landing and taking off from water. Fig. 2-124 shows both the S-61 with its boat hull and the Model 107 landing at New York's West 30th Street Heliport [316].

The arrival of twin-engine helicopters led to the U.S. Civil Aeronautics Board (CAB) creating the transport helicopter portion (Part 7) of its Civil Air Regulations. Both the S-61 and Model 107 were certificated to the Category A performance requirements (paragraphs 7.110 through 7.118) of the regulation [318]. The applicant in this category was, in 1956, directed to select the weights, altitudes, and temperatures his aircraft would be tested at to show compliance. Both the S-61 and Model 107 were certificated to a takeoff gross weight of 19,000 pounds at sea level on a standard day. At other altitudes and temperatures, the takeoff gross weight was lower as the flight manuals showed. The general takeoff paragraph (7.112) reads as follows:

“The takeoff performance shall be determined and scheduled in such a manner that, in the event of one engine becoming inoperative at any point after the start of takeoff, it shall be possible for the rotorcraft either to return to and stop safely on the takeoff area, or to continue the takeoff, climb out, and attain a rotorcraft configuration and airspeed at which compliance with the climb requirement of paragraph 7.115 (a) (2) is met.”

The takeoff trajectory, as you have just read, was undefined. But the requirement to climb at least 100 feet per minute [paragraph 7.115 (a) (1)] with one engine inoperative was very defined. Furthermore, paragraph 7.115 (a) (2) of the regulation required climb at 150 feet per minute with the critical engine out and the remaining engine(s) operating at maximum continuous power. Thus, a tri-engine helicopter configuration was expected.

When you look at the Boeing-Vertol Model 107 landing at the 30th Street heliport, think about the takeoff. Imagine a vertical takeoff up to, say, 100 to 150 feet. Suppose at this pinnacle, one engine fails. The pilot might choose a near vertical descent right back down to the heliport. Of course controlling and stopping the vertical descent could be a problem. The pilot would have the option to transition into forward flight. He would have his initial altitude plus maybe another 15 to 20 feet, which is the height of that heliport above the water, to make this transition. Given that the pilot could get to the speed for minimum power required and just skim the water, the helicopter would then need to climb at a minimum of 100 feet per

**Table 2-23. The Third Generation of Helicopters**

<b>Basic Aircraft Information</b>	<b>Sikorsky HH-52 (S-62)</b>	<b>Sikorsky CH-3C (S-61)</b>	<b>Boeing Vertol YHC-1A (M 107)</b>
<b>Type Certificate Data Sheet</b>	H8SO [319]	1H15 [320]	1H16 [321]
<b>References</b>	[89, 317]	[206, 317]	[187, 317] & [322]
<b>Power Installed</b>	<b>Single</b>	<b>Twin</b>	<b>Twin</b>
Engine Model	GE T-58-GE-8B	GE CT58-110-1	GE CT58-110-1
OEI (30 sec)		1,350 @ 21,275 rpm	1,350 @ 21,275 rpm
OEI (2-1/2 min)		1,250 @ 21,275 rpm	1,250 @ 21,275 rpm
Takeoff Rating at Sea Level (hp)	730 @ 20,960 rpm	1,250 @ 21,275 rpm	1,250 @ 21,275 rpm
Military Rating (30 min) (hp)			
Normal (Continuous) Rating (hp)	670 @ 20,960 rpm	1,050 @ 21,275 rpm	1,050 @ 21,275 rpm
<b>Power Limits</b>			
Transmission (30 min) (hp)			2,010 @ 270 rpm
<b>Weights</b>		10491	10425
Empty (full oil, trapped fuel) (lb)	5,600	11,228	12,168
Extra Equipment (lb)	345	819	403
Crew (lb at 200 lb/man)	200	400	400
Minimum Operating (lb)	6,145	12,647	13,171
Fuel Full at 6 lb/gal (lb)	1,950	2,460	2,100
Passengers (lb at 200 lb/man)	2,400 (12)	5,600 (28)	5,000 (25)
Category A Takeoff Weight (lb)	n/a	19,000	17,900
Category B Takeoff Weight (lb)	8,300	19,000	19,000
<b>Dimensions</b>			
<b>Main Rotor(s)</b>	<b>One</b>	<b>One</b>	<b>Two</b>
Diameter (ft)	53.0	62.0	48.33 each rotor
Disc Area (ft <sup>2</sup> )	2,206	3,019	1,835 each rotor
Blade Chord (in.)	16.4	18.25	18.0
Number of Blades	3	5	3 each rotor
Solidity	0.06215	0.0777	0.0594
Airfoil	NACA 0012	NACA 0012	NACA 0012
Projected disc area (ft <sup>2</sup> )	n/a	n/a	3,310
Distance Between Hubs (ft)			33.33
<b>Tail Rotor</b>	<b>One</b>	<b>One</b>	<b>None</b>
Diameter (in.)	106	124	
Blade Number	2	5	
Blade Chord (in.)	10.5	7.34	
Solidity	0.1261	0.1401	
Airfoil	NACA 0012	NACA 0012	
<b>Airframe</b>			
Nose-to-Tail Length (ft)	44.17	61.42	44.57
Height (ft)	15.83	16.08	16.83
Vertical Stabilizer Area (ft <sup>2</sup> )			
Horizontal Stabilizer Area (ft <sup>2</sup> )			
<b>Center of Gravity Limits</b>			
Forward (in.)	6.3 rotor hub	6.3 rotor hub	28.0 CL between rotor
Aft (in.)	10.4 rotor hub	10.4 rotor hub	10.0 CL between rotor

## 2.4 FORWARD-FLIGHT PERFORMANCE



**Fig. 2-124.** The helicopter airlines bought twin, turbine-engine-powered helicopters in the early 1960s. The Sikorsky S-61L (top) was type certificated on November 2, 1961 [320]. The Boeing-Vertol Model 107-II (bottom) was type certificated on January 26, 1962 [321].

minute. This criterion is quite interesting. At a takeoff gross weight of 19,000 pounds, additional power available in the amount of

$$(2.227) \text{ Climb Power} = \frac{\text{weight (lbs)} \times \text{rate of climb (ft/sec)}}{550} = \frac{19,000(100 / 60)}{550} = 57 \text{ hp}$$

would be required. The climb trajectory would have to be well planned. Suppose the helicopter had to climb to 500 feet to clear obstacles. That would mean a climb time of 5 minutes (300 seconds) at, say, 60 miles per hour (88 feet per second), which is 26,400 feet—a distance of 5 miles! Locating heliports around water or on long runways with plenty of clear space was certainly attractive in the early 1960s.

Both the S-61 and Model 107 had much better climb performance than the Federal Aviation Agency (FAA) required around 1960 as I will show you shortly.

In 1991, a rather careful study of the airspace required for a one-engine-operative situation was prepared by Systems Control Technology, Inc. for the FAA [323]. This study surveyed performance data from eight helicopters and selected five helicopters<sup>77</sup> for detailed study. The conclusion was that current guidance for heliport design was “inadequate to cover the range of helicopters and conditions that are encountered during rejected takeoff or climb out with one engine inoperative.” The report was critical of the FAA in that its “policy on takeoff and landing requirements for scheduled rotorcraft air carrier operations has been inconsistently applied over the years from 1952 through 1990.”

The FAA (previously the CAB) and the manufacturers worked diligently to improve the regulations. By 2006, the FAA had produced Section 29, which was much more quantitative in its requirements for multi-engine-powered transport category rotorcraft. The most stringent takeoff trajectory is shown in Fig. 2-125. The operational approach is to take off backwards keeping the heliport (the landing surface) in view. The takeoff can be aborted, following one engine failure, all the way up to the takeoff decision point (TDP), which is on the order of 125 feet and well aft of the emergency landing point. With one engine failure at the decision point, a transition into forward flight must allow the helicopter to clear an obstacle some 15 feet above the heliport pad. Hopefully, the pilot can reach a safe takeoff speed ( $V_{\text{TOSS}}$ ) and can climb to 200 feet. At that point in the trajectory, the pilot accelerates to the speed for best rate of climb ( $V_Y$ ), which would be about the speed for minimum power required. Then the objective is to get to an altitude of 1,000 feet above the takeoff point.

The first question that Fig. 2-125 raises deals with the loss in height in reaching 45 knots. Following the discussion about power-off landing starting on page 23, a relatively simple approximation can be made. Suppose at the 125-foot hovering decision point, one engine quits, and suppose the remaining engine (or engines) do nothing more than keep rotor speed at 100 percent. Then the height can be traded for forward speed. Simplistically, the requirement means that

---

<sup>77</sup> The helicopters were the Aerospatiale 355F and 332C, the MBB BO-105 CBS, the Sikorsky S-76A, and the Boeing Vertol 234 LR.

## 2.4 FORWARD-FLIGHT PERFORMANCE

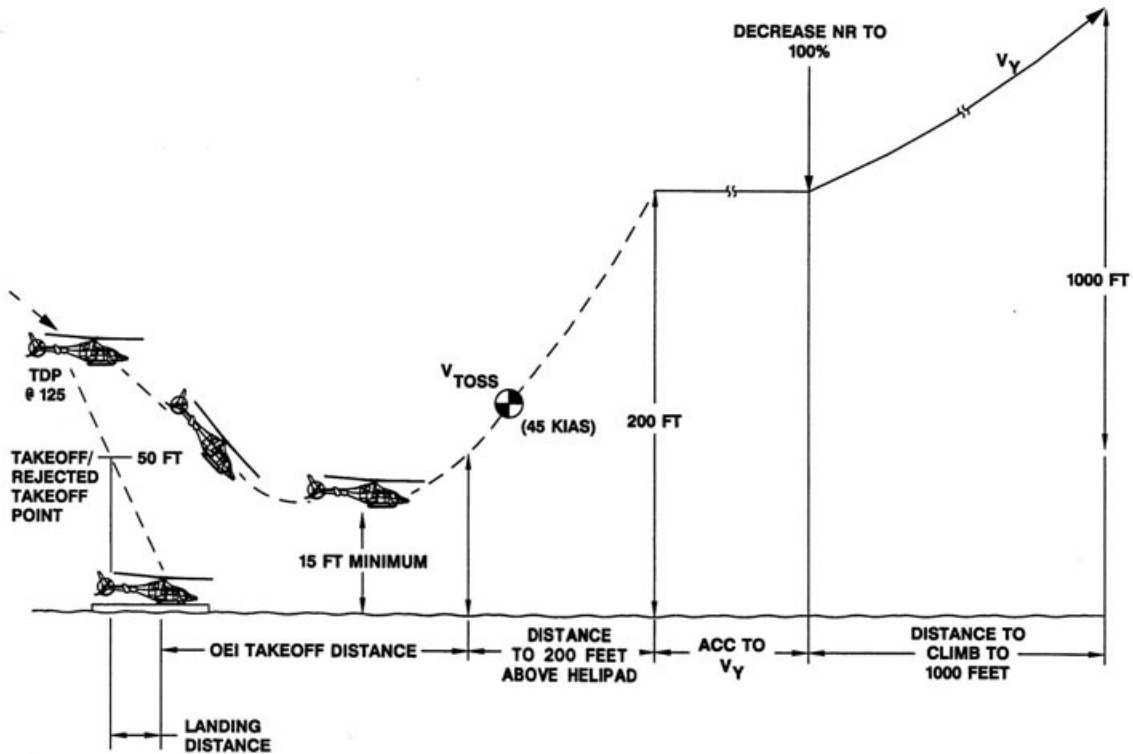


**Fig. 2-125. The takeoff trajectory given a one-engine-out situation at the takeoff decision point (TDP), some 125 feet above the heliport.<sup>78</sup>**

$$(2.228) \quad h_1 - h_2 \geq \frac{2}{g}(V_2^2 - V_1^2)$$

where ( $h_1$ ) is the initial hovering height, 125 feet, and ( $h_2$ ) is the clearance height, 15 feet. The helicopter is initially at zero speed (i.e.,  $V_1$  is 0), but must accelerate to ( $V_2$ ), which is 45 knots or 76 feet per second. The FAA calls my  $V_2$  ( $V_{TOSS}$ ), which stands for takeoff safety speed. The gravity constant ( $g$ ) is 32.2 feet-per-second squared. On this basis, you have

$$(2.229) \quad 125 - 15 = 110 \geq \frac{2}{32.2}(76^2 - 0^2) = 89,$$

which shows that a 125-foot hovering starting point is rational because to reach 45 knots only requires a drop of 89 feet from the 125-foot TDP. Equation (2.229) shows that a 50-foot “takeoff rejection takeoff point” is perhaps a little low because it is only at 89 + 15 feet that the pilot will be able to get to 45 knots. Of course power from the remaining engine (or engines) can do more than keep rotor speed at 100 percent. On the other hand, the pilot must pull out of the dive and then start climbing to reach the 200-foot altitude above the helipad.

<sup>78</sup> This figure is courtesy of Tom Wood, now the Director of Preliminary Design at Bell Helicopter Textron. I left Boeing in mid-1977 and became Chief of Aerodynamics at Bell. Tom immediately became my right hand in managing the group. I know very few engineers with his outstanding grasp of fundamental helicopter technology and his knowledge of what it takes to develop and certificate a rotorcraft.

## 2.4 FORWARD-FLIGHT PERFORMANCE

The distances to be determined in Fig. 2-125 are not too difficult to estimate. The helicopter could return to the landing pad from the 125-foot TDP along, say, a 45-degree slope. That would mean that the TDP is 125 feet aft of the landing pad, should one engine quit. The pilot, by putting the nose down quickly, might get a horizontal acceleration of 0.15 g or about 4.8 feet-per-second squared. That acceleration would get him to 45 knots in about 16 seconds (i.e.,  $V = at$ ) and requires a distance of 600 feet (i.e.,  $S = \frac{1}{2} at^2$ ) from the TDP. Therefore, the OEI takeoff distance would be  $600 - 125 = 475$  feet. At that distance from the landing pad, the pilot must climb at 100 feet per minute until reaching the 200-foot altitude, which means roughly 2 minutes at 45 knots (76 feet per second or greater) or about 9,100 feet (1-3/4 miles). At the 200-foot altitude, the pilot accelerates to the speed for minimum power required ( $V_Y$ ), say on the order of 75 knots, which would take 10 seconds and a distance of some 200 feet if the horizontal acceleration is again 4.8 feet-per-second squared. The climb to 1,000-foot altitude from 200 feet, at a minimum of 150 feet per minute, would take a little over 5 minutes. And at 75 knots, the aircraft would travel another 7-1/2 miles.

The preceding airspace that this *19,000-pound* helicopter would need, therefore, breaks down as shown in Table 2-24.

Clearly, it takes about 2 to 2-1/2 minutes and some 9,000 feet to gather up a helicopter that just meets the minimum FAA requirements. This is really not, in my opinion, a vertical takeoff and landing aircraft comparable to the DC-1 that TWA paid for in the mid-1930s.

This example illuminates a need for considerably improved one-engine-out performance of a twin-engine helicopter safely taking off with a full passenger and fuel load. Fortunately, this need was slowly filled by the engine manufacturers. They qualified their new engines with power ratings above the takeoff rating. The Sikorsky S-61 was certificated to the then CAB one-engine-out requirement using a 30-second engine output rating of 1,350 horsepower versus the twin-engine takeoff rating of 1,250 horsepower per engine as Table 2-23 shows. While only 100 more horsepower, this power increment is significant—on the order of 175-feet-per-minute rate of climb following Eq. (2.227). Consider, for example, the S-61 and Model 107 II power required versus true airspeed shown in Fig. 2-126. (In lieu of actual flight test data for the commercial versions of the two helicopters, I used interpolated flight test data for the CH-3C [206] and the YHC-1A [187] to construct Fig. 2-126. The data is, I believe, quite representative for this example.)

**Table 2-24. Airspace Needed by 1960's Helicopters to Meet Minimum CAB (FAA) One-Engine-Out Takeoff Operation**

Flight Phase	Distance (ft)	Altitude (ft)	Airspeed (knots)	Time (sec)
At TPD	125 aft	125	0	0
OEI Takeoff Distance (ft)	475	15	45	16
Climb to 200 feet	9,100	200	45	120
Accelerate to 75 knots	200	200	75	10
Climb to 1,000 feet	39,600	1,000	75	300
Total Airspace	49,500 (9.4 miles)	125 to 1,000	0 to 75 knots	446 (7.5 min)

## 2.4 FORWARD-FLIGHT PERFORMANCE

Fig. 2-126 shows that both helicopters could hover at the TDP at sea level on a standard day at their certificated takeoff gross weight of 19,000 pounds within engine and transmission limits. With one engine failure at the TDP, the pilot would drop collective, move the cyclic pitch stick forward, and begin a controlled free fall using the loss in altitude to gain forward speed. To pull out, say, at about 30 knots, the pilot would pull in collective pitch and bring the operating engine up to its 30-second temperature limit, which provides 1,350 horsepower. This would clear the 15-foot height above the heliport required by the FAA and get the helicopter to 45 knots (or faster). Clearly, the S-61 could maintain steady, level flight at 45 knots and would be able to accelerate to the minimum power-required speed, say 70 knots. At 70 knots, the S-61 would have about 220 horsepower (for 30 seconds) in excess of the 1,130 horsepower required to maintain steady, level flight at 70 knots. This translates into 385-feet-per-minute rate of climb, so the 200-foot-altitude requirement would be reached in about 30 seconds (i.e., 200 – 15 feet at 385 feet per minute is about one-half of a minute). Flying at 70 knots for 30 seconds, the S-61 would cover about 3,500 feet or about two-thirds of a mile. This is considerably less airspace than the 9,100 feet suggested in Table 2-24.

Getting from an engine failure at the TDP to 200-foot altitude and 70 knots would mean that the operating engine had given its all at the 1,350-horsepower OEI rating. The prudent pilot would reduce power to 1,250 horsepower and begin his climb from 200- to 1,000-foot altitude. This would reduce the excess power to 120 horsepower (i.e., 1,250 – 1,130) and the rate of climb would drop from 385 to 210 feet per minute. Therefore, the 1,000-foot altitude would be reached in about 3.8 minutes, and the S-61 would cover 27,000 feet or about 5 miles.

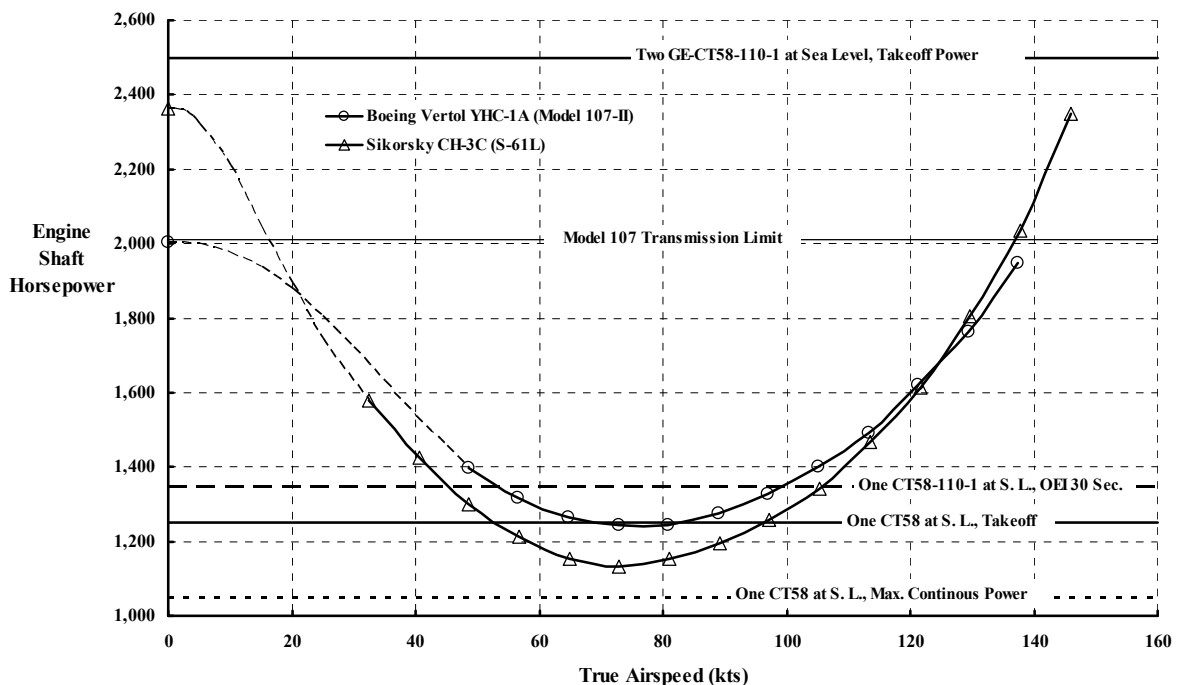


**Fig. 2-126. Engine power required and available at sea level on a standard day for the 25- to 29-passenger helicopters certificated for passenger service in early 1960.**

The preceding discussion justifies Systems Control Technology's concern [323] that the FAA had a mismatch between helicopter OEI performance and heliport designs, even in the early 1990s.

The Boeing Vertol Model 107 power required versus airspeed data shown in Fig. 2-126 raises two interesting questions. To begin with, the Model 107 tandem rotor helicopter hovers at 19,000 pounds using only 2,000 engine shaft horsepower. The S-61, at the same takeoff gross weight, requires 2,360 horsepower. The primary reason for this difference is, of course, the difference in disc area between the two machines, which accounts for about 10 percent of the difference. The S-61's tail rotor adds to the difference. The other question is even more interesting: If a profitable operating airplane, say the DC-3, could take off from TWA's Albuquerque airport on one engine, why shouldn't the modern helicopter do the same? To meet this criteria, the Model 107, with 25 passengers and full fuel tanks, would need two engines rated at 2,000 horsepower for takeoff at sea level on a standard day.

Just to see the value of a design that can hover on one engine, consider the Model 107 at the takeoff decision point. Both engines would be loafing at 50 percent of takeoff power. The loss of one engine would force the remaining engine to quite quickly pick up the slack. The helicopter would lose some altitude and rotor speed because of pilot and engine reaction time, but the pilot could confidently descend back to the heliport. Or, if warranted, he could continue with a relatively normal takeoff. A simplistic analysis of this relatively normal takeoff is rather easy to construct using the energy method of Eq. (1.31), repeated here for convenience (with a positive sign convention associated with climb, not descent) as

$$(2.230) \quad \int_0^{t=t_f} 550 \text{ HP } dt = \int_{h_1}^{h_2} W \, dh + \int_{V_1}^{V_2} W/g \, V \, dV + \int_{\Omega_1}^{\Omega_2} I_R \, \Omega \, d\Omega$$

$$= W(h_2 - h_1) + W/g \frac{1}{2}(V_2^2 - V_1^2) + I_R \frac{1}{2}(\Omega_2^2 - \Omega_1^2)$$

Suppose, following the loss of one engine, that the pilot pushes forward on the cyclic and quickly develops a horizontal acceleration, then forward speed, and then climbs. The helicopter would reach 70 knots in some final time ( $t_f$ ) in seconds. Now tackle the integral of power that Eq. (2.230) requires. To keep it simple, let the excess power available increase linearly with airspeed. That is, assume at time zero, when hovering, that there would be zero excess power available. However, at 70 knots there would be 750 excess horsepower available, which is the difference between minimum power required and 2,000 horsepower available from the operating engine. Therefore, horsepower (HP) would vary with true airspeed ( $V$ ) as

$$(2.231) \quad \text{HP} = KV = \left( \frac{750 \text{ hp}}{70 \text{ knots}} \right) \left( \frac{V \text{ fps}}{1.69} \right) = 6.34(V \text{ fps}).$$

The velocity ( $V$ ) in feet per second is obtained by assuming some average acceleration ( $a_{\text{avg}}$ ) in feet-per-second squared times time. That is,  $V = a_{\text{avg}} \cdot t$ . Therefore, the variation of horsepower with time is simply

## 2.4 FORWARD-FLIGHT PERFORMANCE

$$(2.232) \quad \text{HP} = \text{KV} = \left( \frac{750 \text{ hp}}{70 \text{ knots}} \right) \left( \frac{\text{V fps}}{1.69} \right) = 6.34 (a_{\text{avg.}} t).$$

It follows that the horsepower integral, which is total energy, is on the order of

$$(2.233) \quad \int_0^{t_f} 550 \text{ HP} dt = \int_0^{t_f} 550 (6.34 a_{\text{avg.}} t) dt \quad \text{in foot-pounds of energy}$$

$$= (550)(6.34) \left( \frac{a_{\text{avg.}}}{2} \right) t_f^2$$

$$= (550)(6.34) S_f$$

Remember that  $V = a_{\text{avg.}} t$  so from simple calculus, horizontal distance traveled ( $S$ ) equals  $\frac{1}{2} a_{\text{avg.}} t^2$ . Then, the energy solution for takeoff is simply

$$(2.234) \quad (550)(6.34)S_f = W(h_2 - h_1) + (W/g)\left(\frac{1}{2}\right)(V_2^2 - V_1^2) + I_R \frac{1}{2}(\Omega_2^2 - \Omega_1^2).$$

Now, assume a takeoff gross weight ( $W$ ) of 19,000 pounds, an initial height ( $h_1$ ) of 100 feet, a final height ( $h_2$ ) of 1,000 feet, an initial speed ( $V_1$ ) of zero, and a final speed ( $V_2$ ) of 70 knots or 118 feet per second. Furthermore, assume no change in rotor speed (i.e.,  $\Omega_2 = \Omega_1$ ). The gravitational constant ( $g$ ) is 32.2 feet-per-second squared. You, therefore, have

$$(2.235) \quad S_f = \frac{19,000(1,000 - 100) + \frac{19,000}{64.4}(118^2 - 0^2)}{(550)(6.34)} = 6,082 \text{ feet} \approx 1.15 \text{ mile}.$$

This ability to hover with one engine out at the takeoff decision point (TDP) means that airspace around a heliport must consider the height of objects, man-made or natural, within a 1-mile radius of the heliport and less than 1,000 feet tall. This is a considerable reduction from the 9.4-mile radius arrived at in Table 2-24. (The horizontal distance to reach 45 knots and 200-foot altitude, using Eq. (2.234), is just a little over 1,000 feet.)

Now think about the average acceleration and time associated with the 6,082 feet of distance traveled and the final speed reached of 70 knots. Because velocity and distance are related to average acceleration and final time as

$$(2.236) \quad S_f = \frac{1}{2} a_{\text{avg.}} t_f^2 \quad \text{and} \quad V_2 = a_{\text{avg.}} t_f,$$

it follows that

$$(2.237) \quad a_{\text{avg.}} = \frac{1}{2S_f}(V_2)^2 = \frac{1}{2(6,082)}(1.69 \times 70)^2 = 1.15 \text{ ft/sec}^2 = 0.036g,$$

which is a relatively comfortable acceleration. The 1,000-foot/70-knot point would be reached in 103 seconds. The pilot would hardly have enough time to compose a simple explanation to the passengers for returning to the heliport! In fact, considering the very short distances that the three early helicopter airlines were flying (less than 30 miles), the pilot could elect to continue flying the scheduled route.

Before leaving the discussion of the Boeing Vertol Model 107-II, you should know that this helicopter, which began as the YHC-1A, became the CH-46 series for the U.S. Marines. The Marines funded continual upgrades leading to the E model [188]. The helicopter has been stretched to 45 feet, 8 inches. The rotor diameter is now 25.5 feet. Most importantly, the transmission has been updated to 2,800 horsepower, and the General Electric engines are now T-58-GE-16s with a takeoff rating of 1,870 shaft horsepower each. At 19,000 pounds, the helicopter can nearly hover at sea level on one engine. If the helicopter airlines had had the CH-46E helicopter as a commercial version 30 years ago, they and the FAA might have seen the need for subsidy disappear. Furthermore, the airspace needed for heliports would have been reduced dramatically.

There is no question that the industry sees the performance benefit of twin-engine helicopters with engines that can provide a one-engine-inoperative (OEI) rating well above the twin-engine takeoff rating. Perfect evidence of this fact was reported by Cole [324].<sup>79</sup> The technical discussion in Cole's paper is well worth your time to read and understand.

There is much more to be learned about helicopters in the commercial world as you will read in the purchase price, operating costs, and accident record chapters of this volume.

#### 2.4.5 Closing Remarks

Without doubt, the calculation of induced power of a rotor in steady forward flight has been a thorn in the side of rotorcraft engineers for decades. Glauert started the industry off with his well-known approximation so that the industry relied on

$$(2.238) \text{ Induced RHP}_{\text{mr}} = \frac{Wv_i}{550} = k_i \frac{W}{550} \left[ \sqrt{\frac{V^4}{4} + \left( \frac{W}{2\rho\pi R^2} \right)^2} - \frac{V^2}{2} \right]^{\frac{1}{2}}.$$

The inclusion of an induced power correction factor ( $k_i$ ) is the rotorcraft equivalent of the Oswald efficiency factor for airplanes. A useful, but crude, approximation [211] developed after free-wake calculation could routinely be made is

$$(2.239) \quad k_i = 1.075 \cosh(7.5\mu^2).$$

The question many of us have asked [325-327] for a long time has been, "Given that an elliptical lift distribution gives the minimum induced drag for a fixed wing (as Prandtl and Glauert found), what is the answer for a rotary wing?" We got the answer at the 2010 AHS Forum held in Phoenix, Arizona. Kenneth and Steven Hall [328] gave us the answer with one figure—Fig. 2-127. This figure says that if we could build it, our best articulated rotor would (at the high advance ratios typical of today's helicopters) be anywhere between 3 and 10 times

---

<sup>79</sup> Jeffrey Cole first presented his paper at the American Helicopter Society 53rd Annual Forum held at Virginia Beach, Virginia, from April 29 through May 1, 1997. His paper was finally accepted for publishing in the AHS Journal in October of 2000. The final paper was published in the April 2001 issue of the AHS Journal. To me, this is rather slow publishing—for whatever reason—of such a good paper dealing with such an important aspect of the industry's business.

## 2.4 FORWARD-FLIGHT PERFORMANCE

worse than a fixed wing having a span equal to the rotor diameter. And furthermore, more blades than two are better. I am very glad this answer came in time to be included in this volume.

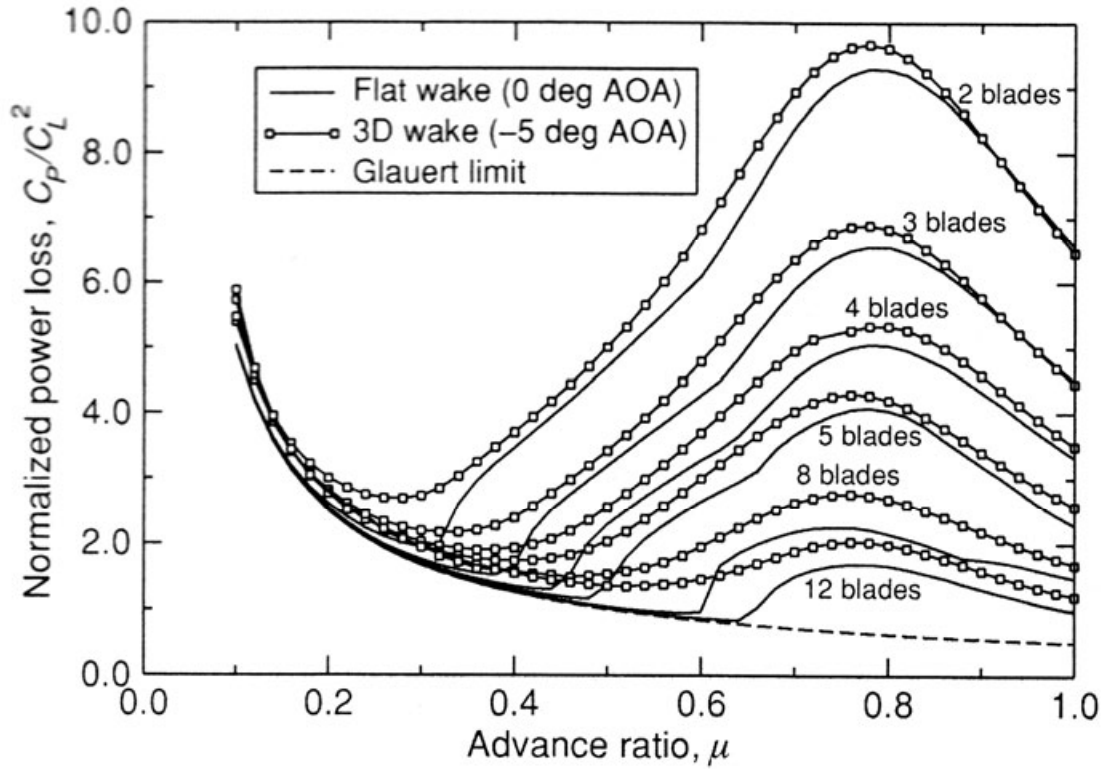
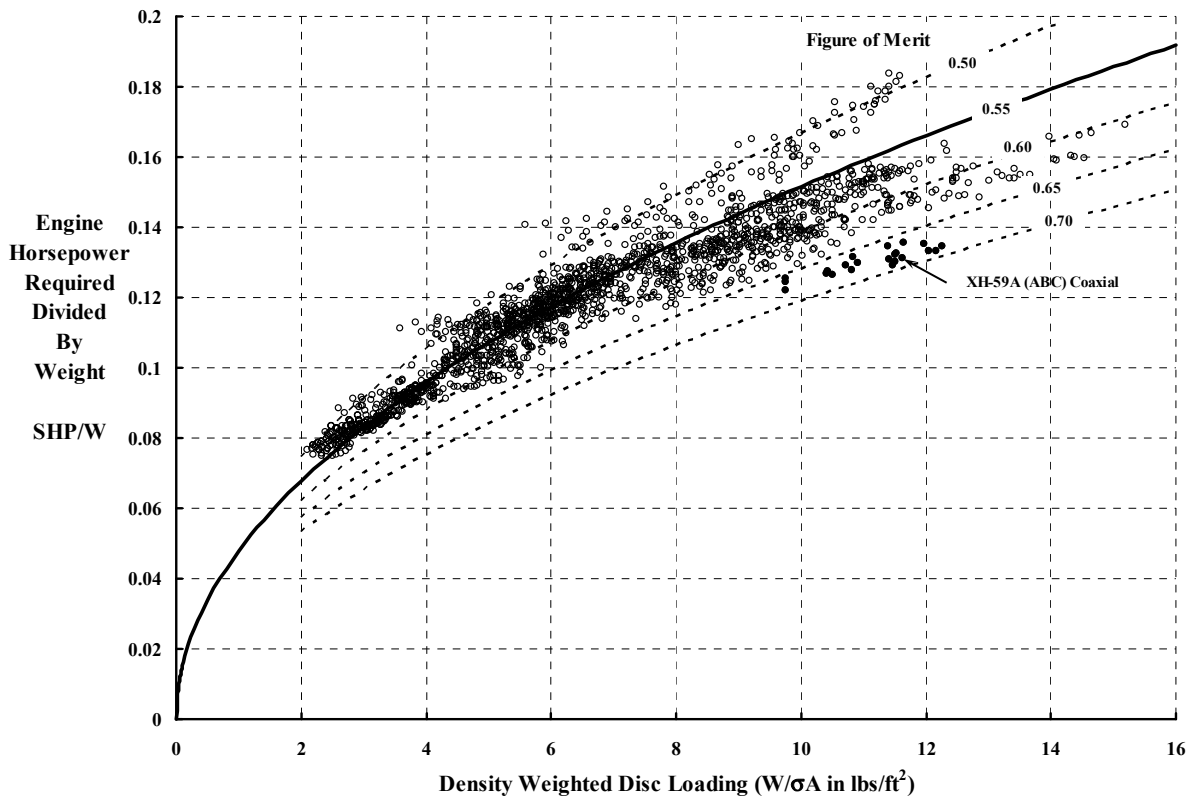


Fig. 2-127. Normalized induced power of the ideal articulated rotor [328]

## 2.5 FUEL EFFICIENCY

Aircraft of all types obtain energy from burning fuel to create lift and propulsion, and perform. Of all the aircraft, the helicopter is the most fuel efficient hovering machine man has yet invented. It achieves this hovering fuel efficiency by obtaining lift and propulsion with the least amount of energy imparted to the air. In forward flight, on the other hand, the helicopter is one of the most, if not *the* most, fuel *inefficient* aircraft flying. Consider fuel efficiency in hover first and then fuel inefficiency in forward flight second.

A measure of fuel efficiency in hover is endurance, which is measured in hours. The hours a helicopter can hover depends on the helicopter's engine shaft horsepower required to hover, the engine's specific fuel consumption (SFC) in pounds of fuel burned per hour per horsepower, and the amount of fuel that the fuel tanks hold. Consider this simple approach to estimating endurance. The power required per pound of weight to hover (SHP/W), as Fig. 2-128 shows, depends—to a reasonable approximation—on Figure of Merit (FM), disc loading (weight divided by rotor disc area), and the density altitude at which the helicopter is hovering. Fig. 2-128 was created from data provided by references [108, 109, 115, 116, 118, 121, 124, 125, 133, 170-188, 190-206] and [207-210].



**Fig. 2-128. Engine hover power required per pound of gross weight vs. density-weighted disc loading for 50-plus helicopters. A Figure of Merit of 0.55 is typical.**

## 2.5 FUEL EFFICIENCY

You will recall from Eq. (2.45) that FM is simply the ratio of ideal power to actual power, from which it follows that

$$(2.240) \quad \text{Actual SHP} = \frac{\text{Ideal Power}}{\text{Figure of Merit}} = \frac{1}{550 \text{ FM}} \left( W \sqrt{\frac{W}{2\rho A}} \right)$$

and, therefore,

$$(2.241) \quad \frac{\text{SHP}}{W} = \frac{1}{550 \text{ FM}} \left( \sqrt{\frac{W}{2\rho A}} \right) = \frac{1}{550 \text{ FM}} \left( \sqrt{\frac{W}{2\rho_o (\rho/\rho_o) A}} \right) = \frac{0.02637}{\text{FM}} \left( \sqrt{\frac{W}{\sigma A}} \right)$$

where the ratio of engine shaft horsepower required (SHP) divided by gross weight (W) depends on the density ratio ( $\sigma = \rho/\rho_o$ ,  $\rho_o = 0.002378$  slugs-per-foot cubed) and the density-weighted disc loading ( $W/\sigma A$ ). For this example, the single (or coaxial or synchropter) rotor area (A) is  $\pi R^2$ , and the tandem rotor area is  $2\pi R^2$ .

Hover endurance also depends on the engine's fuel consumption rate. This rate is generally expressed in pounds of fuel burned per hour, which, for the turbine engine, increases in nearly a linear fashion as Eq. (2.23) suggests. For this example, I have chosen to illustrate the fuel burn rate with engine SFC following Eq. (2.22). Typical results for a representative set of engines is shown in Fig. 2-129.

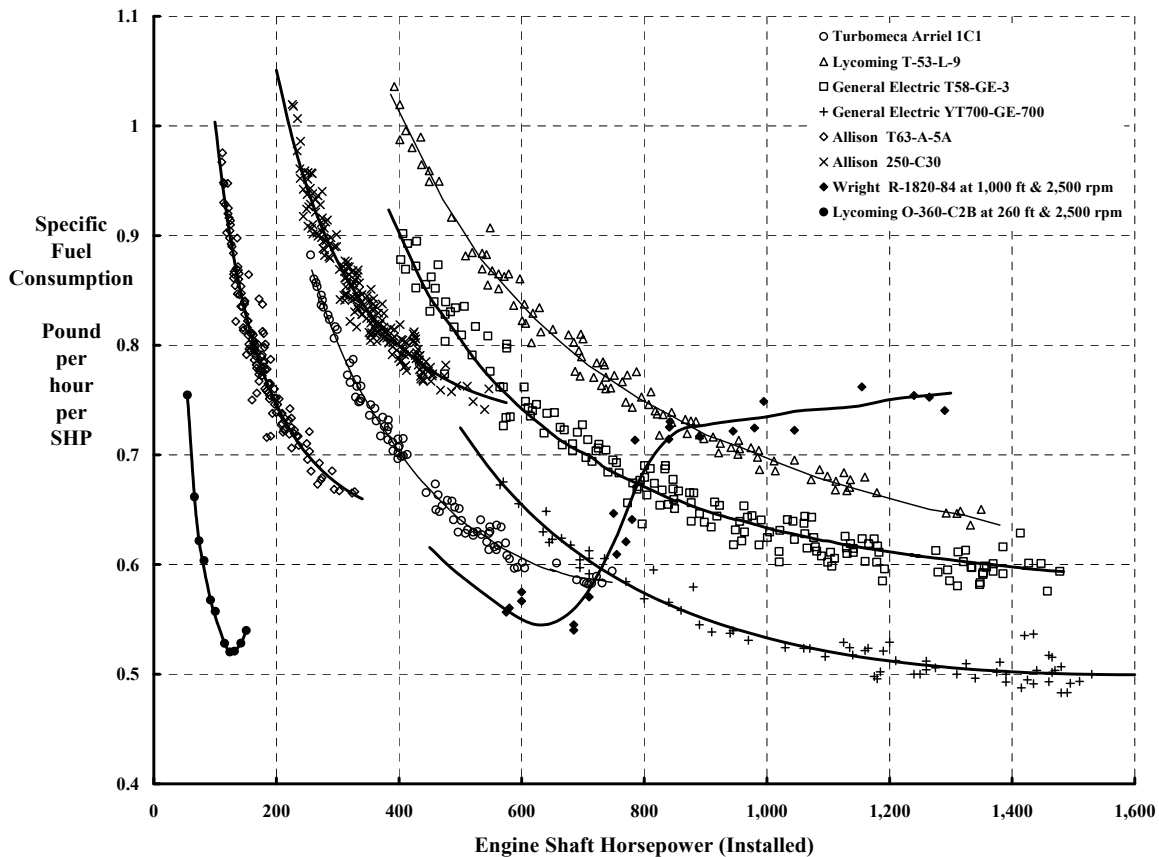


Fig. 2-129. Engine specific fuel consumption in hover ranges between 0.50 and 0.65.

With these two key parameters (FM and SFC) in hand, calculate the hover endurance (E) in hours as follows:

$$(2.242) \text{ Endurance} = - \int_{\text{initial weight}}^{\text{final weight}} \frac{1}{\text{fuel burned in pounds/hour}} dw .$$

Now, fuel burned per hour is simply

$$(2.243) \text{ lbs/hr} = (\text{SFC})(\text{SHP}) = \text{SFC} \left[ \frac{0.02637}{\text{FM}} W \left( \sqrt{\frac{W}{\sigma A}} \right) \right] = \text{SFC} \left( \frac{0.02637}{\text{FM}} \frac{W^{3/2}}{\sqrt{\sigma A}} \right).$$

The endurance is then calculated with the integral

$$(2.244) E = - \int_{\text{initial weight}}^{\text{final weight}} \frac{1}{\text{SFC} \left( \frac{0.02637}{\text{FM}} \frac{W^{3/2}}{\sqrt{\sigma A}} \right)} dW = - \int_{\text{initial weight}}^{\text{final weight}} \frac{\sqrt{\sigma A} \text{FM}}{0.02637 \text{SFC}} W^{-3/2} dW .$$

Suppose the initial weight is the takeoff gross weight (W), and the final weight is 0.9 W. Then you have

$$(2.245) E = 4.1 \left( \frac{\text{FM}}{\text{SFC}} \right) \sqrt{\frac{1}{W/\sigma A}} \text{ in hours and for fuel equal to 0.1 of takeoff gross weight.}$$

Now, from Fig. 2-128, a representative FM from the last 50 years is 0.55. And from Fig. 2-129 engine manufacturers can produce engines with an SFC of 0.55, which means the hover endurance has the first approximation of

$$(2.246) E = \frac{4.1}{\sqrt{W/\sigma A}} \text{ in hours and for fuel equal to 0.1 of takeoff gross weight.}$$

Of course the FM ranges from a low of 0.5 to about 0.7, and the specific fuel consumption can vary from 0.5 to about 0.7, so the ratio of FM to SFC can range from a high of 1.40 to a low of 0.70. Nevertheless, for a given technology Fig. 2-130 shows that the lower the disc loading, the greater the hovering endurance.

Just for the fun of it, I took a moment to research the United States and world records that Sikorsky set with his VS-300 in 1941. From Bill Hunt's fascinating first-person story of working with Sikorsky during the pioneering era [329], I read that on April 7, 1941, Sikorsky practiced for the records, staying up for exactly 30 minutes and using nearly all the fuel in the 6-gallon tank located on the port side of the VS-300C-5a. Hunt notes that "there was still sufficient fuel left for another 6/8 min before having to take fuel from the new tank (located on the starboard side), which meant there would be no fuel problem for at least a full hour." That statement and some photographs suggest to me that the "new tank" was quite likely another 6-gallon tank. At that time the VS-300C, in its -5a configuration, had a 30-foot-diameter rotor and two, aft, laterally displaced rotors on outriggers, plus the tail rotor. At takeoff the helicopter weighed approximately 1,200 pounds, which would be a disc loading of about 1.7 pounds per square foot. Assuming that the port 6-gallon tank was filled with

## 2.5 FUEL EFFICIENCY

6-pounds-per-gallon, 80-octane fuel, the VS-300C-5a must have been consuming fuel at the rate of 36 pounds per 37 minutes, or roughly 58 pounds per hour.

On April 15, 1941, Sikorsky captured the U.S. endurance record of 1 hour, 5 minutes, and 14-1/2 seconds. On that day Sikorsky benefited from a 15-mile-per-hour wind as well as ground effect. At 15-minute intervals Sikorsky “would return to the starting point and have the fuel consumption checked (from the ground by binoculars). The wind was obviously contributing to the noticeable amount of extra fuel remaining at each check-in, so at the third check-in Igor unhesitatingly said he was going for the one-hour mark.” Officials of the National Aeronautics Association witnessed and recorded this endurance. This little-noticed step to the world’s endurance record is rarely mentioned.

On May 6, 1941, Heinrich Focke’s F. 61 world endurance record of 1 hour, 20 minutes, and 49 seconds established on June 25, 1937 [7], was surpassed by Sikorsky with a performance, according to Hunt, of 1 hour, 48 minutes, and 56.1 seconds. Apparently the

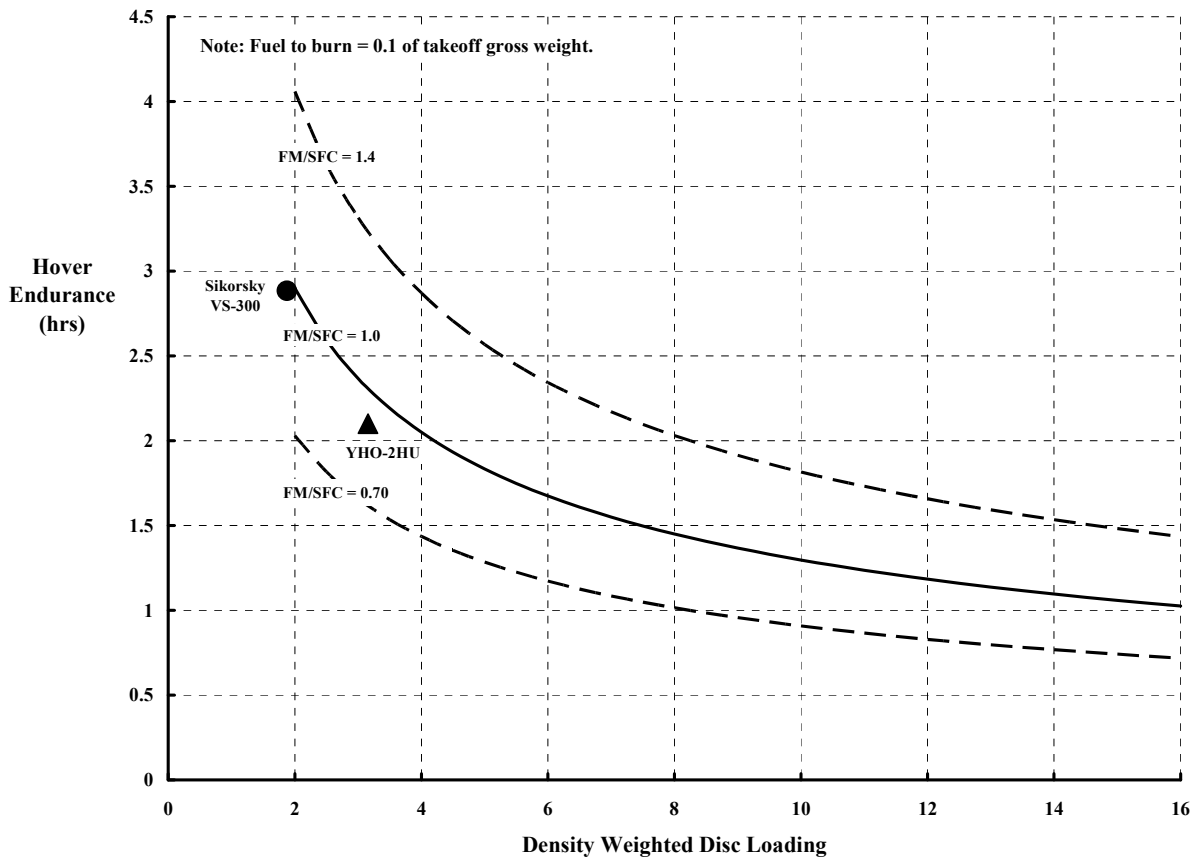


**Fig. 2-130. Helicopters, with their low disc loading, have the greatest hovering endurance of any aircraft man has developed yet (fuel = 0.1 TOGW). Note the Sikorsky VS-300 point shown at endurance with more fuel than used to set the world record of 1 hour and 32 minutes.**

National Aeronautics Association's witness only credited the event with 1 hour, 32 minutes, and 26.1 seconds, which is what history books generally quote. Hunt notes that "an elliptical saddle-type extension [an extra 3-1/2-gallon tank] was fitted on to the outer profile of the starboard tank." He later quotes the extra fuel at 30 pounds, which is a little confusing because 3-1/2 gallons would weigh more like 21 pounds. Nevertheless, Sikorsky landed the VS-300C-5a at the 1-1/2-hour (or 1-3/4-hour) point because there was a change in engine noise, which the group decided was reason enough to call a halt. The noise change was caused by a blown exhaust gasket.

In a private exchange with John Kowalonek, the archivist at the Sikorsky Historical Archives [330], I learned that "the takeoff gross weight for this record flight was 1,325 pounds, and included an extra fuel tank for a total fuel capacity of 14.7 gallons at takeoff. The amount of fuel at the end of the 1-hour-and-32-minute flight was 2.5 gallons." On this basis, 12.2 gallons of fuel weighting about 73 pounds was burned, which is 47.7 pounds per hour.

If you accept that 47.7 pounds per hour was the fuel consumption rate for the world record, Sikorsky took off at 1,325 pounds, burned about 73 pounds of fuel in 1-3/4 hours, and landed at about 0.95 of his takeoff weight. Following Eq. (2.244), I calculate that the ratio of Figure of Merit (FM) to specific fuel consumption must have been on the order of 0.962. Imagine now that Sikorsky had taken off at 1,325 pounds and burned 132 pounds of fuel (stored in larger fuel tanks), which gives a final landing weight of 0.9 of the takeoff weight. Then his world record would have been 2 hours and 53 minutes. I put this point in Fig. 2-130, just for the fun of it.

A more concrete example from the early 1960s is also shown in Fig. 2-130. The Hughes YHO-2HU [111], a very small, two-man helicopter with a 1,550-pound takeoff gross weight, used the Lycoming O-360-C2B engine with a fuel flow rate of about 75 pounds per hour at high power. This 25-foot-rotor-diameter machine had a 25-gallon fuel tank, which at 6 pounds per gallon is 155 pounds of fuel. Assume that the helicopter hovered out of ground effect at sea level with no wind and landed after running the tank dry (i.e., 155 pounds of fuel equals 0.1 times the takeoff weight, which is the basis of Fig. 2-130.). The hover endurance would be about 2.1 hours at a disc loading of 3.16. In fact, the ratio of FM to specific fuel consumption (SFC) is about 0.9.

Now let me proceed to helicopter fuel efficiency in forward flight. The measure of this fuel efficiency is most frequently quoted by the general public in miles traveled per gallon when they talk about their cars. In aviation, however, the measure is more commonly quoted in nautical miles (nm) traveled per pound of fuel burned. The simplest calculation of nautical miles per pound is obtained from the Bréguet range equation [331],<sup>80</sup> which can be easily

---

<sup>80</sup> My first encounter with the Bréguet range equation came from an aero course I took in 1955 at Rensselaer Polytechnic Institute using Perkins & Hage [284]. In October 2006 Mustafa Cavcar published a fascinating paper [332] tracing the origin of Bréguet's equation back to 1918. Cavcar suggested that while "we" all quote the equation, "nobody" ever gives a specific reference other than Bréguet's paper [331] and then only occasionally.

## 2.5 FUEL EFFICIENCY

derived. For general use, distance traveled or range (R) in nautical miles is simply velocity (V) in knots times time (t) in hours. But range depends on the pounds of fuel burned. That is,

$$(2.247) \quad R = \int_{t_{\text{final}}}^{t_{\text{initial}}} V \, dt = \int_{W_{\text{final}}}^{W_{\text{initial}}} V \frac{dt}{dW} dW = \int_{W_{\text{final}}}^{W_{\text{initial}}} \frac{V}{dW/dt} dW \approx \int_{W_{\text{final}}}^{W_{\text{initial}}} \frac{V}{\Delta W/\Delta t} dW$$

where the initial weight ( $W_i$ ) is the takeoff gross weight of the aircraft, and the final weight ( $W_f$ ) is the landing weight. The difference in the two weights is the pounds of fuel burned. The rate of fuel consumption ( $\Delta W/\Delta t$ ) has the units of pounds per hour.

Now, fuel burn rate is specific fuel consumption (SFC) times shaft horsepower (SHP) so that

$$(2.248) \quad \frac{\Delta W}{\Delta t} = (\text{SFC})(\text{SHP})$$

and, in forward flight, the engine power required is calculated as

$$(2.249) \quad \text{SHP} = \frac{D_{a/c} V}{550} = \frac{V_{\text{fps}}}{550} \left( \frac{D_{a/c}}{L} \right) W = \frac{1.69 V_{\text{kts}}}{550 (L/D)_{a/c}} W = \frac{V_{\text{kts}}}{326 (L/D)_{a/c}} W,$$

so that

$$(2.250) \quad \frac{\Delta W}{\Delta t} = (\text{SFC}) \left[ \frac{V_{\text{kts}}}{326 (L/D)_{a/c}} W \right].$$

To arrive at fuel burn rate, I have grouped the propeller efficiency with the aircraft drag ( $D_{a/c}$ ) to create an apparent drag in pounds. This apparent drag is divided by aircraft lift (L), which gives an aircraft lift-to-drag ratio  $[(L/D)_{a/c}]$ . In steady flight, lift equals weight (W). (It is worth noting that 1 hp = 550 foot-pounds per second just to keep the units correct.)

The range equation (2.247) now becomes

$$(2.251) \quad R \approx \int_{W_{\text{final}}}^{W_{\text{initial}}} \frac{V_{\text{kts}}}{(\text{SFC}) \left[ \frac{V_{\text{kts}}}{326 (L/D)_{a/c}} W \right]} dW = 326 \int_{W_{\text{final}}}^{W_{\text{initial}}} \frac{(L/D)_{a/c}}{(\text{SFC})} \frac{1}{W} dW \quad \text{in nm.}$$

The integration is performed by assuming that average values for specific fuel consumption (in pounds per hour per horsepower) and aircraft lift-to-drag ratio are adequate for a first-order approximation. In fact, on a maximum range test, a pilot would slowly climb and adjust speed at each altitude to (1) keep maximizing the aircraft's lift-to-drag ratio, and (2) ensure the lowest rate of fuel consumption. Therefore, range in nautical miles, becomes

$$(2.252) \quad R \approx 326 \left[ \frac{(L/D)_{a/c}}{\text{SFC}} \right]_{\text{avg.}} \int_{W_{\text{final}}}^{W_{\text{initial}}} \frac{1}{W} dW = 326 \left[ \frac{(L/D)_{a/c}}{\text{SFC}} \right]_{\text{avg.}} \ln \left( \frac{W_{\text{initial}}}{W_{\text{final}}} \right).$$

Range in statute miles is simply Eq. (2.252) with the constant 326 increased to 375. It is helpful to remember that there are 5,280 feet per statute mile and 6,076 feet per nautical mile.

Before converting Bréguet's range equation into fuel efficiency, let me give you two interesting examples of maximum range. The first example is Charles Lindbergh's flight from Long Island, New York, to Paris. An early discussion and somewhat technical analysis of the flight written by August Von Parseval was published in "Motorwagen" on May 31, 1927, translated into English by Dwight Miner, and published in the United States as NACA TM No. 423 [333]. In July 1927 the N.A.C.A. published the technical preparation of the Spirit of St. Louis (Fig. 2-131) for the flight; it was written by Donald Hall, the chief engineer of Ryan Airlines, Inc., who built the airplane [334]. Hall's detailed engineering report is an absolute gold mine of data, if you are interested. According to Parseval's somewhat premature article and Hall's rather complete engineering data, Charles Lindbergh's Spirit of St. Louis took off weighing 5,250 pounds with 450 gallons of fuel, which, at 6.12 pounds per gallon, is 2,750 pounds. He was in the air 33 hours and 47 minutes, and traveled about 3,130 nautical miles (3,600 statute miles) if there was no tail wind. Hall's data suggests that Lindbergh landed with about 180 pounds of fuel left, which means that 2,570 pounds of fuel was consumed. I will guess the initial 25 gallons of oil was down to 10 gallons at landing, so at 7 pounds per gallon, he lost another 100 pounds. I suggest, therefore, that the landing weight was 2,580 to 2,700 pounds.

Using Bréguet's range equation, it appears that the Spirit of St. Louis flew across the Atlantic at an  $(L/D)_{a/c}$ -to-SFC average ratio of 13.5. That is,

$$(2.253) \quad R = 326 \left[ \frac{(L/D)_{a/c}}{\text{SFC}} \right]_{\text{avg.}} \ln \left( \frac{5,250}{2,580} \right) = 326 [13.5]_{\text{avg.}} (.71) = 3,130 \text{ nautical miles.}$$

In terms of miles per pound of fuel burned, that would be 3,130 nautical miles divided by 2,570 pounds—about 1.2 nautical miles per pound or 1.4 statute miles per pound. The average fuel flow was near 12.5 gallons per hour. (I am sure my analysis is off a bit, but the example illustrates the use and first-order accuracy of Bréguet's range equation.)



**Fig. 2-131. Charles Lindbergh's Spirit of St. Louis (photo courtesy of Loftin Collection, NASA Langley Research Center).**

## 2.5 FUEL EFFICIENCY

The second example you should know about concerns an equally impressive nonstop, non-refueled, record-setting flight with a small helicopter [147]. The Hughes YOH-6A (Fig. 2-132), piloted by Bob Ferry, took off from Culver City, California, at 2:20 p.m. on April 6, 1966, and landed at Ormond Beach, Florida, 15 hours and 8 minutes later. Ferry's YOH-6A took off at an overload gross weight of 3,235 pounds, burned 1,850 pounds of fuel, and landed with about 10 pounds of fuel leftover. As fuel burned off, Ferry climbed (roughly linearly with time) to near 25,000-foot altitude over Jacksonville, Florida. From there he rapidly descended to Ormond Beach. The flight established a new, straight-line distance record of 2,213 statute miles (1,923 nautical miles), although the actual distance was 2,277 statute miles.

Using Bréguet's range equation, Ferry flew the YOH-6A across the United States at an  $(L/D)_{a/c}$ -to-SFC average ratio of 8.2. That is,

$$(2.254) \quad R = 326 \left[ \frac{(L/D)_{a/c}}{SFC} \right]_{\text{avg.}} \ln \left( \frac{3,235}{3,235 - 1,850} \right) = 326 [8.2]_{\text{avg.}} (0.848) = 2,277 \text{ nm.}$$

In terms of nautical miles per pound of fuel burned, that would be 2,277 nautical miles divided by 1,850 pounds—about 1.23 nautical miles per pound or 1.42 statute miles per pound. The average fuel flow was near 20.4 gallons per hour.



**Fig. 2-132. Hughes YOH-6A set the world distance record on April 6–7, 1966 [147] (photo from author's collection).**

The contrast between the Spirit of St. Louis and the YOH-6A is noteworthy. The 1927 airplane's ratio of  $(L/D)_{a/c}$  to SFC was 13.5; the 1966 helicopter's was 8.2. Furthermore, the helicopter was powered by the Allison T63-A-5A, which from Fig. 2-129 had an average SFC during the flight on the order of 0.8. This suggests that the average lift-to-drag ratio of the helicopter was about 6.5. In contrast, the airplane was powered by the Wright J-5-C giving 223 brake horsepower at 1,800 rpm. Hall's report [334] indicates an SFC of about 0.5, which gives the airplane an average lift-to-drag ratio of 6.5.

I have three conclusions from these two examples: (1) the two aircraft had comparable lift-to-drag ratios, as long as you include propeller efficiency as a drag; (2) the piston engine's specific fuel consumption was nearly half that of the turbine engine; and (3) nothing beats a tail wind, which, I am confident, was different for the two record-making flights.

Now let me address fuel efficiency expressed in nautical miles (nm) per pound (lb) of fuel burned (nm/lb). This ratio is frequently referred to as specific range (SR). Range divided by the fuel consumed to travel that distance is a measure of the average specific range. Therefore,

$$(2.255) \quad SR = \frac{R}{W_{\text{fuel}}} = 326 \left[ \frac{(L/D)_{a/c}}{\text{SFC}} \right]_{\text{avg.}} \left[ \left( \frac{1}{W_{\text{fuel}}} \right) \ln \left( \frac{W_{\text{initial}}}{W_{\text{initial}} - W_{\text{fuel}}} \right) \right],$$

and when the natural logarithm is expanded, you have, with some rearrangement,

$$(2.256) \quad SR = \frac{R}{W_{\text{fuel}}} = 326 \left[ \frac{(L/D)_{a/c}}{\text{SFC}} \right]_{\text{avg.}} \frac{1}{W_{\text{initial}}} \left[ 1 + \frac{1}{2} \left( \frac{W_{\text{fuel}}}{W_{\text{initial}}} \right) + \frac{1}{3} \left( \frac{W_{\text{fuel}}}{W_{\text{initial}}} \right)^2 \right].$$

From Eq. (2.256) you can see that for a normal ratio of fuel consumed to takeoff weight—in the range of 0.1 to 0.15—that specific range is inversely proportional to the takeoff gross weight. A quite adequate approximation is simply

$$(2.257) \quad SR = \frac{R}{W_{\text{fuel}}} = 350 \left[ \frac{(L/D)_{a/c}}{\text{SFC}} \right]_{\text{avg.}} \frac{1}{W_{\text{initial}}} \quad \text{in nautical miles per pound.}$$

In essence, this result says the heavier the machine (for a given aircraft and engine technology), the poorer the miles per gallon, which I expect you already knew.

The immediate value of Eq. (2.257) is the comparison of fuel efficiency for many helicopters. There is a wealth of data in industry literature that give takeoff weight, range, and fuel capacity, etc., for any given helicopter. Some of the data are “apples and oranges” of course. However, from a survey of some 550 helicopters,<sup>81</sup> you will see in Fig. 2-133 that

---

<sup>81</sup> I have a list of over 550 helicopters in my personal collection. This unpublished list occupies a Microsoft® Excel® spreadsheet some 590 rows deep and 50 columns wide. Not all the technical data blanks are filled in yet, therefore not all the sub-calculations are complete. Many of the helicopters on my list are derivatives of basic models, so the number of really different helicopters is much less than 550.

## 2.5 FUEL EFFICIENCY

specific range does, in fact, decrease with increasing takeoff weight as Eq. (2.257) dictates. Furthermore, 50 years of modern helicopter history is summed up, *from a fuel efficiency point of view*, concisely with

$$(2.258) \quad SR = \frac{R}{W_{\text{fuel}}} = 350 [4.0 \text{ to } 7.5]_{\text{avg.}} \frac{1}{W_{\text{initial}}} \quad \text{in nm/lb.}$$

Fig. 2-133 shows that with a few exceptions, the industry's best efforts have produced helicopters with  $(L/D)_{a/c}/SFC$  equal to 7.5. This is the solid line that captures the top of the data scatter in the figure. The bottom of the scatter is captured with a long, dashed line calculated using Eq. (2.257) with the lift-to-drag ratio divided by engine specific fuel consumption equal to 4.0.

Cammack, the author of the paper about the YOH-6A World Record Program [147], closes the portion of his paper describing the cross-country flight with this key statement:

“It is interesting to note that this distance was achieved using a turbine engine with an SFC of approximately 0.7. If small turbine engines with SFC's of approximately 0.5 become available, distances 40 percent greater will be possible. The resulting still air range, based on the closed circuit distance record (Flight 7) would be 2440 miles (1740 miles  $\times$  1.4 = 2440 miles)—virtually the West Coast to Honolulu Ferry Range that has been a goal for the past decade.”

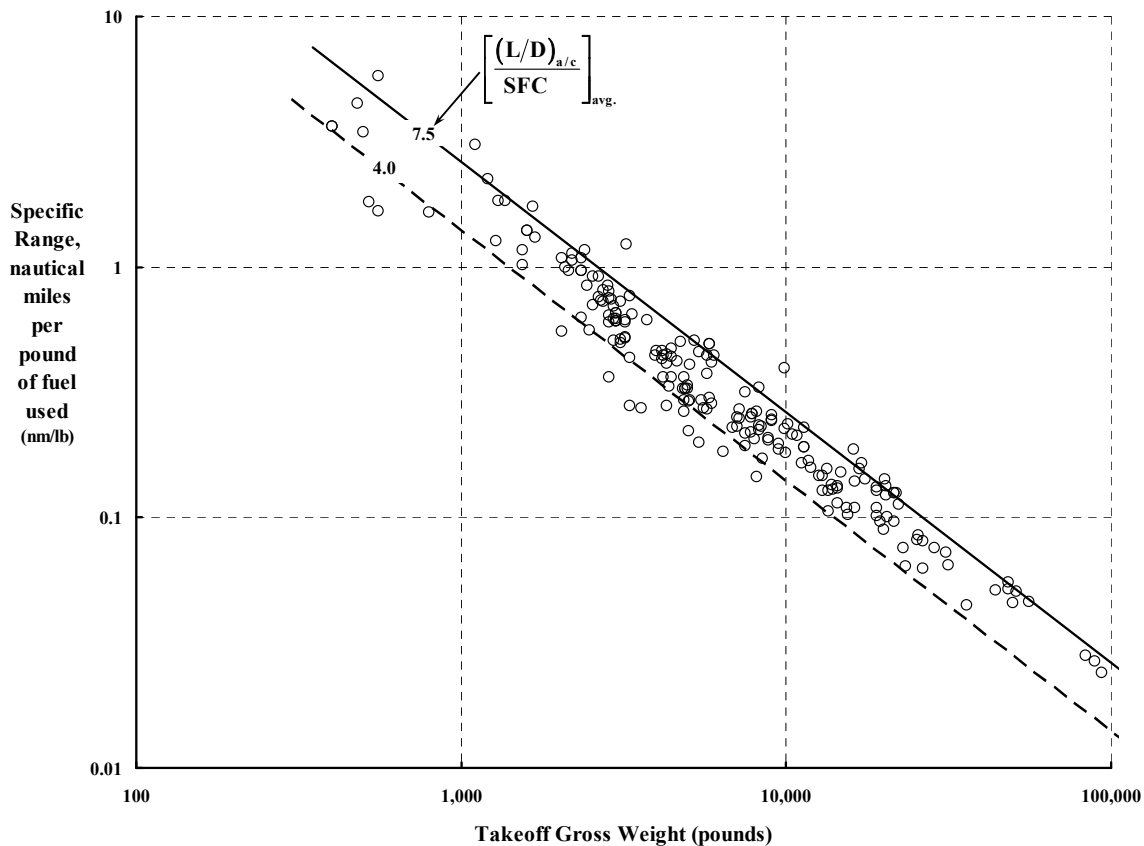


**Fig. 2-133. Helicopter fuel efficiency after 60 years of development.**

As of 2012, no small turbine engine with an SFC close to 0.5 has arrived. And, just as important, no helicopter airframe manufacturer has made a 40 percent improvement in the aircraft maximum lift-to-drag ratio. Furthermore, the nonstop, non-refueling helicopter flight from the West Coast of the United States to Honolulu has yet to be made.

### 2.5.1 Helicopter Lift-to-Drag Ratio (L/D)

Helicopter lift-to-drag (L/D) ratio, whether average or maximum, can be a sore subject to bring up with members of the rotorcraft industry. Sixty years ago, helicopter pioneers steadfastly insisted that no real barrier existed in achieving airplane-like L/Ds. But, try as they might, succeeding generations have made very little progress toward this goal. The purpose of this section of the book is to look at helicopter L/D in the cold light of day after 60 years.

An aircraft's L/D is quite easy to define given Eq. (2.47). For a helicopter in steady, level flight, it is simply

$$(2.259) \quad \frac{L}{D} = \frac{W}{550 \text{SHP} / V} = \frac{W V}{550 \left( \frac{\text{RHP}_{\text{Main Rotor(s)}}}{\eta_{\text{Main Rotor(s)}}} + \frac{\text{RHP}_{\text{Tail Rotor(s)}}}{\eta_{\text{Tail Rotor(s)}}} + \text{SHP}_{\text{Acc.}} \right)} = \frac{C_{w\mu}}{C_{P-\text{Engine}}}$$

where flight weight ( $W$ ) is in pounds, and velocity ( $V$ ) is in feet per second. Using anything other than the engine (or engines) total shaft horsepower (SHP) required to fly seems, to me, quite unreasonable. You have been exposed to rotor horsepower (RHP) and engine power used to drive accessories earlier in this discussion of modern helicopter results.

References [108, 109, 115, 116, 118, 121, 124, 125, 133, 170-188, 190-206] and [207-210] provide a reasonable amount of flight test data with which to calculate L/D for these several helicopters. The results of this calculation are displayed in Fig. 2-134.

The L/D ratio for the Sikorsky UH-60A has been examined in detail in Fig. 2-135. Let me discuss the three upper lines in Fig. 2-135 first and then address the parasite drag of helicopters in a separate paragraph.

As you can see, the highest L/D ratio comes when the drag of only the main rotor blades alone is considered. You will recall (Volume I, paragraph 2.11.3, pages 225–234) that in 1927 Glauert held little promise that an isolated rotor would ever achieve a maximum L/D much greater than 8.0. For a number of reasons he did not imagine, he turned out to be right. The L/D of an isolated rotor in forward flight was given in Volume I, Eq. 2.289, page 232 as

$$\frac{L_R}{D_R} = \frac{L_R}{\frac{L_R^2}{2\rho A V_{FP}^2} + \frac{\rho A \sigma V_t^3}{8V_{FP}} C_{d\min} (1 + 3\mu_{hp}^2)}$$

## 2.5 FUEL EFFICIENCY

For the UH-60A this 1927 theory is shown as the dashed line in Fig. 2-135 using  $C_{d_{min}} = 0.008$ . With a better understanding of profile drag and the effect of nonuniform downwash [211], this favorable 1927 main-rotor-blades-alone estimate becomes more realistic as the estimate labeled 1980 shows.

The influence of accessory power, transmission efficiency, and the tail rotor cannot be ignored. These items decrease the maximum L/D ratio by two points! The decrement is of the same order as the 26 square feet of equivalent flat plate area, which I will now discuss.

### 2.5.2 Equivalent Parasite Drag Flat Plate Area ( $f_e$ )

Equation (2.259) calculates the lift-to-drag ratio of a helicopter. This ratio depends on the main rotor(s) horsepower required ( $RHP_{Main\ Rotor(s)}$ ). As discussed in Volume I, page 64, the autogyro era showed that this main rotor power could be calculated using the energy method, which says that

$$(2.260) \text{ Power} = Q\Omega = T_{hp}v - (T_{hp} \sin \alpha_{hp} + H_{hp} \cos \alpha_{hp})V_{FP} + \frac{\rho(\pi R^2)V_t^3 \sigma C_{do}}{8} (1 + 3\mu_{hp}^2),$$

and that  $(T_{hp} \sin \alpha_{hp} + H_{hp} \cos \alpha_{hp})$  is just rotor drag that an autogyro's propeller had to overcome. When applied to the helicopter, the rotor is both lifting and propelling so that rotor drag becomes a propulsive force. This propulsive force is, to the first approximation, equal to the parasite drag of the helicopter. The parasite drag of the helicopter, as is customary for airplanes, is nothing more than  $f_e = D/q$  where  $q = \frac{1}{2} \rho V^2$ . Therefore, it follows that

$$(2.261) T_{hp} \sin \alpha_{hp} + H_{hp} \cos \alpha_{hp} = -f_e q.$$

On this basis, the main rotor or rotors require power from the engine in the amount of

$$(2.262) \text{ Power} = T_{hp}v + f_e q V_{FP} + \frac{\rho(\pi R^2)V_t^3 \sigma C_{do}}{8} (1 + 3\mu_{hp}^2).$$

As I related in Volume I, pages 258 and 259, the Royal Aircraft Establishment (RAE) had obtained a Cierva C.30 Autogyro in 1934 to conduct an end-user evaluation. A report was ultimately published in March 1939 [335]. Following extensive flight testing, the RAE concluded that

“the experiments do not suggest any very obvious method of improving performance of the aircraft [the C.30] except by reducing the parasitic drag of the fuselage. It has been estimated that the reduction of solidity and increase of blade angle as compared with the C.6 autogyro has increased the L/D ratio of the rotor at top speed from 5.9 to 8.8 and it seems unlikely that much further improvement in the aerodynamic performance of the rotor can be obtained.”

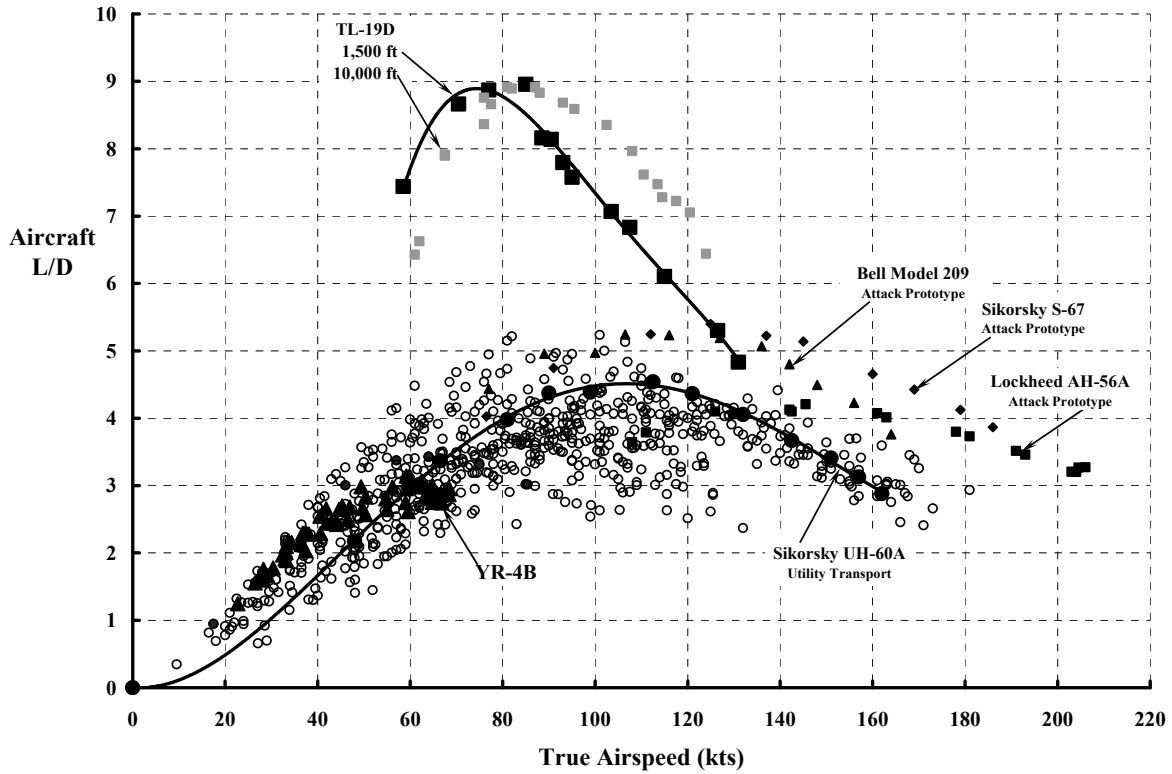


Fig. 2-134. Helicopter lift-to-drag ratio after 60 years of development.

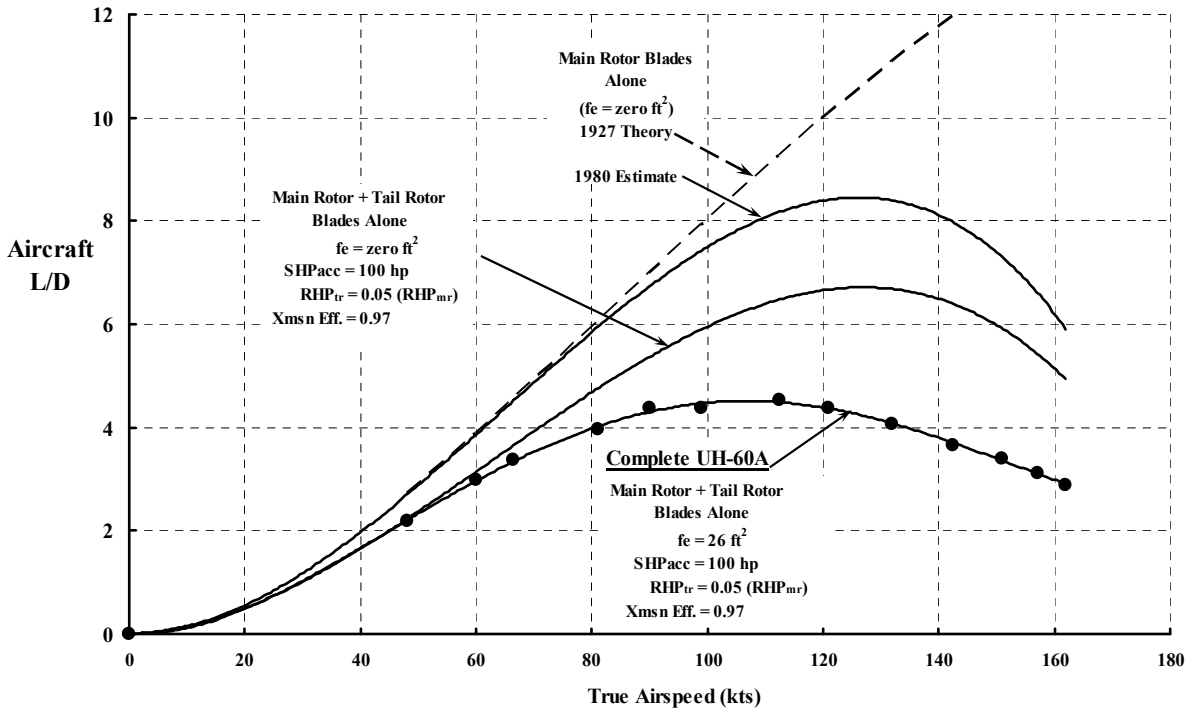


Fig. 2-135. Estimate of the elements that make up the L/D of a UH-60A (gross weight 15,500 pounds, altitude 2,060 feet, and main rotor speed 244 rpm).

## 2.5 FUEL EFFICIENCY

Based on model wind tunnel testing, it was concluded that the 1,800-pound-gross-weight Cierva C.30 had a parasite drag area of  $f_e = 7.57$  square feet. The distribution of drag area by component is provided in Table 2-25. The reference gross weight is 1,800 pounds.

With the onset of World War II and the 6 years that followed, the attention of the rotorcraft industry was riveted on developing a helicopter. The primary effort was to just get a helicopter flying—never mind its aerodynamic efficiency. There was, of course, general agreement that the machines all had high parasite drag, but reliability, stability, control, and hovering performance shortcomings were of much greater importance than the inadequate performance in forward flight.

I do not mean to infer any lack of attention to parasite drag with the preceding paragraphs. In fact, just the opposite. Each of the pioneering companies had ongoing efforts to find the equivalent parasite drag area for its helicopters. As one example, consider what the Kellett Aircraft Corporation engineering group documented in February 1945.

In February 1945 the Kellett Aircraft Corporation had completed the transition from autogyros and was pursuing the XR-8, a synchropter (Fig. 2-136) that first flew on August 7, 1944. The XR-8 was followed by the much larger XR-10. As part of that transition, Gordon Fries prepared a Kellett engineering report [336] titled *A Summary of References, Methods and Procedures Useful in Estimating Parasite Drag*. Following a thorough and careful step-by-step calculation used in parasite drag estimating at the time, Gordon established the drag breakdown for the Kellett YG-1B autogyro, the Kellett XR-8 helicopter, and the Sikorsky YR-4B.<sup>82</sup> To construct the comparison summarized in Table 2-26, Gordon used over 20 different references dealing with aircraft component drag estimating methods and data.<sup>83</sup>

**Table 2-25. C.30A Drag Breakdown Based on 1/8-Scale-Model Tests**

Component	Drag at 100 fps (lb)	Parasite Area ( $f_c$ in sq ft)	Percent
Undercarriage and Its Wheels	29	2.44	32
Engine and Exhaust Ring	17	1.43	18
Fuselage With Vertical Fins	11	0.93	12
Pylon	10	0.84	11
Rotor Hub	10	0.84	11
Tail Plane	7	0.59	8
Windscreens	4.5	0.38	5
Tail Wheel	1.5	0.13	2
<b>Total</b>	<b>90</b>	<b>7.57</b>	<b>100</b>

---

<sup>82</sup> I count Gordon as a longtime friend. His report was checked and approved by Wayne Wiesner, another longtime friend. When the Kellett brothers' (Rodney and Wallace) company failed after the XR-10 crashed in New Jersey in 1947, the brothers decided to manufacture frozen food containers for grocery stores. The need became apparent when frozen food became a new product in the United States. To stay in the rotorcraft industry, Gordon moved to Piasecki and Wayne moved to Hiller. Gordon started to round out my aerodynamics education at Rensselaer Polytechnic Institute when I moved from Preliminary Design to the Aerodynamics group in 1957.

<sup>83</sup> When I started doing parasite drag estimates I had Dr. Sighard Hoerner's book [337], *Fluid-Dynamic Drag* (my first-edition May 1951 copy was just titled *Aerodynamic Drag*), as primary reference.



**Fig. 2-136. The Kellett XR-8 synchropter was patterned after the Flettner Fl-265, which had its first flight in Germany in 1938 (photo courtesy of Wayne Wiesner).**

The N.A.C.A. continued its rotorcraft research program by transitioning from an emphasis on autogyros to an emphasis on helicopters. In early 1945 the Bureau of Aeronautics and the Air Technical Service Command (the Army Air Corp) requested flight testing research on the Sikorsky YR-4B by the Langley Memorial Aeronautical Laboratory. The Navy provided an HNS-1 (its version of the Army YR-4B) and in March and April 1945, Fred Gustafson published two reports [47, 48]. The first report documented level flight performance and the second covered hovering and vertical flight performance. In analyzing the forward-flight performance of the YR-4B, Gustafson used initially unpublished lift, drag, and pitching moment data that Dick Dingeldein and Ray Schaefer obtained for a full-scale YR-4B in the Langley 30- by 60-foot open throat wind tunnel. The test results were later published [271]. This landmark data is reproduced here as Fig. 2-137. Note that with the camera not installed, the airframe parasite drag area varied from a minimum of (0.0172 times 1,134) 19.6 square feet to nearly 23.8 square feet at a nose-down angle of attack of  $-16$  degrees.

2.5 FUEL EFFICIENCY

**Table 2-26. Kellett Parasite Drag Area Breakdown for Three Rotorcraft (February 1945)**

Component	YG-1B	XR-8	YR-4B
Fuselage and Pylon	5.74	5.71	5.67
Landing Gear	1.97	9.09	5.13
Rudder	0.05	0.15	0
Tail Rotor Structure	0.00	0.00	0.62
Stabilizer and Fin	0.66	1.15	
Blade Roots and Hub	1.78	4.61	5.47
Other	0.00	1.30	2.99
Interference Effects	0.51	0	0
<b>Total</b>	<b>10.71</b>	<b>22.00</b>	<b>19.89</b>
<b>Reference Gross Weight</b>	<b>2,800</b>	<b>2,975</b>	<b>2,540</b>

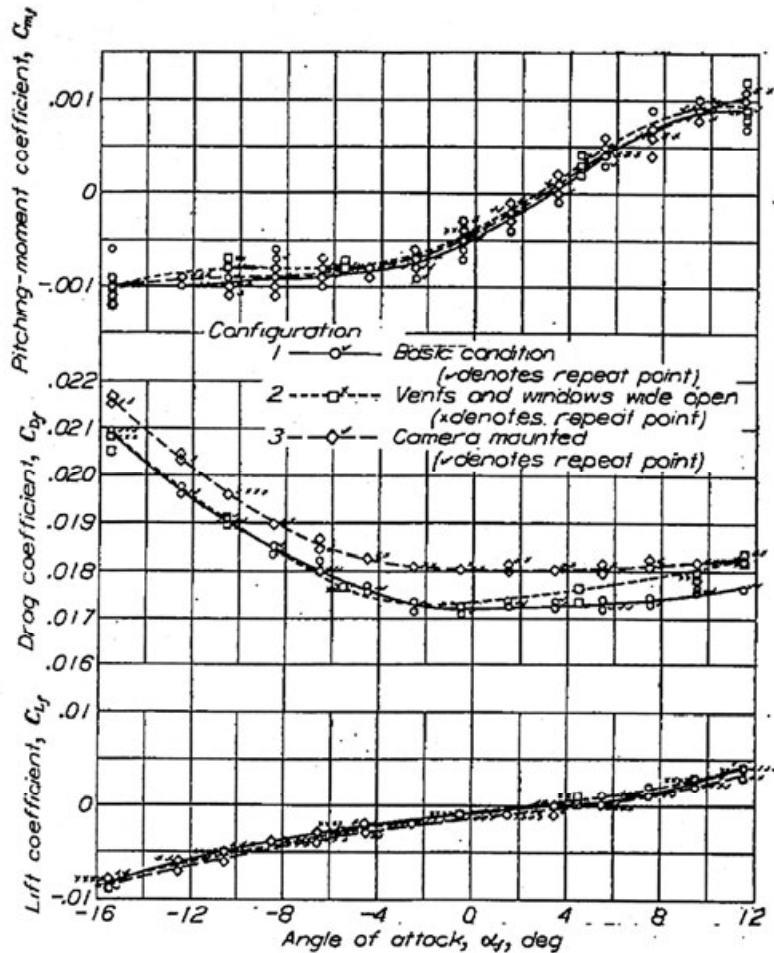


**Fig. 2-137. The Sikorsky YR-4B airframe aerodynamic properties with main- and tail-rotor blades removed. Coefficients based on the main rotor area of 1,134 square feet [271].**

In using the Dingeldein data, Gustafson added 0.4 square feet of drag to account for the “cylindrical blade shanks.”<sup>84</sup> Furthermore, he corrected the wind-tunnel angle of attack to account for the main rotor downwash, which he computed as

$$(2.263) \quad \Delta\alpha_f = 57.3 \left( \frac{W + L_f}{\frac{1}{2} \rho V^2 \pi R^2} \right).$$

This main-rotor-interference angle of attack ( $\Delta\alpha_f$ ) in degrees was added to the helicopter’s pitch attitude (in degrees), which was “determined by means of a pendulum inclinometer.”

The thoroughness of Fred Gustafson’s 1945 work set a high standard for those of us who followed.

By 1954 helicopter development had overcome many of the early mechanical deficiencies, and Robert Harrington of the N.A.C.A. Langley Memorial Aeronautical Laboratory published NACA TN 3234 [338]. In my opinion, his summary and introduction represented a call to action on reducing parasite drag. In August 1954 he wrote the following:

#### “SUMMARY

A reduction in helicopter parasite drag is possible but not profitable except in those cases where high speed and long range are primary requirements. For some of the factors causing drag, reduction in parasite-drag area may result in increased weight whereas, in other cases, it does not. The final design, however, must be a compromise between the reduction of drag and the increase in weight.

#### INTRODUCTION

In the past, there has been little consideration given to the problem of helicopter parasite drag. Many more serious problems such as vibration, stability, and even adequate hovering performance have required the full attention of the designer. In any event, parasite drag becomes important only in the higher speed range.

Now, however, there are certain uses of the helicopter where high speed and long range are important. Wherever this is the case, it appears that significant benefits can be realized from reductions in parasite drag. The purpose of this paper is to indicate the order of magnitude of these possible benefits and to discuss a few of the ways by which parasite drag can be reduced.”

To make his points, Harrington hypothesized a 10,000-pound helicopter having a parasite drag area of 40 square feet, which he “chose as representative of current practice for helicopters of this size.” He then proceeded to use several references for drag reduction from fixed-wing drag reduction efforts to concluded that a reduction of 25 square feet of parasite area could be obtained. He estimated that 20 square feet of drag reduction could be obtained just from applying fixed-wing lessons learned about landing gears and wheels. He explained his reasoning as follows:

---

<sup>84</sup> It is worth noting that the minimum parasite drag area of 19.6 square feet that Dingeldein obtained, plus the 0.4 square feet Gustafson added for “blade shanks” (equaling 20.0 square feet), compares quite favorably with the 19.89 square feet Fries estimated as shown in Table 2-26.

## 2.5 FUEL EFFICIENCY

“Landing-gear installation. Shown in figure 2 [reproduced here as Fig. 2-138] are sketches of the landing-gear installations on three different helicopters in the general weight range which is being considered. Past experience with airplanes indicated that the landing gear contributed from one-third to one-half the total drag. Calculations of the parasite drag of helicopter landing gears such as these indicate a parasite-drag area of about 20 square feet. When available drag data for wheels, struts, and tubing are used, a parasite-drag area of 15 square feet is obtained if no interference losses are considered. Experience indicates that the interference drag of the various strut intersections, the strut-fuselage intersection, and the wheel-strut intersection would probably add at least another 5 square feet and thus give a total area of 20 square feet. All this drag increment could be saved by use of a fully retractable landing gear. In some cases it may be impractical or undesirable to retract the gear fully. In that event, significant drag reductions, possibly equal to the sum of all these other items, may still be realized by proper fairing of the wheels and struts. Some data on landing-gear fairings are presented in references 5 [see NACA Report 485] and 6 [see NACA Report 518]. It should be mentioned that there will probably be some weight penalty involved in retracting or fairing the gear. This weight increase would somewhat reduce the estimated power saving.”

As it turned out, smaller helicopters (e.g., the Bell H-13 and Hiller H-23) changed to skid gears to satisfy U.S. Army field operation requirements, but nonretractable, wheeled landing gear continued as standard on heavier machines until the late 1970s.

Harrington’s August 1954 report was quite timely because the U.S. Army began a search for a new Light Observation Helicopter (LOH) to replace aging Bell OH-13 and Hiller OH-23 first-generation helicopters. In October 1960 the U.S. Navy, acting for the Army Chief of Transportation, sent out a request for proposals for a four-seat, turbine-powered LOH. Some 25 aircraft companies were solicited. In October 1961 the contenders were narrowed down to the Bell YOH-4, the Hiller YOH-5, and the Hughes YOH-6.

### TYPICAL HELICOPTER LANDING GEAR INSTALLATIONS

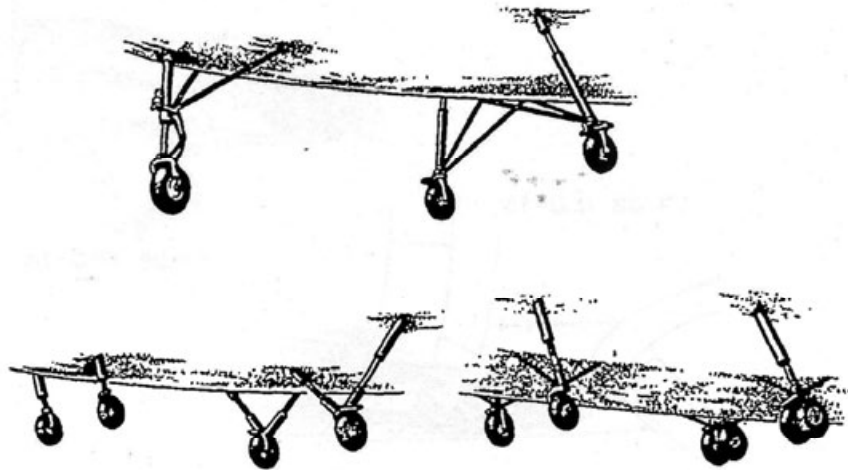


Figure 2

Fig. 2-138. Harrington’s examples of “current” landing gear installations [338].

One of the companies solicited for an LOH proposal was the Vertol Division of the Boeing Company. At that time Jack Diamond was Chief of Preliminary Design at the division. In July 1960 Jack had written a letter to George Dausman (Assistant Chief of Aerodynamics of the Airborne Support Systems, Engineering Division, Air Force) asking for helicopter drag data. Mr. Dausman responded with a letter [339] which read in part:

“A search of our old files for helicopter drag data has resulted in the attached tabulation of equivalent drag areas. Many of the values are estimates based upon preliminary drag build-ups and the remainders are calculated from Edwards flight test data. Generally, drag values for the H-19 and more recent machines are from test data.”

The tabulation Dausman included is reproduced here as Table 2-27. I have added columns for the manufacturer and the nominal gross weight as given by Lambermont and Pirie [89].

Let me stop for a moment to look at a graphical summary of the parasite drag area accumulated in Tables 2-25, 2-26, and 2-27. This data is summarized in Fig. 2-139. First of all, the somewhat limited data suggests that helicopter parasite area varies as nominal gross weight raised to the two-thirds power. That is, it appears that

$$(2.264) \quad f_e = K(GW / 1000)^{2/3}.$$

Accepting this approximation, the industry decreased parasite drag by a factor of 2 in about 15 years after the Sikorsky R-4B began flying, which is to say that K went from 8.6 to 4.2 in 15 years. Quite interestingly to me, the helicopter drag levels appear to have overcome the advantage autogyros offered with their  $K = 5.2$ .

**Table 2-27. Survey of Parasite Drag Area as of July 1960**

Model Designation	Manufacturer	Equivalent Drag Area (ft <sup>2</sup> )	Nominal Gross Weight (lb)
R-4B	Sikorsky	23.1	2,540
H-5	Sikorsky	17.9	4,900
H-10	Kellett	29.4	11,000
H-12	Hiller	16.6	2,700
H-13G	Bell	10.6	2,350
XH-15	Bell	15.4	2,777
XH-16	Piasecki	54.0	33,577
YH-16	Piasecki	54.0	46,750
XH-17	Hughes	128.0	52,000
YH-18	Sikorsky	15.3	2,100
H-19	Sikorsky	26.0	7,200
H-21	Piasecki	30.0	11,500
H-26	American Helicopter	4.4	875
H-34	Sikorsky	34.0	13,000
H-37	Sikorsky	75.0	31,000
XH-40	Bell	18.0	8,500
YH-40	Bell	36.0	8,500
YH-41	Cessna	9.0	3,000
LZ-5	Doman	20.4	5,200

## 2.5 FUEL EFFICIENCY

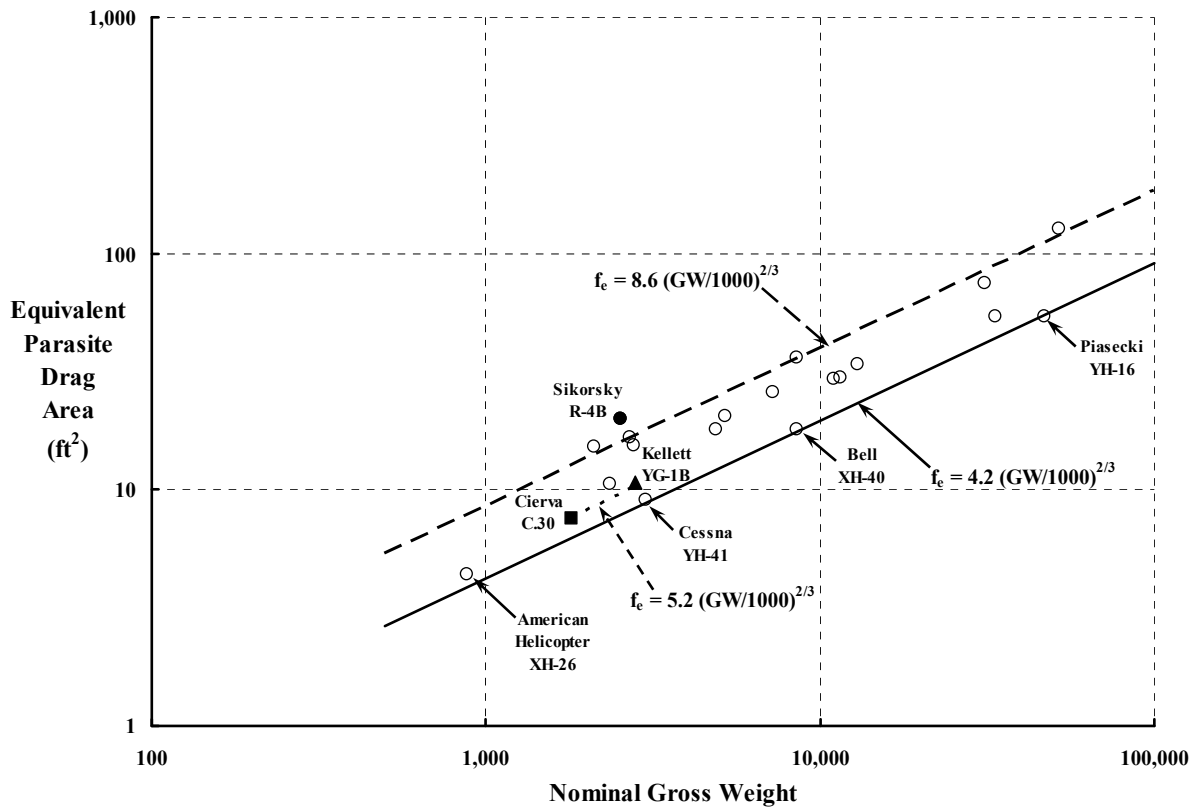


**Fig. 2-139. From 1945 to the late 1950s, the rotorcraft industry decreased helicopter parasite drag area by a factor of two.**

As part of the forthcoming LOH competition the U.S. Army wanted their own assessment of parasite drag. In May 1960 they assigned a research program to what was then the U.S. Army Transportation Research Command (USATRECOM) located at Fort Eustis, Virginia. A project engineer was assigned (Lt. Herbert H. Moser<sup>85</sup>) and the wind tunnel services of NASA Langley Research Center were enlisted. NASA obtained both a 1/5-scale and a full-scale model of what could be a four-place LOH, and these models were tested. Preliminary NASA reports [340, 341] were made available in December 1960.<sup>86</sup> Lt. Moser published the results of the research program in the American Helicopter Society Journal in January 1961 [342], which was quite timely for the competition.

<sup>85</sup> When Herb completed his service he came to Boeing Vertol for several years. If my memory serves me correctly, Herb became a project engineer in Preliminary Design for Jack Diamond. The report Herb wrote is an absolute must-read paper.

<sup>86</sup> These preliminary reports, which I have copies of, were given NASA L-1469 and L-1470 numbers. They later were published as NASA TN D-1363 and NASA TN D-1364 in July 1962, but with slightly different titles.

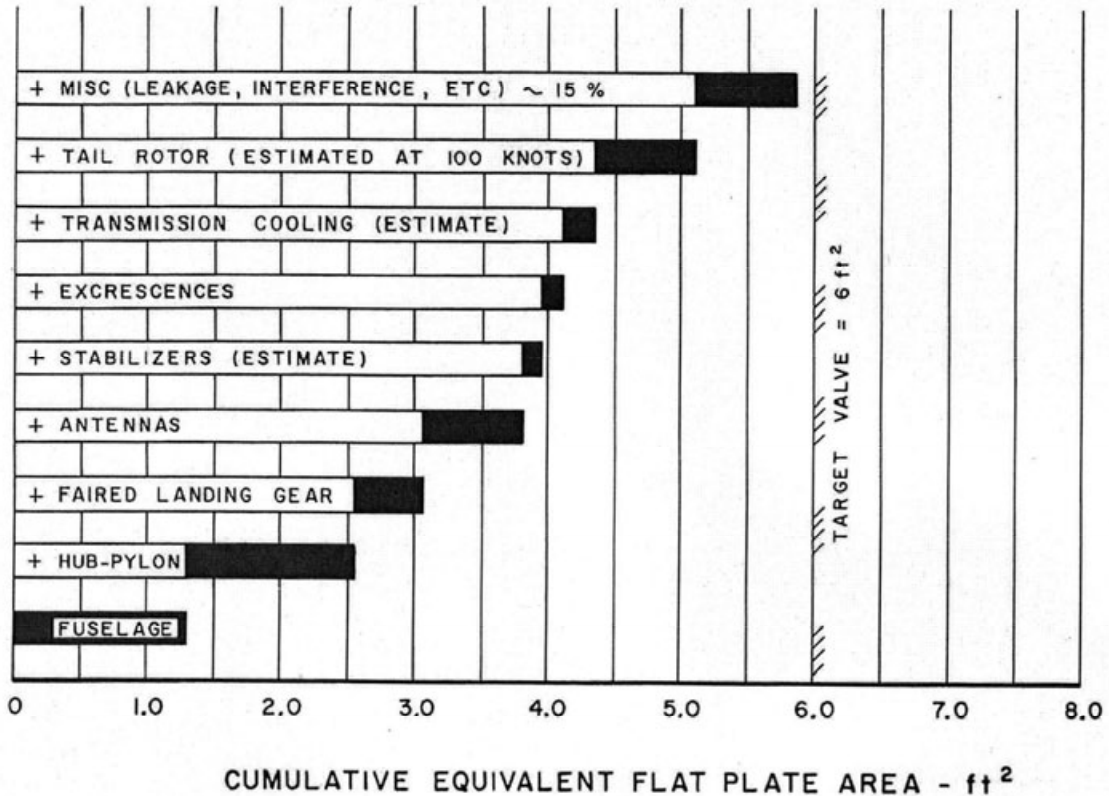


**Fig. 2-140. Parasite drag breakdown for the U.S. Army version of the Light Observation Helicopter [342].**

As Lt. Moser reported, the U.S. Army felt, based on their estimates of the LOH configuration, that a 2,400-pound gross weight with a parasite drag area of 6.0 square feet should be achievable by the industry. This meant that they expected a K of 3.35 computed from Eq. (2.264) as

$$(2.265) \quad K = \frac{f_c}{(GW/1,000)^{2/3}} = \frac{6}{(2,400/1,000)^{2/3}} = 3.35.$$

In essence the Army was expecting industry to come up with a configuration that lowered the parasite drag constant (K) from 4.2 to 3.35. Lt. Moser stated the situation quite clearly in the introduction of his report when he wrote:

“Subsequent to the issuing, in May 1960, of the Military Characteristics pertaining to the LOH, there arose a great deal of controversy with regard to the obtainability of the desired performance in a practical, four-place helicopter configuration with the then prescribed power plant [the Allison T-63 turboshaft engine rated at 250 horsepower at sea level standard and 206 horsepower at 4,000 ft on a 95° F day].”

Based on the NASA wind tunnel results, Lt. Moser used a summary chart showing a drag breakdown to convince industry that the Army target value of 6 square feet was rational. I have reproduced his summary chart here as Fig. 2-140. The Army configuration is illustrated in Fig. 2-141. The full-scale-model test report [341] gives the Run Number 28, Army configuration as:

## 2.5 FUEL EFFICIENCY

“Run 28: Model C with curved element pylon, three-blade articulated hub - disk plane 21 inches above fuselage, streamlined landing skids, F.M. homer, A.D.F. sensor, F.M. communication, V.H.F. communication, V.O.R. split loop, door outlines, door handles, and rotating beacon (mounted behind hub on the pylon).”

The message that the U.S. Army sent to LOH competitors (via Lt. Moser<sup>87</sup>) was loud and clear. The parasite drag area target was 6 square feet—at least at zero fuselage angle of attack. Any discussion about drag increase with nose-down angle of attack, as Fig. 2-142 shows, was quite muted. It is important to note that Lt. Moser’s drag area buildup required faired skid gear to make the target. While the three-blade articulated hub (plus pylon) only accounted for about 1.6 square feet, the difference between faired and unfaired skid gear was 2.4 to 2.6 square feet of parasite drag area.

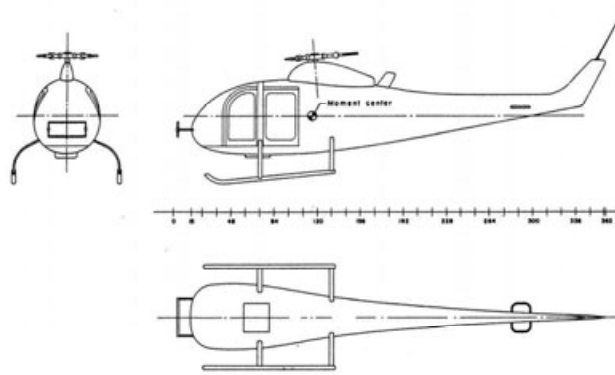


**Fig. 2-141. U.S. Army version of the Light Observation Helicopter [341].**

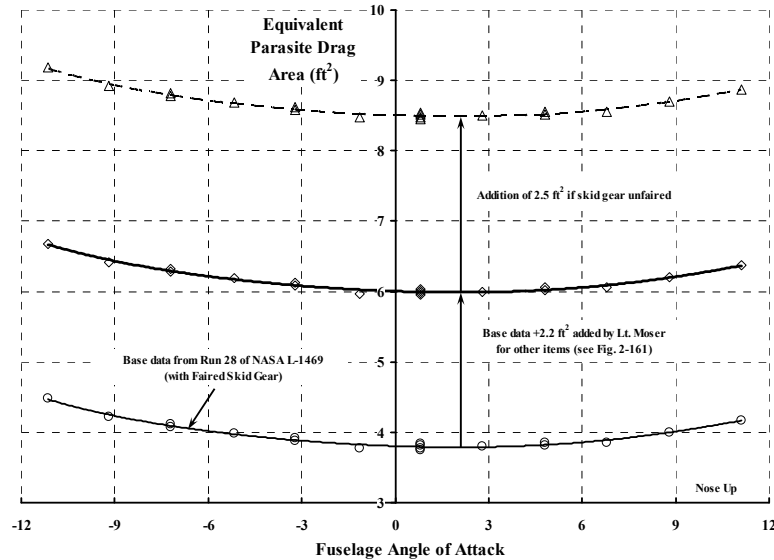


**Fig. 2-142. Parasite drag breakdown for the U.S. Army version of the Light Observation Helicopter.**

<sup>87</sup> Lt. Moser noted at the bottom of the first page of his AHS Journal paper that “the opinions expressed in this paper are those of the author and do not necessarily reflect those of the Department of the Army or any other Government agency.” It is not often you read those kinds of words in the Journal of the American Helicopter Society.

As you read earlier, Hughes won the LOH competition with its YOHO-6. Then finally, in 1968, a complete full-scale helicopter (then an OH-6A) was tested in the NASA Ames 40-by 80-foot wind tunnel. The installation is shown in Fig. 2-143, and note that the test was conducted with the rotor system powered by its own turboshaft engine. The test was primarily directed at measuring stability and control parameters. The test results were published in a Hughes Tool Company Aircraft Division report in May 1970 [343].

Try as I might, I have never obtained a quoted parasite drag area closer than 5.7 to 6.4 square feet for this 2,800-pound LOH winner. Being an optimistic aerodynamicist on this occasion, I choose the 5.7-square-foot number because the skid gear was faired.



**Fig. 2-143. A Hughes OH-6A Light Observation Helicopter installed in the NASA Ames 40- by 80-foot wind tunnel (photo courtesy of Bill Warmbrodt, Ames Research Center).**

## 2.5 FUEL EFFICIENCY

In 1978 Bell Helicopter Textron also made use of the NASA Ames full-scale wind tunnel. Its Model 222, the first Bell helicopter with retractable gear, is shown installed in the tunnel in Fig. 2-144. A 1/5-scale model was tested in the Vought Corporation 7- by 10-foot wind tunnel to clarify tare and interference effects. The full-scale aircraft was not powered. The drag polar that was reported [344] is shown in Fig. 2-145.



**Fig. 2-144. A Bell Model 222 installed in the NASA Ames 40- by 80-foot wind tunnel (photo courtesy of Bill Warmbrodt, Ames Research Center).**

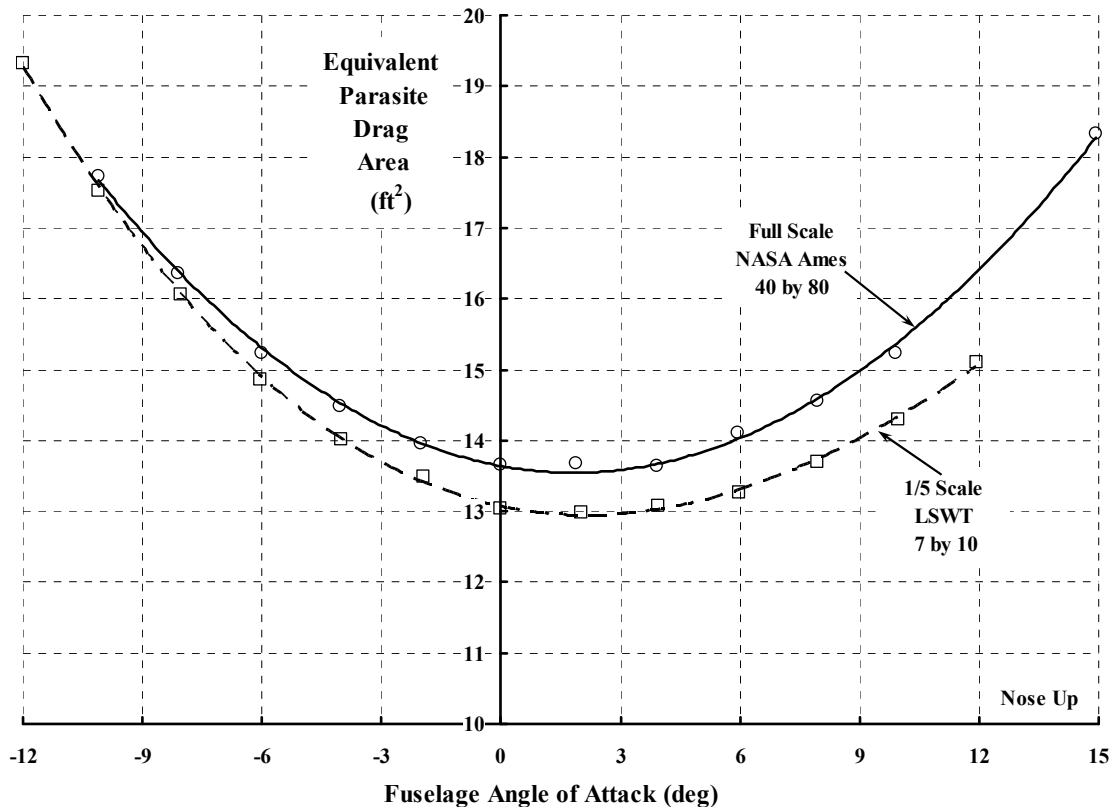


**Fig. 2-145. Bell Model 222 drag polar with gear retracted [344].**

Next the industry had a chance to apply what had been learned up to the early 1970s. First off the U.S. Army sought new utility and attack helicopters to replace the older Bell UH-1 (the Huey) and Bell AH-1 (the Cobra). The competition ultimately led to today's Sikorsky UH-60 (the Black Hawk) and the Hughes AH-64 (the Apache). On the commercial side, Sikorsky came out with the S-76 and Bell started delivery of its Model 222. Both of these commercial products had retractable landing gear. Just as importantly during this decade, the American Helicopter Society created an Ad Hoc Committee on Helicopter Parasite Drag in May 1974. The committee chairman, Bob Williams, delivered the final report on May 14, 1975 [345].

The Ad Hoc Committee report was a compilation of 15 papers authored by top aerodynamic engineers in the rotorcraft industry. To me this collection, plus the supplement of rotorcraft drag bibliography, is of such importance that I have included the key material in Appendix C. The bibliography itself lists over 150 references. Appendix C provides at least a starting point to appreciate the rotorcraft industry's efforts in parasite drag reduction.

By 1990 the industry had created enough products to, in my opinion, truly summarize the parasite drag area progress—even to the inclusion of helicopters with retractable landing gear. My assessment of the progress and state of the art is shown in Fig. 2-146, which adds to the data shown earlier in Fig. 2-139.

## 2.5 FUEL EFFICIENCY

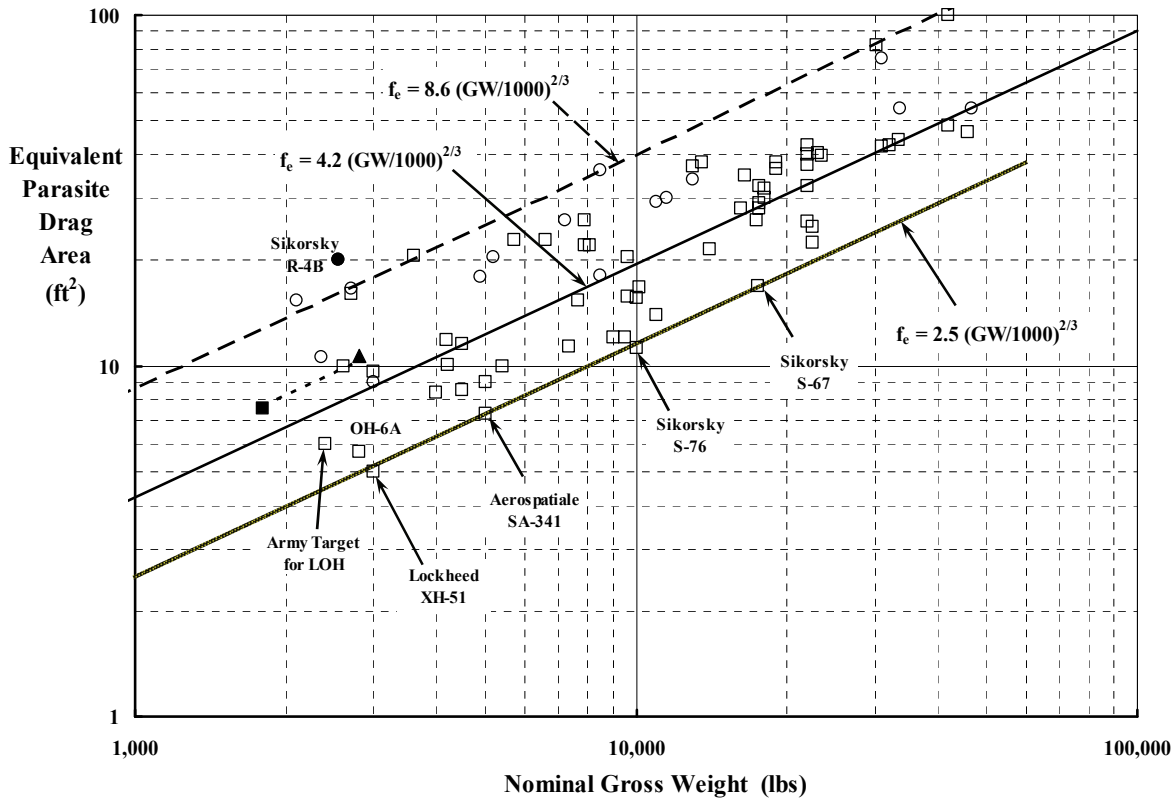


**Fig. 2-146. Reduction in parasite drag area from 1945 to 1980.**

As Fig. 2-146 shows, my assessment is that advanced commercial helicopters with *retractable landing gear* should be able to achieve a parasite drag area on the order of

$$(2.266) \quad f_c = 2.5(GW/1000)^{2/3}.$$

By 1990 the rotorcraft industry saw that retractable gear easily paid for itself. This was a decision point that the fixed-wing industry encountered in the mid-1930s. They responded with the Boeing Model 247 and the Douglas DC-1, -2, and -3. For helicopters below 8,000-pounds gross weight, a retractable skid gear seems worthwhile. For heavier machines, the natural choice is retractable, wheeled gear. Certainly the Lockheed XH-51 (Fig. 2-147) and the Sikorsky S-76 (Fig. 2-148) are prime examples. Time will tell if new utility helicopters such as the AW 101, the NH 90, and the S-92 shown in Fig. 2-149, Fig. 2-150, and Fig. 2-151, respectively, have applied available knowledge. Aerodynamic knowledge abounds (see Appendix C) about streamlining the fuselage, improving engine inlets and exhausts, minimizing protuberances, and sealing gaps, etc. I suggest reading Evan Fradenburg's paper [297] about the Sikorsky S-76, the superb paper about development of the Agusta A-109 [346], and the paper about Westland Helicopter's efforts to set a new speed record of 216.3 knots on August 11, 1986 [347].

Given that airplane lessons can now be applied to helicopters, it seems to me that reducing rotor hub parasite drag area is the next improvement that must be made to raise lift-to-drag ratios to the maximum that industry can hope to obtain with the helicopter.



**Fig. 2-147. The Lockheed XH-51 shows what can be achieved when attention is paid to parasite drag area (photo from author's collection).**



**Fig. 2-148. The Sikorsky S-76 shows what can be achieved when attention is paid to parasite drag area (photo from author's collection).**

## 2.5 FUEL EFFICIENCY



**Fig. 2-149.** The Agusta Westland 101 in a civilian role (photo from author's collection).



**Fig. 2-150.** The NH Industries 90 in a military role (photo from author's collection).



**Fig. 2-151.** The Sikorsky S-92 in a flight test role (photo from author's collection).

### 2.5.3 Rotor Hub Parasite Drag Area

Unlike the streamlined attachment of wings to a fuselage evolved by members of the fixed-wing world, the rotary wing industry has had to deal with a very high drag, mechanically complex attachment—a rotor hub. Jeffrey Jones [348] stated in the 13th Lanchester Memorial Lecture that “the hub is untidy.” Perhaps that is a little too simplistic. As you can see from Fig. 2-152, the rotary wings are indeed attached to a hub, but then the hub is solidly attached to a rotor mast, a rotating component. The rotor mast is an output shaft from a transmission. It is the transmission, finally, that is attached to the fuselage. In a converse sense, the fixed-system controls emerge from the fuselage and attach to the nonrotating ring of the swashplate. The swashplate (recall Fig. 2-44 on page 101 of Volume I) transfers the nonrotating control input to the rotating ring to which the bottom of each pitch link is attached with a rod end bearing. The top of each pitch link is attached to a pitch arm, and thus the pilot’s control motion finally feathers each blade. More than one fixed-wing aerodynamicists has said, “And you want to clean that claptrap up!” Frequently, a rotorcraft designer will respond with, “Maybe you could find some sort of fairing that will cut the parasite drag area in half?” But then the rotorcraft champion will immediately add, “Of course the fairings must permit easy access to all components for a mechanic’s inspection and servicing.”

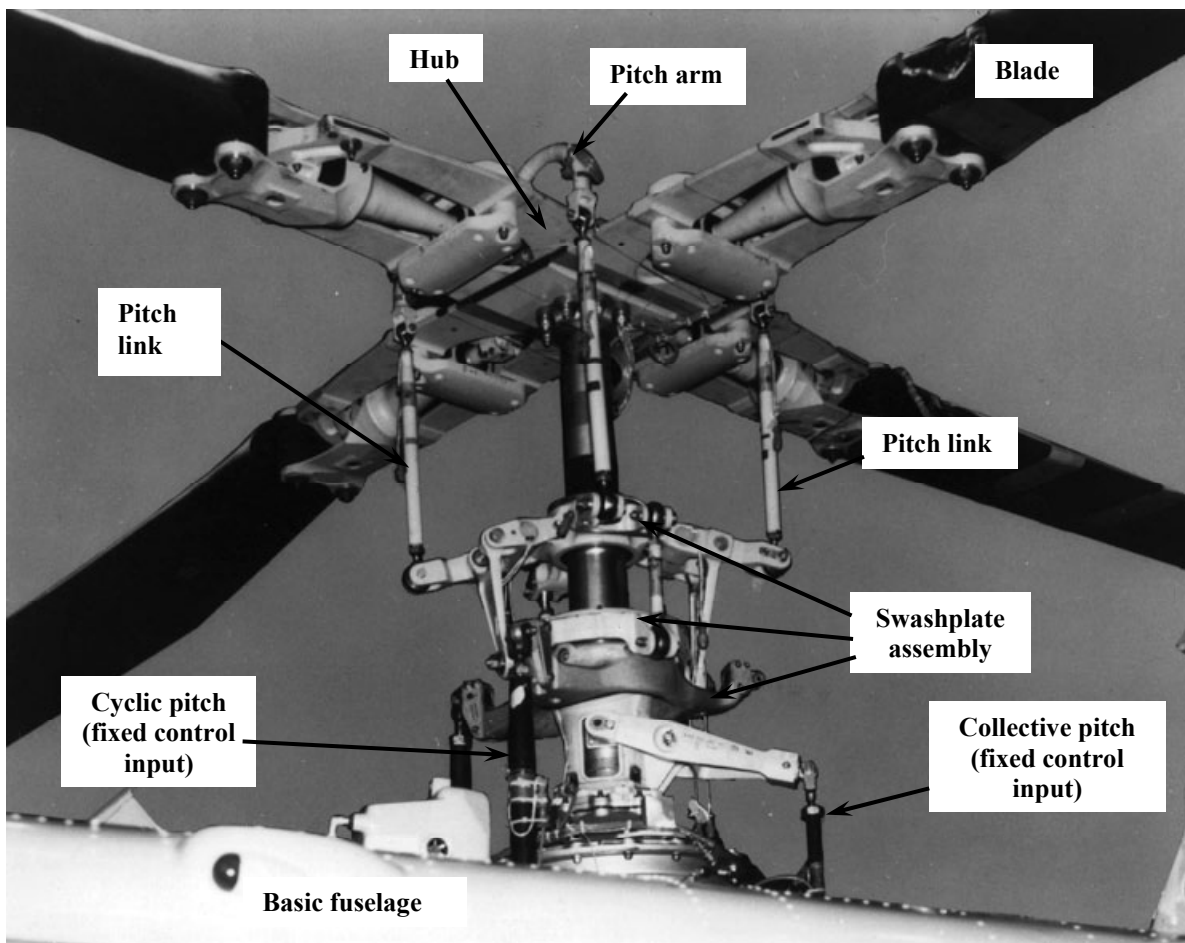


**Fig. 2-152. The Bell Model 412 rotor system with pylon fairing off (photo from author’s collection).**

## 2.5 FUEL EFFICIENCY



**Fig. 2-153. The first step taken in “hub” parasite drag reduction is some sort of pylon fairing (photo from author’s collection).**

A pylon fairing is a natural first step taken to shield some of the components. The Bell Model 412 pylon fairing is shown in Fig. 2-153. When you look at any number of helicopter photos in the popular press and trade magazines, you will invariably see a pylon fairing.

Given a pylon fairing, the question immediately comes up as to what can be done to further reduce the parasite drag area of the hub and control system. One immediate effort began with a wind tunnel test of an all-encompassing fairing around the hub and upper control system of the Sikorsky S-51. This was the first Sikorsky helicopter to be certificated by the Civil Aviation Authority. The wind tunnel test was conducted by the McCulloch Motors Corporation under Air Force contract. A report [349] was published in April of 1955.<sup>88</sup> This effort at fairing was not promising enough to try in flight test.

Two additional efforts at complete fairing were carried through to flight test in the mid-1950s. One was the McDonnell XV-1 [350], a compound helicopter that I will discuss in greater deal in Volume III. The other was the Lockheed CL-475 (Fig. 2-154), which was developed under the inventive direction of Irv Culver at the Lockheed Skunk Works [351].

---

<sup>88</sup> This report is unclassified but restricted to authorized U.S. Government agencies and their contractors. A little over protection I would say since rumor had it that the fairing was a large-diameter spherical enclosure. Because the configuration was so unsatisfactory, I have made no effort to get an unrestricted copy so that a photo could be included in this volume.



**Fig. 2-154. The Lockheed CL-475 was used to demonstrate a bearingless rotor system in 1955. The rotor system was quite well suited to a hub fairing on top of the pylon fairing (photo from author's collection).**

The CL-475 was Lockheed's first venture into the rotorcraft world. The primary purpose of this experimental helicopter was to demonstrate a *bearingless hub* [352, 353], which I will discuss in detail shortly. The rotor hub itself proved worthy of follow-on development and led to the Lockheed XH-51, the very low drag helicopter shown earlier in Fig. 2-147. As you can see, the bearingless hub was carried forward on the XH-51, but the hub fairing was not.

So far the several efforts at parasite drag reduction with hub fairings, including work done in the 1980s [354, 355], were never carried through to production helicopters. In fact, the pylon fairing configuration was more determined by separated flow considerations as they affected tail rotor and empennage vibration than by drag reduction.

However, one experiment that is of note was conducted by the Vertol Division of the Boeing Airplane Company and reported by Ed Gabriel [356] in June of 1962.<sup>89</sup> The question was one of reducing the drag of the blade root ends on the HC-1B helicopter, the prototype of the CH-47. The situation is illustrated in Fig. 2-155. The approach was to use a series of elliptical cross sections. The 1/3-scale-model test was conducted in the University of Maryland's 7- by 10-foot wind tunnel during the week of April 16, 1962 (Fig. 2-156). Ed used Scotch<sup>®</sup> tape to attach Helence nylon tufts and got some terrific flow visualization photos as Fig. 2-157 shows.

<sup>89</sup> I have kept this report all these years because it was a fine piece of experimental work done by Ed Gabriel. Unfortunately, the fairings were never flight tested, which I always thought was an oversight. Obtaining a practical mechanical *and* low-drag rotor hub aerodynamic fairing is, in my opinion, a very, very difficult engineering task.

## 2.5 FUEL EFFICIENCY

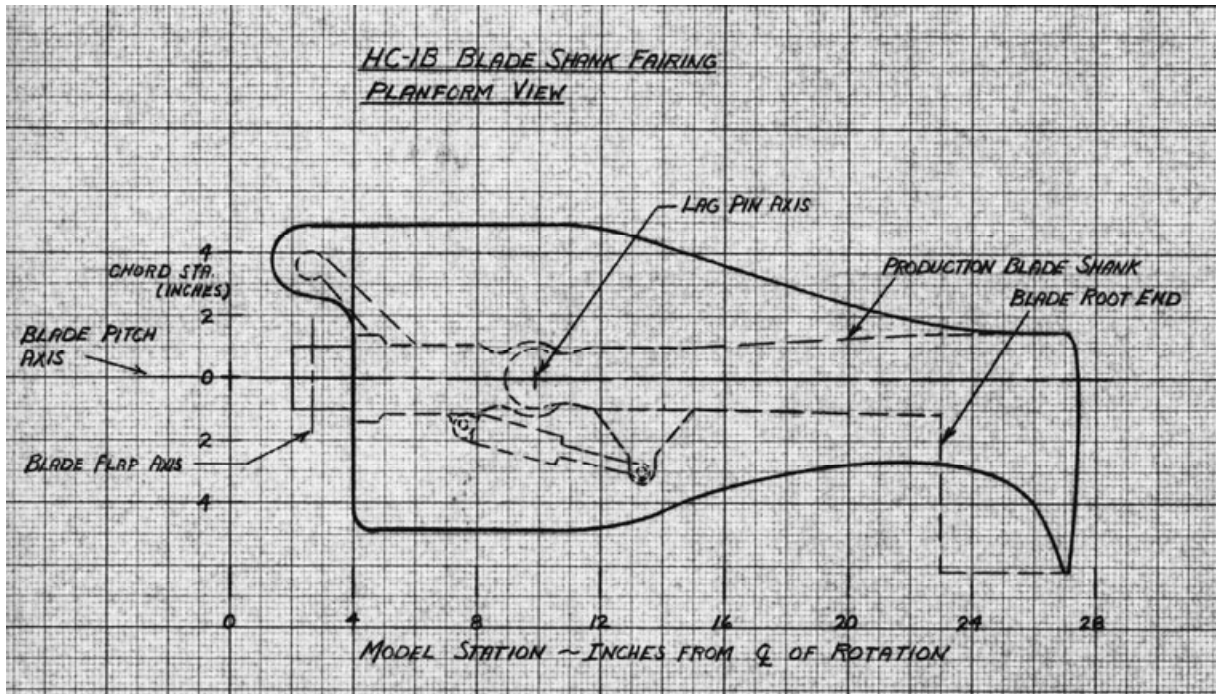


Fig. 2-155. A blade shank fairing tested in 1962 [356].

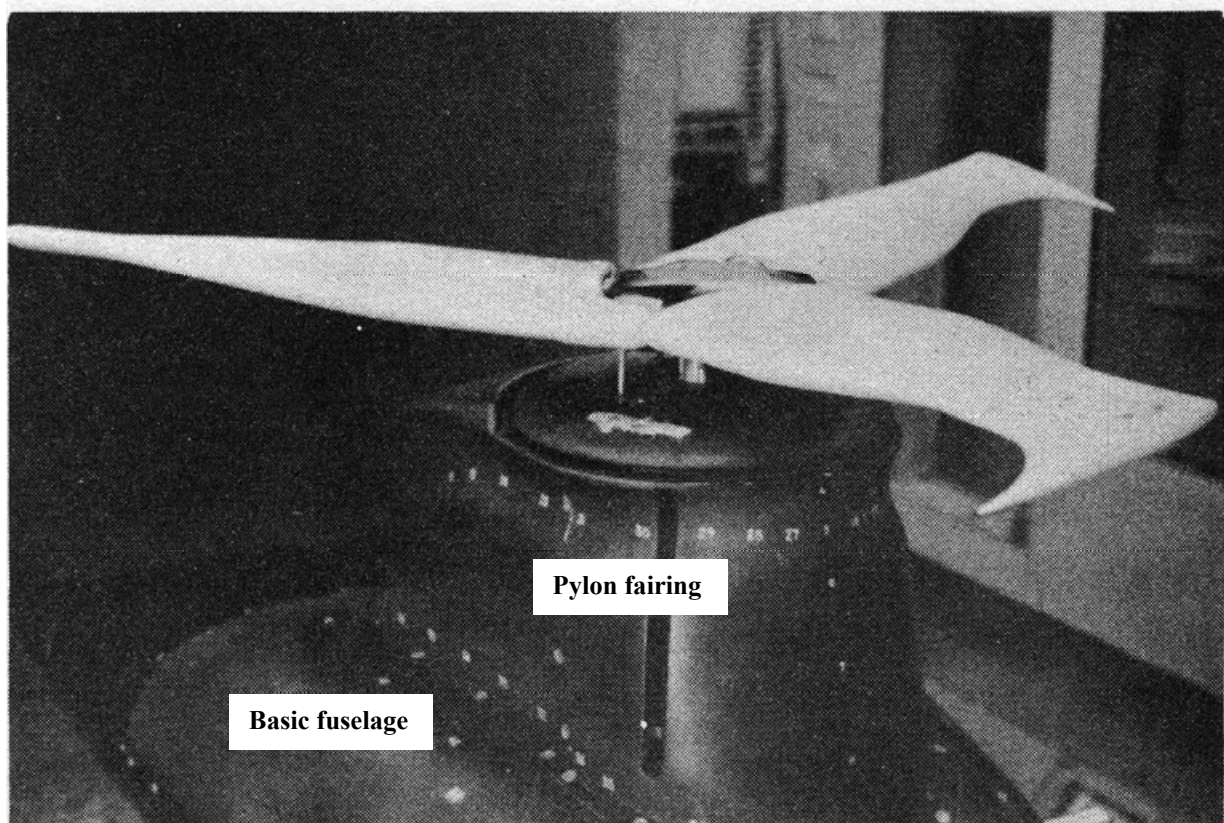


Fig. 2-156. The 1/3-scale model of a CH-47 in the University of Maryland wind tunnel [356].

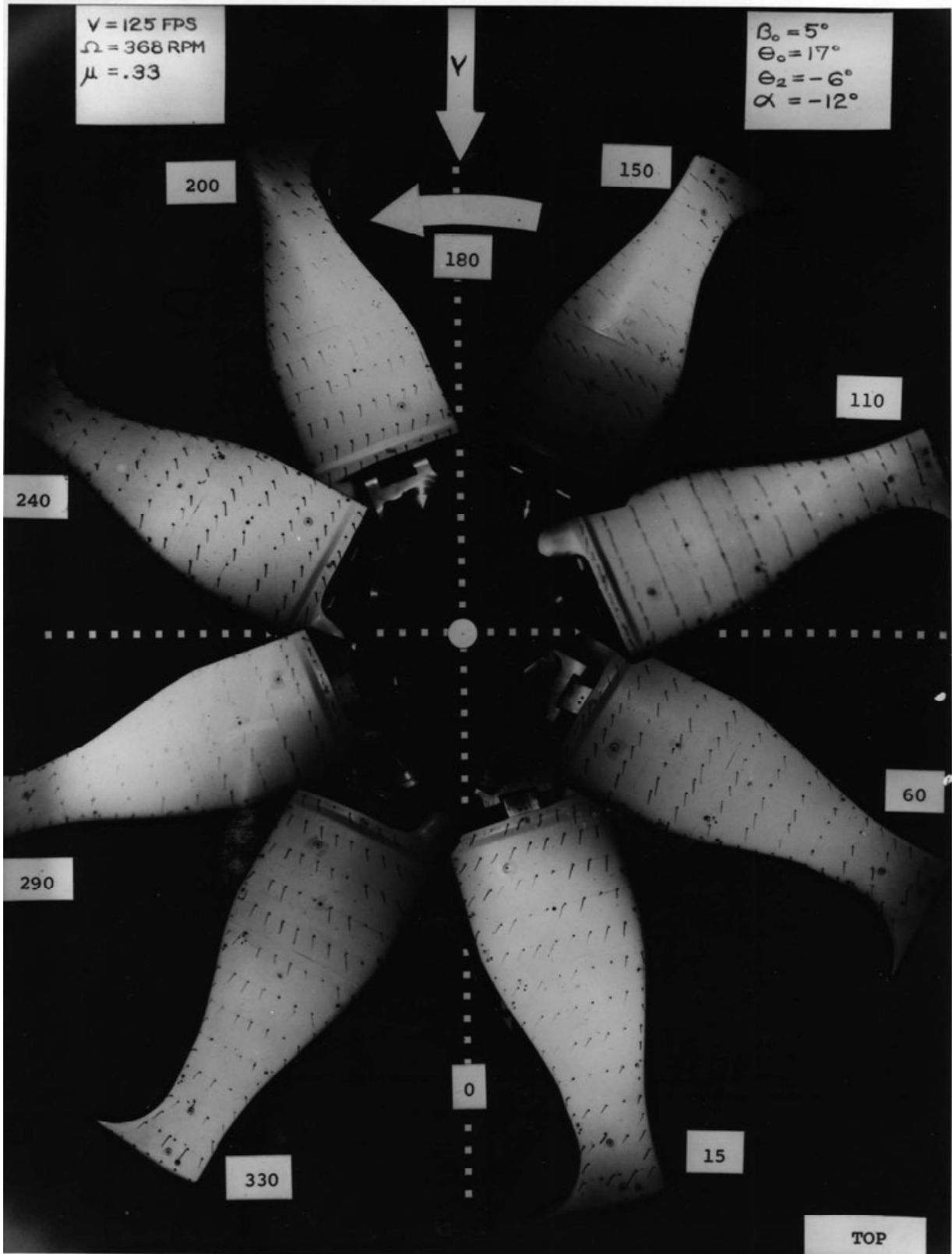


Fig. 2-157. Tufts showing flow angularity [356].

## 2.5 FUEL EFFICIENCY

Searches for a fairing around the root of a blade to reduce shank drag were ongoing well into the late 1980s. In this decade, the U.S. Army Research and Technology Laboratories located at Ft. Eustis, Virginia, joined with NASA Ames Research Center to develop an Integrated Technology Rotor/Flight Research Rotor (ITR/FRR) [357]. As part of that effort, some members of the aerodynamic staff at Bell Helicopter Textron, led by Phil Alldridge, performed a wind tunnel test to compare potential cuff (or shank, or blade inboard radial section if you prefer) fairings for their ITR [358]. Phil concluded that elliptical airfoils offered the least drag at high speed.

Now let me address the hubs themselves. The first thing to know is that many, many different hub types have reached flight test and even production status. Many, but hardly all, of them are illustrated in Appendix D. This collection of hub types has been compiled from my own files and three other sources:

1. Bill Bousman's collection [359]. Bill collected photos of many hubs from several manufacturers. Then he had the NASA Ames graphic arts department create line drawings on vellum. He had the drawings framed. They were mounted on the second floor wall in building 215 at the NASA Ames Research Center. At my request, Bob Ormiston's secretary, Pat Horn, had 8-1/2- by 11-inch copies made, and Pat sent the beautiful artwork to me in June 1993. They are included in Appendix D.
2. Schindler and Pfisterer's AGARD paper [360], which I consider an exceptionally thorough piece of work. These two men classified hub types as shown here in Fig. 2-158.
3. Tom Hanson's small, extremely valuable book titled *A Designers Friendly Handbook of Helicopter Rotor Hubs*, which he published himself [361].

The paper by Schindler and Pfisterer [360] captures the major focus of rotor system hub designers as Fig. 2-159 shows. Schindler and Pfisterer also concluded that rotor hub weight as a percentage of nominal gross weight dropped from about 7 percent to about 2 percent over three decades. A particularly important improvement along the way was the development and recommended application of elastomeric bearings by the Lord Manufacturing Company. Fig. D-2 and Fig. D-11 in Appendix D give you some idea of how shim stock plus rubber laminates can replace complicated roller or needle bearing assemblies to provide blade articulation in flap, lag, torsion, and centrifugal force reaction. Mosinskis and Schneider of the Vertol Division of the Boeing Company showed [362] quite specifically that a CH-47 hub parts count was reduced from 408 parts to 48 parts, and the need for lubrication relative to 233 parts was reduced to zero. The successful application of elastomeric bearings was a stunning breakthrough and spread throughout the rotorcraft industry rather quickly.

Despite their design differences, few, if any, rotor hub designers have been able to incorporate aerodynamic attention to parasite drag reduction. The emphasis ever since the demonstration of the autogyro nearly eight decades ago has been on a design philosophy "that

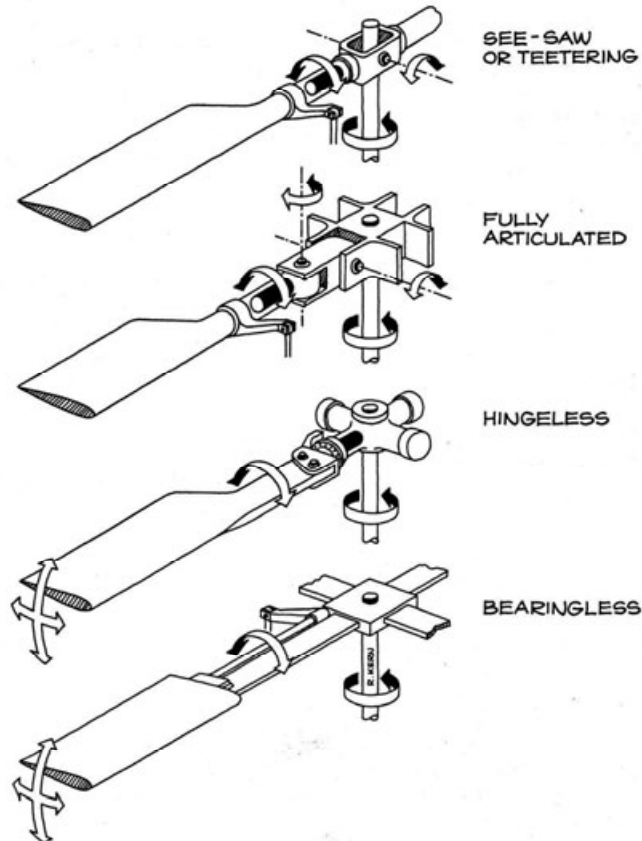


Fig. 2-158. The four basic hub configurations developed between 1936 and 2010 [360].

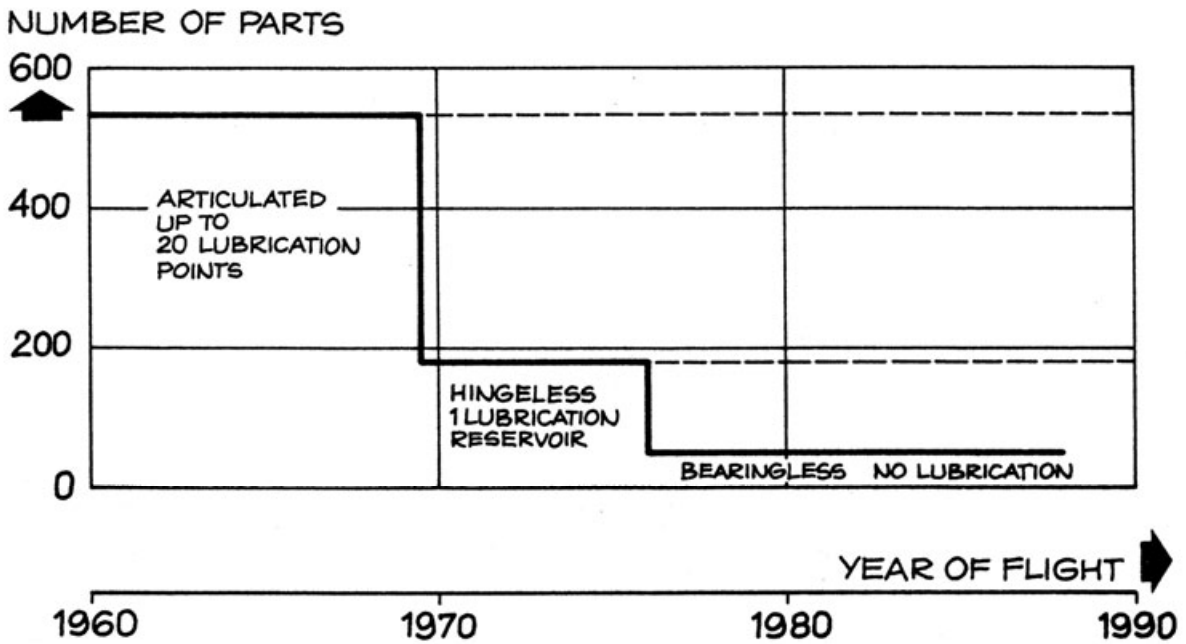


Fig. 2-159. Emphasis on reduced parts count and improved maintainability has been the primary focus of rotor system hub designers [360].

## 2.5 FUEL EFFICIENCY

thou shall not fail.” Beyond that, the design effort has been on improving reliability, extending times between overhaul, decreasing maintenance, lowering parts count, lowering cost, improving flying qualities, and not introducing aeroelastic instabilities.

The problem in achieving a low-drag hub is all wrapped up, primarily, in the feathering motion a hub must provide for a blade that exerts an enormous centrifugal force. A secondary factor is the blade-to-hub attachment joint that generally requires some provision for blade folding. These two features dictate the frontal area of all hubs that I know of. To illustrate this very important primary point, consider Fig. 2-160, which comes from Tom Hanson’s book [361]. Three of the five ways (b, c, and d) to provide blade feathering motion under centrifugal load have the frontal area set by the diameter of the pitch housing. In fact, the twistable straps illustrated in Fig. 2-160 (a) give the initial impression that a very low frontal area has been achieved. However, a close look at the Hughes OH-6 hub in Appendix D, Fig. D-29, shows that a large-diameter pitch housing is required to control blade angle. This is also true for the Hughes (then McDonnell and now Boeing) AH-64 rotor hub, an enlargement of the OH-6 approach. Furthermore, lead-lag motion is accommodated with a vertical pinned hinge, and lead-lag dampers are required.

The first hingeless rotor hub was developed by E. Burke Wilford and flown on his 1932 autogyro. You read this story in Volume I, starting on page 73. An excellent photo of the hub was shown in Volume I, Fig. 2-35. The second hingeless hub (see Appendix D, Figs. D-37, 38, and 39) was developed for the then Messerschmitt-Bölkow-Blohm BO-105, which made its first flight in February 1967.<sup>90</sup>

This brings me to the bearingless main rotor (BMR) hub<sup>91</sup> shown by Hanson in Fig. 2-160 (e). The illustration is also representative of several bearingless tail rotor hubs. The first BMR was created by Fred Doblhoff and Kurt Hohenemser, who were the core of a Helicopter Group within the McDonnell aircraft company. They came up with a compound helicopter—the XV-1 shown in Fig. 2-161. Note that both pylon and hub fairing drag-reduction aerodynamic technology was applied in this early 1950’s machine. The XV-1 stiff inplane hub configuration is seen in Appendix D, Figs. D-42, 43, and 44. The second BMR was invented by Irv Culver [363] and tested on the Lockheed CL-475 (Fig. 2-154, and Appendix D, Fig. D-34). The follow-on was the Lockheed XH-51 bearingless hub [364], shown in Appendix D, Fig. D-35. Then in November 1975, the Boeing Vertol Company submitted a proposal to the U.S. Army Air Mobility Research and Development Laboratory (AVLABS) at Ft. Eustis, Virginia. This proposal was well received and a contract (DAAJ02-76-C-0026) was awarded in June of 1976. The Boeing Vertol BMR (Appendix D, Figs. D-16 and D-17) was designed, fabricated, and tested on a BO-105 [365-368].

---

<sup>90</sup> The 5,500-pound normal gross weight BO-105 was the first light helicopter to have twin engines. A key engineering figure who got the BO-105 into a production run of over 1,400 helicopters was Günter Reichert. When we first met in Brussels for a week-long course on rotorcraft held at the Von Karman Institute in 1973, we cemented our relationship by exchanging sons for a few weeks in the summers of 1974 and 1975.

<sup>91</sup> Evan Fradenburgh, a key drag-reduction advocate during the development of the Sikorsky S-76 [297], made a comment to me at the 34th AHS Forum in 1978 that I have never forgotten. He said, “What’s wrong with bearings?” I do not think Evan was in favor of the bearingless hub.

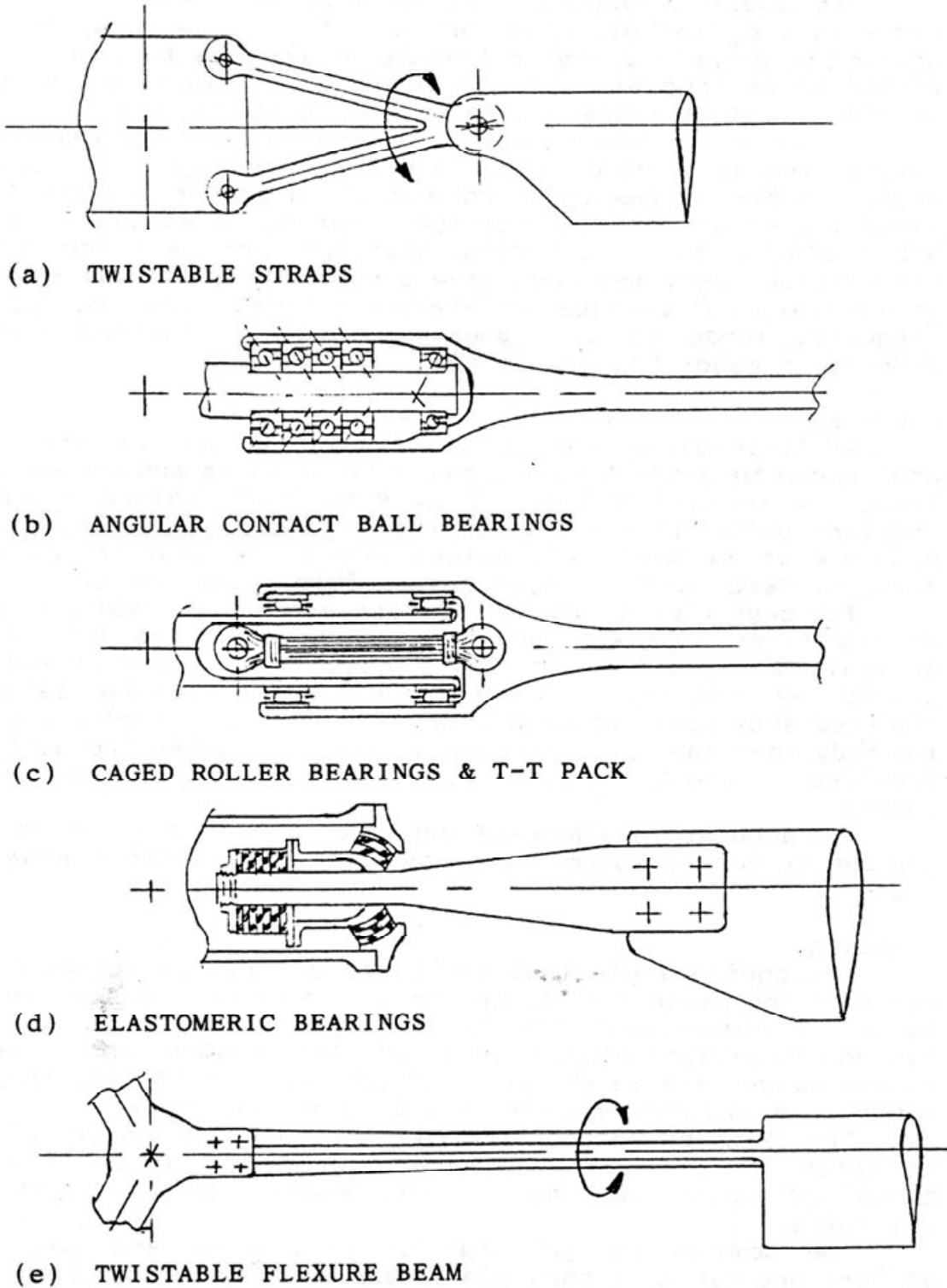


Fig. 2-160. Five ways of accommodating blade feathering under a centrifugal load. Note that the actual components required to feather the blade are not shown [361].

## 2.5 FUEL EFFICIENCY



**Fig. 2-161. The first liftoff of the XV-1 (Feb. 1954) was followed by the first official flight in July 1954. The XV-1 was free of aeroelastic instabilities, but aircraft drag was greater than predicted despite efforts during 1952 testing in the NASA Ames Full-Scale Wind Tunnel [350]. (Photo courtesy of David Peters from Kurt Hohenemser's files.)**

The upshot of the Lockheed and Boeing Vertol BMRs was rotor systems of marginal aeromechanical stability that precipitated additional experiments [369]. In short, neither configuration had lead-lag dampers, and the damping provided by aerodynamic and structural forces was insufficient for a production helicopter. The difference between the modern BMRs and the more successful XV-1 of the early 1950s was that the XV-1 was stiff inplane and the modern versions were soft inplane. The words stiff and soft refer to the natural frequency in the first lead-lag mode as was discussed in Volume I.

As the industry continued with BMR development,<sup>92</sup> the torque tube approach to control blade feathering by Lockheed and Boeing Vertol was replaced with a large pitch housing frequently called a cuff. The cuff was designed to carry some lead-lag motion to a snubber/lead-lag damper. The Bell Model 680 BMR shown in Appendix D, Fig. D-15, is an adequate example. This inboard component is nothing more than a variation on a blade root end fairing. The cuff and snubber/lead-lag damper arrangement made the Hughes' rotor from the Hughes' Advanced Rotor Program (HARP) work on its Model 500E; the Bell 680 rotor worked on its Model 430, UH-1Y, and AH-1Z; and the Sikorsky BMR rotor [371] worked on its RAH-66. Huber relates this progress in his very thorough paper, *Will Rotor Hubs Lose Their Bearings?* [370]. While considerable progress was made by aeroelasticians [372-375], there was no hub parasite drag reduction with any of the BMRs as far as I know. In fact, I dare say BMRs increased hub parasite drag.

---

<sup>92</sup> An excellent paper recounting nearly all the industry's BMR efforts was written by Helmut Huber [370] and published in 1992. He followed in Günter Reichert's footsteps at Messerschmitt-Bölkow-Blohm (MBB), which then became Eurocopter Deutschland GmbH. Helmut's paper actually uses the words "drag reduction" in a number of places.

With the preceding synopsis of rotor hub development, let me go back to 1959. In February of that year, Gary Churchill and Robert Harrington at NASA Langley published a report about their measurements of rotor hub drag [376]. The five hubs were tested on a long shaft sticking up from a very streamlined body. There was no pylon fairing, which minimized body-to-rotor-hub interference. Their summary results shown in Fig. 2-162 indicated that the primary variable was hub frontal area.

Churchill and Harrington's "available to all" experiment initiated a ground swell of experimenting all through the 1960s and well into the 1970s. Both model and full-scale testing was in full swing. This led to the 1975 Ad Hoc Committee's report [345] on rotorcraft drag submitted to members of the American Helicopter Society as mentioned earlier. By mid-1978, the Boeing Vertol Company [377] and Sikorsky Aircraft [378] had begun to quantify hub drag, pylon/hub interference drag, exposed control system drag, and rotor mast (or shaft) drag. In March of 1978, Chuck Keys and Hal Rosenstein of Vertol published what many thought was a summarizing bible on hub drag. Their report [379] showed that this member of the rotorcraft industry had 23 internal memos about experiments conducted between 1953 (with a full-scale H-21 hub) and 1974 (with a 1/12-scale of a heavy-lift helicopter hub). Much of this work was supported by NASA and the U.S. Navy and Army. Keys and Rosenstein included MBB's fruitful work with an elliptical fairing on the BO-105 hingeless main rotor hub [380], which is shown in Fig. 2-163.

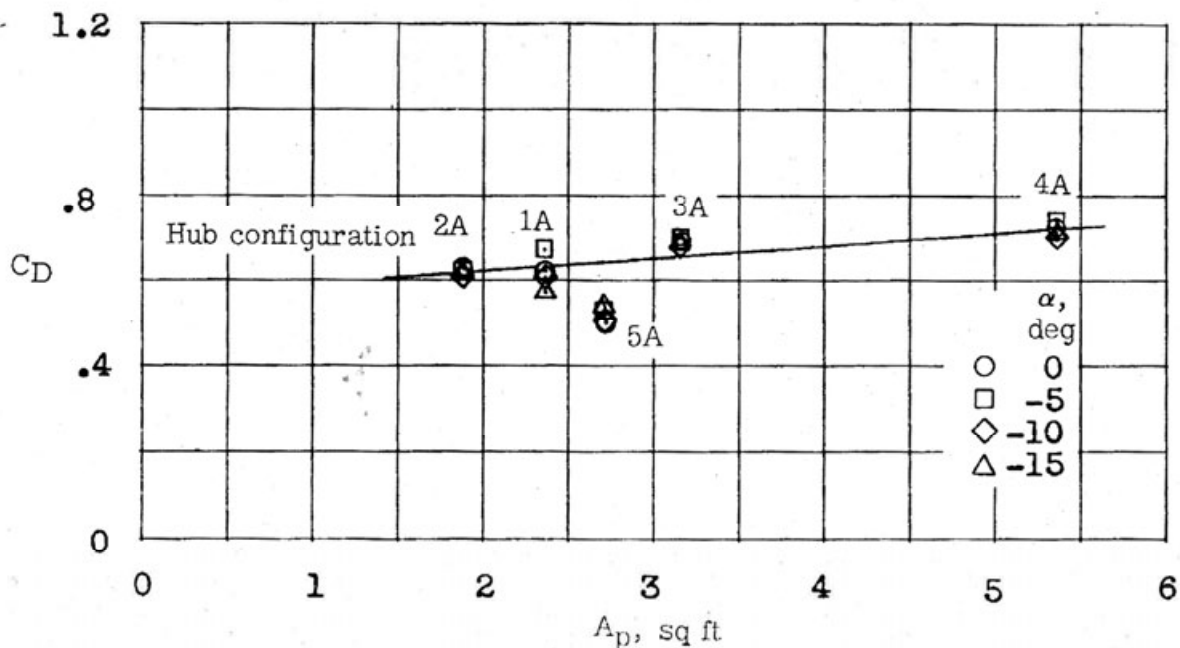


Fig. 2-162. By 1959 the industry began to relate rotor hub drag to hub frontal area although the drag coefficient did appear to be dependent on hub configuration [376].

## 2.5 FUEL EFFICIENCY



**Fig. 2-163. The BO-105 hingeless rotor hub reduced parasite hub drag by 1.1 square feet based on power-required measurements. No treatment of the blade root ends was applied (photo from author's collection).**

In the Sikorsky report [378] submitted by Tom Sheehy, Tom extended Churchill and Harrington's summary, Fig. 2-162, and boldly suggested that the drag of unfaired hubs trended as

$$(2.267) \quad f_e = A_p (0.582 + 0.0349A_p - 0.00057A_p^2).$$

It may be splitting hairs with Sheehy's figure 3 data, but my review of his unfaired hub parasite drag (shown in Fig. 2-164) suggests that

$$(2.268) \quad f_e = A_p (0.4618 + 0.0719A_p - 0.0024A_p^2).$$

This may adequately represent the majority of large, frontal area hubs presented in Appendix D. To this 1977 state of the art represented by Eq. (2.268), one must add 25 percent for all interferences and then another 15 percent for everything not accounted for. In my opinion, a conservative estimate of the hub drag, when operating with blades attached and installed on an operational helicopter, would be to just increase the hub parasite drag area given by Eq. (2.268) by 50 percent.

From the latter half of the 1970s on up to the turn of the century, the rotorcraft industry concentrated on incorporating bearingless main rotor hubs onto production helicopters and improving hingeless main rotor hubs. Helicopters such as the UH-60 and AH-64 were brought to production for the U.S. Army, and new commercial helicopters were brought to the market place. Ames Research Center continued exploration of hub fairings and fairings suited to bearingless and hingeless hubs. To me, it seemed like a 20-year lull in hub drag reduction.

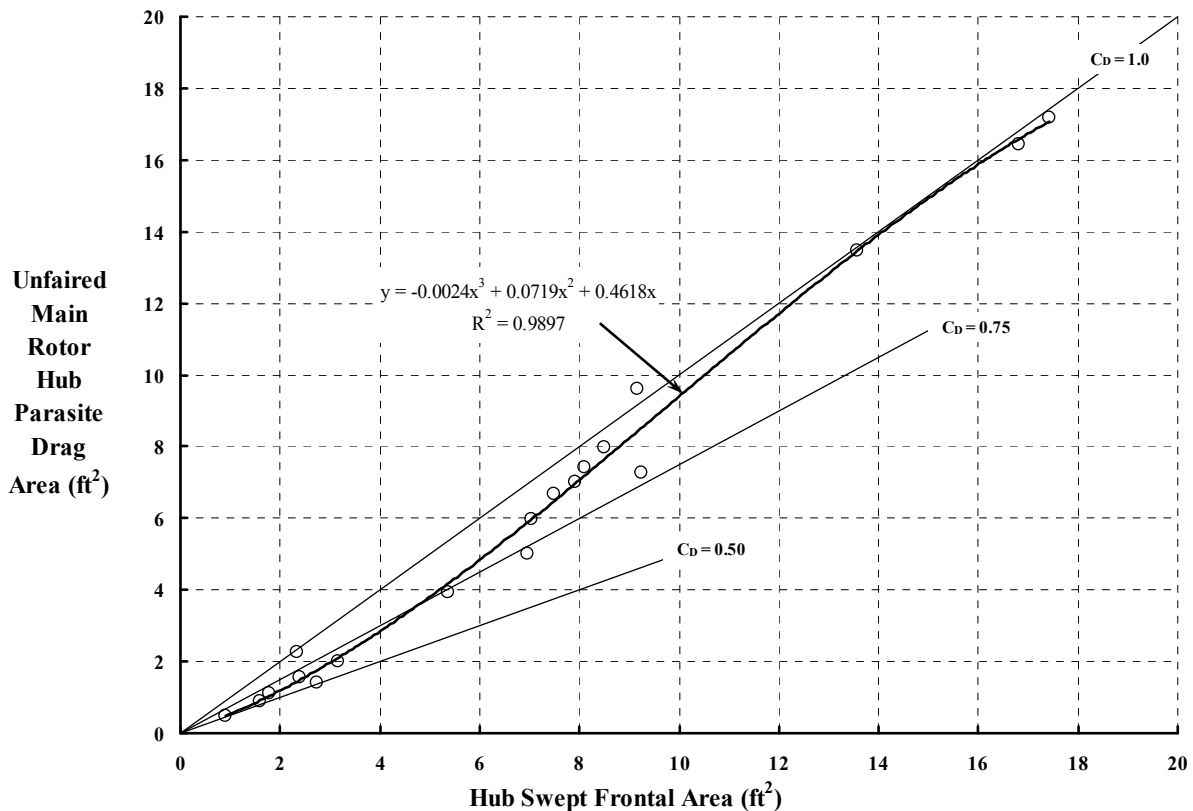


**Fig. 2-164. By 1977 rotor hub drag (before accounting for hub/pylon interference) suggested that the lowest drag would come when inventors and designers reduced hub frontal to zero!**

In fact, there really was not a lull because Larry Young, Bob Stroub, and their small team at Ames Research Center kept hub and pylon drag reduction research going. In 1989 they published results from a definitive experimental study of hub fairings [355]. In 1993 NASA and Bell Helicopter Textron conducted a joint hub and pylon drag reduction program. A 1/5-scale model of the Bell 222 with the blade cuffs of a Bell 680 bearingless rotor (Appendix D, Fig. D-15) was tested in the NASA Ames 7- by 10-foot wind tunnel as shown in Fig. 2-165. The reported experimental results [381] led to the conclusion that “the total model drag was reduced by 20.8 % as compared to the unfaired rotor hub and mast configuration” shown in Fig. 2-165. Roughly speaking, hub-plus-pylon-plus-cuff parasite area drag could be reduced at least 1.5 to 2.0 square feet below what Bell was contemplating in full scale. Unfortunately, a flight research program was not conceived, but improvements did find their way onto the Bell Model 430 with its 680 bearingless rotor system as shown in Fig. 2-166.

This discussion about hub parasite was summarized by Evan Fradenburgh in his 1994 Nikolsky Lecture [382]. Evan related hub fairings and pylon tailoring testing at Sikorsky. He included the rotor head fairing for the Sikorsky S-67, Fig. 2-167, which set a world speed record of 191.9 knots in December 1970. This effort, along with wind tunnel testing on an S-61 hub and pylon [383], led Evan to write in 1995:

## 2.5 FUEL EFFICIENCY



**Fig. 2-165.** A 1/5-scale Model 222 with blade root end cuffs simulating the Model 680 rotor system was the baseline for a NASA/Bell hub and pylon drag reduction effort (photo courtesy of Larry Young).



**Fig. 2-166.** The Bell Model 430 used the Model 680 bearingless rotor system. Some aerodynamic attention was given to the pylon shape, but no hub fairing was used. The Bell Model 430 could be bought with retractable gear or a nonretractable skid gear (photo from author's collection).

“Some of the more modern rotor heads for an aircraft of this size [S-61] are better, but not by a lot. Even the latest “bearingless” rotor head designs, while certainly simpler in terms of parts count, have large frontal areas and do not represent any aerodynamic improvement....The downside [to the S-61] concept was that it added weight, complexity, and made rotor head maintenance checks difficult.”

After 1995 through to 2009, the literature is virtually devoid of pylon and hub parasite drag reduction discussions.<sup>93</sup> For that matter, I found no new data points to add to the trends shown in Fig. 2-168. It seems that aerodynamicists know what to do, but trying to make a “silk purse out of a sow’s ear” does not satisfy the rotorcraft industry. Unlike retractable landing gear, the tradeoff of weight, complexity, and maintenance for drag reduction by fairing virtually all of the large frontal area hubs in Appendix D is not a serious consideration. I say *virtually all* because there are two hubs that have the lowest frontal area that need further discussion. These hubs are called simply doorhinge hubs.

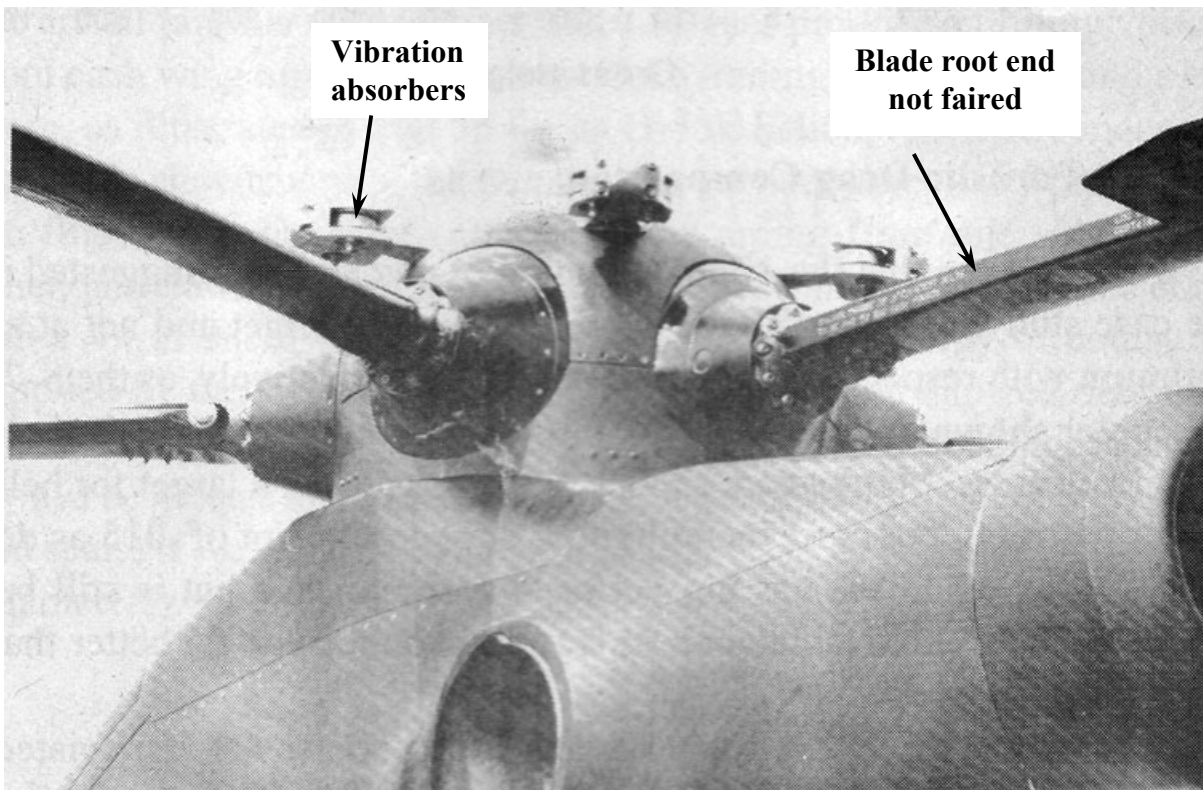


**Fig. 2-167. The S-67 pylon and hub fairing. This aircraft achieved 192 knots in level flight in 1970 and held the speed record for 8 years. Note that no fairing of the blade root end (or shank) was incorporated. Note also that the S-61 bifilar vibration absorbers were not removed [382].**

<sup>93</sup> I say virtually devoid because the one exception I found [384] was wind tunnel testing by the Fuji Heavy Industries company in support of the Fuji Bearingless Rotor for the Kawasaki OH-1 armed observation helicopter, which first flew in August of 1996. The tunnel testing was conducted with 1/4-scale models using the Bell Model 412 hingeless hub as the baseline.

## 2.5 FUEL EFFICIENCY

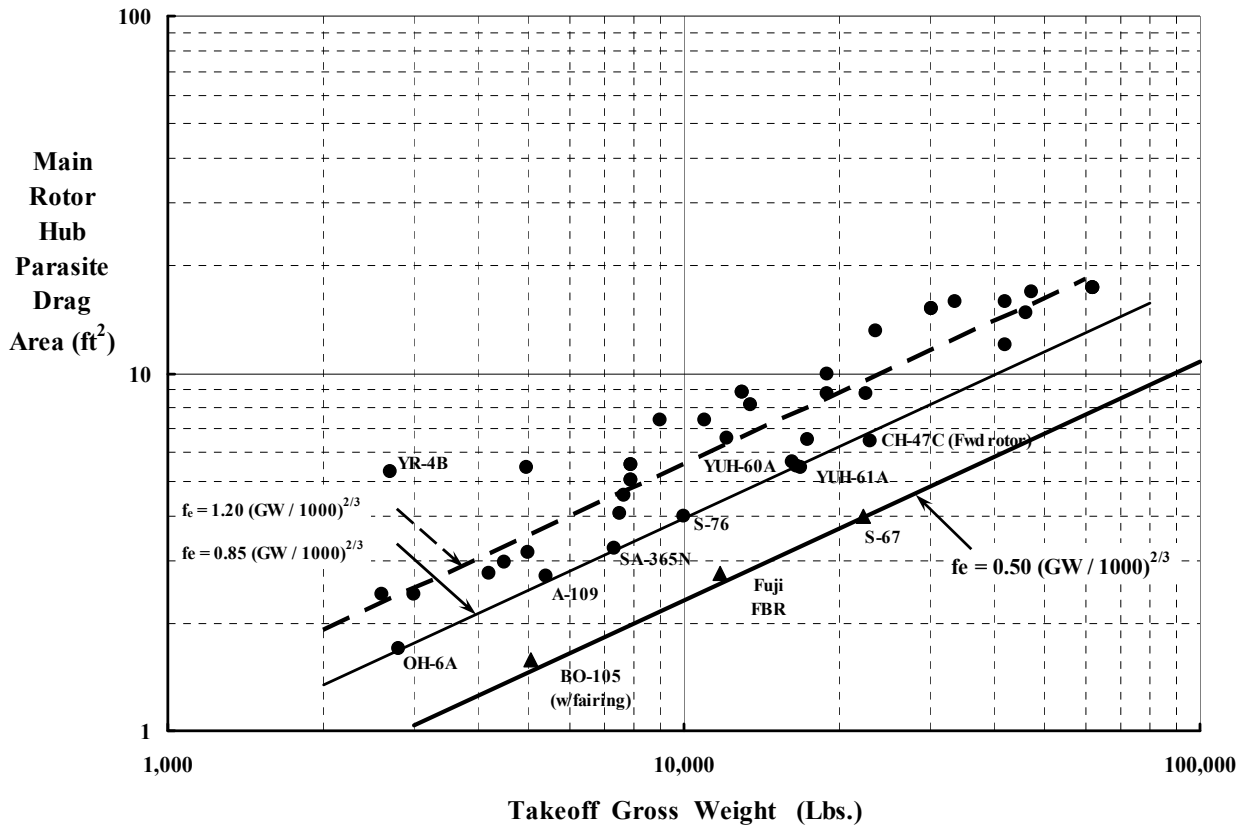


Fig. 2-168. Harris hub drag perspective in 1998.

### 2.5.4 The Doorhinge Rotor Hub

The doorhinge rotor hub was invented by Bob Metzger in the early 1960s. Bob was a key member of the Bell Helicopter engineering department. The configuration is shown in Fig. 2-169. Bob and Jan Drees received a patent (U.S. number 3,280,918) on October 25, 1966. Bob Lynn notes in the 37th Cierva Memorial Lecture he delivered to the Royal Aeronautical Society in October 1996 [385] that “the airframe of this formidable configuration [the UH-1B Huey gunship] was later improved to the UH-1C model [in service September 1965] with the introduction of the ‘doorhinge rotor.’ The new rotor was needed for the higher gross weight required by the machines’ new role.” Bob Lynn adds in a footnote that “Robert Metzger, the inventor/developer of the [doorhinge rotor] system named the design ‘doorhinge’ much to the chagrin of the marketing people, because that is where he got the idea of how to increase the rotor’s inplane stiffness.” The Bell doorhinge rotor hub, Fig. 2-169, was designed around the teetering rotor approach.

The doorhinge concept found another advocate rather quickly. The advocate was the Lockheed Corporation. In late 1965 the U.S. Army awarded a contract to Lockheed for an Advanced Aerial Fire Support System (the AAFSS). In winning the competition for an advanced gunship to replace the Bell AH-1 fleet, Lockheed applied the doorhinge concept to a

stiff inplane, hingeless rotor hub for its AH-56 (Fig. 2-170). This aircraft, named the Cheyenne by the U.S. Army,<sup>94</sup> flew first in September 1967. The normal gross weight of the AH-56 was 18,300 pounds with a maximum takeoff weight of 25,880 pounds. It demonstrated 215 knots in level flight and reached 245 knots in a dive.

The AH-56 was a very promising aircraft, but the program was cancelled. There is no better summary of Lockheed's venture into rotorcraft than what Ray Prouty and Al Yackle published in 1992 [386]. Their paper is, in my opinion, a factual account written in a very straightforward manner. As they recount, the aircraft experienced control-system problems with its initial configuration. The problems were found and ultimately fixed, but not fast enough to satisfy the Department of Defense and the U.S. Army. Lockheed itself was experiencing problems in several other major program areas. The outcome was a new start by the U.S. Army that yielded the Hughes AH-64 Apache<sup>95</sup> and ultimately, in 1995, the merger of the Lockheed Corporation with Martin Marietta.

As you can see from Fig. 2-171 and Fig. 2-172 (plus other details included in Appendix D), the Lockheed hub was simplicity itself—and it minimized the frontal area because of the doorhinge concept and the compact tension-torsion arrangement necessary for blade retention against centrifugal force. A gyro system was mounted above the rotor hub in the initial AH-56 configurations. The gyro added mechanical stability augmentation improvement to flying qualities.



**Fig. 2-169. The Bell doorhinge rotor hub was invented and developed by Robert Metzger, and patented in October 1966. It was an integral part of the Bell AH-1 Cobra fleet (photo courtesy of Burkhard Domke via Troy Gaffey).**

<sup>94</sup> The Lockheed AH-56 was not a pure helicopter. It was, in fact, a compound helicopter, which I will discuss in more detail in Volume III.

<sup>95</sup> There were several lessons learned during the AH-64 program that were recorded by Ken Amer, Ray Prouty et al. [387]. Ken notes that the paper was written in 1987, but the DOD delayed release until 1992.

## 2.5 FUEL EFFICIENCY



**Fig. 2-170.** The AH-56 was a compound helicopter. The gyro above the hub created rotor control problems in the original design. A pusher propeller and wing were used for forward flight. The landing gear retracted aft (photo from author's collection).



**Fig. 2-171.** A revised control system called the Advanced Mechanical Control System left a spider on top of the hub and put the gyro below the transmission [386]. All control rods went up through the main rotor shaft (photo courtesy of Barry Lakinsmith, AFDD).

As I come to the end of this discussion, and with Appendix D and Fig. 2-173 in front of me, I am convinced that the Lockheed stiff inplane, hingeless rotor evolved in the late 1960s gets my vote as the winner. It deserves to be resurrected, improved with advanced materials, redesigned perhaps, built, wind tunnel tested, and for sure, flight tested.

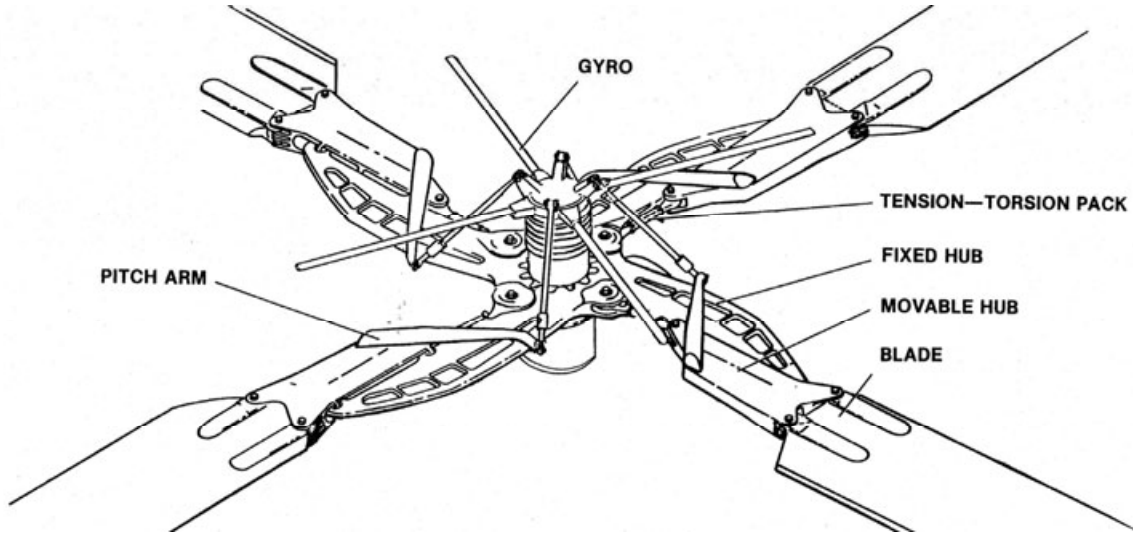


**Fig. 2-172. The Lockheed hingeless hub as used on the AH-56. A control gyro was mounted on top of the hub for mechanical flight stability (courtesy of Bill Bousman).**

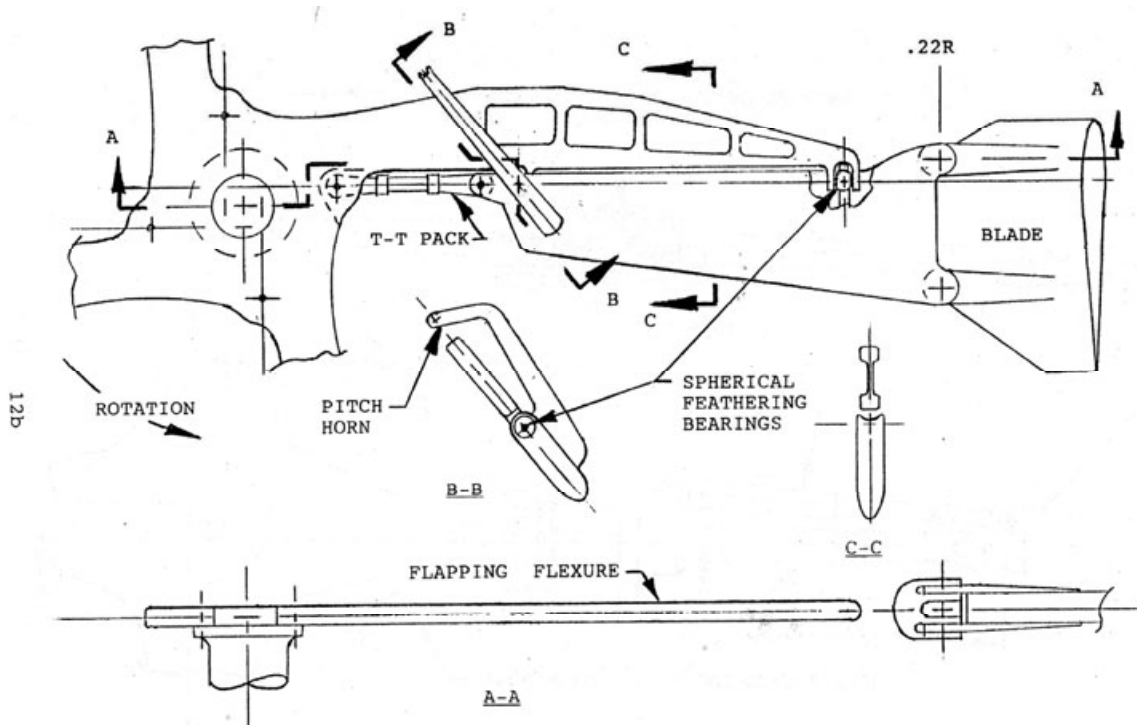


**Fig. 2-173. Tom Hanson's drawing of the Lockheed hingeless hub with the gyro system removed [361]. The pitch horn could easily be trailing as Fig. 2-171 shows.**

## 2.5 FUEL EFFICIENCY

### 2.5.5 Closing Remarks

This discussion of fuel efficiency, aircraft lift-to-drag ratio, and equivalent parasite drag area would be incomplete if two other points were not addressed more thoroughly.

First reconsider Fig. 2-146 on page 292 for a moment. There are a moderate number of data points showing equivalent parasite drag area as a function of a nominal gross weight. A few of the points were obtained by drag estimating methods. A few more have come from scale model testing in a wind tunnel, but the majority have come from flight test. Of course each point can be criticized if for nothing more than being associated with the wrong gross weight. Beyond that, time after time scale model testing has led to an optimistic result, and a drag buildup by calculations based on similarity has frequently been just as optimistic. Finally, an equivalent parasite drag area derived from flight test is just as suspect [388], which leads me to a key point.

The aircraft parasite drag area ( $f_c$ ) can be obtained from flight test. That is true. Consider the situation where the main rotor shaft has been instrumented to measure torque. Then, given the rotor speed, main rotor horsepower is immediately available. Now accept for the moment that Eq. (2.262) is correct. It is a simple matter to solve for the parasite drag area as

$$(2.269) \quad f_c = \frac{550 \text{ RHP}_{\text{main}} - T_{\text{hp}} v - \frac{\rho (\pi R^2) V_t^3 \sigma C_{\text{do}}}{8} (1 + 3\mu_{\text{hp}}^2)}{q V_{\text{FP}}}$$

The assumption here is that the induced power ( $T_{\text{hp}} v$ ) and the profile power (the last term in the numerator) can be calculated accurately. This assumption is not true for any point in Fig. 2-146. The reason I say this is that the ability to calculate nonuniform induced velocity was just being developed when the helicopters shown reached flight test. Furthermore, the industry did not begin to calculate profile power without the use of tabulated airfoil lift, drag, and pitching moment (i.e., CFD) in a comprehensive “code” until the beginning of this century. Of course each manufacturer’s engineering department had helicopter performance theories to correlate with measured data [389, 390]. But calculation of accurate, main rotor induced and profile power was, and still is, a semiempirical art guided by correction factors.

Now the second point. On the horizon one can see computational fluid dynamics (CFD) making considerable progress. In the first decade of the 21st century, computations of rotor blade airloads and improving blade response were demonstrated [391-393]. Then, with encouragement from John Berry’s 1997 report [394] on velocity measurements behind a model rotor hub, the industry began applying CFD to the hub drag problem [395-397].<sup>96</sup> It is my hope that a doorhinge rotor along the lines of that shown in Fig. 2-173 will have its drag calculated with CFD in the not too distant future.

---

<sup>96</sup> Virtually no quantitative data can be gleaned from these reports. Apparently hub drag values are as guarded by industry as weight data. Frankly, I cannot imagine any reason for this secretive behavior given Fig. 2-164, Fig. 2-168, and Fig. 2-173.

## 2.6 VIBRATION

Vibration, caused by rotating and reciprocating components in particular, has been a thorn in the side of inventors, engineers, and humans in general, since the dawn of time. The rotary wing world has most certainly not been immune to vibration problems. You will recall from the discussion of vibration in Volume I that Cierva wrote in his 1935 paper [398] that

“perhaps the most irritating of the secondary difficulties met with in the autogiro developments have been those of a dynamical [vibration] nature.”

This “most irritating” of problems carried over to helicopter development. The fall 2006 issue of *Vertiflite*<sup>97</sup> included an article by Harry Moore [399]. He wrote about his recollections from the early days of flying the Sikorsky R-4 (Fig. 1-2) in 1945, the first production helicopter in the United States. He recalled that

“the R-4 was a very demanding aircraft to fly cross-country. It cruised at about 60 miles per hour and carried only enough gasoline for about an hour and a half. In addition to the extremely limited range, it could not be trimmed up for cruising flight, but required constant hands-on attention at all times. The pilot had to hold constant pressure on the cyclic pitch stick to keep moving in the desired direction. It had no radio and the pilot had to stay below 700 feet above the ground if he wore no parachute. In addition to these inconveniences, *the noise and vibration were fierce* [my italics]. This all added up to pretty tough navigation. The R-4 was not your ideal cross-country aircraft. In spite of these shortcomings, every one of us loved to fly this demanding machine. It may have demanded full-time attention, but it gave a bountiful return in satisfaction to the pilot who mastered it. It was surely precision flying at its very best.”

As Moore stated, the vibration was “fierce,” and this situation prompted action by the Wright Air Development Center (WADC) located at the then Wright-Patterson Air Force Base in Ohio. In 1954 they contracted with Eugene Liberatore (then employed by the Prewitt Aircraft Company) to prepare and edit an 18-volume series on rotorcraft. Volume 7 was a *Vibration Handbook for Helicopters* written by Bob Wagner, who later moved to Hiller Aircraft Corporation. This volume [400] has 149 references. There is not one aspect of helicopter vibration that aeromechanic engineers study today that is not touched on in this handbook.

From 1954 on, it seems that there has been a continuing series of meetings and articles that restate that helicopter vibration is a problem and ask what can be done about it. Many of these meetings and articles describe solutions that mitigate vibration somewhat. For example, in 1957 the *Journal of the American Helicopter Society* (AHS) [401] included the article titled *How Can Helicopter Vibrations be Minimized?* Contributors to this article all gave “their opinions on the current state of the art, on what can be done now to improve the situation, and on what remains to be done towards solving the helicopter vibration problem.” By 1963, when the Cornell Aeronautical Laboratory and the U.S. Army Transportation Research Command (TRECOT) sponsored a symposium about helicopter and V/STOL dynamics loads [402], the situation had not improved.

---

<sup>97</sup> The American Helicopter Society’s *Vertiflite* magazine is a marvelous addition to any engineering library. The diversity of articles is quite amazing because each issue—almost from inception—contains some fascinating history, and the technical data included in the history articles is of considerable value.

## 2.6 VIBRATION

Then, in February 1974, the AHS and NASA Ames Research Center convened a specialists' meeting on rotorcraft dynamics [403]. This was a milestone meeting. The general chairman was Ted Carter (a rotorcraft statesman in his own right) from Sikorsky. The technical chairman was Bob Ormiston (still a powerful voice in the aeromechanics community). Ted closed his opening remarks with the following statement:

“For the next two days we'll be assessing the state of the art and our ability to handle each of these problems and on Friday we will have a chance to back off and overview the whole situation. Bob Ormiston's paper [see pages 284 to 302] in this final session is, as far as I know, unique in the comparison it makes between all of our competitive methods addressed to a single problem. Finally, in the panel sessions, our ultimate customers, the designers and the service users will be given an opportunity to tell us what we're doing wrong.”

The presenters and attendees at this 1974 milestone meeting reaffirmed the fact that, despite our best efforts, helicopter vibration was still a problem, but for the first time the detailed scope of the vibration problem was laid out in a quantitative manner by a large group of experts.<sup>98</sup>

Seven years later, in November 1981, an AHS Specialists' meeting was held in Hartford, Connecticut. The subject of that meeting was Helicopter Vibration. At that meeting, Dick Gabel from Boeing gave the keynote address [404], which he titled *When Helicopter Smooth Surpasses Jet Smooth*. Dick's address covered the full spectrum of helicopter vibration with about 200 slides and was, in my opinion, absolutely outstanding. In particular, he described vibration mitigating devices in use by every member of the rotorcraft industry.

Three years later, Bob Loewy was given the honor of presenting the 4th Nikolsky Lecture at the 40th Annual Forum of the AHS. His lecture subject was *Helicopter Vibrations—A Technology Perspective* [405]. The last sentence of Dr. Loewy's conclusions in 1984 reads as follows:

“As a problem of complexity and challenge, reducing helicopter vibrations still must be counted in the first rank. Great progress has been made as shown in fig. 48 and much still remains to be done, as shown in fig. 49 (both from Ref. 2). I believe the years ahead will show continued progress of this kind.”

The two figures Bob refers to are included here as Fig. 2-174.<sup>99</sup> Whether the industry fulfilled the projections he and Dick Gabel hoped for in the early 1980s is still to be determined.

---

<sup>98</sup> This 1974 meeting report [403] contained comments from the audience. At that meeting I was a rather obscure but outspoken aerodynamics attendee. It was a dynamics meeting, but my impression was that the real solution would come when airloads could be accurately predicted. In the meantime, I thought the experts in solving the  $F = ma$  problem should get the “ma” side of the equation right, which the meeting showed was not in great shape. It was not until the first decade of the 21st century that accurate prediction of blade airloads was obtain by a tenacious group of aeromechanic experts using computational fluid dynamics. The technical chairman of this quiet group, which held its 20th get-together in February 2011, is Bob Ormiston.

<sup>99</sup> It seems that Dick Gabel's keynote address was not included in the meeting proceedings. Fortunately, Bob Lowey had a copy, which he was able to send to me. I forwarded it to several other researchers because it deserved to be resurrected.

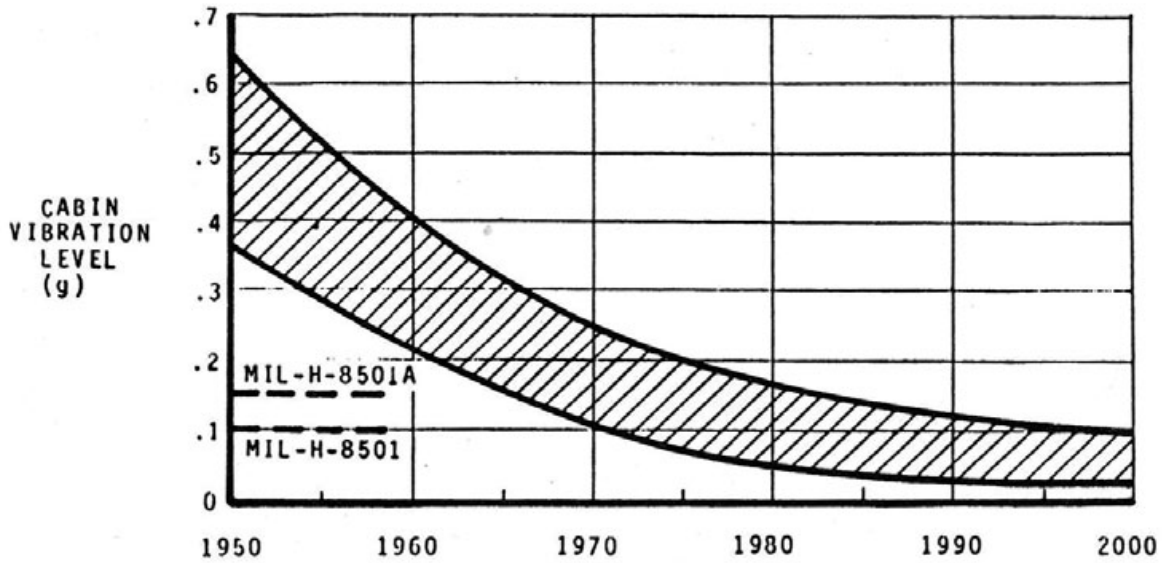


**Fig. 48** Trend of helicopter vibration relative to Mil specs (from Ref. 2).

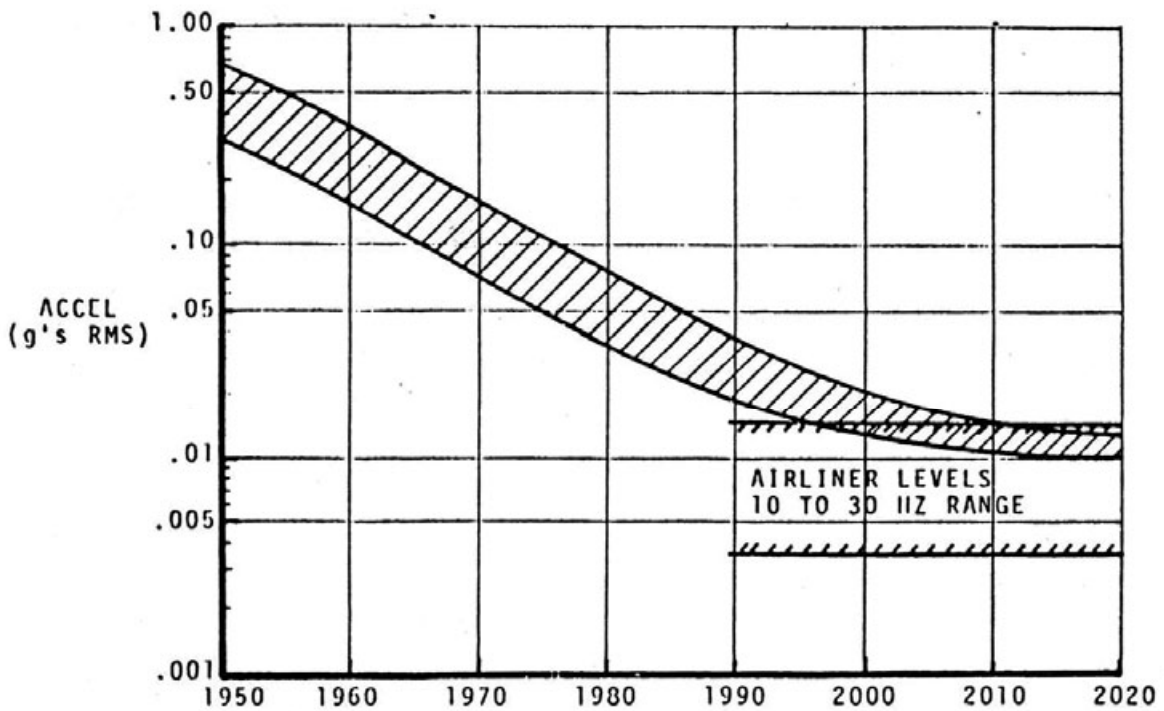


**Fig. 49** Trend of helicopter vibration relative to jet airliners (from Ref. 2).

Fig. 2-174. From *When Helicopter Smooth Surpasses Jet Smooth* [404] by Dick Gabel.

## 2.6 VIBRATION

Then, in May of 1993, the AHS Dynamics Committee agreed to support a workshop on rotor dynamics analysis. Groundwork was laid during the following year, and in May 1994 the Workshop was ready to correlate vibratory hub load predictions from eight different codes with data measured on a Westland Lynx helicopter. Active participants from eight organizations worked steadily through until June 1996. At the AHS forum that year, Bob Hansford and John Vorwald presented [406] the group's results. The summary conclusion was not very encouraging because the workshop concluded that

“on average, codes are not able to predict vibratory loads to an accuracy any greater than 50% of the Lynx measured loads.”

So now it is March 2011, and as I write this book, vibration of a new helicopter still cannot be predicted. Fortunately, absolutely no one has given up trying. Furthermore, as you will read shortly, computational fluid dynamics (CFD) tools are being used on the blade airloads with considerable success.

The preceding hop, skip, and jump through this introduction to vibration leads me to Fig. 2-175. Of course, this is a very simplified presentation of the helicopter vibration problem. I have left out all the interconnecting lines such as aircraft response effects, blade airloads, and the fact that vibrating pilots can make undesirable control inputs, which starts another feedback loop. Still, Fig. 2-175 is a useful guide to keep in mind during the following discussion. Let me start with the human aspects and work backwards to blade airloads, which have been the unsolved source of the helicopter vibration problem.

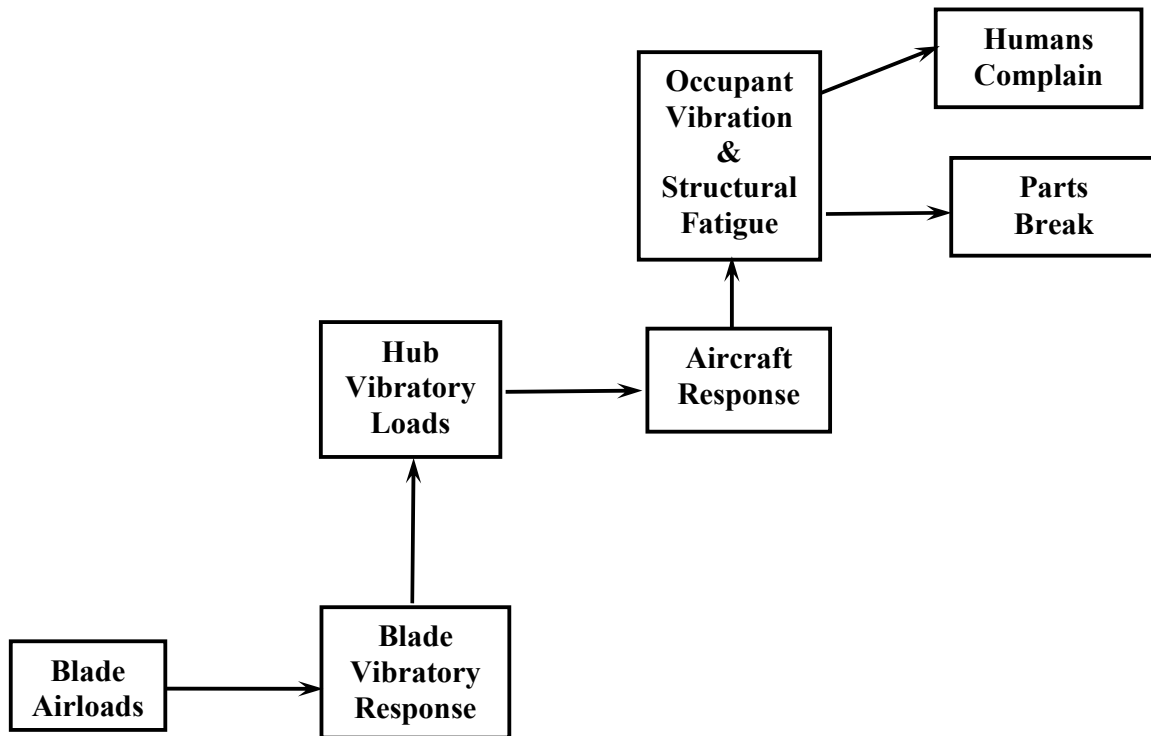


**Fig. 2-175. The path from airfoil airloads to human and structural complaints.**

### 2.6.1 Occupant Vibration, Humans Complain

In my mind there is no question that a human is the most sensitive “sensor” shown in Fig. 2-175. He or she can quite quickly describe, with any number of adjectives, any vibratory experience. Unfortunately, engineers do not deal very well with adjectives as design criteria. Low-frequency vibration, on the order of 1 cycle per second, can cause seasickness. High-frequency vibration, upwards of 60 cycles per second, can hurt eardrums, and vision begins to blur. When you think of a human (Fig. 2-176) as a relatively nonrigid structure comprised of 90 to 95 percent liquid, the vibratory response seems more like a bowl of jelly with some lumps. Still, the desire to quantify human response to vibration has been, and continues to be, a fascinating subject for human factors researchers. One example of their work is the nearly 1,000-page *Handbook of Human Vibration* compiled by Griffin [407], which contains about 1,500 references. It would not be easy to compile that many references even dealing with all the other helicopter vibration aspects shown in Fig. 2-175!

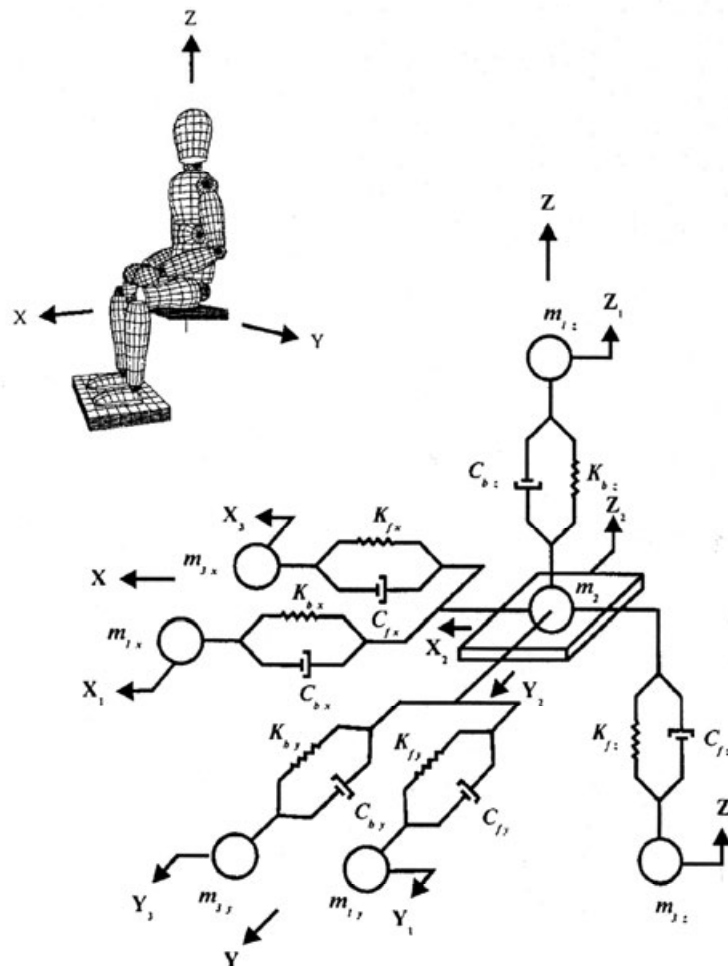


Fig. 1 Lumped parameter model of a seated human body with three separate vibration axes

Fig. 2-176. A human is not an easy component to model with classical structural dynamics tools [408].

## 2.6 VIBRATION

There does, however, seem to be a general consensus among human factors researchers that a human has a natural frequency. This frequency appears to be around five cycles per second when a seated person is shaken vertically. Human factors engineers immediately qualify this broad, generalized opinion with statements that hands, arms, feet, legs, eyeballs, head, etc., can respond at other frequencies. This group does associate five cycles per second with “whole body response” in their shake test experiments. In this sense, a human is like a seismic recording instrument, which is a well-known dynamics problem.

Consider a human sitting on a *cushioned* seat that is rigidly attached to a vibrating floor. This would mean that underneath the seat cushion shown in Fig. 2-176 is a metal seat with, say, four legs extending down to the floor where the human’s feet are resting. This metal seat has a back to support the seat-back cushion that, in turn, supports the human in an upright position. Imagine that the seat cushions are “comfortable.” A design criterion would be, of course, an attachment of the metal seat to the floor with crash attenuation components. To a helicopter engineer, this would seem to be a rigid floor-to-human connection that is quite solid. Suppose now that the floor (subscript F) where the seat is attached vibrates up and down according to

$$(2.270) \quad Z_F = A \sin(\omega_F t) = A \sin(2\pi f_F t).$$

This would be a sinusoidal motion of amplitude (A) in feet and a floor forcing frequency ( $\omega_F$ ) in radians per second. It is quite common to express the frequency in cycles per second, which is called hertz (Hz) and is denoted by (f).<sup>100</sup> That is,  $\omega = 2\pi f$  as shown in Eq. (2.270).

This displacement of the floor is not a realistic measurement. Instead, engineers today use accelerometers that measure the second derivative of the displacement, which can then be integrated to give displacement. An accelerometer can be mounted to the floor under the seat. The output of this sensor would be

$$(2.271) \quad \frac{d^2 Z_F}{dt^2} = -A\omega_F^2 \sin(\omega_F t) = -\omega_F^2 Z_F$$

with units of feet-per-second squared. One integration of this acceleration would be velocity or

$$(2.272) \quad \frac{dZ_F}{dt} = A\omega_F \cos(\omega_F t)$$

with units of feet per second. Another integration of acceleration gives the displacement described by Eq. (2.270).

To humans sitting in seats (say a pilot and a copilot), the preceding engineering is of absolutely no interest. In fact, this engineering design and analysis is not a reasonable approximation at all. To illustrate this, just think of riding up and down all day in an elevator.

---

<sup>100</sup> The term hertz was named after Heinrich Hertz. The name was established by the International Electro-technical Commission in 1930. The General Conference on Weights and Measures replaced cycles per second (cps) with Hz in 1960. Thus, 5 cycles per second equals 5 Hz in modern notation. Furthermore, 5 Hz equals  $2\pi(5)$  or about 31.4 radians per second.

This is, admittedly, a very slow vibration. Without the display showing the floor number, you have no reference to displacement. Furthermore, it really is only when you decelerate to stop at a floor (or accelerate towards a different floor) that you have a sense of velocity, and this is really a change in velocity, which is acceleration.

Using adjectives, a human feels, thinks, and expresses his perception of the acceleration in a vibration environment. The human's evaluation is not in relation to the quantitative floor displacement. There are, of course, exceptions. For example, you hear comments that during an earthquake, the "building swayed." Another example occurs when a pilot says, "The instruments are a blur." I doubt, however, that that would be how a pilot would describe what was being experienced overall.

Human factor researchers [407, 408] do have a structural dynamics model of a seated human. Most simplistically, a human is a lump of mass (weight/32.174) in slugs, connected to the floor by a spring of stiffness ( $k$ ) in pounds per foot and a damper ( $c$ ) in pounds per foot per second, as Fig. 2-177 suggests. With this model, the human's whole body displacement (his center of gravity) relative to the floor ( $z_b$ ) is governed by the simple  $F = ma$  equation of

$$(2.272) \quad m \frac{d^2 z_b}{dt^2} + c \frac{dz_b}{dt} + k z_b = -m \frac{d^2 Z_F}{dt^2} = m (\omega_F)^2 A \sin(\omega_F t).$$

When Eq. (2.272) is divided through by mass, you have

$$(2.273) \quad \frac{d^2 z_b}{dt^2} + \frac{c}{m} \frac{dz_b}{dt} + \frac{k}{m} z_b = (\omega_F)^2 A \sin(\omega_F t),$$

which has the solution for displacement of

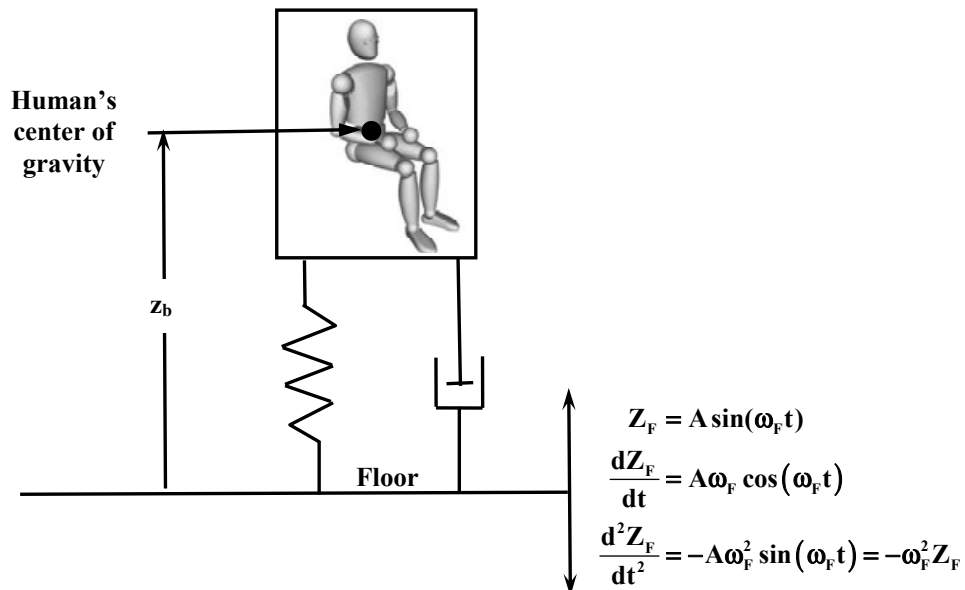


**Fig. 2-177. An extremely simple representation of a human flying in a helicopter that has a vibrating floor.**

## 2.6 VIBRATION

$$(2.274) \quad z_b = (\omega_F)^2 A \left\{ \left[ \frac{\left(\frac{k}{m} - \omega_F^2\right)}{\left(\frac{k}{m} - \omega_F^2\right)^2 + \left(\frac{c}{m} \omega_F\right)^2} \right] \sin(\omega_F t) - \left[ \frac{\left(\frac{c}{m} \omega_F\right)}{\left(\frac{k}{m} - \omega_F^2\right)^2 + \left(\frac{c}{m} \omega_F\right)^2} \right] \cos(\omega_F t) \right\}.$$

The first derivative of displacement is velocity so

$$(2.275) \quad \frac{dz_b}{dt} = (\omega_F)^3 A \left\{ \left[ \frac{\left(\frac{k}{m} - \omega_F^2\right)}{\left(\frac{k}{m} - \omega_F^2\right)^2 + \left(\frac{c}{m} \omega_F\right)^2} \right] \cos(\omega_F t) + \left[ \frac{\left(\frac{c}{m} \omega_F\right)}{\left(\frac{k}{m} - \omega_F^2\right)^2 + \left(\frac{c}{m} \omega_F\right)^2} \right] \sin(\omega_F t) \right\}$$

and, most importantly, the acceleration is the second derivative of displacement so

$$(2.276) \quad \frac{d^2 z_b}{dt^2} = -\omega_F^4 A \left\{ \left[ \frac{\left(\frac{k}{m} - \omega_F^2\right)}{\left(\frac{k}{m} - \omega_F^2\right)^2 + \left(\frac{c}{m} \omega_F\right)^2} \right] \sin(\omega_F t) - \left[ \frac{\left(\frac{c}{m} \omega_F\right)}{\left(\frac{k}{m} - \omega_F^2\right)^2 + \left(\frac{c}{m} \omega_F\right)^2} \right] \cos(\omega_F t) \right\}.$$

It is very important to remember that what the human feels is the sum of the floor movement, the seat movement, and the seat cushion movement, and his or her response to the total components' movements. This means that the total acceleration of the seated human is Eq. (2.271) plus Eq. (2.276). This body total acceleration can be expressed in units of gravity, so that

$$(2.277) \quad \text{Body total acceleration in g's} = \left( \frac{d^2 Z_F}{dt^2} + \frac{d^2 z_b}{dt^2} \right) \frac{1}{32.174}.$$

Given the preceding discussion, let me show you three examples. To begin with, the human's whole body natural frequency is  $\omega_b = \sqrt{k/m}$ , which, in radians per second, is  $2\pi f_b$ . If the frequency ( $f_b$ ) is 5 Hz, which human factors engineers say is not unreasonable, you have  $\omega_b = \sqrt{k/m} = 2\pi(5) = 31.4$  radians per second. On page 380, Griffin's Handbook [407] states that vibrating humans respond as if they have a critical damping ratio ( $c/c_c$ ) of about 0.475. This means that  $c/m = 2\sqrt{k/m} (c/c_c)$ , which gives  $c/m = 29.8$ . Therefore, in Eqs. (2.273) to (2.276),  $k/m$  equals 987 and  $c/m = 29.8$ .

Now suppose three floor movements are examined as defined by the following table:

Parameter	Symbol	Unit	Case 1	Case 2	Case 3
<b>Floor</b>	F				
Vibration Frequency	f	Hz	1	5	20
Vibration Frequency	$\omega_F$	rad/sec	6.28	31.4	125.6
Amplitude	A	ft	0.0814977	0.00325990	0.000203744
<b>Human</b>	b				
Natural Frequency	$\omega_b$	rad/sec	31.4	31.4	31.4
Damping	c/m	1/sec	29.8	29.8	29.8

Note for these three cases that as the frequency of the floor vibration increases, the floor displacement amplitude goes down. I have chosen these proportions to ensure that the maximum floor acceleration remains constant at  $\pm 0.1 \text{ g}$  (i.e.,  $3.2174 \text{ ft/sec}^2$ ) for each case. One-tenth of a g vibration can be quite uncomfortable for a human to withstand.

The time history of vibration expressed as acceleration in units of gravity for the three cases are shown in Fig. 2-178, Fig. 2-179, and Fig. 2-180. Consider the lowest frequency vibration case first. The human feels that he (or she) hardly moves relative to the floor. All the floor vibration passes nearly directly to the body. Because the body is nearly synchronized with the floor, the total body maximum acceleration is only slightly greater than the floor's maximum acceleration. The second case, Fig. 2-179, is a case where the floor is vibrating at the human's natural frequency of 5 Hz. This is the classical case of resonance. Because the human body acts like it has damping (internal parts do not actually slosh around *too* much), the body's acceleration relative to the floor is not amplified excessively. The maximum total body acceleration is greater than the floor's maximum acceleration by a factor of slightly more than 0.04 g. That is, the amplification factor (the ratio of total body to floor maximum accelerations) is  $0.145/0.1$ . Note that the total body waveform is not in phase with the floor waveform. The third case is with the floor vibrating at 20 Hz. Now the body-relative-to-floor waveform is nearly completely out of phase with the floor. As the floor goes down, the body goes up. The two accelerations nearly cancel. The results are that the maximum total body acceleration is much less than the maximum floor acceleration. The amplification factor is about  $0.0254/0.1$ . The human feels like his (or her) body is only being shook by a very small floor movement, albeit a very fast movement—something like a buzz.

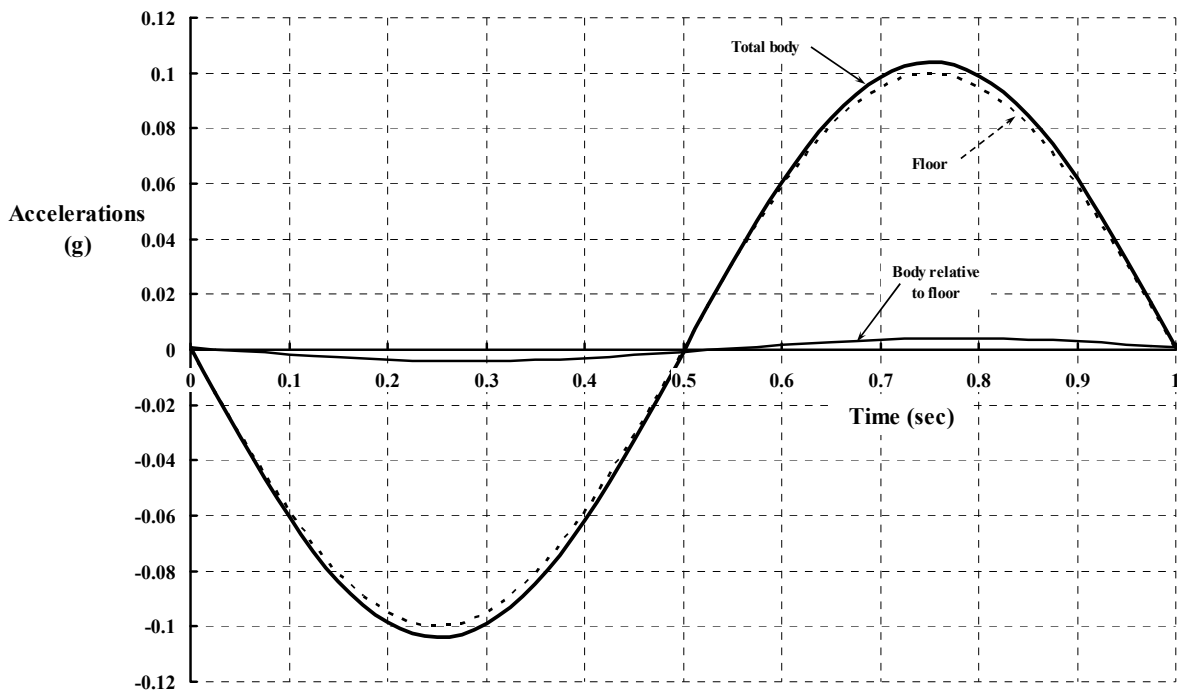
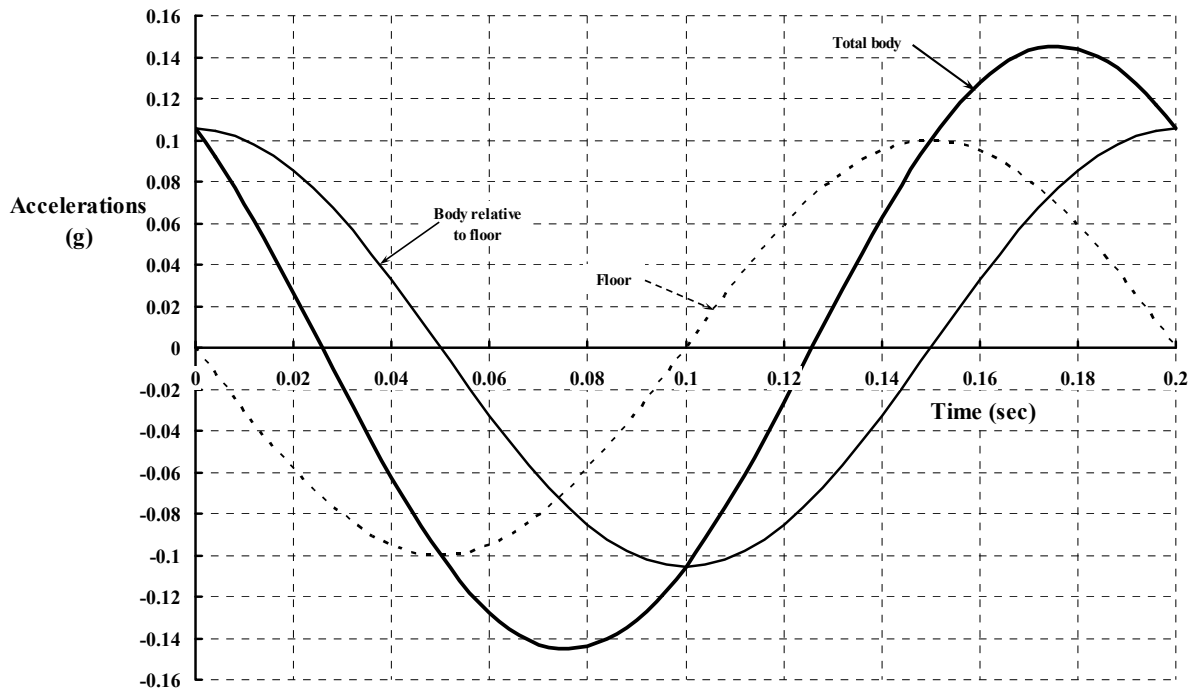
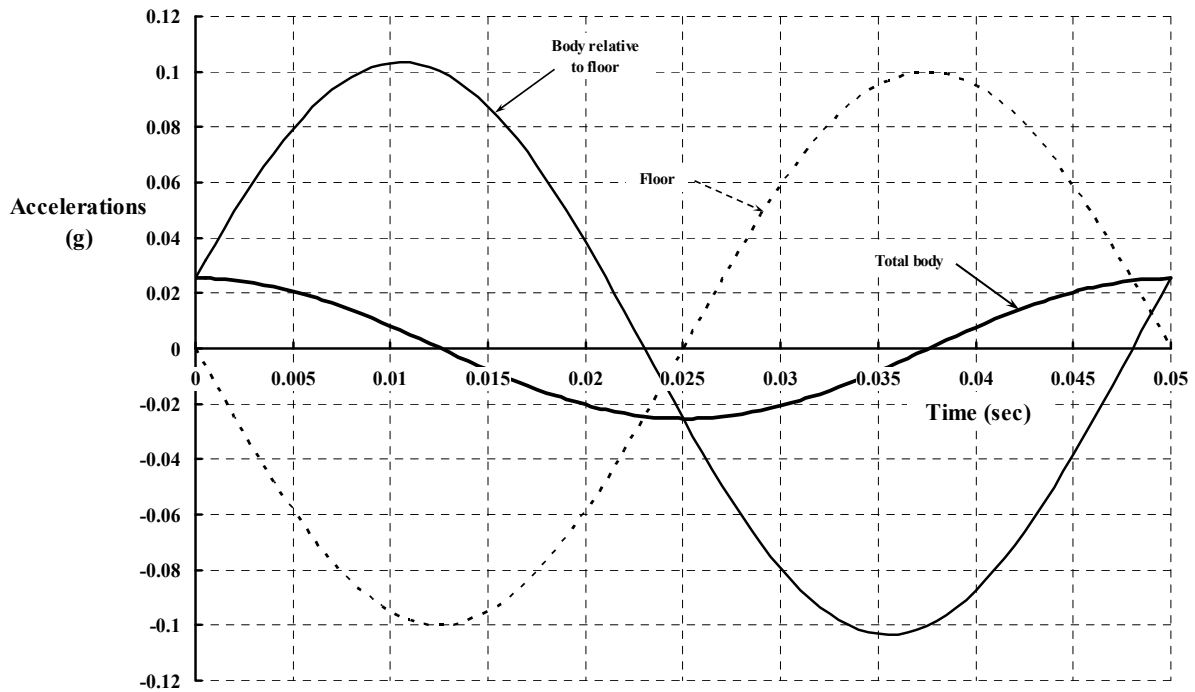


Fig. 2-178. The floor vibrates at 1 Hz with an amplitude of 0.5 g.

## 2.6 VIBRATION



**Fig. 2-179.** The floor vibrates at 5 Hz with an amplitude of 0.5 g. This is a case of the floor moving at the natural frequency of the human, which is called resonance.



**Fig. 2-180.** The floor vibrates at 20 Hz with an amplitude of 0.5 g.

The preceding three cases are points along the maximum acceleration curve shown in Fig. 2-181. Keep in mind that at all floor vibration frequencies, the acceleration of the floor is given as

$$(2.278) \quad \frac{d^2 Z_F}{dt^2} = -(0.10g) \sin(\omega_F t).$$

Note that Fig. 2-181 can be used as an amplification curve for a human for any value of maximum floor/seat acceleration simply by multiplying the vertical scale by 10 and then multiplying by the different chosen floor acceleration. Furthermore, the maximum total body acceleration for floor vibration frequencies beyond 20 Hz is approximated as

$$(2.279) \quad \left( \frac{d^2 z_b}{dt^2} + \frac{d^2 Z_F}{dt^2} \right)_{\max} = \pm \frac{\omega_F^4 A}{32.174} \left[ \frac{\left( \frac{c}{m} \omega_F \right)}{\left( \frac{k}{m} - \omega_F^2 \right)^2 + \left( \frac{c}{m} \omega \right)^2} \right] \quad \text{in g's}.$$

It is worth remembering that vibration at 20 Hz is near the bottom of human hearing. An 88-key piano plays a frequency of about 27 Hz when struck on the lowest key. The highest key broadcasts at just under 4,200 Hz when struck. Of course, many people have “felt” thumps on the chest from loud notes coming from large drums.

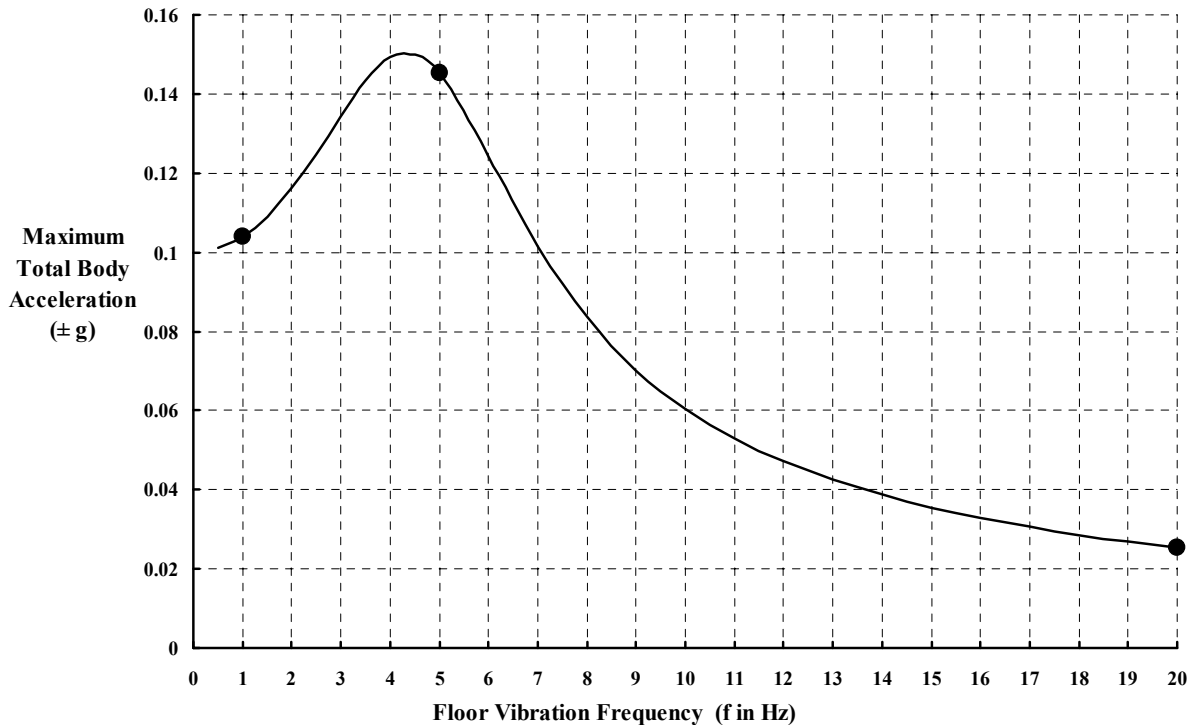


**Fig. 2-181.** A human feels that the floor vibration is the worst when the floor/seat vibrates at about 4.5 Hz (computed with a maximum floor acceleration of ±0.1 g at all frequencies).

## 2.6 VIBRATION

With this background, the question immediately arises as to just how much vibration a human can tolerate. (Keep in mind that *tolerating* is a far cry from *accepting* and that *accepting* is a further cry from *not perceiving*.) This is the key question that needs to be answered by all engineers creating products used by humans. Unfortunately, despite such reference material as Griffen's Handbook [407], the design criteria are hardly definitive (perhaps that is a little too harsh, considering the complexity of a human and the diverse experiments that Griffen examines). That is not to say that helicopter design criteria for vibration limits are not available, re-examined, and proposed in the literature; however, there is an abundance of diverse opinions.

The rotorcraft industry has depended on military specifications for acceptable helicopter vibration boundaries. These specifications have depended, in turn, on the International Organization for Standardization (ISO),<sup>101</sup> and specifically on ISO 2631, *Guide for the Evaluation of Human Exposure to Whole-Body Vibration*. Of course, particular countries still do some tailoring to serve their individual needs. In 1978, the ISO had decided on and published vibration criteria or boundaries at which human proficiency was decreased. The group quantified the boundaries in terms of acceleration in meters-per-second squared versus the time the vibration was endured, and they chose the frequency range of 4 to 8 Hz as the normalizing reference for a family of curves. Their collective view of this normalizing reference is shown here as Table 2-28.

The then current view was that vibration below 4 Hz and above 8 Hz would differ from the reference according to three simple equations. That is, from 4 to 1 Hz, the vibration tolerance would increase as  $K = 2/\sqrt{f}$ . Over the frequency range from 4 to 8 Hz,  $K = 1$ , and for  $f = 8$  to 80 Hz,  $K = f/8$ . Thus, the *allowable* (if you will) vertical vibration in units of g appears as shown in Fig. 2-182. Note that this figure gives three straight line segments because it is graphed in a log-log axis system. In a linear axis system, the 1978 ISO 2631 appears as Fig. 2-183, which I think is more useful for this discussion.<sup>102</sup>

Be aware that similar logic has created similar criteria for lateral and longitudinal vibration. Furthermore, Griffen discusses the situation for individual parts of the body. His Handbook is very careful to point out that the actual situation, based on work as late as 1990, is far from hard lines on a graph. All humans are not the same, and tests have only been conducted with a very small sample of them.

**Table 2-28. Reference Acceleration for Degraded Proficiency for Vertical Vibrations in the Frequency Range of 4 to 8 Hz**

Time	24 hr	16 hr	8 hr	4 hr	2.5 hr	1 hr	25 min	16 min	1 min
Acceleration (m/sec <sup>2</sup> )	0.14	0.212	0.315	0.53	0.71	1.18	1.8	2.12	2.8
Vertical g's	0.0143	0.0216	0.0321	0.0540	0.0724	0.1203	0.1835	0.2162	0.2855

<sup>101</sup> The ISO came into being through a succession of meetings that began in 1945. By April 1947 a constitution was hammered out and ratified by over 15 interested bodies from many countries.

<sup>102</sup> Griffen devotes chapter 10 to a number of vibration standards, only one of which is ISO 2631 and its growth from 1978 to the modern era.

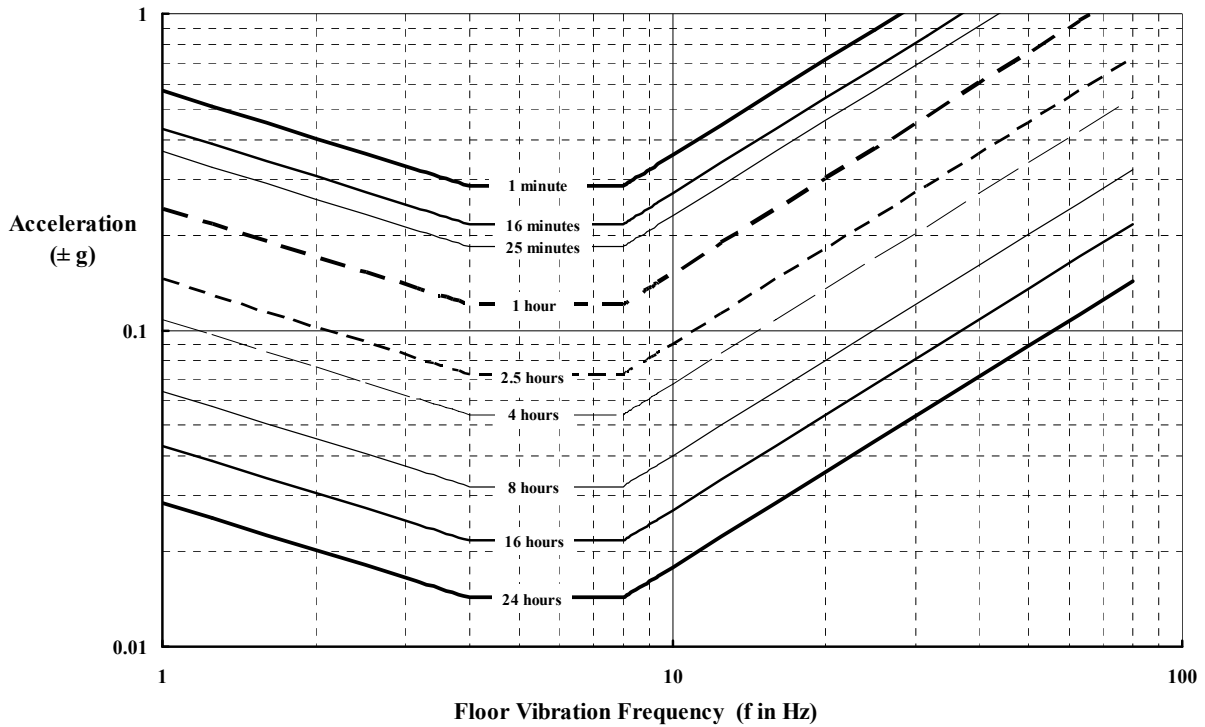


**Fig. 2-182. Human proficiency is reduced after exposure to vertical floor vibration at varying accelerations and time (log-log axis).**

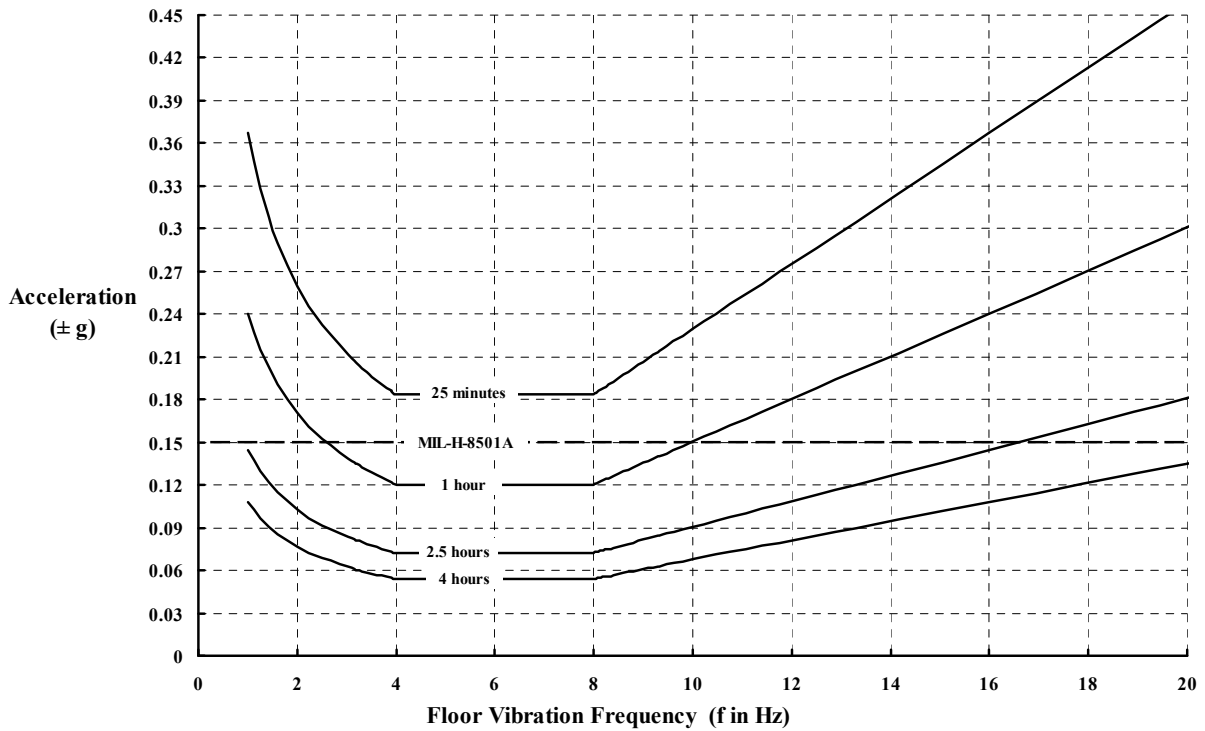


**Fig. 2-183. Human proficiency is reduced after exposure to vertical floor vibration at varying accelerations and time (linear axis).**

## 2.6 VIBRATION

The United States military created MIL-H-8501 for helicopters in November 1952 [409]. Shortly thereafter (September 1961) this original specification was revised to MIL-H-8501A [410], which states in part in paragraph 3.7, *Vibration characteristics*, that

- “1. Vibration accelerations at all controls in any direction shall not exceed 0.4 g for frequencies up to 32 cycles per second.
2. Vibration accelerations at the pilot, crew, passenger, and litter stations at all speeds between 30 knots rearward and  $V_{cruise}$  shall not exceed 0.15 g for frequencies up to 32 cycles per second. From  $V_{cruise}$  to  $V_{max}$  the maximum vibratory accelerations shall not exceed 0.2 g up to 36 cycles per second.
3. Vibration characteristics at the pilot, crew, passenger, and litter stations shall not exceed 0.3 g up to 44 cycles per second during slow and rapid linear accelerations or deceleration from any speed to any other speed within the flight envelope.”

You might note in passing that Dick Gabel’s upper graph in Fig. 2-174 shows that the revised 8501A raised acceptable vibration from 0.10 to 0.15 g for paragraph (2). A hint that the upward revised allowable vibration was a step in the wrong direction came in November of 1970. In that year, Dick Gabel and two coauthors presented a paper [411] at a symposium dealing with environmental effects on VTOL designs. Their second conclusion is of particular importance because they wrote:

“(2) The multi-harmonic nature of helicopter vibration presents a special problem. In any given situation, the levels at each of the component rotor harmonics can be well within acceptable limits and still combine to produce an unacceptable comfort level. Since the frequencies are harmonic, both the amplitude and phase are important and it becomes extremely difficult to identify the offending frequency or combination of frequencies. It is recommended, therefore, that comfort criteria for a generalized multi-axis, multi-frequency environment be developed for helicopter applications. Since the sensitivity of the hands and feet differ from the remainder of the body, criteria for independent stimulation of the hands and feet are required in addition to whole body vibration in the seated position. Modifying effects of noise, temperature, and humidity should also be considered.”

In 1977, Dan Schrage (then a Captain in the U.S. Army) presented a paper [412] that showed the industry’s problems with vibration on two major U.S. Army development programs (the UTTAS leading to the UH-60 and the AAH leading to the AH-64). The four helicopter companies (Bell, Boeing, Hughes, and Sikorsky) were unable to meet the Army’s low-vibration requirements and, furthermore, the requirements left something to be desired as well. A few years later, at the 37th Annual Forum of the AHS held in May 1981, Dave Kidd of Bell Helicopter presented an exceptionally clear story leading to an assessment of helicopter vibration criteria. His paper is well worth your reading time because he traces work on human vibration comfort criteria from 1931 up to 1981 and deals directly with words like acceptable and unacceptable. Finally, in March 1992, Ray Prouty (in his invaluable, clarifying style) wrote a 1-1/2-page article [413] for *Rotor & Wing* magazine that we layman could grasp. He illustrated his article with a figure similar to Fig. 2-183.

By 2006, Sam Crews (Chief of the Aeromechanics Division at the U.S. Army Aviation Engineering Directorate) had compiled enough knowledge to introduce a new vibration criteria tailored to rotorcraft. This military requirement for rotorcraft vibration specifications, modeling, and testing was published as an Aeronautical Design Standard [414] known as

ADS-27A-SP.<sup>103</sup> This ADS deserves your attention because many of the issues raised by industry, including Dick Gabel's second conclusion quoted previously, were addressed.

Let me conclude this discussion about humans with a few comments about the helicopters that the humans are flying in. This is, as you will see, the unfortunate side of the human-helicopter interface. Turn your attention to Fig. 2-184. In this figure I have shown the fundamental forcing frequency of many helicopters. This fundamental frequency is the once-per-revolution (1/rev) frequency computed as  $f = \frac{V_t/R}{2\pi}$  in Hz, where ( $V_t$ ) is the rotor tip

speed in feet per second and (R) is rotor radius in feet. The main rotors of a large number of helicopters fall in the 4- to 8-Hz range that ISO 2631 singles out as its reference range (as Fig. 2-183 shows). This immediately raises the point that if the main rotor is out of balance, or the blades are out of track, a 1/rev frequency will be passed from the main rotor hub to the airframe floor, and then to the seated human, and the human (let's say the pilot) will complain. This facet of vibration was discussed in detail in Volume I. Fortunately, both the manufacturer and mechanics in the field can exercise considerable control of main rotor track and balance, which generally keeps this source of vibration well below 0.05 g.

On the other hand, as you learned from Volume I, main rotors pass vibration at blade number (b) times the fundamental 1/rev frequency, which is to say b(1/rev). Furthermore, main rotors pass vibration at twice the blade number times the fundamental 1/rev, which amounts to n[b(1/rev)] where n goes up as 1, 2, 3, 4, etc. To illustrate, Fig. 2-184 shows the widely used Sikorsky S-70, known as the UH-60 Black Hawk by the U.S. Army. Because it has four blades, the main rotor passes significant vibration at 4 times 4.3 Hz equals 17.2 Hz. According to ISO 2361 and MIL-H-8501A per Fig. 2-183, the pilots and passengers should remain proficient for 2.5 hours *if* the vibration at 17.2 Hz is no higher than  $\pm 0.15$  g. This is a big *if* that I will address shortly.

Tail rotors can also be a source of vibration for single rotor helicopters. Take the Sikorsky UH-60 for example. It has a tail rotor that has a fundamental 1/rev frequency (see Fig. 2-185) of just under 20 Hz. This means that vibration caused by an unbalanced tail rotor might be mistaken (or added to or subtracted from) the main rotor 4/rev vibration, which is at 17.2 Hz.

With the preceding background, you should be able to read and appreciate a recent AHS Journal paper [416]. This outstanding paper was devoted to the structural dynamics of helicopter seats and how vibration can be mitigated for the pilot and copilot. The research program was supported by the Canadian military and the Canadian National Research Council. The test helicopter used in the research was a Bell Model 412, which is the Canadian military Model CH-146. The pilot and copilot were instrumented at their helmets, shoulders, and thighs. Additional accelerometers were mounted on the seat frames, seat cushions,

---

<sup>103</sup> The U.S. Army's intentions were conveyed to the rotorcraft industry by Sam at the 1981 AHS National Specialists' Meeting on Helicopter Vibration in Hartford, Connecticut. In that paper [415], an intrusion index was suggested, which came to pass in ADS-27A-SP. Explaining the intrusion index, however, is beyond the intent of this volume.

## 2.6 VIBRATION

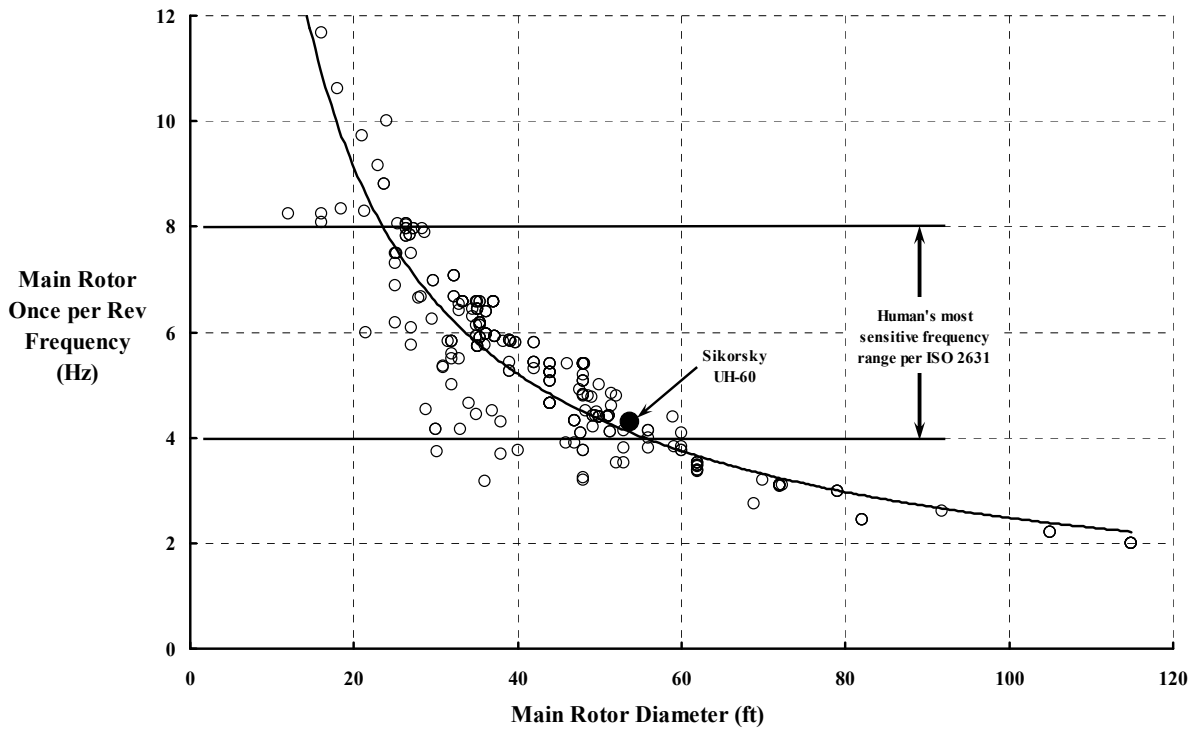


**Fig. 2-184.** Many helicopters have their fundamental 1/rev frequency in the range where humans are most sensitive to vibration.

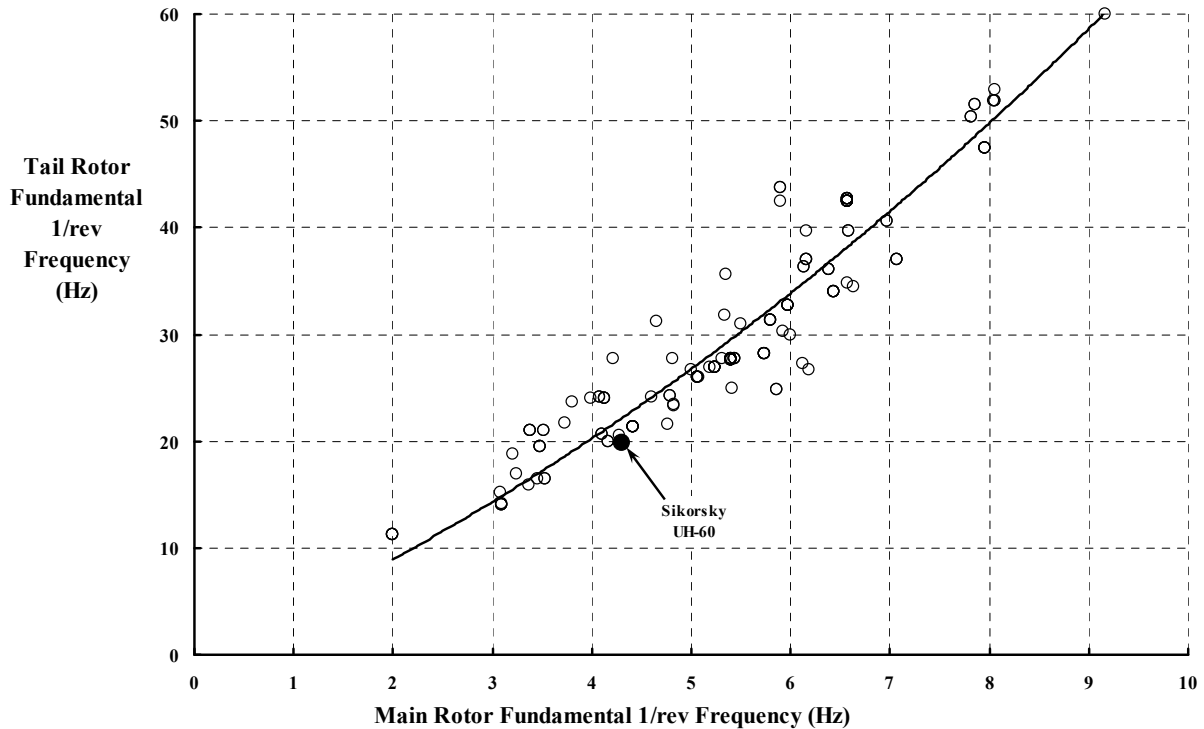


**Fig. 2-185.** Unbalanced and out-of-track tail rotors can cause vibration at their 1/rev frequencies.

seat bases, and on the floor rails. Interestingly, the authors found that “the original in-service seat cushion provided effective vibration isolation at high frequencies, but the low-frequency vibration at 1/rev was amplified by the seat.” In laboratory tests with a mannequin, they showed that by using active seat-to-floor rails struts, the vibration levels could be virtually cut in half, which was considerably better than results obtained with nine different types of seat cushions. This AHS Journal paper is well worth your reading time. Finally, if you are an aircraft engineer you will appreciate the fact that, with Table 2-28 and Fig. 2-182, the human factors researchers have created a curve of allowable stress versus number of cycles (i.e., an S-N curve) for humans. The stress is measured in units of gravity, and the number of cycles is frequency (cycles per second or hertz) times time. Suppose from Table 2-28 or Fig. 2-182 you choose the lowest g level within the frequency range of 4 to 8 Hz, and then you choose the maximum human whole body response frequency of 4.5 Hz from Fig. 2-181. These choices let you create a “human structural fatigue S-N curve,” which I have done with Fig. 2-186. Note that a log scale is used for the x-axis (number of cycles).

A human’s proficiency is reduced when he or she is vibrated at accelerations above the line shown in Fig. 2-186. It appears that the vintage 1978 ISO 2631 criteria may be somewhat in doubt for cycles below the 16-minute point because of the rather sharp break leading from the 16-minute point to the 1-minute point. The inference is that below the line a human is more tolerant of the vibration. However, given the small sample of humans reflected in the data leading to the ISO 2631 criteria of 1978, you should imagine that the line shown on Fig. 2-186 is probably the centerline of a broad band of scattered data.

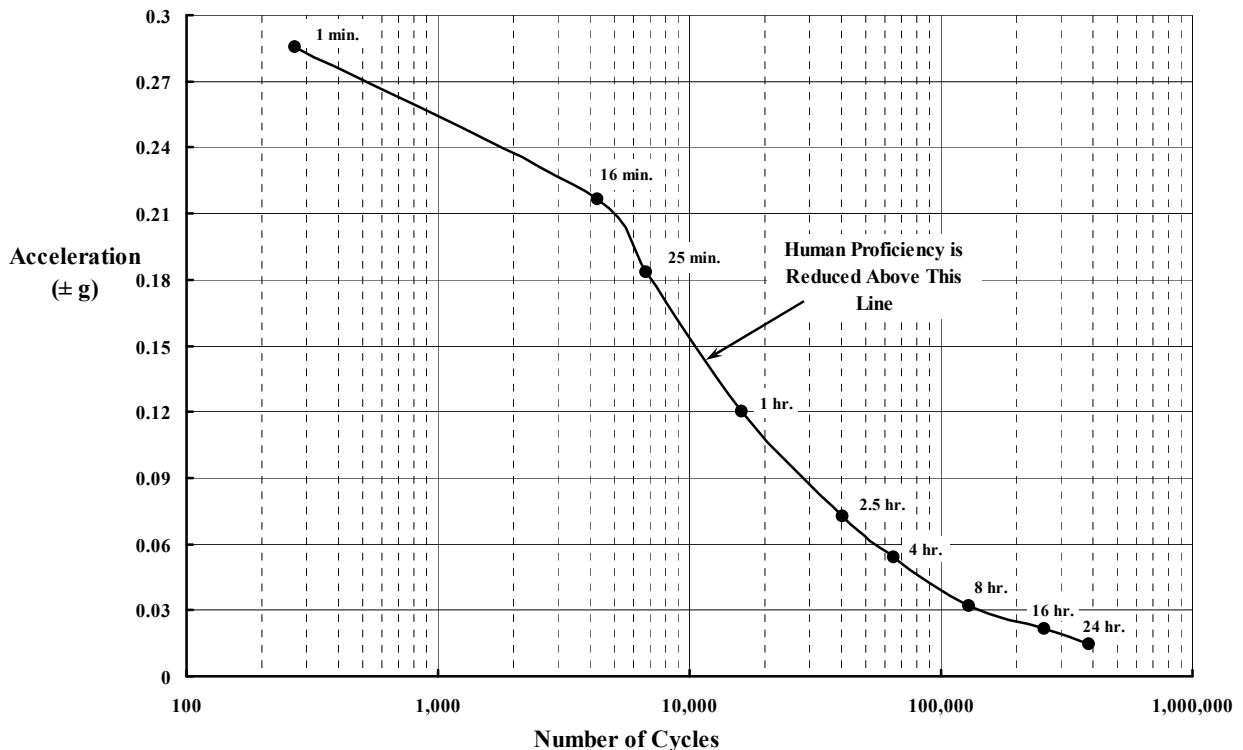


Fig. 2-186. An S-N curve for a human (vibration at 4.5 Hz).

## 2.6 VIBRATION

### 2.6.2 Structural Fatigue, Parts Break<sup>104</sup>

Besides humans, vibration affects every part in a helicopter, and just consider how many parts there are in a modern helicopter such as the Sikorsky UH-60 shown in Fig. 2-187. It is absolutely necessary to make calculations and perform tests to establish how many cycles any part can absorb before the part breaks due to fatigue. Of course, design experience can be used for many of the parts, but there is no question that bench fatigue tests must be completed at the subassembly and assembly level before production begins.

Experimental data about material fatigue strength has been accumulating at least since the King of England's coach springs kept failing. Now, after several centuries, a sufficient amount of data has been collected in several U.S. Department of Defense (DoD) handbooks [417-422] so that a designer has at least a starting point for material selection. The metals handbook [417] gives an explanatory example of fatigue stress versus number of cycles for a representative test specimen, which I have include here as Fig. 2-188. There are 50 such figures associated with steel alone in the 1,700-page handbook.

As you look at Fig. 2-188, you can see that the general trend of any one line is the lower the stress, the greater the number of cycles that the material can sustain before failure. Notice also that a log scale is used for the fatigue life, but not for the maximum stress.

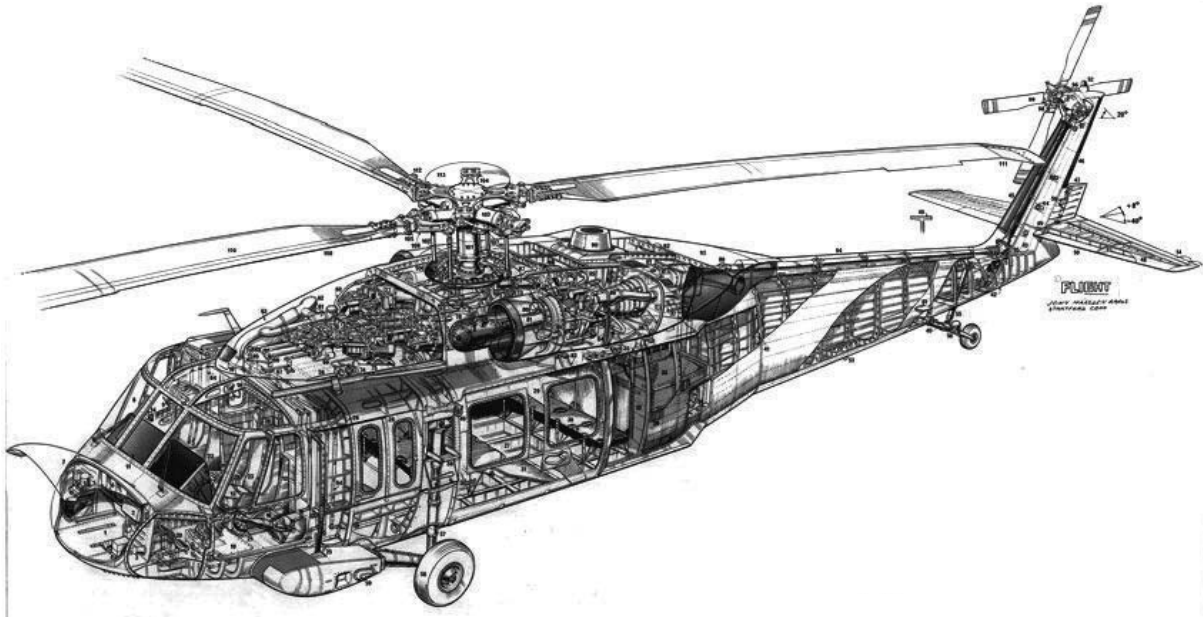


**Fig. 2-187. Cutaway artist's rendition of the Sikorsky UH-60 (courtesy of Flight International Inc.).**

<sup>104</sup> In my mind, all you can do with a part is cut it in two—or attach it to another part. By this standard, a nut and a bolt are two parts. When the nut is screwed onto a bolt, you have a subassembly. When a large group of subassemblies are put together, you have an assembly. A rotor system is an assembly to me. A large group of assemblies—when put together—gives you a flyable helicopter. In my experience, nothing beats a drawing tree, a parts list, and exploded view assembly drawings to understand a helicopter. In short, an aircraft needs to be understood at the part level.

Furthermore, very few of the test results in this example show data much beyond 10-million ( $10^7$ ) cycles. The authors of MIL-HDBK-5J used data from their figure 2.3.1.2.8 (d) to create this presentation example, which happens to be for steel. The property of steel is such that no damage is found in practice for millions more cycles if the stress is below the endurance limit. This is called a runout and is shown on the graphs for steel with the little arrows attached to data points at the end of each line. (*Aluminum does not exhibit this characteristic.*) Notice in the box on Fig. 2-188 that all figures in the metals handbook include a description of the material (i.e., Material = A), which is 4130 steel in this example. The importance of notches in the test specimen is given as  $K_t$ , which can vary from  $K_t = 1$  for no notch, up to at least 4. Imperfections such as notches create concentrated stresses and thus reduce fatigue strength. For this example,  $K_t = 4$ . The type of notch is also important, and this is defined by a few words in each box. Finally, the test material can be loaded by both a mean and an alternating force. This information is conveyed by either a value of mean stress or a stress ratio, because the specimen load is applied such that

$$(2.279) \quad S_{(t)} = S_{\text{mean}} + S_{\text{alternating}} \sin(\omega t)$$

where the time varying stress ( $S_{(t)}$ ) is defined by a mean stress ( $S_{\text{mean}}$ ) and a sinusoidal component of amplitude ( $S_{\text{alternating}}$ ). For the example case, it so happens that Level 1 equals a mean stress of 0 pounds per square inch (psi), Level 2 = 10,000 psi, Level 3 = 20,000 psi, and Level 4 = 30,000 psi. When the loading condition is defined by a stress ratio (SR), the

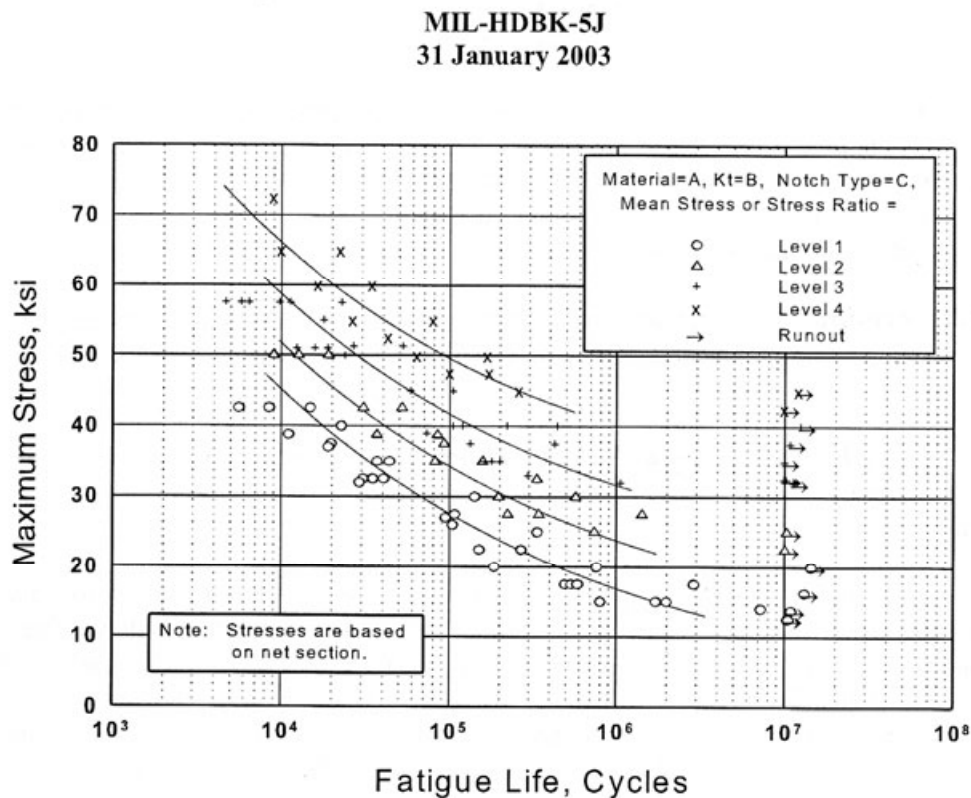


Fig. 2-188. An S-N curve for a structural material.

## 2.6 VIBRATION

handbook means

$$(2.280) \quad SR = \frac{S_{\min}}{S_{\max}}$$

from which it follows that if  $SR = -1$ , the mean must be zero and the fatigue stress is simply  $S_{\text{alternating}}$ . Obviously you can calculate backwards to find the mean and the alternating stresses given  $S_{\max}$  and  $SR$ .

An important aspect of fatigue is that as the mean stress is increased, the material can withstand less alternating stress. To illustrate this point, imagine a part is to have a life of  $10^5$  cycles. Reading from Fig. 2-188, you have the following table:

Mean Stress (psi)	Maximum Stress (psi)	Alternating Stress (psi)
0	27,000	27,000
10,000	34,000	24,000
20,000	41,000	21,000
30,000	49,000	19,000

One example of this fatigue aspect is illustrated in the design of a rotor blade spar. This part has a mean load created by centrifugal force and an alternating bending moment created by airloads.

MIL-HDBK-5J makes an effort to collapse the data in Fig. 2-188 to a single line using an empirical formula of the form

$$(2.281) \quad S_{\text{eq}} = S_{\max} (1 - SR)^n .$$

The presentation example, Fig. 2-189, shows one of the better “consolidations” with  $n = 0.63$  in this case. Note that when the mean stress is zero (i.e.,  $SR = -1$  and  $S_{\max} = S_{\text{alternating}}$ ), then the alternating stress is simply

$$(2.282) \quad S_{\text{alternating}} = \frac{S_{\text{eq}}}{1.547} .$$

With this approach you see that the *endurance limit* for this notched specimen is on the order of  $S_{\text{eq}} = 22,000$  pounds per square inch, which means an endurance limit of about 14,000 pounds per square inch.

The influence of a notch (which represents deliberate damage to a part) is serious because a designer must make some allowance for both manufacturing defects and field damage. Fatigue limits for an unnotched test specimen are shown in Fig. 2-190. This figure is directly comparable to Fig. 2-188. With no notch ( $K_t = 1.0$ ), this steel alloy has an endurance limit of about 45,000 pounds per square inch if the mean stress is zero, which is more than three times the endurance limit of the notched specimen ( $K_t = 4.0$ ) if the mean stress is zero. The prudent designer of a rotor blade spar made with 4130 alloy sheet (0.075-inch-thick) steel must “knock down” the design stress from 45,000 pounds per square inch to some lower value. The question has always been how much of a knock down factor should he (or she) use. In practice, a fatigue test would be conducted with several manufactured spars.

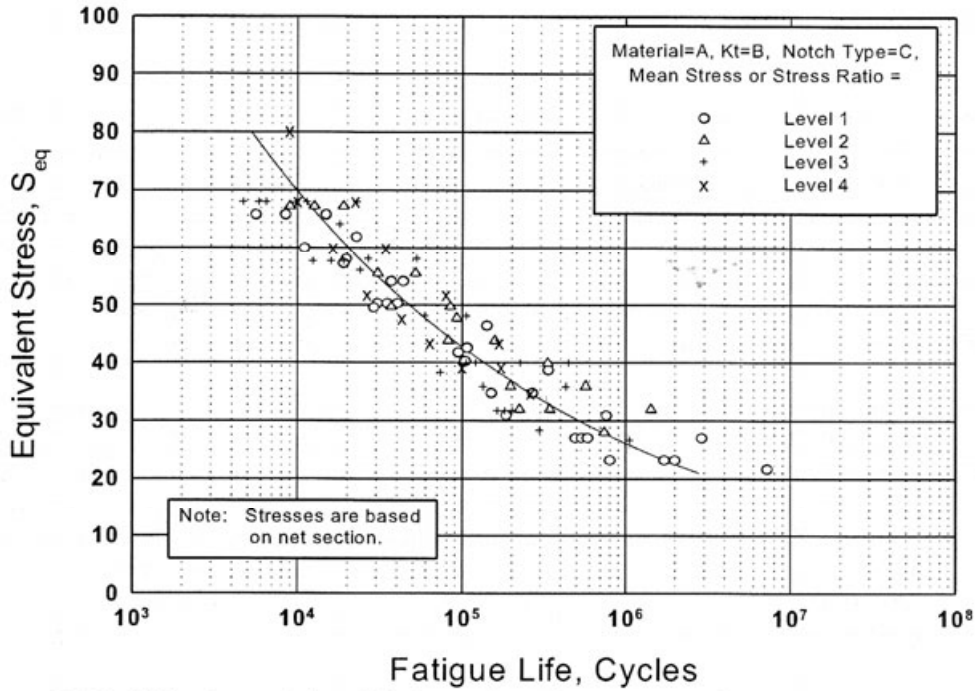


Figure 1.4.9.2(b). Consolidated fatigue data for a material using the equivalent stress parameter.

Fig. 2-189. An  $S_{eq}$ -N curve for a structural material.

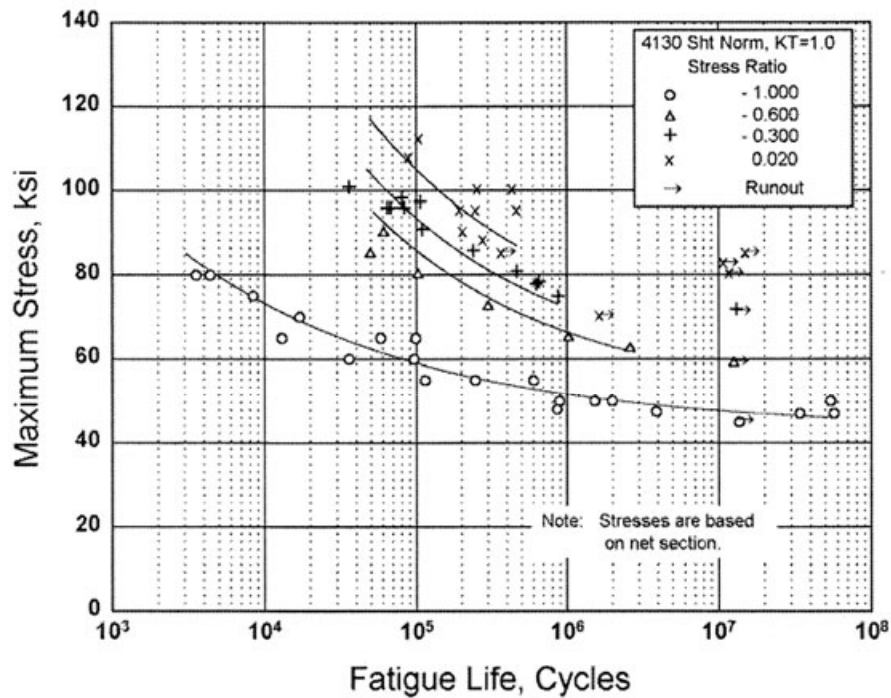


Figure 2.3.1.2.8(a). Best-fit S/N curves for unnotched 4130 alloy steel sheet, normalized, longitudinal direction.

Fig. 2-190. An S-N curve for a notch-free structural material.

## 2.6 VIBRATION

Appendix E contains a useful reminder about metal fatigue that crossed my desk in 1974. I've referred to that article throughout my career whenever some helicopter part became a problem.

Perhaps a little more background about fatigue stresses and cycles to failure would be of interest.

A simple example about structural fatigue is a ground-air-ground cycle. Imagine that a military helicopter flies 600 hours a year, or a commercial helicopter flies 1,200 hour a year. Imagine that a typical mission is 1 hour from start to finish. That would be 600 to 1,200 cycles per year acting on the landing gear. Whether retractable or fixed, one might expect the landing gear to last 30 years with minimum maintenance. That amounts to 18,000 to 36,000 cycles.<sup>105</sup> As another example, think of the axles and wheels and other associated parts of a car. If driven at 50 miles per hour for 100,000 miles, a car accumulates about 2,000 hours. Who knows how many cycles the springs and shock absorbers experience in 2,000 hours? But then think about the car's engine turning at 2,000 revolutions per minute (i.e., about 33 Hz) at 50 miles per hour for 100,000 miles or 2,000 hours. That means that the engine crankshaft accumulates 240,000,000 or  $2.4 \times 10^8$  cycles. An even more astounding example is the human heart. At a pulse rate of 60 beats per minute (1 Hz), the heart has accumulated  $2.4 \times 10^9$  cycles after 75 years. That is 10 times the life of a car engine!

This brings me to the subject of materials used in aircraft. The primary question, of course, is how many cycles can various materials such as wood, metals, and modern composites absorb before they break due to an alternating load. It is well known that early airplanes were constructed primarily of wood frames. Furthermore, George Rosen's book [288] about the history of propellers describes many early wooden propellers including those for sale in 1910 (Fig. 2-191). According to Rosen, "The typical service life of a wooden propeller generally lasted no more than six months." These early aircraft were, however, powered by the internal combustion engine, which the aviation pioneers borrowed from the budding auto industry that was rapidly encountering part failures due to metal fatigue.

The move to propellers made of sheet steel riveted along the edges was disappointing, to say the least. Caldwell [423] shows 7 figures of early efforts where the metal propellers ran 5 minutes or less, at about 1,440 revolutions per minute, before destruction. Rosen notes that by the fall of 1921, Dr. Sylvanus Albert Reed had developed and successfully flight tested the forged duralumin (aluminum plus copper) two-bladed propellers. Reed's success earned him instant fame in the aviation world and the Collier Trophy.

With the addition of variable pitch, the thin-tipped propeller (with any number of blades) that we know today came into its own. Then, as you learned in Volume I, Cierva developed rotor blades using a round, steel tube spar with a built-up set of ribs to achieve the

---

<sup>105</sup> It is more likely that a landing gear would be designed for crash landing rather than fatigue. However, you will remember that the British de Havilland Comet lost several commercial jets in 1954. The losses were caused by metal fatigue due to repeated pressurization and depressurization of the aircraft cabin.



**Fig. 2-191. The first U.S. propeller manufacturer ran this ad in a 1910 issue of *Aircraft* magazine [288].**

rotary wing. These vintage, 1930's rotor blades had a service life of 75 hours on the Cierva C.30 Autogiro. The C.30 37-foot-diameter rotor operated at a nominal tip speed of 370 feet per second. This is a 1/rev frequency of 3.18 Hz, so 75 hours amounts to about 860,000 cycles, slightly under 1 million or  $10^6$  cycles.

World War I saw the beginning of the end of wooden airframes and the start of widespread use of aluminum and steel tubes and sheets. As Nelson notes in his introduction to his report about wooden beams used for the main structure of airplane wings [424]:

“The present war [WWI] has caused an unprecedented demand for selected spruce for airplane construction. The increased demand has necessarily caused a greatly increased output. However, the magnitude of the requirements and methods of construction, whereby a large part of the selected stock is wasted in the construction of the one-piece beams, makes the problem of furnishing sufficient selected stock a very serious one, even with the enlarged output.

The remedy for this condition lies either in the discovery of a perfectly satisfactory substitute for the spruce now used, or in the development of some method of construction which will conserve the present supply by utilizing more of the selected material.”

## 2.6 VIBRATION

By 1931, rather thorough experiments and analyses [425] were showing that aluminum and steel were viable candidates for fuselage tubular structures, about which a doped canvas skin could be attached. With the coming of World War II, the need for a substitute for wood became even more acute. This accelerated the transition from wood to metal; this story is well told by Eric Schatzberg [426]. Then a landmark paper establishing Miner's Law for fatigue was published in September 1945. Milton Miner, a structural test engineer at the Douglas Aircraft Company, titled his paper *Cumulative Damage in Fatigue* [427]. While modern studies have questioned some of Miner's assumption, his "law" has been (and continues to be) applied to fatigue damage of many aircraft parts subjected to alternating loads of several magnitudes.

In 1950, a paper [428] was published in the Journal of the Helicopter Association of Great Britain.<sup>106</sup> The paper was titled *Materials and the Fatigue Aspect* and presented by a Mr. W. E. Cooper. Mr. Cooper primarily addressed rotor systems after writing "that fuselages, engines and transmissions could be designed and built by established procedures." He provides a very interesting table, which I have reproduced here as Table 2-29. This table refers first to U.T.S., which stands for ultimate tensile strength. Endurance limit refers to a level of vibratory stress at which the material will not be damaged with no less than the number of cycles listed. In fact, some materials behave *as if* the part will never break *if* the alternating stress never exceeds the endurance limit. This behavior is referred to as a run-out. The unit of tons is (I believe) a long ton, which is 2,240 pounds, not the 2,000 pounds per ton

**Table 2-29. A 1950's View of Material Fatigue Endurance Limits**

<i>Material</i>	<i>U.T.S. tons/sq. in.</i>	<i>Endurance Limit tons/sq. in.</i>
Mild Steel S.21	32	±14 at 20 × 10 <sup>6</sup> cycles
Medium C Steel S.1	35	±15 " "
Ni-Cr-Mo Steel S.11	60	±32 " "
Ni-Cr-Mo Steel DTD.331	85	±42 " "
Ni-Cr-Mo Steel S.28	100	±41 " "
Duralumin Bar L.1	28	± 9½ " "
Duralumin Forging DTD.150	23	± 5½ " "
Light Alloy Bar L.40	28	+ 9 " "
Mahogany		±1.45 at 50 × 10 <sup>6</sup> cycles
Jablo		±4½ " "
Jicwood		±4½ " "
Spruce		±1.4 at 10 × 10 <sup>8</sup> cycles

<sup>106</sup> Spurred on by the founding of the American Helicopter Society in 1943, a similar body was founded in Great Britain. The champions were members of the Royal Air Force who met on July 10, 1945. In September of that year, Memorandum and Articles of the Association were signed. The first annual general meeting was held on March 23, 1946, and 54 members were elected. The Association's Journal was published quarterly and Volume 1, Number 1, came out in September 1947. In January 1960, the Association merged with the Royal Aeronautical Society and became the Rotorcraft Section of the Society. There is a wealth of historically significant data in the Association's Journals.

used in the United States today. Thus, the 42 long tons per square inch equates to about 94,000 pounds per square inch. There are only a few modern steel alloys offered by MIL-HDBK-5J [417] that achieve this high of an endurance limit with the mean stress equal to zero. You will note from Volume I that Cierva used the highest strength steel listed in Table 2-29.

Because commercial autogyros and helicopters were being used in several countries by the early 1950s, the subject of airworthiness became a serious topic. The British Air Ministry created the Air Registration Board in 1936, and in 1951, Mr. J. K. Williams, a member of that Board, offered the Helicopter Association his views about certification requirements for a helicopter. He titled his paper, *The Fatigue Problem With Emphasis on the Airworthiness Aspects* [429]. In his opening remarks, Williams notes that “the designers of civil aeroplanes contemplate that their aircraft may be in service for at least 10,000 hours or so.” Then he sympathizes with helicopter designers because “when so little is still known about the fundamental nature of the fatigue of materials and the extreme difficulty of ascertaining the effect of varying external loads on a structure, the helicopter designer is presented with the problem of fatigue at his doorstep even at this comparatively early stage in helicopter development.” Nevertheless, Williams insists that “the principle must be established that having determined the range of stresses under all possible ground and flight conditions, then the *service* life of each critical component should be so determined as to ensure continuous safe operation—the service life being well below the fatigue life—of the component.”<sup>107</sup> Then, after commenting on fatigue testing and explaining the concept of cumulative damage theory (later to become Miner’s law), Williams suggests that

“very little research work has been carried out to date to substantiate the damage rule and what work has been carried out seems to indicate that the application of a number of stress cycles above the endurance limit lowers the life of the specimen under subsequent applications of a lower stress. In addition, if a number of stress cycles below the endurance limit is applied then the fatigue life under subsequent applications of a higher stress is improved.

Stated simply this means that the fatigue limit can be lowered by overstressing and raised by understressing which belies the cumulative damage rule. All these disadvantages to the application of the cumulative damage rule can be compensated to some extent by:

- (a) Carrying out tests on at least six specimens of each component to cover the scatter effect.
- (b) Introducing a multiplying factor for the magnitude of the stress cycle and this it is suggested should be (1.3).
- (c) Introducing a reduction factor to the fatigue life obtained on test in order to determine the service life. This reduction factor it is suggested should be (0.5).

The component is to be removed from service and replaced by a new component at the expiration of the service life. It is suggested that the service life as obtained by the above method should not exceed two to three thousand hours, especially for rotor blade components.

---

<sup>107</sup> It continually amazes me when I see the word “all” or the words “all possible” in specifications, regulations, and requests for proposals. The size of “all” is absolutely mind-boggling to me; so much so that I equate “all” with infinity. A work statement for “all” cannot be written nor can the cost of “all” be estimated. Of course, a schedule for “all” cannot be laid out. In my opinion, “all” is a very dangerous word.

## 2.6 VIBRATION

If the results of the laboratory tests indicate that the most critical factored stress cycles are all below the endurance limit of the component, then the component should still be replaced at a nominally agreed period and this period it is suggested should be in the region of four thousand hours.”

Williams concludes with two key statements:

“Finally all that has been mentioned in this paper to date leads to the inevitable conclusion that for the reduction of the possibility of fatigue failure to a minimum in helicopters there must be:

*First class design* of component parts with special emphasis on the elimination of high stress concentrations which can have such a calamitous effect on the fatigue endurance of a structural component. These stress concentrations can be induced in various ways.

- (1) *By design*—Sharp angles, changes of section (re-entrant angles), screw threads.
- (2) *Machine shop*—Rough turning, accidental tool marks on the surface. Grinding cracks. Identification and inspection stamp marks.
- (3) *Fabrication*—Slag blowholes and cracks in welded construction. Press fits and shrink fits.
- (4) *Heat treatment*—Cracks due to hardening stresses.
- (5) *Manufacture of material*—Importance of surface finishing (use of shot peening process) because practically all fatigue failures originate at the surface.

In addition, the workmanship and standards of maintenance and inspection on these components have to be of a very high order indeed. Lately we have come to realize that the design, manufacture and inspection of these vital component parts of the helicopter, the failure of anyone of which in flight may have such unfortunate consequences, must be of a standard even higher than that for aircraft engines. That is to say, much higher than the standards for the design and manufacture of fixed wing aircraft. This may yet prove to be the most important of all the preventatives of fatigue failure on helicopters.”

The helicopter industry took these 1951 airworthiness requirements to heart as it grew to the industry we know today. Understanding fatigue and how to avoid the pitfalls Williams enumerated (plus many others) has been a number-one priority of stress men, load calculating engineers, designers, builders, and operators, and caution has been a byword as new materials such as titanium and fiberglass have been introduced.

By 1951, the budding helicopter industry was experiencing a growing number of unexplained rotor blade fatigue failures. At that time, blade structural design technology was only able to estimate blade bending frequencies and mode shapes. Calculating actual bending moments and stresses was hardly attempted. The technology situation had, in fact, hardly improved from the autogyro era. The thought was that at and near operating rotor speed, the calculated natural frequencies of the vibrating beam (i.e., a rotor blade) should not be close to integers of rotor speed. (You learned about this aspect of blade design in Volume I, pages 139 to 191, in relation to autogyros.) At that time, little attention was given to bending modes above the second flapwise mode, but with the number of blade fatigue failures growing, the Air Research and Development Command at the Wright Air Development Center (WADC) decided that action was required. The Rotary Wing branch of the Propeller Laboratory, with Captain Paul Simmons acting as project engineer, placed a research contract with the Aero-Mechanics Department of Cornell Aeronautical Laboratory.

The research contract called for designing, building, whirl tower testing, and then flight testing three sets of blades on a Sikorsky H-5 production helicopter. The H-5 was designated by the U.S. Navy and the Marines as an HO3S (Fig. 2-192). The 5,500-pound gross weight was supported by a 48-foot-diameter rotor and powered by one Pratt and Whitney R-985-AN-7 450-horsepower engine. The seating was one plus three-in-a-row. Sikorsky sold the model commercially as an S-51.

The research program was named the “H-5 Variable Stiffness Blade Program.” The results of the program were published in six parts [430], and the principal authors were Harold Hirsch and James Kline. The project pilot and flight engineer was Hans Weichsel, Jr.<sup>108</sup> The background paragraphs provided in Part 3 show just how advanced this program was and are of significant historical value. They read as follows:

**“Program Initiation** The need for, and organization of, the so-called ‘H-5 Variable Stiffness Blade Program,’ from which the results presented in this paper are extracted, was conceived jointly by W.A.D.C. Rotary Wing Branch personnel, and engineers of the Cornell Aeronautical Laboratory. Approaching the problem with the limited theoretical and experimental data available at the time the project was conceived, it is frankly admitted that the existence of higher mode resonant bending was not then foreseen. In fact, at the time there were no proven arguments to refute the popular opinion that the role of blade bending stiffness in determining blade motions and stresses was of secondary importance. This opinion, while now proven false as a generalization, can be justified with some logic for the case of first mode bending, by the fact that the centrifugal stiffening effect realized with normal blades will be four or five times as great as that due to their structural stiffness. In view of this fact, and anticipating only quasi-static bending in the first bending mode, with, perhaps some amplification, it was felt that the differences between data, measured with blades possessing the limited amount of stiffness variation obtainable with conventional blade’ construction, would be too small to be accurately determined. Design requirements were, therefore, established for blades which would provide a four-to-one stiffness range, yet possess approximately the same mass and aerodynamic characteristics [as standard H-5 blades]. Further, the blades were to possess 1/2, 1, and 2 times the stiffness of standard H-5 blades, and be flyable on an H-5 helicopter. With a four-to-one stiffness range, it was anticipated that stiffness variation effects would be sufficiently large so that they could be measured.

**Fiber Glass Blade Design** Extensive preliminary studies (ref 5) of various blade designs revealed only one which met the four-to-one stiffness range requirement. The proposed design called for the development of three separate sets of blades, one of each stiffness, employing a fiber glass shell, die molded integrally to a balsa wood core. By employing the high strength-to-weight ratio of fiber glass, in conjunction with the ability to vary the elastic modulus of the fiber glass skin by selectively orienting the fiber direction, the required stiffness range was provided. Whirl test blades were first constructed to prove the fiber glass design, and, after they successfully passed Propeller Laboratory tests, the three sets of flight test blades were manufactured. Detailed information concerned with the design and manufacture of the fiber glass blades may be obtained from reference 6 and 7. A further description of the blades, together with a detailed analysis of their mass, structural, and dynamic characteristics is also available (ref 8). The finished appearance of the blades is shown in figure 1, p. 4.”

---

<sup>108</sup> Hans left Cornell Labs in 1960 and joined Bell in 1965. When I arrived at Bell in 1977, I had the good fortune to be influenced by him on several new product development programs. Hans was a gentleman of the old school, had a tremendously good intuition for practical engineering, and a feeling for the needs of the commercial marketplace that I thought was unmatched by anyone I had ever met.

## 2.6 VIBRATION



**Fig. 2-192. The H-5 served in South Korea from 1950–1953 during the Korean war (photo from author’s collection).**

To me, this research into blade frequency placement to avoid resonance with periodic airloads was a milestone. The fact that bending in the third flapwise mode was very important, particularly at low speeds associated with transition, was quite an eye-opener. The Cornell Aeronautical Lab researchers discovered this fact using *fiber glass blades* in 1951. The three sets of blades each had one blade with flap bending strain gauges located at blade radius stations of 72, 108, 135, 162, 189, 216, 234, 252, and 272 inches on the 24-foot-radius blades. When you read this report, I am sure you will be struck by the conclusions, which were, in part:

“While the good correlation obtained, between predicted and measured results indicates that it should be possible to predict resonant conditions during the design stage it is unfortunately found that little can be done to avoid coming close to one or another resonant point, it appears that the best that can be done at least until the nature of the resonance is understood is to make provision in the design so that the natural frequencies may be shifted in such manner that the resonant conditions do not coincide with normal operating conditions.

Attention is called to the necessity of providing sufficient data stations, when conducting blade strain surveys so that information will be obtained at all critical blade stations. Equally important it is necessary that the stations be judiciously chosen, so that they do not fall at node points, and thereby fail to detect important higher mode contributions.

Finally, anticipating the probability of some higher order bending content, it is important that the blade designer recognize the critical role which resonant conditions may play in determining the fatigue life of blades. Since the blade resonant frequencies are harmonic multiples of the rotor speed it is important to anticipate that the load cycles applied to the blade will be proportional to the product of total rotor revolutions and the exited harmonic orders and that the peak stresses and vibratory moment amplitudes will be larger than predicted by current theory.

It is believed that this report completely substantiates the existence of the rotor blade higher mode bending phenomenon and that it discloses the most important manifestations of the problem. It is recognized that no answers are provided to many of the questions raised by the results presented. Such answers are not yet available. It is hoped however that the problem will occasion sufficient interest, and concern so that it will receive the attention which it merits, and that additional work aimed at providing the required answers will be undertaken.”

The blade problem *has* “received the attention” as you can well imagine.

### 2.6.3 Hub Vibratory Loads, Aircraft Response

The heart of the helicopter vibration problem lies behind the five words that title this section. Simplistically, the problem falls in the category of forced vibration of a structural beam. In fact, despite some six-plus decades of intense effort, members of the rotorcraft community have only a general idea of the rotor system vibratory forces and moments that are applied to the structural beam called a helicopter. Even when given the “virtually” exact applied loads, the response of the beam has only been approximately estimated with an extremely detailed theory that relies totally on the modern computer.

You will find a simple analysis of the vibrating beam problem in Appendix F. It should help you understand the key engineering terms and concepts used by dynamists.

To give you more insight into the overall problem, let me first discuss some flight test vibration measurements for a few helicopters, then secondly, delve deeper into what are commonly called ground shake tests and analyses of helicopters. The progress made in actually calculating the hub vibratory loads will be taken up in a later paragraph.

#### 2.6.3.1 Some Flight Test Results

The pioneering efforts of the U.S. Army to select the helicopter rather than the autogyro for its future needs led Sikorsky to develop the R-4, R-5, R-6, and the commercial S-51. Then Bell developed the now familiar Bell Model 47 (Fig. 2-110). This helicopter received the world’s first civil certification (from the then CAA) on March 8, 1946. With the Korean War on the horizon, the Army began procuring light, two-place, side-by-side-seating helicopters in small lots in 1948. Significant quantities of both Bell H-13s (Model 47) and Hiller H-23s (Model 360 or UH-12) were procured during fiscal year 1951, the first year of the Korean War. These military helicopters were flight tested at the Air Force Flight Test Center located at Edwards Air Force Base in California.

Reported flight test results for both H-13 and H-23 helicopters included vertical vibration measurements on the floor between the pilot’s and passengers’ seats. The measurements were made with accelerometers, which give an output in feet-per-second squared. The general practice is to divide the accelerometer output by the gravity constant (32.174 feet-per-second squared) to convert vibration to units of g.

This first example provides vibration data for the H Model of the Bell H-13 [171]. The primary result is vibration versus calibrated airspeed.<sup>109</sup> The once-per-revolution (1/rev) vibration for this helicopter is given in Fig. 2-193 and, because the H-13 has a two-bladed rotor, vibration at 2/rev is given in Fig. 2-194. The nominal main rotor speed is 344 rpm, which is 5.7 Hz and, therefore, 2/rev equals 11.4 Hz. Note that vibration at 1/rev is on the order of 0.03 g or less. Based on the 1978 ISO 2631 standards shown in Fig. 2-183, the crew should remain proficient for at least 4 hours. In contrast, the 2/rev vibration can reach at least

---

<sup>109</sup> See footnote 65 on page 212 for calibrated and true airspeeds.

## 2.6 VIBRATION

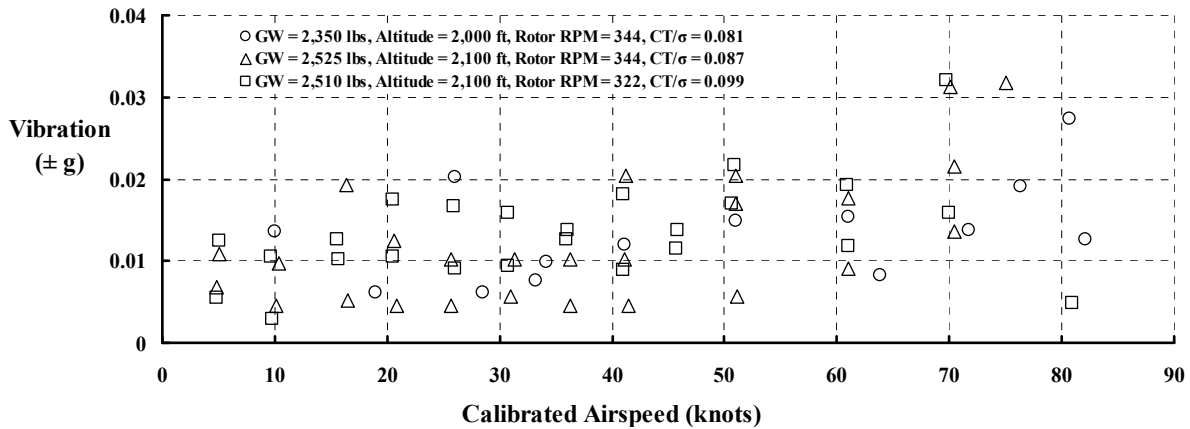


**Fig. 2-193. Bell H-13H 1/rev vibration at the pilot's floor [171].**

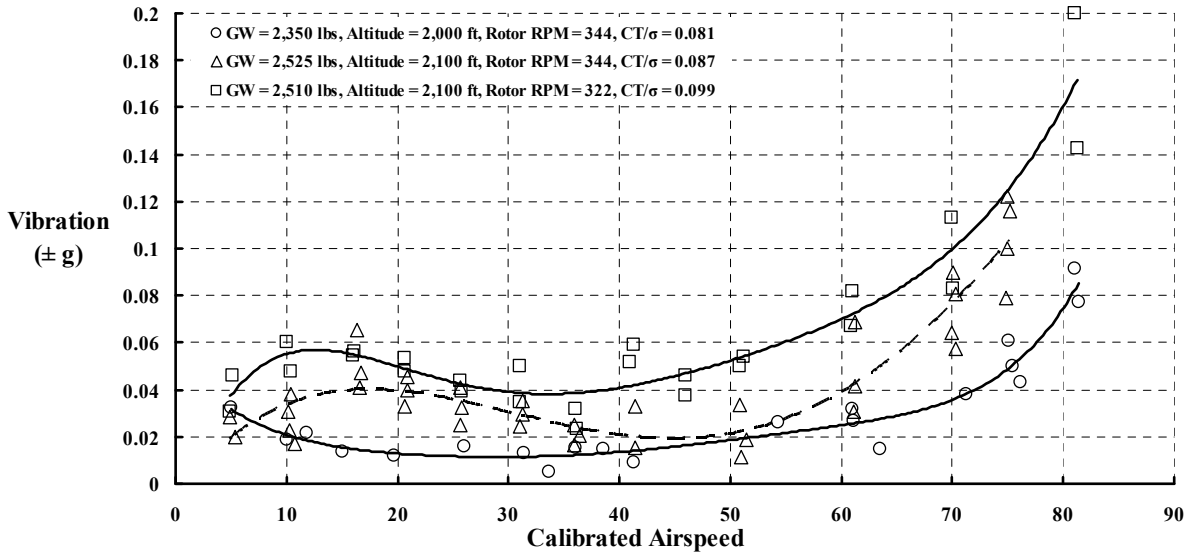


**Fig. 2-194. Bell H-13H 2/rev vibration at the pilot's floor [171].**

0.2 g at 80 knots. Using ISO 2631 standards (with 0.2 g at 11.4 Hz), crew proficiency would begin to deteriorate within an hour or less. Of course, the pilot can drop off speed by 10 knots and obtain a more tolerable ride.

Fig. 2-194 raises a serious point about performance. If the maximum speed or, worse yet, the cruise speed is accompanied by quite high vibration, then the helicopter will have a crew-imposed speed limit. This is a very serious deficiency for any rotorcraft. It might be tolerated for a military mission, but this situation would never be tolerated in commercial operations.

The second helicopter of particular interest is a very small U.S. Army machine obtained from Hughes in the late 1950s. This helicopter began commercially as the Hughes Model 269 and ultimately became the Schweizer Model 300. Along the way, the initial Army model was designated as the YHO-2HU (Fig. 2-195), later to become the T-55 Osage.

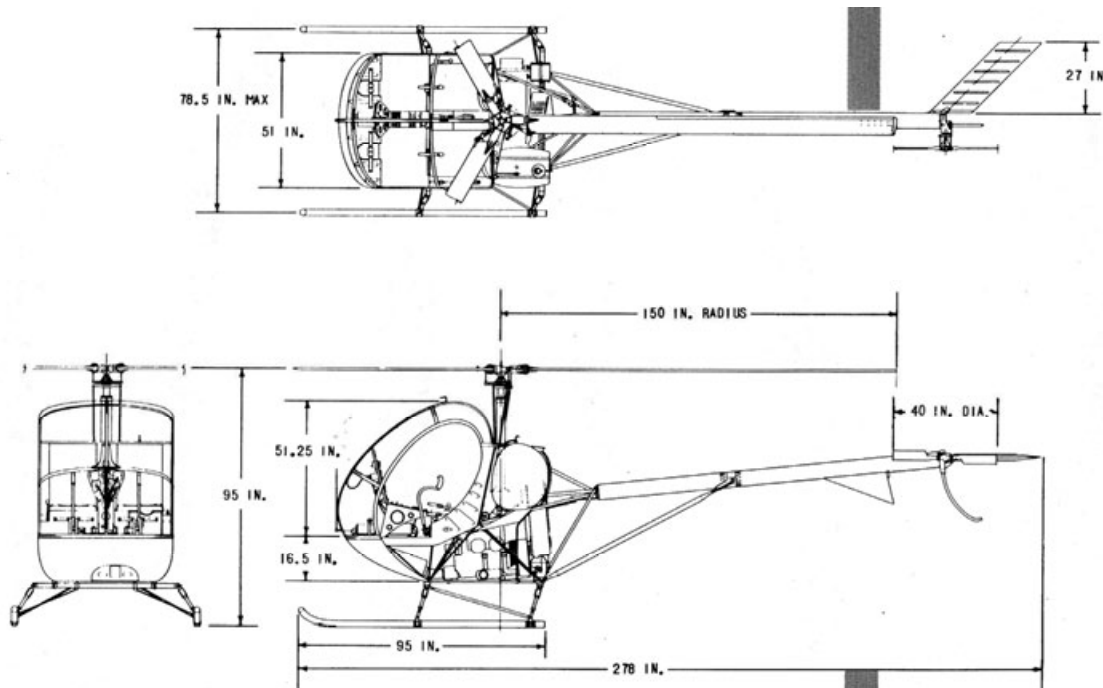


**Fig. 2-195. The Hughes Model 269 became the T-55 primary flight training helicopter for the U.S. Army and is now, with improvements, the Schweizer (now part of Sikorsky) Model 300 [111].**

The T-55 became the standard Army training helicopter until the late 1980s. Some 60,000 Army aviators were trained to fly in this machine. The 25-foot-diameter rotor operated normally at 450 rpm, which is a 1/rev of 7.5 Hz. The takeoff gross weight was 1,550 pounds, and the aircraft was powered by a 180-hp Lycoming HIO-360-B1A piston engine.

The primary vibration reported by Ken Ferrell [111] was at 3/rev or 22.5 Hz because of the three-bladed rotor system. The section of the report dealing with vibration spoke quite favorably about the vibration levels of the YHO-2HU saying:

“The vibration characteristics in level flight are very good and compare favorably with the smoothest helicopters. The vibration was found to be greater for the heavy weight than for the light weight condition. The magnitude also increased as the engine speed was decreased. Vibration levels at the pilot’s seat were greater than those measured at the rotor mast, *indicating that the cabin structure was amplifying the vibration in the cockpit.* [My italics.]

The vibration levels vary with airspeed and in general are at a minimum for airspeeds of 30 to 50 knots TAS. The following illustration [see Fig. 2-196] shows a typical variation of vibration with airspeed: As the airspeed is increased and blade stall is encountered the vibration levels increase. The vertical vibration is greater than the lateral for both locations, with the exception of the low altitude heavy-weight conditions.”

What is very interesting about the “illustration” shown next is that the vibration is virtually twice what MIL-H-8501A [410] allowed as noted in Fig. 2-183. In fact, when all the reported data is gathered up on one chart as I have done with Fig. 2-197, the summary “illustration”

## 2.6 VIBRATION

appears rather optimistic. Furthermore, the T-55 exhibited a very substantial lateral vibration at the pilot's seat as Fig. 2-198 shows. That these vibration levels (which exceed MIL-H-8501A) might be considered "very good and compare favorably with the smoothest helicopters" can only be explained by ISO 2631 standards provided in Fig. 2-182. According to those standards, 0.4 g at 22.5 Hz (i.e., 3/rev) should be tolerable for somewhere between 25 and 60 minutes.

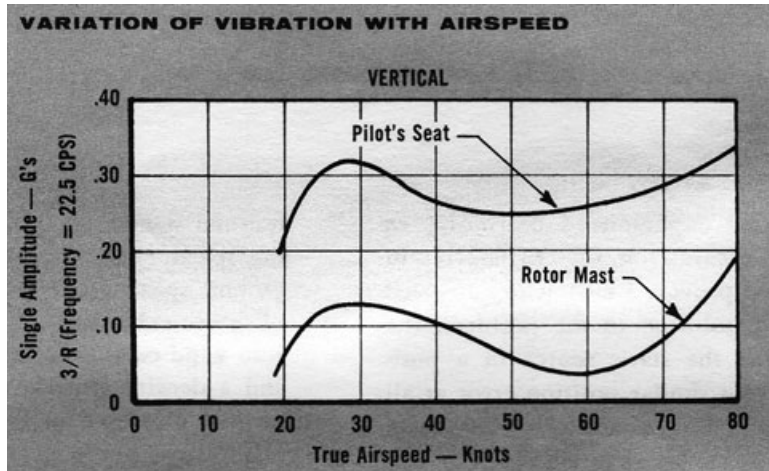


Fig. 2-196. The summary opinion of the U.S. Army about the vertical vibration of the T-55 at the pilot's seat and at the rotor mast [111].

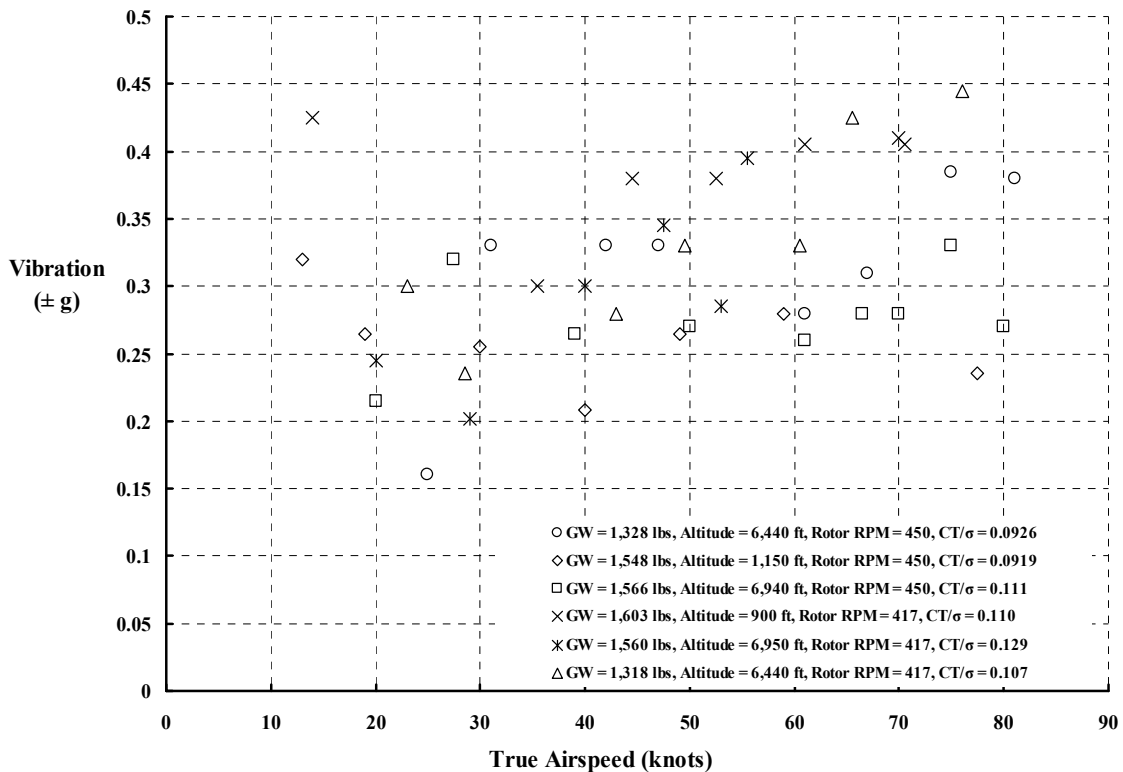


Fig. 2-197. The vertical vibration data at the pilot's seat of the T-55 for a number of weights, altitudes, and main rotor speeds [111].

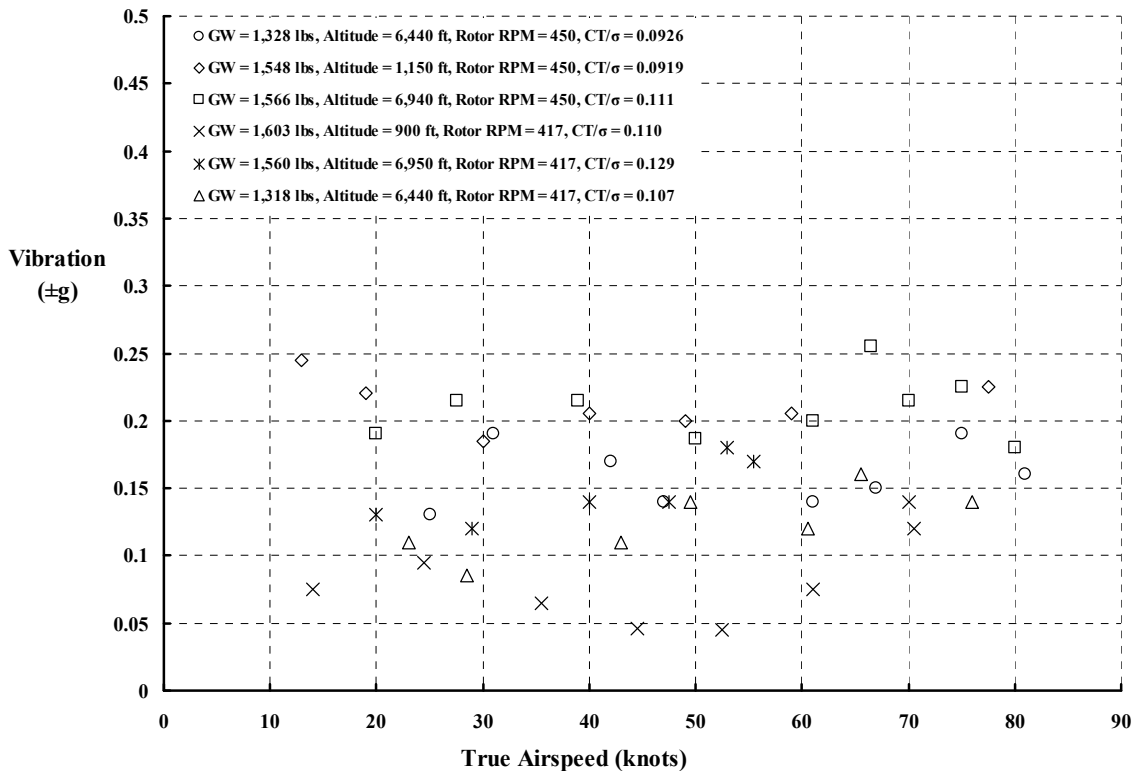


Fig. 2-198. The *lateral* vibration data at the pilot's seat of the T-55 for a number of weights, altitudes, and main rotor speeds [111].



Fig. 2-199. The B model of the H-21 was used by the U.S. Air Force. The C model was the Army's version (photo from author's collection).

The Piasecki H-21B shown in Fig. 2-199 is the next helicopter of particular interest. This tandem rotor helicopter was the result of Frank Piasecki's first step into production. The B and C models had a three-bladed, 44-foot-diameter rotor with the front rotor turning

## 2.6 VIBRATION

counterclockwise when viewed from above. The rotors did not intermesh. In its final grow version, the gross weight was 15,000 pounds. A major marketing point was that the tandem rotor helicopter had a much wider center-of-gravity range than a corresponding single rotor machine such as the Sikorsky H-34. This feature allowed greater flexibility in cargo and troop loading. I must tell you, however, that this marketing debate has gone on for decades.

An Air Force flight test report [109] written by Jim Hayden<sup>110</sup> provided vibration data at three center-of-gravity positions within the gross weight to center of gravity (GW-c.g.) envelope<sup>111</sup> for a gross weight of 15,000 pounds. The mid center of gravity for the test was at fuselage station 339 inches, which was 15 inches forward of the centerline between rotors. The forward center of gravity for this test was at fuselage station 328 inches, and the aft center of gravity was at fuselage station 347 inches. The flight test data provided in Fig. 2-200 shows that the aft and mid center-of-gravity vertical vibration at the pilot's floor station (along the main beam) was significantly lower than at the forward center-of-gravity location. At the test main rotor speed of 258 rpm, the 1/rev frequency was 4.3 Hz, which means that the 3/rev vibration shown in Fig. 2-200 was at 12.9 Hz.

This H-21 test report states that “every pilot who assisted in the qualitative evaluation commented on the low vibration of the test aircraft. Some stated that it was the smoothest H-21 that they had ever flown.” This statement is, of course, quite different than saying that “the test aircraft” was the *smoothest helicopter* they had ever flown.

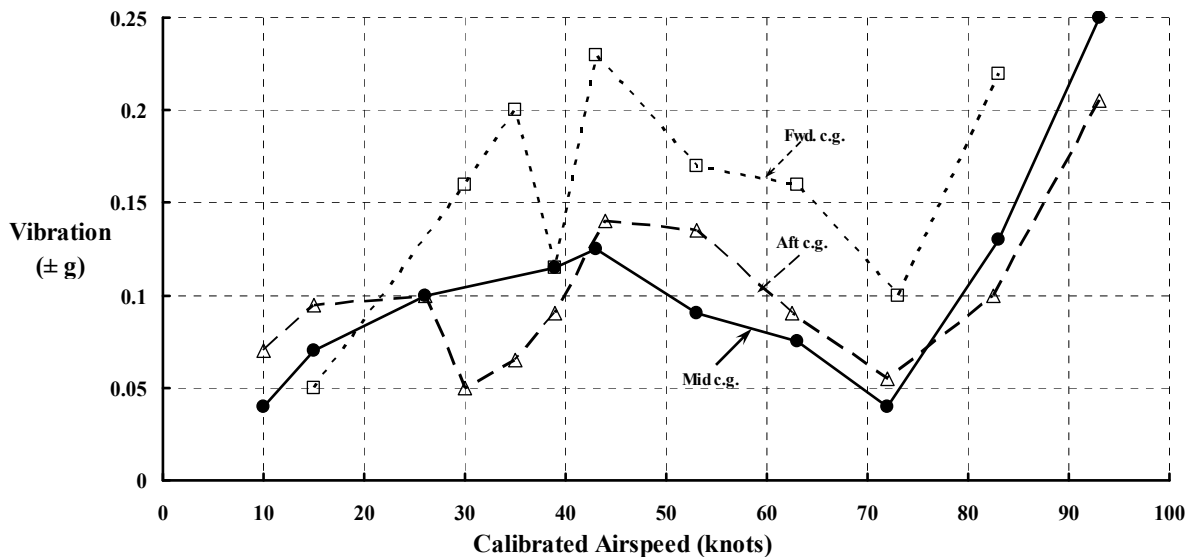


**Fig. 2-200. Pilot 3/rev vertical vibration for the tandem rotor H-21B (gross weight 14,800 lb, density altitude 3,000 ft, main rotor speed 258 rpm, and  $C_T/\sigma = 0.106$  [109]).**

<sup>110</sup> When Jim left the Air Force he came to Vertol (later Boeing Vertol) and was a flying qualities expert—and a very good friend.

<sup>111</sup> The aircraft's center of gravity ranged from about 4 inches aft of the centerline between rotors to 25 inches forward of the centerline for gross weights at or below 13,500 pounds. The center of gravity range decreased to about 15 inches at a gross weight of 15,000 pounds.

While on the subject of tandem helicopters, I should point out that the other early tandem rotor helicopter that came to production with Piasecki's leadership was the HUP (see Fig. 2-80). This helicopter was chosen by the N.A.C.A. for flight test and analytical study [431] because it "was known to have a high vibration level under certain conditions." Tests were made with both wood and metal blades. The test approach was to use an in-flight shaker to excite coupled rotor/airframe response. Vibration at both 3/rev and 6/rev with the three-bladed rotor systems was very high (approaching 0.8 g) near the forward hub in the low-speed range. This report is a very important piece of work that was done in 1957.

Using flight evaluation of the Boeing Vertol CH-47D as the measure [432], the vibration situation for tandem rotor helicopters since the 1957 HUP has shown only modest improvement over the years. From test data acquired all through 1983, the report states (from paragraph 94 b) that "the high level of cockpit vibration at and above cruise airspeed (about 140 knots calibrated airspeed) is a shortcoming.<sup>112</sup> However, attenuation of the cockpit vibrations is not planned due to the limited mission profile time spent above cruise airspeed, the weight penalty, and the complexity of attenuation systems." This flight evaluation included a qualitative vibration rating scale, which I have reproduced here as Fig. 2-201. The crew rated the CH-47D in the 7 to 9 range at speeds above cruise.

DEGREE OF VIBRATION	DESCRIPTION <sup>1</sup>	PILOT RATING
No vibration		0
Slight	Not apparent to experienced aircrew fully occupied by their tasks, but noticeable if their attention is directed to it or if not otherwise occupied.	1 2 3
Moderate	Experienced aircrew are aware of the vibration but it does not affect their work, at least over a short period.	4 5 6
Severe	Vibration is immediately apparent to experienced aircrew even when fully occupied. Performance of primary task is affected or tasks can only be done with difficulty.	7 8 9
Intolerable	Sole preoccupation of aircrew is to reduce vibration level.	10

<sup>1</sup>Based upon the Subjective Vibration Assessment Scale developed by the Aeroplane and Armament Experimental Establishment, Boscombe Down, England.

**Fig. 2-201. The vibration rating scale frequently quoted by flight test pilots.**

<sup>112</sup> In U.S. Army lingo, a shortcoming is defined as an imperfection or malfunction occurring during the life cycle of equipment that must be reported and that should be corrected to increase efficiency and to render the equipment completely serviceable. It will not cause an immediate breakdown, jeopardize safe operation, or materially reduce usability of the material or end product. Next comes a deficiency. A deficiency is an unacceptable red flag, to me, and requires immediate action by the chief engineer.

## 2.6 VIBRATION

The next helicopter of interest is the experimental model of what became the Bell Huey. The test report [115] deals with the Bell XH-40, which laid the foundation for the U.S. Army UH-1 series and Bell commercial Models 204 and 205. The first flight of this experimental single rotor, turbine-powered helicopter was made in late October 1956. By May 1958, the Air Force Flight Test Center at Edwards Air Force Base was able to publish a flight test evaluation. The flying portion of the program was accomplished between April 30th and June 21st of 1957. In discussing vibration, Keith Putnam (the project engineer) and Bob Ferry (an Air Force Captain and the project pilot)<sup>113</sup> had this to say:

“As expected with a two-bladed rotor, the frequency of the predominant vibration harmonic was two oscillations per rotor revolution (two-per-rev). Under some flight conditions the four-per-rev component was also significant. Vibration was recorded in the lateral and vertical directions at the center of gravity, between the pilots’ seats and at the extreme sides of the cockpit beside pilots’ seats. Lateral vibration in the cockpit and vertical vibration at the cg did not exceed 0.1g in amplitude and therefore has not been presented in appendix I. Since vibration at the left and right sides of the cockpit was found to be similar, only vibration data obtained at the right side has been presented.

Vertical vibration in the cockpit was in all cases greater than at the center of gravity. This indicates that the vibration input from the rotor to the airframe is being amplified by the cockpit structure to amplitudes that become unacceptable in the high speed range. Vibration at the pilots’ station was also found to increase with distance from the centerline of the aircraft. It is therefore suggested that the vibration experienced by the pilots at high speed (as induced by blade stall), at the altitudes tested, could be reduced considerably by changing the response characteristics of the cockpit structure.

The helicopter was very smooth in hovering flight. Vibration under most conditions was less than 0.1g. The H-40 exhibited an unusually low vibration level during stabilized flight in the transition region (10 to 30 knots CAS), an area where many helicopters are quite rough. At speeds above transition, vibration decreases and remains at acceptable levels (less than 0.2g) until the onset of blade stall for the altitudes at which vibration data was gathered — 6,000 to 11,500 feet. As blade stall progresses the vibration level in the cockpit increases sharply with speed and quickly becomes unacceptable.”

There is no question that in terms of recorded vibration data, the XH-40 was giving the pilot and copilot a rough ride at the high-speed, high-altitude conditions and low main-rotor speed. While the gross weight ranged from a low of 5,290 to 5,400 pounds (nominally the design gross weight), the tests were conducted at three main-rotor speeds of 294, 304, and 314 rpm. Only two nominal altitudes were flown: the low altitude was around 6,000 feet and the high altitude was about 11,000 feet. The blade loading coefficient ( $C_T/\sigma$ ) ranged from 0.094 to 0.124.

---

<sup>113</sup> Keith and Bob took this experimental helicopter right to its limits in 30.5 hours of flying. At the design gross weight of 5,400 pounds, they tested up to 105 knots true airspeed at 11,500-foot-density altitude. Their concluding view was that “The XH-40 in the state of development tested is unacceptable for service use. Correction of its present deficiencies, however, will result in a helicopter with excellent performance compared to current helicopters.” With improvements, total production exceeded 15,000, which put this helicopter in the class of the Douglas DC-3 and its military equivalent, the C-47.

The highest vibration was measured on the cockpit floor, just to the right of the pilot's seat.<sup>114</sup> This conclusion is suggested by Fig. 2-202 and Fig. 2-203. Putnam and Ferry stated that "at speeds above transition, vibration decreases and remains at *acceptable levels (less than 0.2 g)* [my italics] until the onset of blade stall..." This "less than 0.2 g" criteria was met for five of the six test data sets as Fig. 2-202 shows. From Fig. 2-203 you can see that the right side of the cockpit floor has about  $\pm 0.078$  g more vibration than the floor between the crew members. This suggests that the helicopter had a lateral hub vibratory force that was rocking the machine about its longitudinal axis. The onset of blade stall appears to create both excessive 2/rev and 4/rev vertical vibration as Fig. 2-204 shows.

The onset of blade stall as indicated by the vibration of the Bell XH-40 was addressed by Putnam and Ferry in their flight evaluation report [115]. They took a very direct approach stating:

"In a manner analogous to the development of the expression for stall in a fixed wing aircraft the following equation may be derived to express the relation between the variables affecting retreating blade stall in a helicopter.

$$\sqrt{W} = K\sqrt{\sigma}(V_{rot.} - V_{fwd. stall})$$

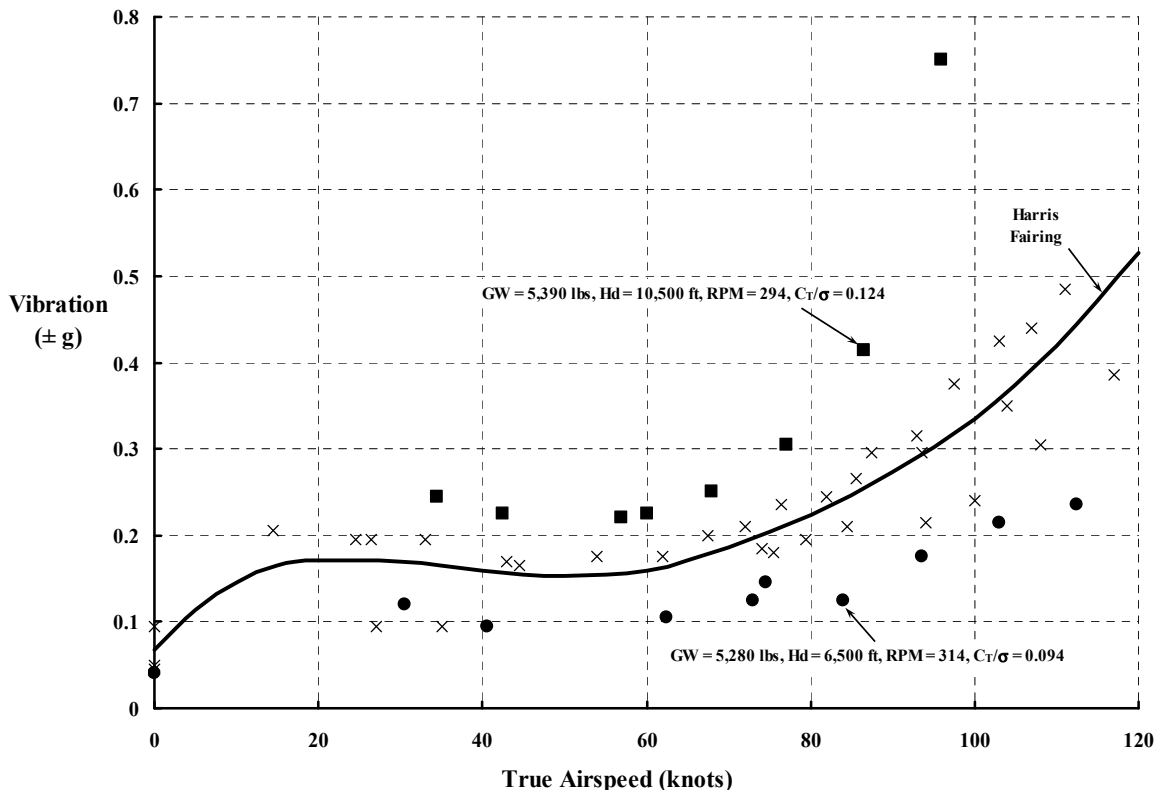


Fig. 2-202. Pilot 2/rev vertical vibration for the XH-40 [115].

<sup>114</sup> The cockpit station for a two-man crew frequently places the pilot's seat on the starboard side of the helicopter. This differs from fixed-wing practice where the pilot in command is placed on the port side of the aircraft.

## 2.6 VIBRATION

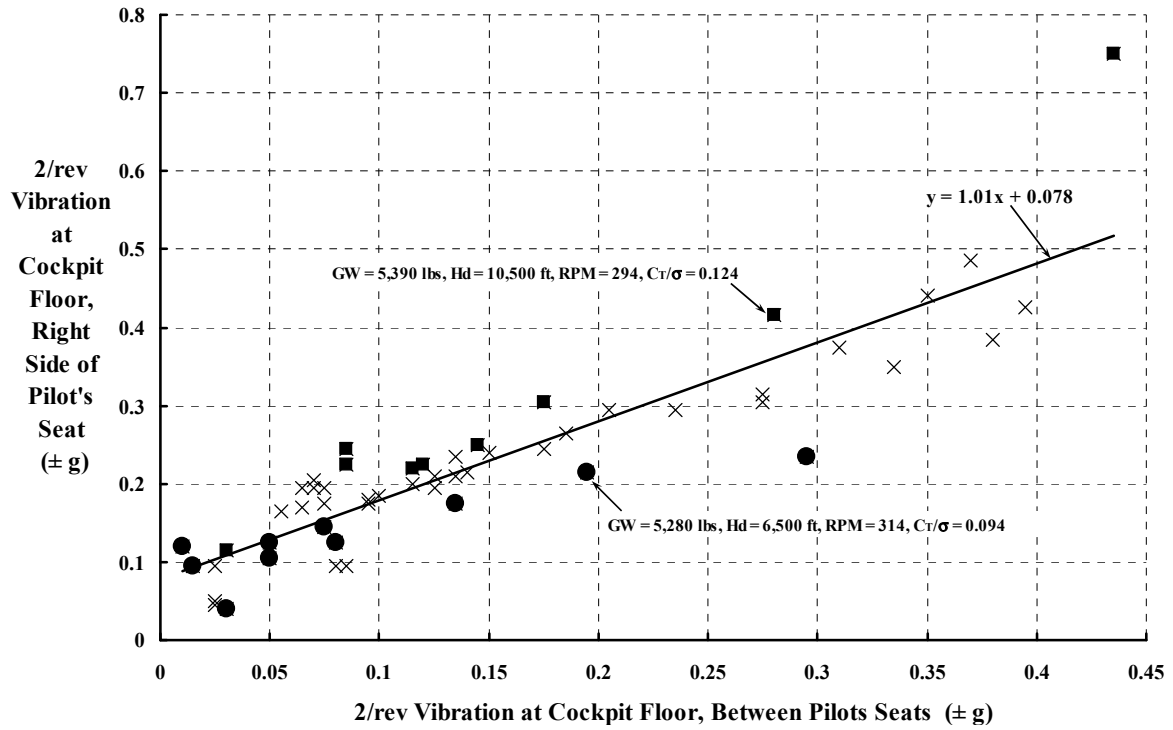


Fig. 2-203. Cockpit floor 2/rev vertical vibration for the XH-40 [115].

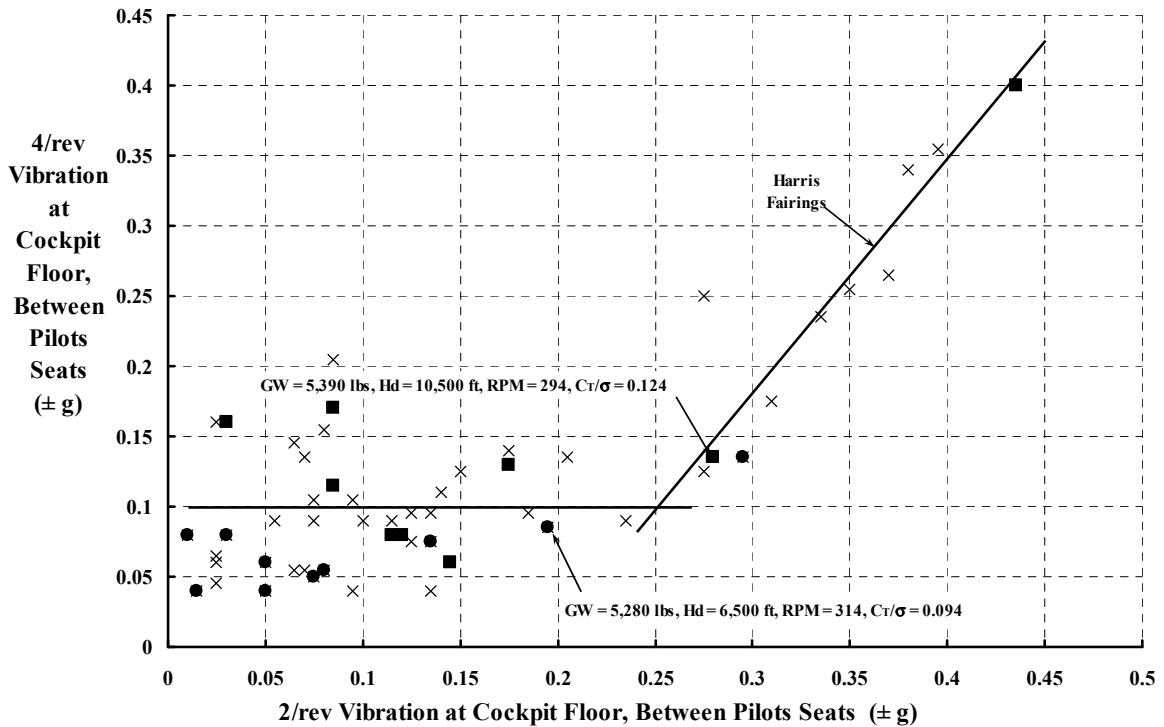


Fig. 2-204. Cockpit vertical vibration above  $\pm 0.25$  g was an indication to the flight crew of blade stall onset for the XH-40 [115].

where

$W$  = gross weight at which stall occurs, lb.

$\sigma$  = ratio of air density at which stall occurs to air density at sea level

$V_{rot.}$  = tip speed of rotor due to rotational velocity, fps =  $\frac{2\pi}{60} N_R R$

$N_R$  = rotational speed of rotor, rpm

$R$  = rotor radius, ft

$V_{fwd. stall}$  = true forward speed at which stall occurs, fps.

$K$  = constant determined by flight test

As discussed in the Level Flight section of the Test Results it was very difficult for the pilot to distinguish between vibration due to blade stall because vibration from other sources was also present. In analysis of the vibration data it was observed that at high altitudes (6,000 to 11,000 feet) a sharp increase in vibration level occurred at certain airspeeds. It was reasoned that perhaps at these altitudes the only phenomena causing this increase in vibration level was retreating blade stall. If this were true then the airspeeds at which a given level of vibration occurred might correlate with the stall equation. A level of 0.25g was chosen since this is the beginning of the unacceptable vibration range and in all cases was above the airspeed at which the sharp increase in vibration occurred. This data correlated quite well, as may be seen in the following plot, considering the wide variation in density and rotor speed between the individual points. All stall predictions in this report were made from the line faired through these points."

The "plot" Putnam and Ferry refer to is reproduced here as Fig. 2-205. They accompanied the plot with a note that "each data point was taken at a vibration level of 0.25 G." This is the first and only example I have of someone trying to closely relate (in a quantified manner) blade stall onset to increasing vibration.

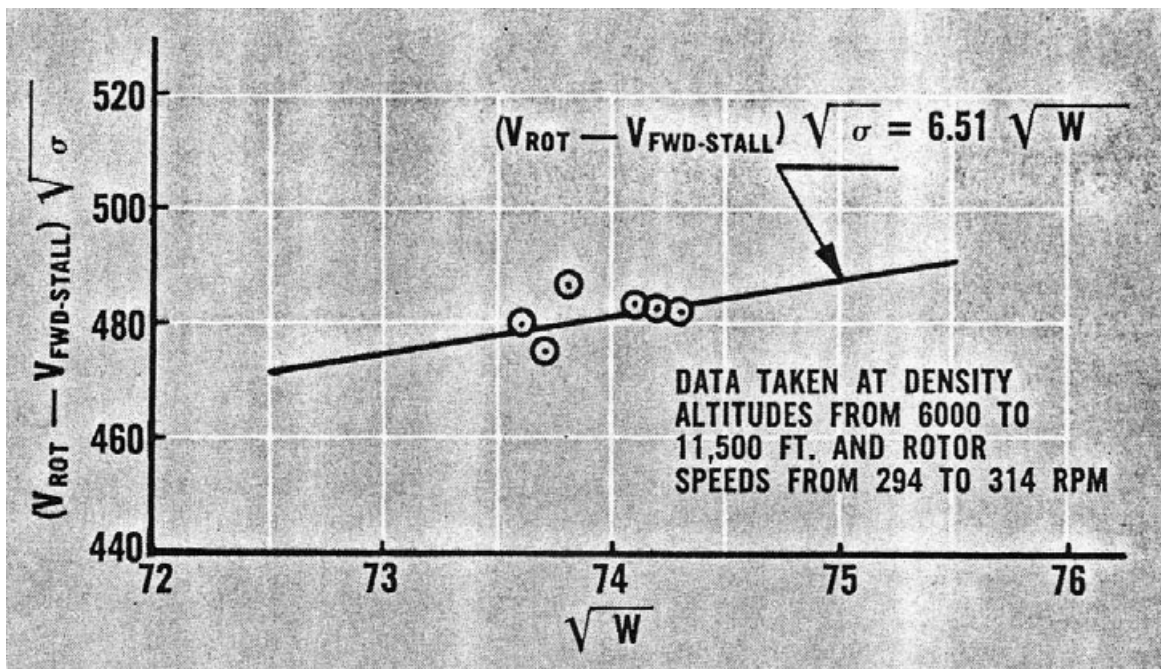


Fig. 2-205. Blade stall onset as determined by cockpit vertical vibration for the XH-40 [115].

## 2.6 VIBRATION

Before proceeding to examine the final helicopter, let me stop in the mid-1970s. At the May 1973 Annual Forum of the American Helicopter Society, a senior flight test engineer, (Emmett J. Laing) of the USAASTA located at Edwards Air Force Base in California, presented a broad review of Army helicopter vibration. Laing's follow-on AHS Journal paper [433] is a real milestone in my mind. He began the paper saying, in part:

“It has long been suspected that the helicopter vibration environment contributes to instrument, avionics, and other component failure rates and degrades crew performance. However, accurate evaluation of the effects of helicopter vibration on components and crewmembers has been hampered by a lack of sufficient vibration data. To better understand the helicopter vibration environment, the United States Army Aviation Systems Test Activity (USAASTA), with the assistance of the United States Army Air Mobility Research and Development Laboratory, Eustis Directorate, and Northrop Corporation, Electronics Division, is conducting a comprehensive vibration survey on present United States Army helicopters. This test project was initiated to determine the vibration environment of Army helicopter cockpit instruments and avionics. However, it was rapidly expanded to include human factors and reliability and maintainability considerations for many other components. Testing has been conducted on the OH-58A, UH-1H, CH-54B, and OH-6A helicopters and will be completed on the AH-1G and CH-47C helicopters, hopefully in 1973.”

Laing's paper was just the very beginning of a massive vibration survey conducted on six U.S. Army helicopters. He finish the AH-1G report in 1974 and the CH-47C report in 1975, which completed the program.<sup>115</sup>

Laing's vibration summary of the UH-1H<sup>116</sup> (one of the several Huey models that followed from the XH-40) is reproduced here as Fig. 2-206. What I find so helpful from Laing's several year effort is his gathering of data from what must have been miles of digital tapes. He was able to create a mean of the maximum of the maximums from tens of accelerometers to produce the worst-case situation. Then, on top of that, he reduced the data to a mean plus 3-sigma graph of vibration versus frequency at several stations as shown in Fig. 2-206. (He noted that the “mean plus 3-sigma is a statistically calculated acceleration below which 99.87 percent of all data falls.”) The pilot station data in Fig. 2-206 shows that maximum vibration from all flight conditions was at or below  $\pm 0.34$  g at 2/rev, below  $\pm 0.40$  g for 4/rev, and below  $\pm 0.36$  g for 6/rev. You can get a feeling about Laing's data analysis by selecting just the highest measured XH-40 vibration points from Fig. 2-202, Fig. 2-203, and Fig. 2-204 and quoting those points as the XH-40's vibration.

In his AHS Journal paper, Laing was able to quantify (from four helicopters) the overall vibration that avionic components were subjected to. His assessment is reproduced here as Fig. 2-207.

Finally, it is well worth quoting Laing's conclusions because they ultimately contributed to revisions in Army specifications and design standards, such as the introduction in 2006 of ADS 27 by Sam Crews, as I mentioned earlier. Laing's conclusions in 1974 were:

---

<sup>115</sup> Laing's six reports became a valuable source for other researchers including the Army Aeromedical Research Laboratory located at Fort Rucker, Alabama [434].

<sup>116</sup> See Laing's *Vibration and Temperature Survey Production UH-1H Helicopter* [435].

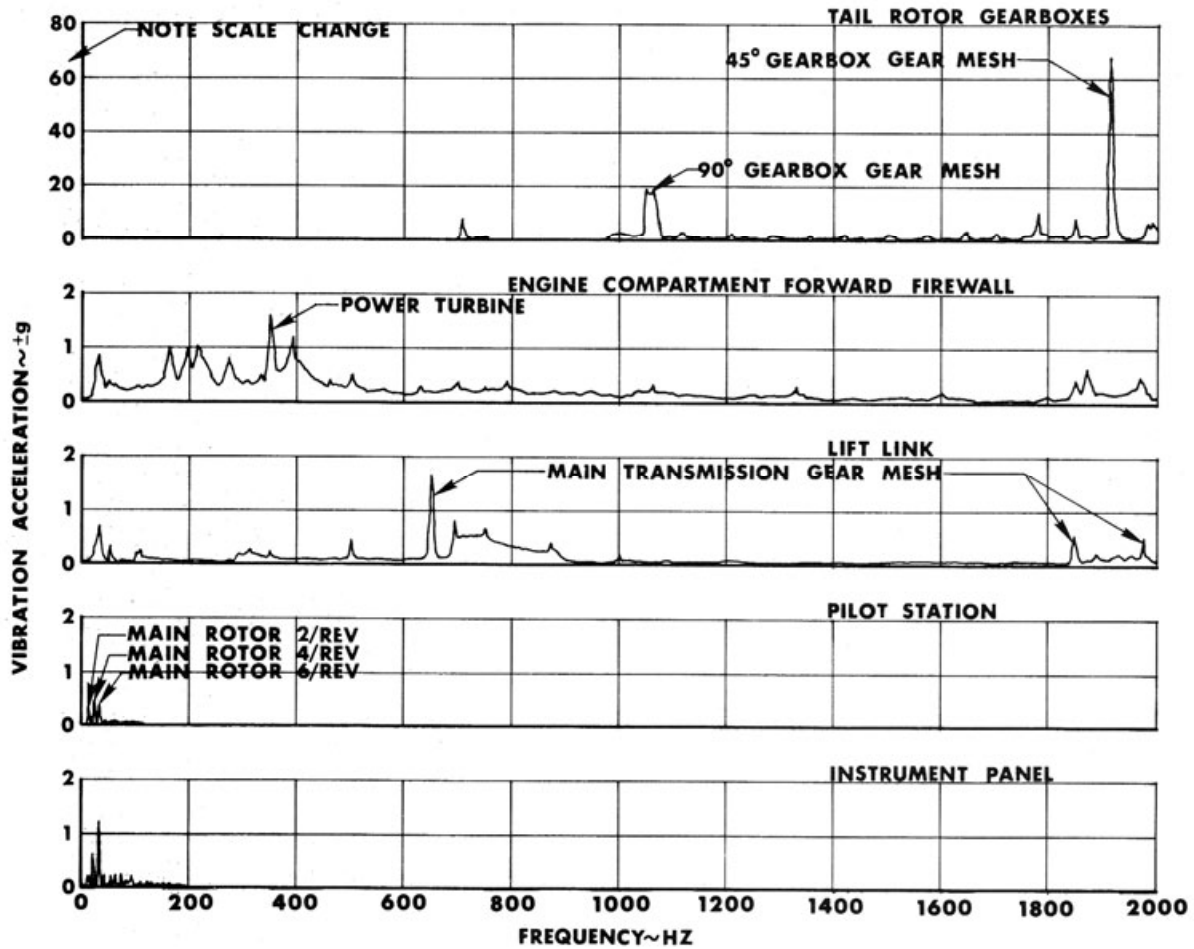


Fig. 2-206. UH-1H maximum vibration environment [433].

Flight Condition	Mean Plus 3-Sigma Acceleration (~ ±g)								
	OH-58A		UH-1H		CH-54B		OH-6A		
	2/rev	4/rev	2/rev	4/rev	6/rev	12/rev	1/rev	4/rev	8/rev
Ground run	--	--	.30	.11	.46	.02	.26	.12	.01
Hover	.12	.17	.16	.26	.55	.04	.26	.67	.09
Level flight	.21	.35	.28	.35	.40	.03	.24	1.29	.12
Climb	.13	.21	.27	.40	.40	.05	.34	1.31	.08
Descent	.21	.31	.33	.43	.46	.04	.30	.71	.14
Maneuvering	.29	.42	.28	.35	.50	.12	.30	1.28	.28
Transition	--	--	.34	.34	.80	.09	.25	.97	.50

<sup>1</sup>All axes combined. All avionics accelerometer locations combined.

Fig. 2-207. Avionic equipment installed in helicopters can be subjected to severe vibration [433].

## 2.6 VIBRATION

“This paper has presented data which describe the vibration environment of the current generation of Army helicopters. It has been shown that

1. Statistical methods can be used to summarize large quantities of vibration data.
2. Helicopter vibrations are primarily sinusoidal, with the main rotor and gunfire the primary instrument and avionics vibration sources.
3. Rotating equipment such as gearboxes and shafts also cause significant vibrations when components are mounted close to these sources.
4. Improved vibration isolator and seat cushion design may reduce vibrations transmitted to the avionics and crew.
5. The laboratory test requirements of MIL-STD-810B present generally adequate acceleration limits, but present an inadequate frequency range.
6. Consideration should be given to specifying the pilot station vibration limits of MIL-H-8501A as a function of frequency below 32 Hz.

Much more data are available from USAASTA in the engineering test reports on each helicopter and on digital computer tape. It is anticipated that this data will increase the understanding of the helicopter vibration environment, and can be used to define realistic vibration qualification requirements for helicopter instruments, avionics, and other components.”

I was particularly drawn to Laing’s sixth conclusion because in the general discussion about pilot station vibration data he said, “The highest vibration levels recorded were on the UH-1H helicopter at frequencies of 7.2 Hz and 32 Hz and the 7.2-Hz vibration was judged more severe than the 32-Hz vibration of equal amplitude.” The vibration at 7.2 Hz amounted to  $\pm 0.3$  g at a main rotor speed of 220 rpm during ground run-up in a 20-knot wind. The 32-Hz vibration ( $\pm 0.5$  g) at the 6/rev frequency of the main rotor was obtained during flight.

Now let me conclude this discussion of flight test results with the Sikorsky UH-60A as the example helicopter. First of all, you will recall that the then Boeing Vertol and Sikorsky competed in the U.S. Army competition for a new utility helicopter to replace the Bell UH-1 Huey. Government flight test reports for both helicopters were published in November 1976 [124, 125]. Perhaps the deciding technical issue was vibration, and this deciding issue hinged on the Army requirement that the new utility helicopter must be transportable in an Air Force C-130. Boeing took the requirement to heart (Fig. 2-208).<sup>117</sup> Sikorsky, faced with the same situation, put in a shaft extension to raise the main rotor (Fig. 2-209), which significantly reduced its vibration problem—but significantly increased disassembly and reassembly times for air transportability by C-130.<sup>118</sup>

---

<sup>117</sup> As I recall the situation, there was disagreement between Chuck Ellis (a longtime mentor and program manager for the YUH-61A) and Ken Grina (chief of engineering who also corrected my design approach on the Boeing Vertol Bearingless Main Rotor research program). The Army had placed air transportability very high on the list of requirements, and Chuck felt that Boeing Vertol could win the competition with the low rotor position and then fix the vibration. As vibration became more of a deciding issue, the YUH-61A main rotor plane was raised (which did reduce vibration), but it was too little too late.

<sup>118</sup> Chapter 7 of Ray Leoni’s terrific book *Black Hawk* [162] tells a detailed story of reducing vibration after the early flights established that their aircraft did not meet U.S. Army vibration specifications by a country mile. When this occurs in a vigorous competition, it takes nerves of steel and absolute confidence in the outcome to watch solutions come along in time to win.



**Fig. 2-208.** The main rotor of the Boeing YUH-61A was mounted close to the fuselage to meet the requirement for air transportability in an Air Force C-130. Vibration was severe due to rotor-fuselage aerodynamic interference (photo from author's collection).



**Fig. 2-209.** On the YUH-60A, Sikorsky reduced rotor-fuselage aerodynamic interference by increasing the separation distance between the main rotor and fuselage. Note the problem of designing a fuselage with a big hole in it (photo from author's collection).

Even after Sikorsky won the UTTAS competition on December 23, 1976, vibration reduction efforts continued. The Army conducted airworthiness tests on the third and fourth production UH-60A helicopters from October 27, 1979, to October of the following year. The flight test report [161] was published in September 1981. This report was approved for public release and showed that Sikorsky was on the way to achieving a low-vibration machine. The Army was, however, not satisfied, writing in the report's abstract that "the vibrations were found to be quite high in several areas and were considered to be excessive for *a new generation helicopter*" [my italics]. It took the use of several vibration suppression devices, but early in production Fig. 2-210 shows that the pilot was getting one of the lowest vibration environments one might hope for at that stage in a program. Furthermore, vibration at the center of gravity of the aircraft was generally low as Fig. 2-211 shows. As Leoni relates on page 147 of *Black Hawk* [162], it took the "combined effects of the raised rotor, 4P absorbers, and airframe nose-stiffening to reduce cockpit levels to near 0.05 g."

## 2.6 VIBRATION

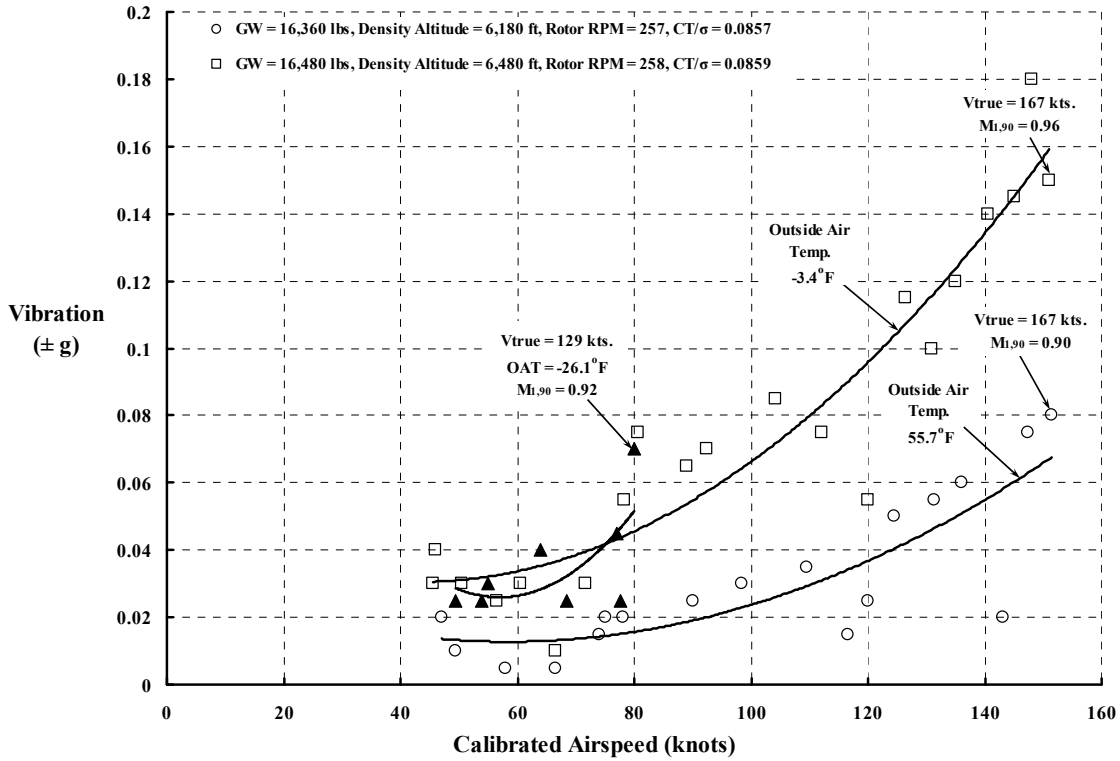


Fig. 2-210. Pilot station vertical vibration was encouragingly low on the early UH-60A.

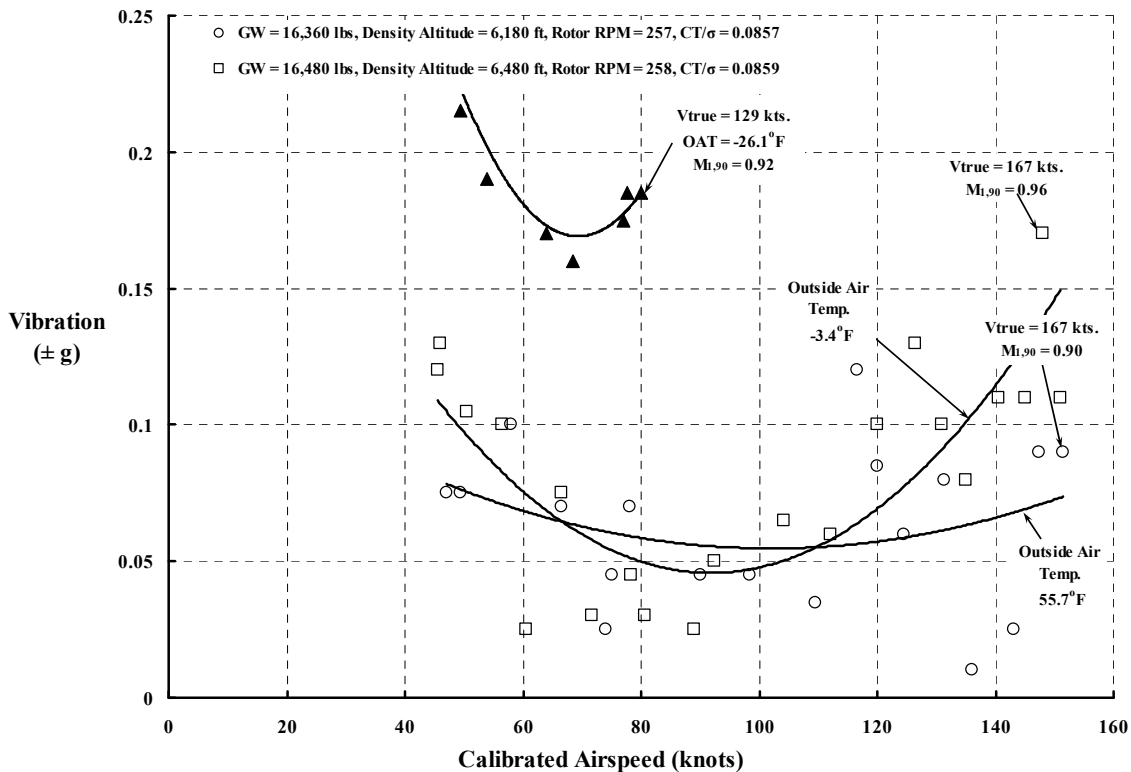


Fig. 2-211. Vertical vibration at the center of gravity showed that more work was needed after the flight testing of an early production UH-60A was completed.

When you read the several paragraphs in the *Vibration Characteristics* section of the UH-60A airworthiness report [161], you will find several noteworthy sentences. For example, I thought these comments were quite valuable:

1. Para. 114. “Only 4/rev vibration data test results are presented in figures 113 through 124, appendix E, as the other harmonics were not significant.”

2. Para. 115. “During the test program, many modifications were made to the test aircraft by Sikorsky Aircraft personnel in their effort to update the aircraft to a production model. These changes included such items as spindle assembly, dampers and damper bolts, etc., which may cause a variability of vibration characteristics. Because of these changes, the aircraft exhibited different vibration characteristics. Therefore, throughout the test program, the vibrations were qualitatively assessed [with] VRS<sup>119</sup> ratings ranging from 2 to 7. The vibration characteristics did not meet the requirement of paragraph 3.2.1.1.3.1.4 of the PIDS [Prime Item Development Specification]. Future tests should be conducted on a current production UH-60A in order to obtain vibration data that would be more representative of the aircraft.”<sup>120</sup>

3. Para. 116. “Vibration levels at the cg of the aircraft during level flight tests are presented in figures 116 through 118, appendix E. At the heavy weight condition as shown in figure 118, the vertical acceleration exceeded 0.2 g at 55 KCAS and fails to meet the requirements of paragraph 3.2.1.1.3.1.4 of the PIDS. The lateral and longitudinal accelerations were below 0.05 g at all airspeeds. At 16,480 pounds (approx primary mission gross weight), below 56 KCAS and above 120 KCAS the vertical acceleration exceeded 0.1 g with a peak of 0.17 g at 148 KCAS (fig. 117). The lateral and longitudinal accelerations were essentially below 0.05 g at all airspeeds.”

4. Para. 117. “The vibration characteristics of the pilot's and copilot's instrument panel were qualitatively evaluated throughout the test program. The pilots were able to read the instruments and no blurring was ever experienced.”

5. Para. 118. “Comparing the lower rotor speed data [minimum power-on rotor speed of 245 RPM] at heavy and primary mission gross weights to the higher rotor speed at similar conditions, show essentially no difference in vibration level at the pilot's station. The vertical vibration levels at the aircraft cg, minimum power-on rotor speed, airspeeds below 50 KCAS at both gross weights and above 138 KCAS at the primary mission gross weight, exceeds 0.15 g and does not meet the requirements of paragraph 3.2.1.1.3.1.4 of the PIDS.”

6. Para. 119. “Vibration test results near primary mission gross weight and aft cg during maneuvering flight are presented in figures 123 and 124, appendix E. At 118 KCAS, the highest 4/rev vibration level was 0.24 g laterally at the pilot seat, which occurred at a bank angle of 45 degrees or 1.4 g normal acceleration. The 60 degree left and right maneuvering stability flight was difficult to perform because the airspeed fluctuated  $\pm 10$  KIAS and pilot workload increased significantly (HQRS 6).”<sup>121</sup>

7. Para. 120. “The vibrations were excessive during descents and translations from forward flight to hover, as well as in those areas previously mentioned. The excessive vibrations significantly increased pilot work load during certain maneuvers, and are a shortcoming.”

---

<sup>119</sup> The vibration rating scale (VRS) created by the flight test crew was shown in Fig. 2-201.

<sup>120</sup> No matter how encouraging, vibration measurements on one aircraft out of a fleet can hardly be considered representative, but at least it is a start.

<sup>121</sup> The Handling Qualities Rating Scale (HQRS) also helped pilots convey their feelings to rotorcraft engineers.

## 2.6 VIBRATION

Ray Leoni points out in his terrific book *Black Hawk* [162] that some 25 years after these early UH-60A tests were reported, Sikorsky developed an active vibration control system for its commercial S-92. Sikorsky applied this vibration suppression system to a growth version of the UH-60A Model to obtain the UH-60M, which first flew in 2003 and began delivery in mid-2006. As Ray describes it:

“This new system utilizes an active vibration control system (AVCS) to reduce 4/rev vibration throughout the airframe. The AVCS eliminates the need for the passive spring-mass units carried in all prior Black Hawk models, thereby significantly reducing weight. The AVCS further maintains consistent vibration performance when rotor speed deviates from its nominal 100% value and avoids the loss of effectiveness characteristic of passive absorbers when operating at off-design frequencies.

The AVCS achieves lower vibration at lower weight because it is a distributed system able to attenuate vibration in selected zones within the airframe. Force generators of the AVCS can be located wherever necessary throughout the fuselage to generate forces to cancel out local vibrations. The heart of the system is a closed-loop algorithm that calculates the force generator commands required to minimize vibrations as measured by accelerometers located throughout the cockpit and cabin. A feedback control algorithm processes a tachometer signal, providing frequency and phase information, and also processes accelerometer signals that feed back local vibration conditions.

The AVCS computer calculates the required force generator commands and sends them digitally to an electronic unit. This unit then converts the digital signals to analog signals, which then are sent to electric motors within the force generators. These motors drive counter-rotating eccentric masses to generate forces of appropriate magnitude and frequency to cancel fuselage vibrations.

In the UH-60M, a force generator capable of producing 1000 lb is located in the forward cabin overhead, replacing a heavy spring-mass absorber. In addition, generators able to produce 450 lb are located one in the left landing-gear stub wing and one in the cockpit nose. Figures 199-201 show where the major AVCS components are located in the M model.”

What I find so interesting about efforts to reduce helicopter vibration is that there are (so far) two basic approaches to helicopter vibration reduction and even elimination. The first is to reduce the vibration at the source, which is in the rotating system. The second approach is to suppress and even cancel the vibratory response of the fuselage in selected regions, which is done in the nonrotating system. The latter approach is where the AVCS system falls [436]. With either approach significant weight is added, cost goes up, and more parts need maintenance. In 1971 and again in 1981, Dick Gabel and Bob Lowey speculated [404, 405], or perhaps you could say hoped, that the rotorcraft industry would produce helicopters with a “jet smooth ride” in the foreseeable future. We have not achieved that goal yet, but we are getting there.

As deliveries of the Sikorsky UH-60 series grew, NASA and the U.S. Army found another use for the machine. They initiated [437, 438] a new, and the most comprehensive, program the world had ever seen to measure and analyze just about everything associated with vibration on a UH-60A.<sup>122</sup> This helicopter was considered modern and very much state

---

<sup>122</sup> I intend to use data from this program throughout the rest of this vibration discussion to illustrate points related to Fig. 2-175.

of the art in the mid-1980s. As the program progressed from its start in 1986, every researcher in the rotorcraft industry came to know about the UH-60 Airloads Program. By February 1994, the flight test phase was completed, and experimental results began to be published [167]. One of the first detailed results, provided by NASA's Karen Studebaker [439], was three-axis pilot vibration versus advance ratio. This data is shown in Fig. 2-212. You might note that data for vertical vibration at the flight crew station is considerably lower for the early production UH-60A (Fig. 2-210) than for the UH-60A helicopter as modified for the Airloads Program. Some of the difference can be explained by ground shake test and analysis of the fuselage response, which is the next subject to be discussed.

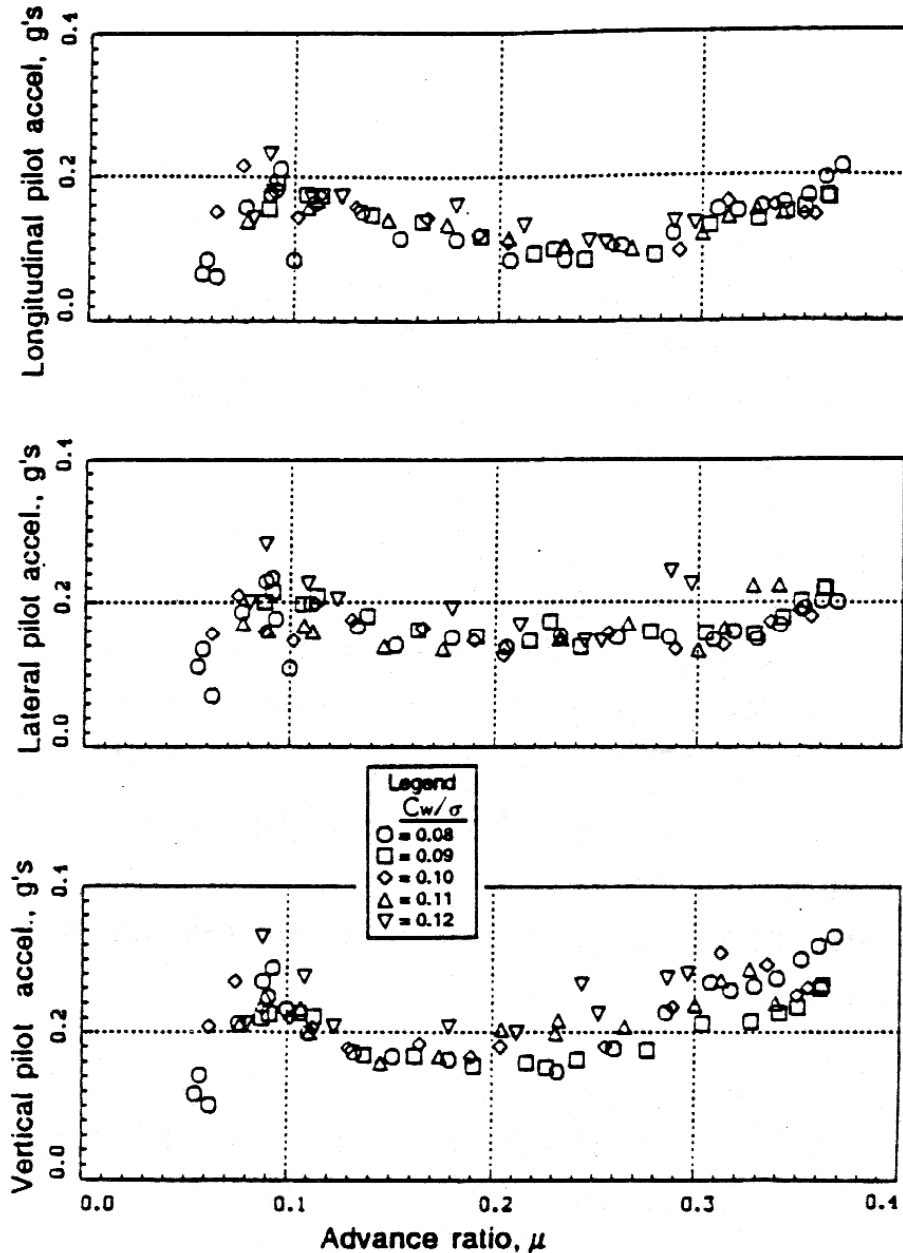


Fig. 2-212. Pilot seat vibration for the UH-60A as configured for the UH-60 Airloads Program [439].

## 2.6 VIBRATION

### 2.6.3.2 Fuselage Response Given Exact Hub Vibratory Loads

You read in Volume I that the rotorcraft industry first encountered ground resonance during development of the autogyro. You also learned in Volume 1, appendix C, some basic dynamics of ground resonance, and the importance of aircraft pitch and roll frequencies required to avoid this very destructive behavior. What I did not emphasize was that, in order to obtain the aircraft frequencies, ground shake tests were performed as a matter of airworthiness qualification and safety. When it became obvious that the helicopter produced severe vibration in flight, the industry's only recourse was cut-and-try fixes. By the late 1950s, structural dynamists turned to fuselage shake tests in the laboratory to understand the behavior of the helicopters that designers were creating. While there was no clear ability to calculate the hub loads that shook the machine, structural dynamists could at least experimentally determine how each newly developed helicopter responded to known applied hub loads. These on-ground tests in a laboratory were referred to as shake tests.

While I have no doubt that all helicopter developers conducted (and still conduct) some form of shake testing with their designs, the first published experiment and analysis that I know of came out as a N.A.C.A. report on June 18, 1957.<sup>123</sup> This report [431] was written by John Yeates, George Brooks, and John Houbolt, all of whom I came to know and respect. In John Yeates' portion of the report, he captured the essence of the vibration situation. In 1957 he wrote:

“In some of the early designs, attempts were made to lower the vibration level by setting the natural frequencies of the helicopter components, such as the blades, fuselage, and engine, between the multiples of rotor speed. This approach to the problem was only partially successful. Some calculations indicated that coupling of rotor blade bending and fuselage bending might bring about structural resonance at frequencies where none was apparent from considerations of each component separately. It became apparent that the helicopter must be treated as a coupled system and that the effect of the interaction of the components (blades, fuselage, engine, etc.) is important. The problem is to design and calculate more accurately so that determination of the coupled response frequencies of the structure is possible before the prototype is built.”

With that said, John launched first into the shake test helicopter and its setup, which is shown in Fig. 2-213. The location of vibration pickups and the number of components measured is shown in the boxed numbers in Fig. 2-214. As you can see from Fig. 2-213, the machine was suspended at the rotor hubs. The suspension shock cords were, in effect, very soft springs. The natural frequency of this setup was less than 1 Hz. A mechanical shaker was mounted on the front rotor transmission, just above the heads of the crew. The shaker applied a vertical sinusoidal vibratory force ( $F$ ) with an amplitude of 0.45 (frequency in Hz squared) up to its limit of 75 pounds.

Notice immediately in the shake test setup that no rotor blades were attached. This promptly raises a basic question. Because the vibration solution depends on the coupled response of the whole helicopter (blades and fuselage), how do you represent the blades? The

---

<sup>123</sup> I remember that month well because it was on Saturday, June 22, 1957, that Susan Bullis and I were married in Center Church on the Green in New Haven, Connecticut. Suddenly, rotorcraft became my second love.



Fig. 2-213. Shake test setup for the Piasecki HUP, which had 35-foot-diameter tandem rotors (photo courtesy of NASA from NACA LAL 85686.1).

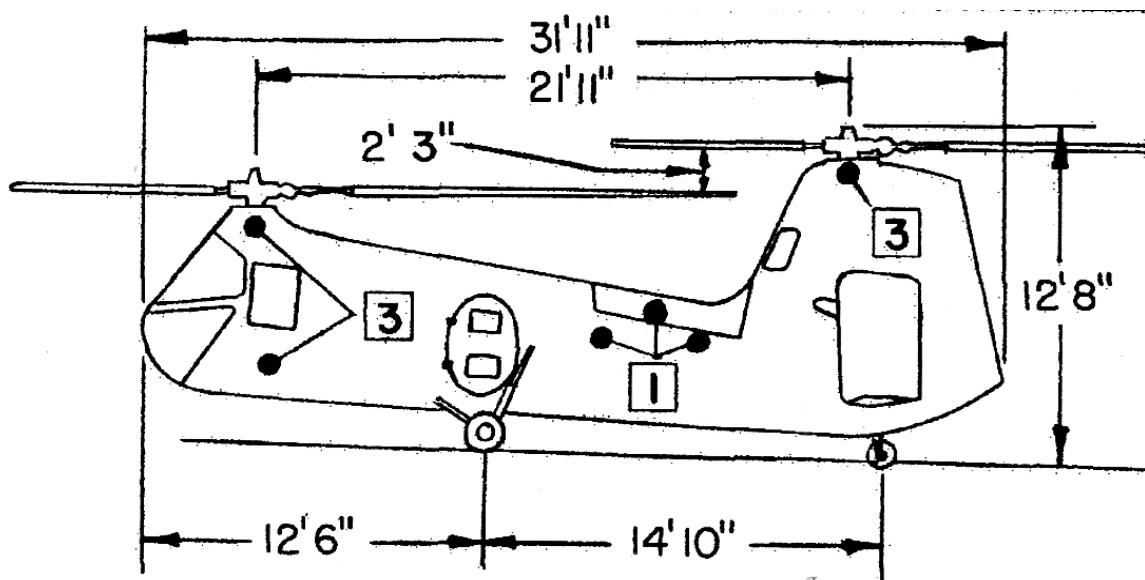
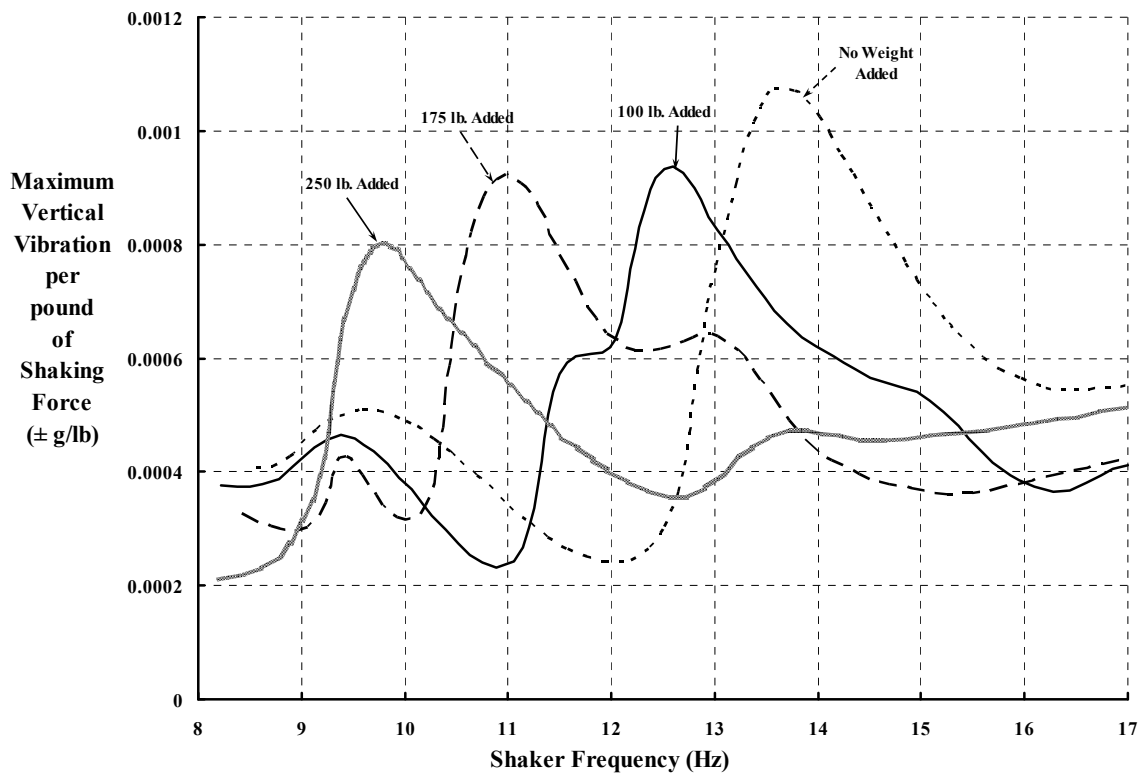


Fig. 2-214. The location of vibration pickups and the number of components measured is shown in the boxed numbers [431].

## 2.6 VIBRATION

researchers, in chapter I of their groundbreaking report [431], replaced the blade assemblies with several pounds of dead weight. The blade assemblies *from the flapping hinge outboard* were replaced by zero weight first, and then by 100, 175, and 250 pounds per rotor head. The authors did not mention the actual weight of the blade assemblies removed; however, my files give the weight of six blades and hinges at about 450 pounds. Therefore, the dead weight added per rotor station would be 225 pounds. You might think that the 250-pound additional dead weight would have been the most accurate representation of the missing blade assemblies. However, the theory available at the time said that the blade assemblies *do not* act as dead weight. Rather, the blade motion in the coupled fuselage-rotor vibration problem makes the blade assemblies appear to have an *effective* weight that is considerably less. The calculations at the time suggested that 100 pounds per rotor head was the more correct simulation. As you will see shortly, flight test results confirmed this view. The reason for this effective weight comes about because of the flapping and bending motion allowed by the flapping hinges. When the hub vibrates up, the blades tend to cone down, much like an umbrella closing, and when the hub vibrates down, the blades act like the umbrella is opening up again. Of course, the actual theory is more complicated, but that is about the best way I can describe the blade assemblies coupled motion in this introduction.

The shake test was performed by varying the shaker frequency over the range of 8 to 17 Hz. The shaker gave a sinusoidal input at the front rotor, and the fuselage response at the front rotor was recorded (i.e., at the upper solid black dot from the box with a 3 in it on



**Fig. 2-215. Shake test results as a function of dead weight added to each rotor head to simulate blade and hinge assemblies removed.**

Fig. 2-214). For this experimental program, the fuselage response was measured in units of velocity in inches per second. This was a standard sensor at the time; it was later replaced by accelerometers in more modern times. I have taken the liberty of converting the velocity measurements into accelerations in units of gravity following Eqs. (2.274) to (2.276). My interpretation of these N.A.C.A. initial shake test results is shown in Fig. 2-215.

The report by Yeates, Brooks, and Houbolt [431] contains the results from the HUP flight test where the aircraft was shook in flight. They took data with the shaker operating and turned off and, in effect, subtracted the results to give the results shown in Fig. 2-216, which I have recast into acceleration in gravity units per pound of shaker force. Their interpretation was that the two peaks in the flight test results versus the one peak in the ground test indicated coupled motion between the fuselage and the rotor.

The basic message that the authors were trying to convey seems simple to me. Suppose the fuselage structural analysis, without considering the blades, suggests that the fuselage first bending mode would have maximum vibration if its frequency was at, say 14 Hz. Then everyone would want to reduce (or increase) the fuselage stiffness to move the natural frequency to a lower (or higher) frequency. However, that design move could (in flight) land the experimental machine right on one of the twin peak vibration points of the coupled fuselage-rotor blade assemblies. Brooks and Houbolt were able to reinforce this point with their analysis, which is carried out in chapter II of their report [431]. Their theory led to solving eight equations in eight unknowns, which is beyond the intent of this vibration discussion.

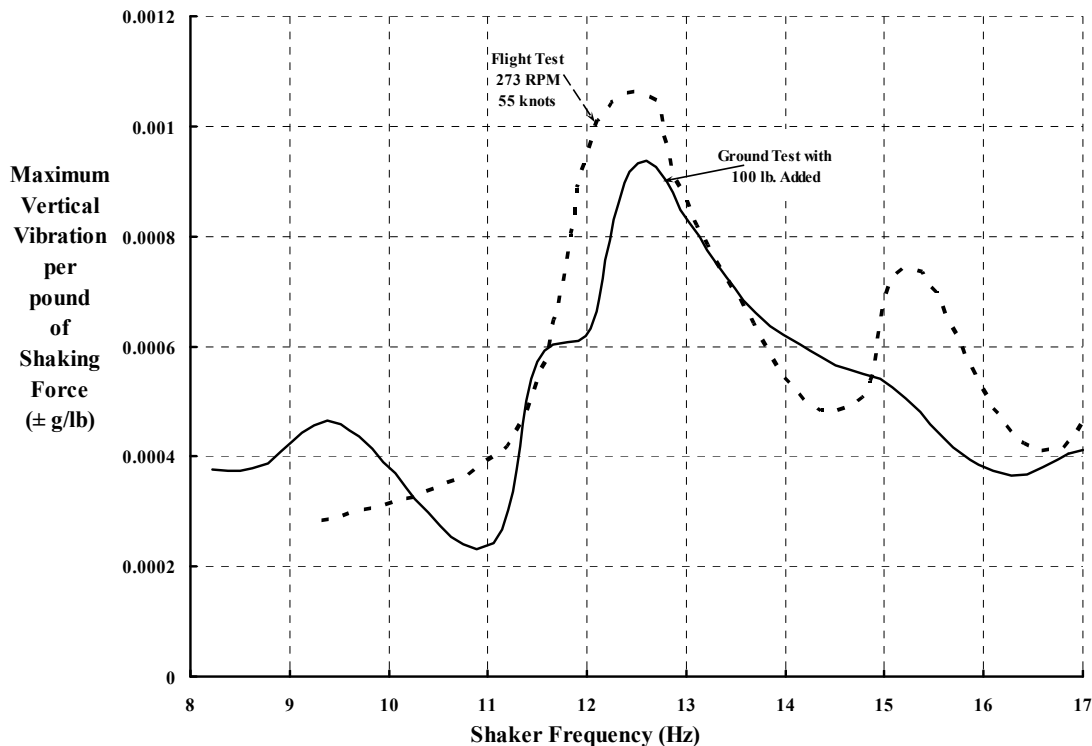


**Fig. 2-216. Flight test revealed that coupled fuselage-rotor system analysis was absolutely required for solving helicopter vibration problems.**

## 2.6 VIBRATION

NASA's basic research and understanding of helicopter vibration did not stop with the groundbreaking effort of Yeates, Brooks, and Houbolt. The immediate follow-on was the construction, test, and analysis of a basic research dynamic model. The objective was to measure and calculate coupled frequencies and mode shapes for a 1/8-scale model. This basic research was reported by Milton Silveira and George Brooks in December of 1958 [440].

In Volume I, you learned about natural frequencies and mode shapes of rotor blades. Appendix C of this volume provides an introduction to the natural frequencies and mode shapes of a simple beam, which has no rotor system attached. What Silveira and Brooks did was build an absolutely beautiful, simple dynamics model (Fig. 2-217), at small scale, where all the structural properties necessary for analysis were easily obtained. The four-bladed rotor was 66 inches in diameter and had the approximate dynamic properties (I think) of a Sikorsky S-58, which is the U.S. Army's H-34. The "fuselage" was made of two welded magnesium angles that form a box cross section. The construction and properties of the rotor pylon and shaft can be found in the report [440]. The overall model, mounted on a very rigid I-beam, was softly attached to the I-beam so that only vertical, horizontal, and pitch degrees of freedom were permitted. The test was only conducted in hover outside a wind tunnel.

The researchers first obtained the natural frequencies and mode shapes of the individual components. This allowed them to construct the uncoupled natural frequencies for the basic model. Then, by shaking the model with the rotor operating at several different rotor speeds, they experimentally obtained the coupled (rotor plus fuselage plus pylon plus rotor shaft) system frequencies, which I have reproduced here as Fig. 2-218. The modes, called out by number on the figure, are as follows:

Mode 1 Fuselage rigid body pitching  
 Mode 3 Blade first bending  
 Mode 5 Fuselage first elastic bending  
 Mode 7 Pylon bending

Mode 2 Fuselage horizontal translation  
 Mode 4 Shaft translation  
 Mode 6 Blade second elastic bending

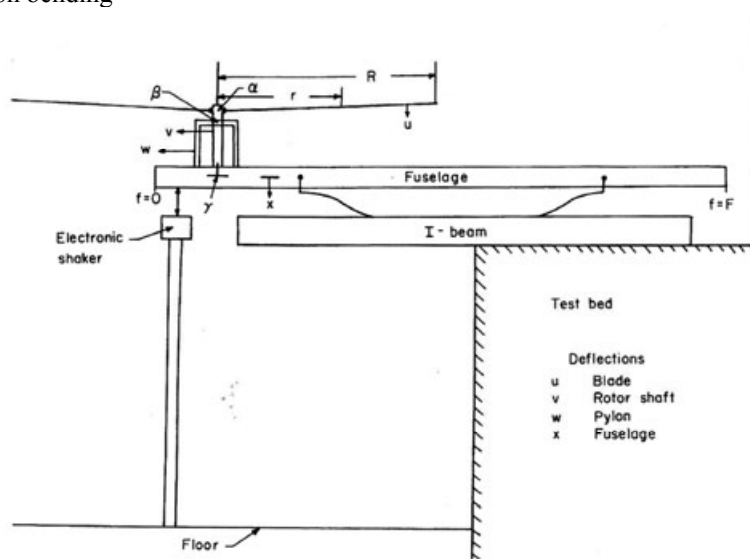


**Fig. 2-217. The exploration of coupled system frequencies and mode shapes was done with a beautiful, simple dynamics model [440].**

The mathematically tractable analysis used a seven-degree-of-freedom set of equations, and the calculated coupled system frequencies were in quite reasonable agreement with the experimentally obtained data as Fig. 2-218 shows.

The work of these N.A.C.A. researchers clearly established the need for the rotorcraft industry to attack helicopter vibration as a coupled system problem. It was the last conclusion of Silveria and Brooks' report that set the next step for the industry. They wrote that "(t)he coupled natural frequencies and mode shapes can be determined by the analytical procedure presented herein with sufficient accuracy if the mass and stiffness distributions of the various helicopter components are known." There was a big *if* in that conclusion.

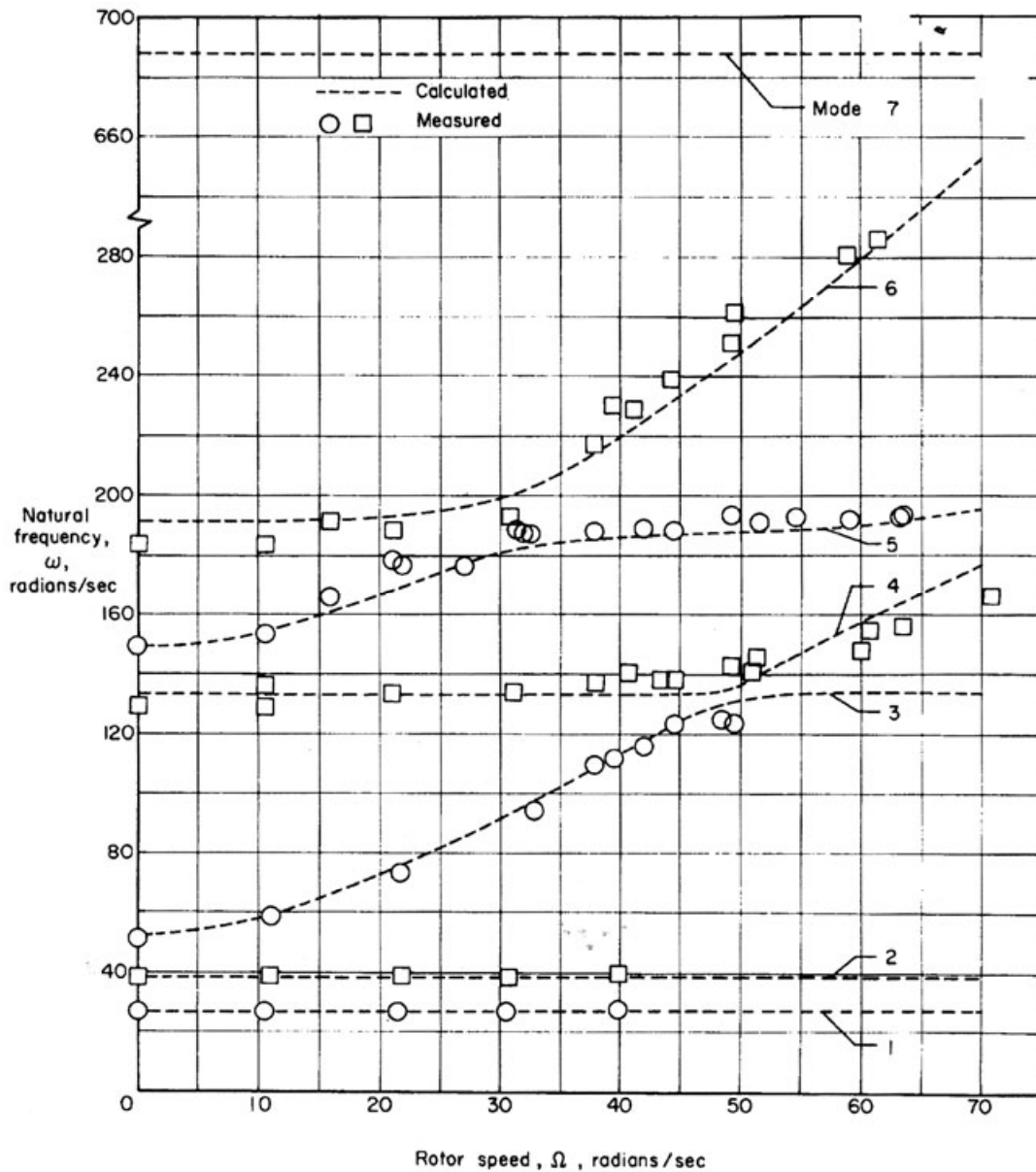


Fig. 2-218. Coupled mode frequencies of the simple research model [440].

## 2.6 VIBRATION

The investigation of tandem rotor helicopter vibration did not stop with the N.A.C.A. research by Yeates, Brooks, and Houbolt. The idea that shake testing, both on the ground and in flight, was a valuable approach to basic understanding was applied at the Vertol Division of the Boeing Company, which was then located in Morton, Pennsylvania. This approach was used on the H-21B in 1961. The results were reported by Bob Ricks to the Aeronautical Systems Division of the Air Force Systems Command in 1962 [441]. Then, with delivery of the CH-46A (Boeing Model 107) to the U.S. Marines, vibration in excess of MIL-H-8501A was, as you might have guessed, a problem. The Model 107 had some vibration problems that Bob Loewy and Dick Gabel were able to solve. However, in converting the 107 to the CH-46A, automatic blade folding was added and vibration increased, requiring a renewed, 2-year vibration reduction effort.

CH-46A vibration was tackled with the most thorough effort that the industry had ever, in my opinion, mounted. The author of the final report [442] was Dick Gabel who was then the Chief Dynamics Engineer at Vertol and was well respected throughout the industry.<sup>124</sup> Dick opened this nearly 900-page report with a crystal clear AVID Summary. He wrote in the opening Background and Purpose section that

“AVID, acronym for Advanced Vibration Development was conceived by BuWeps [Navy Bureau of Weapons] and the Contractor to provide a better understanding of the sources of helicopter rotor vibratory loads and the mechanism of the fuselage response to these loads. This basic knowledge type program followed two years of hardware programs on the CH-46A, which through fuselage stiffening and absorbers had brought vibration down to acceptable levels, and in fact to MIL-H-8501A requirements. AVID, was intended to provide a deeper knowledge of the vibration sources than was heretofore possible in the usual ‘fix’ type program.

AVID was thus contracted to provide a step forward in the state-of-the-art as regards an in-depth understanding of helicopter vibration. Although it was never intended to develop or test any vibration reduction hardware here, it was intended to recommend those avenues which showed most promise for successful vibration control at least weight. Specifically, it was hoped by those associated with production and user activities of the CH-46A that results of AVID would lead to successful light weight hardware recommendations and the subsequent removal of all vibration absorbers.”

The AVID program used analysis and ground and in-flight shake testing, measured structural loads and blade airloads, and made more than a few hardware changes to ferret out the sources of vibration. One of the key hardware effects was the impact of blade folding hardware. Testing of a Canadian CH-113A (which has no automatic blade folding hardware and has an 883-pound rotor hub weight) versus the CH-46A (which weighs 1,144 pounds) showed that the rotor longitudinal load (measured by shaft bending) was cut in half with the lighter hub.

The AVID program laid the groundwork for a broader industry program called DAMVIBS, which I will discuss in detail shortly.

---

<sup>124</sup> Dick was—and I still feel is, even in retirement—a good friend who could explain any dynamics phenomena so that even I understood it. Dick replaced Bob Loewy in the fall of 1962 when Bob went to the University of Rochester. The AVID report had rather limited distribution, but Bob Loewy, Wayne Johnson, and Bob Ormiston have copies. I borrowed Bob Ormiston’s copy, and Mike Scully and I spent an afternoon in May 2011 making a Portable Document Format (PDF) copy.

It took several more years, plus the invention of the digital computer, before a structural analysis that could model a helicopter fuselage and all of its internal components became available.<sup>125</sup> This analysis was called NASTRAN, which is a contraction of NASA Structural Analysis. It was funded by NASA under contract number NASA-10049 from June 29, 1966, to March 2, 1970, when a final report for the project [444] was submitted by Computer Sciences Corporation to NASA Goddard Space Flight Center.

Compared to the early N.A.C.A. efforts led by George Brooks where a few components (as counted on Fig. 2-217) were examined with seven degrees of freedom (i.e., the modes), NASTRAN can have over 40,000 components and 65,000 degrees of freedom. This “the sky is the limit” powerhouse tool became a factor in nearly every engineering design from buildings to cars to space vehicles and, of course, a major tool for the rotorcraft industry. Finally, structural dynamists could “model” the fuselage of a helicopter, in a computer. An example of this NASTRAN model for the Sikorsky UH-60A primary structure is shown in Fig. 2-219. Notice the likeness of the NASTRAN model to the cutaway artist’s rendition of the Sikorsky UH-60 shown in Fig. 2-187. References [445-447] provide an enormous amount of detail about how such a model was constructed and how close the engineers came to experimental shake test results using NASTRAN. The experimental shake test of the UH-60A (Fig. 2-220) and its test setup (Fig. 2-221) was very carefully conducted.

It is worth a moment to discuss the NASTRAN model shown in Fig. 2-219. I visualize the model as being constructed from a Tinker Toy set. Every little stick (individual wood dowels of different lengths) becomes, in NASTRAN parlance, a finite element. Each stick has uniform stiffness and uniform mass. The sticks are joined together with the round Tinker Toy wooden spools having holes all around so that loads go from stick to stick through a joint. Each joint becomes a reference point in a NASTRAN model. With NASTRAN the whole assembly can be covered with a metal or composite skin to complete the basic model. Then other components (e.g., engine, fuel tank, rotor pylon, shafts, hubs, etc.) can build up the detail. At that point, the engineer can analytically apply either static or vibratory loads, such as vibratory hub loads. Clearly, building such a math model is not done overnight, and actual drawings of as many parts as possible are required. As of now, the NASTRAN model evaluates the helicopter’s structural properties *after* the designers’ drawings are done. The ultimate step, I believe, is to have NASTRAN create the satisfactory design and then translate the results to drawings to be released to manufacturing.

Soon after the arrival of NASTRAN, NASA Langley Research Center embarked on an industry-wide determination of airframe structural properties for several helicopters

---

<sup>125</sup> In the intervening period, the rotorcraft industry began to expand on vibration analysis of coupled modes with what came to be called a “comprehensive analysis.” The prototype of the comprehensive analysis was created by research at Bell Helicopter and, with U.S. Army support, evolved in 1967 into a computer program simply named C-81. This program modeled the complete helicopter with, for the time, detailed structural dynamics and aerodynamics of both fixed and rotating components. Of course, simpler and very informative studies of coupled rotor-fuselage vibration continued as Mike Rutkowski demonstrated in 1983 [443]. This report is well written, well illustrated with mode shapes and calculated frequencies, and can serve as a primer if you want to delve deeper into helicopter vibration.

## 2.6 VIBRATION

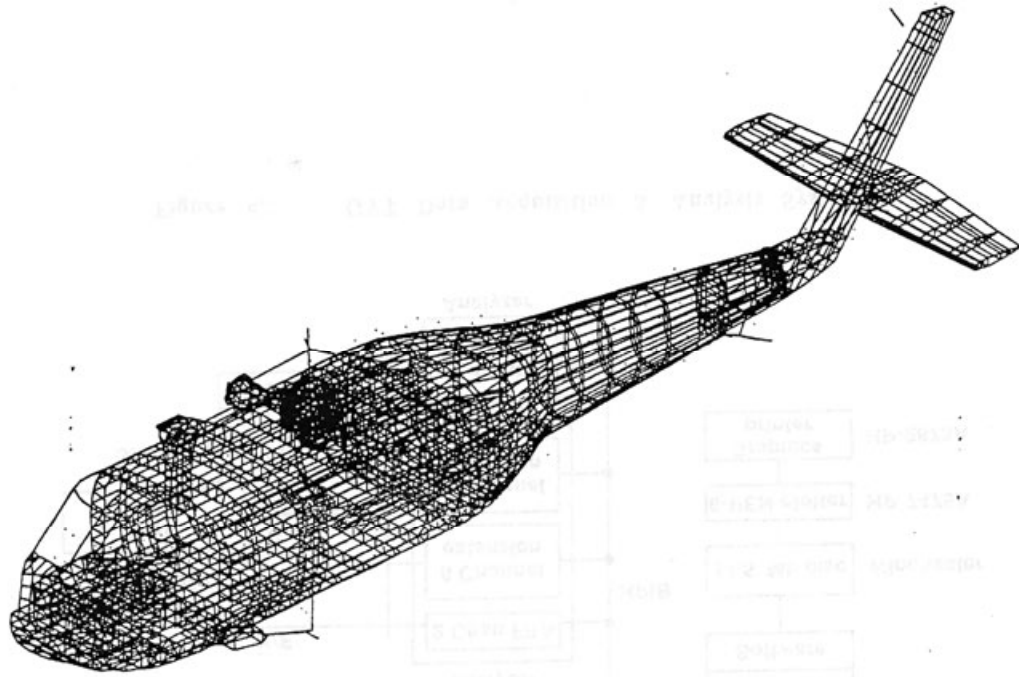


**Fig. 2-219. NASTRAN model of the primary structure of a Sikorsky UH-60A.**



**Fig. 2-220. Shake test setup for experimental study of the Sikorsky UH-60A (photo courtesy of Ashish Bagai and Sikorsky Aircraft).**

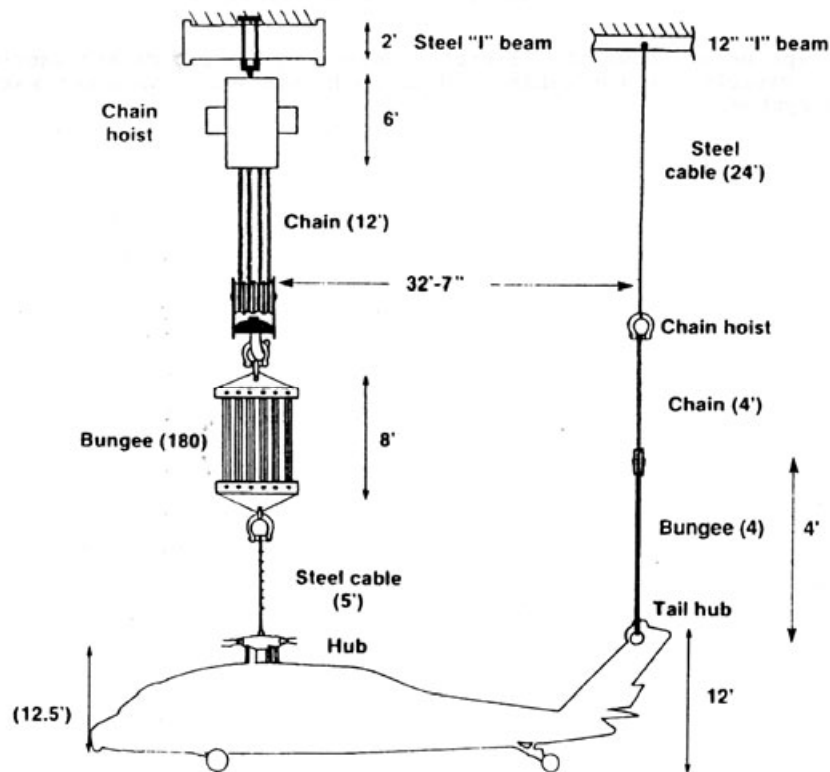


Fig. 2-221. Shake test setup for experimental study of the Sikorsky UH-60A [446].

manufactured by several companies. This renewed attack on vibration by NASA was conceived and supervised by William C. Walton, Jr., until his retirement in 1984. Technical guidance was provided by Eugene Naumann and Raymond Kvaternik. When Bill retired, Ray stepped in as program manager. Bill Walton gave the program its name, DAMVIBS, a contraction of **D**esign **A**nalysis **M**ethods for **V**ibrations program. *This was much stronger language than Cierva used in 1935.* By any standard, the DAMVIBS program yielded a giant step forward in the rotorcraft industry's attack on helicopter vibration. A workshop environment let participants freely interchange NASTRAN models and share company engineering data in an unprecedented manner. The key players, acknowledged by Ray in his final program overview [448] in April 1992, deserve much wider remembrance:

#### "Acknowledgements

John F. Ward was Manager of Rotorcraft Technology at NASA Headquarters during the definition of the DAMVIBS Program and provided the initial support and encouragement to get the program started. William C. Walton, Jr. and Eugene C. Naumann led in the definition, implementation, and management of the activity which resulted in the CH-47D study. Mr. Walton later led in the definition and implementation of the DAMVIBS Program and prepared coworkers to manage the program in anticipation of his retirement in June 1984. John H. Cline has served as the Technical Representative of the Contracting Officer for the four DAMVIBS task contracts since 1984. Robert J. Huston was Manager of Rotorcraft Research and Technology at Langley during the formative phase of the program and provided advocacy and support when it was needed most. James D. Cronkhite (Bell), Richard Gabel (Boeing), Mostafa Toossi (McDonnell Douglas), and William J. Twomey (Sikorsky) were the project engineers who headed up the respective industry teams."

## 2.6 VIBRATION

You can appreciate just how comprehensive the DAMVIBS program was from Fig. 2-222, which I have reproduced from Ray's June 1989 progress report [449]. The study of basic airframes showed that prediction of measured frequencies "was good up to about 10 Hz, only partly satisfactory between 10–20 Hz, and generally unsatisfactory above 20 Hz." Depending on your view, these results were only a good start because these helicopters had three or four blades, and this meant that response to 3/rev or 4/rev (in the range of 15 to 30 Hz) was not predicted close enough for engineering purposes. The DAMVIBS participants decided that much more detail about how to include engines (and drivetrain, stores, armament, crew, fuel, doors, avionics, instrument panels, control system access panels, fairings, canopy, couplings, secondary structure covers, etc.) to the primary NASTRAN models was going to be required. In short, virtually nothing could be left out of the model until it was proven to be a small effect. To mount this second phase, they tasked Jim Cronkhite at Bell to shake test an AH-1G in its fully assembled configuration and then systematically remove subassemblies, repeating shake testing at each step. Each of the eight steps produced new insight until Bob Domka from Bell was able to report in detail [450], at the 44th AHS Forum in 1986—and Jim could later summarize in 1993 [451]—that "the

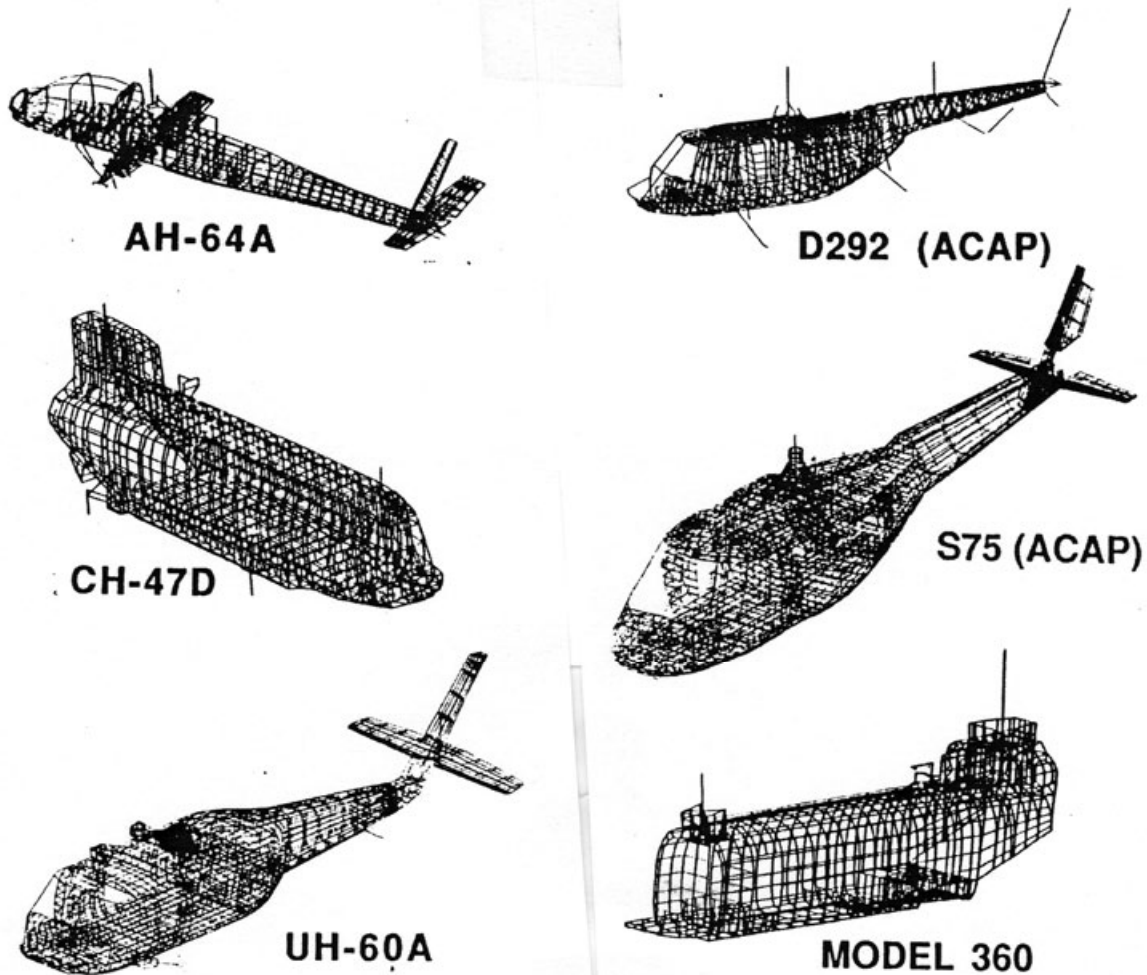


**Fig. 2-222. Both metal and composite airframes were examined during the DAMVIBS program [449].**

natural frequency correlation at the higher frequencies was improved from 20 % error to less than 5 % error for frequencies up to 30 Hz ( $4/\text{rev} = 21.6$  Hz for the AH-1G) by adding more detail in the tailboom and by including tightly fastening panels, doors, and secondary structure in the forward fuselage.” I believe that Bob Domka’s paper [450] is worth its weight in gold. The message as I saw it then (and still think) was that joints of any type are not rigid.<sup>126</sup> This must make you wonder about how field service will cause a deterioration of a well-manufactured, metal airframe *after* the helicopter is delivered.

With finally a rather adequate NASTRAN model of the AH-1G, the DAMVIBS participants went on to predict vibration measurements from flight test for this helicopter. Four reports came out in the 1989–1990 time frame that made the logical effort to combine the AH-1G NASTRAN response model with vibratory loads calculated by each of the DAMVIBS participants’ “comprehensive” rotor loads programs. You will read about this effort and its results shortly.

The DAMVIBS program also spun off a key ingredient for the future UH-60 Airloads Program that you read about earlier. The ingredient was a “much better” NASTRAN model of the UH-60A than was available during the DAMVIBS program. By way of background, during the DAMVIBS program the test configuration was a UH-60A at virtually a weight empty of 10,000 pounds. The DAMVIBS shake test details and results as published by Sikorsky’s Howland, Durno, and Twomey [446] showed that 72 accelerometers were located at many positions on the fuselage as Fig. 2-223 shows.

The vibration in g’s per pound of hub shaking force is a common output from a shake test. The primary independent variable is the shaker frequency. As a simple example from many graphs of data from Howland, Durno, and Twomey, consider just the vibration at two locations. I have chosen two positions on the right-hand side of the floor (see location 3 and 7 on Fig. 2-224) to show only vertical response to vertical hub shaking force. Keep in mind that there can be vertical response to lateral and longitudinal hub vibratory forces as well. In fact, when you think about it, at any given location the full story appears more like Table 2-30 below (and you are only being introduced here to 2 locations and 1 of the 18 data possibilities that are stored in Sikorsky’s files). With 72 locations and 18 possibilities, you need to be prepared to look at 1,296 graphs for just *one* helicopter in the DAMVIBS program files. Theory versus test adds another 1,296 curves.

**Table 2-30. Loads and Responses to be Considered in the Vibration Problem**

Location Response	Hub Vertical Force	Hub Lateral Force	Hub Longitudinal Force	Hub Pitching Moment	Hub Rolling Moment	Hub Torsional Moment
Vertical						
Lateral						
Longitudinal						

<sup>126</sup> During the DAMVIBS program, I was deeply involved in technology at Bell. To make sure that I never lost my basic understanding of vibration, and appreciation for the efforts and progress Jim and his research team were making, I would frequently re-read NACA TN 2884, which was published in January 1953 [452]. The work was performed and reported to the N.A.C.A. by the National Bureau of Standards.

## 2.6 VIBRATION

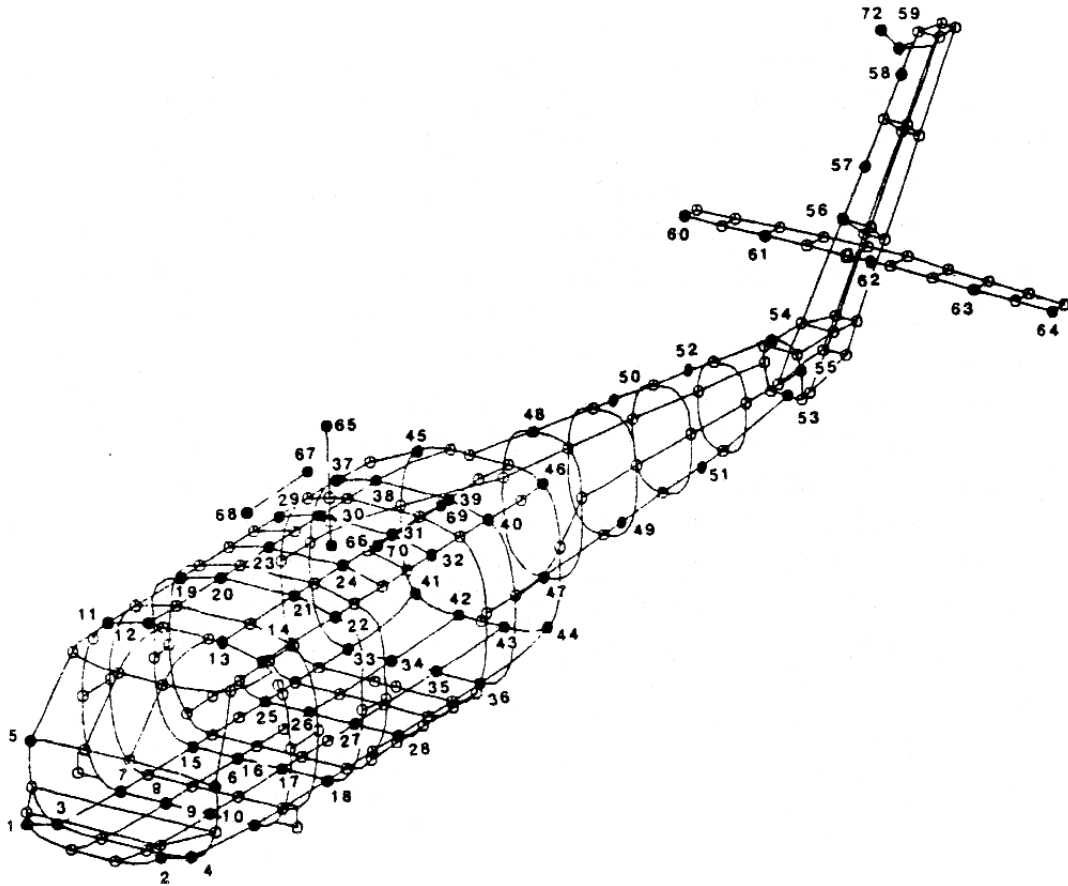


Fig. 2-223. During the DAMVIBS program, 72 accelerometers were placed on the UH-60A fuselage. The floor vibration was associated with locations 3 through 36 [446].

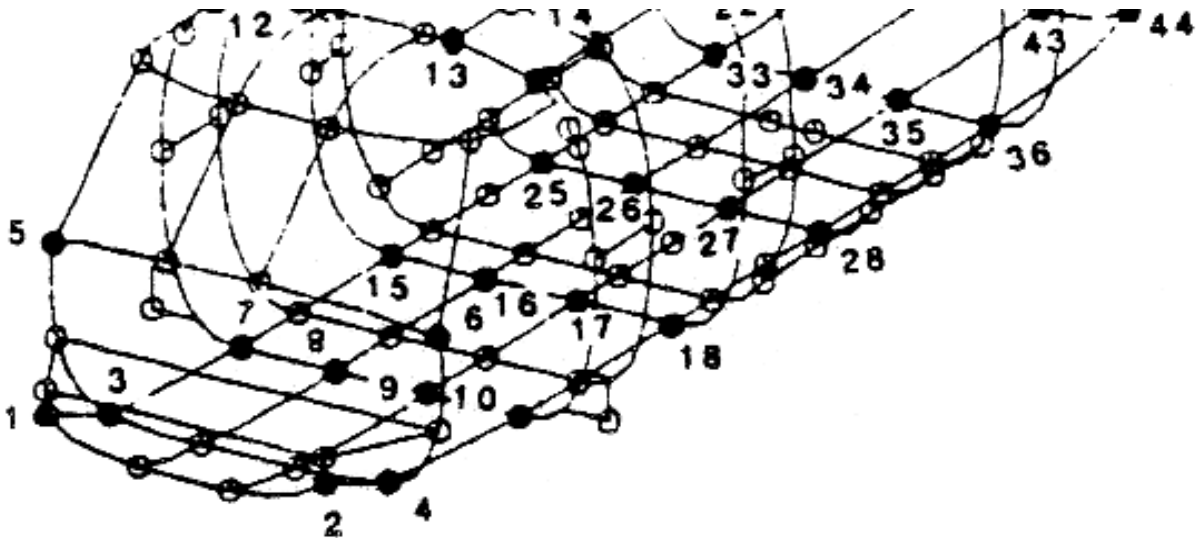
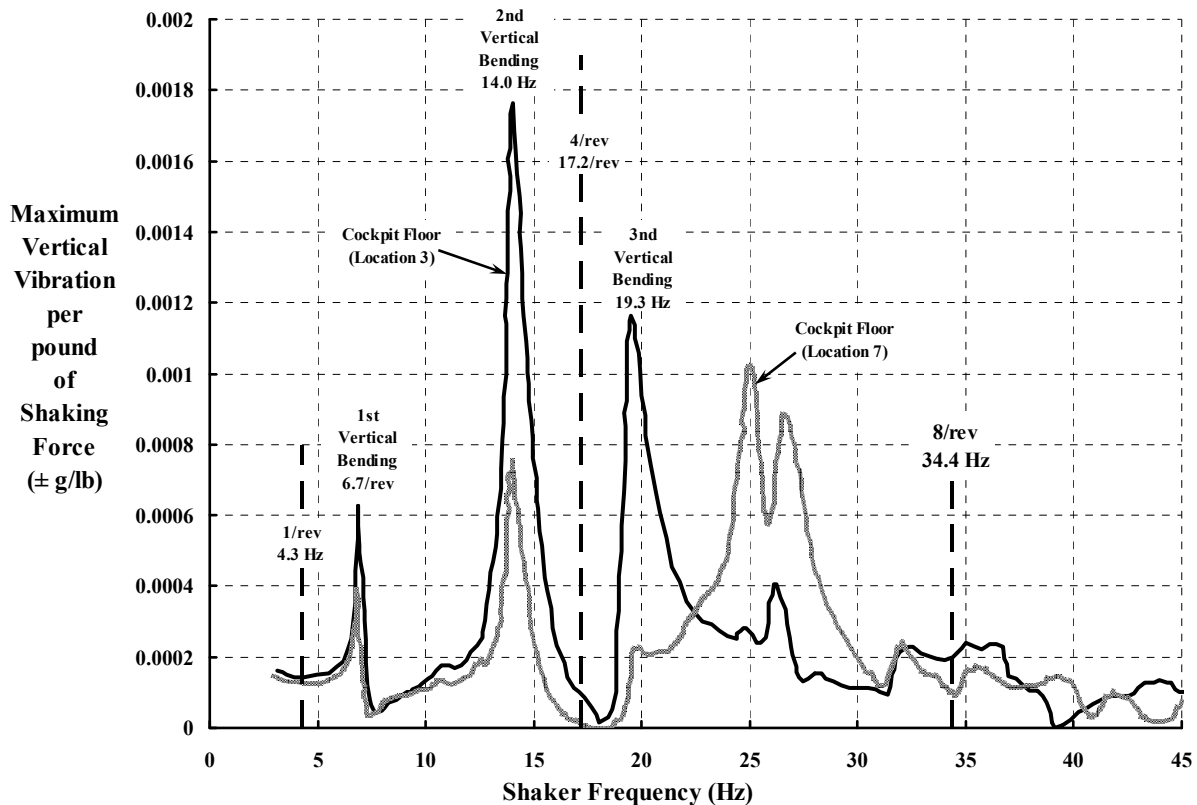


Fig. 2-224. The pilot's and copilot's seats are approximately above locations 7, 8 and 9, 10 for the UH-60A DAMVIBS shake test of the primary airframe [446].



**Fig. 2-225. Vertical response to vertical hub shaking force at two points on the floor of the UH-60A<sup>127</sup> [446].**

A sample of the wealth of data in the Howland, Durno, and Twomey report is shown here in Fig. 2-225. The basic data is frequently called a response curve, but I tend to think of the graph as a calibration curve. Without including the fuselage-rotor coupled result, you might say that a vertical hub vibratory load at 4/rev of 1,000 pounds (about one-tenth of the weight empty) will produce about  $\pm 0.1$  g at location 3 on the cockpit floor (i.e.,  $\pm 0.0001$  g per pound times  $\pm 1,000$  pounds). The primary airframe shows that there would be imperceptible vibration at location 7, which is along the light gray line in Fig. 2-225.

The first vertical bending mode of this UH-60A result appears to be right around 6.7 Hz as Fig. 2-225 suggests. The next critical mode has a peak acceleration at 14.0 Hz, and the experimenters associated this frequency with the second vertical bending mode. With Fig. 2-225 before you, just imagine your reaction if this second mode had its peak at 4/rev. Then the vibration to the pilot near location 7 (the light gray line) would be, for 1,000-pounds hub vertical shaking force, about  $\pm 0.7$  g. According to ISO 2631 criteria (Fig. 2-182),  $\pm 0.7$  g at 17.2 Hz would cause loss of pilot proficiency in about 1 minute!

<sup>127</sup> I reproduced this graph from Howland's report [446], page 153. The report's summary graphs are very small, so I used a program called GrabIt to read points from the small graph into a Microsoft<sup>®</sup> Excel<sup>®</sup> spreadsheet. I took this approach because I was afraid to bother engineers at Sikorsky for the original artwork. After all, the report is over 20 years old. I felt lucky to have a good PDF file from which to make a reasonably accurate, nice-sized graph for this discussion.

## 2.6 VIBRATION

The comparison of NASTRAN model results to each manufacturer's helicopter during this 1980s time frame was, as Ray Kvaternik suggested, not too bad in the lower frequency range, but prediction of frequencies at which peak vibration was found was  $\pm 20$  percent. The situation Sikorsky researchers were able to benchmark is shown here in Fig. 2-226. The second bending mode is predicted to be at 12.4 Hz, while test data shows 14.0 Hz. This is an error of about 12 percent. At these respective frequencies, the maximum acceleration was 0.0022 g per pound of shaking force versus 0.0018 g per pound, a 22 percent error.<sup>128</sup>

You might argue that this example correlation between test and theory shown below is not good enough for detail design, and I would agree with you, but counter with this: The rotorcraft industry had nothing in the early 1950s. Some 30 years later, the DAMVIBS participants and their respective companies had a solid rock from which to make significant improvements.

Of course, just having the helicopter response, given exact shaking forces, is only half the battle. The accurate prediction of in-flight vibration is the objective, and this is the subject you will read about next.

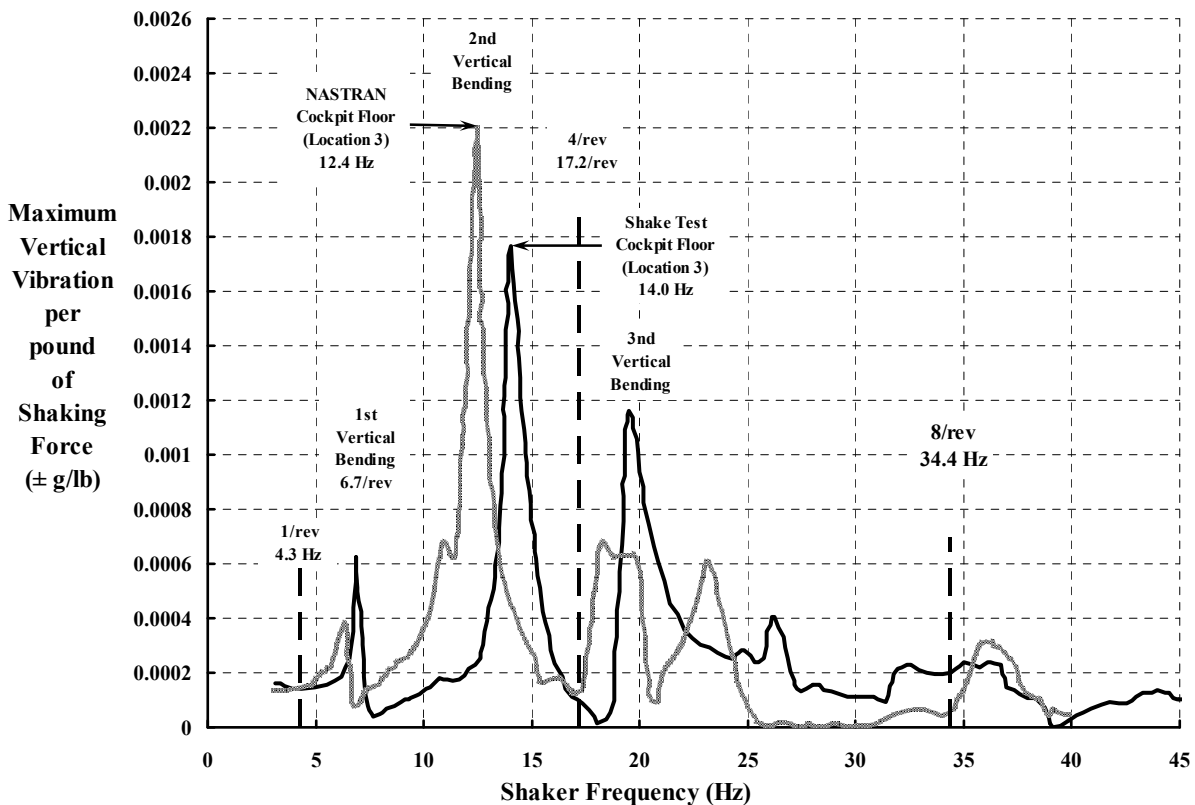


**Fig. 2-226. NASTRAN vs. shake test results for the UH-60A for vertical response to vertical hub shaking force at location 3.**

<sup>128</sup> I remember thinking at the time that the DAMVIBS participants had achieved a miracle to just get the NASTRAN predictions to fall on the same graph with the shake test results.

### 2.6.3.3 AH-1G Vibration, Theory Versus Test

With this background, the DAMVIBS participants went the final step of predicting flight test vibration measurements for the AH-1G. This task required coupling predicted hub vibratory loads to the best NASTRAN model of the complete helicopter that Bell had to offer. Four reports came out in the 1989/1990 time frame that documented this logical effort to combine the AH-1G NASTRAN response model with vibratory loads calculated by each of the DAMVIBS participants' "comprehensive" rotor loads programs. The four participants were Bell Helicopter Textron [453], Boeing Helicopters [454], McDonnell Douglas Helicopter Company [455], and Sikorsky Aircraft [456]. Their approach to this final theory-versus-test comparison is summarized in Fig. 2-227.

The effort depended heavily on two sets of data that were furnished by Bell. The first data set was the AH-1G NASTRAN model. This necessary data was packaged in two volumes totaling slightly over 1,000 pages [457]. The second data set was the flight-measured vibration of the AH-1G (ship number 20391) that the four companies were to correlate with [458]. This flight test data, taken from a loads survey done in 1976 [459], amounted to six points in a level flight speed sweep. The selected flight number from the loads survey was 35A, and the counters were 610 through and including 615, which covered true airspeeds of 67, 85, 101, 114, 128, and 142 knots. This flight was flown at a pressure altitude of 5,000 feet and an outside air temperature of 82.4 °F, which is a density altitude of 2,600 feet. The main rotor speed was 324 rpm. The test gross weight was 8,320 pounds.

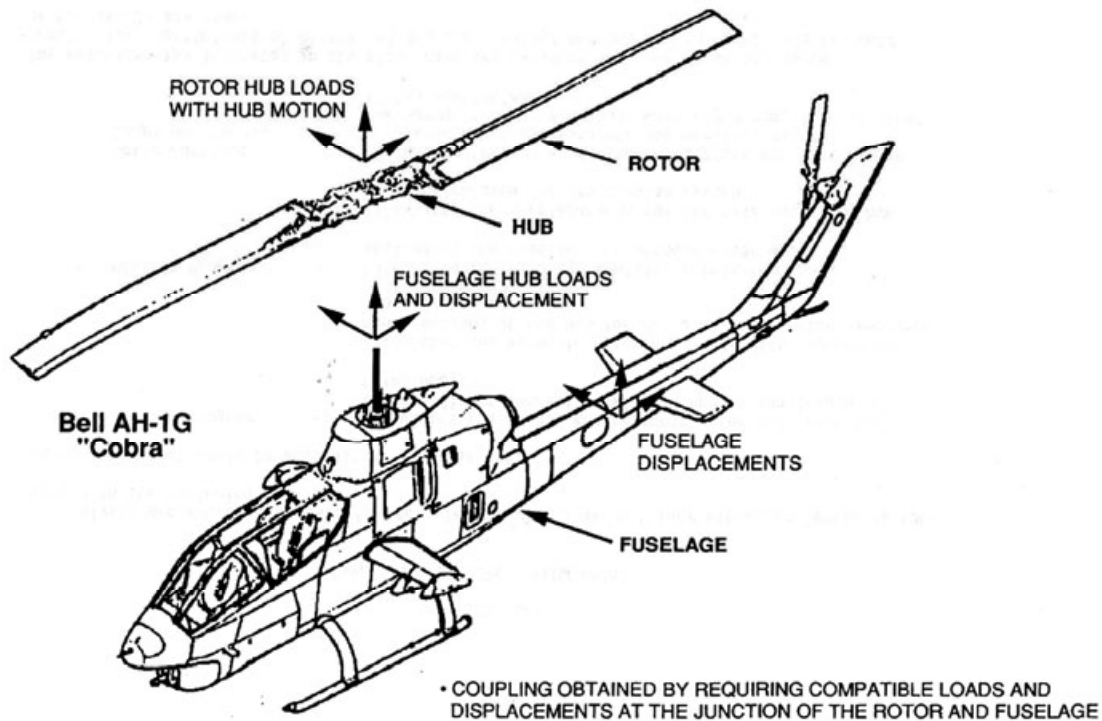


**Fig. 2-227. AH-1G theory vs. test approach at the end of the DAMVIBS program (example from reference [454]).**

## 2.6 VIBRATION

Along with a great deal of aircraft geometry, structural and aerodynamic properties, and sensor locations, Bob Dompka and Jim Cronkhite [458] passed loads and vibration in harmonic coefficient form to the three other major DAMVIBS participants. This tabulated data of mean plus the next six harmonics was placed in appendix A of their report. This appendix was titled OLS<sup>129</sup> Harmonic Data for Correlation and was grouped into:

1. Hub Accelerations (Mast Top F/A, Mast Top Lateral, Mast Top Vertical)
2. Fuselage Vertical Accelerations (Nose Sta. 46, Gunner Sta. 100, Pilot Sta. 146, Engine Deck Sta. 249, Tail Boom Sta. 297, Tail Boom Sta. 485, 90 Deg Gearbox Sta. 518, Tail Boom Fin Load Sta. 521, Left Wing-tip Sta. 195, and Right Wing-tip Sta. 195)
3. Fuselage Lateral Accelerations (Nose Sta. 46, Gunner Sta. 100, Pilot Sta. 146, Engine Deck Sta. 249, Tail Boom Sta. 297, Tail Boom Sta. 400, Tail Boom Fin Load Sta. 521)
4. Main Rotor (Red Blade)—Chord Bending Moments (31%, 50%, 70% of 264 inches)
5. Main Rotor (Red Blade)—Beam Bending Moments (31%, 50%, 70%, 90% of 264 inches)
6. Main Rotor (Red Blade)—Torsion Moments (31%, 50%, 70%, 90% of 264 inches)
7. Axial Forces (Cyclic F/A Boost Cylinder, Cyclic Lateral Boost Cylinder, Collective Boost Cylinder, M/R Red Pitch Link, M/R White Pitch Link, Lift Link, M/R Red Drag Brace)
8. Pylon Vertical Displacements (Left Fwd, Right Fwd, Left Aft, Right Aft)
9. Vehicle Performance Data (Hub Flapping Angle, Hub Feathering Angle, A/C Roll Attitude, A/C Pitch Attitude, A/C Yaw Attitude)

This was a small, but key, sample of the nearly 60 channels of data available. Just think about it. The above 9 items give 46 data channels for each of 6 speeds. Each data channel has a mean plus 6 sine and 6 cosine amplitudes. This is a total of  $46 \times 6 \times 14$ , which equals 3,864 points on a whole bunch of graphs, and then you are ready to start correlation!

There are three specific areas of correlation results I want you to appreciate. The first is the difficulty that each of the four players had in predicting the helicopter's trim and blade motions. The second is predicted versus measured vibration at the AH-1G nose, which was none too good. The third is the general conclusions and recommendations from the effort.

Each of the four reports [453-456] explained their comprehensive rotor analysis computer programs, and the aircraft trim and control positions that were predicted. The rotor analyses were known as:

Bell—C-81

Boeing—C-60

McDonnell—RACAP for Rotor Airframe Comprehensive Aeroelastic Program

Sikorsky—RDYNE for Rotorcraft Dynamics Analysis

---

<sup>129</sup> OLS stands for Operational Loads Survey and was the common acronym for reference [459].

These computer programs were, in my mind, second-generation comprehensive analysis tools that tailored their program input to each company's product line. (These tools grew out of the 1955 groundbreaking computer program [460] developed by Alfred Gessow and Almer Crim of N.A.C.A. Langley, which I consider the first generation). Each company's comprehensive analysis grew from a basic rotor-alone model in the mid-1960s to inclusion of elastic fuselage motions by the mid-1980s. However, because the AH-1G was a two-bladed Bell product [459, 461], the engineering staffs from the other three companies were not able to exactly represent the machine. One particular design aspect that Bell was quite aware of was the bending of the rotor mast and the underslung hub as illustrated in Fig. 2-228. This required work-arounds by the other three DAMVIBS participants. Nevertheless, the DAMVIBS team plunged ahead with openness that can only be fostered in a workshop environment. I will discuss these and other programs that calculate airloads and blade vibratory loads shortly.

The calculation of trim parameters was somewhat different for each of the four major DAMVIBS participants, and only three reported their results. What was reported was not very encouraging. In determining trim, say in the plane of symmetry, the sum of forces along and perpendicular to the flight path must be zero. Of course, the pitching moment about the aircraft center of gravity must also be zero. The AH-1G situation was not much better than the Cierva C.30 problem that was discussed in Volume 1. For example, the fuselage lift, drag, and pitching moment contributions to aircraft trim were only an educated guess. This was because the flow about the fuselage, including the rotor-induced velocities, was not available. Just as important, accurate airloads that deflected the blade, particularly in torsion, were only being calculated at the rudimentary level. This meant that the rotor's contribution to aircraft trim was also an unknown. In short, the AH-1G trim problem was a case of having three equations with two very interactive unknowns and a raft of variables.

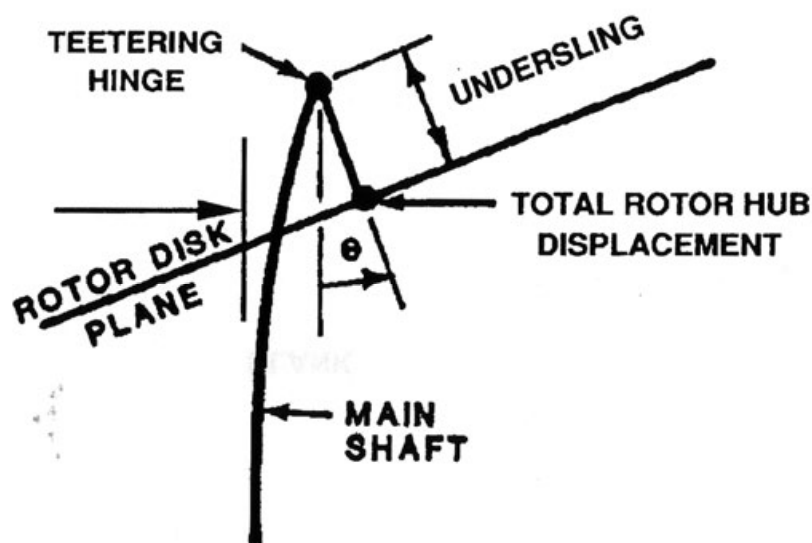


**Fig. 2-228.** The AH-1G had a rather limber, main-rotor mast and an underslung rotor hub. This Bell design approach was not a configuration choice in the second-generation comprehensive analyses of other manufacturers [454].

## 2.6 VIBRATION

The participants had the initial job of predicting the measured fuselage pitch attitude ( $\theta_{fus}$ ),<sup>130</sup> the measured blade root feathering angle ( $\theta_{root,\psi} = \theta_{mean} + B_{1s} \sin \psi + A_{1s} \cos \psi$ ), and the measured hub teetering angle ( $\beta_{root,\psi} = \beta_{mean} + \beta_{1sin} \sin \psi + \beta_{1cos} \cos \psi$ ).<sup>131</sup> The problem was attacked by Bell engineers, who had the most knowledge of their own product, using an iteration scheme that they called full aircraft trim. Both Boeing and Sikorsky engineers chose to input the measured fuselage pitch attitude. Boeing engineers then chose to vary the side force and propulsive force until the calculated values of flapping ( $\beta_{1sin}$  and  $\beta_{1cos}$ ) matched the measured values. This approach solves for the cyclic control angles ( $B_{1s}$  and  $A_{1s}$ ). Sikorsky engineers chose to input measured cyclic control angles and solve for the hub teetering angles. Neither analyses by Boeing nor Sikorsky could obtain a trim solution for the highest speed of 142 knots. All three groups allowed the mean root feathering angle to vary until a semblance of forces equal to zero was obtained. Of course, the solution process then required poetic license and considerable engineering judgment (and still does).

First, let me show you some results for fuselage pitch attitude (Fig. 2-229). Bell's prediction with its iteration scheme falls within  $\pm 1$  degree, which is not, in my opinion, very good. However, the fact that the fuselage pitches nose-down to obtain increased forward

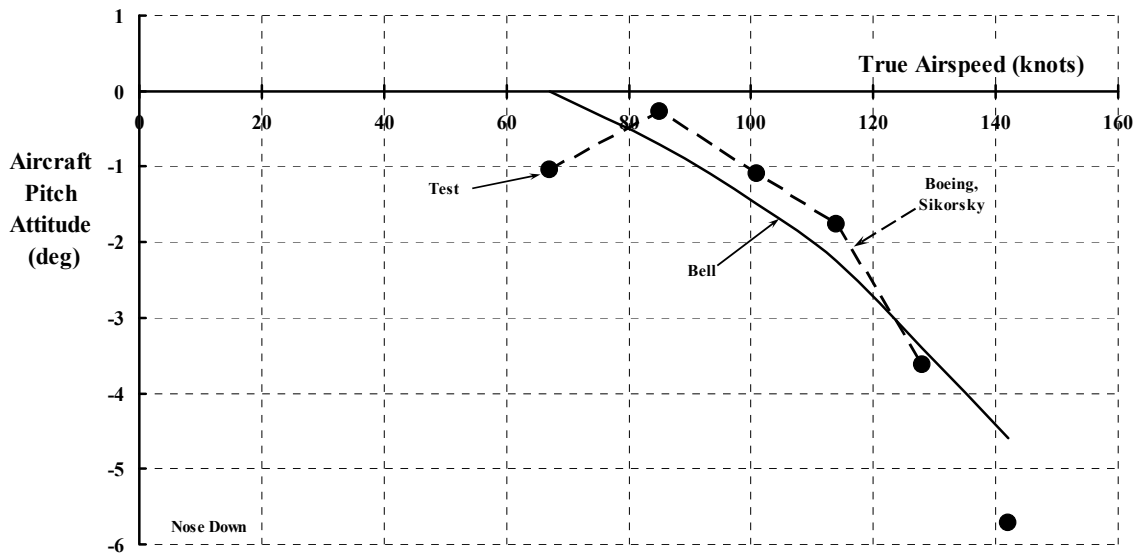


**Fig. 2-229. The AH-1G fuselage pitch attitude trend with forward speed was captured by Bell's C-60 analysis. Boeing and Sikorsky used the measured data as input to their comprehensive analyses.**

<sup>130</sup> Keep in mind that with mast bending, shaft angle of attack and fuselage angle of attack are not the same. Furthermore, fuselage angle of attack and fuselage pitch attitude are also not the same.

<sup>131</sup> The sign convention for the Fourier series representing blade feathering and hub teetering is not standardized within the industry. Some members use a carryover from the autogyro era while others use a mathematically pure form. In addition, the words longitudinal and lateral are represented by many different symbols and subscripts. Finally, plus and minus frequently can be misinterpreted. I can only suggest that you take extraordinary care when dealing with these aspects of helicopter trim.

speed is a fact that is captured. You should know that pilots and passengers do not like to fly tilted nose-down, and they will complain if the tilt is more than  $-2$  or  $-3$  degrees.

Next, consider the longitudinal ( $B_{1s}$ ) and lateral ( $A_{1s}$ ) blade feathering components in Fig. 2-230 and Fig. 2-231 below. Bell and Boeing predicted longitudinal cyclic to within  $\pm 1$  degree. Sikorsky chose the test data as an input to its comprehensive analysis. Keep in mind that all three participants used fuselage attitude as an input to their comprehensive analyses.

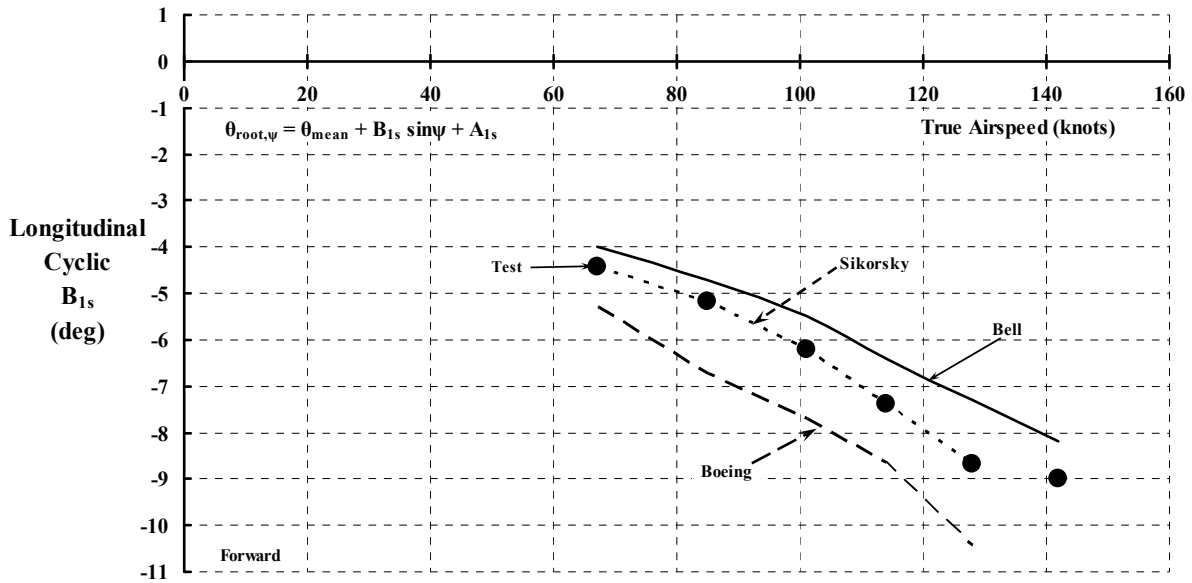


**Fig. 2-230. Bell and Boeing predicted longitudinal cyclic to within  $\pm 1$  degree. Sikorsky chose the test data as an input to its comprehensive analysis.**

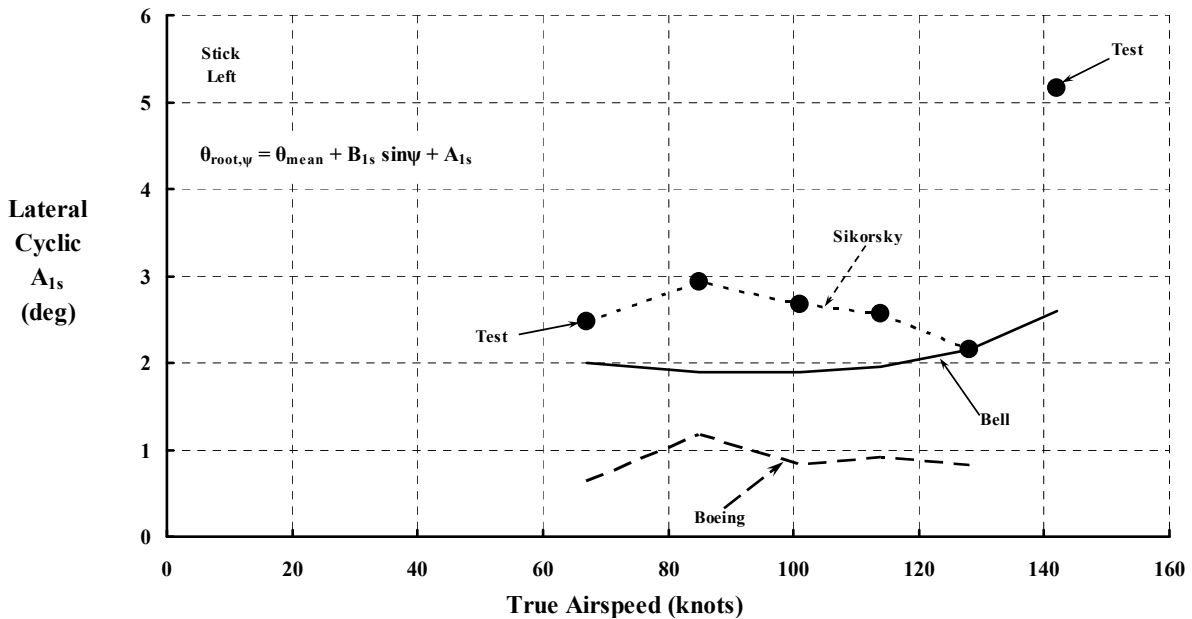
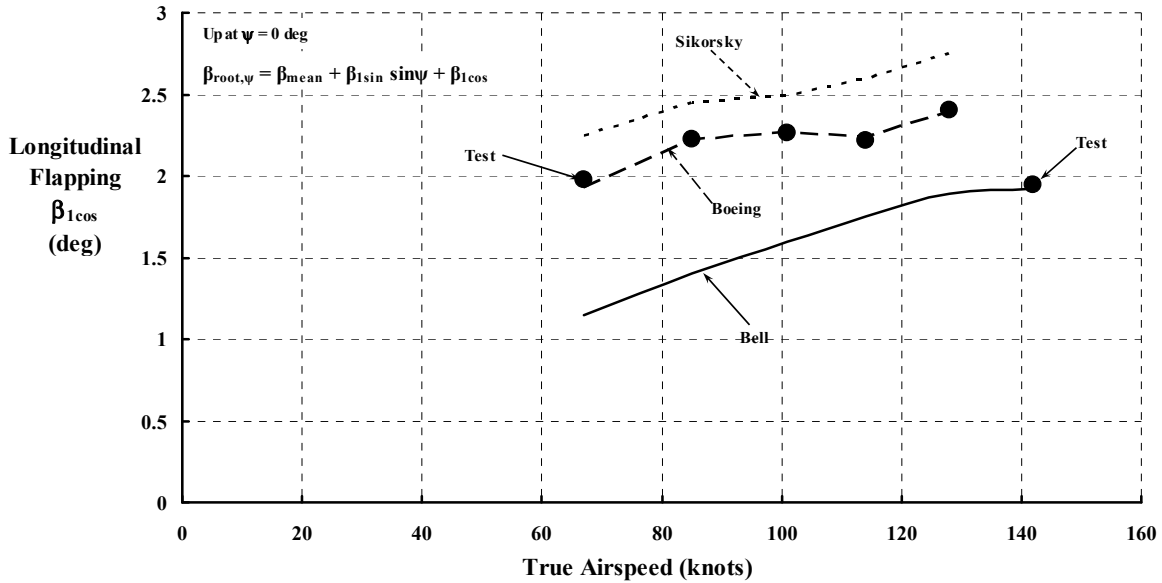


**Fig. 2-231. Bell and Boeing underpredicted lateral cyclic.**

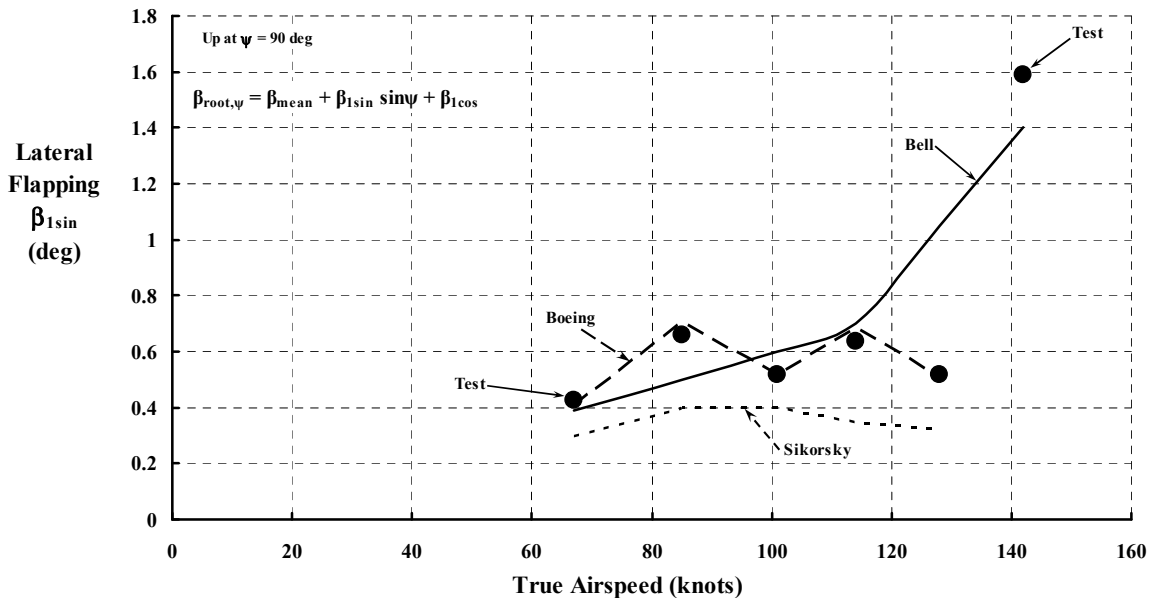
## 2.6 VIBRATION

Fig. 2-231 shows that lateral cyclic was underpredicted. Lastly, consider the hub teetering angle (perhaps you prefer the once-per-revolution flapping angle) provided in Fig. 2-232 and Fig. 2-233.

Prediction of trim angles is a mandatory first step in analyzing any aspect of helicopter behavior. The DAMVIBS participants were able to demonstrate the state of the art in the 1980s. Their results showed that the rotorcraft industry was making progress but that the comprehensive analyses of the time were still falling short.



**Fig. 2-232. Bell and Sikorsky predicted longitudinal flapping to within  $\pm 0.75$  degree. Boeing chose the test data as an input to its comprehensive analysis.**



**Fig. 2-233. Bell and Sikorsky predicted longitudinal flapping to within  $\pm 0.5$  degree. Boeing chose the test data as an input to its comprehensive analysis.**

The accurate prediction of vibration was the objective of the DAMVIBS participants, but as Fig. 2-234 and Fig. 2-235 show, this objective was not met. I have selected results from just one fuselage station, the AH-1G nose, to support this conclusion. *However, saying that the objective was not met is not to say that the DAMVIBS program was a failure. It was far from it. Industry and NASA researchers threw every element of 1980's advanced technology they had at the helicopter vibration problem. There were two major contributions that stand*

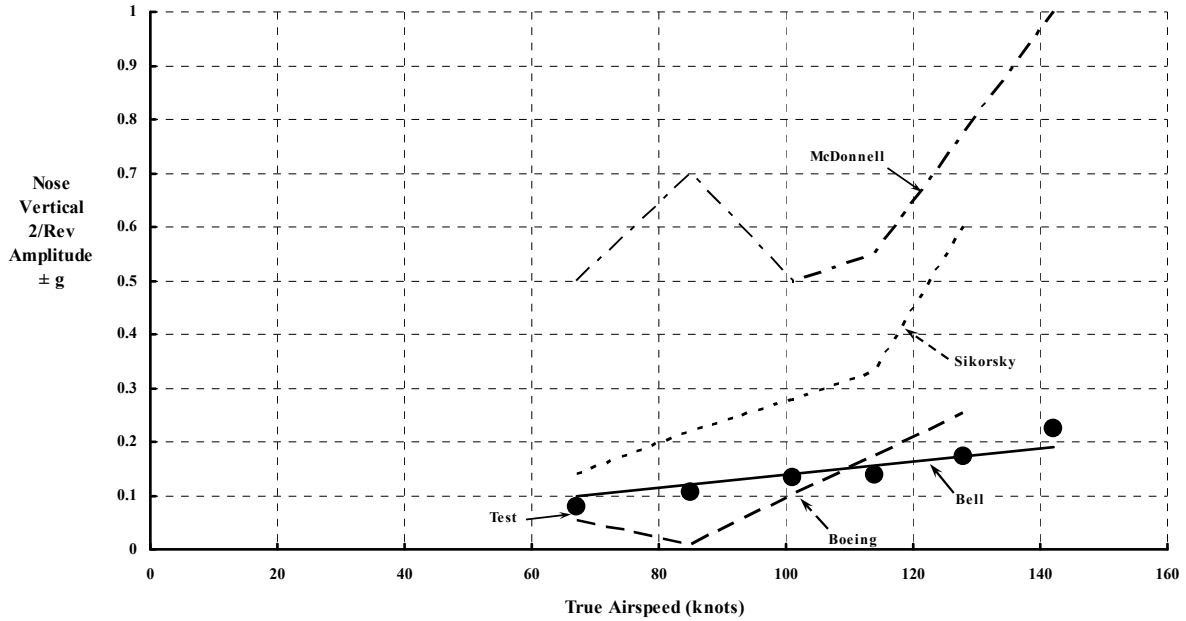


Fig. 2-234. AH-1G nose vertical vibration prediction during the DAMVIBS program.

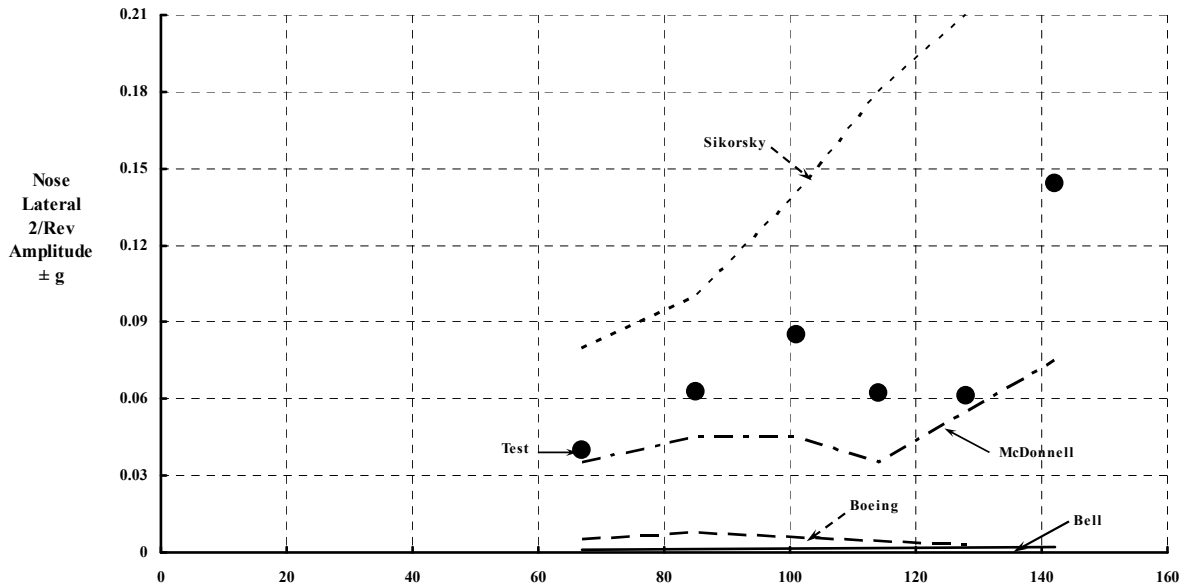


Fig. 2-235. AH-1G nose lateral vibration prediction during the DAMVIBS program.

## 2.6 VIBRATION

out. The first contribution was a giant leap forward in adapting NASTRAN to rotorcraft's needs. The DAMVIBS participants established the minimum level of depth required to obtain the accurate natural frequencies and mode shapes of their current and future products. The second contribution was clear evidence that none of their comprehensive analyses could predict basic rotor system loads and deflections at the accuracy level required by the NASTRAN analysis in order to calculate vibration throughout the helicopter.

In January of 1993 Ray Kvaternik of the NASA Langley Research Center compiled and published a summary of the DAMVIBS program [462], which had been initiated in 1984. Ray's summary view along with contributing papers from Bell, Boeing, McDonnell, and Sikorsky are included in this NASA publication. The conclusions reached by each participant are of immense value, and I have included several key points (in quotes, along with my additional thoughts without quotes) as follows:

1. NASA—"Provided the leadership role and focal point for the type of structural dynamics research which was needed by the industry." The workshop environment let the researchers exchange results and plan follow-on steps without compromising their competitive positions in the market place.
2. Bell—"A detailed build-up FEM [NASTRAN finite element modeling] of the tail boom (rather than an elastic line) improved higher frequency correlations. The effects of secondary structure, non-structural panels, and canopy should be considered during the design phase. In the future, aeroelastic rotor analysis improvements are needed in the representation of rotor downwash and the calculation of hub loads for multi-bladed rotor systems." In short, nothing can be overlooked in the NASTRAN model and that includes damping. Problems with calculating hub loads need to be fixed.
3. Boeing—"A non-linear response with force was observed during shake testing. The frequency at the peak responses tended to decrease with increasing force level. The amplitude increased, but not proportionally with force level. Frequency shifts up to nearly 1 Hz and amplitude changes up to 35% were observed for a 2 to 1 change in force level. The changes were neither uniform across the spectrum nor consistent with frequency. Attachment of large concentrated weights or lumped masses to the airframe can be critical. The attachments must correctly transmit loads into the structure. Mass modeling in general has been treated rather superficially compared to stiffness. Considering the modal complexity of the higher order natural frequencies near  $b/rev$ , much more detailed modeling is needed. Modeling of a composite aircraft is more difficult than a comparable metal aircraft because of the need to determine equivalent physical properties for multi-ply structures of varying ply orientations, thicknesses and material types. The Stress group, as a general practice, needs to adopt modeling procedures which are compatible with both static and dynamic modeling requirements. Cost of the effort to provide a model for both static and dynamic analysis is 5 % of the airframe design effort. Cost of the static model alone is 4 % so the dynamic model costs only add an additional 1 %."
4. McDonnell—"The proper modeling of the mass distribution and representation of secondary and non structural components is essential to accurate vibration modeling. Prior to performing the [shake] test, magnitude and types of excitation loads should be studied using FEM. Excellent correlation with AH-64 shake test results was obtained at most measurement locations up to 13 Hz. Automated DMAP procedures enhance the analysts capabilities to do [NASTRAN] model checkout and verification." The first rule of Roger's Rules for Rangers is 'Don't forget noth'en.' This rule seems to be particularly true when building a NASTRAN

finite element model. Application of AH-1G NASTRAN modeling to the AH-64 was off to a good start.

5. Sikorsky—“The development of a finite element model of the UH-60A airframe having a marked improvement in vibration-predicting ability has been traced. A new program, PAREDYM, which automatically adjusts an FEM so that its modal characteristics match test values, has been developed at Sikorsky. This program has shared in the improvement of the UH-60A model. Along with the closer look at finite element modeling, which was engendered by the DAMVIBS program, came also a closer look at the shake test data which were being used for model verification. A preliminary investigation showed important effects on the airframe test data of the bungee system used to suspend the test article, effects not normally accounted for in finite element modeling. The objective of the DAMVIBS program was to raise the level of the finite-element modeling of helicopter airframes to the point where it would be taken seriously in its ability to predict vibration and in its ability to bring low vibration into the airframe design process. DAMVIBS has succeeded in doing this. Although much improvement remains to be done, it has brought respectability to the analytical prediction of inflight helicopter vibration, and its stated goal of bringing low vibration into the design process of helicopter airframes has been seriously begun.”

These conclusions confirm the major step forward in obtaining accurate fuselage response given “exact” hub vibratory loads, as in a shake test or an analytical experiment using NASTRAN. At the end of the DAMVIBS program, the problem of how to get accurately calculated hub loads was squarely on the table.

The data and accomplishments of the DAMVIBS program were not lost on other members of the rotorcraft industry. In particular, Hyeonsoo Yeo<sup>132</sup> and Inderjit Chopra<sup>133</sup> at the University of Maryland tackled AH-G vibration prediction using a comprehensive analysis known as UMARC, which is short for University of Maryland Advance Rotor Code. They took considerable care in modeling the limber main-rotor mast and an underslung rotor hub shown in Fig. 2-228 because, as they stated in the abstract to their Journal of Aircraft paper [463], “Modeling of pylon flexibility is essential in the two-bladed teetering rotor vibration analysis.” Furthermore, they carefully accounted for the fact that Bell’s AH-1G transmission is mounted to the fuselage on elastomeric springs, which allow both lateral and longitudinal rocking, and a degree of main rotor inplane loads isolation from the fuselage.

When you read Yeo and Chopra’s vintage 1999 paper you will see that prediction of the rotor control angles required for trim were no better than what the four DAMVIBS participants were able to achieve, yet they obtained predicted 2/rev vibration at the pilot’s seat, both vertically and laterally, well within a factor of two. Unfortunately, their success did not carry over to prediction of pilot vibration levels at 4/rev.

---

<sup>132</sup> Hyeonsoo (Dr. Yeo as I like to call him because of his many contributions at such an early age) wrote this paper when he was a graduate research assistant to Inderjit. After serving his apprenticeship, he became (and still is) a valuable member of the U.S. Aeroflightdynamics staff located at NASA Ames Research Center.

<sup>133</sup> When the U.S. Army and NASA began the Rotorcraft Center of Excellence program in 1985, grants were awarded to several universities. Because of Inderjit’s leadership, the University of Maryland received financial support, and the result has been a string of outstanding young men and women quite capable of improving rotorcraft technology well beyond the level imagined by our pioneers. The same can be said about results from Georgia Tech, Rensselaer Polytechnic Institute, Penn State, and other universities that have participated in the Centers of Excellence program.

## 2.6 VIBRATION

### 2.6.3.4 An Introductory UH-60A Example

As the NASA Langley Research Center sponsored DAMVIBS program drew to a close, NASA Ames Research Center took up the flight testing of a heavily instrumented UH-60A [167, 437]. The program, as you read about earlier, was called the UH-60A Airloads Program and included full-scale flight testing and full-scale, rotor-alone, wind tunnel testing. Bill Bousman was honored to give the 31st AHS Nikolsky lecture at the 67th Annual Forum of the American Helicopter Society in May of 2011. Bill traced the history of helicopter testing for airloads (and blade loads and deflections) from 1954 up to the conclusion of the UH-60A Program in 2010. Because of Bill's excellent lecture [464], the UH-60A Program, and the progress made in calculating airloads using computational fluid dynamics (CFD), I decided to have a little fun on the side. My motivation came to a head when Ethan Romander (who works for Bill Warmbrodt at the Flight Vehicle Research and Technology Division of Ames Research Center) presented a paper at the May 2011 Forum [465]. Ethan's paper showed excellent correlation of rotor-alone *performance* with the UH-60A airloads rotor as tested in the 40- by 80-Foot Wind Tunnel at Ames Research Center. The task I gave myself was to predict UH-60A flight-measured vertical vibration at the flight crew station due only to vertical hub vibratory loads over a speed range using a very limited amount of resources.<sup>134</sup>

The resources available for this task were relatively simple. First of all, the measured UH-60A vibration at the crew station had been published by Karen Studebaker as you saw in Fig. 2-212. To augment this data, I prevailed on Bob Kufeld (at Ames Research Center) to pull out the vibration waveforms that would give more depth to the overview that Karen had provided. Second, the UH-60A configured for the Airloads Program had been shake tested by Sikorsky [466], and a NASTRAN model had been created [467]. The shake test data provided a ballpark for cockpit vertical g response per pound of vertical hub load. Third, Ethan Romander had shown very encouraging prediction of power required versus wind tunnel speed. Given that level of correlation, I decided to bet that maybe Ethan's calculated hub loads would be adequate for this simple example. Ethan was kind enough to respond to every one of my requests.

Now let me relate the fun I had. Bob gave me vertical, lateral, and longitudinal vibration data for the pilot and copilot at several speeds. I chose to restrict my task to predicting only vertical vibration for the pilot. The pilot's location corresponds to the measurement point labeled 7 on Fig. 2-224. The 7 speed points Bob picked (from a total of 23) were obtained in steady, level flight at a weight coefficient solidity ratio of  $C_w/\sigma = 0.08$ . Thus, I began with Table 2-31. To get a sense of what the pilot's vertical vibration waveform looked like, I chose two data points: 8515 corresponding to a true airspeed of 47 knots and 8534 corresponding to 158 knots. The time histories for both vertical vibratory responses extended over a 2-second period. Fig. 2-236 and Fig. 2-237 shows this "raw" data for eight revolutions within the 2 seconds. On the surface, these two figures look like an oscillograph

---

<sup>134</sup> It is my belief that—in the not too distant future—the AVID and DAMVIBS attacks will be repeated using the UH-60A Airloads Program data. The improvements in hub load prediction and NASTRAN modeling will then be applied, and the rotorcraft industry will have a new baseline for its capability to predict helicopter vibration.

strip-out that I grew up with. In those days we would quickly draw horizontal lines that showed the approximate minimum and maximum values, and then take an average to get a vibration amplitude. I would estimate from these two figures that at 47 knots the pilot was feeling  $\pm 0.20$  g. At the higher speed, it looks to me like the pilot was feeling about  $\pm 0.32$  g. This is about what Karen showed in Fig. 2-212. It is clear that the extremes of vibration are not constant over the eight revolutions.

**Table 2-31. Experimental Data Points for Harris' UH-60A Vibration Example**

Data Point	Boom Indicated Airspeed (knots)	True Airspeed (knots)	Advance Ratio ( $V_t = 726$ fps)	Weight Coefficient $C_w = \frac{W}{\rho AV_t^2}$
8515	35	47.33	0.110	0.00652
8513	55	64.97	0.151	0.00654
8511	75	88.11	0.205	0.00656
8526	95	111.75	0.260	0.00652
8528	115	132.09	0.308	0.00653
8531	127	145.89	0.340	0.00654
8534	138	157.93	0.368	0.00651

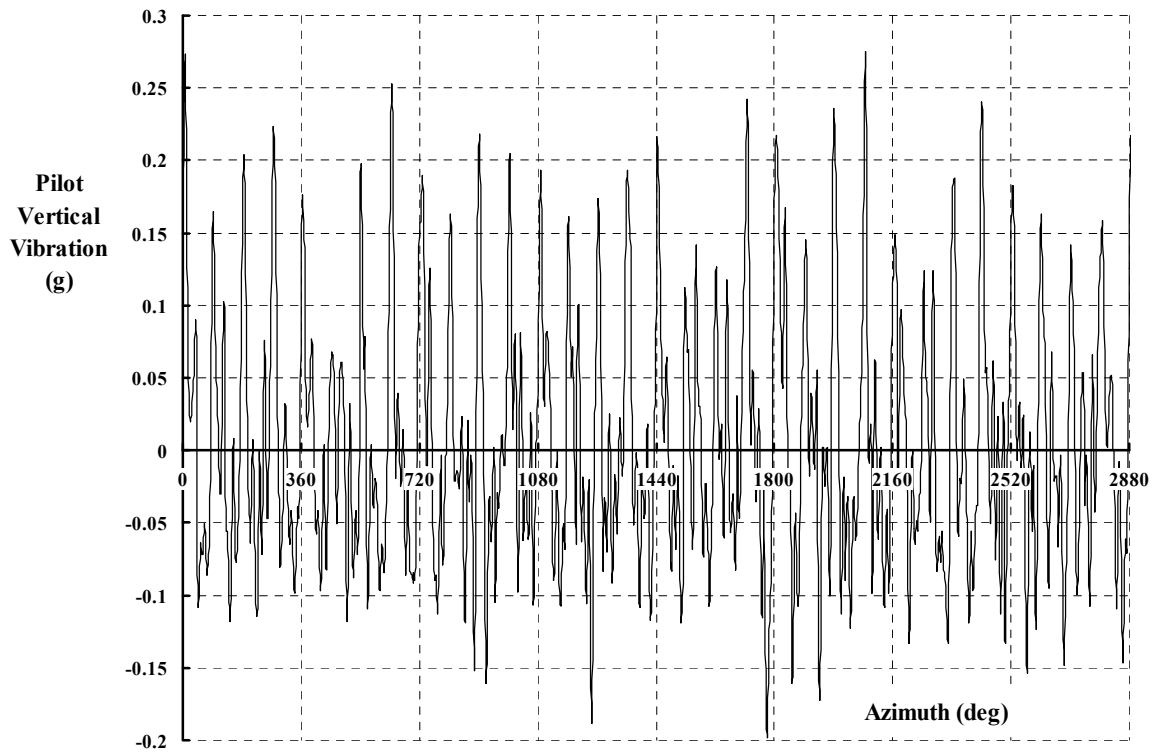


**Fig. 2-236. UH-60A pilot vertical vibration at 47 knots over 8 revolutions.**

## 2.6 VIBRATION

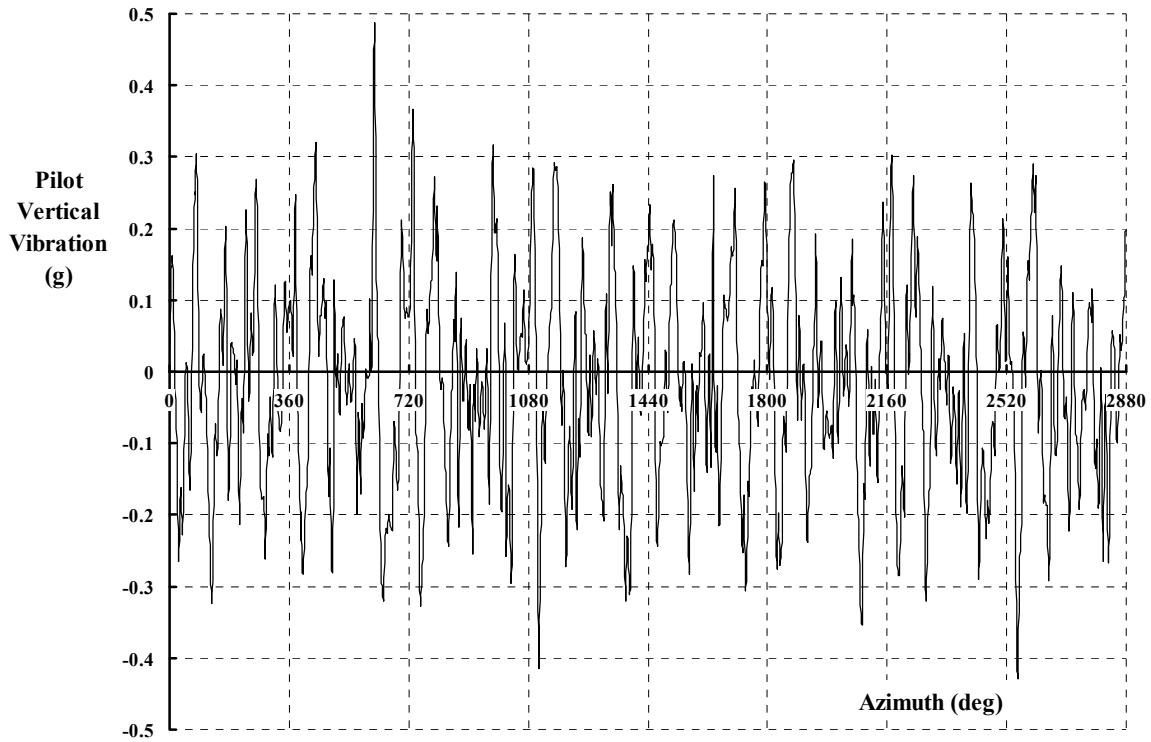


Fig. 2-237. UH-60A pilot vertical vibration at 158 knots over 8 revolutions.

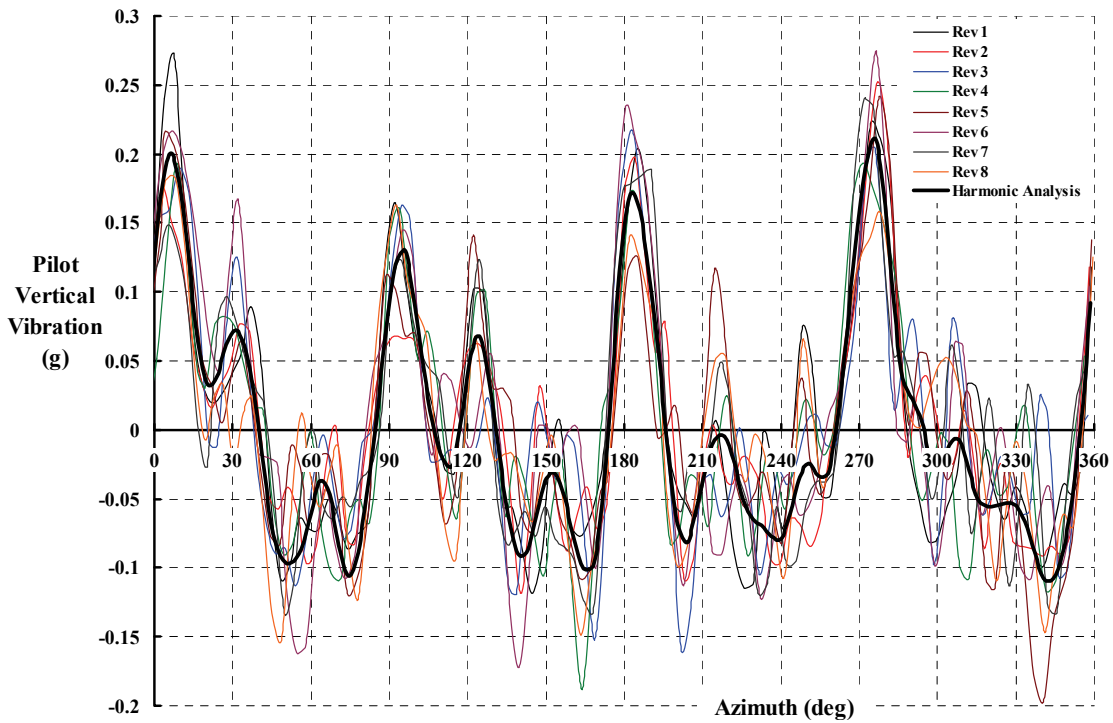
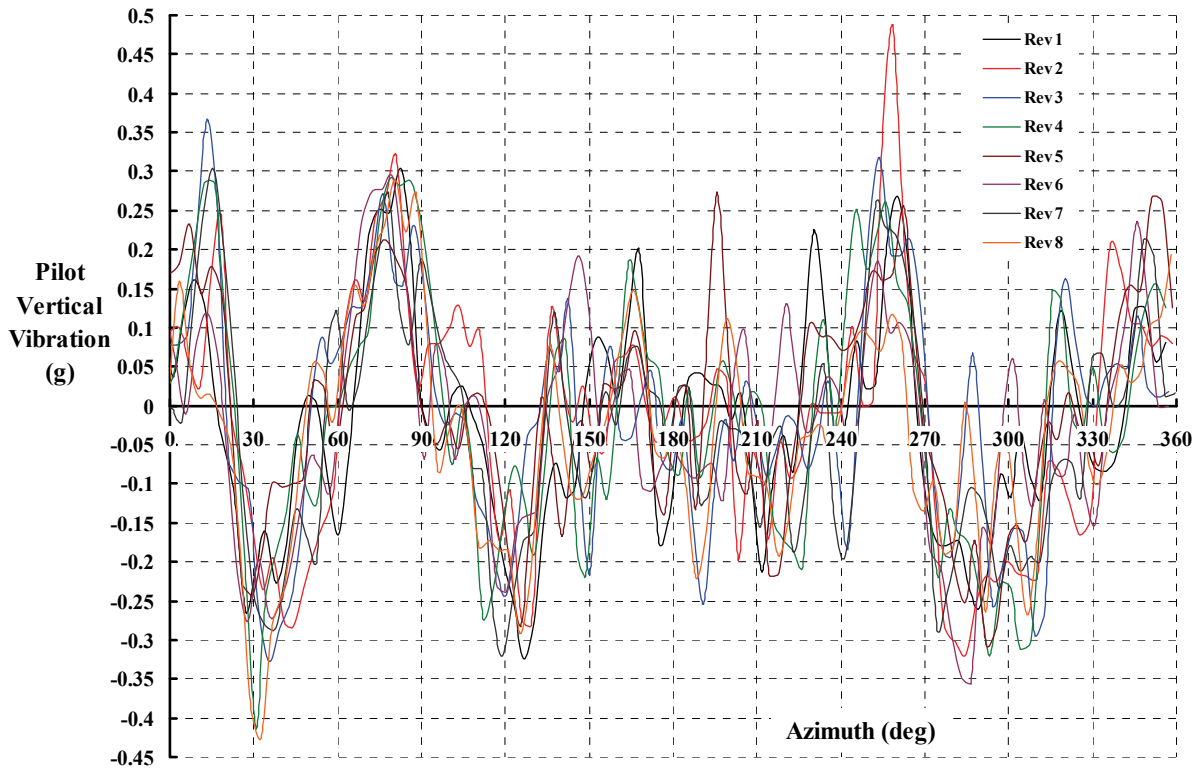


Fig. 2-238. Eight revolutions of UH-60A pilot vertical vibration at 47 knots.



**Fig. 2-239. Eight revolutions of UH-60A pilot vertical vibration at 158 knots.**

It would be nice, of course, if the eight revolutions of data repeated themselves in a very orderly manner. In my experience, this has never been the case with experimental time histories. These UH-60A pilot vertical vibration time histories are certainly no exception as Fig. 2-238 and Fig. 2-239 show. Of course, there is a sense of a 4/rev component in both figures, but the higher harmonics are clearly “contaminating” the waveforms.

Fig. 2-238 includes a heavy black line, which is the result of a Fast Fourier Transform (FFT) analysis over the eight revolutions of data. An FFT analysis is a statistical averaging process that assumes the data is “reasonably” repetitive and, therefore, can be represented by a Fourier series of the form

$$(2.283) \quad y = a_0 + \sum_{i=1}^N [a_i \cos(i\psi) + b_i \sin(i\psi)] = a_0 + \sum_{i=1}^N A_i \cos(i\psi - \phi_i)$$

where  $A_i = \sqrt{a_i^2 + b_i^2}$  and  $\phi_i = \arctan(b_i/a_i)$ . You can solve backwards for the harmonic coefficients ( $a_i$  and  $b_i$ ) when given the amplitude ( $A_i$ ) and the phase angle ( $\phi_i$ ) using the fact that  $a_i = A_i \cos \phi_i$  and  $b_i = A_i \sin \phi_i$ . Of course,  $i$  goes from 1 to whatever you want.

The heavy black line on Fig. 2-238 includes harmonics up to and including the 30th. The line might be considered a mean curve fit to the flight point. Because the experimental waveforms are so unsteady, you do not get a very comforting mathematical representation.

## 2.6 VIBRATION

However, Fig. 2-240 shows that vibration at 4/rev is a major contributor to the overall magnitude. The magnitudes of the other harmonics are caused, in part, by the dissimilar blades used on the UH-60A as configured for the Airloads Program. One of the four blades was heavily instrumented for pressure measurements; another blade had a multitude of strain gauges. Vibration from other components cannot be ruled out. But keep in mind that flight test is measuring a situation that is hardly constant from one instant in time to the next, even in the smoothest of air.

The second facet of the problem—cockpit vertical g response per pound of vertical hub load—came from the paper [466] authored by Durno, Howland, and Twomey from Sikorsky Aircraft, and presented at the 43rd AHS Forum in May of 1987. On figure 32 of their paper, they contrasted DAMVIBS shake test results with the UH-60A Airloads Program configuration. The DAMVIBS configuration was tested at a weight of 9,500 pounds. The UH-60A Airloads Program configuration was shake tested at 17,800 pounds. The contrast between pilot vertical response to a vertical hub shaking force for the two configurations is provided here in Fig. 2-241.

The results published by Durno and his coauthors included a preliminary opinion about why the two configurations had different responses. They wrote that

“in order to investigate the differences between the empty DAMVIBS and a flight configuration, an additional test was conducted. The configuration was chosen to simulate the flight test vehicle to be used for the NASA/AEFA BLACK HAWK rotor loads test program. The aircraft weight was 18,800 lbs [468] and was made up by distributing the weights shown below.

Weight	Lbs	Location
Pilot	240	Sta 253
Co-pilot	220	Sta 253
Instrumentation	75	Sta 264
Instrumentation	275	Sta 389
Cargo	4550	Sta 360
Fuel	2300	

Figure 32 [Fig. 2-241] presents a comparison of the frequency response at the cockpit floor in the vertical direction due to a vertical excitation. It is evident that there is considerable difference in the responses. The predominant modes below 4P are labeled on the figure. The most significant shift is in the third vertical bending mode of the DAMVIBS configuration. This mode appears to have shifted down from 19.3 Hz to 13 Hz. This large shift seems possible due to the shape of the DAMVIBS third vertical mode which has a lot of motion in the cabin center. This is where the mass was placed to increase the gross weight of the AEFA [early identification of the Airloads Program UH-60A] configuration.

The modal frequencies that have been abstracted from analysis are presented in figure 33 [reproduced here as Table 2-32]. These results are actually preliminary until all of the AEFA data has been analyzed and mode shapes generated. Again, the largest difference between the empty and flight configurations is in the 13 to 19 Hz range.”

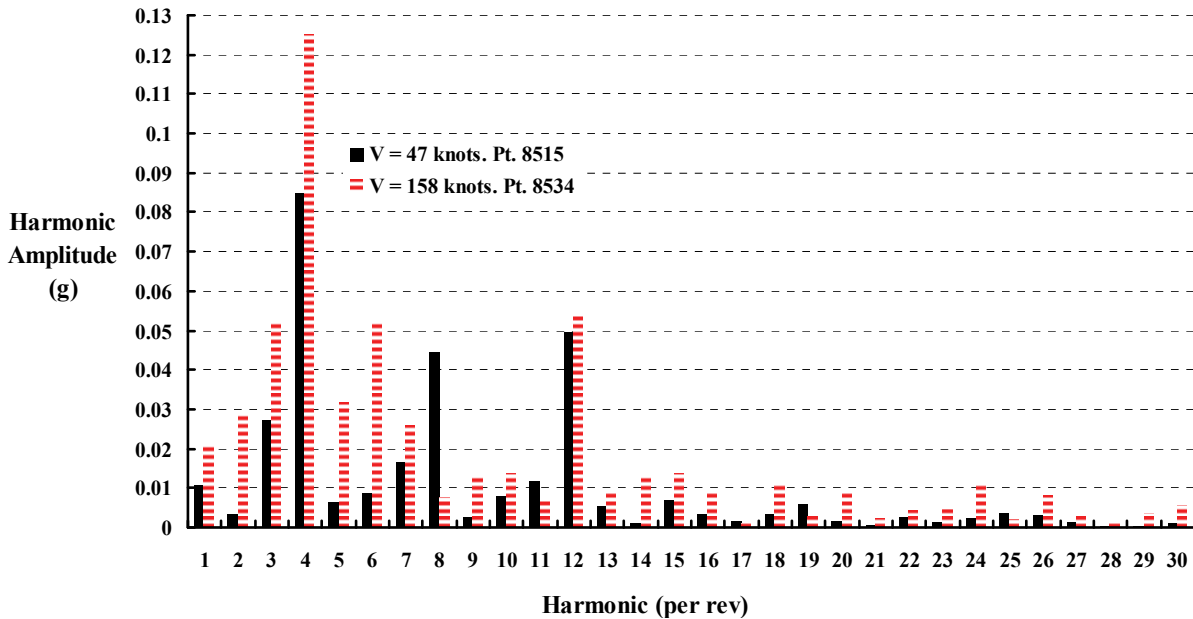


Fig. 2-240. Harmonic amplitudes for UH-60A vibration at 47 and 158 knots true airspeeds from 20 revolutions.

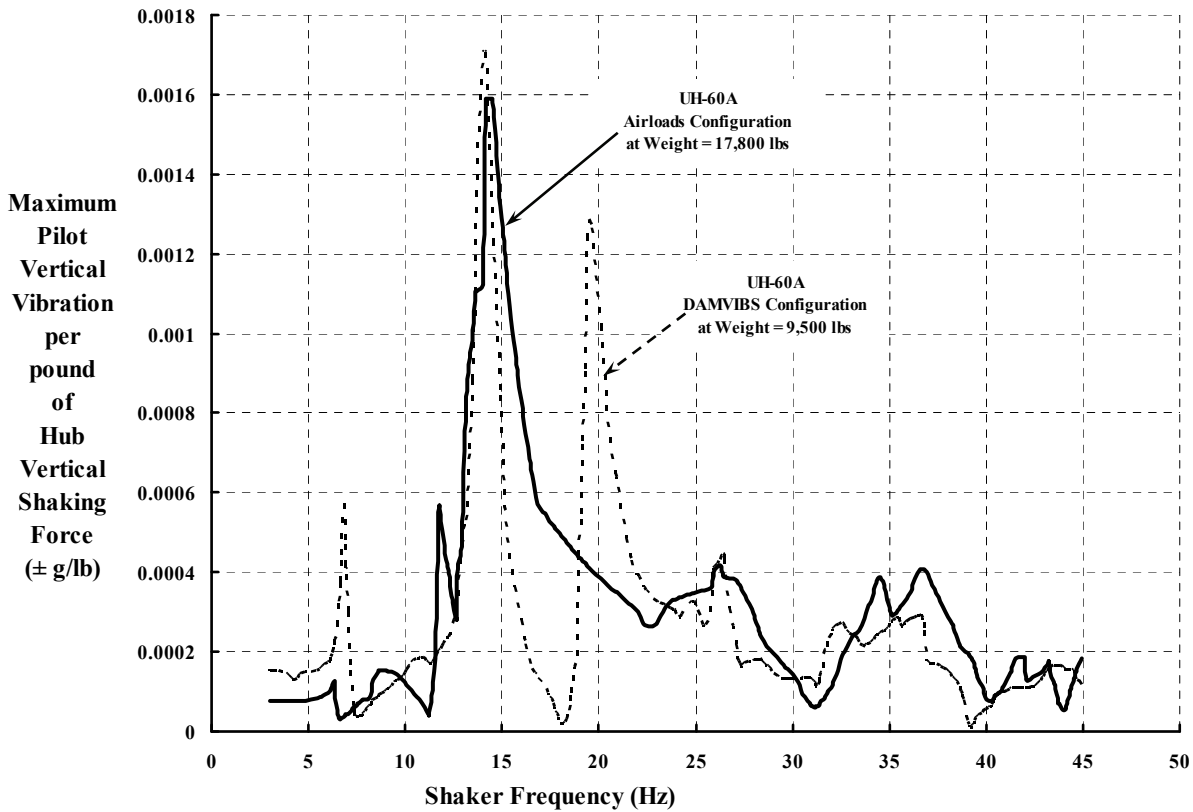


Fig. 2-241. The UH-60A used in the Airloads Program at 17,800 pounds had a substantially different shake test response than did the DAMVIBS configuration at 9,500 pounds [466].

## 2.6 VIBRATION

**Table 2-32. Comparison of Empty vs. Flight Configuration, Modal Frequencies**

Mode Description	DAMVIBS	NASA/AEFA
1st Lateral Bending	5.5	5.4
1st Vertical Bending	6.7	6.3
Nose Vertical	n/a	8.3
Stabilator Yaw/Roll	10.6	n/a
Stabilator Roll/Yaw	11.9	n/a
2nd Vertical Bending	12.3	11.6
Transmission Roll/2nd Lateral	13.8	n/a
Nose Vertical/Tail Vertical	14.0	14.5
Cockpit/Cabin Roll	15.4	15.3
Stabilator Yaw/Pylon Torsion	16.1	n/a
3rd Vertical/Transmission Vertical	19.3	13.0
Stabilator Bending	25.2	25.9

In the updated shake testing of the UH-60A in its Airloads Program configuration, Goodman reported [468] in 1990 that

“ground vibration testing of the NASA/AEFA configuration was conducted as a follow-on to testing of a lower gross weight configuration which was supported by the NASA DAMVIBS program (Ref(c)). Both tests were conducted with the same UH-60A helicopter (S/N 86-24507). In preparation for shake testing, the following aircraft rotor head components and equipment were removed:

Main Rotor Blades	Tail Rotor Blades
Spindles	Tail Rotor Hub
Bearings	Cabin Troop Seats
Dampers	Bifilar
Tail Gearbox Cover	Intermediate Gearbox Cover
Nose Absorber Access Cover	Lower Pylon Fairing
Fuel	

The fairings and covers were removed to provide access to measurement locations. These are considered to be secondary structure having little or no impact on aircraft structural dynamics. The main rotor and tail rotor hubs were replaced by ones modified for compatibility with the shake test suspension system. With the hardware listed above removed and with the test hub installed, the test article weight was 9500 lbs with c.g. at Station 360". A total of 640 lbs were then added to the rotor hub to simulate 50% of the rotor flapping mass and the bifilar mass. This 640 lbs was comprised of 240 lbs of shaker hardware and 400 lbs of steel plates attached to hub arms. With the addition of the 640 lbs the total weight reached 10,140 lbs with c.g. at Station 359". This was the configuration tested under the DAMVIBS contract and is designated as the DAMVIBS configuration. Note that the rationale behind attaching 50% percent of the main rotor flapping mass and the bifilar mass is that this roughly simulates the 4/rev rotor impedance of a UH-60A, and consequently will yield modes near 4/rev with properties similar to the modes of an aircraft in flight which have frequencies in the vicinity of 4/rev.

At the completion of DAMVIBS testing the aircraft was re-configured for NASA/AEFA testing. A full fuel load of 2,300 lbs was added, as well as 5,360 of miscellaneous weight (locations shown in Figure 1), yielding a total weight of 17,800 lb. Note that the weight reported in Ref (b) for the NASA/AEFA configuration was reported incorrectly as 18,800 lb. *For both the NASA/AEFA and the DAMVIBS configurations, the nose, forward cabin, and aft cabin absorbers were installed, but the leaf springs were blocked, rendering the absorbers inactive.* [My italics]

Then in 1993, a NASTRAN model of the UH-60A configured for the Airloads Program was completed by Idosor and Seible at the University of California under a NASA Ames Research Center contract. Their report [467] clarified many configuration details and is a particularly well-written piece of theoretical and related experimental work. Their NASTRAN analysis identified 12 modes in the 0- to 20-Hz range. However, despite the many improved details, comparison of test to theory showed that an accurate NASTRAN model had still not been achieved.

Now for the third facet of the vibration prediction task. This portion of the task required some hub loads. As I mentioned earlier, Ethan Romander's use of computational fluid dynamics (CFD) (plus computational structural dynamics (CSD)) to predict performance of the UH-60A rotor-alone encouraged me to ask for (and receive) his calculated hub loads. This was "betting on the come" that maybe the calculated hub loads would be in the "ballpark." But to hedge my bet, I prevailed on Tom Norman (at Ames Research Center) to give me his "preliminary" 40- by 80-ft wind tunnel measured hub loads (from the balance) so that I might have a possible range for the "real" hub loads. With these two data sets in hand, I made the comparison shown in Table 2-33. To be reasonably sure that 1/rev, 4/rev, and 8/rev loads would be adequate for this introductory example, I examined the harmonic vertical vibratory loads of the test data at advance ratios of 0.15 and 0.40. As you can see from Fig. 2-242, in a more thorough analysis every harmonic up to and including 12/rev, and even up to 30/rev, might someday become important. Because I only had pilot vertical response up to 45 Hz (about 10/rev for 258 rpm) from Fig. 2-241, I had to forgo including the rather large 12/rev load at an advance ratio of 0.40.

**Table 2-33. Theory and Test Vertical Vibratory Hub Loads for UH-60A Vibration Example (nominal rotor speed of 258 rpm (4.3 Hz) and nominal thrust of 20,000 lb)**

<b>(A) Theory From CFD + CSD</b>									
<b>Advance Ratio</b>	<b>1/Rev Cosine</b>	<b>1/Rev Sine</b>	<b>1/Rev Amp</b>	<b>4/Rev Cosine</b>	<b>4/Rev Sine</b>	<b>4/Rev Amp</b>	<b>8/Rev Cosine</b>	<b>8/Rev Sine</b>	<b>8/Rev Amp</b>
0.15	0.0	0.0	0.0	827.4	314.1	885.0	-102.8	-186.9	213.3
0.20	0.0	0.0	0.0	580.4	36.8	581.5	-193.5	-76.4	208.0
0.30	0.0	0.0	0.0	51.1	-217.8	223.7	-228.6	730.3	765.3
0.37	0.0	0.0	0.0	-205.8	-552.0	589.1	-173.1	344.1	385.2
0.40	0.0	0.0	0.0	-219.2	-468.6	517.3	-30.3	292.5	294.1
<b>(B) Test From Run 52 of the 40- by 80-Foot Wind Tunnel Test Number Air Force 010</b>									
<b>Advance Ratio</b>	<b>1/Rev Cosine</b>	<b>1/Rev Sine</b>	<b>1/Rev Amp</b>	<b>4/Rev Cosine</b>	<b>4/Rev Sine</b>	<b>4/Rev Amp</b>	<b>8/Rev Cosine</b>	<b>8/Rev Sine</b>	<b>8/Rev Amp</b>
0.15	476.3	-6.9	476.4	634.2	26.8	634.8	373.1	178.9	413.8
0.20	651.2	-39.8	652.5	311.6	-62.9	317.8	473.8	60.5	477.7
0.30	1006.6	79.1	1009.7	-230.5	-502.8	553.1	-404.0	-234.7	467.2
0.37	1328.1	636.9	1472.9	-485.0	-1052.4	1158.8	-15.5	-224.5	225.0
0.40	1287.0	1047.9	1659.6	-152.5	-882.8	895.9	-163.3	-227.2	279.8

## 2.6 VIBRATION

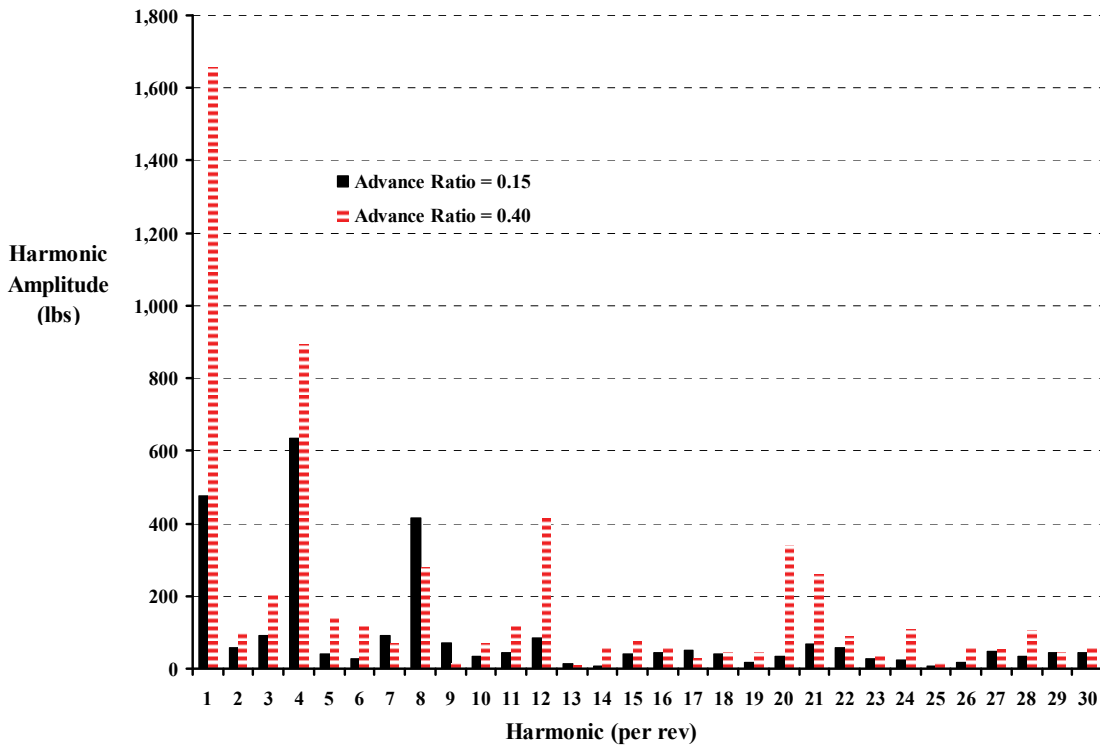


**Fig. 2-242. Rotor-alone test of vertical vibratory hub loads up to 30/rev as measured by the rotor balance (note: balance not calibrated for vibration).**

Given hub loads (Table 2-33) and pilot response to the hub loads (Fig. 2-241), the actual prediction was rather simple. The pilot response to a vertical hub load at 4/rev (i.e., 17.2 Hz at 258 rpm) is 0.00054 g per pound. At 8/rev (34.4 Hz), the pilot response is 0.00038 g per pound. The pilot vertical vibration, therefore, becomes simply

$$(2.283) \quad V_{\text{pilot}} = (0.00054) [a_{4\cos} \cos(4\psi) + b_{4\sin} \sin(4\psi)] \\ + (0.00038) [a_{8\cos} \cos(8\psi) + b_{8\sin} \sin(8\psi)]$$

which, of course, neglects 1/rev vibration. The results of applying this equation with both theory and test values of 4/rev and 8/rev vertical hub loads is shown in Fig. 2-243. As you can see, I have used all of Karen Studebaker's data from Fig. 2-212. I have bounded her UH-60A Airloads Program data with lower and upper lines around her points, and then added the results from Eq. (2.283) as the red solid circles (theory hub loads) and black solid squares (40- by 80-ft wind tunnel test hub loads). Frankly, I was rather pleased to obtain results that were only off by a factor of two, using such a woefully incomplete method.

Fig. 2-243 shows that at an advance ratio of 0.30, the prediction of pilot vertical vibration with theoretical vertical vibratory hub loads is "spot on." This led me to examine comparisons of theory and test waveforms for this point at 128 knots true airspeed. The comparison is shown in Fig. 2-244. Note first that the harmonic analysis (the heavy black line) of the eight revolutions is rather representative of the flight test measurements.

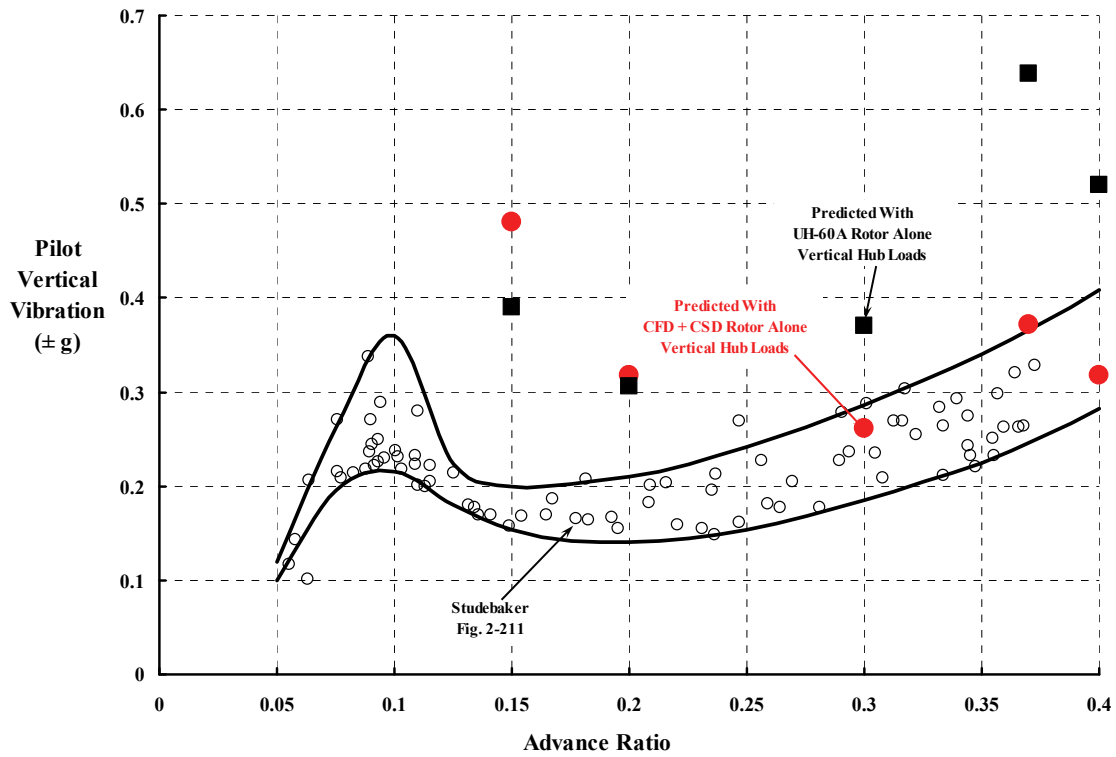


Fig. 2-243. Pilot vertical vibration predicted with calculated and measured 4/rev and 8/rev vertical vibratory hub loads.

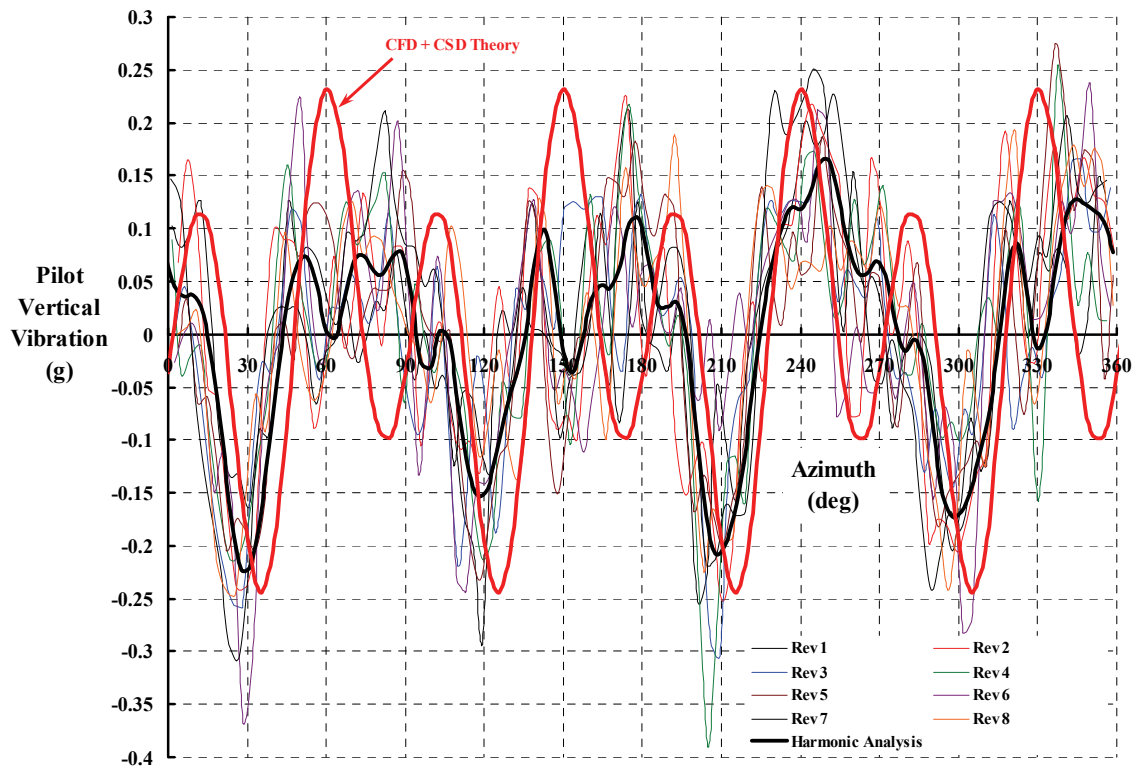


Fig. 2-244. Predicted and measured pilot vertical vibration at 132 knots true airspeed.

## 2.6 VIBRATION

Admittedly, you must stare at Fig. 2-244 for a while before you believe this, but more importantly, note that the predicted vibration using Ethan's CFD + CSD vertical vibratory hub loads (the heavy red line) is, remarkably, just as representative of the flight test data.

This introductory example of the UH-60A vibration in the Airloads Program configuration is, of course, quite incomplete. You know this because of Table 2-30 on page 373. Furthermore, theory used by Ethan Romander did not include coupled fuselage-rotor dynamics because it was a rotor-alone study. Of course, an analysis that assumes all blades are identical precludes any prediction of harmonic loads other than 4/rev, 8/rev, 12/rev, etc.

### 2.6.4 Blade Vibratory Response, Hub Vibratory Loads

The fixed system (i.e., nonrotating) hub vibratory loads used in the preceding analysis of helicopter vibration are created by rotating system, blade root, and vibratory loads. As you learned in Volume I, each blade element has a vertical force, an inplane force, a radial force, and a torsional moment. You learned early in Volume I (pages 14 and 15) that when these forces are summed over the blade length and averaged over a revolution you will obtain the primary performance of the rotor. This process of averaging over a revolution hides a great deal of information about any specific blade element. It is precisely because of this radial integration and azimuthal averaging that rotor performance and fundamental behavior has been obtained with considerable accuracy for so many decades. The vibration problem, however, requires that the loads of each blade, obtained at each azimuth, be correct. This means that not only must the azimuthal average be correctly predicted, but the distribution of blade root loads at each azimuth must be correct as well. It is a saving grace that it is just the radial integration at each azimuth that must be correct; that means that some of the errors at each blade element will be self-cancelling as the sum from blade root to blade tip is taken—one hopes.

Consider, if you will, the problem presented in Fig. 2-245, which shows the loads from one blade acting at the coincident flapping, lagging, and feathering hinge of a UH-60A hub. The blade itself is not shown, but imagine it is connected to the vertical pins located at the end of the basic hub arm and along the spanwise root shear force vector ( $RS_{\text{spanwise}}$ ). There is an x, y, z coordinate system that rotates with the hub, and the z-axis is parallel to the shaft (vertical). The x- (spanwise) and y- (chordwise) axes lie in a plane perpendicular to the shaft.<sup>135</sup> The 0, 0, 0 point of the axis system is located at the exact center of the hub. The blade torsional moment is reacted at the root by the pitch link, which passes a vibratory load ( $PL_{\text{load}}$ ) to the airframe. In the world of torsion, it is very important to remember that the blade torsion moment is reacted by a force couple. This means that some of the vertical root shear contains the reaction to the pitch link load.<sup>136</sup>

---

<sup>135</sup> Over the years I seem to have adopted the notion that the radial dimension of the blade is associated with x and that  $x = r/R$ . I am quite sure that this thinking is not universal; the sign convention is more important.

<sup>136</sup> I have purposely left out considering the lead-lag damper load path in this introductory discussion. As you can see from Fig. 245, the lag damper bridges the elastomeric bearing and contributes loads primarily in the spanwise direction. Comprehensive analyses such as CAMRAD II place the shears at the hub centerline.

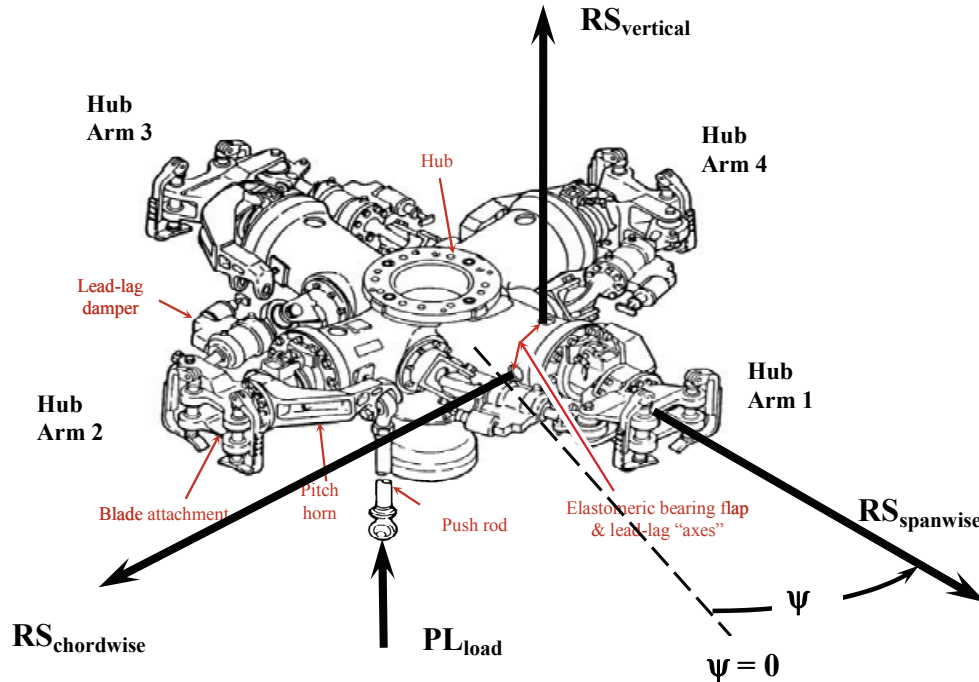


**Fig. 2-245. Rotating blade root shears and pitch link load acting on a UH-60A hub (basic hub picture courtesy of Bill Bousman and Bob Ormiston, AFDD).**

The rotating root shears and pitch link load for a single blade, *once you have calculated them*, are resolved into the nonrotating hub loads as you learned in Volume I. That is,

$$\begin{aligned}
 \text{Thrust} &= \text{Hub } F_Z = RS_{\text{vertical}} + PL_{\text{load}} \\
 (2.284) \quad \text{H-force} &= \text{Hub } F_X = RS_{\text{spanwise}} \cos \psi + RS_{\text{chordwise}} \sin \psi . \\
 \text{Y-force} &= \text{Hub } F_Y = RS_{\text{spanwise}} \sin \psi - RS_{\text{chordwise}} \cos \psi
 \end{aligned}$$

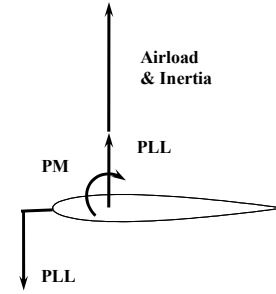
Suppose now that you want to calculate the vertical shear load ( $RS_{\text{vertical}}$ ) and the two inplane shear loads ( $RS_{\text{spanwise}}$  and  $RS_{\text{chordwise}}$ ). It is a simple matter to write the basic equation for the vertical root shear, which you encountered in Volume I. Based on Fig. 2-84 on page 170 in Volume I, you later came to Eqs. 2.230 and 2.231 on page 199 of that volume, which I have reintroduced (with some symbol changes) here as

$$\begin{aligned}
 RS_{\text{vertical}} &= \int_0^R d(L_{r,t}) - \int_0^R d(I_{r,t}) - PL_{\text{load}} - w_b \\
 (2.285) \quad &= \int_0^R \left( \frac{dL_{r,t}}{dr} \right) dr - \int_0^R (m_r) \left( \frac{\partial^2 z_{r,t}}{\partial t^2} \right) dr - PL_{\text{load}} - w_b
 \end{aligned}$$

where the blade weight ( $w_b$ ) is 255.6 pounds for one UH-60A blade. Do not forget that a blade torsional moment is resisted by force couple. That is why the vertical root shear in Eq. (2.285) includes the  $PL_{\text{load}}$  term. This means that the pitch link load ( $PL_{\text{load}}$ ) has an equal and opposite

## 2.6 VIBRATION

shear force located somewhere. For the UH-60A, this shear force acts at the coincident flap, lag, and feathering bearing. The little sketch at the right reinforces this point. This a load that must be considered in the design of bearings.



Because the blade element loads are known to be periodic (i.e., harmonic) in simple analytical cases, Eq. (2.285) can be rewritten in terms of azimuth ( $\psi$ ) with the substitutions

$$\psi = \Omega t \text{ or } \frac{1}{dt^2} = \Omega^2 \frac{1}{d\psi^2}$$

to give

$$(2.286) \quad RS_{\text{vertical}} = \int_0^R \left( \frac{dL_{r,\psi}}{dr} \right) dr - \int_0^R (m_r) \Omega^2 \left( \frac{\partial^2 z_{r,\psi}}{\partial \psi^2} \right) dr - PL_{\text{load}} - w_b.$$

In a similar manner, equations for the inplane root shears are written as

$$(2.287) \quad \begin{aligned} RS_{\text{chordwise}} &= \int_0^R \left( \frac{dD_{r,\psi}}{dr} \right) dr + \int_0^R \Omega^2 (m_r) y_{r,\psi} dr - \int_0^R \Omega^2 (m_r) \left( \frac{\partial^2 y_{r,\psi}}{\partial \psi^2} \right) dr \\ RS_{\text{spanwise}} &= \int_0^R \left( \frac{dF_{r,\psi}}{dr} \right) dr - \int_0^R 2\Omega (m_r) \left( \frac{\partial y_{r,\psi}}{\partial \psi} \right) dr + \int_0^R (m_r) \Omega^2 r dr \end{aligned}$$

and the pitch link load ( $PL_{\text{load}}$ ) becomes

$$(2.288) \quad \begin{aligned} \text{Pitch arm} \times PL_{\text{load}} &= \int_0^R \left( \frac{dPM_{r,\psi}}{dr} \right) dr - \int_0^R I_{\theta} \Omega^2 \frac{d^2 \theta_{r,\psi}}{d\psi^2} dr - \int_0^R I_{\theta} \Omega^2 \theta_{r,\psi} dr \\ &\quad - \int_0^R \frac{dL_{r,\psi}}{dr} y_{r,\psi} dr + \int_0^R \frac{dD_{r,\psi}}{dr} z_{r,\psi} dr \\ &\quad + \int_0^R (cg - pa) \Omega^2 m_{r,\psi} \frac{d^2 z_{r,\psi}}{d\psi^2} dr + \int_0^R (cg - pa) \Omega^2 m_{r,\psi} z_{r,\psi} dr \end{aligned}$$

You can delve deeper into the derivation of these first-order equations by reading pages 421 to 429 in Wayne Johnson's book, *Helicopter Theory* [235]. You might note in passing that I have taken considerable poetic license in using  $dL_{r,\psi}/dr$ ,  $dD_{r,\psi}/dr$ , and  $dF_{r,\psi}/dr$  as blade element forces in the z-, y-, and x-axis directions. This requires a belief that all angles are small and, as you will soon see, is a very poor and unnecessary assumption in the study of rotorcraft vibration.<sup>137</sup>

What I do want you to appreciate is that the blade element airloads of lift ( $dL_{r,\psi}/dr$ ), drag ( $dD_{r,\psi}/dr$ ), radial ( $dF_{r,\psi}/dr$ ), and moment ( $dM_{r,\psi}/dr$ ) drive the blade out-of-plane bending

<sup>137</sup> The blade element forces must be resolved into the z-, x-, and y-axis directions and then be given new symbols. Let me wait a bit before switching to the correct description.

$(z_{r,\psi})$  and inplane bending ( $y_{r,\psi}$ ). Furthermore, out-of-plane bending and inplane bending are directly connected as well. Of course, elastic twisting ( $\theta_{r,\psi}$ ) under the blade element forces and pitching moments leads to the pitch link load and alters the airloads, and to top it off, inplane motion is quite dependent on the lead-lag damper. The solution situation appears pictorially in Fig. 2-246. The rotorcraft industry has had this complex, highly coupled, computational problem for decades and has never given up improving successive solutions.

The perfect circle that you see in Fig. 2-246 implies an ultimately exact computational solution that agrees with experiment to a level well suited to reasonably accurate rotorcraft design. This goal has not been achieved as I write these words, however major accomplishments have been made over the last several decades. One set of milestones was published by Wayne Johnson [469]. Wayne was given the honor of presenting the 30th Nikolsky Lecture at the 2010 Annual Forum of the American Helicopter Society.<sup>138</sup> As he pointed out, each successive milestone he examined improved the capabilities that aeromechanics researchers are reaching for. In reading Wayne's excellent summary, you will note that major improvements were made in CSD methods to obtain the blade elastic deflections (i.e.,  $z_{r,\psi}$ ,  $y_{r,\psi}$ , and  $\theta_{r,\psi}$ ). These CSD improvements came well before comparable improvements were made in calculating blade element aerodynamic forces and moments using CFD.

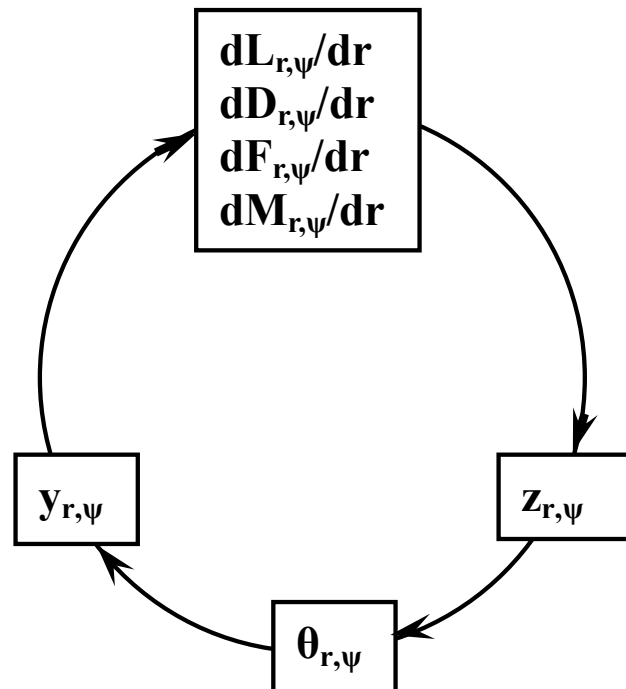


**Fig. 2-246. The rotorcraft industry has faced this vicious computational circle for over eight decades.**

<sup>138</sup> Somehow Wayne was able to capture the history of 19 milestones using only 298 references in his lecture, which makes his published paper [469] a milestone in itself.

## 2.6 VIBRATION

In my opinion, the success in applying CFD to obtain the blade element airloads that was achieved by Frank Caradonna, Chee Tung, and Andre Desopper in 1982 [470] was like the door opening in a very unpleasant, dark room. The icing on the cake came 2 years later when Wayne Johnson succeeded in coupling CFD to CSD (his well-known CAMRAD II comprehensive computer program [471]). This new foundational aeromechanics tool (CFD + CSD) reinvigorated rotorcraft researchers [465, 472-475] to a level that I cannot ever remember feeling or seeing.

The application of the CFD + CSD comprehensive analysis to the UH-60A Airloads Program flight test data (and the follow-on rotor-alone wind tunnel experiment) enabled Ethan Romander [465] to make computations leading to Fig. 2-243, and specifically to Fig. 2-244.

Now let me give you a measure of how accurate a vintage 2010 advanced theory is in relation to the most comprehensive, full-scale, rotor-alone wind tunnel experiment ever conducted. For the theory, I will use the CAMRAD II + Overflow 2 comprehensive analysis as reported by Romander [465]. For the test, I will use data obtained from the UH-60A Airloads rotor-alone as tested in the 40- by 80-Foot Wind Tunnel at Ames Research Center. Specifically, this was Air Force test number 10, run 52. I have selected Points 30 and 31 for theory-test comparison, which are for an advance ratio of 0.3. I selected this advance ratio because the CFD + CSD theory appeared (in Fig. 2-243) to fall within the range of measured pilot vibration. The performance parameters for this 0.3 advance ratio case are provide in Table 2-34.

In the first place, the full-scale UH-60A Airloads rotor was mounted on the NASA Large Scale Rotor Test Apparatus, commonly called the LRTA. This assembly was then installed in the 40- by 80-Foot Wind Tunnel as shown in Fig. 2-247. The LRTA is, indeed, a large-scale piece of test equipment. The body-of-revolution fairing encloses a number of very heavy subassemblies as you can see from Fig. 2-248. A brief description [476] states that

“the LRTA (Figs. 1 and 3) is a special-purpose drive and support system designed to test helicopters and tilt rotors in the NFAC. Developed for NASA and the U.S. Army by Dynamic Engineering, Inc., the LRTA is capable of testing rotors at thrust levels up to 52,000 lb. Its primary design features include 1) a drive system powered by two 3000 HP motors, 2) a five-component rotor balance to measure steady and unsteady rotor hub loads, along with an instrumented flex-coupling to measure rotor torque, 3) a six-component fuselage load-cell system to measure steady fuselage loads, 4) a complete rotor control system (including console) with primary and higher harmonic control, and 5) an output shaft assembly with a replaceable upper shaft for mating with different rotor systems.”

Of course, the balance is the heart of any test rig such as the LRTA. As Fig. 2-249 shows, the balance of the LRTA is quite large in diameter, but really not very tall. Calibrating the balance required enormous fixtures in themselves [477], and then both a static calibration and a dynamic calibration had to be completed [478]. This dynamic calibration was, in effect, a vibration test similar to the shake testing of helicopters that you read about earlier. The objective was to get balance output per pound of rotor vibratory forces and moments.

**Table 2-34. UH-60A Rotor Performance Parameters for Theory vs. Test Analysis at an Advance Ratio of 0.3. Theory Required to Closely Match Thrust, Rolling Moment, and Pitching Moment at Test Shaft Angle of Attack by Adjusting Controls**

Parameter	Symbol	Unit	Test Value	Theory Value	Notes
Density	$\rho$	slug/ft <sup>3</sup>	0.002298	Same	
Speed of Sound	$a_s$	ft/sec	1,117.0	Same	temp = 519.217 °R
Forward Speed	V	ft/sec	217.8	Same	129 knots
Tip Speed	$V_t$	ft/sec	726.0	Same	
Shaft Angle of Attack	$\alpha_s$	deg	-4.202		forward (physical)
Shaft Angle of Attack	$\alpha_{s\text{corr}}$	deg	-3.495	Same	forward (includes wall correction)
Collective Pitch	$\theta_0$	deg	10.02	13.888	at coincident hinge, + nose up
Longitudinal Cyclic	$\theta_{\text{sin}}$	deg	-7.55	-7.422	at coincident hinge, + nose up
Lateral Cyclic	$\theta_{\text{cos}}$	deg	1.32	0.848	at coincident hinge, + nose up
Thrust	T	lb	20,466	20,458	+ up
H-force	H	lb	-101.1	200.47	+ towards $\psi = 0$ deg
Y-force	Y	lb	-530.8	125.49	+ towards $\psi = 90$ deg
Rolling Moment	$M_{\text{roll}}$	ft-lb	-1,658	-1,716	+ starboard side up
Pitching Moment	$M_{\text{pitch}}$	ft-lb	-3,010	-3,021	+ nose up
Total Horsepower	RHP	hp	1,786	1,757	
Induced + Profile	$HP_{\text{ind} + \text{profile}}$	hp	n/a	1,218	CFD + CSD cannot separate
Propulsive	$HP_{\text{propulsive}}$	hp	n/a	539	



**Fig. 2-247. Tom Norman (left) and Patrick (Rick) Shinoda inspect the UH-60A Airloads rotor system as installed on the LRTA in the Air Force 40- by 80-Foot Wind Tunnel located at NASA Ames Research Center.**

2.6 VIBRATION

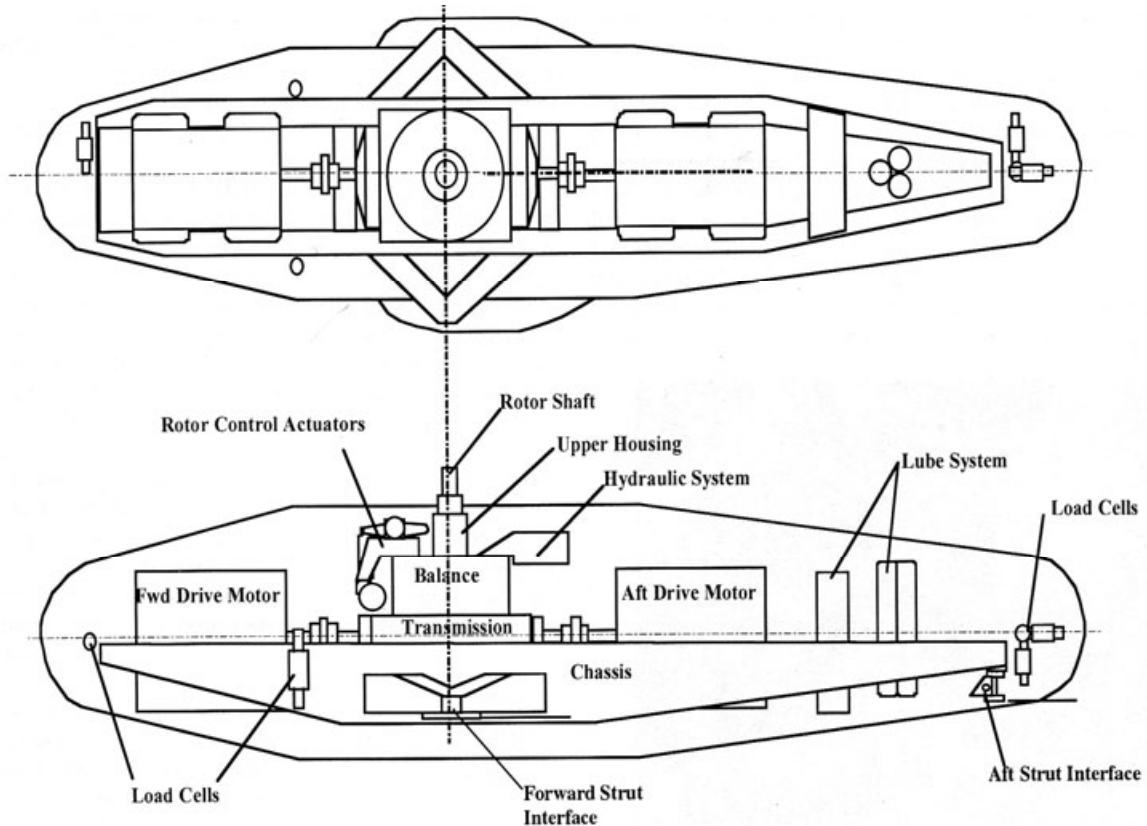


Fig. 2-248. The 40-foot-long NASA LRTA. Two 3,000-hp electric motors can provide up to 165,000 ft-lbs of torque at rotor speeds up to 320 rpm [476].

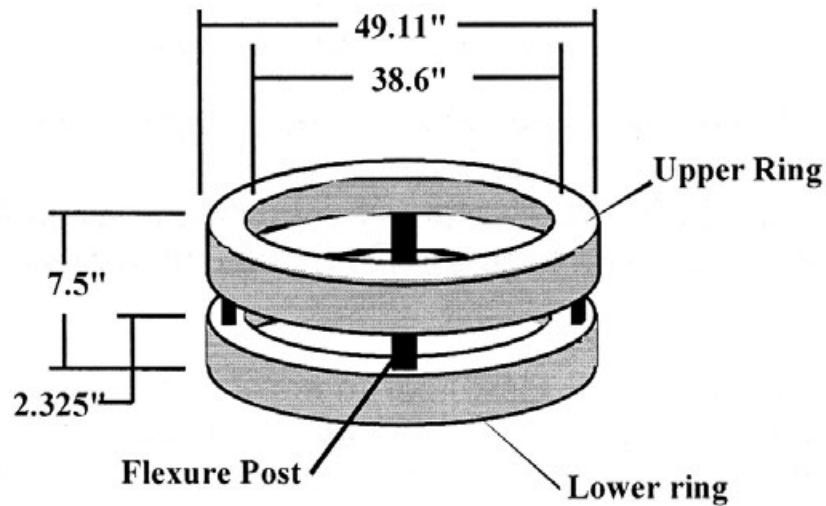
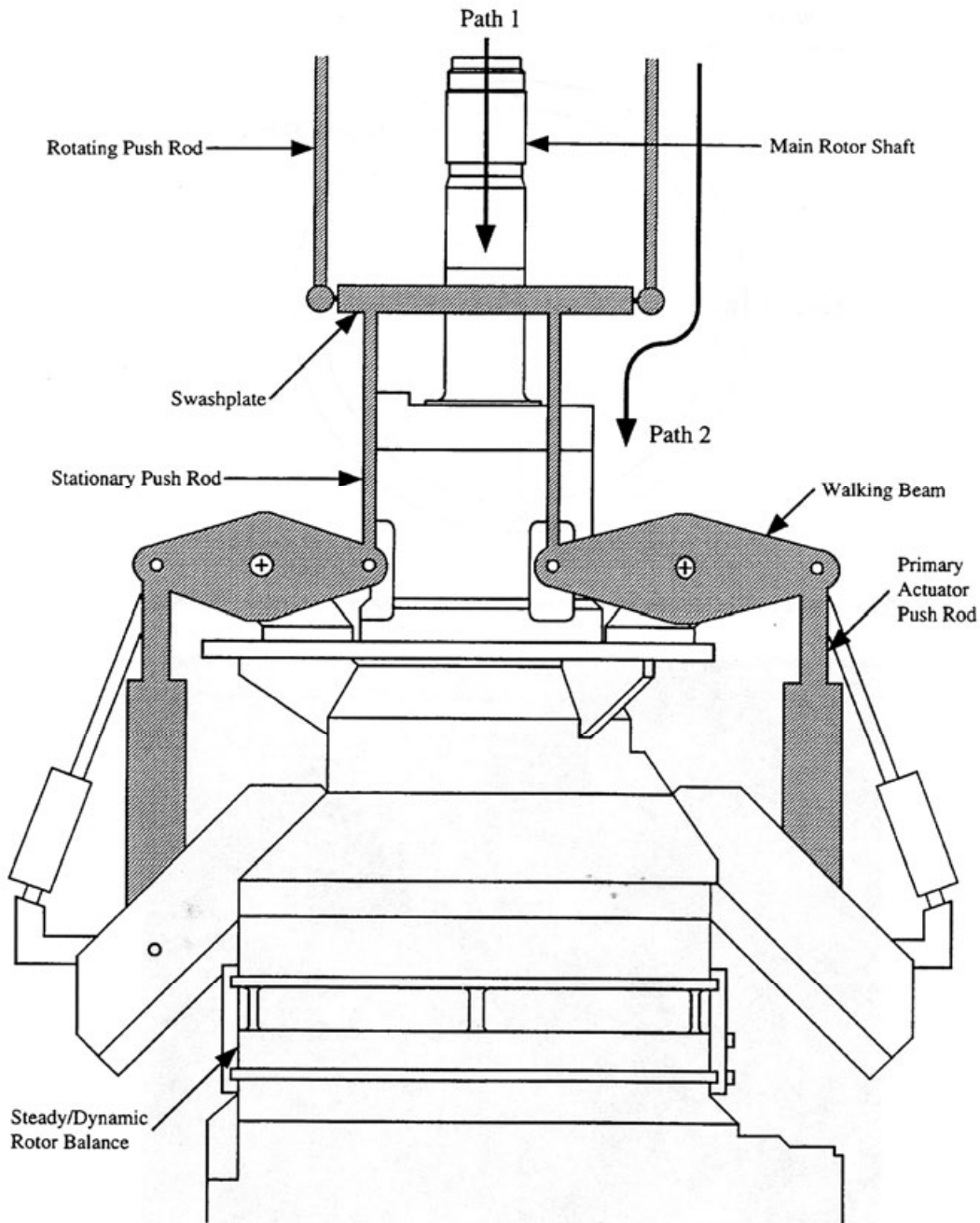


Fig. 2-249. The key component of the LRTA is the balance. Thrust up to 52,000 lb and an inplane force up to 15,000 lb can be accurately recorded. The flexure posts are designed for a resultant moment of 125,000 ft-lbs at the balance center [478]. The distance from the balance center to the hub center was 61.5 in. for the UH-60 Airloads rotor wind tunnel test.

Fig. 2-245 showed rotor hub forces (and, of course, moments, which are not shown) and pitch links, which must be transmitted to the balance. These loads follow two different paths as Fig. 2-250 shows. In the case of steady, vertical loads with the four-bladed UH-60 rotor, the balance reads the sum of vertical root shears ( $RS_{\text{vertical}}$ ) from hub arms 1, 2, 3, and 4 plus the pitch link loads ( $PL_{\text{load}}$ ) from the four blades, which follow the gray shaded parts noted as Path 2 on Fig. 2-250. This sum is rotor thrust, which is a force acting directly normal to the upper ring of the balance.



**Fig. 2-250. Hub loads and pitch link loads follow different paths to the balance of the LRTA [478].**

2.6 VIBRATION

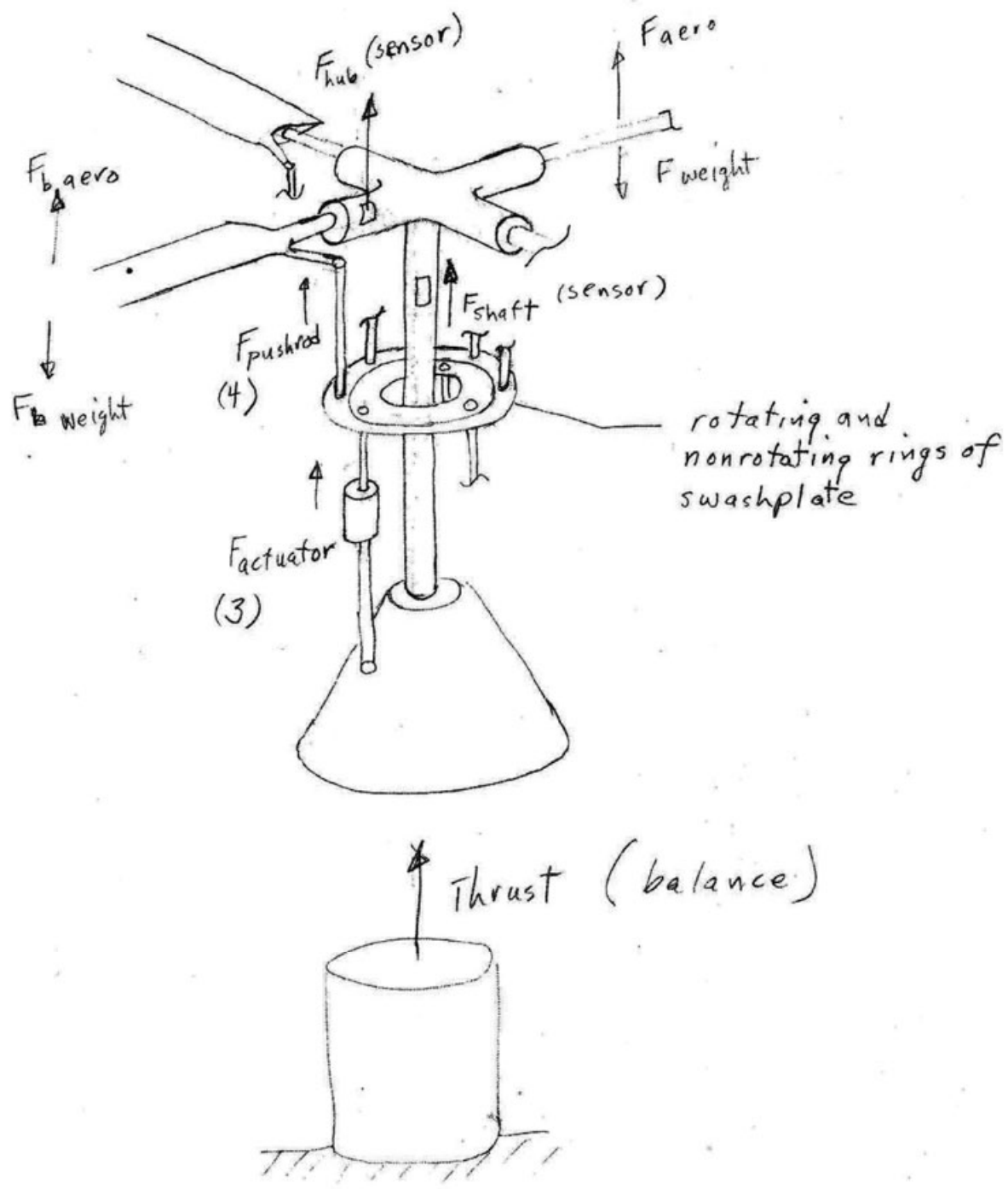


Fig. 2-251. Bob Ormiston's and my working sketch.

The UH-60A Airloads rotor-alone test that I am using in this discussion is noteworthy because of one additional measurement that has rarely been included in past experiments. Measurements were made of the vertical shear in each arm of the hub. Strain gauges were applied along the neutral axis of each hub arm. The radial location of these shear gauges was approximately 15 inches from the center of rotation, which is the station taken as the focal point of the flap, lag, pitch bearing. These gauges provide a direct measurement of vertical shear as given by Eq. (2.286).

It is worth a moment to examine in more detail the two vertical load paths to the balance noted in Fig. 2-250. As you study Fig. 2-251,<sup>139</sup> you can see rather quickly that the vertical shear loads from the four individual hub arms find their way to the balance by way of the shaft. The four individual pitch links load the rotating ring of the swashplate (see Fig. 2-44 on page 101 in Volume I for a more detailed drawing). The rotating ring loads transfer through ball bearings to the nonrotating ring, which is supported by three stationary actuators. The three actuator loads then collectively load a plate attached to the balance. Numerically, the result is that the balance reads a force normal to the balance equal to

$$(2.289) \quad \text{Balance normal force} = \sum_1^4 RS_{\text{vertical}} + \sum_1^4 PL_{\text{load}} = \sum_1^4 RS_{\text{vertical}} + \sum_1^3 F_{\text{actuator}} .$$

The fact that during this comprehensive test the hub arms were strain gauged for vertical shear is a terrific additional piece of instrumentation. The reason I say this is because several checks on the overall system accuracy can be obtained. Just take the steady normal force that the balance records as an example. *The balance steady normal force is rotor thrust to the performance engineer.* This statement is obviously true because pitch link loads cannot lift the helicopter and, of course, inertia loads cannot lift the helicopter. All that pitch link loads and inertia loads can do is break parts and vibrate the machine—and make noise while doing it.

Now that you have some idea of the test equipment, consider experimental results for the rotor forces as a function of the azimuth angle of hub arm 1. These forces are in the nonrotating system. If the balance was mounted to the helicopter roof, they would be the shaking force that the airframe feels. Hub arm 1 is the master blade in the reference system for this test. The balance normal force is vertical and along the shaft ( $B_Z$  positive up). The balance longitudinal force ( $B_X$ ) is perpendicular to the shaft and directed aft towards the tail rotor (if it were there). The balance lateral force ( $B_Y$ ) is perpendicular to the shaft and directed towards the azimuth position of 90 degrees, which would be to starboard because the UH-60 main rotor rotates counterclockwise when viewed from the top. The steady (i.e., mean) value of these forces, which vary with master blade azimuth, are the rotor's aerodynamic thrust ( $T$ ), and H-force and Y-force—so important to the performance engineer.

The primary force, the balance vertical force that supports the machine, is examined in Fig. 2-252. Right away you can see an important difference between flight and wind tunnel

---

<sup>139</sup> After trying seven times to make my version of Fig. 2-251, I gave up and called Bob Ormiston for his help. We spent several hours discussing his sketch, which was ten times clearer than any I had made. There are several subtleties involved in how each load and its reaction can be drawn, and he knew how to steer clear of any unnecessary complications. Finally, we arrived at a rough draft of the figure.

## 2.6 VIBRATION

testing. Here 64 revolutions of vertical force data have been superimposed to create the gray, shaded band you see. You will recall from the UH-60 flight test data that no such repeatability was apparent—at least in my mind. Furthermore, the average waveform, shown with the solid red circles obtained from the tabulated Fourier series coefficients, does appear to be a reasonable base for a test-versus-theory comparison.

The balance longitudinal and lateral forces are provided in Fig. 2-253 and Fig. 2-254, respectively. You can see that the repeatability over 64 revolutions is even better than for the balance vertical force shown in Fig. 2-252.

I would be sadly remiss if I did not emphasize that no dynamic calibration corrections have been made to the three balance force data figures you have before you. A dynamic calibration of the sort performed on the LRTA's smaller cousin—the NASA Rotor Test Apparatus, reported in 1996 [478]—was completed in June of 2009, and the data reduction and report are in work as I write this. Until then, the rotor performance data (the balance and rotor-alone steady forces and moments) are considered satisfactory for theory-test comparisons as Romander reported [465]. Despite this unfinished work, I believe that this “hot-off-the-press” data is such a benchmark activity that you will find it referenced many times in the future. Therefore, you should be quite aware of this milestone in aeromechanics development.

You will note tabulation along the bottom of each figure. These tabulations provide the Fourier series coefficients that reproduce the red, solid circles you see on top of the gray bands of experimental data for 64 revolutions. To me, it is the objective of any advanced comprehensive analysis to predict these vertical, longitudinal, and lateral forces. As you will see shortly, we cannot make an accurate prediction yet, but with the data from this comprehensively instrumented UH-60 Airloads rotor and the advances obtained with CFD + CSD analyses—and continued hard work by the rotorcraft industry—I have no doubt that we will.

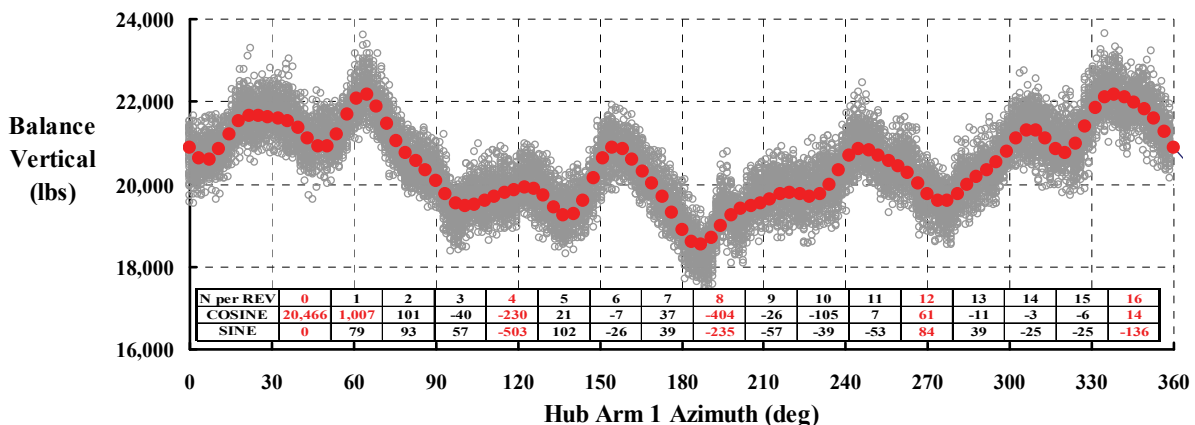


**Fig. 2-252. Balance vertical force for 64 revolutions at an advance ratio of 0.3.  
(Note: no dynamical calibration applied.)**

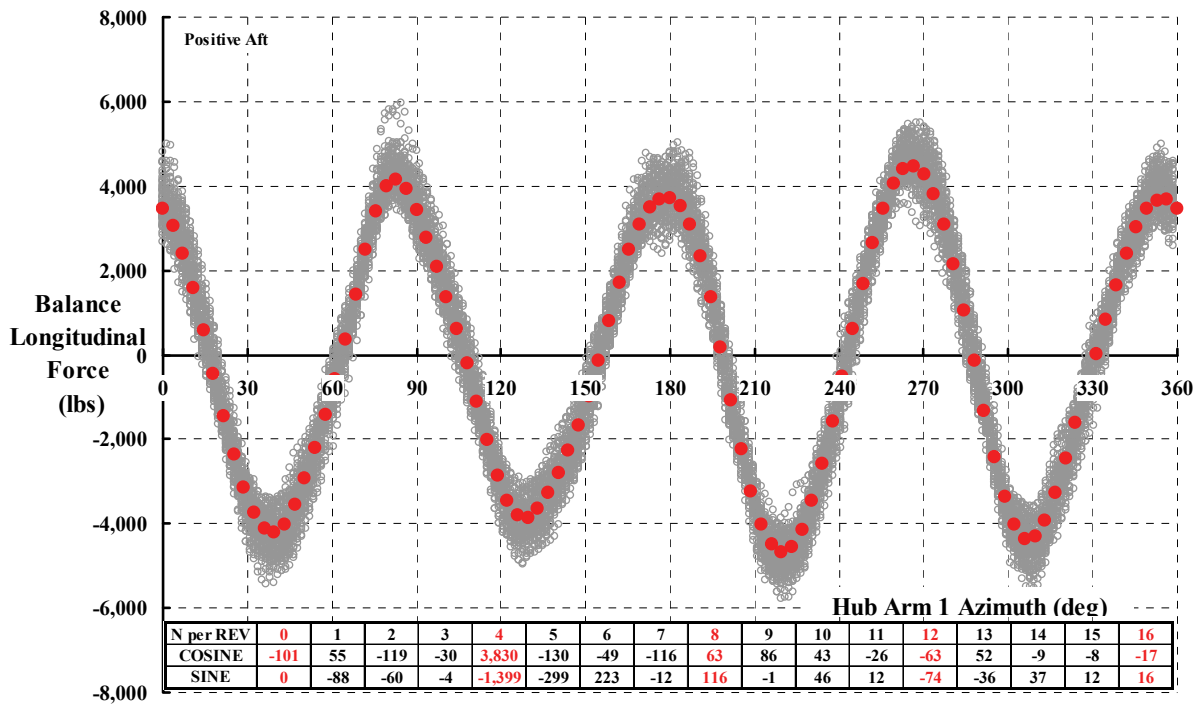


Fig. 2-253. Balance longitudinal force for 64 revolutions at an advance ratio of 0.3.  
(Note: no dynamical calibration applied.)

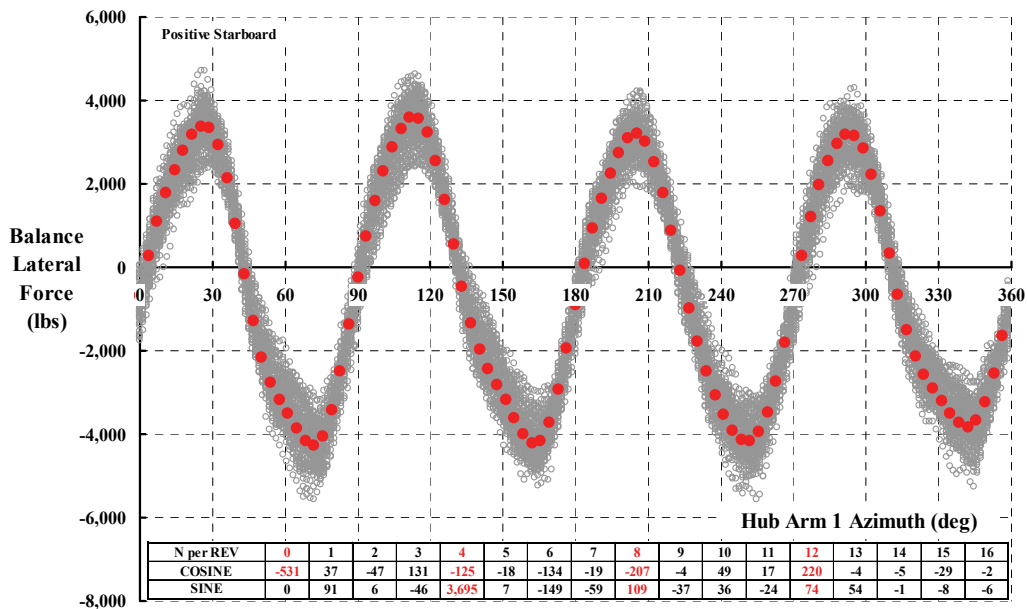


Fig. 2-254. Balance lateral force for 64 revolutions at an advance ratio of 0.3.  
(Note: no dynamical calibration applied.)

## 2.6 VIBRATION

### 2.6.4.1 Dynamic Calibration of LRTA Balance

You have noted, I am sure, that the three balance vibratory force measurements (Fig. 2-252, Fig. 2-253, and Fig. 2-254) have not been corrected for system dynamic response. Preliminary analysis of the dynamic calibration of the LRTA completed in June 2009 does show that the correction to balance vertical vibratory forces will be reasonably accurate. You can see this from Fig. 2-255 where amplification factors range from 0.9 to 1.4 for integer harmonics up to 8/rev. Unfortunately, the situation for the inplane balance vibratory forces presents a real challenge. Both Fig. 2-256 and Fig. 2-257 show that the primary 4/rev vibration characteristic of a four-bladed rotor system is severely amplified by a lack of stiffness within the hub to balance load path.

As you have learned, resonance peaks in situations where there is little damping are accompanied by very steep gradients on either side of the maximum. This makes obtaining accuracy in determining amplification factors quite difficult. In this UH-60A Airloads rotor test example, the 4/rev vibratory inplane forces are tabulated in Fig. 2-253 and Fig. 2-254 as being over  $\pm 3,500$  pounds, which must be reduced by a factor of 10 for the longitudinal force and a factor of 5.5 for the lateral force. Roughly speaking then, the inplane vibration *is not* the  $\pm 4,000$  pounds shown in Fig. 2-253 and Fig. 2-254, but more on the order of  $\pm 350$  to  $\pm 400$  pounds when the dynamic calibration is ultimately applied. The importance of this experimental situation cannot be overstated. It means that theory-versus-test comparisons for inplane vibratory forces are not, as I write this, very informative. Such has been the story of vibration for seven decades, but in this example, a great deal can be learned about vertical force.

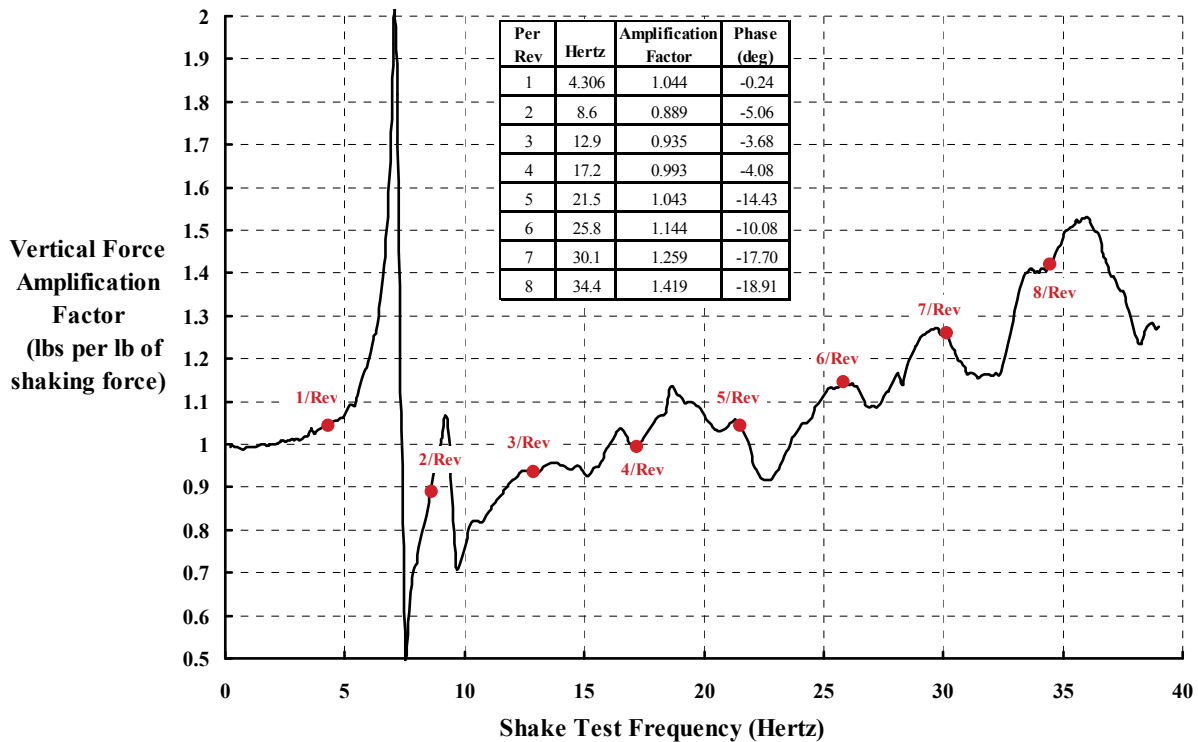


Fig. 2-255. Vertical force dynamic calibration (per revolutions based on 258.33 rpm).

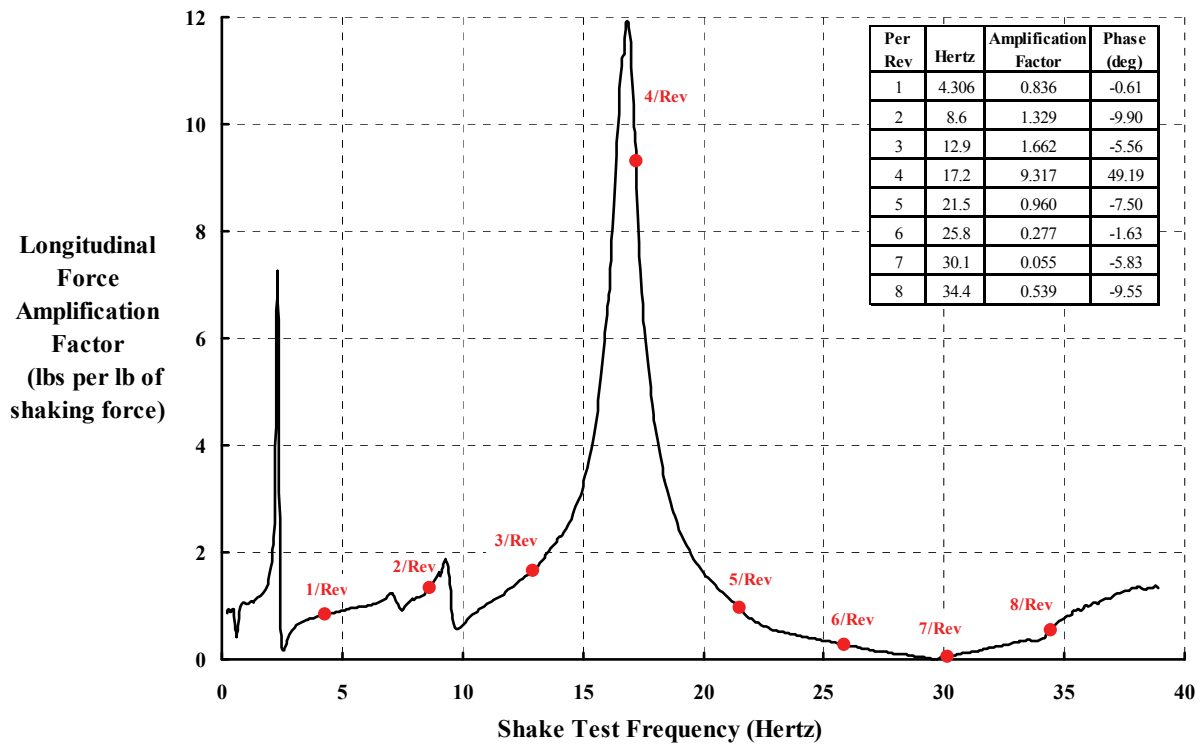


Fig. 2-256. Longitudinal force dynamic calibration (per revolutions based on 258.33 rpm).

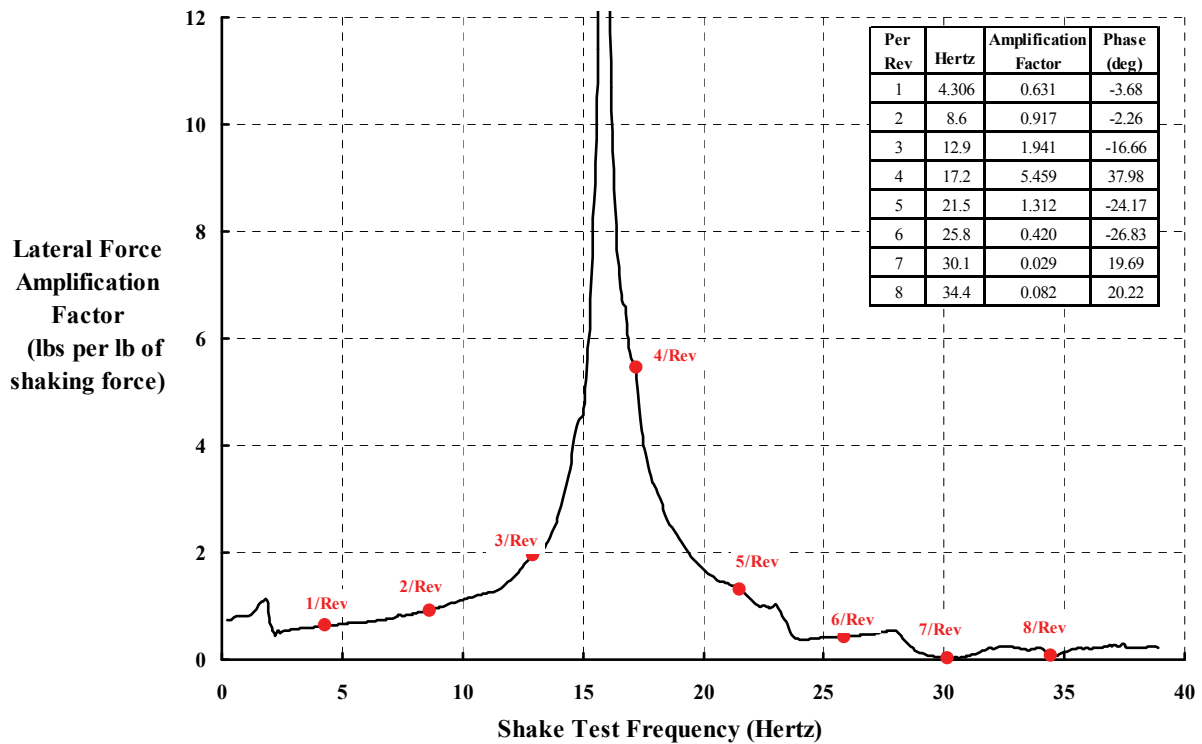


Fig. 2-257. Lateral force dynamic calibration (per revolutions based on 258.33 rpm).

## 2.6 VIBRATION

### 2.6.4.2 Vertical Forces

While an immediate correlation between theory and test cannot be made now with the balance data, there is a much more informative comparison to be seen. As mentioned earlier, data from four vertical shear strain gauges were obtained during this very comprehensive experiment. A comparison of theory to the measured vertical shear ( $RS_{\text{vertical}}$ ) of each hub arm and associated blade pitch link load ( $PL_{\text{load}}$ ) is more than fascinating.<sup>140</sup> The reason that these data channels are so vital is that the contribution of each individual blade to the balance vertical force can be examined. *This is particularly important when the research blades are not identical, as in this case.* In this UH-60A rotor-alone test with mismatched blades due to instrumentation, the situation was that:

- Hub arm 1 had a pressure blade attached, colored red
- Hub arm 2 had a standard blade attached, colored black
- Hub arm 3 had a strain-gauged blade attached, colored green
- Hub arm 4 had a standard blade attached, colored blue

The following discussion entails graphs of data for each blade, using one page per blade. The four examples show theory versus test for vertical shear and pitch link load. Both theory and test make the vertical shear calculation according to Eq. (2.286), which is repeated here for convenience as

$$(2.286) \quad RS_{\text{vertical}} = \int_0^R \left( \frac{dL_{r,\psi}}{dr} \right) dr - \int_0^R (m_r) \Omega^2 \left( \frac{\partial^2 z_{r,\psi}}{\partial \psi^2} \right) dr - PL_{\text{load}} - w_b .$$

There is a little bookkeeping done with blade weight, which I will discuss after you have reviewed the graphs (Fig. 2-258 through Fig. 2-265) on the following several pages.

It is important, however, for you to realize that steady loads (also called mean loads) that lead to the rotor thrust are derived from Eq. (2.286) as

$$(2.290) \quad \text{Rotor Thrust 1 Blade} = \int_0^R \left( \frac{dL_{r,\psi}}{dr} \right) dr = RS_{\text{vertical}} + PL_{\text{load}} + w_b .$$

The steady load of the inertia term in Eq. (2.286) must, by the laws of physics, be zero, and pitch link loads cannot lift the machine, as I pointed out earlier.

With these thoughts in mind, you will immediately notice in Fig. 2-258 and Fig. 2-259 that vertical shear waveforms between theory and test are encouragingly similar. Furthermore, the pitch link load waveforms show primarily that the predictions have a steady load nearly three times more negative (nose down) than the experimental results. Fig. 2-259 shows that the advancing side of the blade travel is remarkably well predicted in waveform shape, but the retreating side (i.e., from 180 degrees back to 360 degrees azimuth) is clearly not well predicted at all. I would suggest that because the CFD model did not include a bent-up trailing edge tab, these earlier results will improve significantly in the near future.

---

<sup>140</sup> No similar instrumentation was included for the inplane shears, but I am sure that some future experiment will add this important data.

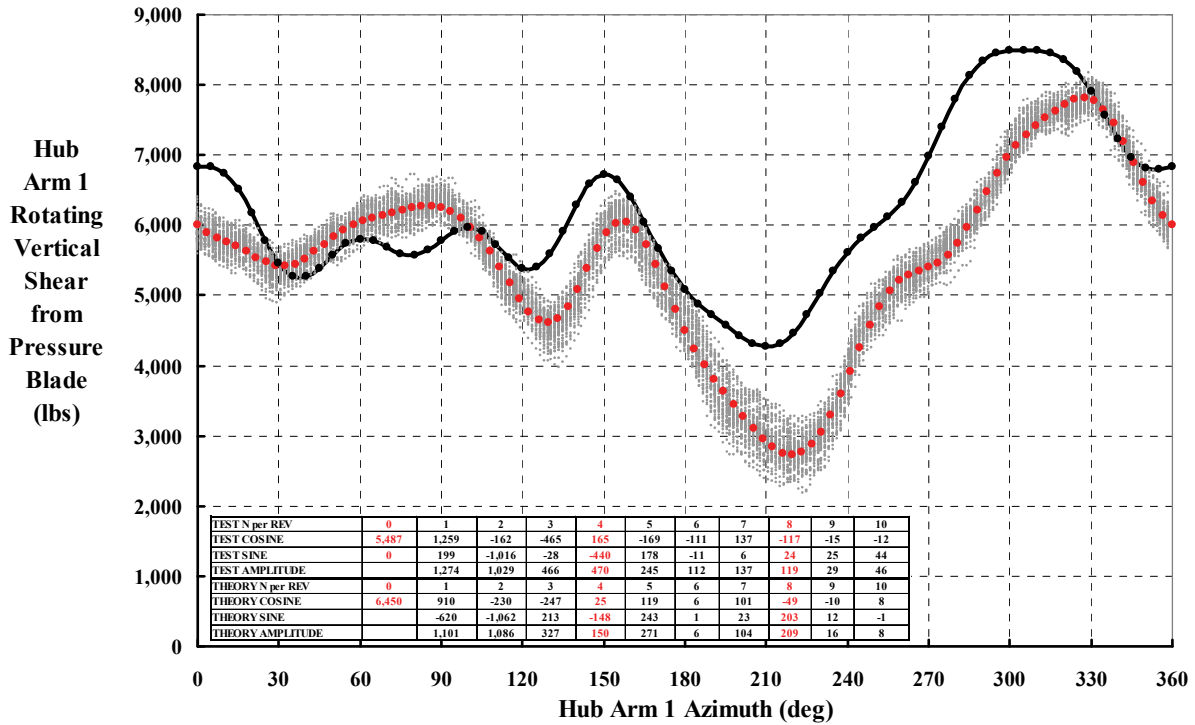


Fig. 2-258. Pressure blade on hub arm 1.

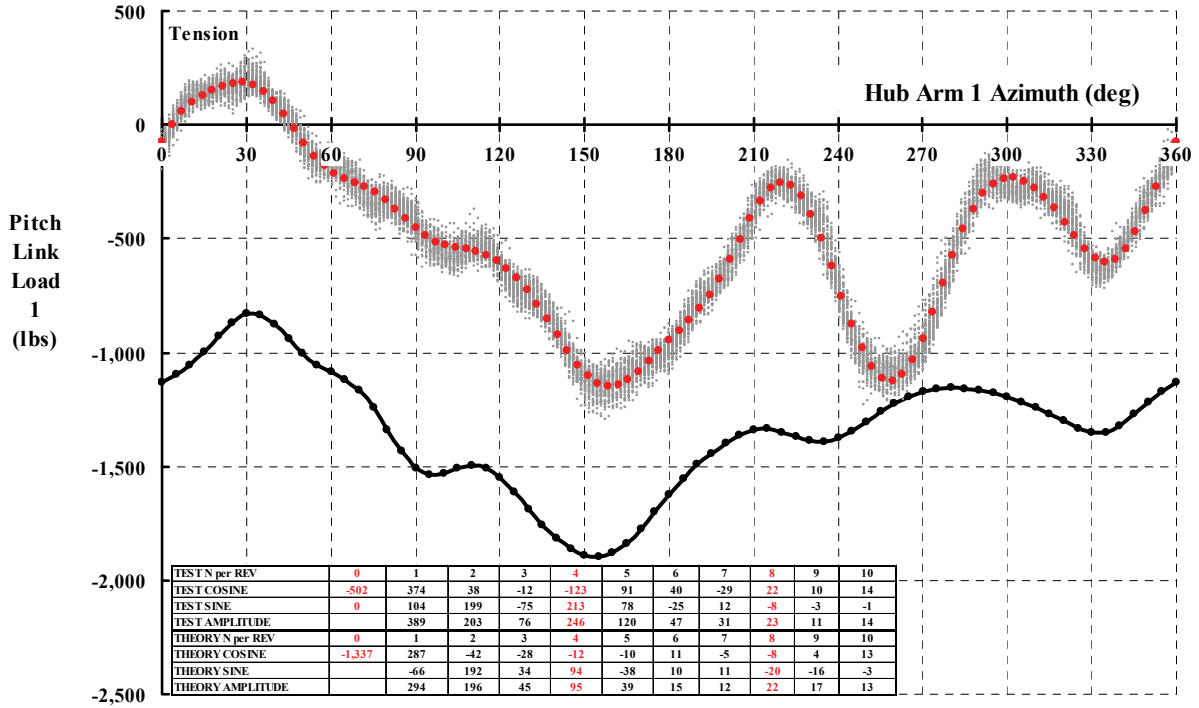


Fig. 2-259. Pressure blade on hub arm 1.

## 2.6 VIBRATION

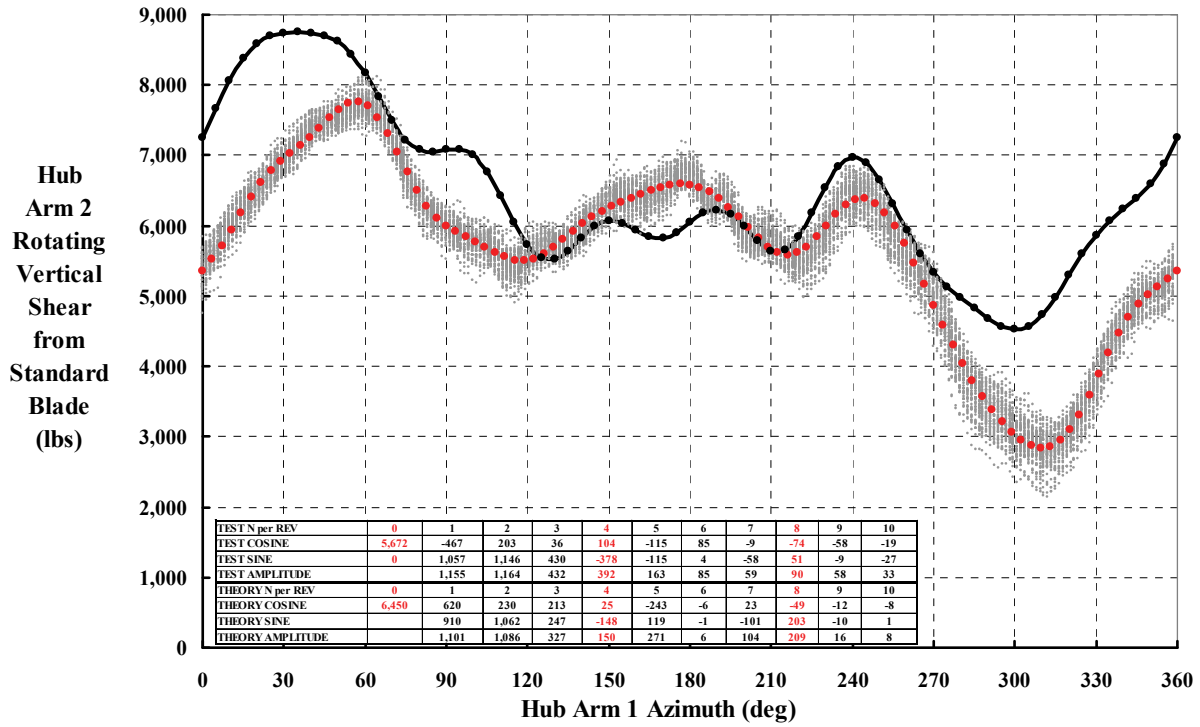


Fig. 2-260. Standard blade on hub arm 2.

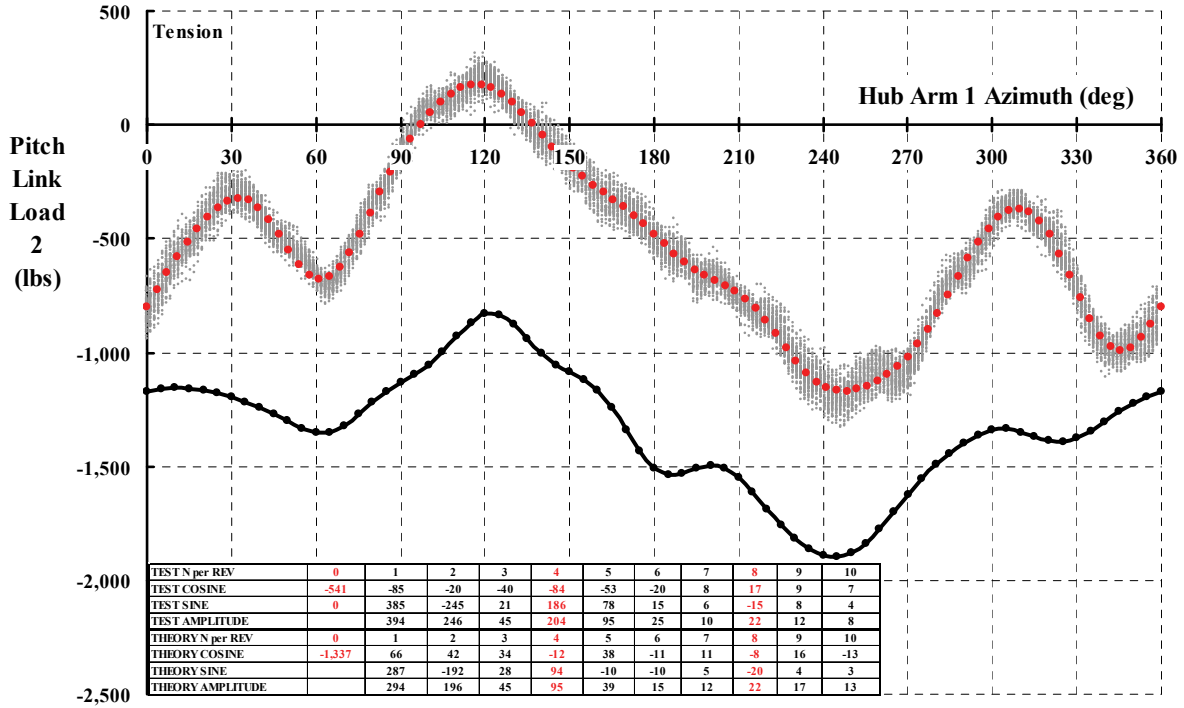


Fig. 2-261. Standard blade on hub arm 2.

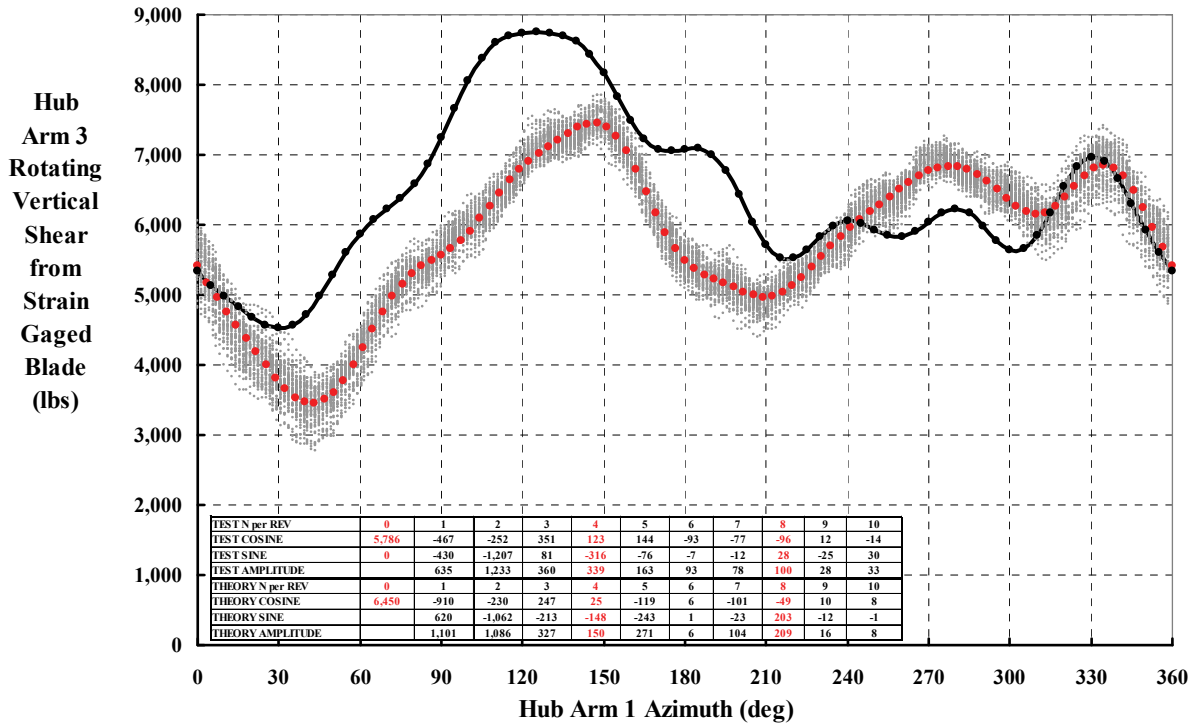


Fig. 2-262. Strain-gauged blade on hub arm 3.

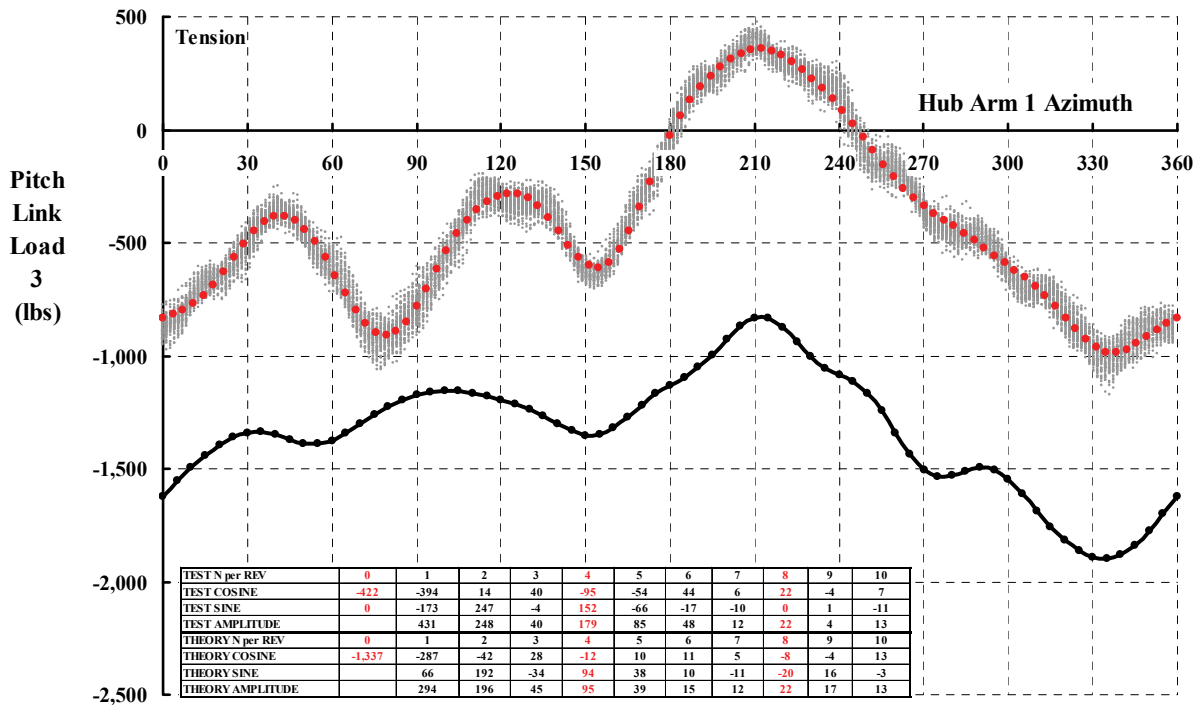


Fig. 2-263. Strain-gauged blade on hub arm 3.

## 2.6 VIBRATION

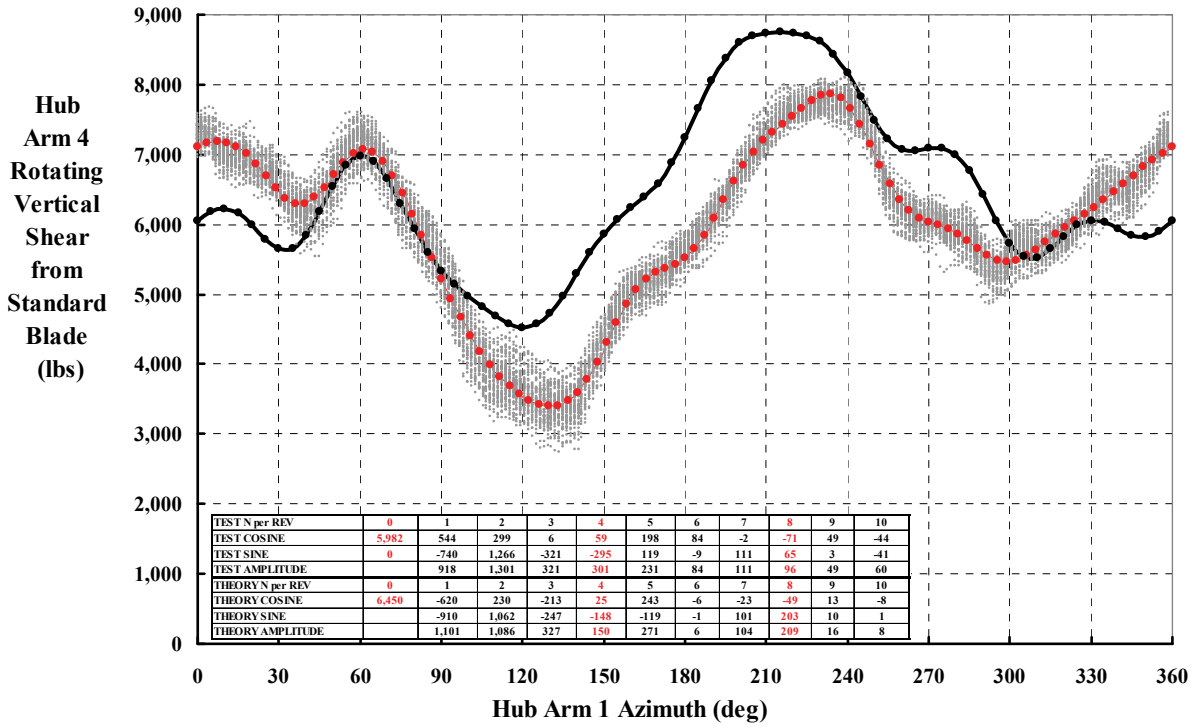


Fig. 2-264. Standard blade on hub arm 4.

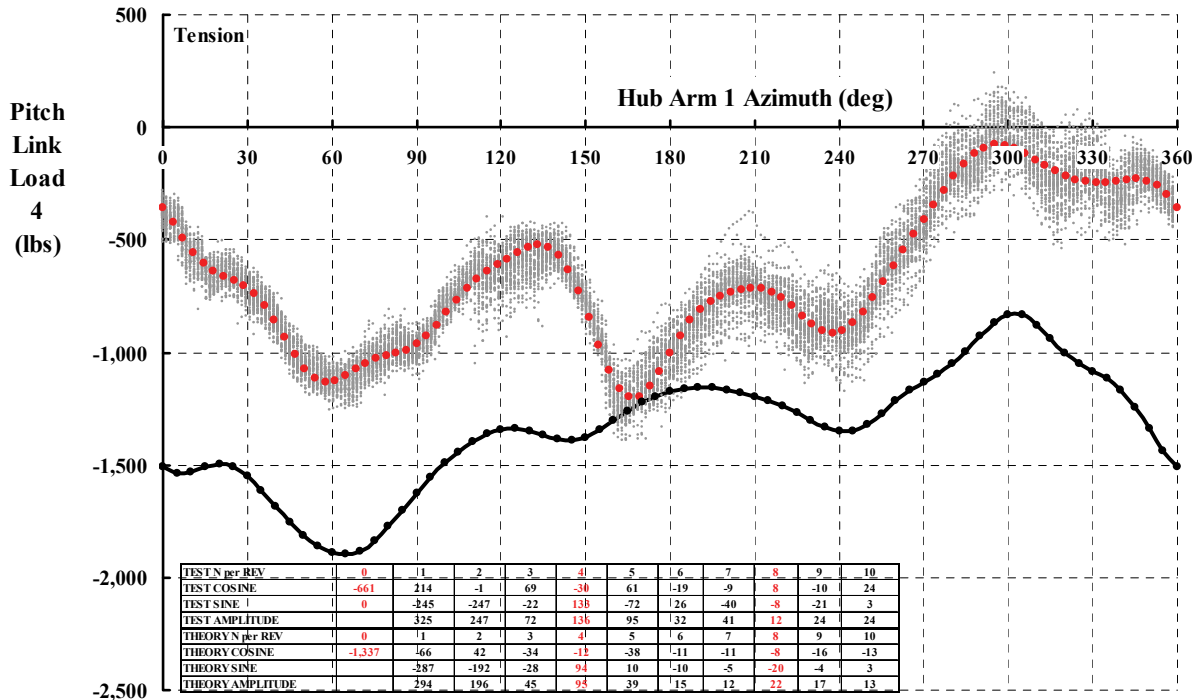


Fig. 2-265. Standard blade on hub arm 4.

To make the four preceding comparisons, I had to change the bookkeeping of the blade weight ( $w_b$ ), which is 255.6 pounds. Data reduction for the test placed the blade weight in the balance wind-off weight tares, which means that in Eq. (2.286), blade weight is assumed to be zero. In contrast, the CFD + CSD theory correctly accounts for blade weight according to Eq. (2.286), and so I added the 255.6 pounds back in (by hand). This juggling leads to the comparison of mean loads shown in Table 2-35.

In my experimental experience, I have never seen the absolute accuracy of mean (i.e., steady) loads that you have before you in Table 2-35. The rotor thrust has been obtained directly by the balance and by data from both paths shown in Fig. 2-250. The balance says that the rotor thrust is 20,466 pounds, and the sum of vertical shears and pitch link loads says that the rotor thrust is 20,801 pounds. This difference of 335 pounds out of roughly 20,000 pounds is a difference of 1.6 percent, which I consider extraordinary and a very real compliment to the team that put this comprehensive UH-60A rotor test together. Note that the theory (20,452 lb) matches the balance (20,466 lb), which was the ground rule for this trim condition at an advance ratio of 0.3.

Now let me take a moment to compare the results from the individual blades to each other. It has always been the task of the manufacturing side of the rotorcraft industry to make blades and other key components of the rotor system assembly identical. However, the drawings released from engineering always include  $\pm$  tolerances. The accumulation of these generally small tolerances has frequently led to an out-of-tolerance system and real problems on the delivery line. This is particularly true when matching blades, so the customer flies away in a machine with very low, 1/rev vibration.

When you look at blade-to-blade results from the vertical shear measurements in Fig. 2-266, you immediately see that the standard blades are, in fact, not very well matched, but then neither are the pressure- and strain-gauged blades. However, taken as a group, these experimental results are extremely encouraging. It is just the theory (the black, solid circles) that really stands out. I suggest that when agreement between test and theory for the pitch link loads (Fig. 2-267) is obtained, then the vertical shear graph comparison in Fig. 2-266 will be considerably more attractive.

**Table 2-35. UH-60A Steady Vertical Shear and Pitch Link Load Comparison at an Advance Ratio of 0.3 and a Blade Loading Coefficient ( $C_T/\sigma$ ) of 0.09**

Item	Vertical Shear ( $RS_{\text{vertical}}$ in lb)	Pitch Link Load ( $PL_{\text{load}}$ in lb)	Contribution to Thrust (lb)
Test Balance Thrust	n/a	n/a	20,466
Test Hub Arm 1	5,487	-502	4,985
Test Hub Arm 2	5,672	-541	5,131
Test Hub Arm 3	5,786	-422	5,364
Test Hub Arm 4	5,982	-661	5,321
Test Total Thrust	22,927	-2,126	20,801
Theory 1 Hub Arm	6,450	-1,337	5,113
Theory 4 Hub Arms	25,800	-5,348	20,452

## 2.6 VIBRATION

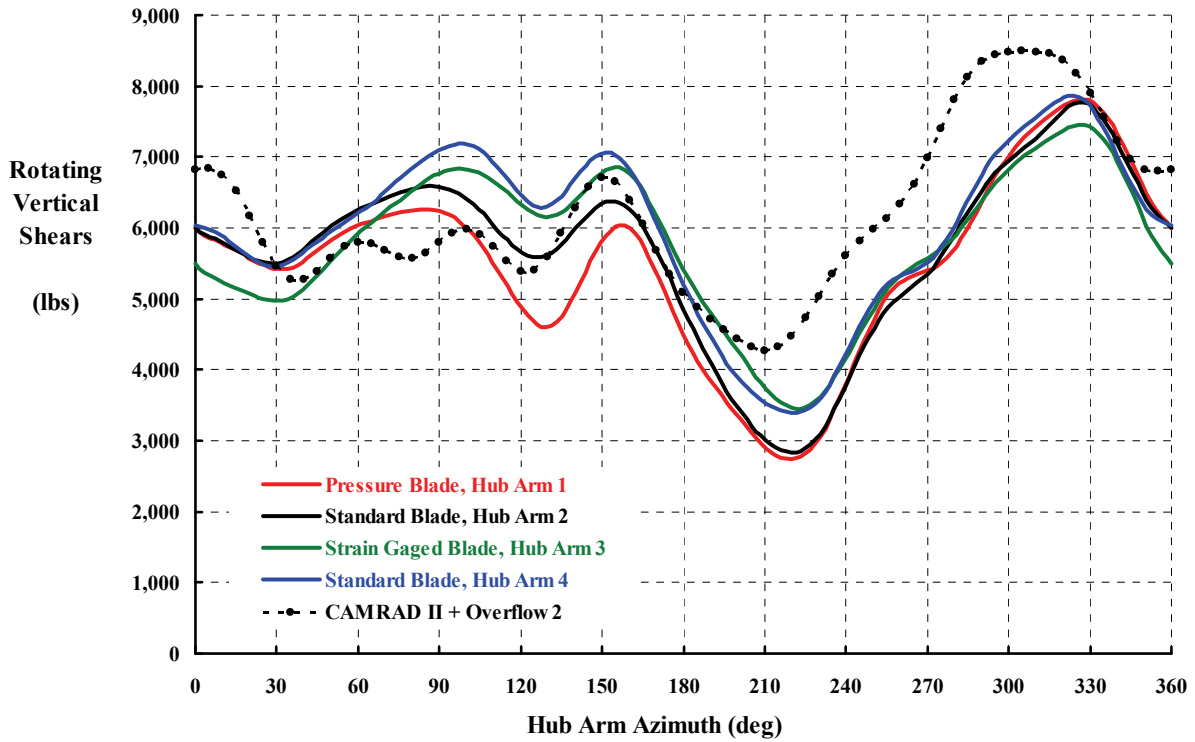


Fig. 2-266. Blade-to-blade comparison of rotating vertical shear at an advance ratio of 0.3 and a blade loading coefficient ( $C_T/\sigma$ ) of 0.09.

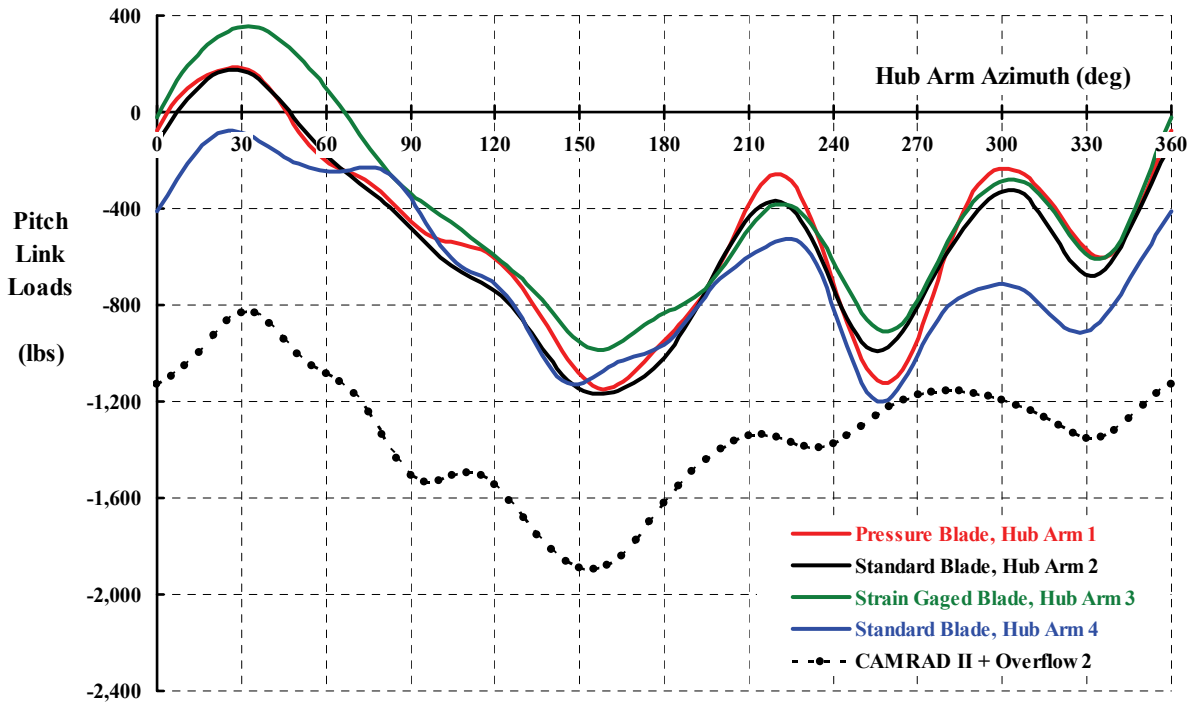
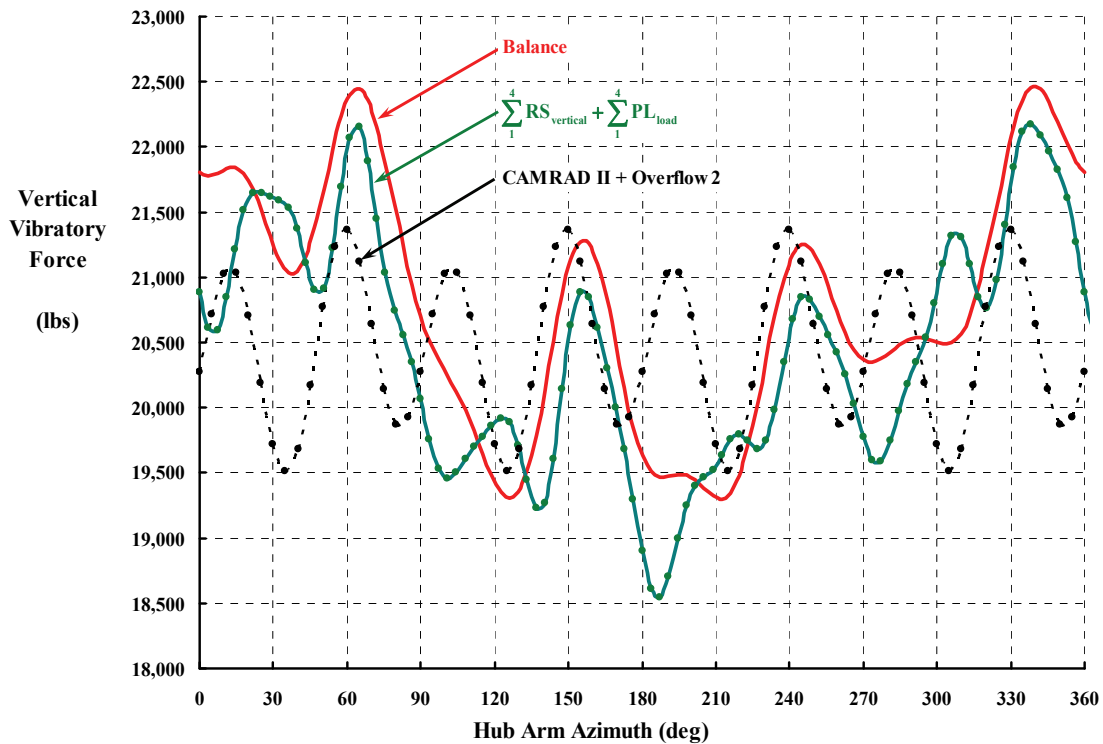


Fig. 2-267. Blade-to-blade comparison of pitch link load at an advance ratio of 0.3 and a blade loading coefficient ( $C_T/\sigma$ ) of 0.09.

To conclude this discussion of vertical force measurements and theory, take a look, if you will, at the three curves shown in Fig. 2-268. The balance reading is the vertical force that would shake the UH-60 in flight, in my view. The summation of vertical forces from the root shear gauges ( $RS_{\text{vertical}}$ ) and the pitch links ( $PL_{\text{load}}$ ) appears to add some distortion in the comparison because of differences in higher harmonic coefficients. The theory is, clearly, far from adequate and contains an excessive amount of 8/rev content in its waveform. In terms of overall amplitude, you can see that the balance is showing  $\pm 1,550$  pounds about a steady load of 20,446 pounds. The same load obtained by component force summation is  $\pm 1,825$  pounds about a steady load of 20,801 pounds. Finally, the theory is only estimating  $\pm 950$  pounds about the steady load of 20,452 pounds.

You might be discouraged by the concluding result given in Fig. 2-268. You should not be. I say this because, in my experience, just getting theory to fall on the same scale as test has often seemed a miracle when dealing with vibration problems, and remember, this has been a review of “hot-off-the-press” data from the most comprehensive test of a full-scale rotor in a wind tunnel. I have great confidence that the current group of aeromechanics researchers will scrutinize data from this experiment in detail, improve shortcomings of current theories, and produce far better comparisons over the complete range of speeds, thrusts, and shaft angles of attack that this UH-60 Airloads rotor was tested at.

Now consider the analysis of inplane forces, which you were introduced to with Fig. 2-253 and Fig. 2-254.



**Fig. 2-268. Vertical vibratory force comparison between theory and test at an advance ratio of 0.3 and a blade loading coefficient ( $C_T/\sigma$ ) of 0.09.**

## 2.6 VIBRATION

### 2.6.4.3 Longitudinal and Lateral Inplane Forces

There is no doubt that rotor system vibratory inplane loads are every bit as important as vertical forces. You read about this in the vibration chapter in Volume I. In fact, you can see from Fig. 2-253 and Fig. 2-254 that the overall amplitude of inplane vibratory loads *might* be nearly two to three times higher than the vertical vibratory loads shown in Fig. 2-252. (I say *might* be, because the balance inplane forces from this test have yet to be corrected for dynamic response.) Of course, the proportions between vertical and inplane forces vary considerably with flight conditions, but for this UH-60 Airloads rotor example at an 0.3 advance ratio, inplane loads are certainly not negligible—though I really doubt they can be as large as I have reported in Fig. 2-253 and Fig. 2-254.

The longitudinal and lateral vibratory forces were obtained in two ways during this wind tunnel test of the full-scale UH-60A Airloads rotor system. The primary way was directly from the balance, which is in the nonrotating world. (Remember, the balance loads have yet to be corrected for dynamic response, which may, in future reports, alter the waveform you see in Fig. 2-253 and Fig. 2-254.) The second path comes from resolving, to the nonrotating world, the rotating shears created by the hub loads associated with  $RS_{\text{longitudinal}}$  and  $RS_{\text{spanwise}}$  shown in Fig. 2-245. This is done following Eq. (2.284). Somewhat indirect measurements of these forces were obtained by shaft-bending-moment strain gauges mounted to the shaft several inches below the hub center as shown in Fig. 2-251. It would be nice if the comparison between test and theory were in reasonable accord for the inplane vibratory forces. Unfortunately, at this time neither longitudinal nor lateral experimental forces are well predicted as Fig. 2-269 and Fig. 2-270 clearly show.

To help you appreciate the difficulties in measuring vibratory forces even at full scale, you might consider reading two reported efforts with wind tunnel models [479, 480]. The first effort was aimed at a Sikorsky H-37 and was the most thorough seen in the literature up to 1967. Then, in 1982, a comprehensive attack (led by Dick Gabel at Boeing Vertol) with a model of a tandem rotor machine led to the following conclusions:

- “1) The rotor balances did not adequately measure vibratory loads due to poor dynamic response characteristics, large rotor cross coupling.
- 2) The hub accelerometers provided a good qualitative assessment of vibratory loads but the results were sensitive to centrifugal accelerations when the accelerometers were not exactly at the center of rotation.
- 3) The shaft bending gauges provided a good method for determining vibratory hub loads. They were able to measure both inplane forces and hub moments, but not vertical loads.
- 4) The hub balance proved effective in measuring vertical hub loads, but large interactions and damaged gauges did not permit adequate measurement of inplane loads.
- 5) The generalized coordinate analysis gave reliable vertical hub loads.
- 6) A careful check calibration must be made on each measurement system used to insure the dynamic loads recorded are reliable. Even though a system has been used successfully on previous models, poor dynamic response characteristics can distort the true results.
- 7) Vibratory hub loads were obtained that could be used to define the expected aircraft vibratory loads as a function of airspeed and gross weight that will prove useful in the full scale design process.”

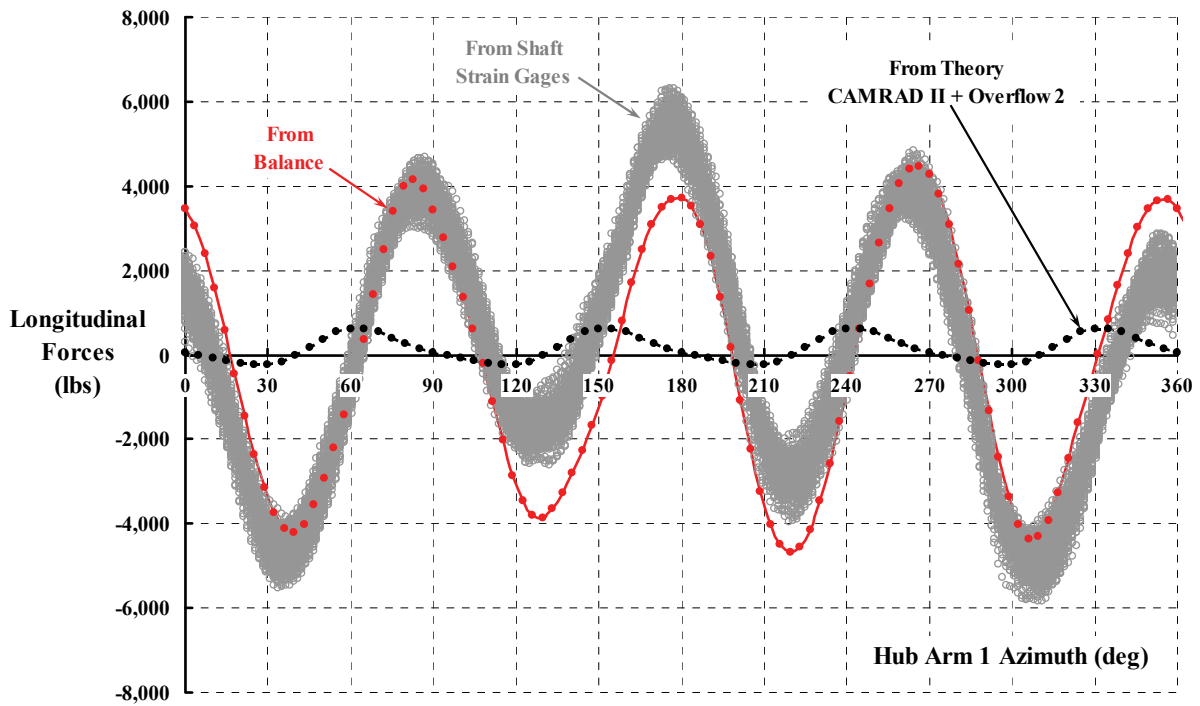


Fig. 2-269. Longitudinal vibratory force comparison.

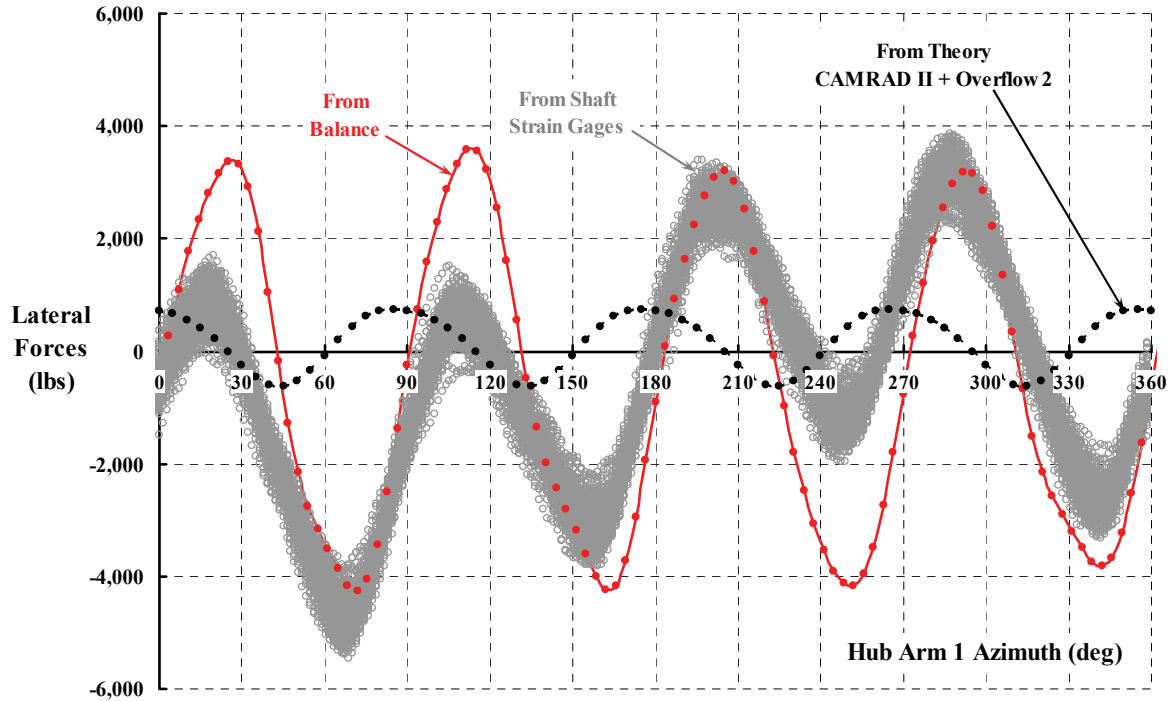


Fig. 2-270. Lateral vibratory force comparison.

## 2.6 VIBRATION

### 2.6.5 Blade Airloads, Blade Vibratory Response

You have now come to the crux of the vibration problem. Because of the most recently completed UH-60A Airloads rotor test [481]<sup>141</sup> (which I am constructing this discussion on) you can see more clearly than ever how theory and test compare. So let me start with a dissection of the vertical shear ( $RS_{\text{vertical}}$ ) first. Unfortunately, a deeper look into inplane loads will have to wait for future analyses, and published papers and reports by others.

#### 2.6.5.1 Dissecting Hub Arm Vertical Shear

The analysis of vertical shear that you are about to review will convince you, I hope, that some fundamentals of vibration are, after seven decades, becoming much clearer. My objective here is to show you how the components of the vertical shear vary with azimuth. The starting point is Eq. (2.286), which is repeated here for convenience

$$(2.286) \quad RS_{\text{vertical}} = \int_0^R \left( \frac{dL_{r,\psi}}{dr} \right) dr - \int_0^R (m_r) \Omega^2 \left( \frac{\partial^2 z_{r,\psi}}{\partial \psi^2} \right) dr - PL_{\text{load}} - w_b,$$

and the data under discussion is summarized in Fig. 2-271. To begin with, the vertical shear comparison between test (the red, dashed line) and theory (the heavy, solid black line) shows that, after seven decades, aeromechanics researchers now have come close enough to start digging deeper. The theory (CAMRAD II + Overflow 2) waveform differs slightly in just where the peaks and valleys fall in azimuth, but the character and key harmonics are, indeed, captured.

With this encouragement, consider the airload,  $\int_0^R \left( \frac{dL_{r,\psi}}{dr} \right) dr$ , contribution to the vertical shear. This integral is available from the blade that was instrumented with pressure taps at eight radial stations. (The pressures at the  $r/R = 0.55$  station are currently in question.) The chordwise array of the pressure taps at each radius station allowed computation of the airfoil's normal force ( $dN_{\text{pressure}}/dr$ ), the chordwise force ( $dC_{\text{pressure}}/dr$ ), and the pitching moment—all loads due to the pressure distribution about the airfoil's surface. As mentioned earlier, I have taken poetic license in referring to the blade element force as  $dL_{r,\psi}/dr$ . When you look at Fig. 2-272, you can see why. I have really been referring to  $dT/dr$ . Elemental lift is, as you know, a force normal to the local velocity ( $V_{\text{local}}$ ). In comparing theory to test, you must now be more exact because CAMRAD II + Overflow 2 rigorously includes all CFD computed terms so that

$$(2.291) \quad \text{Theory} \int_0^R \frac{dT_{r,\psi}}{dr} dr = \int_0^R \left[ \begin{array}{l} \frac{dN}{dr} \cos(\theta_{\text{geometric}} + \theta_{\text{control}} + \theta_{\text{elastic}}) \\ - \left( \frac{dC_{\text{pressure}}}{dr} + \frac{dC_{\text{skin friction}}}{dr} \right) \sin(\theta_{\text{geometric}} + \theta_{\text{control}} + \theta_{\text{elastic}}) \end{array} \right] dr.$$

<sup>141</sup> This paper by Tom Norman and his coauthors is an absolutely must-read document in order to appreciate the enormous step forward made in rotor wind tunnel testing.

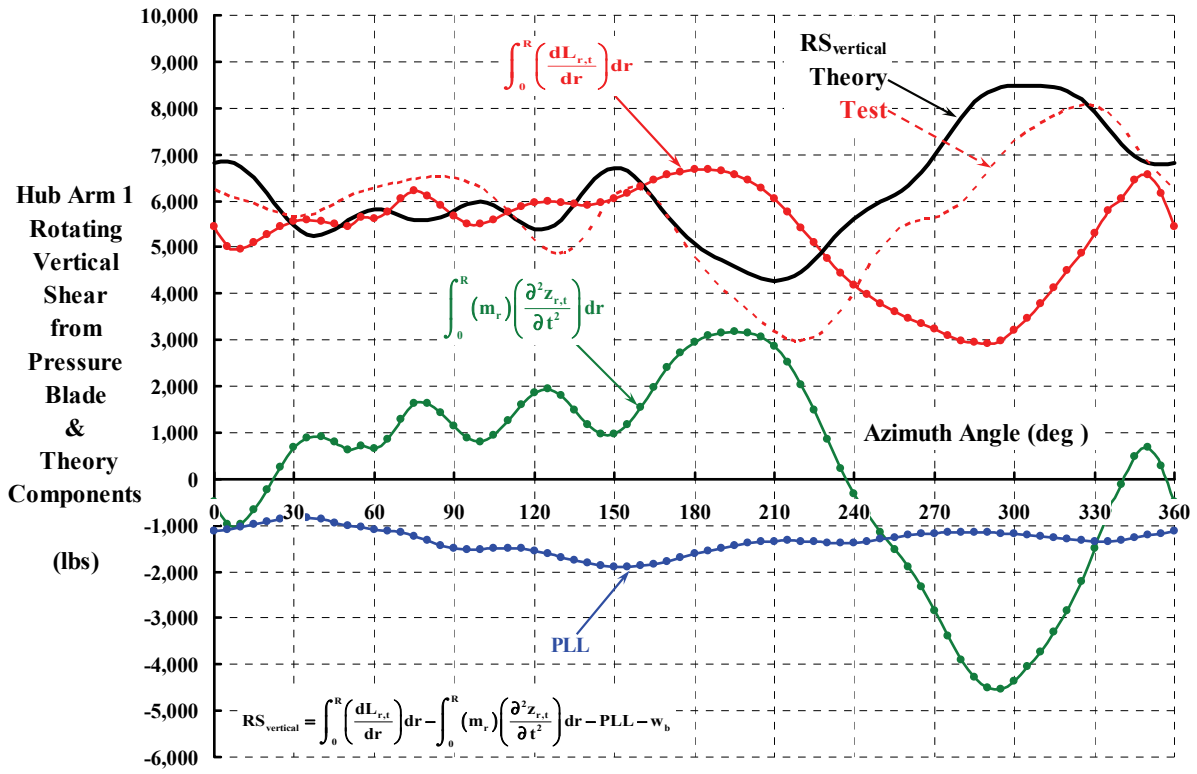


Fig. 2-271. Theory components of vertical shear.

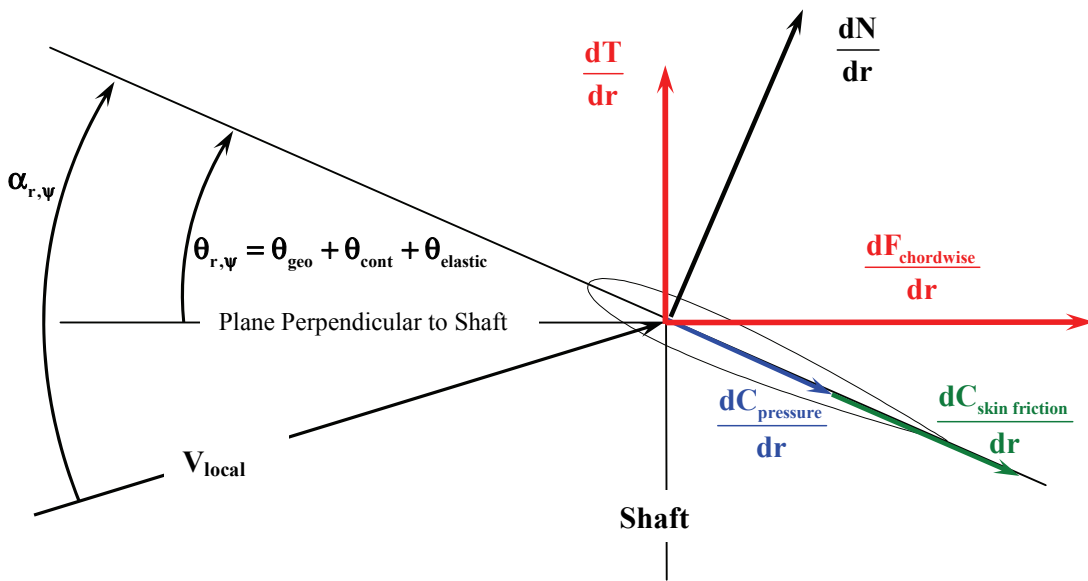


Fig. 2-272. Blade element forces and angles.

## 2.6 VIBRATION

In contrast, the preliminary integration from this “hot-off-the-press” experimental program computes the blade elemental thrust integral as

$$(2.292) \quad \text{Test Preliminary} \int_0^R \frac{dT_{r,\psi}}{dr} dr = \int_0^R \left[ \frac{dN_{\text{pressure}}}{dr} \cos(\theta_{\text{geometric}} + \theta_{\text{control}}) \right] dr .$$

Data reduction at this point in time does not include the chordwise force due to pressure nor is elastic twisting ( $\theta_{\text{elastic}}$ ) accounted for. This UH-60A rotor test had no instrumentation to obtain the skin friction force.

Despite these somewhat “apples-to-oranges” current computations, let me proceed anyway. You can see from Fig. 2-273 that a very encouraging result has been obtained. In fact, I have never seen results comparable to Fig. 2-273 in all my years in the rotorcraft industry. You should particularly note that the mean loads (or steady loads, if you like) are within 200 pounds of each other. That is, the test steady load is 5,470 pounds and the CAMRAD II + Overflow 2 has a mean load of 5,270 pounds. Furthermore, the first three harmonics dominate the waveforms as the tabulation on the figure shows.

Now consider the contribution of the inertia term,  $\int_0^R (m_r) \Omega^2 \left( \frac{\partial^2 z_{r,\psi}}{\partial \psi^2} \right) dr$ , to the vertical shear ( $RS_{\text{vertical}}$ ). Theory and test for this major force are compared in Fig. 2-274. The inertia load contribution shown in Fig. 2-274 is not directly measured in test or calculated

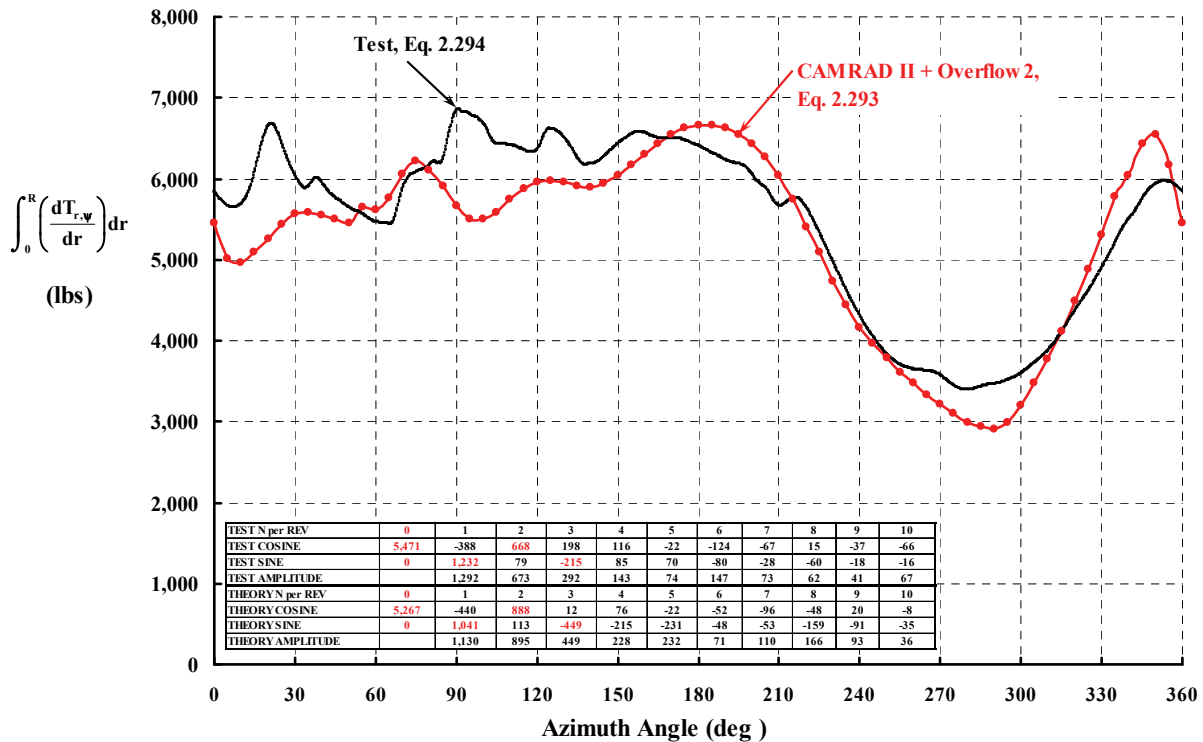


**Fig. 2-273. Theory and test for the root thrust are in closer agreement than I have ever seen.**

by the theory. It is derived from Eq. (2.286) for both test and theory as

$$(2.293) \int_0^R (m_r) \Omega^2 \left( \frac{\partial^2 z_{r,\psi}}{\partial \psi^2} \right) dr = \int_0^R \left( \frac{dT_{r,\psi}}{dr} \right) dr - RS_{\text{vertical}} - PL_{\text{load}} - w_b .$$

In test, the thrust integral was found by integrating the measured pressure distributions at eight radial stations to give the blade element normal force as Eq. (2.292) suggests<sup>142</sup>; the hub arm vertical shear and the pitch link load were all measured. Thus, the residual must be the inertia force. This approach charges all the experimental error to the inertia term. What is so interesting is that the steady load in the inertia integral should theoretically be zero, not the 489 pounds given by the tabulation. Coming this close is, to me, a remarkable achievement.

In backing out the inertia integral using theoretical results, you see that the steady load is 154 pounds, which is a measure of the theoretical error. This is a quite satisfactory result in my view.

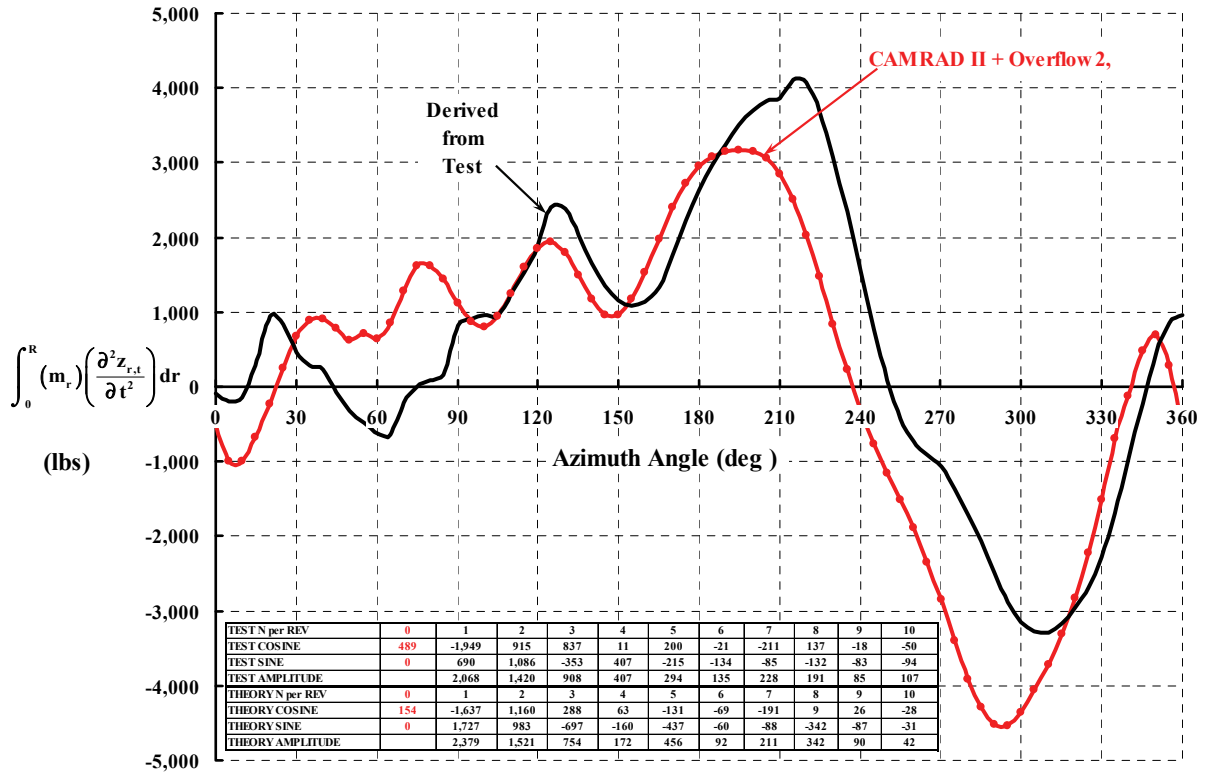


**Fig. 2-274. Theory and test for the inertia response of the blade to the airload are remarkably close.**

<sup>142</sup> Randy Peterson, who works for Bill Warmbrodt at NASA Ames Research Center, performed the integration of Eq. (2.292) using somewhat more than 200 pressure gauges—no mean trick in my book. This means that airloads at only eight radial stations were available. You can read more about how Randy did it in Tom Norman’s paper, *Full-Scale Wind Tunnel Test of the UH-60A Airloads Rotor* [481].

## 2.6 VIBRATION

The third contribution to the vertical shear ( $RS_{\text{vertical}}$ ) is the pitch link load ( $PL_{\text{load}}$ ). Here the disagreement between test and theory is quite significant as Fig. 2-275 shows. Not only is there disagreement in the steady load by nearly a factor of three, the test data clearly shows considerably more response at the 4/rev harmonics. This strongly suggests that not modeling the trim tab of the blade in the computational fluid dynamics (CFD) model is a situation to be rectified in the future. I would also suggest that the computational structural dynamics (CSD) model of the blade may be slightly off in the 4/rev frequency range.

The oscillation is clearly at 4/rev in the 220- to 330-degree azimuth angle, which might be considered the retreating blade stall region of the rotor. However, the advance ratio ( $\mu = 0.3$ ) and blade loading coefficient ( $C_T/\sigma = 0.09$ ) generally constitute a flight condition somewhat below blade stall onset as Romander [465] shows in his figure 14.

### 2.6.5.2 Blade Airloads—Test Versus Theory

To conclude this vibration discussion, consider the airload measurements from the UH-60A Airloads pressure blade obtained during the 40- by 80-Foot Wind Tunnel testing<sup>143</sup> and provided here in Fig. 2-276 and Fig. 2-277. Let me draw your attention first to the distribution along the blade of the steady blade element aerodynamic pitching moment

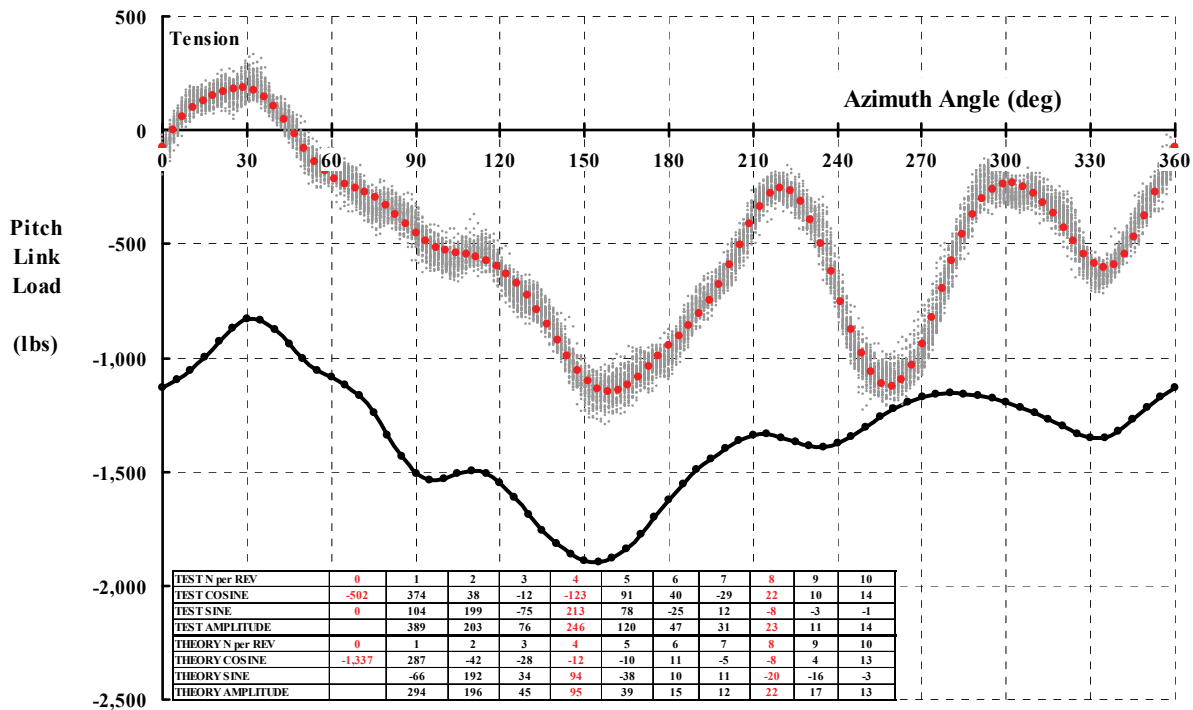


**Fig. 2-275. CAMRAD II + Overflow 2 provide a very poor prediction of pitch link load at the present time.**

<sup>143</sup> Just for future reference, the data is from Air Force test entry Number 10, Run 52, Data Point 31.

( $dPM/dr$ ) shown in Fig. 2-276. The integral from the 5-foot radius to the blade tip of the experimental pitching moments is a blade root aerodynamic pitching moment of about  $-565$  foot-pounds. The radial distribution of elemental pitching moment of the CAMRAD II + Overflow 2 theory is noticeably different, and the integral from root to tip is  $-400$  foot-pounds. These moments are resisted by the pitch link load, which acts at a 7.2-inch moment arm. Thus, the pitching moment airload contributes a compressive load of some  $-940$  and  $-500$  pounds, respectively, because the pitch arm/pitch link upper rod end-bearing is leading the blade. You should keep in mind that the pitching moment airload is not the only steady load that the pitch link must react with. For instance, the blade element thrust ( $dT/dr$ ) times inplane deflection from the torsion axis, and the blade element inplane force ( $dF_{inplane}/dr$ ) times an out-of-plane deflection from the torsion axis are also significant contributors as Eq. (2.288) reminds you. (You also learned this in Volume I, appendix D, fig. D-6 on page 377.)

Now consider an example of a blade element pitching moment as the blade completes one revolution. I have chosen the blade element at the 20.8-foot radius station as the example. This radius station corresponds to the 0.775 radius station based on the UH-60A radius of 322 inches or 26.3333 feet. I have chosen this specific radius station because so many past rotor studies have used the 3/4 radius station as a representative average of the whole blade. The example waveform of element pitching moment ( $dPM/dr$ ) in foot-pounds per foot is shown in Fig. 2-277.

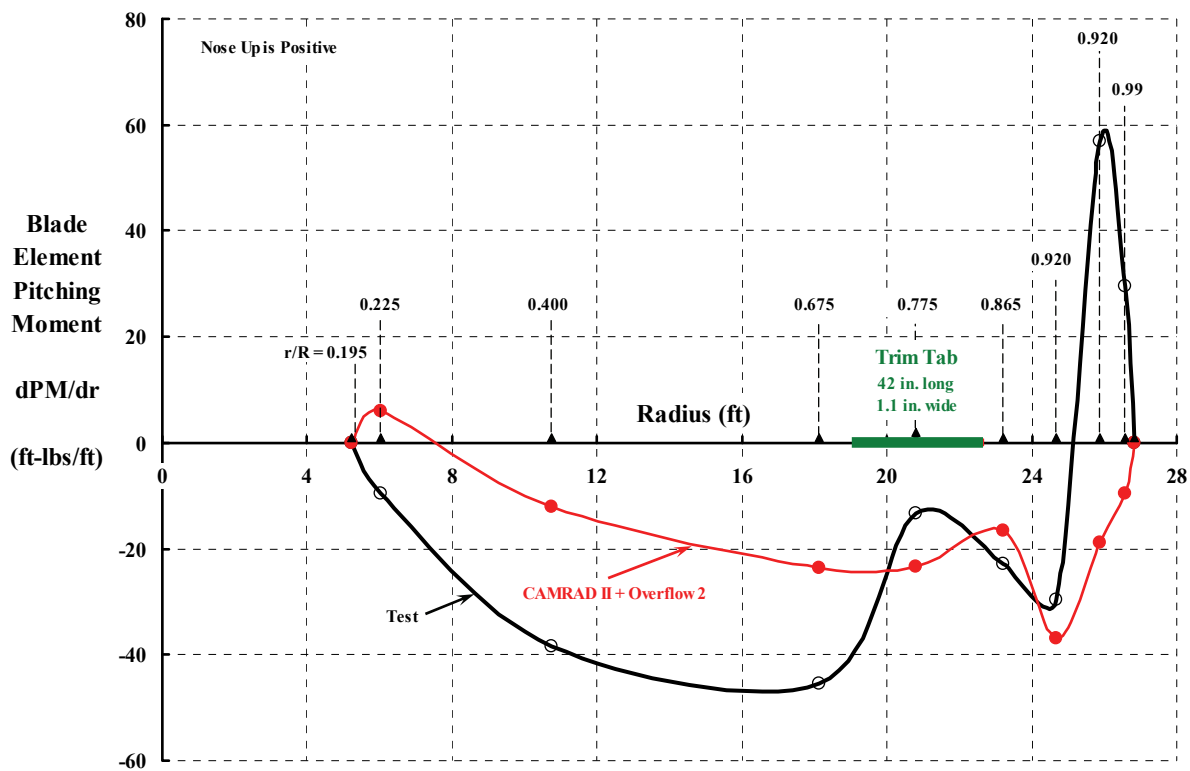


Fig. 2-276. Distribution along the blade of steady blade element pitching moment.

## 2.6 VIBRATION

You should immediately notice the similarity between the elemental pitching moment waveform in Fig. 2-277 and the pitch link waveform shown in Fig. 2-275—particularly in the first half of the blade’s revolution (i.e., from 0 to 180 degrees of azimuth angle). You might also agree that as the blade continues its revolution to the 270-degree azimuth angle, the similarity is still quite evident. However, in the final quadrant of azimuth angle, the pitch link load shows a marked oscillation that is only hinted at in the aerodynamic pitching moment. It is also clear in Fig. 2-275 that the CAMRAD II + Overflow 2 theory is at odds with test results in the 210- to 330-degree azimuth angle range. It is this azimuth angle range that has been historically [482-484] identified as the “retreating blade stall” region. In this UH-60A case where advance ratio equals 0.3 and the blade loading coefficient ( $C_T/\sigma$ ) equals 0.09, blade stall is definitely evident. However, the amount of separated flow is not sufficient to particularly impact the primary aerodynamic behavior of the rotor system. Were the UH-60A experiencing severe retreating blade stall, the pitch link load waveform shown in Fig. 2-275 would be completely dominated by the oscillation in the 210- to 330-degree azimuth angle region. The domination would be so great that the alternating load (i.e., the maximum peak to minimum peak) would dictate the fatigue load and part life for design purposes.

The pitching moment behavior of this blade element at the 0.775 radius station can be examined in relation to the normal force ( $dN/dr$ ) waveform of the element, which you see in Fig. 2-278. To do this, let me nondimensionalize the aerodynamic force and moment into the more familiar airfoil coefficient form. This requires some estimate of the local velocity illustrated in Fig. 2-272. I say estimate because, for a rotor blade, the actual velocity is not presently available in either the test pressure data or CFD theories.<sup>144</sup> Not to be dissuaded, I have chosen to define the local velocity as

$$\Omega r + V \sin \psi ,$$

which is the first equation you encountered in Volume I (on page 13). On this basis, it follows that

$$(2.294) \quad C_N = \frac{dN / dr}{\frac{1}{2} \rho (\Omega r + V \sin \psi)^2 c} \quad \text{and} \quad C_M = \frac{dPM / dr}{\frac{1}{2} \rho (\Omega r + V \sin \psi)^2 c^2} ,$$

which some more experienced aerodynamic engineers in the rotorcraft industry might take offense to because of my use of local velocity as  $\Omega r + V \sin \psi$ . However, having taken this step, it is possible to show you graphs of approximately correct  $C_M$  and  $C_N$  versus azimuth angle. Of course, I am using the normal force coefficient ( $C_N$ ) as an approximation to the more correct blade element lift coefficient ( $C_L$ ), which some readers may also take offense to considering Fig. 2-272.<sup>145</sup>

---

<sup>144</sup> This is not to say that serious attempts to deduce both local angle of attack and velocity have not been made [485]. Hank Tanner reported his effort in reference [486], which also included radial flow velocity measurements with a “boundary layer button.”

<sup>145</sup> I have to admit that ignoring the local *induced* velocity is only acceptable for radius stations well outside of the reverse flow region (defined by  $x = -\mu \sin \psi$ ) and is of doubtful use for advance ratios above 0.5. Including the induced velocity is not currently possible because neither test nor CFD + CSD theory will tell us what this velocity is! You might find the tutorial about rotor-induced velocity that I wrote in 2006 [487] of some interest.

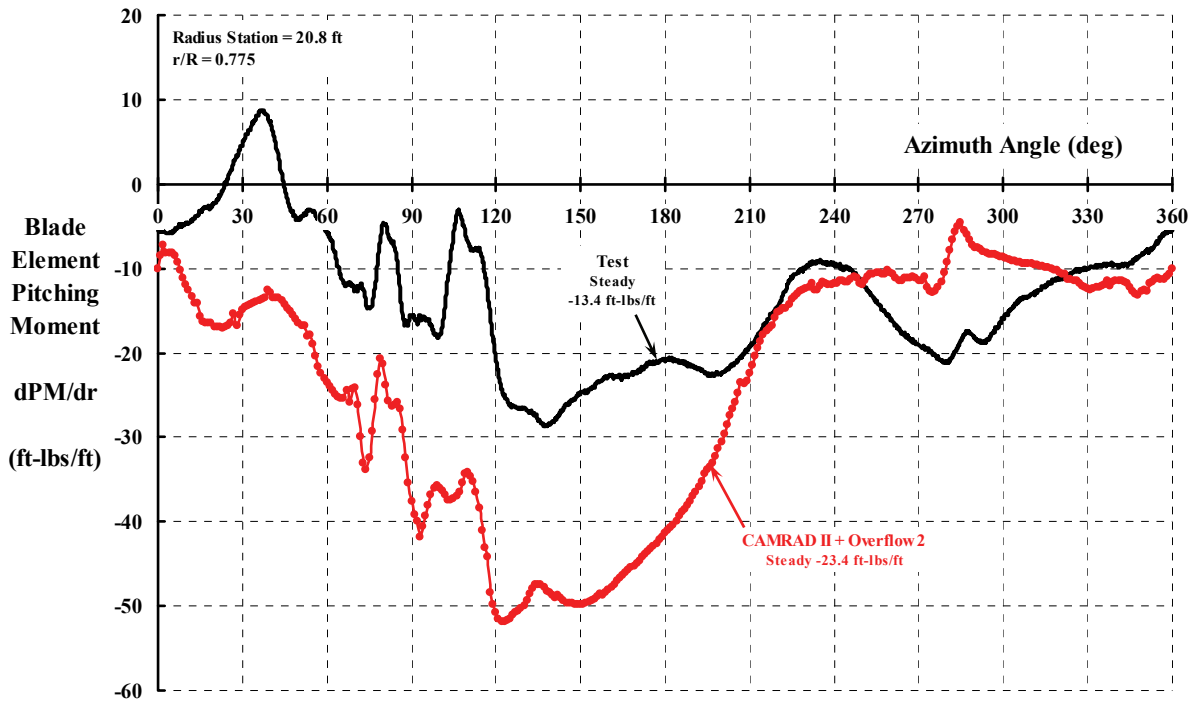


Fig. 2-277. Blade element pitching moment behavior with azimuth angle.

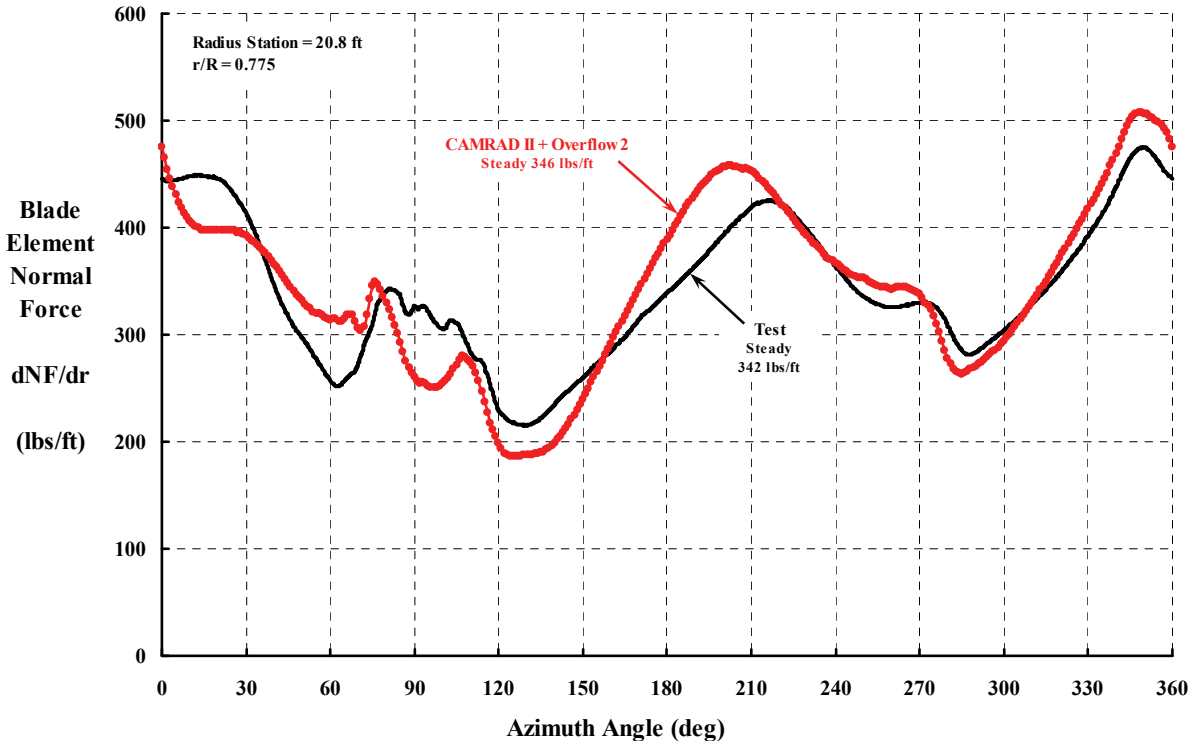


Fig. 2-278. Blade element normal force behavior with azimuth angle.

## 2.6 VIBRATION

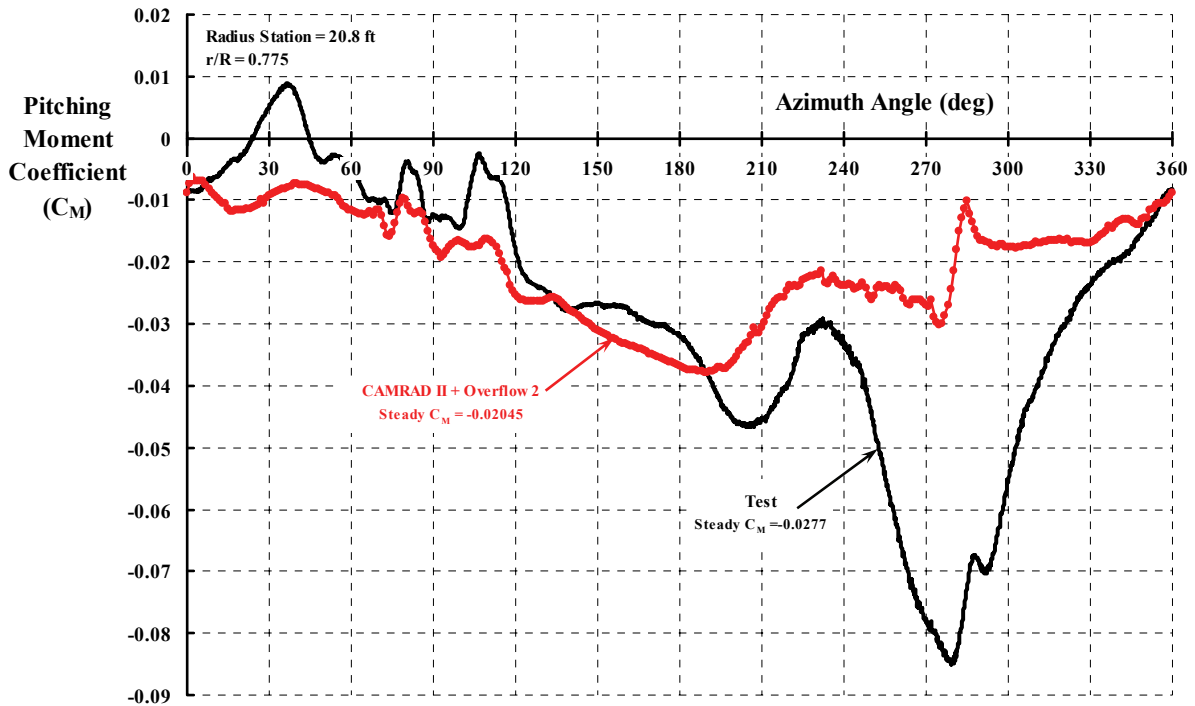


Fig. 2-279. Pitching moment coefficient behavior with azimuth angle.

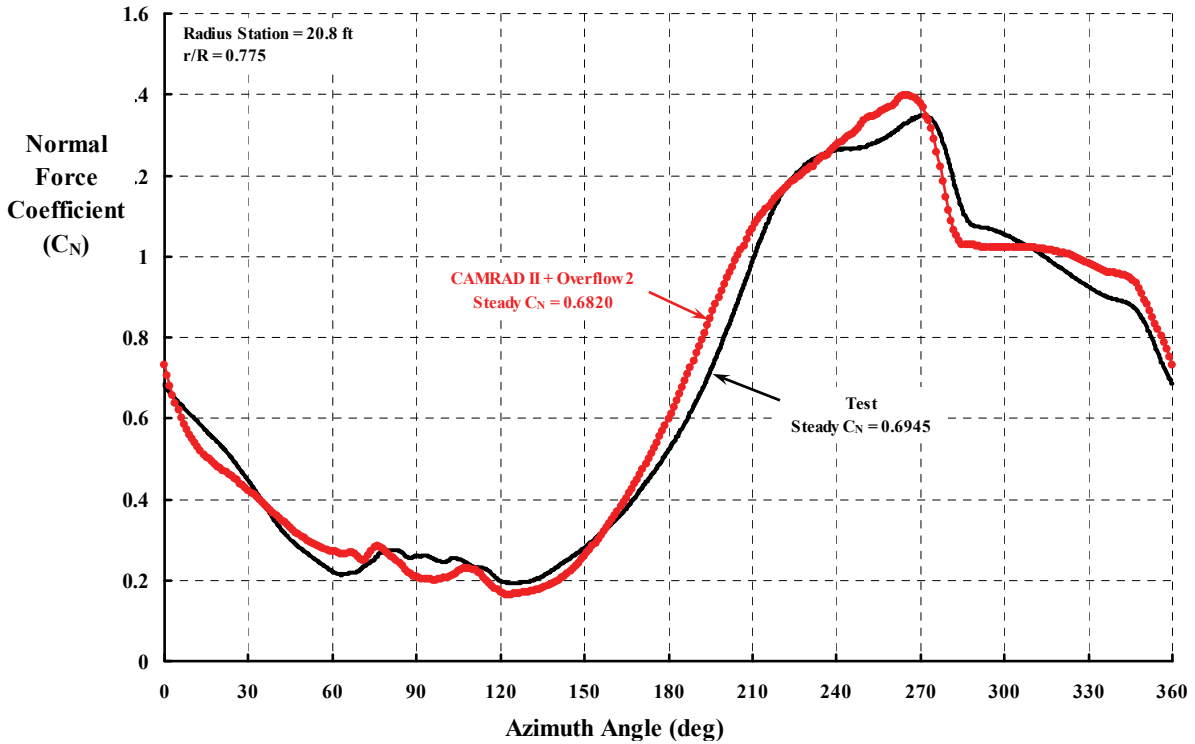


Fig. 2-280. Normal force behavior with azimuth angle.

The results of converting normal force ( $dN/dr$ ) and ( $dPM/dr$ ) from dimensional to customary airfoil coefficients ( $C_N$  and  $C_M$ ) are shown in Fig. 2-279 and Fig. 2-280. The comparison between theory and test of the normal force coefficient is quite favorable; the comparison of pitching moment coefficients is quite unfavorable in the azimuth angle range from 240 to 360 degrees. This brings me to the subject of blade stall.

In Fig. 2-281, I have shown you how  $C_M$  varies with  $C_N$ . The lemniscate-shaped figure that the blade element traces out during a revolution has two distinct loops. The larger loop that lies below a normal force coefficient of 1.0 is quite typical of the behavior predicted by classical unsteady aerodynamics. This is the shape you saw in Volume I, appendix B. The smaller loop that lies in the region above  $C_N = 1.0$  exhibits the behavior that rotorcraft engineers have come to call “dynamic stall.” The subject of dynamic stall and rotor blade response, particularly in control loads growth, has been studied in so much depth and breadth since the late 1950s that it is beyond this introduction. I believe a book could be written just on this one aspect of rotorcraft design. However, a paper written by Jing Yen and Mithat Yuce [488] published in October 1990 will give you a particularly good starting point. These authors examined the effect of blade stall on pitch link loads, and Mithat Yuce included a very unique way to calculate the amplitude of pitch link loads when blade stall is severe.

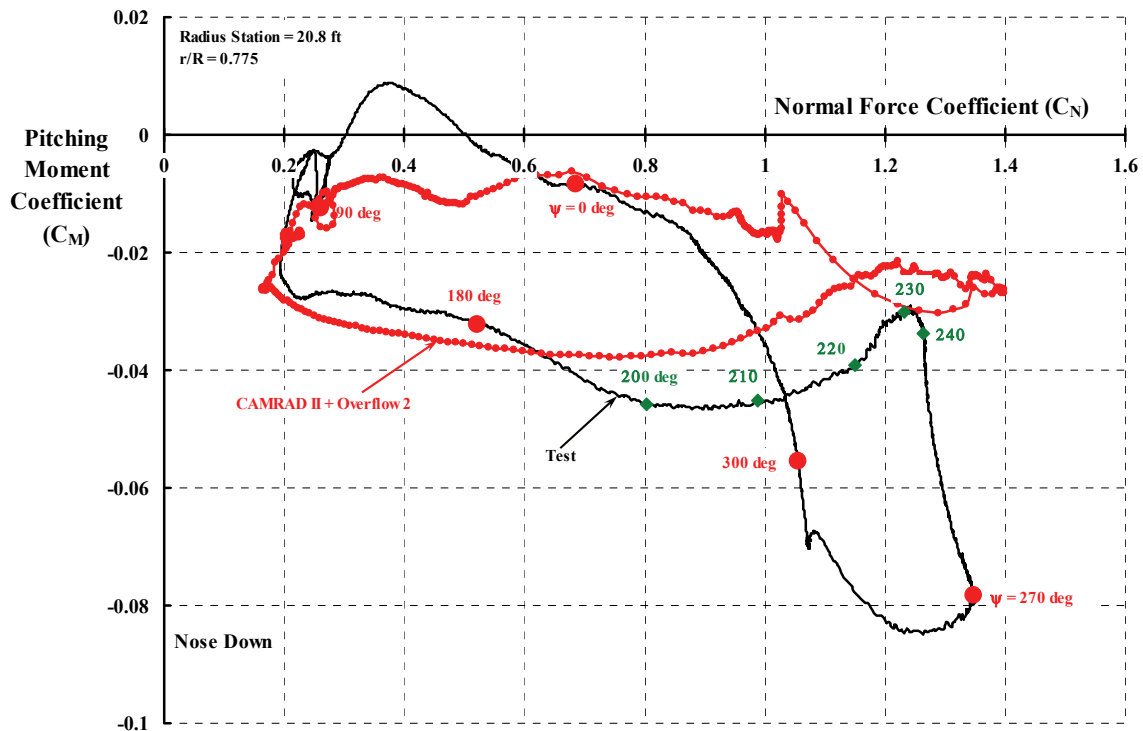
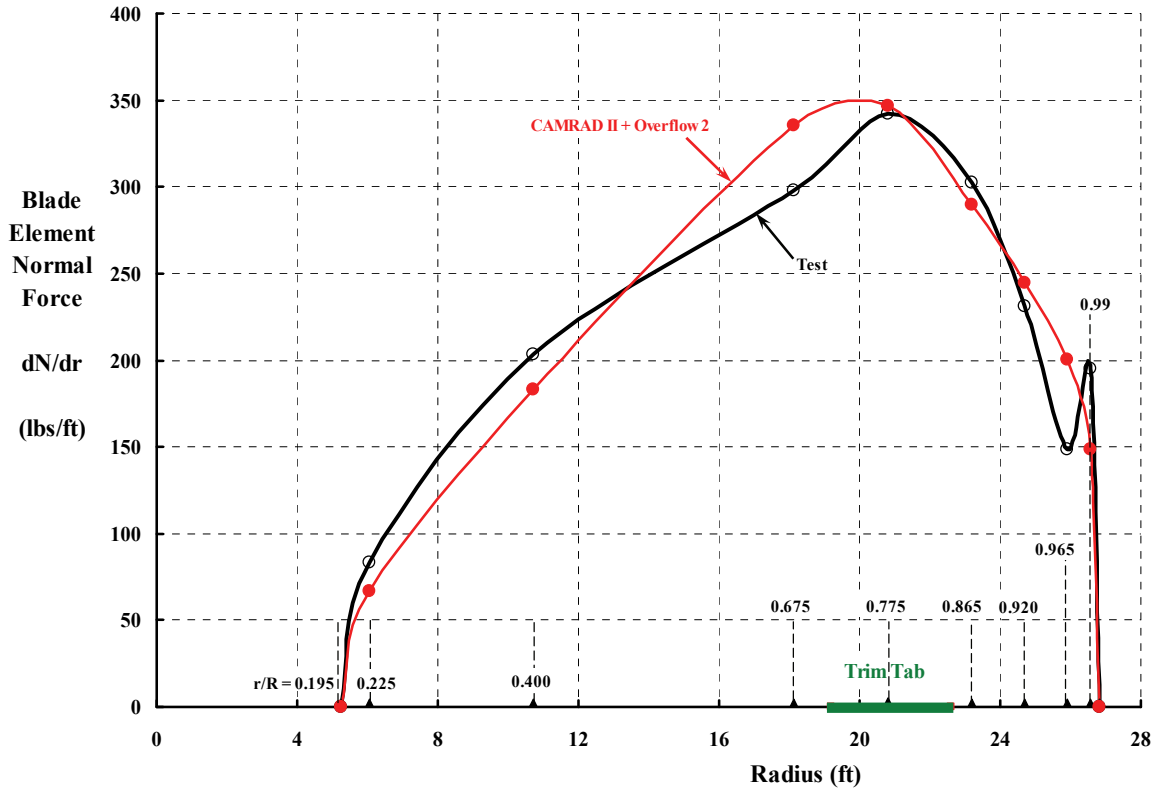


Fig. 2-281. The UH-60A blade element at the 0.775 radius station exhibits retreating blade stall at about 230-degree azimuth angle. Reattached flow appears complete during the last 30 degrees of rotation.

## 2.6 VIBRATION



**Fig. 2-282. The UH-60A blade element at the 0.775 radius station exhibits retreating blade.**

I would be more than remiss if you did not have the most fundamental blade element test versus theory comparison to review. This fundamental comparison is, in my view, the steady thrust distribution versus radius station, which you now have with Fig. 2-282.

### 2.6.5.3 Synthesized Airfoil Aerodynamic Characteristics

The general view of *rotorcraft engineers* using CFD is that the theory does not produce aerodynamic properties of rotor blade airfoils. An airfoil surface produces forces that can, so far, only be resolved through known geometric angles using CFD. The angle of attack of a blade element is not presently a known angle in the CFD world of rotor blades nor, as I mentioned, is the local velocity of a blade element. This is very disturbing to many aeromechanic researchers who have spent many years developing and applying blade element theory, which *does* calculate both angle of attack and local velocity. Given the local velocity and angle of attack, two-dimensional airfoil aerodynamic characteristics can then be obtained, and all behavior of the elastic rotor blade can be determined. The result of this progress has been that no direct bridge between classical blade element and CFD theories currently exists.

The even more practical problem is that in comprehensive computer programs today (such as Johnson's CAMRAD II) 1,000 flight conditions can be analyzed during a new helicopter design. In contrast, with the more advanced programs, say CAMRAD II + Overflow 2, the chief engineer would be lucky to get 10 conditions analyzed in the same time.

Of course, with the seemingly endless development of faster computers, the industry should expect that advanced CSD + CFD approaches will become everyday tools within the near future.

To help bridge the gap between blade element and CFD airload estimates, let me suggest the following objective and approach. The objective is to obtain airfoil aerodynamic characteristics from CFD calculated results. That is, I want to derive the “equivalent” two-dimensional airfoil angle of attack ( $\alpha$ ), lift coefficient ( $C_l$ ), and drag coefficient ( $C_d$ ) from the CFD computed normal force ( $dN_{\text{pressure}}/dr$ ), chordwise pressure force ( $dC_{\text{pressure}}/dr$ ), and chordwise skin friction force ( $dC_{\text{skinfriction}}/dr$ ). In short, I want to synthesize airfoil aerodynamic characteristics from CFD results after first obtaining the angle of attack of the blade element.

The basic premise to obtain angle of attack is that, according to potential flow theory, an airfoil has no drag regardless of its lift. This fundamental premise is illustrated by the black vectors in Fig. 2-283. In potential flow theory it is customary to assume the chordwise pressure force as positive when directed towards the leading edge of the airfoil. Thus, lift is made up of a normal force due to pressure (shown as the red vector) and the chordwise pressure force (shown as the black vector).<sup>146</sup> On this basis, the blade element angle of attack ( $\alpha_{\text{BE}}$ ) in radians can be estimated as

$$(2.295) \quad \alpha_{\text{BE}} \approx \text{arc tangent} \left( \frac{-dC_{\text{pressure}}/dr}{dN_{\text{pressure}}/dr} \right) = \text{arc tangent} \left( \frac{dC_{\text{pressure}}/dr}{dN_{\text{pressure}}/dr} \right).$$

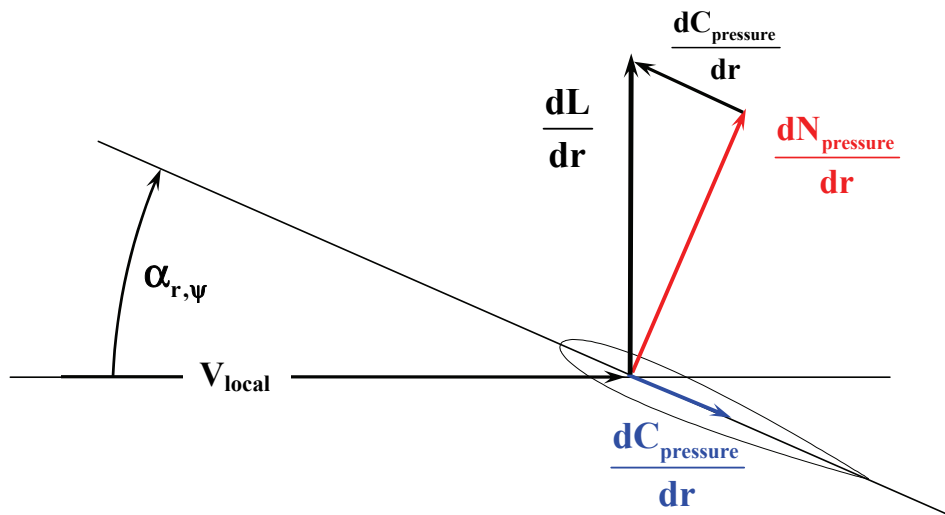


Fig. 2-283. Blade element forces due to pressure distributions.

<sup>146</sup> I hope I have not confused you by leaving the blue vector for  $dC_{\text{pressure}}/dr$  in the figure. I think of chordwise forces in the sense of drag, which is positive when directed towards the trailing edge. Most CFD calculators take all chordwise forces as positive towards the leading edge, a fact I must continually remind myself of.

## 2.6 VIBRATION

The corollary to this premise is that the blade element lift coefficient can then be calculated as

$$(2.296) \quad C_\ell = \frac{\sqrt{\left(-\frac{dC_{\text{pressure}}}{dr}\right)^2 + \left(\frac{dN_{\text{pressure}}}{dr}\right)^2}}{\frac{1}{2}\rho(\Omega r + V \sin \psi)^2 c}$$

and, therefore, lift coefficient can be plotted versus angle of attack, which follows what you learned in Volume I, appendix B. The results of applying this approach are illustrated in Fig. 2-284 and Fig. 2-285. Here I have used Ethan Romander's CAMRAD II + Overflow 2 computed results corresponding to the UH-60A Airloads rotor test associated with Run 52, Point 31, which is at an advance ratio of 0.3 and  $C_T/\sigma = 0.09$ . The radius station is 0.775 R.

Fig. 2-285 shows that unsteady aerodynamics play a significant role in rotary wing airloads even for such a fundamental characteristic as airfoil lift coefficient. While the nominal lift curve slope is 0.1088 per degree, the unsteady aerodynamics create what are frequently called hysteresis loops. The effect, as you saw in Fig. B-10 on page 321 of Volume I, is that lift lags behind angle of attack when the angle of attack is decreasing. Conversely, lift leads angle of attack when the angle of attack is increasing. Mathematically, an airfoil in unsteady flow has lift coefficient behavior approximately as

$$(2.297) \quad C_\ell = A\alpha + B\frac{d\alpha}{dt},$$

and this is what you see in Fig. 2-285.

Suppose that now you want to synthesize the airfoil drag coefficient ( $C_d$ ). Following the vector diagram shown on Fig. 2-272, you can see that

$$(2.298) \quad C_d = \frac{\left(\frac{dN}{dr}\right) \sin \alpha + \left(\frac{dC_{\text{pressure}}}{dr} + \frac{dC_{\text{skin friction}}}{dr}\right) \cos \alpha}{\frac{1}{2}\rho(\Omega r + V \sin \psi)^2 c} = C_N \sin \alpha + C_C \cos \alpha,$$

which can be derived from the CAMRAD II + Overflow 2 results because both chordwise pressure and skin friction forces are calculated. (This is not possible with the UH-60A Airloads rotor because no instrumentation measuring the skin friction force was used.)

The influence of unsteady aerodynamics on blade element drag coefficient is substantially greater than on lift coefficient as Fig. 2-286 shows. You see immediately that the total drag coefficient is the difference between two large components that are shown with blue lines in Fig. 2-286. The normal force component ( $C_N \sin \alpha$ )—the dashed blue line—is generally positive while the total chordwise component ( $C_C \cos \alpha$ )—the solid blue line—is generally negative. Both components are roughly 10 times the magnitude of the total drag coefficient. This is one of those small differences in big numbers problems that engineers frequently have to deal with. And this is why, even in steady flow, pinning down, experimentally, the drag coefficient of an airfoil has historically been so difficult. Whether it can be done with experimental data from an instrumented blade element in a rotor blade remains to be seen.

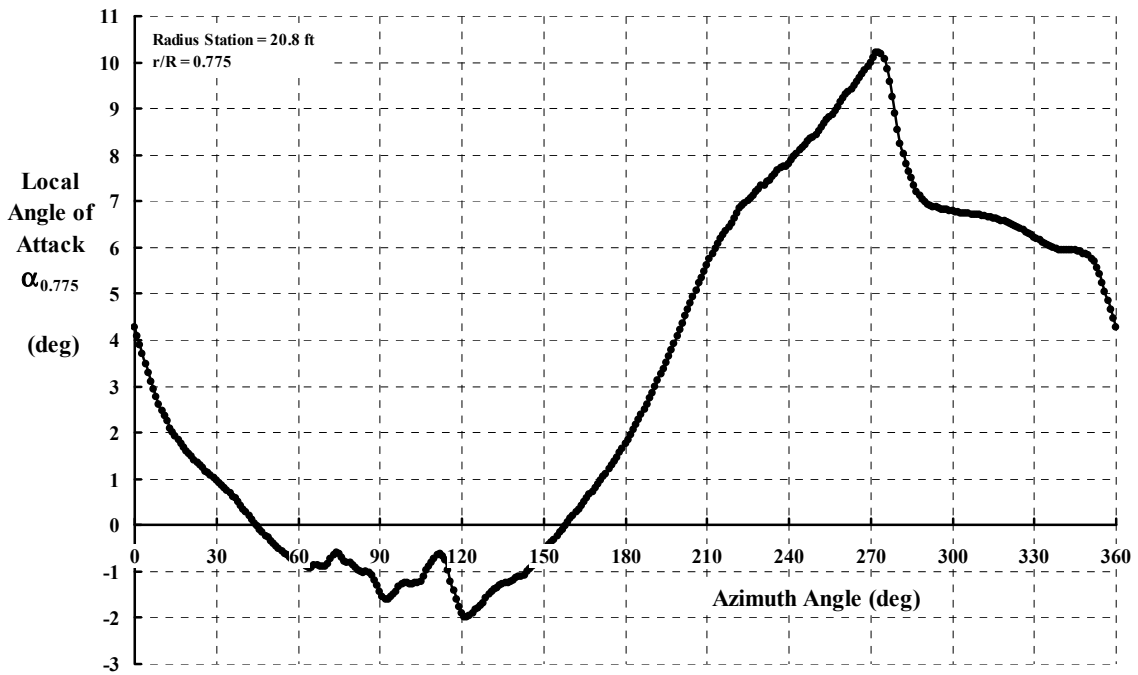


Fig. 2-284. Estimated airfoil angle of attack for the blade element located at the 0.775 radius station for  $\mu = 0.3$  and  $C_T/\sigma$ .

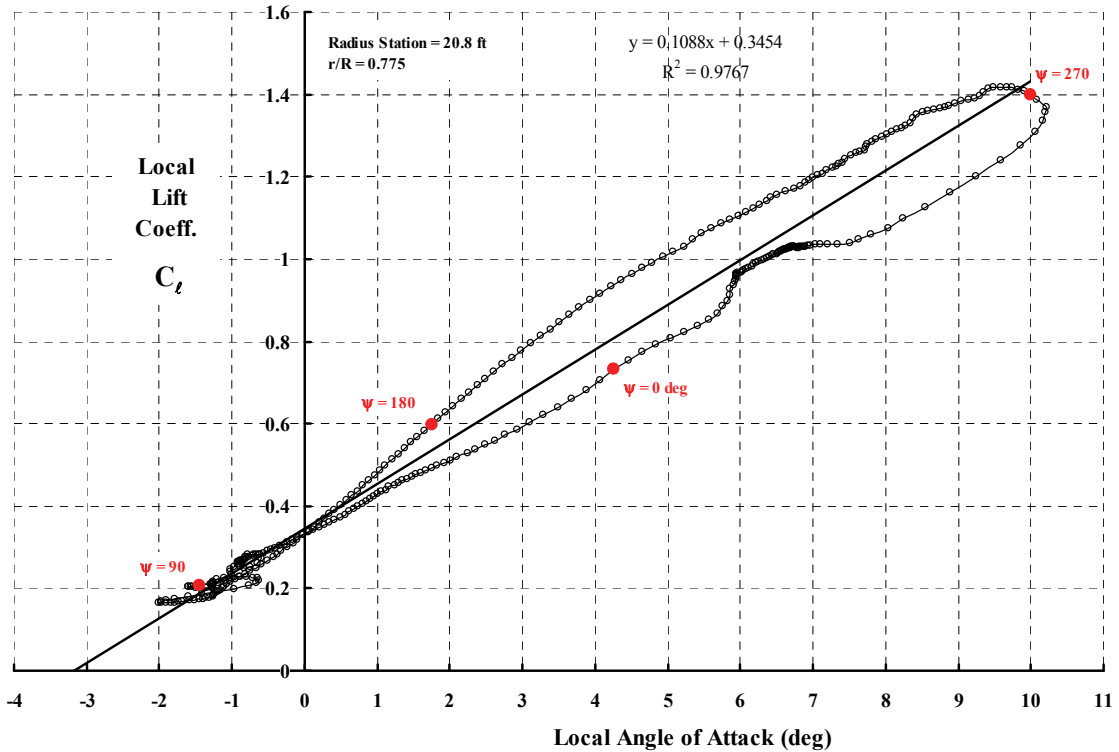


Fig. 2-285. Lift coefficient vs. angle of attack reflects unsteady aerodynamic behavior.

## 2.6 VIBRATION

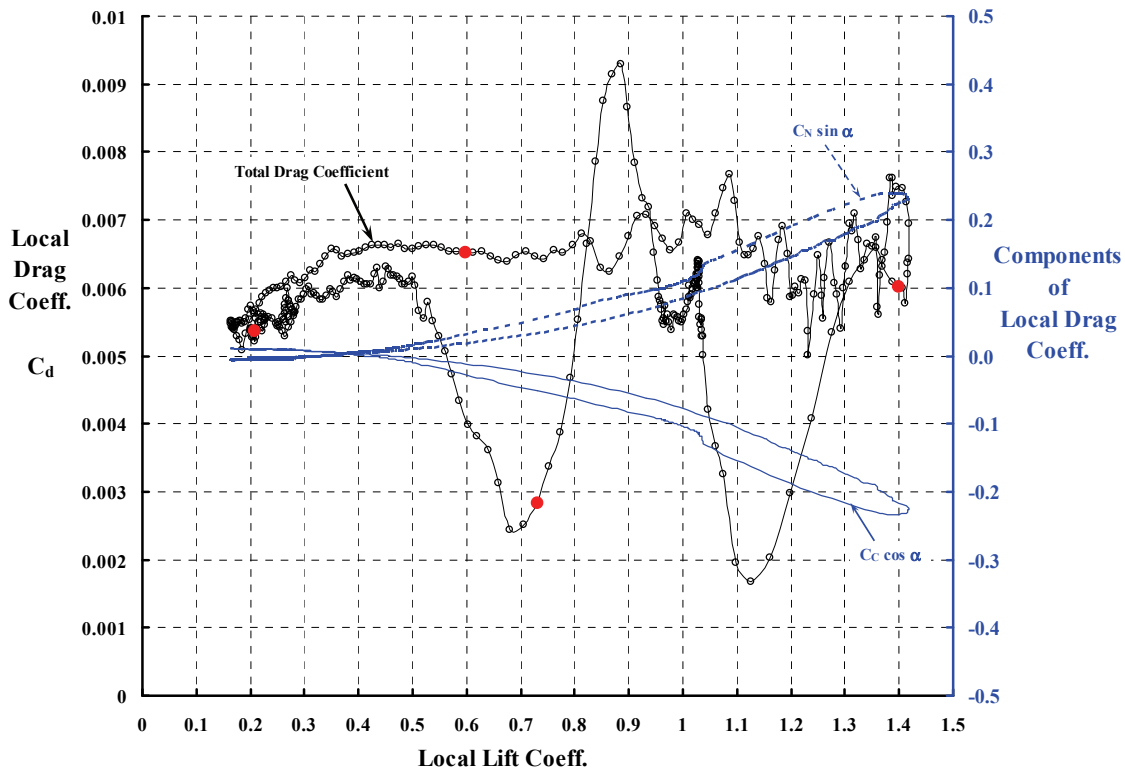


Fig. 2-286. The influence of unsteady aerodynamics on blade element drag coefficient.

### 2.6.6 Closing Remarks

Helicopter vibration problems are a continuation of those experienced by the autogyro pioneers, which you read about in Volume I. As Cierva wrote in his 1935 paper [398]:

“Perhaps the most irritating of the secondary difficulties met with in the autogyro developments have been those of a dynamical [vibration] nature.”

Now you have come forward seven and one-half decades to August 2012, and the rotorcraft industry still has the same opinion.

There is no question that there has been a considerable reduction in the vibration that occupants of a helicopter must tolerate. However, this improved ride quality has been achieved, in my opinion, by cut-and-try fixes with minimal help from theory. It has, in fact, been the use of many different types of anti-vibration devices, added to the basic machine by each manufacturer, that has saved the day as the rotorcraft industry expanded.

You should now appreciate the tenacity of aeromechanic researchers in evolving improvements to theory so that calculations before first flight could be relied on. The importance of a coupled rotor-fuselage attack became clear in the 1950s. Comprehensive theory, begun with a computer program called C-81 by Bell Helicopter, spread quickly throughout the industry in the 1960s and 1970s. This more complex theory appeared to still be

inadequate when tested against flight test results throughout the next 40 years. Almost every paper during this 40-year period decried the lack of reliable aerodynamic forces and moments that rotor systems respond to. It has taken the development of CFD coupled to available (and quite satisfactory) CSD computer programs to renew industry expectations of breakthroughs in the foreseeable future.

It now appears that a very comprehensive flight and wind tunnel program [489] using a Sikorsky UH-60A Black Hawk helicopter has provided new foundational experimental data. This data, compared to one CFD + CSD theory (CAMRAD II + Overflow 2) as you have seen, appears to have captured prediction of vertical vibratory forces. However, the prediction, to the accuracy of the vertical forces, of the more difficult inplane vibratory forces has not been achieved yet.

Generally I am not one to make speculations about future progress,<sup>147</sup> but if I were a betting man, I would bet that by August 2025, aeromechanic researchers—using the recently obtained UH-60A Airloads Program data provided by NASA Ames Research Center and its U.S. Army cohorts—will demonstrate quite useable correlation between test and theory for this widely used helicopter. Then, successful application of the newfound knowledge to a new helicopter design *with confirmation from flight test* will signify a very long awaited grasp of rotorcraft vibration. With luck, vibration levels at the “jet smooth level” Dick Gabel described in reference [404], without the current penalties in weight, cost, reliability, and maintenance [490], will become a reality, and *then* the rotorcraft industry can say that the helicopter’s vibration problem has been solved.

---

<sup>147</sup> Harry Gray, a CEO of United Technologies, placed a full-page statement in the Wall Street Journal (in the 1970s, I think). All it said in big print was, “Don’t promise what you can’t deliver.” I keep that thought in mind.



## 2.7 NOISE

People within a range of 1,500 feet of an operating helicopter frequently say that the noise is loud, and even intolerable, for long periods of time. They say sometimes they even need to put their hands over their ears. They say they do not want helicopters flying around their homes or places where they work, and this is just the tip of the iceberg of the list of noise complaints about helicopters. The situation was summed up quite well in 1955 [491]. There are only two exceptions to these thoughts about helicopter noise: one is in civil and military medevac situations and the other is in military operations such as close air support. There *are* times when the noise of an approaching helicopter can be music to the ears.

In the discussion of helicopter noise that follows, I want you to appreciate the human ear and how sound is perceived, understand how noise is measured, and to be able to calculate helicopter noise in hover and forward flight. Finally, I want you to know about government efforts regulating helicopter noise levels and flight paths within the world of aviation.

### 2.7.1 Sound, Noise, and Human Hearing

Sound and noise are words defined in the Random House Dictionary of the English Language [492] as follows:

**sound** n. 1. the sensation produced by stimulation of the organs of hearing by vibrations transmitted through the air or other medium. 2. mechanical vibrations transmitted through an elastic medium, traveling in air at a speed of approximately 1100 feet per second at sea level. 3. the particular auditory effect produced by a given cause: the sound of music. 4. any auditory effect; any audible vibrational disturbance.

**noise** n. 1. sound, especially of a loud, harsh, or confused kind: deafening noises. 2. a nonharmonious or discordant group of sounds.

For this discussion, it is not important for you to know much more, medically, about the human ear than what is conveyed by Fig. 2-287. One thing you should note in Fig. 2-287 is that ambient pressure on the ear drum is balanced by two sources. One source is air pressure acting through the ear canal onto the *outer surface* of the ear drum. The second source is air pressure acting up the Eustachian Tube onto the *inner surface* of the ear drum. Thus, the pressure difference across the ear drum is zero. To expand this point, suppose you go up from sea level to Denver Colorado, a mile-high city. This is a reduction in ambient pressure from 2,116 pounds per square foot to 1,744 pounds per square foot, but because the ear drum has a two-sided pressure balance, the ear drum remains completely un-deflected, and the brain does not perceive this situation as sound. This is quite different from a balloon being blown-up at sea level and then carried up to Denver. In that case, the balloon would expand to reduce the inner pressure until it again balances the lower pressure at the higher altitude. Of course, most of us have experienced ear pain when the Eustachian Tube is partially blocked as with a cold and stuffy nose. When that happens, our ears do begin to take on the characteristics of a balloon because of a pressure difference between the outer and inner surfaces of the ear drum.

## 2.7 NOISE

Sound and noise create a *vibrational pressure* having the simplest form of

$$(2.299) \text{ sound pressure wave for a pure tone} = p_t = p_o \sin[(2\pi f)t].$$

This constitutes the vibratory pressure that comes into the outer ear and deflects the eardrum in and out a very, very small amount. This type of air pressure is not balanced by the Eustachian Tube, therefore a vibratory auditory signal is transmitted to the brain. This auditory signal is transmitted from the ear drum into the middle ear, and then into the inner ear. The complete signal is then transmitted by nerves to the brain, which processes the signal into what we call sound. To me, an ear is nothing more than a microphone.

Equation (2.299) describes a single tone having a frequency ( $f$ ) in hertz. When you hit a piano key you hear a note, which is a tone. The amplitude of the vibration is ( $p_o$ ) in any one of several units. Using a piano key as an example, a soft touch will create a low amplitude of vibration pressure. Conversely, striking the key quite hard will create a large value of  $p_o$ . The most common unit of pressure in acoustics studies is newtons per square meter. One newton per square meter is called a pascal. When the pressure is in units of pascals, it is generally noted as ( $p_a$ ). I am still stuck in English units, so for the discussions that follow, you should remember that one pascal equals 0.020885434273 pounds per square foot, or if you prefer, 50 pascals equals about 1 lb/ft<sup>2</sup>.

Human factors research on hearing became quite serious in the United States shortly after Alexander Graham Bell was awarded a patent for the electric telephone by the United States Patent Office in 1876. By 1899, American Telephone & Telegraph (AT&T) Company was in business. AT&T had four major divisions, one of which was Bell Telephone Laboratories (more commonly called Bell Labs) that conducted research and development. Two members of Bell Labs were Harvey Fletcher and Wilden A. Munson. Fletcher was a physicist and director of the physical research department at Bell Labs, and Munson was an engineer in Fletcher's department. In 1933, they published a landmark paper [493] in the Journal of the Acoustical Society of America. Their paper contained a definition of loudness, its measurement, and an often referenced graph showing lines of constant loudness, which you will see shortly.

A key facet of Fletcher and Munson's work established the threshold of hearing based on a group of young people with very good hearing. From a helicopter engineer's point of view, I think the subject of sound and noise begins with this hearing threshold that Fletcher and Munson set forth in 1933 and that was updated in 2003 [494]. You see from Fig. 2-288 that this threshold of hearing for a pure tone, such as given by Eq. (2.299), is presented as a line on a graph of the root mean square (rms) of vibratory pressure ( $p_{rms}$  in lbs/ft<sup>2</sup>) versus frequency ( $f$ ) in hertz. The root mean square of pure tone vibratory pressure is calculated simply as

$$(2.300) \quad p_{rms} = p_o / \sqrt{2}.$$

Using Fletcher and Munson's updated starting point (but in English units for pressure), you see in Fig. 2-288 that a human's ear is rather sensitive in the frequency range from 500 to 8,000 hertz. That is, if you are a young person with average to better-than-average hearing,

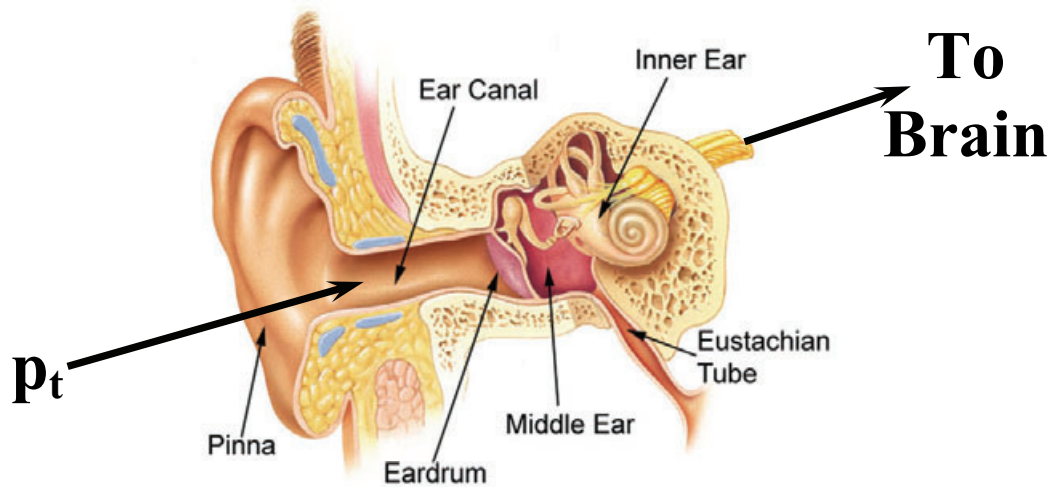


Fig. 2-287. A simplified schematic of a human's hearing device.

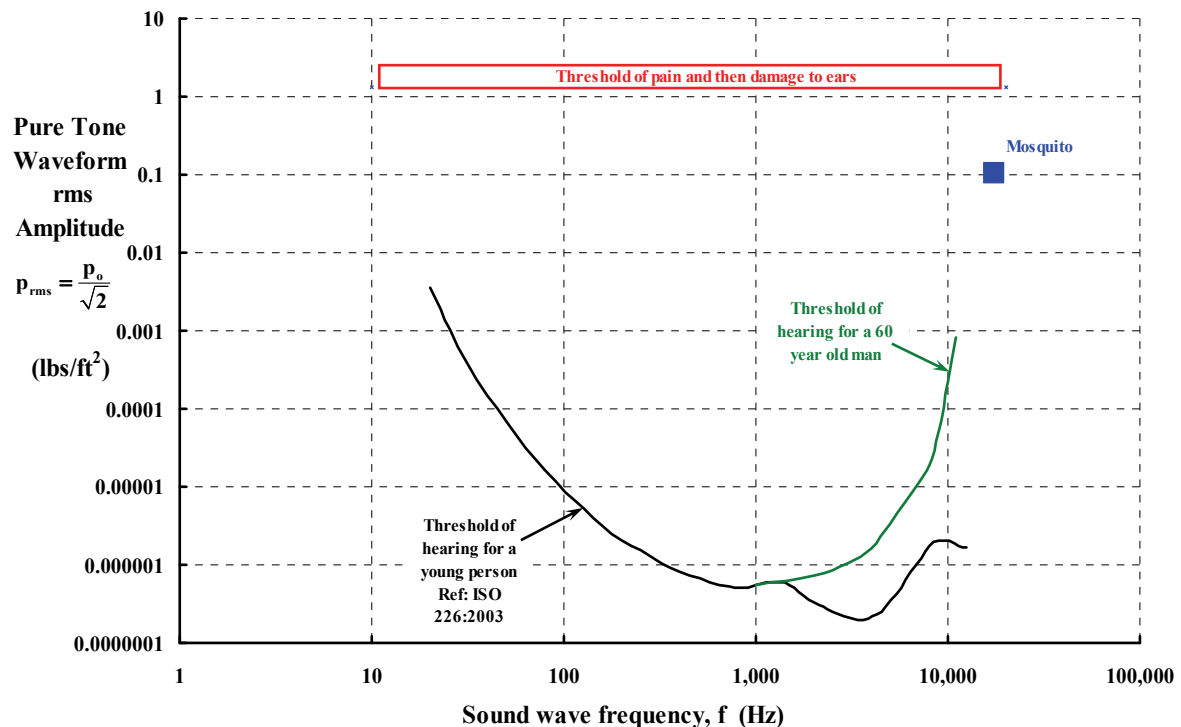


Fig. 2-288. Thresholds of hearing and pain found with pure tones going into headphones worn by the human being tested. Converted from ISO 226:2003 [494].

you can easily hear a mosquito. At the other end of the frequency scale, a human's hearing becomes very much less sensitive. At 10 to 20 hertz, a human may feel the sound rather than hear it. Hearing deteriorates with age [495], and typically by age 60 a male no longer can hear a mosquito or (in my case at age 77) a fly. (Apparently, young people are now taking advantage of this acoustical situation by using the sound of a mosquito as a ringtone for their cell phones. This ploy clearly obviates a great deal of adult interference in young people's lives.)

## 2.7 NOISE

### 2.7.2 Loudness Curves, Sound Pressure Level, and the Decibel

The ground work that Fletcher and Munson laid in 1933 created the first graph of constant loudness levels. You cannot get very far into reading about acoustics before encountering their often-reproduced graph, which you see here as Fig. 2-289. The ordinate axis is sound pressure level (SPL) in decibels, a unit that I will discuss shortly. The abscissa is pure tone frequencies in hertz (cycles per second). The lines represent sound at constant or equal loudness as determined from a group of “subjects.” Imagine you are a “subject” in a loudness experiment. You put on earphones and the technician turns a knob that generates a reasonably quiet, pure tone sound per Eq. (2.299) at, say, 1,000 hertz (cycles per second). You tell the technician that the sound you hear is your reference loudness and call it a loudness of 40 (never mind the units for now). The technician will write down 40 decibels. The technician then turns the frequency to 100 hertz—*without changing the volume*. You say that the volume went down. The technician then says he (or she) will slowly turn up the volume until you say it sounds as loud as before (i.e., at 1,000 hertz). At your call, he (or she) will stop raising the volume and record, say, 62 decibels.

Following this experimental procedure, you and the technician can create one line that Fletcher and Munson labeled a loudness of 40. (A unit for loudness called a phon was later coined, and the 40 became 40 phons.)

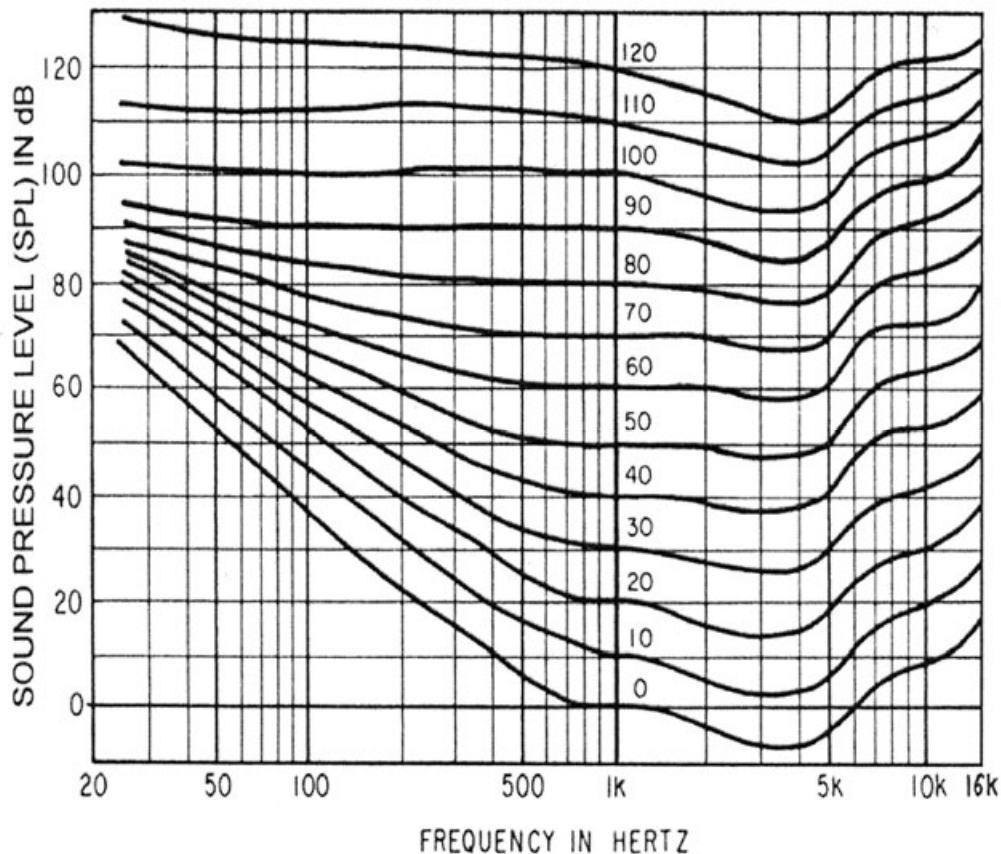


Fig. 2-289. Fletcher and Munson’s loudness graph of 1933 [493].

As you noticed in Fig. 2-289, the ordinate is sound pressure level (SPL) in decibels, which is the number the technician wrote down when you selected the reasonable volume at 1,000 hertz (i.e., 40) as your reference. Remember he wrote down 62 at 100 hertz, the increased volume that you said sounded as loud as the volume at 1,000 hertz. A decibel is the favored unit for measuring sound pressure levels. My use of pounds per square foot as on the vertical axis of Fig. 2-288 will most certainly be frowned upon by many readers. I should have at least used pascals, you might be saying, but keep in mind that many helicopter engineers unfamiliar with the subject of noise think of vibratory pressure in pounds per square foot—and it is to those interested engineers that I am writing.

There is no question that using so many zeros on the vertical scale of Fig. 2-288 before a number appears is unwieldy—even in the engineering world. So enter the decibel. Quite simply, a decibel is nothing more than a re-referencing of the pressure axis on Fig. 2-288. A sound pressure level (SPL) in decibels is mathematically defined as

$$(2.301) \quad \text{SPL decibel (dB)} \equiv 10 \left[ \log_{10} \left( \frac{p_{\text{rms}}}{p_{\text{reference}}} \right)^2 \right]$$

where, *for a pure tone*, the root mean square pressure ( $p_{\text{rms}}$ ) is given with Eq. (2.300). You should notice immediately that a decibel has no units because  $p_{\text{rms}}$  is divided by a reference pressure ( $p_{\text{ref}}$ ). The International Organization of Standardization appears to have settled on a value of the reference pressure as 0.00002 pascals (or  $2 \times 10^{-5}$  Pa, or 20 micro pascals), which converts to  $4.17708684662 \times 10^{-7}$  pounds per square foot. This “universal” value was established as the reference hearing level at a frequency of 1,000 hertz. Thus, when the root mean square pressure ( $p_{\text{rms}}$ ) equals the reference pressure ( $p_{\text{ref}}$ ) you have the  $\log_{10}$  of 1, which is zero.

The loudness curves that Fletcher and Munson published in 1933 opened the door to a human factors search for refinements to their curves—and a loudness scale. After seven decades of human factors research,<sup>148</sup> the International Organization for Standardization (the same group that was involved in vibration as you read earlier) settled on a new set of loudness curves, which they identified as ISO 226:2003 [494]. I have included this modern standard here as Fig. 2-290 for the sake of completeness.

The researchers’ logic and approach to creating a loudness scale appears rather straight forward. If “corrections” to a set of loudness curves were established that turned the curves of a loudness graph into straight lines parallel to the X-axis, then a human’s perception of loud could be quantified by a number. In fact, electronic sound meters could be developed and manufactured that displayed a digital readout of loudness for all to see and record. Keep in mind that not all humans have the same hearing ability, so efforts at standardizing by human factors researchers have produced results with considerable scatter. Still, the group has met with some success.

---

<sup>148</sup> A step along the way was the paper published by Robinson and Dadson [495]. They show the variation in the threshold of hearing from several studies.

## 2.7 NOISE

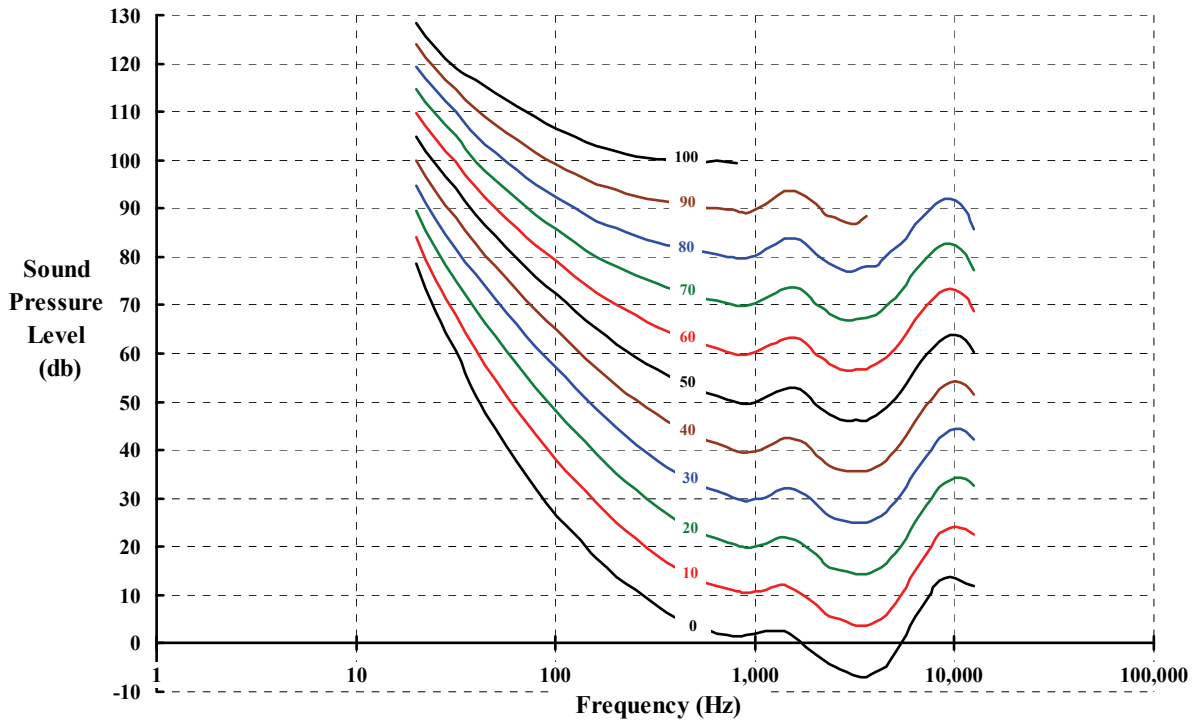


Fig. 2-290. Modern equal loudness curves of 2003 published as ISO 226:2003.

### 2.7.3 Weighted Loudness Curves

The “corrections” (i.e., weighting) that the audio industry created are called in the literature, A-weighted, B-weighted, and C-weighted sound pressure levels (SPLs). The game has been to make each curve in Fig. 2-290 flat, which is to say nearly independent of frequency. That means a large correction at low frequency tapering down to zero correction at 1,000 hertz, which has been taken as the reference frequency. In fact, you can see from Fig. 2-290 that a “correction” curve must subtract decibels as a function of both frequency and loudness. This could amount to a rather complicated function. The industry was not prepared to tackle that complexity given electronics in the pre-digital world, so they selected only three loudness corrections (i.e., A, B, and C) at which to be reasonably accurate with a “correction” dependent only on frequency—for pure tones.

The creators applied some simple mathematics to arrive at the three weighting curves. They said,

$$\begin{aligned}
 \text{Weighted SPL decibel (dB)} &\equiv 10 \left[ \log_{10} \left( \frac{p_{\text{rms}}^2}{p_{\text{ref}}^2} \times g(f) \right) \right] \\
 (2.302) \qquad \qquad \qquad &= 10 \log_{10} \left( \frac{p_{\text{rms}}^2}{p_{\text{ref}}^2} \right) + 10 \log_{10} [g(f)] \\
 &= \text{SPL}_{\text{Unweighted}} + W_{\text{Weighting factor}}
 \end{aligned}$$

where the multiplying factor  $[g(f)]$  would approximately flatten the loudness curves.<sup>149</sup> It was then a simple step to subtract any type of weighting factor (i.e.,  $W_A$ ,  $W_B$ , or  $W_C$ ) from a measured, pure-tone SPL and display a number that approximately quantified a human's opinion of noise—in decibels. The convention was adopted that these weighted SPLs would be designated dB(A), dB(B), and dB(C).

They constructed the A-weighting from the 40-phon levels, the B-weighting from the 70-phon levels, and the C-weighting from the 100-phon levels. It appears that B-weighting has fallen into disuse and the A-weighting and C-weighting are applied to any measured sound pressure level to convert to a 1-number readout in decibels. Many audio equipment firms sell sound meters (Fig. 2-191) that display noise level (or sound level if you prefer) in decibels followed by A, B, and C. These meters generally include a selection between A- and C-weightings.

Let me illustrate how the three weightings are applied. This calculation is important because so many sound meters are used to measure noise in the world, and the readouts are used by many government bodies to regulate noise environment.

The A-, B-, and C-weightings are calculated from the following equations:

$$(2.303) \quad W_A = 2.0 + \log_{10} \left\{ \frac{12,200^2 f^4}{(f^2 + 20.6^2)(f^2 + 12,200^2) \sqrt{(f^2 + 107.7^2)(f^2 + 737.9^2)}} \right\},$$

$$(2.304) \quad W_B = 0.17 + 20 \log_{10} \left\{ \frac{12,200^2 f^3}{(f^2 + 20.6^2)(f^2 + 12,200^2) \sqrt{(f^2 + 158.5^2)}} \right\}, \text{ and}$$

$$(2.305) \quad W_C = 0.06 + 20 \log_{10} \left\{ \frac{12,200^2 f^2}{(f^2 + 20.6^2)(f^2 + 12,200^2)} \right\}.$$

The offsets (2.0, 0.17, and 0.06 for  $W_A$ ,  $W_B$ , and  $W_C$ , respectively) ensure that at 1,000 hertz, no weighting occurs.

<sup>149</sup> Do not forget that  $\log_{10}(x + y)$  does not equal  $\log_{10}(x) + \log_{10}(y)$ . Rather  $\log_{10}(xy) = \log_{10}(x) + \log_{10}(y)$ .



**Fig. 2-291. A modern, commercially available sound meter.**

## 2.7 NOISE

Graphically, the three weighting curves described by Eqs. (2.303), (2.304), and (2.305) appear as shown in Fig. 2-292. When the weightings are applied to three of the loudness curves, you see the results in Fig. 2-293, which may take you aback as I have often been. If the objective was to get three curves that were nearly flat, then by helicopter engineering standards the objective was not met. Nevertheless, that is today's precision as built into many sound meters. A constraint has been that many sound meters still use pre-digital electronics.

This brief introduction to acoustics really just brings you forward from 1933 to about 1960. After that, acoustic engineers applied their energy to the entertainment world. Hi-Fi<sup>150</sup> became a popular source for music, then stereo, and now you have surround sound and home theaters—a multibillion-dollar industry. It almost seems that noise created by airplanes and helicopters was inconsequential—at least until after World War II.

The proliferation of airplanes after WWII caused an awareness of noise “pollution” from both propeller- and jet-driven aircraft. It was quickly found that pure tone, A-weighted loudness measurements did little to quantify aviation noise. Then, in 1959, a new scale that quantified the annoyance of aviation sounds was introduced [496] and later refined [497] by Karl Kryter<sup>151</sup>. He introduced Perceived Noise Level (PNL), which went on to become a worldwide parameter when discussing aircraft noise. I will tell you more about PNL later.

### 2.7.4 Propellers and Rotors at Zero Speed

You might be wondering why I have included a short discussion on airplane propellers in this volume dealing with helicopters. First of all, a great deal of propeller noise technology became the foundation for helicopter rotor noise studies. Even during World War I, fighter and bomber aircraft were quite noisy. In fact, propeller tip speeds frequently exceeded sonic Mach number. Then, when United States airlines were started in the early 1920s (funded by the U.S. Post Office [498]), frequent complaints really began (Fig. 2-294). Secondly, several of the early N.A.C.A. reports illustrate some noise fundamentals quite clearly based on propeller static testing. Thus, I can offer you some insight about data and test procedures that carried over to early helicopter main-rotor-noise test results in hover. In this section, you will see several test results from propellers and rotors obtained in the mid-1950s through the 1960s. Static propeller noise measurements can be considered akin to those of a hovering helicopter's tail rotor. I will take up noise prediction in the next section.

---

<sup>150</sup> After graduating from RPI in 1956 and getting a job at Vertol, I quickly saved enough money to build my own hi-fidelity system from Heath kits. At that time, The Heath Company was located in Benton Harbor, Michigan. From their kits, I built a tube-type preamplifier, 15-watt amplifier, and an AM/FM radio, and splurged on a terrific turntable to play 33-1/3 records. I built two solid-mahogany cabinets, one for the electronics and the other for the bass reflex speaker system, which used three Altec Lansing speakers and crossover networks. Now *that* was a real home entertainment system.

<sup>151</sup> Kryter worked at Bolt Beranek and Newman, Inc. in Cambridge, Massachusetts. In October 2009 this well-known and respected research organization became a wholly owned subsidiary of Raytheon.

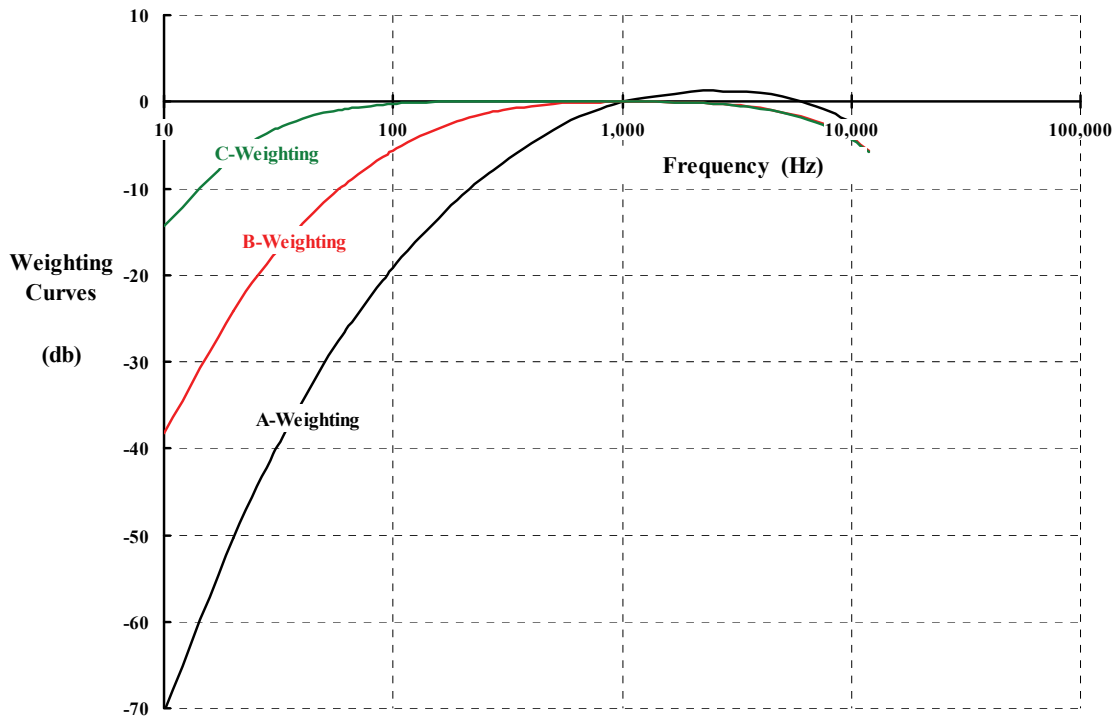


Fig. 2-292. Weighting curves to correct measured sound pressure levels to one digital readout of noise.

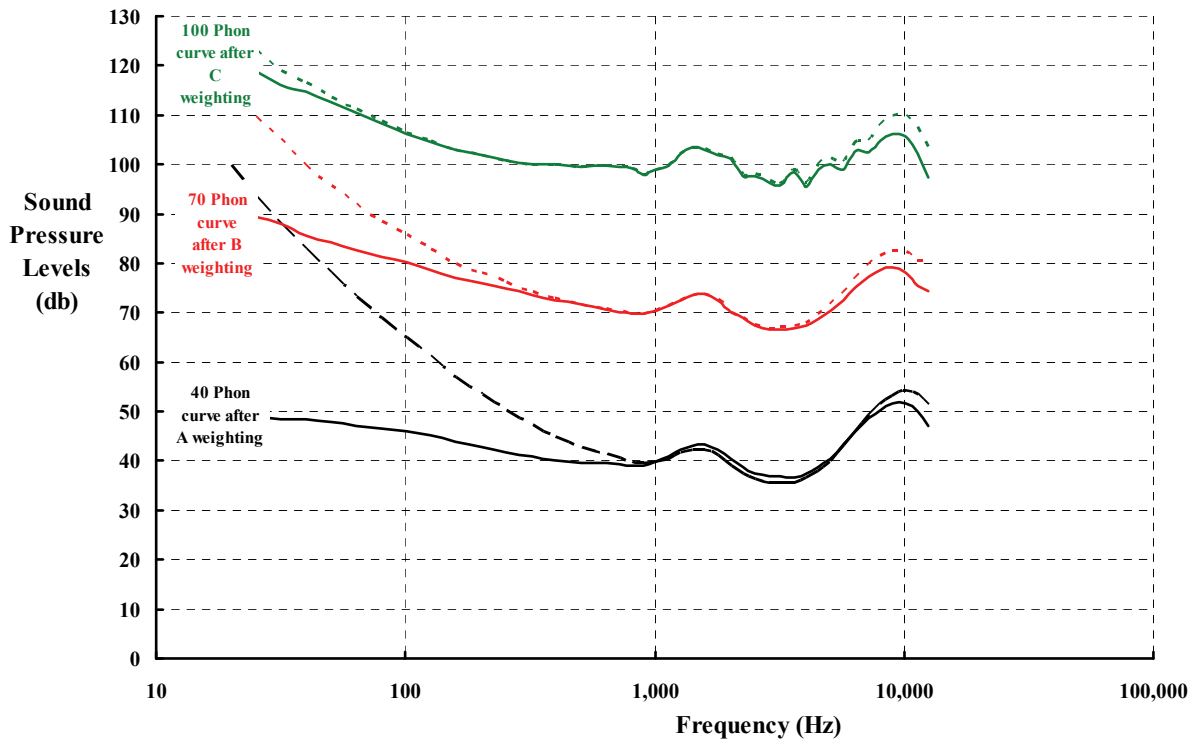


Fig. 2-293. Loudness curves corrected by weighting curves.

FROM SCRAPBOOK OF LEON CUDDEBACK  
CHIEF PILOT OF VARNEY AIRLINES FOUNDED IN 1926

*Dear Aviators One and All  
Please have sense enough to  
stay off from the very pickers as  
the pickers get the lead ache and  
are unable to pick berries on the  
count of your God Damned racket  
By  
Berrie Raisers of Ada County*

Fig. 2-294. Varney Airlines, located in Boise, Idaho, later became part of United Airlines [316]. (Found on the Internet at Stanford.edu under noise.)



Fig. 2-295. The joint Air Force–Navy–NACA supersonic propeller flight research vehicle of the 1950s. Two Westinghouse J-34-W-34 jet engines plus afterburners and one Allison XT-38-A-5 turboprop engine. Prop speeds of 1,700 and 3,600 rpm ground adjustable on gear box assembly. Conventional, maximum 10-foot-diameter prop shown. I believe the prop is shown stopped and feathered in this photo [499].

There is now little question that the propeller of a small, light airplane, all the way up to propellers on the Douglas DC-3 to -7 series and the Lockheed Constellation series, are very loud—no matter what the measurement scale is. This situation was a serious consideration as the transition from propeller-driven to jet-driven commercial transport airplanes was being made during the 1950s and early 1960s. Of course, the maximum speed for efficient propellers was a major point during very vigorous debates about the pros and cons of the two propulsion systems that raged on in that period. But, as airports expanded, many aspects of commercial airplane noise, and its effect on the nearby neighborhoods, became a serious concern. It was a case of wanting increased propulsive efficiency *and* lower noise; one of those cases of wanting our cake and eating it too.

In the 1950s, the N.A.C.A. joined with the Air Force and Navy to conduct flight research on propellers designed for nearly Mach 1 flight speeds. The flight research vehicle was the McDonnell XF-88B shown in Fig. 2-295. The program was declassified in 1958. In the first report about the program [499], the authors stated in their introduction that

“several years ago the National Advisory Committee for Aeronautics realized there was a need for providing continuous research on propellers designed for high efficiency for airplanes of maximum range at speeds up to Mach number 1.0. These propellers would be utilized on airplanes on which range and efficiency of operation were paramount, such as long-range strategic bombers, tankers, long-range assault transports, maximum endurance tactical-fighter bombers, and passenger transports. In order to study the problem as a whole, including operation under installation conditions with a turbopropeller engine providing the driving power, a propeller flight-research program was planned. The airplane chosen for this study was a McDonnell XF-88 turbojet airplane. The research program is a joint Air Force-Navy-NACA effort. The airplane and continuing propeller research equipment are supplied by the U. S. Air Force. The Department of the Navy supplies the turbojet and turboprop engines. The research program and its execution are the responsibility of the NACA.”

The program included noise measurements during ground operation of several propellers [500-505] designed for maximum propeller efficiency at very high advance ratios ( $V/nD$ ) and high flight Mach number. These carefully conducted noise measurements of static propeller operation correspond to the helicopter operating in hover. From these tests, I have selected three propeller noise tests that Max Kurbjun and others reported. The first example comes from NACA TN 3422 in July of 1955 [500] where a “conventional” propeller (the largest at 10-foot diameter) was tested at a tip speed of 877 feet per second. The second example [501] provides noise data at a tip speed of 1,319 feet per second. The third example [503] was the smallest diameter propeller (6.85 feet), and it was tested at a tip speed of 613 feet per second.

The primary data Kurbjun reported in NACA TN 3422 was overall sound pressure levels, which I will discuss shortly, as obtained with a microphone and a tape recorder. The test was a “static” propeller test. Imagine the propeller research airplane (Fig. 2-295) tied down (i.e., static) as if it were running up the propeller prior to beginning a takeoff. Noise was recorded at many azimuth points around the compass rose. The nose was taken as zero degrees, and the noise data was recorded at 15-degree increments in a clockwise sense. Basically, Kurbjun marched around the propeller hub at a 75-foot radius taking data as he went. Kurbjun was also very thorough in describing the sound recording equipment he used.

## 2.7 NOISE

Kurbjun noted in his report that “the 10-foot-diameter propeller investigated in the present report is typical of designs used in today’s aircraft, and the tip Mach number and power loading investigated are representative of those used in current operations.” He noted that the static propeller thrust was 2,080 pounds, the horsepower delivered to the propeller shaft was 1,250 at 1,675 rpm (tip Mach number of 0.79 and tip speed of 877 feet per second), and that the blade angle at the 0.7 radius station was 19.50 degrees. The atmospheric temperature was 47 degrees Fahrenheit and the barometric pressure was 30.27 inches of mercury (Hg). As Fig. 2-296 shows, the four propeller blades each had a constant chord of 1 foot from the 0.4 radius station to the tip, and inboard made a transition to a 4.8-inch cylinder. Kurbjun did not mention the airfoil or the propeller manufacturer.

The measured overall sound pressure levels (OSPLs) Kurbjun recorded are reproduced here in Fig. 2-297 (from figure 4 of his NACA TN 3422). Notice that slightly aft of the propeller plane, close to 115 decibels was recorded, but for all intents and purposes of my discussion here, the noise is about 110 decibels all around the propeller. The predicted noise [506] was derived from two classic reports, both translations from foreign reports: Gutin’s work of 1936 [507] and Yudin’s work of 1944 [508].

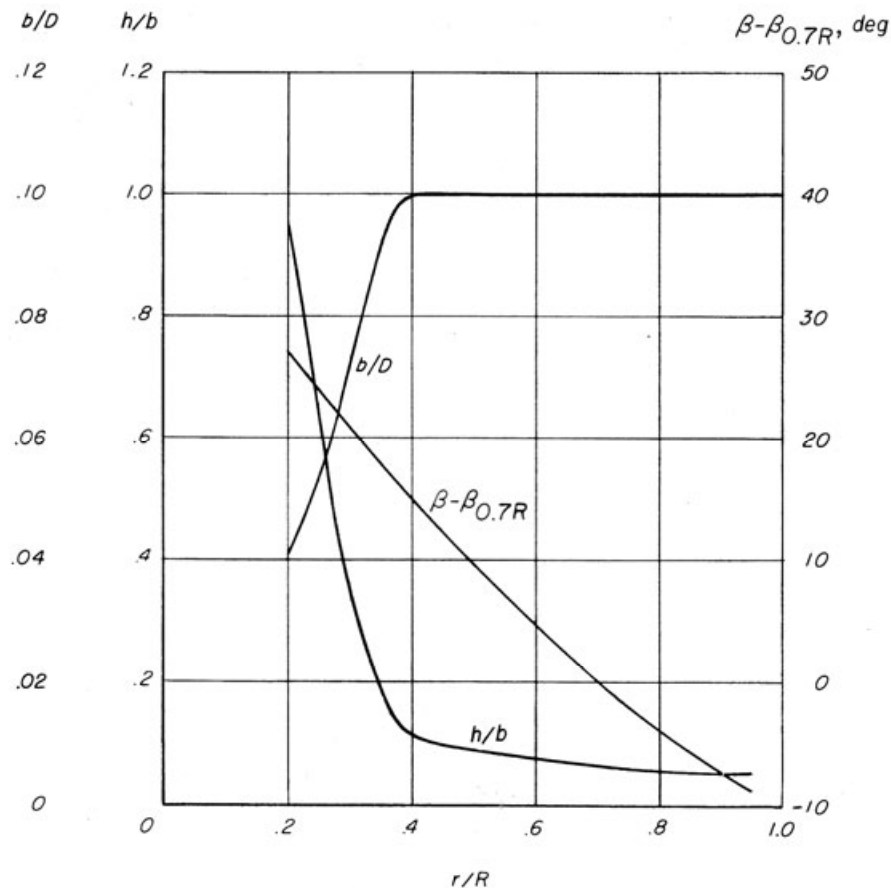


**Fig. 2-296. Four-bladed, 10-foot-diameter propeller blade geometry. Chord is  $b$ , thickness is  $h$ , and diameter is  $D$ . The blade twist,  $\beta - \beta_{0.7R}$ , is nearly linear [500].**

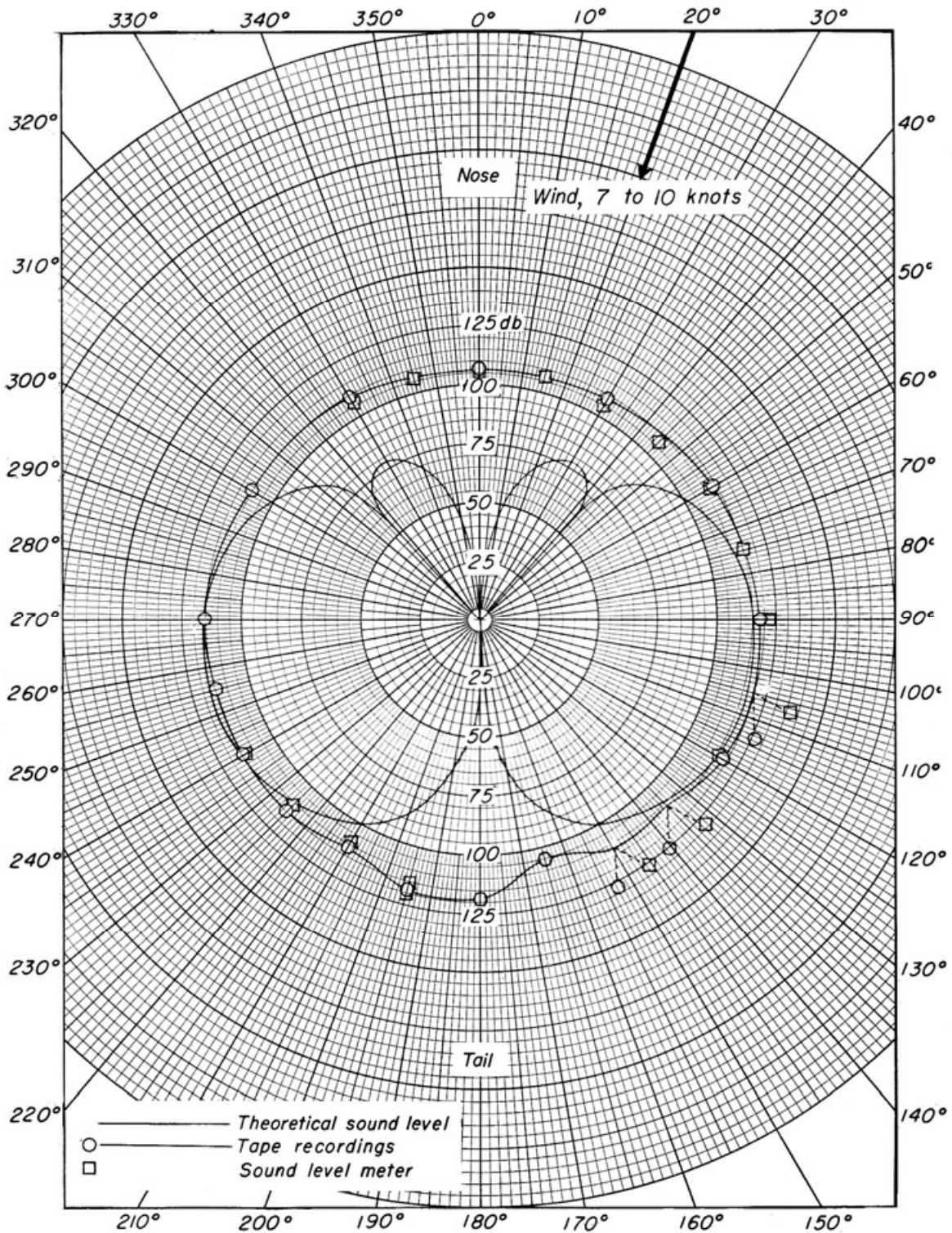


**Fig. 2-297. Overall sound pressure levels at a 75-foot radius from the propeller hub with the propeller operating at 2,080-lb thrust and absorbing 1,250 hp at 1,675 rpm. Tip Mach number of 0.79 [500].**

## 2.7 NOISE

The second propeller [501] was “designed for a forward flight Mach number of 0.95 at an altitude of 40,000 feet.” It had considerably different blade geometry from the “conventional” propeller as you can see by comparing Fig. 2-298 to Fig. 2-296. In this report, Kurbjun made a point of comparing the overall sound pressure levels between this “supersonic” propeller and the “subsonic” propeller as Fig. 2-299 shows. He concluded that a 14-decibel penalty was incurred by the supersonic design, but was careful to note that that “is slightly high as the difference measured was between a three-bladed supersonic propeller and a four-blade subsonic propeller.”

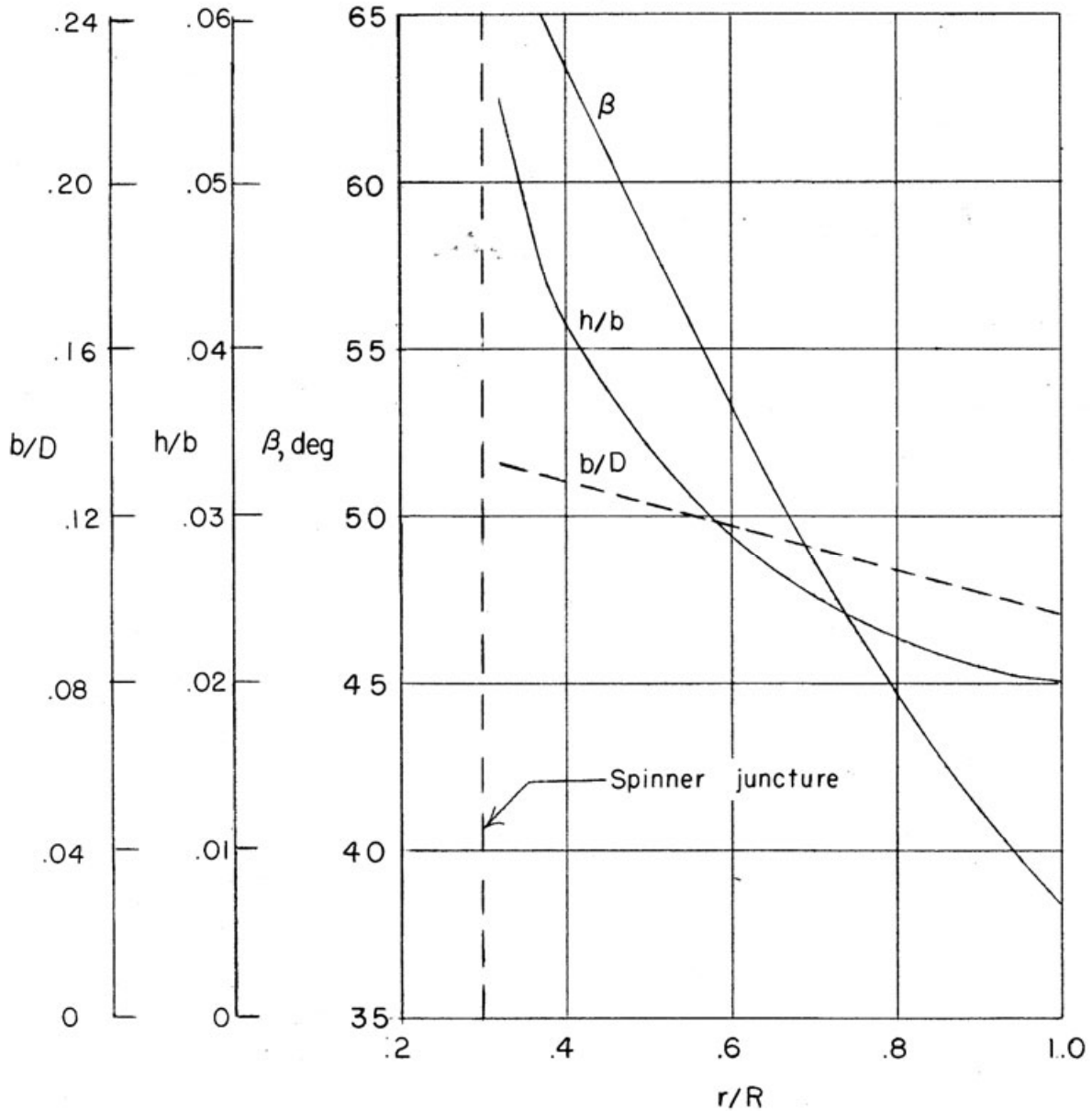


**Fig. 2-298. Three-bladed, 7.2-foot-diameter propeller blade geometry. Chord is  $b$ , thickness is  $h$ , and diameter is  $D$ . The blade twist,  $\beta - \beta_{0.7R}$ , is nearly linear [501].**

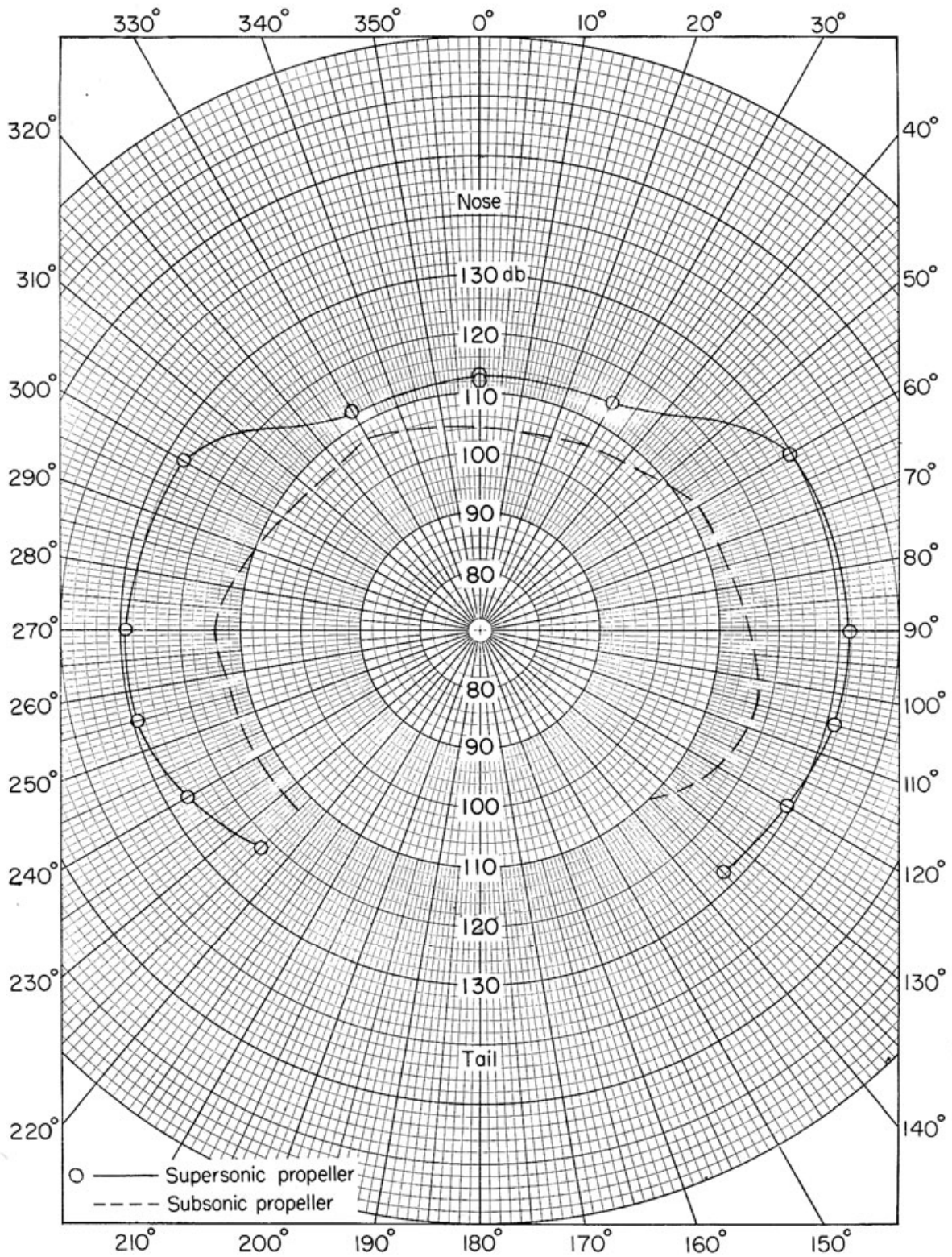


**Fig. 2-299. Overall sound pressure levels at a 100-foot radius from the propeller hub with the propeller absorbing 1,400 hp at 3,500 rpm. Tip Mach number of 1.2 [501].**

## 2.7 NOISE

The third propeller tested [503] was referred to by Kurbjun as a transonic propeller, which had the blade geometry shown in Fig. 2-300. He very conveniently provided a table comparing the several propellers, which I have reproduced here as Table 2-36. The conventional propeller was not included, but he did include a “modified supersonic” type, which I have not included as one of my examples. From Fig. 2-301 you can see that the transonic propeller, designed for an advance ratio of 4.0, was the lowest static noise configuration and nearly on a par with the conventional propeller in Fig. 2-297.

**Table 2-36. Kurbjun’s Propeller Comparison**

Data Source	Propeller Type	Design Forward Mach Number	Design Altitude (ft)	Advance Ratio $J=V/nD$	Solidity at 0.7 R $\sigma_{0.7R} = \frac{Bb}{2\pi r}$	Tip Airfoil Thickness Ratio	Airfoil Thickness Ratio at the Spinner	Tip Mach Number
NASA Memorandum 4-18-59L	Transonic	0.82	35,000	4.0	0.195	0.02	0.070	0.55
NACA TN 4059	Supersonic	0.95	40,000	2.2	0.154	0.02	0.042	1.20
NACA TN 4172	Modified supersonic	0.95	40,000	3.2	0.154	0.02	0.055	0.80

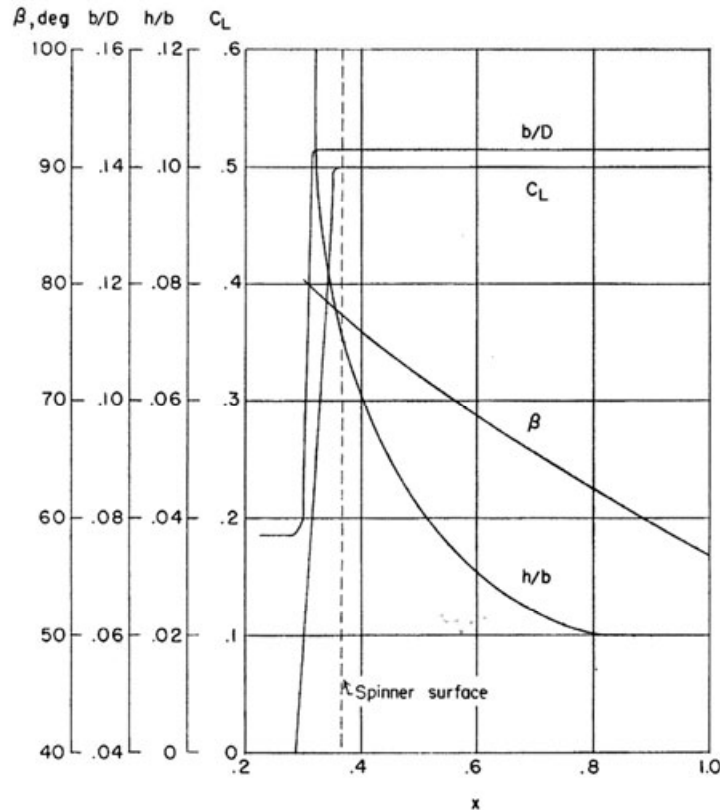


**Fig. 2-300. Three-bladed, 6.85-foot-diameter transonic propeller blade geometry. Chord is  $b$ , thickness is  $h$ , and diameter is  $D$ . The blade twist,  $\beta - \beta_{0.7R}$ , is nearly linear [503].**

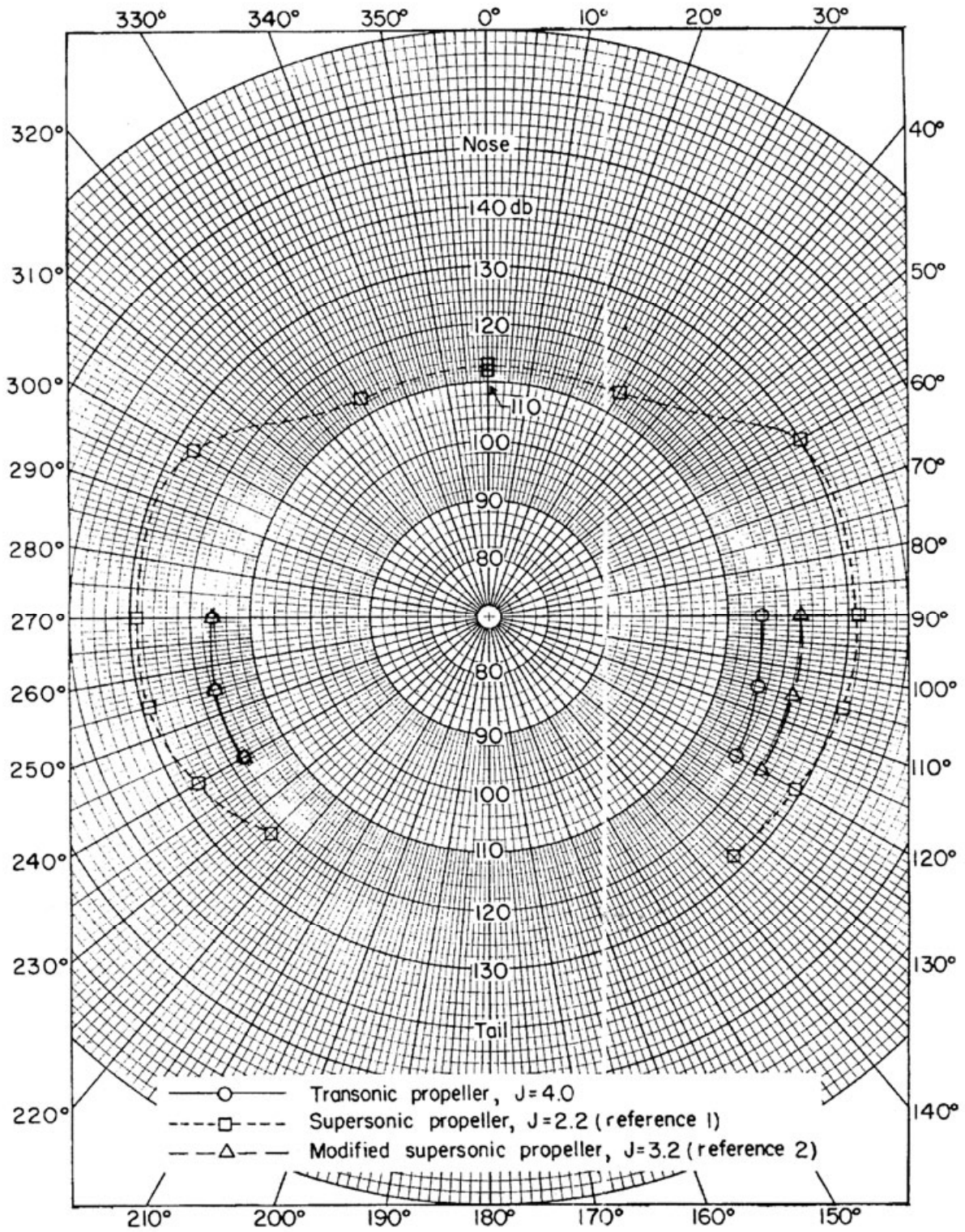


Fig. 2-301. Overall sound pressure level of the transonic propeller nearly achieved the static noise level of the conventional propeller [503].

## 2.7 NOISE

This discussion of propeller noise would not be complete without showing you some forward flight performance. The transonic propeller design appeared most promising with respect to noise at the beginning of a takeoff as Fig. 2-301 shows. This encouraged NASA (the follow-on to the N.A.C.A.) to obtain forward flight performance data. The flight test results were reported by Tom O'Bryan and Jerry Hammack in NASA Memorandum 4-19-59L in May of 1959 [504]. They summarized the transonic efficiency with two charts, one of which I have reproduce here as Fig. 2-302. This data is presented in propeller coefficient form, which was defined in Table 2-15, page 229.

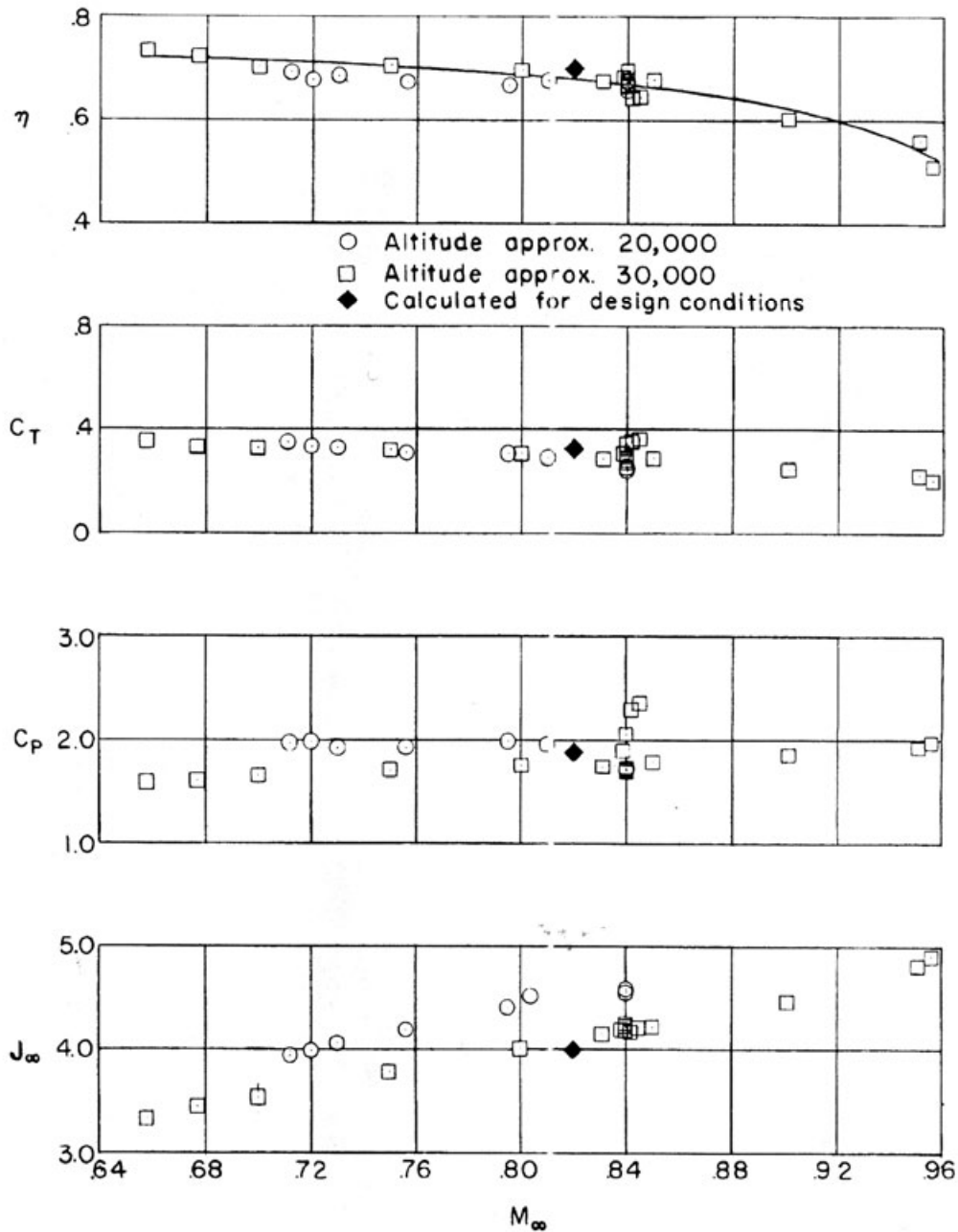


Fig. 2-302. Forward flight performance of the transonic propeller was not great [504].

The forward flight propulsive efficiency of the transonic propeller showed that there would be an appreciable reduction from conventional propeller levels at flight Mach numbers associated with commercial jet transports then being introduced to the airlines. While the noise might have been comparable to the current propeller-driven fleet, the performance demonstrated by the program was not good enough to continue the effort.<sup>152</sup> I will mention that propeller efficiency ( $\eta = C_T J / C_P$ ) was obtained by direct measurement of shaft torque and RPM, but thrust was obtained from integration of propeller wake pressures measured with probes [511]. To me, this always made the thrust coefficient suspect because the wake included airframe interference effects. This, in turn, might have shortchanged the actual thrust leading to a lower propulsive efficiency. I note in passing that the Wright Brothers' propellers achieved an estimated efficiency of 0.66 at about 20 miles per hour (i.e., Mach number of 0.02), so getting the same efficiency at a flight Mach number of 0.84 must constitute real progress!

Lest you think that efforts to reduce propeller noise were not producing results, consider a solution demonstrated by the N.A.C.A laboratory at Langley in 1946 (Fig. 2-303). James Hanson, in his terrific history about the Langley Research Center from 1917 to 1958 [512], included these photos with the caption:

“Langley modified a Stinson L-5 to show that a quiet airplane could be developed. During the lunchtime of the NACA’s annual inspection in 1946, the modified (lower photograph) and the standard aircraft were flown separately over the conference building. Those who witnessed the demonstration were astonished by the relative quiet of the modified L-5.”

I wonder what the berry pickers in Ada County, Idaho would have thought.

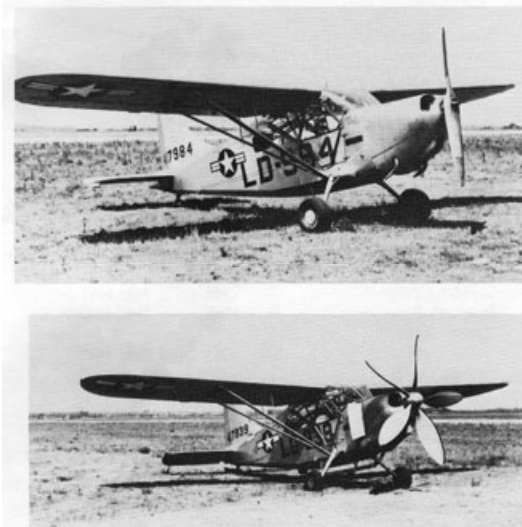


**Fig. 2-303. Noise reduction approach on a Stinson L-5 [513].**

<sup>152</sup> This is not to dismiss an earlier experiment [509]. Here a three-bladed, 9.75-foot-diameter propeller was tested in a wind tunnel up to a free-stream Mach number of 0.96. I found the test results particularly interesting [295] because of potential applications to tiltwing and tiltrotor configurations. And keep in mind that the concerns about the Middle East oil embargo of 1973 and national fuel consumption in the 1970s and 1980s led to a renewed effort to improve turboprop performance with very advanced blade geometry [510]. This program got off to a quick start—flight demonstrated major improvements—and the NASA Lewis Research Center and the entire NASA/Industry advanced turboprop team were awarded the 1987 Collier Trophy.

## 2.7 NOISE

Now let me turn your attention to helicopters and the noise their rotors make.

The recording of early helicopter noise followed much the same patterns and procedures as those used to obtain propeller noise data. In helicopter noise testing, the machine was hovered (generally in ground effect) and measurements were obtained around a compass rose with zero degrees taken off the helicopter's nose. Now let me show you examples of U.S. Air Force and Army noise measurements taken during comprehensive flight evaluation of six helicopters that include two, small tip-driven helicopters. I have also chosen two NASA sets of more detailed results reported in 1973. The time frame of these experiments was from 1958 to 1973.

The ten figures that follow are sequenced according to Table 2-37. The overall sound-pressure-level data for each aircraft show a range of from 75 decibels for the very light OH-6A (hovering out of ground effect at 15 meters, about 50 feet) at a distance of 210 feet from the helicopter's center of gravity, to 140 decibels for the tip ramjet YH-32 at a distance of 50 feet.

The operating conditions for each machine is sketchy at best. In fact, I do not mind saying that noise measurements seemed just an afterthought when compared to cockpit arrangement, aircraft performance, vibration, etc. Therefore the values of parameters in Table 2-37 are, in too many cases, my best educated guess. In general, hover height and tip speeds are clearly reported. After that, I can only share your disappointment in the poor documentation. I have added other comments for each figure.

The following ten figures (Figs. 2-304 through 2-313) constitute a data bank that I will summarize and then use for an overall sound-pressure-level analysis including a test-versus-theory graph.

**Table 2-37. Helicopters Included in Noise Study**

Parameter	Symbol	Units	YHO-2HU	OH-6A	YUH-1D	YUH-1D	S-62A	SH-3A	YH-32	Djinn
Reference			[111]	[514]	[133]	[179]	[515]	[516]	[517]	[518]
Power Source			Piston	Turbine	Turbine	Turbine	Turbine	Turbine	Tip Ramjet	Tip Cold Cycle
Engine			Lycoming 0-360-C2B	Allison T63-A-5A	Lycoming T53-L-9	Lycoming T53-L-9	One CT58-100-1	Two T58-GE-8B	Hiller	Palouste IV
Gross Weight	T	lbs	1,550	2,100	6,600	6,600	7,500	15,600	1,080	1,545
Horsepower	SHP <sub>install</sub>	hp	180	252	1,100	1,100	730	2,500	na	240
Main Rotor										
Diameter	D	ft	25.0	26.33	44	48	53.0	62.06	23.0	36.09
Disc Loading	T/A	lbs/ft <sup>2</sup>	3.16	3.86	4.34	3.65	3.40	5.16	2.60	1.51
Normal RPM			450	470	324	324	228	203	545	380
Tip Speed	V <sub>t</sub>	ft/sec	589	648	746	814	633	659	656	718
Tip Mach Number	M <sub>t</sub>	nd	0.527	0.580	0.669	0.729	0.567	0.590	0.588	0.643
Blades	b	nd	3	4	2	2	3	5	2	2
Chord	c	ft	0.5625	0.5625	1.750	1.750	1.357	1.520	0.7917	0.775
Airfoil Thickness Ratio	t/c	nd	0.15	0.15	0.12	0.12	0.12	0.12	0.12	0.18
Blade Aspect Ratio	R/c	nd	22.22	23.40	12.57	13.71	19.53	20.34	14.53	46.45
Twist	θ <sub>t</sub>	deg	-8.0	-8.0	na	na	-8.0	-8.0	na	-4.0
Tail Rotor										
Diameter	D	ft	3.33	4.25	8.50	8.5	8.75	10.0	2.67	na
Normal RPM			4,131	3,120	1,562	1,562	na	1,243	3,600	na
Tip Speed	V <sub>t</sub>	fps	698	694	695	695	na	669	503	na
Tip Mach Number	M <sub>t</sub>	nd	0.625	0.623	0.623	0.623	na	0.600	0.451	na
Blades	b	nd	2	2	2	2	2	5	1	na
Chord	c	ft	0.2917	0.401	0.701	0.701	na	0.61	0.2917	na
Airfoil Thickness Ratio	t/c	nd	0.15	0.14	0.15	0.15	0.165 to 0.12	0.12	0.15	na
Blade Aspect Ratio	R/c	nd	11.42	5.24	6.06	6.06	na	8.19	4.57	na
Twist	θ <sub>t</sub>	deg	0.0	-5.4	0.0	0.0	na	0.0	na	na
Tethered					Yes	Yes				
Wheels/Skids to Rotor Plane	Hr	ft	7.9	7.2	11.96	11.96	14.2	15.0	7.83	8.6

2.7 NOISE

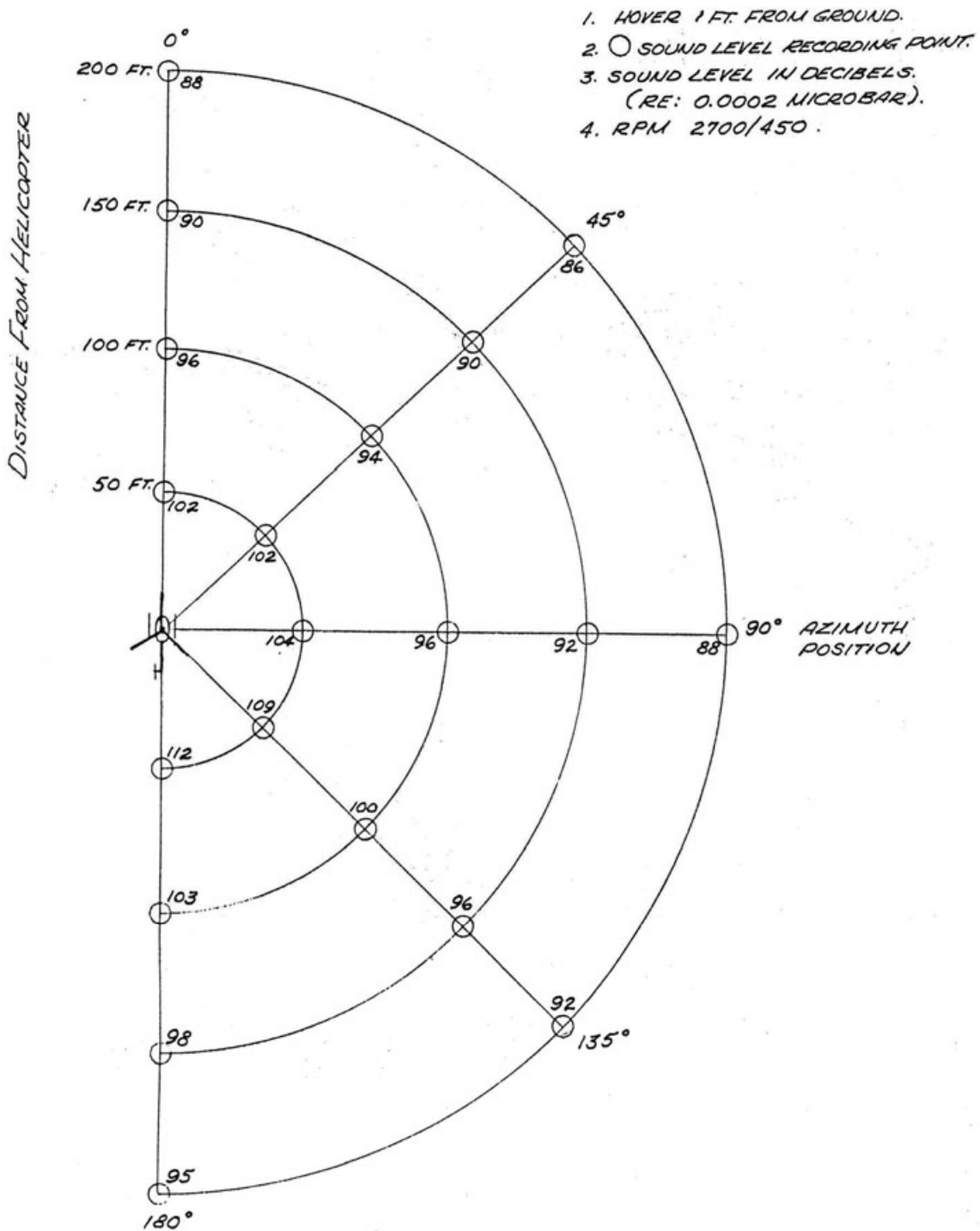


**Fig. 2-304. Noise survey of YHO-2HU in hover at 1-foot skid height. Notice that there is a 10-dB difference between the nose and tail noise at the 50-foot distance. The weight, power, pressure altitude, and outside temperature were not quoted. This data presentation is typical of early U.S. Air Force reports. You will find a dimensioned 3-view of this helicopter on page 345, Fig. 2-195 [111].**

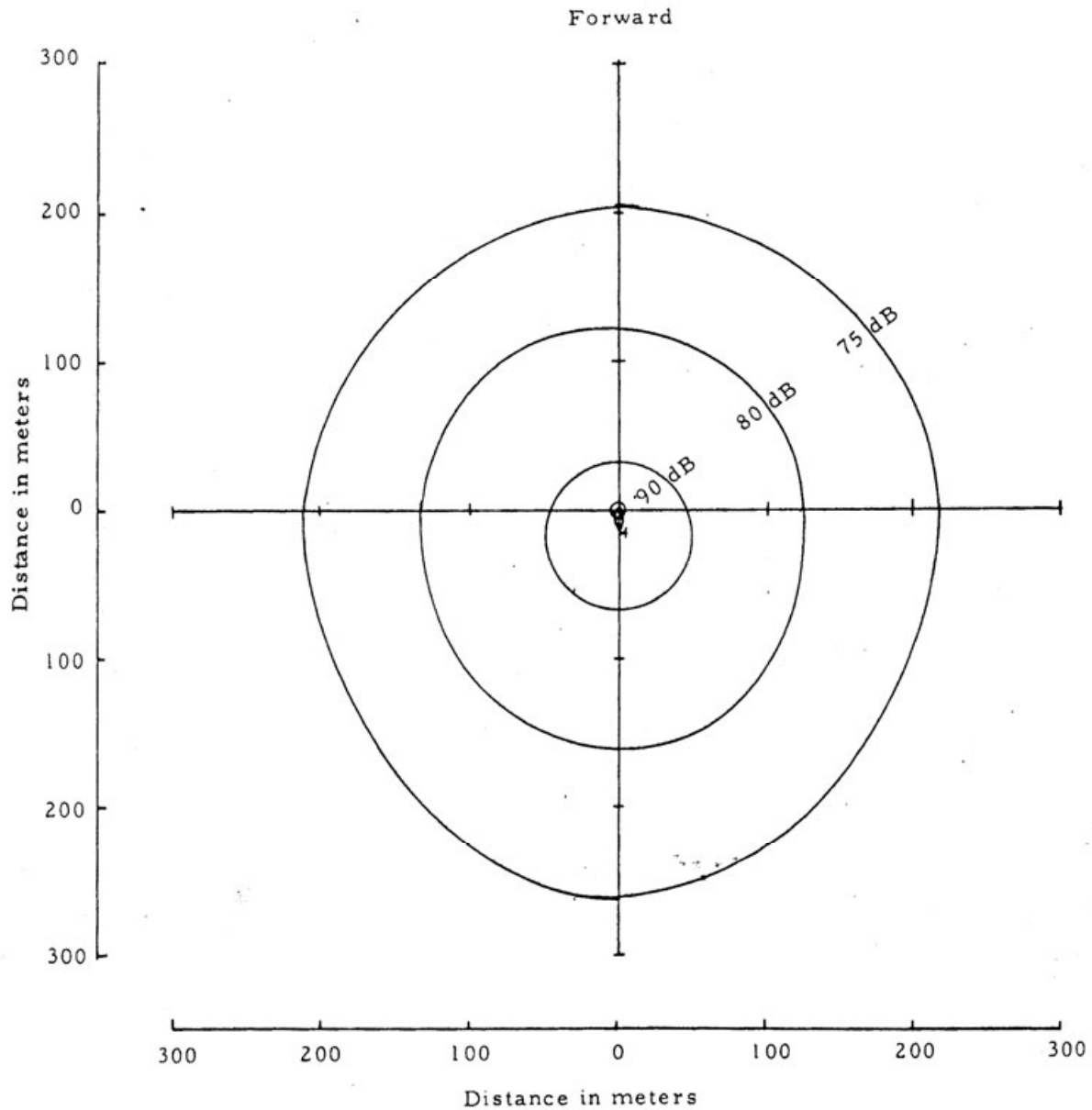


**Fig. 2-305. Noise survey of OH-6A in hover at 15-meters (49-foot) skid height. Note lines of constant decibels format; this was the data presentation format used in the NASA report of the OH-6A and the SH-3A. The weight, power, pressure altitude, and outside temperature were not quoted [514].**

2.7 NOISE

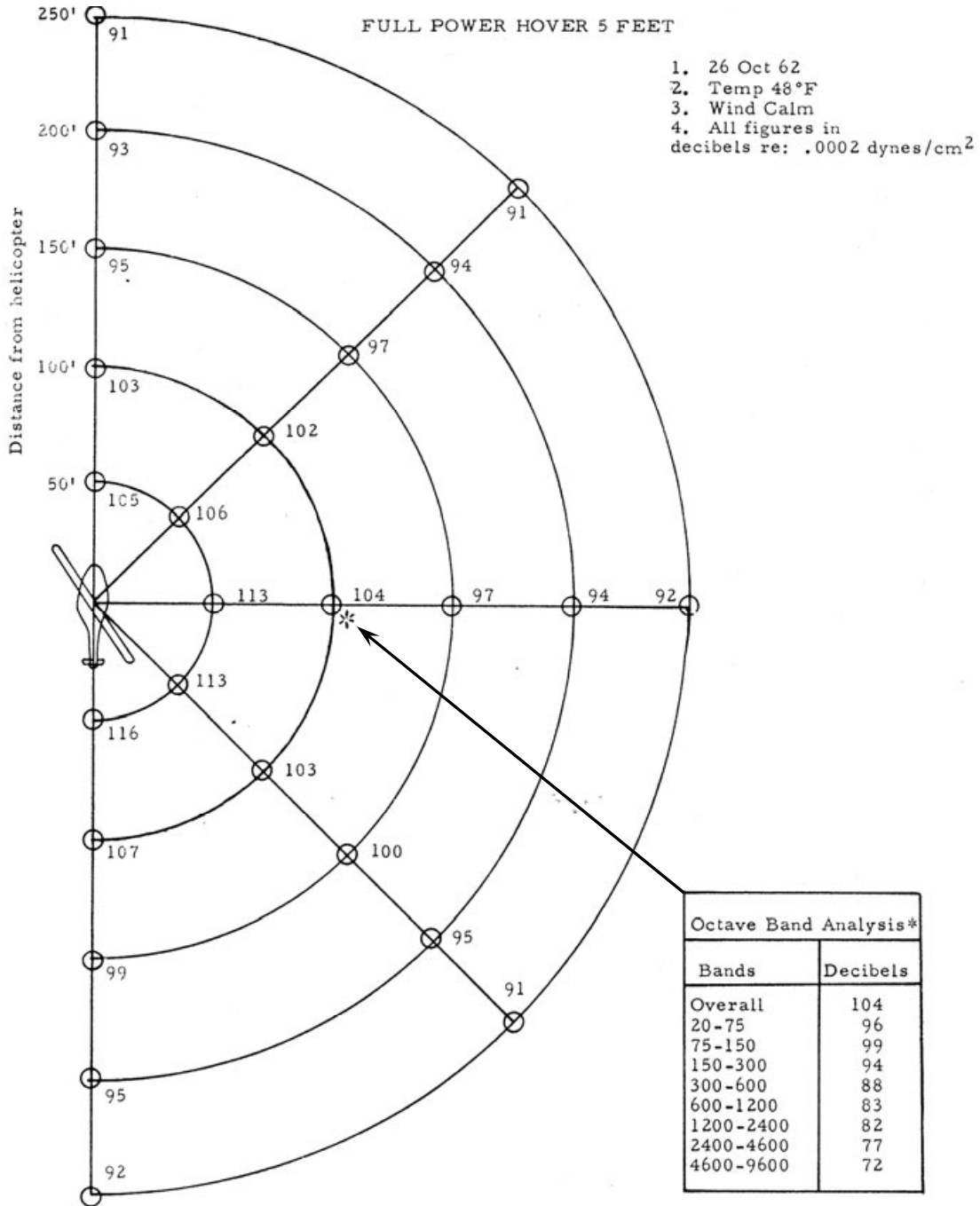


**Fig. 2-306. Noise survey of the 44-foot-diameter YUH-1D in hover at 5-foot skid height. The helicopter was tethered and full power was applied. The thrust and power given in Table 2-37 are my estimates assuming standard density. Note that the outside air temperature was 48°F. I will discuss the octave band analysis (the tabulated data) shortly, but for now note that the data only goes with one circled point at the 100-foot distance to the starboard side of the aircraft. The YUH-1D was also tested with a 48-foot-diameter rotor, which is shown in the next figure [133].**

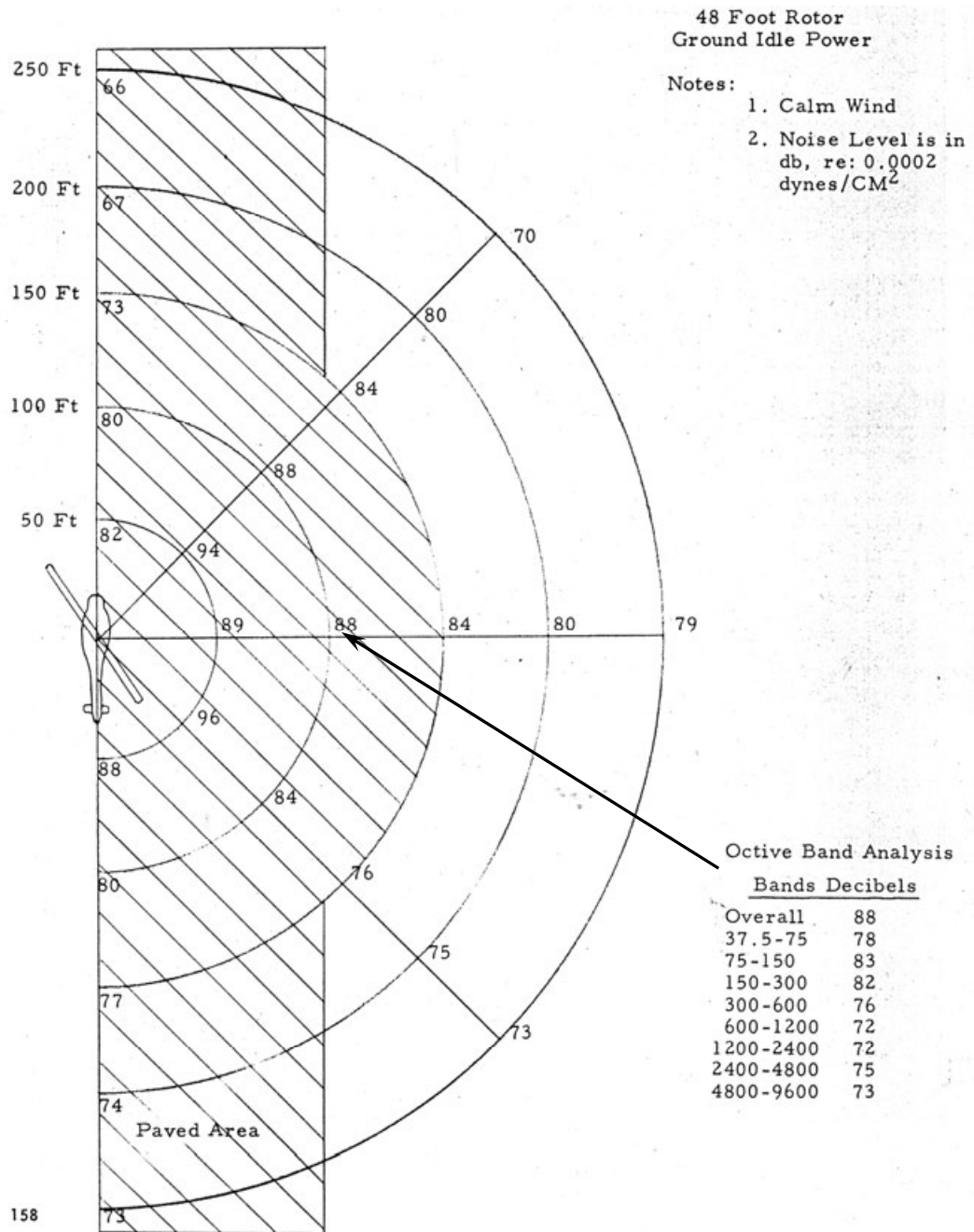
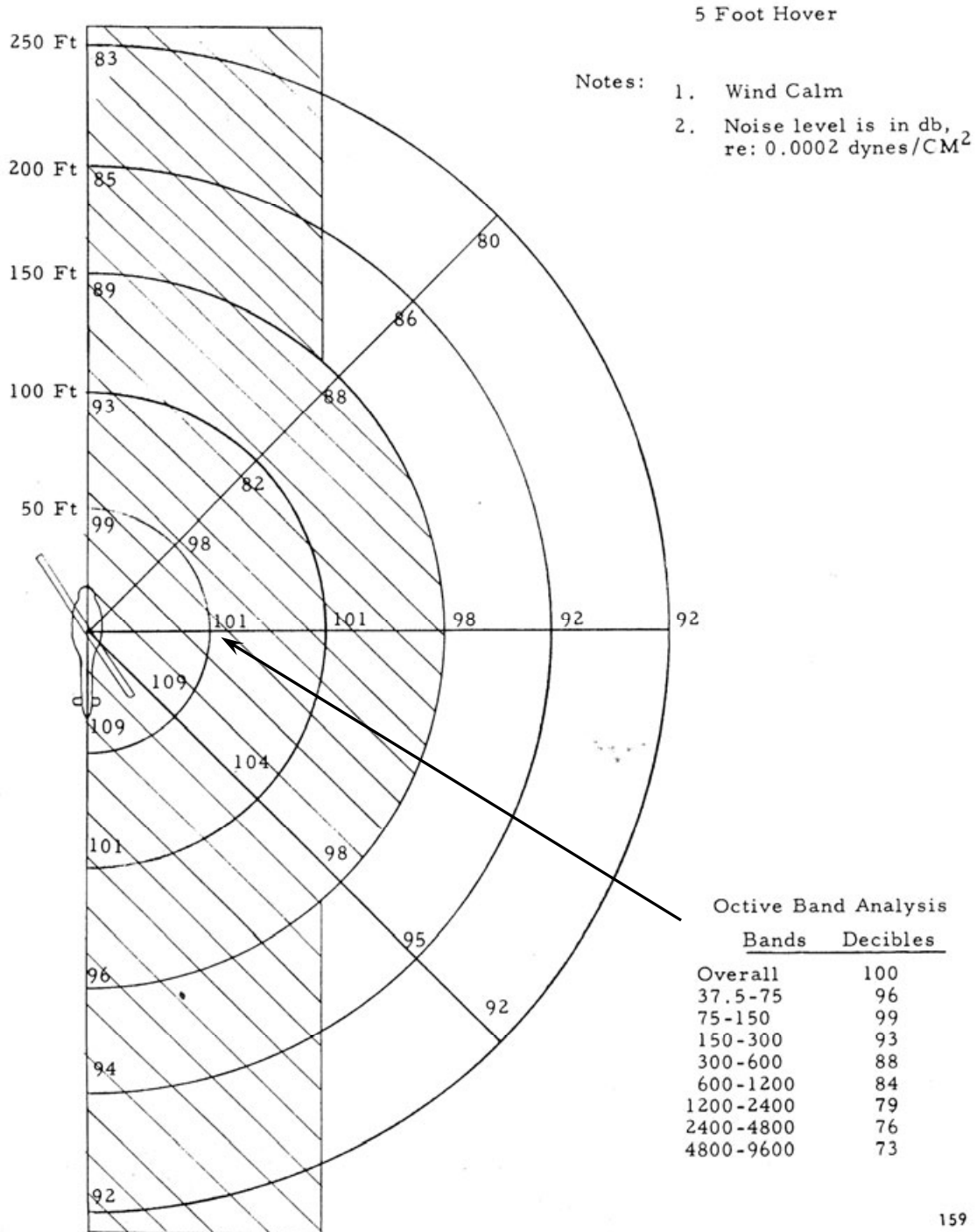


**Fig. 2-307. Noise survey of 48-foot-diameter YUH-1D at ground idle. The thrust should be assumed as zero. My best guess at the ground-idle-power rotor speed is from the pilot's -10 manual, which says 62 percent of 324 rpm [179].**

## 2.7 NOISE



159

**Fig. 2-308. Noise survey of 48-foot-diameter YUH-1D in hover at 5-foot skid height. The helicopter was tethered and full power was applied. The thrust and power given in Table 2-37 are my estimates assuming standard density. Note that the outside air temperature was 48°F. I will discuss the octave band analysis (the tabulated data) shortly, but for now note that the data only goes with one circled point at the 100-foot distance to the starboard side of the aircraft [179].**

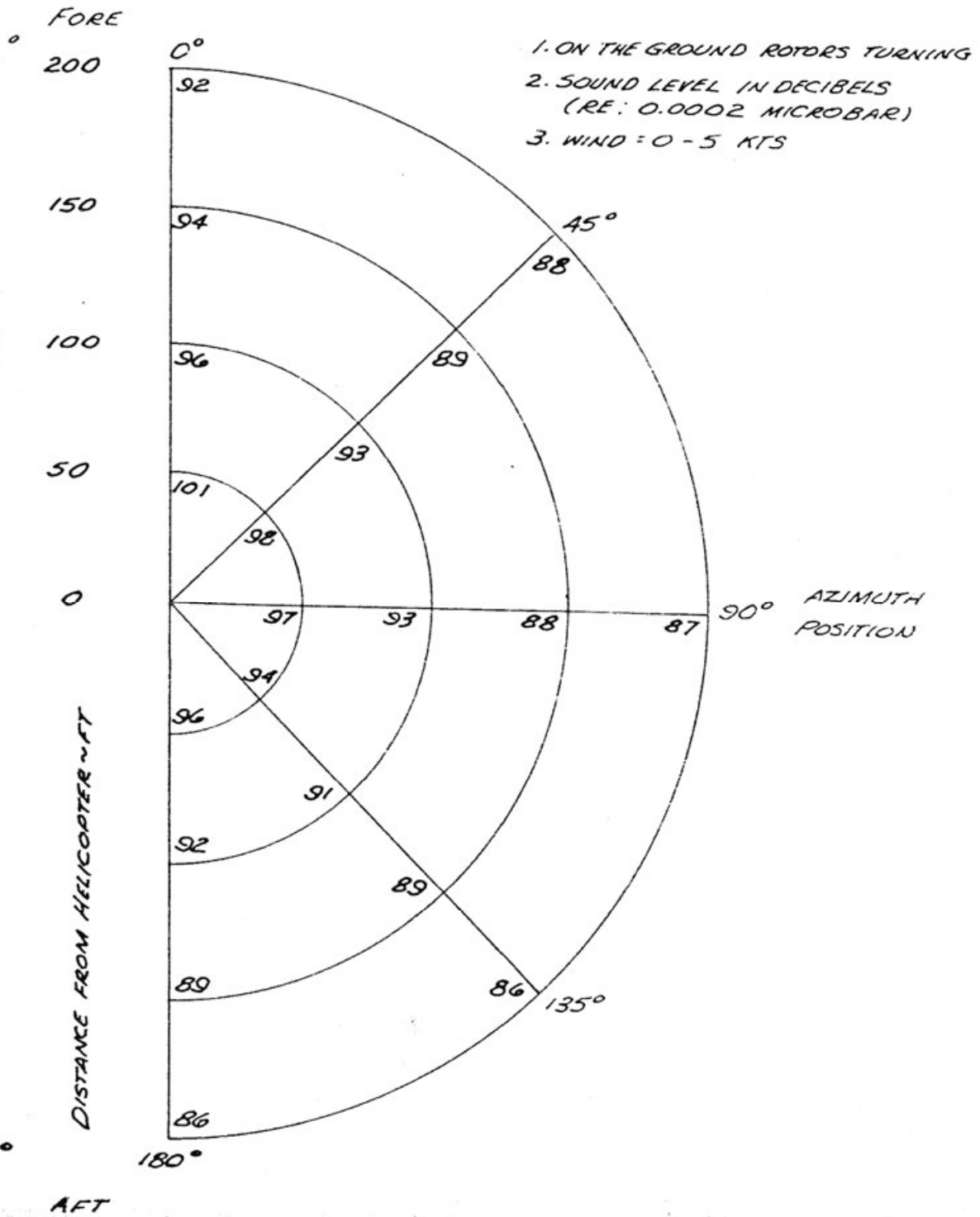


Fig. 2-309. Noise survey of S-62A on the ground, maybe at ground idle, which I would assume is about 60 percent turbine speed [515].

2.7 NOISE

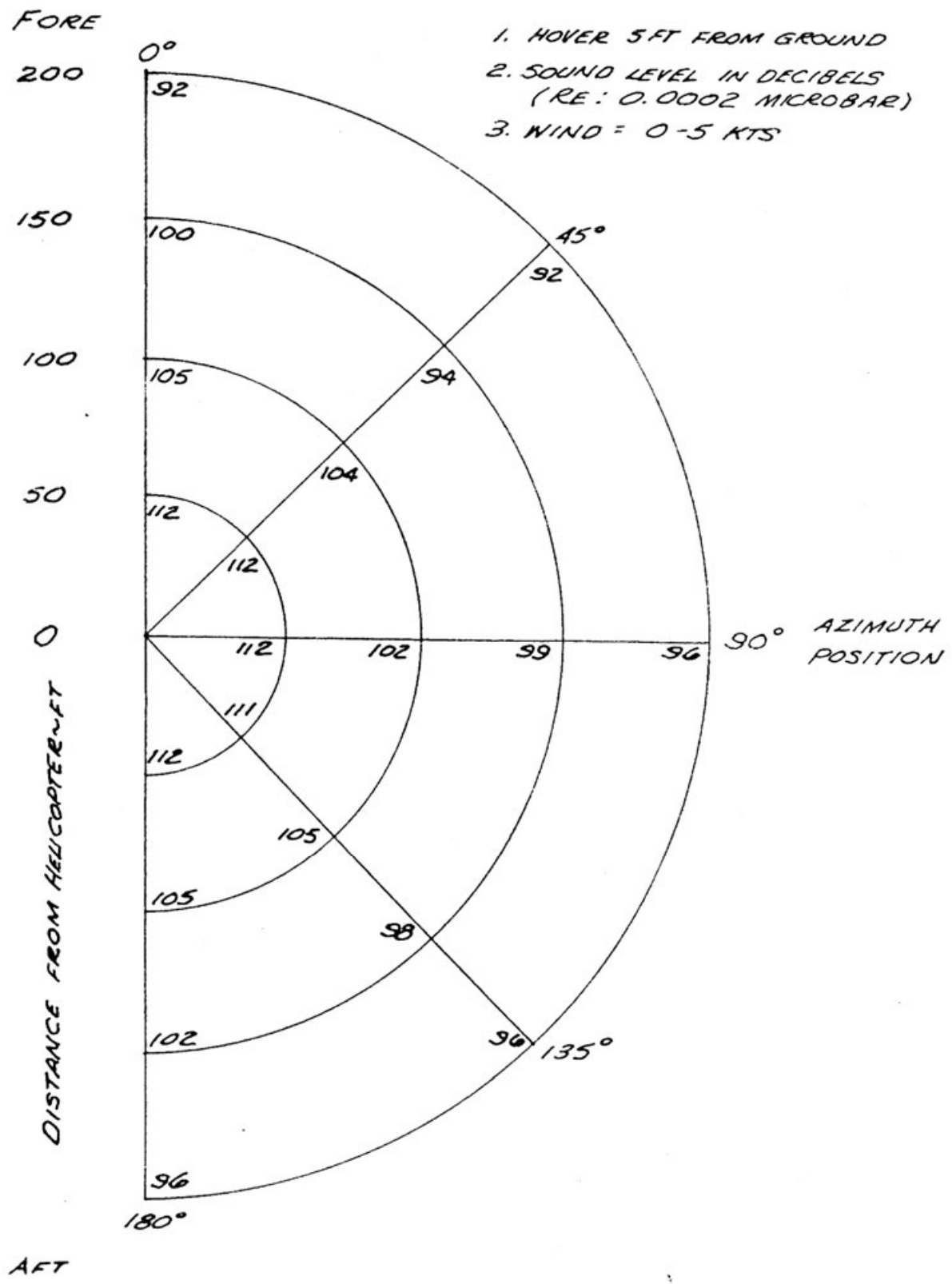
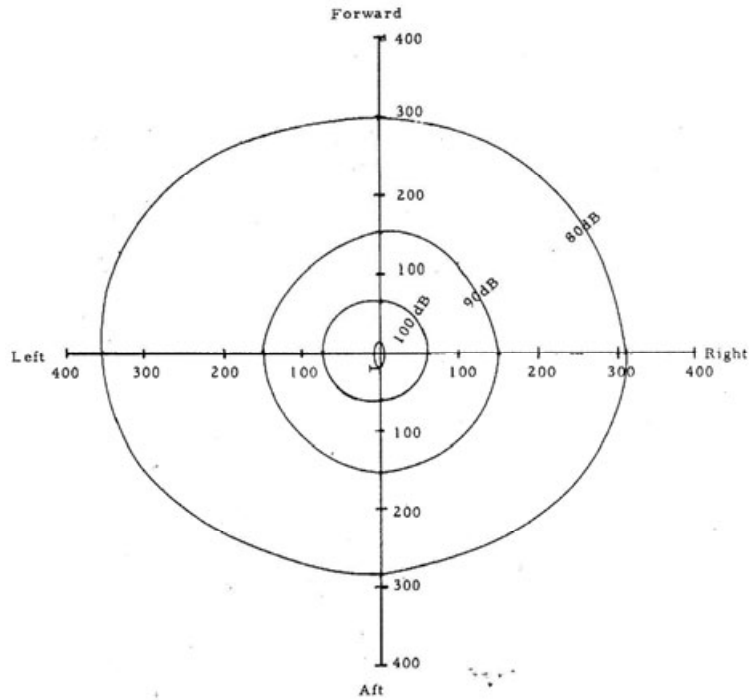
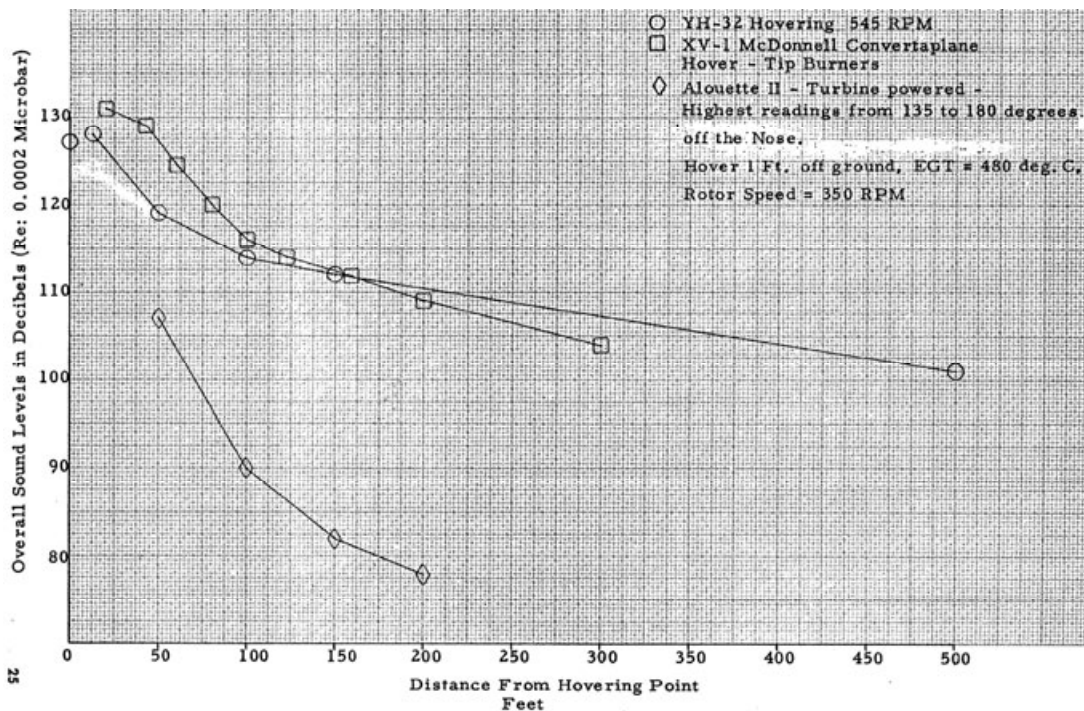


Fig. 2-310. Noise survey of S-62A in hover at 5-foot skid height [515].



**Fig. 2-311. Noise survey of SH-3A in hover out of ground effect at 100-foot skid height. Note: distances in meters [516].**



**Fig. 2-312. Noise survey of YH-32 in hover at 1-foot skid height. This small helicopter had a one-bladed tail rotor. Note: data for XV-1 (a tip-driven compound, which I will discuss in Volume III) and for the French Alouette II was included for comparison [517].**

2.7 NOISE

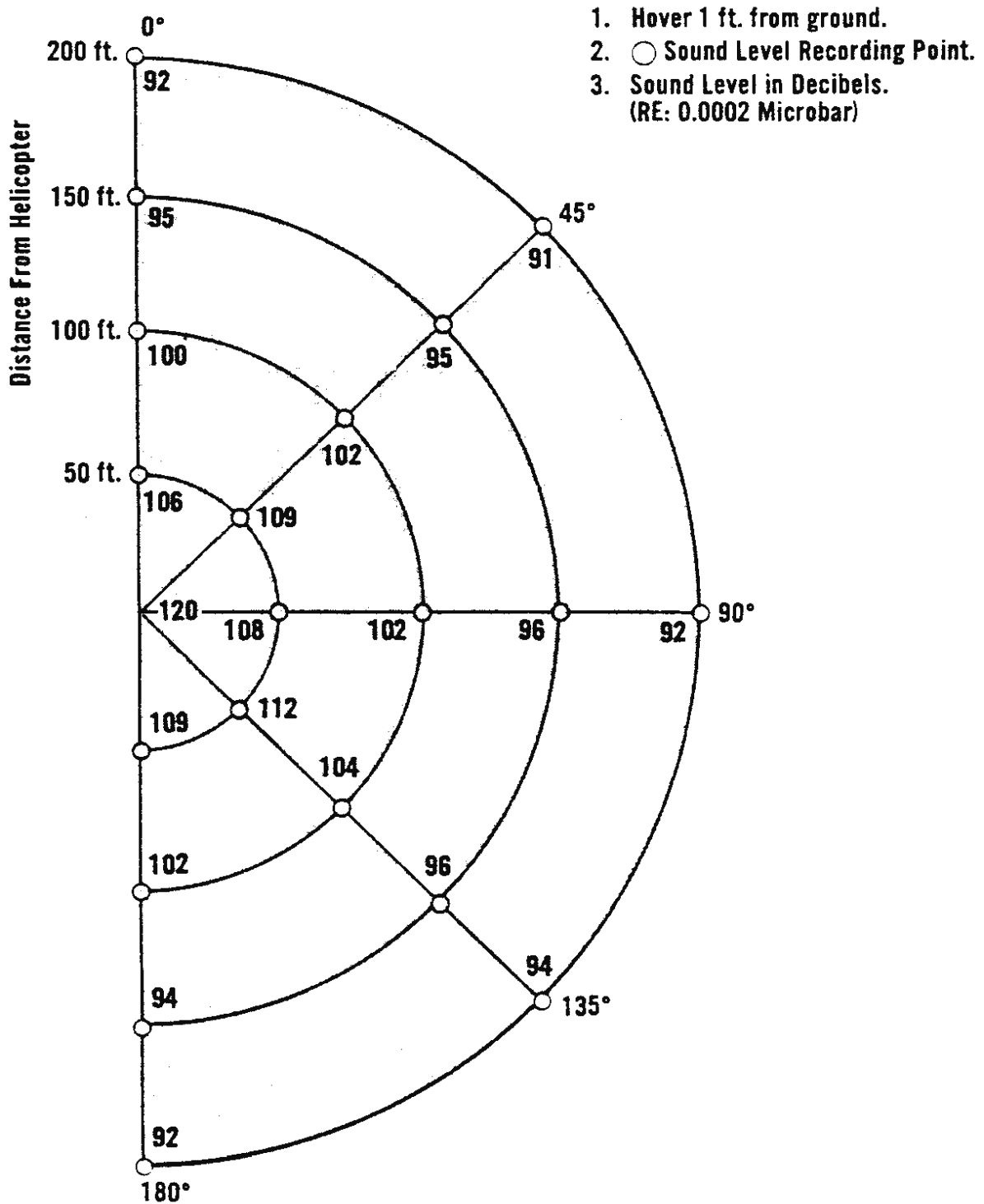


Fig. 2-313. Noise survey of Djinn in hover at 1-foot skid height. The Djinn used a cold cycle, tip-driven main rotor; it had no tail rotor [518].

Now that you have perused the previous ten figures, let me offer one summary shown with Fig. 2-314. Here, I have compared the overall sound pressure levels at the 90-degree compass rose azimuth versus distance from the sound source (approximately each helicopter's center of gravity) for the ten examples.

Note that I have included noise descriptions commonly associated with what people can encounter in their day-to-day lives. Also be aware that ear protection at 95 decibels and above is required by military regulations.

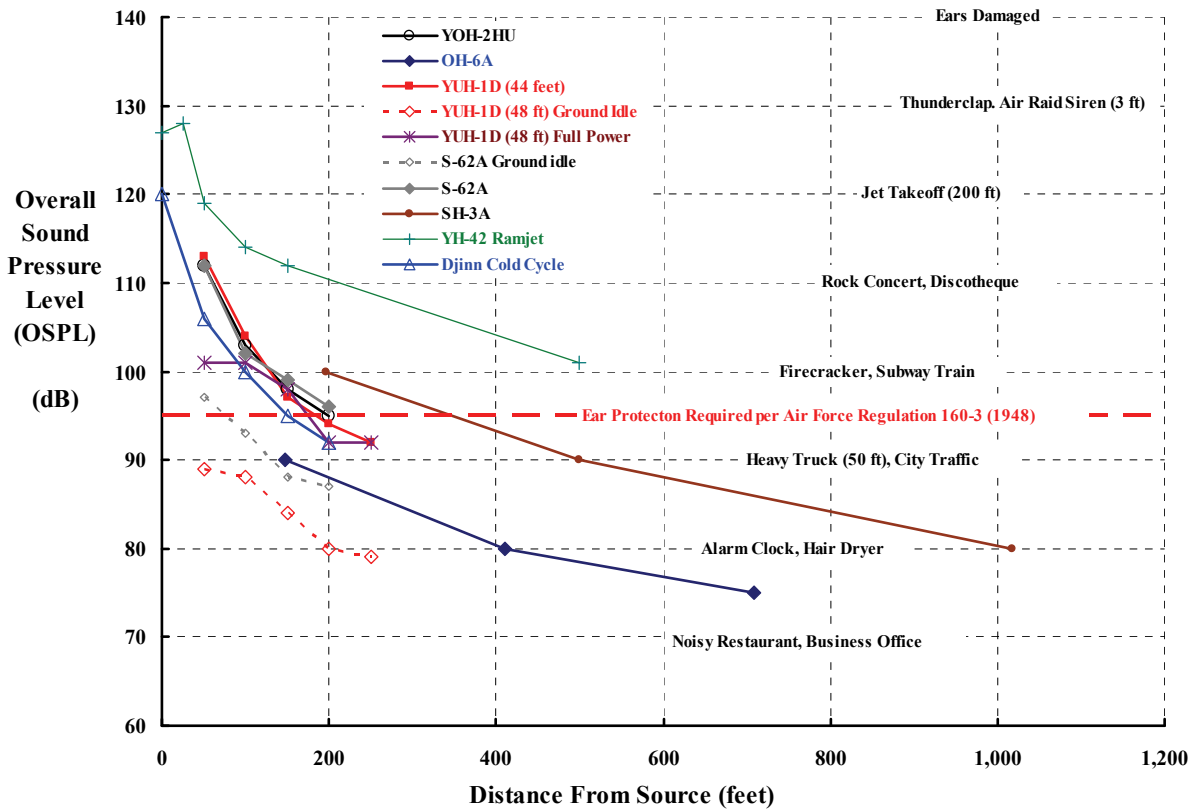


Fig. 2-314. Survey of noise results from several helicopters hovering in ground effect.

**2.7.5 Overall Sound Pressure Level (OSPL) in Hover**

Without going too far back in time, many acoustical engineers believe that the groundwork needed for calculating overall sound pressure level became available in the United States when the N.A.C.A. released translations of two reports [507, 508]. The first of these two reports was written by L. Ya. Gutin (a German); it came out in 1936 and was republished in 1948 as NACA TM 1195. The second, written by E. Ya. Yudin (a Russian), came out in 1944 and was republished in 1947 as NACA TM 1136. These early theories were put to good use at the N.A.C.A. Langley Laboratory and, in fact, throughout the aviation industry.

As a beginning, I think you will find Arthur Deming’s report [519] from 1940 quite helpful. His introduction defines the categories of noise clearly enough to convey with a simple organization chart, which you see in Fig. 2-315. Deming expands his perception, writing:

“The rotation noise is due to the pressure wave enveloping each blade and moving with it; the vortex noise is due to pressure variations on the blade as a result of variations of circulation [thrust]. It may be simply stated that the rotation noise is due to the constant air force on the blades and that the vortex noise is due to the vortices shed in the wake.”

In the 1940s, and for a decade or two more, Deming’s adaption [519] of Gutin’s work to everyday engineering was immensely valuable. Noise (at least due to torque and thrust) could be calculated with a slide rule. Deming and his coauthor, Stowell, also attacked vortex noise [520] following Strouhal’s 1878 work. You will find this report about vortex noise particularly simple, clear, and enjoyable because of the history the authors included.

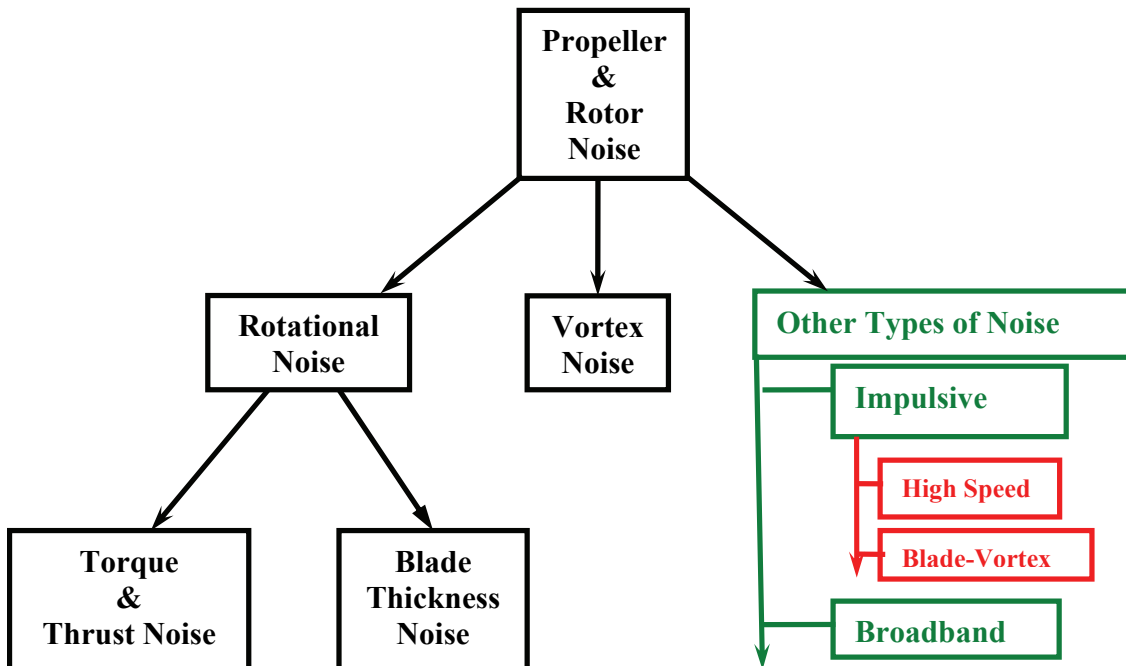


**Fig. 2-315. The noise categories in 1940 with some modern additions.**

A major theoretical step forward came in May of 1969. In that year, J. E. Ffowcs Williams and D. L. Hawkings published *Sound Generation by Turbulence and Surfaces in Arbitrary Motion* in the Philosophical Transactions of the Royal Society of London [521]. This new and firmer foundation to the basic equations needed to calculate how sound waves are propagated was embraced by the acoustic community. (I, however, was simply bowled over by the theoretical derivations because of my totally inadequate set of mathematical skills). Then, in 2003, an application of Williams and Hawkings' work to helicopters by Ken Brentner and Feri Farassat [522] was published, which was (in my opinion) a major contribution. Over a decade of effort by the acoustic community is described in Brentner and Farassat's paper. While the authors note in their paragraph on Preliminaries that "to learn and apply acoustic theory requires considerable mathematical maturity," their inclusion of several theory-versus-test examples brings the whole acoustic field closer to the practicing helicopter engineer. In fact, a useable engineering computer program called WOPWOP was born that has progressed, at Pennsylvania State University under Ken Brentner's guidance, to PSU-WOPWOP [523]. Then a paper that really fell within my level of "mathematical maturity" was published by Gaurav Gopalan in 2008 [524]. Gopalan's paper reduced calculation of helicopter rotor *rotational* noise in hover to an introductory level where computations can be made with a Microsoft® Excel® spreadsheet. Because of Gopalan's work, you have a step-by-step example in this volume of how to arrive at overall sound pressure levels for a helicopter rotor in hover—at least at the introductory level of rotational noise.

There must be several hundred papers and reports dealing with rotorcraft noise as you will quickly conclude from just literature searches [525, 526], conference proceedings [527, 528], and status reports [529, 530]. Several reports having more practical engineering use because of the experimental data included with some theory are references [531-543]. Within this group, there are, in my opinion, three reports that became available between the 1940s and the early 1990s that you might begin with [533, 535, 541].

You should also know that in 1991 Harvey Hubbard compiled and edited NASA Reference Publication 1258 [544], which covered (in Chapter 2) the subject of Rotor Noise written by Fred Schmitz [545]. At that time, Fred was Director of Aeronautics at NASA Ames Research Center. Fred has been an acknowledged expert in the acoustic field for decades.<sup>153</sup> The first six pages of Fred's contribution contain a broad discussion of rotor noise that is immensely valuable. The improvements in measuring equipment, Fred explains, give the insight you see here as Fig. 2-316, which is Fred's third figure. Modern digital electronics allowed seeing the details making up OSPL. A recorded time history of noise could be frequency analyzed in very small frequency bands so rotor noise at each harmonic became quite clear [545]. Furthermore, as Fig. 2-316 shows, noises from other helicopter components were readily identified.

---

<sup>153</sup> When I retired from Bell Helicopter Textron in January 1992 (somewhat after the SuperTeam lost the LHX bid in April 1991), Fred extended an offer to come to NASA Ames. At that time Sue and I were living in Fountain Hills, Arizona. Moving to northern California turned out to be unreasonable in terms of the expensive housing, but the chance to extend my career was very attractive. Fred set me up to go frequently to Ames and make further contributions by working at home. The opportunity to concentrate again on rotorcraft technology was then, and is still, just plain fun. The relationship that contributed to Volume I has now led to this Volume II.

## 2.7 NOISE

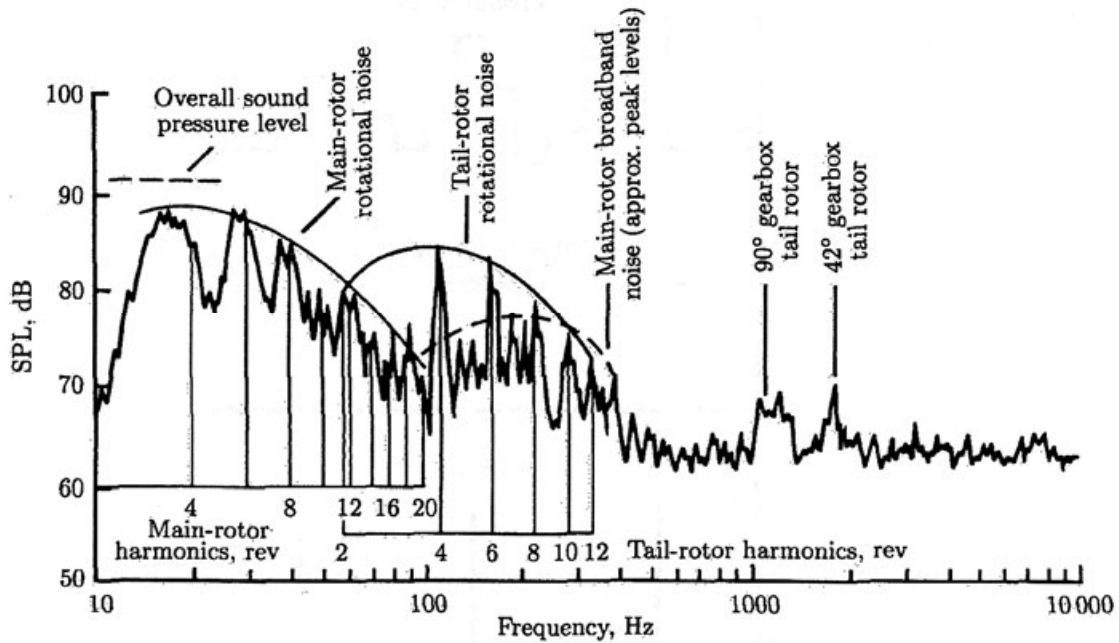


**Fig. 2-316.** The noise generated by a two-bladed Bell UH-1A [545, 546].

You can see from Fig. 2-316 that helicopter overall noise is made up of many tones (i.e., frequencies).<sup>154</sup> Thus, the sound pressure level (SPL) is far from the single-tone hearing experiments that human factors researchers have conducted and analyzed for decades. This multitone character seems to have led to inserting “overall”—the “O” in front of SPL. Overall sound pressure level is calculated with a deceptively simple equation, which is

$$(2.305) \quad \text{OSPL} = 10 \log_{10} \left\{ \frac{1}{p_{\text{ref}}^2} \left[ \frac{1}{T_2 - T_1} \int_{T_1}^{T_2} (p_t^2) dt \right] \right\}.$$

The unit of OSPL is decibels. The reference pressure ( $p_{\text{ref}}$ ) has been somewhat arbitrarily taken as 0.00002 pascals for decades. The sound pressure time history ( $p_t$ ) is measured with a microphone, or calculated by theory, or reported as “racket” by some people.

Sound pressure is displayed as a time history, but because rotor or propeller sound pressure is theoretically periodic, a time history of sound pressure as recorded versus time can be displayed as sound pressure versus an azimuth angle. The waveform may “dance” around a little bit as you saw in Fig. 2-258 through Fig. 2-265 starting back on page 411. This causes a blurring in the waveform, but the basic waveform is generally quite clear, especially in static and wind tunnel testing where an acoustic chamber has been created. Once you have a digitized sound pressure history with time, today’s computer technology makes the sky the limit for analysis questions. Frequently, the waveform is Fourier analyzed to give virtually

<sup>154</sup> When I was plying my trade and when it came to discussing helicopter noise, Harvey Hubbard (NACA), Fred Schmitz (NASA), Charles Cox (Bell), Harry Sternfeld (Boeing Vertol), Ron Schlegel (Sikorsky), Bob Wagner (Hughes), and John Leverton (University of Southampton, before coming to the U.S. to continue his career) were absolute giants in the rotorcraft industry.

exact amplitudes at any harmonic. Acoustic engineers generally do not demand such exact accounting as a Fourier series gives and are satisfied when the periodic sound pressure peaks are clearly visible as in Fig. 2-316.

As a first step, let me introduce you to the OSPL calculations in hover. In a later section, I will discuss the situation in forward flight.

### 2.7.5.1 Thickness, Torque, and Thrust Noise From an Ideal Rotor

The approach to calculating rotor sound pressures that a microphone records *really* became much clearer to me in January of 2008. In that year, Gopalan from the University of Maryland (under Fred Schmitz's encouragement) presented a paper [524] at the AHS Specialists' Conference on Aeromechanics, which was held in San Francisco. Gopalan<sup>155</sup> arrived at a simple engineering result that I think you will find is absolutely perfect for an introductory calculation of overall sound pressure level due to rotational noise.

Gopalan, using some very creative applied mathematics, translated the fundamental theory Williams and Hawkins offered in 1969 [521] into very useable engineering equations. He restricted his work to calculating sound pressure only in the far field, which meant that the distance  $(S = \sqrt{X^2 + Y^2 + H^2})$  from the rotor hub to the observer (obs) in Fig. 2-317 is considerably greater than the rotor radius (R).

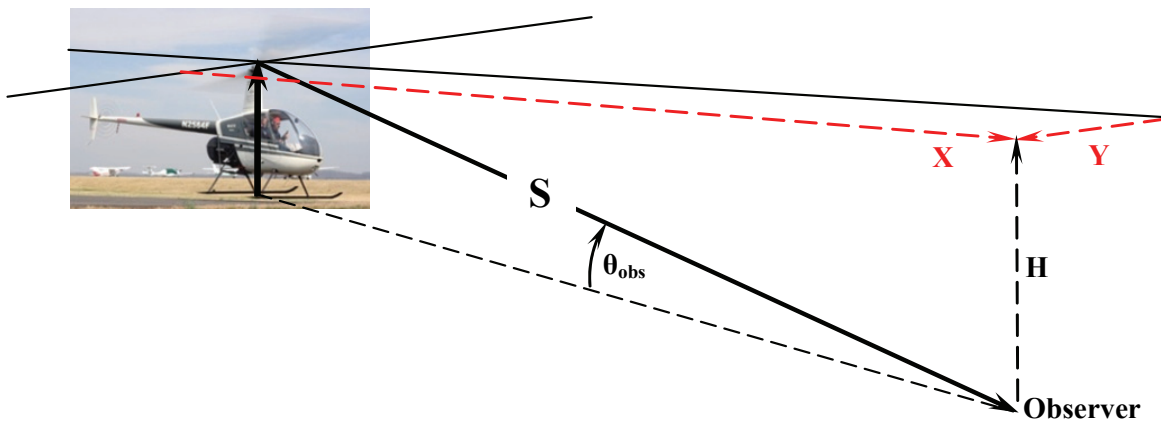


**Fig. 2-317.** The distance between the main rotor hub and the observer is considerably greater than the rotor radius in the prediction of noise in the far field. Note that  $\theta_{obs} = \arcsin (H/S)$ .

<sup>155</sup> Gaurav Gopalan met with a very unfortunate death in September 2011. Fred Schmitz' tribute to Gaurav's life and accomplishments was published in the Winter 2011 issue of the AHS *Vertiflite* trade magazine [547]. We lost an exceptionally valuable contributor that I was quite ready to place in the group offered in the preceding footnote.

## 2.7 NOISE

To illustrate the application of Gopalan's work, let me start with calculating thickness sound pressure. Thickness pressure is created because all real propeller and rotor blades have airfoils with thickness-to-chord ratios ( $t/c$ ) varying between 0.02 and 0.18. You proceed as follows for this component of rotational noise:

$$(2.306) \text{ Thickness } p_{\psi} = K_{\text{thickness}} (F_{M,\psi}) \text{ for one blade}$$

where the variation of thickness pressure ( $p_{\psi}$ ) with the master blade's azimuth ( $\psi$ ) is also dependent on an "equivalent" Mach number ( $M = M_{\text{tip}} \cos \theta_{\text{obs}}$ ) so that ( $F_{M,\psi}$ ) is computed as

$$(2.306) F_{M,\psi} = \frac{M^3}{(1 - M \sin \psi)^4} \left[ \begin{array}{l} M(40 + 10 \cos^2 \psi + 28M^2 \cos^2 \psi + 11M^2 \cos^4 \psi) \\ - \sin \psi (30 + 10M^2 + 6M^4 \cos^2 \psi + 35M^2 \cos^2 \psi - 18M^4 \cos^4 \psi) \end{array} \right]$$

Gopalan found that he could account for an observer who was not exactly in the plane of the rotor by defining the ( $M$ ) in Eq. (2.306) as  $M = M_{\text{tip}} \cos \theta_{\text{obs}}$ . The configuration constant ( $K$ ) is calculated as

$$(2.307) K_{\text{thickness}} = \rho a_s^2 \left[ \frac{S_f \left( \frac{c}{R} \right)^2 \left( \frac{t}{c} \right)}{240 \pi \left( \frac{S}{R} \right)} \right]$$

where the parameters are defined by Table 2-38 on page 476. You might immediately note in this equation for the configuration thickness constant ( $K_{\text{thickness}}$ ) that Gopalan put all blade geometry and the observer distance as ratios, and therefore everything within the [ ] of Eq. (2.307) is dimensionless. To me this is a sign of a good engineer. This makes the units of  $K$  solely dependent on the density and the speed of sound. Gopalan states in his list of symbols that density (on a standard day) is, in the metric system, 1.225 kilograms per cubic meter, and the speed of sound is 340.29 meters per second. Thus, the product ( $\rho a_s^2$ ) becomes 142,360 newtons per square meter, which is 142,360 pascals.<sup>156</sup>

The sound pressure created by the rotor thrust and the torque (actually just the ideal induced torque) was also estimated by relatively simple equations when you follow Gopalan's work. Thrust sound pressure is my shorthand for what helicopter acoustic engineers call "out-of-plane loading" noise. The plane these engineers refer to is the tip path plane. For thrust sound pressure *per blade*, Gaurav offered the following approximation:

$$(2.308) \text{ Thrust } p_{\psi} = L_{\text{thrust}} (D_{M,\psi}) \text{ for one blade}$$

where the variation of thrust sound pressure ( $p_{\psi}$ ) with the azimuth ( $\psi$ ) of the master blade is also dependent on the equivalent Mach number ( $M = M_{\text{tip}} \cos \theta_{\text{obs}}$ ), so that ( $D_{M,\psi}$ ) is computed as

---

<sup>156</sup> In the English system of units, you have 0.002378 slugs per cubic foot for density and 1116.45 feet per second for the speed of sound, which results in 2,962 pounds per square foot on a standard day.

$$(2.308) D_{M,\psi} = \frac{M^2 \cos \psi [20 - 20M \sin \psi + 9M^2 \cos^2 \psi]}{(1 - M \sin \psi)^3}.$$

The configuration constant ( $L_{\text{thrust}}$ ) is calculated as

$$(2.308) L_{\text{thrust}} = (\rho a_s^2) \left( \frac{T/A}{\rho a_s^2} \right) \left( \frac{R}{120 bS} \right) (\tan \theta_{\text{obs}}).$$

For the sound pressure created by applying torque to turn the rotor (called “inplane loading” noise), Gopalan gave the approximation that

$$(2.308) \text{Torque } p_{\psi} = L_{\text{torque}} (H_{M,\psi}) \text{ for one blade}$$

where

$$(2.308) H_{M,\psi} = \frac{\cos \psi \left[ \begin{array}{l} 60 + 30M^2 \cos^2 \psi - 120M \sin \psi - 30M^3 \sin \psi \cos^2 \psi \\ + 80M^2 \sin^2 \psi + 9M^4 \sin^2 \psi \cos^2 \psi - 20M^3 \sin^3 \psi \end{array} \right]}{(1 - M \sin \psi)^3}.$$

The configuration constant for torque ( $L_{\text{torque}}$ ) is calculated as

$$(2.309) L_{\text{torque}} = (\rho a_s^2) \left( \frac{T/A}{\rho a_s^2} \right)^{3/2} \left( \frac{R}{120\sqrt{2} bS} \right) (\cos \theta_{\text{obs}}).$$

There are, of course, several restrictions to the broad use of Gopalan’s equations that you must be aware of. The most important restrictions are:

1. The rotor being analyzed is an ideal rotor, which is to say that the induced velocity is uniform over the whole rotor disc. This uniform induced velocity ( $v$ ) is calculated as  $v = \sqrt{T/2\rho A}$  as you learned from momentum theory. A rectangular blade having a twist distribution of  $\theta_x = \theta_{\text{tip}}/x$  will theoretically produce uniform induced velocity in hover as Gessow and Myers demonstrate on pages 57 and 58 of their classic book, *Aerodynamics of the Helicopter* [234].
2. The rotor blades are represented by a lifting line, not a lifting surface, in the calculation of thickness noise so an approximation to a real airfoil is introduced in Eq. (2.307) using the airfoil constant ( $S_f$ ), which is equal to 0.685 for the NACA 00xx series airfoils.
3. The rotor blades are required to be rectangular (i.e., constant chord) and have a relatively high aspect ratio because of the lifting line assumption. Most helicopter main rotor blades fit this criteria, but this restriction tends to bring most tail rotor blades somewhat into question.
4. The rotor blades are required to have a constant thickness airfoil from root to tip.

To me, this is a small list of restrictions to a set of sound pressure estimating equations that can easily be solved using a simple spreadsheet calculator such as Microsoft® Excel®.

## 2.7 NOISE

The last point I want you to understand deals with the addition of pressures when there is more than one blade. The noise from, say, a three-bladed rotor is not just three times the noise calculated for one blade. Sound pressures are added at the observer location, not the source (i.e., hub) location. It takes time for the sound pressure waves to go from each blade (i.e., an individual sound source) to the observer (i.e., the microphone and onto a digital tape). While a stroboscope will show you where the blades are in azimuth, your stopwatch will be the real abscissa in graphing pressure versus time. This is similar to seeing a lightening flash, but hearing the thunder a short time later. An oscillograph recording the microphone's response would show a graph of pressure versus *observer* time. Fortunately, observer time is related to blade azimuth (i.e., the source's reference) by the following simple relationship:

$$(2.310) \quad t_{\text{obs}} = \left( \frac{S}{a_s} + \frac{R \cos \psi}{a_s} + \frac{\psi}{\Omega} \right) - \left( \frac{S}{a_s} + \frac{R}{a_s} \right) = \frac{R(\cos \psi - 1)}{a_s} + \frac{\psi}{\Omega}.$$

Here, I have taken Gopalan's expression and made time be zero when the master blade is at zero azimuth, which is generally taken as over the tail boom for a single rotor helicopter. You might wonder about the term  $(\cos \psi - 1)$ . This reflects the distortion in the waveform that is caused by the Doppler effect. The Doppler effect creates the difference in sound *tone* (not just noise level) that you hear from a train's horn when the train is coming towards you and when it is leaving your observer position.

Frankly, I found it much more informative to express observer time ( $t_{\text{obs}}$ )—which would be digitized time in seconds with modern instrumentation—as a pseudo azimuth angle in degrees. That is, Eq. (2.310) can be multiplied through by rotor speed ( $\Omega$ ), and then you have

$$(2.311) \quad \psi_{\text{obs}} = \Omega t_{\text{obs}} = \frac{\Omega R(\cos \psi - 1)}{a_s} + \psi = M_{\text{tip}}(\cos \psi - 1) + \psi,$$

which illuminates the tip Mach number ( $M_{\text{tip}} = V_t/a_s$ ) as the measure of how long it takes for the sound to leave its source until the digitizing microphone signal is recorded—not counting any instrumentation delays. An example of this difference in sending and receiving “time” expressed in degrees is shown in Fig. 2-318 for a rotor having a tip Mach number of 0.60.

Note on Fig. 2-318 that a stroboscope might show the master blade at a source azimuth of 150 degrees, but your ears and the instrumentation would perceive the noise coming from the blade when it was at 60 degrees. In short, in the time it takes for the blade's noise, broadcasted at a source azimuth of 60 degrees, to reach you, the blade will already have passed. Of course, one revolution is one revolution.

The Doppler effect leads to a relatively minor scaling problem when adding noise from other blades. The situation, as I see it, is that it is more convenient to do the adding of sound pressure from all blades in a reference observer time (or azimuth,  $\psi_{\text{obs}}$ ) domain, but Gopalan's equations use source azimuth ( $\psi$ ) as the input parameter. My approach has been to

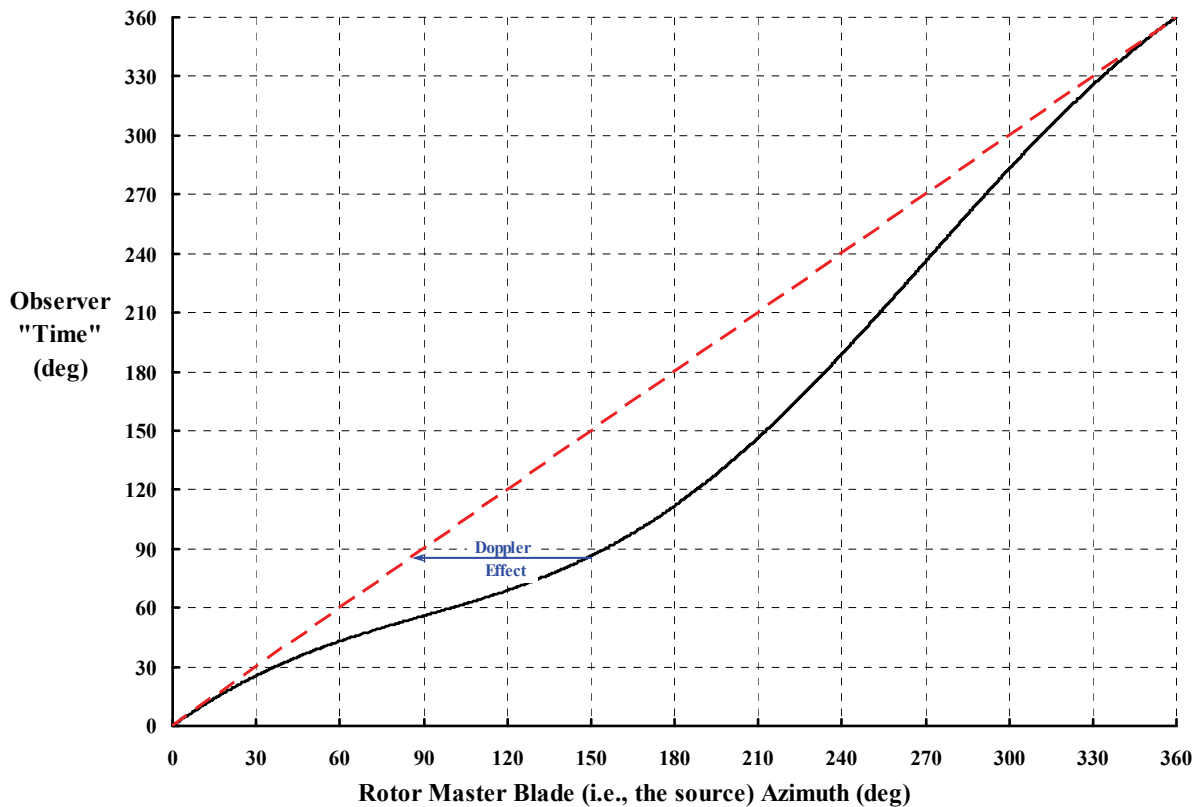


**Fig. 2-318. The Doppler effect per Eq. (2.311) for a tip Mach number of 0.60.**

choose equal steps in observer time, solve for corresponding source azimuth,<sup>157</sup> and then calculate the sound pressure waveform for the master blade. Given the total pressure waveform for the master blade, the waveform can be slid in observer azimuth for each blade in the rotor system. That is, for a three-blade rotor, the master blade begins its waveform at an observer azimuth of zero degrees. The second blade pressure from the master blade's observer time of 120 degrees is placed at an observer azimuth of zero degrees. Similarly, the third blade sees the master blade's observer time at 240 degrees placed at an observer azimuth of zero degrees. Then the pressure from the blades can be added.

The graphical results you will see next all came from calculations made on an Excel® spreadsheet.

Let me now show you a sample of what the calculated sound pressure waveforms look like for a three-bladed, *ideal* rotor in hover, and then the overall sound pressure level according to Eq. (2.305) can be calculated. I have chosen the basic geometry of the YHO-2HU helicopter's main rotor for this example. The inputs to Gopalan's equations are provided in Table 2-38.

<sup>157</sup> To compute  $\psi$  given equal increments in  $\psi_{\text{obs}}$  requires solving Eq. (2.311) backwards. This equation is really a transcendental equation. My approach was to make a column of  $\psi_{\text{obs}}$  and use the goal seek tool in Excel® to find the corresponding input azimuth ( $\psi$ ). I wrote a simple macro to perform the repetitive goal seek operation.

## 2.7 NOISE

**Table 2-38. Configuration Parameters Associated With Thickness Noise**

Parameter	Symbol	English Units	YHO-2HU Geometry	YHO-2HU Metric Units	Notes
Density	$\rho$	slugs/ft <sup>3</sup>	0.002378	1.225 kg/m <sup>3</sup>	Sea level, standard
Speed of Sound	$a_s$	ft/sec	1,116.437	340.29 m/sec	Sea level, standard
Airfoil Shape Factor	$S_f$	na	0.685	same	NACA 0015
Chord/Radius Ratio	$c/R$	na	0.045	same	
Airfoil Thickness Ratio	$t/c$	na	0.15	same	
Tip Mach Number	$M_{tip}$	na	0.53	same	
Elevation Angle	$\theta_{obs}$	rad.	0	same	
Observer Distance	$S$	ft	200	60.96 meters	
Blade Radius	$R$	ft	12.5	3.81 meters	
Blade Number	$b$	na	3	same	
Thrust	$T$	lb	1,600	7,117 newtons	
Disc Loading	$T/A$	lb/ft <sup>2</sup>	3.26	156.06 n/m <sup>2</sup>	

With the parameters provided in Table 2-38, you obtain the three configurations constants as

$$\begin{aligned} K_{thickness} &= 0.0024466 \text{ pascals} \\ L_{thrust} &= 0.0 \text{ pascals} \\ L_{torque} &= 0.00063549 \text{ pascals.} \end{aligned}$$

You might note that there is no noise from thrust in this example because I have placed you, the observer, in a plane that contains the rotor's tip path plane. In short, you see the rotor tip path plane as a thin line and the elevation angle is zero.

The thickness sound pressure (in pascal units) calculated in this example is shown in Fig. 2-319. Here you have the sound pressure for each individual blade as the red, blue, and green curves. The total for all three blades is the heavy black line. The thickness sound pressure is characterized by rather narrow negative spikes as you can see. These negative spikes become narrower but greater in maximum negative peak value as Mach number increases. The peak negative value *for any one blade* is approximated as

$$(2.312) \quad \text{Peak Negative } P_{thickness} = K_{thickness} \left[ M^3 \frac{(3-M)}{(1-M)^3} \right].$$

The tip Mach number for this introductory, sea-level standard YHO-2HU example is 0.53, which corresponds to a tip speed of 592 feet per second. (Remember that  $M = M_{tip} \cos \theta_{obs}$  and that  $\theta_{obs} = 0$  for this example.) This is a rather low tip speed, but also typical of small, piston-powered helicopters of the era. At this Mach number of 0.53, the [ ] term in Eq. (2.312) is 3.54. If the tip speed were up at larger, turbine-powered helicopter values of, say, 700 feet per second, the tip Mach number would be about 0.63 and the [ ] becomes 11.74. Whether the sound pressure level would be around three times as great would depend, of course, on the relative values of  $K_{thickness}$ . With a simple scaling up of the YHO-2HU, the larger machine would need to be 600 feet away from you to have the same level of sound pressure as the smaller machine at a distance of 200 feet.

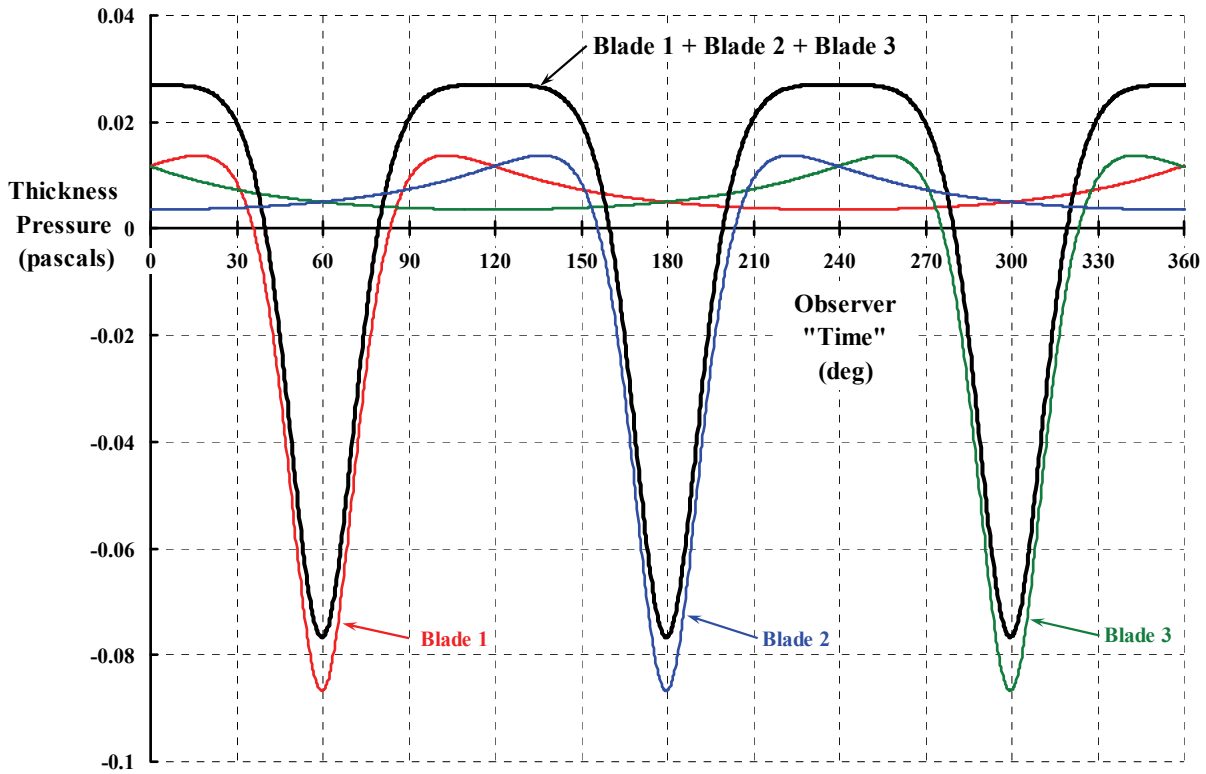


Fig. 2-319. Thickness sound pressure for the YHO-2HU main rotor assumed to be ideal.

Now consider the thrust and torque sound pressure waveforms shown in Fig. 2-320. Because I have chosen to place the microphone exactly inplane with the rotor disc ( $\theta_{\text{obs}} = 0$ ), the thrust contribution to the waveform is zero as you can see from Eq. (2.308). Thus, Fig. 2-320 gives only the torque contribution to the recorded sound pressure level. The total sound pressure from the three blades is clearly a three-per-rev waveform, but fortunately this contribution is not completely in phase with the sound pressure waveform created by thickness. Unfortunately, you will find from your own calculations that when the evaluation angle ( $\theta_{\text{obs}}$ ) is 10 or 20 degrees, the thrust and torque contributions are much closer in phase and are very additive. You might note from Eq. (2.308) that if the observer is *above* the rotor plane, then the elevation angle is negative and the thrust contribution begins to cancel the torque contribution to the sound pressure waveform. For the sake of completeness, you should note that the peak negative sound pressures for thrust and torque are, respectively,

$$(2.313) \quad \text{Peak Negative } P_{\text{thrust}} = L_{\text{thrust}} \left[ \frac{-16 + 13.5M}{(1-M)^2} \right] \text{ and}$$

$$(2.314) \quad \text{Peak Negative } P_{\text{torque}} = L_{\text{torque}} \left[ \frac{-60 + 115M - 84M^2 + 28M^3}{(1-M)^2} \right].$$

## 2.7 NOISE

These two components, when added together—*assuming they are completely in phase, which is a somewhat conservative assumption*—mean that the loading (i.e., thrust and torque contributions) is of the approximate magnitude

$$(2.315) \quad \text{Peak } P_{\text{loading}} = \pm (\rho a_s^2) \left( \frac{T/A}{\rho a_s^2} \right) \left( \frac{R}{120 \text{ bS}} \right) (\cos \theta_{\text{obs}}) \left\{ \begin{array}{l} \left[ \frac{-60 + 115M - 84M^2 + 28M^3}{\sqrt{2}(1-M)^2} \right] \\ + (M_{\text{tip}}^2 \sin \theta_{\text{obs}}) \left[ \frac{-16 + 13.5M}{(1-M)^2} \right] \end{array} \right\}.$$

It is worth noting that the negative peak and positive peak of loading sound pressure, which is the sum of torque and thrust pressures, are equal.

Now take the next step, which is to add thickness, thrust, and torque sound pressures all together. This result is shown in Fig. 2-321. This is the input required to calculate the overall sound pressure level (OSPL). You should know that the total pressure waveform can be represented by a Fourier series. A Fourier analysis of the waveform described by Fig. 2-321 shows that

$$(2.316) \quad \begin{aligned} p_t = & 0.032742 \sin(3\psi) + 0.042379 \cos(3\psi) - 0.006269 \sin(6\psi) - 0.02244 \cos(6\psi) \\ & + 0.001114 \sin(9\psi) + 0.009060 \cos(9\psi) - 0.000121 \sin(12\psi) - 0.003247 \cos(12\psi) . \\ & + \text{etc.} \end{aligned}$$

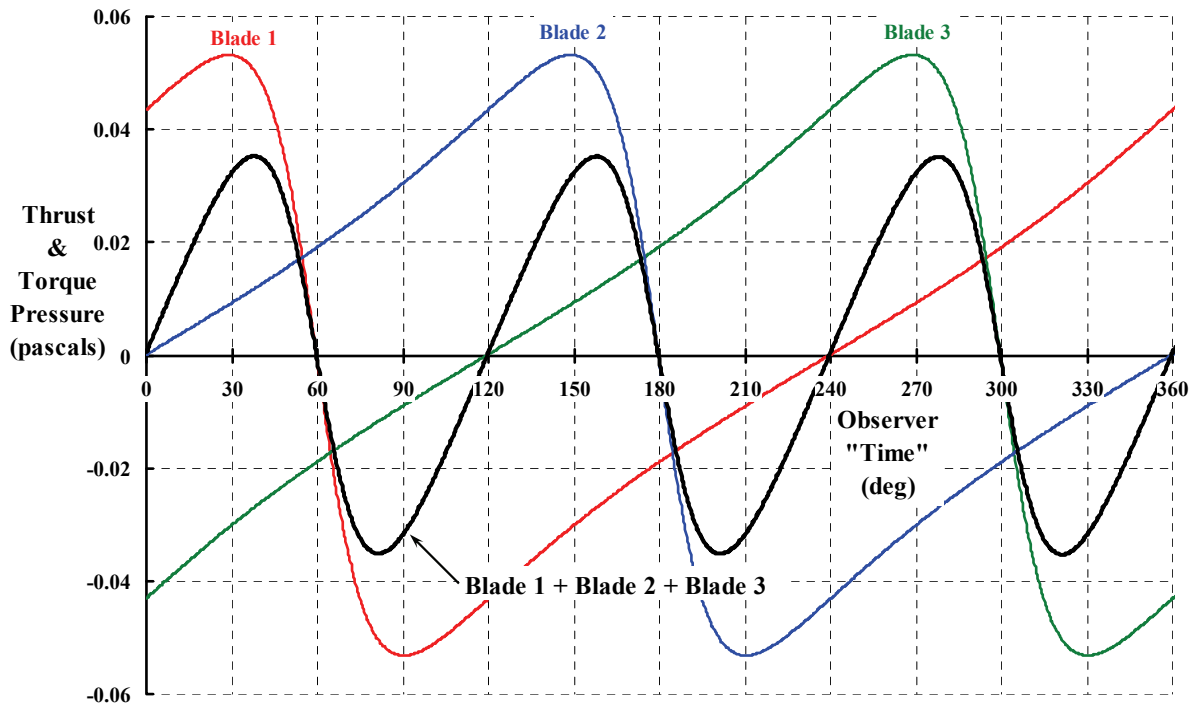
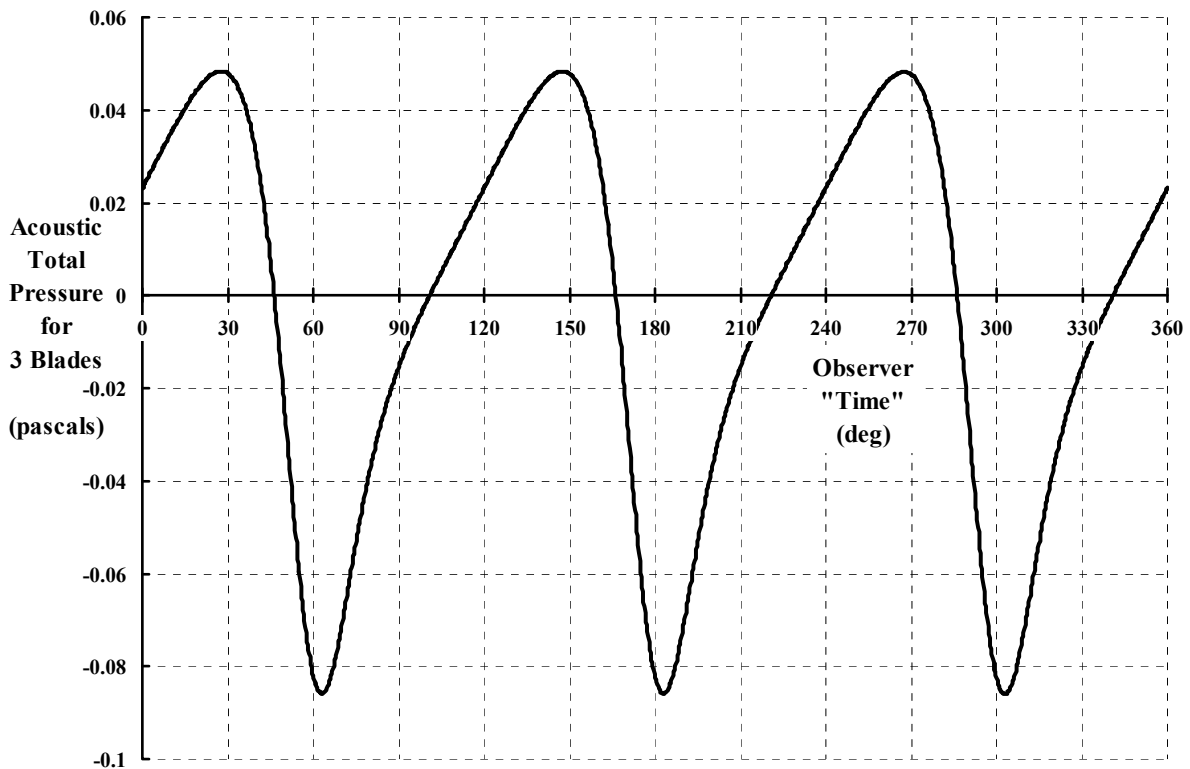


Fig. 2-320. Thrust and torque sound pressure for the YHO-2HU ideal rotor example.



**Fig. 2-321. Total sound pressure for the YHO-2HU ideal rotor example.**

Now take the final step where OSPL is calculated by Eq. (2.305), which is repeated here for convenience as

$$(2.317) \quad \text{OSPL} = 10 \log_{10} \left\{ \frac{1}{p_{\text{ref}}^2} \left[ \frac{1}{(T_2 - T_1)_{\text{obs}}} \int_{\text{obs}T_1}^{\text{obs}T_2} (p_t^2) dt_{\text{obs}} \right] \right\}.$$

This step requires that the sound pressure level from Fig. 2-321 be squared and plotted versus observer time (in seconds). You see this graphical result here as Fig. 2-322.

In creating the sound pressures leading to Fig. 2-322, I used a time step of .00007374 seconds, which corresponds to 0.2 degrees of observer azimuth, and yields 1800 ordinates over one rotor revolution. To perform the integration, I was satisfied with trapezoidal area approximations for each time step of the revolution. Thus, this YHO-2HU example, *assuming an ideal rotor-induced velocity distribution over the disc*, arrives at an overall sound pressure level of 66.4 decibels.

## 2.7 NOISE

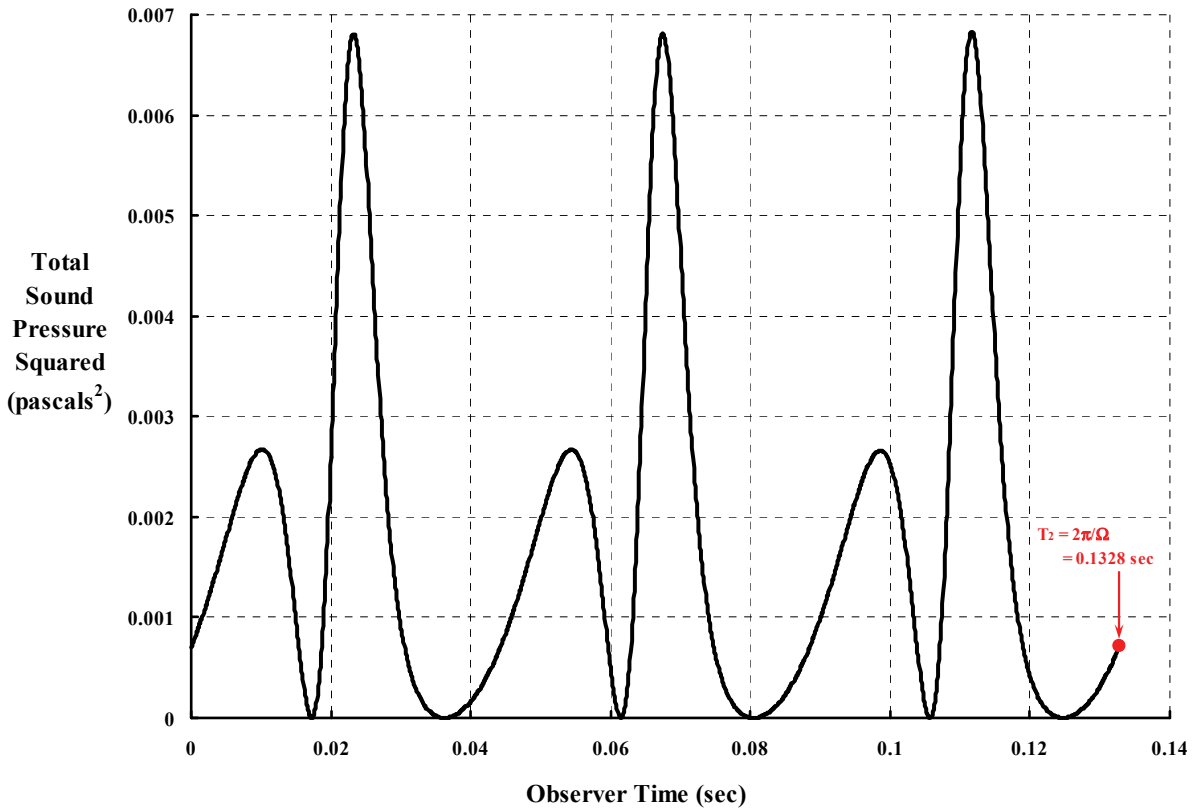


**Fig. 2-322. Integrating total sound pressure squared over one rotor revolution for the YHO-2HU ideal rotor example yields an OSPL of 66.4 decibels (using  $p_{\text{ref}}$  of 0.00002 pascals).**

### 2.7.5.2 Extending Gopalan's Work to a Conceptual Design Tool

In Gopalan's first paper [524], he examined parameters that affect maximum pressures. My purpose here is to extend his work to the calculation of overall sound pressure levels (OSPLs) for rotors having 2 to 8 blades operating at tip Mach numbers from 0.5 to 0.75. To apply Gopalan's work, I have provided a virtually exact equation for the total sound pressure level of *one* blade. With that result in hand, the sound pressure level for any number of blades up to eight is expressed in terms of the result for one blade. I have chosen to deal with noise created when the observer angle ( $\theta_{\text{obs}}$ ) is zero, which is near enough to the maximum noise for illustration purposes.

Equation (2.317) shows that the first step to obtaining OSPL for *one* blade with a zero observer angle requires evaluation of the pressure integral

$$(2.318) \quad \frac{1}{(T_2 - T_1)_{\text{obs}}} \int_{\text{obs}T_1}^{\text{obs}T_2} (p_t^2) dt_{\text{obs}}$$

where the sound pressure ( $p_t$ ) is given by Gopalan per Eqs. (2.306) and (2.307) for thickness pressure, and Eqs. (2.308) and (2.309) for inplane loading pressure, as

$$(2.318) \quad p_t = K_{\text{thickness}} F_{M,\psi} + L_{\text{torque}} H_{M,\psi}.$$

Because the pressure is for just one blade, the integration can be carried out over one revolution in the source azimuth (i.e., blade azimuth) coordinate system. That is, from the definition of observer time according to Eq. (2.310), you have

$$(2.319) \quad \frac{dt_{\text{obs}}}{d\psi} = \frac{1}{\Omega} - \frac{R}{a_s} \sin \psi = \frac{1}{\Omega} (1 - M \sin \psi),$$

and because  $T_1$  can be taken as zero for a reference and  $T_2$  equals  $2\pi/\Omega$  for one revolution, you can transform the pressure integral of Eq. (2.318) from observer time to source azimuth to obtain

$$(2.320) \quad \frac{1}{2\pi} \int_0^{2\pi} (p_t^2) d\psi = \frac{1}{2\pi} \int_0^{2\pi} (K_{\text{thickness}} F_{M,\psi} + L_{\text{torque}} H_{M,\psi})^2 (1 - M \sin \psi) d\psi.$$

The squared expansion of the sound pressure leads to three integrals that must be evaluated. Thus,

$$(2.321) \quad \begin{aligned} \text{Blade 1} \quad \frac{1}{2\pi} \int_0^{2\pi} (p_t^2) d\psi &= \frac{K_{\text{thickness}}^2}{2\pi} \int_0^{2\pi} F_{M,\psi}^2 (1 - M \sin \psi) d\psi \\ &+ \frac{2K_{\text{thickness}} L_{\text{torque}}}{2\pi} \int_0^{2\pi} (F_{M,\psi} H_{M,\psi}) (1 - M \sin \psi) d\psi \\ &+ \frac{L_{\text{torque}}^2}{2\pi} \int_0^{2\pi} H_{M,\psi}^2 (1 - M \sin \psi) d\psi \end{aligned}$$

Using the mathematical software called Mathematica<sup>®</sup>, I evaluated the three integrals and found that a quite adequate engineering result for Mach numbers up to 0.8 is

$$(2.322) \quad \begin{aligned} \text{Blade 1} \quad \frac{1}{2\pi} \int_0^{2\pi} (p_t^2) d\psi &= K_{\text{thickness}}^2 \left[ \frac{450M^6}{(1-M^2)^{9/2}} \left( 1 + \frac{22}{9}M^2 - \frac{17}{18}M^4 + \frac{59}{192}M^6 - \frac{447}{1280}M^8 \right) \right] \\ &+ L_{\text{torque}}^2 \left[ \frac{1800}{(1-M^2)^{3/2}} \left( 1 - \frac{1}{3}M^2 - \frac{3}{8}M^4 - \frac{1}{16}M^4 + \frac{1}{1280}M^4 \right) \right] \end{aligned}$$

where, you will note, the product term  $2K_{\text{thickness}} L_{\text{torque}}$  conveniently comes out exactly zero. To repeat, the configuration constants for one blade and zero elevation angle are

$$K_{\text{thickness}} = \rho a_s^2 \left[ \frac{S_f \left( \frac{c}{R} \right)^2 \left( \frac{t}{c} \right)}{240\pi \left( \frac{S}{R} \right)} \right] \quad \text{and} \quad L_{\text{torque}} = (\rho a_s^2) \left( \frac{T/A}{\rho a_s^2} \right)^{3/2} \left( \frac{R}{120\sqrt{2}S} \right).$$

## 2.7 NOISE

Now for a rotor system having two or more blades, you compute the thickness and torque sound pressures integrals by selecting from the following pairs:

$$b = 2, \int P_{\text{thickness}}^2 = 2 \left( \int P_{\text{thickness}}^2 \right)_{b=1}$$

$$b = 2, \int P_{\text{torque}}^2 = (-0.04091 M^2 + 0.68223 M - 0.13392) \left( \int P_{\text{torque}}^2 \right)_{b=1}$$

$$b = 3, \int P_{\text{thickness}}^2 = (28.9283 M^3 - 64.5194 M^2 + 47.9753 M - 8.8891) \left( \int P_{\text{thickness}}^2 \right)_{b=1}$$

$$b = 3, \int P_{\text{torque}}^2 = (0.48787 M^2 - 0.12254 M - 0.00879) \left( \int P_{\text{torque}}^2 \right)_{b=1}$$

$$b = 4, \int P_{\text{thickness}}^2 = (46.3691 M^3 - 113.5021 M^2 + 92.2180 M - 20.8876) \left( \int P_{\text{thickness}}^2 \right)_{b=1}$$

$$b = 4, \int P_{\text{torque}}^2 = (0.70555 M^2 - 0.55217 M + 0.11572) \left( \int P_{\text{torque}}^2 \right)_{b=1}$$

$$b = 5, \int P_{\text{thickness}}^2 = (6.3916 M^3 - 52.8966 M^2 + 69.3612 M - 20.0193) \left( \int P_{\text{thickness}}^2 \right)_{b=1}$$

$$b = 5, \int P_{\text{torque}}^2 = (0.72823 M^2 - 0.69278 M + 0.17031) \left( \int P_{\text{torque}}^2 \right)_{b=1}$$

$$b = 6, \int P_{\text{thickness}}^2 = (-117.8000 M^3 + 178.9898 M^2 - 67.2027 M + 5.2442) \left( \int P_{\text{thickness}}^2 \right)_{b=1}$$

$$b = 6, \int P_{\text{torque}}^2 = (0.99622 M^3 - 1.25498 M^2 + 0.53448 M - 0.07624) \left( \int P_{\text{torque}}^2 \right)_{b=1}$$

$$b = 7, \int P_{\text{thickness}}^2 = (-299.7618 M^3 + 537.7901 M^2 - 294.5375 M + 51.4713) \left( \int P_{\text{thickness}}^2 \right)_{b=1}$$

$$b = 7, \int P_{\text{torque}}^2 = (1.28199 M^3 - 1.90795 M^2 + 0.96434 M - 0.016495) \left( \int P_{\text{torque}}^2 \right)_{b=1}$$

$$b = 8, \int P_{\text{thickness}}^2 = (-477.9969 M^3 + 905.6624 M^2 - 538.8664 M + 103.6451) \left( \int P_{\text{thickness}}^2 \right)_{b=1}$$

$$b = 8, \int P_{\text{torque}}^2 = (1.38764 M^3 - 2.21825 M^2 + 1.19569 M - 0.21679) \left( \int P_{\text{torque}}^2 \right)_{b=1}$$

Once the blade number configuration is selected, the calculation of overall sound pressure level is quite simple because

$$(2.323) \quad \text{OSPL}_b = 10 \log_{10} \left\{ \frac{1}{P_{\text{ref}}^2} \left[ \int P_{\text{thickness}}^2 + \int P_{\text{torque}}^2 \right] \right\}.$$

Let me give you an example using the YHO-2HU configuration described in Table 2-38. The primary variables are Mach number ( $M = M_{tip} = 0.53$  because  $\theta_{obs} = 0$ ) and blade number ( $b = 3$ ). Calculating the sound pressure for one blade at a tip Mach number of 0.53 using Eq. (2.322) gives

$$(2.324) \quad \text{Blade 1} \quad \frac{1}{2\pi} \int_0^{2\pi} (p_t^2) d\psi = K_{thickness}^2 [71.115] + L_{torque}^2 [2584.007].$$

Then the correction factor for blade number is applied using the  $b = 3$  set on page 482 evaluated at a Mach number of 0.53. Thus,

$$(2.325) \quad \left[ \int P_{thickness}^2 + \int P_{torque}^2 \right]_{b=3} = K_{thickness}^2 [71.115](2.721) + L_{torque}^2 [2584.007](0.063306) \\ = 193.5K_{thickness}^2 + 163.6L_{torque}^2$$

Given that in this example

$$(2.326) \quad K_{thickness} = \rho a_s^2 \left[ \frac{S_f \left( \frac{c}{R} \right)^2 \left( \frac{t}{c} \right)}{240 \pi (S/R)} \right] = 0.00244658, \text{ and}$$

$$(2.327) \quad L_{torque} = (\rho a_s^2) \left( \frac{T/A}{\rho a_s^2} \right)^{3/2} \left( \frac{1}{120\sqrt{2} (S/R)} \right) = 0.0019051$$

you then have

$$(2.328) \quad OSPL_{b=3} = 10 \log_{10} \left\{ \frac{1}{(0.00002)^2} [0.0011583 + 0.0005946]_{b=3} \right\} = 66.42 \text{decibels}$$

and, therefore, the overall sound pressure level is 66.42 decibels.

There are, of course, many other approaches to extend Gopalan's work and gain more insight to hovering rotor noise. I chose the preceding approach after spending considerable time in omphaloskepsis.

### 2.7.5.3 Insight Gained From Gopalan's Work

When you look closer at Eqs. (2.325) through (2.328), you can see that the ratio of observer distance ( $S$ ) to rotor radius ( $R$ ) is common to both  $K_{thickness}$  and  $L_{torque}$ . You will also note that the atmospheric condition ( $\rho a_s^2$ ) is common and so is the reference sound pressure ( $p_{ref}$ ). This suggests that the overall sound-pressure-level equation can be rewritten to take a somewhat different form. Therefore, let me suggest the following:

## 2.7 NOISE

$$(2.329) \quad \text{OSPL}_b = 10 \log_{10} \left\{ \frac{1}{(S/R)^2} \left( \frac{\rho a_s^2}{p_{\text{ref}}} \right)^2 \left\{ \left[ S_f \left( \frac{c}{R} \right)^2 \left( \frac{t}{c} \right) \right]^2 \left( \frac{f_{(b,M)}}{240^2 \pi^2} \right) + \left( \frac{T/A}{\rho a_s^2} \right)^{3/2} \left( \frac{g_{(b,M)}}{2 \times 120^2} \right) \right\} \right\}.$$

This form illuminates an observer position parameter (S/R) and an atmospheric condition, and leaves the rotor itself as a constant, for a given tip Mach number, within the brackets. Furthermore, logarithmic properties of products and powers can be employed. For instance, the effect of distance for a given blade configuration and disc loading (T/A) shows you that overall sound pressure level should vary inversely, with distance squared, from the noise source. Said another way, OSPL should decrease as the  $\log_{10} (S/R)$  increases. That is,

$$(2.330) \quad \text{OSPL}_b = 10 \log_{10} \left\{ \frac{\text{Constant}}{(S/R)^2} \right\} = 10 \log_{10} \{ \text{Constant} \} - 20 \log_{10} (S/R).$$

The constant, as you have noted, is

$$(2.331) \quad \text{Constant} = \left( \frac{\rho a_s^2}{p_{\text{ref}}} \right)^2 \left\{ \left[ S_f \left( \frac{c}{R} \right)^2 \left( \frac{t}{c} \right) \right]^2 \left( \frac{f_{(b,M)}}{240^2 \pi^2} \right) + \left( \frac{T/A}{\rho a_s^2} \right)^{3/2} \left( \frac{g_{(b,M)}}{2 \times 120^2} \right) \right\}.$$

Now, referring back to Fig. 2-314 on page 467, you can see that OSPL does decrease with increasing distance from the helicopter. However, the comparisons between helicopters should be analyzed in terms of distance divided by radius. This insight suggests a revision of the horizontal axis of Fig. 2-314 to a semi-log scale, using (S/R) as the scaling parameter. You see the result of this rescaling and using a semi-log abscissa with Fig. 2-323.

There are a number of observations to be made about Fig. 2-323. First off, using Eq. (2.330), I have superimposed four heavy lines on top of the helicopter data to help in this discussion. You can immediately see at the top that the loudest machine is the Hiller YH-42 rotor that was tip-driven by ramjets and has, apparently, a constant of  $2,000 \times 10^{10}$ . The noise of the YH-42 clearly diminishes with distance as Eq. (2.330) prescribes. Scanning down Fig. 2-323, it appears that all the other helicopters (including the Djinn with its cold cycle tip drive) fall within a band where the constant in Eq. (2.330) is between  $10 \times 10^{10}$  and  $100 \times 10^{10}$ . Two of the helicopters had noise data obtained while operating at ground idle, and the associated constant is about  $1 \times 10^{10}$ . It appears that going from ground idle to hover raises the noise level by 10 decibels for both the YUH-1D (48 ft) and the S-62A.

Next, when you follow the constant's magnitude up the OSPL scale at  $S/R = 10$ , you should note that a factor of ten in the constant equals just 10 decibels. This is the behavior of the logarithm. More importantly, it means that achieving a noticeable noise reduction requires substantial changes to the current fleet, which I will discuss shortly.<sup>158</sup>

---

<sup>158</sup> I am sorry to say that not all flight test data leading to Fig. 2-323 was quantified in enough configuration and flight condition detail for me to show how accurate Eq. (2.331) might be. However, in the 1970s, the Quiet Helicopter Program was completed, and quantified data for the Hughes OH-6A and the Sikorsky S-62A were obtained. I will discuss that program and its results later.

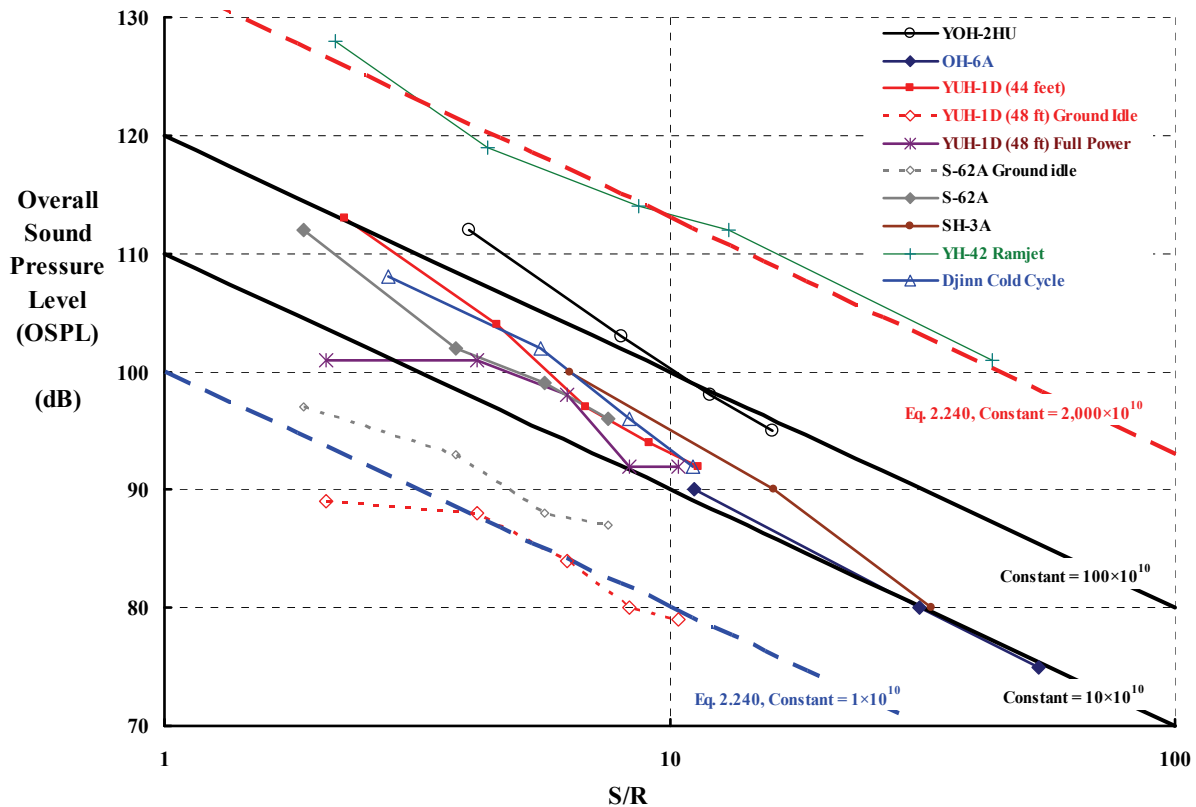


**Fig. 2-323. Comparison of noise signatures from several helicopters hovering in ground effect.**

There is one very important last point that has to do with the reflections of sound waves off the ground and other nearby surfaces. The experimental data shown in Fig. 2-323 is for helicopters hovering in ground effect or at ground idle. Therefore, parts of the sound waves emanating from the helicopter reflect off the ground. According to Hicks and Hubbard [532], “In general ground reflection causes a doubling of the sound intensities at the ground level.” This means that the pressure squared as given by Eq. (2.329) should be multiplied by 4. That is to say, if reflected waves are a factor, then the term  $1/(S/R)^2$  in Eq. (2.329) should be increased to  $4/(S/R)^2$ . This is the equivalent of adding 6 decibels to a solution with no reflection (i.e.,  $10 \log_{10} 4 = 6$ ).

The difficulties presented by ground reflection were brought to the industry’s attention again in 1973 as part of the Quiet Helicopter Program. Testing of a standard and modified Sikorsky SH-3A included noise measurements at four hovering heights. Bob Pegg and his coauthors [516] included one figure illustrating how the frequency content of the sound pressure level in decibels varied with frequency. I have included their figure here as Fig. 2-324. In their report they noted that

“narrow-band frequency analyses (4-Hz bandwidth) from both the standard and modified helicopters were made from data taken while the helicopters were hovering at four heights. All of the narrow-band frequency data for both modified and standard aircraft showed evidence of a ground-plane-reflection effect. This effect became more severe with increasing

## 2.7 NOISE

hover height. A typical example of ground reflection or image interference is shown in figure 17. In this figure the increasing effects of cancellation and re-enforcement are evident in the narrow-band spectra in the form of peaks and valleys in the noise levels. This effect makes analysis of hovering data at altitude extremely difficult.”

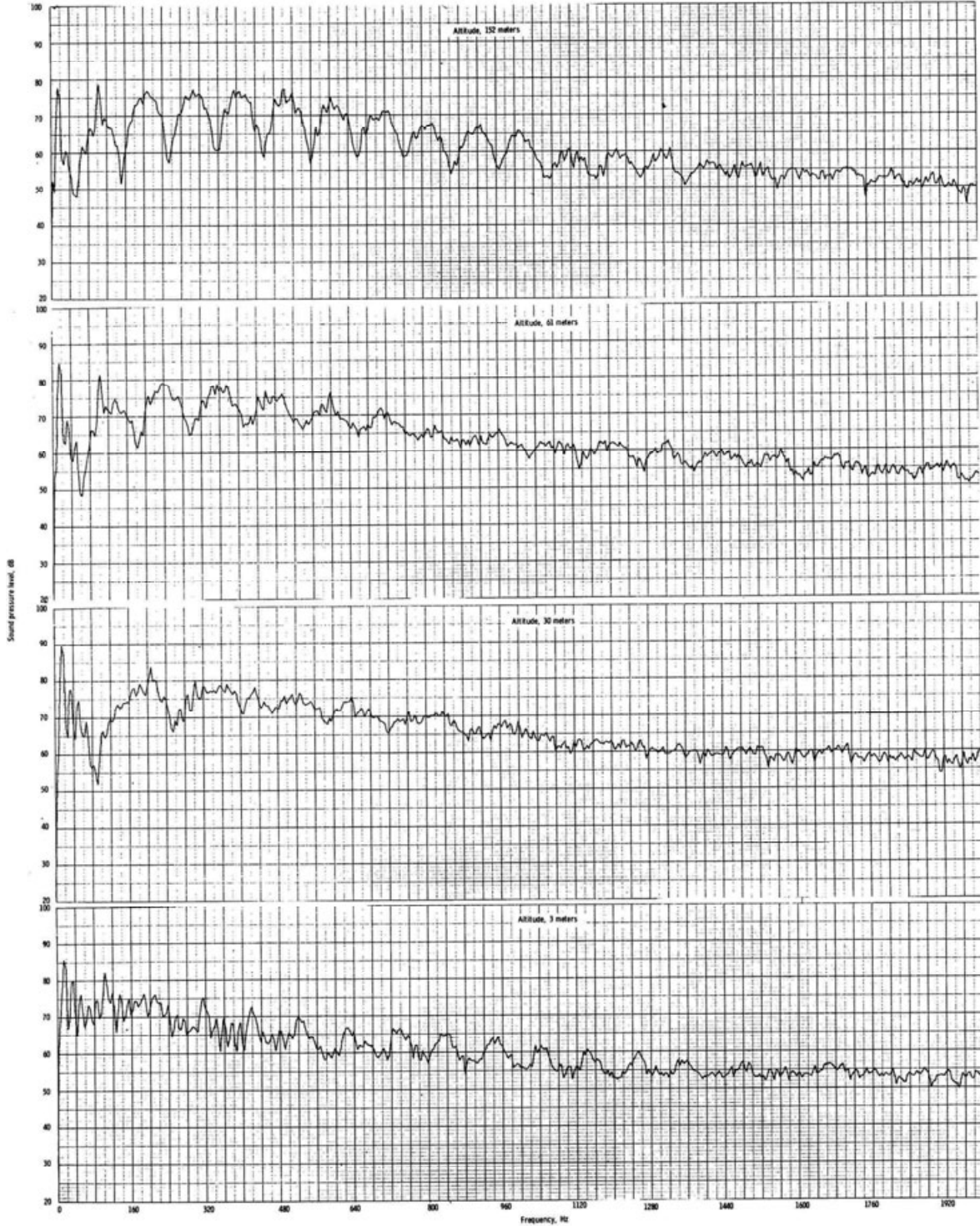


**Fig. 2-324. SH-3A noise signatures in hover at several altitudes [516].**

Although Fig. 2-324 is of poor quality, it is only at the lowest hovering altitude of 3.1 meters that the individual harmonics of the rotor noise are clearly seen. Pegg and his coauthors used the data at the lowest altitude to identify the first 11 harmonic peaks of the main rotor and the first 2 noise peaks due to the tail rotor. I have included their detailed analysis here as Fig. 2-325 to illustrate how difficult it can be to find these noise source harmonics from hovering measurements made when ground reflections are a factor. You should note that the largest noise harmonic is from the tail rotor.

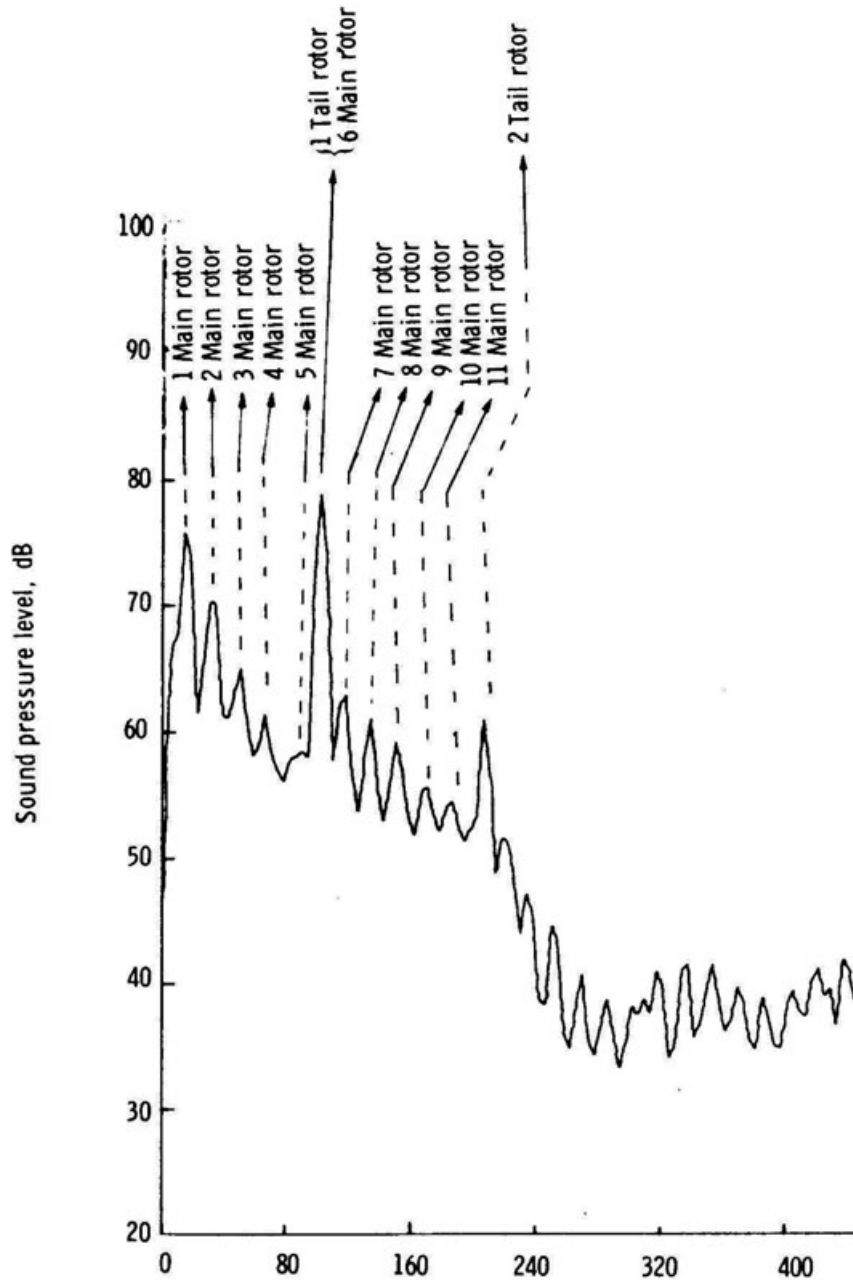


Fig. 2-325. SH-3A noise signatures in hover at 3.1 meters altitude [516].

## 2.7 NOISE

### 2.7.5.4 Test Versus Rotational Noise Theory (Only) Using In-Ground-Effect Data

Now you have some test data from several helicopters in front of you (i.e., Fig. 2-323), and you have an introductory method of calculating main-rotor rotational noise *alone* due to thickness and torque. The natural question is, “How close does this *main rotor alone* noise theory come in predicting the *total helicopter* noise?” The answer is shown in Fig. 2-326.

Your immediate reaction to this correlation of test and theory provided by Fig. 2-326 may well be one of disappointment, but when you look closer, you can see that the basic pattern for each data set is that each set lies nearly parallel to the line of perfect correlation. The implication of this observation is that each helicopter can be described mathematically with a simple constant (K) times the main-rotor-alone sound pressure. That is, following Eq. (2.329), assume that the total helicopter noise behaves as

$$(2.332) \quad \text{OSPL}_b = 10 \log_{10} \left\{ \frac{K}{(S/R)^2} \left( \frac{\rho a_s^2}{p_{\text{ref}}} \right)^2 \left\{ \left[ S_f \left( \frac{c}{R} \right)^2 \left( \frac{t}{c} \right) \right]^2 \left( \frac{f_{(b,M)}}{240^2 \pi^2} \right) + \left( \frac{T/A}{\rho a_s^2} \right)^{3/2} \left( \frac{g_{(b,M)}}{2 \times 120^2} \right) \right\} \right\}$$

from which it follows from the logarithm of a product that

$$(2.333) \quad \text{OSPL}_b = 10 \log_{10} \left\{ \frac{1}{(S/R)^2} \left( \frac{\rho a_s^2}{p_{\text{ref}}} \right)^2 \left\{ \left[ S_f \left( \frac{c}{R} \right)^2 \left( \frac{t}{c} \right) \right]^2 \left( \frac{f_{(b,M)}}{240^2 \pi^2} \right) + \left( \frac{T/A}{\rho a_s^2} \right)^{3/2} \left( \frac{g_{(b,M)}}{2 \times 120^2} \right) \right\} \right\} \\ + 10 \log_{10} \{K\}$$

Therefore, each helicopter’s overall sound pressure level in decibels equals its main rotor noise (i.e.,  $K = 1$ ) plus some additional decibels due to a multitude of possible sound pressure sources. On this basis, you can see that the OSPL of the YUH-1D, with a 48-foot-diameter rotor, appears to be well predicted based solely on its main-rotor-alone rotational noise. That is,  $K = 1$ , in which case  $10 \log_{10}(K = 1)$  equals zero. At the other extreme, the YH-43 with its ramjet tip drive will show virtually exact correlation if  $K = 3,694!$  That is,  $10 \log_{10}(K = 3,694) = 35.6$  dB. Thus, the red, open diamonds for the YH-43 move to the right on the abscissa by 35.6 decibels, which puts the YH-43 right on the perfect correlation, green dashed line.

Let me draw your attention to the Hughes OH-6A shown with the blue open diamonds in Fig. 2-326. This helicopter’s data can be translated to the right by 15.5 decibels to achieve near perfect correlation. This corresponds to  $K = 37$ . According to Hicks and Hubbard [532] as discussed previously, ground reflection might easily double the sound pressure. This suggests that 6 decibels of the 15.5 decibels could be just ground reflection, and therefore other helicopter components might only contribute about 10 decibels. I raise this conjecture because during the Quiet Helicopter Program, the OH-6A was rather thoroughly examined for individual component noise contributors. I will discuss this aspect of the program shortly.

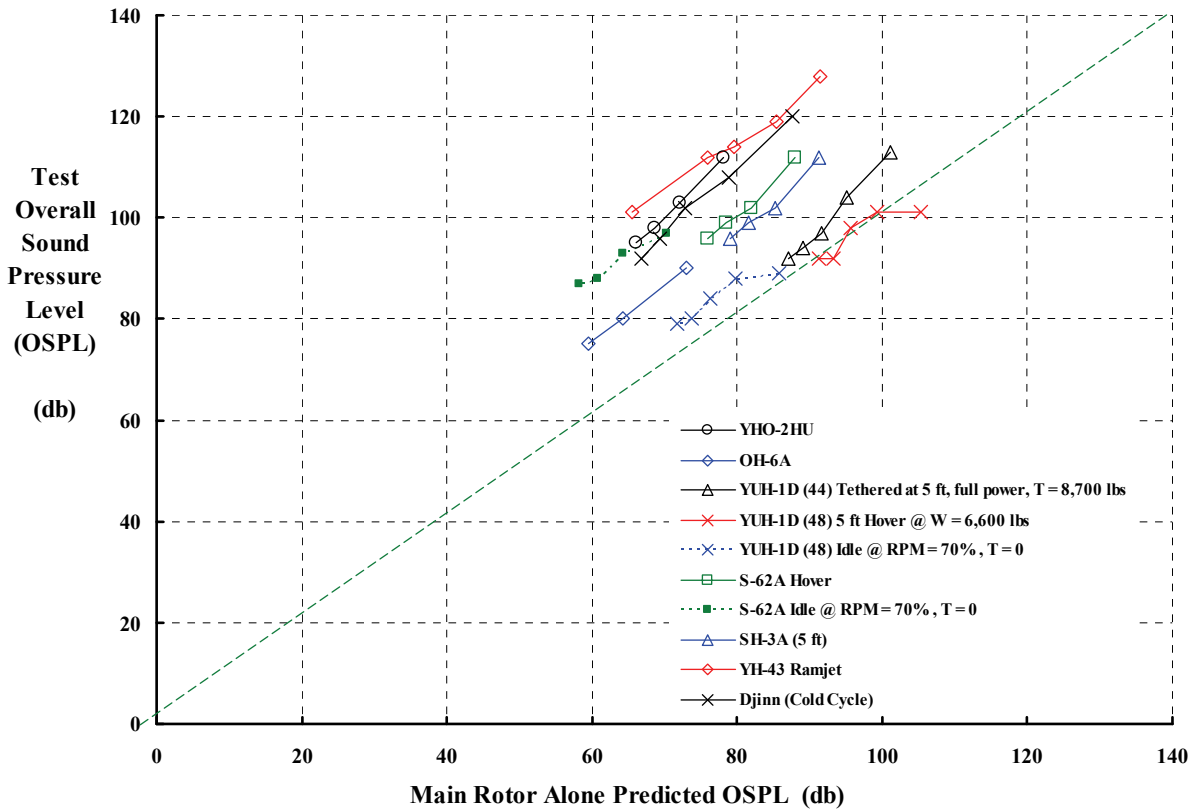


**Fig. 2-326. Test versus rotational noise theory (only) for helicopters hovering in ground effect.**

The message from this correlation example is quite clear. The main rotor is a major contributor to noise emanating from a hovering helicopter. After all, for the turbine-powered machines such as the OH-6A, the S-62A, and the SH-3A examples, about 80 decibels out of 100 can be attributed to the main rotor. It appears that in some cases such as the YUH-1D, the very simple theory provided by Gopalan may capture the whole noise signature for a helicopter hovering in ground effect. Of course, all the other assemblies of the machine (i.e., tail rotor, engine, gear boxes, engine exhaust pipe, airframe, generators, hydraulic pumps, auxiliary power supply, etc.) must remain as possible contributors to the noise signature until proven to be inconsequential by experiment or at least some predictive theory.

**2.7.5.5 UH-60 Noise Sensitivity Trade Study**

Let me now examine how sensitive OSPL is to the first-order configuration parameters that Gopalan established. As a baseline, consider the main rotor of a U.S. Army UH-60A, more commonly known as the Black Hawk. This helicopter has a four-bladed, 53.67-foot-diameter rotor. The rotor turns at 258 rpm, which gives a tip Mach number of 0.65 at sea level on a standard day. The rotor solidity is 0.0826, which translates to a blade chord-to-radius ratio ( $c/R$ ) of 0.06487. The nominal airfoil thickness-to-chord ratio ( $t/c$ ) is 0.10, and I have assumed the airfoil shape parameter ( $S_f$ ) to be 0.685. At a rotor thrust of 23,400 pounds, the

## 2.7 NOISE

disc loading ( $T/A$ ) for this baseline example is 10.34 pounds per square foot. Because  $\rho a_s^2$  equals 2,964 pounds per square foot, it follows that  $T/A/\rho a_s^2$  equals 0.00349. I will assume that noise is to be measured at an observer distance of about 200 feet, which means  $(S/R)$  is on the order of 7.5. I will also assume that the UH-60 is hovering out of ground effect (say at a height of 100 feet) and that you, the observer, are in a 100-foot tower. This means you are in the rotor plane and that there is (presumably) little noise reflected from the ground.

Given this UH-60 input, let me now follow the calculations made for the YHO-2HU example. Calculating the sound pressure for one blade at a tip Mach number of 0.65 using Eq. (2.322) gives

$$(2.334) \quad \text{Blade 1} \quad \frac{1}{2\pi} \int_0^{2\pi} (p_t^2) d\psi = K_{\text{thickness}}^2 [753.349] + L_{\text{torque}}^2 [3230.101].$$

Then the correction factor for blade number is applied using the  $b = 4$  set on page 482 evaluated at a Mach number of 0.65. Thus,

$$(2.335) \quad \left[ \int P_{\text{thickness}}^2 + \int P_{\text{torque}}^2 \right]_{b=3} = K_{\text{thickness}}^2 [753.349](0.0394) + L_{\text{torque}}^2 [3230.101](1.708) \\ = 193.5 K_{\text{thickness}}^2 + 163.6 L_{\text{torque}}^2$$

For the UH-60

$$(2.336) \quad K_{\text{thickness}} = \rho a_s^2 \left[ \frac{S_f \left( \frac{c}{R} \right)^2 \left( \frac{t}{c} \right)}{240 \pi (S/R)} \right] = 0.00723174 \text{ and}$$

$$(2.337) \quad L_{\text{torque}} = (\rho a_s^2) \left( \frac{T/A}{\rho a_s^2} \right)^{3/2} \left( \frac{1}{120\sqrt{2} (S/R)} \right) = 0.0229791,$$

and so you have

$$(2.338) \quad \text{OSPL}_{b=4} = 10 \log_{10} \left\{ \frac{1}{(0.00002)^2} [0.15104 + 0.09378]_{b=4} \right\} = 87.87 \text{decibels}.$$

Note here that the relative contributions of torque loading pressure and thickness pressure are in the ratio of 0.09378 to 0.15104, or about 0.62. This dominance of thickness pressure over the inplane loading pressure is only slightly greater than what you saw for the YHO-2HU. It appears that the current helicopter fleet, worldwide, shares this characteristic.

It is helpful to see the total pressure waveform and its components, so I have included this data on Fig. 2-327. Here you can see that the large negative spikes due to thickness noise are quite dominant. When you compare this UH-60 result to the YHO-2HU result shown in Fig. 2-319 and Fig. 2-320, you might conclude, as I have, that helicopter noise reduction must first deal with thickness contributions before there is a high payoff for reducing what is commonly called rotational noise created by thrust and torque.

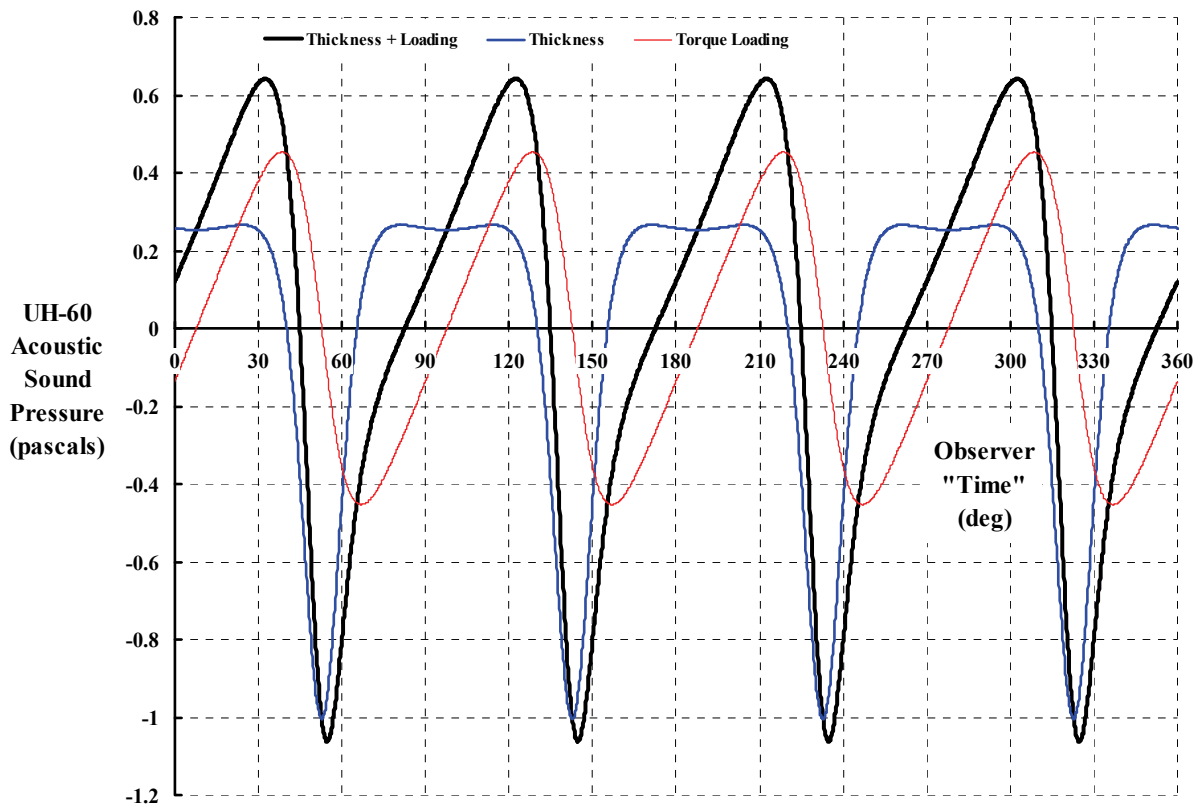


**Fig. 2-327. UH-60 noise contributions to sound pressure at the baseline condition.**

The overall sound pressure level is 87.87 decibels for this UH-60 example, which is some 20 decibels louder than the small, piston-powered YHO-2HU helicopter—at *equal observer to helicopter distance of 200 feet*. But do not be completely fooled. The YHO-2HU example was calculated at a distance-to-radius ratio of  $S/R = 16$ , and this UH-60 calculation was made at  $S/R = 7.5$ . When this UH-60 estimate is made at  $S/R = 16$ , the OSPL becomes 81.3 decibels. Another way to look at it is this: the UH-60 would sound about like the YHO-2HU (at an observer distance of 200 feet) if the observer was about 2,400 feet away from the UH-60 at an  $S/R$  of 90.

It is clear that helicopter noise disappears with distance. A more pertinent question is what changes to the UH-60 (or YHO-2HU for that matter) could be made to lower its noise in hover. One change that is immediately available is to lower the rotor tip speed. High tip speeds were known to create noise ever since the invention of the propeller. Consider this analytical experiment. Suppose that the pilot of a UH-60 reduces rotor RPM while maintaining a steady hover 100 feet above the ground at a main rotor thrust of 23,400 pounds. Of course, he must increase collective pitch and probably over-torque the transmission and possibly over-temp an engine to do this, but assume that no restrictions are imposed during this experiment. Naturally, the rotor  $C_T/\sigma$  will increase, but starting from a  $C_T/\sigma$  of 0.10 at the normal 258 rpm, the rotor speed might be decreased to, say, 182 rpm (i.e., 70 percent of normal) before the rotor reaches a  $C_T/\sigma$  of 0.2. That would be, I suggest, on the ragged edge of complete blade stall in hover. Accepting this scenario, the results of this trade study are

## 2.7 NOISE

shown in Fig. 2-328, which suggests that noise would drop from 87.87 decibels to 76.9 decibels. The sensitivity to Mach number amounts to 7.6 decibels per 0.1 M as the red dashed line on Fig. 2-328 shows. You can get a quick feel for the sensitivity to a change in tip Mach number by using the red dashed line, which behaves as

$$(2.339) \quad \Delta \text{OSPL} = 10 \log_{10} \left\{ \left( \frac{182 \text{rpm}}{258 \text{rpm}} \right)^n \right\} = 10n \log_{10} \left\{ \left( \frac{182}{258} \right) \right\} = 10n(-0.152).$$

The overall sound pressure level drops from 87.87 decibels at 258 rpm (i.e.,  $M = 0.65$ ) to about 75 decibels at 182 rpm. This is a change in OSPL of roughly  $-13$  decibels so  $(n)$  in Eq. (2.339) becomes about 8.6. The conservative rule of thumb, lacking a more detail calculation, is to use  $n = 6$ .

The UH-60 might be changed more extensively by increasing the number of blades while holding the rotor solidity ( $\sigma = bc/\pi R$ ) constant at 0.0826 and the rotor thrust constant at 23,400 pounds. By keeping rotor speed at 258 rpm, the  $C_T/\sigma$  would remain at 0.10, which would at least satisfy the aerodynamic community (but probably not those interested in the selling price or weight empty of the redesigned machine). Still, the noise would be reduced as Fig. 2-329 shows. I would suggest that rotor blade aspect ratios ( $R/c$ ) approaching 23 would

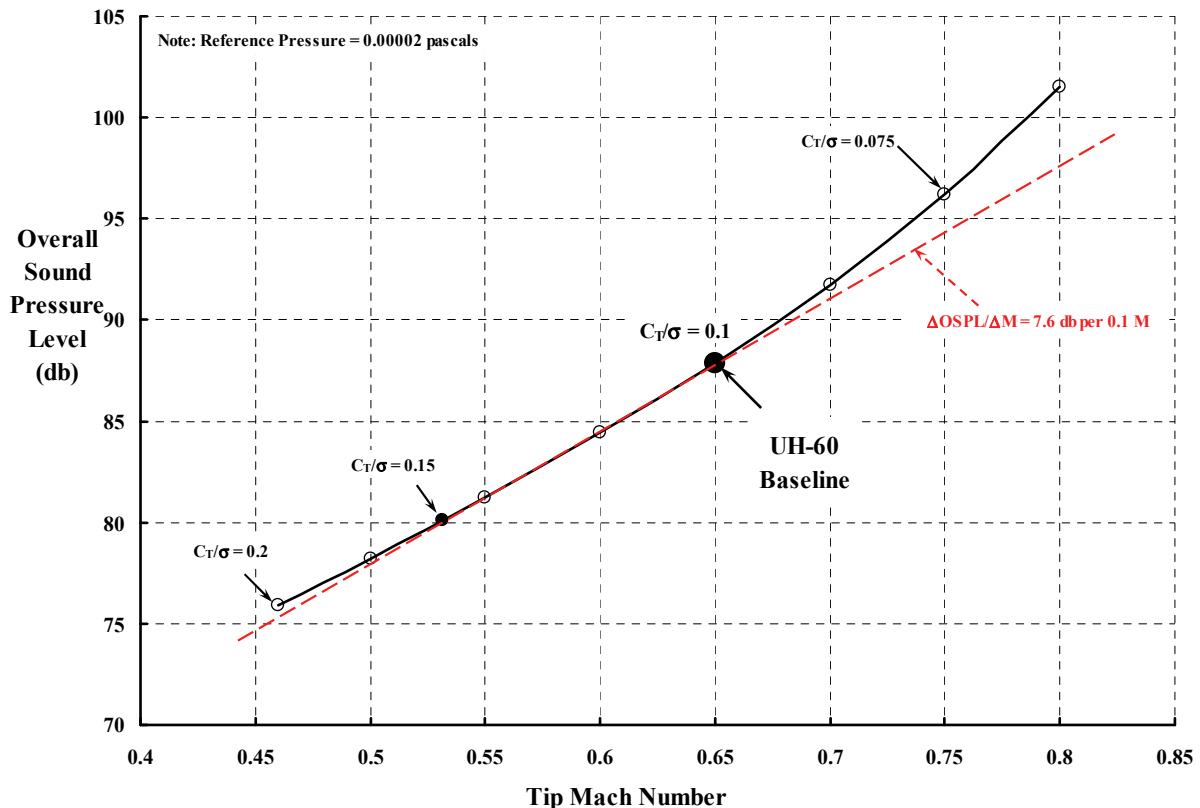


**Fig. 2-328. UH-60 noise reduction with reduced tip speed at a constant rotor thrust of 23,400 pounds at sea level on a standard day.**

present a serious challenge to rotor blade designers and aeromechanic engineers because of blade torsional deflections and even unsolvable instabilities. Remember that rotor blades are really flying wings with control at just one wing tip.

You might consider keeping the four-bladed rotor system as is but redesigning the blades with very thin airfoils. This approach would address thickness noise in an effort to make  $K_{\text{thickness}}$  smaller as Eq. (2.336) suggests. The results of this approach are shown in Fig. 2-330. It is interesting to note here that with a zero-thickness-ratio airfoil, only the noise due to torque is left, and this amounts to about 84 decibels. The meaning here is clear; if the thickness noise is greater than the torque noise contribution, then making  $L_{\text{torque}}$  smaller with a reduction in disk loading will not appreciably reduce noise.

To emphasize this last point, consider the impact of halving the rotor thrust at several levels of thickness noise. You see the effect from the green line on Fig. 2-330. I bring this point to your attention because the noise solution that Gopalan provided is very interactive in the weighting between thickness and torque contributions. Clearly, thickness noise can mask rotational noise reductions. It is not until the thickness noise is relatively quite small that a simple change in thrust is perceptible. You might have guessed this from Fig. 2-319, Fig. 2-320, and Fig. 2-321.

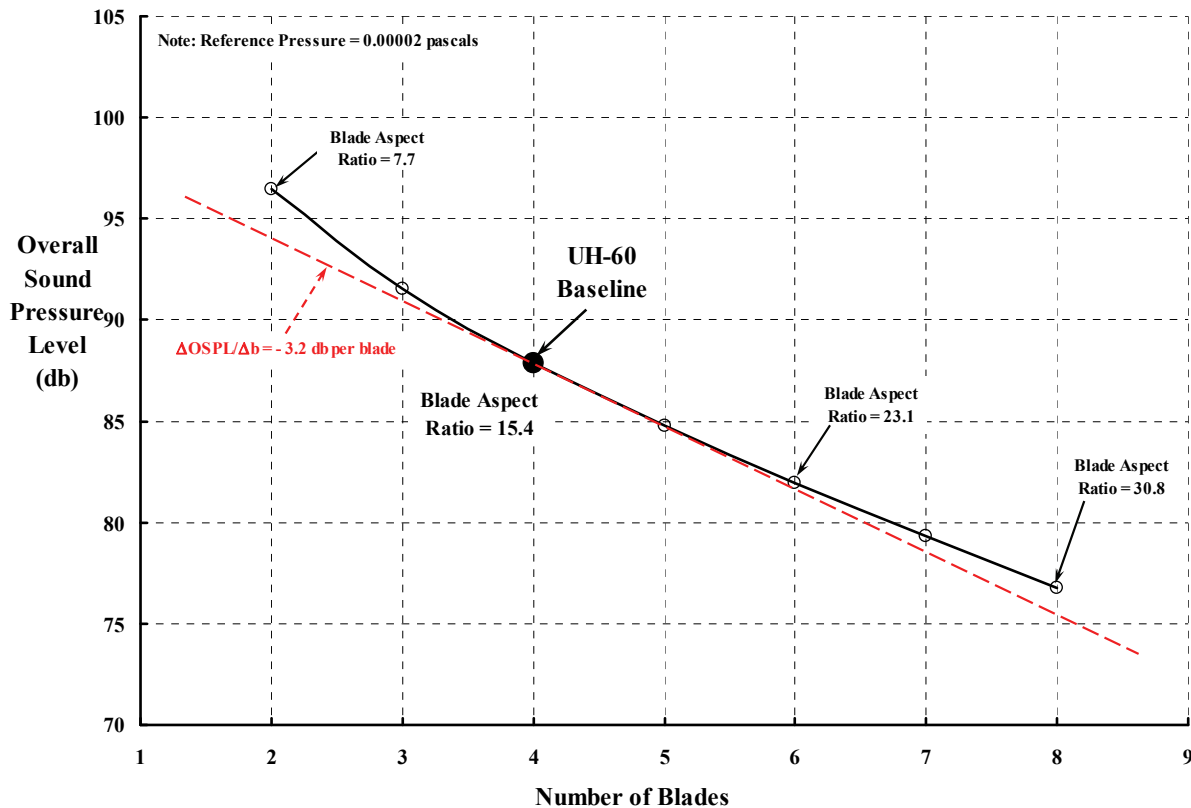


**Fig. 2-329. UH-60 noise reduction with increased blade number at constant solidity, tip Mach number, and constant rotor thrust of 23,400 pounds at sea level on a standard day.**

## 2.7 NOISE

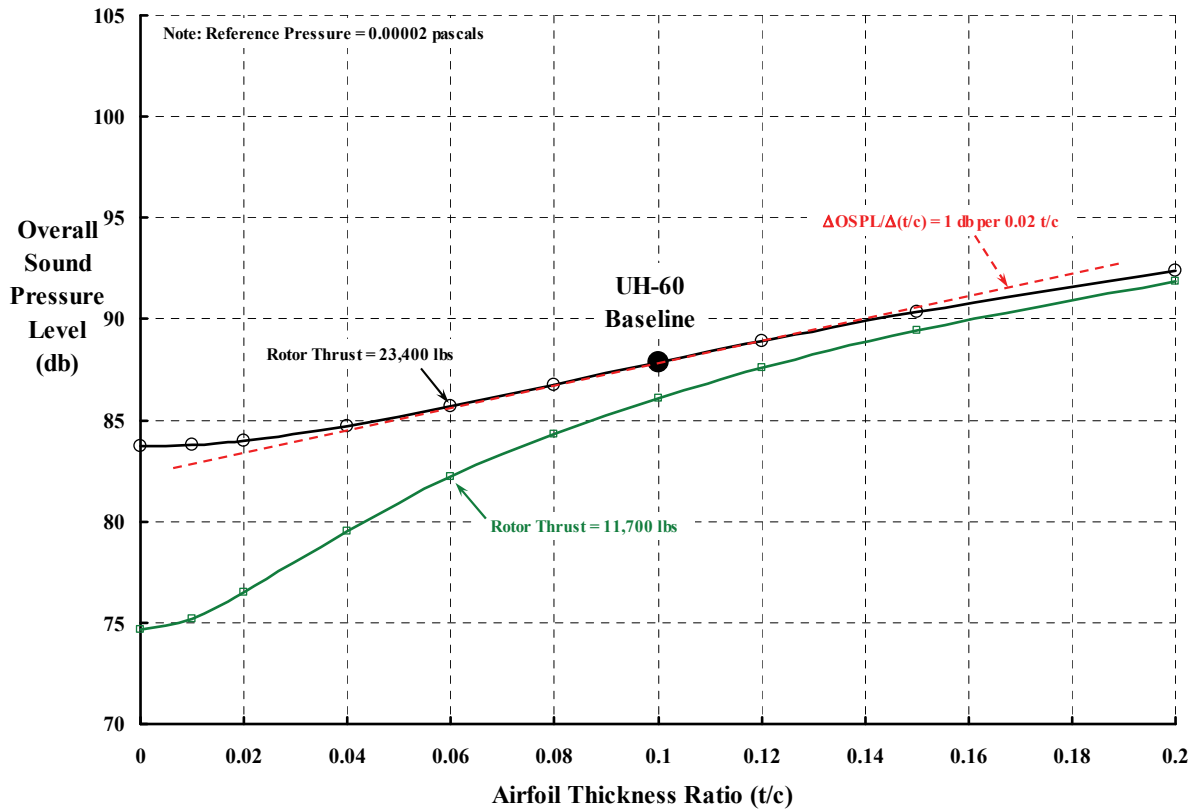


**Fig. 2-330. UH-60 noise reduction with decreasing airfoil thickness ratio alone for two main rotor thrusts. Thickness noise is zero when  $t/c$  is zero.**

### 2.7.5.6 Thickness and Torque Noise From a Real UH-60 Rotor

Using the ideal rotor in the preceding UH-60 example should, I hope, please helicopter performance engineers. After all, that has been their goal (perhaps dream would be a better word) for decades. However, practically speaking, the majority of helicopter main rotors that are flying have simple linear twist and rectangular blades. Tail rotors for the single-main-rotor machines are even further from ideal because they generally have zero twist and rectangular blades. For other than the ideal rotor, which you will recall has a twist distribution of  $\theta_x = \theta_{tip}/x$ , the nice closed-form equations for the torque and thrust sound pressure comparable to what Gopalan obtained for the ideal rotor have yet to be published. As a result, I will begin one step back from the integrated equations Gopalan gave to recalculate the sound pressure of the UH-60 main rotor taking account of its production blade geometry.

Geometric twist does not change the thickness sound pressure—at least within the first order of magnitude being addressed in this introduction—but the rotational noise charged to torque and thrust sound pressure is influential. To illustrate just how large this influence might be, consider just the torque sound pressure calculation. This sound pressure is obtained from the more fundamental, pre-integrated equation Gopalan gave. I have rearranged his result slightly to read

$$(2.340) \quad p_{\text{torque}} = \frac{M_{\text{tip}}}{4\pi S} \int_0^1 \left( \frac{dD}{dr} \right)_{\text{per blade}} \left\{ \frac{\cos(\psi - \phi)}{[1 - Mx \sin(\psi - \phi)]^3} \right\} dx .$$

It is from this equation that Gopalan obtained the closed form integrations for the ideal rotor. He was able to do this for the ideal rotor because the blade element inplane drag ( $dD/dr$ ) is constant and can be taken outside the integral. If you work in English units as I do, then for Eq. (2.340) the rotor speed ( $\Omega$ ) is in radians per second, the speed of sound ( $a_s$ ) is in feet per second, and the distance between observer and the rotor hub ( $S$ ) is in feet. You will have to divide the final result by 0.02088 to convert from pounds per square foot to pascals. The complexity of Eq. (2.340) increases because the phase angle ( $\phi$ ) must be included. This angle accounts for the Doppler effect and is found from

$$(2.341) \quad \phi = -M \left[ \frac{(1-x) \cos \psi}{(1 - Mx \sin \psi)} \right] .$$

Suppose now that the blade element drag ( $dD/dr$ ) in pounds per foot is not constant for the blade under consideration. Then a more complicated representation must remain a part of the integrand. The immediate task is to define blade element drag. To obtain a calculated distribution of blade element thrust and drag, I turned to Wayne Johnson who used his CAMRAD II comprehensive program to produce Fig. 2-331. My intention here is to calculate the torque noise with a real blade element drag distribution and compare the results to the ideal UH-60 case that you have just finished reading.

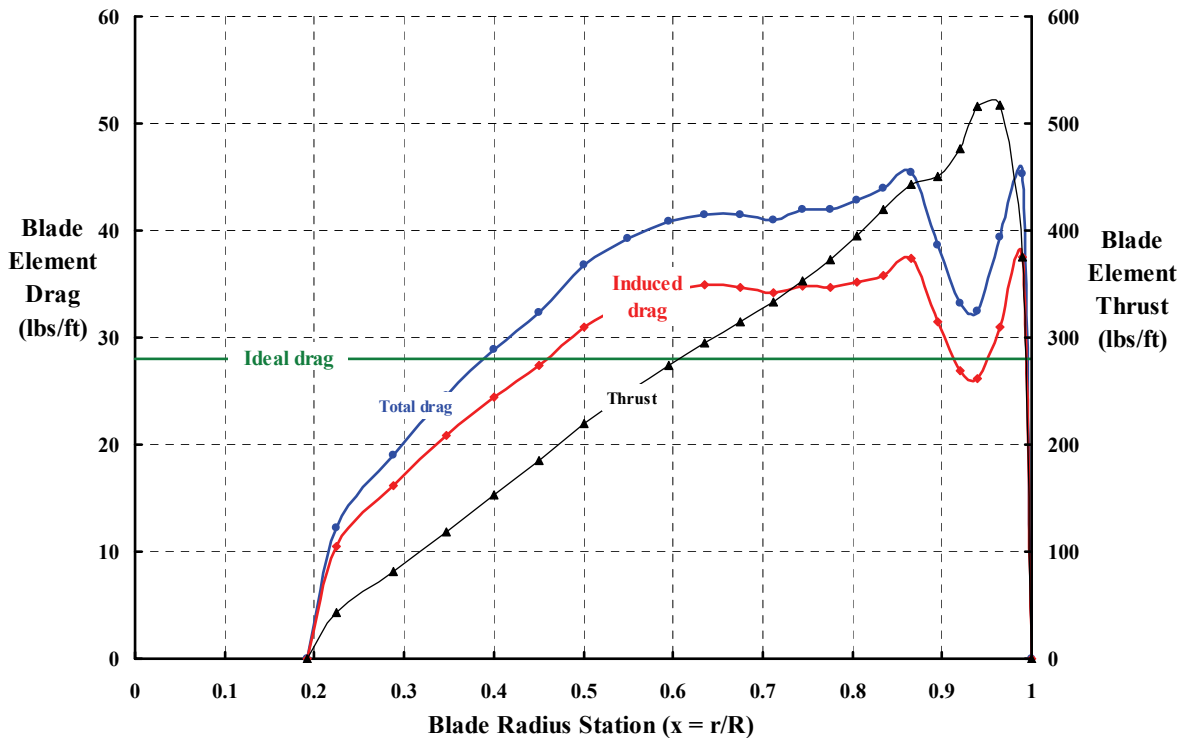


Fig. 2-331. UH-60 blade element forces (23,400-lb thrust, 258 rpm, sea level, standard day).

## 2.7 NOISE

It is worth a moment to calculate the ideal blade element drag per foot to provide a comparison to the CAMRAD result shown in Fig. 2-331. Assuming small angles,

$$(2.341) \left( \frac{dD_{\text{ideal}}}{dr} \right)_{\text{per blade}} = \frac{v}{\Omega r} \left( \frac{dT}{dr} \right)_{\text{per blade}} = \frac{1}{b} \left[ \frac{v}{\Omega r} (4\pi\rho r v^2) \right] = \frac{4\pi\rho}{b\Omega} (v^3) = \frac{4\pi\rho}{b\Omega} \left( \frac{T}{2\rho A} \right)^{3/2}.$$

The blade element thrust ( $dT/bdr$ ) given by momentum theory is rotated through the blade element induced velocity angle ( $v/\Omega r$ ) to create an induced blade element drag ( $dD/dr$ ). For this UH-60 example, the rotor thrust is 23,400 pounds at sea-level standard. This is a disc loading ( $T/A$ ) of 10.345 pound per square foot. The rotor speed, 258 rpm, corresponds to  $\Omega = 27.04$  radians per second. Therefore, the ideal induced blade element drag is slightly over 28 pounds per foot. This drag level is shown as the horizontal line on Fig. 2-331. It is also worth comparing the induced velocity distribution along the blade span, which you see in Fig. 2-332.

To continue then, Fig. 2-333 shows the comparison of the inplane torque loading pressure when the blade element drag distribution is a constant (i.e., ideal) and when the drag distribution reflects a comprehensive code (i.e., CAMRAD II) best estimate. The small change in loading pressure due to a practical, twisted blade has virtually no effect on the noise because the thickness noise is so dominant. The calculated OSPL for the UH-60, assuming an ideal blade element drag distribution, is 87.87 decibels; for what I would call a production blade, the OSPL is 88.34 decibels!

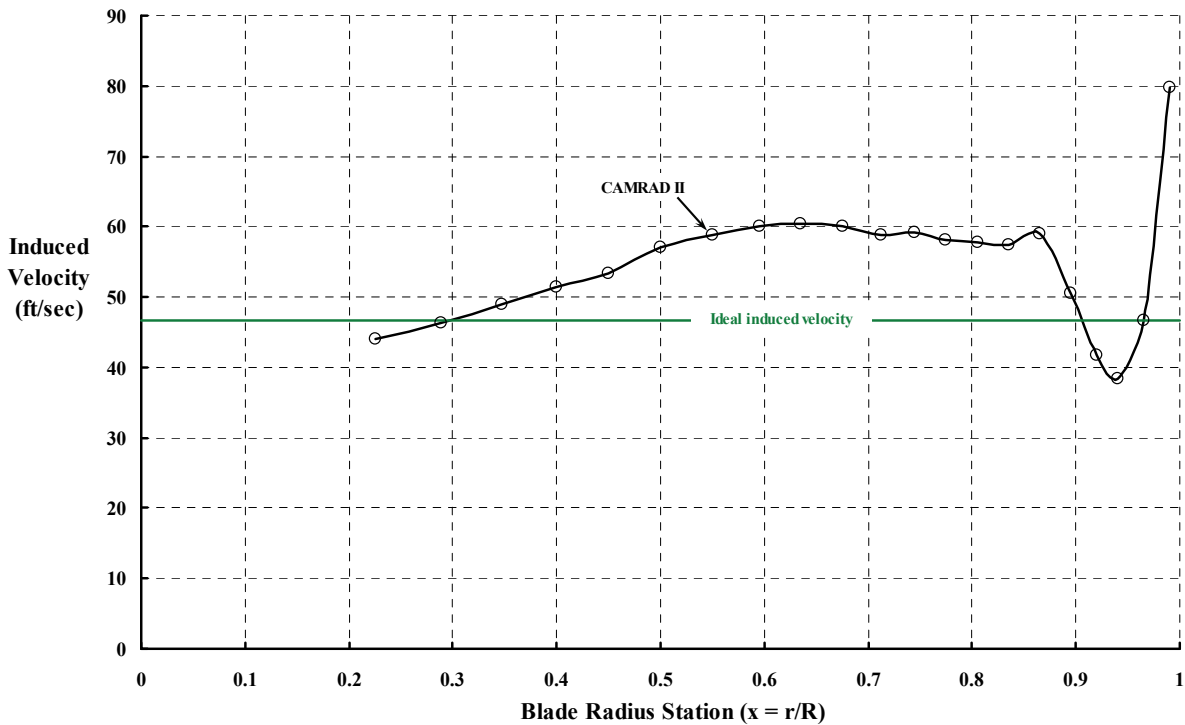


**Fig. 2-332. Induced velocity at UH-60 blade elements (23,400-lb thrust, 258 rpm, sea level, standard day).**

That is not quite the whole story though. The blade elements of a real rotor have both pressure drag *and* skin friction drag.<sup>159</sup> However, my few UH-60 calculations of inplane torque pressure, and then the overall sound pressure level, showed that the UH-60 OSPL would increase to only about 89 decibels when the total blade element drag distribution shown in Fig. 2-331 is used in the calculation.

In closing this discussion of how to get 90 percent of the right estimate of rotor rotational noise in 10 percent of the time, I have come to the conclusion that helicopter main-rotor noise broadcasted radially to an observer nearly in the main rotor plane is dominated by thickness sound pressure. It appears that for many of today's helicopters, thickness sound pressure is so dominant that loading sound pressure is a minor factor. Thus, rotor blade parameters of radial chord and airfoil distributions offer the greater potential for helicopter noise reduction—at least noise created by nearly inplane sound pressure. Unfortunately, I have only touched briefly on noise that reaches an observer when the helicopter is hovering well above the observer. Still, when you look back at Fig. 2-303, you can see that blade planform, number of blades, and tip Mach number are worth several more rotary wing experiments. Of course, cost, maintenance, weight, and performance trade-offs must be made before a significant departure from what is flying can be sold to the industry.

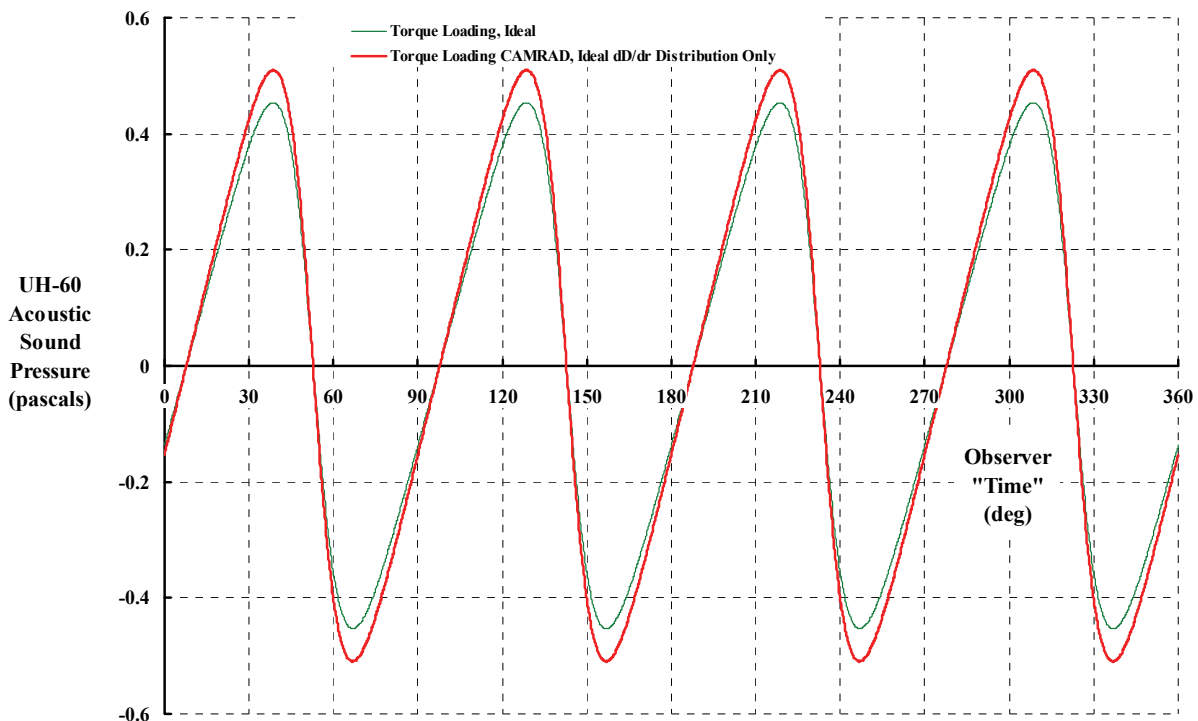


**Fig. 2-333. Differences between ideal and realistic blade element drag distributions do not appear to be a major factor in inplane loading sound pressure.**

<sup>159</sup> In discussing this skin friction aspect of noise with Ken Brentner in mid-January of 2012, he pointed out that skin friction does add noise, but it is generally neglected because it is small.

## 2.7 NOISE

### 2.7.6 The Quiet Helicopter Program

“The high noise level of the present-day helicopter reduces its tactical effectiveness. The element of surprise made possible by the mobility of helicopter-supported operations is negated to a large extent by early aural detection. The possibility of a helicopter-quieting program was the subject of a May 1968 meeting at the Institute for Defense Analyses in Washington, D. C. As a result of this meeting, a research and development program was initiated by the Advanced Research Projects Agency under the direction of Dr. C. J. Wang and technically administered by Mr. R. C. Dumond, Eustis Directorate, USAAMRDL.

In 1969, three helicopters – the Sikorsky SH-3A, Kaman HH-43B, and Hughes OH-6A – were modified for low-noise operation. The NASA Langley Acoustics Branch conducted acoustics measurements of the noise characteristics of the three helicopters. The OH-6A achieved the greatest overall noise reduction of the three helicopters tested.

The approach for the Phase I program was to concentrate on quieting the major noise producer in the OH-6A helicopter – the tail rotor. By incorporating a four-bladed tail rotor (in lieu of a two-bladed) and a low-speed tail rotor gearbox, the aircraft was safely operated at 70 percent  $N_2$  with minimum gross weight (1450 pounds nominal), thus attaining overall sound pressure level reduction of 11 decibels in hover and 11.5 decibels in forward flight. This achievement represents a sound pressure decrease of approximately 73 percent.

In April 1970, a contract was awarded for a Phase II program to obtain a maximum reduction of the sound pressure level (SPL) of all noise sources on the OH-6A helicopter. Descriptions of the modifications, the test programs, and the results obtained are included in this report.”

The above quotation was the introduction that began a report by William Barlow and his coauthors concerning the OH-6 Phase II Quiet Helicopter Program [548]. This report came out in September of 1972. About a year later, the NASA Langley Acoustic Branch released unclassified noise measurement data for the Sikorsky SH-3A [516] and the Hughes OH-6A [514]. A report of the Kaman HH-43B results was released with a NASA Confidential restriction in February of 1971 [549]. The SH-3A and OH-6A reports were declassified by the end of 1973, but for some reason the HH-43B report still remains classified—perhaps because the modified configuration showed very little noise reduction and/or no request for declassification has been made. All three reports note that the activity was a joint project of the Eustis Directorate, U.S. Army Air Mobility Research and Development Laboratory (USAAMRDL), the Advanced Research Projects Agency (established in 1958; became DARPA in 1972 with the addition of the D), and the NASA Langley Research Center.

In the initial selection process, ARPA wanted a Bell UH-1 helicopter based on Bell’s milestone work reported in 1962 [546], but with the production requirements for the Vietnam War, Bell could not be responsive to the desired schedule. This led to the inclusion of the Hughes OH-6A modified helicopter. It is the Hughes OH-6A modifications to the standard machine, and the results obtained, that I want to convey in this discussion of the Quiet Helicopter Program. The primary emphasis of this discussion is on hover.

But first I should mention that a limited edition of the highly modified OH-6A allowed a very covert, secret mission to be conducted on December 5 and 6, 1972. The story came to light when James Chiles published an article in the Smithsonian Air & Space Magazine dated March 1, 1980 [550], which you can read on the Internet. The limited edition OH-6A became known as the Hughes 500P and carried the name "The Quiet One." What I found interesting was that Barlow's report [548] contains not only the highly modified configuration description, but also the equivalent of a mini-flight program suited to a flight safety release. The mini-flight program was conducted from April 1970 to April 1971, and apparently testing was also conducted at the now well-known Area 51. Chiles reports that "Hughes shipped two 500P helicopters to Taiwan in October 1971 and flight training was completed in June 1972." And then Air America and the CIA really went to town. Chiles' article really is quite interesting and well worth your reading time.

While all this Black program was going on, Hughes was carrying out its basic Quiet Helicopter Program. They provided a standard OH-6A and three modified configurations as reported in the NASA unclassified report [514] authored by Henderson, Pegg, and Hilton. A summary of the modifications tested in 1969 as part of the Phase I program, and another, more highly modified configuration that arrived during Phase II and was tested in 1971, are shown in Table 2-39 below, which I have reproduced directly from Henderson's report.

**Table 2-39. Three Modifications to the Standard OH-6A Were Tested by NASA Langley in Two Phases of the Hughes Quiet Helicopter Program [514]**

(a) 1969 modifications

Configuration	Modifications
A	Standard OH-6A helicopter at 658 kg gross weight
B	*Four-blade tail rotor (Chord = 0.122 m) with blade phasing of 60°/120° Main-rotor speed reduced from 484 rpm to 328 rpm New tail-rotor gear box; tail-rotor speed reduced from 3120 rpm to 1630 rpm Power turbine governor was employed to allow engine governing at reduced speeds
C	*Two-blade tail rotor (Wide chord = 0.244 m) Main-rotor speed reduced from 484 rpm to 328 rpm New tail-rotor gear box; tail-rotor speed reduced from 3120 rpm to 1630 rpm Power turbine governor was employed to allow engine governing at reduced speeds

(b) 1971 modifications

Configuration	Modifications
D	Standard OH-6A helicopter at 726 kg gross weight
E	A five-blade main rotor Trapezoidal blade tip cap attached to each main-rotor blade Main-rotor speed was reduced from 468 rpm to 314 rpm Four-blade tail rotor (Chord = 0.122 m) with blade phasing of 75°/105° Tail rotor speed reduced from 3120 rpm to 1272 rpm by using a new tail-rotor gear box A noise suppressor for engine exhaust Modified gearing for main-rotor gear box Damping material added to some of the shafting and gearing Acoustic blanket material applied to transmission and engine compartment

\*The same helicopter (airframe) was employed for both the wide-chord tail rotor and four-blade tail rotor modification.

## 2.7 NOISE

The preliminary work that the Hughes team accomplished during Phase I of the program identified the usual culprits associated with helicopter noise. These culprits are the tail and main rotors, which demand a much slower tip speed than that found when minimum weight empty is the performance objective. The Phase I program leading to the 1969 modifications was limited to those that could easily be made to a standard helicopter. One tail rotor issue that was settled was that at equal solidity ( $\sigma = 0.24$ ) and tip speed ( $V_t = 363$  fps), four narrow-chord blades (Fig. 2-335) were quieter than two wide-chord blades (Fig. 2-336). Furthermore, scissoring the four-bladed tail rotor to a 60-degree acute angle rather than the common 90-degree orthogonal arrangement offered a measurable improvement. There was no question that the reduced rotor speeds were required to achieve the lower noise signature. Henderson and his coauthors concluded that

“a field noise measurement program has been conducted on a standard OH-6A helicopter [Fig. 2-334] and two OH-6A helicopters modified to reduce the external noise levels. The purpose of this study was to document the noise characteristics of each helicopter during flyover, hover, landing, and take-off operations. The 1969 modifications were limited to those which could easily be made to a standard helicopter. The 1971 modifications consisted of extensive modifications of an OH-6A helicopter to have low external noise characteristics.

Based on the analysis of the measured results, the average noise levels associated with the final modified helicopter (configuration E) are 14 dB lower than the standard helicopter (configuration D) while operating at an altitude of 30 meters with an airspeed of 70 knots in level flight.

Narrow-band spectra data of the hovering helicopters show that there was a general reduction of harmonic content with the modified aircraft. Noise reductions at frequencies below 80 Hz are associated with main rotor modifications, those between 80 Hz and 630 Hz with tail rotor modifications, and those above about 630 Hz with engine and gearing modifications.”

What I found rather interesting about these conclusions is that comparative OSPL data from the 1969 results were not even mentioned in the conclusions. It is as if enthusiasm was brimming over to get to the next step, which was Configuration E shown in Fig. 2-337.



**Fig. 2-334. Standard Hughes OH-6A. Configurations A and D (courtesy of Bill Warmbrodt and NASA Langley Research Center).**



**Fig. 2-335. Configuration B modification to the OH-6A. Four-bladed, scissor-tail rotor (courtesy of Bill Warmbrodt and NASA Langley Research Center).**



**Fig. 2-336. Configuration C modification to the OH-6A. Two-bladed, wide-chord tail rotor (courtesy of Bill Warmbrodt and NASA Langley Research Center).**



**Fig. 2-337. Configuration E modification to the OH-6A, which was called The Quiet One and later identified as the Hughes Model 500P. The “P” stood for Penetrator (courtesy of Bill Warmbrodt and NASA Langley Research Center).**

## 2.7 NOISE

I have chosen just one chart from Henderson's report [514] to summarize the noise signature from the OH-6A and its several modified configurations. As you can see from Fig. 2-338, detection time is reduced considerably. Think of it this way: if a standard OH-6A is first heard at -20 seconds, then a person would hear the machine (traveling at 40 knots or 67.5 feet per second) when it is about 1,400 feet away—about a quarter of a mile. In contrast, The Quiet One (configuration E) becomes audible (assuming the same OSPL level in decibels) at about 3 seconds before arrival when it is about 200 feet (or two-thirds of a football field) away. It is easy to see why the Hughes Model 500P was selected for the covert operation carried out in early December of 1972.

To fully appreciate how The Quiet One came about, you would do well to review two reports. The first is William Barlow's report titled *OH-6A Phase II Quiet Helicopter Program* [548]. This report's abstract, with my notes in [ ], is quite informative:

"This report presents the results of the Phase II Quiet Helicopter Program. A Hughes OH-6A Light Observation Helicopter (LOH) was extensively modified to obtain a maximum of quieting. The purpose was to apply the latest known sound-suppression techniques available to industry to an actual helicopter and then to measure the results. An acoustic goal was set which required a balanced treatment of each noise-producing source throughout the full frequency range. Noise reductions ranged from 14 to 20 dB depending on the flight conditions.

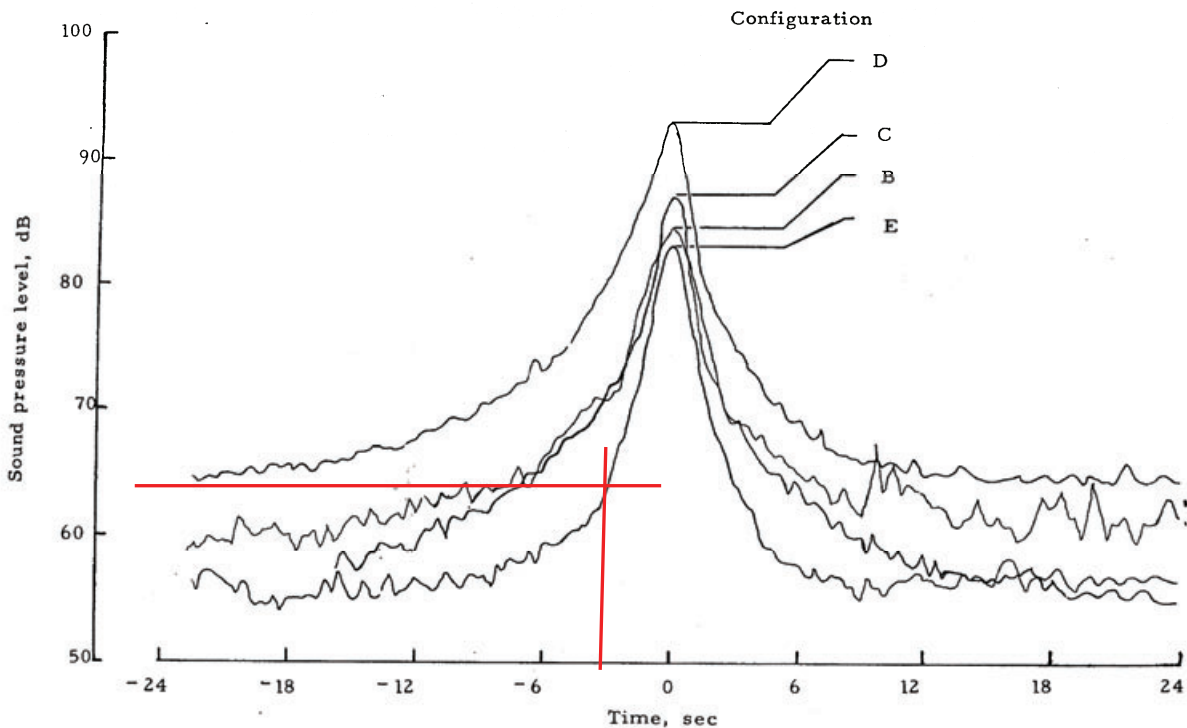


**Fig. 2-338.** The Quiet One (configuration E) offered a dramatic reduction in noise when compared to the Standard OH-6A (configuration D). Measurement made as helicopter approaches, passes directly overhead, and departs. Flight at 1,600 pounds, speed of 40 knots, altitude of 100 feet [514].

The report describes the detailed configuration changes, the test and development programs, and the final sound level measurements compared to the standard OH-6A.

The concept involved the adding of main and tail rotor thrust capacity [4 to 5 blades on main rotor and 2 to 4 blades on tail rotor] to permit operation at reduced RPM and propulsion system quieting to match the overall sound level goals. The additional rotor capacity at full RPM permitted a large net gain in payload and forward speed. Two flight modes were developed: a very quiet low-RPM mode [0.67 times 645 fps main rotor tip speed and 1,600 pounds gross weight] and a quiet high-performance mode [0.78 times 645 fps and 2,400 pounds gross weight]. The pilot changes modes, in a few seconds, by trimming RPM in flight.”

The natural question to ask is what was the weight-empty penalty paid to achieve this very significant reduction in noise signature. In discussing the weight and balance of The Quiet One, Barlow reported that

“the basic weight of the helicopter was increased 192 pounds with the incorporation of the quieting features. This represents a 15 percent loss in useful load for the standard OH-6A, which has a maximum Army-approved gross weight of 2400 pounds. However, the added rotor capability at 100 percent N2 will permit increasing the gross weight to 3150 pounds – a payload increase of more than 85 percent.

The permissible longitudinal center-of-gravity range for the Quiet Helicopter is from 4 inches forward to 7 inches aft of the main-rotor centerline (stations 97 to 107). Since most of the weight was added aft of the main-rotor centerline, the center of gravity of the aircraft moved from station 109 to station 114.9, making it necessary to carry forward ballast when operating at 1600 pounds to remain within the aft limit. Ballast is not required, however, when operating the aircraft at heavier gross weights with the usual avionics equipment installed in the forward areas.”

The basic weight of the OH-6A is given [117] as 1,145.5 pounds, the primary mission weight is 2,163 pounds, an alternate mission weight is 2,400 pounds, and the structural limit is 2,700 pounds. Barlow states that the modifications to the OH-6A amounted to 192 pounds, of which 71 pounds went to engine and engine compartment treatment. Thus, the basic weight increased to 1,337 pounds, a 17 percent increase. To offset that penalty, Hughes was prepared to increase the maximum takeoff gross weight from 2,400 to 3,150 pounds. You might think that was rather aggressive, but keep in mind that Hughes proceeded to grow the Model 500 series rather quickly to the five-bladed 500 D, which was FAA certified in early December of 1976 with a weight empty of 1,414 pounds and a maximum gross weight of 3,000 pounds. *I believe any competent helicopter manufacture could duplicate Hughes' efforts at quieting their products. It only requires management of weight empty and selling price. Clearly the technology existed in the early 1970s.*

The second report to read was written by Frank Robinson and titled *Component Noise Variables of a Light Observation Helicopter* [541]. This NASA-sponsored effort was a ground test of an OH-6A and several individual components. In this experiment, first a standard OH-6A and then the evolving Quiet One were attached to a test rig as shown in Fig. 2-339. Robinson's report includes only data measured at just the one microphone location shown. Some 255 runs were made covering such variables as rotor speed, thrust, engine and engine

## 2.7 NOISE

compartment muffling, and many sub-configurations. Frank Robinson's report is, in my opinion, a gold mine.<sup>160</sup>

The test setup included several unique features and components as Robinson points out. Four key points I selected for you are:

1. At the rear of the [test rig] unit is the dynamometer which can be connected to the aircraft's power plant by means of a drive shaft with universal joints at each end. The Allison T-63 engine has provisions for driving from either end which allows the dynamometer drive shaft to be connected without disturbing the aircraft's regular drive system. The dynamometer cooling system consists of three automotive radiators, with electrically driven automotive fans, a cooling water reservoir, and an electrically driven circulating pump. The dynamometer was able to absorb full engine power. There was, however, a noise frequency recorded which corresponded to the RPM of the dynamometer drive shaft.
2. A separate large tank muffler, or [engine] silencer, was also fabricated and can be seen at the extreme right of figure 2. For those test runs requiring the engine to be silenced, this tank muffler was connected to the engine exhaust with a long insulated duct, also visible in fig. 2.
3. When mounted on the test rig, the helicopter could be run with any combination of its major components either removed or silenced. The tail rotor could be removed and the engine silenced so only the main rotor could be heard. The main rotor could be removed and the engine silenced so only the tail rotor could be heard. Both the main and tail rotors could be removed with the dynamometer absorbing the power so only the engine could be heard.
4. The test aircraft was equipped with precision visual instrumentation for reading engine torque, tail rotor torque, tail rotor thrust, collective pitch and tail rotor pitch. The aircraft was flown in free hover at a 6-foot skid height and a variety of gross weights and rotor speeds to obtain calibrated readings. This enabled the pilot to duplicate the various rotor thrust and power conditions with the helicopter mounted on the test rig by setting-up the same values for collective pitch, etc., as those recorded during free hover.”

Now let me show you what I think was the starting point for what led to The Quiet One. Following point 4 above, an overall sound pressure level of 87.0 decibels in free hover was measured. The aircraft was at a gross weight of 2,400 pounds, the main rotor tip speed was 666 feet per second, and the tail rotor tip speed was 692 feet per second. These tip speeds correspond to 103 percent of design engine operating speed. When mounted to the test rig at the same control settings, the measured OSPL was 88.5 decibels. For reference then, the narrow band frequency content of noise for this base case is shown in Fig. 2-340. Note that I have added a red line, to the right of which a human is likely to hear the OH-6A. Thus, the first noise peak at about 31 Hz—a 4 per rev from the main rotor—should be readily heard.

---

<sup>160</sup> Frank Robinson was not able to interest any of his employers (Cessna, McCulloch, Kaman, Bell, and finally Hughes) in his concept for a small, low-cost helicopter, so he resigned from Hughes and in June of 1973 founded Robinson Helicopter Company in his Palos Verdes home. The first R22 prototype was built in a tin hangar at the nearby Torrance Airport, and in August of 1975, Robinson flew the R22 on its first flight. In 1979, after 3-1/2 years of testing and technical analysis, the R22 received its FAA Type Certificate. The first R22 was delivered in late 1979 and soon became the world's top selling civil helicopter. His four-seat R44 was FAA certified in late 1992. His R66, a turbine-powered machine, was certified in October 2010. In June 2010, with FAA certification of the R66 eminent, Frank Robinson retired at the age of 80. The company publicly announced his resignation as President and Chairman in August 2010. Now *that* is a story that easily matches those of our pioneers.

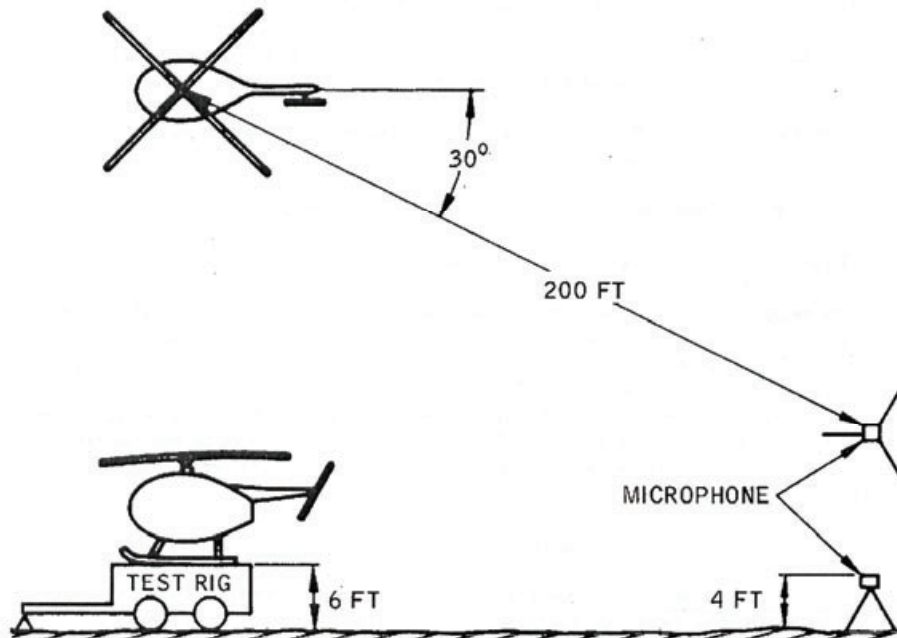


Fig. 2-339. Tie-down test rig used during OH-6A component noise measurement program placed the main rotor plane 14.2 feet above ground level [541].

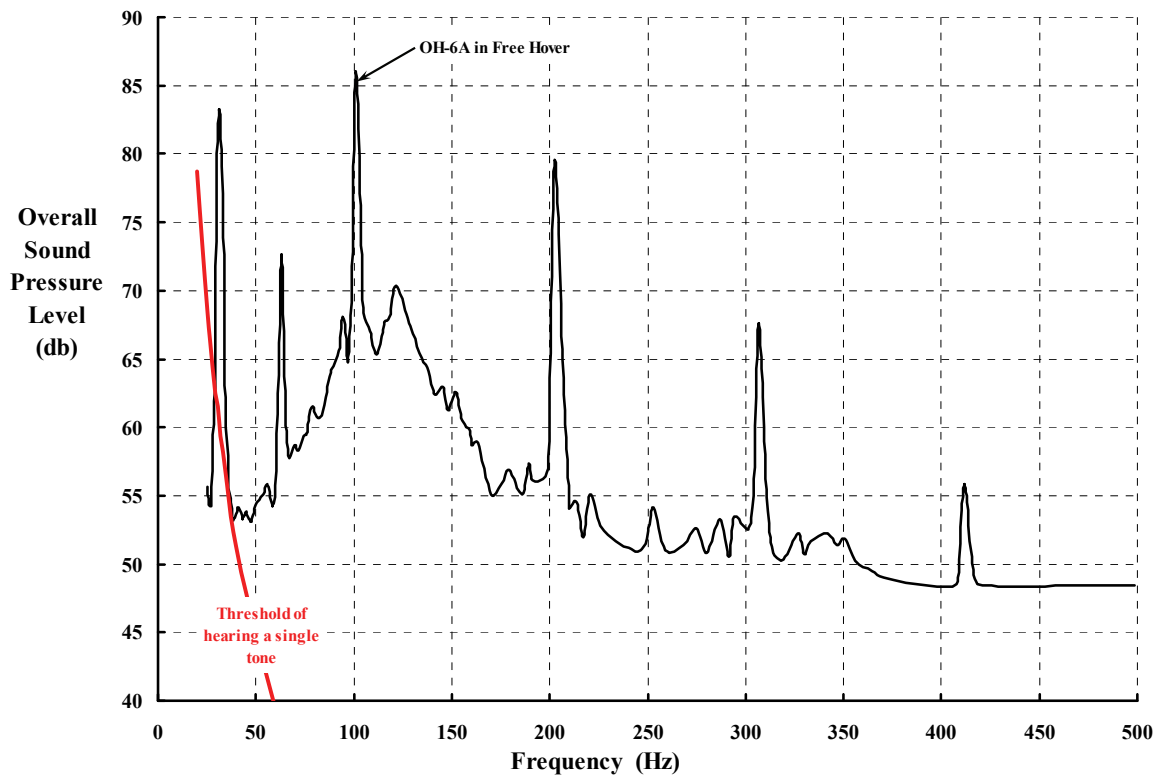


Fig. 2-340. Narrow band frequency content of OSPL for the OH-6A in free hover at an altitude of 6 feet (gross weight 2,400 lb, 103 percent engine rpm). The helicopter's OSPL was 87.0 decibels [541].

## 2.7 NOISE

Now consider the three major components and their individual contribution to the OH-6A noise signature that you see in Fig. 2-341, Fig. 2-342, and Fig. 2-343. The testing of the engine alone (Fig. 2-341) required the dynamometer to absorb 215 horsepower at 103 percent N<sub>2</sub> because both the main and tail rotors were not installed. No acoustic treatment of the engine or the engine compartment was applied at this point, nor was the low-noise exhaust pipe installed. This was just the noise of a production Allison T63-A-5A as installed in a production OH-6A. Well, that is not quite right because the drivetrain was still operating as if the rotors were installed. However, drivetrain noise signatures only became obvious above 1,000 hertz as you will see when you read Barlow's report [548].

The main rotor's contribution to the OH-6A noise signature (Fig. 2-342) at a thrust of 2,400 pounds (206 hp) and tip speed of 666 feet per second shows that it was only very apparent at the 4 and 8 per revolutions of the main rotor. Beyond that, the engine and tail rotor noises are dominant and mask all higher harmonics. Notice the orderly progression of the noise spikes at multiples of  $1 \times 4/\text{rev}$ ,  $2 \times 4/\text{rev}$ ,  $3 \times 4/\text{rev}$ , etc.; this follows fundamental acoustic theory.

Finally, the tail rotor's contribution to the OH-6A noise signature (Fig. 2-343) at a thrust of 130 pounds (18.9 hp) and 692 feet per second tip speed shows that it was very apparent at its fundamental two-bladed frequency and for several multiples of  $2/\text{rev}$ , even above the 500-hertz range I have chosen to examine in this introduction.

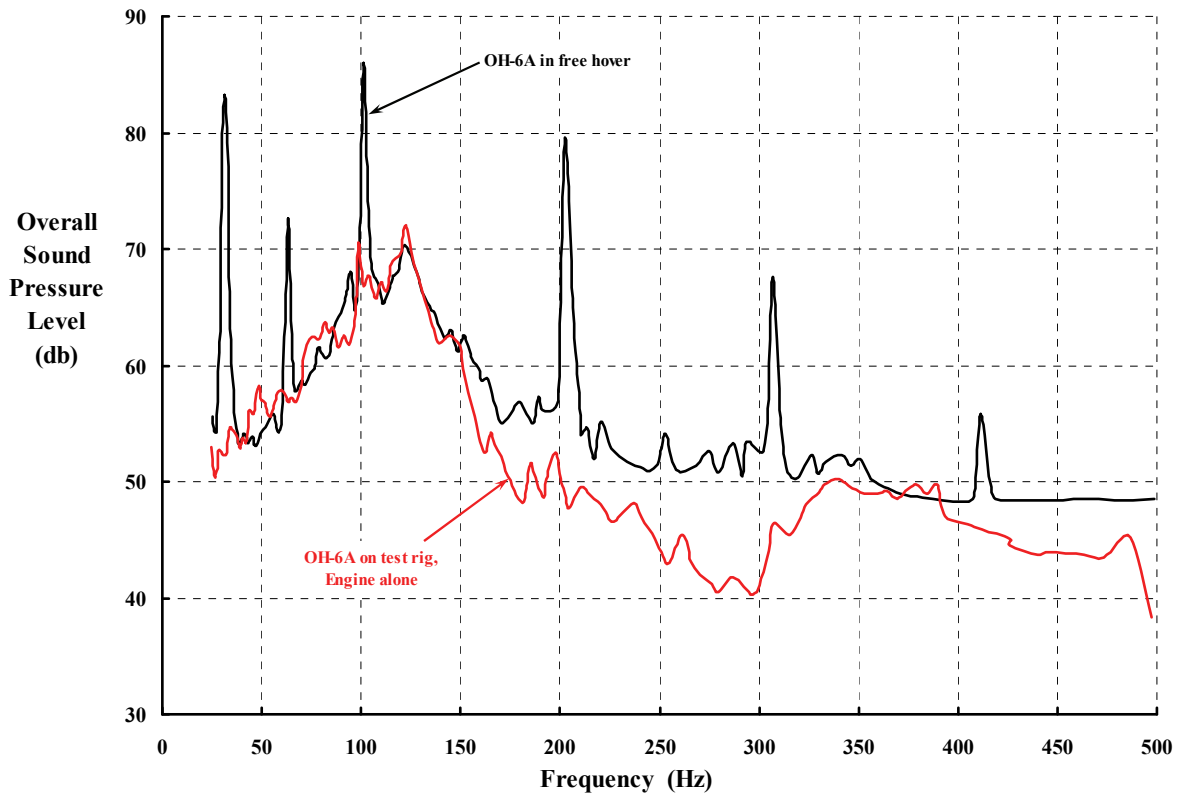


**Fig. 2-341. Engine-alone frequency content of OSPL for the OH-6A. The OSPL of just the engine alone was 83.5 decibels [541].**

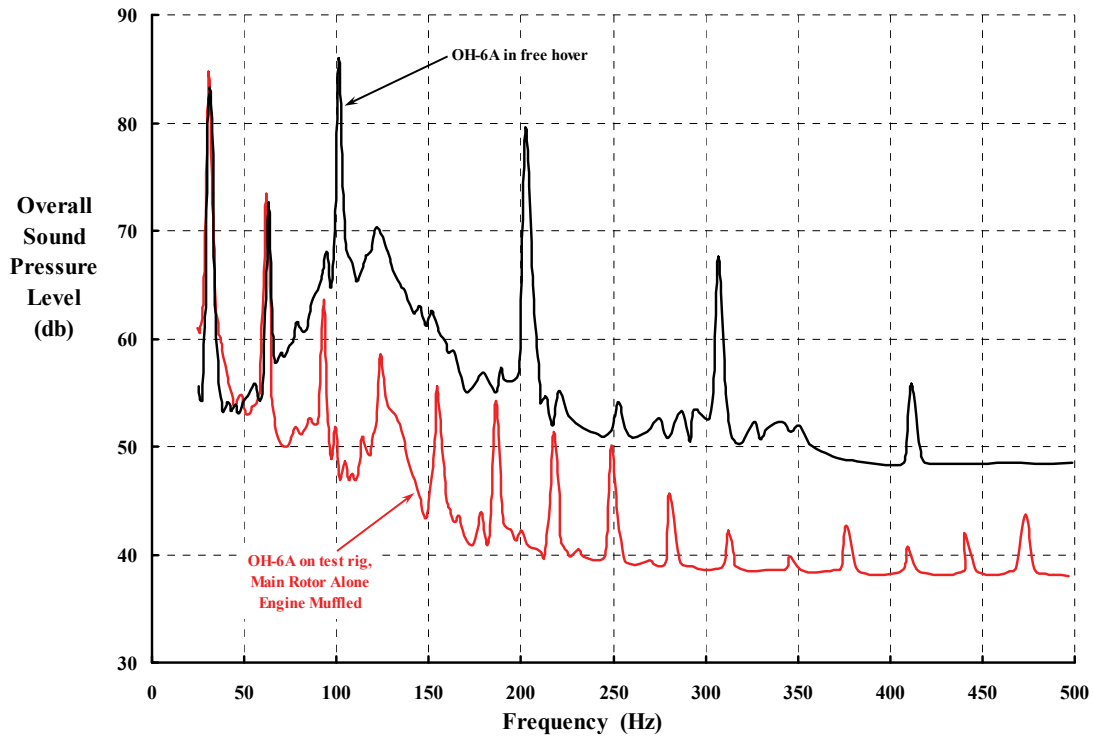


**Fig. 2-342. Main-rotor-alone frequency content of SPL for the OH-6A. The OSPL of just the main rotor alone was 86.0 decibels [541].**

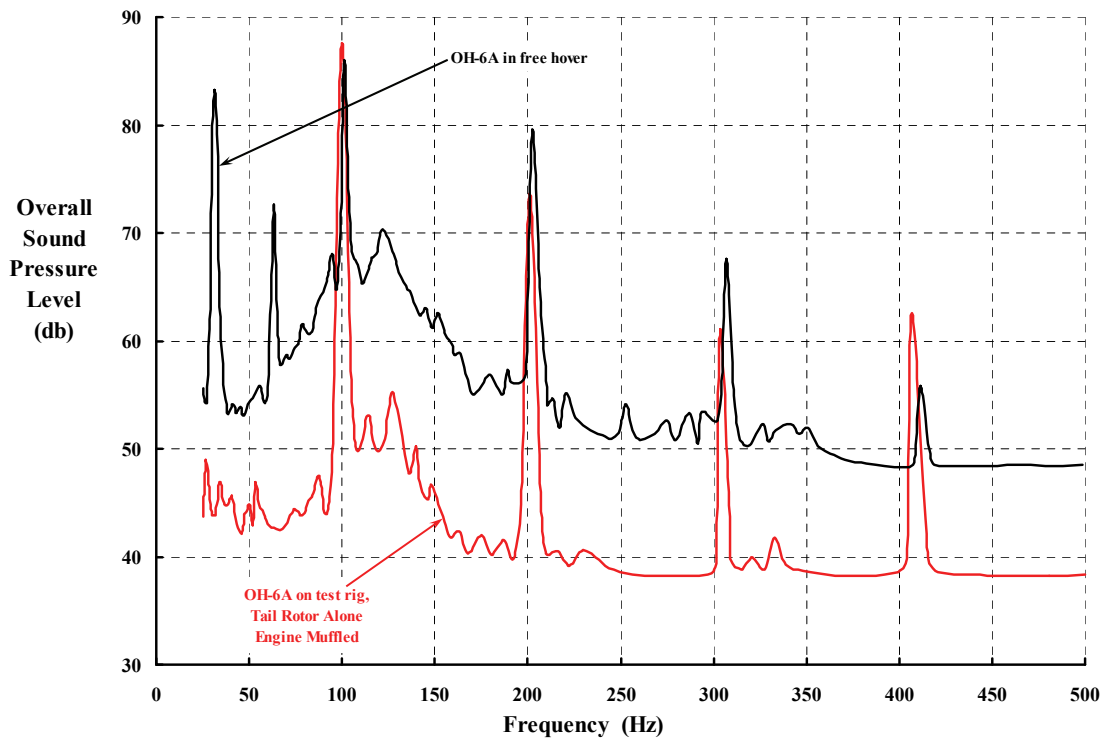


**Fig. 2-343. Tail-rotor-alone frequency content of SPL for the OH-6A. The OSPL of just the tail rotor alone was 86.0 decibels [541].**

## 2.7 NOISE

As you can quickly appreciate from the three preceding figures, the attack on OH-6A noise had to include silencing of the engine and its compartment, and many of the drivetrain components (to be able to operate the aircraft at a low RPM), and then tackling the noise spikes that became apparent. I find it very interesting that the body of Barlow's report [548] was a very packed 54 pages, 23 pages of which were devoted to engine and drivetrain details. Five pages were used to discuss the tail rotor, and only 4 pages covered the main rotor. Two charts in Barlow's report stand out, in my opinion, as summarizing the comparison of The Quiet One versus the standard OH-6A before the aircraft were shipped to NASA Langley. Most impressive is the reduction in aural detection distance by a factor 6, which is shown in Fig. 2-344. The noise reduction demonstrated in hover is shown here as Fig. 2-345.

Taking Barlow's and Robinson's work to heart, it seems clear to me that there is no assembly in any helicopter now flying, or that is yet to be conceived and put into production, that can be overlooked if the objective is to significantly reduce noise. Furthermore, I would suggest that the place to start is with the engine and drivetrain areas, which may be less glamorous than studies of main and tail rotor noise, but offer high payoff for considerably less time and money spent. And in closing, I think that Hughes' accomplishments equal what NASA showed could be done with a Stinson L-5, which you saw earlier in Fig. 2-303.

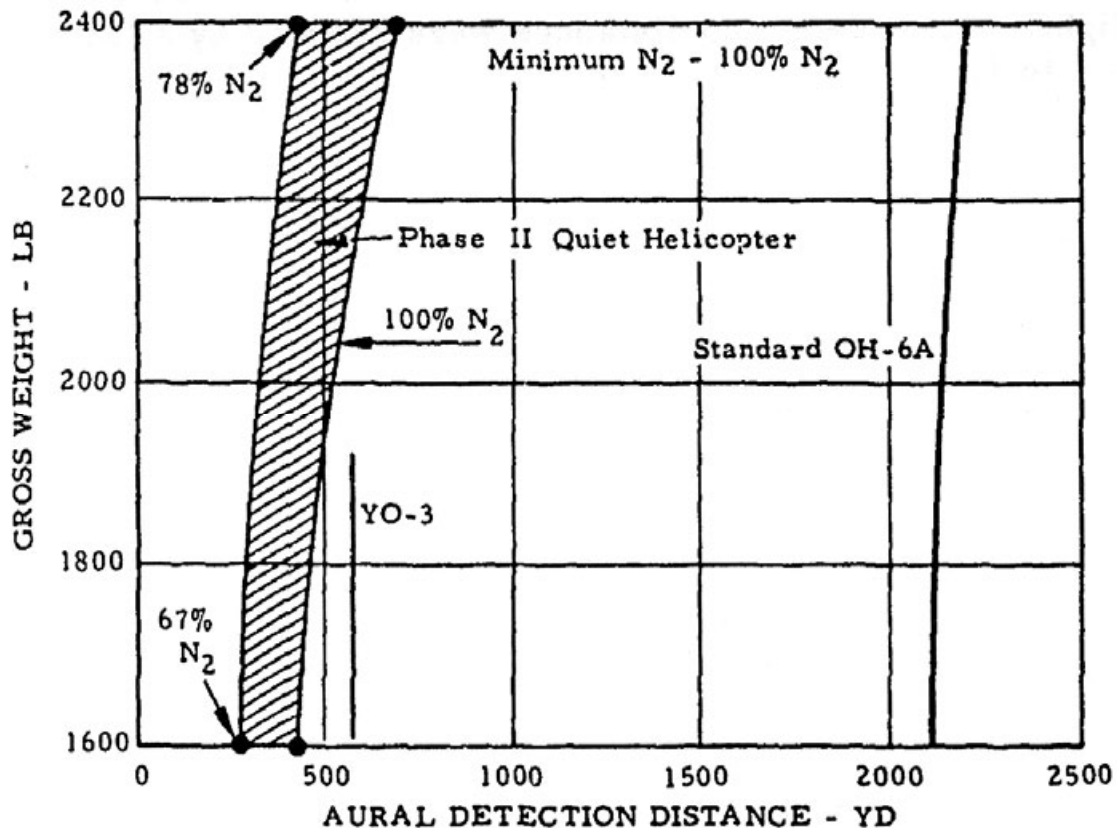


Fig. 2-344. Reduction in OH-6A aural detection distance achieved by Hughes during Phase II of the Quiet Helicopter Program [548].

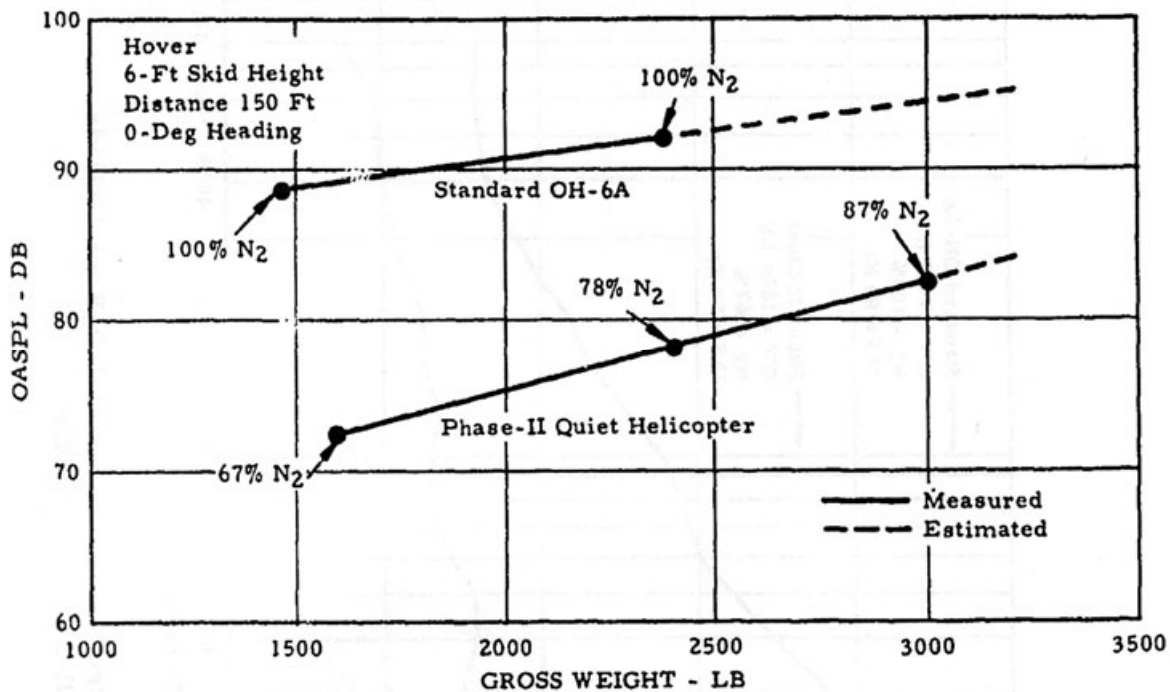


Fig. 2-345. Reduction in standard OH-6A hover noise achieved by Hughes during Phase II of the Quiet Helicopter Program [548].

### 2.7.7 Government Noise Regulations for Helicopters

Shortly after the completion of The Quiet Helicopter Program, the war in Vietnam came to an end.<sup>161</sup> The number of helicopters then being sold in the world was climbing by leaps and bounds. In the United States alone, The Federal Aviation Administration (FAA) was (a) experiencing an overwhelming number of applications for airworthiness certificates, and (b) providing helicopter registrations at the rate of 500 per year as Fig. 2-346 shows. But then, in the late 1970s, the general public started to have enough helicopters flitting about that people began noticing them—and the noise they produced. It was simply a repeat of what happened when the airplane came on the scene in the mid-1920s, only now there were more people complaining than just berry pickers near Boise, Idaho. National authorities of several nations, including the U.S., began to prepare draft regulations that would restrict operations of helicopters in highly populated areas—just the areas that the helicopter was designed to service. In fact, the FAA issued a Notice of Proposed Rulemaking on July 19, 1979, outlining proposed noise certification procedures and limits [551].

About this time, the International Civil Aviation Organization (ICAO), supported by the FAA and most European nations, established a working group to develop helicopter noise certification standards. Faced with the certainty of some ill-conceived regulations, the industry, and the Helicopter Association International (HAI) in particular, offered a different approach. At this point, let me quote directly from the HAI *Fly Neighborly Guide* [552]:

<sup>161</sup> Saigon fell on April 30, 1975.

## 2.7 NOISE

“The industry, and HAI in particular, felt that a better approach would be for the industry to develop voluntary guidelines to control the noise impact by operational means. After a number of FAA/industry meetings, the FAA, in the fall of 1981, agreed to withdraw its initial NPRM related to helicopter noise certification while additional technical data were acquired.<sup>162</sup> This was done with the understanding that the helicopter industry would develop new technology—creating quieter, more advanced equipment, and implement a voluntary noise abatement program. This resulted in the establishment of the HAI Fly Neighborly Program based on an earlier program developed by Bell Helicopter Textron [553-555].

ICAO initially issued international noise standards in 1981, as a part of the International Standards and Recommended Practices, Environmental Protection, Annex 16 to the Convention on International Civil Aviation. These were not adopted by many nations before they were relaxed in 1985. Since that time, the standards have been amended a number of times. The FAA subsequently issued helicopter noise certification standards in 1988. These have been revised over the years. They are defined in 14 CFR Part 36.”

You can download the HAI *Fly Neighborly Guide* [552] (only 28 pages, all for free) and I am sure you will have no trouble grasping its content. The reason I say that is because the technical content has been obtained from key rotorcraft engineers reinterpreting much of their noise measurements so that even laymen get the points. In stark contrast, the ICAO’s set of aircraft noise standards is slightly over 200 pages [556] and costs \$180 with shipping, and then you have the FAA’s regulations about rotorcraft noise [557, 558], which spell out the certification procedure in nearly infinite detail. For example, precise microphone placement and noise measurements for three flight profiles must be obtained. The profiles cover takeoff (Fig. 2-347), flyover (Fig. 2-348), and landing (Fig. 2-349). Then the recorded data is reduced to a pass/fail grade using a most detailed set of equations [558]. (Further discussion of ICAO and FAA requirements relative to noise is definitely beyond the scope of this discussion.)

The HAI *Fly Neighborly Guide* gets to the heart of the helicopter noise problem. If you will take a moment to review Fig. 2-315 on page 468, you will note that listed under Other Types of Noise are High-Speed Impulsive noise and Blade-Vortex Impulsive noise. The combination of basic research and operational experience during the late 1970s and early 1980s disclosed that some airfoils along a rotor blade could experience transonic flow at certain operating conditions. At high speed, severe noise became quite clear to an observer on the ground as the tip of an advancing blade began to exceed a critical Mach number. It was as if the blade tip was breaking the “sound barrier.” You will recall that when an airplane breaks the sound barrier, people hear only one loud bang or crack, and then the airplane is gone. Low-speed helicopters take considerably longer to pass the observer, but the observer hears many rotor revolutions before the helicopter is out of sight, and each revolution produces mini sonic booms from every blade. Rotorcraft aero-acousticians have labeled this high-advancing-tip Mach number noise as high-speed impulsive noise.

---

<sup>162</sup> The initial proposed regulation would have required retrofitting all helicopters in the fleet. This would have required an enormous amount of research, time, and money. In essence, the helicopter industry would have had to ground virtually every machine. The revised regulations basically grandfathered what was flying, which gave industry the time to meet the new regulations with much quieter machines.

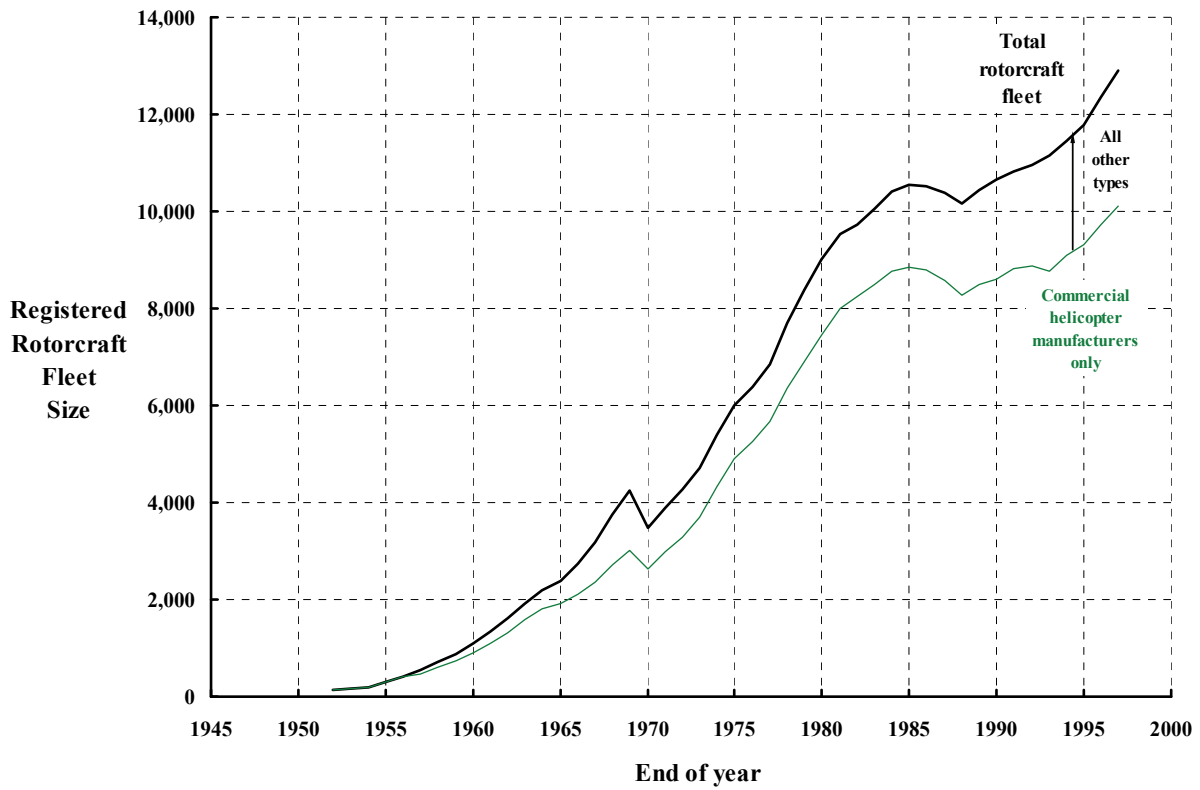


Fig. 2-346. Growth in the U.S. rotorcraft fleet.

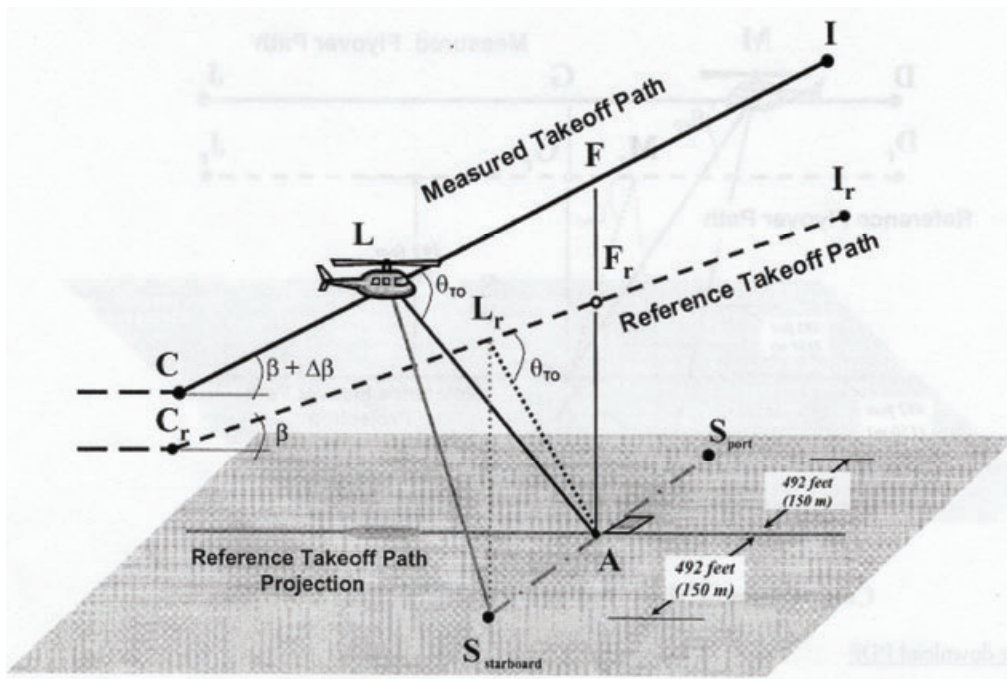


Fig. 2-347. FAA takeoff flight profile for noise certification [557].

## 2.7 NOISE

The other very annoying noise came when a helicopter was descending at relatively low speed as in an approach to landing. The magnitude of this noise was on par with high-speed impulsive noise that came with transonic Mach numbers of rotor blade tips, but was, upon research, associated with the wake from an upstream blade impinging on a following blade. Testing and analysis led to calling this wake-blade interaction situation Blade-Vortex Interaction and adopted the shorthand notation of BVI. The HAI *Fly Neighborly Guide* had

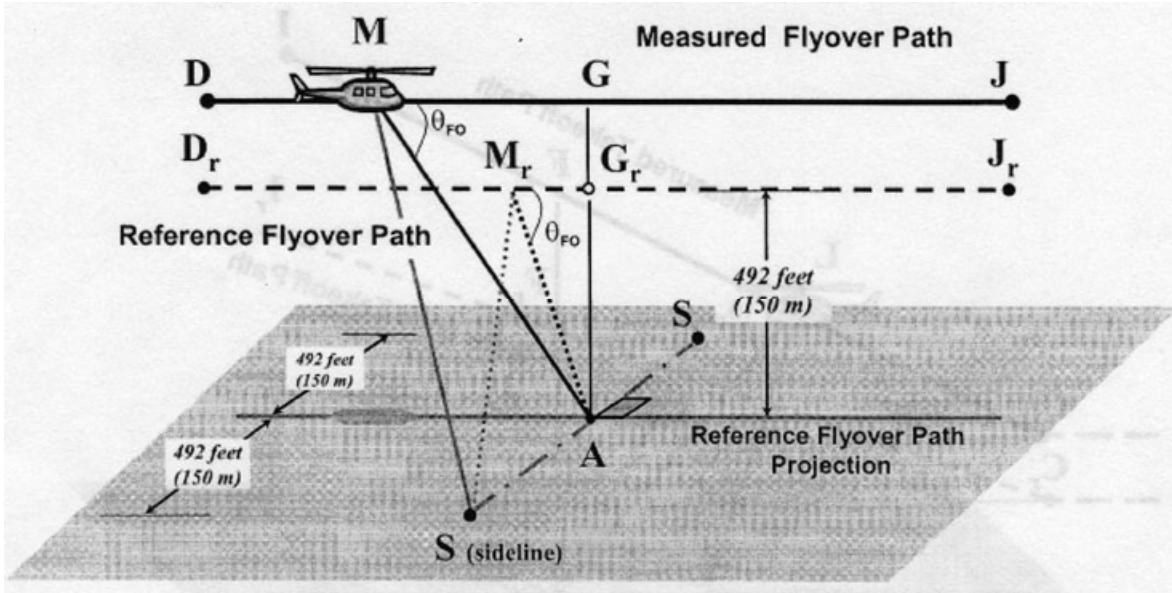


Fig. 2-348. FAA flyover flight profile for noise certification [557].

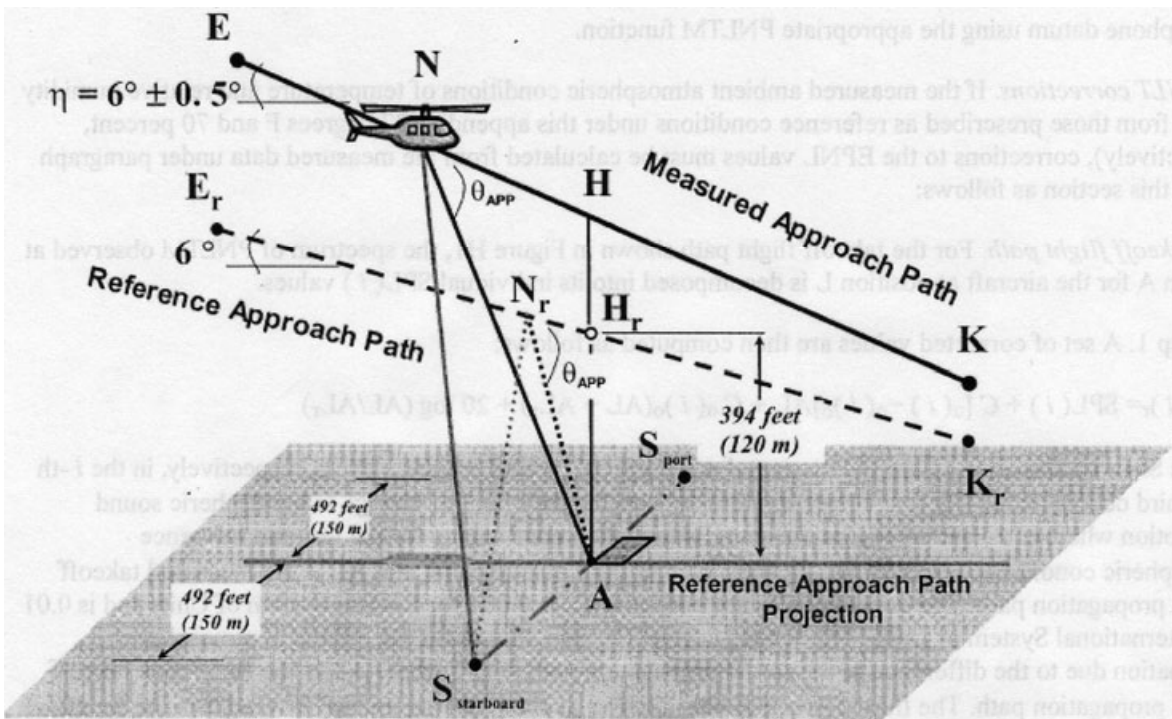


Fig. 2-349. FAA landing flight profile for noise certification [557].

this to say about the operating noise characteristics:

“For a typical small/light helicopter, the most annoying noise mechanism impulsive noise (BVI) occurs during partial power descents and in sharp/high-rate turns. For a typical medium or large/heavy helicopter, they can occur in low-speed level flight, during partial power descents, and in sharp/high-rate turns. Figures 1, 2 and 3 show the flight conditions under which you can expect main rotor impulsive noise to occur.

The impulsive noise boundary for your particular helicopter may be somewhat larger than that shown in Figures 1 and 2 because the main rotor may generate impulsiveness intermittently when it encounters wind gusts, or during a rapid transition from one flight condition to another. Although the sound produced at these descent rates is not extremely loud to crewmembers inside the helicopter, they can, in most cases, recognize it and, thereby, define the impulsive noise boundaries for their particular helicopter. However, in some cases, the impulsive BVI noise cannot be detected in the cockpit. Of course, people on the ground hear impulsive noise grow more intense as the helicopter descends.”

I have included here as Fig. 2-350, the first two of the three figures that the *Fly Neighborly Guide* refers to.

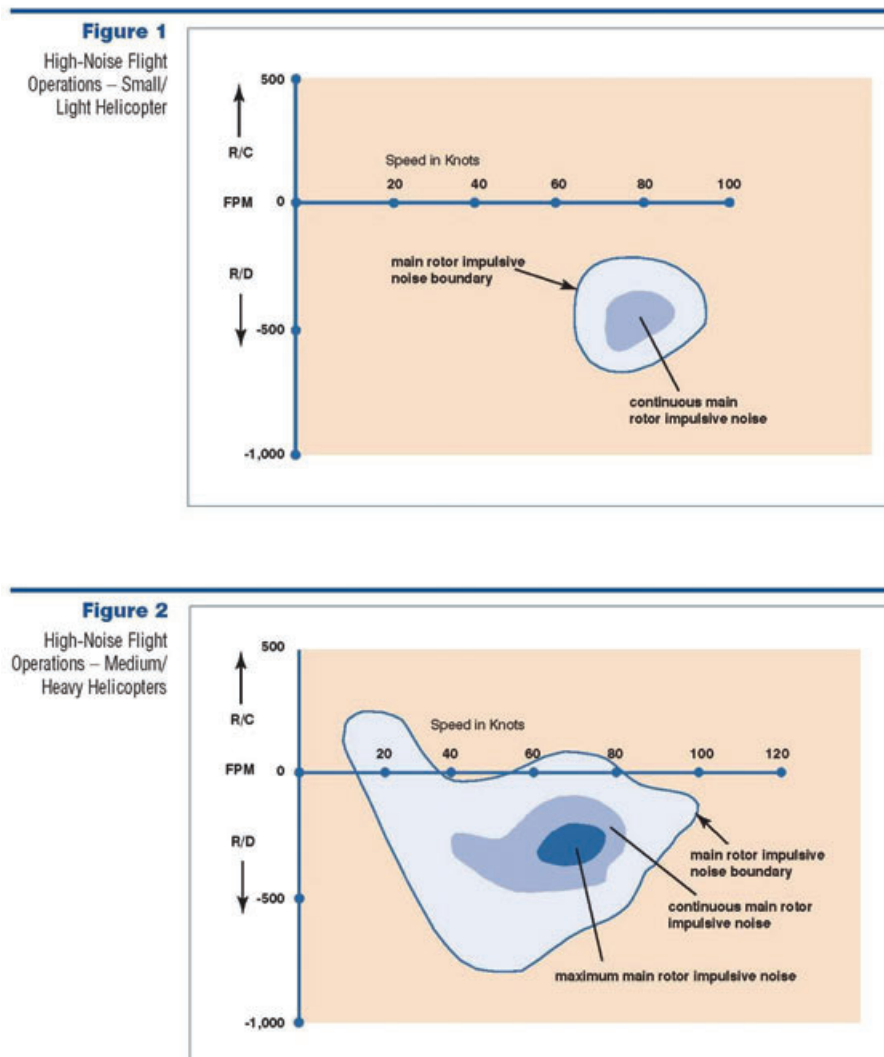


Fig. 2-350. Regions of high blade-vortex interaction (BVI) to be avoided [552].

## 2.7 NOISE

The HAI *Fly Neighborly Guide* goes on with a discussion about how to make the approach to landing so as to fly around the blade-vortex interaction region. Because the BVI region is less pronounced for small and light helicopters, the *Fly Neighborly Guide* suggests two ways around the BVI region, but for medium and heavy helicopters the guide suggests skirting around the BVI region so the approach would be made at a rate of descent of about 900 to 1,000 feet per minute. I have added the FAA's 6-degree required approach for certification to both figures (Fig. 2-351 and Fig. 2-352). Personally, it appears to me that lower noise will be produced using an approach glide slope more like 12 degrees. In fact, the guide makes this very point with its figure 7, which you see here as Fig. 2-353.

### 2.7.8 Noise in Forward Flight

At this point in the discussion,<sup>163</sup> it would be nice to write that understanding and prediction of helicopter noise in forward flight is complete, but even after nearly four decades of research, noise created by blade-vortex interaction (BVI) and/or transonic advancing blade tip speeds has only recently become predictable. You may wonder then how the HAI could publish such clear advice in graphical form as shown in Fig. 2-351 and Fig. 2-352. The answer is rather simple: the HAI suggestions are based on a collection and simplification of a large body of experimental data. This is not to infer that no theoretical progress has been made. In fact, quite the opposite is true as I will now summarize.

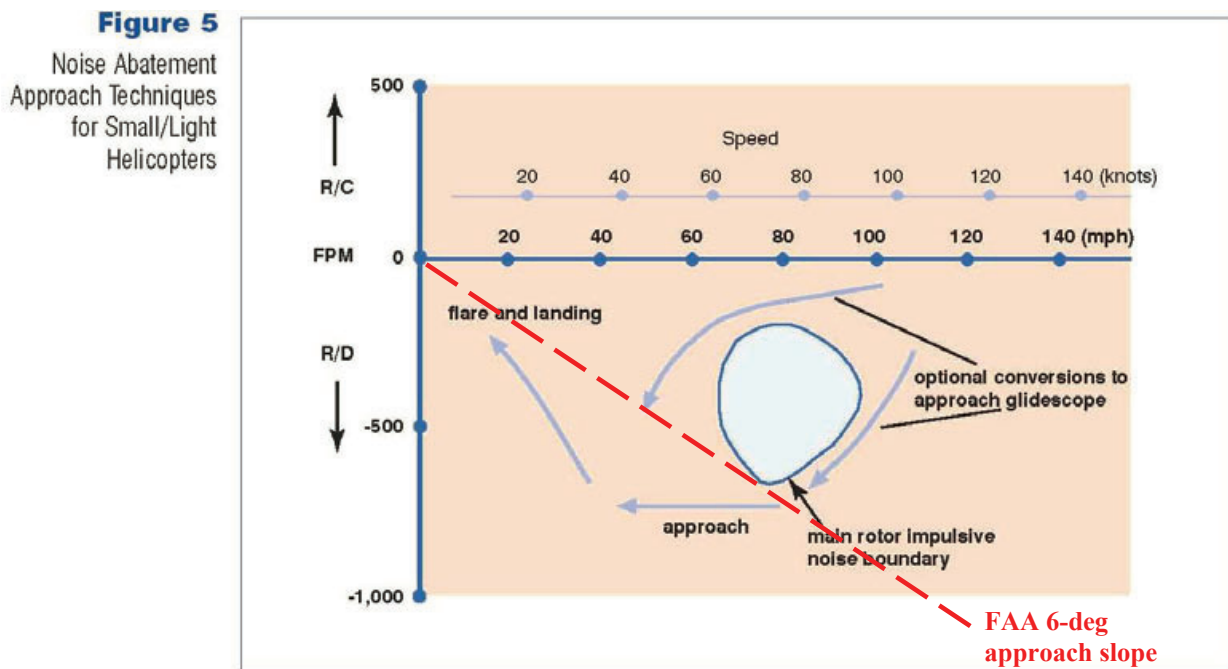


**Fig. 2-351. The HAI *Fly Neighborly Guide* for noise abatement with small/light helicopters [552].**

<sup>163</sup> As of February 14, 2012.

**Figure 6**  
Noise Abatement  
Approach Technique  
for Medium and  
Heavy Helicopters

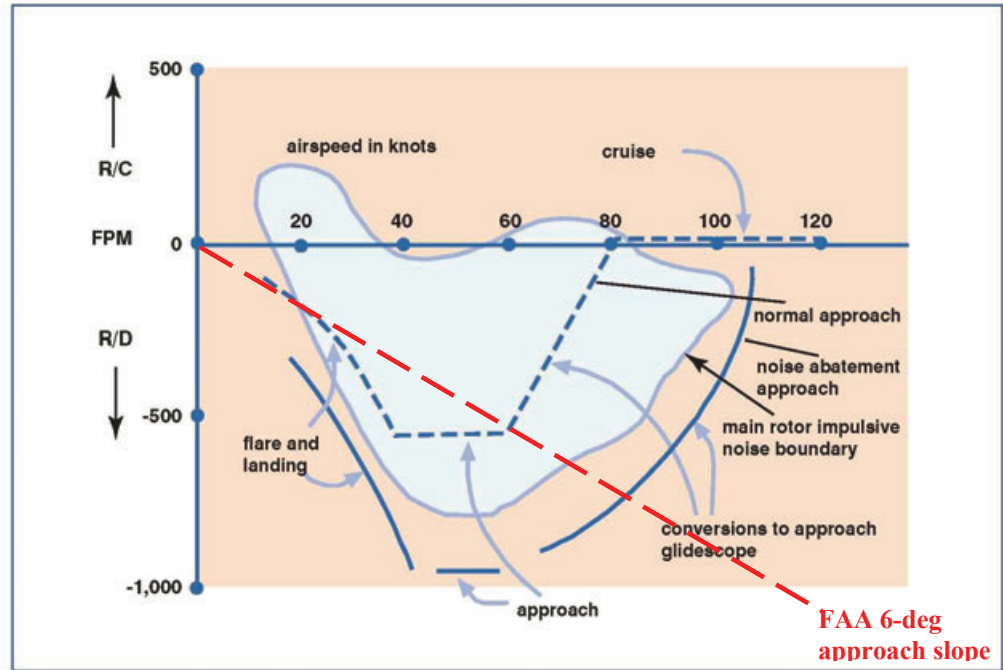


**Fig. 2-352.** The HAI *Fly Neighborly Guide* for noise abatement with larger helicopters [552].

**Figure 7**  
Ground Noise  
Exposure Footprint

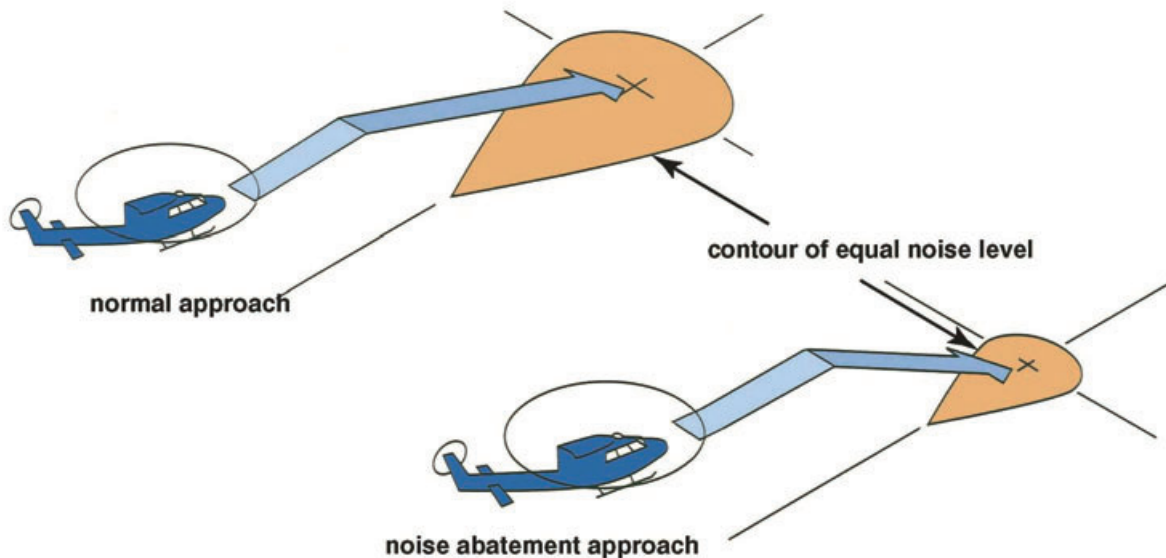


**Fig. 2-353.** The HAI *Fly Neighborly Guide* suggests that a lower noise footprint can be achieved operationally with steeper approaches than the 6 degrees specified by the FAA for certification purposes [552].

## 2.7 NOISE

The research that has gone on since 1970 has not concentrated on what a person on the ground hears. That is the task that regulatory bodies have concentrated on. Rather, noise research has concentrated on the sound pressure levels emanating from the sources on the helicopter. While regulatory bodies have worked to quantify annoying noise in terms of a decibel,<sup>164</sup> researchers have been deciphering particular noise signatures from pressure waveforms plotted as a time history (with pressure being in pascals or sometimes in dynes per square centimeter; note that 10 dynes/cm<sup>2</sup> equals one pascal). And the research that has gone on has been, rather specifically, on the most annoying rotor noises, which are high speed and blade-vortex impulsive and broadband. To guide this summary, let me refer you to the classifications of rotor noise you saw earlier, which I have repeated here as Fig. 2-354.

To provide you with some insight into progress in noise research, I intend to draw the story primarily from four papers and two status reports. These publications were compiled by very knowledgeable researchers:

1. Fred Schmitz and Don Boxwell's 1976 landmark AHS Journal paper [559].
2. Fred Schmitz and Yung Yu's 1979 follow-on AHS Journal Paper [560].
3. Fred Schmitz's Chapter 2 in Volume 1 of Harvey Hubbard's two volumes, which came out in 1991 [545].
4. Ken Brentner and Feri Farassat's two papers, one from 1994 [561] and the other from 2003 [522].
5. Mike Watt's Chapter 3 from the September 2009 NASA status report compiled by Gloria Yamauchi and Larry Young [530].

By the late 1960s, engineers had a good handle on rotational noise. This progress came about primarily because of research on fixed-wing propeller noise. Then in the early 1970s, research on helicopter noise began in earnest despite little industry interest or serious requests from either the military or civil marketplaces. The motivation came from the theoretical work published by Ffowcs Williams and Hawkings [521] in 1969 and the germ of an idea to record in-flight helicopter noise, which came to Fred Schmitz in 1974.<sup>165</sup>

In my opinion, experimental noise research took a giant step forward when Fred Schmitz and Don Boxwell published [559] the first results of helicopter in-flight noise measured by a very quiet fixed-wing aircraft flying in formation with the helicopter under investigation. This first-of-its-kind experiment used a U.S. Army UH-1H helicopter trailing

---

<sup>164</sup> I myself would suggest that the units of annoying noise should be the number of kids and/or grandkids awoken from an afternoon nap.

<sup>165</sup> As Fred related the story to me, he was in Europe training pilots of Hueys to fly quietly when operating near their airbases, which were generally close to cities. He happen to see an icing rig used to spray ice in flight onto a following aircraft. He asked Dick Lewis (then working at Edwards), "Why can't we mount a microphone on a OV-1 and record helicopter noise?" Dick thought it could be done. Despite several naysayers (including Fred's boss, Irv Statler) Fred made it happen. Later, Fred used his persuasive powers to obtain an FBI YO-3 airplane for extensive testing of many other helicopters at NASA Ames Research Center. Much of the data is still classified.

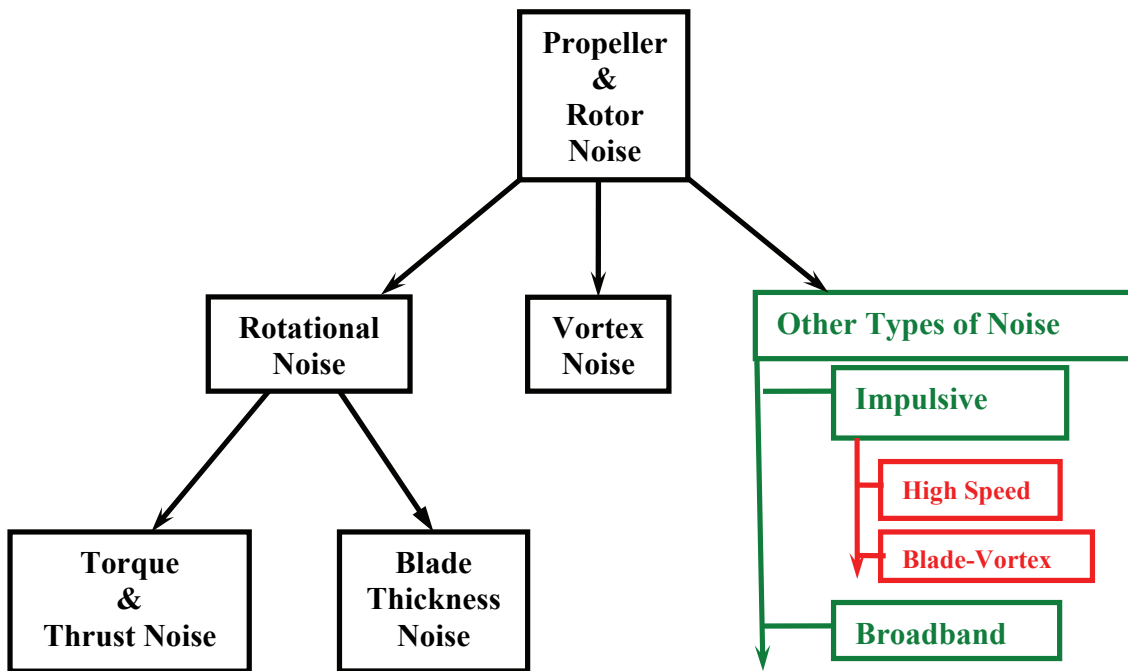


Fig. 2-354. The noise categories in 1940 with some modern additions.

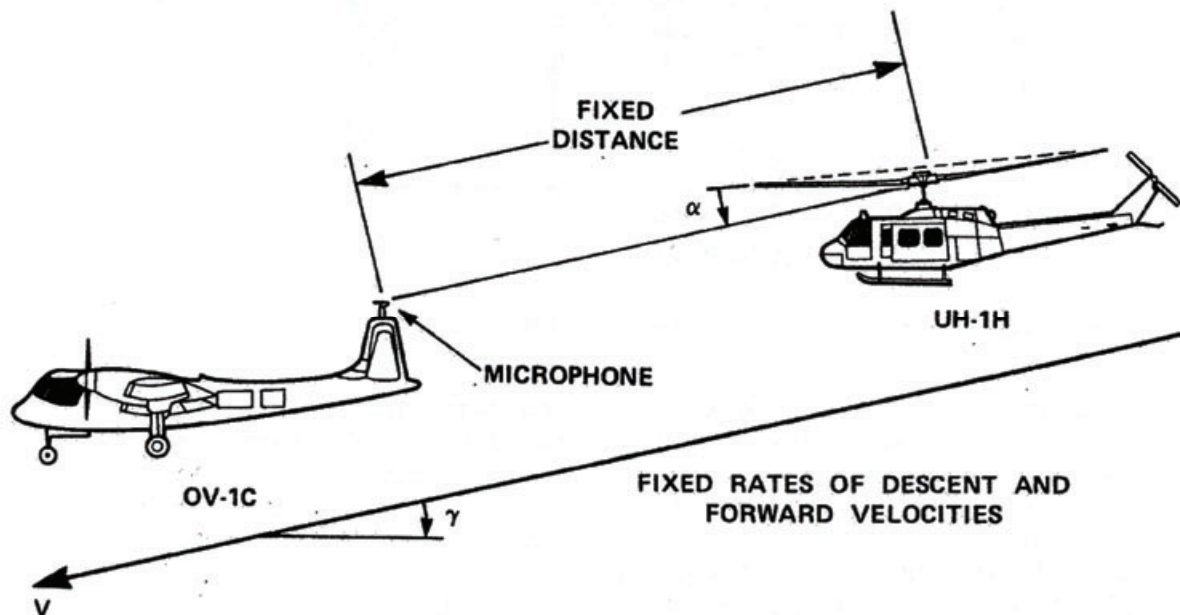


Fig. 2-355. The first in-flight measurements of helicopter noise must be credited to a team led by Fred Schmitz and Don Boxwell [559].

2.7 NOISE

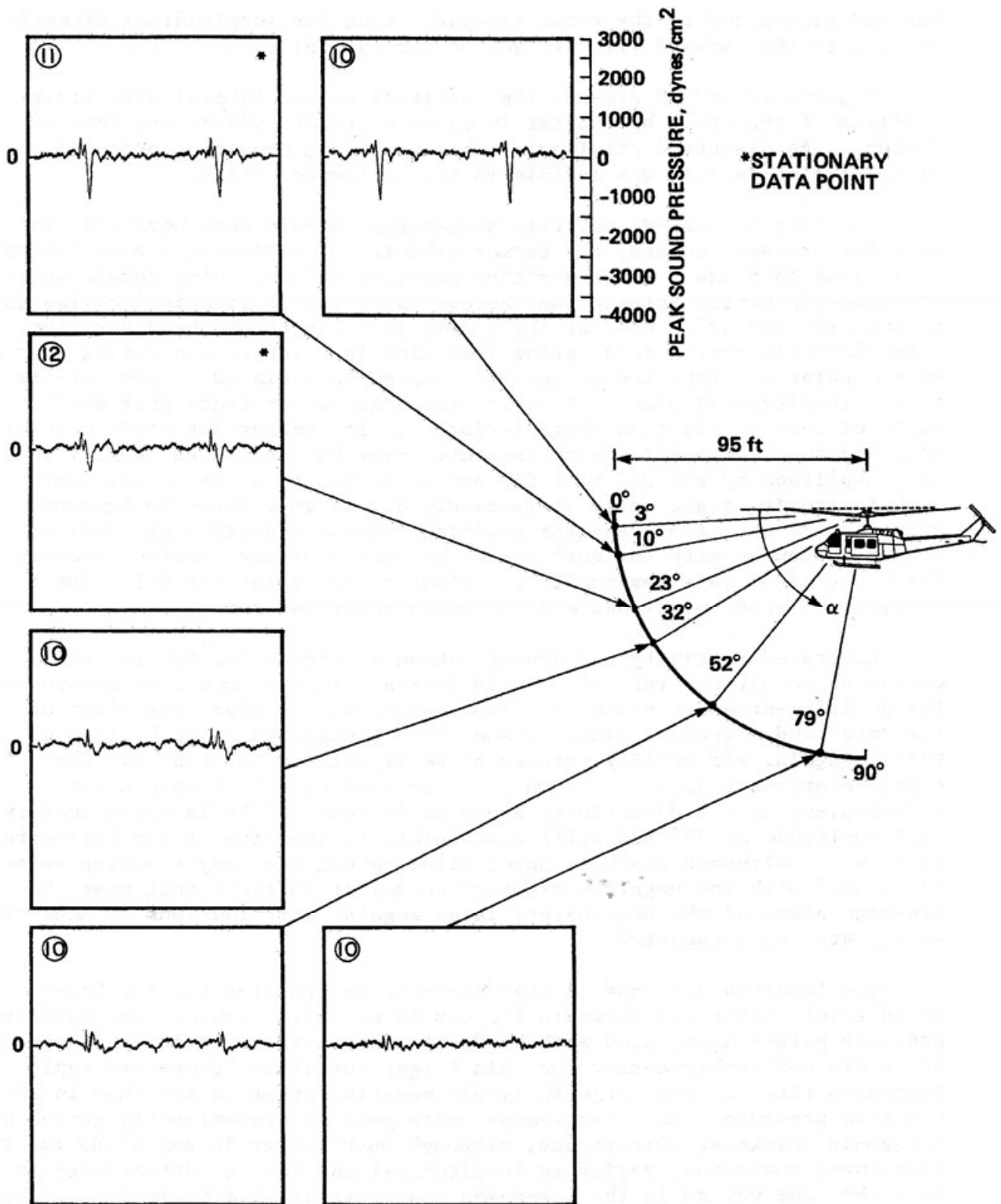


Fig. 2-356. UH-1H sound pressure waveforms with the helicopter at 80 knots indicated airspeed and at a rate of descent of 400 feet per minute. Time scale is for one revolution [559].

behind a U.S. Air Force OV-1C. The geometry of the test procedure is illustrated in Fig. 2-355, and results are shown in two forms. The first form is shown here in Fig. 2-356. By maneuvering the OV-1C carefully around the UH-1H, sound pressure levels and characteristic waveforms were obtained at several radiating angles. To the searching eye, distinct pressure impulses were quite evident, and this began identification of blade-vortex interaction and high-speed, impulsive noise waveform signatures.

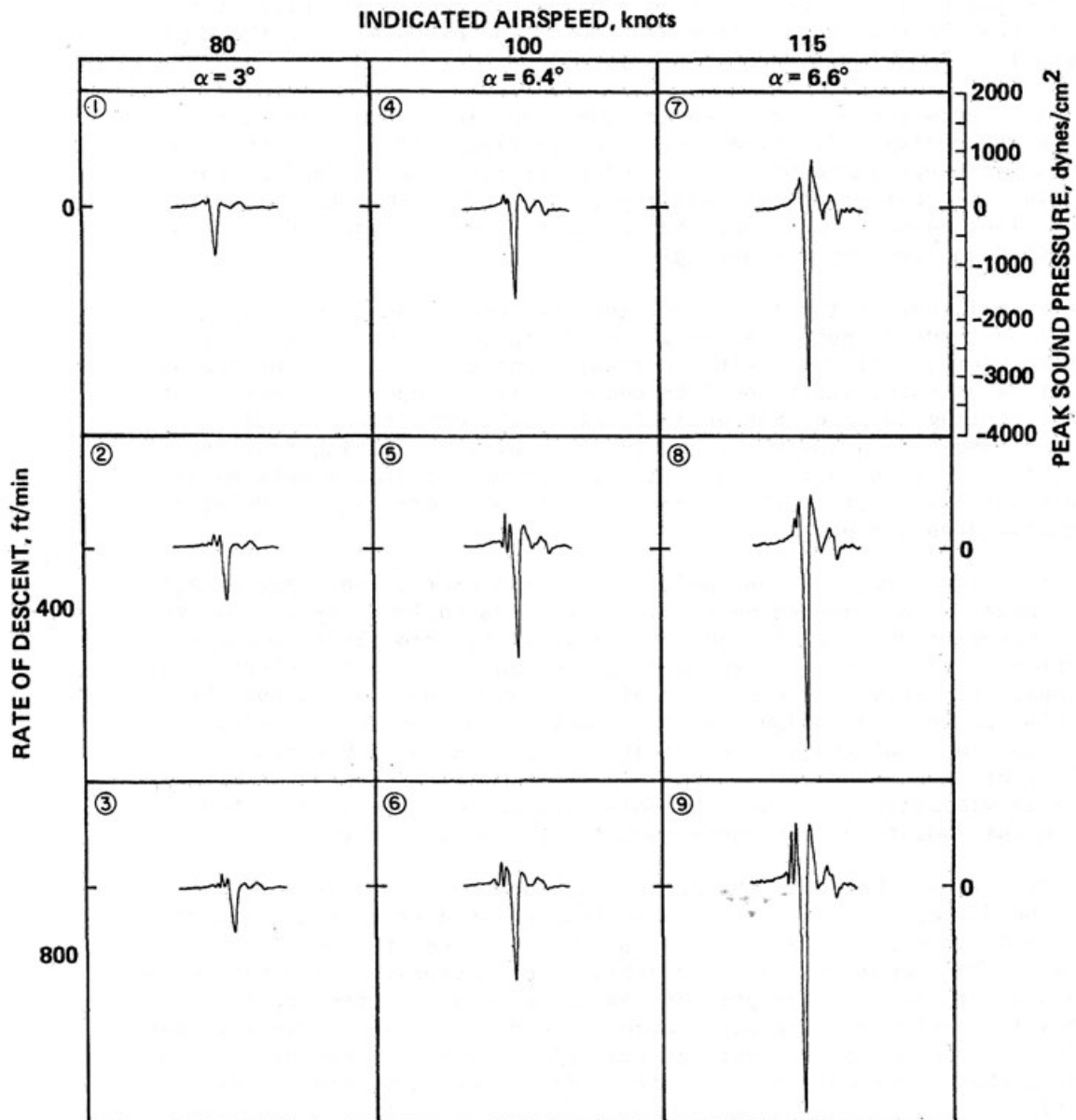


Fig. 2-357. UH-1H sound pressure waveforms for a small matrix of indicated airspeeds and rates of descent. Time scale is one-half of a revolution [559].

## 2.7 NOISE

The second form provide by Fred and Don's paper [559] is a sparse airspeed and rate-of-descent matrix of sound pressure waveforms. This data is shown here in Fig. 2-357. Now you see the influence of advancing tip Mach number, which clearly dominates the pressure waveform. Given that the UH-1H tip speed is about 814 feet per second, the advancing tip Mach number is calculated as  $M_{x=1, \psi=90^\circ} = M_{at} = (V_{FP} + V_t)/a_s$ , and so it follows that 80 knots equates to an advancing tip Mach number of about 0.85, 100 knots to 0.88, and 115 knots to 0.90, assuming that the speed of sound ( $a_s$ ) is 1116.4 feet per second. You can see that the noise impulse creates a very large pressure spike approaching 3,000 to 4,000 dynes per square centimeter at 115 knots. That is equivalent to 300 to 400 pascals.

It is worth a moment to crudely estimate the overall sound pressure level produced by such massive impulses as Fig. 2-357 shows. Suppose I make use of the fundamental equation that calculates overall sound pressure level (OSPL) in decibels that you encountered earlier. That is, let me apply

$$(2.305) \quad \text{OSPL} = 10 \log_{10} \left\{ \frac{1}{p_{\text{ref}}^2} \left[ \frac{1}{T_2 - T_1} \int_{T_1}^{T_2} (p_t^2) dt \right] \right\}$$

to the time history of sound pressure ( $p_t$ ) shown in Fig. 2-358. Here I have assumed a UH-1H two-bladed main rotor having a tip speed of about 814 feet per second. A tip speed of 814 feet per second corresponds to nearly 5.4 revolutions per second or, more usefully, one revolution in 0.186 seconds. The two-bladed UH-1H will have two sound pressure impulses for every revolution. As Fig. 2-358 shows, the two impulses will occur over a very short time increment of  $T_3 - T_1$  and  $T_6 - T_4$ . I will assume that between the two spikes the sound pressure is zero. On this basis, the OSPL equation is used in this example as follows:

$$(2.341) \quad \text{OSPL} = 10 \log_{10} \left\{ \frac{1}{p_{\text{ref}}^2 (T_7 - T_0)} \left[ \int_{T_0}^{T_1} (p_{0 \rightarrow 1}^2) dt + \int_{T_1}^{T_2} (p_{1 \rightarrow 2}^2) dt + \int_{T_2}^{T_3} (p_{2 \rightarrow 3}^2) dt + \text{etc.} \right] \right\}.$$

Now suppose the pressure drop is linear with time. That is, from  $T_1$  to  $T_2$  the time history behaves simply as a straight line so that  $p_t = At+B = p_{\text{max}}(t-T_1)/(T_2-T_1)$ . Note that the pressure drop occurs during the first half of the impulse time so that  $T_2 = T_1 + (T_3 - T_1)/2$ . Assume the rise in pressure from  $T_2$  to  $T_3$  is a mirror image of the pressure drop. Thus, a pressure impulse is modeled as two right-triangles placed back to back on the long side. Finally, assume the second pressure impulse is a duplicate of the first. This makes four right-triangles to be accounted for with a two-bladed rotor.

With this two-bladed impulse model, you have, in effect, four pressure segments (the left and the right hands of two spikes, if you will) and the OSPL calculation is reduced to

$$(2.342) \quad \text{OSPL} = 10 \log_{10} \left\{ \frac{4}{p_{\text{ref}}^2 (T_7 - T_0)} \left[ \int_{T_1}^{T_2 = \frac{T_3 + T_1}{2}} \left[ \frac{p_{\text{max}}}{(T_2 - T_1)} (t - T_1) \right]^2 dt \right] \right\}$$

and the integration result is simply

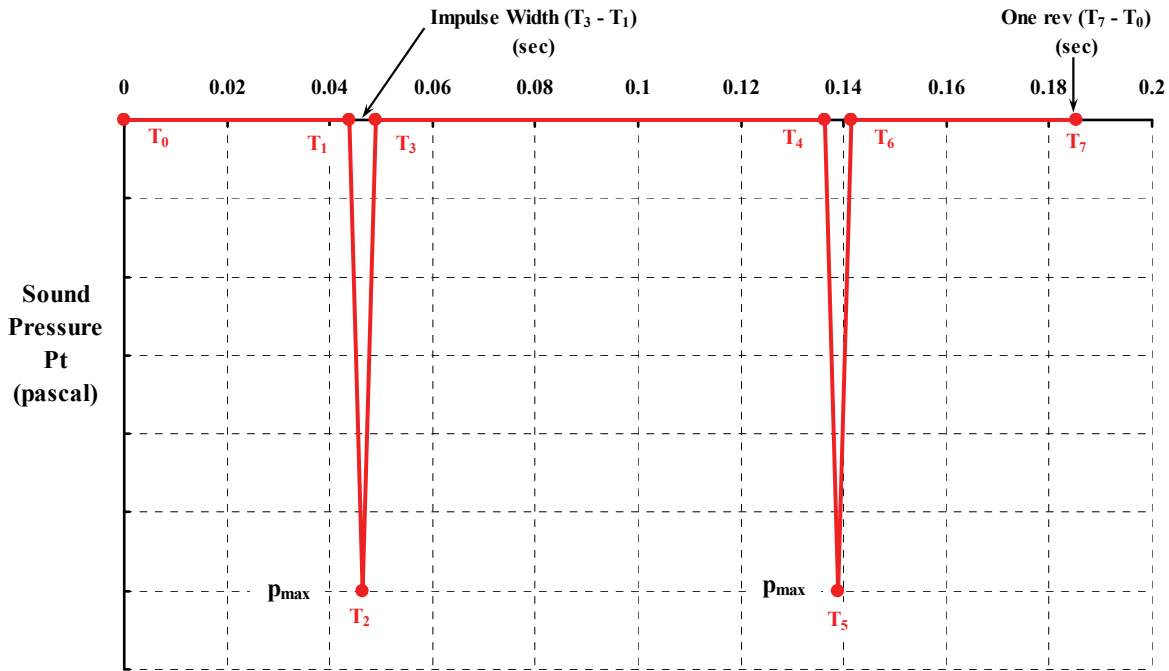


Fig. 2-358. UH-1H sound pressure waveforms for a small matrix of indicated airspeeds.

$$(2.343) \quad \text{OSPL} = 10 \log_{10} \left\{ \frac{2 p_{\max}^2}{3 p_{\text{ref}}^2} \left( \frac{\text{impulse time}}{\text{time of 1 rev}} \right) \right\}.$$

Now consider a numerical result using the UH-1H data at 115 knots in level flight as provided in Fig. 2-357. Here the peak sound pressure ( $p_{\max}$ ) is on the order of 3,000 dynes per square centimeter (or 300 pascals). The reference pressure ( $p_{\text{ref}}$ ) is the industry standard of 0.0002 dynes per square centimeter, so the ratio ( $p_{\max}/p_{\text{ref}}$ ) is about  $15 \times 10^6$ . The time of one rotor revolution at 814-feet-per-second tip speed is 0.186 seconds. Suppose for simplicity's sake that the impulse time is 1.86 milliseconds, which is 0.00186 seconds. Then the ratio of impulse time to the time of 1 rotor revolution is about 0.01. With these approximate values, you will calculate that the overall sound pressure level (OSPL) is 122 decibels.

Do not forget that in this experiment, the 122 decibels just arrived at is associated with a microphone mounted on the vertical tail of the OV-1C, which was about 100 feet away from the noise source. The UH-1H has a radius of 24 feet, which means the distance-to-radius ratio ( $S/R$ ) is about 4. Making use of Eq. (2.330), which gives the influence of distance on OSPL, you can see that the UH-1H at 115 knots creates an OSPL about in accordance with

$$(2.344) \quad \text{OSPL}_b = 10 \log_{10} \left\{ \frac{2.4 \times 10^{13}}{(S/R)^2} \right\} = 10 \log_{10} \{2.4 \times 10^{13}\} - 20 \log_{10} (4) = 122.$$

Suppose now that a person was 1,000 feet from the UH-1H. Then Eq. (2.344) estimates that that person would experience an OSPL of 102 decibels. Even at a distance of one statute mile, the OSPL would be 87 decibels, which is still quite annoying.

## 2.7 NOISE

Here is an interesting point. Suppose a UH-1H is coming to save you and you are in the open (say the middle of the desert), and suppose the pilot is going flat out at 115 knots (130 miles per hour or 11,646 feet per minute) with a rate of descent of 800 feet per minute. This is a flight path angle to the ground of just under 4 degrees. Say you first hear him 2 minutes before he is right there with you. Two minutes means the UH-1H is about 2 miles away when you first hear it. The closing distance (S) in Eq. (2.344) would be

$$(2.345) \text{ Closing distance} = S = S_{t=2} - 11,646(t),$$

and your time (t) starts at zero when you become aware of the helicopter. The question I am leading up to is this: "How does the noise increase as you wait?" The answer comes by using Eq. (2.344) and plotting OSPL versus time since awareness, which you see in Fig. 2-359. You might note in passing that this figure is quite similar to Fig. 2-338 on page 502. Only the noise created as the machine slows down and comes to hover is lacking.

Now let me go back to a key speculation that Fred and Don made in their 1976 paper. They took a hard look at the pressure waveform that you see in box 9 of Fig. 2-357, which you can associate with an airspeed of 115 knots and a rate of descent of 800 feet per minute.

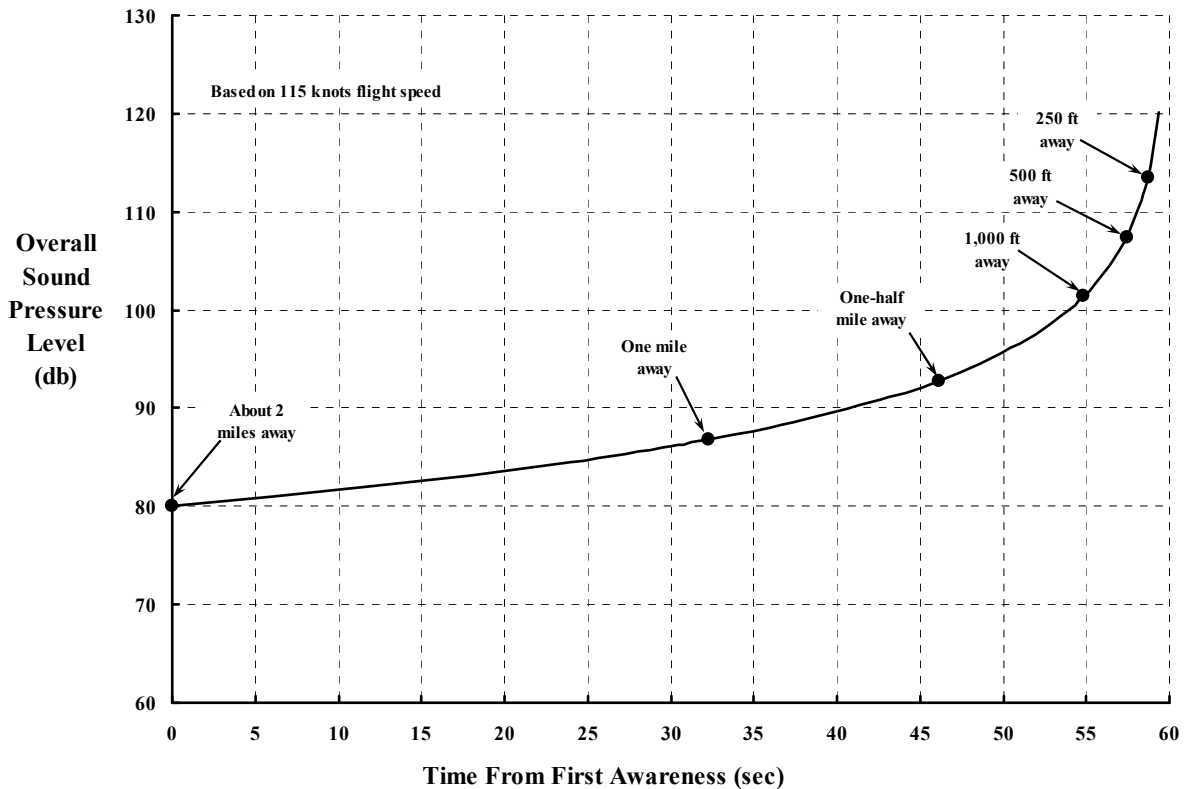


**Fig. 2-359. UH-1H overall sound pressure level as a function of distance from the observer.**

They took representative data and made what they called a composite illustration, which I have reproduced here as Fig. 2-360. You might first notice that here the negative pressure is plotted in the opposite direction from what you probably use. They made the point that “the convention established by early high-tip-speed propeller researchers is adhered to: a pressure decrease (negative pressure) is indicated upward and a pressure increase (positive pressure) downward.” I thought that *that* little bit of history was rather interesting because in all subsequent reports and papers, pressure data was plotted the “right” way. But back to the key speculation. Their speculation in 1976 was that

“the composite waveform model illustrates three predominant pressure disturbances observed in the data. They are shown in the same relative sequence and approximate pulse width that were characteristic of the measured data. Typically, the sequence began with one or two successive increases in positive pressure of “triangular” pulse shape (fig. 4, no. 1). These positive pressure peaks were followed by a large near-triangular negative pressure pulse. At high advance ratios, the negative pressure rise (fig. 4, no. 2) increased in amplitude slightly slower than its subsequent rapid decrease (fig. 4, no. 3) and the waveform is represented more by a saw-tooth or half-triangular pulse. Finally, when it was observed to occur, an extremely narrow positive pressure spike followed immediately after or as a result of the extremely rapid increase in pressure. Although it is not the intent of this paper to relate in detail the potential

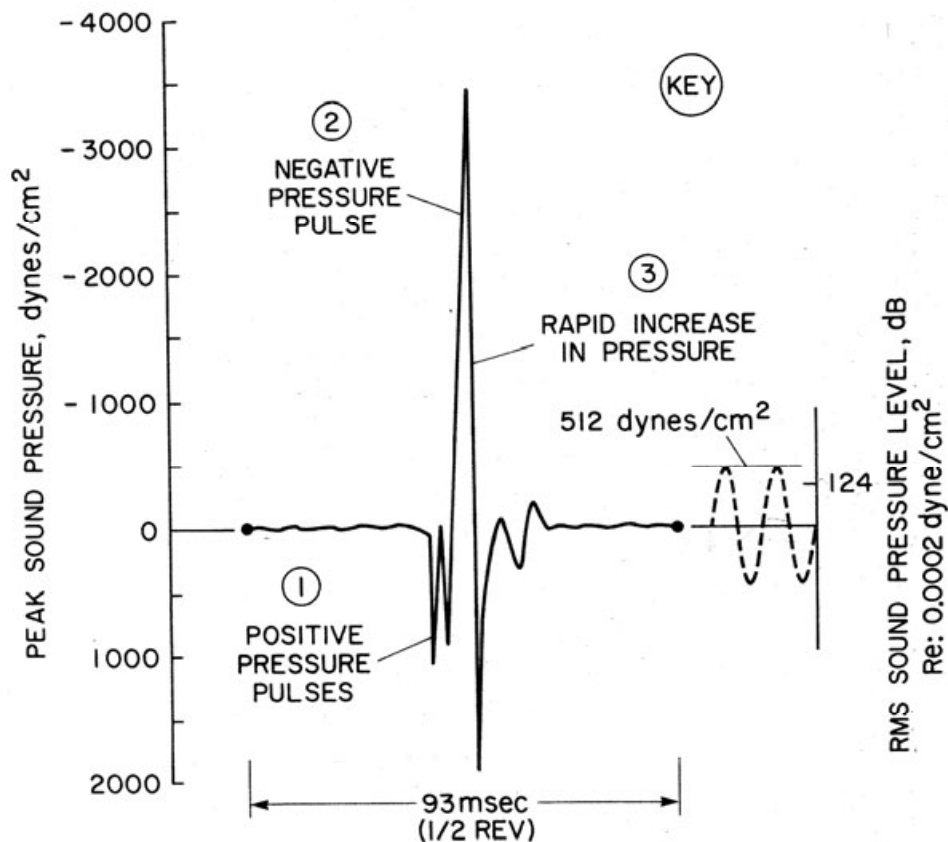


Figure 4. Composite illustration showing dominant UH-1H acoustic waveform features.

Fig. 2-360. Dissecting a sound pressure waveform [559].

## 2.7 NOISE

design causes of the radiated noise to the acoustic time history, some discussion and general observations are in order. It is the authors' hypotheses that the initial series of positive pulses (fig. 4, no. 1) is a direct result of blade-tip vortex interaction and that the remainder of the impulsive noise waveform features are associated with high advancing-tip Mach numbers. The large rise in negative pressure (fig. 4, no. 2) is thought to be attributable to "thickness" effects, while the following sharp increase in pressure (fig. 4, no. 3) is related to a radiated shock wave being shed from the advancing rotor blade. No attempt at theoretical justification of these hypotheses is attempted in this work; the primary intent is to furnish a consistent set of acoustic impulsive noise data."

You will note on the right axis of Fig. 2-360 a translation of 512 dynes per square centimeter into a sound pressure level. The pressure waveform is shown as a dashed line conveying two cycles of sine wave. The message here is that if the sound wave went on forever with an amplitude of 512 dynes per square centimeter, you would hear a continuous noise of 124 decibels. (In the 1979 paper by Fred and Yung Yu, the 512 was corrected to 448). The sound pressure level in decibels of a pure tone is calculated according to Eq. (2.301), so you have

$$(2.346) \quad \text{SPL decibel (db)} \equiv 10 \left[ \log_{10} \left( \frac{p_{\text{rms}}}{p_{\text{reference}}} \right)^2 \right] = 10 \left[ \log_{10} \left( \frac{448/\sqrt{2}}{0.0002} \right)^2 \right] = 124.$$

By 1979, Fred and Yung Yu concluded that the earlier speculation was correct and, in the intervening period, the OV-1/UH-1H test done at Edwards was repeated using a YO-3A (borrowed from the FBI!) and a UH-1H. This follow-on testing was conducted at NASA Ames Research Center. This effort was reported through an AHS Journal paper [560] and included a graph of peak negative pressure versus advancing tip Mach number, which you can see here as Fig. 2-361. As you can see, test data from the two different sites and recording airplanes was in close enough agreement for engineering purposes. The cause for concern was that theory and test data did not agree—at all.

This disagreement between theory and test (hardly an uncommon situation) sent noise researchers off in three directions. The *first* direction was to obtain in-flight noise data for a Bell AH-1S attack helicopter and later a multitude of other machines. The *second* direction was to step back from full-scale testing in flight and obtain data for model rotors in hover. The *third* direction was, of course, to start improving the theory, which was, at that time, quite embryonic. Let me briefly discuss each of the three directions in turn.

### 2.7.8.1 In-Flight Noise Measurements

The step that incorporated the AH-1S into a growing noise database allows me to show you the comparison in Fig. 2-362. Here you have both full-scale AH-1S and 1/7-model-scale AH-1S data [562] compared to the full-scale UH-1H. Fred notes [545] that "the model-scale acoustic data were taken in the DNW (Deutsch-Niederländischer Windkanal) anechoic wind tunnel and are of very high quality." In a 1983 report [563] by Fred and Yung Yu, the authors

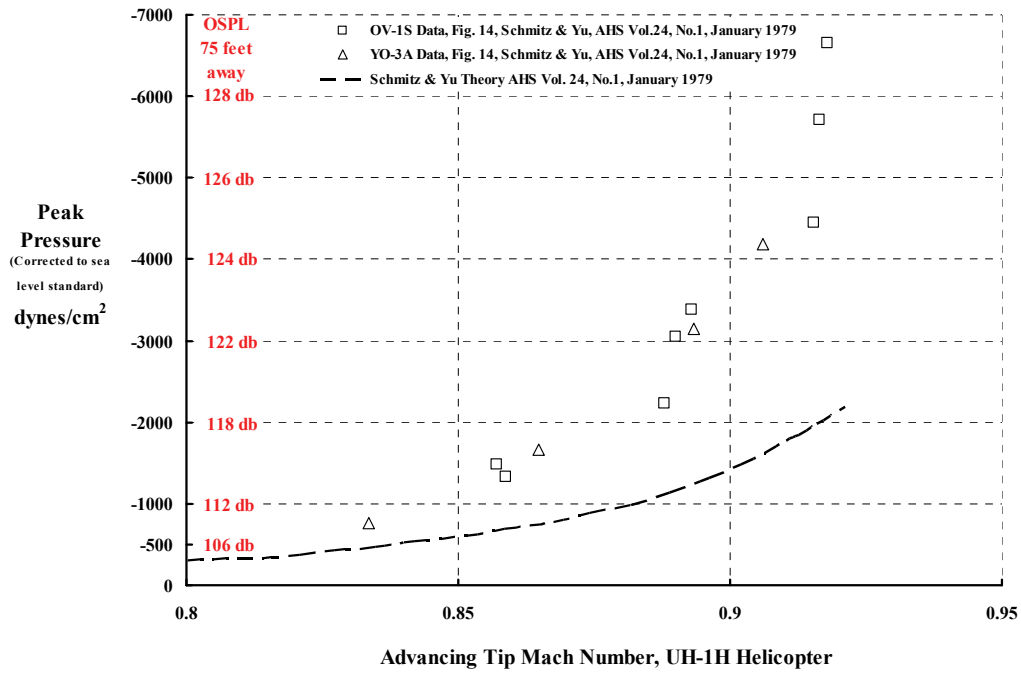


**Fig. 2-361. 1979 theory did not predict UH-1H peak negative pressure-spike increases with advancing tip Mach numbers. I have added the red decibel scale following the discussion surrounding Fig. 2-358.**

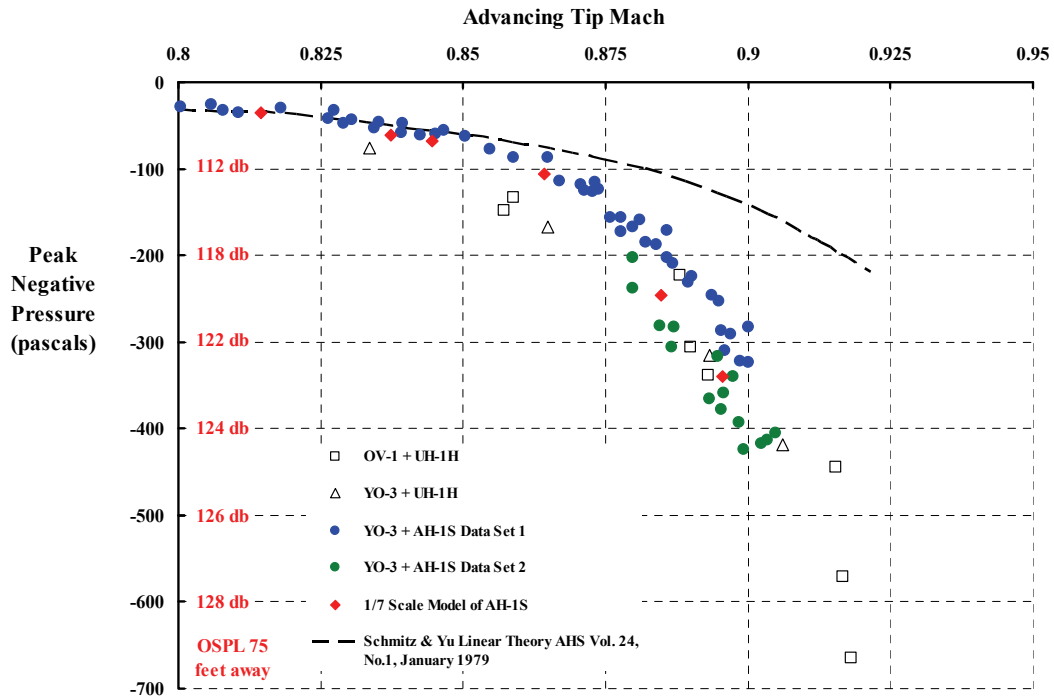


**Fig. 2-362. In-flight noise test data for full-scale UH-1H and AH-1S helicopters plus 1/7-scale model of the AH-1S clearly show that low tip Mach numbers reduce high-speed impulsive noise.**

## 2.7 NOISE

note that testing of a scale model UH-1H showed that the “dominant” parameter for high-speed impulsive noise is advancing tip Mach number and that advance ratio was a minor player—at least over an advance ratio range of 0.091 to 0.264. They also became aware of a significant difference in pressure waveform as the advancing tip Mach number was increasing (Fig. 2-363). They reported as follows:

“Perhaps the most interesting aspect of high-speed helicopter noise is the development of the saw-toothed waveform at high advancing-tip Mach numbers. This is shown in figure 36 [reproduced here as Fig. 2-363] together with a plot of the peak pressure versus advancing-tip Mach number ( $M_H$  is constant and  $\mu$  is varying) (ref. 13). In case A ( $M_{AT} = 0.867$ ), a near-symmetrical pulse is observed; the subjective qualities could be described as a loud thumping. As the advancing-tip Mach number is increased, the symmetrical pulse becomes saw-tooth in character (case B,  $M_{AT} = 0.90$ ); the waveform consists of a large decrease in pressure followed by an extremely sharp increase in pressure ( $\Delta P/\Delta t \cong 4 \times 10^6$  dynes/cm<sup>2</sup>/sec). Crispness (many harmonics) and intensity of the acoustic signature are its dominant features. At still higher advancing-tip Mach numbers (case C,  $M_{AT} = 0.925$ ), the peak negative pressure becomes very large, and the sudden rise in pressure becomes nearly instantaneous ( $\Delta P/\Delta t \cong 1 \times 10^7$  dynes/cm<sup>2</sup>/sec). Some overshoot can be seen, part of which is real and part of which is due to instrumentation bandwidth limitations. The noise generated by this latter waveform is rich in higher harmonics and can be subjectively classified as harsh and extremely intense.

It is known that this rapid increase in pressure (case C) is a radiating shock wave. Early indications of its formulation can be seen in case B at the lower advancing-tip Mach number. Of course we know that local shock waves do exist near the tip of the rotor blade throughout this Mach number range. However, this acoustic plot suggests that these local shock waves ‘delocalize’ at a certain ‘delocalization Mach number’ and propagate to the acoustic far-field. Below the delocalization Mach number (0.9 for the NACA 0012 airfoil), all shock waves are confined to the blade. Above the delocalization Mach number, shock waves on the surface of the blade radiate as shock waves to the acoustic far-field (see refs. 20 and 22).”

In-flight measurements were gathered on many helicopters as part of the NASA In-Flight Rotorcraft Acoustic Program, and the YO-3 airplane was put to very productive use. Most of the data obtained with military helicopters is still classified. However, one investigation of blade tip geometry effects on noise was published in the appendix of reference [564]. The blade geometry testing was accomplished with the YO-3/AH-1S combination. On the civil side, you will find some very interesting reports. For example, a Sikorsky S-76 helicopter was tested behind a YO-3 to obtain data that could be compared to test results obtained with an isolated main rotor in the 80- by 120-foot wind tunnel at NASA Ames Research Center [565]. This work was directed at learning more about blade-vortex interaction noise. While only a small range in thrust, rate of descent, and advance ratios was covered, this in-flight test provided a very clear picture of the sound pressure created by blade-vortex intersections on a four-blade rotor system as Fig. 2-364 shows. This particular data is associated with a helicopter rotor thrust coefficient ( $C_T$ ) of 0.00778, an advance ratio ( $\mu$ ) of 0.167, a true airspeed of 65.8 knots, and a rate of descent of 748 feet per minute. This figure shows the clear difference between the blade-vortex signature and the signature due to high advancing tip Mach number (Fig. 2-363). Watch the scales here and remember that a pascal is 10 dynes per square centimeter. Incidentally, the overall sound pressure level for this data point was 106.2 decibels. Other recorded data showed OSPLs ranging from 99.9 to 109.6 decibels. These measured waveforms gave the small band of noise researchers even more food for thought.

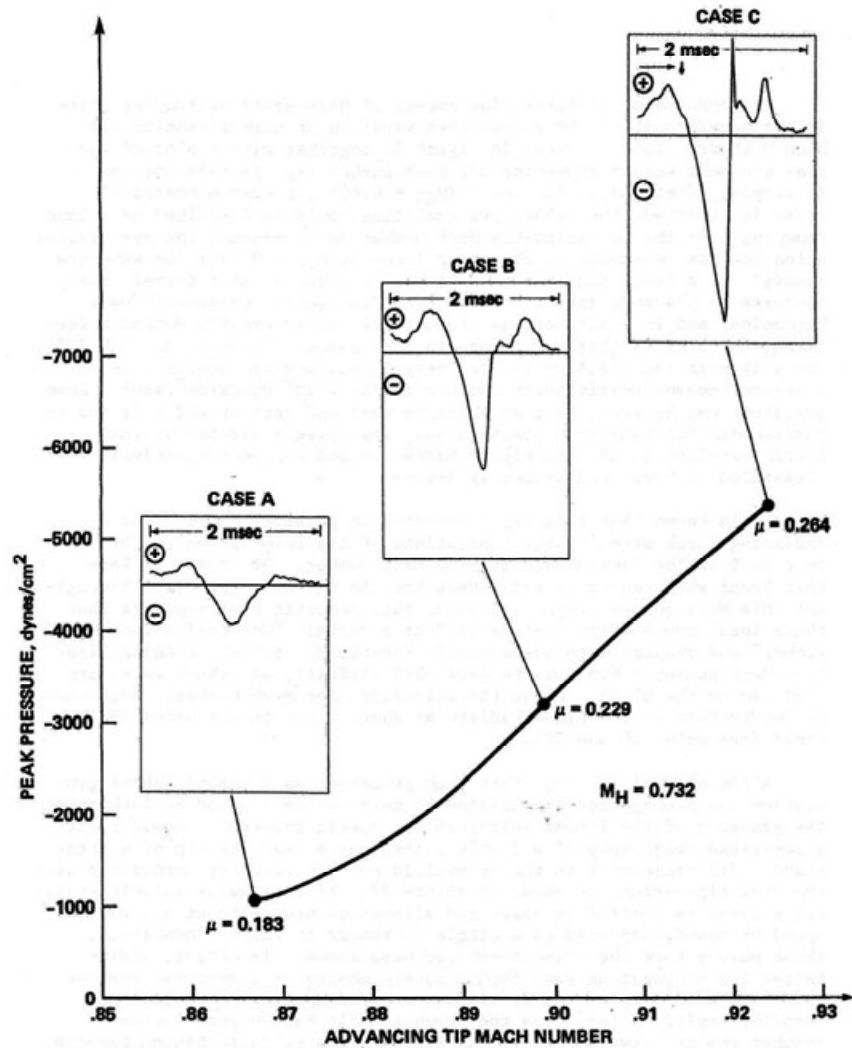


Fig. 2-363. Compressibility creates severe sound pressure spikes [563].

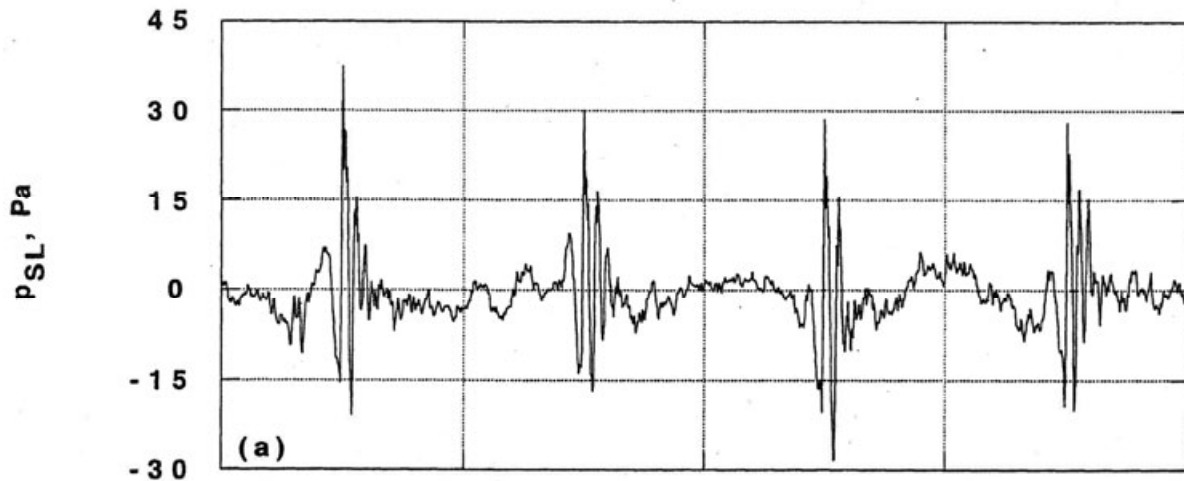


Fig. 2-364. Blade-vortex interaction sound pressure waveform for the Sikorsky S-76. Time period is one revolution [565].

## 2.7 NOISE

An even more comprehensive test program was conducted with an MBB BO-105 and reported in 1994 [566]. However, the authors reported some rather discouraging findings in the abstract to their paper, saying in part that

“acoustic measurements of a Messerschmitt-Bölkow-Blohm (MBB) BO-105 helicopter in flight are compared with acoustic measurements of a full-scale BO-105 rotor tested in the 40- by 80-Foot Wind Tunnel at NASA Ames Research Center and with acoustic measurements of a small-scale BO-105 rotor tested in the Deutsch–Niederländischer Windkanal (DNW).

Significant differences are seen in both the magnitude and shape of the blade-vortex interaction (BVI) events in the 40- by 80-Foot Wind Tunnel data and DNW data, as compared to the flight data. The rotor wakes in the 40-by 80-Foot Wind Tunnel and DNW are concluded to be different from the rotor wake occurring in flight. The differences in the respective wakes are primarily attributed to different trim conditions, wind tunnel wall effects, different shaped bodies underneath the rotors, and wind tunnel turbulence levels. The free-wake calculation results are generally consistent with the measured flight test acoustic data, and provide valuable insight into the kinematics of blade-vortex interactions.”

The rotor model was a 0.4 scale of the BO-105.

One important action item that got closed in 1984 was how to scale model-noise data to full-scale data and vice versa. This task was reported in reference [567].

Then in 1986, noise researchers got probably the highest-quality model database obtained up to the end of the 1980s [568]. The introduction to this paper (authored by Russ Zinner, Don Boxwell, and Bob Spencer) could hardly contain the enthusiasm of the noise researchers' community. It read in part:

“Helicopter noise was recognized as a problem as early as 1954 when Hubbard and Lassiter wrote their paper entitled ‘Some Aspects of the Helicopter Noise Problem.’ Although Hubbard and Lassiter were primarily describing engine and transmission noise, external noise is of even greater concern with today’s helicopters. Helicopter noise was officially addressed in 1979 when the International Civil Aviation Organization (ICAO) Committee on Aircraft Noise established limits on the amount of external noise a helicopter could produce under different flight conditions. This new set of standards required manufacturers to produce helicopters that reduced noise below the levels established by the ICAO.

One way to ensure that new helicopters produce noise below the ICAO limits is to use accurate acoustic prediction codes in the early design stages. The confidence level of these prediction codes needs to be high to keep the acoustician an integral part of the design team. One of the most important steps in code development is code validation, for which a high-quality rotor acoustic data base is essential. Unfortunately, only limited high-quality acoustic data have been available for use in validation, often consisting of merely a single point or a single flight condition. This dearth of acoustic data is one of the factors limiting the rapid progress of acoustic prediction codes.

A new rotor acoustic data base is now available to the aeroacoustic research community in a 25-volume, 11-report set. This data base, inspired by a joint agreement between the U.S. Army Aeroflightdynamics Directorate and Boeing Helicopters (BH), was collected in the Duits-Nederlandse Windtunnel (DNW) in 1986. This experimental test was one in a series of tests under the Army’s Aerodynamic and Acoustic Testing of Model Rotors (AATMR) program and used a dynamically scaled, blade-pressure-instrumented -of the forward rotor on the BH 360 helicopter.

This paper collates and summarizes the validated acoustic data base in an order that gives careful attention to four areas of current rotor acoustic research: 1) high-speed impulsive (HSI) noise, 2) blade-vortex interaction (BVI) noise, 3) low-frequency noise, and 4) broadband noise (BBN). Each of these basic rotor-noise sources was identified in validating the BH 360 data base, and the data for each are presented and arranged in terms of trends using critical scaling parameters. These scaling parameters are the same as those already reported in the literature. Also to be discussed is the extent to which distinct features of each source exist in this data base, including some known anomalies and deficiencies of which users should be aware when including this data base in specific areas of their rotor acoustic predictive work.”

The first sentence of the authors’ conclusions was italicized and said, “*High-quality data necessary for acoustic code validation are now available.*” You definitely want to read this report. Then if you want to go into all the data that was recorded, you will need to tackle the 25-volume data contained in the 11 reports, which are available but only on a limited basis.

The value and quality of noise data obtained in the DNW wind tunnel quickly spread throughout the industry. For example, the Army’s Aerodynamic and Acoustic Testing of Model Rotors (AATMR) program included testing of a dynamically similar model of the McDonnell Douglas HARP composite bearingless main rotor and a Model 369 tail rotor [569]. Sikorsky obtained data for an S-76 model rotor that was reported in 1990 [570], also under the AATMR program. Then in 2001, a follow-on BO-105 model rotor was tested at the DNW. Results from this second entry, referred to as HART II, with a more extensive objective were reported [571] by Yung Yu and his nine coauthors. In the abstract to their paper, the authors state:

“In a major cooperative program within the existing US-German and US-French Memoranda of Understanding/Agreements (MOU/MOA), researchers from German DLR, French ONERA, NASA Langley, and the US Army Aeroflightdynamics Directorate (AFDD) conducted a comprehensive experimental program in October 2001 with a 40% geometrically and aeroelastically scaled model of a B0-105 main rotor in the open-jet anechoic test section of the German-Dutch Windtunnel (DNW). This international cooperative program carries the acronym HART-II (Higher harmonic control Aeroacoustics Rotor Test).

The main objective of the program is to improve the basic understanding and the analytical modeling capabilities of rotor blade-vortex interaction noise with and without higher harmonic pitch control (HHC) inputs, *particularly the effect of rotor wakes on rotor noise and vibration* [My italics]. Comprehensive acoustic, rotor wakes, aerodynamic, and blade deformation data were obtained with pressure-instrumented blades. The test plan has been concentrated on measuring extensive rotor wakes with a 3 component Particle Image Velocimetry (PIV) technique, along with measurements of acoustics, blade surface pressures, and blade deformations.

The prediction team with researchers from DLR, ONERA, NASA-Langley and AFDD was actively involved with the pre-test activities to formulate a test plan and measurement areas of the PIV technique. The prediction team predicted all the test results in advance before performing the wind tunnel test. This was done to obtain the best quality of test data, to improve the speed of measurements, and to determine the necessary measurement information for code validation. In this paper, an overview of the HART-II program and some representative measured and predicted results are presented.”

## 2.7 NOISE

As you may be sensing by now, after the original in-flight noise testing opened the book on helicopter rotor noise research, the database has been continually expanded and the data quality has been continually improved. Much of the data has found its way into the open literature as you read this. You can also appreciate that the small band of very knowledgeable noise researchers has grown—not enough in my opinion, but grown. This group has decided that high-speed impulsive noise (i.e., the advancing blade tip Mach number noise) needs to be studied, understood, and predicted in hover before dealing again with forward flight. On the other hand, they have concluded (a) that blade vortex interaction (BVI) noise is clearly a rate of descent at low speed problem, and (b) comprehensive free-wake theories are required to provide airloads leading to BVI analytical noise calculations and numerical results useful to the working engineer. It is interesting to me that rotor blade airloads are even more important to the prediction of noise than to vibration predictions. It appears that computational fluid dynamics (CFD) is the fundamental tool required for helicopter design work.

### 2.7.8.2 More Study of Noise in Hover and Forward Flight

The second direction taken (to deal with high-speed impulsive noise) was to step back from full-scale testing in flight and obtain data for model rotors in hover. The attack was led by the Aeromechanics Laboratories, a part of the U.S. Army R & T Laboratories (AVRADCOM) located at NASA Ames Research Center. The first step was to turn the test cell used to measure hovering rotor performance into an Anechoic Hover Chamber. This facility improvement was accomplished under the leadership of Andy Morse.<sup>166</sup> The transformation is illustrated here in Fig. 2-365. The more detailed description of the transformation [572] stated:

“The data presented in this paper were gathered in a unique anechoic hover test facility which was designed primarily to gather acoustic and aerodynamic data on hovering rotors. The test chamber has been lined with polyurethane foam and has been designed to be anechoic (without acoustic reflections) down to 110 Hz. As illustrated in figure 1, aerodynamic recirculation is avoided by allowing quiescent air to be drawn into the room through acoustically lined ducts, collecting the wake of the hovering rotor through an annular diffuser, and exhausting the wake to the outside. In its current configuration, the test chamber can accommodate rotors from 1.5 to 2.4 m in diameter.”

The early testing in the improved hover chamber was done with 1/7-scale rotor models of the UH-1H. As Fig. 2-366 shows, this model was tested first with blades having the full scale twist ( $\theta_t$ ) of  $-10.9$  degrees. Fred and Yung Yu noted [563] then that

“one of the same rotors used in the scaling tests (a 1/7 scale of a UH-1H main rotor) was run for these high-speed hover tests (ref. 15). The geometrically scaled rotor has a NACA 0012 airfoil section with a root-to-tip washout of  $10.9^\circ$ . Because thrust appeared to be unimportant in the high-speed noise generation process, a second set of untwisted but geometrically scaled rotor blades was run at near-zero net thrust. Some small positive net thrust was required to avoid shed-wake interference effects. The data were taken with a microphone located within the tip-path-plane of the rotor at a distance of 1.5 rotor diameters ( $r/D = 1.5$ ) from the hub. This in-plane microphone position is consistent with that used in previous in-flight and wind tunnel tests and is in a position to measure the most intense high-speed impulsive signature.”

---

<sup>166</sup> During this period, Irv Statler was the “chief” of the laboratory and Andy Morse reported to him.

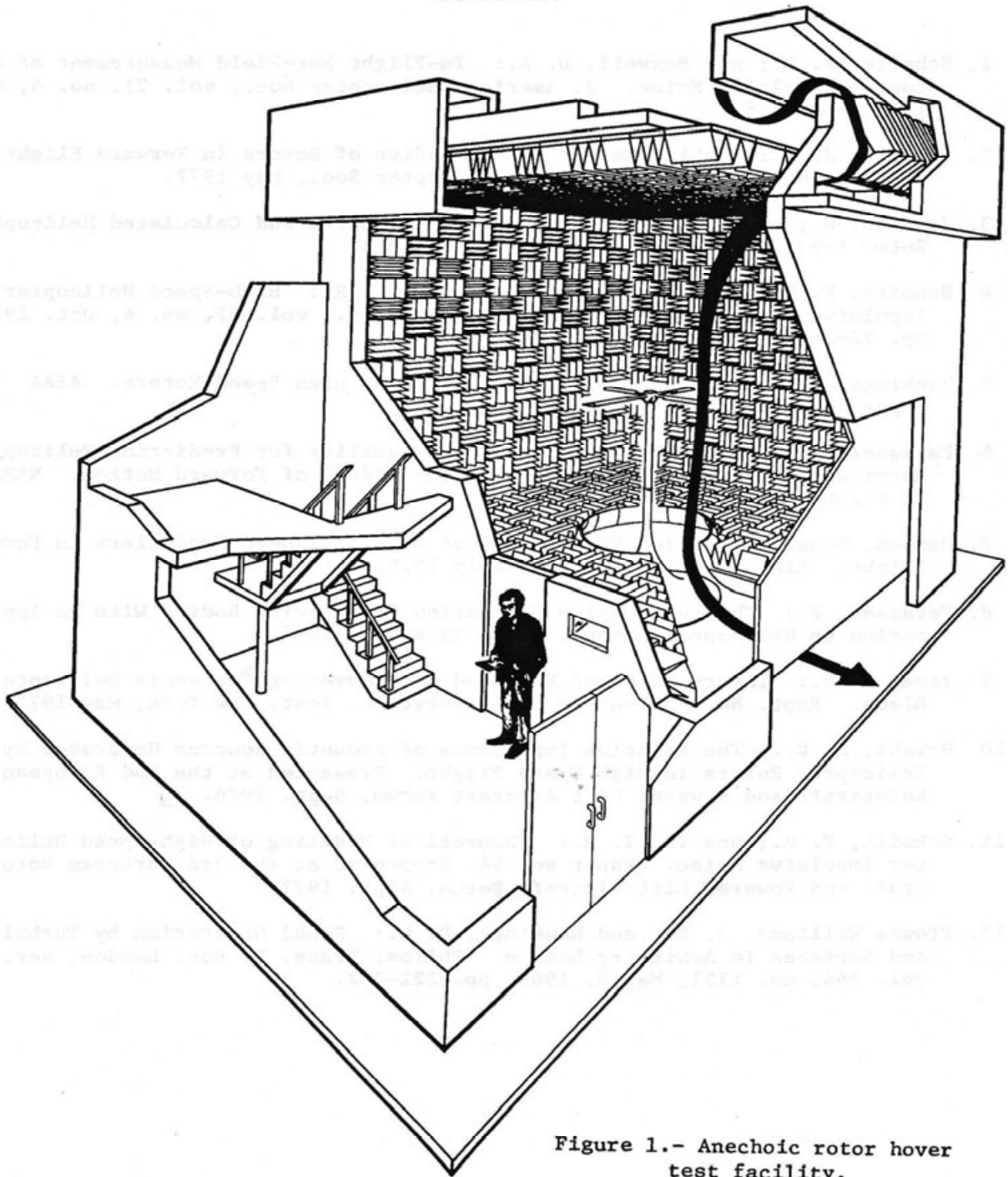


Figure 1.- Anechoic rotor hover test facility.

Fig. 2-365. The Anechoic Hover Chamber located at the U.S. Army Laboratory at NASA Ames Research Center [572].

2.7 NOISE

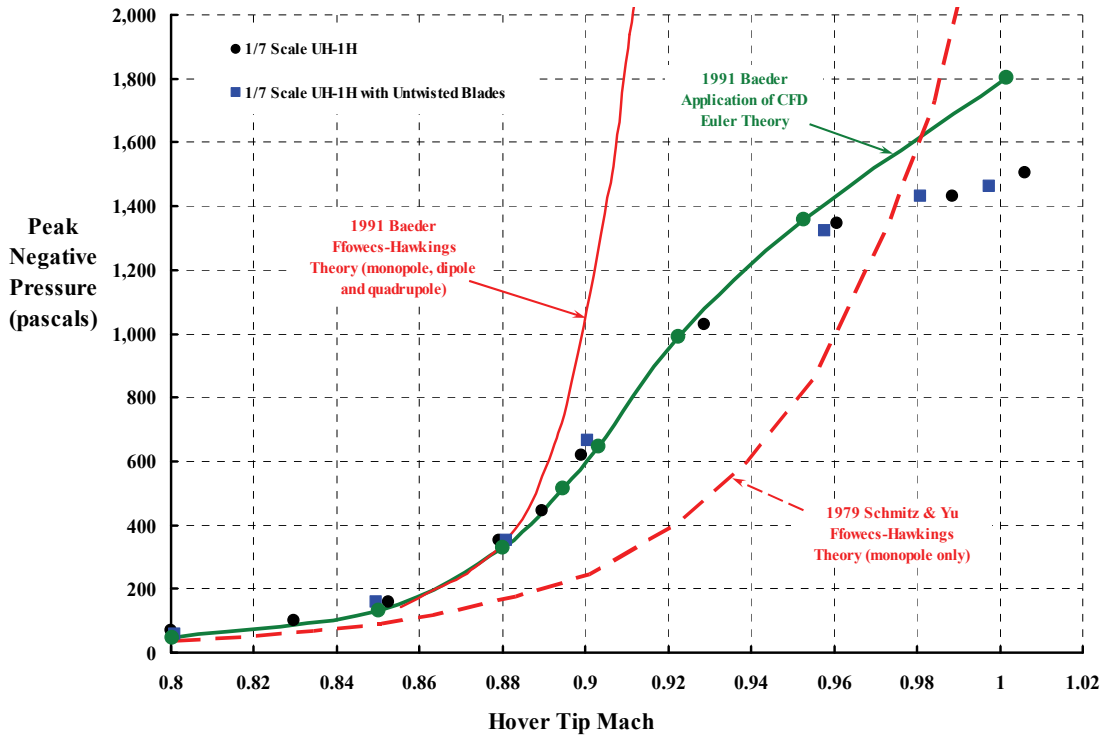


Fig. 2-366. Theory (versus test) has improved in the prediction of impulsive noise due to high tip Mach number.

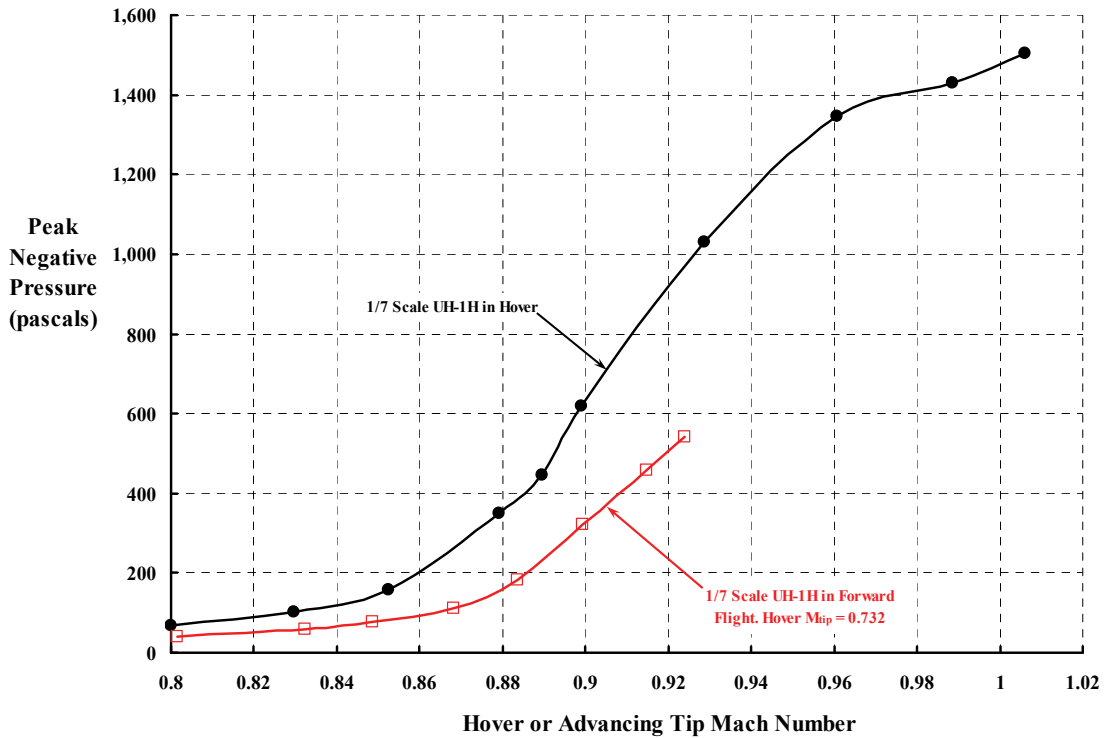


Fig. 2-367. Blades with the NACA 0012 airfoil probably should not be flown above an advancing tip Mach number of 0.80—if noise is a consideration.

After the 1/7-scale UH-1H testing was completed in hover, the model was tested in the NASA Ames 7- by 10-foot wind tunnel [553] located next to the Anechoic Hover facility. The test section of the tunnel was lined to a depth of 3 inches with “Scottfelt” (a polyurethane foam) to provide a measure of acoustic isolation. The model was tested at a hover tip Mach number of 0.732, and the advance ratio varied from 0.093 to 0.264 so that data over a reasonable range in advancing tip Mach number was obtained. The rotor thrust coefficient ( $C_T$ ) to solidity ( $\sigma$ ) ratio was maintained at 0.064, and the angle of the tip path plane ( $\alpha_{\text{tip}}$ ) was trimmed to a  $-2$  degrees forward. This simulated flight test data. The comparison of noise in hover versus noise in forward flight is, I think, quite interesting as Fig. 2-367 shows. Apparently, serious impulsive noise will be broadcasted above an advancing tip Mach number of 0.80 for blades having the NACA 0012 airfoil over the outer portion of the blade.

### 2.7.8.3 Theory is Improving

The first payoff for the growing and broadening attack on predicting rotor noise at its source was in the area of high-speed impulsive noise. Two perfect examples are the results Jim Baeder achieved in 1991 with direct calculation of noise using CFD [573] and the extension of the Ffowcs Williams–Hawkings theory (by adding a quadrupole<sup>167</sup>) to the WOPWOP analysis as Ken Brentner and Feri Farassat review in reference [522]. You will note in Fig. 2-366 that I have include the predictions of these two tools compared to hover noise measurements of a model UH-1H [563]. (I cannot yet, however, show you a theory-versus-test comparison of the UH-1H data you saw in Fig. 2-362.) In discussing the two approaches with several engineers familiar with high-speed impulsive noise, I came to three conclusions as of this writing. The first conclusion is that it is a very encouraging step forward that impulsive noise can now be predicted at least up to Mach numbers in the transonic range. The second conclusion is that taking the propeller approach of thin tips, reducing the design tip speed, sweeping the blade tip, and giving the helicopter operator a low-tip-speed option as Hughes did with The Quiet One is the only way to deal with such an undesirable noise signature. The implication of this second conclusion is that not only does advancing tip Mach number pose some limitations on desirable performance, it also poses an operating restriction for quiet as Fig. 2-368 suggests. The third conclusion is that this is going to still be a very hard sell to customers (and upper management) considering (a) the implied increases in weight empty, (b) a potential loss in useful load, (c) selection of a more powerful engine, and (d) an unfavorable increment in selling price. As I write this, it is not clear how to have our cake and eat it too, but it is clear that very innovative engineering, marketing, and pricing will be required.

The second payoff from this 25-plus-year effort has come in predicting blade vortex interaction (BVI) *and* broadband noise. Here the progress is also quite impressive despite the very detailed knowledge required about rotor wake geometry and the individual blade elastic

---

<sup>167</sup> The Ffowcs Williams–Hawkings theory calculates noise using monopoles, dipoles, and quadrupoles to model the pressure waves emanating from the rotor blade airfoils. The clearest discussion I found about these pulsating pressure “devices” was on the Internet at <http://www.acs.psu.edu/drussell/Demos/rad2/mdq.html>. The author is Daniel A. Russell. I never studied these mathematical techniques in sufficient depth to adequately discuss them, so you are better off reading what a person with a Ph.D. has to say on this topic.

## 2.7 NOISE

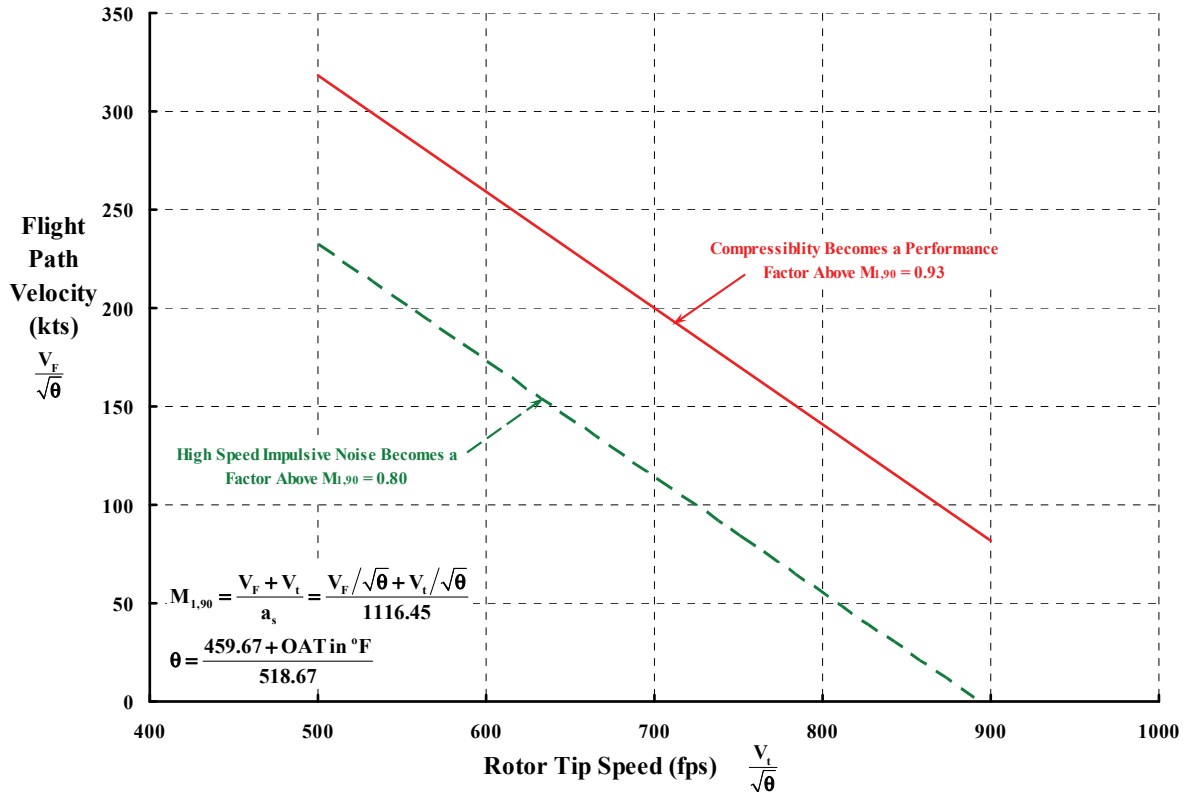


**Fig. 2-368. Advancing tip Mach number should be both a performance and impulsive noise design consideration.**

deflections. In the April 2000 Journal of the American Helicopter Society, Thomas Brooks and his coauthors [574] developed a connected group of tools, which they named TRAC (Tilt Rotor Aeroacoustic Codes—even though it can do helicopters too). Their block diagram describing the code is reproduced here as Fig. 2-369. You can see that CAMRAD is used to obtain the rotor trim and then a computational fluid dynamics (CFD) code derives the rotor blade loading. An alternate loading can be obtained from the HIRES code. At this point there is enough information to give WOPWOP details to compute noise, which is the final pressure waves and magnitude in pascals.

Brooks and his coauthors compared their TRAC program to BO-105 data obtained during the HART II program and a sample of their achievement is shown here with Fig. 2-370. While many refinements can be expected, these sample results published in April 2000 are, in my opinion, quite impressive. The group followed up with more progress, which you can read about in references [575, 576].

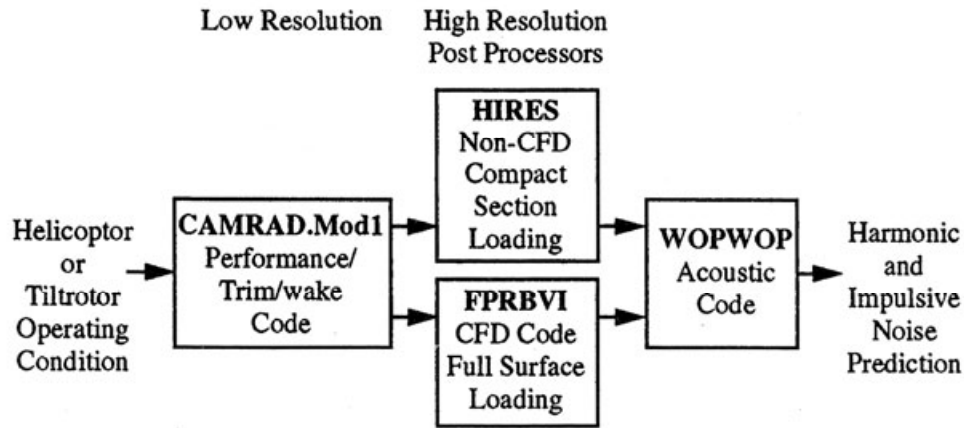


Fig. 2-369. The TRAC analysis created by a NASA Langley team [574].

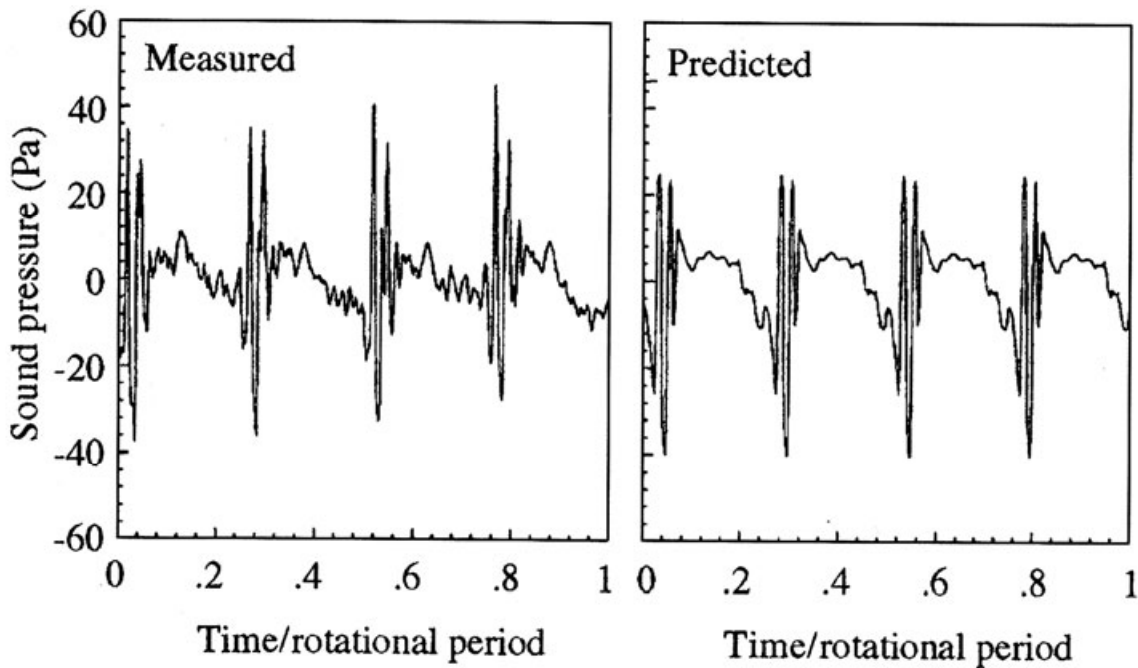


Fig. 2-370. Sound pressure waveforms in low speed are predictable [574].

### 2.7.9 Closing Remarks

In closing, I must first apologize for not including all of the noise reduction efforts that have been made in England and Europe. Those efforts have easily been on par with what I have related to you here in this limited discussion.

Helicopter noise comes from many sources as Fig. 2-371 suggests. What you have just finished reading has only dealt with external noise (and just rotor noise at that), which earthbound people and animals find very annoying. Space limitations have kept me from

## 2.7 NOISE

discussing interior noise in detail, but you can read a very good summary in Mike Watt's chapter on noise that Gloria Yamauchi and Larry Young included in reference [530]. Also, I found the report [577] describing how interior noise in a Sikorsky CH-53A was reduced from 115 dB in its untreated military configuration (!) to 87 dB, after the cabin was acoustically treated, quite instructive. The authors closed their summary with the statement that "Specifically, a reduction of 12 dB from the first-stage planetary gear clash in the main gear could result in an interior environment which is only slightly higher than that in current narrow-body jet transports." This work was done in 1977.

There is no question that a quarter century of research by a relatively small core of very talented and dedicated individuals has provided the rotorcraft industry with foundational tools that can help design less annoying helicopters. In my opinion, the next step is to be able to calculate, during the preliminary design phase, the machine's noise levels relative to regulations required by certifying bodies (such as the FAA in the United States). As you saw from Fig. 2-347, Fig. 2-348, and Fig. 2-349, the noise during takeoff, flyover, and landing must be calculated in advance of a commitment to production. Currently the FAA has defined "not to exceed" noise levels as a function of rotorcraft gross weight. These limits are shown in Fig. 2-372 with the solid lines. Wayne Johnson prepared<sup>168</sup> this figure from two references [578, 579]. You will note that the noise unit for FAA certification is EPNdb, which is shorthand for Effective Perceived Noise in decibels. As you read earlier, this parameter is spelled out by the FAA in considerable detail [557, 558].

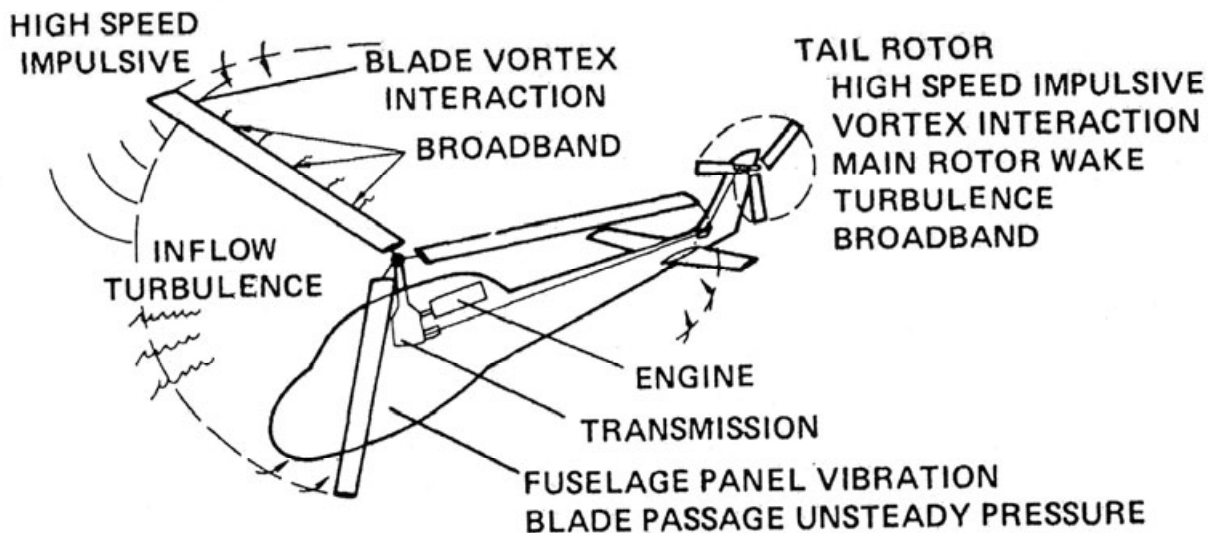


**Fig. 2-371. The many sources of both external and interior noise created by a helicopter.**

<sup>168</sup> Wayne prepared this figure for inclusion in his soon-to-be-published book titled *Rotorcraft Aeromechanics*. He kindly gave me permission to include the figure in advance of his publication.

Finally, the question I think a chief engineer needs answered during preliminary design of a new rotorcraft is, “Where does the design team’s configuration fall on Fig. 2-372?” There is, in fact, test data that noise researchers can use to compare analysis, when it is created, to test. You can begin to address this need by reviewing the paper that David Conner, Casey Burley, and Charles Smith presented at the 2006 American Helicopter Society Annual Forum [580].

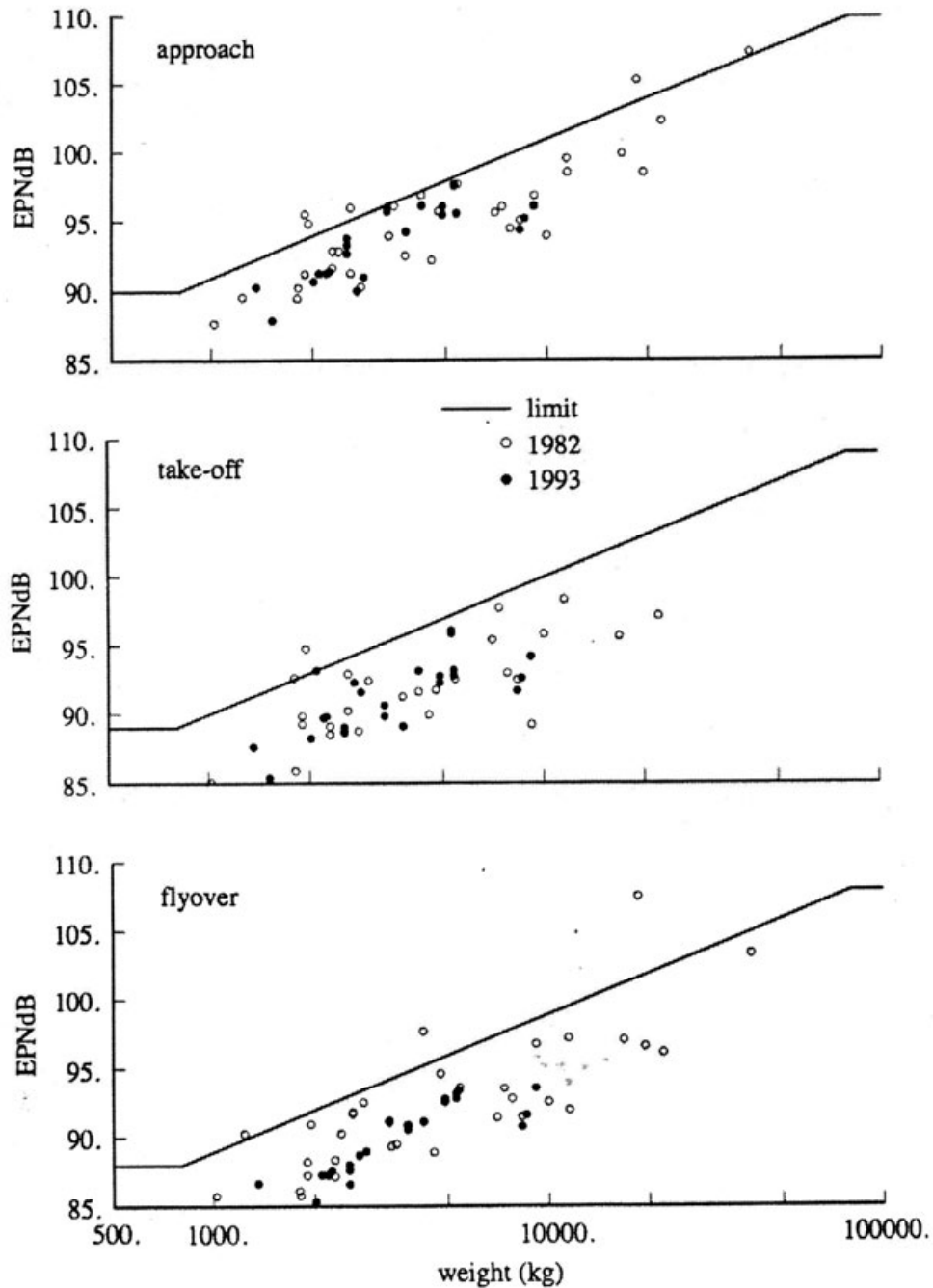


**Fig. 2-372. The FAA’s not-to-exceed noise levels if aircraft is to be certificated in the U.S. (courtesy of Wayne Johnson).**



## 2.8 PURCHASE PRICE

Consumers, in the course of shopping, frequently look at an item and wonder, “How much does this cost?” With a little effort they search and find a price tag, or maybe a clerk comes forward with a computer scan showing the price. Now think about the use of those two words: cost and price. The consumer is really asking about how much he or she must pay to purchase the item. The consumer is not asking how much the manufacturer has spent to put the item before the consumer, and therein lies the reason for titling this chapter *Purchase Price*.

In this chapter you will be reading primarily about the *list price* of helicopters and very little about manufacturing *costs*. The reason for this is that manufacturers do not readily divulge their costs. In fact, cost data is not even spread around the company—in my experience. However, in military procurement situations manufacturers do provide financial data as requested by the government (at least in the United States). And, frankly, my experience has been to often wonder if the larger helicopter manufacturing companies really even know the accurate cost of producing any given aircraft they are delivering to a customer. The situation may be different for companies dealing only in the civil marketplace. They may know their product costs quite accurately, as would smaller cost centers that pursue pure research and development. Very productive groups such as the Lockheed Skunk Works [581] clearly demonstrate they know their costs. Of course, the difference between cost and price reflects some measure of profit, depending on how the books are kept.

In 1984 I bought the second edition of *Augustine’s Laws* [582], which introduced me to a number of Department of Defense (DoD) trends that I had never thought too much about. One of the trends, and Norm Augustine’s caption for it, caught my eye, and I have included it here as Fig. 2-373.<sup>169</sup> This one book inspired me to delve into (a) the selling price of helicopters in the civil marketplace, and (b) military procurement of helicopters. The next several pages discuss these two topics.

### 2.8.1 Civil Marketplace

The marketplace for civil helicopters is worldwide as you can easily imagine. The “list price” of helicopters in this marketplace is quite variable as you can also easily imagine. But there is one source that captures prices for almost all civil helicopters that have been sold over several decades. That source is HeliValue\$, Inc. [583] located in Wauconda, Illinois. For years this company has published *The Official Helicopter Blue Book*<sup>®</sup>, and this collection is truly a gold mine of data used in the buying and selling of new and used machines.<sup>170</sup>

---

<sup>169</sup> You will find *Augustine’s Laws* very thought provoking. Norm Augustine has been accorded many honors and has been a major figure serving this country both in the government and as a leader in industry as you can read from articles on the Internet. Incidentally, his Law XVI (in the 1984 edition) states that “In the year 2054, the entire defense budget will purchase just one aircraft.”

<sup>170</sup> Mike Scully and I used data from this source and some others to write a paper [584] which we titled *Rotorcraft Cost Too Much*. In this paper, we offered a helicopter price estimating equation.

## 2.8 PURCHASE PRICE

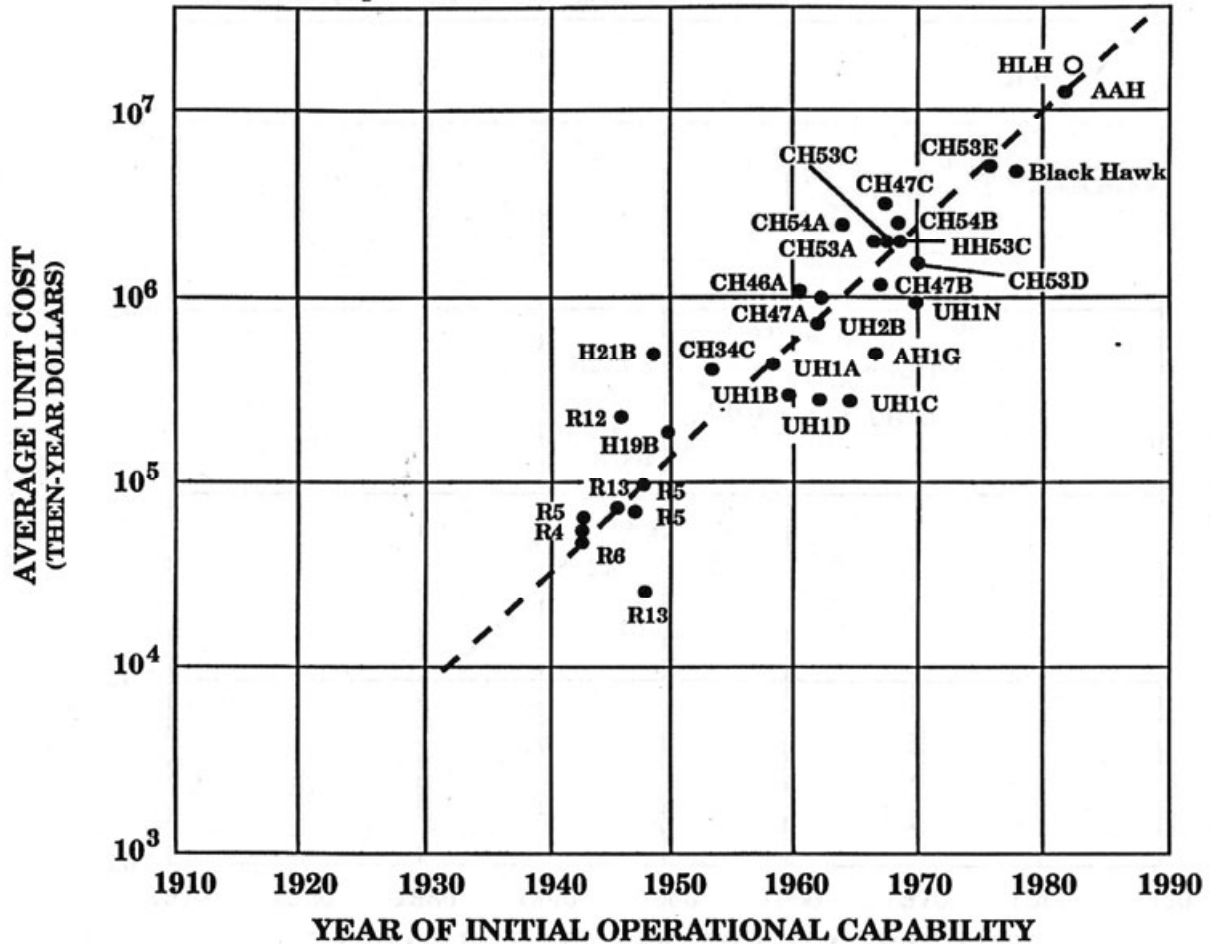


Fig. 2-373. Norm Augustine captioned his figure 11 with: “The slope of the unit cost vs. time curve for rotary wing aircraft is the same as for fixed-wing aircraft, albeit getting off to a somewhat belated start” [582].

When you study the trend of civil helicopter prices you will be immediately struck by the fact that one of Augustine’s Laws, shown here as Fig. 2-373, is just as applicable to the increase (over several years) in the selling price—perhaps list price would be a better term—for any one specific helicopter model. One thing you should be aware of is that almost all civil helicopters contain engine, drivetrain, and rotor subassemblies developed, at least in part, with government money. An exception is the Robinson Helicopter Company’s R-22, R-44, and R-66 lines. Bell Helicopter’s Model 206B Jet Ranger is a more typical example.

You will recall that Bell participated in the U.S. Army Light Observation Helicopter competition with Hughes and Hiller, which Hughes won in the prototype fly-off because of a very competitive machine and very aggressive per-unit pricing. Bell’s submittal, shown in Fig. 2-374, lost. Bell immediately turned their design into a civilian machine shown in Fig. 2-375, and proceeded to sell over 7,300 206B-II and 206B-III, and U.S. Army OH-58A and OH-C versions over nearly four decades.



**Fig. 2-374.** Bell Helicopter's YOH-4 prototype for the Light Observation Helicopter competition during the 1960s. First flight was December 8, 1962 (photo from author's collection).



**Fig. 2-375.** Bell Helicopter capitalized on the YOH-4 engine, drivetrain, and rotor systems with a civil marketplace fuselage. This began the Model 206 Jet Ranger series. FAA certificated October 20, 1966; first sale January 13, 1967 (photo from author's collection).

The primary difference between the 206B II and 206B III (or OH-58A and OH-58C) is a slightly increased takeoff rating of the Allison (now Rolls Royce) Model 250 C-20 gas turbine engine. A secondary difference is that the growth versions had a slightly larger diameter tail rotor (5.2 feet increased to 5.42 feet). It is very hard to pinpoint any other significant changes in the basic configuration of this helicopter over its production life of four decades. What did improve was the time between overhaul (TBO) of many of the helicopter's expensive parts.

## 2.8 PURCHASE PRICE

The Bell Model 206B was introduced to the civil marketplace in 1967 at a factory list price of \$89,500 in its base configuration.<sup>171</sup> Of course, you could have it factory equipped with VHF, VOR, ADF, transponder, flight instruments, dual controls, and heater, but then your purchase price was \$105,500.<sup>172</sup> Bell delivered 115 Jet Rangers in 1967, which, I am sure, was a very positive indication that the civil marketplace was ready for small gas-turbine-powered helicopters even though they cost more than the piston-powered versions.

As the number of Bell Jet Rangers produced grew (Fig. 2-376), the list price also kept growing (Fig. 2-377). This fact may fly in the face of many cost estimators who swear by the relatively well-known “learning curve,” which I will discuss in more detail later. The point to grasp here is that there is a large group, at least in the United States, that claims some skill in estimating cost. However, as I have pointed out, price is different than cost, and the group that sets the selling price of helicopters is very, very small indeed.

In my opinion, the single most critical decision required from the president of a civil helicopter manufacturing company is illustrated by Fig. 2-376. As you can see from this figure, Bell did not produce a constant number of the Model 206Bs each year. This is a significant difference between military and civil production rates. Fulfilling a military contract generally entails producing a large quantity over several years, at so many a year and even so many a month. With this kind of assurance, a very stable production line can be set up, and production costs can be lowered as everyone learns the job. But when the number of machines to be produced each year varies as much as Fig. 2-376 shows, production proceeds in a jerky manner, the manufacturing staff is not constant from year to year, and learned skills can disappear—only to be required all over again next year.

Now assume you are the president of, let’s say, Bell Helicopter, and you must make the critical decision about how many Model 206Bs are to be produced next year. Keep in mind that if you release more for production than can be sold, the number of aircraft sitting outside the final assembly line building becomes unsold inventory, and you may not even cover the cost of production for that year. If you release too few for production and the marketplace demand for your product is particularly high, you will be sold out before the end of the year, and with helicopter production you cannot get additional machines to sell just at the snap of your fingers, even if you are the president. In fact, the lead time between your decision about how many aircraft are to be produced and the resulting first additional finished helicopter is about 18 months. Just think about the cost implications of Fig. 2-376, and then think about how you would set the average selling price for each year’s production batch.

If you let your imagination search for the many other factors involved in the difference between cost and price, you may conclude, as I have, that a chief engineer has a relatively easy job. All the engineering department has to do is release drawings (to manufacturing) for a world-class design that beats the competition at every turn. Let me examine this point with Fig. 2-378.

---

<sup>171</sup> *The Official Helicopter Blue Book*<sup>®</sup> provides factory list prices for helicopters in both base and equipped configurations. Sharon Desfor, the president of this company, is a delight to talk to, and she has all kinds of sources that could be tapped should you want to delve more deeply into the civil marketplace.

<sup>172</sup> This is the kind of experience you have when buying a new car!

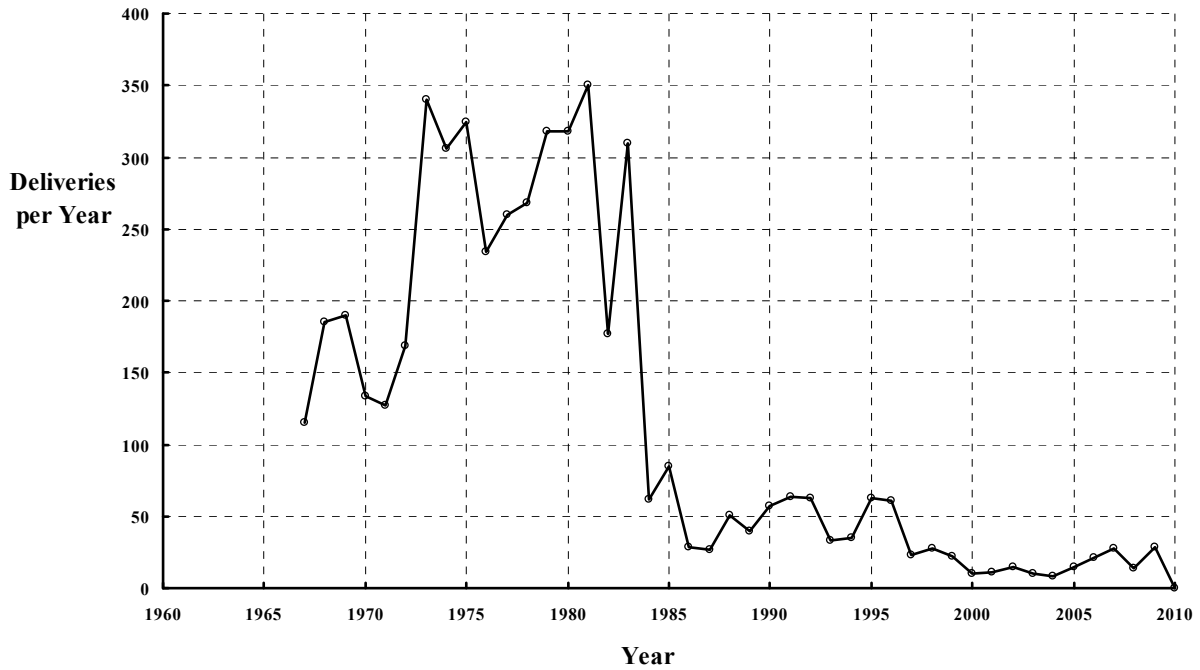


**Fig. 2-376.** Per-year production of the Bell Model 206B was hardly constant over its four-decade life.

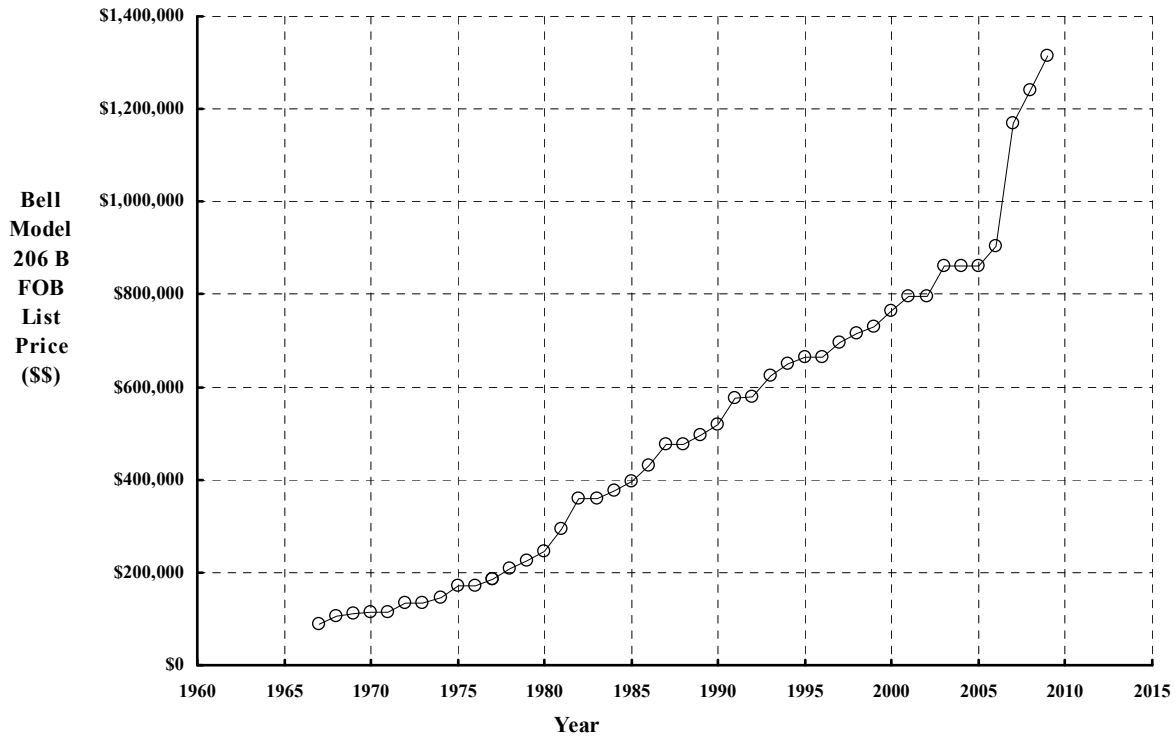


**Fig. 2-377.** Base configuration factory list price of the Bell Model 206B Jet Ranger has increased over the years, primarily due to inflation. (Excerpted from *The Official Helicopter Blue Book*<sup>®</sup>, with permission from HeliValue\$, Inc.)

## 2.8 PURCHASE PRICE

The accumulating income to Bell for selling about 5,000 Model 206B Jet Rangers is shown in Fig. 2-378. The 5,000 aircraft constitute serial numbers 1 through 2,283 of the -II model, the rest being the -III model. In essence, this is the cumulative number of Jet Rangers listed in *The Official Helicopter Blue Book*<sup>®</sup>, which you see distributed by year in Fig. 2-376. I took the product of each year's batch times the list price for that year (Fig. 2-377), and then summed it to arrived at Fig. 2-378. This does not include income from U.S. military sales of about 2,300 OH-58 helicopters.

You can see that from an initial investment of, say, \$60 million over the 4-year span (from first flight of the YOH-4 and first sale of the 206B), Bell had a cumulative income of \$1.4 billion. Of course, when the cost of producing the 5,000 aircraft is subtracted (say \$1.3 billion) and income tax on the \$0.1 billion is paid, Bell might have had \$600 million available to invest in a new product or even to do more research and development for, say, a V-22 tiltrotor.<sup>173</sup> From the chief engineer's point of view, he must use the initial \$60 million to manage the program that gets the product line to that first sale. In the early 1960s, \$60 million was a lot of money and, with inflation, is about \$600 million today. Also keep in mind that the YOH-4 research and development to first flight was funded by the U.S. Army, so Bell had a running start on its commercial derivative of the engine, drivetrain, and rotor systems.

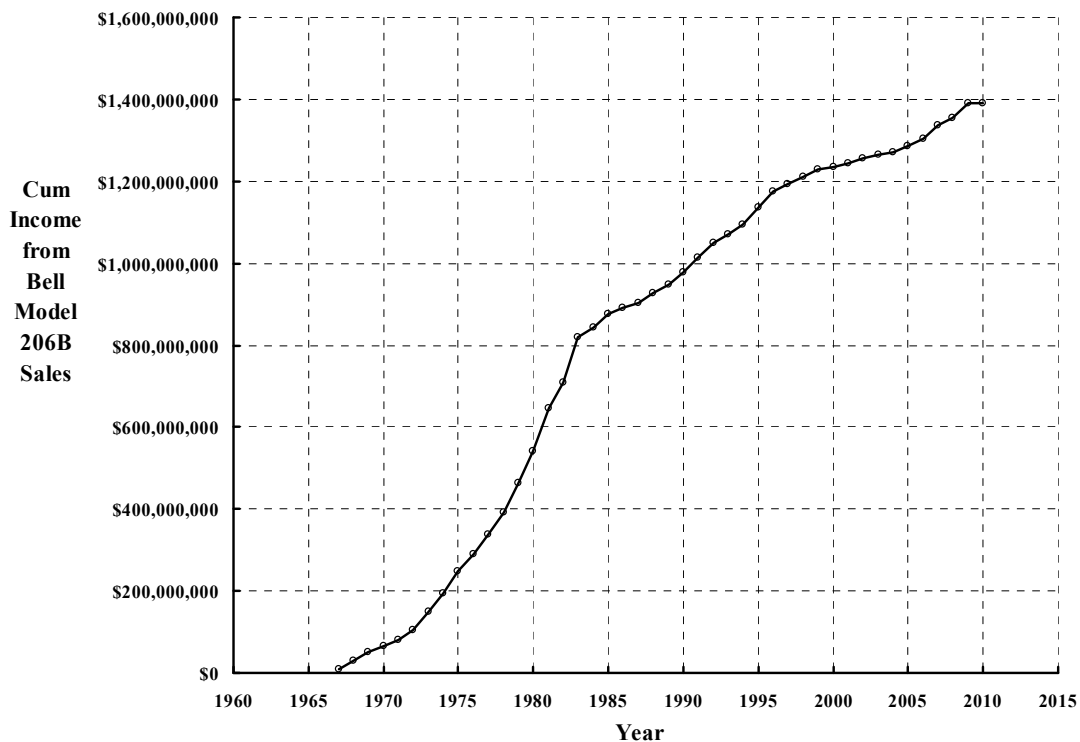


**Fig. 2-378. Cumulative income to Bell Helicopter as Model 206B sales were made over a four-decade production life.**

<sup>173</sup> In Bell's case, they had to return some money to their parent corporation, Textron, so that Textron could pay stockholders a dividend and have some money left over for other investments in any of their many other companies like E-Z-GO golf carts. Of course, Textron also had to advance Bell some more money so that Bell could develop the Bell Model 206 L, which became the 206 Long Ranger.

### 2.8.1.1 Estimating Purchase Price

During the mid-1990s, Mike Scully and I worked very intensely to develop an equation that reasonably predicted factory list price. Our work came to a conclusion when reference [584] was published in January of 1998. One motivation for our effort was a joint feeling that pricing (or costing) a helicopter on the basis of dollars per pound of weight empty was quite questionable,<sup>174</sup> so we began to accumulate an Excel® file of selling prices. From that file, we established an average curve of inflation for helicopters, and then we indexed the price of all the listed helicopters to 1994. Of course, it was then quite easy to create Fig. 2-379, which showed us just how *inaccurate* estimating factory list price by weight empty alone was.

As we continued to expand [585] and refine and correct our database, we began a year-long search for an equation that would reduce the scatter in any price estimating relationship. Early efforts showed that a regression analysis using up to 13 parameters was not producing major improvements. The problem was that with 13 parameters, the regression analysis had statistical confidence in only a few parameters. This led us to selecting weight empty (WE) in pounds, total engine(s) rated horsepower (THP) in horsepower, and number of blades (b) per rotor as the primary variables. We relegated other influential parameters to a constant (H).

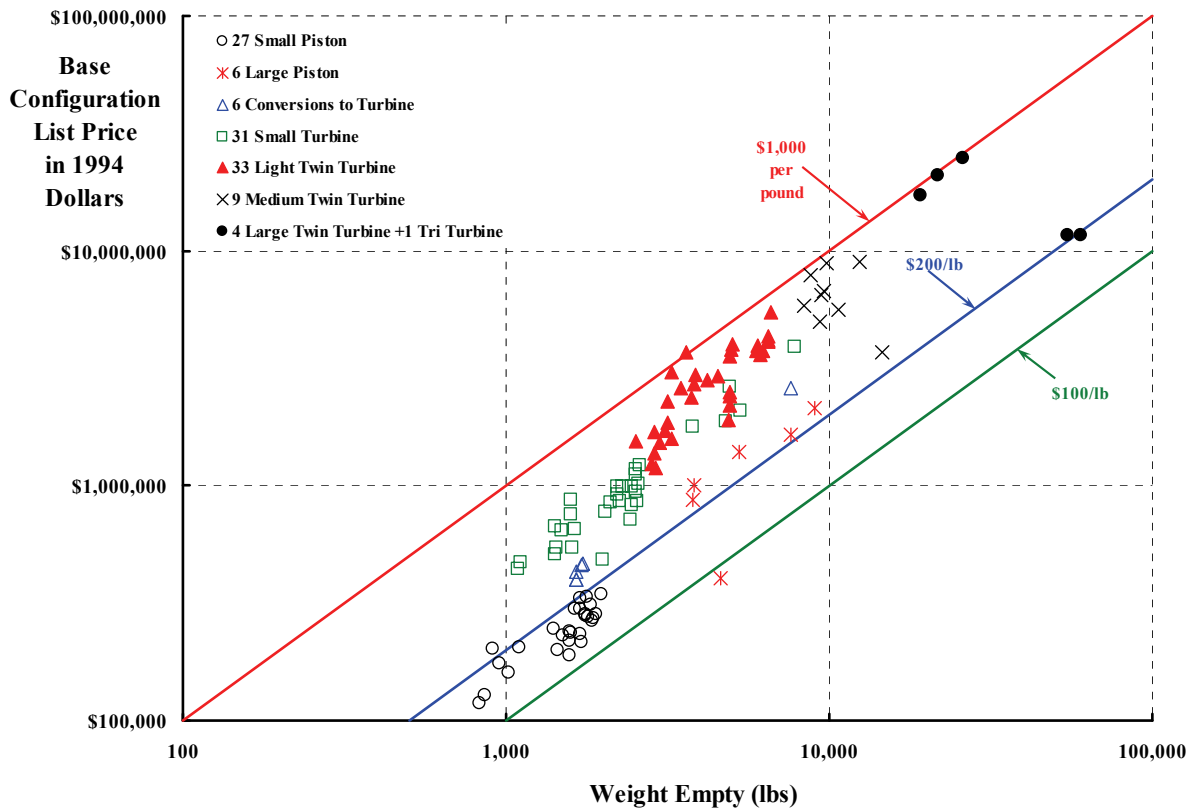


Fig. 2-379. List prices are not accurately estimated by weight empty alone [584].

<sup>174</sup> Mike and I are of the same mind-set. We do not like to base a quantitative number on feelings.

## 2.8 PURCHASE PRICE

The final price-estimating relationship was keyed to 1994 U.S. dollars. With slightly abbreviated nomenclature, you now have

$$(2.347) \quad \text{Base List Price} = \$269(H)(WE)^{0.4638} (THP)^{0.5945} (b)^{0.1643}$$

where H is the product of five factors and is computed as:

$$(2.348) \quad H = \text{Engine Type} \times \text{Engine No.} \times \text{Country} \times \text{Rotors} \times \text{Landing Gear.}$$

The factors (found by regression analysis) used in computing H are:

<b>Engine Type</b>		<b>Engine Number</b>		<b>Country</b>	
Piston	1.000	Single	1.000	U.S. Commercial	1.000
Piston (geared supercharged)	1.398	Multi	1.344	Russia	0.362
Piston (converted to turbine)	1.202			France/Germany	0.891
Gas Turbine	1.794			Italy	1.056
				U.S. Military	0.883

<b>Number of Main Rotors</b>		<b>Landing Gear</b>	
Single	1.000	Fixed	1.000
Twin	1.031	Retractable	1.115

The predictive accuracy of Eqs. (2.347) and (2.348) is shown in Fig. 2-380. If the relationship were 100 percent accurate, every symbol in this figure would fall precisely on the diagonal line. Many data symbols nearly touch the diagonal line indicating this estimating relationship has very high assurance that it can at least come within 20 percent of the “actual” price 106 out of 121 times, or about 88 percent of the time. Quotations are used around the word “Actual” on the y-axis label on Fig. 2-380 for two reasons. First, purchase price (whether base or equipped) frequently was negotiable in the year the helicopter was bought. Secondly, we assumed the same inflation regardless of country, manufacturer, or helicopter model.

Try as we might, Mike Scully and I could do no better than what you see in Fig. 2-380. We had reasonable engineering confidence (a) that helicopters powered with a gas turbine engine were clearly more expensive than those powered with a piston engine—at equal total rated power, (b) that twin engines were more expensive than a single-engine configuration—at equal total rated power, (c) that the economic situation in Russia made their product very attractive from a selling point of view, and (d) that the U.S. military got a price break *if they purchased large numbers in multi-year lots*.

Let me leave you with one additional thought. The increase in list price when the base helicopter is equipped with modern avionics can easily amount to 20 percent, as we showed in the published paper. When you think about it, pricing avionics on a dollar-per-pound basis seems quite unreasonable. On a dollar-per-pound basis, a diamond, for example, just does not fit on Fig. 2-379. The trend over the last two decades seems (to me) to be to equip a basic air vehicle (i.e., the platform) with a growing suite of avionics that does not weigh very much—and the avionics price is disproportional to the air vehicle price. Therefore, some additional effort that identifies how many avionics’ dollars are included in the “base” factory list price may well alter the price estimating relationship we offered in January of 1998.

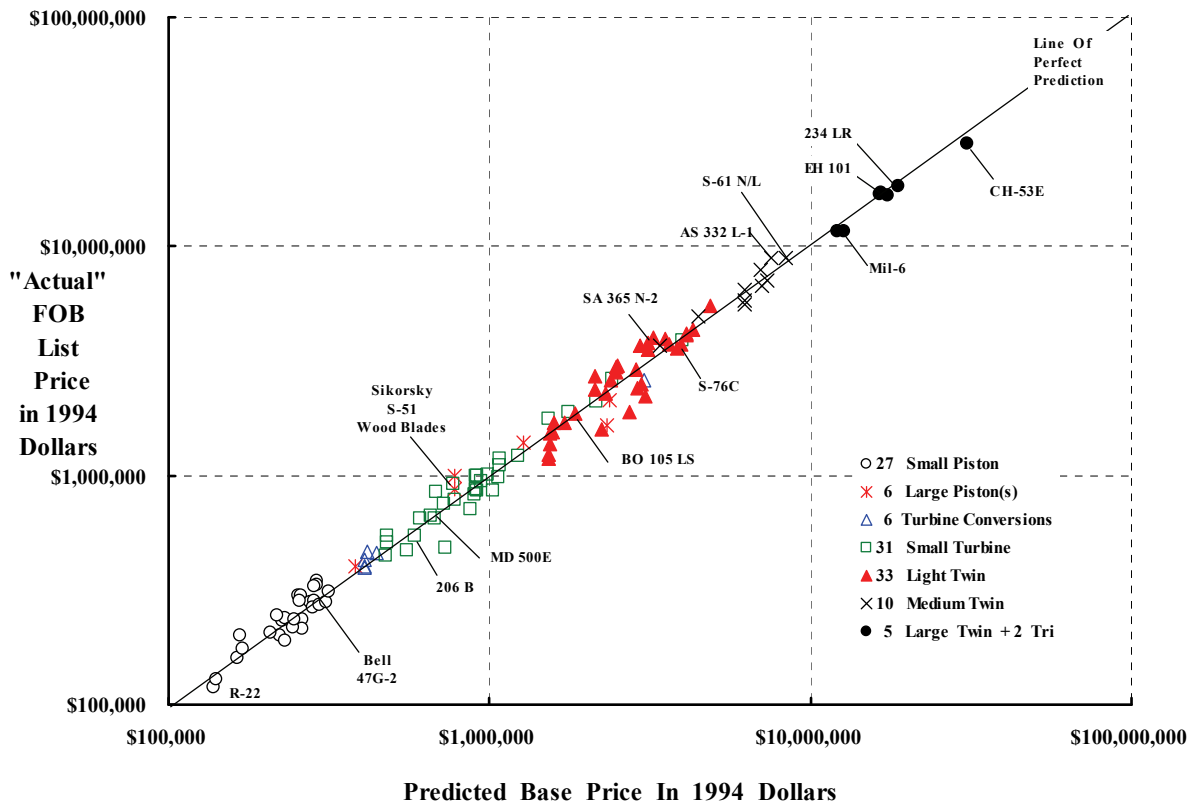


Fig. 2-380. Out of 121 helicopters, 106 are price predicted to within ±20 percent [584].

2.8.1.2 Productivity Per “Buck”

You will recall reading about productivity starting on page 115 in the discussion of weight. On page 116 you read that the industry frequently used an assumption that

$$\text{Productivity Per Dollar} \propto \frac{\text{Payload} \times \text{Speed}}{\text{Weight Empty}} = \frac{PV}{WE}$$

and that weight empty could be used as a stand-in for cost. The basic assumptions were that (1) helicopter manufacturing costs, (2) the purchase price, (3) the user or operator’s costs, and (4) the end benefactor cost (say a passenger’s ticket price) ALL are proportional to the helicopter’s weight empty. In footnote 42 I pointed out that saying I am not in favor of these assumptions would be an understatement! On more than one occasion I have seen the focus placed solely on reducing weight empty regardless of the manufacturing or material costs. Sidestepping the issue of rotorcraft costs is not something I recommend.

Given some reasonably concrete list price data now available to you, it is possible to redefine productivity in terms of list price rather than weight empty. Of course, a customer would most certainly want to know what other financial considerations there are (such as operating costs). In fact, total life cycle costs passed on to the paying customer would be an even more comprehensive parameter to replace weight empty. For now, let me show you the

## 2.8 PURCHASE PRICE

trend of productivity per “buck.” For the numerator, productivity, I choose useful load (i.e., the difference between takeoff gross weight and weight empty) times economical cruise speed. This product has the units of pound-knots or ton-knots. For the denominator, let me use factory list price for the *equipped* configuration in 1,000 dollars. Thus,

$$(2.349) \quad \text{Productivity Per Dollar} \equiv \frac{\text{Useful Load} \times \text{Cruise Speed}}{\text{Equipped List Price in } \$1,000}$$

The trend of productivity in ton-knots per \$1,000 is shown in Fig. 2-381. As you can see, I have added my suggestion of the boundary that few helicopters have exceeded. Notwithstanding my interpretation, however, it does appear that increased speed over the decades has not increased productivity per “buck” with edgewise flying rotors. The move from piston-powered helicopters (i.e., the black open circles) to turbine-engine-powered machines (i.e., the green open squares, the red solid triangles, the black x’s, and the solid black circles) raised useful load and cruise speed—but not enough to offset the accompanying increase in list price. Fig. 2-381 does, of course, raise the basic question of the value of speed. This question is not answered by the productivity per “buck” parameter chosen here.

To conclude this discussion of productivity, let me show you a figure that compares helicopters to fixed-wing aircraft. This comparison, shown in Fig. 2-382, is a somewhat different view than what Mike Scully and I offered in reference [584]. I must mention that Evan Fradenburgh<sup>175</sup> was a great help to us when he read a draft of our work and initial thoughts about productivity per “buck.” In Fig. 2-382 you see that the fixed-wing aircraft have increased productivity per dollar by increasing speed. In quite sharp contrast, the helicopter industry has not achieved a similar result. You will note that the Type B Wright Flyer of 1911–1912, the Douglas DC-3, and The Lockheed Electra (the turboprop one) are convincing evidence that this segment of the transportation industry has capitalized on speed.

The reason that the helicopter has the adverse trend shown in Fig. 2-382 was explained in reference [584] as follows:

“The helicopter industry offers users increased productivity if they will pay more as figure 2 shows. The productivity that a 1994 dollar will buy is described by the simple, empirical equation

$$\text{PRODUCTIVITY (ton-knots)} = 0.00425 (1994 \text{ Dollars})^{0.75}$$

This equation is the dark solid line near the top of the open and solid circle symbols on figure 2 and represents current technology and business pricing offered by the rotorcraft industry. The helicopter’s starting technology is measured by the dotted line lying below most of the circle symbols on figure 2 and approximated by the equation

$$\text{PRODUCTIVITY (ton-knots)} = 0.00215 (1994 \text{ Dollars})^{0.75}$$

---

<sup>175</sup> Evan Fradenburgh was a superb engineer at Sikorsky whom I could turn to for advice on any rotorcraft subject. I thought his aerodynamic cleanup of the Sikorsky S-76 was quite a remarkable feat. His Nikolsky Lecture [382] was a very well deserved honor, and the paper is well worth your reading time. I felt the loss of a good friend when he died in May 2006.

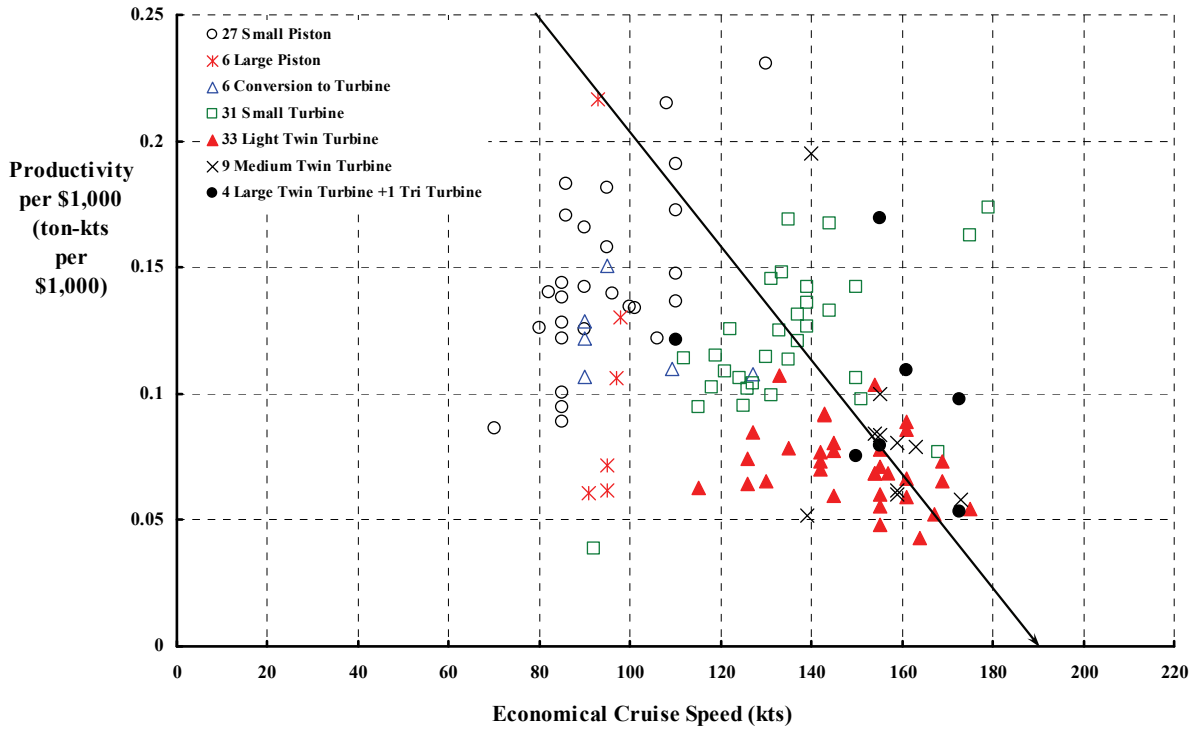


**Fig. 2-381. Increasing size and speed, and adding features, has not increased productivity per “buck.” Just the opposite has happened.**

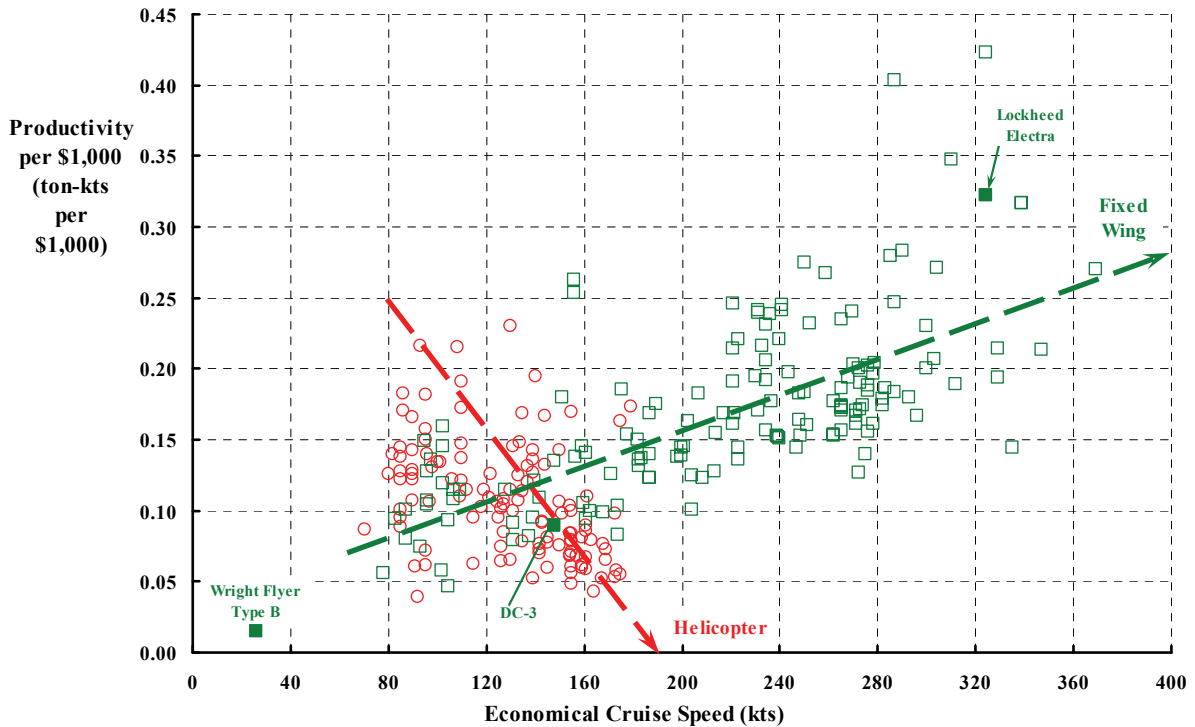


**Fig. 2-382. I really do not have an adequate explanation for the helicopter’s disappointing trend (but edgewise flying rotors may be at the heart of the matter).**

## 2.8 PURCHASE PRICE

These measures of the equipped helicopter's place in the transportation world show that our industry has doubled productivity per 1994 dollar since our start with the Bell 47 and Sikorsky S-51. This progress is reflected by the constant 0.00215 increasing to 0.00425 in the above equations. The S-51 offered 1,500 pounds of useful load and 70 to 80 knot cruise speed for about \$114,000 in 1953. Escalating 1953 dollars to 1994 dollars, following Figure 1, would make the S-51's price today approximately \$1.0 million. Today's helicopter has almost twice the cruise speed for the same useful load which accounts in large measure for the increased productivity.

The rotorcraft industry justifiably takes pride in maturing the helicopter over the last five decades. However, a fixed wing advocate might point out that today's modern gas turbine helicopter is about on par with such pre World War II airliners as the Ford Tri-motor and the legendary Douglas DC-3. Of course, this simple measure of productivity ignores (1) the helicopter's unique ability to operate from very small vertiports and (2) the airliner's need for long runways and dedicated terminal area airspace.

The downside to our efforts in maturing the helicopter is that productivity per "buck" has gone down as we have offered larger and more sophisticated products. This fact is demonstrated with a little simple math as follows:

$$\frac{\text{Productivity}}{1994 \text{ Dollar}} = \frac{0.00425 (1994 \text{ Dollars})^{0.75}}{1994 \text{ Dollar}} = \frac{0.00425}{(1994 \text{ Dollar})^{1/4}} \propto \frac{1}{(\text{Size \& Features})^{1/4}}$$

This formula says that the productivity per "buck" of a \$1,000,000 equipped helicopter is about 134 ton-knots per \$1M. However, for a \$10,000,000 equipped helicopter, the productivity per "buck" goes down to 76 ton-knots per \$1M. This adverse trend may well explain the slow sales of large, sophisticated, fully equipped helicopters."

### 2.8.2 Military Procurement

There is little question that selling helicopters in the civil marketplace is very, very different from fulfilling a military procurement request. After all, a commercial customer is buying off-the-shelf, so to speak. In contrast, the military most frequently asks for a replacement of an aging helicopter model in its fleet. Thus, satisfying the military frequently requires starting with a clean sheet of paper, and this requires application of research, new technology, and extensive development, all in a very competitive environment.<sup>176</sup>

In his book titled *Stephen Morris* [586], Nevil Shute (Norway)<sup>177</sup> added an additional thought about the difference between the two purchasers. He has his fictional character (in England, just after World War I) saying:

"Two days later Morris started work in the design office of the Rawdon Aircraft Company (1919) Ltd. He did not find the work very difficult after the first few days. The whole business of designing an aeroplane he found to run on certain very definite lines. First

---

<sup>176</sup> I suggest again that you read *Augustine's Laws* [582] to get a more complete view. It is more than a tongue-in-cheek story of what must be considered in Department of Defense procurement.

<sup>177</sup> Nevil Shute (Norway) is, by far, my favorite author. He was an aeronautical engineer by day and an author by night until his worldwide popularity became so great that he gave up the aviation industry to write full time. He used his full name in his engineering career and "Nevil Shute" as his pen name in order to protect his engineering reputation.

of all, certain broad considerations governing the design of the machine came to the designer. Thus if it were a passenger machine for an air line, the air line had certain definite ideas as to what they wanted; the carrying capacity, the speed, the landing speed, and the “ceiling” or maximum height that it was possible for the machine to attain. Such considerations as these would be settled in conference with the designer, who would indicate tactfully where they were asking for technical impossibilities. If the machine were a military one for the Air Force the procedure was, in general, much the same, with the difference that the purchaser had a habit of asking for technical impossibilities and refusing to discuss the matter. This made the design of military machines a very specialized business.”

As president of a publically held company that only sells commercial helicopters, you are responsible for your employees while answering to your customers, your board of directors, and your stockholders. Now think about who you also answer to if you are the president of a company that designs and manufactures helicopters for, say, the United States Army. Now you are faced with several layers of authority, which I am suggesting in Fig. 2-383. As the military contractor, you face three immediate constraints: namely cost, schedule, and performance. Cost as used here means the price that the Army will pay for the sum of development, production, operation, and support; in effect, life cycle cost to the taxpayers. Schedule includes such meaningful points as first flight date and when the helicopter is introduced into service. Performance as used here is not just helicopter aerodynamic performance. Rather, performance may also include kill probability, system reliability, and many other parameters found in a system specification.

A military contractor takes several risks (over and above normal business risks) when doing business with the U.S. Government. Before discussing a number of these risks, you should be aware that there are two very common contractual arrangements that the

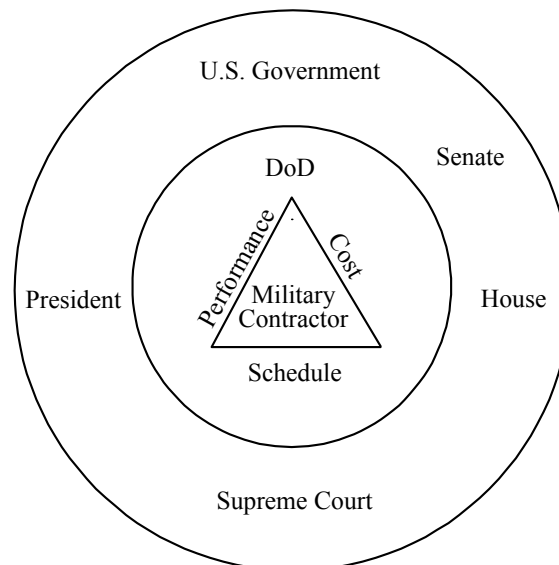


**Fig. 2-383. Military contractors must meet the specification, stay within budget, and deliver on schedule. Unfortunately, it is a very rare occurrence when this happens. The reasons for this rarity are enumerated by Norm Augustine in *Augustine’s Laws* [582].**

## 2.8 PURCHASE PRICE

Department of Defense enters into. The most risky for a military contractor is a fixed-price contract.<sup>178</sup> The less risky type is a cost-plus-fee contract (the sum equals price). In the former, you, as president, may really be “betting your company” that your team can deliver what you promise within the time, and for the price, you quoted. If you underrun your quoted price, you will make a handsome profit. If you overrun your quoted price, your company may be deep in debt when the dust settles.

With a cost-plus-fee contract the U.S. Army (in my example) can expand the work statement by demanding many specification changes not originally envisioned, and the government pays the increased cost. Your company is financially protected (but maybe not your reputation), and you still receive the negotiated fee, *but* the program may be cancelled before you get the chance to make good on the finished product because of “requirements creep,” technical problems, cost growth, and schedule slippage.<sup>179</sup>

A number of risks that a military contractor must take when entering either type of contract were discussed in the Boeing Company 2011 Annual Report to stockholders [589]. With my paraphrasing, you must, as president, be prepared for at least the following:

1. Your funding is subject to congressional appropriations and the government may modify, curtail, or terminate your contract(s) without prior notice *and at its convenience*.
2. Your contract costs are subject to government audits. If the audit results are not satisfactory to any particular audit agency, you have the start of trouble.
3. Your business is also open to potential government inquiries and investigations, any one of which could result in fines or even prevent you from a future military business opportunity.
4. All of your government work is subject to a raft of procurement regulations.
5. You may well be overly dependent on subcontractors and suppliers, as well as on the availability of raw materials and components.
6. Your risk assessment and cost and schedule estimates may be somewhat in error, or even just plain wrong.
7. You have no assurance that you can successfully compete against current or future competitors.

The above list is, of course, incomplete. One program that was successful, despite the odds, created the U.S. Army UH-1 series, which was produced by Bell Helicopter.

---

<sup>178</sup> Bell Helicopter entered into this contract type with the Army Helicopter Improvement Program (AHIP), which fielded the OH-58D [145]. Incidentally, the unpublished full-length copy of this conference paper [145] is available from the author.

<sup>179</sup> This is what happened to the RAH-66 Comanche program. You will find more detail about lessons learned from the Comanche program on the 12 CDs compiled by Bill Harper and Mike Richey [587]. Also, a case history about the LHX/RAH-66 program was published as a master thesis by Jason Galindo while at the Naval Postgraduate School in Monterey, California [588]. His review stops just before the RAH-66 development program was cancelled.



2.8 PURCHASE PRICE

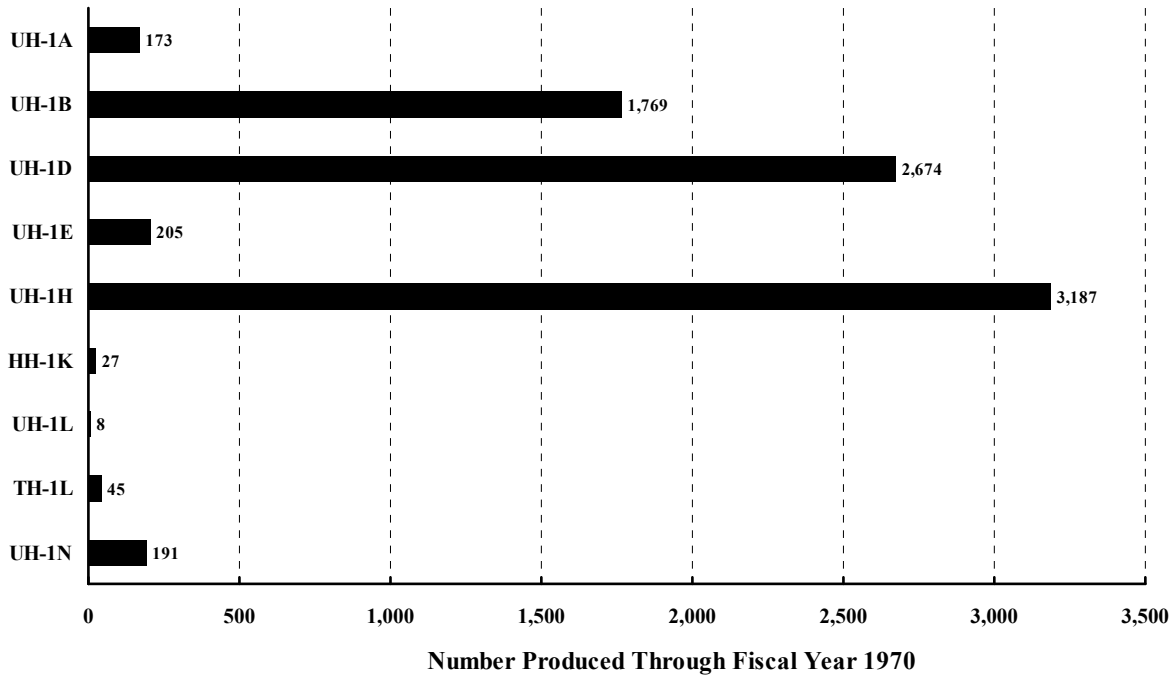


Fig. 2-385. Nearly 8,300 Hueys were produced through fiscal year 1970.

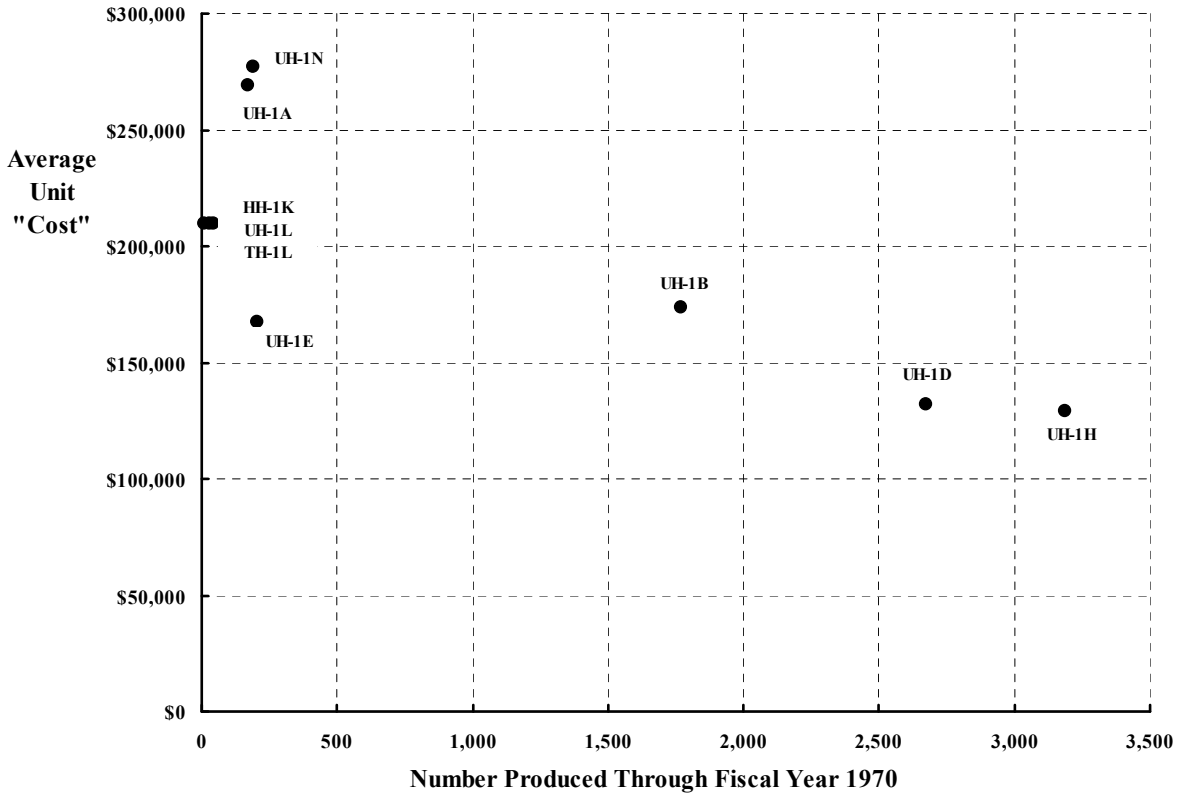


Fig. 2-386. Bell could agree to lower its average unit cost (maybe price?) when the U.S. Army ordered large quantities of Hueys, as they did during the Vietnam War.

It is not often that an engineer stumbles across financial data of significant value, but during the later part of my career I did [590]. This report dealt primarily with weight-empty growth for several helicopters, which was my particular interest at the time, but, can you imagine, it included Huey development and production cost data by contract number. The report has no distribution list or notes about why it was created, and I can find no reference to it so I suspect it was not widely distributed. The authors did note, however, that

“in a request for cost history of the UH-1, the AVSCOM procurement directorate provided an itemized list of 33 procurement contracts from FY 1955 through FY 1970.”

Because of the inclusion of this data in reference [590], you can appreciate some quantified dollars and cents historical information that is quite interesting.

For example, it was pointed out that the U.S. Air Force was the contracting service for the Army’s start of the Huey development. The table included in the report [590] is reproduced here as Table 2-40 and lists not only Huey models but also the YAH-1G attack helicopter, popularly known as the Cobra. What you should particularly note is getting from the XH-40 (three experimental aircraft) through to nine preproduction HU-1As consumed just over 29 million dollars of Department of Defense (DoD) money. This research and development investment, plus another \$20 million for 16 more models, allowed the Army to procure the nearly 8,300 Hueys shown in Fig. 2-385. For this production quantity, the DoD paid Bell \$1,176 billion. Just think about these numbers for a minute or two. A production line amounting to \$1,176 billion for a very successful helicopter was established, and the initial Research and Development investment was \$49 million, which is 4.2 percent of the total cost.

Do not forget, however, that this is an example during a wartime situation. The Vietnam War led to a very large requirement for several models of Hueys, which, in turn, led to Bell learning how to produce in quantity more and more efficiently. This learning allowed Bell to reduce the average cost of a Huey, as I have illustrated in Fig. 2-386. Here I have just graphed the tabulated data provided by reference [590]. This is a parallel example to how the United States dealt with production during World War II. Certainly, it is a parallel to how Douglas Aircraft learned to produce DC-3s [314].

This brings me to the subject of a “learning curve.”

**Table 2-40. R&D Contracts Leading to Huey Production**

Contract No.	Type	Model	Qty	Unit Price	Total Contract Price
AF33(600)30229	CPFF R&D	XH-40	3	4,418,460.00	13,255,382.00
AF33(600)33710	CPFF R&D	YH-40	6	1,681,614.00	10,089,684.00
AF33(657)34920	CPFF R&D	HU-1A	9	643,393.11	5,790,538.00
AF33(600)39616	CPFF R&D	HU-1B	5	1,350,285.20	6,751,426.00
AF33(600)41636	CPFF R&D	YUH-1D	7	1,707,137.14	11,949,960.00
AF33(657)9777	CPFF R&D	UH-1E	4	423,007.25	1,692,029.00
DA23-204-AMC-04075	CPIF Supply	YAH-1G	2	3,795,000.00	7,590,000.00

## 2.8 PURCHASE PRICE

### 2.8.2.2 The Learning Curve

You can see from Fig. 2-386 that as the number of helicopters produced increases, it appears that the cost per unit decreases. An observation of this sort was publically stated in February 1936 by Mr. T. P. Wright.<sup>182</sup> His paper, which you will find in the Journal of the Aeronautical Sciences (now the A.I.A.A.) [591], is fascinating for two reasons. I suppose the first reason is that his paper must be referenced in every follow-on discussion of aircraft costs and cost estimating that has ever been published. More importantly, his compilation of factors affecting the cost of airplanes has stood the test of time. Wright provided evidence that, among other factors, quantity affects airplane costs. While he never uses the words “learning curve” in his 1936 paper, those are the descriptive words used by every author who studied this particular factor.

Wright says in his introduction that

“the effect of quantity production on cost, particularly, requires study as in this respect more than in others, there exists a lack of appreciation of the variation which occurs. Recently the matter became of increasing interest and importance because of the program sponsored by the Bureau of Air Commerce for the development of a small two-place airplane which, it was hoped, could be marketed at \$700 assuming a quantity of ten thousand units could be released for construction.

The present writer started his studies of the variation of cost with quantity in 1922. A curve depicting such variation was worked up empirically from the two or three points which previous production experience of the same model in differing quantities made possible. Through the succeeding years, this original curve, which at first showed the variation in labor only, was used for estimating purposes and was corrected as more data became available. The form which this curve takes when plotted on plain cross-section paper is shown in fig. 1 [shown here as Fig. 2-387]. On this figure there is also shown the variation of the ratio of labor to raw material as quantity varies. The correcting of curves of this type by new points of actual experience resulted in data which permitted other curves to be plotted, showing the variation of raw material, purchased material, and finally, of the whole airplane, against quantity.”

After discussing the influence of design factors, tooling, changes, and size, he notes that

“in developing the curve which shows variation of labor cost with production quantity, it became evident that its form was of the type depicted by the formula  $F = N^x$ .”

and the formula became known as the Wright’s Learning Curve.

The cost sum of labor, material, and tools gave Wright the dashed line shown in Fig. 2-387, which he elected to approximate with his  $F = N^x$  formula. More specifically, Wright points out with his dashed line that his experience strongly suggests that the behavior is calculated as

$$(2.350) \quad \frac{\text{Approximate Cost of the Last Machine of a Series}}{\text{Cost of the First Machine}} = \frac{1}{N^x}$$

---

<sup>182</sup> At the time, Theodore Paul Wright was Chief Engineer and Manager of the Curtiss–Wright plant in Buffalo, New York. Wright was head of the Civil Aeronautics Administration from 1944 to 1948. He died in August of 1970.

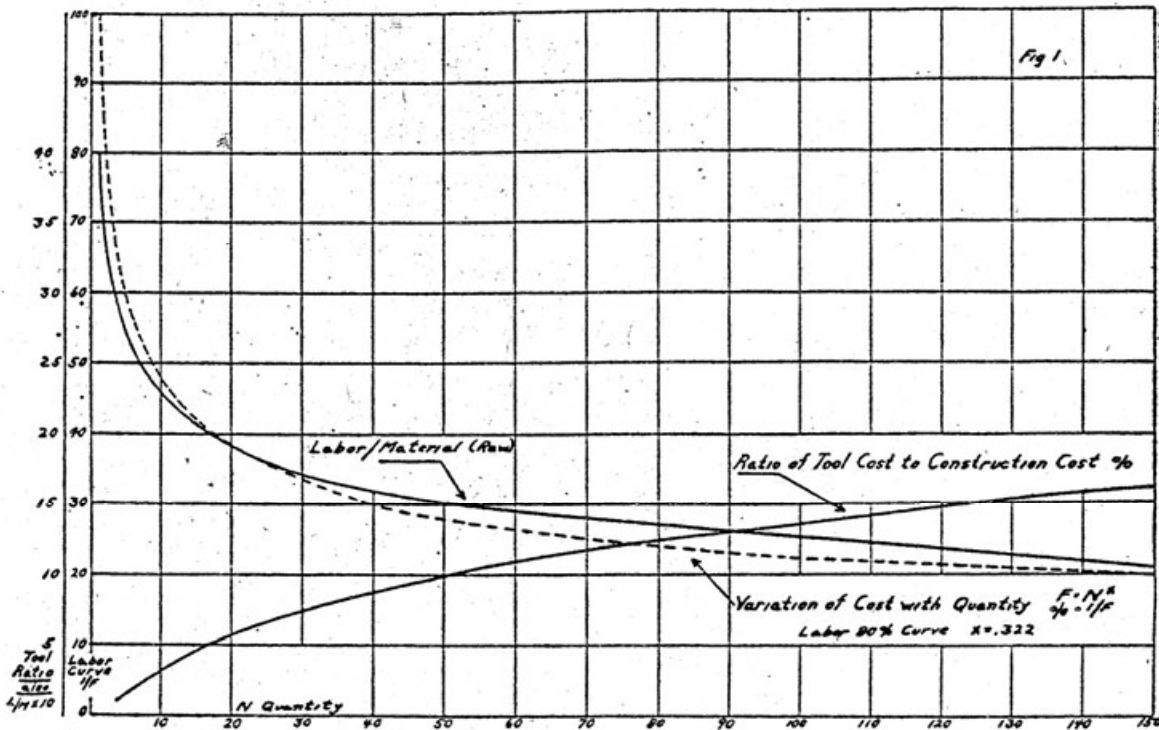


Fig. 2-387. T. P. Wright’s starting point for the “learning curve.”

where (N) is the number of the last machine in the production lot, and (x) is some number that fits a manufacturer’s experience, or perhaps hope, or perhaps a military negotiated expectation. The dashed line in Fig. 2-387 that Wright uses as an example assumes  $x = 0.322$ . Thus, if  $N = 40$ , then the approximate cost of the 40th machine, as fraction of the cost of the first machine, will be  $1/40^{0.322}$ , which equals 0.305.

As Wright’s observations became apparent to other manufactures, particularly during World War II, a number of other ways to mathematically say the same thing came into the economic literature. Personally, I prefer stating Wright’s observation as

$$(2.351) \quad \text{Cost of Aircraft } N = \text{First Aircraft Cost}_{(N=1)} \left[ \text{LCF} \right]^{\left( \frac{\log N}{\log 2} \right)}$$

where [LCF] stands for learning curve factor. This factor ranges from perhaps as low as 0.70 to hopefully no more than 1.0. In this form, the dashed line in Fig. 2-387 has an  $\text{LCF} = 0.8$ . You will frequently hear cost estimators say, “Let’s assume a learning curve of 80 percent as part of our cost estimate.” You should keep in mind that while Eq. (2.351) uses the word “Cost,” the learning curve can apply to labor hours, or price, or many other units. Wright made his initial observation from labor hours as Fig. 2-387 shows.

As you read Wright’s milestone paper, you will begin to realize that he is about to debunk the Bureau of Air Commerce’s objectives for its Small Plane program. The Bureau was saying that the total number of airplanes to be built was to be 10,000 and that anyone

## 2.8 PURCHASE PRICE

could buy one for \$700 (i.e., the price). As Wright's reasoning unfolds, he tackles (at the end of his paper) the \$700 airplane Small Plane program that the Bureau of Air Commerce was proposing. He first suggests that the general specifications for a "small two-place airplane" would be:

Useful Load	700 lb
Weight Empty	1,100 lb
Gross Weight	1,800 lb
Structural Weight	800 lb
Engine	100 to 125 h.p.
High Speed	125 to 150 m.p.h.
Speed Range	3 [This is the ratio of maximum speed to stall speed]
Material	All metal

Then, to make his point, he assumes that the price estimate in a small production lot of 25 would be on the order of:

Cost (1,100 lb weight empty @ \$6/lb)	\$6,600.00
Profit (manufacturing, at 10%)	\$660.00
<u>Sales Discount (20%)</u>	<u>\$1,815.00</u>
Price	\$9,075.00

which he rounds off to \$9,000 by expecting to get a break on the engine cost. Then, pricing production in several lot sizes assuming the price for the first article is \$16,356 and a constant LCF of 0.83, he tabulates (with my editing)<sup>183</sup>

Quantity	25	100	500	1,000	10,000
Selling Price by Lot Size	\$9,000	\$6,372	\$4,184	\$3,481	\$1,880
Total Income (P×Q)	\$225,000	\$637,200	\$2,092,00	\$3,480,500	\$18,797,000

With these financial figures on the table, Wright concludes:

"We thus see that for a plane of these specifications and in the original quantity cited by the Bureau of Air Commerce when commencing its \$700 Small Plane program, [the airplane] would have to be priced at about three hundred percent more than was hoped. Perhaps some reductions from the estimate could be effected by altering construction, design, and reducing sales discounts and profits (although by so doing the ten thousand units would probably never be sold) but in the quantity of ten thousand units which is under consideration, it is doubtful whether a price of less than \$1,750 could possibly be attained."

You should note that the total cost (or total income in this case) is computed simply as

$$\begin{aligned}
 (2.352) \quad \text{Cost of } N \text{ Aircraft} &= P \times Q = \sum_1^N \text{Cost of Aircraft } N \\
 &= \text{Cost 1}^{\text{st}} \text{ Aircraft} \left\{ 1 + \text{LCF}^{(\log 2 / \log 2)} + \text{LCF}^{(\log 3 / \log 2)} + \dots + \text{LCF}^{(\log N / \log 2)} \right\}
 \end{aligned}$$

and that the selling price for each aircraft in a given lot (i.e., P) can be closely approximated with

<sup>183</sup> Wright appears to have obtained his approximate figures with graphs and a slide rule. I used Excel®.

$$(2.352) \quad P = \text{Cost 1}^{\text{st}} \text{ Aircraft} \left\{ \text{LCF}^{1.573(\log N) + 0.693(\log N)^2 - 0.0692(\log N)^3} \right\}.$$

When I first became interested in the “learning curve,” I came across an article in the November 1952 copy of *Aero Digest* written by a Mr. W. A. Raborg, then employed by Northrop Aircraft, Inc. Several paragraphs from his paper stuck with me and you may also find them interesting (because a few hundred thousand papers and reports have been published trying to extend, refine, make more complex, and apply Wright’s original work). For example, Raborg wrote [592] in 1952 (with my editing and additions in brackets) that

“by the end of World War II, the major aircraft companies had rather generally recognized the value of the [learning] curve by its application to their own particular production data. The smaller companies, however, comprising most of the sub-contractors, had little knowledge of its use. The United States Government had also come to recognize the importance of the learning curve. In order to strengthen the aircraft industry for future military requirements, the *Government distributed World War II aircraft production data to all contributing companies* [my italics]. In addition, the Government sponsored several research projects with private organizations to develop further the application of the theory. Probably the best known of these was the work done by the Stanford Research Institute which was later made available to the various Aircraft companies.”

The World War II aircraft production data that Raborg mentions was published with the title *Source Book of World War II Basic Data: Airframe Industry, Volume I—Direct Man-Hours – Progress Curves* [593]. No date shows on this 200-page document, but data is included from January 1940 through December 1945, so for reference purposes I have used 1946. This Source Book is the foundation for nearly all studies applying and extending Wright’s Learning Curve. The Source Book tabulates labor man-hours for the Boeing B-29 through to Sikorsky’s R-4, R-5, and R-6. One thing I have found absolutely fascinating (over and above the four massive tables) is the Direct Labor Progress Curves (i.e., learning curves) that show actual data for direct man-hours per airframe unit weight plotted versus cumulative plane number. Table 3 of the Source Book states that

“airframe Unit Weight is the airplane weight empty minus the total weight of the following items:

- engine (dry weight);
- propeller hubs, blades, power control and governor;
- wheels, brakes, tires, and tubes;
- auxiliary power plant;
- turbo-superchargers;
- radio receivers, transmitters, radar and removable units, but not installation parts and wiring;
- starter;
- battery;
- generator, turrets and power-operated gun mounts.

The source of these data is the Airframe Unit Weight reports which were issued periodically by predecessors of the Air Materiel Command. Changes in Airframe Unit Weight from one month to the next may indicate a change in the basic model. Where variations of the same basic model with different airframe unit weights (such as A-20G and A-20H at Douglas—Santa Monica) were accepted in the same month, a weighted average airframe unit weight figure was calculated, weighted by the number of acceptances. The data from the Airframe Unit Weight Reports are rounded to the nearest hundred; the weighted average data are not rounded off.”

## 2.8 PURCHASE PRICE

On each figure you have the facility, the aircraft model, and the airframe unit weight noted. The accumulated data from bombers, fighters, transports, light planes, helicopters, etc., really does not support the use of man-hours per pound as a fundamental parameter as you will conclude, as I have, after thumbing through the 129 figures. But because the unit airframe weight varies so much with aircraft type, and to a lesser extent with what factory was building that type,<sup>184</sup> the parameter is useful in keeping the same scales for all types.

Let me give you an example of learning curve data from two aircraft that you will find in table 4 of the Source Book, with associated graphs in the Source Book's appendix. Keep in mind that it is World War II production data that is under discussion. First of all, you can see from Fig. 2-388 that learning curve data is almost always plotted on a log-log axis system, which Wright pointed out in his original work is preferable. This axis system is particularly handy because the basic hypothesis given by Eq. (2.351) becomes an intercept and a slope. You see this when you take the logarithm of both sides of Eq. (2.351)

$$(2.353) \quad \log(\text{Cost of Aircraft } N) = \log\left(\text{First Aircraft Cost}_{(N=1)} [\text{LCF}]^{\left(\frac{\log N}{\log 2}\right)}\right),$$

which gives you

$$(2.354) \quad \log(\text{Cost of Aircraft } N) = \frac{\log(\text{First Aircraft Cost}_{(N=1)})}{\log 10} + \left[ \frac{\log(\text{LCF})}{(\log 2)(\log 10)} \right] \log N .$$

$$= A + B \log N$$

You will note on Fig. 2-388 that I have “eyeballed” linear lines that I think best fit the learning curves for these two aircraft. From the lines, I calculated the learning curve factor (LCF) quite simply as

$$(2.355) \quad \text{LCF} = \left[ \frac{\text{Cost of Aircraft } N}{\text{First Aircraft Cost}} \right]^{\left(\frac{\log 2}{\log N}\right)} .$$

Using the Boeing B-29 as an example, you have

$$(2.356) \quad \text{LCF} = \left[ \frac{0.27 \text{ mh/lb}}{28 \text{ mh/lb}} \right]^{\left(\frac{\log 2}{\log 10,000}\right)} = \left[ \frac{0.27}{28} \right]^{\left(\frac{0.301}{4}\right)} = 0.705 \quad \text{for B-29,}$$

and for the Sikorsky R-6 (built in quantity by Nash-Kelvinator in Detroit, Michigan) you obtain an LCF of 0.715.

It should be clear that estimating cost (in any units) of the N<sup>th</sup> aircraft a priori can be simply an educated guess, but given some previous actual data, the guess may, with considerable luck, not be in error by more than  $\pm 25$  percent [594].

---

<sup>184</sup> For example, the Boeing B-29 was built by Boeing in Renton, Washington, and Wichita, Kansas; by Bell Aircraft Corporation in Marietta, Georgia; and by the Glenn L. Martin Company in Omaha, Nebraska. Clearly the factories were quite dispersed and not always near what we would call headquarters.

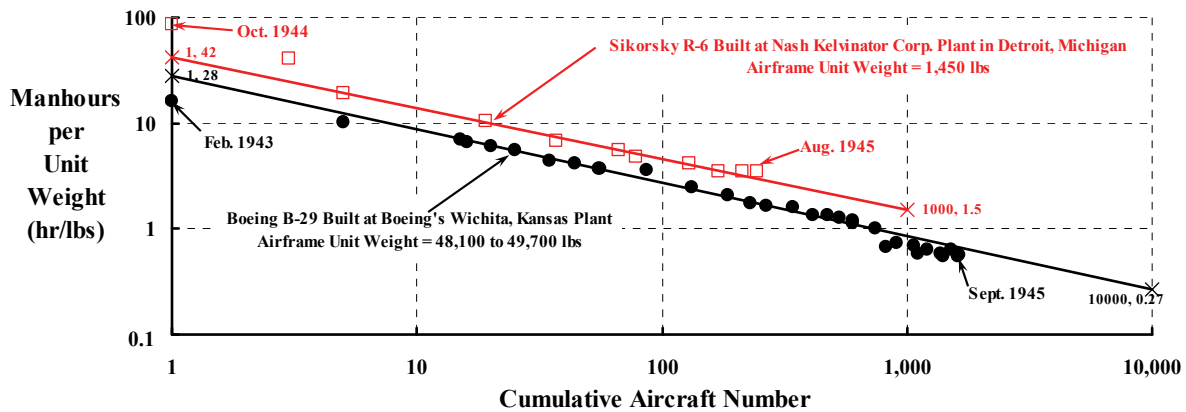


**Fig. 2-388. T. P. Wright’s observations about how quantity affects cost were reaffirmed based on data gathered during World War II [593].**

In view of what you have read, let me now reexamine the Bell Huey data provided in Fig. 2-386. The points shown in this figure came from the following tabulated information (Table 2-41) [590]. There are a few points to be made about this data. First of all, this is data for a cost-plus-fee type of contract. What the actual numbers at contract completion were are probably available—in some file somewhere. Second, I do not know if the engine (and other assemblies) were furnished to Bell, and therefore they may not be included in the unit price.<sup>185</sup>

**Table 2-41. Some Production Contracts for Hueys [590]**

Fiscal Year	Contract No.	Model	Qty	Unit Price	Total Contract Price	Cum Qty	Cum Dollars
	AF33(600)36024	HU-1A	47	414,342	19,474,100	47	19,474,100
	AF33(600)38615	HU-1A	110	217,726	23,949,921	157	43,424,021
	AF33(600)40447	HU-1A	16	197,360	3,157,764	173	46,581,785
	AF33(600)40447	HU-1B	74	270,553	20,020,947	247	66,602,732
	AF33(600)41900	HU-1B	118	246,178	29,048,958	365	95,651,690
	AF33(657)7001	UH-1B	315	183,379	57,764,490	680	153,416,180
	AF33(657)10000	UH-1B	289	254,707	73,610,237	969	227,026,417
	AF33(657)11111	UH-1B	272	135,771	36,929,712	1241	263,956,129
	AF33(657)11111	UH-1B	18	132,701	2,388,629	1259	266,344,758
	AF33(657)7001	UH-1B(MAP)	8	183,394	1,467,150	1267	267,811,908
	AF33(657)11111	UH-1B(RAN)	3	171,902	515,706	1270	268,327,614
1965	DA 230204-AMC-02805(Y)	UH-1B	149	125,833	18,749,117	1419	287,076,731

<sup>185</sup> Webb Joiner, whose first job at Bell was assistant to then Bell CFO Jim Atkins, mentioned in private correspondence [595] that “The early contracts, that covered the major part of the aircraft deliveries, were fixed price target incentive contracts. At the beginning of the contract we negotiated a target cost and a target profit along with a sharing factor (rate) for overruns on cost and normally a different sharing factor for underruns. As we worked the contract we filed quarterly estimates to adjust interim cash flow to Bell and at the end of the contract we had a second contract negotiation to determine final cost and contract price. The final price of each contract was different from the original price. This final price was incorporated into the contract by an amendment. I also want to remember that some of the later contracts were pure fixed price.” Webb also told me that “The engines, I believe in every contract, were Government Furnished Equipment (GFE) to Bell; also avionics, small dollar amounts—primarily radio equipment, was also GFE to Bell. So the cost of these items was not in Bell’s contract values.” Jim Atkins, then Jack Hoerner, and then Webb Joiner later became presidents of Bell, and it was my good luck to have worked at Bell during the period of their outstanding leadership.

2.8 PURCHASE PRICE

Table 2-41. (continued)

Fiscal Year	Contract No.	Model	Qty	Unit Price	Total Contract Price	Cum Qty	Cum Dollars
1965	DA 230204-AMC-02805(Y)	UH-1B	8	130,976	1,047,808	1427	288,124,539
1965	DA 230204-AMC-02805(Y)	UH-1B	6	145,419	872,514	1433	288,997,053
1965	DA 230204-AMC-02805(Y)	UH-1B	1	133,342	133,342	1434	289,130,395
1965	DA 230204-AMC-02805(Y)	UH-1B	4	129,294	517,176	1438	289,647,571
1965	DA 230204-AMC-02805(Y)	UH-1B	1	160,024	160,024	1439	289,807,595
1966	DA 23-204-AMC-03501(T)	UH-1B	500	127,498	63,749,000	1939	353,556,595
1966	DA 23-204-AMC-03501(T)	UH-1B	1	119,835	119,835	1940	353,676,430
1967	DAAJ01-67-C-0025(B)	UH-1B	2	167,694	335,388	1942	354,011,818
	AF33(657)7001	UH-1D	30	436,764	13,102,930	1972	367,114,748
	AF33(657)11111	UH-1D	410	172,952	70,910,320	2382	438,025,068
1965	DA 230204-AMC-02805(Y)	UH-1D	571	136,711	78,061,981	2953	516,087,049
1965	DA 230204-AMC-02805(Y)	UH-1D	4	133,302	533,208	2957	516,620,257
1965	DA 230204-AMC-02805(Y)	UH-1D	45	121,590	5,471,550	3002	522,091,807
1966	DA 23-204-AMC-03501(T)	UH-1D	1613	114,599	184,848,187	4615	706,939,994
1966	DA 23-204-AMC-03501(T)	UH-1D	1	122,003	122,003	4616	707,061,997
	AF33(657)9779	UH-1E	29	265,097	7,687,805	4645	714,749,802
	AF33(657)11112	UH-1E	48	156,361	7,505,328	4693	722,255,130
1964	DA 23-204-AMC-02897(X)	UH-1E	24	137,574	3,301,776	4717	725,556,906
1964	DA 23-204-AMC-02897(X)	UH-1E	28	142,755	3,997,140	4745	729,554,046
1966	DA 23-204-AMC-04011	UH-1E	31	144,042	4,465,302	4776	734,019,348
1966	DA 23-204-AMC-04011	UH-1E	27	145,433	3,926,691	4803	737,946,039
1967	DAAJ01-67-C-0030(B)	UH-1E	18	171,259	3,382,500	4821	741,328,539
1967	DAAJ01-67-C-0025(B)	UH-1H	769	130,401	100,278,369	5590	841,606,908
1967	DAAJ01-67-C-0025(B)	UH-1H	1	141,745	141,745	5591	841,748,653
1967	DAAJ01-67-C-0025(B)	UH-1H	3	138,223	414,669	5594	842,163,322
1967	DAAJ01-67-C-0025(B)	UH-1H	9	156,345	1,407,105	5603	843,570,427
1967	DAAJ01-67-C-0025(B)	UH-1H	2	133,317	266,634	5605	843,837,061
1967	DAAJ01-67-C-0025(B)	UH-1H	3	133,346	400,338	5608	844,237,399
1967	DAAJ01-67-C-0025(B)	UH-1H	4	138,060	552,240	5612	844,789,639
1967	DAAJ01-67-C-0025(B)	UH-1H	10	141,605	1,416,050	5622	846,205,689
1968	DAAJ01-67-C-0566	UH-1H	528	125,952	66,502,656	6150	912,708,345
1968	DAAJ01-67-C-0566	UH-1H	1	132,242	132,242	6151	912,840,587
1968	DAAJ01-67-C-0566	UH-1H	4	130,691	522,764	6155	913,363,351
1968	DAAJ01-67-C-0566	UH-1H	1	133,710	133,710	6156	913,497,061
1968	DAAJ01-67-C-0566	UH-1H	2	131,333	262,666	6158	913,759,727
1968	DAAJ01-67-C-0566	UH-1H	6	125,952	755,712	6164	914,515,439
1968	DAAJ01-67-C-0566	UH-1H	16	148,117	2,369,872	6180	916,885,311
1968	DAAJ01-67-C-0566	UH-1H	3	125,952	377,856	6183	917,263,167
1968	DAAJ01-67-C-0566	UH-1H	1	131,326	131,326	6184	917,394,493
1968	DAAJ01-67-C-0566	UH-1H	11	129,202	1,421,222	6195	918,815,715
1968	DAAJ01-67-C-0566	UH-1H	4	125,952	503,808	6199	919,319,523
1968	DAAJ01-67-C-0566	UH-1H	8	125,952	1,007,616	6207	920,327,139
1968	DAAJ01-67-C-0566	UH-1H	546	125,952	68,769,792	6753	989,096,931
1968	DAAJ01-67-C-0566	UH-1H	6	125,592	755,712	6759	989,852,643
1968	DAAJ01-67-C-0566	UH-1H	12	125,592	1,511,424	6771	991,364,067
1968	DAAJ01-67-C-0566	UH-1H	11	125,592	1,385,472	6782	992,749,539
1969	DAAJ01-69-C-0028(2B)	UH-1H	1226	130,409	159,881,730	8008	1,152,631,269
1968	DAAJ01-68-C-1911(B)	HH-1K	27	209,688	5,661,563	8035	1,158,292,832
1968	DAAJ01-68-C-1911(B)	UH-1L	8	209,698	1,677,500	8043	1,159,970,332
1968	DAAJ01-68-C-1911(B)	TH-1L	45	209,688	9,435,938	8088	1,169,406,269
1969	DAAJ01-69-C-0085(2B)	UH-1N	79	265,000	20,935,000	8167	1,190,341,269
1970	DAAJ01-70-C-0205 (Navy)	UH-1N	62	302,112	18,731,000	8229	1,209,072,269
1970	DAAJ01-70-C-0234 (Canadian)	UH-1N	50	265,000	13,250,000	8279	1,222,322,269

Notwithstanding some reservations about data contained in reference [590], let me proceed with a simple analysis. In Fig. 2-389 you see the accumulating contract awards to Bell (in millions of dollars) plotted versus aircraft numbers to be delivered. Excel’s regression analysis (i.e., the trendline tool) of this data offered the opinion that

$$(2.357) \quad \text{Cum Dollars} = \$809,600(N)^{0.80632} \quad R^2 = 0.9988.$$

I chose to round off the price of the first aircraft (i.e.,  $N = 1$ ) at \$800,000. Then I applied Eq. (2.352), adjusting the LCF until the resulting line on Fig. 2-389 looked “close enough.” This process gave an LCF of 0.857. On this basis, you have the opinion that the learning curve for Bell, while producing the Huey over the fiscal years 1960 to 1970, was

$$(2.358) \quad \text{Price of Huey } N = \$800,000 \left[ 0.857 \right]^{\left( \frac{\log N}{\log 2} \right)}.$$

It is quite important for you to appreciate that the analysis arriving at Eq. (2.358) includes the influence of inflation. During World War II, prices were fixed, but during the decade of the 1960s, helicopter selling prices slightly exceeded the U.S. Consumer Price Index as figure 1 of reference [584] illustrates. Using a value of unity in 1950, this reference arrived at an inflation factor of 1.292 in 1960 and 1.855 in 1970. This means that the price of the 8,000th Huey of about \$108,180 reflected about a 43 percent increase over the 10-year period. That is, the price of the 8,000th Huey should have been, without inflation, only about \$61,660. This means that the LCF was actually closer to 0.815, which is considerably better than the LCF of 0.857 you see with Eq. (2.358).

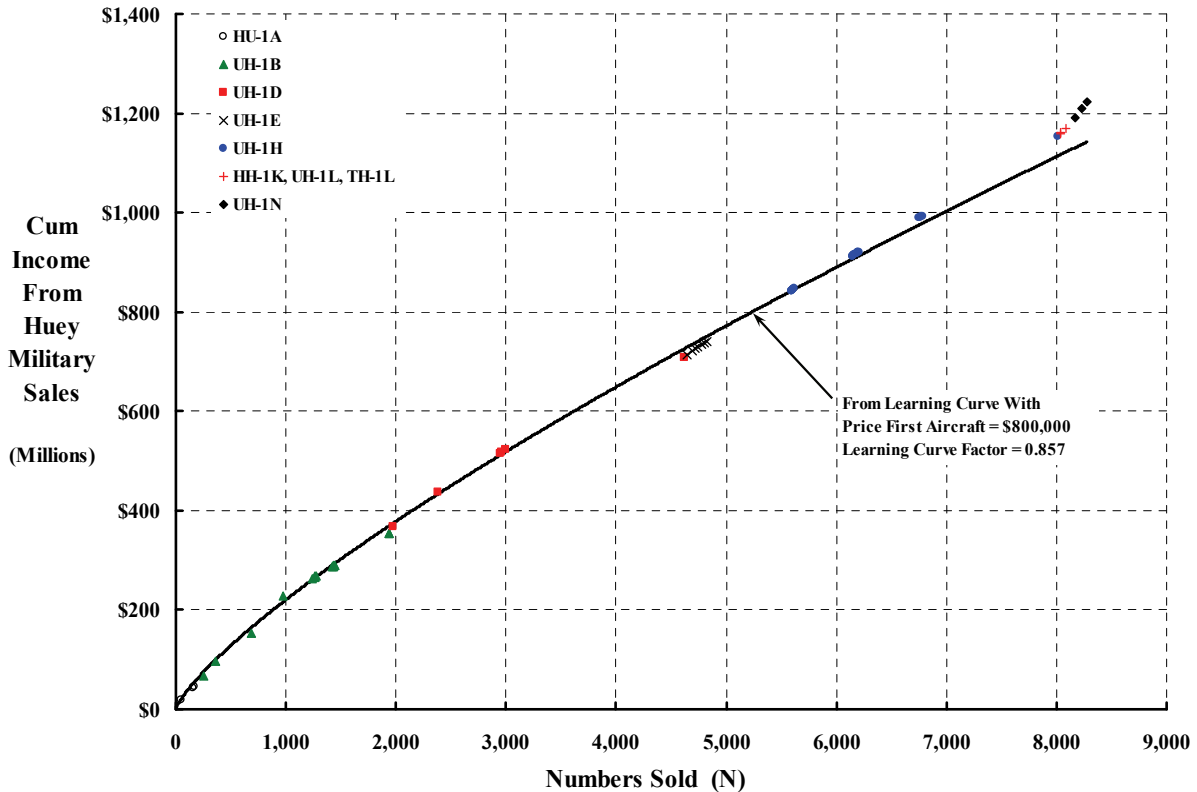


Fig. 2-389. Bell Helicopter’s approximate income from military sales of the Huey.

## 2.8 PURCHASE PRICE

Let me conclude this discussion with other paragraphs Mr. Raborg [592] included in his 1952 Aero Digest article:

“The staff organizations of the aircraft companies, which had become familiar with the applications of the learning curve during World War II, however, dwindled to skeleton forces during the post war period of reduced production. Now, as the industry is expanding its production again, much of the experience gained in World War II must be repeated for, or at least brought to the attention of, the newer employees. Relatively few persons understand the application of the learning curve, and there are few accurate references on the subject.

The problem is even more serious now than before. During the growth of airplane manufacture from 1940 to 1945, the learning curve was used almost exclusively by management and its staff groups, and little interest in its use appeared anywhere in the line organization. Today, however, the general acceptance of the curve by management and by the Government has led to its recognition by the shop as well. Production departments, that is, personnel on the line, knowing that it is a tool which they are expected to use, are now accepting the theory and asking for technical assistance in its use. Probably the most versed persons on the subject are still among management, and certainly one of the prerequisites for production management positions is a thorough understanding of its application.

Some idea of the importance of the learning curve may be seen from the fact that:

- (1) Military planners use the learning curve to estimate the nation's aircraft mobilization expansion potential. Air Force equipment, pilots, ground crews and supporting personnel, training schools, etc., are all closely coordinated with aircraft production, and therefore reflect the reliability of the learning curve theory;
- (2) The Government uses the learning curve to measure [an] aircraft manufacturer for efficiency and production;
- (3) The Government checks [an] aircraft manufacturer's bids for accuracy and reasonableness. This examination is largely based upon statistical analysis of the manufacturer's own record with respect to general industry production performance;
- (4) Aircraft manufacturers use the learning curve in preparing bids for new business;
- (5) Aircraft manufacturers use the learning curve in developing labor loads, area and equipment requirements, shop efficiency measures, budgets, and often standards; and
- (6) Aircraft manufacturers use the learning curve to measure the progress of active contracts. This is often the basis for contract payments and loans.”

The statements Mr. Raborg made seem to me to be every bit as applicable today as they were in 1952. In fact, his statement that “relatively few persons understand the application of the learning curve, and there are few accurate references on the subject” may be even more correct today. It is absolutely amazing to me how successive investigators have cast Wright's simple observation [596, 597] into many different (and more complex) forms. However, there is, I think, one noteworthy exception published in 1959 by John Nichols of Hiller Aircraft Corporation [598].

### 2.8.2.3 Design to Cost

T. P. Wright's paper can certainly be classified as a milestone because it introduced the learning curve, but stop for a moment. His application was, in fact, to the Bureau of Commerce plan to create a market for a \$700 small plane in 1936. To me, this was a very early example where designing to meet a price was the objective. The whole concept of designing to meet a selling price was finally put into a major Department of Defense policy statement and labeled Design to Cost. This policy [599] was released in October 1977 with the title *Joint Design-to-Cost Guide, Life Cycle Cost as a Design Parameter*. This guide starts with a one-page foreword (dated 9 January 1976) signed by three generals and one admiral<sup>186</sup> who said:

“We approve this revised ‘Guide on Design to Cost’ for use within our commands. It provides information and guidance for application of the Design to Cost concept.

Since the first edition of this Guide in October 1973, there have been numerous applications of Design to Cost in both major and non-major system, sub-system and component developments. The great majority of these applications have been limited to ‘unit production cost.’ Although no Design to Cost program has yet matured to the point at which "lessons learned" can be garnered from factual cost data, we are convinced from evidence in hand that the concept works and will be of great benefit.

However, the concept can and must be expanded beyond unit production cost to include operating and support costs. Approaches which concentrate on those operating and support costs which are design sensitive are currently available even in the absence of a uniform, useable and historical data base for all operating and support costs.

We seek a favorable balance among the elements of life cycle cost, (development, production, operating and support costs) and the performance of every system.

There are no easy steps in designing a complex weapon system to established cost goals. The DOD and contractors must be committed, effectively communicate and maintain essential effort toward achieving the established Design to Cost goals.

Supplemental instructions may be issued by the individual commands.”

The guide further notes that “several cost effective weapon systems have recently been developed which, because of their cost, were not affordable in adequate numbers to satisfy mission requirements, necessitating additional lower cost developments.” The purpose of the guide (to solve this problem) was, and still is, “to establish life cycle as a design parameter during a system’s design and development phase and provide a cost discipline to be used throughout the acquisition of a system.” The trend Augustine provided earlier (Fig. 2-373) sums up the whole situation quite clearly—as far as I am concerned in this introductory volume.

The guide also introduced the Work Breakdown System (WBS) in its appendix A. The purpose of the WBS was to ensure that performance, cost, and schedule (see Fig. 2-383) of future system acquisitions would be more carefully monitored. By 2011, appendix A of the

---

<sup>186</sup> General John R. Deane, Jr. as Commander of the U.S. Army Material Command; General William J. Evans as Commander of the Air Force System Command; General F. W. Rogers as Commander of the Air Force Logistics Command; and Admiral F. H. Michaelis for the Naval Material Command.

## 2.8 PURCHASE PRICE

guide had grown to a 251-page document and had become a military standard now known as MIL-STD-811C [600].

On a personal note: The guide has been the “bible” for over four decades, yet I have not found any quantitative evidence that the DoD and its contractors’ basic problem has been solved by using the Design-to-Cost Guide (but then, I have hardly made a thorough search). My view is that the guide does not address human frailties, misbehaving hardware (be it mechanical or electronic), or computer software that has gone off course. In being a part of the team that fielded the OH-58D [145], I rarely viewed the WBS as anything more than data for economic historians. To me, successful *development* is *only* accomplished by a small team lead by a great designer like Kelly Johnson [581] or Ed Heinemann [601], and only then if they are unencumbered by monitors, accountants, watchers, calendars, and WBS computer printouts. To me, successful *production* is *only* accomplished by a company having very strong engineering and manufacturing voices, and led by someone like Donald Douglas [314] or William M. Allen, who was president of Boeing from September 1945 to April 1968, and later chairman of the board. I am convinced that creating a *guide* and a *system* that models men like the ones I have acknowledged cannot be done.

In the 1970s, a number of papers and reports were published that (a) aimed at more accurate cost estimating [602], (b) suggested how to establish a designer’s cost target [603], (c) described planning a product [604], and (d) dealt with tradeoffs between cost and performance [605], etc. Much of this information was derived from commercial practices even for general aviation products [604], which is the category where the FAA places commercial helicopters.

In the papers and reports just referenced, you will read comments that the product’s price is nearly set in concrete during the conceptual design phase. I firmly believe this to be absolutely true. Consider this upfront decision: when a military or commercial customer chooses a helicopter instead of a fixed-wing aircraft for his mission, he has already accepted a 50 percent surcharge for the vertical takeoff and landing capability—according to reference [584].

But let me proceed, given the decision by military planners that a new helicopter is required. The next two major cost decisions are whether to use a piston or a gas turbine engine and whether to have one or two engines. By making state-of-the-art decisions of *twin* gas turbines, you increase the lowest cost configuration by factors of 1.344 and 1.794, respectively, as Eq. (2.348) shows. The expectation from these two decisions is, of course, that life cycle cost savings over, let’s say, 30 years, will easily cover the higher unit cost.

With these three major cost-driving decisions made, put yourself in a very high-level position and you must give U.S. Army go-ahead approval for development and production of a new helicopter. For example, say you are in Mr. James Ambrose’s shoes<sup>187</sup> and wrestling with the new Light Helicopter (LHX) that the Army Training and Doctrine Command

---

<sup>187</sup> James Ambrose was the Under Secretary of the Army (from October 1981 to February 1988) who approved the LHX go-ahead.

(TRADOC) says is required in the near future. This was, in fact, exactly what happened during the birth of the LHX program that led to the RAH-66 Comanche. At that time the configuration was presented as having a weight empty of 7,500 pounds, powered with two gas turbines each rated at 1,300 horsepower, and the average price (perhaps you would prefer cost) of \$5.3 million (capped by Congress) in a fielding of up to 7,000 machines.<sup>188</sup> The 7,000 LHXs were to replace Hueys, OH-58s, OH-6s, and the AH-1 Cobras. The total development and production program (including the yet to be developed engine!) was estimated at \$37 billion [606].

Now take a minute to reflect on the baseline that 7,000 LHXs are to be delivered at an average price of \$5.3 million each, for a total of \$37.1 billion. Given Bell Helicopter's performance in delivering over 8,000 Hueys, let me assume an LCF of 0.857, which includes some inflation. Working backwards using Eq. (2.352), you will find that the price of the first production RAH-66 is \$29.6 million and that the price estimate of the N<sup>th</sup> RAH-66 will be as follows:

$$(2.359) \quad \text{Price of the } N^{\text{th}} \text{ RAH-66} = \$29,593,000 \left[ 0.857 \right]^{\left( \frac{\log N}{\log 2} \right)}.$$

It is quite interesting to compare the first Huey aircraft price of \$0.8 million obtained with Eq. (2.358) to the first RAH-66 aircraft price of \$29.6 million arrived at with Eq. (2.359). This is a first-aircraft price ratio of 37 to 1. No doubt many readers will be simply taken aback and left wondering if the RAH-66 would have provided the military with a correspondingly better machine (if the program not been cancelled). However, at least four major design-to-cost factors created this price ratio. I believe the major design-to-cost factors are:

1. General inflation of helicopter prices (quite apparent in the commercial world),
2. Significant basic helicopter configuration changes,
3. Addition of major advancements in mission equipment, and
4. Procurement quantities.

Let me discuss each design-to-cost factor in turn.

First of all, inflation, from the early 1960s when Hueys became available to the U.S. Army to the mid-1990s when the RAH-66s were to have arrived on the scene, amounted to about a factor of 9 [584]. This would mean that the \$0.8 million would realistically become \$7.2 million 35 years later. Thus, inflation becomes a factor in applying past performance to current cost estimates. In this Huey-based example, the first aircraft ratio should be thought of as more like 29.6/7.2, which is 4.1.

---

<sup>188</sup> As I remember it, in the early 1980s Secretary Ambrose legislated that the LHX go-ahead was based on a weight empty of 7,500 pounds, a unit cost of \$7.5 million, and replacement of all the aging utility, reconnaissance, and attack helicopters then in the Army's fleet. I do not recall the Secretary's numbers being supported by any significant industry input. I thought at the time that all his numbers did was set the goal in concrete and hold the Army's and industry's feet to the fire. The Secretary never wavered in his position much like Nevil Shute had his character, Stephen Morris, saying: "If the machine were a military one for the Air Force the procedure was, in general, much the same, with the difference that the purchaser had a habit of asking for technical impossibilities and refusing to discuss the matter."

## 2.8 PURCHASE PRICE

Secondly, the Huey was the first turbine-powered helicopter to enter U.S. Army service, and it was powered with a single engine. The RAH-66 was powered by twin turbines incorporating state-of-the-art technology. The effect of this and other basic configuration differences can be estimated using the price estimating relationships provided by Eqs. (2.347) and (2.348). As applied to the RAH-66 program, you first obtain the factor (H), *which is based on the major decisions made before any real designing has begun*. Thus,

$$(2.360) \quad \begin{aligned} \text{RAH-66 H factor} &= \text{Engine Type} \times \text{Engine No.} \times \text{Country} \times \text{Rotors} \times \text{Landing Gear} \\ &= (1.794)(1.344)(0.883)(1.000)(1.115) = 2.374 \end{aligned}$$

The same major decisions for the Huey were quite different. For the Huey you calculate an H factor of

$$(2.361) \quad \begin{aligned} \text{Huey H factor} &= \text{Engine Type} \times \text{Engine No.} \times \text{Country} \times \text{Rotors} \times \text{Landing Gear} \\ &= (1.794)(1.000)(0.883)(1.000)(1.000) = 1.584 \end{aligned}$$

Then there is the difference in weight empty of the two aircraft, the difference in installed power, and the difference in number of blades to consider. *A designer can, within the bounds of fundamental physics, control the outcome here. However, a design constraint of air transportability in an Air Force C-130, or requiring the machine to fit in a space allocated on some U.S. Navy ship, is very limiting.* Looking at the complete story and using reference [116] for HU-1A data, you see that the basic configuration differences create an air vehicle (i.e., the platform) first aircraft factor of

$$(2.362) \quad \left( \frac{\text{RAH-66}}{\text{Huey}} \right)_{\text{1stA/C}} = \left( \frac{\$269(2.374)}{\$269(1.794)} \right) \left\{ \left( \frac{7,500}{3,900} \right)^{0.4638} \left( \frac{2 \times 1,300}{1 \times 860} \right)^{0.5945} \left( \frac{5}{2} \right)^{0.1643} \right\} \\ = 4.02$$

On this basis, the inflated Huey first aircraft price of \$7.2 million becomes \$28.8 million, which I believe can be compared to the RAH-66 first aircraft price of \$29.6 million.

The third item of mission equipment package differences between the Huey and the RAH-66 must, therefore, amount to \$800,000. Commercially, in 1994, Bell sold the Model 412EP for \$4,400,000 in its base configuration [583]. If you wanted the machine with factory installed equipment, the price jumped to \$4,800,000 [583]. The inference here is that the military-equipped RAH-66 had all the standard items such as autopilot, flight instruments, copilot package and heater, *plus* special avionics, radios, self-protection devices, weapon, etc., all for a total price of about \$800,000.

The fourth design-to-cost factor has more to do with total program price. If this is the design constraint, the number of aircraft becomes the major program price-driving factor. You can appreciate this factor from Table 2-42. The original selling point to the Army itself and to Congress was that up to 7,000 LHXs were going to be bought—some in utility configuration, some in reconnaissance configuration, and some in an attack helicopter configuration. As the program marched on to an RAH-66 development contract award on April 1, 1991, things started going south during development—much like Augustine recounts [582]. By May of

2001, the weight empty had grown to over 9,500 pounds (Fig. 2-390 [587]), the airframe had run out of space—within its stealth-dictated outer mold lines—for mission equipment additions, and the LHTEC team of Allison and Garrett was being asked to uprate its T800 engines from 1,300 to 1,563 horsepower. Any thought of a \$5.3 million price per RAH-66 ceased to be real, and the total program price of \$37 billion began to fall into the unaffordable range as development dragged on. What the final outcome would have been had the program not been cancelled on February 23, 2004, will, of course, never be known.<sup>189</sup>

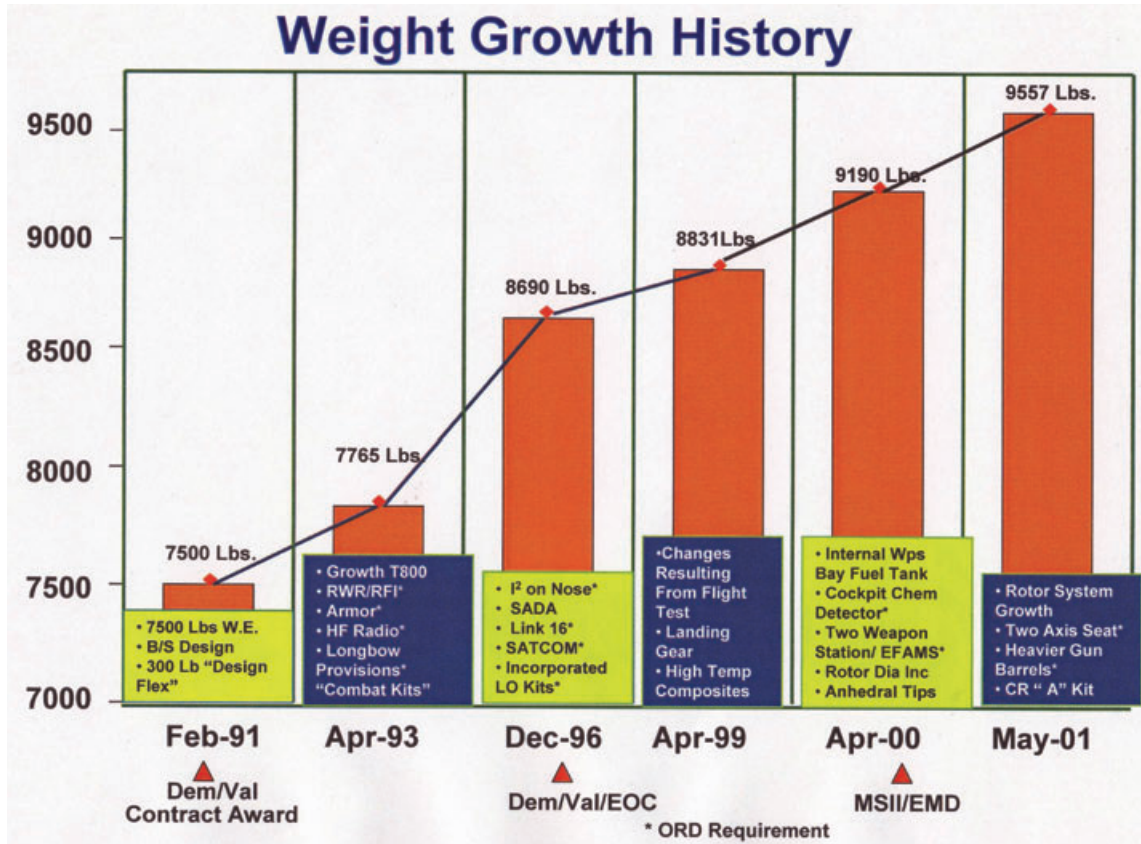


Fig. 2-390. RAH-66 weight-empty growth over 10 years of development [587].

Table 2-42. Effect of Lot Size on Program Price

Lot Size	Average Price (\$ millions)	Total Production Price (\$ billions)
7,000	5.300	37.10
3,500	6.088	22.83
1,750	7.208	12.62
1,000	8.159	8.16
500	9.054	4.75
250	11.061	2.77
100	13.481	1.35
25	17.971	0.45

<sup>189</sup> More than enough has been written about the LHX/RAH-66 program and lessons learned about [587, 588, 606-617].

## 2.8 PURCHASE PRICE

### 2.8.3 Concluding Remarks

On one occasion<sup>190</sup> after Mike Scully and I had published our *Rotorcraft Cost Too Much* paper [584], I was approached by Marat Tishchenko, the very prominent Russian chief engineer.<sup>191</sup> He said that he was quite disappointed that Mike and I had not separated out engine costs before doing the regression analyses leading to Eqs. (2.347) and (2.348). Of course, I had to agree with him, but I also explained that engine manufacturers were even more reluctant to divulge cost data than the prime U.S. helicopter manufacturers were. Marat simply smiled. But it does raise the point for future study—a study that I hope someone will tackle. In 2003, Marat published a paper [618] that examined the effect of disc loading on preliminary design of transport helicopters using methodology developed by the Mil Design Bureau. He notes his concerns about Eqs. (2.347) and (2.348) writing:

“It should be noted that the above formula [Eqs. (2.347) and (2.348)] is based on the sale price of helicopters and includes a (variable) profit element that is not the same for all helicopters. A factor of 1.16 is included to account for an annual inflation rate of 2.5% (from 1994 to 2000). The coefficient H is equal to 2.40576 for helicopters with payloads of 4, 10 and 20 metric tons (single rotor). Figure 4 shows the price (in current dollars) vs. disk loading for different payloads and number of blades. The price increases with disk loading for all the values of payload considered. This indicates that the lowest practical disk loading should be selected in order to keep the purchase price low. However, in Eq. (31) [Eqs. (2.347) and (2.348)], a key factor that influences the price is total engine power, which in turn increases rapidly with increase in disk loading. *Such a sharp growth of the price due to a change of power seems to be an overestimation of this effect and requires modifications to the formula for the price. One possible reason for this could be that Eq. (31) reflects the prices of helicopters for which parameters are already optimized and vary gradually within limits.*” [My italics]

When a chief engineer of Marat’s stature and successful track record (he was the leader for the MIL-26 program!) has some misgivings, you better take notice.

In late 2011, as I was thumbing through *Jane’s All the Worlds Aircraft for 2011-2012* [619], I came across the price of Sikorsky’s new S-92 quoted at \$21.333 million for the “typically equipped” helicopter. Out of curiosity, I calculated what the S-92 would have sold for in 1994 using the price estimating relationship that Mike and I devised as follows:

$$(2.363) \quad \begin{aligned} \text{S-92 H factor} &= \text{Engine Type} \times \text{Engine No.} \times \text{Country} \times \text{Rotors} \times \text{Landing Gear} \\ &= (1.794)(1.344)(1.000)(1.000)(1.115) = 2.688 \end{aligned}$$

and then in 1994, the unequipped price would be

$$(2.364) \quad \begin{aligned} \text{S-92 Base List Price} &= \$269(H)(WE)^{0.4638} (THP)^{0.5945} (b)^{0.1643} \\ &= \$269(2.688)(16,752)^{0.4638} (2 \times 2,520)^{0.5945} (4)^{0.1643} \\ &= \$13.13 \text{ million} \end{aligned}$$

---

<sup>190</sup> I cannot remember specifically, but would guess it was at an AHS Forum in 1998 or 1999.

<sup>191</sup> At age 39 Marat Tishchenko became the head of the Mil Moscow Helicopter Plant when the founder, Mikhail Mil, passed away January 31, 1970. He remained as plant manager and chief engineer until retiring in 1991. Through the auspices of Inder Chopra and the Alfred Gessow Rotorcraft Center, Marat became a Minta Martin Visiting Research Scholar, which led to his many contributions here in the United States.

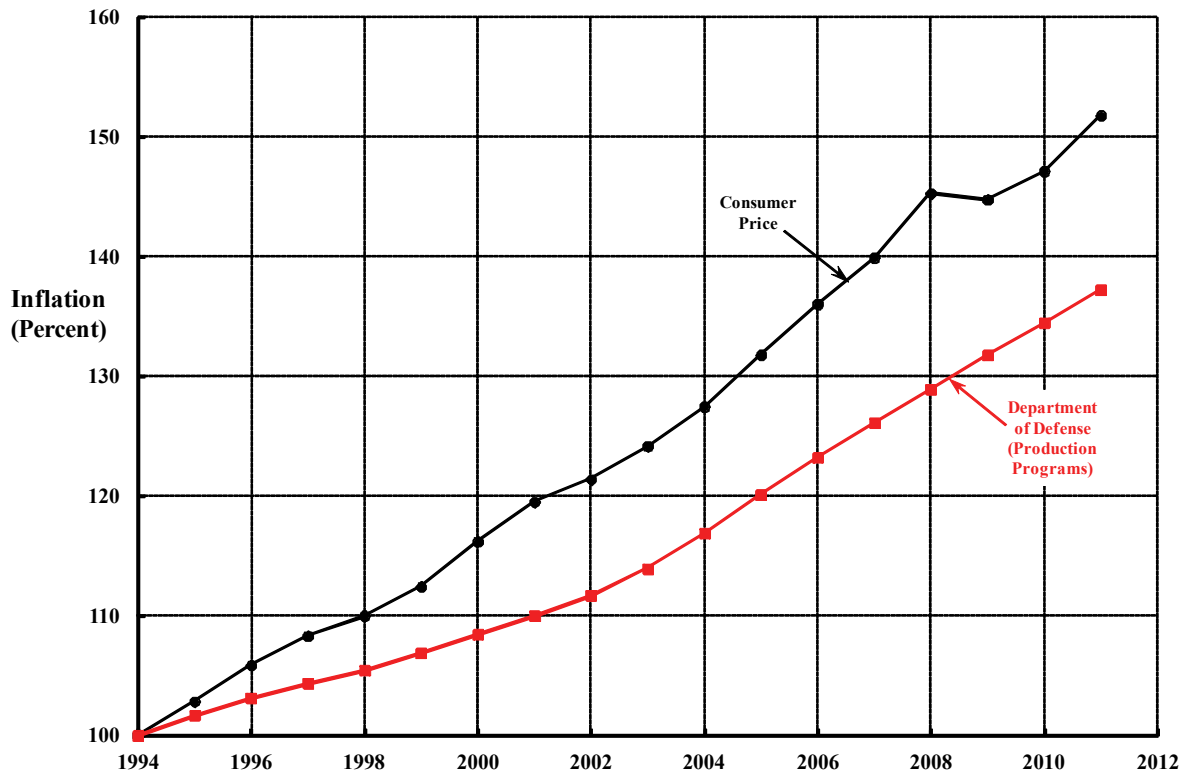


**Fig. 2-391. Two views of inflation since 1994.**

Following figure 10 of reference [584], the most that equipping adds (i.e., top of scatter) to the price is 20 percent, which yields the estimate for an equipped S-92 of \$15.75 million in 1994 dollars. A recent study by Wayne Johnson using two sources [620, 621] has yielded the inflation from 1994 through 2011 data shown here as Fig. 2-391. You can see that the consumer price index suggests that an inflation factor of 1.4 to 1.5 is not unreasonable. Therefore, the \$15.75 million should escalate to around, say at most, \$23.6 million. This suggests to me that Sikorsky might be selling its new S-92 at a bargain!

Looking at the military side of helicopter procurement over the last 50 years, I would say that the U.S. Army and industry did not acquit themselves at all well on the LHX/RAH-66 and, to a lesser extent, the AH-56 programs. This is in distinct contrast to the CH-47, OH-6, OH-58, UH-60, AH-64, and OH-58D development and production programs. Harper and Richey, in their 12-lesson, roughly 1,500-slide PowerPoint® presentation [587], make the statement that “we did everything right and still we failed,” which can be summarized here with just one of their charts, Fig. 2-392. Personally, I would disagree with their statement. My view is that the LHX/RAH-66 program did everything “by the book” and *this* caused the U.S. Army and industry to fail. That says to me that the “book” should be thrown away.

The book came into being because of the long period between the early 1970’s start on UH-60 and AH-64 developments, and the LHX/RAH-66 program, which had its competition decided on April 1, 1991. You may figure the gap differently, but in that period *system*

## 2.8 PURCHASE PRICE

*engineering* came into its own. The corollary to system engineering was Integrated Product Teams (IPTs—occasionally referred to as silos). Before long the people writing about how to develop and produce helicopters had never designed, developed, and/or produced anything. The product of these system engineering proponents was nothing more than guidelines, work management schemes, DoD directives, MIL standards, and a ton of ancillary conceptual flowcharts, none of which deserve to be referenced in this volume.<sup>192</sup>

Frankly, even the discipline labeled as *system engineering* is incomprehensible to me because the “discipline” is too far removed from words like designing, releasing drawings, preparing subassembly specifications, and then building, flight testing, qualifying, and delivering. I believe that the rise of system engineering destroyed the practice of having a chief designer (I prefer chief engineer) and a director of manufacturing, and giving them the power, resources, and any additional support needed to do the job. *Regardless of the complexity of the ultimate product*, I believe that for a *development program* an organization need be no more unrecognizable than what you see here as Fig. 2-393. Then you select these leaders based on their skill breadth and track record, and then you trust them.

When a helicopter worth producing is obtained from development, the organization for development must be altered to emphasize the director of manufacturing, and the emphasis on engineering should be substantially reduced.

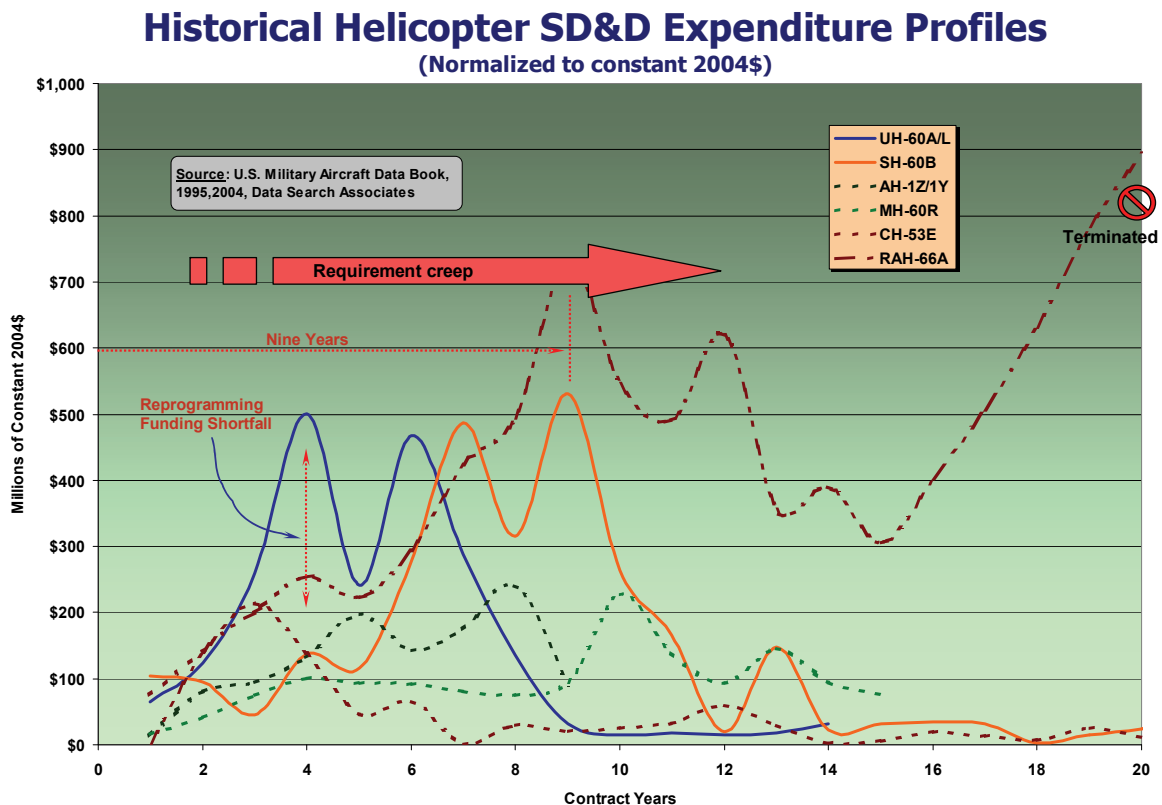
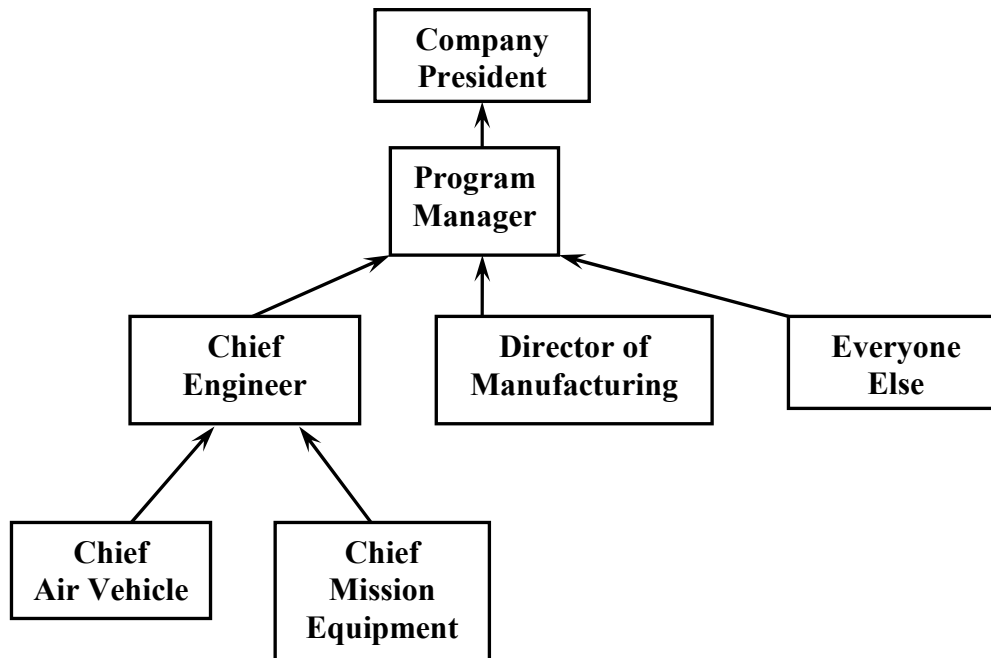


Fig. 2-392. The LHX/RAH-66 program was in trouble almost from the start [587].

<sup>192</sup> I have strong opinions about system engineering.



**Fig. 2-393. On a development program, system engineering is no substitute for a team made up of a chief engineer, a chief of air vehicle (i.e., the platform), and a chief of mission equipment—no matter how complex the product is.**

A little earlier you read that I do not think much of the Work Breakdown System (WBS). It was hardly in vogue during the UH-60 and AH-64 programs (as I remember them) and those programs can hardly be called failures. On the other hand, the WBS definitely was a burden placed on the AHIP/OH-58D program, which I had the privilege to be a part of in the position of chief engineer. When you review the WBS [600], you will see that cost is measured by time. Money spent is presumed to equate to tasks completed. Tracking can be made, to pick an extreme, at the pennies and seconds level thanks to data entries made into a computer on a weekly basis. But, as the OH-58D chief engineer during development, after a month or so I found that the WBS could not tell me what was happening on any given day. Nor could it tell me what the problem of the day (or even of the week) was, and it offered no insight about a coming crisis. In fact, the WBS very much inhibited me from walking around and talking to the men (and a few women) at drawing boards and computer screens, or making parts on the shop floor, or struggling with subcontractors—all the people who were actually doing work and producing something.

As related in the more complete, unpublished version of reference [145], I described the Milestone Done-Done (MD<sup>2</sup>) method of tracking what was going on (at least in engineering) during the AHIP/OH-58D development program. With some of my additional thoughts in brackets, this is what I wrote:

## 2.8 PURCHASE PRICE

“The Bell AHIP Engineering team [leaders, Mike Kawa for Air Vehicle, Jack Floyd for Mission Equipment, and myself] actually managed their business on a day-to-day and week-to-week basis using primarily the Milestone Done-Done (MD<sup>2</sup>) method rather than relying very much on the MCS [Bell’s government-approved WBS version] cost and schedule variance weekly report or the monthly historical report. This statement of fact may come as a disappointment to the originators and proponents of the WBS. The MD<sup>2</sup> engineering business management method was introduced to AHIP by the author, based on some success with an earlier program that is reported in reference 24. Doing business by the MD<sup>2</sup> method follows from the primary management chart shown in figure 53 [seen here as Fig. 2-394] and focuses almost entirely on “what is and isn’t getting done.” Comparatively little engineering attention is given—in the MD<sup>2</sup> management method—to gathering man-hours-spent data or the time of day since this information is readily supplied by an overabundance of accountants, calendars and watches.

The MD<sup>2</sup> method requires Engineering to completely define and vigorously manage the accomplishment of a meaningful set of detailed milestones. For AHIP there were 669 detailed milestones and the what, who, how much and when for each was completely described. With this tabulated plan [and a drawing tree], the more commonly used graphs of (1) milestones done versus time and (2) man-hours spent versus time become quite secondary. The primary management view (of the plan and tracking to the plan) is graphically presented in the form shown by figure 53. Three reasons for choosing the format of figure 53 are: Engineers generally prefer graphs to tables. A good plan or line will require Engineering to define quite a few milestones or the graph will plot as a series of large step functions which engineers do not like. If milestones are not getting done and man-hours are being spent, the line of actual performance goes straight up which is graphically disturbing to any engineer.

The MD<sup>2</sup> management method has only one corollary and that is to set the standard for being done. This is an important point because no credit is given for partial completion of a milestone (i.e., Engineering’s “percent complete” is formed by the ratio of the two whole numbers of milestones done divided by total milestones). The standard, given a plan with many milestones, is very simple: a milestone is not done if words like “..... is done except” are used. Thus, the standard says that “done” and “except” cannot be used together. The standard replaces “except” with “done” and that is why the method is referred to as Milestones Done-Done, or MD<sup>2</sup>.

The actual performance of the Bell Engineering Department is shown on Figure 53. All engineering relating to the contractual milestones shown by figure 53 is done except (notice that “all” and “except” do not go well together either) FSED [Full Scale Engineering Development] is not done-done. As of March 14, 1986, even with the DD250 (i.e., the Government Acceptance form) of several production aircraft, there were three milestones still left undone and expenditures stood at 637,232 man-hours.<sup>193</sup> In fact, FSED activity is at the trickle level, but getting the last few milestones done-done is like pulling teeth.”

---

<sup>193</sup> The department’s budget, as allocated by Program Management, was 528,700 man-hours. As an aside, this budget was the proverbial “success-oriented budget” and, in Engineering’s view, only addressed the known-known tasks in the AHIP program. Following suggestions from Augustine’s Laws [582], Engineering had prepared a broader view that included known-unknown tasks (620,000 man-hours) and an even broader view that included unknown-unknown tasks. This latter estimate was made with the thought that if Bell Engineering exceeded 800,000 man-hours to complete their portion of AHIP, there was a disaster in the making.

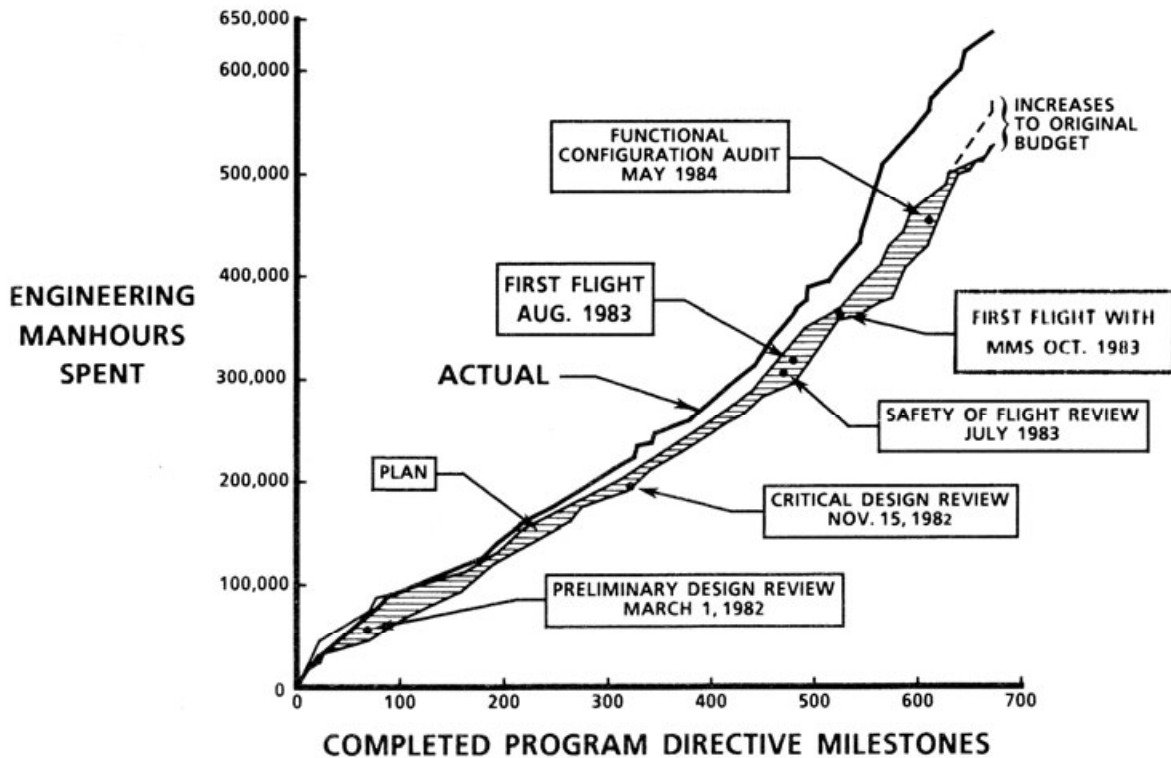


Figure 53. Management by Milestones Done-Done

**Fig. 2-394. The Work Breakdown System should be thrown away on development programs and replaced with the MD<sup>2</sup> system.**

Please keep in mind that the AHIP/OH-58D program was a relatively simple program (compared to LHX/RAH-66 and, say, the V-22 tiltrotor) because all the major assemblies of the air vehicle had been demonstrated to be ready—through flight testing. In contrast, the mission equipment package was all new from the ground up. Had a mockup in which to locate the many electronic subassemblies (and associated wiring bundles) *and* a mission equipment system integration laboratory not been in place in a timely manner, I believe there would have been real trouble on the program.

This, in my estimation, was one of several major factors causing the LHX/RAH-66 program to get off to a less than satisfactory start. The U.S. Army overall approach was to have the first several aircraft be virtual prototypes of the full-up production product. Thus, all-new air vehicle technology, an all-new engine, and an all-new mission equipment architecture were on the table at the same time for two competitors, and then selection of a winner from the two competitors was based primarily on paper designs. The whole past lesson of “try (or is it fly) before you buy” was dismissed because of a misguided perception that all the design and analysis tools were infallible. Following a system engineering organization, the concept of Integrated Product Teams (ITPs) and relying on WBS accounting for program status just ensured failure.

## 2.8 PURCHASE PRICE

I think one real lesson is that a bare bones air vehicle must be demonstrated by flight testing as a satisfactory platform. Then the machine can be stuffed with mission equipment that meets the mission needs. All of the mission equipment can be demonstrated in a system integration laboratory while the basic air vehicle is being debugged in flight testing. Then, and only then, should the mission equipment installation in the air vehicle be completed. After installation, the system can be debugged and made ready for customer acceptance.

There are many who think the reason why the AHIP/OH-58D development program was reasonably successful was because it was a fixed-price contract. In my opinion, they are all wrong. The key factor was that *the specification and work statement were fixed* so adding all manner of emerging mission equipment after contract award could not be done on anyone's whim or an even stronger urging. Furthermore, increasing the number of fatigue specimens or some other airworthiness activity was not allowed. During the AHIP/OH-58D program, the word *no* by Army and Bell program management (Colonel Bud Forster, who later became a Lieutenant General, and Teddy Hoffman, respectively) meant *no* with a period.

There are two additional thoughts that came my way. Both thoughts deal with some UTTAS history. The first was offered to me by Colonel Clarence (Bud) Patnode, retired,<sup>194</sup> and I am very glad to include it in these concluding remarks. After reading this chapter, Bud wrote me an e-mail [623] saying in part:

“Based on my six years in the UTTAS program (three years as the Department of the Army Systems Staff Officer (DASSO) and three years in the PM shop leading up to the fly off) and my four years in the AAH PM shop as the PM for TADS/PNVS I will offer some comments.

Single vs. twin engine. The UTTAS was the only system of the Army's Big Five (UTTAS, AAH, XM-1 Tank, Bradley Armed Personnel Carrier, Patriot Air Defense System) to be approved by the Defense Systems Acquisition Review Council on its first attempt. During that formal DSARC review, the USAF and some DOD folks challenged the need for twin engines. Although the requirement for twin engines had been well substantiated in the extensive analysis done in Concept Formulation, it became a potential show stopper during this final review to approve program start. LTG Robert Williams set those analysis aside and in an eloquent way stated to the effect that it sometimes comes down to trying to answer the parents of a soldier lost in an accident as to why the Army did not value their lives enough to provide the added safety of twin engines. Much to the surprise and pleasure of many of us in attendance, LTG Williams replaced hundreds of pages of analysis with a brief convincing statement. Certainly, the UTTAS twin engine configuration was a major cost driver and decision.

Fixed Price and Fixed Requirements. Throughout the UTTAS Concept Formulation and Development, the army medical corps continued to try to force a major change in the dimensions of the fuselage to accommodate their belief of a better way to transport patients. During Concept Formulation LTG Williams made it very clear to the medics that they would be flying Hueys for a very long time if they in some way caused a change in the UTTAS requirements. He had to stomp their butts to keep them from causing a major change to the requirements. During the early years of development, BG Leo Turner, PM UTTAS continued

---

<sup>194</sup> Bud and I became friends around the start of the AHIP/OH-58D days. His wise council has kept me out of more trouble than I care to admit. Bud's story [622] about how the army and then DOD reached a decision to develop the UTTAS is fascinating.

holding off the medics who would have killed the program had they prevailed. A great example of fixed requirements. BG Turner was one tough Texan who continued to block changes to the requirements.

The concept of design to cost does not address the up-front decisions that the customer already has made his mind up about. For example, a chief designer is not likely to be able to convince U.S. Army aviation leaders or a commercial customer that an airplane or autogyro will do the job and cost him less than a helicopter, or that maybe a piston engine might do, or that a single gas turbine saves purchase price when compared to a twin-engine choice. Of course, overrunning a legislated budget and delivering late to a prescribed schedule with an underperforming product does not enhance a reputation. However, in my view, after over 55 years, performance, cost, and schedules have always finally been negotiated without including known-unknowns and unknown-unknowns. The differences between plan and reality created by executive amnesia are still quite amazing to me.

It is a setup for continued failure when you do not include known-unknowns and unknown-unknowns when selling a program.

Now as to the second thought that came my way. There is one question that has been on my mind for several years. It deals with designing to cost, or, as the military prefers, Design to Unit Production Cost (DTUPC). If cost data is held so close to the vest by top management, how does engineering get concrete dollar numbers and targets to do its detailed design work? In struggling with this question relative to the military, I turned to Bud Forster (retire Lieutenant General, U.S. Army, and a friend) and asked if the 1970's Department of Defense design-to-cost policy [599] helped improve performance on military procurements. With Bud's permission, here is his reply (with a little of my editing):

“DTUPC worked well in the 1980s when we had Program Managers, and subsequently Program Executive Officers, as well as TRADOC<sup>195</sup> System Managers and School Commandants with a fair degree of operational experience. We had lived through the early days of Vietnam with equipment designed for use against the USSR in Europe. We no longer could accept the point solution—nor could we intentionally set out to design lightweight, but lethal tanks for the jungle nor helicopters that could only survive against crew served machine guns. Key to DTUPC were some enlightened School Commandants, like Don Parker and Lou Wagner, who would listen to Program Managers explain why [a] AHIP could not afford the weight of a cargo hook, [b] why Apache was barely affordable and manufacturable while barely meeting its performance requirements, and [c] they would ban the trade of fuel tankers to enhance the M1 tank. To these School Commandants, maintaining schedule and unit production costs were key because of the pressure on the Army budget following Vietnam and the competition for peacetime dollars with a Navy and Air Force that appeared to be much more favored in the Office of the Secretary of Defense. So any changes to the approved requirement had to be assessed in light of DTUPC impact and few changes were approved by the School Commandants.

The tight link between TRADOC School Commandants, TRADOC System Managers, and Program Managers was weakened with the advent of the Acquisition Corps. Program Managers no longer had the operational experience, and therefore rapport, with

---

<sup>195</sup> U.S. Army Training and Doctrine Command

## 2.8 PURCHASE PRICE

School Commandants. Also School Commandants, for reasons I don't understand fully, became less and less involved in acquisition decisions. Perhaps this was because of pressures to train and retrain for Desert Storm, Iraqi Freedom, and Enduring Freedom. The fact that TRADOC System Managers became part of the Acquisition Corps and became more and more civilianized may have contributed to less rigor in enforcing requirements stability.

During the Army Acquisition Review of late 2010/early 2011 almost every example of success we used was from the 1980s. The exception I remember was the Block 2 upgrade of the Apache AH-64D, which seemed to have recreated the Program Manager and TRADOC System Manager link to operational experiences. This Apache program was managed to a dollar level that kept it out of the spotlight and was executed quickly enough to avoid death by "good ideas" and "help from higher up."

Bud's short note says to me that when the tight links between the war fighter and the rest of us are broken, things go to "hell in a hand basket" very quickly. I think that replacing excellent leadership traits and skills learned by experience with some directive or handbook just never seems to work.

Let me add, perhaps, a less philosophical note. A most recent paper [624] that derived list price estimating methodology for fixed-wing aircraft was brought to my attention by Wayne Johnson. The authors of this paper are all affiliated with the Institute of Aeronautics and Astronautics located in Aachen, Germany. Their paper is titled *Aircraft Cost Model for Preliminary Design Synthesis*. These authors were able to examine list price at the airframe component level. The work is an example of what I believe needs to be done in the rotorcraft industry. I hope somebody takes up the challenge.

Finally, you should be aware that there are many "cost estimating methods" that try to estimate purchase price, operating costs, and even life cycle costs. For helicopters currently operating in the commercial fleet, you have Conklin & de Decker, Inc. that offers very popular software products, one of which I will introduce you to shortly. For military helicopters you have no place to turn. Of course, each major manufacturer has its own ability to estimate purchase price, operating costs, and life cycle costs in response to a military request. And, of course, the U.S. Department of Defense has the ability in all service branches to make a reasonable estimate of what something "should cost" just to keep suppliers from straying too far from reality. I can, however, suggest one paper that may be of interest to you. Although it deals only with fixed-wing aircraft, J. Wayne Burns' paper [625] gives you a feeling of the breadth and detail you need just to become familiar with the world of cost estimating.

## 2.9 OPERATING COSTS

One of the major factors in the mind of a potential buyer of a transportation product is the cost (to the buyer) of operating the machine. In the United States today, for example, an automobile buyer is most certainly concerned about what fuel mileage the car that he (or she) wants is going to get. The same is most certainly true in the world of rotorcraft. But beyond the question of fuel efficiency, a potential helicopter buyer must also consider total operating costs for each future year. Total operating cost is frequently broken down into fixed costs (like hanger rental for a year) and variable costs, which are costs that are incurred every time the helicopter is flown. Before discussing helicopter operating costs in detail, and then reviewing two examples of maintenance, it helps to have some background about fixed-wing and rotary wing airlines.

### 2.9.1 Airplanes

To begin with, let me quote from one of my favorite books about how the airline business got started and the aircraft that made it possible. This book, written by Peter W. Brooks who captured many details about autogyros [4] that you read about in Volume I, is titled simply *The Modern Airliner* [626].<sup>196</sup> He wrote on page 43:

“During the first 10 years after the end of the First World War the centre of gravity of transport aircraft development remained in Europe, where all the major countries were soon engaged in the creation and expansion of passenger-carrying scheduled air services. During the greater part of this period, U.S. transport aircraft remained inferior to European designs, although the Americans produced two notable series of radial air-cooled engines, the Wright Whirlwind and Pratt & Whitney Wasp. Not until the Ford Tri-Motor appeared in 1926 did American transport aircraft begin to be competitive with those in Europe. The United States’ most important contributions to the first 10 years of air transport’s development were in the operational field. Because their operations were confined to mail carriage, they had a powerful incentive to undertake bad-weather and night flying as soon as possible—night flying was introduced in 1923—and to achieve the highest possible standards of regularity and punctuality, even at the expense of safety. As a result, instrument and night flying and the development of navigational aids made more rapid progress in the United States than it did in Europe. An exception to this was ground-to-air radio communication, which was in general use in Europe for several years before it was adopted in the United States. The Americans’ lead in most of these fields was to have important repercussions later, when the all-weather capabilities of passenger carrying aircraft increased rapidly in the early 1930s. It was, in fact, one of the factors which helped to create the ascendancy which the Americans were to win in the 1930s and which they retain to this day.”

The ascendancy in air transport that Brooks refers to is traced with great clarity by R. E. G. Davies in his classic book titled *Airlines of the United States Since 1914* [316]. This story and two other more technical classics [628, 629] all make the point that the Ford Tri-Motor (Fig. 2-395 and Fig. 2-396) exposed the public to air travel for business and pleasure. However, this 1926 airplane did not make any airline operationally feasible without government subsidies. That freedom came 10 years later with the Douglas DC-3 (Fig. 2-397 and Fig. 2-398).

---

<sup>196</sup> This 176-page book came out in 1961, and Brook’s followed it in 1962 with an absolutely superb, technical-fact-filled 585-page book dealing with both fixed-wing and rotary wing aircraft in use by the airline industry [627]. Peter Brooks was an Englishman; he died January 17, 1996, at the age of 76.

## 2.9 OPERATING COSTS



**Fig. 2-395.** Vibration and noise were just barely tolerable in the Ford Tri-Motor (Internet photo).



**Fig. 2-396.** The Ford Tri-Motor could maintain flight on two engines when operating near sea level (photo from author's collection).



**Fig. 2-397. The Douglas DC-3 provided the minimum level of comfort passengers have come to expect (photo courtesy of Ben Wang).**



**Fig. 2-398. The Douglas DC-3 could maintain flight on one engine, even at altitude (photo from author's collection).**

## 2.9 OPERATING COSTS

Edward Pearson Warner<sup>197</sup> was a prominent (and unbiased) figure in aviation as the airlines and aircraft manufacturers were reaching their first plateau. In 1938, while a member of the National Advisory Committee for Aeronautics (N.A.C.A), he delivered five lectures at Norwich University located in Northfield, Vermont. In his third lecture he spoke about airliner technical development and its effect on air transportation [630]. The lecture was published by the university as a small book, and it became a classic reference for later authors and historians. What is so interesting to me about this 42-page book is that Warner laid out operating cost data in a few major categories. Warner's discussion (about six early aircraft used by airlines) is an invaluable starting point to learn about operating cost.

### 2.9.1.1 E. P. Warner's Direct Operating Cost (DOC) Analysis

To begin with, imagine it is the late 1930s and you have decided to start an airline—just a small one to start with, of course. Say you are guessing that you can make a handsome profit with three Douglas DC-3s and charging very reasonable fares. You have decided that a route from Washington D.C. to Huntsville, Alabama, with several intermediate stops, is an ideal niche to fill because American, TWA, Eastern, and United (Fig. 2-399) are not interested (perhaps because they want to expand their transcontinental route structures). You figure the D.C.–Huntsville route is about 900 miles outbound and 900 miles retracing your steps, including some margin (Table 2-43). What you want to know now is how much it will cost to operate your company each year and, more specifically, how much it will cost to operate each of the three DC-3 aircraft for one year. Then you can contemplate what your fare structure will be. You have read E. P. Warner's thin book [630] cover to cover and are going to make your estimates based on his bookkeeping.<sup>198</sup> You are particularly interested in the comparison that Warner made between the Ford Tri-Motor and the Douglas DC-3 aircraft. However, based on what you have heard about the new Douglas machine, you are fairly certain that you will not make a profit with the Ford Tri-Motor. The deciding factor appears to be a 10-seat machine priced at \$6,800 per seat versus the Douglas DC-3 aircraft priced at \$5,240 per seat. Still, you have decided to let the operating cost comparison make up your mind. Of course, Warner has made it clear that his numbers are primarily for making a comparison and may not apply to the route and airline you are planning; still it is a start.

There is, of course, a great deal of preliminary input data you need to have before starting your accounting calculations. With some help from the Douglas Company, you summarize your basic information about their DC-3 as shown here in Table 2-44.

---

<sup>197</sup> Edward Pearson Warner (November 9, 1894–July 11, 1958) was an American pioneer in aviation and an aeronautical engineering teacher. He became a member of the U.S. Civil Aeronautics Board at its founding in 1938, a delegate to the 1944 Chicago Conference for the Convention on International Civil Aviation, and an international civil servant. Edward Warner's achievements are commemorated in the world's civil aviation community by the international award that bears his name.

<sup>198</sup> In offering this example, I recreated Warner's example from pages 33 to 42 of his little book. It took some fill-in estimates on my part because his details are left to the reader's imagination in several categories. Warner was making the point that technical progress made between the Ford Tri-Motor and the Douglas DC-3 provided a way for airlines to become profitable without subsidies from the Postal Department for carrying mail. His story and analysis support that view quite well.

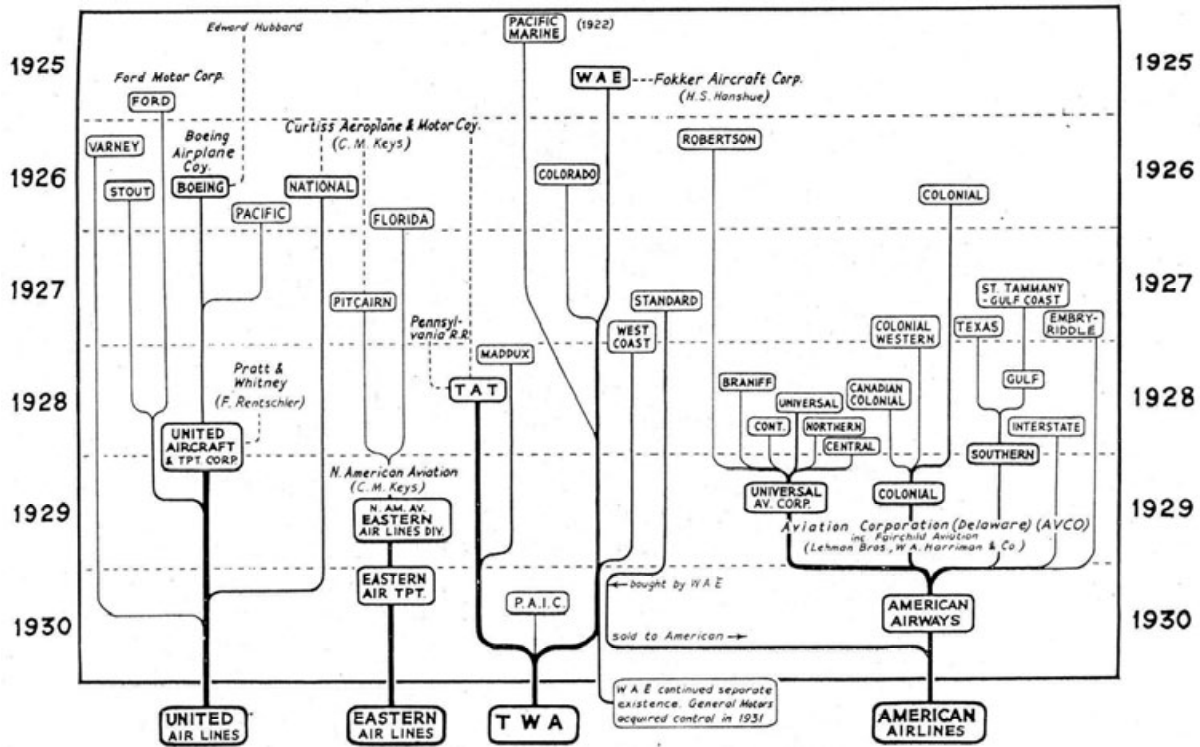


Fig. 16. Genealogy of the Big Four, 1925-1930.

Fig. 2-399. How United, Eastern, TWA, and American came into being [316].

Table 2-43. Planned Route Structure for Your Startup Airline

Segment No.	Leave	Arrive	Statute Miles	Minimum On-Ground Time
1	Washington, D.C.	Norfolk, VA	143	4 at Norfolk
2	Norfolk, VA	Elizabeth City, NC	44	4 at Elizabeth City
3	Elizabeth City, NC	Rocky Mount, NC	91	4 at Rocky Mount
4	Rocky Mount, NC	Raleigh-Durham, NC	57	4 at Raleigh-Durham
5	Raleigh-Durham, NC	Greensboro, NC	66	4 at Greensboro
6	Greensboro, NC	Winston-Salem, NC	16	30 at Winston-Salem (refuel)
7	Winston-Salem, NC	Charlotte, NC	75	4 at Charlotte
8	Charlotte, NC	Ashville, NC	89	4 at Ashville
9	Ashville, NC	Knoxville, TN	88	4 at Knoxville
10	Knoxville, TN	Chattanooga, NC	87	4 at Chattanooga
11	Chattanooga, NC	Huntsville, AL	83	Overnight at Huntsville
<b>Total</b>			<b>840</b>	

## 2.9 OPERATING COSTS

**Table 2-44. Input Data for Operating Cost Analysis**

Input	Units	Ford	Douglas	Notes
Model		5-AT Tri-Motor	DC-3A	
Engine		3 P&W Wasp C	2 P&W	R-1830-S1C3G
Total installed horsepower	hp	1,260	2,400	Pratt & Whitney spec
Max takeoff gross weight	lbs	13,250	25,200	Douglas spec
Weight empty	lbs	7,576	16,860	Your requirement
Number of passenger seats	number	10 to 15	21 to 28	Your requirement
Horsepower at cruise ( $HP_{cr}$ )	hp	750	1080	Douglas flight test
Cruise speed ( $V_{cr}$ )	mph	125	180	Douglas flight test
Payload	tons	1.6	2.5	Your requirement
Range	miles	625	900	Your requirement
Cruise time	hrs	5.00	5.00	Your requirement
Fuel flow (SFC)	lbs/hr per hp	0.50	0.44	Pratt & Whitney spec
Fuel price	cents/gallon	11.0	12.5	Current price
Fuel density	lb/gallon	6.0	6.0	Aviation gas spec
Pilot	number	Yes	Yes	Your requirement
Co-pilot	number	Yes	Yes	Your requirement
Price of complete airplane	dollars	\$68,000	\$110,000	Douglas list price
Price of airframe	dollars	\$50,000	\$90,000	Douglas list price
Depreciation rate for airframe	years	5	5	Your requirement
Price of engines	dollars	\$18,000	\$20,000	Pratt & Whitney list price
Engine life	hrs	3,500	5,000	Pratt & Whitney spec
Engine life in miles flown	miles	437,500	900,000	(engine life) $\times$ $V_{cr}$
Flying time per year	hrs	2,000	2,000	Your requirement
Miles flown per year	miles	250,000	360,000	(yearly hours)(cruise speed)
Miles per crash	number	3,500,000	7,000,000	Your safety plan

**Table 2-45. Fuel Cost for the 900-Mile Trip Equals \$53.10 for the DC-3**

Fuel Cost	Units	Ford	Douglas	Notes
Fuel burn rate in cruise	gallons/hr	62.5	79.2	$(SFC \times HP_{cr}) / (\text{fuel density})$
Gallons used in cruise	gallons	313	396	(gallons per hour)(cruise time)
Other gallons used	gallons	34	29	about 10% of cruise fuel
Fuel used for 5 hours	gallons	347	425	sum all gallons
Fuel cost per 5 hours	cents	3,813	5,310	(gallons used)(fuel price)
Fuel cost per mile	cents/mile	6.10	5.90	(fuel cost)/(miles traveled in 5 hours)
Cost per ton-mile	cents/ton-mile	3.81	2.36	(cents per mile)/(payload in tons)
Cost per hour	dollars/hr	\$7.63	\$10.62	(cents per mile)( $V_{cr}$ )/100
Cost per available seat-mile	cents/seat-mile	0.61	0.28	(cents per mile)/(no. of seats)
<b>Fuel cost per 900 miles</b>	<b>dollars</b>	<b>\$54.90</b>	<b>\$53.10</b>	<b>(cents per mile)(900 miles)/100</b>

You immediately see from Table 2-44 that three DC-3A aircraft are going to cost you \$330,000. No spares are included, and the Douglas price is F.O.B. Santa Monica, California, which means it will cost another \$20,000 to get them back to Washington National Airport (now Reagan National), which is scheduled to be completed in June of 1941.

Warner's approach to estimating the cost to operate one aircraft requires a detailed accounting in five cost categories: namely fuel, crew, maintenance, depreciation, and insurance plus crash reserve. In each category, you want data about cost per mile, cost per payload miles in ton-miles, cost per hour, cost per available seat-mile, and cost for one 900-mile trip. So you start with the fuel cost estimate. For this item Warner wrote that

“the first of the major cost items is fuel, and fuel involves three variables. The improving aerodynamic efficiency of the airplane has yielded a steady increase in speed for a given power loading, which in turn has meant the accomplishment of more ton-miles of work per horsepower-hour. Improvement in engine design and improvement in fuel have reduced specific consumption. But improvement in fuel has also increased the price per gallon at which fuel must be bought.”

The step-by-step calculations appearing in Table 2-45 show that fuel cost per the 900-mile trip favors the DC-3 slightly, but on a per-seat basis, the Ford costs \$5.49 per seat while the DC-3 costs just \$2.53 per seat. It makes you begin to wonder though if all the seats that are available on each aircraft will always be filled with paying passengers. If the DC-3 is making trips with only one-half of the available seats filled, then it may be a losing proposition compared to the Ford machine flying with all seats filled on every trip.

The cost of manning the two aircraft with both a pilot and a copilot is shown in Table 2-46. On this cost element, Warner says that

“the rate of pilot compensation is now fixed by a formula established by the National Labor Board in 1934, and subsequently given the force of law by specific reference in the Air Mail Act of 1934. Under that ruling, pilots receive a base pay plus an additional sum for each hour of flight, the rate of accumulation of this supplementary portion being dependent on the speed of the airplane. Until that provision was adopted, they were paid either a flat sum per mile or a flat sum per hour in addition to their base pay. In the first case, assuming the number in the crew always to be the same, the personnel cost per mile would be substantially the same for every airplane. Under the second alternative, the cost per mile would be inversely proportional to the speed of the plane. The Labor Board ruling establishes in effect a compromise between the two, the cost per mile going down with increasing speed but not so rapidly as the speed goes up.”

**Table 2-46. Crew Cost for the 900-Mile Trip Equals \$64.80 for the DC-3**

Crew Salaries	Units	Ford	Douglas	Notes
Crew cost per mile	cents/mile	9.3	7.2	Warner's numbers
Cost per ton-mile	cents/ton-mile	5.8	2.9	(cents per mile)/(payload in tons)
Cost per hour	dollars/hr	\$11.63	\$12.96	(cents per mile)(cruise speed)/100
Cost per available seat-mile	cents/seat-mile	0.93	0.34	(cents per mile)/(no. of seats)
<b>Crew cost per 900 miles</b>	<b>dollars</b>	<b>\$83.70</b>	<b>\$64.80</b>	<b>(cents per mile)(900 miles)/100</b>

## 2.9 OPERATING COSTS

Warner also makes a point about stewardesses saying they are “a passenger service, rather than a direct operating cost. Present-day transports could be operated without stewardesses, were it felt that passengers were more interested in a little additional economy than in personal service; and conversely, stewardesses could at any time have been put onto any airplanes large enough to have an aisle along which they could move.”

Warner also makes a further comment about crew size saying that

“there is, of course, another factor which has played some part in the economic history; that of the size of the crew. Even after passengers began to be carried, the single pilot remained for some time the common rule; and when a co-pilot was taken it was more as a safety measure, in the event of sudden illness of the pilot, than because he had any definite duties to perform. Not until about 1934 did the functions of the cockpit become so multifarious and so elaborately organized that they had to be distributed between two men and kept them both forever busy. On Pan-American oceanic flying boats the operating crew numbers four or even five, and it is likely to grow to three on the domestic airlines with the introduction of four-engine planes such as the DC-4 or the Boeing 307; but for the purposes of this analysis the DH-4, the Boeing 40, and the Lockheed Vega will be treated as single-pilot craft, while the other three parties to the comparison will each be charged with a co-pilot.”

The third category is maintenance cost provided here in Table 2-47. Here Warner offers a warning saying that

“maintenance is much less determinate. We find ourselves limited to very general speculation based on the required frequency of overhaul of various engines, the complexity of the rigging of the various airplane structures, and the relative rapidity of deterioration of the materials of which they were composed. Engine overhaul periods have increased from about 120 flying hours of the Liberty [which powered the DH-4], as used by the Post Office in 1924, to about 500 hours at present [1938]. The internally braced metallic structures of the present day require much less routine rigging attention than did the wire-braced biplanes that preceded them; and the metal is inherently less likely to deteriorate than was the wooden structure of the past, and especially plywood wing covering, though the difference in that respect in temperate climates is much less than is commonly supposed. Maintenance costs were kept low on the Liberty engines by the availability of large stocks of parts from the Army’s wartime accumulation at a nominal charge; but that was an abnormal factor dependent on a special and temporary situation [World War I] and in no way inherent in the nature of the equipment, and I have excluded it from the accounting. I have assumed costs on the Liberty engine and the DH-4 planes, both in figuring maintenance and in estimating a depreciation allowance, as they would have been if the equipment had been built up especially for commercial use and purchased directly from a manufacturer. It must be emphasized once more that the values so tabulated assume modern maintenance organization, in every case, and an equal degree of managerial competence throughout.”

**Table 2-47. Maintenance Cost for the 900-Mile Trip Equals \$45.00 for the DC-3**

Maintenance	Units	Ford	Douglas	Notes
Airplane and engine	cents/mile	8.70	5.00	Warner's numbers
Cost per ton-mile	cents/ton-mile	5.44	2.00	(cents per mile)/(payload in tons)
Cost per hour	dollars/hr	\$10.88	\$9.00	(cents per mile)(cruise speed)/100
Cost per available seat-mile	cents/seat-mile	0.87	0.27	(cents per mile)/(no. of seats)
<b>Maintenance cost per 900 miles</b>	<b>dollars</b>	<b>\$78.30</b>	<b>\$45.00</b>	<b>(cents per mile)(900 miles)/100</b>

Let me interject here that maintenance costs for helicopters are frequently provided by the helicopter manufacturer. In my experience, the operators rarely seem to achieve the manufacturer's claims. Later, you will read in some detail just what the maintenance manual for a Robinson R-22 has to say.

The fourth operating category is depreciation (Table 2-48) about which Warner said

“involves assumptions on equipment life, number of hours flown per year, and first cost. Life is dependent principally on the rate at which technical progress crowds existing equipment over the edge of obsolescence; but that is one of the variables that it is hard to project into the present day, and it can hardly be regarded as inherent in the particular piece of equipment under analysis. It seems fair then to take a uniform life of five years for the airplane, a length of time well within the sheer physical survival capacity of any of them; but for the engines, for which life is determined primarily by actual wear and so is measured in operating hours, a reasonable total of time has risen from 1,200 hours with the Liberty to 3,500 with the early air-cooled types, and to 5,000 at the present time. The hours of flying per year were extravagantly low in the days of the government-operated mail service, when each pilot had his own machine permanently assigned. They probably did not average above 600; but if the same equipment were being operated now, the standards of its employment would be less prodigal, and the hours would be limited by the time that schedules required on the ground between trips and by the time necessary for mechanical servicing. Projecting all types into the present, I would take 1,200 hours a year as reasonable for the DH-4, 1,700 for the Boeing Model 40, and 2,000 for each of the other types. First costs on a commercial basis, at present price levels, should be about as tabulated.”

This price data, as well as cruise speed, is tabulated in Table 2-44.

The fifth and last operating cost category is insurance and reserving money in a crash account (Table 2-49). Warner decided to assume a self-insured choice and made it clear that by

“assuming self-insurance, no factor of insurance company operating expense or profit enters into the calculation. The approximating of insurance and crash reserve again involves a difficult projection. The DH-4 flew without even a radio receiver; and the [Lockheed] Vega, the Ford, and the early Boeing Model 247 all operated in a period when the radio beam was unknown or virtually unused, and when contact flying in bad weather had to remain the rule. Faithful to my oft-repeated purpose of restricting these cost variations to the factors inherent

**Table 2-48. Depreciation Cost for the 900-Mile Trip Equals \$65.00 for the DC-3**

Depreciation	Units	Ford	Douglas	Notes
Airframe loss per year	dollars	\$10,000	\$18,000	(purchase price)/number of years
Airplane	cents/mile	4.00	5.00	(airframe loss price)/(miles flown per year)
Engine	cents/mile	4.11	2.22	(engine price)/(miles flown per engine life)
Depreciation per mile	cents/mile	8.11	7.22	Warner's numbers
Cost per ton-mile	cents/ton-mile	5.1	2.9	(cents per mile)/(payload in tons)
Cost per hour	dollars/hr	\$10.14	\$13.00	(cents per mile)(cruise speed)/100
Cost per available seat-mile	cents/seat-mile	0.81	0.34	(cents per mile)/(no. of seats)
<b>Depreciation cost per trip</b>	<b>dollars</b>	<b>\$73.03</b>	<b>\$65.00</b>	<b>(cents per mile)(900 miles)/100</b>

## 2.9 OPERATING COSTS

in the equipment, I have assumed that each of the six [aircraft] types being compared is being operated at the present time and fitted with as much instrumental and communication equipment as it could reasonably hold. Obviously it would be impossible, both because of space limitations and because of the concentration of all the responsibility in a single pilot, to put as many navigational devices and radio sets into a Boeing Model 40 as are being planned for the DC-4, for example; but I have supposed that even the DH-4, if reincarnated and set to prove itself economically, would have the benefit of two-way communication and beam reception.”

Warner goes on to say that “the principal differentials of hazard, in addition to the difference in the amount of equipment to be carried, would then lie in the number and reliability of the power-plants and in the ability to get down into bad fields without the likelihood of damage to the airplane. Making what seems to be due and reasonable allowance on those accounts, I set the probability at a loss of the total value of one DH-4 airplane by crash (whether in a single complete washout or in a larger number of accidents of less individual destructiveness) for every 800,000 miles; for the Boeing Model 40, at one every 2,000,000 miles; for the Ford, 3,500,000; for the Vega, 1,500,000; and for the Boeing 247 and the DC-3, 7,000,000.”

**Table 2-49. Insurance and Reserve Cost for the 900-Mile Trip Equals \$12.60 for the DC-3**

Insurance + Crash Reserve	Units	Ford	Douglas	Notes
Insurance cost per mile	cents/mile	1.90	1.40	Warner's numbers
Cost per ton-mile	cents/ton-mile	1.19	0.56	(cents per mile)/(payload in tons)
Cost per hour	dollars/hr	\$2.38	\$2.52	(cents per mile)(cruise speed)/100
Cost per available seat-mile	cents/seat-mile	0.19	0.07	(cents per mile)/(no. of seats)
<b>Insurance and reserve cost per trip</b>	<b>dollars</b>	<b>\$17.10</b>	<b>\$12.60</b>	<b>(cents per mile)(900 miles)/100</b>

It is only necessary now to show the total of the five categories to get Warner’s comparative estimates of direct operating cost (DOC) for the Ford Tri-Motor and the Douglas DC-3A. The sum, reproduced here as Table 2-50, shows that the most common DOC benchmark, cost per available seat-mile, was reduced from 3.41 to 1.27 cents per available seat-mile. This is more than a 50 percent reduction because of Douglas’ technology.

**Table 2-50. DOCs used by E. P. Warner to Show the Role Technology Played in Making Air Transportation Profitable Without Government Subsidies**

DOC Parameters	Units	Ford Tri-Motor	Douglas DC-3A
Cost per mile	cents/mile	34.11	26.72
Cost per ton-mile	cents/ton-mile	21.32	10.69
Cost per hour	dollars/hr	\$42.64	\$48.10
Cost per available seat-mile	cents/seat-mile	3.41	1.27
<b>Cost per 900-mile trip</b>	<b>dollars per trip</b>	<b>\$307.03</b>	<b>\$240.50</b>

In 1970 Ronald Miller and David Sawers<sup>199</sup> superb research about aircraft and airlines was published in the United States [628]. It is probably coincidental that the title of their book, *The Technical Development of Modern Aviation*, somewhat mirrors Edward Warner's 1938 lecture titled *Technical Development and its Effect on Air Transportation* [630]. Be that as it may be, the depth of research from airline files, the number of aircraft manufacturers contacted, and the list of contributors they acknowledge, allowed them to gather an enormous amount of technical data and DOC data. For example, in appendix I, they provide detailed DOCs in the standard form (CAB Form 41) for over 18 aircraft in airline use up to 1966. Fig. 2-400 is my summary of their work. It is clear that the Douglas Aircraft Company produced aircraft with the lowest DOC from just before the start of World War II until turbojet fixed-wing aircraft came on the scene and proved themselves, say by 1963.

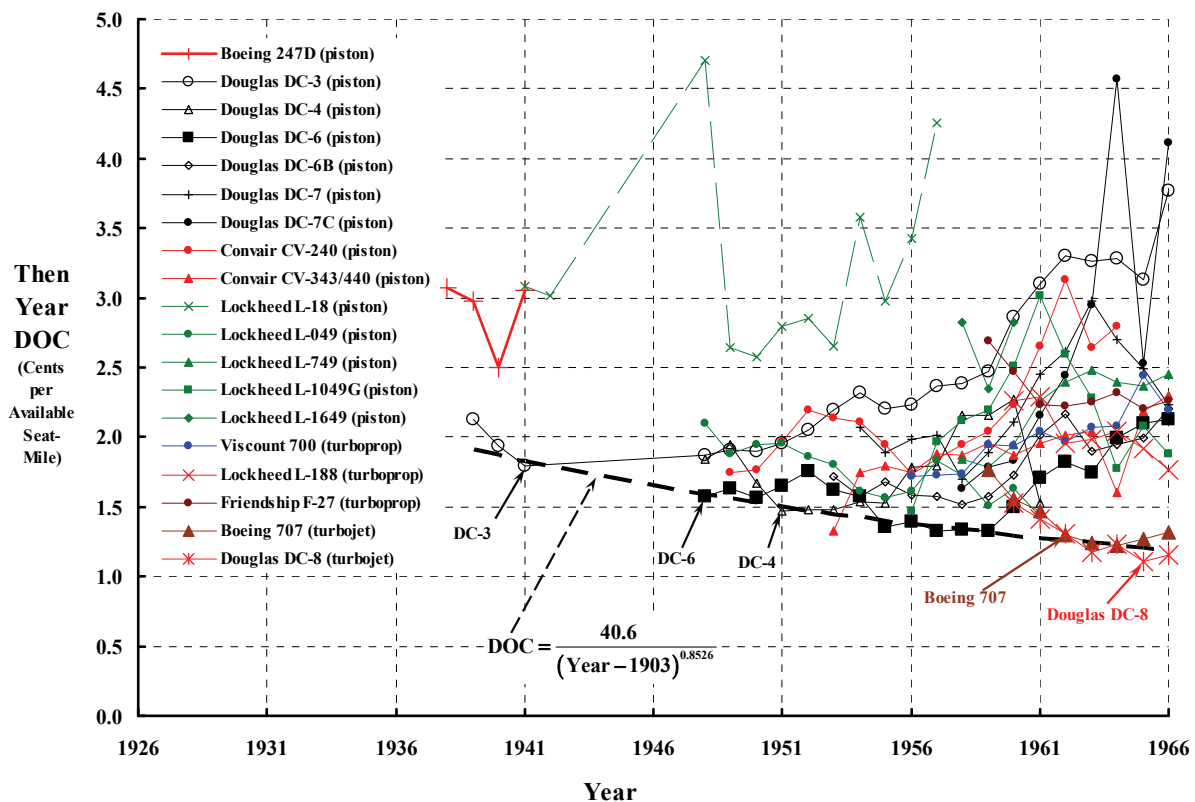


**Fig. 2-400. Historical view of direct operating costs (DOCs) in then year dollars for airlines. (Note: includes the effect of inflation.)**

<sup>199</sup> The book's jacket states that "Ronald Miller spent his undergraduate years at Harvard and went on to obtain his doctorate at Princeton after writing a dissertation on the application of modern mathematical techniques to airline scheduling (published as *Domestic Airline Efficiency* by MIT Press in 1963). He is now an associate professor at the University of Pennsylvania.

David Sawers spent three years at Oxford, then became research assistant to Professor John Jewkes, helping him in the writing of *The Sources of Invention*. From 1959 to 1964, he was a member of the editorial staff of *The Economist*. He then spent eighteen months at Princeton, as a visiting fellow in the Department of Economics, working on this book."

## 2.9 OPERATING COSTS

As I have noted on Fig. 2-400, this direct operating cost summary compiled by Miller and Sawers includes the effect of inflation. The authors, in appendix III of their book, provided an interesting data set about inflation. They wrote:

“To be able to make allowances for changes in the prices of various goods and services used in operating an airplane, a composite Index of Input Prices has been constructed. Deflating the unit operating cost series of various aircraft by this index will thus remove the purely monetary effects of changing prices. The four items for which reasonably useful price material is available are: flying personnel, fuel and oil, mechanics and the aircraft themselves.

(a) Flying personnel. This series reflects the trend in salaries of pilots, co-pilots and other flight personnel. Wage rate data, rather than annual earnings, would be preferable; because of the complexities of individual airline contracts with their pilots, this ideal was not feasible. Instead, the numbers of people in the Federal Aviation Agency’s classifications: pilots and co-pilots, and other flight personnel, for each of the years, were divided into the total annual payrolls for these two groups.

(b) Fuel and oil. The total annual expenditure on fuel consumed by domestic carriers is divided by a composite figure—total gallons of gasoline and oil (and jet fuel, from 1955 onward)—to produce an average annual cost of fuel-and-oil per gallon.

(c) Mechanics. The trend in average annual earnings of mechanics is used as a measure of changes in the costs of performing aircraft (airframe and engine) maintenance. The same reservations regarding the use of annual earnings instead of a wage rate apply here as with flying personnel.

(d) Aircraft. The index of aircraft prices which was used is explained in detail in section B of this appendix.

In order to combine these separate series into one composite index, weightings were adopted based on the total annual expenditures by scheduled domestic air carriers on the different items. In the case of aircraft, the weighting employed was the annual expenditure on depreciation. In so far as the quality of each of these items has been improved over the years, this index probably rises too rapidly. In the case of human resources, both flying personnel and mechanics, such changes are extremely difficult to measure. The octane rating does provide an index of quality improvement for gasoline, but it has not been possible to incorporate it in the fuel and oil series. The aircraft index does attempt to remove the influence on prices of newer model airplanes, concentrating on changes in the price of an ‘unchanged type’ over the years. (See below, section B.) The composite index and its component parts are shown in table I, below.”

The table Miller and Sawers are referring to is reproduced here as Table 2-51.

You might notice that if Fig. 2-400 was corrected for inflation, then the rise in DOC each year exhibited by some aircraft would not be very apparent. In fact, when the Boeing 707 was introduced in 1959, its DOC was 1.77 cents per available seat-mile. But in 1948 dollars, Miller and Sawers’ data suggest that the Boeing 707’s DOC would have been about 1.07 cents per available seat-mile versus 1.87 for the Douglas DC-3. This suggests that if the Douglas DC-3 achieved one-half of the DOC of the Ford Tri-Motor and that made the airlines profitable, then the turbojet-driven, swept-wing aircraft—having 5 to 10 times the number of available seats (and nearly three times the cruise speed!)—should have really lowered air transportation fares. That, of course, is exactly what has happened. In the summer of 2008, I

presented a seminar [631] about aviation history to several interns working for Bill Warmbrodt at NASA Ames Research Center. An introductory slide that seemed to go over well is shown here as Fig. 2-401. When I asked if any of the interns had come to NASA by cross-country flying, two interns said they had paid about \$450 and made the trip in less than 6 hours flying time—by modern jet aircraft.

**Table 2-51. Trends in Inflation [628]**

Year	Flying Personnel	Fuel and Oil	Mechanics	Aircraft	Composite Index
1939	65	77	42	74	65
1940	63	76	41	68	63
1941	67	78	45	70	66
1948	100	100	100	100	100
1949	102	107	109	111	107
1950	106	108	118	127	114
1951	115	106	124	129	118
1952	124	109	130	137	124
1953	137	114	132	144	130
1954	144	120	144	147	137
1955	144	115	142	151	136
1956	148	113	145	160	139
1957	153	117	144	176	145
1958	167	117	154	187	152
1959	185	99	176	217	166
1960	198	85	172	225	168
1961	211	79	189	225	173
1962	223	74	191	236	177
1963	234	70	197	258	187

**Three Major Steps in Transcontinental Passenger Air Service**

**Ford Tri-Motor, 1929**



48 hours with 10 stops. 10 passengers.  
2,000 miles by air at 90 mph and  
1,000 miles by train at 50 mph  
\$351.94 in 1929 = \$4,220 in 2008

**Douglas DC-3, 1936**



18 hours with 3 stops. 21 passengers.  
\$149.95 + \$4.00 for swivel seats  
+ \$8.00 for sleeper berth  
\$149.95 in 1936 = \$2,220 in 2008

**Lockheed L-1049G, 1955**



8 hours with no stops.  
66 seats at 41-inch pitch  
92 seats at 38-inch pitch  
\$158.85 in 1955 = \$1,210 in 2008

**Fig. 2-401. It was the successive introduction of faster aircraft with more seats that led to the growth of airlines [631].**

## 2.9 OPERATING COSTS

Now let me conclude this discussion about direct operating costs.

The preceding tables and discussion show you the bare-bones bookkeeping of what is generally called direct operating costs or DOC, a common acronym you hear more than occasionally. Warner is careful to point out that “these, of course, are the totals for the direct costs alone, and indeed only for a selected group of the major items among them. To give an idea of the scale of charges or of Government assistance at which an airline could cover expenses, a total for all costs of operation, including the overhead, is required.” This second grouping has been called *indirect* operating costs.

### 2.9.1.2 E. P. Warner’s Indirect Operating Cost Analysis

Your airline will require ground crews, main office staff (from president to janitor), and all other costs that support the flying operations. Warner called this major cost category Indirect Operating Costs, saying that “of the items not so far individually taken into account, some are roughly proportional to the totals tabulated above being the minor direct costs that may be expected to vary on much the same scale as the major ones. Some are proportional to the total mileage flown, and largely independent of the characteristics of the airplane. Some are proportional to the product of mileage by size, or to the total volume of traffic handled. Some examination of the manner of variation of individual elements of indirect cost and of traffic-handling cost has led me to the rough rule that total [operating] cost can be taken as 1.2 times the total just tabulated [i.e., the five line items associated with direct aircraft operating cost leading to Table 2-50] plus 14 cents a mile, plus 9 cents a ton-mile (of payload) times payload.” Warner’s estimate means that the indirect operating cost is

$$(2.366) \quad \begin{aligned} \text{Indirect Operating Costs} &= 0.2(\text{DOC in cents per mile}) \\ &+ 14 \frac{\text{cents}}{\text{mile}} + \left( 9 \frac{\text{cents}}{\text{ton-mile}} \right) (\text{useful load in tons}) \end{aligned}$$

Accepting Warner’s estimates of your airline’s probable indirect operating costs, you would find for the Ford Tri-Motor that

$$\begin{aligned} \text{Indirect Operating Costs} &= 0.2(34.11) + 14 \frac{\text{cents}}{\text{mile}} + \left( 9 \frac{\text{cents}}{\text{ton-mile}} \right) (1.6) \\ &= 35.22 \text{ cents/mile} \end{aligned}$$

and for the Douglas DC-3A, that

$$\begin{aligned} \text{Indirect Operating Costs} &= 0.2(26.72) + 14 \frac{\text{cents}}{\text{mile}} + \left( 9 \frac{\text{cents}}{\text{ton-mile}} \right) (2.5) \\ &= 41.84 \text{ cents/mile} \end{aligned}$$

### 2.9.1.3 Summary Results of E. P. Warner’s Total Operating Cost Analysis

Now having both direct and indirect operating costs, you can draw a comparison of total operating costs between a Ford Tri-Motor and a Douglas DC-3A. Your results, shown here in Table 2-52, immediately tell you the minimum what-to-charge story. Both aircraft

**Table 2-52. Operating Cost Summary**

Item	Units	Ford Tri-Motor	Douglas DC-3A
Direct operating cost	cents/mile	34.11	26.72
Indirect operating cost	cents/mile	35.22	41.84
Total	cents/mile	69.33	68.56
Other measures			
<b>Cost per ton-mile</b>	<b>cents/ton-mile</b>	<b>43.3</b>	<b>27.4</b>
<b>Cost per hour</b>	<b>dollars/hr</b>	<b>\$86.67</b>	<b>\$123.41</b>
<b>Cost per available seat-mile</b>	<b>cents/seat-mile</b>	<b>6.93</b>	<b>3.26</b>
<b>Cost per 900-mile trip</b>	<b>dollars per trip</b>	<b>\$624.01</b>	<b>\$617.06</b>

can fly your 900-mile trip at a virtually identical cost of about \$620. If you use the Ford with only 10 seats, you will have to charge a fare of \$62 per passenger. The 21-seat Douglas DC-3A lets you charge only \$30 per passenger. Of course, these are just-break-even numbers; too many empty seats on the trip probably mean you will not make payroll that week! How you factor in (a) flying a trip at less than a 100 percent load factor, or (b) what weather might do, or (c) what happens if your aircraft is forced down in a farmer's field thus creating some unscheduled maintenance are just a few of the decisions that you must make as president.

Now let me complete this example considering the fact that you have three DC-3As in your fleet. Suppose you want to provide 365-days-a-year service. You want to have one aircraft leaving Washington, D. C. in the morning, West bound for Huntsville, and a second aircraft leaving Huntsville in the morning at the same time, but East bound for Washington, D. C. That leaves you one aircraft in reserve at all times. Thus, one aircraft is always flying 5 hours per day times 365 days per year, which equals 1,825 hours a year. This is well within the 5,000-hour life of the Pratt & Whitney engine that Warner used in his direct operating cost analysis. This would also be somewhat less than the 2,000-hours-per-year utilization Warner suggests as typical. Based on the \$617 dollars per 900-miles-one-way trip from Table 2-52, your cost could be as high as two aircraft times \$617 per day times 365 days per year, or about \$450,000. The third aircraft might be available for some charter work but otherwise it is a "hanger queen" that, let me guess, only costs you 300 hours per year at \$123 per hour, or about \$50,000 per year. Your cost for the first year is, therefore, \$500,000, even if nobody bought a ticket all year!

Just think about these costs for your first year. If you go to a bank and borrow the \$350,000 to pay the Douglas Aircraft Company, you might get a loan of \$250,000, provided the bank loan officer is convinced that you and your backers have a very feasible business plan. He would, I imagine, take the three new DC-3As as collateral and also insist that real insurance (not the self insurance you used in your DOC computations) be obtained. Say the loan officer offers you a 7-year loan at 4.5 percent interest (compounded annually). This deal means a monthly payment of

$$\text{Monthly payment} = (\$250,000) \left[ \frac{0.045}{12} + \frac{0.045/12}{(1 + 0.045/12)^{7 \times 12} - 1} \right] = \$3,900,$$

## 2.9 OPERATING COSTS

and this means that your fare structure must provide for another \$46,800 per year. This is just one example of the “extra” costs that you must consider to get your airline up and running.

To close this discussion about direct and indirect operating costs (i.e., total operating costs) of running an airline, you should be aware that more than a few papers and reports have been published about how to estimate operating costs [632-635]. Fortunately, an accounting structure, negotiated between the Department of Commerce’s Civil Aeronautics Board (CAB) and the airlines in the 1940s, was refined over the years. In 1999, I tried my hand at creating an economic model for certificated airlines [636] using CAB/FAA Form 41 data that came from the Department of Commerce through Data Base Products<sup>200</sup>. The Form 41 has several schedules that provide you with detailed data. (Form 41 and its schedules are very much like the Internal Revenue Service Form 1040 and its schedules that the IRS requires each year.) The major accounting line items are shown in Fig. 2-402. You can see here that E. P. Warner’s bookkeeping of direct operating costs (DOCs) has been slightly rearranged and relabeled as “Total Aircraft Operating Expenses,” and that his indirect costs have been carefully expanded. I gave indirect operating costs a label of “All Other Operating Expenses” in reference [636] because Form 41 did not seem to have one.

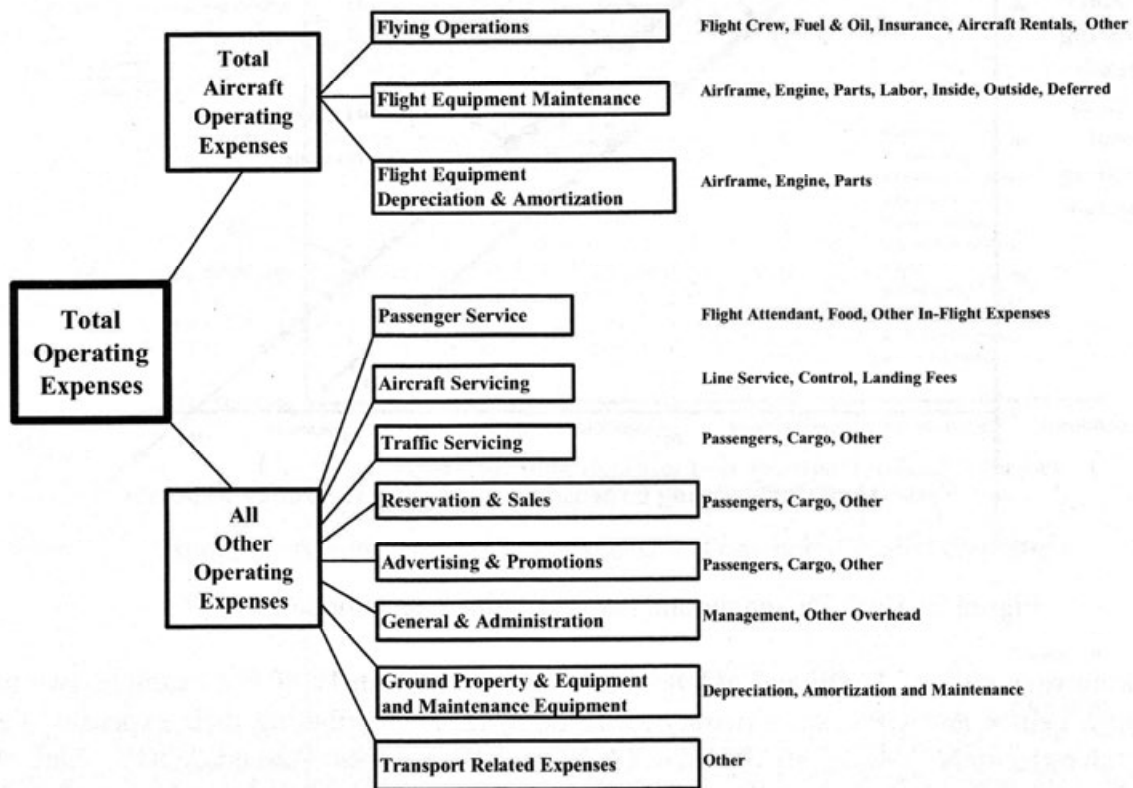


**Fig. 2-402. Accounting tree for total operating expenses [636].**

<sup>200</sup> My contact at Data Base Products is Lucretia Frederich. I believe she knows more about Form 41 and Data Base’s manual and CD products [637] than anyone. She was unbelievably helpful as I worked to produce reference [636].

### 2.9.2 Helicopters

The founders and the leaders of our rotorcraft industry who followed, from Cierva to today, have always had a dream. Many early proponents believed that there could be a helicopter in every garage.<sup>201</sup> The more practically minded believed that some sort of helicopter shuttle service around cities would be the ideal use of the helicopter. And today many believe that a helicopter operating between two nearby congested areas (such as between New York City and Boston in the United States, or between Tokyo and Osaka in Japan) will best serve national transportation needs. There are, of course, others who believe that high-speed rail is the most cost-effective solution for congestion.

An example of the high-speed rail view was offered by none other than Ronald Edwards George (R. E. G.) Davies, an Englishman born on July 3, 1921, who “wrote the book” on airline history in the United States [316]. His view [638] is very definitely worth your reading time because Davies was a lifelong aviation enthusiast right up until the day he died (July 30, 2011). He adapted his contribution to Aviation Week’s *Handbook of Airline Economics* from a lecture he gave before the Wings Club in New York City in May of 2000. At that time, he was the Curator of Air Transport at the National Air and Space Museum in Washington D.C. Davies “emphasize[d] four main criteria for long-range planning:

1. 650-seat airliners will be in service
2. Supersonic airliners will not
3. Airport planning for 2020 must start now [in 2000]
4. Major airports must incorporate high-speed rail.”

Davies’ chapter in the Aviation Week *Handbook* is 25 pages long, and he makes a very strong argument for his view based on projections in population growth. He does not suggest that scheduled airline service with helicopters, or any other rotorcraft, is just around the corner. Davies was right on his first two points and may yet be right on the last two points.

You might think that R. E. G. Davies was unaware of helicopters and what they offered the transportation system. You would be wrong. He did, in fact, devote nearly 12 pages out of 678 pages of his most referenced book [316] to a section he titled “*Helicopter Experiments*.” The primary experiment he describes concerned the CAB’s subsidy of Los Angeles Airways, Chicago Airways, and New York Airways from their certificated inception (May 1947, August 1949, and December 1951, respectively) to when the subsidy was “formally terminated on 11 April 1965.” One bright spot in this era was the start of San Francisco and Oakland Helicopter Airlines that began service in June of 1962. Davies makes the point that “a striking initial feature of the San Francisco helicopter operation was its independence of subsidy and, because of this demonstrated viability, it received in November 1963 from the C.A.B. the first permanent C.A.B. certificate to be awarded to any helicopter carrier.” As Davies comes to the end of his story, he writes:

---

<sup>201</sup> Can you imagine a couple of hundred Saturday morning grocery shoppers coming by helicopter to land at a Walmart?

## 2.9 OPERATING COSTS

“After twelve years of passenger operations, therefore, the Helicopter Carriers had been given a good chance to prove the efficiency of rotor-driven aircraft, but had failed to make their case. When the subsidy was withdrawn, they had to seek other artificial support. There was no great wave of protest from the American public as a whole, and very few sympathizers from the airline world itself, except from the interested sponsors like Pan American, United, TWA, and American.

Senator T. H. Kuchel, the Californian Republican, wrote to the C.A.B. Chairman in April 1965 (when the subsidy was cut off) suggesting that Los Angeles Airways should be reclassified as a Local Service airline, and thus qualify for subsidy and a share of the \$60,000,000 which was allocated annually to those carriers. But nothing came of this. Possibly the C.A.B. did not regard the type of service provided by LAA as a true social amenity, benefiting as it did only a minority of privileged citizens who wished to save a little time on the congested freeway system in the vast Southern Californian metropolis.

The Board had held serious doubts about helicopters for several years. On 17 May, 1960, simultaneously with the renewal of New York Airways’ certificate for seven years, it affirmed that the type of equipment offered by helicopter operators need not be confined to rotary-winged aircraft in the true sense of the word. This was interpreted as permitting the use of VTOL (Vertical Take-off and Landing), STOL (Short Take-Off and Landing), and other direct-lift aircraft.”

Despite what I think was a heroic effort, Los Angeles Airways had to give up in July of 1971, Chicago Helicopter Airways ceased operations December 31, 1965, and New York Airways, though carried on by Pan American for a while, closed its doors in 1972. By then, each of these pioneering efforts had experience with twin-turbine helicopters—the Boeing Vertol Model 107 II, the Sikorsky S-62, and then the Sikorsky S-61N. This step forward in helicopter progress by the manufacturers was still not great enough to make the helicopter airlines profitable without government subsidy. The helicopter industry just could not make the giant step that Donald Douglas provided with the DC-3.

There is, of course, still more to this story, which I will get to shortly, but first let me discuss the Federal Aviation Agency’s (FAA’s) view of helicopter airlines up to 1960 and what they forecasted for the future.

### 2.9.2.1 Project Hummingbird

The “Helicopter Experiment” that R. E. G. Davies referred to was named Project Hummingbird by the FAA [315]. The experiment began in October 1947 when Los Angeles Airways (LAA) was given a temporary certificate to carry mail and property. LAA began service almost immediately, and their small fleet started to accumulate aircraft miles rather quickly as Fig. 2-403 shows. Chicago Helicopter Airways (CHA), the next helicopter airline to carry mail, quickly added their helicopters to the budding experiment. Three years later, New York Airways (NYA) came online as the last mail carrier to participate in Project Hummingbird. In Appendix G you will find a copy of the FAA’s report about the experiment that gives results through 1959.<sup>202</sup> This report provides enormous insight into how the FAA

---

<sup>202</sup> You would think such a milestone report would have received wide distribution, but when I checked to see if you could get a copy easily, I found it so buried away that I thought it was better to include it herein.

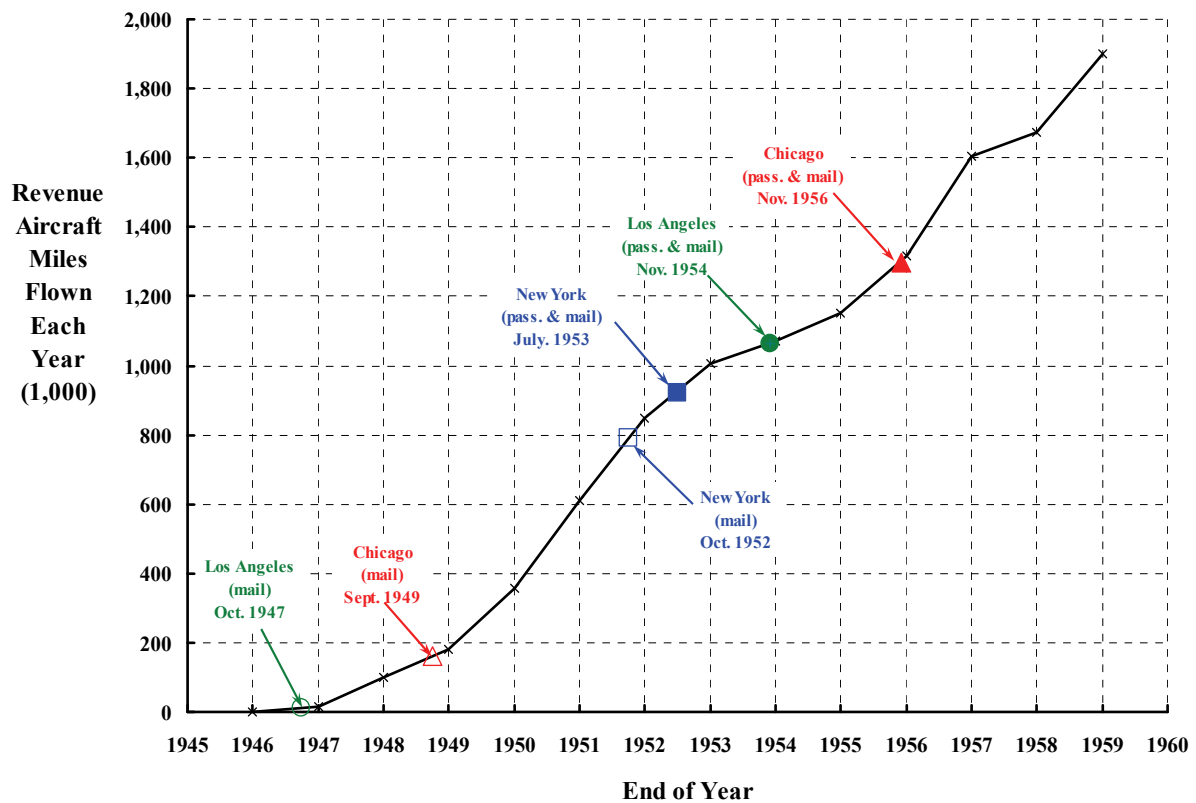


**Fig. 2-403. Helicopter airlines steadily increased miles flown [315].**

followed the same path that was taken in the creation of the fixed-wing airline industry. That is, build a route structure using helicopters to carry mail, and subsidize the adventure until the industry can stand on its own two feet and make a profit carrying passengers without government assistance.

The three helicopter carriers began with five different helicopter models: the Sikorsky S-51, S-55, and S-58; the Bell Model 47, and the Vertol Model 44. During the one year of 1959, the three airlines, each with a very small fleet, had expanded to the point that they put nearly two million aircraft miles on their combined fleet. Because each successive helicopter came with more seats, the three airlines quickly found themselves transporting an ever increasing number of passengers each year. In fact, being well subsidized so fares would be competitive with ground transportation, the growth in paying customers was exponential (Fig. 2-404), and the trend suggested even better things to come in the 1960s. Of course, the trip miles each passenger was transported was rather short—the average trip distance being only about 20 miles in 1959. This was, in part, due to the FAA restricting the helicopter airlines to a radius of 50 to 60 miles about their respective cities. The FAA made it very clear that they did not want the helicopters encroaching on the routes of trunk-line and short-haul carriers that they were already subsidizing to the tune of \$60,000,000 a year (Fig. 2-405).

## 2.9 OPERATING COSTS

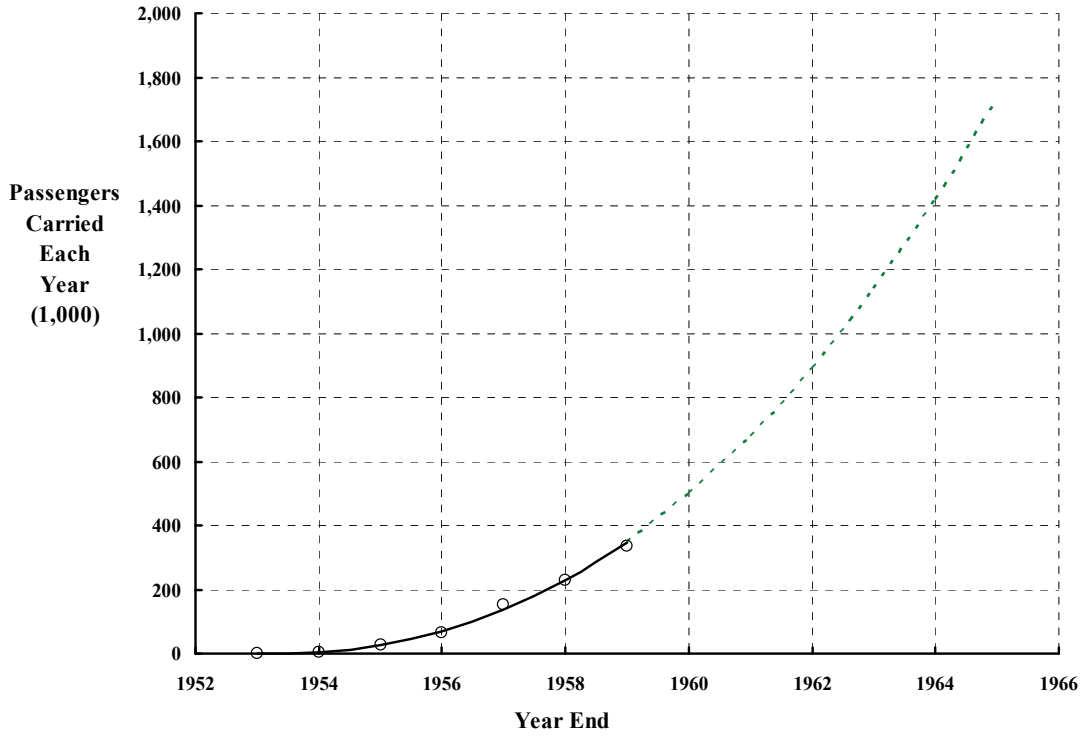


**Fig. 2-404. The helicopter airlines got off to a very good start, and the projections through 1965 looked rosy [315].**

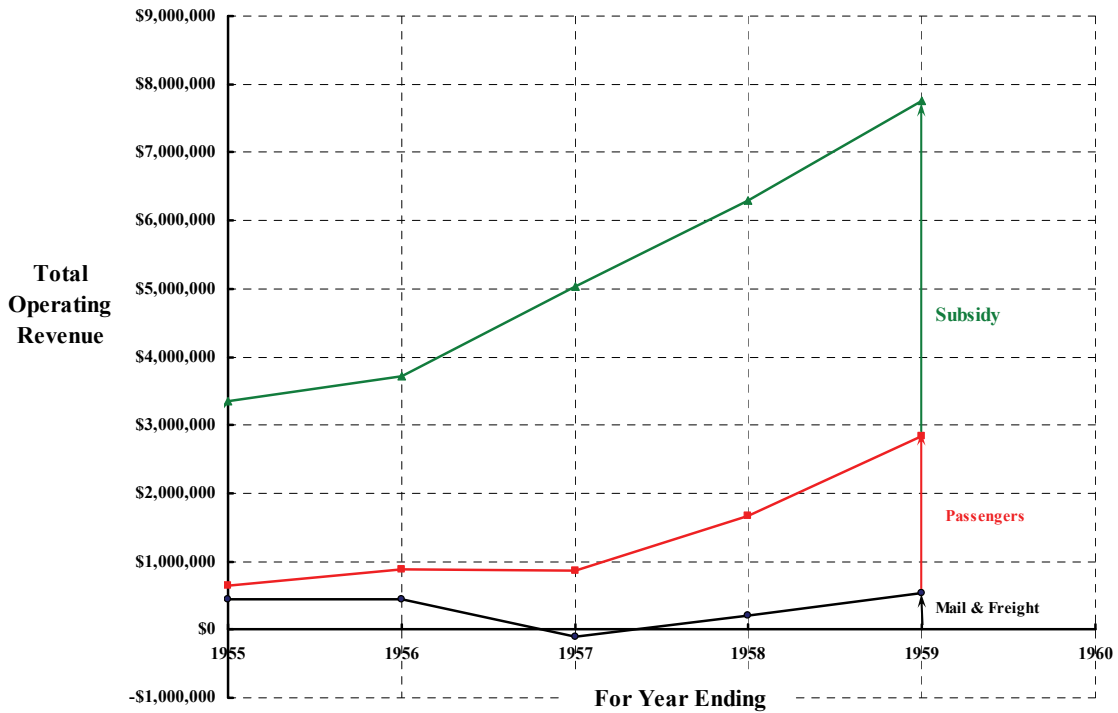


**Fig. 2-405. CAB/FAA subsidy amounted to over 60 percent of what the three helicopter airlines needed to break even [315].**

The revenue from carrying passengers quickly exceeded that coming from carrying mail and other property. Unfortunately, the direct and indirect costs (i.e., the total operating costs) far exceeded the revenue coming in from fares and mail carrying operations. The situation—as I interpret it from reading the report on Project Hummingbird included here in Appendix G—is shown in Fig. 2-406. It appears that the total operating costs for each of the first 5 years was running at \$14.61 for every passenger carried. This is the slope of the line shown in Fig. 2-406 going through the solid green boxes. The data points are from table 13 of the Project Hummingbird report and the abscissa, of passengers carried each year, is from table 4. The trip distance is on the order of 20 miles, as an average. Therefore, the approximate cost per paying passenger seat-mile is 73 cents (i.e., 1461/20), which is a more pessimistic way of looking at the 5-year period than the several tables in Appendix G show.

Of the total \$14.61 per passenger required to just break even, the helicopter airlines were only charging their passengers \$6.67 per average trip. You might note in reading Appendix G that the actual operating costs were coming down (see table 15 in Appendix G), and the helicopters finally reached a point in 1959 where half of the seats were filled on an average trip (see table 7 in Appendix G). However, weather-related problems kept the fleet grounded about 12 percent of the time the aircraft were scheduled to fly. Still, everyone thought that progress was being made.

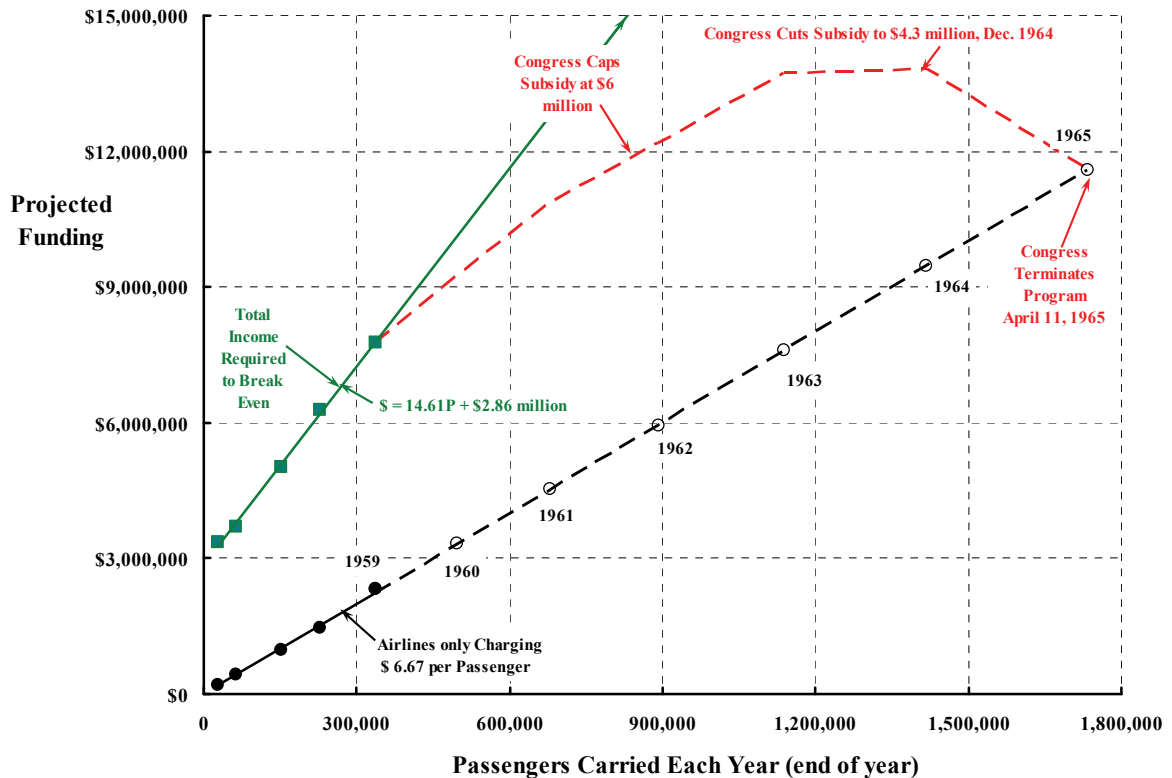


**Fig. 2-406. The helicopter airlines had total operating costs far in excess of what they were charging their customers [315].**

## 2.9 OPERATING COSTS

What seems to be of great concern was the out-year projection of how many passengers might be expected. If the subsidy stayed at \$7.94 per passenger and the number of passengers transported continued to climb, then there would be a considerable drain on the U.S. Treasury. In essence, if the helicopter airlines continued to attract the traveling public as the projections were suggesting, the helicopter airlines would break the bank.

As you read the Project Hummingbird report [315] included here in Appendix G, you will see that the CAB thought that helicopter operating costs were *the problem*. The statement is repeated several times and, most discouragingly, they did not see a helicopter currently in development that would alter the outlook. The suggestion was also made by the CAB that the helicopter airlines might raise their fares so the subsidy could be reduced. However, the airlines felt that the current levels were “in the judgment of airline management” at just the right level “to produce the maximum gross revenues while meeting requirements to be competitive with limousine and cab fares and to contribute to traffic development.”

The helicopter airline management pointed at the soon-to-be-available Boeing Vertol 107 and Sikorsky S-61 as twin-turbine helicopters that would reduce direct operating costs when compared to the then current fleet. *The problem*, as summarized by the CAB in table 16 of their report, is included here as Table 2-53. To explain the helicopter situation to fixed-wing advocates, the report (see table 14 in Appendix G) shows that domestic trunk and local-service airlines had *total operating costs* in 1959 of \$0.28 and \$0.51, respectively, per available ton-mile, as compared to total operating costs of \$4.05 per available ton-mile for the helicopter airlines as a group in 1959. This comparison was startling to some and showed just what a tall mountain the helicopter airline advocates had to climb.

The CAB was careful to point out that *the problem* was not just direct operating cost. Their report included table 15, provided here as Table 2-54, which must have, I am guessing, sealed the fate of those pioneers of helicopter airlines. As you can see, even if the direct operating costs of all of the helicopters in operation were reduced to zero, the indirect operating costs were still way out of line with comparable fixed-wing trunk and short-haul carriers.

**Table 2-53. Direct Operating Cost of Helicopters Operating in Certificated Airline Service for Years Ending June 30, 1958, and September 30, 1959**

Helicopter Type	Year Entered Service	DOC Per Hour Flown (\$)	DOC Per Available Ton-Mile (\$)	DOC Per Available Seat-Mile (\$)
Sikorsky S-51*	1947	—	—	—
Bell B-47	1949	54.37 to 54.75	4.95 to 5.33	—
Sikorsky S-55	1952	77.97 to 142.10	2.38 to 7.35	0.28 to 0.35
Sikorsky S-58	1956	208.05 to 260.92	1.67 to 3.02	0.20 to 0.33
Vertol V-44B	1958	256.28 to 260.35	3.35 to 3.47	0.36 to 0.40

\*The S-51 was flown too few hours for any meaningful cost experience.

While the Postal Department was quite willing to subsidize fixed-wing airline development for nearly three decades,<sup>203</sup> the CAB was not going to recommend nurturing helicopter airlines for any more than the 18 years between 1947 and 1965. I had two feelings from the Project Hummingbird report: (1) they did not foresee a step comparable to the replacement of the Ford Tri-Motor with the Douglas DC-3 even by 1970, and (2) mass transit was not ever going to be the helicopter's (the report mentions V/STOL configurations<sup>204</sup>) strong suit.

It is interesting that the helicopter airlines were carried for several more years after the Hummingbird report came out, but I think that this was just a gesture to the proponents who felt that the operational data from the new twin-turbine helicopters might cast a whole new light on the economic situation. You get this feeling from the first paragraph in the *Unit Costs and Fares* section (page 914 of Appendix G), which says:

“In addition to greatly improved performance characteristics, the new twin-turbine helicopters ordered by the three certificated operators are also expected to provide important reductions in unit costs. Actual operating experience with the new turbocopters is lacking, of course, but available estimates show a range of about 10 cents to 16 cents for direct operating costs per available seat mile. Comparatively, direct operating costs of the piston-powered S-58 are 20 cents per seat mile. If these unit cost estimates are realized, they will therefore represent a substantial improvement over current levels which suggest the possibility of lower fares as a factor which will promote traffic growth.”

I read the FAA report as saying that they did not want to call a halt to the “helicopter experiment” until the next-generation helicopter was given a chance to demonstrate that it would cut direct operating costs by as much as 50 percent. The helicopter that the helicopter airline pioneers were pinning their hopes on was the Sikorsky S-61.

I hope you read the full Project Hummingbird report included in Appendix G of this volume.

**Table 2-54. Direct and Indirect Operating Costs of Certificated Helicopter Airlines From 1955 to 1959**

Year	Dollars Per Available Ton-Mile			Dollars Per Revenue Ton-Mile		
	Total	Direct	Indirect	Total	Direct	Indirect
1955	6.75	3.62	3.13	15.22	8.16	7.06
1956	6.37	3.22	3.15	12.96	6.55	6.41
1957	4.82	2.93	1.89	11.50	6.99	4.51
1958	3.98	2.47	1.51	10.04	6.22	3.82
1959	4.05	2.54	1.51	8.29	5.20	3.09

<sup>203</sup> The story is well told by F. Robert van der Linden [498].

<sup>204</sup> The Project Hummingbird report makes reference to compound helicopters and short takeoff and landing aircraft, which are configurations I will discuss in Volume III: Other V/STOL Aircraft.

## 2.9 OPERATING COSTS

### 2.9.3 A Direct Operating Cost (DOC) Calculator

You have just read that the three helicopter airlines, LAA, CHA, and NYA, needed a helicopter that would cut their direct operating costs by at least 25 percent, and hopefully even in half. You can appreciate the giant step that was being taken just by looking at LAA's effort from starting with the 4-passenger-seat Sikorsky S-51 in 1947 (Fig. 2-407), to 15 years later when the 26-passenger-seat (in a full airline interior) Sikorsky S-61 (Fig. 2-408) came online. As I read the history, I began to wonder if, in fact, the S-61 did lower DOCs. My searching (as of this writing) has not turned up an answer, though I imagine that archives somewhere have the answer. So I thought it would be fun to see if a reasonable estimate might be obtained. That is the purpose of the following: to use a DOC calculating method of that time to estimate the DOC for a Sikorsky S-55 and compare it to an S-61, both operating in 1967.

One of the earliest methods for estimating helicopter operating expense, that I am aware of, was published by Bob Stoessel and Jack (John E.) Gallagher<sup>205</sup> in October of 1967 [639]. They were offering a more realistic approach to estimating DOC for Vertical Takeoff and Landing (VTOL) aircraft. Their paper briefly traces development of the Air Transport Association of America's (ATA's)<sup>206</sup> DOC calculation method from its beginnings in 1944. What Stoessel and Gallagher proposed was a tailoring of the ATA method for use in comparing and estimating DOC of VTOL aircraft. At that time, exploration of many VTOL types was in full swing. Jack Gallagher, as President of New York Airways, was able to contribute "accurate maintenance data [for the Sikorsky S-61 and Boeing V-107] in sufficient detail to be useable as a base or anchor points." The major distinction between fixed-wing and rotary wing aircraft that was addressed was maintenance costs. Stoessel and Gallagher proposed adding to the then current ATA method consideration in more depth of "costs incurred per flight cycle and costs incurred per engine shutdown."

I will use the Stoessel and Gallagher DOC estimating method of 1967 to compare the Sikorsky S-55 (10 passenger, piston powered) to the Sikorsky S-61 (26 passenger, turboshaft powered). In deference to Jack Gallagher, this example will use the New York Airways inter-airport shuttle flight path route (Fig. 2-409), schedule (Fig. 2-410), and fares (Fig. 2-411) as the operation for each helicopter to complete. Of course, any scenario could be studied. The three *primary* cost categories (and their next-level breakdown) that contribute to DOC will be those addressed by Stoessel and Gallagher. They are:

- Flying operations (flight crew, fuel and oil, insurance)
- Direct maintenance of flight equipment (accounting for per rotor hour, per flight cycle, and per engine shutdown)
- Depreciation of flight equipment (including spares)

---

<sup>205</sup> Jack Gallagher was an instrumental figure in New York Airways. I was put in touch with Jack Gallagher Sr. by his son (also named Jack Gallagher) who worked in program management at Bell Helicopter Textron while I was there.

<sup>206</sup> The ATA was the first, and remains the only, trade organization of the principal U.S. airlines.



**Fig. 2-407. LAA, the first helicopter airline, began airmail carrying operations with the Sikorsky S-51 on October 1, 1947 (photo from author's collection).**



**Fig. 2-408. LAA was the first to use the Sikorsky S-61; it was introduced into service on March 1, 1962 (photo courtesy of Ed Coates).**

2.9 OPERATING COSTS

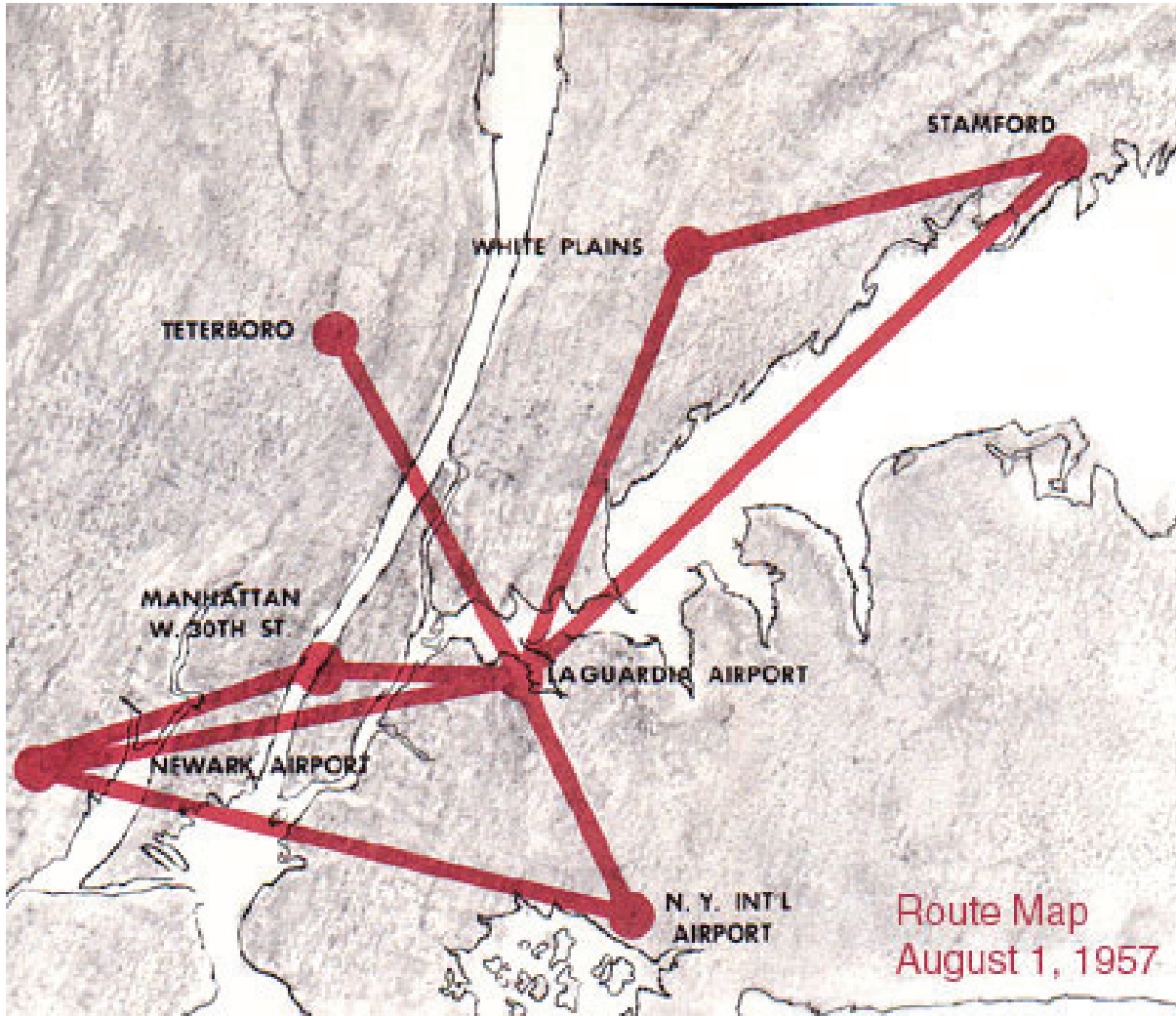


Fig. 2-409. NYA route map during its early startup years (author's collection).

**PASSENGERS ASSEMBLE TEN MINUTES BEFORE SCHEDULED DEPARTURES OF ALL FLIGHTS**

*Hourly Schedules*

**INTER-AIRPORT SHUTTLE FLIGHTS  
N. Y. INTERNATIONAL-LA GUARDIA-NEWARK AIRPORTS**  
Eastern Daylight Saving Time

FLIGHT No.	355	361	566	32	582	590	598	606	25‡	614	622	630	26‡	638	646	654	662	38†	680	682
	A.M.	A.M.	A.M.	A.M.	A.M.	A.M.	P.M.	P.M.	P.M.	P.M.	P.M.	P.M.	P.M.	P.M.	P.M.	P.M.	P.M.	P.M.	P.M.	P.M.
N. Y. INT'L Lv.			8:00	9:00	10:00	11:00	12:00	1:00		2:00	3:00	4:00	4:10	5:00	6:00	7:00	8:00	9:00	10:18	10:45
LAGUARDIA Ar.			8:10	9:10	10:10	11:10	12:10	1:10		2:10	3:10	4:10	4:20	5:10	6:10	7:10	8:10	9:10	10:28	10:55
LAGUARDIA Lv.	6:50	7:30	8:15	9:15	10:15	11:15	12:15	1:15	1:20	2:15	3:15	4:15		5:15	6:15	7:15	8:15	9:18	10:30	
NEWARK Ar.	7:10	7:50	8:35	9:41	10:35	11:35	12:35	1:35	1:40	2:35	3:35	4:35		5:35	6:35	7:35	8:35	9:44	10:50	

**NEWARK-LA GUARDIA-N. Y. INTERNATIONAL AIRPORTS**

FLIGHT No.		360	366	374	382	390	398	406		414	422	430		438	446	454	462	474	478	486
		A.M.	A.M.	A.M.	A.M.	A.M.	P.M.	P.M.		P.M.	P.M.	P.M.		P.M.	P.M.	P.M.	P.M.	P.M.	P.M.	P.M.
NEWARK Lv.		7:20	8:00	9:00	10:00	11:00	12:00	1:00		2:00	3:00	4:00		5:00	6:00	7:00	8:00	9:39	10:00	11:00
LAGUARDIA Ar.		7:57	8:17	9:17	10:17	11:17	12:17	1:17		2:17	3:17	4:17		5:17	6:17	7:17	8:17	9:56	10:17	11:17
LAGUARDIA Lv.		7:40	8:20	9:20	10:20	11:20	12:20	1:25		2:25	3:20	4:20		5:20	6:20	7:25	8:20	9:58	10:25	
N.Y. INT'L Ar.		7:50	8:30	9:30	10:30	11:30	12:30	1:35		2:35	3:30	4:30		5:30	6:30	7:35	8:30	10:08	10:35	

*All flights daily except Sundays and Holidays.*

‡ Monday through Friday only. Passengers must check in ten minutes before flight time at United Air Lines Passenger Service counters.  
† Passenger Service on Flight 38 from LaGuardia to Newark will start May 19th.

Fig. 2-410. NYA hourly schedules for inter-airport show how short the in-flight travel times were using the Sikorsky S-55 (author's collection).

HELIPORT TO HELIPORT—ONE-WAY FARES							
	LaGUARDIA	N. Y. INT'L	NEWARK	TETERBORO	NEW BRUNSWICK	WHITE PLAINS	STAMFORD
N. Y. Int'l	4.09						
Newark	8.64	8.64					
Teterboro	5.45	8.64	5.45★ 8.64†				
New Brunswick	9.09	9.09	9.09	9.09			
White Plains	7.73	8.18	8.86	8.86	9.77		
Stamford	7.95	8.18	9.09	9.09	10.23	5.45	
Trenton	10.00	10.00	10.00	11.14	5.45	11.14	11.59

Joint Tariff Fares with Northwest Orient Airlines.  
 All fare plus tax—Half-fare for children under 12 years of age.  
 All schedules and fares subject to change without notice.  
 ★ From Teterboro to Newark.  
 † From Newark to Teterboro by way of LaGuardia.

**Fig. 2-411. NYA fare structure using the Sikorsky S-55 was thought to be competitive with ground transportation in August of 1957 (author's collection).**

You will see that I have based all costs on one trip. This takes some poetic license with Stoessel and Gallagher's published work, but you will see results in terms of DOC per hour and DOC per seat-mile in the summary.

### 2.9.3.1 Flight Profile

The example flight profile I have constructed envisions leaving New York International Airport (now John F. Kennedy Airport) for LaGuardia Airport, and then continuing on to Newark Airport. Then a return trip is made by retracing the outbound route. You have, therefore, the following flight profile scenario:

Start rotors turning at 7:45 a.m.

Lv. N.Y. Int'l at 8:00 a.m. after 15 minutes of ground operation with rotors turning

Ar. LaGuardia at 8:10 a.m. after 10 minutes at cruise

Lv. LaGuardia at 8:15 a.m. after 5 minutes of rotor-turning ground operation

Ar. Newark at 8:35 a.m. after 20 minutes at cruise

Lv. Newark at 9:00 a.m. after 25 minutes of ground operation (5 minutes of ground operation with rotors turning + 20 minutes in shutdown and restart)

Ar. LaGuardia at 9:20 a.m. after 20 minutes at cruise

Lv. LaGuardia at 9:25 a.m. after 5 minutes of rotor-turning ground operation

Ar. N.Y. Int'l at 9:35 a.m. after 10 minutes at cruise.

Shutdown for 15 minutes, refuel, and be ready to take the 10:00 a.m. trip with a rotor startup at 9:50 a.m.

## 2.9 OPERATING COSTS

This postulated flight profile provides several important parameters necessary for calculating the DOC. These parameters are:

1. Time spent at cruise is  $10 + 20 + 20 + 10$  minutes = 1.0 hour
2. Time spent in rotor-turning ground operation is  $15 + 5 + 5 + 5$  minutes = 0.50 hour
3. Total rotor-turning time per trip = 1.5 hour/trip
4. Number of flight cycles (i.e., ground-air-ground) per trip = 4
5. Number of engine startup and shutdown cycles = 2
6. Total round-trip time (leave at 8:00 a.m. and return at 9:35 a.m.) = 1.58 hours
7. Total round-trip distance traveled = 85 statute miles

While the S-61 cruises faster than the S-55 on paper, I have chosen to assume that both helicopters fly the same schedule. This may potentially penalize the S-61 in fuel used, but the distances are so short, and the possibility of traffic control holdups so real in this example, I doubt that the S-61's cruise speed benefit would be seen in the final numbers.

The question of how many trips are made in a year is particularly important to distributing yearly costs of insurance and depreciation. When you look at the inter-airport shuttle service that New York Airways offered (Fig. 2-410), you can count about 16 round-trips scheduled for each day. The schedule offers this service 6 days a week for 52 weeks, skipping Sundays and holidays. This means that rotor-on time each day could be on the order of 16 trips times 1.5 hours per trip or 24 hours! Clearly, this would leave no time for scheduled maintenance (never mind unscheduled maintenance), and this means the fleet must consist of more than one helicopter. Therefore, let me assume that *one* helicopter makes 3 round trips per day, in which case the number of trips in 1 year is calculated as 3 trips/day  $\times$  6 days/week  $\times$  52 weeks/year or 936 trips per year. This assumption means the rotor-on time is about 1,400 hour per year, which is, in fact, a very high utilization rate for helicopters. On the other hand, there are 8,760 hours in a year, and this leaves about 6.25 maintenance hours for every rotor-turning hour.

With the above background in place, let me proceed with the DOC calculation.

### 2.9.3.2 Flight Crew Costs

In discussing the cost of a flight crew, Stoessel and Gallagher did not reference a year, but let me assume it is 1967. Because this example is a comparison in the same year, the actual year is relatively unimportant. They said in their paper that

“the formulas for flight crew represent an average for the U. S. helicopter air carriers. They account for the following factors:

- Size of crew
- Crew pay differential
- Average crew utilization
- Credit (or duty) hour increment
- Travel and incidental expense
- Check pilots' pay increment
- Retirement, payroll tax, and insurance contribution increment”

and proceeded to use the estimating formula as:

$$(2.365) \quad \frac{\$}{\text{Trip}} = \left[ \$45 + 0.03 \left( \frac{\text{GW}}{1,000} \right) + 2.00 \left( \frac{V_{\text{cr}}}{100} \right) \right] \left( \frac{\text{Rotor time}}{\text{Trip}} \right)$$

where GW is the maximum certificated gross weight in pounds, and  $V_{\text{cr}}$  is the average cruise speed in miles per hour. For the S-55, you have  $\text{GW} = 7,200$  pounds and an economical cruise speed of 75 miles per hour. For the S-61, you have  $\text{GW} = 20,500$  pounds and an economical cruise speed of 115 miles per hour. Therefore, the flight crew costs for the two helicopters amount to:

S-55 equals \$70.07 per trip for flight crew

S-61 equals \$71.87 per trip for flight crew.

### 2.9.3.3 Fuel and Oil Costs

To approximate fuel and oil costs, Stoessel and Gallagher showed computations for both U.S. domestic and international cases. Here, I will only deal with the U.S. domestic case where Jet A fuel was being bought by the airlines for \$0.11 per gallon, and oil was considerably more at \$7.50 per gallon.<sup>207</sup> Following their proposed method, fuel and oil costs are calculated as

$$(2.365) \quad \frac{\$}{\text{Trip}} = \left( \frac{\text{Fuel used in lbs}}{\text{Trip}} \right) \left( \frac{1}{\text{lbs/gal.}} \right) \left( \frac{\$}{\text{gal. Avgas}} \right) + 0.13 \left( \frac{1}{\text{lbs/gal.}} \right) \left( \frac{\$}{\text{gal. oil}} \right) (\text{No. of engines}) \left( \frac{\text{Rotor time in hours}}{\text{Trip}} \right)$$

Stoessel and Gallagher noted that Jet A fuel had a density of 6.7 pounds per gallon and that oil for turbine engines was 8.1 pounds per gallon. They did not suggest prices and densities for piston engines. Therefore, I will use approximate values of Avgas at 6.1 pounds per gallon and oil for piston engines at 8.1 pounds per gallon. For 100-octane Avgas, I will guess the price at about \$0.13 per gal and oil at \$7.50 per gallon.

An accurate estimate of fuel burned per trip requires, of course, a thorough understanding of the performance of both helicopters, but as representative values, let me use:

Helicopter	Fuel Flow at Cruise (gal./hr)	Economical Cruise Speed (mph)	Fuel Flow at Flight Idle (gal./hr)
S-55	40	75	5
S-61	160	115	20

From the flight profile, 1 hour is spent at cruise and 1/2 hour is spent at ground idle. Therefore, the S-55 uses  $40 + 2.5$  or 42.5 gallons, or 260 pounds, in one round-trip; the S-61 uses  $160 + 10$  or 170 gallons, or 1,139 pounds in one round-trip. This information shows the fuel and oil costs for the two helicopters being compared as:

<sup>207</sup> In early 2012, Jet A fuel was selling for \$5.63/gal. and Avgas for \$6.04/gal. The respective engine oils were selling for \$57.18/gal. and piston engine oil for \$64.42/gal.

## 2.9 OPERATING COSTS

S-55 equals \$5.71 per trip for fuel and oil

S-61 equals \$19.06 per trip for fuel and oil.

### 2.9.3.4 Insurance

Stoessel and Gallagher's view on insurance was that

“the annual rate of insurance is usually high for the initial service period of a new ‘family’ of aircraft where there are major innovations in technology or state of the art. The initial rate for a new type of aircraft similar to one already operational is also somewhat higher, but not as high as for a new family. The following are representative variations in insurance rates with service experience:

<u>Year after Initial Operation</u>		<u>Insurance Rate</u>
<u>of the Family</u>	<u>of the Type</u>	
1		3.0 x stabilized rate
2	1	2.0 x stabilized rate
	2	1.5 x stabilized rate
3 and subsequent	3 and subsequent	stabilized rate

When VTOL transport aircraft become widely used for short-haul operation, the insurance rates will become equivalent to those for conventional fixed-wing or [conventional takeoff and landing] CTOL aircraft. Therefore, a stabilized rate of 2 percent, which would be attained by the third year of operation, is used. Using this recommended rate, the insurance cost after the third year of operation is:

$$(2.365) \quad \frac{\$}{\text{Trip}} = \frac{0.02 (\text{Cost of complete aircraft in dollars})}{\text{Trips per year}}$$

According to HeliValue\$, Inc. [132] data, in 1967 an S-55 sold for about \$350,000, and an S-61N sold for about \$1,200,000 (both being in the equipped configuration). Accepting the estimate that one helicopter in the fleet does 936 trips per year, you arrive at:

S-55 equals \$7.27 per trip for insurance

S-61 equals \$24.92 per trip for insurance.

### 2.9.3.5 Direct Maintenance

Stoessel and Gallagher believed that considerably more detailed estimating was required in the area of direct maintenance cost of flight equipment. They offered the opinion that both labor man-hours and repair parts' costs must be accounted for on a per-rotor-hour basis, a per-flight-cycle basis, and a per-engine shutdown and restart basis. They wrote in their introduction (with some condensing and editing on my part):

“Introduction. The basic philosophy employed in the derivation of maintenance labor and materials formulas is that (1) it is valid to project VTOL aircraft maintenance costs from data on existing rotary wing aircraft provided that rational adjustment factors are introduced and

(2) the best base from which to project such costs is the experience of commercial helicopter airlines, particularly those with comprehensive detailed records of maintenance.

New York Airways uses the Air Transport Association's Specification 100 System for segregating and recording maintenance labor and material cost. As sufficient statistical information becomes available, the following grouping is recommended for comparative maintenance cost analyses:

1. Airframe
  - Aircraft (less engines, rotors & controls and drive system)
  - Rotors & Controls
  - Drive System (transmissions & shafts)
2. Engines

However, when analyses are made for initial concepts and for parametric studies, just the two major groupings—of airframe and of engines—are recommended. This is the case, also, when brochure and other descriptive data are utilized to supply input for such studies, because these seldom provide information in sufficient detail to warrant separation of the airframe into its major components.

When the VTOL aircraft now in commercial air carrier service are compared with their CTOL or fixed wing counterparts from the standpoint of maintainability characteristics, it is apparent that the time element is of greater significance than the cyclic one. Two reasons for this appear to be:

1. The greater amount of vibration—even with rotors operating in ground-idle.
2. Decreased maintenance requirements for landing gear structure, wheels, tires and brakes (a function of flight cycles, or wheels-off to wheels-on).

Rotor time (the total time of rotor operation) has been selected as a measurement of the "time" factor because (1) most of the systems are functioning completely when rotors are engaged (this includes a greater amount of engine power than for ground idle with CTOL aircraft) and (2) there is such a wide variation in the ratio of rotor hours to flight hours, from a low of 1.09 for one of the helicopter operations analyzed to a high of 1.78 for another.

As for measurement of maintenance cost as a function of engine shutdowns (engine start, operation at some temperature or temperatures, and shutdown), there are generally only four elements of the aircraft so affected. These are (1) engine, (2) engine starting system, (3) engine exhaust system and (4) rotor brake."

#### **2.9.3.5.1 Airframe Maintenance Costs**

Stoessel and Gallagher prefaced their equations for estimating airframe maintenance with a brief discussion of the parameters involved. They wrote:

"Parameters. The basic parameters considered desirable for comparative analyses of VTOL airframes are:

- a. Cost and weight of
  - Basic Airframe (less rotors & controls, and drive system)
  - Rotors & Controls
  - Drive System (transmissions & shafts)
- b. Cabin area (for determination of maintenance costs for 'payload accommodations')

For analyses involving initial concepts and parametric studies, the foregoing requirements are reduced to:

## 2.9 OPERATING COSTS

- a. Weight of aircraft, less engines
- b. Cost of aircraft, less engines

A maintenance burden ratio of 1.8 times direct labor is now recommended for general operating expense comparisons of CTOL [Conventional Takeoff and Landing] aircraft. Nevertheless, the ratio recommended for VTOL aircraft is 1.3, because this is more in line with current averages for helicopter and for local service carriers. As for direct labor rates, an hourly rate of \$4.00 per manhour is recommended. This is identical to the rate used in the forthcoming ATA method for CTOL aircraft.”

I have regrouped Stoessel and Gallagher’s equations into one equation so that you now have the following for the estimate of airframe maintenance labor man-hours per trip:

$$(2.365) \quad \frac{\text{Man-hours}}{\text{Trip}} = \left[ 3.0 + 2.0 \left( \frac{W_{af}}{1,000} \right)^{1/2} \right] \left( \frac{\text{Rotor hours}}{\text{Trip}} \right) + \left[ 0.2 + 0.2 \left( \frac{W_{af}}{1,000} \right)^{1/2} \right] \left( \frac{\text{Flt. cycles}}{\text{Trip}} \right) + \left[ 0.1 + 0.1 \left( \frac{W_{af}}{1,000} \right)^{1/2} \right] \left( \frac{\text{Engine shutdowns}}{\text{Trip}} \right)$$

And for airframe materials per trip, Stoessel and Gallagher offered:

$$(2.366) \quad \frac{\text{Dollars}}{\text{Trip}} = \left[ 4.0 + 4.0 \left( \frac{\text{Cost}_{af}}{10^6} \right) \right] \left( \frac{\text{Rotor hours}}{\text{Trip}} \right) + \left[ 0.6 + 0.6 \left( \frac{\text{Cost}_{af}}{10^6} \right) \right] \left( \frac{\text{Flt. cycles}}{\text{Trip}} \right) + \left[ 0.3 + 0.3 \left( \frac{\text{Cost}_{af}}{10^6} \right) \right] \left( \frac{\text{Engine shutdowns}}{\text{Trip}} \right)$$

Of course, the man-hours per trip, Eq. (2.365), needs to be expressed in dollars per trip. This conversion introduces one of the most widely sought numbers in any evaluation of a new aircraft’s maintenance program. This parameter is maintenance man-hours per flight hour (MMH/FH). You see its importance because

$$(2.367) \quad \frac{\text{Dollars}}{\text{Trip}} = \left( \frac{\text{MMH}}{\text{FH}} \right) \left( \frac{\text{FH}}{\text{trip}} \right) \left( \frac{\text{Direct Labor Rate}}{\text{mh}} \right) (\text{Overhead rate}) \\ = \left( \frac{\text{MMH}}{\text{trip}} \right) \left( \frac{\text{Direct Labor Rate}}{\text{mh}} \right) (\text{Overhead rate})$$

Maintenance man-hours per flight hour for the helicopters flying today range from a low of 0.5 to as much as 6 MMH/FH, although a few of the most recent, larger helicopter models are below 5 MMH/FH as you will see shortly. Please take note that Stoessel and Gallagher addressed the parameter not as man-hours per flight hours, but rather as man-hours per rotor-turning hours.

Now let me introduce some specific numbers to make a comparison between the S-55 and the S-61. First of all, you have the flight profile information that there are 1.5 rotor hours per trip, four flight cycles per trip, and two engine shutdowns per trip. Furthermore, Stoessel and Gallagher observe that the direct labor rate in 1967 is \$4.00 per hour, and they recommend the overhead rate (i.e., the maintenance burden ratio) of 1.3. On this basis, only the airframe weight ( $W_{af}$ ), which is the weight empty less the engine weight and the airframe

cost ( $Cost_{af}$ ), again not including the engine, are required before the calculation can be completed. The weights, of course, are available from many sources (though not many sources agree). The airframe and engine cost-split making up the selling list price is not so easy to come by, as I have mentioned before. For this example, I have assumed the total power plant(s) cost is one-fourth of the selling list price. It is useful to have the numbers in a small table, which I have included here as Table 2-55.

From here on out, the calculations are straightforward arithmetic, and you will find that “airframe” direct maintenance costs for one trip amount to:

S-55 equals \$53.31 per trip for airframe direct maintenance (\$41.95 labor; \$11.36 materials)

S-61 equals \$68.27 per trip for airframe direct maintenance (\$51.17 labor; \$17.10 materials).

**Table 2-55. S-55 and S-61 Data for DOC Calculations**

Type	No. of Engines	Weight Empty (lb)	List Price (\$)	Airframe Weight (lb)	One Engine Weight (lb)	Airframe Cost (\$)	One Engine Cost (\$)
S-55	1	5,250	0.35 mil	4,400	850	0.2625 mil	0.0875 mil
S-61	2	12,460	1.20 mil	11,700	340	0.90 mil	0.150 mil

**2.9.3.5.2 Engine Maintenance Costs**

Here again Stoessel and Gallagher preface their equations for estimating engine maintenance with a brief discussion of the parameters involved. They wrote:

“Parameters. The engine parameters considered satisfactory for use in evaluation of operating expenses of VTOL aircraft are basic parameters considered desirable for comparative analyses of VTOL airframes:

- a. Number of engines
- b. Equivalent shaft horsepower per engine [at rated takeoff power, sea level on a standard day]
- c. Cost per engine

As in the case of VTOL airframes, the following assumptions can be used for engine maintenance:

- a. Labor rate—\$4.00 per manhour
- b. Maintenance burden—30 percent of direct labor”

and suggested that for engines without gearboxes the estimating equation would be:

$$\begin{aligned}
 \frac{\text{Man-hours}}{\text{Trip}} = & \left[ 0.5N_{\text{eng}} + 0.02N_{\text{eng}} \left( \frac{\text{SHP}_{\text{TO rated}}}{1,000} \right) \right] \left( \frac{\text{Rotor hours}}{\text{Trip}} \right) \\
 (2.368) \quad & + \left[ 0.2N_{\text{eng}} + 0.02N_{\text{eng}} \left( \frac{\text{SHP}_{\text{TO rated}}}{1,000} \right) \right] \left( \frac{\text{Flt. cycles}}{\text{Trip}} \right) \\
 & + \left[ 0.1N_{\text{eng}} + 0.01N_{\text{eng}} \left( \frac{\text{SHP}_{\text{TO rated}}}{1,000} \right)^{\frac{1}{2}} \right] \left( \frac{\text{Engine shutdowns}}{\text{Trip}} \right)
 \end{aligned}$$

Quite interestingly, they differentiate between engine drivetrains where there is an engine gearbox attached to the engine. I suspect this reflects the difference between a Boeing Vertol

## 2.9 OPERATING COSTS

107 and a Sikorsky S-61 as Gallagher experienced at New York Airways in 1967. To account for “engines with gearboxes” they only changed one number in Eq. (2.368), which had to do with the man-hours per rotor hours. They suggested that the configuration differences should increase

$$\text{from } \left[ 0.50N_{\text{eng}} + 0.02N_{\text{eng}} \left( \frac{\text{SHP}_{\text{TO rated}}}{1,000} \right) \right] \text{ to } \left[ 0.55N_{\text{eng}} + 0.02N_{\text{eng}} \left( \frac{\text{SHP}_{\text{TO rated}}}{1,000} \right) \right].$$

Stoessel and Gallagher then gave their equation for engine materials per trip offering:

$$(2.369) \quad \frac{\text{Dollars}}{\text{Trip}} = \left[ 2.1N_{\text{eng}} \left( \frac{\text{Cost}_{\text{eng}}}{10^5} \right) \right] \left( \frac{\text{Rotor hours}}{\text{Trip}} \right) + \left[ 1.3N_{\text{eng}} \left( \frac{\text{Cost}_{\text{eng}}}{10^5} \right) \right] \left( \frac{\text{Flt. cycles}}{\text{Trip}} \right) + \left[ 0.7N_{\text{eng}} \left( \frac{\text{Cost}_{\text{eng}}}{10^5} \right) \right] \left( \frac{\text{Engine shutdowns}}{\text{Trip}} \right)$$

The configuration description provided in Table 2-55 only needs the added information that the S-55 had only one engine ( $N_{\text{eng}} = 1$ ), a Pratt & Whitney Wasp R-1340-57, rated at a  $\text{SHP}_{\text{TO rated}}$  of 600 horsepower takeoff at sea level on a standard day. The S-61 was a twin-turboshaft-powered machine ( $N_{\text{eng}} = 2$ ). One engine was rated at  $\text{SHP}_{\text{TO rated}}$  equal 1,400 horsepower. Neither helicopter had engines delivered with gearboxes, so Eqs. (2.368) and (2.369) apply in this comparison.

Again, from here on out the calculations are straightforward arithmetic, and you will find that “engine” direct maintenance costs for one trip amount to:

S-55 equals \$18.04 per trip for engine direct maintenance (\$9.51 labor; \$8.53 materials)

S-61 equals \$49.34 per trip for engine direct maintenance (\$20.09 labor; \$29.25 materials).

### 2.9.3.5.3 Total of Direct Maintenance Costs

The contributions of airframe and engine maintenance costs can be summarized as you see here in Table 2-56.

This summary would, of course, be incomplete without highlighting what many perceive as the key parameter of man-hours per flight hour. You no doubt realize that Stoessel and Gallagher chose instead man-hours per rotor-turning hour based, I would assume, on New York Airways’ operational data. They apparently felt that it made little difference to maintenance costs whether the rotor was turning in flight or running at ground idle.

**Table 2-56. S-55 and S-61 Direct Maintenance, \$/Trip Data for DOC Calculations**

Helicopter	Total	Airframe Total	Airframe Labor	Airframe Material	Engine Total	Engine Labor	Engine Material
S-55	71.35	53.31	41.95	11.36	18.04	9.51	8.53
S-61	117.62	68.27	51.17	17.10	49.34	20.09	29.25

To emphasize what I believe was their main point, they included two graphs showing how maintenance man-hours could accumulate when flight cycles, and engine shutdowns and restarts, are added to man-hours required because of rotor-turning time. These two pieces of information are included here as Fig. 2-412 and Fig. 2-413. These two figures show that using a helicopter (or any other VTOL machine, for that matter) on very short-haul trips, like a bus or perhaps even commuter trains, can require as many labor man-hours due to stopping and starting as are required because of cruising.

Before going on to depreciation, the last operating cost line item, there is one thing I might add. It bothers me that the curves shown in Fig. 2-412 and Fig. 2-413 do not go through zero-zero. In fact, the dominant man-hour cost in the airframe group says that even if the

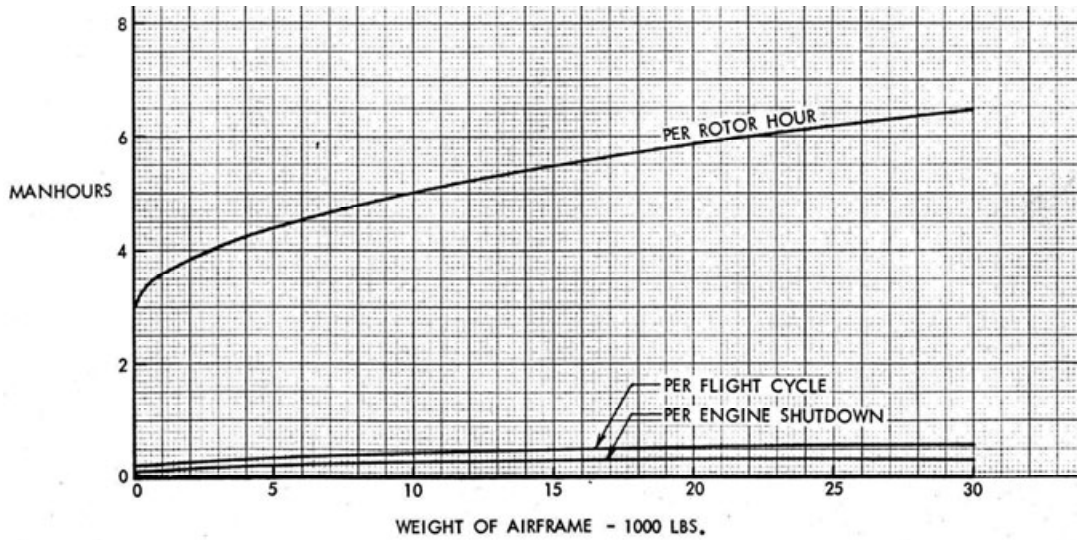


Fig. 2-412. Airframe maintenance labor man-hours are a function of airframe weight (i.e., weight empty less engine(s) dry weight) [639].

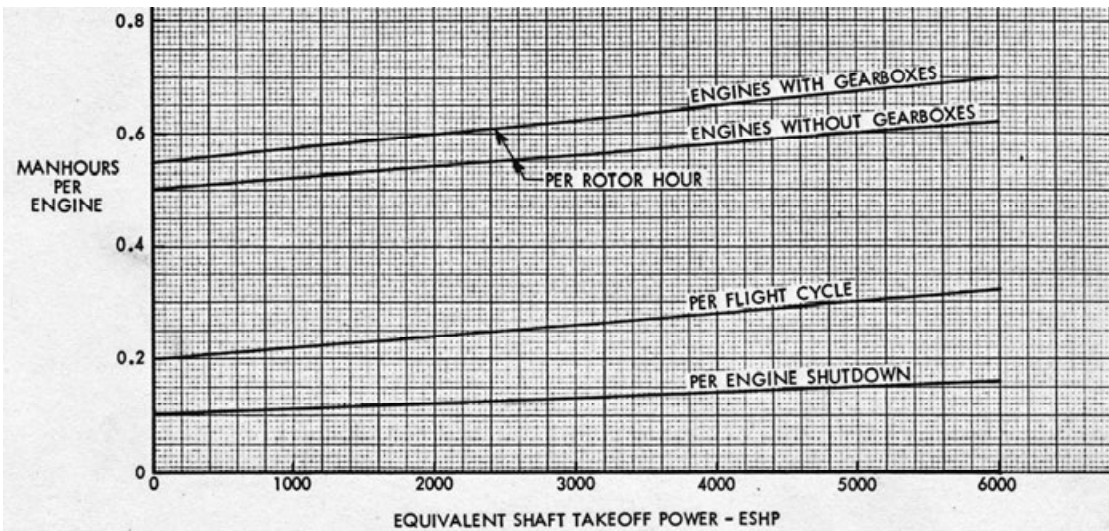


Fig. 2-413. Engine maintenance labor man-hours are a function of the engine's sea-level standard takeoff rating [639].

## 2.9 OPERATING COSTS

airframe weight (which includes the rotor systems) is zero, it still takes 3 man-hours per rotor-turning hour. This assumption implies that small, 2- or 3-seat helicopters will be severely penalized. Therefore, I would suggest that Stoessel and Gallagher's curves deserve some attention. The curves may be quite satisfactory for the Boeing Vertol 107- and Sikorsky S-61-size machines of the 1960s, and even for larger VTOL configurations. However, an extrapolation to helicopters of twice the size must surely be open to question. Frankly, the situation today is that the rotorcraft industry is still having considerable trouble establishing believable maintenance man-hours per flight hour even after detail design is completed.

### 2.9.3.6 Depreciation of Flight Equipment

In approaching direct operating costs due to depreciation, Stoessel and Gallagher took the position that "there seems to be no reason for VTOL aircraft to have shorter useful lives than comparable CTOL aircraft. Therefore, a 12-year depreciation period is used herein for VTOL aircraft, with a zero residual value. This is the equivalent of: 9 years to 25 percent residual value or 10 years to 16-2/3 percent residual."

Stoessel and Gallagher also noted that "larger fleets require less spares than smaller fleets, if other factors such as the degree of spares pooling and the number of enroute (or through) and turnaround stops remain substantially unchanged. For analyses involving a single-based shuttle service, and also for a multi-base inter-city operation, the following spares provisioning allowances are recommended: (1) airframe spares, as a percent of aircraft cost, less engines [should be] 10 percent and (2) engine spares, as a percent of engine costs [should be] 40 percent."

With those thoughts in mind, they offered the following equation for estimating depreciation including spares

$$(2.370) \quad \frac{\text{Dollars}}{\text{Year}} = \frac{(1 + K_{\text{af spares}}) \text{Cost}_{\text{af}} + (1 + K_{\text{eng spares}}) N_{\text{eng}} \text{Cost}_{\text{eng}}}{\text{Depreciation period}}$$

and recommend that the airframe spares constant ( $K_{\text{af spares}}$ ) be 0.10, and the engine spares constant ( $K_{\text{eng spares}}$ ) be 0.40. They seemed quite comfortable (in 1967) with a depreciation period of 12 years.

On this basis, you have the comparable depreciation (including spares) yearly expenses of \$117,500 per year for the S-61 and \$34,270 per year for the S-55. Fortunately, these yearly costs can be spread over 936 trips per year. You might note in passing that you are, in effect, buying the helicopters and spares all over again every 12 years. This is a cost line item that CPAs probably understand better than I do. At any rate, you have:

S-55 equals \$36.61 per trip for depreciation (including spares)

S-61 equals \$125.53 per trip for depreciation (including spares).

### 2.9.3.7 DOC Calculation Summary

Looking at a summary table obtained with the Stoessel and Gallagher DOC calculator lets you draw some very interesting conclusions. As you see here in Table 2-57, the direct operating cost to fly the S-61 on one trip is just about 1.9 times the cost of flying the S-55 on one trip. This is hardly unexpected because the S-61 is powered by twin-turboshaft engines and has 26 seats available. The piston-powered S-55 has only 10 seats available.

The more common parameter for decision making is DOC per available seat-mile. Because the flight profile has been done for a route that totals 85 miles, you can quickly see that the S-61, with 16 additional seats, does offer an economical improvement over the S-55. That is, for the S-55 you will estimate

$$S-55 = \frac{\$191.22}{10 \text{ seats} \times 85 \text{ miles}} = 22.5 \text{ cents per available seat-mile,}$$

and for the S-61 you see hope because

$$S-61 = \frac{\$359.73}{26 \text{ seats} \times 85 \text{ miles}} = 16.3 \text{ cents per available seat-mile.}$$

This comparison certainly provides a basis for going to the Project Hummingbird program managers and pleading for an extension of temporary certification (along with its subsidy) to Los Angeles Airways, Chicago Helicopter Airways, and New York Airways.

However, the extensions ultimately were not granted, and this first voyage by rotorcraft into the airline business came to an end in April of 1965.

**Table 2-57. S-55 and S-61 Direct Operating Costs, \$/Trip Data Comparison**

DOC Line Item (\$/Trip)	S-55	S-61
DOC total	191.22	359.73
Flying operation	83.26	116.57
Flight crew	70.07	71.87
Fuel and oil	5.71	19.06
Insurance	7.48	25.64
Maintenance	71.35	117.62
Airframe	53.31	68.27
Engine	18.04	49.34
Depreciation (including spares)	36.61	125.53

## 2.9 OPERATING COSTS

### 2.9.4 S-61 Direct Operating Costs in 2011

You might be interested in seeing what time has done to the direct operating costs of flying a Sikorsky S-61 in 2011. This updating will change your perspective about what cost items are the big drivers. You have seen in Table 2-57 that direct operating costs for the S-61 amounted to \$359.73 per trip. The situation in 2011 is somewhat different, primarily because of inflation.

To build the direct operating cost story in 2011, let me introduce you to a very refined source that you should be aware of. This commercially available source arose from work started by Alan Conklin and Bill de Decker in the mid-1970s. Their efforts created a company (Conklin & de Decker Associates, Inc.) that has grown into an industry source of aviation information. They have a software product available today that evaluates aircraft operating costs. I purchased the computer program *Aircraft Cost Evaluator (ACE)* [640] because it includes variable operating costs, fixed operating costs, and total operating costs<sup>208</sup> of nearly 100 helicopters currently in operation. The company has not added a capability to predict costs of an aircraft in design and development, but with all their current insight, I imagine they could.

The Sikorsky S-61N is one of the helicopters in the *Aircraft Cost Evaluator* data bank. The cost line items in this evaluation tool are not directly comparable to the classic DOCs used in the world of fixed-wing aircraft operating in today's airlines. (I will discuss the cost line items preferred in the world of helicopter operations in more detail later.) However, all the data required to make a nearly apples-to-apples comparison to what you have learned so far is there. You will recall that I expressed DOC in dollars per trip and that a trip was 85 statute miles, not nautical miles, which is the preferred unit today. The 1967 versus 2011 comparison shown in Table 2-58 is quite interesting. Notice immediately that the proportions of the three major line items (i.e., flying operations, maintenance, and depreciation) do not appear to have changed significantly. But within flying operations, fuel has become nearly one-half of the cost versus being less than one-fifth of the cost in 1967. Notice also that maintenance costs per trip have increased by a factor of 12. (Let me discuss maintenance in

**Table 2-58. S-61 DOC, \$/Trip Cost Comparison Between 1967 and 2011**

DOC Line Item (\$/85-Statute-Mile Trip)	S-61 in 1967	S-61 in 2011
DOC total	\$359.73	\$3,443.57
Flying operation	116.57	1,438.53
Flight crew	71.87	315.77
Fuel and oil	19.06	887.47
Insurance	25.64	235.29
Maintenance	117.62	1,482.18
Depreciation (including spares)	125.53	522.86

---

<sup>208</sup> The bookkeeping of operating cost line items is somewhat different from that used by Stoessel and Gallagher who patterned their line items on the Air Transport Association's Report 100.

more detail shortly.) Finally, you can see that depreciation has increased by a factor of 5, primarily because in 1967 the S-61 had a list price of \$1,200,000, which translates to a list price of \$3,187,500 in 2011. Overall, there appears to be a growth factor of 10 in total DOCs over the 45-year period. It is worth noting that when configured in an airliner interior with 26 seats for passengers, the calculated DOC per available seat-mile is 16 cents (i.e., \$359.73 divided by 85 and 26) when the S-61 was operating for New York Airways in 1967. Today that cost is estimated to be \$1.56. When comparing helicopter DOCs in 1967 per available seat-mile of 16 cents to fixed-wing aircraft as shown on Fig. 2-400, even I get a little discouraged about ever seeing large fleets of helicopters carrying millions of passengers from city center to city center.

### 2.9.5 Fuel and Maintenance DOCs in 2011

Because Table 2-58 shows that, today, fuel and maintenance costs are big-ticket items within flying operations, they deserve more detailed discussion. I have chosen to address these two cost line items in the paragraphs that follow. The discussion will draw on the data bank embedded in the *Aircraft Cost Evaluator* by Conklin & de Decker Associates, Inc., because the data bank has been created from broad surveys of many helicopter operators.

Today you will encounter direct operating costs expressed in dollars per hour, particularly when comparing a number of different helicopters. You will also find that the dollars-per-flight-hour convention is used by the *Aircraft Cost Evaluator*, so let me discuss fuel and maintenance direct operating costs in those units.

#### 2.9.5.1 Fuel and Oil Operating Costs in 2011

Consider fuel (and oil) costs first. This line item cost per flight hour depends, to the first approximation, on only two parameters. Simplistically, you can state that

$$(2.371) \quad \frac{\text{Fuel DOC}}{\text{Hour}} = \left( \frac{\text{Gallons of fuel used}}{\text{Flight hour}} \right) \left( \frac{\text{Fuel price}}{\text{Gallon}} \right) = (\text{Fuel Flow}) \left( \frac{\text{Fuel price}}{\text{Gallon}} \right).$$

It is true that books have been written about aviation fuel. However, for my purposes here in August of 2012, it is sufficient to say that Jet A gas used for turbine engines costs about \$6.67 per gallon and has a density of 6.7 pounds per gallon. For piston engines, you have AvGas at \$7.29 per gallon with a density of 6.1 pounds per gallon.

A helicopter operator (and the chief engineer, as well) are at the mercy of the world's commodities markets for the price of fuel on any given day (see Fig. 2-414). Furthermore, both interested parties must accept what chemical engineers have achieved in extracting energy per gallon of fuel. The only thing left that will lower fuel costs is to burn less fuel for any given job. To the user this means buying helicopters that are the most fuel efficient.<sup>209</sup>

---

<sup>209</sup> To the practicing helicopter engineer, this means increasing specific range, which is the name these engineers give to pounds of fuel burned per nautical mile flown. You encountered this very important parameter earlier in the discussion about fuel efficiency in Section 2.5, starting on page 267 of this volume.

## 2.9 OPERATING COSTS

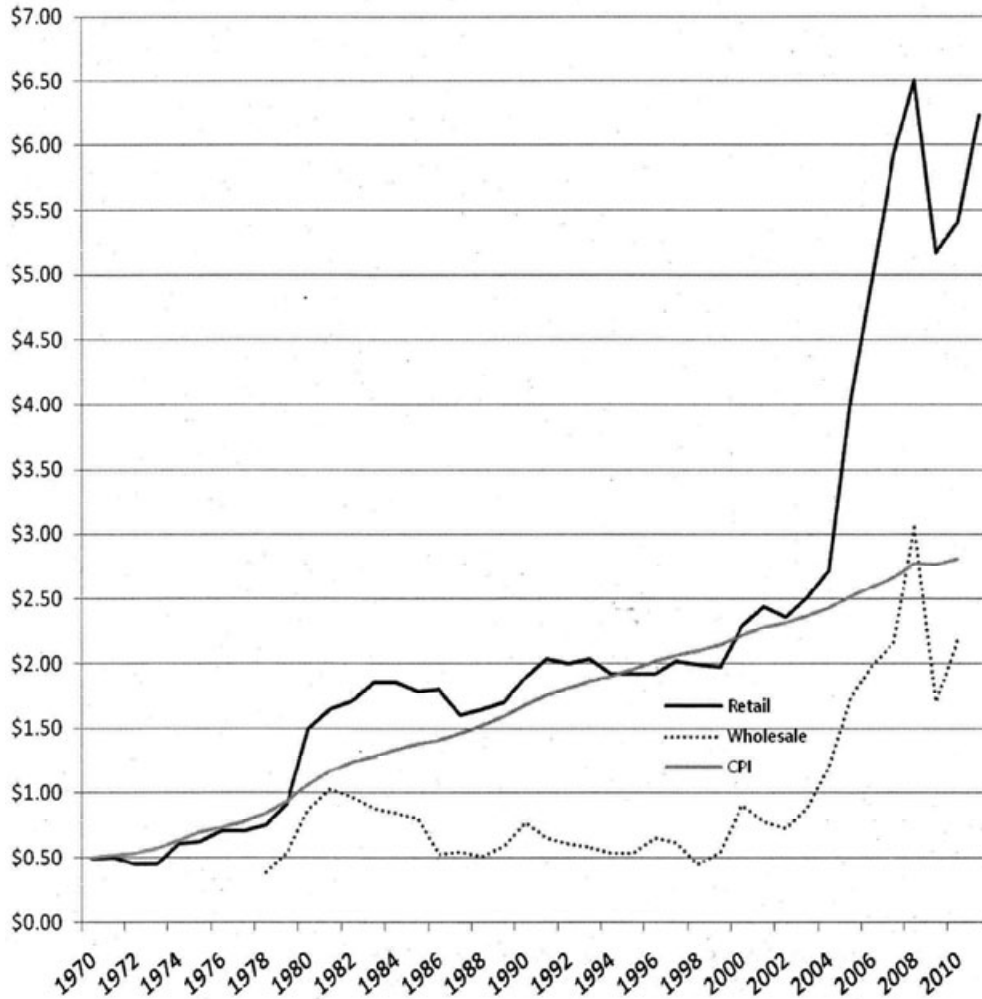


**Fig. 2-414. You are probably well aware of this dollars-per-gallon trend because the cost of gasoline for a car simply parallels this data for Jet A fuel used by gas turbine engines (courtesy of Conklin & de Decker Associates, Inc.).**

The gallons per hour (i.e., fuel flow) that a helicopter uses in a given job depends, of course, on the job. Hovering for an hour can be very expensive as opposed to cruising at the most economical speed for an hour. To examine fuel and oil contributions to DOC in this discussion, let me assume a passenger-carrying job between two cities that are 50 nautical miles apart. Imagine the trip begins with a taxi, takeoff, and climb, and then cruises 50 nautical miles. The trip ends with a descent, landing, and taxiing to where the passengers can get out. I will assume that when in cruise, the speed is, say for an S-61, 110 knots, which means in-flight time is about three-quarters of an hour. The actual time the rotor is turning adds, to keep things simple, about 15 percent of the cruise time for such a short-distance flight. The passengers think the trip is just under an hour, and they would compute the average speed at about 100 knots. The S-61 pilot would read from his instruments that this helicopter was burning fuel at roughly 175 gallons per hour. With Jet A fuel selling for \$6.67 per gallon, that 1-hour trip incurs fuel expenses amounting to \$1,167. Within the accuracy of the numbers, I will say that oil is included in the \$1,167 at about 3 percent, or roughly \$35.

You can see that fuel flow (i.e., gallons of fuel burned per hour) is a very influential parameter. Fortunately, the *Aircraft Cost Evaluator* has nominal fuel-flow data for nearly 100 helicopters in its data bank. This practical operational data, when graphed as shown here in Fig. 2-415, gives you a very good idea of what today’s current civil helicopter fleet experience is. The lowest line on Fig. 2-415 represents, in my opinion, helicopters with 1990s technology doing 150- to 200-nautical-mile trips, such as offshore oil rig support [641]. The middle line is a regression analysis result for all turbine-powered helicopters. I see this line as representing all helicopters in a general utility role. The highest line is my view of what the first generation of turbine-powered helicopters achieved. The combination of improved turbine engine technology and attention to helicopter parasite drag has improved fuel efficiency from a coefficient of 0.036 to 0.023, which, by my calculation, is a 37 percent improvement (i.e.,  $0.023/0.036 = 0.63$ ). On the other hand, all the progress that engineers can make to helicopter fuel efficiency (and thus lower fuel DOC) in a decade or two gets wiped out when the price of a gallon of Jet A fuel jumps by a factor of two or three, as Fig. 2-414 shows can happen. This makes fuel efficiency even more important.

It is, of course, possible to get into a discussion that splits hairs about (a) not accurately accounting for all segments of a flight profile, or (b) not following FAA rules for fuel reserves, or (c) simply lumping oil used as a percentage of fuel used. In my opinion, if selling a new helicopter to a potential civil customer requires this kind of discussion, the design is most certainly too marginal. Most importantly, as demonstrated so far, the helicopter lacks the fuel efficiency that operators of fixed-wing aircraft have come to expect. This fact was even clear during the autogyro era as Fig. 2-125 on page 261 of Volume I shows.

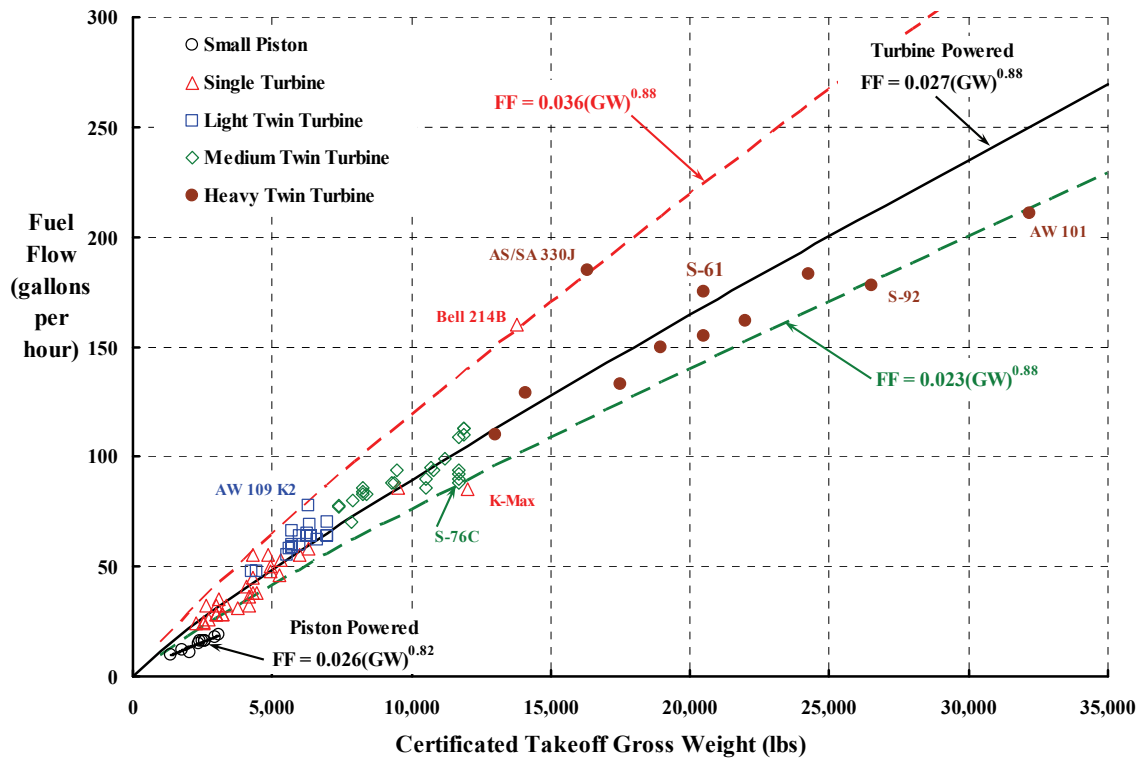


Fig. 2-415. Fuel efficiency of today’s civil helicopter fleet [640].

## 2.9 OPERATING COSTS

In dealing with direct operating costs, I prefer to express the costs as dollars per available seat-mile (however, you should remember that dollars per flight hour is a very popular metric.) Because dollars per available seat-mile has been a well-used parameter within the transportation world, I find it less confusing; once you have the dollars per mile (be it statute or nautical) it is a simple step to see how the helicopter's interior might be configured for the lowest DOC. Of course, a helicopter configured with a limited-seating executive interior will always show a higher DOC per available seat-mile than a helicopter configured for a commercial or utility job.

The fuel flow data in Fig. 2-415 can be transposed to fuel cost per nautical mile quite easily just by dividing fuel DOC per hour by cruise speed. That is,

$$(2.372) \quad \frac{\text{Fuel DOC}}{\text{Nautical mile}} = \frac{(\text{Fuel flow}) \left( \frac{\text{Fuel price}}{\text{Gallon}} \right)}{\text{Cruise speed in nautical miles per hour}} = \frac{\text{Fuel DOC/Hour}}{V_{cr} \text{ in knots}}.$$

An additional step can be taken to show the fuel efficiency parameter that helicopter performance engineers are most accustomed to using. This parameter is called specific range and has the units of nautical miles traveled per pound of fuel burned. Thus,

$$(2.373) \quad \text{Specific Range} = \frac{\text{Nautical mile}}{\text{Pound of fuel used}} = \frac{V_{cr}}{(\text{Fuel flow})(\text{Fuel density})}.$$

Specific range for the current civil helicopter fleet is shown in Fig. 2-416. This is the helicopter engineer's way of seeing the fuel flow data shown in Fig. 2-415. Unfortunately, it is quite rare to see engineering fuel efficiency results that include the price of fuel.

You can see in Fig. 2-416 that quite a few turbine-powered helicopters define the top of scatter in this important parameter. This top of scatter line is, in my mind, the fuel efficiency that all future helicopters should meet or exceed. On the undesirable side, you see several helicopters are performing rather poorly in the field. [As an aside, I would suggest that the goal of a new design should be at the top of scatter; but to marketing (and the customer) I would base fuel and oil costs derived by using the bottom of scatter. This would give a better than 50-50 chance of delivering what is promised, keep engineering's focus on what is possible, and offer hope that the new helicopter would perform above the mean of scatter. Of course, this approach to quoting fuel efficiency should not be kept a secret; everybody should be aware of it.]

Specific range can be calculated rather accurately for any helicopter design as it progresses from concept to completion of qualification testing. However, the *Aircraft Cost Evaluator* accounts for all aspects of any given job, but only with a first-order approximation. This means that idle, taxiing, hold for traffic, takeoff, climb, and begin cruise, etc., are lumped into an overall specific range value. The data bank does allow a benchmark for a nominal, average specific range of helicopters currently in operation. This benchmark, shown here as Fig. 2-416, is quite valuable when bridging the gap between an engineer and an operator because it tells the engineer to allow for the difference between theory and real-life operator experience.

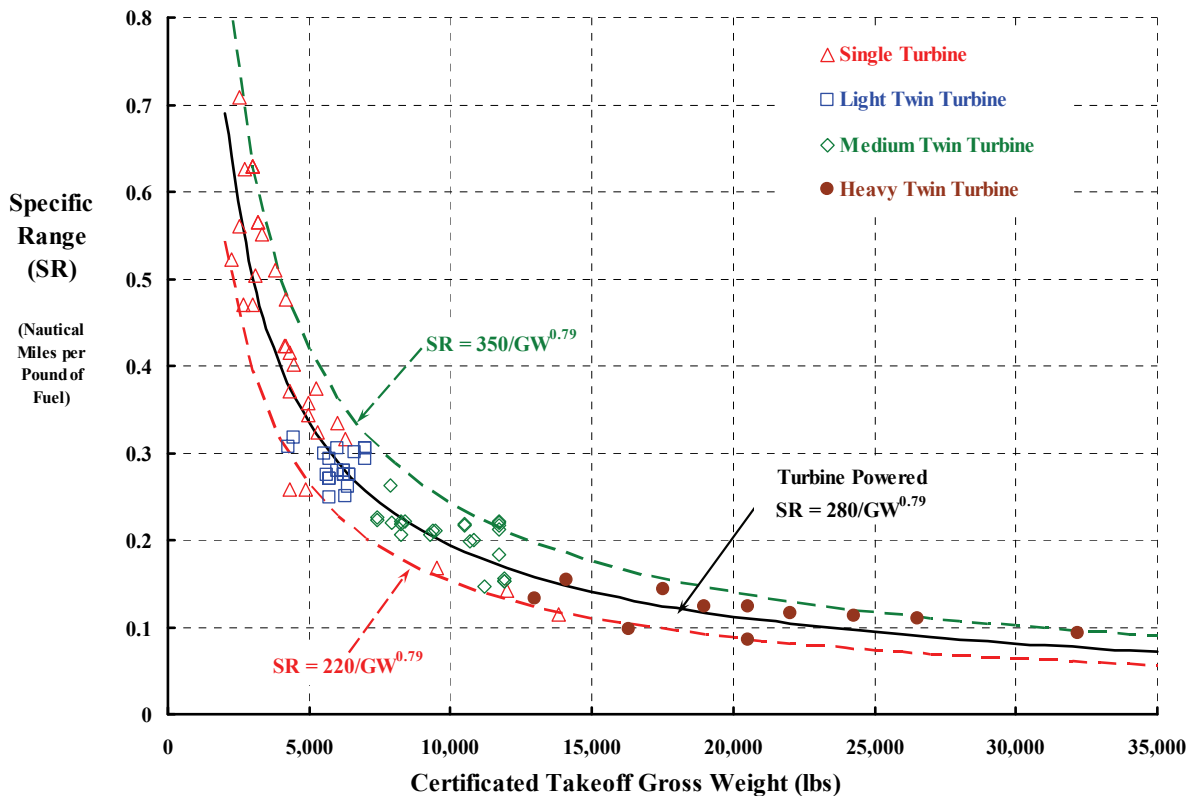


**Fig. 2-416. Specific range in cruise flight of operational, turbine-powered civil helicopters. Derived from Conklin & de Decker’s *Aircraft Cost Evaluator* data bank. Includes 30 percent for reserve and 3 percent for oil.**

There is a fundamental about fuel efficiency that you should be aware of. In helicopter performance calculations for any given helicopter and its engine (or engines), specific range varies (a) with speed at a given weight and altitude, (b) with weight in flight at a given altitude, and (c) with altitude for a given weight. Let me illustrate this important fundamental with Fig. 2-417, which shows specific range varying with speed. Because the S-61 has been used as an example earlier, pretend that Fig. 2-417 is for an S-61 at sea level on a standard day and at its certificated maximum flight weight of 20,500 pounds.

Two views of fuel efficiency are shown in Fig. 2-417. First take a look at what the helicopter performance engineer might present for the efficiency in nautical miles per pound of fuel used—*after the calculation is reduced by about 25 to 30 percent to approximate an operator’s real-life usage*. Performance engineers most frequently want to state nautical miles per pound at a high cruise speed, a practice that comes from dealing with military requirements. Generally, military requirements are weight driven. To find this cruise speed, the maximum nautical mile per pound is multiplied by 0.99, and a horizontal, dashed line is drawn as shown on the figure. This line intersects the specific range curve at two speed points, which, in this example, are at 99 and 113 knots. The engineer will only quote the cruise speed at the 113-knot point. In my experience, it is rare that an engineer will add that the specific range of 0.085 equates to 0.57 nautical miles per gallon given that Jet A fuel

## 2.9 OPERATING COSTS

weighs 6.7 pounds per gallon. Only once in my career have I heard an engineer throw in an “oh, and by the way, Jet A fuel is selling for \$6.67 per gallon so our design spends \$11.67 per nautical mile at 113 knots!”

Now, look at Fig. 2-417 from an operator’s point of view. The lower line (in green) is fuel DOC in dollars per hour, which you read on the right-hand scale. According to the *Aircraft Cost Evaluator* data bank, the typical S-61 operator cruises the machine at about 100 to 115 knots, but generally closer to 100 knots. This speed range is precisely where the fuel DOC per nautical mile is a minimum. The geometry of these statements is illustrated by the straight, dashed line in Fig. 2-417. You can see that this line is just tangent to the fuel-DOC-per-hour curve at about 105 knots. (Keep in mind that dollars per hour divided by cruise speed in knots is dollars per nautical mile.) Furthermore, an operator is likely to choose the lower speed because the fuel DOC per hour is lower.

In short, the civil operator chooses to fly a helicopter at slightly lower speed than a military operator because he does not value speed quite as much as his military counterpart. And, of course, other line items that contribute to DOC benefit by flying a helicopter at reduced power.

This brings me to a discussion about maintenance direct operating costs.

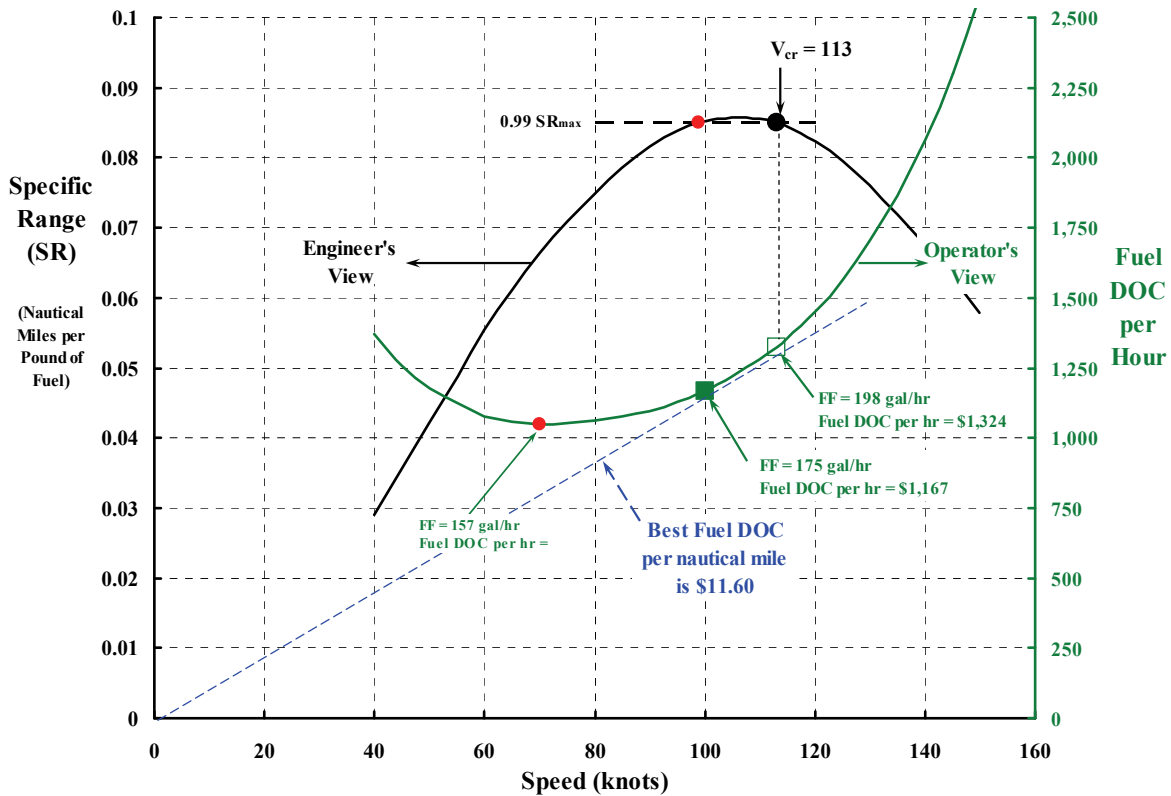


**Fig. 2-417. Engineers and operators frequently see fuel efficiency in quite different ways. Furthermore, the military operator values speed and weight above hourly costs.**

**2.9.5.2 Maintenance Costs in 2011**

The 2011 maintenance cost of the S-61 is estimated in my example at \$1,482 per 85-statute-mile trip as Table 2-58 records. In more conventional terms, this equates to \$17.44 per statute mile (i.e., 1,482/85). In fact, the *Aircraft Cost Evaluator* obtains its estimate of variable costs in terms of dollars per cruise flight hour and uses 100 knots or 115 miles per hour as the average cruise speed for the S-61. (It calculates fixed costs in dollars per year.) This means that a conversion from my DOC example using dollars per 85-statute-mile trip requires division by 85 to get dollars per statute mile and then multiplying by a cruise speed of 115 miles per hour to get maintenance dollars per cruise flight hour. The conversion of total maintenance costs from my 85-statute-mile-trip example to the more often quoted dollars per flight hour, along with some notes, is shown in Table 2-59. All estimates in this example are based on surveys of helicopter operators flying the S-61, and include considerable research and analysis on the part of the Conklin & de Decker group.

Estimating maintenance costs per flight hour before the helicopter has even flown is a relatively new concept to the helicopter industry. It is, of course, not new to the fixed-wing manufacturing industry because they, and the several airlines operating in the United States, have been at it for about nine decades. The airlines, as certificated by the FAA, have a very well developed accounting tree (see Fig. 2-402) and any number of Form 41 financial and economic reports [636] that you could refer to and perhaps follow. They also have the Air Transport Association (ATA), that has acted as a spokesman for the whole airline service industry [642] for just over 75 years. The corresponding organization for helicopters is the Helicopter Association International (HAI) that has, since 1948, been dedicated to promoting the helicopter as a safe and efficient method of transportation, and championing the advancement of the civil helicopter at every opportunity.

Unfortunately, the FAA classifies helicopters as part of the much larger General Aviation group that they keep track of. As such, financial and economic data for helicopters is nowhere near airline data in depth and accuracy. Fortunately, the HAI’s Economic Committee has continually improved its *Guide for the Presentation of Helicopter Operating Cost Estimates*, the latest revision being dated October 2010 [643]. The industry has struggled with a number of questions since the *The Guide* first came out in 1981. The effort to obtain some uniformity in just defining terms and establishing common accounting practices has not been easy. The effort is difficult because of three primary reasons. First, helicopters come in so

**Table 2-59. S-61 Estimated Maintenance Cost Breakdown**

<b>Maintenance Total</b>	<b>\$1,482 Per 85 Statute Miles</b>	<b>\$2,008 Per Flight Hour</b>	<b>Notes</b>
Labor	\$402.16	\$514.82	5.47 man-hours per flight hour; \$94 per labor hour
Parts airframe/engine/avionics	\$216.92	\$293.87	Referred to as just “materials” by some
Engine restoration	\$341.52	\$462.66	Often called engine overhaul
Major periodic maintenance	\$476.86	\$646.01	Daily, 100 hours, 250 hours, etc.
Refurbishing (interior)	\$44.72	\$60.58	10 man-hours per seat per year; labor rate of \$94 per hour

## 2.9 OPERATING COSTS

many different types and sizes. Second, many variables can affect the operating costs, even for a given type helicopter. Third, published operating costs from a variety of sources can represent a variety of assumptions. The HAI envisions that it can ultimately serve as a repository for the developing knowledge of operating cost estimates. Despite the fact that an individual operator considers its operating costs quite proprietary, there has been a great deal of progress as you will see by reading a copy of *The Guide* [643]. Now, let me show you the current civil helicopter fleet's maintenance cost, line item by line item, using the Conklin & de Decker *Aircraft Cost Evaluator* data bank as the most representative and reliable source.

### 2.9.5.2.1 Direct Maintenance Labor Costs in 2011

Invariably, the first line item is the direct operating cost of maintenance labor, which depends on two components and is calculated as

$$(2.374) \quad \frac{\text{Labor DOC}}{\text{Flight hour}} = \left( \frac{\text{Labor hours}}{\text{Flight hour}} \right) \left( \frac{\text{Labor Dollars}}{\text{Labor hours}} \right) = \left( \frac{\text{MMH}}{\text{FH}} \right) \left( \frac{\text{Labor Dollars}}{\text{Labor hours}} \right).$$

It is here that one of the most (if not *the* most) difficult parameters to estimate in the whole set of DOC accounting line items is found. This parameter is maintenance man-hours per flight hour (MMH/FH) and, to this day, accurately pinning down MMH/FH in advance of operating experience seems nearly impossible. This, of course, is a minor difficulty for the military who are very careful to require a potential helicopter contractor to include “design to” values in a system specification. For example, paragraph 3.2.4 of the OH-58D specification (Fig. 2-418) [644] specifically states:

3.2.4 **Maintainability.** The OH-58D system shall be designed to achieve the following maintainability when performing the mission defined in 3.2.1.1.2.d, and operating under the environmental conditions of 3.2.7. Preventive and corrective maintenance tasks shall be assumed to be conducted by Army personnel with a skill level equivalent to that of an Army aircraft maintenance school graduate with 6 months on-the-job experience. Repair tasks or downtime attributable to enemy action or operation of equipment outside of prescribed limits are excluded from stated maintainability.

3.2.4.1 **OH-58D maintenance man-hour to flight-hour ratio.** The OH-58D shall be designed so that maintenance shall not exceed the following direct scheduled and unscheduled productive maintenance man-hour to flight-hour ratio of: (See 6.3.11)

<u>AVUM<sup>1</sup> &amp; AVIM<sup>2</sup></u>	
Helicopter	1.175
MMS	.300
OH-58D	1.475

<sup>1</sup>AVUM = Aviation Unit Maintenance

<sup>2</sup>AVIM = Aviation Intermediate Maintenance

The above maintainability shall be allocated as follows:

	AVUM	AVIM	TOTAL
<b>Unscheduled</b>			
Airframe	.166	.238	.404
Engine	.060	.088	.148
MMS	.075	.225	.300
Other	.079	.114	.193
<b>Scheduled</b>			
OH-58D System Total	.430	-	.430
	.810	.665	1.475

Maintenance at the AVUM is assumed to be performed by no more than two mechanics with tools provided in the general mechanic's tool set and a minimum of special tools. Definitions of MIL-STD-721 and 90 flying hours per month shall apply.

**Fig. 2-418. MMH/FH “design to” requirements for the U.S. Army OH-58D [644].**

You might note that this requirement has a parenthetical note in paragraph 3.2.4.1 to “see 6.3.11.” When you turn to that system specification paragraph, you will find that it is titled *Minimum Performance* and says:

“The performance values referenced in these paragraphs [3.2.4.1 and others] are predicted values to which the contractor [Bell Helicopter] shall design, test and qualify. In the event that demonstrated values fail to confirm the predicted values, the following are the minimum demonstrated values which shall be considered to fulfill the requirements of this specification.”

And in a subparagraph, 6.3.11e, you will read that minimum maintenance values were:

- “(1) Allocation of subsystem values for each of the above paragraphs will be incorporated at the final configuration audit.
- (2) OH-58D system maintenance manhours to flight hour ratio of 1.8.”

In short, the “design to” requirement for the OH-58D system total was an MMH/FH ratio of 1.475. Furthermore, if the OH-58D overall system MMH/FH was at or below 1.8 in operation, Bell was not to be penalized. In my opinion, the U.S. Army’s need was clearly stated, and the latitude they would accept was equally clear.<sup>210</sup>

The military requirement to pay attention to MMH/FH in design is just as important to manufacturers and operators of civil helicopters. The industry’s success is shown in Fig. 2-419. The data is graphed versus weight empty, but it should be clear that MMH/FH

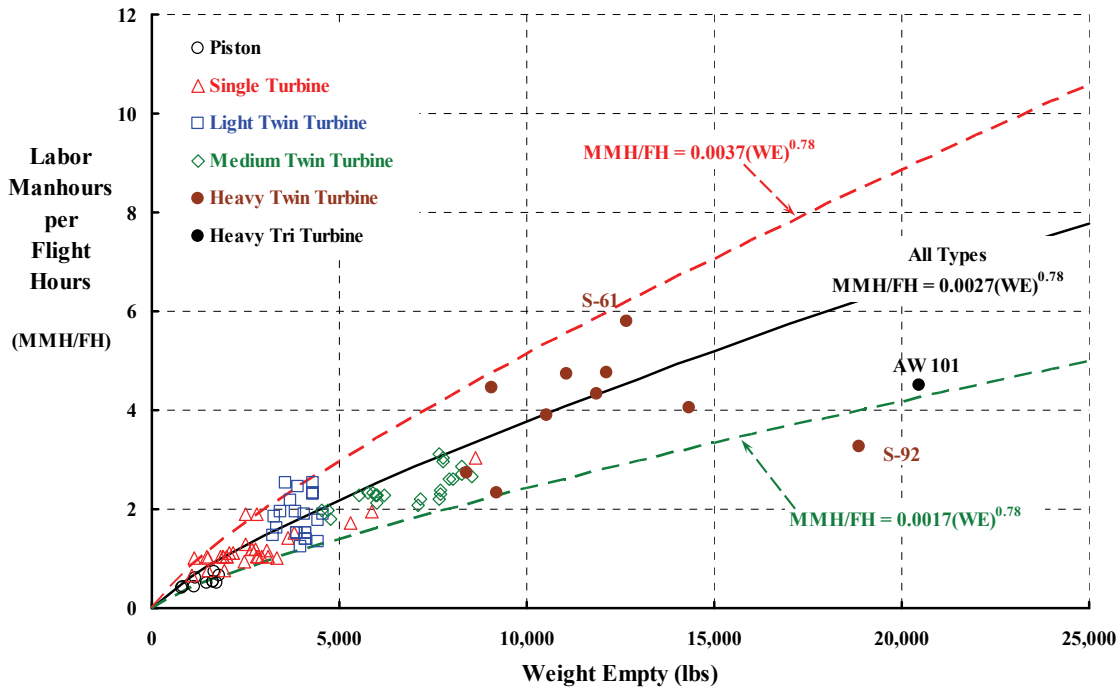


**Fig. 2-419. Direct maintenance labor hours per flight hour (derived from Conklin & de Decker’s *Aircraft Cost Evaluator* data bank).**

<sup>210</sup> The Advanced Helicopter Improvement Program (AHIP) team is quite proud (and happy, as well) that the OH-58D and its several upgrades are still performing well in the field even as I write this volume about helicopters [145].

## 2.9 OPERATING COSTS

depends on many variables besides weight empty. You know this because there is so much scatter in the data. I found from regression analysis that no combination of typical design and configuration data reduced the scatter. Therefore, the use of weight empty as the abscissa in Fig. 2-419 is only a convenient way to summarize the available data. Nevertheless, let me suggest that the lower curve in Fig. 2-419 would be the starting point for a conceptual design.

The only other parameter you need to estimate maintenance labor's contribution to DOC is, following Eq. (2.374), the hourly labor pay rate. As you might guess, the *Aircraft Cost Evaluator* data bank has the trend of this parameter with years, and it is available here as Fig. 2-420. It interesting to me to wonder just how would a chief engineer, and other members of the company, guess maintenance labor costs for a configuration that is just beginning to come together in preliminary design and is probably 3-plus years away from the first delivery to a customer.

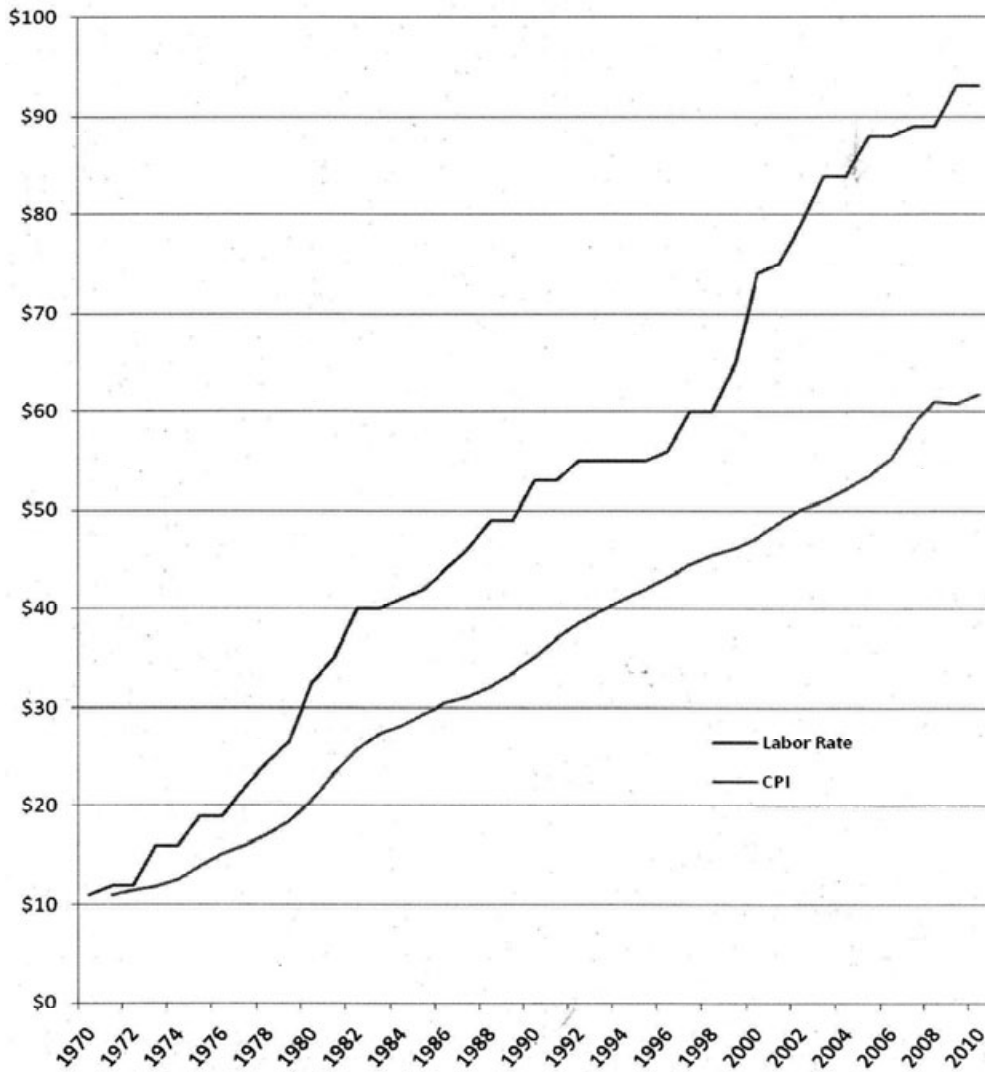


**Fig. 2-420. The trend in labor rates over the past three decades (courtesy of Conklin & de Decker, Inc.).**

You should know that each of the major helicopter manufacturers keep track of their products' performance in the field. Bell Helicopter, for example, has published a quarterly newsletter called Rotor Breeze<sup>211</sup> for many years. Each year, they pick one issue and include an article titled *Direct Maintenance Cost Projection* for that year. An example for 2012 is shown here in Fig. 2-421 [645]. If you look just below the label "Labor Sub-Total" in bold print you see a line labeled "MMH/FH." This is the company's estimate of maintenance man-hours per flight hour based on the operators they have surveyed. It probably will not surprise you to learn that these Bell Helicopter estimates do not agree with MMH/FH estimates embedded in Conklin & de Decker's *Aircraft Cost Evaluator*. Here is the comparison:

<b>Bell Helicopter Textron Inc.</b>				
<b>2012 Direct Maintenance Cost Estimates <sup>(1)</sup></b>				
<b>Airframe</b>	<b>206L4</b>	<b>407</b>	<b>412</b>	<b>429 <sup>(2)</sup></b>
<b>Labor <sup>(3)</sup></b>				
Inspection	\$26.46	\$13.17	\$38.08	\$9.23
Overhaul	\$7.75	\$10.11	\$8.40	\$4.92
Unscheduled and On-Condition	\$24.30	\$60.51	\$33.49	\$76.35
<b>Labor Sub-Total</b>	<b>\$58.51</b>	<b>\$83.79</b>	<b>\$79.97</b>	<b>\$90.50</b>
<i>MMH/FH</i>	<i>0.73</i>	<i>1.05</i>	<i>1.00</i>	<i>1.81</i>
<b>Parts</b>				
Inspection	\$1.60	\$4.18	\$12.94	\$3.83
Retirement Parts	\$56.37	\$36.11	\$127.74	\$67.43
Overhaul	\$29.61	\$53.40	\$55.81	\$23.02
Unscheduled and On-Condition	\$56.73	\$71.63	\$202.24	\$107.27
<b>Parts Sub-Total</b>	<b>\$144.31</b>	<b>\$165.32</b>	<b>\$398.73</b>	<b>\$201.55</b>
<b>Powerplant Direct Maintenance</b>				
Direct Maintenance Costs <sup>(3)</sup>	\$75.04	\$93.07	\$308.42	\$208.70
Line Maintenance labor	\$5.66	\$5.72	\$29.27	\$10.01
<b>Powerplant Sub-Total</b>	<b>\$80.70</b>	<b>\$98.79</b>	<b>\$337.69</b>	<b>\$218.71</b>
<b>Total DMC per FH</b>	<b>\$283.52</b>	<b>\$347.90</b>	<b>\$816.39</b>	<b>\$510.76</b>
<b>Fuel &amp; Lubricants <sup>(4)</sup></b>				
Fuel Flow Rate (Gal/Hr)	38	46	113	76

- Notes:
- (1) Basic VFR helicopter; 600 flight hours per year
  - (2) 429 DMC estimates are based upon preliminary figures and are subject to change
  - (3) Labor costs calculated at US\$80 per maintenance man-hour. Local rates may vary.
  - (4) Engine DMC represents total costs of maintenance including overhauls, accessory maintenance, unscheduled maintenance, and accruals for scheduling maintenance and life limited parts.
  - (5) Hourly fuel costs calculated as (Fuel Flow Rate x Fuel Cost per Gallon)  
Lubrication costs calculated as 1% of hourly fuel costs

**Fig. 2-421. Direct maintenance costs per hour for four Bell helicopters in the first quarter of 2012 [645].**

<sup>211</sup> Bell has published this newsletter for, I think, about 60 years. Today you can see recent copies by going to [http://www.bellhelicopter.com/en\\_US/SupportServices/TechPublications/RotorBreeze.html](http://www.bellhelicopter.com/en_US/SupportServices/TechPublications/RotorBreeze.html)

## 2.9 OPERATING COSTS

Estimator	206L4	407	412	429
Bell Helicopter	0.73	1.05	1.00	1.81
Conklin & de Decker	1.19	1.17	2.31	2.54

It is entirely unproductive to enter a debate about who has the correct values because neither estimate is the definitive estimate, and both estimates fall within the bounds shown in Fig. 2-419. The reason I say this is because I seriously doubt that any two surveys captured all the same operators, and quite probably the jobs each helicopter type is doing vary even for the same operator, as you will see shortly.

Sikorsky is another helicopter manufacturer who keeps in daily contact with operators who fly their products. They publish *Sikorsky Commercial Links* [641]. The July 2005 issue was particularly interesting to me because the focus was on the then newly fielded S-92. One article in the newsletter struck me because it stated operational data obtained by Norsk Helikopter, which service offshore oil rigs in the North Sea. The article is included here as Fig. 2-422.

An accompanying article about Norsk Helikopter in the *Sikorsky Commercial Links* of July 2005 provided some key maintenance data stating that

“from a maintenance perspective, the design of the S-92 is autonomous in the field for ease of maintenance. [Two hundred and fifty] and 500 hour inspections have been performed in the field and were carried out without any noted discrepancies. Reports indicate that the inspections took a total of 5 men and 100 man-hours to complete, approximately 2 days less than the industry standard.”

In my experience, the working (and soon-to-be-working) helicopter engineer does not get enough close looks at the operator’s side of the rotorcraft industry. Newsletters such as Bell’s *RotorBreeze* and *Sikorsky Commercial Links* are quite valuable and can fill a gap. These newsletters deserve more attention by the engineering community, and I believe each issue should be delivered to their desks and be required reading.

### Norsk S-92 Fleet Surpasses 1,000 Flight Hours

Norsk Helikopter achieved an industry milestone June 9 when it became the first S-92 operator in the world to reach 1,000 fleet hours, transporting more than 20,000 passengers to and from North Sea oil fields.

Used for crew change missions from Bergen, Norway, throughout the North Sea, Norsk’s two S-92s began revenue service in February and April 2005 respectively. Through June 9, the two S-92s logged 543 and 462 hours, carrying 10,855 and 9,620 passengers, respectively.

“We are generally highly satisfied with the implementation of the two helicopters. The utilization in our daily flight program is high, and we must conclude that our expectations have been reached,” said Geir Tynning, Norsk’s commercial director.

The robust design, new technology and demonstrated reliability of the S-92 have quickly proven itself ready to meet the demanding needs of Norwegian offshore oil customers. The S-92 is the first in the world certified by the European Aviation Safety Agency/Joint Aviation Authorities to the latest and most rigorous safety standards.



**Fig. 2-422. Sikorsky’s S-92 was a hit right from the start (photo courtesy of Sikorsky Aircraft Corporation).**

When you have questions about the civil helicopter fleet, the best place to turn, in my opinion, is the *Helicopter Annual* [646] that is published by the Helicopter Association International (HAI). Their membership numbers over 2,500. The *Helicopter Annual* issue is just packed full of facts and figures. Using this source, consider two very important questions that companies face when doing a survey of operating costs. The first question deals with how many operators are operating how many helicopters. The answer, for the year 2009, is shown here in Fig. 2-423. You can see at the extremes that there are 219 operators who have just a single helicopter in their fleet. At the other end of the spectrum, there are 14 operators who have 51 or more helicopters in their fleet. Frankly, it is hard for me to imagine that all 622 operators (in 2009) have the same bookkeeping of operating cost line items. On top of that, it is just as hard to imagine that all their helicopters are doing nearly the same job. This is in sharp contrast to certificated airlines whose fixed-wing airliners provide basically one service—transporting people. A broad spectrum in operator fleet size such as Fig. 2-423 enumerates, surely contributes to the wide scatter shown in Fig. 2-419.

The second question that bears on helicopter direct maintenance costs and contributes to the scatter shown in Fig. 2-419 is, “What jobs do all these operators tackle?” Again, HAI’s *Helicopter Annual* [646] has the answer, and it is shown here in Fig. 2-424 for the 2009 snapshot. By my count there are 28 different roles that helicopters play in the transportation world. There are, you might note in passing, several operators whose fleets provide the equivalent of airline passenger service. Certainly Air Taxi/Charter (Part 135), Commuter/Scheduled, Corporate/Not for Hire (Part 91), Executive Transport, and Offshore fall in this airline-like business category. Now let me proceed to the next maintenance cost line item.

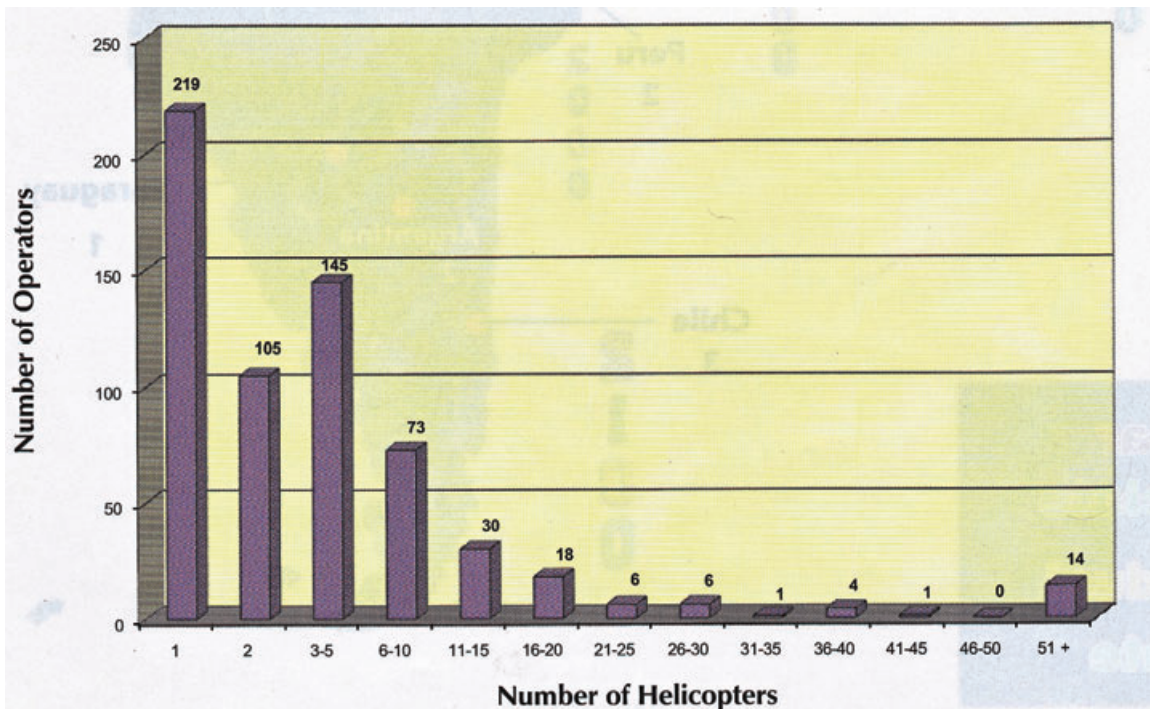


**Fig. 2-423. The number of helicopters that each HAI-member operator has in its fleet (courtesy of the Helicopter Association International).**

## 2.9 OPERATING COSTS

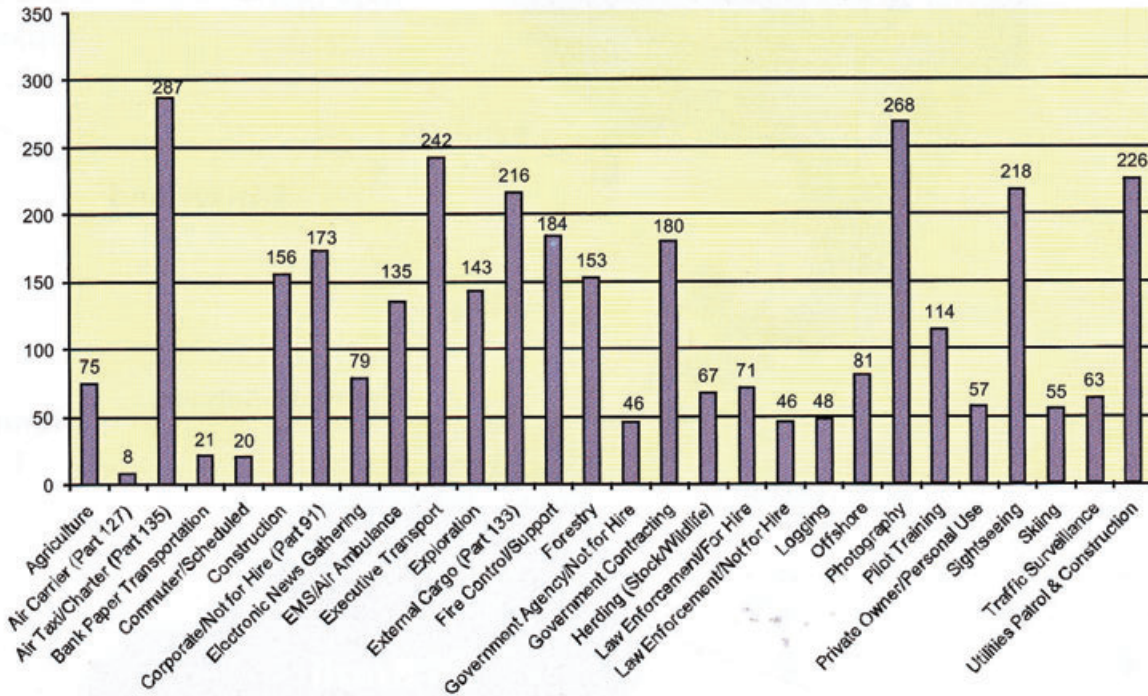


**Fig. 2-424. The number of helicopters used in each of 28 job categories in 2009 (courtesy of Helicopter Association International).**

### 2.9.5.2.2 Parts Airframe/Engine/Avionics

The DOC line item of what was frequently referred to just as “materials” in earlier years is illustrated in Fig. 2-425. These are the parts and pieces that mechanics use to maintain a helicopter on a daily basis. To collect the *Aircraft Cost Evaluator (ACE)* data of parts’ cost per hour, I arbitrarily chose the listed base price of helicopters in 2011. Of course, many helicopters were not sold new in 2011. This meant that helicopters sold new in some past year needed their price inflated to 2011. Therefore, purchase price data from *The Official Helicopter Blue Book*<sup>®</sup> [583] that led to prices in 1994 (as discussed in Chapter 2.8, Purchase Price) had to be further inflated to 2011 using a factor of 1.52 (see Fig. 2-391). Then, from this hodgepodge of *The Official Helicopter Blue Book*<sup>®</sup>, *ACE*, and other data, I selected the 2011 “list” base prices for Fig. 2-425. I am sorry that I could not come up with a more accurate estimate.

You will no doubt notice in Fig. 2-425 that the Bell Helicopter Model 222 series sticks out like a sore thumb. The A model of this series was near its first flight date (August 13, 1976) when I joined Bell in July of 1976 as chief of aerodynamics.<sup>212</sup> The basic helicopter showed great promise, but the Lycoming LTS 101-650 engine was nowhere near mature

<sup>212</sup> I left Boeing Vertol after 20 years because I wanted to work in the civil helicopter world for awhile. It was, in retrospect, a rather short-term prospect because Mr. Jim Atkins suggested that I become chief engineer on the AHIP/OH-58D program [145], which was soon to begin with a competition (between Hughes and Bell) for a new scout helicopter. Mr. Atkins was then President of Bell, and because I had (and still have) so much respect for this man, I put my military helicopter hat on again.

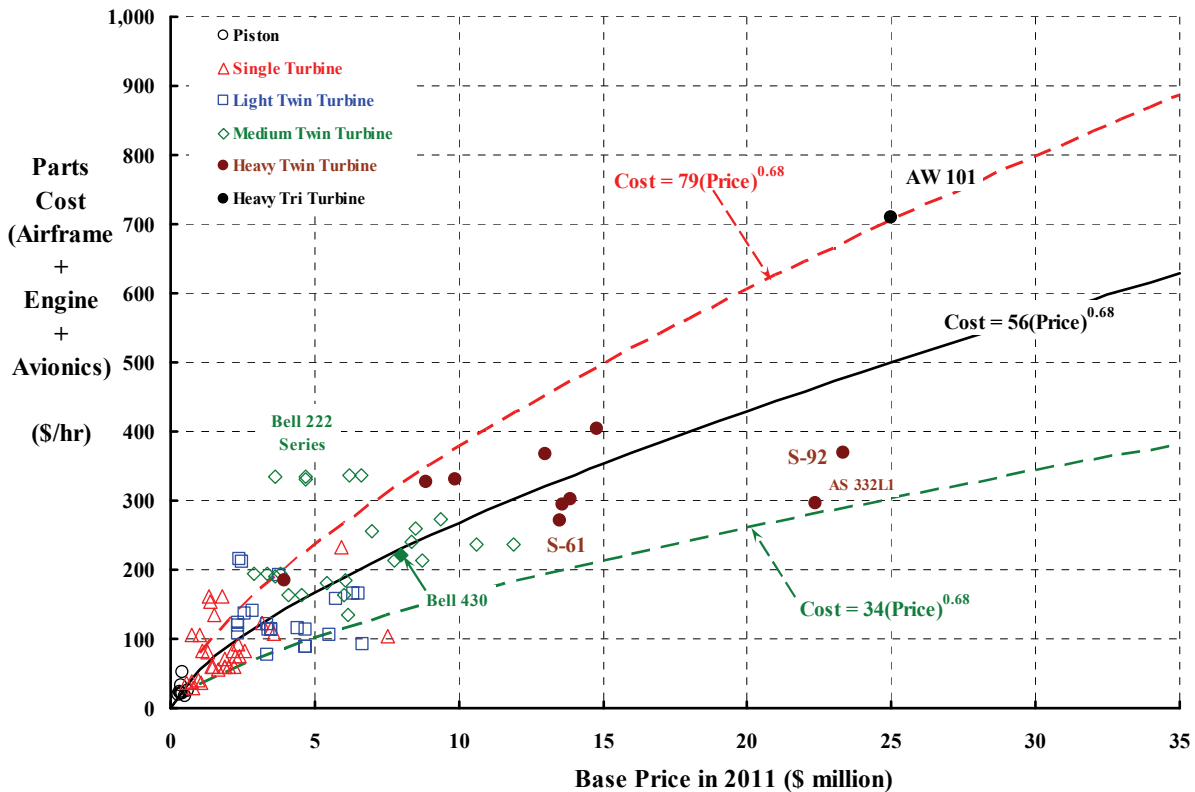


**Fig. 2-425. Costs per flight hour of parts and pieces required in daily maintenance (derived from Conklin & de Decker’s *Aircraft Cost Evaluator* data bank).**

enough for production. The engine problems soon became widely apparent in the civil helicopter world, and this stymied sales despite all efforts by the Bell marketing group. Reduced pricing and improvements made by Lycoming yielded the -750 engine. This engine and several airframe improvements creating the B Model 222 did not turn the helicopter’s sales prospects around. Nor did the introduction of a skid gear version (the Model 222U) recoup the situation. Replacing the two Lycoming LTS 101 engines with two Allison (now Rolls Royce) 250-C30 engines led to the Model 230 and a more realistic, break-even price in the early 1990s, but it was too little too late. Then a switch, from the two-blade rotor system of the Model 230 to a four-blade rotor system and upgrading the Rolls Royce 250-C30 engines to 250-C40 engines, created the Model 430 (first flight in 1994). This helicopter was introduced and the civil helicopter market regained confidence in Bell. It was an expensive lesson.

#### 2.9.5.2.3 Engine Restoration (i.e., Overhaul)

Engine restoration, or overhaul as it is frequently referred to, is also a major maintenance DOC line item. Fortunately, turbine engine manufacturers have improved their product’s time between overhaul (TBO). What started out as 500 to 1,000 hours TBO is now approaching 3,500 hours and, in a few examples, turbine engine manufacturers have adopted a policy called “on condition” inspections before determining that a complete overhaul is required.

## 2.9 OPERATING COSTS

Fig. 2-426 shows my summary of the range in DOCs for engine restoration. Engines offered by General Electric, Rolls Royce, and Pratt & Whitney completely dominate the helicopters surveyed here. Both the General Electric CT7 series and the Rolls Royce 250 series use the “on condition” criteria before a decision to overhaul is made. When you think about it, a 3,000- to 4,000-hour TBO means that new turbine engines do not need a complete overhaul for 5 to 7 years when helicopters are only flying 600 hours a year. This is quite remarkable when you consider that the best high-powered piston engines of World War II required a complete overhaul every 500 to 1,000 hours.

Let me turn your attention to Frank Robinson’s recent certification of his R66. The growth from the piston-powered R44 to the turbine-powered, five-passenger R66 shows, in my view, just how wise a man Robinson is. The turbine engine he selected was the Rolls Royce RR300 shown in Fig. 2-427. This engine is almost a relic in some engineers’ minds because it is a resurrected (but improved, primarily with fewer parts and modern technology) Allison 250-C18, which was the engine the U.S. Army chose in the 1960s to fill their Light Observation Helicopter requirement. The RR300 is a low-cost alternative to piston engines in the 240- to 300-horsepower class. This means that small fixed-wing and rotary wing aircraft *finally* have an entrance-level step to all the benefits of gas turbine engine technology. The price of the RR300 engine still requires a call to Rolls Royce by “serious buyers only,” but with general aviation encompassing such a worldwide market, you have to believe that this engine is going to be a winner. Now let me proceed to the next DOC line item.

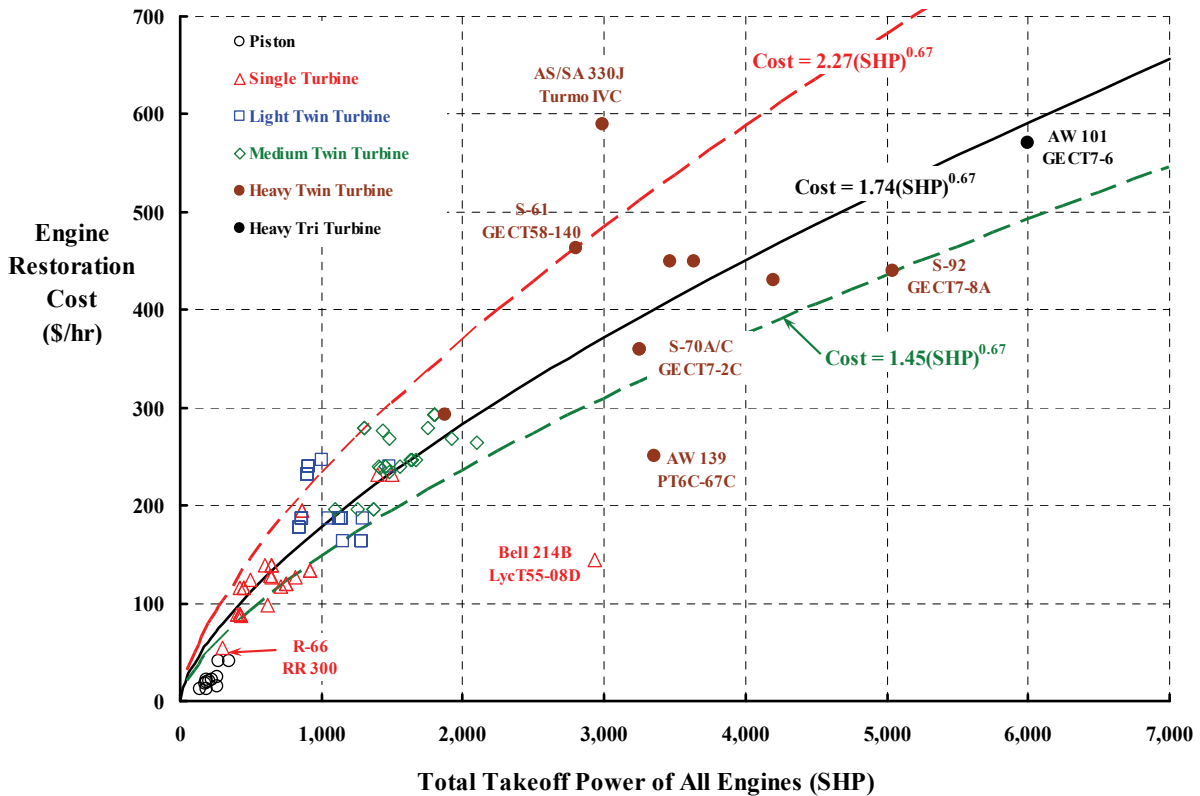


Fig. 2-426. Engine overhaul costs per flight hour (derived from Conklin & de Decker’s *Aircraft Cost Evaluator* data bank).



**Fig. 2-427. Frank Robinson worked with Rolls Royce for nearly 3 years to get a good fit of the RR300 with his R66, 5-passenger helicopter. At the February 2012 Heli Expo held in Dallas, Texas, Rolls Royce announced that the R66/RR300 had over 10,000 flight hours and that support for the engine was growing globally (photo from author's collection).**

#### *2.9.5.2.4 Major Periodic Maintenance*

There is no question, at least in my mind, that engine manufacturers have done their job in reducing maintenance direct operating costs and, from the airframe side of the coin, there is also no question that the cost per hour of major periodic maintenance has been significantly reduced over time. You see this in Fig. 2-428 where I have concluded that major periodic maintenance cost per hour is a fraction of the list base price (in millions of dollars). This DOC line item has gone from a factor of 50, with some of the earliest helicopters, to about 18 for what can be considered the state of the art in the first decade of the twenty-first century. This represents a reduction of nearly 60 percent. The engine manufacturers, according to Fig. 2-426, went from a factor of 2.27 to 1.45, which suggests a reduction of about 36 percent.

There are several noteworthy points made by Fig. 2-428. To begin with, it is quite clear that virtually all of the early helicopters were very difficult to maintain. Statements such as, "It's a nightmare compared to a Piper Cub," or "I have to work 2 or 3 hours for every hour that thing flies" were commonly overheard. Every helicopter to the near or to the left of the red dashed line in Fig. 2-428 falls in this unsatisfactory group. Starting with the A model, the Sikorsky S-76 series had a disproportionately expensive major periodic maintenance cost. What is unique about the S-76 series is that as successive price changes with corresponding

## 2.9 OPERATING COSTS

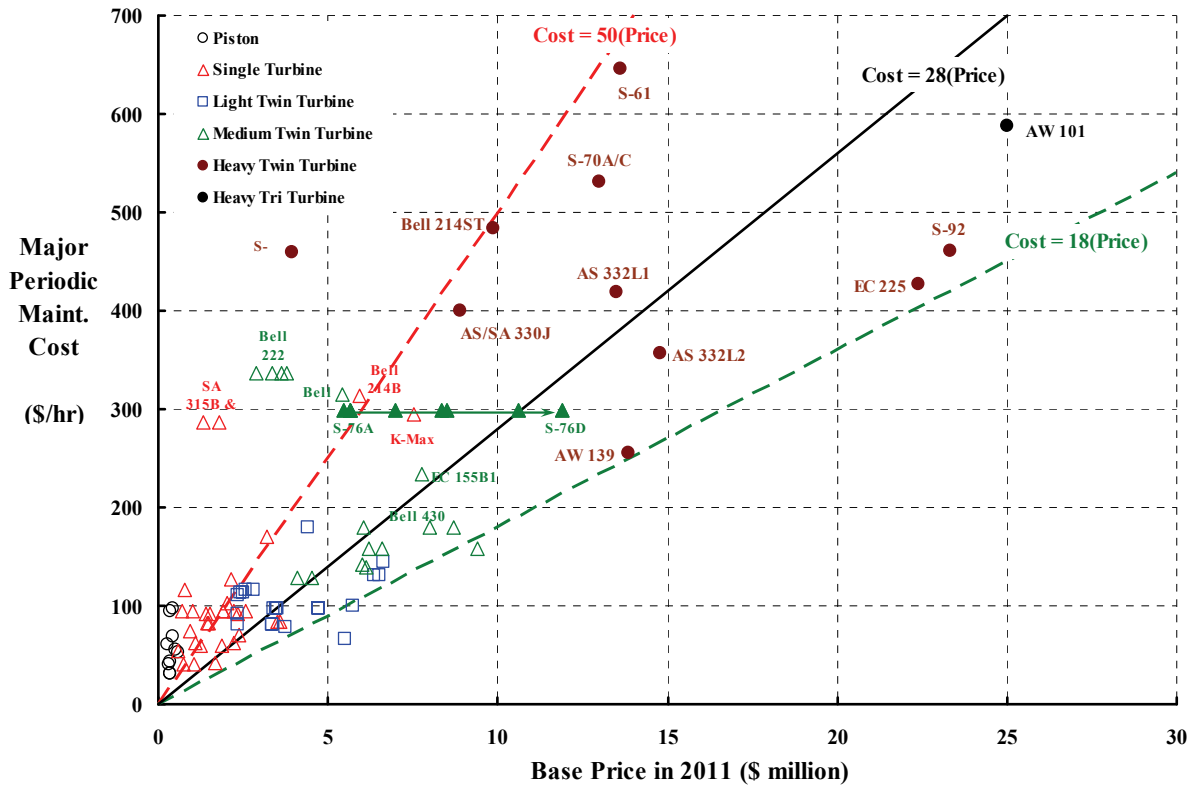


**Fig. 2-428. Major periodic maintenance costs per flight hour (derived from Conklin & de Decker’s *Aircraft Cost Evaluator* data bank).**

model changes drove the purchase price up, the periodic maintenance costs did not rise. Today the S-76D, with all the field experience and the improvements that followed, falls somewhat below the regression analysis result of “Cost equals 28 times Base Price in 2011.”

The Bell Model 222 series presents another interesting example. Here the rather limited field experience was incorporated into the Model 230. Then the change from a two-bladed, classical Bell product to a “modern” four-bladed hingeless rotor system finally created a successful machine, the Bell Model 430.

### 2.9.5.2.5 Refurbishing (Interior)

The last DOC line item embedded in Conklin & de Decker’s *Aircraft Cost Evaluator* data bank is refurbishing, principally of the passenger compartment. The Conklin & de Decker survey for 2011 suggests that this DOC item has a *yearly* cost of 10 maintenance man-hours per passenger seat per year. Accepting this rule of thumb means that

$$(2.375) \quad \frac{\text{Refurbishing DOC}}{\text{Flight hour}} = \frac{\left(\frac{\text{MMH}}{\text{Seat}}\right) \left(\frac{\text{Seats}}{\text{Year}}\right) \left(\frac{\text{Labor Dollars}}{\text{Labor hour}}\right)}{\text{Flight hours/Year}}$$

As a numerical example, consider again the Sikorsky S-61, which has 26 seats in its New York Airways' configuration. This results in 10 times 26 seats, which equals 260 man-hours per year for passenger compartment refurbishing. In 2011, the *Aircraft Cost Evaluator* default labor rate is \$94.00, so the yearly cost is \$24,440 per year. Assuming about 400 hours per year of flight operations, you have \$60.58 per flight hour. This repair for wear-and-tear expense might be more than 10 man-hours per seat if the flight hours per year were 800 hours. Therefore, this refurbishment could, in fact, be a rather fluid expense.

#### 2.9.5.2.6 A Maintenance DOC Near-Term Goal

It is worth a moment to construct a maintenance DOC target for helicopters contemplated in the near future. For example, this future helicopter should minimize the costs in all five maintenance line items just discussed. Using this criterion, the Maintenance DOC in dollars per flight hour would be at or below the following value:

$$\begin{aligned}
 \frac{\text{Maint. DOC}}{\text{Flight hour}} = & \left[ 0.0017(\text{WE})^{0.78} \right] \left( \frac{\text{Labor dollars}}{\text{Labor hour}} \right) && \text{for Labor} \\
 & + 34 \left( \frac{\text{Helicopter list Base Price}}{10^6} \right)^{0.68} && \text{for Parts} \\
 (2.376) \quad & + 1.45 (\text{Total SHP}_{\text{Takeoff}})^{0.67} && \text{for Engine Restoration} \\
 & + 18 \left( \frac{\text{Helicopter list Base Price}}{10^6} \right) && \text{for Major Periodic Maint.} \\
 & + 10 (\text{No. of seats}) \left( \frac{\text{Labor dollars}}{\text{Labor hour}} \right) \left( \frac{\text{Labor hour}}{\text{Flt. hours/year}} \right) && \text{for Refurbishing}
 \end{aligned}$$

It should be obvious that I have simply taken the equation bounding the bottom of scatter from Fig. 2-419, Fig. 2-425, Fig. 2-426, and Fig. 2-428 to create this near-term goal (or target, or design objective, if you prefer).

This near-term goal is hardly out of reach because several helicopters included in Conklin & de Decker's *Aircraft Cost Evaluator* have reached this goal. You can see this conclusion from Fig. 2-429 on the next page. The abscissa on this graph is Eq. (2.376) computed for each helicopter in the *Aircraft Cost Evaluator* data base. The ordinate is the actual survey maintenance DOC for that associated helicopter. Because I have taken bottom of scatter, virtually all data points for helicopters in the current civil fleet lie above the solid, green, diagonal line. A simple linear regression analysis shows that the current civil fleet, as a group, is some 40 percent above the goal. This fact is captured with the red dashed line.

As you look at Fig. 2-429 you can immediately see that the medium twin-turbine helicopter class (the green, open diamonds) has no machine in the current civil fleet even approaching the goal. It appears to me that the reason for this situation is that many of the helicopters in this class are simply re-engined versions of 1980's machines.

## 2.9 OPERATING COSTS

In the heavy twin-turbine class (the round, solid brown circles) you have the Augusta Westland 139 (AW 139), which was designed as a replacement for the Bell Model 212. The first flight of the AW 139 was February 3, 2001. The Eurocopter 225 (EC 225) is a growth version of the 1970's Aerospatiale 332 Puma and was designed to compete with Sikorsky's S-92, which is truly an example of 1990's technology. The Agusta Westland 101 has three turbine engines and was conceived in the early 1980s, but did not enter service until June of 2000.

Considerable progress toward lower maintenance DOCs has been made by manufacturers of light twin-turbine and single-turbine helicopters as Fig. 2-429 suggests.

There are a few things to keep in mind if you use Eq. (2.376). The most important point is that the prediction is very inflation sensitive. Since the time between when a decision is made to offer an all-new helicopter and when the first customer takes delivery can be a decade, a mechanic's pay (with benefits) can increase by a factor of 3 to 3.5 as past history shows (Fig. 2-420). This statement about inflation is just as true for the list base price of the all-new helicopter, and if the selling price inflates, you can be sure that the price of spare parts will escalate as well. On the flip side of the coin, you should at least hope for reductions in maintenance man-hours per flight hour as the A model gives feedback to the manufacturer that can initiate improvements in the B and C models. A good example of this is the increase in time between overhaul—particularly for transmission and rotor hub subsystems. Finally, I expect that continued research and development by the rotary wing industry will introduce technology to all future new machines that will make Eq. (2.376) obsolete.

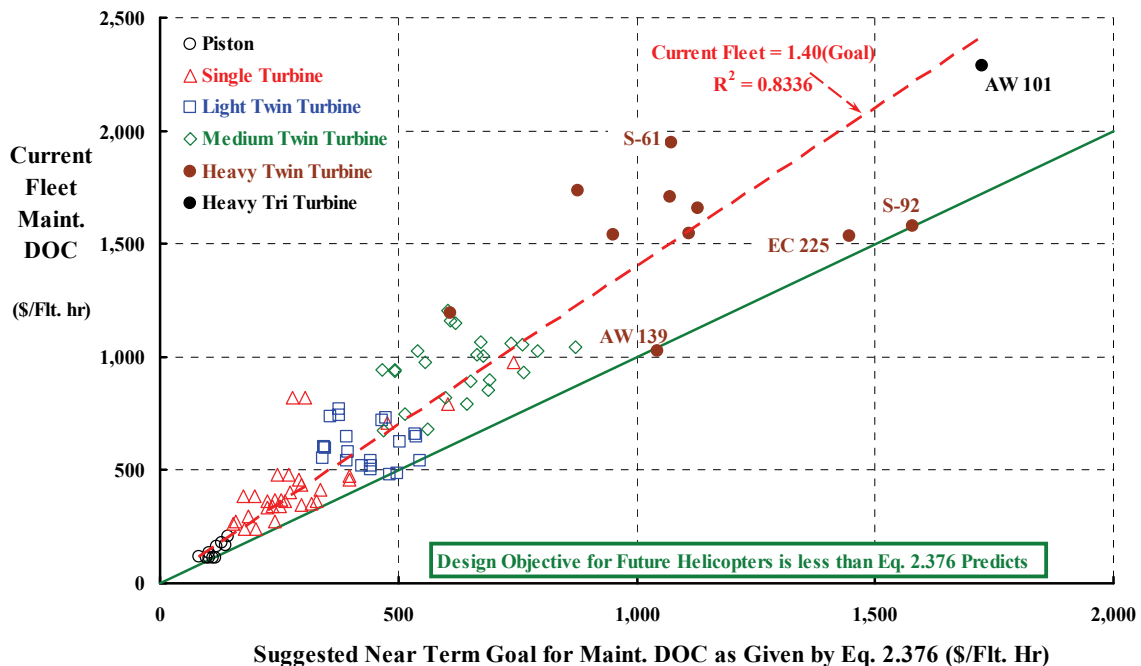


**Fig. 2-429. There is nothing to suggest that maintenance DOC cannot be further reduced as the helicopter continues to mature.**

### 2.9.6 Parts and Prices, Limited-Life Parts, and Scheduled Maintenance

In Volume I: Overview and Autogyros, you were introduced to autogyro maintenance. Appendix K of Volume I included a maintenance manual used by the Royal Air Force for the Cierva C-30, which was identified as the ROTA Gyroplane by the British Air Ministry. I included that maintenance manual for two reasons: the first reason was because of its historical significance, and the second reason was to give you a reference point to which helicopter maintenance could be compared.

It really is not possible to discuss helicopter maintenance, and such key factors as maintenance man-hours per flight hour, without studying maintenance manuals and parts catalogs in detail. Therefore, I have selected one helicopter, the Robinson R22, to discuss in more detail. It seems to me that the Robinson R22 is an ideal candidate because it is a well-developed, two-seat helicopter that parallels the two-seat Cierva C-30 autogyro, both useable in general utility operation. The choice of the Bell 206B Jet Ranger would be a natural choice because it was one of the first turbine-powered machines and because so many have been produced. Perhaps you also sense that the progression is from a piston-powered autogyro to a piston-powered helicopter to a turbine-powered helicopter. Both helicopters have maintenance and parts catalogs available, which I bought or was given. My study of the rather thick books suggests a few major observations that will let you appreciate the tasks operators must complete to keep their helicopters in safe, ready-to-fly condition.

#### 2.9.6.1 Parts Count and Spare Part Prices

The Cierva C-30 parts count was 3,241 as you learned in Volume I. The question that occurred to me was, “How many parts does it take to make a comparable, state-of-the-art helicopter (i.e. the Robinson R22)?” Or, if you care to pursue it, “How many parts are in the most popular, entry-level turbine-powered helicopter (i.e., the Bell Model 206B)?” Both of these helicopters have enjoyed long-term sales, both have well above 100,000 fleet hours, and both have had their initial shortcomings corrected.

It is not hard to get a reasonably accurate parts count for helicopters that are in the civil fleet—simply buy a parts catalog from the helicopter manufacturer. For example, the parts catalog for the R22 comes in a nice blue binder containing approximately 250 pages separated into 16 sections [647]. Each section deals with a major assembly installed on the helicopter such as airframe, power plant, rotor system, etc. Each section has excellent exploded views (illustrations), and the subsystem parts are all numbered.<sup>213</sup>

The Bell 206 series’ Illustrated Parts Breakdown Manual that I have [648] is about 1 foot thick (versus 3 inches for the R22 catalog) and has 67 chapters (versus 13 sections for the equivalent R22 document). One reason the Bell document is larger than the Robinson document is because the Bell document includes five major revisions that update the basic

---

<sup>213</sup> The parts catalog exploded views are just like the one or two sheets Sears Roebuck and Co. gives you with a lawn mower or like a Black & Decker® power tool parts breakdown sheet. All of these types of documents give you some idea about how the machine is assembled.

## 2.9 OPERATING COSTS

May 1996 copy to include the B and B3 versions of the Model 206A. This makes my copy up to date as of November 1, 2001.

Let me restrict the detailed analysis of parts count and the price of spare parts to just the Robinson R22. I have had to do this because it took me a month to analyze this manufacturer's illustrated parts catalog in sufficient detail to reach meaningful conclusions. Let me emphasize here that real and accurate configuration control and management can only be done at the parts level. There is no getting around this fact of real engineering. Configuration management is generally a task included in military contracts for the development of a new machine. It is a task that frequently falls in the "ilities" group that members of the maintainability and reliability profession expect a potential contractor to treat very seriously—particularly during the development phase. Unfortunately, I am sorry to say that in my experience younger engineers seem to scoff at this configuration management task. This is too bad. While it may seem a rather mundane task compared to preliminary and detailed design, and then manufacturing, a chief engineer needs to know his aircraft at the parts level (not some system engineering level) if an outstanding machine is to be produced.

The Robinson R22, Fig. 2-430, is a two-place, piston-powered helicopter. It is built from about 9,000 parts categorized in 11 major assemblies, which you see summarized in Fig. 2-431 and presented with expanded detail in Table 2-60 and Fig. 2-432. All the data that you have before you is for the R22 Beta II and is for an effective date of January 15, 2007.



**Fig. 2-430. The Robinson R22 Beta II is powered by a Lycoming O-360-J2A reciprocating engine. In 2007, a well-equipped configuration, delivered fully assembled, had a list price of \$220,000 [583] (photo from author's collection).**

## 2.9 OPERATING COSTS

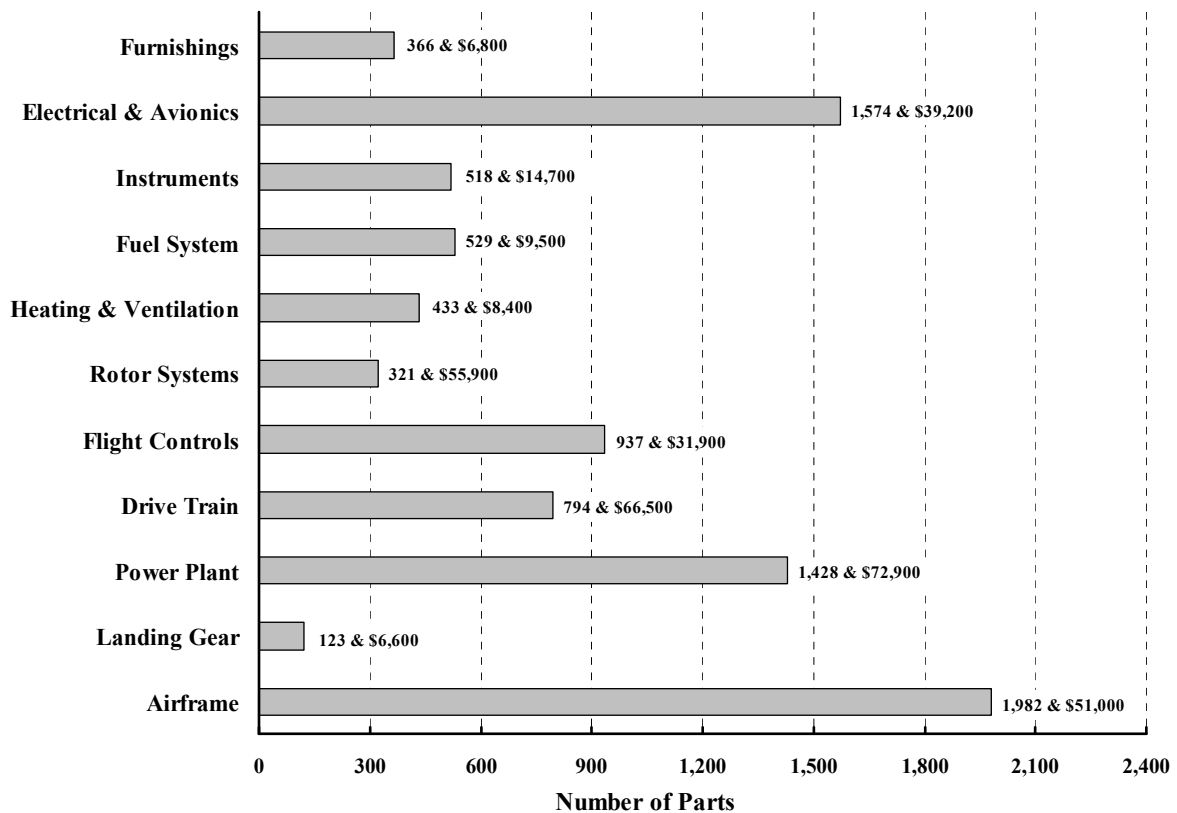


**Fig. 2-431.** The Robinson R22 Beta II, in a well-equipped configuration, has just over 9,000 parts. If built out of spare parts (rather than bought assembled), the price of parts alone would be about \$360,000 in 2007 [647].

**Table 2-60.** Robinson R22 Parts Count and Prices at the Subassembly Level in 2007 [647]

Major Assembly	Subassembly Description	Parts Count	Spare Part List Price
AIRFRAME	CABIN - WINDSHIELDS, COWLING	566	\$9,734
	CABIN - ROOF, WINDSHIELD SUPPORT AND DOOR	106	\$3,712
	CABIN - SKIRT ASSEMBLY	49	\$432
	CABIN - FLOOR, SEAT SUPPORTS	138	\$9,059
	CABIN - BELLY, LOWER EXTERIOR	96	\$1,439
	HORIZONTAL FIREWALL	148	\$1,246
	DOOR ASSEMBLY	120	\$5,160
	MAST FAIRING	207	\$985
	WELDED FRAME	217	\$9,819
	TAILCONE	202	\$4,620
	EMPENNAGE	57	\$3,057
	HARDPOINT/TIE-DOWN INSTALLATION	39	\$1,417
	BAGGAGE COMPARTMENT COVERS	36	\$273
	LANDING GEAR	LANDING GEAR	90
TIE-DOWN INSTALLATION		33	\$973
POWER PLANT	ENGINE INSTALLATION	128	\$41,935
	COOLING SYSTEM	606	\$11,472

2.9 OPERATING COSTS

**Table 2-60 (continued)**

<b>Major Assembly</b>	<b>Subassembly Description</b>	<b>Parts Count</b>	<b>Spare Part List Price</b>
POWER PLANT (cont)	AIR INDUCTION SYSTEM	122	\$6,090
	OIL SYSTEM	84	\$2,578
	OIL FILTER INSTALLATION	29	\$1,705
	ENGINE CONTROLS	244	\$6,597
	CARB HEAT ASSIST AND MIXTURE CONTROL	95	\$647
	CARB HEAT ASSIST BELLCRANK ASSEMBLY	41	\$469
	MUFFLER	77	\$1,391
DRIVETRAIN	MAIN ROTOR GEARBOX AND MAST	125	\$19,210
	MAIN ROTOR GEARBOX INSTALLATION	56	\$1,227
	DRIVE SYSTEM	235	\$23,456
	A041-12 DAMPER	40	\$469
	CLUTCH ASSEMBLY	65	\$7,974
	B021 TAIL ROTOR GEARBOX	50	\$5,628
	BELT TENSION ACTUATOR	86	\$4,801
	ROTOR BRAKE	136	\$3,745
FLIGHT CONTROLS	CYCLIC CONTROL SYSTEM	246	\$8,047
	ADJUSTABLE CYCLIC SPRING ASSEMBLY	51	\$807
	CYCLIC FRICTION ASSEMBLY	69	\$1,010
	COLLECTIVE CONTROL SYSTEM	203	\$8,889
	SWASHPLATE ASSEMBLY	65	\$5,349
	SWASHPLATE BALL INSTALLATION	60	\$2,090
	TAIL ROTOR CONTROL SYSTEM	242	\$5,720
ROTOR SYSTEMS	MAIN ROTOR BLADE ASSEMBLY	85	\$32,572
	MAIN ROTOR HUB	51	\$6,970
	TAIL ROTOR	97	\$11,037
	HUB ASSEMBLY - ELASTOMERIC BEARING	9	\$674
	A029-2 TAIL ROTOR BLADE INSTALLATION (ROUND TIP BLADES)	79	\$4,677
HEATING & VENTILATION	CABIN HEAT SYSTEM - AFT OUTLET	185	\$3,798
	CABIN HEAT SYSTEM - FORWARD OUTLET	199	\$4,115
	CABIN HEAT SYSTEM - DUAL FORWARD OUTLET	38	\$461
	CABIN VENTILATION	11	\$55
FUEL SYSTEM	FUEL SYSTEM	163	\$4,742
	AUXILIARY FUEL SYSTEM	124	\$2,809
	AUXILIARY FUEL COWLING ASSEMBLY	156	\$988
	FUEL PRIMER AND LINES INSTALLATION	86	\$982
INSTRUMENTS	UPPER CONSOLE - SEVEN-INSTRUMENT	167	\$7,057
	LOWER PANEL - SEVEN INSTRUMENT	156	\$4,804
	LOWER CONSOLE AND RADIO INSTALLATION	91	\$930
	PITOT/STATIC LINES INSTALLATION	104	\$1,885
ELECTRICAL & AVIONICS	POSITION AND LANDING LIGHTS INSTALLATION	117	\$1,829
	ELECTRICAL COMPONENTS INSTALLATION	153	\$4,080
	ALTERNATOR AND STARTER INSTALLATION	88	\$3,691
	ELECTRICAL CIRCUIT BREAKER PANEL	80	\$1,101
	ENGINE INSTRUMENT SENDERS AND TEST SWITCHES	53	\$1,011
	TACHOMETER AND LOW RPM WARNING UNIT	68	\$4,021
	NOSE BATTERY INSTALLATION	101	\$1,088
AFT BATTERY INSTALLATION	99	\$1,503	

Table 2-60 (continued)

Major Assembly	Subassembly Description	Parts Count	Spare Part List Price
ELECTRICAL & AVIONICS (cont)	TRANSPONDER AND BLIND ENCODER INSTALLATION	76	\$343
	BELLY ANTENNAS	41	\$1,752
	FM/DME/TRANSPONDER ANTENNAS	22	\$66
	ADF/MARKER BEACON ANTENNAS	42	\$157
	NAV ANTENNA INSTALLATION	28	\$798
	FORWARD TAILCONE ANTENNAS	18	\$1,004
	AFT TAILCONE ANTENNAS	21	\$1,120
	GPS ANTENNAS (COWL MOUNT)	37	\$307
	LORAN ANTENNAS	42	\$57
	VHF COM ANTENNA	23	\$183
	RPM GOVERNOR INSTALLATION	128	\$11,329
	ELECTRICAL WIRE HARNESS	31	\$1,594
	DIGITAL CLOCK INSTALLATION	14	\$295
	ELT INSTALLATION (POINTER)	81	\$1,131
	DME INSTALLATION	64	\$222
	FLOOR TRANSMIT SWITCH INSTALLATION	21	\$254
	PICTORIAL NAVIGATION SYSTEM (HSI)	69	\$133
FLUX GATE INSTALLATIONS	54	\$153	
FURNISHINGS	INTERIOR FURNISHINGS	335	\$6,599
	FIRE EXTINGUISHER INSTALLATION	31	\$160
<b>GRAND TOTAL</b>		<b>9,005</b>	<b>\$363,400</b>

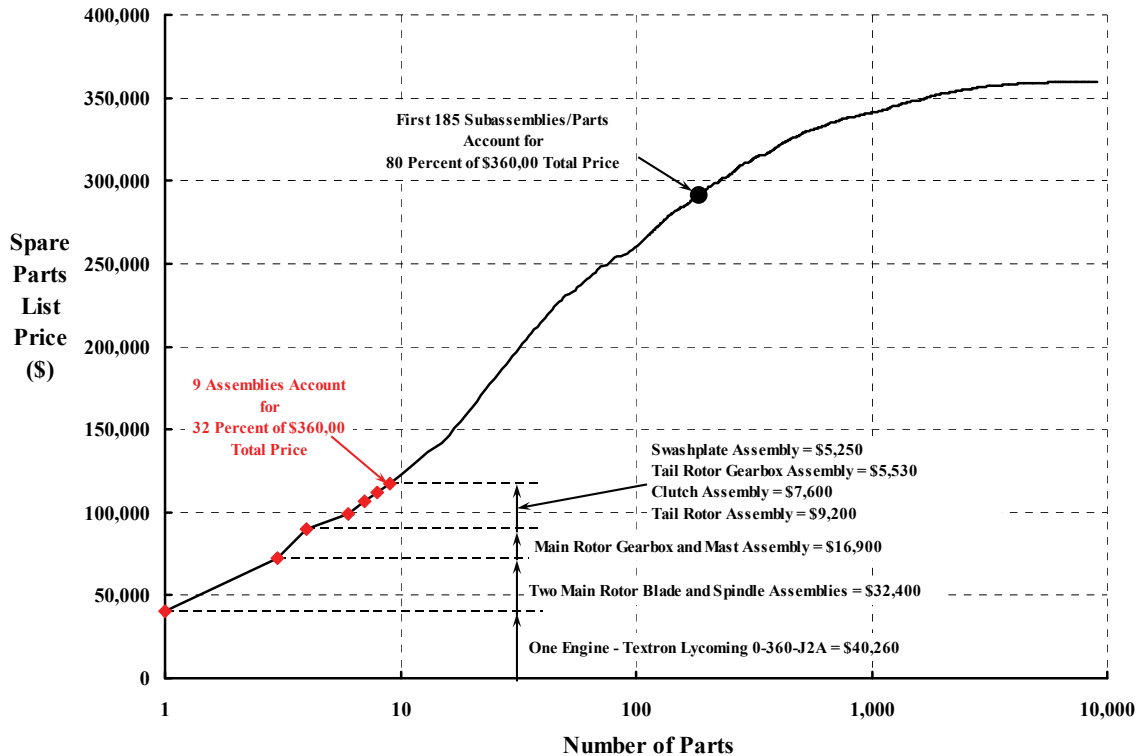


Fig. 2-432. Twenty percent of the assemblies/subassemblies/parts account for 80 percent of the spare parts list price in 2007.

## 2.9 OPERATING COSTS

Naturally the preceding parts count and spare part list prices have to be considered rather approximate. It would, of course, be quite accurate if prepared by a member of the parts department at Robinson Helicopter Company, but I felt that would be too much to ask because their real business is customer service. Despite these thoughts, I believe that the tabulations provided here are the right orders of magnitude.

One thing worth repeating is that the list price of an assembled R22 is \$220,000 [583]. If the helicopter was built up out of spare parts, just the assemblies/parts would cost about \$360,000, and the labor would be an additional cost. The ratio of \$360,000 to \$220,000 is 1.64.

The comparison of the Robinson R22 Beta II to the Cierva C-30 autogyro shows that the R22 is comprised of about 9,000 assemblies/parts and the C-30 contains only about 3,200 assemblies/parts (as you read in Volume I, page 276, table 2-22). The difference is dominated by (a) the instruments plus electrical and avionics major assemblies, which account for nearly 2,000 assemblies/parts, and (b) the airframe itself. This is not quite an apples-to-apples comparison as the 1930's C-30 autogyro certainly did not have the elegant interior furnishings of the R22, its welded tubular fuselage frame was canvas covered versus the R22's all metal skin, and the pilot's C-30 instrument panel was a far cry from what Robinson offers in their seven-instrument panel arrangement shown in Fig. 2-433. You might note in passing that what many buyers would consider as reasonable instruments, avionics, and associated electrical equipment total just under \$54,000 at spares list price. On this basis, and then adding in the Lycoming engine at around \$40,000 (bringing the total to \$94,000 out of \$360,000) roughly one-fourth of the helicopter's \$220,000 list price is spent before you have anything to install the assemblies/parts in. This could be an exaggeration on my part.<sup>214</sup>

### 2.9.6.2 Limited-Life Parts

The Robinson R22 contains about 9,000 parts, and you can see from Fig. 2-432 that some 185 assemblies/parts account for \$290,000 out of the total spares price of \$360,000. Not many of the parts wear out or need to be replaced in the 10 to perhaps 20 (or maybe even longer) years of useful life the machine provides. However, a select few are life limited to 5,000 (up to even 10,000) rotor-turning hours, and even fewer parts are life limited to 2,200 hours in certain critical part cases. Unfortunately for the helicopter operator, these life-limited parts always seem to be the most expensive ones. The result is, of course, that scheduled maintenance becomes more expensive when subassemblies like rotor blades *must be retired*

---

<sup>214</sup> Do not forget that each decal, screw, washer, nut, bolt, etc., is given a part number. The Robinson Helicopter Company's illustrated parts catalog [647] includes a file that occupies about 2,500 rows and 3 columns of a Microsoft® Excel® spreadsheet. The file that I created gives the part number, a description, and the unit price. The bulk of the catalog contains exploded views of a subassembly and attaches an index number for each part in the subassembly. Separate pages list the index numbers, the corresponding part numbers, and the quantity of each part number needed. This allows you to find the spare part price for any one of those particular parts. Then quantity times unit price gives the total price for that particular part.

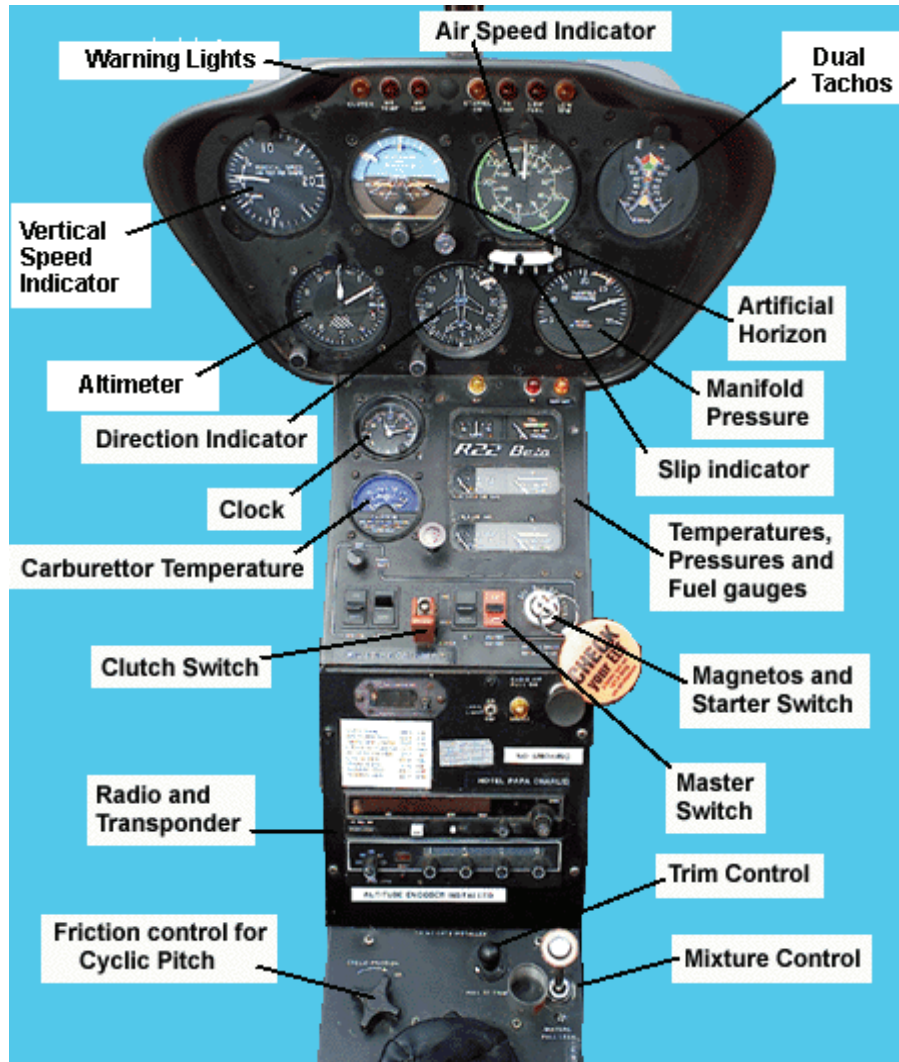
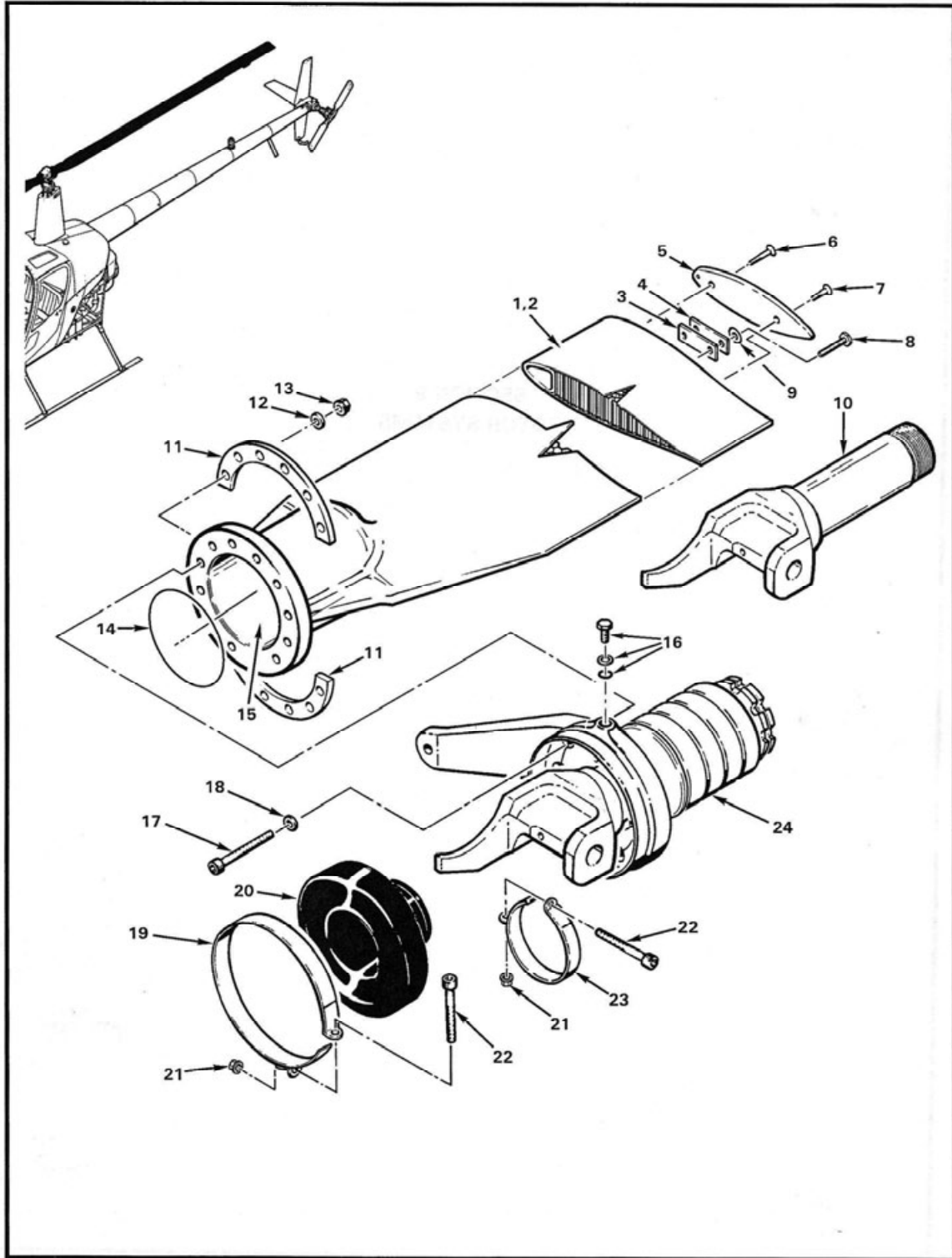


**Fig. 2-433. Robinson offers a quite reasonable package of instruments, avionics, and necessary electrical equipment (photo from author’s collection).**

after, say for example, 2,200 hours. For the Robinson R22, this would mean that a set of two main rotor blades (they must be replaced in pairs) and their spindles (see Fig. 2-434 and Fig. 2-435) priced as spares cost the helicopter owner \$32,400 in parts alone in 2007. (This price has gone up to about \$39,000 as of June 2012, and the price is “subject to change.”)

Stop and think about these numbers for a moment. Suppose you, as an operator, buy your R22 new in June of 2007 and fly it rather casually at 300 hours per year. The blade life of 2,200 hours would be used up in 7 years, in mid-2012. You must start saving for new blades at the rate (guessing inflation) of \$39,000 divided by 2,200 hours, which works out to \$18 per hour. This is just a simple example of what you, as the helicopter owner, must charge any customer who might ask, “How much for an hour flight?”



9.0 FIGURE 9-1 MAIN ROTOR BLADE ASSEMBLY REV APR 2007

Fig. 2-434. Exploded view of a Robinson R22 main rotor blade assembly [647].

**ROBINSON ILLUSTRATED PARTS CATALOG**

**MODEL R22**

FIGURE AND INDEX NUMBER	PART NUMBER	DESCRIPTION	PARTS AVAIL	USABLE ON CODE	QTY PER ASSY
<b>MAIN ROTOR BLADE ASSEMBLY</b>					
9-1-1	A005-6	Main Rotor Blade and Spindle Assembly (Incl items 2, 11 thru 18, and 24) . . . . .	X		2
2	A016-4	Blade Assembly (Ref; Stainless steel skin; must be replaced in matched pairs.) . . . . .	O		1
3	A298-2	Balance Strip (15 grams, 0.125 in. thick steel) . . . . .	X		A/R
4	A298-3	Balance Strip (5 grams, 0.032 in. thick steel) . . . . .	X		A/R
5	A300-2	Tip Cover . . . . .	X		1
6	MS24694-C54	Screw . . . . .	X		1
7	MS24694-C51	Screw . . . . .	X		1
8	A722-4	Screw . . . . .	X		2
9	NAS1149F0332P	Washer (or NAS1149F0363P as required for balance) . . . . .	X		A/R
10	A158-1	Spindle (Ref) . . . . .	O		1
11	A253-1	Spacer (Ref) . . . . .	O		2
12	A141-11	Washer . . . . .	X		12
13	MS21042L4	Nut . . . . .	X		12
14	A215-039	O-Ring (Ref) . . . . .	O		1
15	A257-4	Oil (Type "A" ATF, to fill housing, one-quart bottle) . . . . .	X		A/R
16	B289-2	Bolt (includes washer and o-ring) . . . . .	X		2
17	A722-2*	Screw (Ref) . . . . .	O		12
18	A722-3*	Washer (Ref; chamfered) . . . . .	O		12
19	A165-2	Clamp Assembly (Incl items 21 and 22) . . . . .	X		1
20	A156-1	Boot . . . . .	X		1
21	MS21042L08	Nut . . . . .	X		2
22	NAS1352-08-12P	Screw . . . . .	X		2
23	A165-1	Clamp Assembly (Incl items 21 and 22) . . . . .	X		1
24	A005-3	Spindle Assembly (Ref: Incl items 19, 20, and 23) . . . . .	O		1
*Seal with B270-1 Adhesive.					

REV APR 2007

X - Available as separate spares item  
 O - Available only as part of assembly

9.1

**Fig. 2-435. Tracking index number to part number [647] for the R22.**

## 2.9 OPERATING COSTS

In fact, the Robinson R22 (like so many helicopters currently flying) has a number of parts that are identified as “fatigue life limited.” When these parts are identified during the development program, they become subject to Airworthiness Limitations and require FAA attention. A section of the maintenance manual [649] generally contains one page (hopefully) certifying FAA approval for continued flight airworthiness as long as the operator/owner replaces the helicopter parts in question at the stated times. Fig. 2-436 shows you this very important page for the Robinson R22 [649].

You can immediately see in Fig. 2-436 that 19 subassemblies/parts contained in an R22 are limited to between 2,200 and 6,260 hours of engine run (or flight) time. Because the Bell Model 206B has been in service since the mid-1960s, its maintenance manual [650] has a much more detailed (and longer) list of individual parts that must be retired (i.e., replaced) in order to maintain the machine’s airworthiness. In either example, it may be that only one single ball bearing in a subassembly needs to be replaced, so it is not as if a complete gearbox is replaced. It might interest you to know that main rotor blades for the Bell 206B series are life limited to 5,000 hours, and each blade is list priced at \$47,530 (*per blade*) as of March 15, 2010 [583]. You will recall from Volume I that C-30 blades had a service life of 75 hours.

There is a short list of fatigue life-limited parts for many helicopters currently in service in the United States. This data is included in *The Official Helicopter Blue Book*<sup>®</sup> published by HeliValue\$, Inc. [583]. You will find major subassemblies (such as a main rotor blade or a complete tail rotor gearbox) tabulated in this source. A second column states the quantity required for that helicopter, and a third column provides the factory list price for a new replacement part. For example, the Sikorsky S-76 series’ main rotor blade is life limited to 28,000 hours; then each blade must be replaced at a cost to you, the owner/operator, of \$162,390 (*per blade*). With respect to blades, significant progress has been made with the transition to fiberglass blades. For example, the Bell Model 412 series’ blades do not have a fatigue life limit. Rather the Bell 412 main rotor blade replacement is based on “on condition,” which is, I will admit, somewhat vague but hopefully means at least 10,000 hours barring unusual in-service deterioration. The per-blade cost is \$180,440 (as of January 2009) for a Bell 412 blade, and you need four of them.

I suspect you are getting my drift here. The fatigue life-limited parts and subassemblies are major operating cost drivers. Even with a short list of the more expensive components, you can derive an impression of a minimum cost per flight hour that you must expect just from the costs of parts to be replaced. Of course you must also include the hours of labor required to make the replacement.

Let me add a closing thought. The Robinson Helicopter Company offers an R22 Factory Overhaul at 2,200 hours for \$140,000 (plus upgrades). This works out to \$64 per flight hour, and includes parts and labor. In effect, after buying your new R22 for \$220,000 in 2005, you need to save (accounting for inflation) about \$140,000 over 7 years to put it back into top-notch condition in 2012. Roughly speaking then, you are buying about 64 percent of the helicopter every 7 years assuming 300 hours flying every year. Unfortunately, your original investment is probably depreciating—just like your new car.

AIRWORTHINESS LIMITATIONS

The Airworthiness Limitations section is FAA-approved and specifies maintenance required under 43.16 and 91.403 of the Federal Aviation Regulations unless an alternative program has been FAA approved.

FATIGUE LIFE-LIMITED PARTS

Part Number	Description	Maximum Service Life
A016-2	Main Rotor Blade	2200 Hours or 10 years *
A016-4	Main Rotor Blade	2200 Hours or 12 years *
A020-2	Upper Frame, Rev R and Prior	4200 Hours
A020-2	Upper Frame, Rev S and Subsequent	4400 Hours
A020-84	Lower R.H. Frame	5110 Hours
A023-1,-20,-22, and -23	Tailcone Assembly	4400 Hours
A029-1	Tail Rotor Blade	5525 Hours
A029-2	Tail Rotor Blade	2200 Hours or 12 years *
A030-1	Tail Rotor Hub Assembly	6260 Hours
A046-2	Lower R.H. Frame	5110 Hours
A047-1	Upper Frame	4400 Hours
A062-2	Tail Rotor Hub	6000 Hours
A146-1	Pinion, Main Rotor Gearbox (O-360 Engine)	2200 Hours
A154-1	Main Rotor Hub	4400 Hours
A158-1	Main Rotor Spindle	2415 Hours
B545-1	Gear Set, Tail Rotor Gearbox	2200 Hours
NAS1304-24 (or NAS6604-24)	Tail Rotor Blade Attach Bolt	4430 Hours
NAS630-80 (or MS21250-10080)	Coning Hinge Bolt	2200 Hours
NAS1351-4-20 (or A722-1 or -2)	Pitch Horn Screws	2200 Hours

\* Whichever limit occurs first.

Note: These service lives are based on engine run time as recorded by the oil-pressure-activated hourmeter. If recording flight (skids-up or collective-up) time, multiply recorded hours by 1.12 to determine hours in service.

Approved By:   
 for Manager, Federal Aviation Administration  
Los Angeles Aircraft Certification Office  
 Date of Approval: 5/7/04

FAA Approved: This page constitutes the Airworthiness Limitations Section in its entirety, is considered segregated from the rest of the document, and sets forth the FAA-approved mandatory replacement times for the fatigue life-limited parts listed above.

**Fig. 2-436. The FAA-approved airworthiness page for the R22 listing assemblies and parts that must be replaced after a certain amount of operating time [649].**

## 2.9 OPERATING COSTS

### 2.9.6.3 Scheduled Maintenance

You will recall from Volume I that the Cierva C-30 autogyro maintenance schedule called for “inspection between flights, and inspections (a) daily, (b) every 10 hours, (c) every 20 hours, (d) every 40 hours, and (e) every 120 hours.” The Civet I engine and its “airscrew” required inspection as well, of course. The engine and propeller inspection intervals were identical to the airframe. Furthermore, the aircraft required lubrication at 39 different points on nearly a daily schedule.

The Robinson R22 has a similar list of tasks, albeit with a more liberal schedule. Paragraph 1.101 of the maintenance manual [649] states (with some of my editing) that

“1.101 Scheduled Maintenance. Some helicopters require further maintenance and inspections in addition to the following minimum requirements for new helicopters. Consult aircraft maintenance records, Service Bulletins (SB), aviation regulations, Airworthiness Limitations, and Airworthiness Directives (AD) for specific applicability. Publications listed are subject to revision.

#### Flight Time

- First 29 hours: Change engine oil and filter and inspect oil suction screen and filter per Lycoming SB480E. Check alternator belt tension per Lycoming Service Instruction (SI) 129B. Verify track and balance of drive system. Verify sheave alignment.
- Every 50 hours: Change engine oil and filter and inspect oil suction screen and filter per Lycoming SB480E. Inspect and service engine per Lycoming Operator's Manual and SI1080B.
- First 100 hours: Drain and flush main rotor gearbox (section 1.120) and tail rotor gearbox (section 1.130). Check engine exhaust valve guide clearance per Lycoming SB388C.
- Every 100 hours: Inspect per section 2.400. Inspect and service engine per Lycoming Operator's Manual, SB366, SI1080B, and SI1129B. Inspect and service engine ignition components per TCM SB636, SB643B, SB653, SB658, and SB663A.
- Every 300 hours: Lubricate the clutch actuator's upper and lower bearings (see A181-4 Rev K, Rev L, and Rev M bearings per section 2.502). Lubricate A184 bearing per section 2.503. Inspect valves and check engine exhaust valve guide clearance per Lycoming SB301 B, SB388C, and Operator's Manual.
- Every 500 hours: Drain and flush main rotor gearbox (section 1.120) and tail rotor gearbox (section 1.130). Inspect main rotor blade spindles per FAA AD 88-26-01 R2.
- Every 800 hours: Lubricate the clutch actuator's upper and lower bearings (see A181-4 Rev N bearing per section 2.502).
- Every 2,200 hours: Overhaul helicopter per section 2.7000.

#### Calendar

- Every 4 months: Change engine oil and filter and inspect oil suction screen and filter per Lycoming SB480E.
- Every 12 months: Inspect per section 2.400. Lubricate clutch actuator's upper and lower bearings (see A181-4 Rev K, Rev L, and Rev M bearings per section 2.502.). Lubricate A184 bearing per section 2.503. Inspect emergency locator transmitter (ELT) per FAR 91.207. Clean main rotor gearbox and tail rotor gearbox chip detectors per section 1.115.

## 2.9 OPERATING COSTS

- Every 24 months: Test and inspect transponder per FAR 91.413.
- Every 4 years: Lubricate clutch actuator's bearings (see A181-4 Rev N bearing per section 2.502). Overhaul the engine magnetos per TCM SB643B.
- Every 12 years: Perform 12-year inspection and limited overhaul per section 2.600, or overhaul per section 2.700."

You will see in most maintenance manuals that the first few introductory pages provide *when* to do and *what* to do instructions. The R22 manual follows this vitally important information with a section 2. This section 2, composed of 66 pages, provides more detail about *what* to do and *how* to do it. The rest of the R22 manual (some 400 pages) tells you *how* to do maintenance on each of the major subassemblies listed in Fig. 2-431. The R22 maintenance manual states, in no uncertain terms, that "the helicopter must be inspected periodically to verify it is in airworthy condition. Required inspection intervals are [a] maximum [of] 100 hours time in service or 12 calendar months (annually), whichever occurs first. Fluid leaks, discoloration, dents, scratches, nicks, cracks, galling, chafing, fretting, and corrosion all warrant further investigation. Unairworthy items must be replaced or repaired as allowed by Robinson Helicopter Company. This section contains procedures for performing the required periodic airframe inspections."

It should be apparent now that the schedule for R22 maintenance according to section 1, and the Periodic Maintenance *how to* according to section 2, require many man-hours of time for a qualified technician and/or a mechanic. After taking delivery of your new R22, you must plan your flying so that after the first 29 hours of operation the helicopter power plant (i.e., the Lycoming O-360) and the drivetrain get some attention. After that you get 21 more hours of flying before the first 50-hour servicing must be done. Then flying can continue for another 50 hours at which time the first 100-hour periodic maintenance must be performed. When you graph maintenance man-hours versus flight hours (read the note on Fig. 2-436), you get the accumulating labor hours versus accumulating flight hours shown in Fig. 2-437.

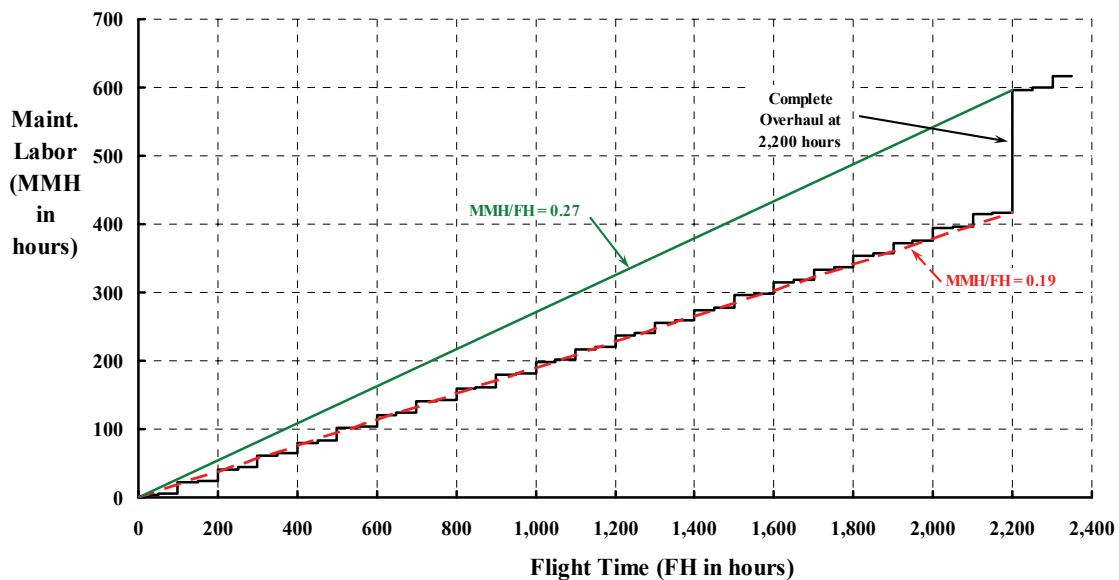


**Fig. 2-437. The ratio of R22 maintenance labor hours to flight hours is about 0.27 when the overhaul task at 2,200 flight hours is included (per the Robinson Helicopter Co.).**

## 2.9 OPERATING COSTS

Data for this figure was arrived at by talking directly to Daniel Huesca, a member of Robinson Helicopter Company's technical representative staff. He kindly quoted labor hours for each of the scheduled maintenance tasks as follows:

R22 Scheduled Maintenance at	Maintenance Man-Hours (hr)
50 hours	2 to 3
100 hours	12 to 16
300 hours	13 to 17
500 hours	14 to 18
800 hours	12 to 16
2,200 hours	180

In constructing Fig. 2-437, I took the upper limit figures that Huesca quoted.

Fig. 2-437 shows that, approximately speaking, the *average* maintenance man-hours per flight hour prior to the 2,200-flight-hours point<sup>215</sup> (when your brand new R22 must be completely overhauled) is just over 0.19. When the 2,200-hour overhaul is included, you have the blue solid line, which says that you should plan on an MMH/FH ratio of 0.27. Additionally, the Robinson Helicopter Company assumes *unscheduled* labor hours at 0.074 per flight hour, which means the total MMH/FH ratio is on the order of 0.344.

There appears to be a difference between maintenance labor hours published by many helicopter manufacturers, and what operators and owners experience in the field. It probably comes as no surprise that the manufacturer-quoted scheduled and unscheduled maintenance hours can be considerably lower than actual field experience. As one example, the Conklin & de Decker's *Aircraft Cost Evaluator (ACE)* [640] bases its maintenance direct operating cost data on an MMH/FH ratio of 0.452 for the R22, which includes both scheduled and unscheduled labor. The explanation for the difference, according to Bill de Decker, the inventor of *ACE*, is primarily due to a simple, scheduled maintenance task frequently revealing additional repairs or some other corrective action that may not be included in all manufacturers' estimates of maintenance labor. These additional, unforeseen tasks can easily increase *unscheduled* maintenance labor and add parts above manufacturers' allocation.

Because Conklin & de Decker have been so successful in gathering and analyzing helicopter maintenance data and specifically MMH/FH, I prevailed on Bill de Decker to share some of his knowledge. (As you will see, the Conklin & deDecker approach requires a manufacturer to provide its MMH/FH for *scheduled* maintenance, and this becomes the baseline.) In response, Bill wrote the following:

“To estimate realistic maintenance labor manhours per flight hour requires the inclusion of a number of factors. The Conklin & de Decker approach includes the following elements:

---

<sup>215</sup> You might keep in mind that today's new cars easily reach 2,000 operating hours after traveling 100,000 miles at, say, 50 miles per hour. A complete overhaul of the car at this time is, in my experience, hardly required.

**Schedule Maintenance (Airframe and Systems)**

This is the maintenance associated with all scheduled inspections and is the labor required to accomplish the scheduled portion of each inspection. This consists usually of removing/replacing access panels, a visual inspection, and often measuring pressure, volts, ohms, flow rate, etc., for specific functions or components. Almost all manufacturers can provide a quite accurate estimate of the typical number of labor hours expended for the scheduled portion of each inspection.

**Unscheduled Maintenance (Airframe and Systems)**

There are two types of unscheduled maintenance. The first is the unscheduled labor required to repair/replace and retest whatever was found during the scheduled inspection to be worn, damaged, or out of specification. The second is the maintenance that is required as a result of “squawks” and maintenance actions that arise in between scheduled maintenance actions. Typically these are the result of a pilot maintenance write-up at the end of a flight.

Some manufacturers can provide an estimate for the required labor that is typically required to accomplish this. In general, a ratio of one hour of unscheduled labor for each hour of scheduled time has proven to be a good rule of thumb.

**Troubleshooting**

Troubleshooting is an integral part of aircraft maintenance, particularly maintenance associated with fixing a “squawk” or pilot write-up. Sometimes the problem is not well described and sometimes it cannot be duplicated on the ground. In addition, the maintenance technician may not be very familiar with the system or component experiencing the stated problem. Conklin & de Decker’s approach, based on experience, is to add a factor that is based directly on the size and complexity of the helicopter, as shown in the following table. As can be expected, the amount of labor expended in troubleshooting is a direct function of the complexity of the systems on the helicopter.

**Troubleshooting Labor Hours Per Flight Hour**

<b>Helicopter Weight Class</b>	<b>Engine Type</b>	<b>Engine Number</b>	<b>MMH/FH</b>
Light	Piston	1	0.30
Light	Turbine	1	0.40
Light	Turbine	2	0.60
Medium	Turbine	1	0.50
Medium	Turbine	2	0.70
Heavy	Turbine	2	0.80

**Engine Maintenance (on Aircraft)**

Engines require both scheduled and unscheduled maintenance in between overhauls and other major maintenance actions. This includes the scheduled 25 or 50 hour oil and filter changes as well as unscheduled maintenance on fuel injectors, fuel controllers, igniter boxes, etc. It also includes the removal and installation of engines sent out for heavy maintenance. As with estimating troubleshooting labor, Conklin & de Decker approaches this cost element by using factors associated with the type, size (SHP) and number of engines, as shown in the following table:

## 2.9 OPERATING COSTS

**Engine On-Aircraft Labor Hours Per Flight Hour**

Helicopter Weight Class	Engine Type	Engine Number	MMH/FH Per Engine	Total MMH/FH
Light	Piston	1	0.15	0.15
Light	Turbine	1	0.15	0.15
Light	Turbine	2	0.15	0.30
Medium	Turbine	1	0.20	0.20
Medium	Turbine	2	0.20	0.40
Heavy	Turbine	2	0.30	0.60
Heavy	Turbine	3	0.30	0.90

### Avionics Maintenance (on Aircraft)

Avionics also require maintenance. However, this maintenance is almost all of the unscheduled variety. And while most radios, navigation receivers and instruments are not repaired on site, they still require removal and installation as well as repairs on associated wiring. Conklin & de Decker uses the same approach as for the engines to estimate the required labor hours per flight hour for this maintenance element. For the avionics the factors that determine the labor effort are the weight class of the helicopter, whether it is a VFR or IFR installation, and whether the helicopter is flown by a single pilot or two pilots, as shown in the following table.

**Avionics On-Aircraft Labor Hours Per Flight Hour**

Helicopter Weight Class	Engine Type	VFR or IFR	Number of Pilots	MMH/FH
Light	Piston	VFR	1	0.10
Light	Turbine	VFR	1	0.15
Light	Turbine	IFR	1	0.20
Medium	Turbine	VFR	1	0.20
Medium	Turbine	IFR	1	0.20
Heavy	Turbine	IFR	2	0.30
Heavy	Turbine	IFR	2	0.30

### Example of Applying These Additive Labor Hours Per Flight Hour

Adding these several additional labor hour per flight hour elements for a particular make and model helicopter yields a total labor hours per flight hour MMH/FH for a particular make and model of helicopter and is quite straightforward. It requires only to obtain the *scheduled* MMH/FH for that particular make and model, which almost all manufacturers can provide. For example, a typical, popular single engine turbine helicopter equipped for VFR operations would have the following total MMH/FH using this analysis:

Scheduled Maintenance	0.33 MMH/FH
Unscheduled Maintenance	0.33
Troubleshooting	0.40
Engine	0.15
Avionics	0.15
<b>Total</b>	<b>1.36 MMH/FH</b>

Actual survey data based on over 200 data points for the Bell 206B and 206L family that Conklin & de Decker has collected over the last 20 years shows that the actual MMH/FH for this popular helicopter averages 1.31 MMH/FH. This is within 5% of the estimated number shown above.”

You must also keep in mind that the final maintenance labor cost depends on the cost of one labor hour, which can range from \$60 to \$90 per hour (currently in 2012). Using the R22 as the example means, therefore, this direct operating cost line item could range from a low of \$60 per hour times an MMH/FH ratio of 0.19 (i.e., \$11.40 per flight hour) to as high as \$90 per hour times an MMH/FH ratio of 0.452 (i.e., \$40.70 per flight hour)!

Finally, there is another source for total maintenance cost per flight hour (i.e., both labor hours and replacement parts' cost); this source is *The Official Helicopter Blue Book*<sup>®</sup> [583]. *The Blue Book* has purchase price data, specifications, other very useful data, and *maintenance costs* for “running the helicopter for one hour.” *The Blue Book* now comes on a CD, which I purchased from HeliValue\$, Inc. The compilers of *The Blue Book* use the acronym HMC for the hourly maintenance cost and state the ground rules for the numbers they publish quite clearly. They say that

“to determine HMCs, it was necessary to make certain assumptions such as:

1. The helicopter will be subjected to no more than two start cycles per flight hour.
2. The average take-offs and landings will not exceed three per flight hour.
3. Other than during take-off and landing, the helicopter will be operated at 75% or less of its maximum continuous power rating.
4. Rotor blades without a scheduled removal interval have been assigned a useful life of 10,000 hours.
5. Mechanical and hydraulic components which do not have a scheduled removal interval are assigned an overhaul interval of 5,000 hours.
6. Operations which increase the number of engine starts, add the higher than average take-offs and landings, or require the helicopter to operate at more than 75% of its maximum power, will increase the HMC.
7. Different components which alter the model number of an aircraft within a series have had their HMCs determined by using an average of the possible variations.”

*The Blue Book* also provides an itemized list of what is not included in their quoted HMC. This line item list basically makes clear that no other cost line items associated with direct operating costs (DOCs) or indirect operating costs are included. Finally, the HMC is quoted as a range rather than one specific number.

### 2.9.7 Total Operating Cost (TOC)

Operating costs that vary with helicopter utilization (say, per flight hour) constitute one major group of accounting line items. The other major group of accounting line items gathers up costs that are not dependent on utilization (e.g., hanger rental fees) and are generally recorded annually. The sum of Variable Costs plus Fixed Costs equals Total Operating Cost (TOC). Giving a cost line item a name has not been, historically, a difficult problem in the helicopter industry. What has been difficult has been to associate the particular cost item as a Variable Cost per flight hour item or as a Fixed Cost per year item. To help standardized assignment to the flight hour group or to the annual group, both operators and manufacturers have turned to their trade organization, Helicopter Association International

## 2.9 OPERATING COSTS

(HAI). Over the years, HAI has been able to guide and improve how cost accounting is done by operators, and airframe and engine manufacturers. Since 1981, HAI has depended on their Economics Committee to periodically improve what is commonly called *The Yellow Book* or *The Guide*.

In 1987, the HAI Economics Committee, reinforced by the Aerospace Industries Association of America, produced the *1987 Guide for the Presentation of Helicopter Operating Cost Estimates*. This very helpful document, the *1987 Guide*, sufficed until early in the first decade of the twenty-first century. By that time the need for improvements became quite clear and, in October 2010, a revised document, still called *The Guide*, was published [643]. The preface of this 2010 edition begins with:

“What does it cost to operate and maintain a helicopter? Upon first read, this is a simple question, but it is one that has created a great deal of debate and confusion for the industry.”

This edition shows particular concern for operators by spelling out some pitfalls that might lead to an operator underestimating TOC. The result of underestimating TOC can, of course, easily cause an operator to undercharge a customer for the use of the helicopter.

When you read *The Guide* for 2010 you will see that (1) operators have a long list of cost items to incorporate when doing their accounting work, and (2) both airframe and engine manufacturers are given guidance in reporting cost estimates for numbers that they are experts in deriving. For example, who is better than the operator to estimate most of the fixed-cost line items, and who is most qualified to define and price, say, the life-limited parts. A key section of *The Guide* deals with defining most of the operating cost categories that have arisen over 30 years. The accounting items, with some editing by me, read as follow:

- II. Operating Cost Categories
  - A. Fuel and Lubricants
  - B. Maintenance
    - 1. Life-Limited Parts
    - 2. Major Overhauls (airframe and engine)
    - 3. Periodic Inspections
    - 4. On-Condition Components
    - 5. Service Bulletins and Air Worthiness Directives (ADs)
    - 6. Unscheduled Maintenance
    - 7. Optional Equipment
    - 8. Sources of Maintenance Cost Estimates
  - C. Insurance
    - 1. Hull
    - 2. Aviation General Liability
    - 3. Workers' Compensation
  - D. Personnel
    - 1. Flight Crew
    - 2. Mechanics and Technicians
    - 3. Office Staff
    - 4. Management Salaries
    - 5. Benefits
  - E. Training
  - F. Depreciation
  - G. Taxes

- H. Finance
- I. Overhead
  1. Rental or Lease Fees (hangar, vehicle, office, storage, etc.)
  2. Utilities (telephone, electricity, water, etc.)

As you can quickly appreciate, *The Guide* is constructing a primer for a small business that operates at least one or two helicopters, which, by the way, require a great deal of “tender loving care.” Furthermore, each line item (i.e., A, B, C, etc.) is addressed in detail.

*The Guide* makes a considerable effort to suggest which cost line items are variable costs and which are more typically fixed costs. In Fig. 2-438, you have one possible assignment of the many cost line items to either the variable- or the fixed-cost groups.

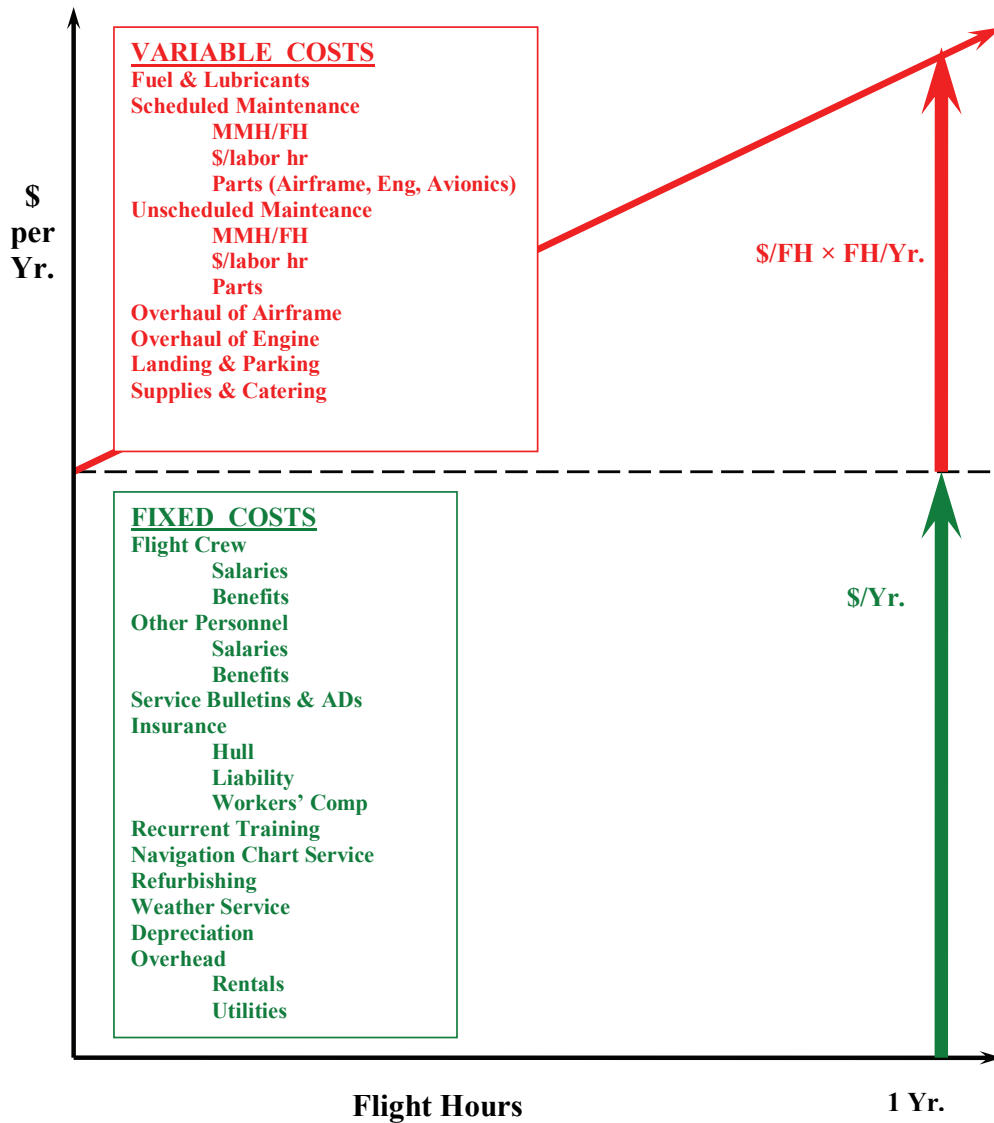


Fig. 2-438. Total operating costs for a year can be divided into two groups: (1) variable (with flight hour) and (2) fixed (typically for a 1-year period).

## 2.9 OPERATING COSTS

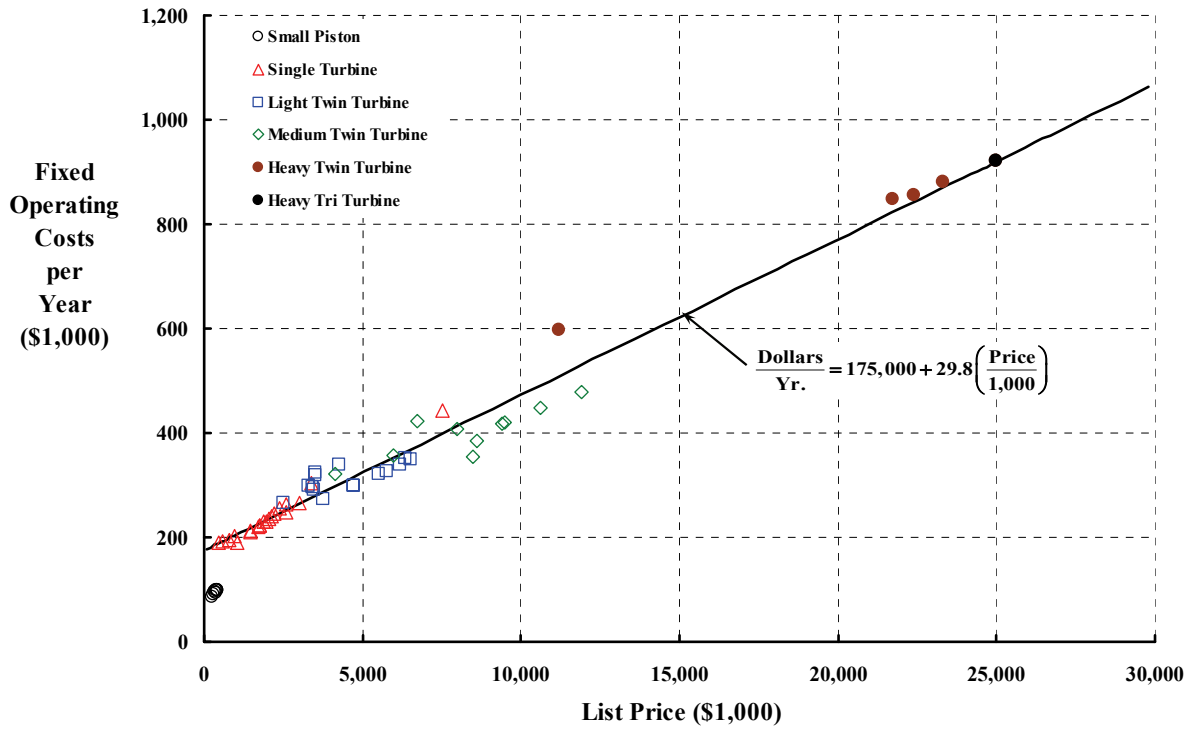


Fig. 2-439. Fixed operating costs per year for newer helicopters (2011 dollars).

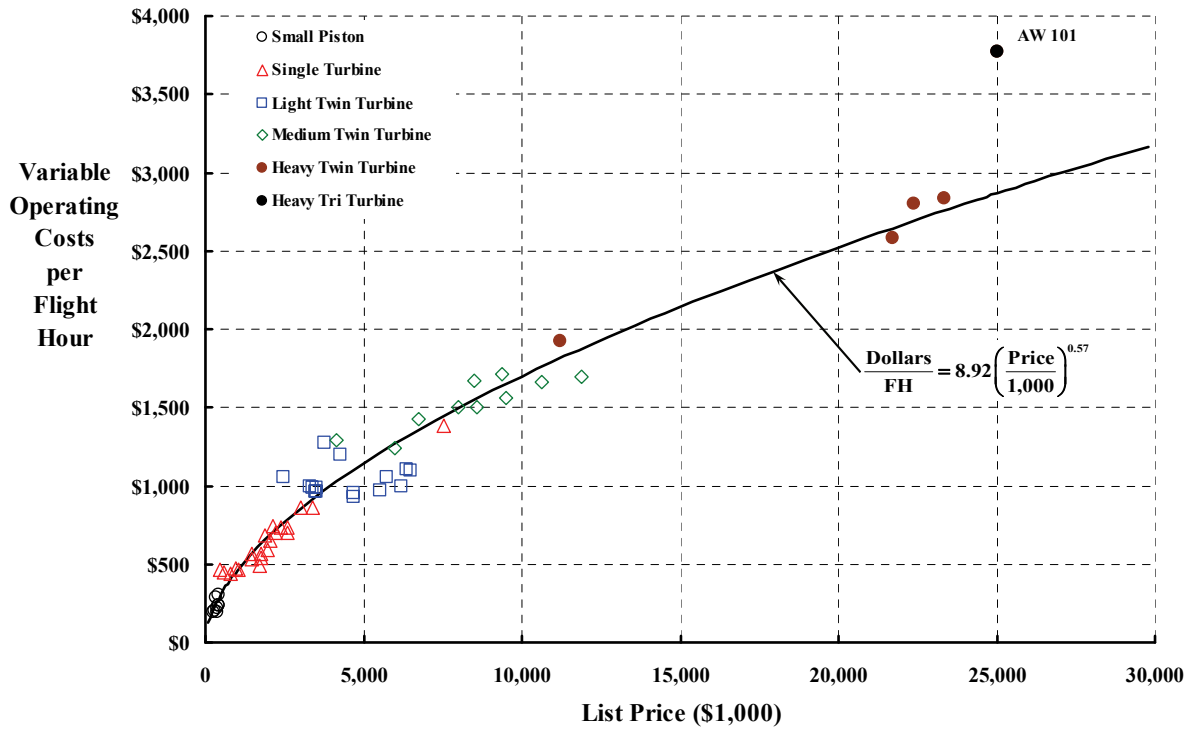


Fig. 2-440. Variable operating costs per flight hour for newer helicopters (2011 dollars).

It is becoming more common in the helicopter industry to define total operating costs as the sum of variable and fixed costs rather than direct and indirect costs.<sup>216</sup> Fig. 2-438 follows this trend, which states, in equation form, that

$$(2.377) \quad \frac{\text{TOC}}{\text{Year}} = \frac{\text{Fixed Costs}}{\text{Year}} + \left( \frac{\text{Variable Costs}}{\text{Flight Hour}} \right) \left( \frac{\text{Flight Hour}}{\text{Year}} \right).$$

This relationship is of the form of a straight line (i.e.,  $y = a + mx$ ). That is, it has an intercept (a), which is fixed costs per year. The slope (m) is variable costs per flight hour, which you also see pictorially in Fig. 2-438.

To give you a rough order of magnitude for the two key parameters (intercept and slope), let me draw upon the data bank embedded in Conklin & de Decker's *Aircraft Cost Evaluator (ACE)*. I selected *only* equipped helicopters introduced into the civil fleet from the year 2000 to 2011 as being representative of "today's state of the art." Beyond that, I accepted factory list price as the primary variable to plot the results. Of course, using list price as the abscissa is absolutely not the only parameter that drives operating costs. For example, you might add number of seats as a variable. Still, for illustration purposes here, it appears adequate. You see the results for fixed costs per year in Fig. 2-439 and variable costs per flight hour with Fig. 2-440.

There is a line and an equation on both Fig. 2-439 and Fig. 2-440. These represent a regression analysis result of just newer turbine-powered helicopters. Using these two approximations, the total operating costs per year can be estimated to the first order simply by substituting the two equations from Fig. 2-439 and Fig. 2-440 into Eq. (2.377), which yields an equation for total operating costs per year. Thus, you have

$$(2.378) \quad \frac{\text{TOC}}{\text{Year}} = \left[ 175,000 + 29.8 \left( \frac{\text{Price}}{1,000} \right) \right] + \left[ 8.92 \left( \frac{\text{Price}}{1,000} \right)^{0.57} \right] \left( \frac{\text{Flight Hour}}{\text{Year}} \right).$$

The underlying assumption here is that the owner/operator has one turbine-powered helicopter in his (or her) company.

The 2010 edition of *The Guide* is very careful to point out that an operator must be aware that TOC per flight hour is very dependent on flight hours flown per year. Ignoring this fact could mean that bidding on a job by using so much per flight hour—based on an incorrect flight-hours-per-year expectation—could mean a substantial loss on a particular job. You can see why *The Guide's* caution is well-founded by looking at Fig. 2-438. Imagine you had a \$5,000,000 helicopter and planned (perhaps hoped would be better) that you would get 400 flight hours worth of business during the forthcoming year. You bid a 1-week job fairly confident that it will take 40 flight hours at \$2,000 per hour, or \$80,000 plus some profit. All

---

<sup>216</sup> Another way for operators to categorize costs is based upon their attachability or traceability to an activity, product, or department within an organization. Two categories are used. The first category is direct costs, which can be traced directly to, say, how much fuel one helicopter uses. The second category is indirect costs, which requires proportioning some yearly fixed cost, say a mechanic's yearly salary, to the time he spends working on that same helicopter.

## 2.9 OPERATING COSTS

you need is 10 jobs like this to meet your goal and make a profit for the year, but then the feast turns to a famine and you only fly 300 hours by the end of the year. In essence, you should have (if you had been clairvoyant) bid the 40-hour job at \$2,300 per hour or \$92,000. You just lost about \$12,000 on that 40-hour job. Naturally, you will bid differently on future jobs and perhaps break even at the end of the year.

You no doubt noticed in Fig. 2-439 that operators with one or two small piston-powered helicopters have fixed costs per year that are about one-half of those for operators of turbine-powered machines. For example, suppose you buy just one Robinson R22 Beta II new on January 1, 2011 for \$258,000. You are likely to have fixed costs of around \$86,000 by the time the year is out—according to the *Aircraft Cost Evaluator* [640]. The same source suggests that the variable cost per flight hour for this modern, two-place helicopter is, on average, just under \$200 per flight hour. Now imagine you accumulate 500 flight hours during the course of the year. That means your total operating costs for 2011 will be \$186,000 (i.e., \$86,000 + 500 × \$200).<sup>217</sup> While these dollar figures may strike you as rather expensive, you should keep in mind that the Robinson Helicopter Company started out selling 7 of the original R22s in 1979 and, by the end of 2009, the company had sold about 4,500 R22s in several versions with no end in sight. It seems to me that when Bell Helicopter stopped

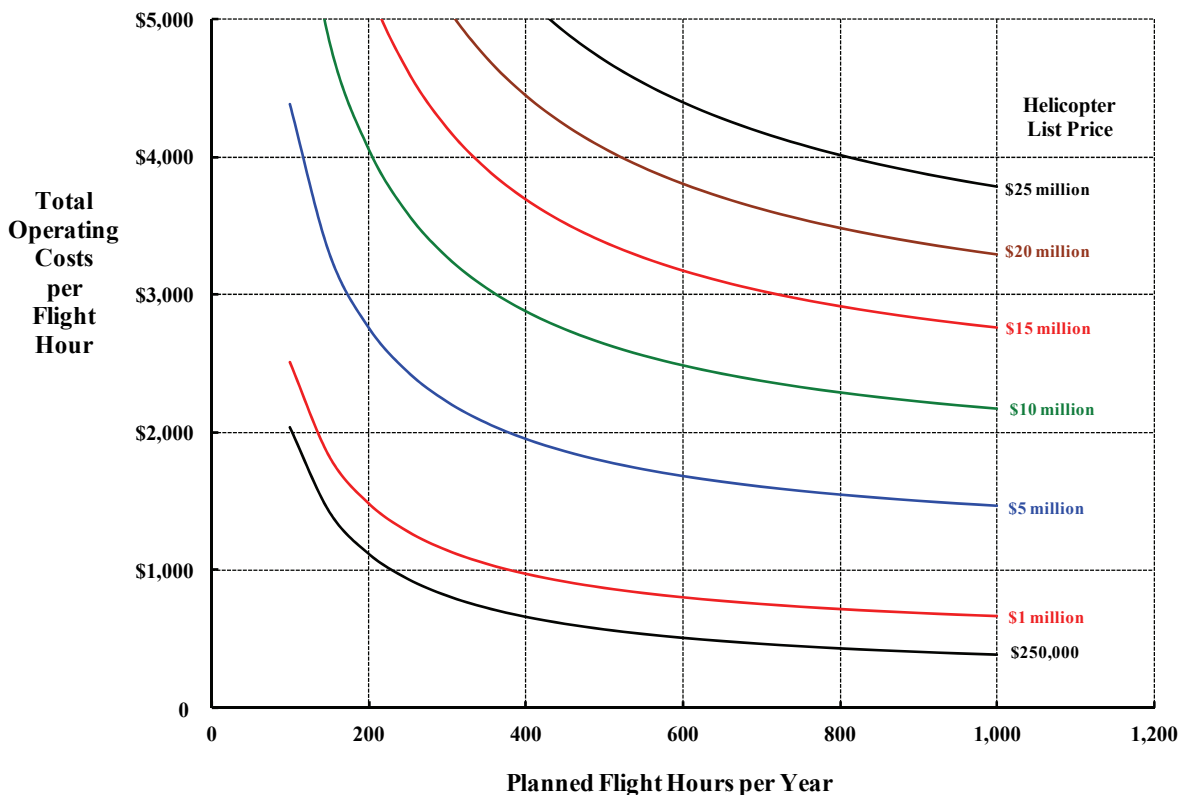


**Fig. 2-441. TOC per flight hour is quite sensitive to the flight hours planned for a year.**

<sup>217</sup> With all deference to our pioneers, this is not the dollar outlay that puts a helicopter in every garage!

## 2.9 OPERATING COSTS

producing its ground-breaking Model 47 in the mid-1970s, Frank Robinson picked up the ball with his R22.<sup>218</sup> There should be no question that the R22 is the helicopter of choice as an entry into the world of helicopter operations.

As a final note, the Robinson R22 total operating costs per year of \$186,000 (assuming 500 hours per year flying) means that you are buying about 72 percent of a new machine each year. This made me wonder about the detailed numbers that Conklin & de Decker found in averaging their survey of many users. Just for the fun of it, I built a TOC cost breakdown to see just what an operator of one R22 should be planning for. My TOC estimate was built upon the estimate dated 15 January 2012 that the Robinson Helicopter company provides on its website [651]. The additional line-item costs used my variation on *ACE* data. I assumed I was both the pilot (\$96/hr) and the mechanic (\$64/hr), albeit a slow one. Table 2-61 gives you my impression of operating costs for an R22.

**Table 2-61. Total Operating Costs for a Robinson Helicopter Company R22 Beta II Bought New for \$274,000 and Flown 500 Hours Per Year**

Cost Line Item	Harris' Estimate	Notes and Assumptions
<b>VARIABLE COSTS Per Year</b>	<b>\$82,690</b>	
Fuel	\$21,400	8 gal./hour, \$5.35/gal. and 500 hours (RHC input)
Lubricants and Fluids	\$430	2% of fuel (RHC input)
Scheduled Maintenance	\$7,680	MMH/FH × \$64 × 500 hrs
MMH/FH	0.24	Fig. 2-437, but slower by 25%. No overhaul included
Unscheduled Maintenance	\$3,840	
MMH/FH	0.12	0.5 times scheduled MMH/FH
Parts (Airframe/Eng/Avionics)	\$10,000	\$20 per flight hour for periodic maintenance parts. <i>ACE</i> input
Engine Restoration	\$6,140	\$12.27/FH (RHC \$27,000 engine exchange program)
Airframe Overhaul	\$31,800	\$140,000/2,200 hr × 500 hr (RHC factory overhaul program)
Landing and Parking	\$750	\$1.50 per hour. No RHC input
Misc	\$650	\$1.30 per hour for catering and misc supplies. No RHC input
<b>FIXED COSTS Per Year</b>	<b>\$85,610</b>	
Crew Salaries		
Base	\$48,000	Harris at \$96/hr. No RHC input
Benefits	\$14,400	Harris at 30% of Base. No RHC input
Aircraft Modernization	\$1,300	<i>ACE</i> input. No RHC input
Hanger	\$2,400	<i>ACE</i> input. No RHC input
Hull Insurance	\$13,700	5% of \$274,000 (I know a guy, and I am a great pilot)
Liability Insurance	\$1,900	1.25% of \$274,000 (I know a guy, and I am a great pilot)
Recurrent Training	\$1,500	<i>ACE</i> input. No RHC input
Navigation Chart Service	\$430	<i>ACE</i> input. No RHC input
Refurbishing	\$1,280	<i>ACE</i> input at 10 labor hours per year per seat × 2 seats
Weather Service	\$700	<i>ACE</i> input. No RHC input
Depreciation	Negligible	RHC input
<b>Total Operating Costs Per Year</b>	<b>\$168,300</b>	

<sup>218</sup> He added the R44 series in 1993 and now has the turbine-powered R66 in production.

## 2.9 OPERATING COSTS

### 2.9.8 Concluding Remarks

Helicopters have become the aircraft of choice for more than two dozen different jobs, as Fig. 2-424 shows, in spite of total operating costs (TOCs) considerably higher than comparative fixed-wing aircraft. Of course, in many, many cases, the job requirements simply exclude fixed-wing aircraft because they cannot hover. Helicopter operators have found that air taxi, charter, offshore oil rig support, and executive transport, for example, are profitable tasks. Where helicopter operators have found that high operating costs simply exclude them from virtually any business is in a head-to-head competition with commercial airlines. The operators have been shut out of even short-haul routes where airports exist, and they have been shut out of city-center-to-city-center routes (even with heliports available) because the unsubsidized ticket price is just too high.

Several generations of helicopter proponents have carried the banner saying that their machines offer just the right addition to the present overall transportation system. The banner states that helicopters now, and future rotorcraft to come, will save the public's time by avoiding growing highway congestion. The more enthusiastic proponents maintain that the whole air traffic system will benefit (and may even avoid collapsing) if the helicopter is introduced. I'm beginning to find the arguments for the helicopter's expanded role rather annoying. I say this because so little reality about operating costs is brought to the table. Project Hummingbird offered the helicopter industry its first try at creating unsubsidized airlines. This first try showed just how small a percentage of the total traveling public would benefit. This first try also showed just what the ticket price would have to be for a helicopter airline to just break even.

Even as late as the mid-1960s, it was not clear to me that helicopter proponents were facing up to their economic obstacles. In December 1963, United Research Inc. prepared a report [652] titled *Outlook for Vertical-Lift Aircraft in Scheduled Commercial Transportation* for the Sikorsky Division of the United Aircraft Corporation, the Vertol Division of the Boeing Company, and for the Small Aircraft Engine Department of the General Electric Company. Let me quote several sentences from the summary of what I consider today to be (1) the best in-depth report ever published studying key aspects of our transportation system and how VTOL aircraft will fit in, and (2) an over-glowing view that keeps being repeated:

“5. As is true in air transport, the subsidy requirements of the helicopter carriers have been related closely to the economic characteristics of their flight equipment. Until the recent introduction of twin-turbine helicopters, the break-even requirements remained well above 100 percent of aircraft capacity. The introduction of twin-turbine equipment has already cut unit operating costs in half and unit costs for turbine operators continue to decline as traffic volume grows. Despite the recent progress which has been made with turbine operations, however, the industry is still heavily dependent upon subsidy support. Subsidy accounts for roughly 50 percent of total operating revenues. Until unit costs are lowered further with an increased scale of operation and load factors raised with higher traffic levels, any substantial reduction in subsidy would cripple the operations of the subsidized carriers at the present time. (Chapter III, pages III-10 through III-27.)

6. The prospects of carriers achieving economic self-sufficiency in the future are good. The nation's intercity and international air travel will continue to expand, and a major part of this travel will be funneled through the airports serving our large metropolitan areas. The pressures which account for severe surface traffic congestion in these urban areas will continue to grow. No technological improvements in surface transportation offering an alternative expedited service are in sight for the near future. Further unit cost reductions can be expected as increasing traffic demand and pending certification of all weather operations increase the utilization of existing facilities, flight equipment and personnel. Although the achievement of economic self-sufficiency is by no means certain, the characteristics of aircraft now available provide the potential for a drastic reduction or possible elimination of subsidy toward the end of a five-year period. (Chapter III, pages III-40 through III-60. )”

This 1963 report has facts and figures in abundance. Unfortunately, if this research were repeated today, I do not believe you would find much has changed. Despite periodic workshops [118], no new argument (in over 35 years) for VTOL airlines came to my attention until the tiltrotor arrived. Then in 1995, at the prodding of Congress, the U.S. Department of Transportation “evaluated the technical feasibility and economic viability of developing civil tiltrotor (CTR) aircraft and a national system of infrastructure to support incorporation of tiltrotor technology into the national transportation system.” [653, 654]. I am not aware of any progress, beyond a recommendation for more studying and more research, that came from the DOT report. The negative views again prevailed.

You may think I have lost all hope of VTOL airlines ever becoming a reality. Nothing could be further from the truth. Keep in mind that commercial airlines sell transportation (seat miles per year) not time in the air (flight hours per year) like General Aviation. Therefore, productivity of V/STOL aircraft (tiltrotor, etc.) may have a significant payoff when compared to a helicopter. While I am disappointed in progress that substantially reduces the purchase price and operating costs of helicopters, the rotorcraft industry has opened a door with the tiltrotor. This VTOL configuration may, in fact, demonstrate the improvement that the Douglas DC-3 gave to the fixed-wing side of the business. At least this gives the rotorcraft industry another chance.

And there is another reason I am always hopeful. It is a quote that I ran across in a report by the American Society of Planning Officials about helicopters in May 1965 [655]. (This group frequently deals with planning for helicopter use in cities.) The short paragraph reads as follows:

“This new vehicle costs too much for everyone. One estimate of initial and maintenance cost for six months is \$5,500. It is unsafe, has no utility, is difficult to operate and expensive to run. There are no adequate service facilities, the insurance costs are extremely high, and there is a most undesirable noise factor. It is practically useless at night and cannot be used in bad weather. Moreover, it compares miserably with the relative cheapness of existing methods of transportation.”

This statement came from a 1907 newspaper article about the automobile. It is not too hard to imagine nearly the exact same words being used to describe the Wright Brothers' invention.



## 2.10 ACCIDENT RECORD

It seems that accidents have been a part of aviation since the dawn of time. First there were tower jumpers, with or without makeshift wings, who were not successful. Then came very rudimentary aircraft of all types that were unstable, uncontrollable, and structurally unsound, not to mention underpowered. Balloons and dirigibles did better, which provided some encouragement until the Hindenburg airship disaster on May 6, 1937, when nearly 100 people were killed. Otto Lilienthal, the German aviation pioneer, was killed on August 10, 1896, after many successful hang glider flights. And in the United States, Wilbur and Orville Wright appeared immune until Orville's crash at Fort Myer on September 17, 1908. The passenger, Lieutenant Thomas E. Selfridge, was killed in that accident. Orville suffered a fractured left leg, four broken ribs, a fractured and dislocated hip, and a back injury. This was the first accident with a powered, heavier-than-air aircraft in which a person died. Orville's accident report to Wilbur by letter on November 14, 1908, traced the initial accident cause to propeller failure. Wilbur wrote a more detailed accident report to Octave Chanute on June 6, 1909, and thus began the practice of accident reporting, all with the purpose of learning how to avoid future accidents.

In this chapter, you will first read some historical background after World War I (WWI) leading up to the last five decades of rotorcraft accidents. These opening remarks include an examination of helicopter accidents per 100,000 flight hours and point out a serious flaw with this commonly quoted accident rate. The second part of this chapter examines 11,426 rotorcraft accidents that the National Transportation Safety Board (NTSB) has reported from January 1, 1964, through 2011. The third part provides a detailed analysis of 8,436 accidents from January 1, 1964, through 1997, and gives a clearer picture of the major human and aircraft deficiencies facing the rotorcraft industry. The concluding remarks offer some specific suggestions that, if taken, will reduce the number of rotorcraft accidents per year by more than half, even as the fleet continues to grow.

### 2.10.1 History, Accident Rate, and Predictions

As WWI drew to a close in late 1918, the major European combatants turned their attention to civil air transportation. Experimental air routes were established in 1919, most with postal service, and passenger acceptance of air travel appeared in 1920. In 1921, the number of passengers significantly increased [656], and traveling by air became an established, but subsidized, industry. France took the lead because of massive government subsidies to its budding airline industry. Great Britain's Government offered little help to its industry until mid-1921. Germany, despite some terms of the armistice, began passenger service as well. In the United States, little national interest beyond air postal service appeared until Charles Lindbergh's nonstop, solo flight across the Atlantic on May 20–21, 1927.

In November 1921, France hosted the Premier Congrès International de la Navigation Aérienne. Two important papers from this conference were translated into English and published in the U.S. by the newly formed National Advisory Committee for Aeronautics, (N.A.C.A.) [657, 658]. The first paper, titled *Organization and Exploitation of Regular Aerial*

## 2.10 ACCIDENT RECORD

*Transportation Lines*, was presented by Tete [657]. Tete comprehensively described commercial aviation growth in France from September 1918 through September 1921. Initial “aerial lines” experimenting began with mail delivery. These experiments quickly showed that “for the regular functioning of aerial transportation lines, it was first necessary to lay out air routes, i.e., to establish airdromes and emergency landing fields, a suitable meteorology service, and a system of communications.” The cooperation of several bureaus within the French Government quickly provided infrastructure, and “at the end of 1919, four French companies were engaged in the regular transportation of passengers and freight” over three major routes. This expansion, illustrated in Fig. 2-442 using tabulated data from Tete’s paper, shows that by the end of 1921, the French airline industry was growing by leaps and bounds. Unfortunately, France’s airlines were covering only about 18 percent of their total operating costs with ticket sales—and this was typical of the world’s air transportation system.

A second paper titled *Aviation and Insurance* [658] was presented by Mayo at the November 1921 conference. Mayo took the position that both France’s and England’s commercial aviation seemed “to be enjoying a considerable degree of prosperity.” But he immediately goes on to say that “in reality the air services in both countries are in a very unsatisfactory condition” because “the air traffic companies of both countries do not pay

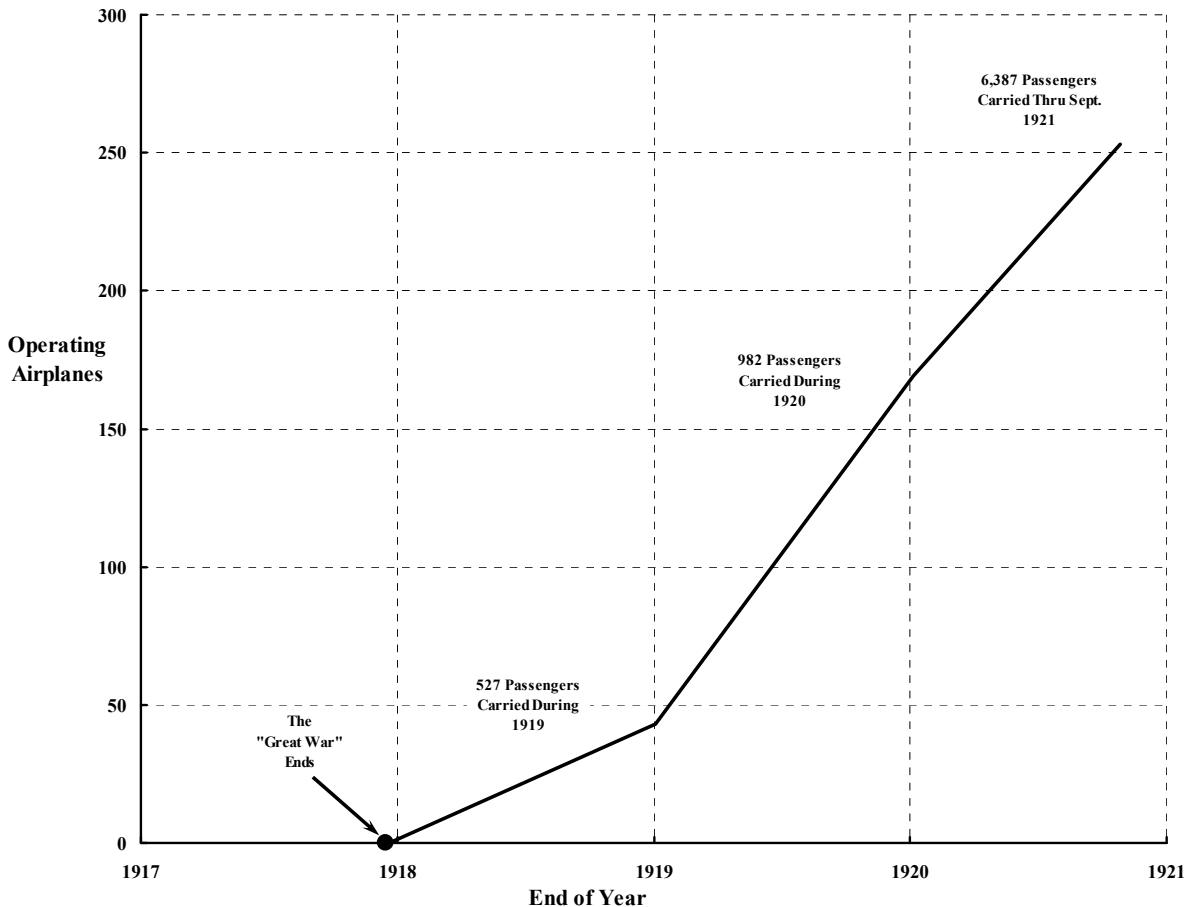


Fig. 2-442. France led the world in developing air transportation.

expenses without aid and will probably not be able to do so for many years to come.” Mayo suggests “many and complex” reasons for this “state of affairs” and then continues saying that “there is, however, one aspect of the question [i.e., the unsatisfactory financial condition] which is all important for the future development of commercial aviation, to wit, aviation insurance.” He makes it very clear that the “existence of satisfactory insurance conditions is indispensable to the commercial prosperity of any enterprise whose capital is invested in anything susceptible of being damaged or destroyed.”

Mayo’s view (just as true today as in 1921) was that if accidents continued at such a high rate, insurance costs would remain high, or go higher, and civil aviation, without continued subsidies, would cease. His “analysis of the statistics of accidents that have happened in civil aviation since the armistice, shows that the number of accidents in which the pilot and passengers were killed or even injured, has been remarkably small. It is doubtless due to this fact that civil aviation has prospered as it has and that the number of passengers carried has risen so rapidly and constantly. The number of airplane accidents, however, has been lamentably high.” Mayo makes it clear that “the [airline] companies must, in their own interest, frankly face the situation and make a determined effort to reduce the number of accidents.”<sup>219</sup>

Mayo alerts the several aviation companies that the insurance industry is well aware of the accident rate and that “several large [underwriters] have been obligated to stop taking aviation risks.” He then points out the “causes of the many accidents which account for the high insurance rates,” stating:

“The frequent accidents to airplanes employed on air routes have been due to widely divergent causes. Probably 90 % of them were due to carelessness and could have been avoided, had the necessary precautions been taken. The principal causes of accidents may be enumerated as follows:

1. Poor piloting;
2. Engine trouble;
3. Lack of system [i.e., not employing top-notch people];
4. Poorly adapted airplanes;
5. Poor airdromes;
6. Unfavorable meteorological conditions.”

In concluding this discussion of civil aviation history up to the end of 1921, I suggest that, with only minor changes, R. H. Mayo’s paper could be presented today at any helicopter (or, for that matter, even general aviation) safety symposium.

Now take a 10-year step forward to aviation and its accident situation in the U.S. The birth of commercial aviation in the U.S. is traced back to 1914 by Davies in *Airlines of the United States* [316] and by van der Linden in his superb book, *Airlines and Air Mail—The Post Office and the Birth of the Commercial Aviation Industry* [498]. As is well known, the

---

<sup>219</sup> It is quite clear that the airline companies of the world have made the “determined effort” Mayo spoke about (as you will no doubt agree)—and they have been remarkably successful. Unfortunately, the results achieved by the rotorcraft industry are not so clear.

## 2.10 ACCIDENT RECORD

post office played a key role in starting commercial aviation in this country. In many ways, the U.S. simply followed France's startup model. What is not so well known is that the growing number of airplane accidents up to the late 1920s became a great concern to several departments of the U.S. Government. Army, Navy, and civilian aircraft pilots were experiencing stalls followed by spins, forced landings following engine failure were all too common and, even with power, landings frequently ended as crashes. By 1928 the situation was serious enough to warrant attention from the Assistant Secretaries for Aeronautics in the Departments of War, Navy, and Commerce.

These departments called upon the N.A.C.A. to establish a special commission that would "prepare a basis for the classification and comparison of aircraft accidents, both civil and military." The commission was formed, and the first meeting was held on March 1, 1928. Finally, after 16 meetings, the committee's work was published on August 15, 1928, as NACA Report No. 308 [659]. This report defined 13 classes of accidents, 4 classes of injuries, and 6 classes of damage to material. Categories of immediate and underlying accident causes were established, and an accident form was adopted. This classification basis was used to analyze 1,432 military and 1,400 civilian accidents that occurred before January 1929. The resulting analysis and associated tabulated data were published one year later in NACA Report No. 357 [660].

In June 1936, a further refinement to definitions and methods of analysis was established with NACA Report No. 576 [661]. This report, titled simply *Aircraft Accidents*, became the standard U.S. reference on the subject and formed the foundation for current NTSB aviation accident reporting. The accident form (Fig. 2-443) had evolved, and it proved to be of immense value. Notice that the "immediate causes of the accident" were divided into four subcategories and the "underlying causes of accident" into only two subcategories. Furthermore, it was not enough to just record pilot error or material failure. The form demanded much more in-depth investigation and reporting.

The form, plus analysis of some 2,800 accidents, led to a table of summary conclusions [660], which is displayed here using the bar chart in Fig. 2-444. There was an immediate payoff for the efforts of the N.A.C.A.-led committee. Analysis of the data revealed major shortcomings in aircraft design and pilot training (e.g., deficiencies in aircraft stability, and control and spin recognition and recovery by pilots) for which corrective actions were developed and implemented. It should be noted that solving these problems did not require computing accidents per flight hour or other ratios that are considered important measures of transportation safety today. The priority then, as now, was to put an end to accidents.

Of course, World War II (WWII) disrupted the orderly and documented study of accidents. However, in October 1944, the U.S. Civil Aeronautics Administration (CAA), the predecessor to the Federal Aviation Administration (FAA), published the first Statistical Handbook of Civil Aviation [662]. This first of many CAA (and then FAA) handbooks pointed out that reported accident statistics were based on definitions and classifications

N.A.C.A. AIRCRAFT ACCIDENT ANALYSIS FORM																																																																																																																																																																																																																																																																																																																																																																																																																																																																																																																																																																																																																																																																																																																																																																																																																																																																																																																																																														
CLASSIFICATION OF ACCIDENT NATURE : ..... RESULTS : ..... PERSONNEL (CLASS) ..... MATERIAL (CLASS) .....			UNDERLYING CAUSES OF ACCIDENT																																																																																																																																																																																																																																																																																																																																																																																																																																																																																																																																																																																																																																																																																																																																																																																																																																																																																																																																																											
			ERRORS OF PILOT							MATERIAL																																																																																																																																																																																																																																																																																																																																																																																																																																																																																																																																																																																																																																																																																																																																																																																																																																																																																																																																																				
			LACK OF EXPERIENCE			PHYSICAL AND PSYCHOLOGICAL				FAULTY INSTRUCTIONS		INSPECTION			MATERIALS		DESIGN																																																																																																																																																																																																																																																																																																																																																																																																																																																																																																																																																																																																																																																																																																																																																																																																																																																																																																																																													
			GENERAL	SPECIAL		DISEASE OR DEFECT	POOR REACTION	TEMPORARY	TEMPORARY	OPERATING	MAINTENANCE	MANUFACTURING	OVERHAUL	MAINTENANCE	UNDETERMINED	ORIGINALLY DEFECTIVE	DETERIORATED	UNDETERMINED	STRENGTH (STRUCTURAL)	ARRANGEMENT	AERODYNAMIC	UNDETERMINED	MODIFICATION	UNDETERMINED																																																																																																																																																																																																																																																																																																																																																																																																																																																																																																																																																																																																																																																																																																																																																																																																																																																																																																																																						
TOTAL	RECENT	TOTAL	RECENT	INHERENT	TEMPORARY	INHERENT	TEMPORARY																																																																																																																																																																																																																																																																																																																																																																																																																																																																																																																																																																																																																																																																																																																																																																																																																																																																																																																																																							
IMMEDIATE CAUSES OF ACCIDENT			PERSONNEL																																																																																																																																																																																																																																																																																																																																																																																																																																																																																																																																																																																																																																																																																																																																																																																																																																																																																																																																																											
			<table border="1"> <tr> <td rowspan="5">%</td> <td rowspan="5">PERSONNEL</td> <td rowspan="5">ERRORS OF PILOT</td> <td>ERROR OF JUDGMENT</td> <td></td><td></td><td></td><td></td><td></td><td></td><td></td><td></td><td></td><td></td><td></td><td></td><td></td><td></td><td></td><td></td><td></td><td></td><td></td><td></td> </tr> <tr> <td>POOR TECHNIQUE</td> <td></td><td></td><td></td><td></td><td></td><td></td><td></td><td></td><td></td><td></td><td></td><td></td><td></td><td></td><td></td><td></td><td></td><td></td><td></td><td></td><td></td> </tr> <tr> <td>DISOBEDIENCE OF ORDERS</td> <td></td><td></td><td></td><td></td><td></td><td></td><td></td><td></td><td></td><td></td><td></td><td></td><td></td><td></td><td></td><td></td><td></td><td></td><td></td><td></td><td></td><td></td> </tr> <tr> <td>CARELESSNESS OR NEGLIGENCE</td> <td></td><td></td><td></td><td></td><td></td><td></td><td></td><td></td><td></td><td></td><td></td><td></td><td></td><td></td><td></td><td></td><td></td><td></td><td></td><td></td><td></td><td></td> </tr> <tr> <td>MISCELLANEOUS</td> <td></td><td></td><td></td><td></td><td></td><td></td><td></td><td></td><td></td><td></td><td></td><td></td><td></td><td></td><td></td><td></td><td></td><td></td><td></td><td></td><td></td><td></td> </tr> <tr> <td colspan="20">ERRORS OF OTHER PERSONNEL</td> </tr> <tr> <td colspan="3" rowspan="20">MATERIAL</td> <td colspan="20">POWER PLANT</td> </tr> <tr> <td colspan="20"> <table border="1"> <tr><td>FUEL SYSTEM</td><td></td><td></td><td></td><td></td><td></td><td></td><td></td><td></td><td></td><td></td><td></td><td></td><td></td><td></td><td></td><td></td><td></td><td></td><td></td><td></td><td></td><td></td></tr> <tr><td>COOLING SYSTEM</td><td></td><td></td><td></td><td></td><td></td><td></td><td></td><td></td><td></td><td></td><td></td><td></td><td></td><td></td><td></td><td></td><td></td><td></td><td></td><td></td><td></td><td></td></tr> <tr><td>IGNITION SYSTEM</td><td></td><td></td><td></td><td></td><td></td><td></td><td></td><td></td><td></td><td></td><td></td><td></td><td></td><td></td><td></td><td></td><td></td><td></td><td></td><td></td><td></td><td></td></tr> <tr><td>LUBRICATION SYSTEM</td><td></td><td></td><td></td><td></td><td></td><td></td><td></td><td></td><td></td><td></td><td></td><td></td><td></td><td></td><td></td><td></td><td></td><td></td><td></td><td></td><td></td><td></td></tr> <tr><td>ENGINE STRUCTURE</td><td></td><td></td><td></td><td></td><td></td><td></td><td></td><td></td><td></td><td></td><td></td><td></td><td></td><td></td><td></td><td></td><td></td><td></td><td></td><td></td><td></td><td></td></tr> <tr><td>PROPELLER AND PROPELLER ACCESSORIES</td><td></td><td></td><td></td><td></td><td></td><td></td><td></td><td></td><td></td><td></td><td></td><td></td><td></td><td></td><td></td><td></td><td></td><td></td><td></td><td></td><td></td><td></td></tr> <tr><td>ENGINE CONTROL SYSTEM</td><td></td><td></td><td></td><td></td><td></td><td></td><td></td><td></td><td></td><td></td><td></td><td></td><td></td><td></td><td></td><td></td><td></td><td></td><td></td><td></td><td></td><td></td></tr> <tr><td>MISCELLANEOUS</td><td></td><td></td><td></td><td></td><td></td><td></td><td></td><td></td><td></td><td></td><td></td><td></td><td></td><td></td><td></td><td></td><td></td><td></td><td></td><td></td><td></td><td></td></tr> <tr><td>UNDETERMINED</td><td></td><td></td><td></td><td></td><td></td><td></td><td></td><td></td><td></td><td></td><td></td><td></td><td></td><td></td><td></td><td></td><td></td><td></td><td></td><td></td><td></td><td></td></tr> </table> </td> </tr> <tr> <td colspan="20">STRUCTURAL</td> </tr> <tr> <td colspan="20"> <table border="1"> <tr><td>FLIGHT CONTROL SYSTEM</td><td></td><td></td><td></td><td></td><td></td><td></td><td></td><td></td><td></td><td></td><td></td><td></td><td></td><td></td><td></td><td></td><td></td><td></td><td></td><td></td><td></td><td></td></tr> <tr><td>MOVABLE SURFACES</td><td></td><td></td><td></td><td></td><td></td><td></td><td></td><td></td><td></td><td></td><td></td><td></td><td></td><td></td><td></td><td></td><td></td><td></td><td></td><td></td><td></td><td></td></tr> <tr><td>STABILIZING SURFACES; STRUTS, WIRES &amp; FITTINGS</td><td></td><td></td><td></td><td></td><td></td><td></td><td></td><td></td><td></td><td></td><td></td><td></td><td></td><td></td><td></td><td></td><td></td><td></td><td></td><td></td><td></td><td></td></tr> <tr><td>WINGS; STRUTS, WIRES, AND FITTINGS</td><td></td><td></td><td></td><td></td><td></td><td></td><td></td><td></td><td></td><td></td><td></td><td></td><td></td><td></td><td></td><td></td><td></td><td></td><td></td><td></td><td></td><td></td></tr> <tr><td>LANDING GEAR; STRUTS, WIRES, FITTINGS, AND RETRACTING MECHANISM</td><td></td><td></td><td></td><td></td><td></td><td></td><td></td><td></td><td></td><td></td><td></td><td></td><td></td><td></td><td></td><td></td><td></td><td></td><td></td><td></td><td></td><td></td></tr> <tr><td>WHEELS, TIRES &amp; BRAKES</td><td></td><td></td><td></td><td></td><td></td><td></td><td></td><td></td><td></td><td></td><td></td><td></td><td></td><td></td><td></td><td></td><td></td><td></td><td></td><td></td><td></td><td></td></tr> <tr><td>SEAPLANE FLOAT OR HULL; STRUTS, WIRES &amp; FITTINGS</td><td></td><td></td><td></td><td></td><td></td><td></td><td></td><td></td><td></td><td></td><td></td><td></td><td></td><td></td><td></td><td></td><td></td><td></td><td></td><td></td><td></td><td></td></tr> <tr><td>FUSELAGE, ENGINE MOUNT, AND FITTINGS</td><td></td><td></td><td></td><td></td><td></td><td></td><td></td><td></td><td></td><td></td><td></td><td></td><td></td><td></td><td></td><td></td><td></td><td></td><td></td><td></td><td></td><td></td></tr> <tr><td>COWLING, FAIRING &amp; FITTINGS</td><td></td><td></td><td></td><td></td><td></td><td></td><td></td><td></td><td></td><td></td><td></td><td></td><td></td><td></td><td></td><td></td><td></td><td></td><td></td><td></td><td></td><td></td></tr> <tr><td>TAIL WHEEL ASSEMBLY AND SKID</td><td></td><td></td><td></td><td></td><td></td><td></td><td></td><td></td><td></td><td></td><td></td><td></td><td></td><td></td><td></td><td></td><td></td><td></td><td></td><td></td><td></td><td></td></tr> <tr><td>ARRESTING APPLIANCES ON AIRCRAFT</td><td></td><td></td><td></td><td></td><td></td><td></td><td></td><td></td><td></td><td></td><td></td><td></td><td></td><td></td><td></td><td></td><td></td><td></td><td></td><td></td><td></td><td></td></tr> <tr><td>MISCELLANEOUS</td><td></td><td></td><td></td><td></td><td></td><td></td><td></td><td></td><td></td><td></td><td></td><td></td><td></td><td></td><td></td><td></td><td></td><td></td><td></td><td></td><td></td><td></td></tr> <tr><td>UNDETERMINED</td><td></td><td></td><td></td><td></td><td></td><td></td><td></td><td></td><td></td><td></td><td></td><td></td><td></td><td></td><td></td><td></td><td></td><td></td><td></td><td></td><td></td><td></td></tr> </table> </td> </tr> <tr> <td colspan="20">HANDLING QUALITIES</td> </tr> <tr> <td colspan="20">INSTRUMENTS</td> </tr> <tr> <td colspan="20">LAUNCHING DEVICES</td> </tr> <tr> <td colspan="20">ARRESTING DEVICES</td> </tr> <tr> <td colspan="3" rowspan="4">MISCELLANEOUS</td> <td colspan="20">WEATHER</td> </tr> <tr> <td colspan="20">DARKNESS</td> </tr> <tr> <td colspan="20">AIRPORT OR TERRAIN</td> </tr> <tr> <td colspan="20">OTHER</td> </tr> <tr> <td colspan="3">UNDETERMINED</td> <td colspan="17"> <p style="text-align: center;">RECOMMENDED BY COMMITTEE ON AIRCRAFT ACCIDENTS JUNE 22, 1936 APPROVED BY EXECUTIVE COMMITTEE NATIONAL ADVISORY COMMITTEE FOR AERONAUTICS JUNE 23, 1936</p> </td> </tr> </table>																				%	PERSONNEL	ERRORS OF PILOT	ERROR OF JUDGMENT																					POOR TECHNIQUE																						DISOBEDIENCE OF ORDERS																							CARELESSNESS OR NEGLIGENCE																							MISCELLANEOUS																							ERRORS OF OTHER PERSONNEL																				MATERIAL			POWER PLANT																				<table border="1"> <tr><td>FUEL SYSTEM</td><td></td><td></td><td></td><td></td><td></td><td></td><td></td><td></td><td></td><td></td><td></td><td></td><td></td><td></td><td></td><td></td><td></td><td></td><td></td><td></td><td></td><td></td></tr> <tr><td>COOLING SYSTEM</td><td></td><td></td><td></td><td></td><td></td><td></td><td></td><td></td><td></td><td></td><td></td><td></td><td></td><td></td><td></td><td></td><td></td><td></td><td></td><td></td><td></td><td></td></tr> <tr><td>IGNITION SYSTEM</td><td></td><td></td><td></td><td></td><td></td><td></td><td></td><td></td><td></td><td></td><td></td><td></td><td></td><td></td><td></td><td></td><td></td><td></td><td></td><td></td><td></td><td></td></tr> <tr><td>LUBRICATION SYSTEM</td><td></td><td></td><td></td><td></td><td></td><td></td><td></td><td></td><td></td><td></td><td></td><td></td><td></td><td></td><td></td><td></td><td></td><td></td><td></td><td></td><td></td><td></td></tr> <tr><td>ENGINE STRUCTURE</td><td></td><td></td><td></td><td></td><td></td><td></td><td></td><td></td><td></td><td></td><td></td><td></td><td></td><td></td><td></td><td></td><td></td><td></td><td></td><td></td><td></td><td></td></tr> <tr><td>PROPELLER AND PROPELLER ACCESSORIES</td><td></td><td></td><td></td><td></td><td></td><td></td><td></td><td></td><td></td><td></td><td></td><td></td><td></td><td></td><td></td><td></td><td></td><td></td><td></td><td></td><td></td><td></td></tr> <tr><td>ENGINE CONTROL SYSTEM</td><td></td><td></td><td></td><td></td><td></td><td></td><td></td><td></td><td></td><td></td><td></td><td></td><td></td><td></td><td></td><td></td><td></td><td></td><td></td><td></td><td></td><td></td></tr> <tr><td>MISCELLANEOUS</td><td></td><td></td><td></td><td></td><td></td><td></td><td></td><td></td><td></td><td></td><td></td><td></td><td></td><td></td><td></td><td></td><td></td><td></td><td></td><td></td><td></td><td></td></tr> <tr><td>UNDETERMINED</td><td></td><td></td><td></td><td></td><td></td><td></td><td></td><td></td><td></td><td></td><td></td><td></td><td></td><td></td><td></td><td></td><td></td><td></td><td></td><td></td><td></td><td></td></tr> </table>																				FUEL SYSTEM																							COOLING SYSTEM																							IGNITION SYSTEM																							LUBRICATION SYSTEM																							ENGINE STRUCTURE																							PROPELLER AND PROPELLER ACCESSORIES																							ENGINE CONTROL SYSTEM																							MISCELLANEOUS																							UNDETERMINED																							STRUCTURAL																				<table border="1"> <tr><td>FLIGHT CONTROL SYSTEM</td><td></td><td></td><td></td><td></td><td></td><td></td><td></td><td></td><td></td><td></td><td></td><td></td><td></td><td></td><td></td><td></td><td></td><td></td><td></td><td></td><td></td><td></td></tr> <tr><td>MOVABLE SURFACES</td><td></td><td></td><td></td><td></td><td></td><td></td><td></td><td></td><td></td><td></td><td></td><td></td><td></td><td></td><td></td><td></td><td></td><td></td><td></td><td></td><td></td><td></td></tr> <tr><td>STABILIZING SURFACES; STRUTS, WIRES &amp; FITTINGS</td><td></td><td></td><td></td><td></td><td></td><td></td><td></td><td></td><td></td><td></td><td></td><td></td><td></td><td></td><td></td><td></td><td></td><td></td><td></td><td></td><td></td><td></td></tr> <tr><td>WINGS; STRUTS, WIRES, AND FITTINGS</td><td></td><td></td><td></td><td></td><td></td><td></td><td></td><td></td><td></td><td></td><td></td><td></td><td></td><td></td><td></td><td></td><td></td><td></td><td></td><td></td><td></td><td></td></tr> <tr><td>LANDING GEAR; STRUTS, WIRES, FITTINGS, AND RETRACTING MECHANISM</td><td></td><td></td><td></td><td></td><td></td><td></td><td></td><td></td><td></td><td></td><td></td><td></td><td></td><td></td><td></td><td></td><td></td><td></td><td></td><td></td><td></td><td></td></tr> <tr><td>WHEELS, TIRES &amp; BRAKES</td><td></td><td></td><td></td><td></td><td></td><td></td><td></td><td></td><td></td><td></td><td></td><td></td><td></td><td></td><td></td><td></td><td></td><td></td><td></td><td></td><td></td><td></td></tr> <tr><td>SEAPLANE FLOAT OR HULL; STRUTS, WIRES &amp; FITTINGS</td><td></td><td></td><td></td><td></td><td></td><td></td><td></td><td></td><td></td><td></td><td></td><td></td><td></td><td></td><td></td><td></td><td></td><td></td><td></td><td></td><td></td><td></td></tr> <tr><td>FUSELAGE, ENGINE MOUNT, AND FITTINGS</td><td></td><td></td><td></td><td></td><td></td><td></td><td></td><td></td><td></td><td></td><td></td><td></td><td></td><td></td><td></td><td></td><td></td><td></td><td></td><td></td><td></td><td></td></tr> <tr><td>COWLING, FAIRING &amp; FITTINGS</td><td></td><td></td><td></td><td></td><td></td><td></td><td></td><td></td><td></td><td></td><td></td><td></td><td></td><td></td><td></td><td></td><td></td><td></td><td></td><td></td><td></td><td></td></tr> <tr><td>TAIL WHEEL ASSEMBLY AND SKID</td><td></td><td></td><td></td><td></td><td></td><td></td><td></td><td></td><td></td><td></td><td></td><td></td><td></td><td></td><td></td><td></td><td></td><td></td><td></td><td></td><td></td><td></td></tr> <tr><td>ARRESTING APPLIANCES ON AIRCRAFT</td><td></td><td></td><td></td><td></td><td></td><td></td><td></td><td></td><td></td><td></td><td></td><td></td><td></td><td></td><td></td><td></td><td></td><td></td><td></td><td></td><td></td><td></td></tr> <tr><td>MISCELLANEOUS</td><td></td><td></td><td></td><td></td><td></td><td></td><td></td><td></td><td></td><td></td><td></td><td></td><td></td><td></td><td></td><td></td><td></td><td></td><td></td><td></td><td></td><td></td></tr> <tr><td>UNDETERMINED</td><td></td><td></td><td></td><td></td><td></td><td></td><td></td><td></td><td></td><td></td><td></td><td></td><td></td><td></td><td></td><td></td><td></td><td></td><td></td><td></td><td></td><td></td></tr> </table>																				FLIGHT CONTROL SYSTEM																							MOVABLE SURFACES																							STABILIZING SURFACES; STRUTS, WIRES & FITTINGS																							WINGS; STRUTS, WIRES, AND FITTINGS																							LANDING GEAR; STRUTS, WIRES, FITTINGS, AND RETRACTING MECHANISM																							WHEELS, TIRES & BRAKES																							SEAPLANE FLOAT OR HULL; STRUTS, WIRES & FITTINGS																							FUSELAGE, ENGINE MOUNT, AND FITTINGS																							COWLING, FAIRING & FITTINGS																							TAIL WHEEL ASSEMBLY AND SKID																							ARRESTING APPLIANCES ON AIRCRAFT																							MISCELLANEOUS																							UNDETERMINED																							HANDLING QUALITIES																				INSTRUMENTS																				LAUNCHING DEVICES																				ARRESTING DEVICES																				MISCELLANEOUS			WEATHER																				DARKNESS																				AIRPORT OR TERRAIN																				OTHER																				UNDETERMINED			<p style="text-align: center;">RECOMMENDED BY COMMITTEE ON AIRCRAFT ACCIDENTS JUNE 22, 1936 APPROVED BY EXECUTIVE COMMITTEE NATIONAL ADVISORY COMMITTEE FOR AERONAUTICS JUNE 23, 1936</p>													
%	PERSONNEL	ERRORS OF PILOT	ERROR OF JUDGMENT																																																																																																																																																																																																																																																																																																																																																																																																																																																																																																																																																																																																																																																																																																																																																																																																																																																																																																																																																											
			POOR TECHNIQUE																																																																																																																																																																																																																																																																																																																																																																																																																																																																																																																																																																																																																																																																																																																																																																																																																																																																																																																																																											
			DISOBEDIENCE OF ORDERS																																																																																																																																																																																																																																																																																																																																																																																																																																																																																																																																																																																																																																																																																																																																																																																																																																																																																																																																																											
			CARELESSNESS OR NEGLIGENCE																																																																																																																																																																																																																																																																																																																																																																																																																																																																																																																																																																																																																																																																																																																																																																																																																																																																																																																																																											
			MISCELLANEOUS																																																																																																																																																																																																																																																																																																																																																																																																																																																																																																																																																																																																																																																																																																																																																																																																																																																																																																																																																											
ERRORS OF OTHER PERSONNEL																																																																																																																																																																																																																																																																																																																																																																																																																																																																																																																																																																																																																																																																																																																																																																																																																																																																																																																																																														
MATERIAL			POWER PLANT																																																																																																																																																																																																																																																																																																																																																																																																																																																																																																																																																																																																																																																																																																																																																																																																																																																																																																																																																											
			<table border="1"> <tr><td>FUEL SYSTEM</td><td></td><td></td><td></td><td></td><td></td><td></td><td></td><td></td><td></td><td></td><td></td><td></td><td></td><td></td><td></td><td></td><td></td><td></td><td></td><td></td><td></td><td></td></tr> <tr><td>COOLING SYSTEM</td><td></td><td></td><td></td><td></td><td></td><td></td><td></td><td></td><td></td><td></td><td></td><td></td><td></td><td></td><td></td><td></td><td></td><td></td><td></td><td></td><td></td><td></td></tr> <tr><td>IGNITION SYSTEM</td><td></td><td></td><td></td><td></td><td></td><td></td><td></td><td></td><td></td><td></td><td></td><td></td><td></td><td></td><td></td><td></td><td></td><td></td><td></td><td></td><td></td><td></td></tr> <tr><td>LUBRICATION SYSTEM</td><td></td><td></td><td></td><td></td><td></td><td></td><td></td><td></td><td></td><td></td><td></td><td></td><td></td><td></td><td></td><td></td><td></td><td></td><td></td><td></td><td></td><td></td></tr> <tr><td>ENGINE STRUCTURE</td><td></td><td></td><td></td><td></td><td></td><td></td><td></td><td></td><td></td><td></td><td></td><td></td><td></td><td></td><td></td><td></td><td></td><td></td><td></td><td></td><td></td><td></td></tr> <tr><td>PROPELLER AND PROPELLER ACCESSORIES</td><td></td><td></td><td></td><td></td><td></td><td></td><td></td><td></td><td></td><td></td><td></td><td></td><td></td><td></td><td></td><td></td><td></td><td></td><td></td><td></td><td></td><td></td></tr> <tr><td>ENGINE CONTROL SYSTEM</td><td></td><td></td><td></td><td></td><td></td><td></td><td></td><td></td><td></td><td></td><td></td><td></td><td></td><td></td><td></td><td></td><td></td><td></td><td></td><td></td><td></td><td></td></tr> <tr><td>MISCELLANEOUS</td><td></td><td></td><td></td><td></td><td></td><td></td><td></td><td></td><td></td><td></td><td></td><td></td><td></td><td></td><td></td><td></td><td></td><td></td><td></td><td></td><td></td><td></td></tr> <tr><td>UNDETERMINED</td><td></td><td></td><td></td><td></td><td></td><td></td><td></td><td></td><td></td><td></td><td></td><td></td><td></td><td></td><td></td><td></td><td></td><td></td><td></td><td></td><td></td><td></td></tr> </table>																				FUEL SYSTEM																							COOLING SYSTEM																							IGNITION SYSTEM																							LUBRICATION SYSTEM																							ENGINE STRUCTURE																							PROPELLER AND PROPELLER ACCESSORIES																										ENGINE CONTROL SYSTEM																							MISCELLANEOUS																							UNDETERMINED																																																																																																																																																																																																																																																																																																																																																																																																																																																																																																																																																																																																																																																																																																																																												
			FUEL SYSTEM																																																																																																																																																																																																																																																																																																																																																																																																																																																																																																																																																																																																																																																																																																																																																																																																																																																																																																																																																											
			COOLING SYSTEM																																																																																																																																																																																																																																																																																																																																																																																																																																																																																																																																																																																																																																																																																																																																																																																																																																																																																																																																																											
			IGNITION SYSTEM																																																																																																																																																																																																																																																																																																																																																																																																																																																																																																																																																																																																																																																																																																																																																																																																																																																																																																																																																											
			LUBRICATION SYSTEM																																																																																																																																																																																																																																																																																																																																																																																																																																																																																																																																																																																																																																																																																																																																																																																																																																																																																																																																																											
			ENGINE STRUCTURE																																																																																																																																																																																																																																																																																																																																																																																																																																																																																																																																																																																																																																																																																																																																																																																																																																																																																																																																																											
			PROPELLER AND PROPELLER ACCESSORIES																																																																																																																																																																																																																																																																																																																																																																																																																																																																																																																																																																																																																																																																																																																																																																																																																																																																																																																																																											
			ENGINE CONTROL SYSTEM																																																																																																																																																																																																																																																																																																																																																																																																																																																																																																																																																																																																																																																																																																																																																																																																																																																																																																																																																											
			MISCELLANEOUS																																																																																																																																																																																																																																																																																																																																																																																																																																																																																																																																																																																																																																																																																																																																																																																																																																																																																																																																																											
			UNDETERMINED																																																																																																																																																																																																																																																																																																																																																																																																																																																																																																																																																																																																																																																																																																																																																																																																																																																																																																																																																											
			STRUCTURAL																																																																																																																																																																																																																																																																																																																																																																																																																																																																																																																																																																																																																																																																																																																																																																																																																																																																																																																																																											
			<table border="1"> <tr><td>FLIGHT CONTROL SYSTEM</td><td></td><td></td><td></td><td></td><td></td><td></td><td></td><td></td><td></td><td></td><td></td><td></td><td></td><td></td><td></td><td></td><td></td><td></td><td></td><td></td><td></td><td></td></tr> <tr><td>MOVABLE SURFACES</td><td></td><td></td><td></td><td></td><td></td><td></td><td></td><td></td><td></td><td></td><td></td><td></td><td></td><td></td><td></td><td></td><td></td><td></td><td></td><td></td><td></td><td></td></tr> <tr><td>STABILIZING SURFACES; STRUTS, WIRES &amp; FITTINGS</td><td></td><td></td><td></td><td></td><td></td><td></td><td></td><td></td><td></td><td></td><td></td><td></td><td></td><td></td><td></td><td></td><td></td><td></td><td></td><td></td><td></td><td></td></tr> <tr><td>WINGS; STRUTS, WIRES, AND FITTINGS</td><td></td><td></td><td></td><td></td><td></td><td></td><td></td><td></td><td></td><td></td><td></td><td></td><td></td><td></td><td></td><td></td><td></td><td></td><td></td><td></td><td></td><td></td></tr> <tr><td>LANDING GEAR; STRUTS, WIRES, FITTINGS, AND RETRACTING MECHANISM</td><td></td><td></td><td></td><td></td><td></td><td></td><td></td><td></td><td></td><td></td><td></td><td></td><td></td><td></td><td></td><td></td><td></td><td></td><td></td><td></td><td></td><td></td></tr> <tr><td>WHEELS, TIRES &amp; BRAKES</td><td></td><td></td><td></td><td></td><td></td><td></td><td></td><td></td><td></td><td></td><td></td><td></td><td></td><td></td><td></td><td></td><td></td><td></td><td></td><td></td><td></td><td></td></tr> <tr><td>SEAPLANE FLOAT OR HULL; STRUTS, WIRES &amp; FITTINGS</td><td></td><td></td><td></td><td></td><td></td><td></td><td></td><td></td><td></td><td></td><td></td><td></td><td></td><td></td><td></td><td></td><td></td><td></td><td></td><td></td><td></td><td></td></tr> <tr><td>FUSELAGE, ENGINE MOUNT, AND FITTINGS</td><td></td><td></td><td></td><td></td><td></td><td></td><td></td><td></td><td></td><td></td><td></td><td></td><td></td><td></td><td></td><td></td><td></td><td></td><td></td><td></td><td></td><td></td></tr> <tr><td>COWLING, FAIRING &amp; FITTINGS</td><td></td><td></td><td></td><td></td><td></td><td></td><td></td><td></td><td></td><td></td><td></td><td></td><td></td><td></td><td></td><td></td><td></td><td></td><td></td><td></td><td></td><td></td></tr> <tr><td>TAIL WHEEL ASSEMBLY AND SKID</td><td></td><td></td><td></td><td></td><td></td><td></td><td></td><td></td><td></td><td></td><td></td><td></td><td></td><td></td><td></td><td></td><td></td><td></td><td></td><td></td><td></td><td></td></tr> <tr><td>ARRESTING APPLIANCES ON AIRCRAFT</td><td></td><td></td><td></td><td></td><td></td><td></td><td></td><td></td><td></td><td></td><td></td><td></td><td></td><td></td><td></td><td></td><td></td><td></td><td></td><td></td><td></td><td></td></tr> <tr><td>MISCELLANEOUS</td><td></td><td></td><td></td><td></td><td></td><td></td><td></td><td></td><td></td><td></td><td></td><td></td><td></td><td></td><td></td><td></td><td></td><td></td><td></td><td></td><td></td><td></td></tr> <tr><td>UNDETERMINED</td><td></td><td></td><td></td><td></td><td></td><td></td><td></td><td></td><td></td><td></td><td></td><td></td><td></td><td></td><td></td><td></td><td></td><td></td><td></td><td></td><td></td><td></td></tr> </table>																				FLIGHT CONTROL SYSTEM																							MOVABLE SURFACES																							STABILIZING SURFACES; STRUTS, WIRES & FITTINGS																							WINGS; STRUTS, WIRES, AND FITTINGS																							LANDING GEAR; STRUTS, WIRES, FITTINGS, AND RETRACTING MECHANISM																							WHEELS, TIRES & BRAKES																										SEAPLANE FLOAT OR HULL; STRUTS, WIRES & FITTINGS																							FUSELAGE, ENGINE MOUNT, AND FITTINGS																							COWLING, FAIRING & FITTINGS																							TAIL WHEEL ASSEMBLY AND SKID																							ARRESTING APPLIANCES ON AIRCRAFT																							MISCELLANEOUS																							UNDETERMINED																																																																																																																																																																																																																																																																																																																																																																																																																																																																																																																																																																																																																																																
			FLIGHT CONTROL SYSTEM																																																																																																																																																																																																																																																																																																																																																																																																																																																																																																																																																																																																																																																																																																																																																																																																																																																																																																																																																											
			MOVABLE SURFACES																																																																																																																																																																																																																																																																																																																																																																																																																																																																																																																																																																																																																																																																																																																																																																																																																																																																																																																																																											
			STABILIZING SURFACES; STRUTS, WIRES & FITTINGS																																																																																																																																																																																																																																																																																																																																																																																																																																																																																																																																																																																																																																																																																																																																																																																																																																																																																																																																																											
			WINGS; STRUTS, WIRES, AND FITTINGS																																																																																																																																																																																																																																																																																																																																																																																																																																																																																																																																																																																																																																																																																																																																																																																																																																																																																																																																																											
			LANDING GEAR; STRUTS, WIRES, FITTINGS, AND RETRACTING MECHANISM																																																																																																																																																																																																																																																																																																																																																																																																																																																																																																																																																																																																																																																																																																																																																																																																																																																																																																																																																											
			WHEELS, TIRES & BRAKES																																																																																																																																																																																																																																																																																																																																																																																																																																																																																																																																																																																																																																																																																																																																																																																																																																																																																																																																																											
			SEAPLANE FLOAT OR HULL; STRUTS, WIRES & FITTINGS																																																																																																																																																																																																																																																																																																																																																																																																																																																																																																																																																																																																																																																																																																																																																																																																																																																																																																																																																											
FUSELAGE, ENGINE MOUNT, AND FITTINGS																																																																																																																																																																																																																																																																																																																																																																																																																																																																																																																																																																																																																																																																																																																																																																																																																																																																																																																																																														
COWLING, FAIRING & FITTINGS																																																																																																																																																																																																																																																																																																																																																																																																																																																																																																																																																																																																																																																																																																																																																																																																																																																																																																																																																														
TAIL WHEEL ASSEMBLY AND SKID																																																																																																																																																																																																																																																																																																																																																																																																																																																																																																																																																																																																																																																																																																																																																																																																																																																																																																																																																														
ARRESTING APPLIANCES ON AIRCRAFT																																																																																																																																																																																																																																																																																																																																																																																																																																																																																																																																																																																																																																																																																																																																																																																																																																																																																																																																																														
MISCELLANEOUS																																																																																																																																																																																																																																																																																																																																																																																																																																																																																																																																																																																																																																																																																																																																																																																																																																																																																																																																																														
UNDETERMINED																																																																																																																																																																																																																																																																																																																																																																																																																																																																																																																																																																																																																																																																																																																																																																																																																																																																																																																																																														
HANDLING QUALITIES																																																																																																																																																																																																																																																																																																																																																																																																																																																																																																																																																																																																																																																																																																																																																																																																																																																																																																																																																														
INSTRUMENTS																																																																																																																																																																																																																																																																																																																																																																																																																																																																																																																																																																																																																																																																																																																																																																																																																																																																																																																																																														
LAUNCHING DEVICES																																																																																																																																																																																																																																																																																																																																																																																																																																																																																																																																																																																																																																																																																																																																																																																																																																																																																																																																																														
ARRESTING DEVICES																																																																																																																																																																																																																																																																																																																																																																																																																																																																																																																																																																																																																																																																																																																																																																																																																																																																																																																																																														
MISCELLANEOUS			WEATHER																																																																																																																																																																																																																																																																																																																																																																																																																																																																																																																																																																																																																																																																																																																																																																																																																																																																																																																																																											
			DARKNESS																																																																																																																																																																																																																																																																																																																																																																																																																																																																																																																																																																																																																																																																																																																																																																																																																																																																																																																																																											
			AIRPORT OR TERRAIN																																																																																																																																																																																																																																																																																																																																																																																																																																																																																																																																																																																																																																																																																																																																																																																																																																																																																																																																																											
			OTHER																																																																																																																																																																																																																																																																																																																																																																																																																																																																																																																																																																																																																																																																																																																																																																																																																																																																																																																																																											
UNDETERMINED			<p style="text-align: center;">RECOMMENDED BY COMMITTEE ON AIRCRAFT ACCIDENTS JUNE 22, 1936 APPROVED BY EXECUTIVE COMMITTEE NATIONAL ADVISORY COMMITTEE FOR AERONAUTICS JUNE 23, 1936</p>																																																																																																																																																																																																																																																																																																																																																																																																																																																																																																																																																																																																																																																																																																																																																																																																																																																																																																																																																											

Fig. 2-443. By mid-1936 the U.S. had an accident reporting form [661].

## 2.10 ACCIDENT RECORD

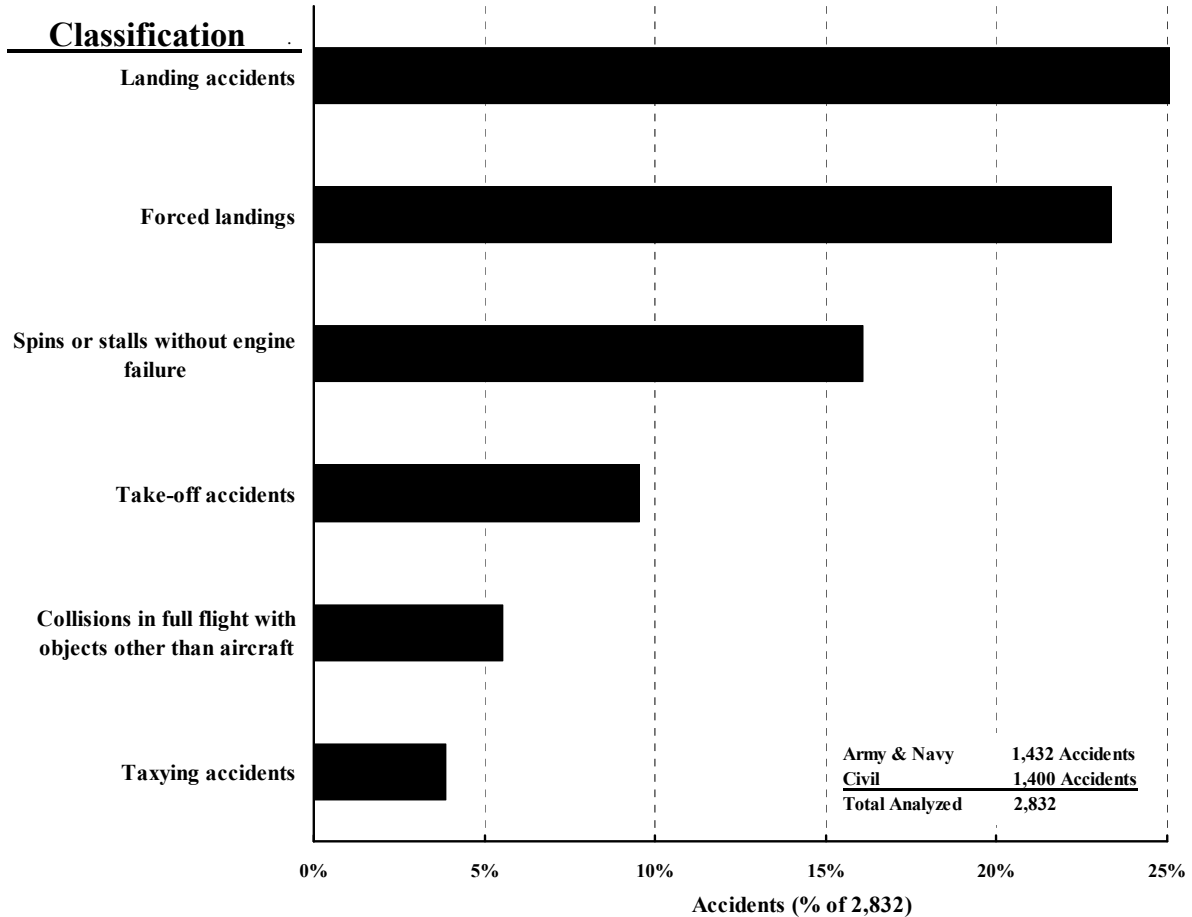


**Fig. 2-444. Accident classification uncovered pilot and airplane deficiencies that needed fixing.**

established by NACA Report No. 576 (although the Statistical Handbook incorrectly referenced the NACA Report as No. 567). This document summarized aviation statistics dating back to 1926, including air carrier and private flying accident statistics compiled by the U.S. Civil Aeronautics Board (CAB), the predecessor to the NTSB. In the introduction, the CAA acknowledged that “There are some gaps in the early statistics [about private flying] because fact-gathering machinery had not been fully organized and it also was extremely difficult to obtain reliable figures from an industry still inchoate.” With respect to private flying, the CAA noted that “because of the dislocation caused by the war, statistics on the amount of private flying during the war years [1942 and 1943] are incomplete.” Despite these reservations, the 1944 CAA handbook provided early examples of detailed tables regarding aircraft operating statistics for both air carriers and private flying. A composite of statistical data from several tables in the 1944 CAA handbook is provided here in Table 2-62.

Historically, Table 2-62 reflects three major events in aviation progress. The first event came with the depression in the early 1930s, which caused the drop in aircraft sold and the demise of several manufacturers. The second event was the rapid rise in air carrier miles flown with fewer aircraft, which came with the transition from Ford Tri-Motors to the Boeing

Model 247 and the Douglas DC-3. The third event was the United State's entry into WWII and the rapid conversion of commercial aircraft to military configurations, which affected statistics in 1942 and 1943.

Despite the upheaving events that are reflected in Table 2-62, the primary aviation safety statistic of the era showed that air transportation safety was improving. The 1944 CAA handbook illustrated this fact with tabulations of statute miles flown per accident, and this historical data is shown in Fig. 2-445. The contrasting trends between air carrier and private flying are quite remarkable. The fare paying public was reading fewer blaring newspaper headlines about fatal airliner crashes and seeing more people boarding airplanes in the movies. Of course, during WWII service men and women in great numbers were exposed to flying in many forms. When these servicemen and women came home, aviation really began the upward trend to become what we know today. As an aside, the New York Yankee baseball team started traveling by airplane in May 1946.

Now jump ahead to today, July 2012, and look back at what has happened in the world of commercial (and amateur) rotorcraft. The modern era of U.S. civil rotorcraft operations officially began on March 8, 1946, with the CAA's certification of the Bell Model 47. In that year, Bell began a first lot production run of 10 helicopters. The two-place Model 47 was followed by the four-place Sikorsky S-51, certificated on April 17, 1947. The S-51 was developed from Sikorsky's R-5 military helicopter and benefited from experience gained with the smaller R-4 and R-6 military models. On October 14, 1948, the CAA certificated the Hiller Model 360, the beginning of the UH-12 series. By the end of 1957, the CAA's Statistical Study of U.S. Civil Aircraft reported 540 registered helicopters in the civil fleet (Table 2-63).

**Table 2-62. Early Aviation Statistical Data in the United States [662]**

Year	Air Carrier Aircraft in Service	Air Carrier Revenue Miles Flown (all services)	Air Carrier Accidents	Private Flying Aircraft in Service	Private Flying Miles Flown	Private Flying Accidents
1926	n/a	4,258,771	n/a	1,300	18,746,640	n/a
1927	n/a	5,779,863	25	2,612	30,000,000	253
1928	268	10,400,239	85	4,779	60,000,000	1,036
1929	442	22,380,020	124	9,315	110,000,000	1,586
1930	497	31,992,634	88	9,218	108,269,760	2,033
1931	490	42,755,417	117	10,090	94,343,115	2,205
1932	456	45,606,354	108	9,760	78,178,700	1,951
1933	406	48,771,553	100	8,780	71,222,845	1,603
1934	417	40,955,396	71	7,752	75,602,152	1,504
1935	356	55,380,353	58	8,613	84,755,630	1,517
1936	272	63,777,226	65	8,849	93,320,375	1,698
1937	282	66,071,507	42	10,446	103,198,355	1,917
1938	253	69,668,827	33	10,718	129,359,095	1,882
1939	265	82,571,523	33	13,217	177,868,157	2,175
1940	358	108,800,436	42	17,253	264,000,000	3,446
1941	359	133,022,679	33	24,124	346,303,400	4,312
1942	179	110,102,860	31	22,329	293,592,580	3,176
1943	194	103,601,443	24	22,323	TBD	3,762

## 2.10 ACCIDENT RECORD

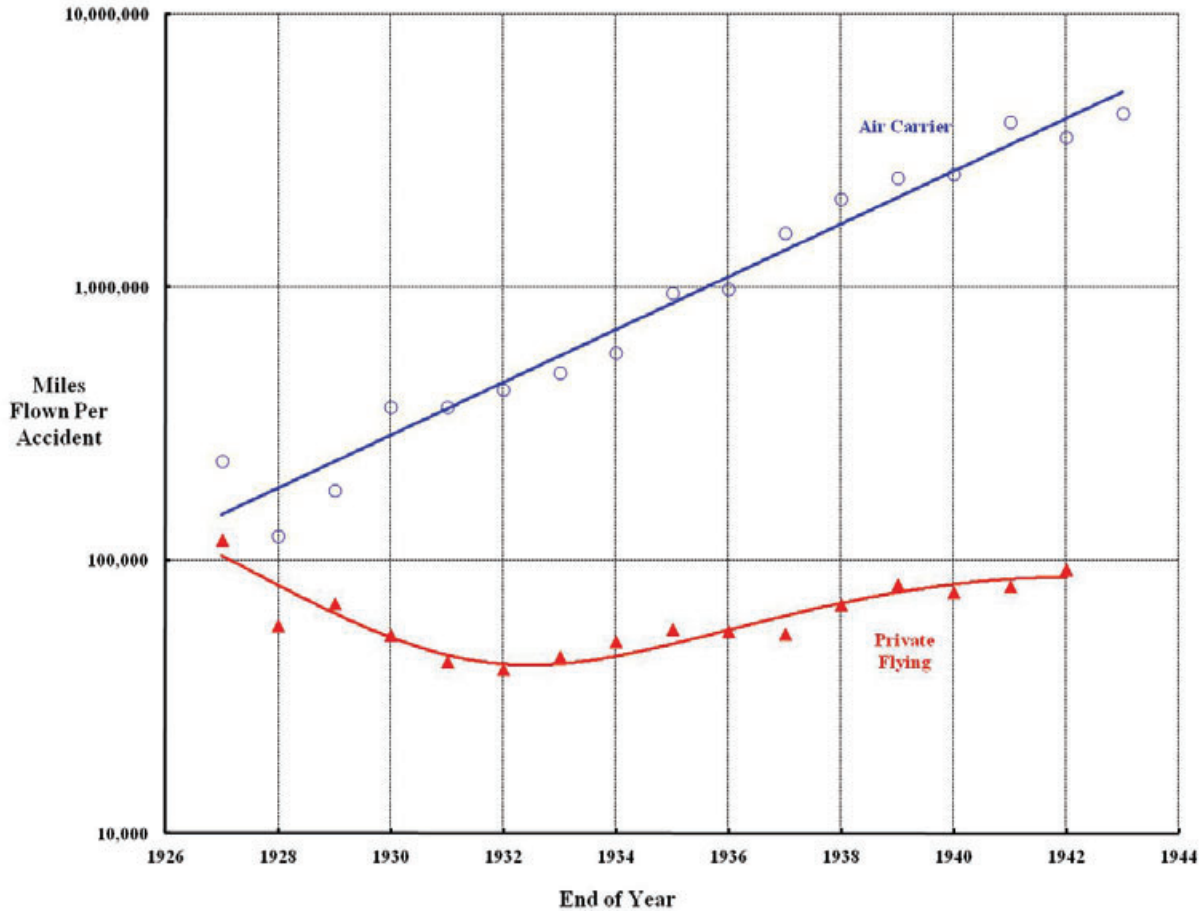


**Fig. 2-445. Early aviation safety statistics in the United States.**

As Table 2-63 shows, the CAA segregated aircraft by “active” and “inactive” based on the following definitions: Active aircraft were those that held a valid certificate of airworthiness, and that had an approved inspection during the previous 12 months *and* were eligible to fly. Aircraft classified as inactive “need not necessarily be in unairworthy condition and may hold a valid airworthiness certificate, but they have not met the periodic inspection requirement.” With only minor variations, these definitions have remained the same for nearly seven decades.

**Table 2-63. The CAA Registered Helicopter Census at the End of 1957**

Manufacturer	Model	Active	Inactive	Total
Bell Aircraft Corp.	47	246	49	295
Hiller Helicopters	UH-12	29	20	49
Sikorsky	R-4, R-6, S-51, S-52	14	25	39
	S-55	27	12	39
	S-58	21	0	21
All others	Various	33	64	97
<b>Total</b>		<b>370</b>	<b>170</b>	<b>540</b>

The size of the helicopter fleet grew substantially after WWII ended, as Fig. 2-446 shows. The FAA made a minor bookkeeping correction to this growth trend in 1970. The growth continued until the early 1980s when the market for new piston- and turbine-powered rotorcraft virtually collapsed. The market began recovering in the early 1990s. At the end of 2005, the FAA Civil Aviation Registry showed a computer listing of nearly 19,000 rotorcraft (mostly helicopters, some autogyros, a couple of compound research helicopters, and two tiltrotors), each with an assigned FAA registry number, or N number as it is commonly referred to. My detailed review of the registry found a significant number of rotorcraft in museums or simply stored. Therefore, a somewhat lower count of active plus inactive rotorcraft is shown in Fig. 2-446 as the Harris count.

Fig. 2-446 raises an interesting point about which there has been growing disagreement for the past two decades. The immediate impression created by Fig. 2-446 is that while more and more rotorcraft have been registered (i.e., bought and N number assigned), the number of rotorcraft actually in use and flying does not seem to have changed appreciably since 1980 or 1981—according to FAA reporting. For example, in the 1980 census, which reported statistics for 1979, the realistic count would be 9,000 active plus inactive rotorcraft. However, the FAA statistically found that only 6,000 flew (at least 1 hour) in 1979. In contrast, by the end of 2003, the active plus inactive count was on the order of 15,000 rotorcraft, but the FAA statistically found only 6,500 were “active.” I find it unimaginable to think that the FAA’s count of active rotorcraft is remotely correct after 1980, particularly because spare parts’ sales have done nothing but increase.

Apparently, even the NTSB began to have some serious misgivings about the FAA civil aviation statistics as well—so much so that they formally expressed themselves in 2005 [663]. Shortly thereafter (July 20, 2010), the FAA decided to address the problem with a new set of rules and regulations [664]. In this Federal Register (vol. 75, no. 138) final rule, starting October 1, 2010, and over the next 3 years, *all* aircraft owners would have to reregister their aircraft, forcing (hopefully) the FAA Master Registry List<sup>220</sup> to become up to date. In the executive summary, the FAA states:

“The FAA estimates that approximately one-third of the 357,000 registered aircraft records it maintains are inaccurate and that many aircraft associated with those records are likely ineligible for United States registration. The inaccuracies result from failures in the voluntary compliance based system. Although aircraft owners are required to report the sale of an aircraft, death of an owner, scrapping or destruction of an aircraft, and changes in mailing address; many have not. Without owner initiated action, there has been no means to correct those records. The FAA has been asked by government and law enforcement agencies to provide more accurate and up-to-date aircraft registration information. [Other interested parties have asked, too.] This rule is intended to support the needs of our system users.”

Time will tell if FAA statistical data accuracy will improve after this new ruling is fully implemented.

---

<sup>220</sup> The FAA Civil Aviation Registry (called the Master List) is maintained at the FAA Mike Monroney Aeronautical Center, 6500 South MacArthur Boulevard, Oklahoma City, OK 73169. The telephone number is (405) 954-4331. The Master List is now available online. This FAA center is about 30 miles away from Piedmont, Oklahoma where Sue and I now live.

## 2.10 ACCIDENT RECORD

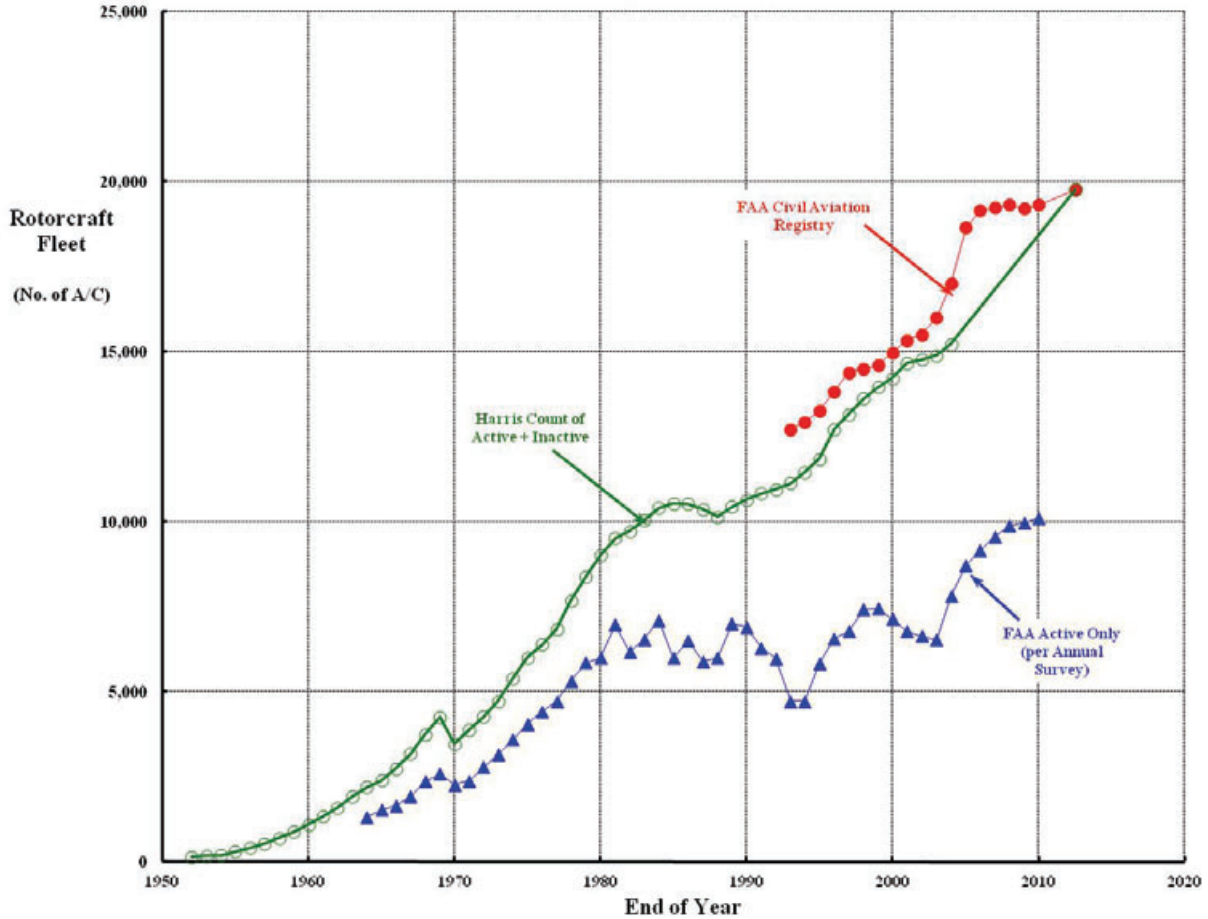


**Fig. 2-446. The FAA-registered rotorcraft fleet has grown, but not all are flying.**

At issue, of course, are the FAA statistics for just how many rotorcraft are “active.” The reason the issue is so important is that the number of flight hours flown by the active aircraft falls in the denominator of the most-quoted safety statistic, which is

$$\frac{\text{accidents}}{100,000 \text{ flight hours}}$$

The numerator, accidents per year, is well documented by the NTSB. The denominator, flight hours per year, is provided by the FAA Statistics and Forecast Branch based on their count of active rotorcraft. By way of background, each year this FAA branch publishes a “Census of U.S. Civil Aircraft.” (Rotorcraft fall in the General Aviation category, which was referred to as Private Flying by the CAA.) The census provides details about the number and types of aircraft currently operating in the U.S. civil aviation fleet, along with other relevant data such as flight hours. Fleet size and flight hour data for General Aviation are obtained by extrapolating data from a survey questionnaire mailed to a sample of registered owners. The validity of this database, to say nothing about the extrapolation, has been questioned occasionally. In fact, the rotorcraft industry requested and received a “one time only” survey. The results [665] did virtually nothing to allay industry concerns about the FAA’s estimate of hours flown per year by the rotorcraft fleet.

The “one time only” rotorcraft activity survey for 1989 [665] chose 10,469 owners from the Registration Master File to mail the standard questionnaire to. There were 1,883 postal returns, which “reflect a seriously out-of-date rotorcraft file.” After three mailings and some culling, the data bank was reduced to 6,724 responses. The survey extrapolation methodology determined that there were 7,488 active rotorcraft in the fleet. Furthermore, the “estimate of total hours flown” by the active aircraft in 1989 was published as 2,828,697—give or take a few minutes. The NTSB recorded 213 rotorcraft accidents in 1989, which means that

$$\frac{\text{Rotorcraft accidents}}{100,000 \text{ flight hours}} = \frac{213}{28.28697} = 7.53 \text{ for 1989.}$$

The official, published rate for 1989 was 8.39 based upon the larger survey of General Aviation for 1989. As an aside, the special rotorcraft survey [665] noted in its table 3.4 that Arizona-based rotorcraft made 113,332 landings on offshore platforms, which at first impression seems ridiculous.

The 47-year trend of accidents per year and active rotorcraft flight hours per year is provided in Fig. 2-447. There has been a noticeable, favorable, and well-documented decline in accidents according to NTSB records. And, according to FAA statistics, fleet flight hours steadily climbed each year from 1964 to 1979; then abruptly began to decline from 1980 onwards to 2002, whereupon a marked increasing trend began to emerge. The abrupt decline in active rotorcraft count (Fig. 2-446) and flight hours (Fig. 2-447) occurred when the FAA changed their survey methodology. A more complete discussion of this methodology change is provided in appendix B of reference [666], *U.S. Civil Rotorcraft Accidents, 1963 through 1997*. Laying aside the FAA’s active aircraft and flight hour dilemma for the moment, the 47-year accident rate (accidents per 100,000 flight hours) history is shown graphically in Fig. 2-448.

Fig. 2-448 gives the impression that the rotorcraft accident rate steadily improved from 1964 to 1979. After 1979, the rotorcraft accident rate remained constant at about 10 accidents per 100,000 flight hours, give or take some randomness. In contrast to the overall fleet statistics, at least two corporations have shown that the national rotorcraft fleet statistics do not apply to them. In an article [667] in the February 1999 issue of *Rotor & Wing*, writer John Persinos explains that Mrs. Carroll Suggs, head of Petroleum Helicopters, Inc., instituted a new and aggressive safety program in 1992. The result of this program was that her company’s “accident rate averaged fewer than one accident per 100,000 flight hours, compared to the national average of more than seven per 100,000 flight hour.” The second company with a published accident rate is CHC Helicopters, Inc. Sylvain Allard, President and CEO of CHC, presented a paper at the September 2005 International Helicopter Safety Symposium [668] where he said that “all accidents are preventable” and that “accidents are a failure of management.” With this forceful commitment from the top, CHC’s accident rate was 0.47 using a 5-year rolling average ending in 2003, which Allard notes is comparable to the average of major airlines.

## 2.10 ACCIDENT RECORD

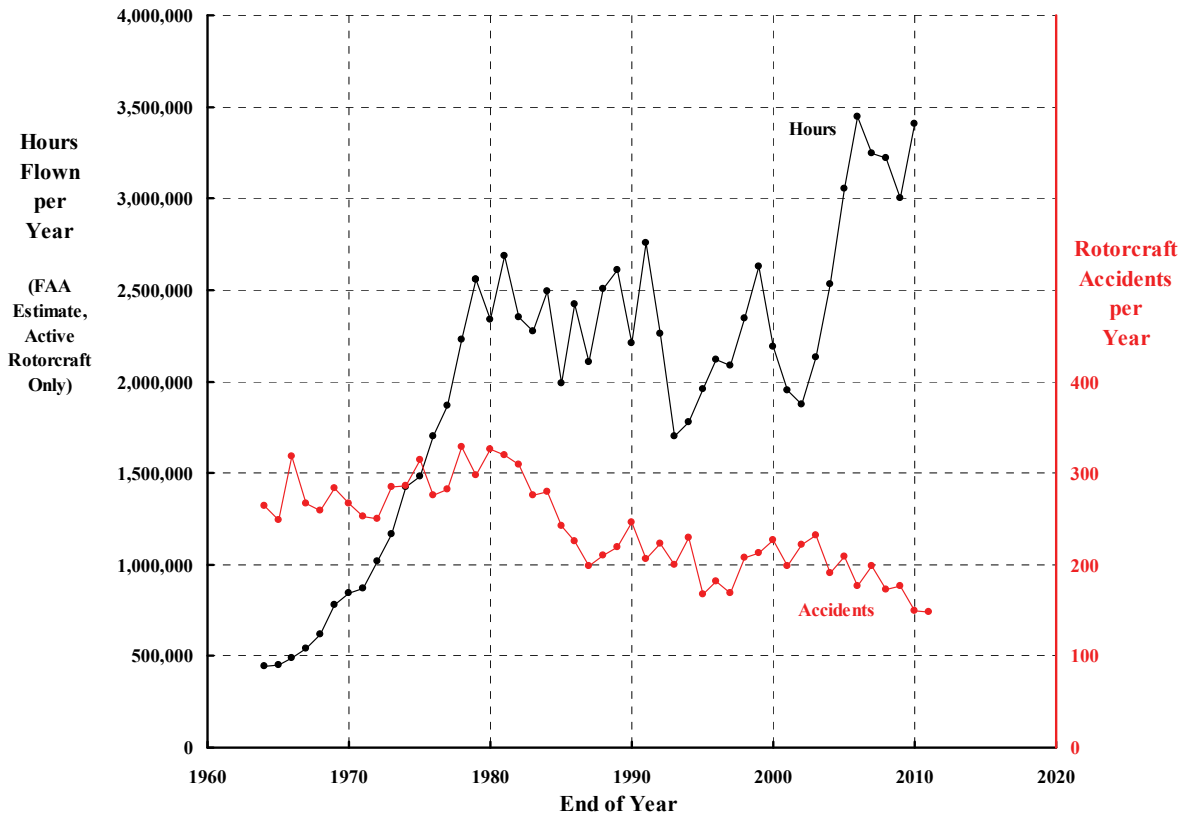


Fig. 2-447. Hours flown and accidents per year used in the accident rate calculation (the FAA's hour-flown data is questionable; the NTSB data is not).

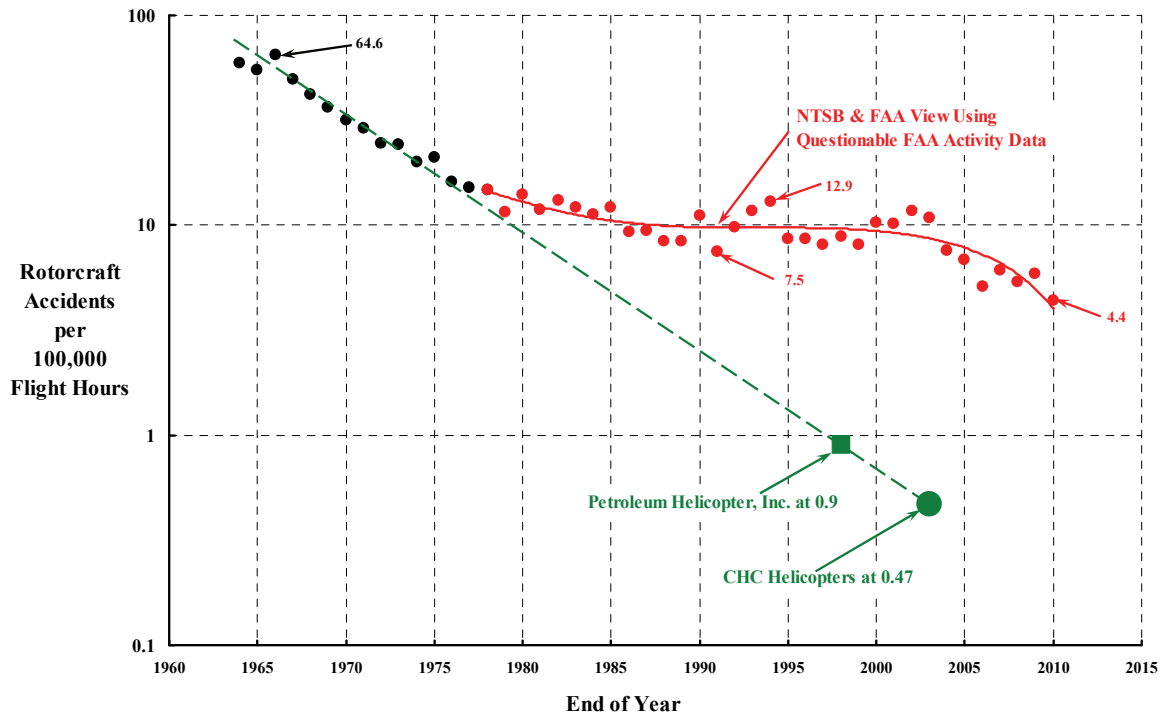


Fig. 2-448. No accidents is the real goal.

The favorable downward trend in rotorcraft accidents per 100,000 flight hours that you see in Fig. 2-448 after 2005 has come about, I believe, because of the formation of the International Helicopter Safety Team (IHST). You should become aware of this worldwide team, and the rotorcraft industry should be grateful for their efforts as well. Dave Downey, Vice President of Flight Safety at Bell Helicopter, wrote some history about the team in *Heliprops* magazine [669], saying:

“The IHST came to life in a meeting at the American Helicopter Society International headquarters in early 2004 with participants from the Helicopter Association International, the FAA, helicopter manufacturers, and others interested in the reduction of helicopter accidents. In order to get the movement going, the first International Helicopter Safety Symposium was held scheduled for everyone to meet in Montreal, Canada in September 2005. Industry interest and attendance was overwhelming.”

He further explains that “the goal of the IHST is to reduce the helicopter accident rate 80 percent by 2016. It is not a complicated goal, however, it is an ambitious one!” The goal was set in September 2005. Accepting a value of 10 accidents per 100,000 hours flown as the reference point according to Fig. 2-448 means, to me, that by 2016 the accident rate should be below 2.0. By my analysis of FAA and NTSB U.S. statistics, the U.S. civil fleet is at 4.4 accidents per 100,000 hours flown at the end of 2011, and a trend has been established. You can read about the IHST in more detail by visiting their website at <http://ihst.org>.

The fact that accident rate is a questionable metric (because the hours flown denominator values available from the FAA are questionable) with which to measure rotorcraft safety *is not* the lesson to be learned from my historical discussion. The real lesson is that correcting human and aircraft deficiencies based on in-depth accident investigation and analysis is where real progress is made. It is the numerator in accident rate that is important. *I believe the only real objective is no accidents at all.*

### **2.10.2 In All, 11,426 Accidents From 1964 Through 2011**

As an overview to detailed accident analysis, consider our accidents-per-year track record over the last 47 years, as shown in Fig. 2-449. NTSB records show that there has been a broadly defined improvement trend. In fact, a very positive spin can be obtained from this data. In 1964, there were 2,196 rotorcraft in the FAA Registry according to the Harris count in Fig. 2-446. The NTSB records count 264 accidents in that year. That works out to about 120 accidents per 1,000 registered rotorcraft in 1964. In 2005, the Harris fleet count was 15,650 rotorcraft and there were only 205 accidents, which is 12 accidents per 1,000 registered rotorcraft. And in 2011, there were 148 accidents in a fleet size of 19,764 rotorcraft, which is 7.5 accidents per 1,000 registered rotorcraft. *Thus, the rotorcraft industry, portrayed in this light, has reduced accidents by more than a factor of 10 from 1964 to 2011—even as the registered fleet increased nearly tenfold.*

A closer examination of accidents during the 47 years discloses, however, two very serious facts that paint the industry in a poor light. The first fact is that the introduction of the single-turbine-powered helicopter was accompanied by a very high yearly accident count, which peaked in 1980. The second fact is that rotorcraft attrition, caused by accidents, has been unacceptably high compared to the commercial airline business.

## 2.10 ACCIDENT RECORD

A more careful examination of Fig. 2-449 shows that between 1972 and 1986 accidents per year did not follow the linear trend shown by the dashed line, which is labeled as the Harris trend. I have put a label to this rise and fall of accidents per year from 1972 to 1986 and called it an “accident bubble.” The accident bubble occurred when single-turbine-powered helicopters were introduced. To see this fact, consider first the fleet growth by rotorcraft type shown in Fig. 2-450. The major growth in single-turbine-powered helicopters clearly occurred between the years 1970 and 1985. The impact of introducing single-turbine-powered helicopters becomes abundantly clear in Fig. 2-451, which documents the accidents per year for helicopters powered with piston or turbine engines. Observe from Fig. 2-451 that accidents per year for single-turbine-powered helicopters increased nearly in proportion to the fleet growth shown in Fig. 2-450.

An even more distressing trend becomes apparent when accumulating accidents are plotted versus fleet growth, as shown in Fig. 2-452. For all intents and purposes, the industry added, in a given year, four helicopters to the FAA Registry and crashed one. And, most distressing, Fig. 2-452 shows no evidence that twin-turbine helicopters are faring better than single turbine-powered helicopters. One hopes that the introduction of future rotorcraft such as tiltrotors will not follow such a disturbing and unacceptable trend.

To complete this overview, it is important to quantify just how costly this accident track record has been over 47 years. In terms of people affected, 3,027 people have been killed in 11,426 accidents, and 2,362 people have been seriously injured. Thankfully, 17,590

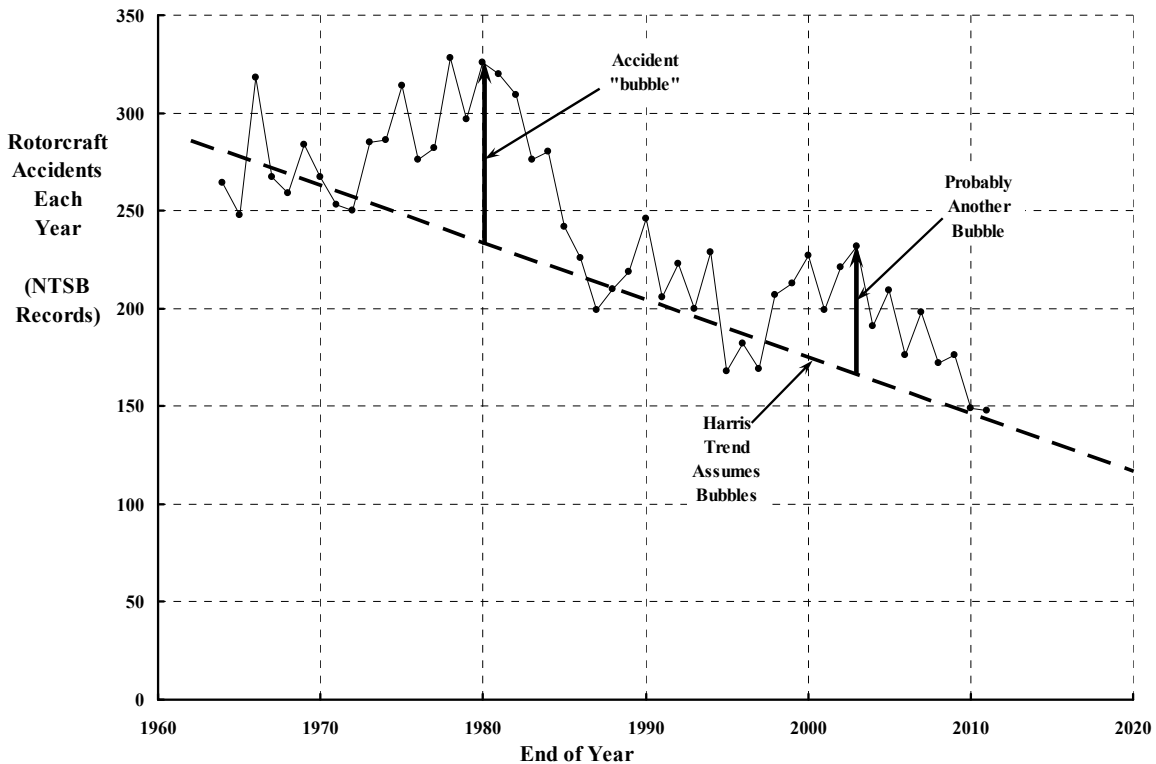


**Fig. 2-449. Accidents per year for the last 47 years (we are doing better, but the goal is no accidents).**

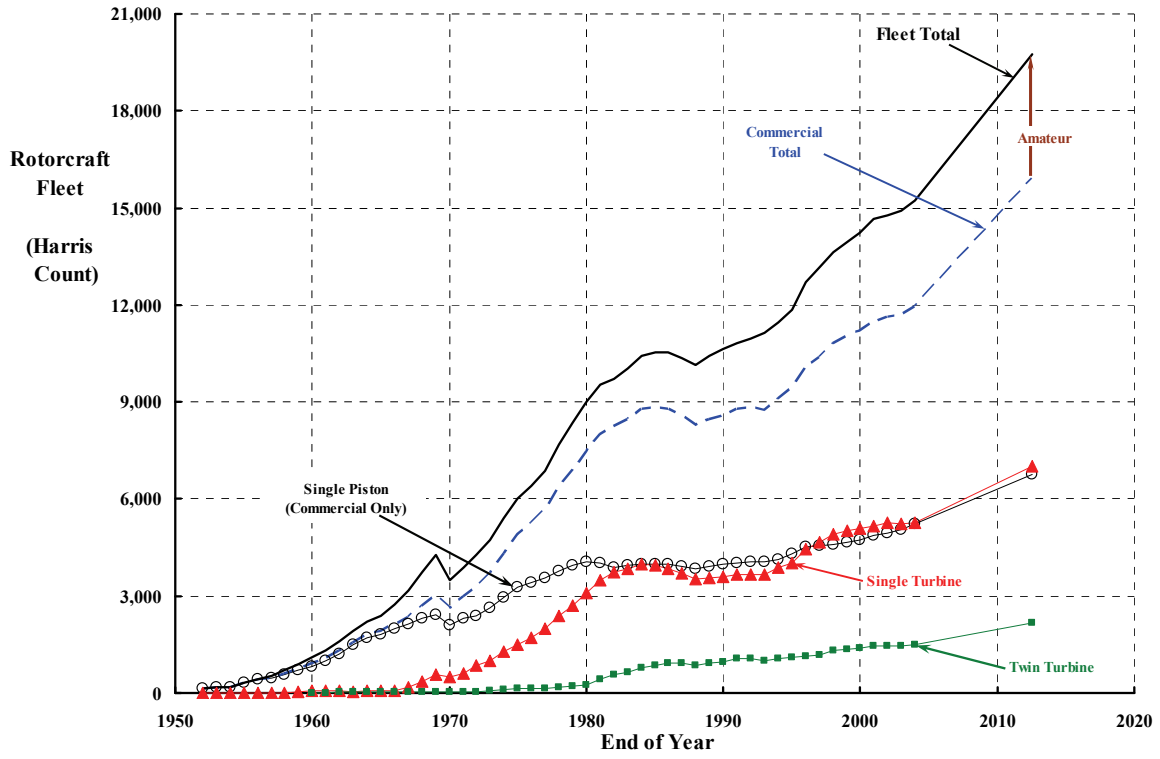


Fig. 2-450. Rotorcraft fleet growth by rotorcraft type.

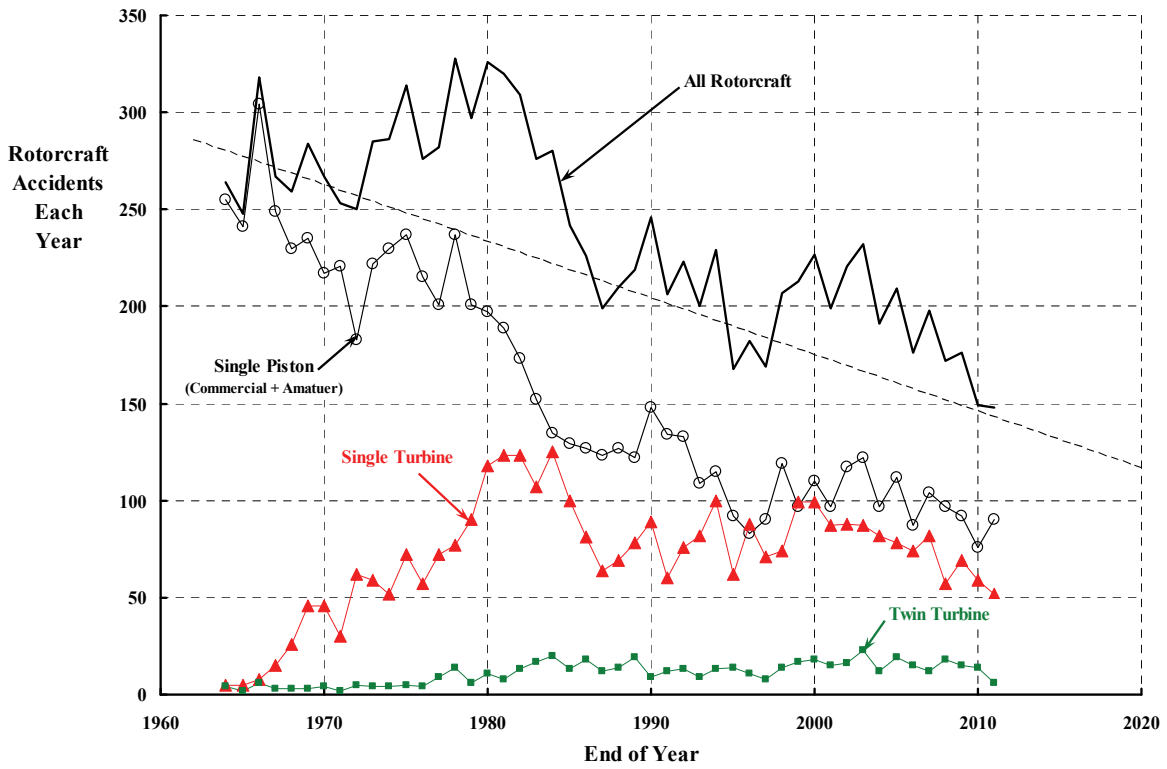
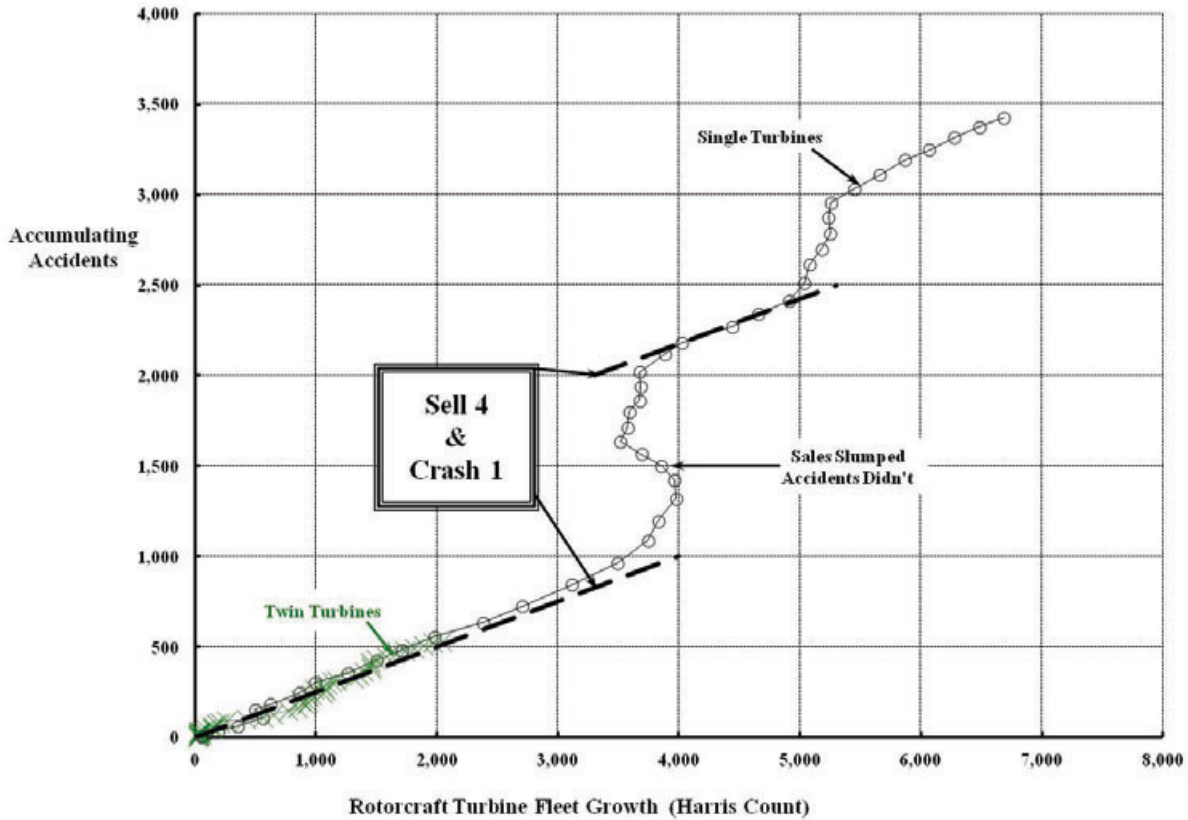


Fig. 2-451. An excessive number of accidents accompanied the introduction of single turbine-powered helicopters.

## 2.10 ACCIDENT RECORD



**Fig. 2-452. Accumulating accidents vs. fleet growth (what a trend—sell four and crash one)!**

people escaped relatively unharmed. Of lesser importance, 2,905 rotorcraft have been destroyed, 8,223 aircraft have been substantially damaged, and only 298 rotorcraft crashed and received minor or no damage.

You might be wondering just how much this track record has cost the rotorcraft industry in cold, hard cash. Let me offer one estimate. The cost of one accident was put at slightly over one million U.S. dollars by the HAI Safety Committee in the spring of 1991 [670]. Walt Lamon, the chairman of the committee, estimated this cost in 1991 as follows:

Operator	\$194,000
(Loss of business, Increase in premiums, Loss of pilot services, Legal expenses, Lost time, etc.)	
Insurance	\$775,000
(Repair or replacement, Claims paid Admin costs, Legal fees, etc.)	
Passengers' Company	\$90,000
(Loss of business, Loss of employees' service, Corporate legal, Lost time, etc.)	
<hr/>	
Cost of One (1) Accident	<hr/> \$1,059,000

On this basis, the 11,426 accidents since 1964 have siphoned off \$12 billion, which is, to me, a staggering amount of lost money for such a relatively small industry—and this estimate does not even consider inflation!

Now let me conclude this overview of rotorcraft accidents investigated and recorded by the National Transportation Safety Board (NTSB) between January 1, 1994, and December 31, 2011, with a summary shown in Fig. 2-453 and Table 2-64.

The NTSB has divided the classification of rotorcraft accidents into 1 of about 21 different groups. One classification, for example, is loss of engine power. You can sense right away that a classification might be called a cause of the accident, but that immediately begs the question, “What caused the loss of power?” The accident investigator might find, for example, that the engine was starved for fuel, but then that leads to the question, “Why wasn’t the fuel getting to the engine?” Of course, an answer here leads to another question, and the answer to that question precipitates another question until, finally, reaching a satisfactory root cause (like maybe the fuel tank was empty). But then someone might ask, “Why was the fuel tank empty?” Just stop a moment and think about the answer to that question. I am sure you can appreciate that the simple act of assigning an accident into a classification is really just the starting point for an NTSB investigator.

To emphasize this one example (i.e., loss of engine power), consider the abbreviated NTSB investigator’s report that follows:<sup>221</sup>

11012 Report Status: Factual NASDAC Database Entry: None  
NTSB Identification: **ERA11CA166**

14 CFR Part 91: General Aviation  
Accident occurred Saturday, February 26, 2011 in Fort Pierce, FL  
Aircraft: ENSTROM F-28C, registration: N5689B  
Injuries: 2 Minor, 1 Uninjured.

[Full narrative available](#)

**ERA11CA166**

The pilot of the helicopter stated that the fuel gauge indicated “one-eighth to one-quarter” full on takeoff. At an altitude of approximately 200 feet, the low fuel pressure light illuminated, followed by a total loss of engine power. The pilot performed a 180-degree autorotation to a parking lot, and the helicopter landed hard, resulting in substantial damage to the left skid and tail boom. During post accident examination, a Federal Aviation Administration inspector drained approximately 3 ounces of fuel from the gascolator. The pilot stated that there were no mechanical malfunctions or anomalies with the helicopter, and that he “ran it out of fuel” by “trusting the gauge.”

---

<sup>221</sup> The NTSB religiously posts their accident reports on their website and you can download the reports. Generally, a preliminary report is available first and is followed later by the final report with a full narrative.

## 2.10 ACCIDENT RECORD

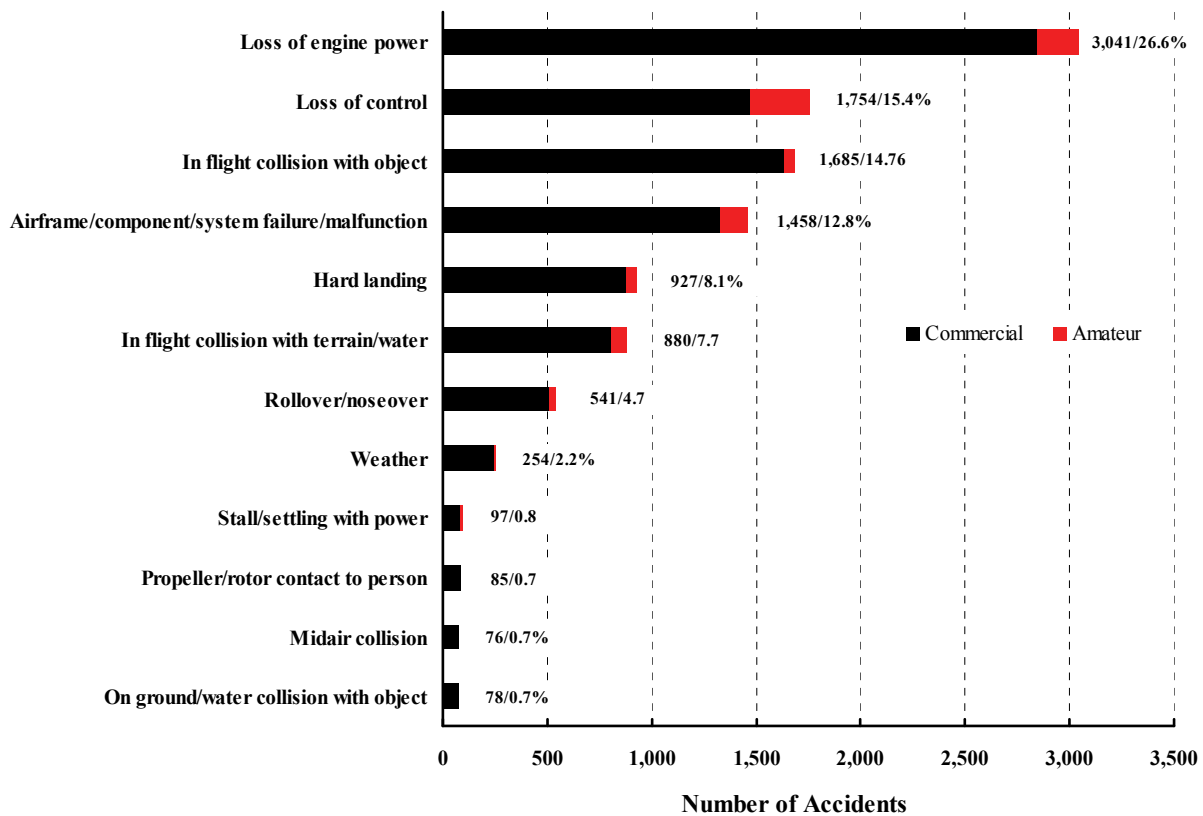


**Fig. 2-453. Ninety-five percent of accidents fall into one of twelve classifications.**

I selected this particular NTSB report (ERA11CA166) because the pilot makes the point that he trusted the fuel gauge. It seems to me that the accident might easily have been traced back to the chief engineer of the company that manufactures the fuel gauge. Of course, if the pilot had some misgivings about the gauge, you might argue that some sort of dip stick could have been used. Perhaps the fuel tank designer might have added a sight gauge. Or you could even argue that the takeoff was made with less than the minimum fuel reserve that the FAA requires.

The classification of 11,426 rotorcraft accidents is shown in Fig. 2-453 for the civil rotorcraft fleet. Here you have the top 95 percent of the 11,426 accidents that have been under study by a small group over the last 18 years.<sup>222</sup> You might notice rather quickly that

<sup>222</sup> You may be curious about how this chapter on safety came to be. During the summer of 1994, I began to wonder about the statement that “virtually all accidents are caused by human error.” To satisfy my curiosity about this often quoted statement, I called the NTSB and asked for a copy of all rotorcraft accident reports going as far back as they cared to give me. The young lady sent me a stack of floppy discs almost in the blink of an eye. That data bank went into a massive Microsoft® Word file and I started reading. Shortly thereafter, Gene Kasper and Laura Iseler at NASA Ames Research Center expressed an interest in this matter. So the three of us took on the task of transferring the Word documents into an Excel® spreadsheet that contained what we thought were key summary data about 8,436 rotorcraft accidents that occurred from late 1963 through 1997. It was a daunting task, frequently accompanied with some very depressing thoughts as the repetition became clear. We

loss of engine power (i.e., a forced landing) accounts for 3,041 accidents, or 26.6 percent of the 11,426 accidents under discussion. That is virtually identical to what airplanes were experiencing in the 1920s and 1930s as you learned from Fig. 2-444. I find the similarity in several classifications (or categories) to what was learned by studying the 2,832 early airplane accidents very interesting.

To begin with, accidents can be grouped by a first-occurrence category. The original accident form (Fig. 2-443) identified these “immediate cause” categories for airplane accidents. Today the NTSB has expanded the number of first-occurrence categories and included categories most associated with rotorcraft. Rotorcraft accidents grouped by the 12 most common first-occurrence categories are shown in Fig. 2-453. Helicopters, with their ability to be flown “low and slow,” experience many more in-flight collisions with objects when compared to airplanes. Interestingly, loss of control is just as prevalent with helicopters as stall-and-spin airplane accidents were in the 1920s. Despite the helicopter’s mechanical complexity, accidents caused by some failure or malfunction of the airframe, or some airframe system, have caused less than 13 percent of accidents. In-flight collisions with terrain and/or water are just as common with helicopters today as with airplanes in the 1920s.

An interesting difference between helicopters and airplanes of the 1920s and 1930s is accidents categorized as hard landings. Fig. 2-444 shows that airplane landing accidents (with power on) were quite prevalent back then, while helicopters—in approximately the same state of development and use—appear one-third as prone to this category of accident. Roll-over and nose-over accidents caused principally by taking off with a skid tied down is, of course, a helicopter trait given its vertical takeoff capability. Finally, weather-related accidents appear about equal for helicopters (Fig. 2-453) and airplanes [660].

Now turn your attention to Table 2-64, which sorts the 11,426 accidents into the commercial (10,540 accidents) and amateur (886 accidents) activities of the industry.

---

published our detailed analysis and opinions in December of 2000 [666]. Then, in May of 2006, I was given the honor of presenting the 26th Nikolsky Lecture, and I chose to speak about rotorcraft accidents [671]. (This was probably not the subject my peers thought I should address; perhaps this book will be some sort of compensation.) The Nikolsky Lecture gave me the chance to update the files to 10,416 rotorcraft accidents, which I could not have done without Gene Kasper’s carefully kept records. And so you come to this last chapter in Volume II, and again, with Gene Kasper’s continued data gathering, you have some insight about 11,426 accidents as of the end of 2011. Gene Kasper is still at Ames Research Center on the U.S. Army side, and he continues to keep the NTSB accident record file in Excel® format current by downloading accident reports from the NTSB website.

Table 2-64. Classification and Number of Rotorcraft Accidents, 1964 Through 2011

Major Category for No. 1 Occurrence	Helicopter Commercial		Helicopter Commercial		Autogyro Commercial		Amateur Helicopter		Amateur Autogyro	
	Piston	Single Turbine	Twin Turbine	Piston	Piston	Single Turbine	Piston	Single Turbine	Piston	Single Turbine
Loss of engine power	1,778	996	65	5	83	4	83	4	110	
In-flight collision with object	1,092	458	83	5	10	0	10	0	37	
Loss of control	897	481	69	23	83	2	83	2	199	
Airframe/component/system failure/malfunction	747	431	134	12	58	0	58	0	76	
Hard landing	634	219	18	5	18	0	18	0	33	
In-flight collision with terrain/water	541	225	36	6	16	2	16	2	54	
Roll-over/nose-over	353	146	7	2	17	0	17	0	16	
Weather	85	131	28	3	1	0	1	0	6	
Stall/settling with power	77	4	2	2	1	0	1	0	11	
Propeller/rotor contact to person	33	38	11	1	0	0	0	0	2	
Midair collision	21	44	9	0	0	0	0	0	2	
On ground/water collision with object	34	28	12	0	0	0	0	0	4	
Fire/explosion	30	17	6	0	2	0	2	0	0	
Abrupt maneuver	13	11	2	1	1	0	1	0	9	
Gear collapsed	16	3	6	1	0	0	0	0	1	
Undershoot/overshoot	17	5	3	1	0	0	0	0	2	
Dragged wing, rotor, pod, float or tail/skid	20	4	2	0	1	0	1	0	0	
On ground/water encounter with terrain/water	8	13	0	0	0	0	0	0	3	
All Others (undetermined, missing, not reported)	131	158	38	3	2	0	2	0	20	
<b>Grand total</b>	<b>6,527</b>	<b>3,412</b>	<b>531</b>	<b>70</b>	<b>293</b>	<b>8</b>	<b>293</b>	<b>8</b>	<b>585</b>	

**2.10.3 Detailed Accident Analysis**

The compilation of data summarized in Fig. 2-453, and examined in more detail in Table 2-64, is the accident record over 47 years. In fact, the distribution of accidents in the several categories (as a percentage) has been changing over the last 47 years. This important fact about rotorcraft accidents is shown in Fig. 2-454. In this figure I have focused on the top four categories or classifications that you see in Table 2-64. These four categories account for 70 percent of all rotorcraft accidents. I have treated the remaining 30 percent as just one group, beginning with hard landings.

Fig. 2-454 is read from the bottom up. That is, the single grouping of accident categories that accounts for 30 percent of accidents each year becomes the base. This group has accounted for virtually a constant 30 percent of yearly accidents for the past 47 years. Accidents caused by some failure or malfunction of the airframe, or some airframe system, add slightly over 12 percent to the base. Fig. 2-454 shows that loss-of-control accidents have more than doubled, as a percentage, since 1964. This is a serious and adverse trend. Helicopters are thought to require a special piloting talent to fly. However, Fig. 2-454 suggests that the basic handling qualities of the aircraft really are poor. Our rotorcraft pioneers

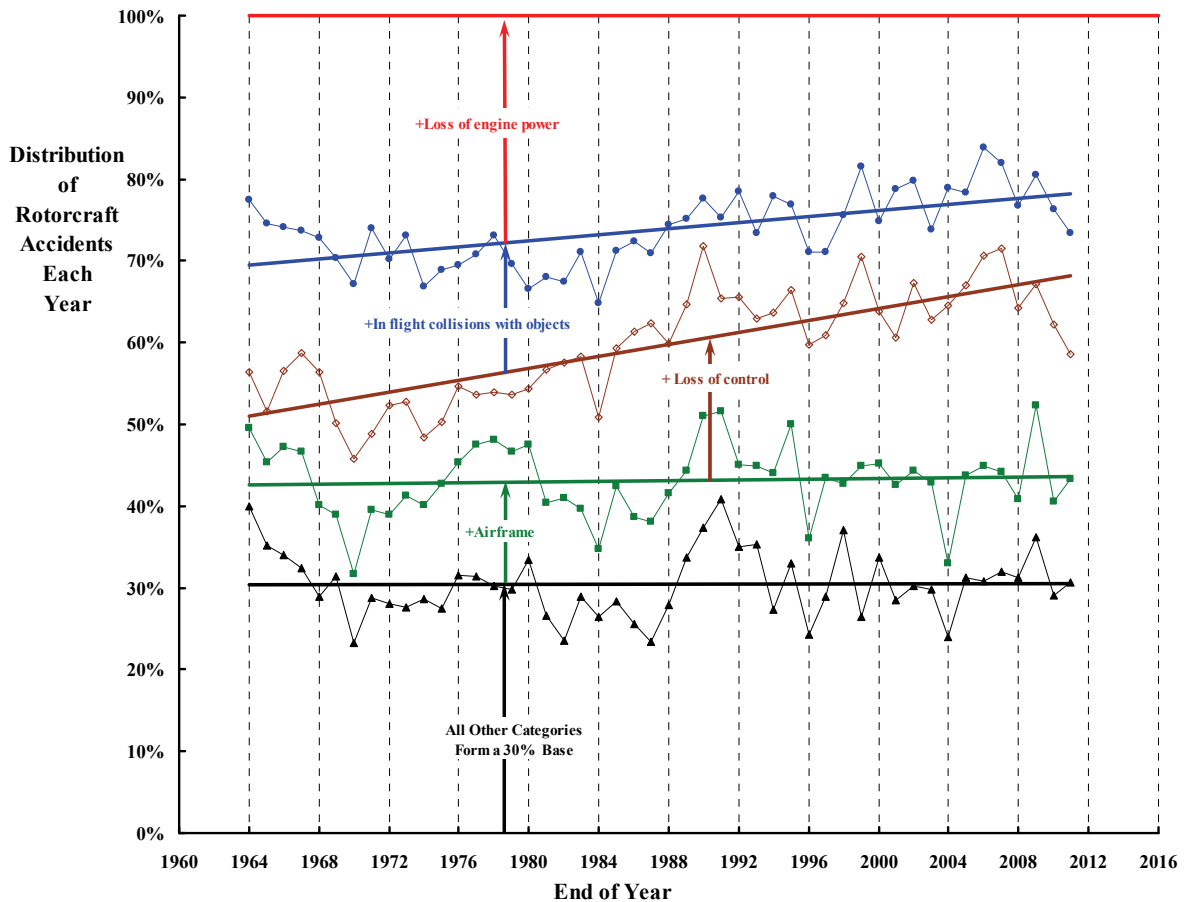


**Fig. 2-454. Loss-of-control accidents are a growing problem.**

## 2.10 ACCIDENT RECORD

dreamed of a helicopter in every garage, and they imagined that a trip to market by helicopter would soon be an everyday occurrence. Frankly, seeing several hundred helicopters flitting in and out of a mall parking lot does not paint a pretty picture to me—given this trend in loss-of-control accidents.

On the positive side, in-flight collision with objects appears to be considerably reduced since 1964, as the shrinking wedge on Fig. 2-454 suggests. Moreover, while not so dramatic, accidents associated with loss of engine power show clear signs of decline.

In the next several paragraphs, I will show you details of just the four accident categories singled out in Fig. 2-454. Details of these four categories, and all the other categories making up the 30 percent base, were first studied and reported in reference [666], which was published in December of 2000. This report dealt with accident analysis up to 1997 and included a study of 8,436 accidents. As Gene Kasper and I read NTSB accident briefs for the period beyond 1997 up through early 2012, we generally agreed that very few new causes of accidents in the four major categories could be highlighted. And so for this chapter, I have “stolen” data, with some updating, from our December 2000 report [666] to bring this Volume II about helicopters to a close. At the risk of repeating myself, it may be disquieting, but the last 47 years of helicopter accidents bear considerable similarities to airplanes in their early stage of development.

### 2.10.3.1 Loss-of-Engine-Power Analysis

So, what causes loss-of-engine-power accidents? More precisely, why did so many engines lose power? NTSB investigators have been able to backtrack toward a root cause for this failure in most of the accidents that began with a loss of power. A simple, first-step analysis of the NTSB accident reports turns up one startling and very disturbing, fact. The fact is that pilots of single *turbine*-powered helicopters are just as prone to loss of engine power as pilots of single *piston*-powered helicopters.

Consider the results of this first-step analysis by looking at Table 2-65, which is data from reference [666]. From 1964 through 1997, there were 8,436 accidents recorded by the NTSB as the rotorcraft fleet expanded. Some 2,408 accidents, about 29 percent of the 8,436 total, were charged to loss of engine power. The accidents are distributed by engine type and divided into commercial and amateur types. This data shows immediately that single turbine-powered helicopters *did not* improve the loss-of-power accident situation relative to single piston-powered helicopters. That is, single piston-powered helicopters experienced 1,554 loss-of-power accidents out of their total 5,371 accidents. This amounts to 29 percent. And, though it may come as a shock, single turbine-powered helicopters fared no better at 31 percent (i.e., 704 out of 2,247 accidents). On the positive side, twin turbine-powered helicopters are showing the promise that many thought would come when single turbine-powered helicopters were introduced. After all, the turbine engine is almost universally thought to be much more reliable than the piston engine.

**Table 2-65. Loss-of-Engine-Power Accident Data, 1964 Through 1997**

Accident Count (1964–1997)	Single Piston	Single Turbine	Twin Turbine	Amateur
8,436 Total	5,371	2,247	302	516
2,408 Loss of Engine Power	1,554 (29 %)	704 (31 %)	39 (13 %)	111 (15 %)

Table 2-65 does not, of course, suggest why engines are losing power. It takes the next analysis step to begin the explanation, and the results of this step are shown in Table 2-66. These results have been taken directly from reference [666] and, therefore, only include analysis of the 8,436 accidents that occurred from January 1, 1964, up to 1997.

To begin with, Table 2-66 shows that actual engine structural failure only caused 495 of the 2,408 loss-of-engine-power accidents, which is one fifth of the loss-of-engine-power accidents. Unfortunately, NTSB data shows that turbine engine structural failure accounts for a larger percentage of failures than piston engines. Perhaps even more worrisome is the number of engine(s) structural failures in the small fleet of twin turbine-powered helicopters.

The primary reason for loss of engine power is fuel/air mixture related. Slightly over 1,000 loss-of-engine-power accidents (some 43 percent of the total 2,408) were traced to incorrect fuel/air mixture. NTSB data shows that pilots of each helicopter class clearly share this fundamental problem. And, believe it or not, fuel exhaustion, which is a polite way of saying that the aircraft ran out of gas, is the culprit. There may be some deeper reason, some root cause, for a forced landing because of fuel exhaustion, but my discussion with many, many fixed-wing and rotary wing pilots did not uncover it. (Running out of gas is an awkward subject to bring up.)

A nearly typical fuel exhaustion accident is illustrated by the experience of a 45-year-old instrument-rated pilot with 2,335 rotorcraft flying hours who was forced to land a Bell 206L-1 on a hazy night after losing power in cruise. NTSB Docket Number 0059/CHI82DA034 reads as follows:

THE ENGINE LOST POWER IN CRUISE DURING A NIGHT FLIGHT WHILE ENROUTE TO OBTAIN FUEL. THE LOW RPM AUDIO AND WARNING LIGHT WERE NOTED WHEN THE LOSS OF POWER OCCURRED. THE PILOT ENTERED AN AUTOROTATIVE DESCENT AND TURNED TO LAND ON AN INTERSTATE HIGHWAY. AS HE STARTED TO DECELERATE FOR LANDING, POWER LINES BECAME VISIBLE IN HIS FLIGHT PATH. HE DUMPED THE NOSE AND DOVE UNDER THE POWER LINES, THEN FLARED AND TOUCHED DOWN AT ABOUT 25 TO 30 MPH. DURING THE LAST PART OF A GROUND SLIDE, THE MAIN ROTOR STRUCK A POLE FOR AN OVERHEAD SIGN AND A SPEED LIMIT SIGN. NO PRE-ACCIDENT ENGINE FAILURES WERE FOUND.

One might guess that the accident investigation uncovered some reason for the loss of engine power. However, no explanation was offered, and this particular accident was counted as one of the 609 in the Undetermined/Other category on Table 2-66. Virtually every one of the 2,408 loss-of-engine-power accidents recorded by the NTSB from the end of 1963 to the end of 1997 resulted in a substantially damaged or destroyed helicopter. Therefore, the fact that power-off landing proficiency is not required by the FAA in order to obtain a helicopter pilot's

## 2.10 ACCIDENT RECORD

certification appears inconsistent with the number of accidents. It also appears that helicopters currently in the civil fleet provide marginal to inadequate autorotational capability for the average pilot to successfully complete the final flare and touchdown to a generally unsuitable landing site. This is, to me, a very large step backward from the capability designed into autogyros. Furthermore, it appears that training in full autorotation landings all the way to touchdown, even to a prepared landing site, is avoided because of both real and perceived risks.

I would say that low rotor inertia of helicopter rotor systems is a serious shortcoming in the current civil fleet. The design issue of trading increased rotor inertia at the expense of increased weight empty, and perhaps aircraft selling price, has been controlled by military designs. I say this because so many civil helicopters have come to the commercial marketplace as derivatives of military machines. It is not that autorotation capability is downplayed as a serious requirement in military designs—far from it. It is just that the requirement to meet a weight-empty goal has overridden, in my opinion, the improvement in safety that comes with a design that the average pilot can successfully land with zero forward ground speed after engine power failure.

This issue of how much autorotational safety can or should be provided in a new helicopter design became particularly important when the gas turbine engine arrived on the

**Table 2-66. Loss-of-Engine-Power Accident Data, 1994 Through 1997 [666].**

Accident Count (1964–1997)	Single Piston	Single Turbine	Twin Turbine	Amateur
2,408 Loss of Engine Power	1,554	704	39	111
495 Engine Structure	263 (17 %)	189 (27 %)	15 (38 %)	28 (25 %)
1,042 Fuel/Air Mixture Related	686 (44 %)	299 (42 %)	17 (44 %)	40 (36 %)
Fuel exhaustion	326	82	1	8
Fuel contamination	97	43	1	4
Fuel starvation	72	26	5	4
Carburetor heat	70	0	0	6
Fuel system	67	92	3	10
Fuel control	42	27	3	7
Fuel improper	6	3	0	1
Induction air system	6	26	4	0
135 Other Systems	101 (6 %)	17 (2 %)	1 (3 %)	16 (14 %)
Ignition system	69	0	0	13
Lubricating system	24	15	1	3
Accessory drive assembly	8	2	0	0
62 Rotor Drive System	53 (3 %)	7 (1 %)	0 (0 %)	2 (2 %)
Clutch assembly	33	1	0	1
Transmission to main rotor	14	1	0	0
Engine to transmission drive	4	4	0	1
Freewheeling unit	2	1	0	0
65 Other Subcategories	54 (3 %)	11 (2 %)	0 (0 %)	0 (0 %)
Simulated power failure	36	8	0	0
Rotor RPM not maintained	18	3	0	0
609 Undetermined/Other	397 (26 %)	181 (26 %)	6 (15 %)	25 (23 %)

scene. With that step forward, low disc loading design approaches almost inherent with piston-engine-powered helicopters were discarded in favor of reduced weight-empty approaches that virtually doubled disc loading. Furthermore, no increase in rotor inertia was made to offset the disc loading increase. The basic issue became important to the military by the mid-1970s as many of their helicopter missions required nap-of-the-earth flying. The loss of engine power while flying very low and slow (just the opposite of what is preached by fixed-wing advocates) became of serious concern with single engine military helicopters. This precipitated a flight test program [75] that clearly established the overall benefits of storing energy for power-off landings in higher rotor inertia. The message, delivered by Tom Wood of Bell Helicopter at the May 1976 American Helicopter 32nd Annual Forum [672], was ignored by both the military and commercial branches of the rotorcraft industry. Instead, a move to twin engines began.

The debates about multi-engine helicopter safety over single-engine machines are almost legendary. Even fixed-wing advocates were demanding three- and four-engine aircraft in the early days. And you will recall that the initial specification for what led to the Douglas DC-3 stated a requirement for three engines. The airline industry and the FAA have finally satisfied themselves that twin-engine-powered aircraft are good enough even for transoceanic passenger-carrying service as witnessed by the Boeing 777.

Part of the multi-engine safety debates has been mathematical probability computations<sup>223</sup> that champion the thought that, with multi-engine redundancy, no one need ever worry about loss of power causing an accident again. Of course, you can see from Table 2-66 that (mathematics be damned) twin-engine helicopters have virtually the same percentage of loss-of-engine-power accidents caused by fuel/air mixture problems as do single-engine helicopters! You might wish that this was not the case, but NTSB data do not support your wish.

The basic argument for multi-engine designs centers on the ability to continue flight with one engine out. Why just *one* of the engines going off-line is the criteria is not at all clear to me, but most studies start with this criteria. A recent example came up during a 2005 NASA study about heavy lift rotor systems [674]. The NASA investigation somewhat paralleled the U.S. Army search for a heavy lift helicopter capable of lifting 20 to 30 tons of payload. The NASA study was, of course, aimed at the technology requirements of a notional, large civil airliner—something in the 120-passenger size and a VTOL aircraft that might enjoy the same commercial success as the Boeing 737.

A portion of this 2005 NASA investigation was carried out by Bell Helicopter and Sikorsky Aircraft who “prepared expositions on autorotation and one-engine-inoperative requirements for heavy lift.” The Sikorsky report by Mark Scott [675] and the Bell report by Tom Wood [676] are two very concise, well-written documents that deserve your undivided attention.

---

<sup>223</sup> Mr. H. L. Price delivered a lecture titled *Safety in Numbers* before The University of Leeds in West Yorkshire, United Kingdom, in November 1966. I was given a copy of the lecture [673] by Dick Carlson during a discussion we were having on probability as it relates to twin-engine safety.

## 2.10 ACCIDENT RECORD

The reports by Wood and Scott focus on two very important points. First of all, it is the FAA who is going to certify any heavy lift vertical takeoff and landing (VTOL) concept. And, between the two authors, you will read that current Part 29 and CAT A requirements may well be made more stringent for any future VTOL configurations of the type under study by NASA and the U.S. Army in 2005. Secondly, heavy lift twin-engine VTOL performance following a loss of one engine is particularly sensitive to the ratio of what horsepower the remaining engine can produce and how long that operating engine can produce that power. Both authors suggest that the emergency rating of the operating engine should be at least 0.9 times the power required to hover. That means that the ratio of an engine's emergency rating should be upwards of 1.8 of the standard takeoff rated power. Again, I recommend both reports for even more detailed discussion.

You should also be aware that the Russian Mil Moscow Helicopter Plant certificated its heavy lift Mi-26 helicopter in mid-1980 for complete twin-engine power failure. The requirement for this 120,000-pound helicopter was to complete autorotational landings to touchdown and to a final stopping of all motion. The paper [677] by Gourgen Karapetyan, Chief Test Pilot for Mil, is quite practical in all the details about meeting this certification requirement. I do not know of a better paper to read on the subject.

As a final note, consider the loss-of-engine-power accident trend shown in Fig. 2-455. The adverse trend that came with the single turbine-powered helicopter was reversed after 1981 when the industry showed what vigorous attention could achieve, but then it appears as if compliancy set in, and the industry failed to follow up.

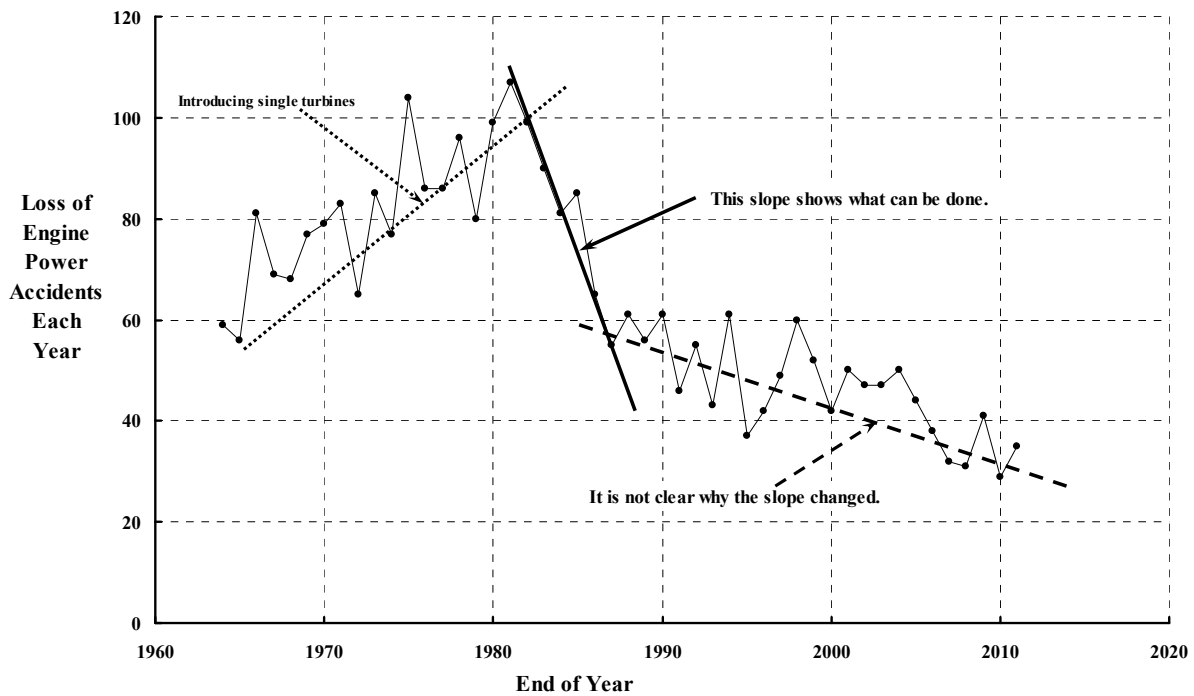


**Fig. 2-455. The introduction of the single turbine-powered helicopter came with a serious increase in loss-of-engine-power accidents.**

**2.10.3.2 In-Flight Collision With Objects**

The preceding NTSB accident synopsis recounting a loss-of-power accident says, in part, that the pilot, as he started to decelerate for landing, saw power lines in his flight path, so he dumped the nose and dove under the wires. He was one of the lucky ones. Unfortunately, in-flight collisions with wires, wires/poles, and trees are a major cause of accidents. The statistics are quite clear as Fig. 2-456 and Table 2-67 show. Unfortunately wires have been, and continue to be, a major threat to helicopter activities, which you learn immediately from Fig. 2-456.

Table 2-67 shows that the major contributor to these in-flight collisions with objects was the single piston-powered helicopter fleet, most frequently during crop dusting. Quite often “crop dusters” appeared to know where the obstacles were relative to a field, but for some reason (e.g., fatigue, sun glare, misjudging distance, etc.) still collided with them. This helicopter type had about equal numbers of main- and tail-rotor strikes.

Unlike piston-powered helicopters, single turbine-powered helicopters were engaged in general utility and passenger service when most of the objects were struck. The single turbine-powered helicopter class, which does relatively little crop dusting, experienced four tail-rotor strikes for every three main-rotor strikes.

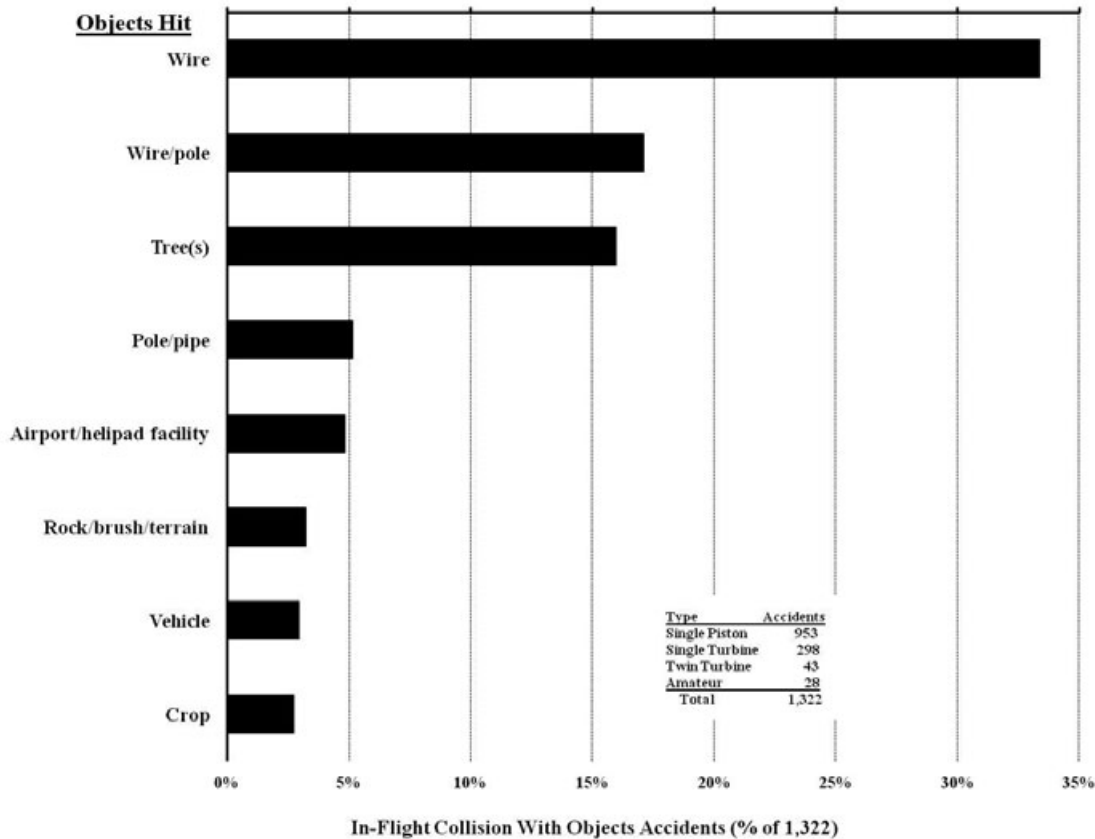


**Fig. 2-456. In-Flight Collision With Objects, 1994 Through 1997 (Pilots Cannot See Wires, Poles, and Trees Well Enough) [666].**

## 2.10 ACCIDENT RECORD

Table 2-67 shows that pilots of twin turbine-powered helicopters were, on a percentage basis, nearly as prone to hitting wires and trees as pilots of single engine helicopters. What stands out is that 12 of the 43 collisions were with airport/helipad facilities. In fact, 9 objects hit were protuberances around the heliport (6 on offshore oil rig platforms, 1 stairwell at a hospital, 1 crane at a building site, and 1 jetway gate). A tail rotor was swung into a hanger, and a barge rising and falling was an inadequate heliport. Twin-turbine helicopters had more than twice as many tail-rotor strikes as main-rotor strikes.

NTSB accident investigators most frequently cite the pilot for failing to see and avoid the object as the cause of the accident. That failure statement is all well and good, but it hardly gets to the root of the problem. Commercially manufactured helicopters are sold primarily because they perform well flying low and slow. Unfortunately, this flight regime places the helicopter pilot in a very hostile environment, populated by many natural and man-made objects. The average pilot's situational awareness of objects that must be avoided is, in fact, significantly impaired because most of the objects are not readily visible. Wires, in particular, are well-known threats to low flying for all aircraft types. It would be very helpful if all man-made objects higher than 500 feet were marked, mapped, and included in electronic databases, such as used in Global Positioning System (GPS) equipment. Perhaps, more practically, a low-price proximity spherical sensor should be developed and certified; a sensor sphere of some large radius should, in effect, cocoon the helicopter and provide the pilot with sufficient warning time to avoid obstacles.

An important reference point is that fuel-/air-mixture-related accidents caused at least 1,042 loss-of-engine-power accidents as Table 2-66 shows. This one area, leading to loss of engine power, equals more than the total amount of accidents caused by rotorcraft pilots running into wires (441), wires/poles (226), and trees (211).

**Table 2-67. In-Flight Collision With Objects Accident Data, 1994 Through 1997 [666]**

Accident Count (1964–1997)	Single Piston	Single Turbine	Twin Turbine	Amateur
8,436 Total	5,371	2,247	302	516
2,408 Loss of engine power	1,554 (29 %)	704 (31 %)	39 (13 %)	111 (15 %)
1,322 In-flight collision with objects	953 (18 %)	298 (13 %)	43 (14 %)	28 (5 %)
441 Wire	310	108	13	10
226 Wire/pole	197	24	0	5
211 Tree(s)	148	50	7	6
68 Pole/pipe	47	19	2	0
64 Airport/helipad facility	32	20	12	0
312 All other objects	219	77	9	7

### 2.10.3.3 Loss of Control

The upward trend in loss-of-control accidents is a very serious concern. In one sense the trend, shown in Fig. 2-457, has been obscured because loss-of-engine-power accidents have had a favorable decline in recent years as has been the case for the total civil fleet. As Fig. 2-453 shows, pilots of the commercial fleet lost control of their helicopters—regardless of their certification level—and this caused 949 of the 7,920 accidents. Pilots of amateur rotorcraft lost control nearly three times as often (on a percentage basis).

Table 2-68 shows that taking off and hovering clearly tax piloting skill. Fig. 2-458 indicates that controlling anti-torque in all flight phases is a root problem with the single-main-rotor helicopter configuration. This is particularly true with the single piston-powered helicopter, where fluctuations in engine RPM occur because of the reciprocating engine's RPM governing system. The turbine engine RPM governing system virtually removed this cause of accidents. However, on a percentage basis, pilots of single turbine-powered helicopters lost directional control twice as often as pilots of single piston-powered helicopters did, which suggests a design deficiency. Equipping some single engine and virtually all twin turbine-powered helicopters with an automatic stability and control system has generally improved the overall loss-of-control situation.

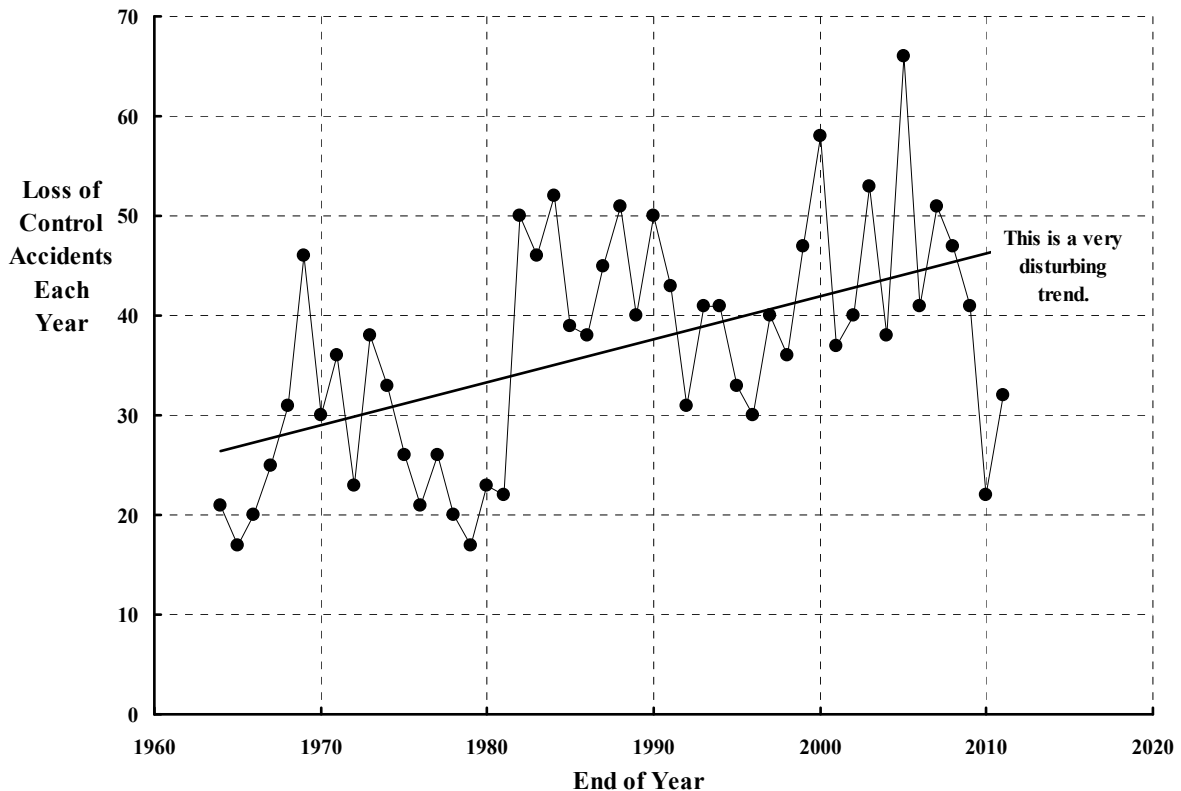


**Fig. 2-457. The trend of loss-of-control accidents presents a very serious situation, 1964 through 2011.**

## 2.10 ACCIDENT RECORD

Perhaps the most misunderstood phase of helicopter flight is taking off, hovering, and landing. These phases rarely (if ever) are flown in a no-wind situation. Fixed-wing aircraft, as you probably know, are particularly sensitive to crosswinds during these critical flight phases,

**Table 2-68. Loss-of-Control Accident Data**

Accident Count (1964–1997)	Single Piston	Single Turbine	Twin Turbine	Amateur
8,436 Total	5,371	2,247	302	516
2,408 Loss of engine power	1,554 (29 %)	704 (31 %)	39 (13 %)	111 (15 %)
1,322 In-flight collision with objects	953 (18 %)	298 (13 %)	43 (14 %)	28 (5 %)
1,114 Loss of control	625 (12 %)	284 (12 %)	40 (13 %)	165 (32 %)
271 Takeoff	148	74	6	43
233 Hover	150	61	5	17
178 Maneuvering	96	39	8	35
122 Landing	79	30	2	11
104 Cruise	43	34	6	21
81 Approach	37	20	8	16
125 All other phases	72	26	5	22

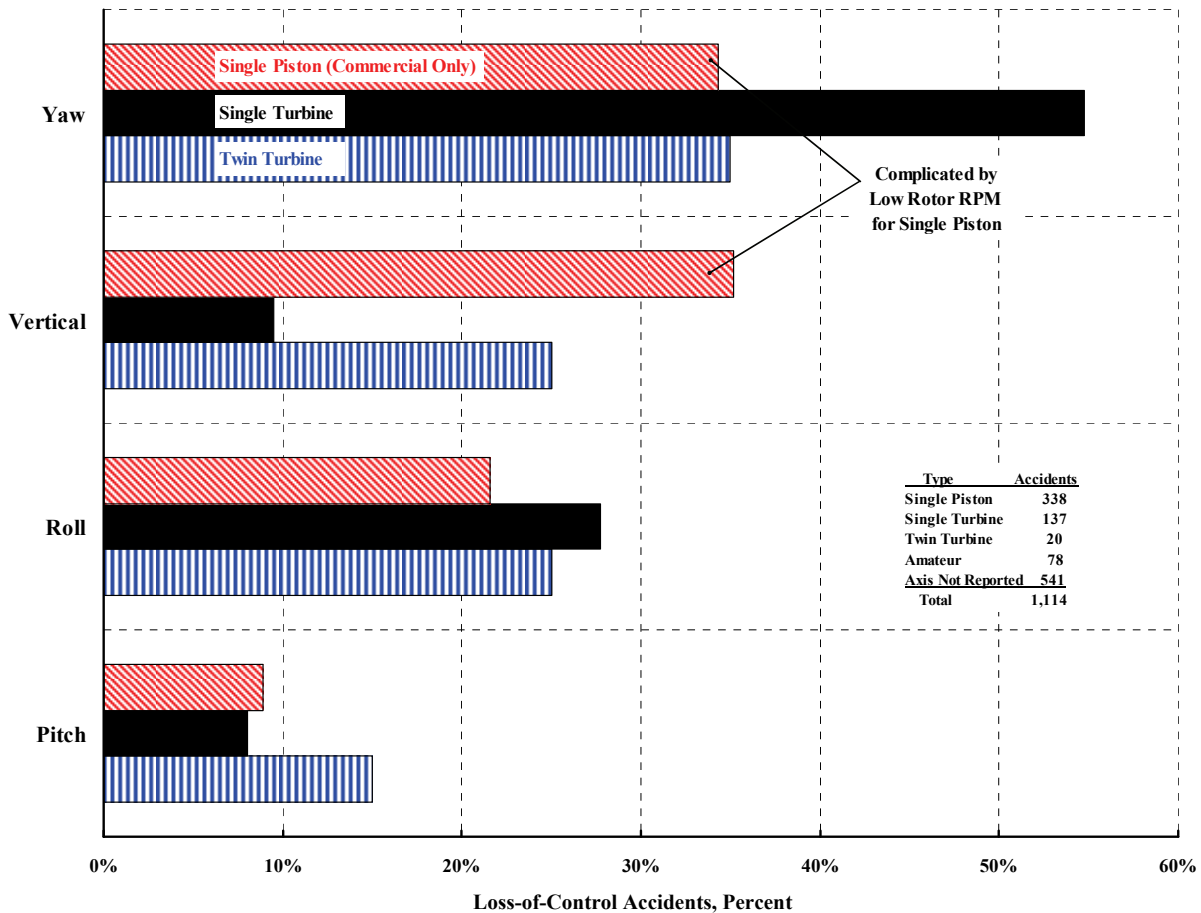


**Fig. 2-458. Controlling yaw is a BIG problem.**

and the single rotor helicopter is, if anything, even more sensitive. The reason is that crosswinds can create unanticipated aircraft yawing because the tail rotor experiences variable climb and descent conditions. It appears that the tail rotor authority of many aircraft in service is inadequate for many of these flight conditions, which can create excessive yaw rates. Certainly this was a serious concern with the Bell Model 206 series. The concern became quite clear after U.S. Army testing of an OH-58 (the military version of the Bell Model 206) revealed the occurrence of an unanticipated right yaw under certain low-speed flight conditions. The army referred to the right yaw characteristic as “loss of tail rotor effectiveness.” This concern was also addressed by Bell Helicopter Textron in a special *RotorBreeze* newsletter article in the May/June 1991 issue [678].<sup>224</sup> In this excellent, two-page article (which might have been saved in the pilot’s flight manual), wind direction from several azimuth angles can place the tail rotor in the wake of the main rotor. This adverse situation can add to or reduce the weather cocking behavior of the single rotor machine. In fact, the main rotor wake can put the tail rotor in a vortex ring condition, which reduces tail rotor control to at least zero or, even worse, gives the helicopter negative weather cocking behavior. This “swapping ends” in a split second is severely disorientating, even to an experienced pilot.

Current single piston-powered helicopters (and turbine-powered helicopters to a somewhat lesser extent) appear inordinately difficult to fly particularly when the average pilot has to devote attention to another task, or has a real or imagined emergency. Cross coupling between the vertical/power/RPM and yaw axes is clearly excessive. The handling qualities design standards applicable to the current helicopter fleet date back to the 1950s. Although generally tolerated, the resulting helicopter stability and control characteristics now appear quite unsatisfactory. This point is driven home in spades by Dugan and Delamer in their excellent paper titled *The Implications of Handling Qualities in Civil Helicopter Accidents Involving Hover and Low Speed Flight* [679]. Handling quality and certification standards for all future helicopters should immediately be raised to levels consistent with what modern technology can provide.

Today there are many radio control model helicopters flying. Many of these models are equipped with Young’s Bell bar or a version of the Hiller servo paddle stabilizing system, which adds stability to the Bell Model 47 and Hiller UH-12 helicopters, respectively. And just as many models are flown with miniature gyro systems to augment stability and control. Furthermore, the number of larger Unmanned Air Vehicles (UAVs) flying under complete autopilot control is impressive. Why this level of stability and control is not a part of every aircraft in the rotorcraft fleet is, quite frankly, very disappointing to me. Surely, it cannot be a cost issue.

One last point concerns the introduction of a new design into the civil fleet. When Frank Robinson got his R22 type certificate (TC H10WE dated March 16, 1979) [680] and sales began to take off, pilots began to experience a rash of “loss-of-control” accidents as the 1980s wore on. Early experience with the R44 began to suggest that both helicopters might

---

<sup>224</sup> The article initially appeared as Bell information letters nos. 206-84-41 and 206L-84-27, dated July 6, 1987. These letters were followed by *RotorBreeze* articles in July/August 1984 and 1987, and as handouts at various safety seminars.

## 2.10 ACCIDENT RECORD

have serious design flaws. The news media, always on the alert for aviation problems, picked up on the increasing number of R22 crashes in July of 1991. In Arizona in that month, KTAR radio traffic reporter Mike Nuetzman was killed when his Robinson R22 helicopter crashed through the roof of a northeast Phoenix house. Then several months later, in the Sunday, November 15, 1992, publication of *The Arizona Republic* [681], I read the special report titled *DANGER in the SKY*, which covered several pages. By 1996, the NTSB had completed its Special Investigation Report [682] of the R22's loss-of-main-rotor-control accidents, an investigation that had backtracked to the early 1980s. Robinson made some design changes to deal with the mast bumping problem that caused the main rotor shaft to be severed, followed by complete loss of the main rotor. Even more important were improvements he made to the flight training program. The R22 and R44 are very low inertia helicopters and, as such, are very sensitive to control inputs, which was not fully realized by many pilots. The NTSB's special report is well worth your reading time because there is much more to this story.

Not to belabor the point, but fuel-/air-mixture-related accidents caused at least 1,042 accidents as Table 2-66 shows. Thus, this one area—leading to loss of engine power—about equals *all* of the accidents caused by loss of control.

### 2.10.3.4 Airframe-Related Failure

Accidents caused by some failure or malfunction of an airframe component or part, or some airframe system, caused 1,083 of the 8,436 accidents (about 12 percent) that occurred from 1964 through 1997. Thus, *all* of the airframe-related failures virtually equal the 1,042 fuel-/air-mixture-related loss-of-engine-power accidents seen in Table 2-66. Table 2-69 shows that main- and tail-rotor systems, which include the rotor itself plus the rotor drivetrain plus the rotor control system, account for over 80 percent of the 1,083 airframe-related failures. Only 182 accidents, less than 20 percent, were caused by failures of other airframe-related components.

Table 2-69 shows that, on a percentage basis, there is little difference between single piston-powered and single turbine-powered helicopter accidents caused by airframe-related failures. That is, both aircraft have contributed about 12 percent (i.e., 639 out of 5,371 accidents) of airframe-related failures to their respective totals. However, early data for twin turbine-powered helicopters suggests that this rotorcraft configuration is experiencing over twice this percentage (about 29 percent) relative to its single engine configuration. This is a disturbing fact coming from NTSB data.

When viewed as subtotals in percent, Table 2-69 shows that there is no significant difference between single engine (piston or turbine) and twin engine helicopters with respect to main- and tail-rotor system failures. Of course, the vast majority of helicopters in the civil fleet are simply outgrowths of military configurations from the 1960s and 1970s. The manufacturers of these helicopters have continually improved successive models, but initial design decisions associated with 30-year-old military design standards are not easily, quickly, or inexpensively changed for civil application. For example, drivetrain components designed for 1,200- to 2,400-hour life for the military help maximize rotorcraft performance in that application. However, that same drivetrain used in a civil helicopter is a contributor to excessive operating costs and, in many civil applications, woefully under designed.

Data from reference [666] provides considerable insight as to the failure modes the NTSB determined for nearly all airframe-related accidents. As might be expected, failures caused by fatigue top the list, followed closely by improper assembly, installation, or maintenance. In the drive system, every component from engine output to transmission (particularly clutch assemblies, free-wheeling units, and tail-rotor drive shafts) has been a constant source of failure. Fatigue failure of rotor blades and hubs (particularly tail rotor components) is still much too prevalent. And, somewhat surprisingly, nonrotating control components (i.e., the so-called lower control systems) failed twice as often as components in the rotating system. Of the 1,083 airframe-related failures, 249 failures were finally traced to fatigue. Another 273 failures were attributed to NTSB descriptions such as material failure, failed, or separated. While these descriptions are less precise than fatigue, the specific component (and even part) are identified and analyzed in reference [666], *U.S. Civil Rotorcraft Accidents, 1963 through 1997*.

Commercial rotorcraft manufacturers have made considerable progress in reducing airframe-related accidents over the past 40 years as Fig. 2-459 shows. Of course, the introduction of single turbine-powered helicopters with their increased performance did require solving new problems and implementing many fixes based on field experience. However, the rotorcraft fleet is approaching 10 times the fleet size of 47 years ago, and airframe-related accidents per year are still declining, albeit slightly, even over the last few decades.

**Table 2-69. Airframe Failure Accident Data, 1964 Through 1997**

Accident Count (1964–1997)	Single Piston	Single Turbine	Twin Turbine	Amateur
8,436 Total	5,371	2,247	302	516
2,408 Loss of engine power	1,554 (29 %)	704 (31 %)	39 (13 %)	111 (15 %)
1,322 In-flight collision with objects	953 (18 %)	298 (13 %)	43 (14 %)	28 (5 %)
1,114 Loss of control	625 (12 %)	284 (12 %)	40 (13 %)	165 (32 %)
1,083 Airframe-related failure	639 (12 %)	282 (12 %)	89 (29 %)	73 (14 %)
192 Tail rotor itself	124	52	10	6
197 Tail rotor drivetrain	119	54	19	5
56 Tail rotor control system	38	11	7	0
445 Tail rotor systems subtotal	281 (44 %)	117 (42 %)	36 (41 %)	11 (15 %)
145 Main rotor itself	57	36	19	33
197 Main rotor drivetrain	127	49	13	8
114 Main rotor control system	63	29	11	11
456 Main rotor systems subtotal	247 (39 %)	114 (42 %)	43 (41 %)	52 (71 %)
118 Airframe	64	41	8	5
32 Landing gear	24	2	2	4
10 Engine*	7	3	0	0
22 Undetermined/other	16	5	0	1
182 Other systems subtotal	111 (17 %)	51 (18 %)	10 (11 %)	10 (14 %)

\* Do not forget the 495 engine structural failures listed in Table 2-66.

## 2.10 ACCIDENT RECORD

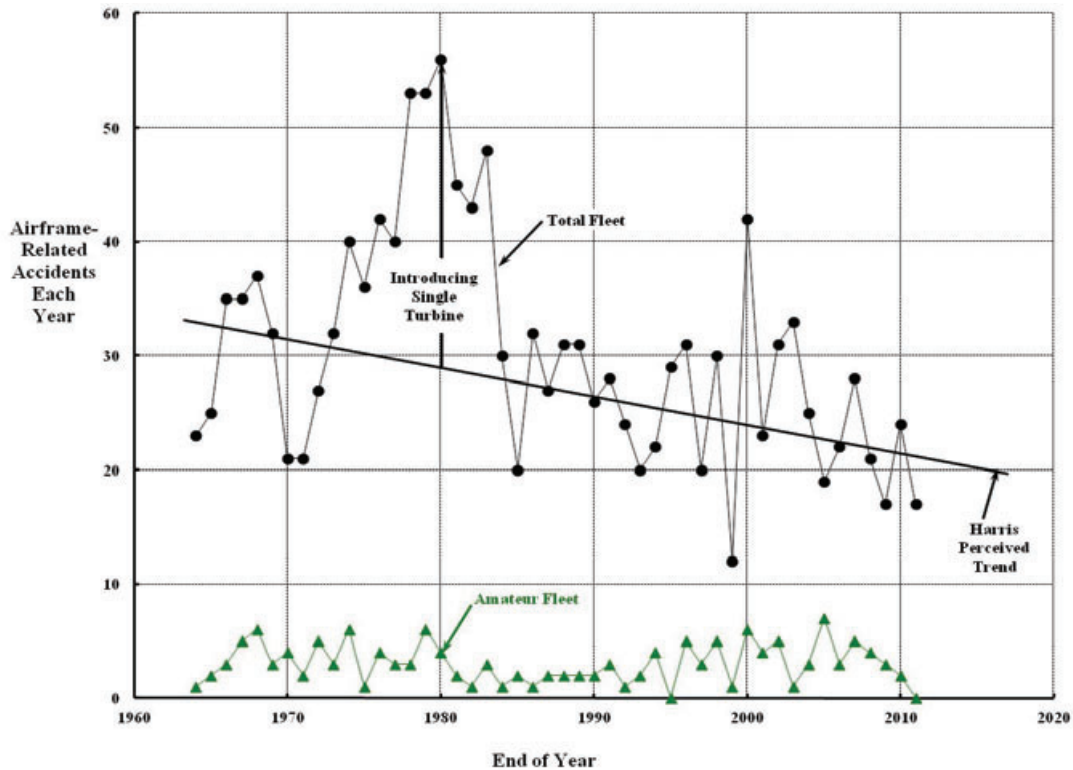


**Fig. 2-459. The introduction of the single turbine-powered helicopter was accompanied by too many accidents.**

### 2.10.4 Concluding Remarks

You read at the beginning of this chapter that fixed-wing aircraft suffered from stall and spin accidents.<sup>225</sup> The accident rate was so alarming that several branches of the U.S. Government sprang into action. This action led to the National Transportation Safety Board being established as part of the Civil Aeronautics Act of 1938. The NTSB began as the Civil Aeronautics Board's Bureau of Safety and became an independent agency within the Department of Transportation in 1967. In 1974, U.S. Congress made the NTSB a completely independent agency from the Department of Transportation (DOT) (and thus from the FAA, as well). As one study authored by the Rand Corporation [684] reported in December of 1999,

“The National Transportation Safety Board (NTSB) is pivotal to the safety of the traveling public in the United States and throughout the world. While it is not a regulatory agency and does not command significant enforcement powers, the NTSB exerts enormous influence based on the independence and accuracy of its accident investigations and the authority of its recommendations. The NTSB is charged with the responsibility of investigating and establishing the facts, circumstances, and probable cause of transportation accidents, and with making safety recommendations to governmental agencies to prevent similar accidents from happening in the future. Fundamentally, the safety board provides a quality assurance function vital to the ongoing safety of all modes of transportation. The

<sup>225</sup> The stall and spin characteristics of even modern day general aviation fixed-wing aircraft have shown to be a very, very difficult problem. The historical overview that Seth Anderson of NASA Ames Research Center published in July of 1979 [683] provides real insight should you care to delve into the subject.

NTSB's unique role in transportation safety is contingent on the ability of the board members and the professional staff to conduct independent investigations of accidents and major incidences and, in so doing, to assure public confidence in the safety of our national transportation systems.”

You might not know that the whole NTSB is staffed by less than 500 full-time people and has a yearly budget of around \$120 million. If there is a more efficient and cost-effective government agency than the NTSB, I am not aware of it. I believe accident investigators are the most dedicated people in the transportation industry, and I take my hat off to each and every one of them. As a member of the rotorcraft industry, I am very sorry that rotorcraft accidents have just added to their workload.

The rotorcraft industry, a relative newcomer to aviation, does not enjoy a particularly good safety record. The record is frequently quoted in terms of rotorcraft accidents per 100,000 flight hours flown by the commercial and amateur fleet. Because the denominator, hours flown, is quite questionable, I have tried to draw your attention to accidents per year and the growing size of the rotorcraft fleet.

The NTSB has recorded 11,426 rotorcraft accidents from January 1, 1964, through December 31, 2011, as the FAA-registered fleet size increased from about 2,200 to virtually 20,000 machines. The study of these accidents that you have read about shows that:

1. The industry's track record is to sell four turbine-powered helicopters and then crash one. This trend applies to twin- as well as single-engine-powered configurations.
2. Accidents classified as loss of control have continually increased at an alarming rate for 47 years.
3. Loss of engine power causes 30 percent of all single-engine-powered helicopter accidents. This is true for both piston and turbine engine configurations. The most frequent reason for the engine's loss of power is not engine structural failure, but an incorrect fuel/air mixture, which accounts for nearly one-half of the 30 percent. The primary cause of incorrect fuel/air mixture is simply running out of gas!

You will recall from Volume I that Henrich Focke [45], when designing the world's first truly successful helicopter, set the number-one design requirement to provide for the “possibility of a forced landing in case of engine failure.” In my view, we have a civil helicopter fleet that does not come even close to providing the autorotational landing capability of the Cierva, Pitcairn, and Kellett autogyros. Power-off, run-on landings may demonstrate to the FAA that any given design meets their requirement, but I submit that this is nowhere near good enough. I believe that we should not design and produce a new single-engine civil rotorcraft with such marginal autorotational capability. The average pilot needs twice as much rotor inertia per helicopter as the current fleet has. Touchdown with virtually zero forward speed should be the minimum design requirement. Doubling current levels of rotor inertia can completely remove the “dead man's curve” (i.e., the height-velocity curve) restriction from flight manuals as Tom Wood reported in 1976 [672]. The impact on a helicopter's weight empty and purchase price appears small enough that this improvement could reasonably be incorporated in growth models of many helicopters in the current commercial fleet.

## 2.10 ACCIDENT RECORD

In 2005 the rotorcraft industry, recognizing that its track record was not improving, began to mount a worldwide, unified attack on accidents associated with their products. The International Helicopter Safety Team (IHST) was formed with the goal of reducing accidents by 80 percent. I have interpreted this goal as reducing accidents from 10 per 100,000 hours flown at the end of 2005 to 2 accidents per 100,000 hours flown by the beginning of 2016. The IHST has already shown that their efforts are paying off, because the trend in accidents per year is clearly downward as Fig. 2-447 shows. There is a wealth of studies about rotorcraft accidents, both military [685, 686] and civil [687-692] that can be reread and the lessons applied. This background, along with the IHST's ongoing investigations, says to me that the industry goal will be met. It seems plausible to look forward to a time where only a few accidents occur in a year—and then maybe we can go a whole year without one accident. That should be our next goal.

This chapter began with a question about the oft-quoted statement that “virtually all accidents are caused by human error.” After reading 11,426 NTSB rotorcraft accident reports, I am forced to agree. Nevil Shute (an aeronautical engineer by day and world famous author by night) wrote in his autobiography *Slide Rule* [693] that

“Aircraft do not crash of themselves. They come to grief because men are foolish, or vain, or lazy, or irresolute, or reckless.\* One crash in a thousand may be unavoidable because God wills it so—not more than that.”

\*Now I would add: or tired, late, pushed by management, sick, broke, distracted, hungover, or overwhelmed, or they just guessed wrong or “just weren't thinking.”

### 3 CONCLUDING REMARKS

The rotorcraft industry completed the transition from autogyros to a helicopter product line by the end of 1945. The helicopter then demonstrated its value during the Korean War (June 1950–July 1953) after which the industry turned to civilian applications. By the end of 1956, the Federal Aviation Agency (FAA) had 540 helicopters in its U.S. registry, although only 370 were actively being flown. This miniscule fleet is lumped into the FAA’s General Aviation category, in a subcategory named rotorcraft with a designation of Code 6. The General Aviation category includes virtually all aircraft over and above those being used in the airline business. As I write these concluding remarks during August of 2012, the FAA’s rotorcraft count is nearly 20,000. The U.S. Department of Defense fleet adds another 6,500 helicopters.

You should be aware that military needs for helicopters have paid for much of the research, development, and field experience that the industry needed to establish its commercial product lines. You can also well imagine that the industry, in producing this growing military and civilian fleet, has had to overcome a multitude of engineering, manufacturing, marketing, product support, and community acceptance problems.

This introduction to helicopters has focused your attention on the major shortcomings of today’s helicopters—at least as I see them. Now let me offer some thoughts about how to overcome these shortcomings. I will discuss these major shortcomings in my order of importance, starting with the accident record and concluding with engines.

If you talk to manufacturers about helping to substantially reduce accidents by modifying their helicopters, it may seem like a dead end. In fact, I have frequently encountered individuals who say, “Safety doesn’t sell.” The next reason you may hear is that “the cost of complete re-certificating to FAA standards is sobering.” Nevertheless, these same manufacturers continue to make major product improvements such as Bell Helicopter’s move from two-bladed rotor systems to multi-bladed (i.e., four) rotor systems. Why some improvements for safety are not included in these product refinements is beyond me. For example, increased rotor inertia can be accomplished along with an increase in engine takeoff ratings. Yes, *some* of the increase in useful load sought may have to be forfeited, and a portion of re-certificating expense will be incurred, but just imagine the marketing advantage a manufacturer would get by being the first to remove the height-velocity restriction from the flight manual.

Loss-of-control accidents are increasing at an alarming rate as Fig. 2-457 showed. The installation of a low-authority stability augmentation system (SAS) (with, at most, 15 percent authority) seems entirely in order, certainly for the next product improvement of single engine helicopters. I suggest that this can also be done as an aftermarket product for helicopters in the current civil fleet. As a bare minimum, pilots need help with directional control, which hardly seems like a tall order.

### 3. CONCLUDING REMARKS

Operating costs of helicopters are, to be blunt, unreasonably high. I believe this situation has come about because military requirements have spilled over on to commercial helicopters. The military only requires components with time between overhauls (TBOs) on the order of 2,000 hours because (I guess) in war the attrition rate can be very high, and in peacetime, relatively little flying goes on. Of course, there can be a weight-empty saving with low TBOs, but operating costs go up. The use of these same military helicopter components (say transmissions, for example) in the civil fleet, which can put 1,000 hours or more per year on a machine, immediately raises operating costs. Anything less than TBOs of 10,000 hours for civil helicopters seems to me to be, as the British say, “penny-wise and pound-foolish.” Another interesting example concerns the use of advanced materials. Rotor blades made with composites have a number of attractive features over metal spar blades, but I am not convinced that their TBO of 10,000 hours (or even “on condition”) justifies the price that manufacturers are charging for spares. In fact, I suggest that graphs of purchase price and operating cost versus TBO would be very, very interesting.

Operating costs are significantly driven by airframe maintenance overhaul prices. The small number of components involved in an overhaul (about 25 to 75), which account for about one-third of yearly maintenance costs, should be redesigned and requalified (if necessary) whenever a model upgrade is considered. A simple weeding-out process over a decade of operational experience should do wonders for this shortcoming. Maybe new designs that are not derived from military components and design requirements, but *really* are driven by what commercial helicopter users so desperately need (even before performance), can produce rotorcraft that would attract major airlines and the short-haul service they could initiate.

Helicopters are just plain too expensive to buy. The 50 percent premium for VTOL over a fixed-wing aircraft is excessive, which seems to keep relegating the machine to niche markets. If it is true that purchase price is driven almost entirely by weight empty and installed power as Eqs. (2.347) and (2.348) on page 546 suggest, then there may be very little that can be done, other than reducing profit margins. On the other hand, it may well be that manufacturing labor hours per pound, or per part count, are too high when compared to the fixed-wing industry—and that might be because rotary wing engineers have learned very little from fixed-wing engineers. Let me suggest, therefore, that a more in-depth examination be done to find out why helicopter prices are so much higher than comparable fixed-wing prices. I would think that an answer to this question would immediately help the rotorcraft industry. Furthermore, an in-depth study could help NASA and the U.S. Army direct their rotorcraft Research and Development (R&D) programs to elements having a much higher return for their dollars.

Noisy helicopters continue to be less and less accepted by an ever-growing number of communities. A small group of researchers now have a reasonable understanding of the many sources of helicopter noise. However, only one helicopter manufacturer (Hughes, in 1972 with *The Quite One*) has demonstrated a practical design approach that *really* lowered helicopter noise [548] *and* that raised useful load at the same time. Hughes’ design approach could be applied today if the rotorcraft industry cared to. Frankly, I would bet (my company,

### 3. CONCLUDING REMARKS

if I had one) that there would be a significant increase in helicopter sales if the industry offered low-noise products across the board.

The fact that helicopter sales remain relatively strong, despite the machine's reputation for vibration, is quite interesting. The way I see it, there is a big gap between what researchers have learned and how much of this knowledge is incorporated into each manufacturer's newest product. For example, tuning both the rotor system *and the fuselage* to avoid amplification of rotor hub loads, before these vibratory loads reach every occupants' seat, is the most fundamental approach to reducing helicopter vibration with today's rotor systems. This is the primary approach I favor. That means fuselage design tools such as NASTRAN [444-446, 457, 466, 467] must be used not only for early stress analysis during preliminary design, but for early vibration analysis as well, which is hardly current engineering practice.

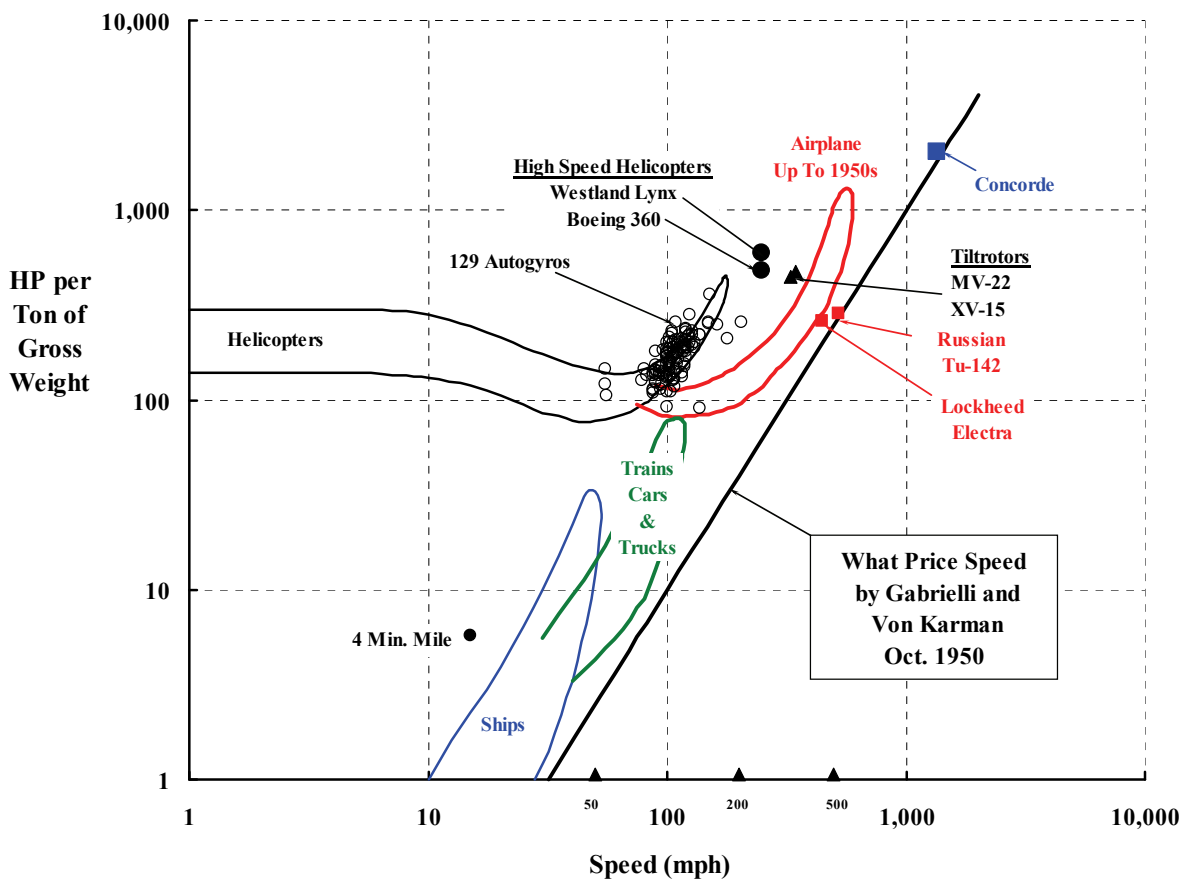
Helicopter performance—including fuel efficiency, and engine and weight-empty subjects—is the most mature technology of all, in my opinion. After seven decades of clearly defining and demonstrating the helicopter's fundamental capabilities, the industry knows where this VTOL aircraft sits in the world of transportation. We know (a) that we can make very large helicopters (like a Russian Mi-26), (b) what ratio of useful load to takeoff gross weight we can offer (with reasonable accuracy), and (c) that we have rather discouraging insight about what we can offer for an economical cruise speed. On virtually every new design, we pick the installed engine takeoff power based on hover performance requirements and then we just accept whatever forward flight performance comes out. Quite frankly, I am tired of spending so much money to raise hovering Figure of Merit. I think the real effort should be to increase cruise and maximum speeds at engine takeoff power by reducing parasite drag of the airframe (including the rotor hub and landing gear). This is the tried and true, aerodynamic approach used by fixed-wing designers for a century. It is time rotary wing designers followed this advice.

It seems to me that we are flogging a dead horse trying to optimize rotor system hovering performance, which can, I admit, be just plain theoretical fun. I believe engine manufacturers can match any hover performance increase obtained by complicated blade geometry at one-tenth of the cost of rotor system "Figure-of-Merit improvements" by airframe manufacturers. Instead, I see research dollars going to hubs designed for low drag (like the AH-56 doorhinge hub) and configurations where landing gears are retracted and fuel is carried internally (like the Sikorsky S-76, to single out just one example).

My perception is that innovation in the helicopter industry has stagnated. We have lived off of civil helicopter derivatives of military designs and components for seven decades. But now (in 2012) we are faced with the likelihood that the military's requirements, and its money, are drying up. Even if the military did want, and could afford, a "new machine," the industry would probably just adapt 1970s and 1980s technology to its need, give or take a modern "glass" cockpit and fuselage shaping for stealth. That is what we did for the LHX/RH-66 Comanche program. This may be good enough for the military, but it is hardly good enough if we really want to increase civil helicopter usage.

### 3. CONCLUDING REMARKS

For the civil marketplace, we cannot continue to coast along perpetuating a commercial fleet with the major shortcomings that I have brought to your attention. If we do continue to coast, I believe the marketplace *and* our pioneers—Cierva, Pitcairn, Kellett, Focke, Sikorsky, Bell's Young and Kelley, Piasecki, Hiller, and Kaman—to name just a few—will be very, very disappointed in us.



**Rotorcraft enjoy a unique position in the transportation industry.**

## 4 REFERENCES

1. Liberatore, E. K.: Helicopters Before Helicopters. Malabar, Fla.: Krieger Publishing Co., 1998.
2. Boulet, J.: History of the Helicopter as Told By Its Pioneers, 1907–1956. Paris, France: Editions France-Empire, 1982.
3. Gablehouse, C.: Helicopters and Autogiros: A History of Rotating-Wing and V/STOL Aviation. Philadelphia, Pa.: J.B. Lippincott & Co., 1967.
4. Brooks, P. W.: Cierva Autogiros: The Development of Rotary-Wing Flight. Washington, D.C.: Smithsonian Institution Press, 1988.
5. Gibbs-Smith, C. H.: The Aeroplane. London, England: Her Majesty's Stationery Office, 1960.
6. Apostolo, G.: The Illustrated Encyclopedia of Helicopters. New York, N.Y.: Bonanza Books, 1984.
7. Coates, S.; and Carbonel, J.-C.: Helicopters of the Third Reich. Surrey, England: Classic Publications, 2003.
8. Anderson, J. D., Jr.: A History of Aerodynamics. Cambridge, United Kingdom: Cambridge University Press, 1997.
9. Pritchard, J. L.: The Dawn of Aerodynamics. The Royal Aeronautical Society, vol. LXI, 1957.
10. Durand, W. F.: Aerodynamic Theory, A General Review of Progress. Mineola, N.Y.: Dover Publications, 1976.
11. Timoshenko, S. P.: History of Strength of Materials. Mineola, N.Y.: Dover Publications, 1983.
12. Dugas, R.: A History of Mechanics. Mineola, N.Y.: Dover Publications, 1988.
13. Betz, A.: The Ground Effect on Lifting Propellers. NACA TM 836, Apr. 1937.
14. Drees, J.: Blade Twist, Droop Snoot, and Forward Spars. Vertflite, Sept./Oct. 1976.
15. Gessow, A.: Standard Symbols for Helicopters. NACA TN 1604, June 1948.
16. Gregory, H. F.: Anything a Horse Can Do: The Story of the Helicopter. New York, N.Y.: Reynal & Hitchcock, 1944.
17. Crocco, G. A.: Inherent Stability of Helicopters. NACA TM 234, 1923.
18. Hohenemser, K.: Dynamic Stability of a Helicopter With Hinged Rotor Blades. NACA TM 907, 1939.
19. Morris, C. L.: Pioneering the Helicopter. New York, N.Y.: McGraw-Hill Book Co., Inc., 1945.
20. Sikorsky, I. I.: The Story of the Winged-S: Late Developments and Recent Photographs of the Helicopter. New York, N.Y.: Dodd, Mead & Co., 1967.
21. Young, A. M.: A New Parameter of Lifting Rotors. Proc. Second Annual Rotating Wing Aircraft mtg. sponsored by the Philadelphia Chapter of the Institute of the Aeronautical Sciences, Philadelphia, Pa., 1939.
22. Young, A.: The Helicopter and Stability. American Helicopter, Mar. 1948.
23. Klemin, A.: Helicopter Engineering: Two-Bladed Rotor by Young. Aero Digest, Apr. 1946.

#### 4. REFERENCES

24. Putnam, V. K.; and Ferry, R. G.: Stability With a Stabilizing Bar. AFFTC-TR-58-4 (see also AD-124128), Air Force Flight Test Center, Edwards Air Force Base, Calif., 1958.
25. Tipton, R. S.: They Filled the Skies. Ft. Worth, Tex.: Bell Helicopter Textron, Inc., 1983.
26. Kelley, B.: Helicopter Stability With Young's Lifting Rotor. Society of Automotive Engineers (SAE) J., vol. 53, no. 12, Dec. 1945 (see also SAE TP 450232, 1945).
27. Kelley, B.: Response of Helicopter Rotors to Periodic Forces. NACA Advance Restricted Report 5A09, Mar. 1945.
28. Anon.: The Bell Rotor System. Report No. 30-929-123, Bell Aircraft Corp., Ft. Worth, Tex., 1954.
29. Spenser, J. P.: Vertical Challenge, The Hiller Aircraft Story. Seattle, Washington: University of Washington Press, 1992.
30. Stuart, J., III: The Helicopter Control Rotor. Proc. 16th Annual Mtg. of the Institute of Aeronautical Sciences, New York, N.Y., Jan. 26–29, 1948.
31. Stuart, J., III: The Helicopter Control Rotor. Report No. 150.1, United Helicopters, Inc., Palo Alto, Calif., Mar. 19, 1947.
32. Stuart, J., III: Analysis of Effect of Lowering a Lifting Rotor Mounted Control Rotor Relative to the Teetering Axis. Report No. 150.2, United Helicopters, Inc., Palo Alto, Calif., 1947.
33. Jacoby, D. R.: Analysis of the Hovering Stability and Control of the UH-12 Helicopter. Report No. 150.3, United Helicopters, Inc., Palo Alto, Calif., Mar. 22, 1948.
34. Klemin, A.: New Ideas in Helicopter Control. Aero Digest, vol. 56, no. 4, Apr. 1948.
35. Miller, R.: Helicopter Control and Stability in Hovering Flight. J. Aeronautical Sciences, Aug. 1948.
36. Sissingh, G. J.: Automatic Stabilization of Helicopters. J. Helicopter Association of Great Britain, vol. 2, no. 3, 1948.
37. Sissingh, G. J.: The Frequency Response of the Ordinary Rotor Blade, the Hiller Servo-Blade, and the Young-Bell Stabilizer. Aeronautical Research Committee R&M No. 2860, 1950.
38. Prewitt, R. H.: Report on Helicopter Developments in Germany. Society of Automotive Engineers (SAE), May 1945.
39. Liptrot, R. N.: Rotating Wing Activities in Germany During the Period 1939–1945. British Intelligence Objectives Sub-Committee Overall Report, vol. 8, Her Majesty's Stationary Office, London, England, 1948.
40. Sissingh, G. J.: Contributions to the Dynamic Stability of Rotary-Wing Aircraft With Articulated Blades, Part I—General Principles. Translation No. F-TS-690-RE, Headquarters Air Material Command, Wright Field, Dayton, Ohio, Aug. 1946.
41. Sissingh, G. J.: The Dynamic Stability of Helicopters With Articulated Rotors. Translation No. F-TS-1002-RE, Headquarters Air Material Command, Wright Field, Dayton, Ohio, Sept., 1946.
42. Guarino, L. S.: Automatic Control and Stabilization of Helicopters. Mid-Eastern Proc. American Helicopter Society, Feb. 19, 1953.

43. Anon.: Automatic Control for Helicopter. *InterAvia*, vol. 6, no. 3, 1951.
44. Burkham, J.: Penni Helicopter. *American Aircraft Modeler*. Jan., 1970.
45. Focke, H.: The Focke Helicopter. NACA TM 858, Apr. 1938.
46. Focke, H.: German Thinking on Rotary-Wing Development. *J. Royal Aeronautical Society*, vol. 69, no. 653, May 1965, pp. 293–305.
47. Gustafson, F. B.: Flight Tests of the Sikorsky HNS-1 (Army YR-4B) Helicopter. 1—Experimental Data on Level-Flight Performance with Original Rotor Blades. NACA WR-L-595, 1945.
48. Gustafson, F. B.; and Gessow, A.: Flight Tests of the Sikorsky HNS-1 (Army YR-4B) Helicopter. 2—Hovering and Vertical-Flight Performance With the Original and an Alternate Set of Main-Rotor Blades, Including a Comparison With Hovering Performance Theory. NACA WR-L-596, 1945.
49. Dingeldien, R. C.; and Schaefer, R. F.: Static-Thrust Tests of Six Rotor-Blade Designs on a Helicopter in the Langley Full-Scale Tunnel. NACA WR-L-101, 1945.
50. Dingeldien, R. C.; and Schaefer, R. F.: Full-Scale Investigation of Aerodynamic Characteristics of a Typical Single-Rotor Helicopter in Forward Flight. NACA Report No. 905, 1948.
51. Cheeseman, I. C.; and Bennett, W. E.: The Effect of the Ground on a Helicopter Rotor in Forward Flight. Report No. A.A.E.E./Res/288, Aeroplane and Armament Experimental Establishment, Minister of Supply, Boscombe Down, July 11, 1955.
52. Heyson, H. H.: Theoretical Study of the Effect of Ground Proximity on the Induced Efficiency of Helicopter Rotors. NASA TM-X-71951, May 1977.
53. Mashman, J.: *To Fly Like a Bird*. Potomac, Md.: Phillips Publishing, Inc., 1992.
54. Glauert, H.: The Theory of the Autogyro. *J. Royal Aeronautical Society*, vol. 31, no. 198, 1927, pp. 483–508.
55. Lock, C. N. H.; and Bateman, H.: Some Experiments on Airscrews at Zero Torque, with Applications to a Helicopter Descending with Engine “Off,” and to the Design of Windmills. Aeronautical Research Committee R&M No. 885, Sept. 1923.
56. Lock, C. N. H.; Bateman, H.; and Townend, H. C. H.: An Extension of the Vortex Theory of Airscrews with Applications to Airscrews of Small Pitch, Including Experimental Results. Aeronautical Research Committee R&M No. 1014, June 1926.
57. Lock, C. N. H.; and Townend, H. C. H.: Wind Tunnel Experiments on a Symmetrical Aerofoil (Gottingen 429 Section). Aeronautical Research Committee R&M No. 1066, Nov. 1926.
58. Glauert, H.: The Analysis of Experimental Results in the Windmill Brake and Vortex Ring States of an Airscrew. Aeronautical Research Committee R&M No. 1026, Feb. 1926.
59. Lock, C. N. H.; and Townend, H. C. H.: Photographs of the Flow Round a Model Screw Working in Water, Especially in the “Vortex Ring State.” Aeronautical Research Committee R&M No. 1043, May 1926.
60. Caygill, L. E.; and Nutt, A. E. W.: Wind Tunnel and Dropping Test of Autogyro Models. Aeronautical Research Committee R&M No. 1116, Nov. 1926.
61. Wheatley, J. B.: Lift and Drag Characteristics and Gliding Performance of an Autogyro as Determined in Flight. NACA TR 434, 1933.

#### 4. REFERENCES

62. Castles, W.; and Gray, R. B.: Empirical Relation Between Induced Velocity, Thrust, and Rate of Descent of a Helicopter Rotor as Determined by Wind Tunnel Tests on Four Model Rotors. NACA TN No. 2474, Oct. 1951.
63. Fitzwilliams, O. L. L.: Engine-Off Landings. *Flight Magazine*, Nov. 13, 1947.
64. Nikolsky, A. A.; and Seckel, E.: An Analytical Study of the Steady Vertical Descent in Autorotation of Single-Rotor Helicopters. NACA TN 1906, June 1949.
65. Nikolsky, A. A.; and Seckel, E.: An Analysis of the Transition of a Helicopter From Hovering to Steady Autorotative Vertical Descent. NACA TN 1907, June 1949.
66. Slaymaker, S. E.; Lynn, R. R.; and Gray, R. B.: Experimental Investigation of Transition of a Model Helicopter Rotor From Hovering to Vertical Autorotation. NACA TN 2648, Mar. 1952.
67. Slaymaker, S. E.; and Grey, R. B.: Power-Off Flare-Up Tests of a Model Helicopter Rotor in Vertical Autorotation. NACA TN 2870, Jan. 1953.
68. Katzenberger, E. F.; and Rich, M. J.: An Investigation of Helicopter Descent and Landing Characteristics Following Power Failure. *J. Aeronautical Sciences*, vol. 23, no. 4, 1956, pp. 345–356.
69. Fradenburgh, E. A.: A Simple Autorotative Flare Index. *J. American Helicopter Society*, vol. 29, no. 3, 1984.
70. Hanley, W. J.; and DeVore, G.: An Analysis of the Helicopter Height Velocity Diagram Including a Practical Method for Its Determination. Federal Aviation Administration Report No. NA-67-1, Feb. 1968.
71. Hanley, W. J.; and DeVore, G.: An Evaluation of the Effects of Altitude on the Height Velocity Diagram of a Single Engine Helicopter. Federal Aviation Agency Report ADS-1, Feb. 1964.
72. Hanley, W. J.; and DeVore, G.: An Evaluation of the Effects of Altitude on the Height Velocity Diagram of a Lightweight, Low Rotor Inertia, Single Engine Helicopter. Federal Aviation Agency Report ADS-46, July, 1965.
73. Hanley, W. J.; DeVore, G.; and Martin, S.: An Evaluation of the Effects of Altitude on the Height Velocity Diagram of a Lightweight, High Rotor Inertia, Single Engine Helicopter. Federal Aviation Agency Report ADS-84, Nov. 1966.
74. Pegg, R. J.: An Investigation of the Helicopter Height-Velocity Diagram Showing Effects of Density Altitude and Gross Weight. NASA TN D-4536, May 1968.
75. Dooley, L. W.; and Yearly, R. D.: Flight Test Evaluation of the High Inertia Rotor System. USARTL TR 79-9, U.S. Army Research and Technical Laboratories, Ft. Eustis, Va., June 1979.
76. Butler, H. K.: *Army Air Corps Airplanes and Observation (1935–1941)*. Saint Louis, Mo.: Historical Office, U.S. Army Aviation Systems, Feb. 1990.
77. Butler, H. K.: *A History of Army Aviation Logistics (1935–1961), Rotary-Winged Aircraft and the Army (1939–1943)*. Saint Louis, Mo.: Historical Office, U.S. Army Aviation Systems Command, Feb. 1990.
78. McClarren, R. H. (Ed.). *Proc. Rotating Wing Mtg.*, Franklin Institute, Philadelphia, Pa., Oct. 28–29, 1938.
79. Ralph McClarren (Ed.): *Proc. Second Annual Rotating Wing Aircraft Mtg.*, Franklin Institute, Philadelphia, Pa., Nov. 30–Dec. 1, 1939.

#### 4. REFERENCES

80. McClarren, R. H.: Personal letter to F. D. Harris; Early Helicopter Meetings at the Franklin Institute Mar. 21, 1993.
81. Klemin, A.: Rotary Aircraft. *Aero Digest*, Dec. 1938,
82. Hardy, C. W.: History of Air Force Development of Rotary-Wing Aircraft. *J. American Helicopter Society*, vol. 1, no. 1, 1956.
83. Gessor, A. J. (Ed.): *American Helicopter Society*, vol. 1, no. 1, 1956.
84. Wiesner, W.: Performance Analysis of U.S. Army Air Force Model XO-60 Rotor Aircraft Equipped With a Jacobs I-6MB-A Engine Rated at 300 H.P. and a Hamilton Constant Speed Propeller. Report No. 130.8, Kellett Autogiro Corp., Upper Darby, Pa., May 1943.
85. Klemin, A.: An Introduction to the Helicopter. NACA TM 340, *J. Mechanical Engineering*, Nov. 1924.
86. Alex, R. P.: Helicopters From "A to Z"—Part I. *American Helicopter Society Newsletter*, vol. 7, no. 10, Oct. 1961
87. Alex, R. P.: Helicopters From "A to Z"—Part II. *American Helicopter Society Newsletter*, vol. 7, no. 11, Nov. 1961.
88. Alex, R. P.: Helicopters From "A to Z"—Part III. *American Helicopter Society Newsletter*, vol. 7, no. 12, Dec. 1961.
89. Lambermont, P. M.; and Pirie, A.: *Helicopters and Autogyros of the World*. New York, N.Y.: A.S. Barnes and Co., 1970.
90. Spenser, J. P.: *Whirlybirds: A History of the U.S. Helicopter Pioneers*. Seattle, Wash.: University of Washington Press, Oct. 1998.
91. Nowarra, H. J.: *German Helicopters, 1928–1945*. West Chester, Pa.: Schiffer Publishing Ltd., 1991.
92. Cobey, W. E.: Evaluation and Tests of the Flettner-282 German Helicopter. Technical Report ATI No. 20283, Headquarters Air Material Command, Wright-Patterson Air Force Base, Dayton Ohio, Sept. 1948.
93. von Gersdorff, K.; and Knobling, K.: *Hubschrauber und Tragschrauber*. Munchen, Germany: Bernard & SeitGraefe Verlag, 1982.
94. Everett-Heath, J.: *Soviet Helicopters*. Surrey, United Kingdom: Jane's Information Group, 1988.
95. Gordon, Y.; Komissarov, D.; and Komissarov, S.: *Mil's Heavylift Helicopters: Mi-6/Mi-10/V-12/Mi-26*. Hinckley, England: Midland Publishing, 2005.
96. Gordon, Y.; and Komissarov, D.: *Mil Mi-8/Mi-17: Rotary-Wing Workhorse and Warhorse*. Hinckley, England: Midland Publishing, 2004.
97. Marshall, C. (Ed.): *The World's Great Military Helicopters*. New York, N.Y.: Aerospace Publishing, 1990.
98. McGuire, F. G.; and McKinnis, M. F.: *Helicopters 1948–1998, A Contemporary History*. Alexandria, Va.: Frank L. Jensen, Helicopter Association International, 1998.
99. Ludvigsen, K.: *The Mercedes-Benz Racing Cars*. Newport Beach, Calif.: Bond/Parkhurst Books, 1971.
100. Scott-Moncrieff, D.: *The Three-Pointed Star, the Story of Mercedes-Benz*. London, England: Gentry Books, Nov. 1979.

#### 4. REFERENCES

101. Marks, L. S. (Ed.): *Mechanical Engineers' Handbook*, 2nd Ed. New York, N.Y.: McGraw-Hill Book Co., Inc., 1924.
102. Taylor, C. F.: *Aircraft Propulsion*. Washington, D. C.: Smithsonian Institution Press, 1971.
103. Setright, L. J. K.: *The Power to Fly: The Development of the Piston Engine in Aviation*. London, England: George Allen & Unwin, Ltd., 1971.
104. Anon.: *Power Progress*. *Aero Digest*, July 1953.
105. Tryckare, T.: *The Lore of Flight*. Gothenburg, Sweden: Trychare, Cagner & Co., 1970.
106. Anon.: *U.S. Standard Atmosphere, 1962*. NASA 63N13176 (see also NACA TR 1235), Dec. 1962.
107. Anon.: *Aviation Week & Space Technology*, Mar. 12, 1979; Mar. 14, 1983; and Mar. 18, 1991.
108. Chabot, W. J.; and Ferry, R. G.: *H-34A Phase IV Performance Test*. AFFTC-TR-56-8, Air Force Flight Test Center, Edwards Air Force Base, Calif., 1956.
109. Hayden, J. S.; and Eggert, W. W.: *H-21 Phase IV Performance and Stability Tests*. AFFTC-TR-57-4, Air Force Flight Test Center, Edwards Air Force Base, Calif., 1957.
110. Odgers, P. W., Major General: *The Air Force Test Center—Cradle of Postwar Aviation*. The Society of Experimental Test Pilots 27th Annual Symposium, Beverly Hills, Calif., Sept. 28–Oct. 1, 1983, pp. 260–268.
111. Ferrell, K. R.: *YHO-2HU Air Force Flight Evaluation*. AFFTC-TR-60-2, Air Force Flight Test Center, Edwards Air Force Base, Calif., 1960.
112. Anon.: *MIL-E-5007. Engines, Aircraft, Turbojet and Turbofan, General Specification for*. Department of Defense, Washington, D.C., 1949.
113. Anon.: *SAE ARP-681B*. Society of Automotive Engineers, 1950.
114. Smith, L. K. (Ed.): *AHS Vertiflite*, vol. 39, no. 5, 1993.
115. Putnam, V. K.; and Ferry, R. G.: *XH-40 Air Force Flight Evaluation*. AFFTC-TR-58-15, Air Force Flight Test Center, Edwards Air Force Base, Calif., 1958.
116. Macpherson, D. F.; and Balfe, P. J.: *HU-1 Performance Evaluation, Addendum I to AFFTC-TR-59-33*. Air Force Flight Test Center, Edwards Air Force Base, Calif., 1960.
117. Nagata, J. I.; and Shapley, J. J.: *Engineering Flight Test of the OH-6A Helicopter (Cayuse) Phase D, Final Report*. USAASTA Project No. 65–37, U.S. Army Aviation Systems Test Activity, Edwards Air Force Base, Calif., 1969.
118. Schroers, L. G.; and Nelson, E. E.: *Engineering Flight Test (Performance Phase) of the OH-5A Helicopter*. USATECOM Project No. 4-3-0250-31/32/33, Edwards Air Force Base, Calif., 1969.
119. Melton, J. R.; and Watts, J. C.: *Engineering Flight Test (Performance Phase) of the OH-4A Helicopter*. USATECOM Project No. 4-3-0250-11/12/13, Edwards Air Force Base, Calif., 1969.
120. Ashley, T. (Ed.): *Flight Magazine—14th Annual Helicopter Edition*, vol. 55, no. 1, 1966.

#### 4. REFERENCES

121. Benson, T. P.; Buckanin, R. M.; Mittag, C. F.; and Jenks, J. E.: Evaluation of an OH-58A Helicopter With an Allison 250-C20B Engine. USAAEFA Project No. 74-48, U.S. Army Aviation Engineering Flight Activity, Edwards Air Force Base, Calif., 1975.
122. Congress, U. S.: Review of Army Procurement of Light Observation Helicopters. Hearings Before the Subcommittee for Special Investigations of the Committee on Armed Services, House of Representatives, 19th Congress, 1st Session, 1967.
123. Nagata, J. I. et al.: Government Competitive Test, Utility Tactical Transport Aircraft System (UTTAS), Sikorsky YUH-60A Helicopter. USAAEFA Project No. 74-06-1, U.S. Army Aviation Engineering Flight Activity, Edwards Air Force Base, Calif., 1976.
124. Winn, A. L., et al.: Government Competitive Test, Utility Tactical Transport Aircraft System (UTTAS), Boeing-Vertol YUH-61A Helicopter. USAAEFA Project No. 74-06-2, U.S. Army Aviation Engineering Flight Activity, Edwards Air Force Base, Calif., 1976.
125. Bender, G. L. et al.: Development Test I, Advanced Attack Helicopter Competitive Evaluation, Bell YAH-63 Helicopter. USAAEFA Project No. 74-07-1, U.S. Army Aviation Engineering Flight Activity, Edwards Air Force Base, Calif., 1976.
126. Steward, R. L. et al.: Development Test I, Advanced Attack Helicopter Competitive Evaluation, Hughes YAH-64 Helicopter. USAAEFA Project No. 74-07-2, U.S. Army Aviation Engineering Flight Activity, Edwards Air Force Base, Calif., 1976.
127. Anon.: Boeing Sikorsky's LH, Now the Army's Comanche. *Rotor & Wing*, vol. 25, no. 5, 1991.
128. Morrocco, J. D.: R & D Shortfall Forces Comanche Changes. *Aviation Week & Space Technology*, Oct. 25, 1993, p. 26.
129. Schrader, E. (Los Angeles Times): Pentagon Scraps Plan for Copter. *San Jose Mercury News*, Feb. 24, 2004.
130. Berger, A.-Y.; and Burr, N.: *Ultralight and Microlight Aircraft of the World*. Somerset, England: Haynes Publishing Group, 1983/84.
131. Carlson, R. M.: The Future of Aerospace. Proc. Symposium in Honor of Alexander H. Flax, National Academy of Engineering, National Academy Press, Washington, D.C., 1993, pp. 45-63.
132. Anon.: *The Official Helicopter Blue Book®*, HeliValue\$, Inc., Wauconda, Ill., various years.
133. Reschak, R. J.; and Baldwin, R. L.: Category II Performance and Limited Handling Characteristics Tests of the YUH-1D With a 44-Foot Rotor. AFFTC Report No. 63-43, Air Force Flight Test Center, Edwards Air Force Base, Calif., 1964.
134. Anon.: MIL-STD-1374A. Weight and Balance Data Reporting Forms for Aircraft (Including Rotorcraft). Department of Defense, Washington, D.C., Sept. 30, 1977.
135. Anon.: MIL-W-25140B. Weight and Balance Control System (for Aircraft and Rotorcraft). Department of Defense, Washington, D.C., Oct. 31, 1977.
136. Prewitt, R. H.: Detailed Specification for Model XR-2 Rotorcraft. Report No. 120.19, Kellett Autogyro Corp., Philadelphia, Pa., Feb. 27, 1941.

#### 4. REFERENCES

137. Prewitt, R. H.: Detailed Specification for Model XR-3 Rotorcraft. Report No. 120.20, Kellett Autogyro Corp., Philadelphia, Pa., Apr. 22, 1941.
138. Anon.: Model Specification, Helicopter, XR-4 (Vought-Sikorsky Model VS-316). Report No. 5536, Vought-Sikorsky Aircraft Div., United Aircraft Corp., Stratford, Conn., Jan. 1, 1942.
139. Anon.: Model Specification, Helicopter, YR-4A and YR-4B (supercedes Report No. 5922 dated May 4, 1942). Report No. 5922A, United Aircraft Corp., Vought-Sikorsky Aircraft Div., Stratford, Conn., Nov. 1, 1944.
140. Anon.: Model Specification, XR-6 (VS-316B). Report No. 5922, Vought-Sikorsky Aircraft Div., United Aircraft Corp., Stratford, Conn., Oct. 20, 1942.
141. Anon.: Model Specification, Helicopter, R-4B. Report No. SER-400B (supercedes SER-400A dated Oct. 10, 1944). Vought-Sikorsky Aircraft Div., United Aircraft Corp., Stratford, Conn., Mar. 10, 1945.
142. Anon.: Model Specification, Helicopter, XR-5. Report No. 5930A, Vought-Sikorsky Aircraft, Div. of United Aircraft Corp., Stratford, Conn., June 1, 1942.
143. Anon.: Model Specification, Helicopter, R-5A. Report No. SER-406, Sikorsky Aircraft, Div. of United Aircraft Corp., Stratford, Conn., Feb. 1, 1944.
144. LePage, L.: Model Specification for Army Air Forces Helicopter Model YR-1A. Engineering Dept. Spec. No. S-144, Platt-LePage Aircraft Co., Eddystone, Pa., Jan. 17, 1944.
145. Harris, F. D.: AHIP: The OH-58D From Conception to Production. Proc. 42nd Annual Forum of the American Helicopter Society, Washington, D.C., June 1986.
146. Kawa, M. M.; and Van Kirk, J. M.: Kiowa Warrior—A Bridge to the Future. Proc. American Helicopter Society 53rd Annual Forum, Virginia Beach, Va., Apr. 29–May 1, 1997.
147. Cammack, S. P.: YOH-6A World Record Program. Proc. 23rd Annual National Forum of the American Helicopter Society, Washington, D.C., May, 1967.
148. Ulnisnik, H.: Private correspondence to F. D. Harris, Nov. 1992.
149. Davis, S. J.; and Wisniewski, J. S.: User's Manual for HESCOMP—The Helicopter Sizing and Performance Computer Program. Report No. D210-10699-1, Boeing Vertol Co., Philadelphia, Pa., Sept. 1973.
150. Schoen, A., H.; and Wisniewski, J. S.: User's Manual for VASCOMP II—The V/STOL Aircraft Sizing and Performance Computer Program. Report No. D8-0375, Vol. VI, Boeing Vertol Co., Philadelphia, Pa., Mar. 1973.
151. Johnson, W.: NDARC-NASA Design and Analysis of Rotorcraft. NASA/TP-2009-215402, Dec. 2009.
152. Crabtree, J. A.; and Amer, K. B.: Helicopter Configuration and Propulsion Systems Study, Part 1. Statistical Weight Analysis. Hughes Tool Co., Aircraft Div., Culver City, Calif., Nov. 1957.
153. Stepniewski, W. Z.: Rotorcraft Weight Trends in Light of Structural Material Characteristics. U.S. Army Aviation Systems Command Technical Report No. TR-87-A-10 (also AD-A186 576), Apr. 1987.

#### 4. REFERENCES

154. Wisniewski, J. S.: The Boeing Model 360 Advanced Technology Demonstrator Helicopter. Proc. 51st Annual Conference of the Society of Allied Weight Engineers, Hartford, Conn., May 18–20, 1992.
155. Stepniewski, W. Z.: A Comparative Study of Soviet vs. Western Helicopters, Part 1: General Comparison of Designs. NASA-CR-3579 (see also AVRADCOM-TR-82-A-9), Mar. 1983.
156. Stepniewski, W. Z.; and Shinn, R. A.: A Comparative Study of Soviet vs. Western Helicopters, Part 2: Evaluation of Weight, Maintainability, and Design Aspects of Major Components. NASA-CR-3580 (see also AVRADCOM-TR-82-A-10), Mar., 1983.
157. Klemm, Lt. A.: Aeronautical Engineering and Airplane Design. New York, N.Y.: The Gardner-Moffat Co., Inc., 1918.
158. Bréguet, L.: The Gyroplane. *J. Royal Aeronautical Society*, vol. 36, no. 8, Sept. 1937.
159. Ferrell, K. R.; Frederick, A. C.; and Kische, J. S.: Flight Evaluation, Compliance Test Techniques for Army Hot Day Hover Criteria. USAASTA Project No. 68-55, U.S. Army Aviation Systems Test Activity, Edwards Air Force Base, Calif., Apr. 1974.
160. Nagata, J. I. et al.: Government Competitive Test, Utility Tactical Transport Aircraft System (UTTAS), Sikorsky YUH-60A Helicopter. USAAEFA Project No. 74-06-1, U.S. Army Aviation Engineering Flight Activity, Edwards Air Force Base, Calif. 1976.
161. Nagata, J. I. et al.: Airworthiness and Flight Characteristics Evaluation, UH-60A (Black Hawk) Helicopter. USAAEFA Project No. 77-17, U.S. Army Aviation Engineering Flight Activity, Edwards Air Force Base, Calif., Sept. 1981.
162. Leoni, R. D.: *Black Hawk: The Story of a World Class Helicopter*. American Institute of Aeronautics and Astronautics, Inc., Reston, Va., 2007.
163. Anon.: UH-60A Weight Report. Sikorsky Aircraft, Stratford, Conn., 1979.
164. Anon.: YUH-60A Weight Report. Sikorsky Aircraft, Stratford, Conn., 1976.
165. Gould, W., et al.: Rotor System Evaluation. AEFA Project No. 85-15, Edwards Air Force Base, Calif., Mar. 1988.
166. Bousman, W.; and Kufeld, R. M.: UH-60A Airloads Catalog. NASA/TM-2005-212827 (see also AFDD-TR-05-003), Aug. 2005.
167. Kufeld, R. M., et al.: Flight Testing the UH-60A Airloads Aircraft. Proc. American Helicopter Society 50th Annual Forum, Washington, D.C., May 11–13, 1994.
168. Kocurek, J. D.; Berkowitz, L. F.; and Harris, F. D.: Hover Performance Methodology at Bell Helicopter Textron. Proc. 36th Annual Forum of the American Helicopter Society, Washington, D.C., May 1980.
169. Lewis, R. B.: Army Helicopter Performance Trends. *J. American Helicopter Society*, vol. 17, no. 2, 1972.
170. Lyle, J. A. et al.: Technology Flight Evaluation of the Aerospatiale SA 365 N-1, Dauphin 2, Helicopter. USAAEFA Project No. 85-06, U.S. Army Aviation Engineering Flight Activity, Edwards Air Force Base, Calif., 1990.
171. Johnson, J. N.; and Ferry, R. G.: H-13H Phase IV Performance Test. AFFTC-TR-57-12 plus Addendum No. 1, Air Force Flight Test Center, Edwards Air Force Base, Calif., 1957.

#### 4. REFERENCES

172. Melton, J. R.; and Watts, J. C.: Engineering Flight Test, Performance Phase of the OH-4A Helicopter. USATECOM Project No. 4-3-0250-11/12/1, U.S. Army Aviation Test and Evaluation Command, Edwards Air Force Base, Calif., Aug. 1964.
173. Yamakawa, G. M.; and Watts, J. C.: Airworthiness and Flight Characteristics Test, Production OH-58A Helicopter, Unarmed and Armed with XM27E1 Weapon System. USAASTA Project No. 68-30, U.S. Army Aviation Systems Test Activity, Edwards Air Force Base, Calif., Sept. 1970.
174. Laing, E. J.; Benson, T. P.; Werner, A. W.; and Broahurst, D. G.: Evaluation of the OH-58A Helicopter With an Allison 250-C20 Engine. USAASTA Project No. 71-24, U.S. Army Aviation Systems Test Activity, Edwards Air Force Base, Calif., Dec. 1972.
175. Yamakawa, G. M.; Buckanin, R. M.; Hagen, J. F.; and Burch, T. E.: Preliminary Airworthiness Evaluation OH-58C Helicopter USAAEFA Project No. 76-11-2, U.S. Army Aviation Engineering Flight Activity, Edwards Air Force Base, Calif., Mar. 1978.
176. Marshall, A. R. et al.: Airworthiness and Flight Characteristics Test of an OH-58C Configured to a Light Combat Helicopter (LCH). USAAEFA Project No. 81-07, U.S. Army Aviation Engineering Flight Activity, Edwards Air Force Base, Calif., 1981.
177. Brown, J. D. et al.: Airworthiness and Flight Characteristics Evaluation of the OH-58D Helicopter. USAAEFA Project No.83-27-1, U.S. Army Aviation Engineering Flight Activity, Edwards Air Force Base, Calif, 1990.
178. Johns, S. L.; and Colvin, G. L.: YUH-1B Category II Performance Tests. AFFTC Report No. 62-21, Air Force Flight Test Center, Edwards Air Force Base, Calif., 1962.
179. Porter, D. W.; and Flanigen, E. G.: Category II Performance Tests of the YUH-1D With a 48-Foot Rotor. AFFTC Report No. 64-27, Air Force Flight Test Center, Edwards Air Force Base, Calif., 1964.
180. Smith, E. D.; and Flanigen, E. G.: UH-1F Category II Performance. AFFTC Report No. 65-05, Air Force Flight Test Center, Edwards Air Force Base, Calif., 1965.
181. Shultz, A.: BHT Hover Performance Methodology. BHTI Report No. 212-099-052, Bell Helicopter Textron, Inc., Ft. Worth, Tex., 1970.
182. Anon.: BHT Hover Performance Methodology for Model 214B. Report No. BHTI 214-099-303 Rev. A, Bell Helicopter Textron, Inc., Ft. Worth, Tex., 1970.
183. Anon.: BHT Hover Performance Methodology for Model 222. Report No. BHTI 222-993-013, Bell Helicopter Textron, Inc., Ft. Worth, Tex., 1978.
184. Kidwell, J. C.; and Foster, J. K.: Engineering Flight Evaluation of the Bell Model 209 Armed Helicopter. USATECOM Project No. 4-6-0300-01, U.S. Army Test and Evaluation Command, Edwards Air Force Base, Calif., 1966.
185. Finnestead, R. L. et al.: Engineering Flight Test, AH-1G Helicopter (Hueycobra) Phase D, Part 2—Performance (also Phase B, Part 6). USAASTA Project No.66-06, U.S. Army Aviation Systems Test Activity, Edwards Air Force Base, Calif., 1970.
186. Nagata, J. I. et al.: Attack Helicopter Evaluation Model 309 Kingcobra Helicopter. USAASTA Project No. 72-10, U.S. Army Aviation Systems Test Activity, Edwards Air Force Base, Calif., 1972.

#### 4. REFERENCES

187. Crawford, C. C.; and Hodgson, W. J.: YHC-1A Flight Evaluation. AFFTC TR-61-1, Air Force Flight Test Center, Edwards Air Force Base, Calif. See also NATC Project TED PTR AD 3097, Naval Air Test Center, Patuxent River, Md., 1961.
188. Dallas, S.; Bumstead, R.; and Tuttle, D. T.: Performance Data and Substantiation Report for the CH-46E Helicopter. Boeing-Vertol Report No. D331-10042-1, Boeing Vertol Co., Philadelphia, Pa., Mar. 14, 1977.
189. McHugh, F.: Letter to F. D. Harris, Aug. 6, 1982.
190. Bender, G. L. et al.: Airworthiness and Flight Characteristics Test (A&FC) of the CH-47D Helicopter. USAAEFA Project No. 82-07, U.S. Army Aviation Engineering Flight Activity, Edwards Air Force Base, Calif., 1984.
191. Koelle, E. A.; and Hodgson, W. J.: YH-41 Performance Evaluation. AFFTC-TR-60-7 Addendum I, Air Force Flight Test Center, Edwards Air Force Base, Calif., 1960.
192. Kidwell, J. C. et al.: High Altitude Evaluation of the Hiller Model 1961 UH-12E. ATO TR-61-3, U.S. Army Aviation Test Office, Edwards Air Force Base, Calif., Mar. 1961.
193. Ferrell, K. R.; and Honaker, J. S.: Category II Performance Tests of the H-43B. AFFTC Report No. 62-11, Air Force Flight Test Center, Edwards Air Force Base, Calif., 1963.
194. Plaks, A.; and Collins, R. E.: Substantiating Data for the SH-2F, Standard Aircraft Characteristics Charts. Kaman Report No. P-65 (see also Nav Air System AIR-530122), Aug. 1, 1973.
195. Johnson, J. N. et al.: Attack Helicopter Evaluation AH-56A Cheyenne Compound Helicopter—Final Report. USAASTA Project No. 72-08, U.S. Army Aviation Systems Test Activity, Edwards Air Force Base, Calif., 1972.
196. Sharon, G. A. et al.: Preliminary Airworthiness Evaluation of the MBB BK-117 Helicopter (Germany/Japan). USAAEFA Project No. 84-22, U.S. Army Aviation Engineering Flight Activity, Edwards Air Force Base, Calif., 1985.
197. Ferrell, K. R.; and Ferry, R. G.: YHO-2HU Air Force Flight Evaluation. AFFTC-TR-60-2, Air Force Flight Test Center, Edwards Air Force Base, Calif., 1960.
198. Nagata, J. I.; and Shapley, J. J.: Engineering Flight Test of the OH-6A Helicopter (Cayuse) Phase D—Final Report. USAASTA Project No. 65-37, U.S. Army Aviation Systems Test Activity, Edwards Air Force Base, Calif., 1969.
199. Webe, J. L. et al.: Airworthiness and Flight Characteristics Test of the OH-6A Configured to a Light Combat Helicopter (JOH-6A LCH). USAAEFA Project No. 81-04, U.S. Army Aviation Engineering Flight Activity, Edwards Air Force Base, Calif., 1983.
200. Webre, J. L. et al.: Airworthiness and Flight Characteristics Evaluation of the McDonnell Douglas Helicopter Corporation (MDHC) 530FF Helicopter, Final Report. USAAEFA Project No. 86-15, U.S. Army Aviation Engineering Flight Activity, Edwards Air Force Base, Calif., 1989.
201. Steward, R. L. et al.: Development Test I, Advanced Attack Helicopter Competitive Evaluation, Hughes YAH-64 Helicopter. USAAEFA Project No. 74-07-2, U.S. Army Aviation Engineering Flight Activity, Edwards Air Force Base, Calif., 1977.

#### 4. REFERENCES

202. Picasso, B. D. et al.: Airworthiness and Flight Characteristics (A&FC) Test of YAH-64 Advanced Attack Helicopter, Prototype Qualification Test—Government (PQT-G), Part 3, and Production Validation Test—Government (PVT-G) for Handbook Verification—Final Report. USAAEFA Project No. 80-17-3, U.S. Army Aviation Engineering Flight Activity, Edwards Air Force Base, Calif., 1982.
203. Ferrell, K. R.; and Honaker, J. S.: H-37A Limited Stability and Control Evaluation. AFFTC-TR-60-15, Air Force Flight Test Center, Edwards Air Force Base, Calif., 1960.
204. Turk, R. N.; and Watts, J. C.: Final Report of Engineering Flight Test of the CH-37 B. USAATA Project No. 62-28, U.S. Army Aviation Systems Test Activity, Edwards Air Force Base, Calif., June 15, 1964.
205. Anon.: Performance Flight Tests of the S-64F (CH-54B) Helicopter for FAA Certification. Sikorsky Aircraft Report No. SER-64511, Sikorsky Aircraft Corp., Stratford, Conn., 1970.
206. Seto, E. I. et al.: Category II Performance Test on the CH-3C Helicopter. AFFTC Report No. 65-39, Air Force Flight Test Center, Edwards Air Force Base, Calif., 1966.
207. Ritter, R. L. et al.: Limited High Altitude Performance Evaluation of the HH-53C Helicopter. AFFTC-TR-71-54, Air Force Flight Test Center, Edwards Air Force Base, Calif., 1971.
208. Anon.: Substantiating Data Report for NATOPS Flight Manual Performance of the Production CH-53E. Sikorsky Aircraft Report No. SER-13441, Sikorsky Aircraft Corp., Stratford, Conn., 1987.
209. Anon.: SA 341/01 Report of Analysis. Aerospatiale RD/DA/MM-H/EV No. 3226, Aerospatiale, Paris, France, 1970.
210. Ruddell, A. J.: Advancing Blade Concept (ABC) Technology Demonstrator. AVRADCOM TR-81-D-5, Aviation Research and Development Command, Ft. Eustis, Va., Apr. 1981.
211. Harris, F. D.: Rotary Wing Aerodynamics—Historical Perspective and Important Issues. Proc. National Specialists' Mtg. on Aerodynamic and Aeroacoustics Sponsored by the American Helicopter Society Southwest Region, Arlington, Tex., 1987.
212. McKee, J. W.; and Naeseth, R. L.: Experimental Investigation of the Drag of Flat Plates and Cylinders in the Slipstream of a Hovering Rotor. NACA TN 4239, 1958.
213. Bousman, W.: Power Measurement Errors on a Utility Aircraft. Proc. American Helicopter Society Aerodynamics, Acoustics, and Test and Evaluation Technical Specialists' Mtg., San Francisco, Calif., Jan. 23–25, 2002.
214. Amer, K. B.; and Gessow, A.: Charts for Estimating Tail-Rotor Contribution to Helicopter Directional Stability and Control. NACA Report 1216, 1953.
215. Lynn, R. R. et al.: Tail Rotor Design, Part I: Aerodynamics. J. American Helicopter Society, vol. 15, no. 4, 1969.
216. Balke, R. W. et al.: Tail Rotor Design Part II: Structural Dynamics. J. American Helicopter Society, vol. 15, no. 4, 1970.
217. Mouille, R.: The “Fenestron” Shrouded Tail Rotor of the SA-341 Gazelle. J. American Helicopter Society, vol. 15, no. 4, 1970.

#### 4. REFERENCES

218. Huston, R. J.; and Morris, C. E. K.: A Note on a Phenomenon Affecting Helicopter Directional Control in Rearward Flight. *J. American Helicopter Society*, vol. 15, no. 4, 1970.
219. Robinson, F.: Increasing Tail Rotor Thrust and Comments on Other Yaw Control Devices. *J. American Helicopter Society*, vol. 15, no. 4, 1970.
220. Huston, R. J.; and Morris, C. E. K.: A Wind-Tunnel Investigation of Helicopter Directional Control in Rearward Flight in Ground Effect. NASA TN-D-6118, Mar. 1971.
221. Wiesner, W.; and Kohler, G.: Tail Rotor Design Guide. USAAMRDL TR 73-99, U.S. Army Air Mobility Research and Development Laboratories, Ft. Eustis, Va., 1974.
222. Sheridan, P. F.: Interactional Aerodynamics of the Single Rotor Helicopter Configuration, Volume I—Final Report. USARTL-TR-78-23A, U.S. Army Research and Technical Laboratories, Ft. Eustis, Va., Sept. 1978.
223. Cook, C. V.: A Review of Tail Rotor Design and Performance. *International J. of Rotorcraft and Powered Lift Aircraft*, vol. 2, no. 3/4, 1978.
224. Yeager, W. T.; Young, W. H.; and Mantay, W. R.: A Wind Tunnel Investigation of Parameters Affecting Helicopter Directional Control at Low Speeds in Ground Effect. NASA TN-D-7694, Nov. 1974.
225. Paul, W. F.; and Zincone, R.: Advanced Technology Applied to the UH-60A and S-76 Helicopters. *International J. of Rotorcraft and Powered Lift Aircraft*, vol. 2, no. 3/4, 1978.
226. Signor, D. B., et al.: Performance and Loads Data from an Outdoor Hover Test of a Lynx Tail Rotor. NASA TM-101057, 1989.
227. Vuillet, A.; and Morelli, F.: New Aerodynamic Design of the Fenestron for Improved Performance. AGARD CP-423, Rotorcraft Design for Operations Symposium, Amsterdam, The Netherlands, Oct. 13–16, 1986.
228. Lehman, A. F.: Model Studies of Helicopter Tail Rotor Flow Patterns In and Out of Ground Effect. USAAVLABS TR 71-12, U.S. Army Aviation Material Laboratories, Ft. Eustis, Va., 1971.
229. Balch, D. T. et al.: Experimental Study of Main Rotor/Tail Rotor/Airframe Interactions in Hover. Volume 1: Text and Figures. NASA-CR-166485, June 1983.
230. Menger, R. P. et al.: Effects of Aerodynamic Interaction Between Main and Tail Rotors on Helicopter Hover Performance and Noise. NASA CR-166477, Feb. 1983.
231. Balch, D. T.; and Lombardi, J.: Experimental Study of Main Rotor Tip Geometry and Tail Rotor Interactions in Hover. Volume 1. Text and Figures. NASA CR-177336-Vol-1, Feb. 1985.
232. Balch, D. T.; and Lombardi, J.: Experimental Study of Main Rotor Tip Geometry and Tail Rotor Interactions in Hover. Volume 2. NASA CR-177336-Vol-2, 1985.
233. Garry, R. M., Col.: French Helicopters. *J. Helicopter Association of Great Britain*, vol. 3, no. 4, 1950.
234. Gessow, A.; and Myers, G. C., Jr.: *Aerodynamics of the Helicopter*. New York, N.Y.: Frederick Ungar Publishing Co., 1967.
235. Johnson, W.: *Helicopter Theory*. Princeton, N.J.: Princeton University Press, 1980.

#### 4. REFERENCES

236. Leishman, J. G.: Principles of Helicopter Aerodynamics. Cambridge, England: Cambridge University Press, 2000.
237. Stepniewski, W. Z.: Introduction to Helicopter Aerodynamics. Morton, Pa.: Rotorcraft Publishing Committee, 1950.
238. Stepniewski, W. Z.; and Keys, C. N.: Rotary-Wing Aerodynamics. Mineola, N.Y.: Dover Publications, 1984.
239. Nikolsky, A. A.: Helicopter Analysis. New York, N.Y.: John Wiley & Sons, Inc., 1951.
240. McCormick, B. W.: Aerodynamics of V/STOL Flight. Orlando, Fla.: Academic Press, 1967.
241. Bramwell, A. R. S.: Helicopter Dynamics. New York, N.Y.: John Wiley & Sons, Inc., 1976.
242. Prouty, R.: Helicopter Performance, Stability, and Control. Boston, Mass.: PWS Engineering, 1986.
243. Knight, M.; and Hefner, R. A.: Static Thrust Analysis of the Lifting Airscrew. NACA TN 626, Dec. 1937.
244. Knight, M.; and Hefner, R. A.: Analysis of Ground Effect on the Lifting Airscrew. NACA TN 835, Dec. 1941.
245. Bhagwat, M. J. et al.: Development and Application of a CFD-based Engineering Analysis of Hover Performance. Proc. American Helicopter Society 62nd Annual Forum, Phoenix, Ariz.. May 9–11, 2006.
246. Landgrebe, A. J.: An Analytical and Experimental Investigation of Helicopter Rotor Hover Performance and Wake Geometry Characteristics. USAAMRDL TR-71-24, U.S. Army Air Mobility Research and Development Laboratories, Ft. Eustis, Va., 1973.
247. Stepniewski, W. Z. et al.: Experimental Investigation of PV-14 Overlap. Part II—Thrust and Power. Piasecki Helicopter Corp. Report No. 14-A-03, 1948.
248. Sweet, G. E.: Hovering Measurements for Twin-Rotor Configurations With and Without Overlap. NASA TN-D-534, Nov. 1960.
249. Crawford, C. C.: Rotorcraft Analytical Improvement Needed to Reduce Developmental Risk—The 1989 Alexander A. Nickolsky Lecture. J. American Helicopter Society, vol. 35, no. 1, 1990.
250. Arents, D. N.: An Assessment of the Hovering Performance of the XH-59A Advancing Blade Concept Demonstration Helicopter. USAAMRDL-TN-25, U.S. Army Air Mobility Research and Development Laboratories, Ft. Eustis, Va., 1977.
251. Mikheyev, S. V. et al.: Ka-50 Attack Helicopter Aerobatic Flight. Proc. 24th European Rotorcraft Forum, Marseilles, France, Sept. 15–17, 1998.
252. Harrington, R. D.: Full-Scale-Tunnel Investigation of the Static-Thrust Performance of a Coaxial Helicopter Rotor. NACA TN 2318, 1951.
253. Coleman, C. P.: A Survey of Theoretical and Experimental Coaxial Rotor Aerodynamic Research. NASA TP-3675, 1997.
254. Stepniewski, W. Z.; and Sloan, L. H.: Experimental Investigation of PV-14 Overlap. Part I—Downwash Distribution. Piasecki Helicopter Corp. Report No. 14-A-03, 1948.

#### 4. REFERENCES

255. Harris, F. D.: Twin Rotor Hover Performance. *J. American Helicopter Society*, vol. 44, no. 1, 1994.
256. Dingeldein, R. C.: Wind-Tunnel Studies of the Performance of Multirotor Configurations. NACA TN 3236, Aug. 1954.
257. Cheney, M. C.: The ABC Helicopter. Proc. AIAA/AHS VTOL Research, Design, and Operations Mtg., Georgia Institute of Technology, Atlanta, Ga., Feb. 17–19, 1969.
258. Burgess, R. K.: The ABC Rotor—A Historical Perspective. Proc. American Helicopter Society 60th Annual Forum, Baltimore, Md., June 7–10, 2004.
259. Phelps, A. E.; and Mineck, R. E.: Aerodynamic Characteristics of a Counter-Rotating, Coaxial, Hingeless Rotor Helicopter Model With Auxiliary Propulsion. NASA TM-78705, May 1978.
260. Felker, F. F., III: Performance and Loads Data from a Wind Tunnel Test of a Full-Scale, Coaxial, Hingeless Rotor Helicopter. NASA TM-81329, Oct. 1981.
261. Stroub, R. H. et al.: An Investigation of a Full-Scale Advancing Blade Concept Rotor System at High Advance Ratio. NASA TM-X- 62081, Aug. 1971.
262. McAlister, K. W. et al.: Experimental and Numerical Study of a Model Coaxial Rotor. Proc. American Helicopter Society 62nd Annual Forum, Phoenix, Ariz., May 9–11, 2006.
263. Leishman, J. G.; and Ananthan, S.: Aerodynamic Optimization of a Coaxial Proprotor. Proc. American Helicopter Society 62nd Annual Forum, Phoenix, Ariz., May 9–11, 2006.
264. Wachspress, D. A.; and Quackenbush, T. R.: Impact of Rotor Design on Coaxial Performance, Wake Geometry, SW and Noise. Proc. American Helicopter Society 62nd Annual Forum, Phoenix, Ariz., May 9–11, 2006.
265. Kussner, H. G.: Helicopter Problems. NACA TM 827, May 1937.
266. Platt, H. H.: The Helicopter: Propulsion and Torque. *J. Aeronautical Sciences*, vol. 3, no. 11, Sept. 1936, pp. 398–405.
267. Zbrozek, J.: Ground Effect on the Lifting Rotor. Aeronautical Research Council R&M No. 2347, July 1941.
268. Hayden, J. S.: The Effect of the Ground on Helicopter Hovering Power Required. Proc. American Helicopter Society 32nd Annual Forum, Washington, D.C., May 10–12, 1976.
269. Tetervin, N.: Airfoil Section Data From Tests of 10 Practical-Construction Sections of Helicopter Rotor Blades Submitted by the Sikorsky Aircraft Div., United Aircraft Corp. NACA WR-L-643, Sept. 1944.
270. Dingeldein, R. C.; and Schaefer, R. F.: Static Thrust Tests of Six Rotor-Blade Designs on a Helicopter in the Langley Full-Scale Tunnel. NACA ARR No. L5F25b, Sept. 1945.
271. Dingeldein, R. C.; and Schaefer, R. F.: Full-Scale Investigation of Aerodynamic Characteristics of a Typical Single-Rotor Helicopter in Forward Flight. NACA TR 905, 1948.
272. Gustafson, F. B.; and Gessow, A.: Analysis of Flight-Performance Measurements on a Twisted, Plywood-Covered Helicopter Rotor in Various Flight Conditions. NACA TN 1595, June 1948.

#### 4. REFERENCES

273. Gessow, A.: Flight Evaluation of Effects of Rotor-Blade Twist on Helicopter Performance in the High-Speed and Vertical-Autorotative-Descent Conditions. Aug. 1948.
274. Ward, J. F.: Rotorcraft Research—A National Effort. J. American Helicopter Society, vol. 32, no. 2, 1986.
275. Phillips, E. H.: Piper—A Legend Aloft. Eagan, Minn.: Flying Books International, 1993.
276. Kitchens, Dr. J. W.: Organic Army Aviation in World War II. Army Aviation Digest, May/June and June/July, 1992.
277. Neel, S. H., Lt. Col.: Helicopter Evacuation in Korea. U.S. Armed Forces Medical Journal, vol. VI, no. 5, 1955.
278. Anon.: Pilot's Flight Operating Instructions for Army Models L-4A, L-4B, and L-4H Airplanes. Yorkshire, England: Air Publications and Forms Store. Sept. 5, 1943 (revised Oct. 25, 1944).
279. Anon.: Erection and Maintenance Instructions for Army Models L-4A, L-4B, L-4H, and L-4J Airplanes. Yorkshire, England: Air Publications and Forms Store. Aug. 25, 1943 (revised Mar. 5, 1945).
280. Anon.: Phase II Flight Test of the Cessna L-19A. WCTSE-WCT-2355, 1951.
281. Kidwell, J. C.; and Clay, W.: Evaluation of L-19A Equipped with Continental O-470-11C1 Fuel Injected Engine. ATO-TR-61-1, 1961.
282. Davidson, J. D.; and Ferry, R. G.: TL-19D Phase IV Performance. AFFTC-TR-57-14, Air Force Flight Test Center, Edwards Air Force Base, Calif., 1957.
283. Oswald, W. B.: General Formulas and Charts for the Calculation of Airplane Performance. NACA TR 408, 1932.
284. Perkins, C. D.; and Hage, R. E.: Airplane Performance, Stability and Control. New York, N.Y.: John Wiley & Sons, Inc., 1949.
285. Diehl, W. S.: The Reduction of Observed Airplane Performance to Standard Conditions. NACA TR 297, 1928.
286. Herrington, R. M. et al.: Flight Test Engineering Handbook. USAF-TR-6273, 1951.
287. Miller, R.; and Sawers, D.: The Technical Development of Modern Aviation. New York, N.Y.: Praeger Publishers, 1970.
288. Rosen, G.: Thrusting Forward: A History of the Propeller. Hartford, Conn.: Hamilton Standard, 1987.
289. Green, W.; and Swanborough, G.: The Great Book of Fighters (an Illustrated Encyclopedia of Every Fighter Aircraft Built and Flown). Osceola, Wis.: MBI Publishing Co., 1994.
290. Durand, W. F.; and Lesley, E. P.: Comparison of Tests on Air Propellers in Flight With Wind Tunnel Model Tests on Similar Forms. NACA TR 220, 1927.
291. Crowley, J. W., Jr.; and Mixson, R. E.: Characteristics of Five Propellers in Flight. NACA TR 292, 1927.
292. Weick, F. E.; and Wood, D. H.: The Twenty-Foot Propeller Research Tunnel of the National Advisory Committee for Aeronautics. NACA TR 300, 1928.
293. Weick, F. E.: Full Scale Tests of Wood Propellers on a VE-7 Airplane in the Propeller Research Tunnel. NACA TR 301, 1928.

#### 4. REFERENCES

294. Weick, F. E.: Full-Scale Wind-Tunnel Tests of a Series of Metal Propellers on a VE-7 Airplane. NACA TR 306, 1928.
295. Harris, F. D.: Performance Analysis of Two Early NACA High-Speed Propellers With Application to Civil Tiltrotor Configurations. NASA CR-196702, Aug. 1996.
296. Jackson, P. (Ed.): Jane's All the Worlds Aircraft 2004–2005. Surrey, United Kingdom: Jane's Information Group Ltd., 2005.
297. Fradenburgh, E. A.: Aerodynamic Design of the Sikorsky S-76 Helicopter. Proc. American Helicopter Society 34th Annual National Forum, Washington, D.C., May 15–17, 1978.
298. Prouty, R.: A Second Approximation to the Induced Drag of a Rotor in Forward Flight. J. American Helicopter Society, vol. 21, no. 3, 1976.
299. Seto, E. I.; and Hodgson, W. J.: Flight Evaluation of the H-21C, HU-1A, and H-34C Equipped with XM-153 Armament Kit. FTC-TDR-62-29, Air Force Flight Test Center, Edwards Air Force Base, Calif., 1962.
300. Boyne, W. J.; and Lopez, D. S.: Vertical Flight—The Age of the Helicopter. Washington, D.C.: Smithsonian Institution Press, 1984.
301. Coleman, R. P.; Feingold, A. M.; and Stempin, C. W.: Evaluation of the Induced Velocity Field of an Idealized Helicopter Rotor. NACA WR-L-126, June 1945.
302. Castles, W., Jr.; and De Leeuw, J. H.: The Normal Component of the Induced Velocity in the Vicinity of a Lifting Rotor and Some Examples of Its Application. NACA TR 1184, 1952.
303. Heyson, H. H.: A Brief Survey of Rotary Wing Induced-Velocity Theory. NASA TM-78741, June 1978.
304. Glauert, H.: A General Theory of the Autogiro. Aeronautical Research Committee R&M No. 1111, Nov. 1926.
305. Heyson, H. H.; and Katzoff, S.: Induced Velocities Near a Lifting Rotor With Nonuniform Disk Loading. NACA TR 1319, 1956.
306. Piziali, R. A.; and Du Waldt, F. A.: A Method for Computing Rotary Wing Airload Distribution in Forward Flight. Cornell Aeronautical Laboratory Report BB-1495-S-1 (see also TCREC TR 62-44), 1962.
307. Crimi, P.: Prediction of Rotor Wake Flows. Proc. CAL/USAAVLABS Symposium, Vol. I, Propeller and Rotor Aerodynamics, Buffalo, N.Y., 1966. (Original work in CAL BB-1994-S, Sept. 1965.)
308. McCroskey, W. J.: Vortex Wakes of Rotorcraft. AIAA Paper No. 95-0530, Proc. AIAA 33rd Aerospace Sciences Mtg. and Exhibit, Reno, Nev., Jan. 9–12, 1995.
309. Huston, R. J.: A Study of the Interference Effects in a Tandem Rotor Helicopter. NASA TM-X-67027, June 1961.
310. Jewel, J. J.; and Heyson, H. H.: Charts of the Induced Velocities Near a Lifting Rotor. NASA Memo 4-15-59L, May 1959.
311. Huston, R. J.: Wind-Tunnel Measurements of Performance, Blade Motions, and Blade Air Loads for Tandem-Rotor Configurations With and Without Overlap. NASA TN-D-1971, Oct. 1963.

#### 4. REFERENCES

312. Pruyn, R. R.; and Alexander, W. T.: USAAVLABS Tandem Rotor Airloads Measurement Program. American Institute of Aeronautics and Astronautics (AIAA) *J. Aircraft*, vol. 4, no. 3, 1967.
313. Pruyn, R. R., et al.: Inflight Measurement of Rotor Blade Airloads, Bending Moments and Motions, Together With Rotor Shaft Loads and Fuselage Vibration, on a Tandem Rotor Helicopter. USAVLABS TR 67-9, U.S. Army Aviation Material Laboratories, Ft. Eustis, Va. (see also Boeing Document D8-0382), 1967.
314. Percy, A.: Douglas Propliners. Shrewsbury, England: Airlife Publishing, Ltd., 1995.
315. Anon.: Project Hummingbird, Economic Report—The Helicopter and Other V/STOL Aircraft in Commercial Transport Service. Federal Aviation Agency, Economic Branch, Office of Plans (Call No. TL 718 1960 U), Nov. 1960.
316. Davies, R. E. G.: Airlines of the United States Since 1914. Washington, D.C.: Smithsonian Institution Press, 1972.
317. Anon.: A Technical Summary and Compilation of Characteristics and Specifications on Steep-Gradient Aircraft. Federal Aviation Agency, Aircraft Branch, Air Commerce Div., Office of Plans (Call No. TL 718 1960 U), 1961.
318. Anon.: Civil Air Regulations, Part 7—Rotorcraft Airworthiness; Transport Categories. Civil Aeronautics Board, Washington, D.C., 1956.
319. Anon.: Type Certificate Data Sheet No. H8SO (Model HH-52A, SH-62). Department of Transportation, Federal Aviation Administration, Washington, D.C., 2003.
320. Anon.: Type Certificate Data Sheet No. 1H15 (Sikorsky S-61L). Department of Transportation, Federal Aviation Administration, Washington, D.C., 2003.
321. Anon.: Type Certificate Data Sheet No. 1H16 (Boeing Model 107-II). Department of Transportation, Federal Aviation Administration, Washington, D.C., 2007.
322. Gerber, P. J.; and Weiland, C.: Detailed Specification, Vertol 107-II-10 Airliner Helicopter (for New York Airways) Twin Turbine Engine, Tandem Rotor. Report No. 107-X-13, Boeing Airplane Co., Vertol Div., Philadelphia, Pa., 1960.
323. Anol, R. K.; McConkey, E. D.; Edwin, D.; and Hawley, R. J.: Helicopter Rejected Takeoff Airspace Requirements. DOT/FAA/RD-90/7, Systems Control Technology Inc., Arlington, Va., Aug. 1991.
324. Cole, J. L. et al.: Development and Qualification of the S-76C+ Helicopter with 30-Second/2-Minute OEI Power Ratings. *J. American Helicopter Society*, vol. 46, no. 2, 2001.
325. Hall, S. R.; Yang, K. Y.; and Hall, K. C.: Helicopter Rotor Lift Distribution for Minimum-Induced Power Loss. American Institute of Aeronautics and Astronautics (AIAA) *J. Aircraft*, vol. 31, no. 4, 1994.
326. Wachspress, D. A.; Quackenbush, T. R.; and Solomon, C. L.: On Minimum Induced Power of the Helicopter Rotor. CDI Report No. 05-04, Continuum Dynamics, Inc., Ewing, N.J., 2005.
327. Rand, O.; Khromov, V.; and Peyran, R. J.: Minimum-Induced Power Loss of a Helicopter Rotor via Circulation Optimization. American Institute of Aeronautics and Astronautics (AIAA) *J. Aircraft*, vol. 41, no. 1, 2004.

#### 4. REFERENCES

328. Hall, K. C.; and Hall, S. R.: A Variational Method for Computing the Optimal Aerodynamic Performance of Conventional and Compound Helicopters. *J. American Helicopter Society*, vol. 55, no. 4, 2010.
329. Hunt, W. E.: *Helicopter*. London, England: Airlife Publishing Ltd., 1998.
330. Kowalonek, J. M.: Email to F. D. Harris; VS-300 World Endurance Record. 2007.
331. Bréguet, L.: Aerodynamical Efficiency and the Reduction of Air Transport Costs. *J. Royal Aeronautical Society*, vol. 26, 1922.
332. Cavcar, M.: Bréguet Range Equation? *American Institute of Aeronautics and Astronautics (AIAA) J. Aircraft*, vol. 43, no. 5, Sept–Oct. 2006.
333. Von Parseval, A.: Lindbergh's Flight. *NACA TM 423*, 1927.
334. Hall, D. H.: Technical Preparation of the Airplane "Spirit of St. Louis." *NACA TN 257*, July 1927.
335. Hufton, P. A.; Nutt, A. E. W.; and Bigg, F. J.: General Investigation Into the Characteristics of the C.30 Autogiro. *Aeronautical Research Committee R&M No. 1859*, Mar. 1939.
336. Fries, G.; and Wiesner, W.: A Summary of References, Methods and Procedures Useful in Estimating Parasite Drag. *Kellett Aircraft Corp. Engineering Report 1430.12*, Feb. 1945.
337. Hoerner, S. F.: *Fluid-Dynamic Drag*. Brick Town, N.J.: Author Published, 1965.
338. Harrington, R. D.: Reduction of Helicopter Parasite Drag. *NACA TN 3234*, Aug. 1954.
339. G. E. Dausman: Private letter to J. Diamond; Helicopter Drag Data. July 25, 1960.
340. Sweet, G. E.; and Jenkins, J. L., Jr.: Wind Tunnel Tests of Four Helicopter Fuselage Models and Various Appendages in the Langley 7- by 10-Foot Wind Tunnel. *NASA Preliminary Data Report L-1470* (see also *NASA TN-D-1363*), 1960.
341. Jenkins, J. L., Jr.; Sweet, G. E.; and Winston, M. M.: Full-Scale Wind Tunnel Tests of an Aerodynamically Clean Helicopter Fuselage and Appendages. *NASA Preliminary Data Report L-1469* (see also *NASA TN-D-1364*), 1960.
342. Moser, H., Lt.: Full-Scale Wind Tunnel Investigation of Helicopter Drag. *J. American Helicopter Society*, vol. 6, no. 1, 1961.
343. Flood, R. L.; Rohtert, R. E.; and La Forge, S. V.: Aerodynamic Tests of an Operational OH-6A Helicopter in the Ames 40' x 80' Wind Tunnel. *HTC-AD Report No. 369-A-8020*, Hughes Tool Co., Aircraft Div., Culver City, Calif. (see also *ASTIA AD 742891*), May 1970.
344. Squires, P. K.: Investigation of Correlation Between Full-Scale and Fifth-Scale Wind Tunnel Tests of a Bell Helicopter Textron Model 222. *NASA CR-166362*, June 1982.
345. Williams, R. M., Chairman: Special Report by the Ad Hoc Committee on Rotorcraft Drag. *Proc. American Helicopter Society 31st Annual National Forum*, Washington, D.C., May 13–15, 1975.
346. Venegoni, M.; Magni, E.; and Baldassarrini, R.: An Industrial Rational for the Aerodynamic Design of the Fuselage for a High Performance Light Helicopter. Paper No. 44, *Proc. Third European Rotorcraft and Powered Lift Aircraft Forum*, Aix-en-Provence, France, Sept. 1977.

#### 4. REFERENCES

347. Perry, F. J.: Aerodynamics of the Helicopter World Speed Record. Proc. 43rd Annual National Forum of the American Helicopter Society, St. Louis, Mo., May 18–20, 1987.
348. Jones, J. P.: The Helicopter Rotor. *J. Royal Aeronautical Society*, vol. 74, no. 719, 1970.
349. Jones, J. R.; and Lund, P. D.: Full-Scale Investigation of Rotor Hub Fairing for a Sikorsky H-5 Rotor Hub. McCulloch Motors Corp. Report No. 55McC103R (ASTIA AD No. 93925), 1955.
350. Harris, F. D.: An Overview of Autogyros and The McDonnell XV-1 Convertiplane. NASA/CR-2003-212799, Oct. 2003.
351. Culver, I. H.: Designing the High-Speed Rigid Rotor Helicopter. *J. Astronautics and Aerospace Engineering*, June 1963.
352. Heppe, R. R.: The Single-Rotor Helicopter With Rigidly-Mounted Blades. *J. Royal Aeronautical Sciences*, vol. 67, no. 634, 1963, pp. 651–663.
353. Hibbard, H. L.; and Heppe, R. R.: Concept and Development of a Simple, Stable, and Economic VTOL Vehicle. IAS Paper No. 62-18, Proc. Institute of the Aerospace Sciences 30th Annual Mtg., New York, N.Y., Jan 22–24, 1962.
354. Logan, A. H.; Prouty, R. W.; and Clark, D. R.: Wind Tunnel Tests of Large- and Small-Scale Rotor Hubs and Pylons. USAAVRADCOTR 80-D-21, U.S. Army Aviation Research and Development Command, Ft. Eustis, Va., 1981.
355. Sung, D. Y.; Lance, M. B.; Young, L. A.; and Stroub, R. H.: An Experimental Investigation of Helicopter Rotor Hub Fairing Drag Characteristics. NASA-TM-102182, Sept. 1989.
356. Gabriel, E.: Wind Tunnel Test and Analysis Report of Flow Visualization Test of a One-Third-Scale HC-1B Rotor Hub with Blade Shank Fairings. Report No. R-285, Boeing Airplane Co., Vertol Div., Philadelphia, Pa., 1962.
357. Bousman, W. G.; Ormiston, R. A.; and Mirick, P. H.: Design Considerations for Bearingless Rotor Hubs. Paper No. A-83-39-62-1000, Proc. 39th Annual Forum of the American Helicopter Society, St. Louis, Mo., May 9–11, 1983.
358. Alldridge, P. J.: High-Speed Rotor Performance Methodology—Investigation of the Aerodynamic Characteristics of the Integrated Technology Hub. BHT Engineering Interoffice Memo 81:PA/dd-1070, Bell Helicopter Textron, Inc., Ft. Worth, Tex., 1986.
359. B. Ormiston: Letter to F. D. Harris; Rotor Hubs. June 30, 1993.
360. Schindler, R.; and Pfisterer, E.: Impacts of Rotor Hub Design Criteria on the Operational Capabilities of Rotorcraft Systems. AGARD CP-423, Rotorcraft Design for Operations Symposium, Amsterdam, The Netherlands, Oct. 13–16, 1986.
361. Hanson, T. F.: A Designer Friendly Handbook of Helicopter Rotor Hubs. Newhall, Calif.: Author Published, 2005.
362. Mosinskis, V. S.; and Schneider, E.: Design and Development of an Elastomeric-Bearing Rotor Hub. Proc. 24th Annual National Forum of the American Helicopter Society, Washington, D.C., 1968.
363. Culver, I. H.; and Rhodes, J. E.: Structural Coupling in the Blades of Rotating Wing Aircraft. IAS Paper No. 62-33, Proc. 30th Annual Mtg. of the Institute of Aerospace Sciences, New York, N.Y., Jan. 22–24, 1962.

#### 4. REFERENCES

364. Cardinale, S.: Soft In-plane Matched-Stiffness/Flexure-Root-Blade Rotor System Summary Report. USAAVLABS TR 68-72, U.S. Army Aviation Material Laboratories, Ft. Eustis, Va., 1969.
365. Harris, F. D.; Cancro, P. A.; and Dixon, P. G. C.: The Bearingless Main Rotor. Proc. Third European Rotorcraft and Powered-Lift Aircraft Forum, Aix-en-Provence, France, Sept. 1977.
366. Dixon, P. G. C.; and Bishop, H. E.: The Bearingless Main Rotor. J. American Helicopter Society, vol. 25, no. 3, 1980.
367. Harris, F. D.; and Dixon, P. G. C.: Boeing BMR Preliminary Design—Volume C, Oral Briefing. Boeing Vertol Report D210-11120-1, Boeing Vertol Co., Philadelphia, Pa., 1976.
368. Staley, J. A.; Gabel, R.; and MacDonald, H. I.: Full-Scale Ground and Air Resonance Testing of the Army-Boeing Vertol Bearingless Main Rotor. Preprint no. 79-23, Proc. 35th Annual National Forum of the American Helicopter Society Washington, D.C., May 21–23, 1979.
369. Dawson, S.: An Experimental Investigation of the Stability of a Bearingless Model Rotor in Hover. Proc. 38th Annual Forum of the American Helicopter Society, Anaheim, Calif., May 4–7, 1982.
370. Huber, H.: “Will Rotor Hubs Lose Their Bearings?” A Survey of Bearingless Main Rotor Development. Paper No. 506, Proc. 18th European Rotorcraft Forum, Avignon, France, Sept. 15–18, 1992.
371. Norman, T. R.; Cooper, C. R.; Fredrickson, C. A.; and Herter, J. R.: Full-Scale Wind Tunnel Evaluation of the Sikorsky Five-Bladed Bearingless Main Rotor. Proc. 49th Annual Forum of the American Helicopter Society, St. Louis, Mo., May 19–21, 1993.
372. Johnson, W.: Recent Developments in the Dynamics of Advanced Rotor Systems. AGARD Lecture Series No. 139, Helicopter Aeromechanics (also see DTIC AD-A155946), Apr. 1985.
373. Harvey, K. W.: Aeroelastic Analysis of a Bearingless Rotor. Symposium on Rotor Technology sponsored by the Mideast Region of the American Helicopter Society, Arlington, Tex., Aug. 11–13, 1976.
374. Nguyen, K.; McNulty, M.; Anand, V.; and Lauzon, D.: Aeroelastic Stability of the McDonnell Douglas Advanced Bearingless Rotor. Proc. 49th Annual Forum of the American Helicopter Society, St. Louis, Mo., May 19–21, 1993.
375. Donham, R. E.; Cardinale, S. V.; and Sachs, I. B.: Ground and Air Resonance Characteristics of a Soft In-Plane Rigid-Rotor System. AIAA Paper No. 69-205, Proc. AIAA/AHS VTOL Research, Design, and Operations Mtg., Atlanta, Ga., 1969.
376. Churchill, G. B.; and Harrington, R. D.: Parasite-Drag Measurements of Five Helicopter Rotor Hubs. NASA Memo 1-31-59L, Feb. 1959.
377. Keys, C. N.; and Wiesner, R.: Guidelines for Reducing Helicopter Parasite Drag. J. American Helicopter Society, vol. 20, no. 1, 1975.
378. Sheehy, T. W.: A General Review of Helicopter Rotor Hub Drag Data. J. American Helicopter Society, vol. 22, no. 2, 1977.
379. Keys, C. N.; and Rosenstein, H. J.: Summary of Rotor Hub Drag Data. NASA CR-152080, Mar. 1978.

#### 4. REFERENCES

380. Teleki, A.: High-Speed Flight Tests With the Bo. 105. *The Aeronautical Journal*, vol. 79, no. 778, Oct. 1975, pp. 425–430. See also DGLR76-222, 9th Annual DGLR mtg., Munich, Germany, Sept. 1976.
381. Martin, D. M.; Mort, R. W.; Young, L. A.; and Squires, P. K.: Experimental Investigation of Advanced Hub and Pylon Fairing Configurations to Reduce Helicopter Drag. NASA TM-4540, Sept. 1993.
382. Fradenburgh, E. A.: The First 50 Years Were Fine...But What Should We Do for an Encore. *J. American Helicopter Society*, vol. 40, no. 1, 1995.
383. Fradenburgh, E. A.: High-Performance Single Rotor Helicopter Study. U.S. Army Transportation Research Command Report No. TREC 61-44, 1961.
384. Obukata, M.; and Nakadate, M.: Aerodynamic Design of Bearingless Rotor Hub. Paper 98 T1-2, Heli Japan 98, Gifu, Japan, Apr. 21–23, 1998.
385. Lynn, R. R.: Fifty Years of Challenge. Royal Aeronautical Society, 37th Cierva Memorial Lecture, London, England, Oct. 1996.
386. Prouty, R. W.; and Yackle, A. R.: The Lockheed AH-56 Cheyenne—Lessons Learned. AIAA Paper No. 92-4278, Proc. AIAA Aircraft Design Systems Mtg., Hilton Head, S.C., Aug. 24–26, 1992.
387. Amer, K. B.; Prouty, R. W.; Korkosz, G.; and Fouse, D.: Lessons Learned During the Development of the AH-56A Apache Attack Helicopter. Proc. 48th Annual Forum of the American Helicopter Society, Washington, D.C., June 3–5, 1992.
388. Yeo, H.; Bousman, W. G.; and Johnson, W.: Performance Analysis of a Utility Helicopter with Standard and Advanced Rotors. Proc. American Helicopter Society Aerodynamics, Acoustics, and Test and Evaluation Specialists' Mtg., San Francisco, Calif., Jan. 23–25, 2002.
389. Harris, F. D.; Kocurek, J. D.; McLarty, T. T.; and Trept, T. J.: Helicopter Performance Methodology at Bell Helicopter Textron. Preprint No. 79-2, Proc. 35th Annual National Forum of the American Helicopter Society, Washington, D.C., May 21–23, 1979.
390. Anderson, W. D.: REXOR Rotorcraft Simulation Model, Volume I—Engineering Documentation. USAAMRDL-TR-76-28A, U.S. Army Air Mobility Research and Development Laboratories, Ft. Eustis, Va., 1976.
391. Potsdam, M. P.; Yeo, H.; and Johnson, W.: Rotor Airloads Prediction Using Loose Aerodynamic/Structural Coupling. Proc. American Helicopter Society 60th Annual Forum, Baltimore, Md., June 7–10, 2004. (Also see *AIAA J. Aircraft*, vol. 43, no. 3, May–June 2006.)
392. Yeo, H.; and Johnson, W.: Prediction of Rotor Structural Loads with Comprehensive Analysis. *J. American Helicopter Society*, vol. 53, no. 2, 2008.
393. Bhagwat, M. J.; and Ormiston, R. A.: Examination of Rotor Aerodynamics in Steady and Maneuvering Flight Using CFD and Conventional Methods. Proc. American Helicopter Society Specialists' Conference on Aeromechanics, San Francisco, Calif., Jan 23–25, 2008.
394. Berry, J. D.: Unsteady Velocity Measurements Taken Behind a Model Helicopter Rotor Hub in Forward Flight. NASA TM-4738, Mar. 1997.

#### 4. REFERENCES

395. Le Chuiton, F.; Kneisch, T.; Schneider, S.; and Kramer, P.: Industrial Validation of Numerical Aerodynamics About Rotor Heads: Towards a Design Optimisation at Eurocopter. Proc. 35th European Rotorcraft Forum, Hamburg, Germany, Sept. 22–25, 2009.
396. Vogel, F.; Brietsamter, C.; and Adams, N. A.: Aerodynamic Investigation on a Helicopter Main Rotor Hub. Proc. 66th Annual Forum of the American Helicopter Society, Phoenix, Ariz., May 11–13, 2010.
397. Bridgeman, J. O.; and Lancaster, G. T.: Physics-Based Analysis Methodology for Hub Drag Prediction. Proc. 66th Annual Forum of the American Helicopter Society, Phoenix, Ariz., May 11–13, 2010.
398. de la Cierva, J.: New Developments of the Autogyro. *J. Royal Aeronautical Society*, vol. 39, no. 8, Dec. 1935.
399. Moore, H.: Twirlybirdings: Recollections From the Early Days of Helicopter Training. *AHS Vertiflite*, vol. 52, no. 3, 2006.
400. Wagner, R. A.: *Vibration Handbook for Helicopters*. Prewitt Aircraft Co., 1954.
401. Gerstenberger, W. et al.: The Rotary Round Table: How Can Helicopter Vibration Be Minimized? *J. American Helicopter Society*, vol. 2, no. 3, 1957.
402. White, R. P.; and Yeates, J. E. (Eds.): Vol I—Propeller and Rotor Aerodynamics; Vol II—Propulsion and Interference; and Vol. III—Aerodynamic Research on Boundary Layers. CAL/USAAVLABS Symposium, Buffalo, N.Y., June 22–24, 1966.
403. Carter, E.S., Jr.: *Rotorcraft Dynamics*. NASA SP-352, Feb. 1974.
404. Gabel, R.: When Helicopter Smooth Surpasses Jet Smooth. Proc. American Helicopter Society Northeast Region National Specialists’ Mtg. on Helicopter Vibration, Hartford, Conn., Nov. 2–4, 1981.
405. Loewy, R. G.: Helicopter Vibrations: A Technology Perspective. *J. American Helicopter Society*, vol. 29, no. 4, 1984.
406. Hansford, R. E.; and Vorwald, J.: Dynamics Workshop on Rotor Vibratory Loads. Proc. 52nd Annual Forum of the American Helicopter Society, Washington, D.C., June 4–6, 1996.
407. Griffen, M. J.: *Handbook of Human Vibration*. London, England: Elsevier Academic Press, 2004.
408. Rosen, J.; and Arcan, M.: Modeling the Human Body/Seat System in a Vibration Environment. *J. Biomechanical Engineering*, vol. 125, 2003.
409. Anon.: MIL-H-8501. Helicopter Flying and Ground Handling Qualities; General Requirements for. Department of Defense, Washington, D.C., Nov. 1952.
410. Anon.: MIL-H-8501A. Helicopter Flying and Ground Handling Qualities: General Requirements for. Department of Defense, Washington, D.C., Sep. 1961 w/amend. Apr. 1962.
411. Gabel, R.; Henderson, B. O.; and Reed, D. A.: Pilot and Passenger Vibration Environment Sensitivity. *J. American Helicopter Society*, vol. 16, no. 3, 1971.
412. Schrage, D. P., Captain; and Peskar, R. E.: Helicopter Vibration Requirements. Proc. 33rd Annual National Forum of the American Helicopter Society, Washington, D.C., May 9–11, 1977.

#### 4. REFERENCES

413. Prouty, R. W.: Vibration Criteria: Finding Discomfort Levels. Rotor & Wing International, Mar. 1992.
414. Crews, S. T.; Lewis, W. D.; and Dulaney, K. E.: Requirements for Rotorcraft Vibration Specifications, Modeling and Testing. U.S. Army Aviation Engineering Directorate, ADS-27A-SP, 2006.
415. Crews, S. T.: Army Helicopter Crew Seat Vibration—Past Performance, Future Requirements. Preprint No. 3, Proc. American Helicopter Society Northeast Region National Specialists' Mtg. on Helicopter Vibration, Hartford, Conn., Nov. 2–4, 1981.
416. Chen, Y.; Wickramasinghe, V.; and Zimick, D. G.: Investigation of Helicopter Seat Structural Dynamics for Aircrew Vibration Mitigation. J. American Helicopter Society, vol. 56, no. 1, 2011.
417. Anon.: MIL-HDBK-5J. Metallic Materials and Elements for Aerospace Vehicle Structures. Department of Defense, Washington, D.C., 2003.
418. Anon.: Composite Materials Handbook, Vol. 1. Polymer Matrix Composites Guidelines for Characterization of Structural Materials: U.S. Department of Defense, Washington, D.C., 2002.
419. Anon.: Composite Materials Handbook, Vol. 2. Polymer Matrix Composites Materials Properties: U.S. Department of Defense, Washington, D.C., 2002.
420. Anon.: Composite Materials Handbook, Vol. 3. Polymer Matrix Composites Materials Usage, Design, and Analysis: U.S. Department of Defense, Washington, D.C., 2002.
421. Anon.: Composite Materials Handbook, Vol. 4. Metal Matrix Composites. U.S. Department of Defense, Washington, D.C., 2002.
422. Anon.: Composite Materials Handbook, Vol. 5. Ceramic Matrix Composites. U.S. Department of Defense, Washington, D.C., 2002.
423. Caldwell, F. W.: Conventional Propeller Calculations. SAE Paper No. 180041, Transactions of the Society of Automobile Engineers, vol. 1, no. 1, 1918.
424. Nelson, J. H.: The Strength of One-Piece Solid, Build-Up and Laminated Wood Airplane Wing Beams. NACA Report No. 35, 1920.
425. Hartman, E. C.: Comparison of Weights of 17ST and Steel Tubular Structural Members Used in Aircraft Construction. NACA TN 378, May 1931.
426. Schatzberg, E.: Wings of Wood, Wings of Metal. Princeton, N.J.: Princeton University Press, 1999.
427. Miner, M. A.: Cumulative Damage in Fatigue. J. Applied Mechanics, vol. 12, no. 3, 1945.
428. Cooper, W. E.: Materials and the Fatigue Aspect. J. Helicopter Association of Great Britain, vol. 4, no. 3, 1950.
429. Williams, J. K.: The Fatigue Problem With Emphasis on the Airworthiness Aspects. J. Helicopter Association of Great Britain, vol. 5, no. 1, 1951.
430. Hirsch, H.; and Kline, J.: An Experimental Investigation of the H-5 Variable Stiffness Blade Program. Part 3. Evaluation of Rotor Resonance Bending Effects. WADC Air Force TR 6329, Part 3. (See AD No. 8445 for Part 1, AD No. 8444 for Part 2, AD No. 6265 for Part 3, AD No. 6161 for Part 4, AD No. 6794 for Part 5, and AD No. 8443 for Part 6), 1952.

#### 4. REFERENCES

431. Yeates, J. E.; Brooks, G. W.; and Houbolt, J. C.: Flight and Analytical Methods for Determining the Coupled Vibration Response of Tandem Helicopters. NACA Report 1326, 1957.
432. Bender, G. L.; Yamakawa, G. M.; Herbst, M. K.; Sullivan, P. J.; Robbins, R. D.; and Williams, R. A.: Airworthiness and Flight Characteristics Test (A&FC) of the CH-47D Helicopter. USAAEFA Project No. 82-07, U.S. Army Aviation Engineering Flight Activity, Edwards Air Force Base, Calif., 1984.
433. Laing, E. J.: Army Helicopter Vibration Survey Methods and Results. *J. American Helicopter Society*, vol. 19, no. 3, 1974.
434. Johnson, J. C.; and Priser, D. B.: Vibration Levels in Army Helicopters—Measurement Recommendations and Data. USAARL Report No. 81-5, U.S. Army Aeromedical Research Laboratory, Biodynamics Research Div., Ft. Rucker, Ala., 1981.
435. Laing, E. J.: Vibration and Temperature Survey Production UH-1H Helicopter. USAASTA Project No. 70-15-2, U.S. Army Aviation Systems Test Activity, Edwards Air Force Base, Calif., 1973.
436. Millott, T. A.; Wong, J. K.; Correia, J. R.; Goodman, R. K.; Welsh, W. A.; and Cassil, C. E.: Risk Reduction Flight Test of a Pre-Production Active Vibration Control System for the UH-60M. Proc. 59th Annual Forum of the American Helicopter Society, Phoenix, Ariz., May 6–8, 2003.
437. Snyder, W. J.; Cross, J. L.; and Kufeld, R. M.: NASA/Army Rotor Systems Flight Research Leading to the UH-60 Airloads Program. Innovations in Rotorcraft Test Technology for the 1990s, Proc. AHS Specialists' Mtg., Phoenix, Ariz., Oct. 8–12, 1990.
438. Watts, M. E.; and Cross, J. L.: The NASA Modern Technology Rotors Program. Paper No. AIAA-86-9788, Proc. AIAA/AHS/CASI/DGLR/ISA/ITEA/SETP/SFE 3rd Flight Testing Conference, Las Vegas, Nev., Apr. 2–4, 1986.
439. Studebaker, K.: A Survey of Hub Vibration for the UH-60A Airloads Research Aircraft. Proc. American Helicopter Society Aeromechanics Specialists' Conference, San Francisco, Calif., 1994.
440. Silveira, M. A.; and Brooks, G. W.: Analytical and Experimental Determination of the Coupled Natural Frequencies and Mode Shapes of a Dynamic Model of a Single-Rotor Helicopter. NASA Memo 11-5-58L, 1958.
441. Ricks, R. G.: A Study of Tandem Helicopter Fuselage Vibration. ASD-TDR-62-284 (AD 0290317), Air Force Systems Command, Aeronautical Systems Div., Wright-Patterson Air Force Base, Ohio, Sept. 1962.
442. Gabel, R.: AVID Program—Advanced Vibration Development. Boeing Vertol Report 107M-D-09 (now 62-0177-f), Boeing Vertol Co., Philadelphia, Pa, 1965.
443. Rutkowski, M. J.: The Vibration Characteristics of a Coupled Helicopter Rotor-Fuselage by a Finite Element Analysis. NASA TP-2118 (see also AVRADCOM TR 82-A-15), Jan. 1983.
444. Anon.: Final Report for NASTRAN Project. NASA CR-112405, Mar. 1970.

#### 4. REFERENCES

445. Dinyovszky, P.; and Twomey, W. J.: Plan, Formulate, and Discuss a NASTRAN Finite Element Model of the UH-60A Helicopter Airframe. NASA CR-181975, Feb. 1990.
446. Howland, G. R.; Durno, J. A.; and Twomey, W. J.: Ground Shake Test of the UH-60A Helicopter Airframe and Comparison With NASTRAN Finite Element Model Predictions. NASA CR-181993, Mar. 1990.
447. Idosor, F. R.; and Seible, F.: NASTRAN Modeling of Flight Test Components for the UH-60A Airloads Program Test Configuration. NASA CR-193614, Feb. 1993.
448. Kvaternik, R. G.: The NASA/Industry Design Analysis Methods for Vibrations (DAMVIBS) Program—A Government Overview. NASA TM-107579, Apr. 1992.
449. Kvaternik, R. G.: Langley Rotorcraft Structural Dynamics Program—Background, Status, Accomplishments, Plans. NASA TM-101618, June 1989.
450. Domka, R. V.: Investigation of Difficult Component Effects on FEM Vibration Prediction for the AH-1G Helicopter. Proc. 44th Annual American Helicopter Society National Forum, Washington, D.C., June 16–18, 1988.
451. Cronkhite, J. D.: A Government/Industry Summary of the Design Analysis Methods for Vibrations (DAMVIBS) Program, Kvaternik, R. G. (Ed.); also see The Nasa/Industry Design Analysis Methods for Vibration (DAMVIBS) Program—Bell Helicopter Textron Accomplishments. Apr. 13–15, 1992.
452. Smith, F. C.; and Howard, D. M.: Calculation and Measurement of Normal Modes of Vibration of an Aluminum-Alloy Box Beam With and Without Large Discontinuities. NACA TN 2884, Jan. 1953.
453. Cronkhite, J. D.; Dompka, R. V.; Rogers, J. P.; Corrigan, J. C.; Perry, K. S.; and Sadler, S. G.: Coupling Rotor/Fuselage Dynamic Analysis of the AH1G Helicopter and Correlation With Flight Vibrations Data. NASA CR-181723, Jan. 1989.
454. DiTaranto, R. A.; and Sankewitsch, V.: Calculation of Flight Vibration Levels of the AH-1G Helicopter and Correlation With Existing Flight Vibration Measurements. NASA CR-181923, Nov. 1989.
455. Sangha, K.; and Shamie, J.: Correlation of AH-1G Airframe Flight Vibration Data With a Coupled Rotor-Fuselage Analysis. NASA CR-181974, Aug. 1990.
456. Sopher, R.; and Twomey, W. J.: Calculation of Flight Vibration Levels of the AH-1G Helicopter and Correlation with Existing Flight Vibration Measurements. NASA CR-182031, Apr. 1990.
457. Cronkhite, J. D.; Berry, V. L.; and Brunken, J. E.: A NASTRAN Vibration Model of the AH-1G Helicopter Airframe. U.S. Army Armament Command Report No. R-TR-74-045 (Vol. I—ADA 009482, Vol. II—ADA 009483), 1974.
458. Domka, R. V.; and Cronkhite, J. D.: Summary of AH-1G Flight Vibration Data for Validation of Coupled Rotor-Fuselage Analysis. NASA CR-178160, Nov. 1986.
459. Shockey, G. A.; Williamson, J. W.; and Cox, C. R.: AH-1G Helicopter Aerodynamics and Structural Loads Survey. USAAMRDL TR-76-39, U.S. Army Air Mobility Research and Development Laboratories, Ft. Eustis, Va., 1976.
460. Gessow, A.; and Crim, A. D.: A Method for Studying the Transient Blade-Flapping Behavior of Lifting Rotors at Extreme Operating Conditions. NACA TN 3366, Jan. 1955.

#### 4. REFERENCES

461. Van Gaasbeek, J. R.: Validation of the Rotorcraft Flight Simulation Program (C81) Using Operational Loads Survey Flight Test Data. USAAVRADCOTR-80-D-4, U.S. Army Aviation Research and Development Command, Ft. Eustis, Va., July 1980.
462. Kvaternik, R. G.: A Government/Industry Summary of the Design Analysis Methods for Vibrations (DAMVIBS) Program. NASA CP-10114, Jan. 1993.
463. Yeo, H.; and Chopra, I.: Coupled Rotor/Fuselage Vibration Analysis for Teetering Rotor and Test Data Comparison. American Institute of Aeronautics and Astronautics (AIAA) *J. Aircraft*, vol. 38, no. 1, Jan.–Feb. 2001.
464. Bousman, W. G.: Rotorcraft Airloads Measurements—Extraordinary Costs, Extraordinary Benefits. Proc. 67th Annual Forum of the American Helicopter Society, Virginia Beach, Va., May 3–5, 2011.
465. Romander, E.; Norman, T. R.; and Chang, I.: Correlating CFD Simulation With Wind Tunnel Test for the Full-Scale UH-60A Airloads Rotor. Proc. 67th Annual Forum of the American Helicopter Society, Virginia Beach, Va., May 3–5, 2011.
466. Durno, J. A.; Howland, G. R.; and Twomey, W. J.: Comparison of Black Hawk Shake Test Results with NASTRAN Finite Element Analysis. Proc. 43rd Annual Forum of the American Helicopter Society, St. Louis, Mo., May 18–20, 1987.
467. Idosor, F. R.; and Seible, F.: NASTRAN Modeling of Flight Test Components for UH-60A Airloads Program Test Configuration. NASA CR-193614, Feb. 1993.
468. Goodman, R.: UH-60A NASA/AEFA Configuration Ground Vibration Test Results. SER-701619, Sikorsky Aircraft, Stratford, Conn., 1990.
469. Johnson, W.: Milestones in Rotorcraft Aeromechanics. NASA/TP-2011-215971, May 2011.
470. Caradonna, F. X.; Tung, C.; and Desopper, A.: Finite Difference Modeling of Rotor Flows Including Wake Effects. *J. American Helicopter Society*, vol. 29, no. 2, 1984.
471. Tung, C.; Caradonna, F. X.; and Johnson, W.: The Prediction of Transonic Flows on an Advancing Rotor. *J. American Helicopter Society*, vol. 31, no. 3, 1986.
472. Datta, A.; Sitaraman, J.; Baeder, J. D.; and Chopra, I.: Prediction of UH-60 Main Rotor Structural Loads Using CFD/Comprehensive Analysis Coupling. Proc. 32nd European Rotorcraft Forum, Maastricht, The Netherlands, Sept. 12–14, 2006.
473. Potsdam, M. P.; Yeo, H.; and Johnson, W.: Rotor Airloads Prediction Using Loose Aerodynamic/Structural Coupling. American Institute of Aeronautics and Astronautics (AIAA) *J. Aircraft*, vol. 43, no. 3, 2006.
474. Datta, A.; Nixon, M.; and Chopra, I.: Review of Rotor Loads Prediction with the Emergence of Rotorcraft CFD. *J. American Helicopter Society*, vol. 52, no. 4, 2007.
475. Lim, J. W.: Improved Performance Prediction for Bo-105 Model Rotor in Cruise Using Computational Fluid Dynamics. Proc. 37th European Rotorcraft Forum, Ticino Park, Italy, Sept. 13–15, 2011.
476. Norman, T. R.; Shinoda, P. M.; Kitaplioglu, C.; Jacklin, S. A.; and Sheikman, A.: Low-Speed Wind Tunnel Investigation of a Full-Scale UH-60 Rotor System. Proc. 58th Annual Forum of the American Helicopter Society, Montreal, Canada, June 11–13, 2002.

#### 4. REFERENCES

477. van Aken, J. M.; Shinoda, P. M.; and Haddad, F.: Development of a Calibration Rig for a Large Multi-Component Rotor Balance. 46th International Instrumentation Symposium of the Instrument Society of America, Bellevue, Wash., Apr. 30–May 4, 2000.
478. Peterson, R. L.; and van Aken, J. M.: Dynamic Calibration of the NASA Ames Rotor Test Apparatus Steady/Dynamic Rotor Balance. NASA TM-110393, Apr. 1996.
479. Bain, L. J.: Comparison of Theoretical and Experimental Model Blade Vibratory Shear Forces. AAVLABS TR66-77, U.S. Army Aviation Material Laboratories, Ft. Eustis, Va., 1967.
480. Gabel, R.; Sheffler, M.; Tarzanin, F.; and Hodder, D.: Wind Tunnel Modeling of Rotor Vibratory Loads. *J. American Helicopter Society*, vol. 28, no. 2, 1983.
481. Norman, T. R.; Shinoda, P.; Peterson, R. L.; and Datta, A.: Full-Scale Wind Tunnel Test of the UH-60A Airloads Rotor. Proc. 67th Annual Forum of the American Helicopter Society, Virginia Beach, Va., May 3–5, 2011.
482. Bailey, F. J., Jr.; and Gustafson, F. B.: Observations in Flight of the Region of Stalled Flow over the Blades of an Autogiro Rotor. NACA TN 741, Dec. 1939.
483. Gustafson, F. B.; and Myers, G. C., Jr.: Stalling of Helicopter Blades. NACA TN 1083, June 1946.
484. Gustafson, F. B.; and Gessow, A.: Effect of Blade Stalling on the Efficiency of a Helicopter Rotor as Measured in Flight. NACA TN 1250, Apr. 1947.
485. Falabella, G.; and Meyer, J. R.: Determination of Inflow Distributions from Experimental Aerodynamic Loading and Blade-Motion Data on a Model Helicopter Rotor in Hovering and Forward Flight. NACA TN 3492, Nov. 1955.
486. Tanner, W. H.; and Wohlfeld, R. M.: New Experimental Techniques in Rotorcraft Aerodynamics and Their Application. *J. American Helicopter Society*, vol. 15, no. 2, 1970.
487. Harris, F. D.: A Note about Self-Induced Velocity Generated by a Lifting-Line Wing or Rotor Blade. NASA/CR-2006-213478, Feb. 2006.
488. Yen, J. G.; and Yuce, M.: Correlation of Pitch-Link Loads in Deep Stall on Bearingless Rotors. *J. American Helicopter Society*, vol. 37, no. 4, 1992.
489. Kufeld, R.; and Loschke, P.: UH-60 Airloads Program: Status and Plans. Proc. AIAA Aircraft Design Systems and Operations Mtg., Baltimore, Md., Sept. 23–25, 1991.
490. Veca, A. C.: Vibration Effects on Helicopter Reliability and Maintainability. USAAMRDL TR 73-11, U.S. Army Air Mobility Research and Development Laboratories, Ft. Eustis, Va., 1973.
491. Richards, E. J.: Problems of Noise in Helicopter Design. *J. Helicopter Association of Great Britain*, vol. 9, no. 1, 1955.
492. Stein, J. (Ed.): *The Random House Dictionary of the English Language*. New York, N.Y.: Random House, Inc., 1967.
493. Fletcher, H.; and Munson, W. A.: Loudness, Its Definition, Measurement and Calculation. *J. Acoustical Society of America*, vol. 5, 1933, pp. 82–108.
494. Anon.: ISO 226:2003. Acoustics—Normal Equal-Loudness-Level Contours. International Organization for Standardization, Geneva, Switzerland, 2003.

#### 4. REFERENCES

495. Robinson, D. W.; and Dadson, R. S.: A Re-determination of the Equal-Loudness Relations for Pure Tones. *British J. Applied Physics*, vol. 7, 1956.
496. Kryter, K. D.: Scaling Human Reactions to the Sound from Aircraft. *J. Acoustical Society of America*, vol. 31, no. 11, 1959.
497. Kryter, K. D.: The Meaning and Measurement of Perceived Noise Level. *Noise Control Engineering Journal (NCEJ)*, Sept./Oct. 1960.
498. van der Linden, F. R.: *Airlines & Airmail—The Post Office and the Birth of the Commercial Aviation Industry*. Lexington Ky.: The University Press of Kentucky, 2002.
499. Hammack, J. B.; Kurbjun, M. C.; and O'Bryan, T. C.: Flight Investigation of a Supersonic Propeller on a Propeller Research Vehicle at Mach Numbers to 1.01. *NACA RM L57E20*, July 10, 1957.
500. Kurbjun, M. C.: Noise Survey of a 10-Foot Four-Blade Turbine-Driven Propeller Under Static Conditions. *NACA TN 3422*, July 1955.
501. Kurbjun, M. C.: Noise Survey of a Full-Scale Supersonic Turbine-Driven Propeller Under Static Conditions. *NACA TN 4059*, July 1957.
502. Kurbjun, M. C.: Noise Survey Under Static Conditions of a Turbine-Driven Full-Scale Modified Supersonic Propeller With an Advance Ratio of 3.2. *NACA TN 4172*, Jan. 1958.
503. Kurbjun, M. C.: Noise Survey Under Static Conditions of a Turbine-Driven Transonic Propeller With an Advance Ratio of 4.0. *NASA Memorandum 4-18-59L*, May 1959.
504. O'Bryan, T. C.; and Hammack, J. B.: Flight Performance of a Transonic Turbine-Driven Propeller Designed for Minimum Noise. *NASA Memorandum 4-19-59L*, May 1959.
505. Hammack, J. B.; and O'Bryan, T. C.: Effect of Advance Ratio on Flight Performance of a Modified Supersonic Propeller. *NACA TN 4389*, Sept. 1958.
506. Hubbard, H. H.: Propeller-Noise Charts for Transport Airplanes. *NACA TN 2968*, June 1953.
507. Gutin, L.: On the Sound Field of a Rotating Propeller. *NACA TM 1195*, Oct. 1948.
508. Yudin, E. Y.: On the Vortex Sound from Rotating Rods. *NACA TM 1136*, Mar. 1947.
509. Evans, A. J.; and Liner, G.: A Wind Tunnel Investigation of the Aerodynamic Characteristics of a Full-Scale Supersonic-Type Three-Bladed Propeller at Mach Numbers to 0.96. *NACA Report 1375*, 1958.
510. Hager, R. D.; and Vrabel, D.: Advanced Turboprop Project. *NASA SP-495*, 1988.
511. Vogeley, A. W.: Flight Measurements of Compressibility Effects on a Three-Bladed Thin Clark Y Propeller Operating at Constant Advanced-Diameter Ratio and Blade Angle. *NACA WR L-505*, 1945.
512. Hansen, J. R.: *Engineer In Charge—A History of the Langley Aeronautical Laboratory, 1917–1958*: *NASA SP-4305*, 1987.
513. Vogeley, A. W.: Sound-Level Measurements of a Light Airplane Modified to Reduce Noise Reaching the Ground. *NACA TR 926*, 1948.
514. Henderson, H. R.; Pegg, R. J.; and Hilton, D. A.: Results of the Noise Measurement Program on a Standard and Modified OH-6A Helicopter. *NASA TN D-7216*, Sept. 1973.

#### 4. REFERENCES

515. Ferrell, K. R.: Limited Stability and Control Evaluation of the S-62A Helicopter. AFFTC-TR-61-8, Air Force Flight Test Center, Edwards Air Force Base, Calif., Mar. 1961.
516. Pegg, R. J.; Henderson, H. R.; and Hilton, D. A.: Results of the Flight Noise Measurement Program Using a Standard and Modified SH-3A Helicopter. NASA TN D-7330, Dec. 1973.
517. Hayden, J. S.; and Lake, W. R.: YH-32 Limited Performance and Stability. AFFTC-TR-58-23, Air Force Flight Test Center, Edwards Air Force Base, Calif., 1958.
518. Hayden, J. S.; and Lake, W. R.: Performance Evaluation of the Djinn Helicopter. AFFTC-TR-60-8, Air Force Flight Test Center, Edwards Air Force Base, Calif., 1960.
519. Deming, A. F.: Propeller Rotation Noise Due to Torque and Thrust. NACA TN 747, Jan. 1940.
520. Stowell, E. Z.; and Deming, A. F.: Vortex Noise From Rotating Cylindrical Rods. NACA TN 519, Feb. 1935.
521. Williams, J. E. F.; and Hawkings, D. L.: Sound Generation by Turbulance and Surfaces in Arbitrury Motion. Philosophical Transactions of the Royal Society of London, vol. 264, no. 1151, May 1969.
522. Brentner, K. S.; and Farassat, F.: Modeling Aerodynamically Generated Sound of Helicopter Rotors. Progress in Aerospace Sciences, vol. 39, 2003, pp. 83–120.
523. Hennes, C. H.; Lopes, L.; Shirey, J.; and Erwin, J.: PSU-WOPWOP 3.3 User's Guide. Pennsylvania State University, University Park, Pa., 2007.
524. Gopalan, G.; and Schmitz, F. H.: Understanding Far Field Near-In-Plane High Speed Harmonic Helicopter Noise in Hover: Governing Parameters and Active Control Possibilities. Proc. American Helicopter Society Specialists' Conference on Aeromechanics, San Francisco, Calif., Jan. 2008.
525. Magliozzi, B.; Metzger, F. B.; Bausch, W.; and King, R. J.: A Comprehensive Review of Helicopter Noise Literature. FAA-RD-75-79, Systems Research and Development Service, Federal Aviation Administration, Washington, D.C., June 1975.
526. Fryer, B. A.: Publications in Acoustics and Noise Control From the NASA Langley Research Center During 1940–1979. NASA TM-80211, Jan. 1980.
527. Anon.: Helicopter Acoustics. NASA CP-2052-PT-1. Proc. International Specialists' Symposium, NASA Langley Research Center, Hampton, Va., May 22–24, 1978.
528. Anon.: NASA CP-2495, Vols. 1, 2, and 3. NASA/Army Rotorcraft Technology. Vol. 1: Aerodynamics, and Dyamics and Aeroelasticity; Vol. 2: Materials and Structures, Propulsion and Drive Systems, Flight Dynamics and Control, and Acoustics; and Vol. 3: Systems Integration, Research Aircraft, and Industry. NASA Ames Research Center, Moffett Field, Calif., 1988.
529. George, A. R.; and Kim, Y. N.: Helicopter Noise: State-of-the-Art. American Institute of Aeronautics and Astronautics (AIAA) J. Aircraft, vol. 15, no. 11, Nov. 1978.
530. Yamauchi, G. K.; and Young, L. A.: A Status of NASA Rotorcraft Research. NASA/TP-2009-215369, Sept. 2009.
531. Deming, A. F.: Noise From Propellers With Symmetrical Sections at Zero Blade Angle, II. NACA TN 679, Dec. 1938.

#### 4. REFERENCES

532. Hicks, C. W.; and Hubbard, H. H.: Comparison of Sound Emission From Two-Blade, Four-Blade, and Seven-Bladed Propellers. NACA TN 1354, July 1947.
533. Hubbard, H. Y. H.; and Lassiter, L. W.: Some Aspects of the Helicopter Noise Problem. NACA TN 3239, Aug. 1954.
534. Hubbard, H. H.: Noise Characteristics of Helicopter Rotors at Tip Speeds up to 900 Feet Per Second. *J. Acoustical Society of America*, vol. 32, no. 9, 1960.
535. Cox, C.; and Lynn, R. R.: A Study of the Origin and Means of Reducing Helicopter Noise. TCREC TR-62-73, Bell Helicopter Textron Inc., Ft. Worth, Tex., Nov. 1962.
536. Powell, A.: Theory of Vortex Sound. *J. Acoustical Society of America*, vol. 36, no. 1, 1964.
537. Schlegel, R.; King, R.; and Mull, H.: Helicopter Rotor Noise Generation and Propagation. USAVALABS TR 66-4, U.S. Army Aviation Material Laboratories, Ft. Eustis, Va., Oct. 1966.
538. Sternfeld, H., Jr.: Influence of the Tip Vortex on Helicopter Rotor Noise. AGARD CP-22, Gottingen, Germany, Sept. 1967.
539. Leverton, J. W.: Helicopter Noise—Blade Slap. Part 1: Review and Theoretical Study. NASA CR-1221, Oct. 1968.
540. Leverton, J. W.: Helicopter Noise—Blade Slap. Part 2: Experimental Results. NASA CR-1983, Mar. 1972.
541. Robinson, F.: Component Noise Variables of a Light Observation Helicopter. NASA CR-114761, 1973.
542. Hubbard, H. H.: Sound Measurements for Five Shrouded Propellers at Static Conditions. NACA TN 2024, Apr. 1950.
543. Hubbard, H. H.; and Lassiter, L. W.: Oscillating Pressures Near a Static Pusher Propeller at Tip Mach Numbers Up to 1.2 With Special Reference to the Effects of the Presence of the Wing. NACA TN 3202, July 1954.
544. Hubbard, H. H.: *Aeroacoustics of Flight Vehicles: Theory and Practice*. Vol. 1—Noise Sources, Vol. 2—Noise Control. NASA RP 1258, Aug. 1991.
545. Hubbard, H. H.: *Aeroacoustic of Flight Vehicles: Theory and Practice*. Volume 1: Noise Sources. NASA RP 1258-Vol-1, Aug. 1991.
546. Cox, C. R.; and Lynn, R. R.: A Study of the Orgin and Means of Reducing Helicopter Noise. U.S. Army Transportation Research Command TREC TR 62-73, 1962.
547. Schmitz, F.: Gaurav Gopalan 1975–2011. *AHS Vertiflite*, vol. 57, no. 4, 2011.
548. Barlow, W. H.; McCluskey, W. C.; and Ferris, H. W.: OH-6A Phase II Quiet Helicopter Program. USAMRDL TR 72-29, U.S. Army Air Mobility Research and Development Laboratories, Ft. Eustis, Va., Sept. 1972.
549. Hilton, D. A.; Henderson, H. R.; and Pegg, R. J.: Ground Noise Measurements During Flyover, Hover, Landing, and Take-off Operations of a Standard and a Modified HH-43B Helicopter. NASA TM X-2226, Feb. 1971.
550. Chiles, J. R.: Air America's Black Helicopter—The Secret Aircraft That Helped the CIA Tap Phones in North Vietnam. *Air & Space*, Mar. 2008.
551. Anon.: Noise Standards for Helicopters in the Normal, Transport, and Restricted Categories. Code of Federal Regulations (CFR) Title 14: Aeronautics and Space; Parts 21 and 36, 1979.

#### 4. REFERENCES

552. Anon.: Fly Neighborly Guide: Helicopter Association International, Alexandria, Va., 2012.
553. Cox, C. R.: Helicopter Noise Reduction and Its Effects on Operations. *J. American Helicopter Society*, vol. 15, no. 1, 1970.
554. Halwes, D.: Flight Operations to Minimize Noise. *AHS Vertiflite*, vol. 17, no. 2, 1971.
555. Cox, C. R.: How to Operate the Medium Helicopter More Quietly. *U.S. Army Aviation Digest*, vol. 19, no. 9, 1973.
556. Anon.: Annex 16—Environmental Protection, Volume I—Aircraft Noise. International Civil Aviation Organization (ICAO), Montreal, Canada. 2012.
557. Anon.: Code of Federal Regulations (CFR) Title 14: Aeronautics and Space; Part 36—Noise Standards: Aircraft Type and Airworthiness Certification, Appendices H and J, 2012.
558. Anon.: Code of Federal Regulations (CFR) Title 14: Aeronautics and Space; Part 36—Noise Standards: Aircraft Type and Airworthiness Certification, Appendix A2, Section A36.4. 2012.
559. Schmitz, F.; and Boxwell, D.: In-Flight Far-Field Measurement of Helicopter Impulsive Noise. *J. American Helicopter Society*, vol. 21, no. 4, 1976.
560. Schmitz, F.; and Yu, Y. H.: Theoretical Modeling of High-Speed Helicopter Impulsive Noise. *J. American Helicopter Society*, vol. 24, no. 1, 1979.
561. Brentner, K. S.; and Farassat, F.: Helicopter Noise Prediction: The Current Status and Future Direction. *J. Sound and Vibration*, vol. 170, no. 1, 1994, pp. 79–96.
562. Boxwell, D. A.; Schmitz, F. H.; Splettstoesser, W. R.; and Schultz, K. J.: Model Helicopter Rotor High-Speed Impulsive Noise: Measured Acoustics and Blade Pressures. NASA TM-85850, Sept. 1983.
563. Schmitz, F. H.; and Yu, Y. H.: Helicopter Impulsive Noise: Theoretical and Experimental Status. NASA TM-84390, Nov. 1983.
564. Boxwell, D. A.; and Schmitz, F. H.: Full-Scale Measurements of Blade-Vortex Interaction Noise. Proc. 36th Annual Forum of the American Helicopter Society, Washington, D.C., May 13–14, 1980.
565. Yamauchi, G. K.; Signor, D. B.; Watts, M. E.; Hernandez, F. J.; and LeMasurier, P.: Flight Measurements of Blade-Vortex Interaction Noise Including Comparisons With Full-Scale Wind Tunnel Data. *J. American Helicopter Society*, vol. 41, no. 4, 1996.
566. Signor, D. B.; Watts, M. E.; Hernandez, F. J.; and Felker, F. F.: Blade-Vortex Interaction Noise: A Comparison of In-Flight, Full-Scale and Small-Scale Measurements. Proc. AHS Aeromechanics Specialists' Conference, San Francisco, Calif., Jan 19–21, 1994.
567. Splettstoesser, W. R.; Schultz, K. J.; Boxwell, D. A.; and Schmitz, F. H.: Helicopter Model Rotor-Blade Vortex Interaction Impulsive Noise: Scalability and Parametric Variations. NASA TM-86007, Dec. 1984.
568. Zinner, R. A.; Boxwell, D. A.; and Spencer, R. H.: Review and Analysis of DNW/Model 360 Rotor Acoustic Data Base. NASA TM-102253, Nov. 1989.
569. Dawson, S.; Jordan, D.; Smith, C.; Ekins, J.; Silverthorn, L.; and Tuttle, B.: HARP Model Rotor Test at DNW. Proc. 45th American Helicopter Society Annual Forum, Boston, Mass., May 22–24, 1989.

570. Liu, S. R.; and Marcolini, M. A.: The Acoustic Results of a United Technologies Scale Model Helicopter Rotor Tested at DNW. Proc. 46th Annual Forum and Technology Display of the American Helicopter Society, Washington, D.C., May 21–23, 1990.
571. Yu, Y. H., et al.: The HART-II Test: Rotor Wakes and Aeroacoustics With Higher-Harmonic Pitch Control (HHC) Inputs—The Joint German/French/Dutch/U.S. Project. Proc. American Helicopter Society 58th Annual Forum, Montreal, Canada, June 11–13, 2002.
572. Boxwell, D. A.; Yu, Y. H.; and Schmitz, F. H.: Hovering Impulsive Noise—Some Measured and Calculated Results. *Vertica—The International Journal of Rotorcraft and Powered Lift Aircraft*, vol. 3, no. 1, 1979.
573. Baeder, J. D.: Euler Solution to Nonlinear Acoustics of Non-Lifting Hovering Rotor Blades. Proc. International Technical Specialists' Mtg., Rotorcraft Acoustics and Rotor Fluid Dynamics, Philadelphia, Pa., Oct. 15–17, 1991.
574. Brooks, T. F.; Boyd, D. D.; Burley, C. L.; and Jolly, J. R.: Aeroacoustic Codes for Rotor Harmonic and BVI Noise—CAMRAD.Mod 1/Hires. *J. American Helicopter Society*, vol. 45, no. 2, 2000.
575. Brooks, T. F.; and Burley, C. L.: Blade Wake Interaction Noise for a Main Rotor. *J. American Helicopter Society*, vol. 49, no. 1, 2004.
576. Burley, C. L.; and Brooks, T. F.: Rotor Broadband Noise Prediction With Comparison to Model Data. *J. American Helicopter Society*, vol. 49, no. 1, 2004.
577. Howlett, J. T.; Clevenson, S. A.; Rupf, J. A.; and Snyder, W. J.: Interior Noise Reduction in a Large Civil Helicopter. NASA TN D-8477, July 1977.
578. Cox, C. R.: Helicopter Noise Certification Experience and Compliance Cost Reductions. Proc. 19th European Rotorcraft Forum, Cernobbio (Como), Italy Sept. 14–16, 1993.
579. Marze, H. J.: Helicopter External Noise: ICAO Standards and Operational Regulations. Proc. Eighth European Rotorcraft and Powered Lift Aircraft Forum, Aix-en-Provence, France, Aug. 31–Sept. 3, 1982.
580. Conner, D. A.; Burley, C. L.; and Smith, C. D.: Flight Acoustic Testing and Data Acquisition for the Rotor Noise Model (RNM). Proc. 62nd American Helicopter Society Annual Forum, Phoenix, Ariz., May 9–11, 2006.
581. Johnson, C. L.: *Kelly—More Than My Share of It All*: Smithsonian Books, Washington, D.C., 1985.
582. Augustine, N. R.: *Augustine's Laws and Major System Development Programs*: American Institute of Aeronautics and Astronautics, 1984.
583. Anon.: *The Official Helicopter Blue Book*<sup>®</sup>, vols. XIV and later: HeliValue\$, Inc., Wauconda, Ill., 2010.
584. Harris, F. D.; and Scully, M. P.: Rotorcraft Cost Too Much. *J. American Helicopter Society*, vol. 43, no. 1, 1998.
585. Lloyd's Aviation Dept. (compiler): *Aircraft Types and Prices*. London, England: Lloyd's of London Press, 1974.
586. Shute, N.: *Stephen Morris. Heather Felicity Norway and Union Trustee Company of Australia, Ltd.*, 1961.

#### 4. REFERENCES

587. Harper, W.; and Richey, M.: Comanche RAH-66: Lessons Learned. U.S. Army Program Executive Office (PEO) Aviation, Ft. Rucker, Ala., 1995.
588. Galindo, J. L.: A Case History of the United States Army RAH-66 Comanche Helicopter. Master's Thesis, Naval Postgraduate School, Monterey, Calif., 2000.
589. McNerney, W. J., President: The Boeing Company 2011 Annual Report. The Boeing Company, Chicago, Ill., 2012.
590. Anon.: Helicopter Growth History Report. Forge Aerospace, Inc., Oct. 1978.
591. Wright, T. P.: Factors Affecting the Cost of Airplanes. *J. Aeronautical Sciences*, vol. 3, no. 4, 1936.
592. Raborg, R. W.: Mechanics of the Learning Curve. *Aero Digest*, vol. 65, no. 5, 1952.
593. Anon.: Source Book of World War II Basic Data: Airframe Industry, Vol. I—Direct Man-Hours – Progress Curves. Army Air Forces, Air Material Command (see also DTIC ADA 800199), 1946.
594. Alchian, A.: Reliability of Progress Curves in Airframe Production. RM-260-1, The RAND Corp., Santa Monica, Calif., Feb. 1950.
595. Joiner, W.: Private correspondance email to Frank Harris dated April 24, 2012.
596. Arrow, K.: The Economic Implications of Learning by Doing. *The Review of Economic Studies*, vol. 29, 1962.
597. Benkard, C. L.: Learning and Forgetting: The Dynamics of Aircraft Production. *The American Economic Review*, vol. 90, no. 4, 2000.
598. Nichols, J. B.: Sources of Helicopter Development and Manufacturing Costs. IAS Report No. 59-11, Proc. IAS 27th Annual Mtg., New York, N.Y., Jan. 26–29, 1959.
599. Anon.: Joint Design-to-Cost Guide, Life Cycle Cost as a Design Parameter. DTIC ADA048254, Departments of the U.S. Army, Navy, and Air Force, 1976.
600. Anon.: MIL-STD-881C. Work Breakdown Structures (WBS) for Defense Material Items. Department of Defense, Washington, D.C., Oct. 2011.
601. Heinemann, E. H.; and Rausa, R.: Ed Heinemann—Combat Aircraft Designer. Annapolis, Md.: Naval Institute Press, May 1980.
602. Anderson, J. L.: Price Determination of General Aviation, Helicopter, and Transport Aircraft. SAWE Paper No. 1224. Proc. 37th Annual Conference of the Society of Allied Weight Engineers, Inc., Munich, W. Germany, May 8–10, 1978.
603. Dubey, M.; and Yackle, A. R.: Establishing a Designer's Cost Target. Preprint No. 712, Proc. 29th AHS Annual National Forum, Washington, D.C., May 1973.
604. Lew, J. N.: Planning a General-Aviation Product. *J. Astronautics & Aeronautics*, Jan. 1977.
605. Dix, D. M.: Projecting Cost-Performance Trade-Offs for Military Vehicles. *J. Astronautics & Aeronautics*, Sept. 1976.
606. Bedard, P.: LHX in Trouble. *Defense Week*, vol. 7, no. 44, 1986.
607. Anon.: DoD Acquisition—Case Study of the Army Light Helicopter Program. GAO/NSIAD-86-45S-1, U.S. General Accounting Office, 1986.
608. Anon.: Defense Update—LH Team Scoring Analyzed. *Rotor & Wing*, June 1991, p. 10.
609. Harvey, D. S.: First Team's Perspective on the LH Competition. *Rotor & Wing*, June 1991, pp. 70–71.

#### 4. REFERENCES

610. Anon.: 1300 Comanches Replace 3100 Old Warriors. Boeing Sikorsky Advertisement in Army Magazine, June 1992.
611. Anon.: Defense Update—Boeing Sikorsky Reveals Design Change for Comanche Rotor. Rotor & Wing, Dec. 1991.
612. Bond, D. F.: Army Boosts RAH-66 Weight by 6%, Plans Extra Equipment. Aviation Week & Space Technology, Jan. 13, 1992.
613. Lytie, T.: Sikorsky's Comanche Helicopter Imperiled. New Haven Register, New Haven, Conn., June 11, 1992.
614. Bolkcom, C.: Army Aviation: The RAH-66 Comanche Helicopter Issue. CRS RS20522, Congressional Research Service, Library of Congress, Jan. 9, 2002.
615. Morris, J.: Army Cancels RAH-66 Comanche Helicopter After 20 Years, \$8 Billion. Aviation Week, Feb. 24, 2004.
616. McDaniels, R.: An Assessment of Developmental Risk for the RAH-66 Comanche Helicopter Development. Personal communication to F. D. Harris, Sept. 1991.
617. McDaniels, R.: The Case for Terminating the RAH-66 Comanche Helicopter Development. Personal communication to F. D. Harris, 1992.
618. Tishchencho, M. N.; Nagaraj, V. T.; and Chopra, I.: Preliminary Design of Transport Helicopters. J. American Helicopter Society, vol. 48, no. 2, 2003.
619. Jackson, P.; Peacock, L.; and Munson, K. (Eds.): Jane's All The World's Aircraft 2011–2012. London, England: Jane's Information Group, May 2011.
620. Anon.: National Defense Budget Estimates for FY 2012 (also called the Green Book). Office of the Under Secretary of Defense (Comptroller), Mar. 2011.
621. Anon.: Consumer Price Index (All Urban Consumers). U. S. Department of Labor, Bureau of Labor Statistics, Washington, D.C., 2012.
622. Patnode, C. A., Jr.: The Decision to Develop the UTTAS—A Case Study. DTIC AD-765 438, U.S. Army War College, Carlisle Barracks, Penn., Mar. 13, 1972.
623. Patnode, C. A., Jr.: Letter to F. D. Harris; comments on UTTAS Program. May 10, 2012.
624. Lammering, T.; Franz, K.; Risse, K.; Hoernschemeyer, R.; and Stumpf, E.: Aircraft Cost Model for Preliminary Design Synthesis. AIAA 2012-0686, Proc. 50th AIAA Aerospace Mtg., Nashville, Tenn., Jan. 9–12, 2012.
625. Burns, J. W.: Aircraft Cost Estimating Methodology and Value of a Pound Derivation for Preliminary Design Development Applications. J. Society of Allied Weight Engineers, Fall 1994.
626. Brooks, P. W.: The Modern Airliner: Its Origins and Development. London, England: Putnam & Co. Ltd., 1961.
627. Brooks, P. W.: The World's Airliners. London, England: Putnam & Co. Ltd., 1962.
628. Miller, R. E.; and Sawers, D.: The Technical Development of Modern Aviation. New York, N.Y.: Praeger Publications, 1970.
629. Loftin, L. K., Jr.: Quest for Performance—The Evolution of Modern Aircraft. NASA SP-468, 1985.
630. Warner, E. P.: Technical Development and Its Effect on Air Transportation: A Lecture: Norwich University, Northfield, Vt., 1938.

#### 4. REFERENCES

631. Harris, F. D.: Some Aviation History. Seminar at NASA Ames Research Center, Moffett Field, Calif., July 23, 2008 (rev. July 29, 2009).
632. Anderson, J. L.; and Andrastek, D. A.: Operating Cost Model for Local Service Airlines. SAWE Paper No. 1098, Index Category No. 29, Proc. Society of Allied Weight Engineers 35th Annual Conference, Philadelphia, Pa., 1976.
633. Maddalon, D. V.: Estimating Airline Operating Costs. NASA TM-78694, 1978.
634. Anon.: Standard Method of Estimating Comparative Direct Operating Costs of Turbine Powered Transport Airplanes. Air Transportation Association of America, Dec. 1967.
635. Brennan, T. J.; and Finizie, L. T.: Gas Turbine Cost Estimating. Proc. AIAA/SAE 12th Propulsion Conference, Palo Alto, Calif., July 26–29, 1976.
636. Harris, F. D.: An Economic Model of U.S. Airline Operating Expenses. NASA/CR-2005-213476, Dec. 2005.
637. Anon.: Operations Manual for Form 41 (inc. CD). Data Base Products, Inc., Dallas, Tex., 1999.
638. Davies, R. E. G.: Air Transport Directions in the 21st Century (The Lessons of History). Handbook of Airline Economics, Aviation Week, Div. of the McGraw-Hill Co., 2002.
639. Stoessel, R. F.; and Gallagher, J. E.: A Standard Method for Estimating VTOL Operating Expense (a More Realistic Approach). AIAA Paper No. 67-828, Proc. AIAA 4th Annual Mtg. and Technical Display, Anaheim, Calif., Oct. 23–27, 1967.
640. Conklin, A.; and de Decker, W.: Aircraft Cost Evaluator—Helicopters. Conklin & de Decker, Orleans, Mass., 2011.
641. Anon.: Sikorsky Commercial Links. Sikorsky Aircraft Corp., July 2005.
642. Anon.: When America Flies, It Works. Air Transport Association (ATA) 2010 Economic Report, Washington, D.C., 2011.
643. Anon.: Guide for the Presentation of Helicopter Operating Cost Estimates. Economics Committee, Helicopter Association International (HAI), Alexandria, Va., 2010.
644. Anon.: OH-58D System Specification AV-SS-NTSH-B10000A (special FCA edition). Bell Helicopter Textron, Inc., Ft. Worth, Tex., May 4, 1984.
645. Anon.: RotorBreeze Q1 issue, Bell Helicopter Textron Inc., Ft. Worth, Tex., 2012.
646. Pociask, M. J. (Ed.): 2009 Helicopter Annual, 27th Edition. The Helicopter Association International (HAI), Alexandria, Va., Jan. 2009.
647. Anon.: R22 Illustrated Parts Catalog: Robinson Helicopter Co. Inc., Torrance, Calif., 2007.
648. Anon.: Bell Model 206A/B/B3 Illustrated Parts Breakdown Manual: Bell Helicopter Textron, Inc., Ft. Worth, Tex., 2001.
649. Anon.: The Official Helicopter Specification Book. HeliValue\$, Inc., Wauconda, Ill., 2004.
650. Anon.: Bell Model 206 Series Maintenance Manual. Bell Helicopter Textron, Inc., Ft. Worth, Tex., 1998.
651. Anon.: R22 Beta II Estimated Operating Costs. Robinson Helicopter Co., Torrance, Calif., 2012.

#### 4. REFERENCES

652. Norling, A. H.: Outlook for Vertical-Lift Aircraft in Scheduled Commercial Transportation. United Research Inc., Cambridge, Mass., 1963.
653. Kruesi, F. E.: Civil Tiltrotor Development Advisory Committee Report to Congress. Volume I: Final Report (see ADA306654). U.S. Department of Transportation, Washington, D.C., Dec. 1995.
654. Kruesi, F. E.: Civil Tiltrotor Development Advisory Committee Report to Congress. Volume 2: Technical Supplement (see ADA306655). U.S. Department of Transportation, Washington, D.C., 1995.
655. Anon.: Helicopters. Report No. 198, American Society of Planning Officials, Chicago, Ill., 1965.
656. Anon.: The World's Air Transportation Services. Data as to Passengers, Mail, and Goods Carried by American and European Transportation Services. NACA TM 108, June 1922.
657. Tete, A.: Organization and Exploitation of Regular Aerial Transportation Lines. NACA TM 83, Apr. 1922.
658. Mayo, R. H.: Aviation and Insurance. NACA TM 93, May 1922.
659. Anon.: Aircraft Accidents—Method of Analysis. NACA TR 308, Aug. 1928.
660. Anon.: Aircraft Accidents—Method of Analysis. NACA TR 357, Jan. 1930.
661. Anon.: Aircraft Accidents—Method of Analysis. NACA TR 576, June 1936.
662. Anon.: Statistical Handbook of Civil Aviation. U.S. Department of Commerce, Civil Aeronautics Administration, Washington, D.C., 1944.
663. Anon.: Current Procedures for Collecting and Reporting U.S. General Aviation Accident and Activity Data. Safety Report NTSB/SR-05/02, PB205-917002 (Notation 7573A), National Transportation Safety Board Safety Report, Washington, D.C., 2005.
664. Anon.: Re-Registration and Renewal of Aircraft Registration. Code of Federal Regulations (CFR) Title 14: Aeronautics and Space; Parts 13, 47, and 91. U.S. Department of Transportation, Federal Aviation Administration, Washington, D.C., 2010.
665. Anon.: Rotorcraft Activity Survey. Executive Resource Associates, Inc., Arlington, Va. (also available as ADA 236698), 1989.
666. Harris, F. D.; Kasper, E. F.; and Iseler, L. E.: U.S. Civil Rotorcraft Accidents, 1963 through 1997. NASA/TM-2000-209597, Dec. 2000.
667. Persinos, J. F.: I Am Not A Compromising Woman. Rotor & Wing, Feb. 1999.
668. Allard, S.: CHC Presentation. International Helicopter Safety Symposium (IHSS), Montreal, Canada, Sept. 2005.
669. Downey, D. A.: The International Safety Team. Heliprops, vol. 20, no. 3, 2008.
670. Lamon, W.: Safety Saves \$\$ as Well as Lives. Rotor, Spring 1991.
671. Harris, F. D.: No Accidents—That's the Objective. J. American Helicopter Society, vol. 52, no. 1, 2007.
672. Wood, T.: High Energy Rotor System. Proc. American Helicopter Society 32nd Annual Forum, Washington, D.C., May 10–12, 1976.
673. Price, H. L.: Safety in Numbers—An Inaugural Lecture, The University of Leeds. West Yorkshire, England: Leeds University Press, 1967.

#### 4. REFERENCES

674. Johnson, W.; Yamauchi, G. K.; and Watts, M. E.: NASA Heavy Lift Rotorcraft Systems Investigation. NASA/TP-2005-213467, Dec. 2005.
675. Scott, M. W.: Aircraft Design Considerations to Meet One Engine Inoperative Safety Requirements. NASA CR-2012-216037, Aug. 2012.
676. Wood, T.: One Engine Inoperative (OEI) and Autorotation for Heavy Lift Rotorcraft System. NASA CR-2012-216038, Aug. 2012.
677. Karapetyan, G.: Mi-26 Autorotational Landings. Proc. American Helicopter Society 48th Annual Forum, Washington, D.C., June 3–5, 1992.
678. Anon.: Low Speed Flight Characteristics Which Can Result in Unanticipated Right Yaw. RotorBreeze, May/June 1991.
679. Dugan, D. C.; and Delamer, K. J.: The Implications of Handling Qualities in Civil Helicopter Accidents Involving Hover and Low Speed Flight. NASA/TM-2005-213473, Nov. 2005.
680. Anon.: Type Certificate Data Sheet (TCDS) No. H10WE, Rev. I. Department of Transportation, Federal Aviation Administration, Washington, D.C., Mar. 16, 1979.
681. Robertson, R.: Danger in the Sky. The Arizona Republic—Final Edition, Phoenix, Ariz., Nov. 15, 1992.
682. Anon.: Special Investigation Report—Robinson Helicopter Company R22 Loss of Main Rotor Control Accidents. NTSB/SIR-96/03, National Transportation Safety Board, Washington, D.C., Apr. 1996.
683. Anderson, S. B.: Historical Overview of Stall/Spin Characteristics of General Aviation Aircraft. AIAA J. Aircraft, vol. 16, no. 7, 1979.
684. Lebow, C.C. et al.: Safety in the Skies—Personnel and Parties in NTSB Aviation Accident Investigations. RAND Publishing, Santa Monica, Calif., Feb. 2008.
685. Boivin, D. L., Lt. Col.; and Forbes, D. T., Jr.: OH-6A Mishap Experience Report USAAAVS, U.S. Army Agency for Aviation Safety, Ft. Rucker, Ala., Oct. 1973.
686. Labun, L. C.: Rotorcraft Crash Mishap Analysis. Safe, Inc., Tempe, Ariz., 2009.
687. Waters, K. T.: Research Requirements to Improve Safety of Civil Helicopters. NASA CR-145260, Nov. 1977.
688. Fox, R. G.: Helicopter Accident Trends. Proc. AHS-FAA-HAI National Specialists' Mtg. on Vertical Flight Training Needs and Solutions, Arlington, Tex., Sept. 17–18, 1987.
689. Fox, R. G.: Measuring Risk in Single- and Twin-Engine Helicopters. American Helicopter Society 2nd Asian Vertiflite Seminar, Singapore, Feb 24, 1992.
690. Fox, R. G.: Measuring Safety Investment Effectiveness Relative to Risks. Proc. American Helicopter Society 54th Annual Forum, Washington, D.C., May 20–22, 1998.
691. Schwirzke, M. F. J.: Near Term Gains in Rotorcraft Safety—Strategies for Investment. Workshop sponsored by NASA Ames Research Center, Moffett Field, Calif., Feb. 1999.
692. Hart, S. G. (Ed.): Final Report of the Helicopter Accident Analysis Team. Flight Control and Cockpit Integration Branch, Army/NASA Rotorcraft Div., NASA Ames Research Center, Moffett Field, Calif. July 1998 (Limited Distribution).
693. Shute, N.: Slide Rule. London, England: William Heinemann Ltd., 1954.

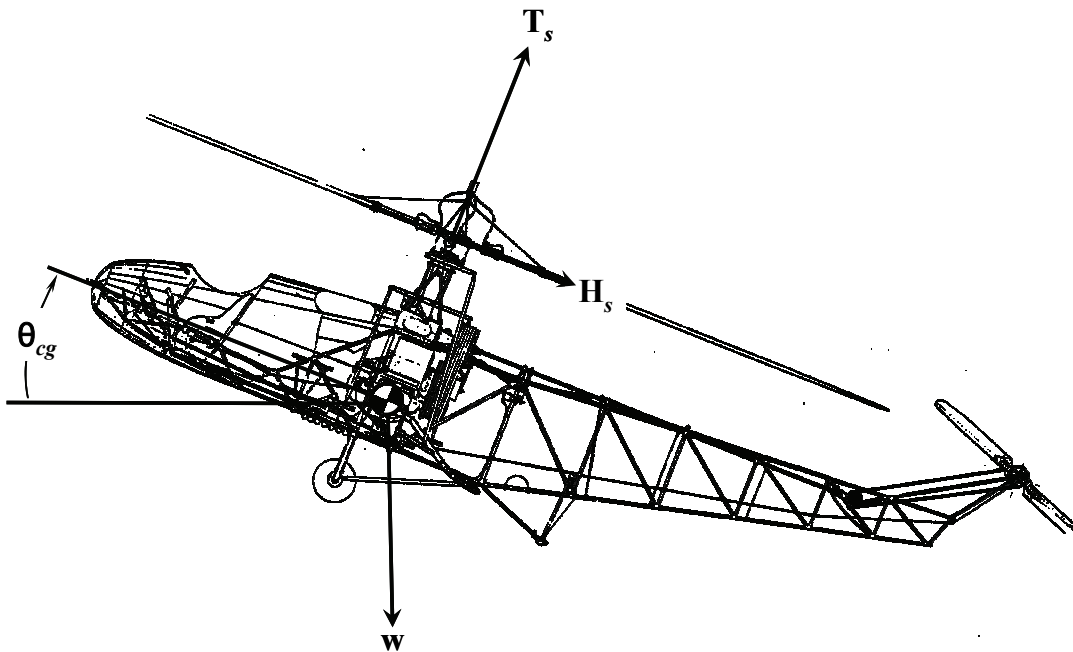
## APPENDIX A

### ROTORCRAFT STABILITY AND CONTROL IN HOVER

For the early helicopters, this subject might be better titled *Control and Instability*. The quadrotor helicopter in and about hover was, however, very nearly stable in both longitudinal/pitch and lateral/roll because of its widely displaced rotors. The tandem rotor helicopter is nearly inherently stable in longitudinal/pitch for the same reason. However the tandem rotor helicopter lacks comparable stability in its lateral/roll motion because both rotor hubs lie in the plane of symmetry. The most inherently unstable helicopter is the single-main-rotor plus anti-torque tail rotor helicopter. Despite this shortcoming, this latter configuration has gained the widest acceptance because of its relative mechanical simplicity. A simple introduction to coupled longitudinal/pitch stability and control for the single-main-rotor helicopter provides considerable insight into the general problem. It also affords a jumping-off point for more advanced study.

#### Longitudinal/Pitch Equations of Motion

The simplified force-and-moment diagram for a single-main-rotor helicopter in hover was shown in Fig. 1-5 on page 10 and is repeated here for convenience.



The primary forces and moments involved in *longitudinal* helicopter stability and control in hover.

## APPENDIX A

The equations for all six components of motion can be reduced, based on more advanced work, to (1) fore and aft or longitudinal motion at nearly constant height and (2) helicopter pitching motion. The two equations describing the motion of this rotorcraft's center of gravity (cg) are

$$(1) \quad \sum F_x = -W \times \theta_{cg} - H_s - \frac{W}{g} \frac{\partial^2 x_{cg}}{\partial t^2} = 0, \text{ and}$$

$$(2) \quad \sum M_{cg} = h \times H_s + M_p - I_{cg} \frac{\partial^2 \theta_{cg}}{\partial t^2} = 0.$$

These two equations of motion assume that rotor thrust ( $T_s$ ) is equal to helicopter weight ( $W$ ) and that the body pitch angle ( $\theta_{cg}$ ) is a small angle. The rotor inplane force, called the rotor H-force ( $H_s$ ), acts in the rotor plane perpendicular to the rotor shaft and is positive when directed aft. Thus, the H-force acts at the hub, which is a distance ( $h$ ) above the center of gravity. The rotor blades can introduce a hub pitching moment ( $M_p$ ).

Small perturbations from a trim condition in both longitudinal displacement ( $x_{cg}$ ) and body pitch angle are usually assumed when solving these simplified equations of motion. Also, it is common to replace the longhand notations of  $\partial^2 x_{cg} / \partial t^2$  and  $\partial^2 \theta_{cg} / \partial t^2$  with  $\Delta \ddot{x}_{cg}$  and  $\Delta \ddot{\theta}_{cg}$  and then dropping the subscript, cg, to study the engineering problem in shorthand. Following this notation practice leads to rewriting Eqs. (1) and (2) as

$$(3) \quad \frac{W}{g} \times \Delta \ddot{x} + \Delta H_s + W \times \Delta \theta = 0, \text{ and}$$

$$(4) \quad I \times \Delta \ddot{\theta} - \Delta M_p - h \times \Delta H_s = 0.$$

The fact that the problem is one of small perturbations is highlighted by using the Greek letter delta ( $\Delta$ ), which also gets dropped later in the analysis as you might have guessed.

The perturbations in the rotor force and moments are created as

$$(5) \quad \Delta H_s = \frac{\partial H_s}{\partial V_{hub}} \times \Delta V_{hub} + \frac{\partial H_s}{\partial \dot{\theta}_{hub}} \times \Delta \dot{\theta}_{hub} + \frac{\partial H_s}{\partial \delta_{cyclic}} \times \Delta \delta_{cyclic}, \text{ and}$$

$$(6) \quad \Delta M_p = \frac{\partial M_p}{\partial V_{hub}} \times \Delta V_{hub} + \frac{\partial M_p}{\partial \dot{\theta}_{hub}} \times \Delta \dot{\theta}_{hub} + \frac{\partial M_p}{\partial \delta_{cyclic}} \times \Delta \delta_{cyclic}.$$

These simplified equations for perturbations in rotor force and moments do not include the effect of body accelerations, which do exist but can be assumed to be of second-order in importance. On the other hand, a provision is made in Eqs. (5) and (6) for the pilot input or control through the longitudinal cyclic stick motion ( $\Delta \delta_{cyclic}$ ).

It is important to note that the velocities at the rotor hub are not necessarily the same as those seen by the rotorcraft center of gravity. While there can be very important structural deformations between these two points within the body, only the geometry of the problem is considered in this elementary analysis. The velocity relations between the center of gravity and the hub as shown in Fig. 1-5 are

$$(7) \quad \Delta\theta_{\text{hub}} = \Delta\theta_{\text{cg}} = \theta,$$

$$(8) \quad \Delta\dot{\theta}_{\text{hub}} = \Delta\dot{\theta}_{\text{cg}} = \dot{\theta}, \text{ and}$$

$$(9) \quad \Delta V_{\text{hub}} = \Delta \dot{x}_{\text{cg}} - h \times \Delta \dot{\theta}_{\text{cg}} = \dot{x} - h \dot{\theta}.$$

The several relationships defined by Eqs. (3) through (9) can now be combined to rewrite the equations of motion a third time. First Eqs. (8) and (9) are inserted in Eqs. (5) and (6). Then the expanded expressions for  $\Delta H_s$  and  $\Delta M_p$  are substituted into Eqs. (3) and (4). Finally, a collection of terms is made. The result of these few steps is

$$(10) \quad \frac{W}{g} \ddot{x} + H_v \dot{x} + (H_{\dot{\theta}} - h H_v) \dot{\theta} + W \theta + H_{\delta} \delta = 0, \text{ and}$$

$$(11) \quad I \ddot{\theta} + [h(M_v + h H_v) - (M_{\dot{\theta}} + h H_{\dot{\theta}})] \dot{\theta} - (M_{\delta} + h H_{\delta}) \dot{x} - (M_{\delta} + h H_{\delta}) \delta = 0.$$

Simplifying this math problem is really quite easy if a less classical approach is taken. You need only differentiate the moment equation, Eq. (11), once with respect to time, which defines the longitudinal acceleration called for in Eq. (10). Then this result, along with the longitudinal velocity from Eq. (11), are substituted into the force equation, Eq. (10). This quickly gives a third-order, ordinary differential equation for the body pitch motion of

$$(12) \quad \frac{W I}{g} \ddot{\theta} + \left[ \frac{W}{g} [h(M_v + h H_v) - (M_{\dot{\theta}} + h H_{\dot{\theta}})] + I H_v \right] \dot{\theta} + (M_v H_{\dot{\theta}} - M_{\dot{\theta}} H_v) \dot{\theta} \\ + W(M_v + h H_v) \theta = \frac{W}{g} (M_{\delta} + h H_{\delta}) \dot{\delta} + (M_{\delta} H_v - M_v H_{\delta}) \delta$$

You have no doubt noticed at this point that some more shorthand has been applied in reaching the preceding result. All the force-and-moment partial derivatives that were written in longhand in Eqs. (5) and (6) have been replaced with a subscript notation. For example,  $\partial H_s / \partial V_{\text{hub}}$  has been replaced with  $H_v$ , and so on.

### Solutions to the Equations of Motion

There are three solutions to Eq. (12) that are of considerable interest. The first solution sheds light on the motion immediately following a wind gust or a pilot's abrupt control input. The second solution investigates the "stick-fixed" inherent stability characteristics. The third solution is obtained when the equations of motion are installed in a flight simulator, and a "pilot is put into the loop." This third solution is more applicable to advanced work and will

not be discussed further here.<sup>1</sup> Generally, however, all three solutions accept the same initial conditions: that at time equals zero, the initial pitch angle and initial pitch rate are both zero (i.e., at  $t = 0$ ,  $\Delta\theta_{cg} = \theta = 0$  and  $d\theta/dt = 0$ ). Consider the time history solution around  $t = 0$  first.

The solution to Eq. (12) for the first several seconds of a time history (i.e., from  $t = 0$  to, say,  $t = 4$  or 5 seconds) is obtained in a very straightforward manner by assuming a Maclaurin power series in time. That is, let

$$(13) \quad (A-13) \quad \theta_{(t)} = \theta_{(0)} + \dot{\theta}_{(0)} \times \frac{t}{1!} + \ddot{\theta}_{(0)} \times \frac{t^2}{2!} + \ddot{\theta}_{(0)} \times \frac{t^3}{3!} + \dots \dots$$

Now consider a common situation where the rotorcraft is hit by a gust of wind ( $V_{gust}$ ) that upsets the vehicle trim. Assume that the gust remains constant over the initial 4- or 5-second time frame of interest. Or perhaps the pilot puts in an initial displacement of longitudinal cyclic stick ( $\delta_{cyclic}$ ) and then holds the stick fixed over these few seconds. This latter case would be a step input that can simulate a gust in a controlled manner. These preceding statements define the initial conditions of the problem in the following way. For  $t = 0$ ,

$$\begin{aligned} x = 0 \quad \theta = 0 \quad \delta_{cyclic} = \delta_{step} \text{ and / or } \dot{x} = V_{gust} \quad \dot{\theta} = 0 \\ \ddot{x} = -\frac{gH_v}{W} V_{gust} \quad (\text{from Eq. 10}) \quad \dot{\delta}_{step} = 0 \\ (14) \quad \ddot{\theta} = \frac{(M_v + hH_v)}{I} V_{gust} + \frac{(M_\delta + hH_\delta)}{I} \delta_{step} \quad (\text{from Eq. 11}) \\ \ddot{\theta} = -\left[ \frac{[h(M_v + hH_v) - (M_\theta + hH_\theta)]}{I} + \frac{g}{W} H_v \right] \ddot{\theta} \\ + \frac{g(M_\delta H_v - M_v H_\delta)}{WI} \delta_{step} \quad (\text{from Eq. 12}) \end{aligned}$$

With these initial conditions, the power series solution approach to finding the rotorcraft pitch response in the first few seconds of motion yields directly

$$(15) \quad \theta = +V_{gust} \frac{(M_v + hH_v)}{I} \left\{ \frac{t^2}{2} - \frac{t^3}{6} \left[ \frac{h(M_v + hH_v) - (M_\theta + hH_\theta)}{I} + \frac{g}{W} H_v \right] \right\} \\ + \delta_{step} \frac{(M_\delta + hH_\delta)}{I} \left\{ \frac{t^2}{2} - \frac{t^3}{6} \left[ \frac{h(M_v + hH_v) - (M_\theta + hH_\theta)}{I} + \frac{g}{W} H_v \right] \right\} + \delta_{step} \frac{g(M_\delta H_v - M_v H_\delta)}{IW} \left\{ \frac{t^3}{6} \right\}.$$

---

<sup>1</sup> A simple solution using a small personal computer plus a “joy stick” will immediately show how hard a helicopter can be to hover. It is also fun!

The longitudinal velocity is defined from Eq. (10) in terms of the pitch angle ( $\theta$ ) and its two derivatives with respect to time as

$$(16) \quad \dot{x} = \left[ \frac{h(M_v + hH_v) - (M_{\dot{\theta}} + hH_{\dot{\theta}})}{M_v + hH_v} \right] \dot{\theta} + \left[ \frac{I}{M_v + hH_v} \right] \ddot{\theta}.$$

The distance the rotorcraft travels from the spot over the ground where the disturbance occurred is the integral of the relative velocity with respect to time. This distance is simply

$$(17) \quad x = \int_0^t (\dot{x} - V_{\text{gust}}) dt.$$

Now consider the second solution for longitudinal and pitch motion when the control is fixed. This is a matter of solving Eq. (12) in its homogeneous form where the right-hand side is set to zero. Information about the dynamic motion such as damping or lack of damping and the associated frequency of any mode that oscillates is generally sought. The solution method is available in any number of mathematical textbooks so only the result is given here:

$$(18) \quad \theta = V_{\text{gust}} \frac{(M_v + hH_v)}{I[(\lambda - R)^2 + \omega^2]} \left[ e^{\lambda t} - e^{Rt} \cos \omega t + \frac{(R - \lambda)}{\omega} e^{Rt} \sin \omega t \right].$$

Again, the longitudinal velocity is defined from Eq. (10) in terms of the pitch angle ( $\theta$ ) and its two derivatives with respect to time. The parameters of  $\lambda$ ,  $R$ , and  $\omega$  that complete the solution are found by finding the roots to the following cubic:

$$(19) \quad \frac{WI}{g} X^3 + \left[ \frac{W}{g} [h(M_v + hH_v) - (M_{\dot{\theta}} + hH_{\dot{\theta}})] + IH_v \right] X^2 + (M_v H_{\dot{\theta}} - M_{\dot{\theta}} H_v) X + W = 0.$$

Given that the basic motion is oscillatory, this cubic will have one real root,  $\lambda$ , and a pair of complex roots,  $R \pm i\omega$ . Solving this cubic is a minor matter in this day and age. The cubic roots from Eq. (19) are, of course, then substituted into Eq. (18), which completes the solution of the stick-fixed stability problem.

### Stability Derivative Approximations

Six rotor stability derivatives must be defined to make practical use of the general solutions given above. The first-order approximations for the rotor H-force and hub pitching moment ( $M_p$ ) were introduced in Volume I as

$$(20) \quad M_p = \frac{F_c r_b b}{2} \times a_{1S}, \text{ and}$$

$$(21) \quad H_S = T_S \times a_{1S} - \left[ \frac{2a \sigma R \lambda_S}{\gamma V_t C_T} \right] \times T_S \times \dot{\theta}_{\text{hub}} + \left[ \frac{\rho b c R V_t^2 C_{d0}}{4} \right] \times \mu_S.$$

## APPENDIX A

You will recall from Volume I that the nomenclature involved here is:

$$\begin{aligned}
 a &= 5.73 \quad \text{per radian, blade airfoil lift curve slope} \\
 C_{d0} &\approx 0.01 \quad \text{blade airfoil drag coefficient} \\
 \sigma &= bcR/\pi R^2 \quad \text{rotor solidity} \\
 \gamma &= \rho acR^4/I_f \quad \text{blade Lock number} \\
 I_f &= \int_0^R r^2 dm \approx 2F_C R^3/3V_t^2 \quad \text{blade moment of inertia} \\
 F_C &= \int_0^R \Omega^2 r dm \approx \frac{L_b}{\beta_0} \approx \frac{W}{b\beta_0} \quad \text{blade centrifugal force} \\
 C_T &= T_s/\rho\pi R^2 V_t^2 \quad \text{rotor thrust coefficient} \\
 \lambda_s &= -\sqrt{C_T}/2 \quad \text{rotor inflow (negative for flow down)} \\
 \mu_s &= \frac{V \cos \alpha_s}{V_t} \approx \frac{V_{\text{hub}}}{V_t} \quad \text{rotor advance ratio}
 \end{aligned}$$

With this nomenclature in mind, the rotor H-force can be put in the more practical form of

$$(22) \quad H_s = W \times a_{1s} + \frac{2W\sqrt{2C_T}}{3\Omega\beta_0} \times \dot{\theta}_{\text{hub}} + \frac{\rho bcR V_t^2 C_{d0}}{4} \times \mu_s.$$

The middle term in the H-force equation accounts for a somewhat reduced level in damping provided to the rotorcraft by this inplane force. This effect was brought to the industry's attention nearly simultaneously in 1950 by Rene Miller<sup>2</sup> and by Ken Amer<sup>3</sup> of the N.A.C.A. Amer's results included the influence of forward speed. Amer showed that a potentially serious roll instability could occur at high speed, even for the single rotor helicopters of that day. Flight test data confirmed the undesirable trait.

The final approximation to have in hand deals with the longitudinal flapping ( $a_{1s}$ ). A reasonably accurate approximation for operation in and about hover is

$$(23) \quad a_{1s} = \left[ \frac{16C_T}{\sigma a} + \sqrt{2C_T} \right] \times \mu_s - \left[ \frac{16}{\gamma\Omega} \right] \times \dot{\theta}_{\text{hub}} - B_{1c}.$$

The six rotor derivatives can be written down almost by inspection, simply by referring to Eqs. (20, 22, and 23) and following the chain rule. An example of the chain rule is

$$M_v = \frac{\partial M_p}{\partial V_{\text{hub}}} = \frac{\partial M_p}{\partial a_{1s}} \times \frac{\partial a_{1s}}{\partial \mu_s} \times \frac{\partial \mu_s}{\partial V_{\text{hub}}}.$$

<sup>2</sup> Miller, R.: *Helicopter Control and Stability in Hovering Flight*. Journal of the Aeronautical Sciences, Aug. 1948.

<sup>3</sup> Amer, K. B.: *Theory of Helicopter Damping in Pitch and Roll and a Comparison with Flight Measurements*. NACA TN 2136, 1950.

Thus, the four stability derivatives are approximated to the first order as

$$\begin{aligned}
 (a) \quad H_v &= W \times \left[ \frac{16C_T}{\sigma a} + \sqrt{2C_T} \right] \times \frac{1}{V_t} + \left[ \frac{\rho b c R V_t^2 C_{d0}}{4} \right] \times \frac{1}{V_t} \\
 (b) \quad H_{\dot{\theta}} &= W \times \left[ \frac{-16}{\gamma \Omega} \right] + \frac{32 W \sqrt{2C_T}}{3 \Omega \beta_0} \\
 (c) \quad M_v &= \frac{F_C r_\beta b}{2} \times \left[ \frac{16C_T}{\sigma a} + \sqrt{2C_T} \right] \times \frac{1}{V_t} \\
 (d) \quad M_{\dot{\theta}} &= \frac{F_C r_\beta b}{2} \times \left[ \frac{-16}{\gamma \Omega} \right].
 \end{aligned}
 \tag{24}$$

In a similar manner, the two control derivatives are approximated to the first order as

$$\begin{aligned}
 (a) \quad H_\delta &= W \times (-1) \times \frac{\partial B_{1C}}{\partial \delta}, \text{ and} \\
 (b) \quad M_\delta &= \frac{F_C r_\beta b}{2} \times (-1) \times \frac{\partial B_{1C}}{\partial \delta}.
 \end{aligned}
 \tag{25}$$

These four rotor stability and two control derivatives can be calculated with any number of successively higher order theories given today's computer power. For example, Wayne Johnson provides state-of-the-art rotorcraft technology in a very comprehensive analysis called CAMRAD II. At the opposite end of the scale is the most rudimentary evaluation found here that accurately captures 90 percent of the fundamental physics in 10 percent of the time.

Two helpful points are illustrated by the rotor-force-and-moment derivatives tabulated by Eqs. (24) and (25). The first is that each derivative depends on rotorcraft weight (in this case, where  $T_s = W$ ). You can see this by noting that centrifugal force in the hub pitching moment per unit of longitudinal flapping can be replaced by  $W/b\beta_0$ . This substitution can be very helpful because a general rule of thumb is that ( $\beta_0$ ), the steady coning angle, is on the order of 0.1 radians. The hub pitching moment ( $M_p$ ) is then restated as

$$(26) \quad M_p = \frac{F_C r_\beta b}{2} \times a_{1S} = \frac{W r_\beta}{2 \beta_0} \times a_{1S}.$$

The second point is that a new rotorcraft parameter is introduced in Eq. (25). This parameter measures the connection between the pilot and the rotor blade. The connection between the longitudinal cyclic stick ( $\delta_{\text{cyclic}}$ ) and the longitudinal blade feathering angle (i.e., the longitudinal cyclic pitch angle,  $B_{1C}$ ) is defined by the control system. Common, everyday engineering practice expresses this key linkage ratio ( $\partial B_{1C} / \partial \delta_{\text{cyclic}}$ ) in degrees of  $B_{1C}$  per inch of  $\delta_{\text{cyclic}}$  travel. The sign convention is that (1) nose-up blade feathering at the advancing blade azimuth of  $\psi = 90$  degrees is created by  $-B_{1C}$ , and (2) the pilot pulling aft on the stick is

## APPENDIX A

+  $\delta_{cyclic}$  travel.<sup>4</sup> Typical ratios are on the order of plus 2 degrees of nose-up blade feathering at  $\psi = 90$  degrees per inch of aft stick travel for rotor systems that have a flapping hinge offset ( $r_\beta$ ). When  $r_\beta = 0$ , the linkage ratio is more like 3 degrees per inch. From the pilot's point of view, he expects that 1 inch of aft stick will tilt the tip path plane 2 or 3 degrees aft.

Studying rotorcraft inherent stability and response in the first 4 to 5 seconds is much more interesting using real numbers from a represented single rotor helicopter. Bramwell<sup>5</sup> suggests a configuration having the following physical properties:

### Example Helicopter

#### Input Data

$$W = 10,000 \text{ lbs}, \quad \rho = 0.002378 \text{ slug} / \text{ft}^3, \quad g = 32.174 \text{ ft} / \text{sec}^2$$

$$I_{cg} = 25,000 \text{ slug} - \text{ft}^2, \quad h = 7 \text{ feet}, \quad r_\beta = 1 \text{ foot}$$

$$R = 25 \text{ feet}, \quad c = 1 \text{ foot}, \quad b = 4 \text{ blades}$$

$$V_t = 685 \text{ ft} / \text{sec} \quad \text{and} \quad \beta_0 = 0.075 \text{ rad} \approx 4.3 \text{ deg}$$

$$\frac{\partial B_{1C}}{\partial \delta_{cyclic}} \approx -2 \text{ deg} / \text{inch} = -0.03491 \text{ rad} / \text{inch}$$

#### Calculated Data

$$\Omega = 27.4 \text{ rad} / \text{sec}, \quad C_T = 0.004564 \quad \text{and} \quad \frac{C_T}{\sigma} = 0.08962$$

$$F_C = 33,333 \text{ lbs}, \quad \gamma = 7.193, \quad I_f = 740 \text{ slug} - \text{ft}^2$$

$$\frac{\partial M_P}{\partial a_{1S}} = \frac{F_C r_\beta b}{2} = \frac{W r_\beta}{2 \beta_0} = 66,667 \text{ ft} - \text{lbs} / \text{rad}$$

Following Eqs. (24) and (25), the six rotor longitudinal derivatives are then calculated as

#### Stability Derivatives

$$H_v = +5.455 \quad \text{lbs per ft} / \text{sec}$$

$$H_\theta = -501.877 \quad \text{lbs per rad} / \text{sec}$$

$$M_v = +33.654 \quad \text{ft} - \text{lbs per ft} / \text{sec}$$

$$M_\theta = -5412.198 \quad \text{ft} - \text{lbs per rad} / \text{sec}$$

#### Control Derivatives

$$H_\delta = +349.066 \quad \text{lbs per inch}$$

$$M_\delta = +2327.106 \quad \text{ft} - \text{lbs per inch}$$

<sup>4</sup> Refer to the discussion in Volume I, pages 76–77.

<sup>5</sup> Bramwell, A. R. S.: *Bramwell's Helicopter Dynamics*. John Wiley & Sons, New York, N.Y., 1976.

It is more convenient to use these first-order stability and control derivatives in the groupings suggested by Eq. (12). This helps to see the key rotorcraft parameters. Therefore, calculate

$$\begin{aligned}
 M_v + h H_v &= +71.841 \\
 M_{\dot{\theta}} + h H_{\dot{\theta}} &= -8925.334 \\
 M_v H_{\dot{\theta}} - M_{\dot{\theta}} H_v &= +12,633.372 \\
 h (M_v + h H_v) - (M_{\dot{\theta}} + h H_{\dot{\theta}}) &= +9428.220 \\
 M_{\delta} + h H_{\delta} &= +4770.567 \\
 M_{\delta} H_v - M_v H_{\delta} &= +947.673
 \end{aligned}$$

### Response in the First 4 to 5 Seconds

The initial response to a wind gust was given in Eq. (15) as

$$(27) \quad \theta = +V_{\text{gust}} \frac{(M_v + h H_v)}{I} \left\{ \frac{t^2}{2} - \frac{t^3}{6} \left[ \frac{h(M_v + h H_v) - (M_{\dot{\theta}} + h H_{\dot{\theta}})}{I} + \frac{g}{W} H_v \right] \right\}.$$

Suppose the example single rotor helicopter is upset by a mild, 5-foot-per-second gust and that this gust remains constant for about 5 seconds. Then the initial response would be for the rotorcraft to pitch up. The pitch angle, numerically expressed in degrees, would be described as

$$\begin{aligned}
 (28) \quad \theta &= +.8232 \left[ \frac{t^2}{2} - \frac{t^3}{6} (.3771 + .0176) \right] = +.4116 t^2 - .05415 t^3 \\
 &= +.4116 t^2 (1 - .1316 t) \quad \text{in degrees}
 \end{aligned}$$

The initial response to a gust is clearly a nose-up pitch motion. The motion increases as the square of time, which is a rather abrupt response. On the other hand, there is some pseudo damping in that the coefficient of  $t^3$  is negative. The pitch-up, therefore, reaches a maximum and then the helicopter begins to return to a level attitude. However, the motion is unstable and the next cycle becomes more extreme.

### Inherent Stability

The early helicopters were clearly unstable in and about hover. The example helicopter illustrates this point quite vividly. The exact solution to the two-degrees-of-freedom flying qualities problem was given as

$$(18) \quad \theta = V_{\text{gust}} \frac{(M_v + h H_v)}{I \left[ (\lambda - R)^2 + \omega^2 \right]} \left[ e^{\lambda t} - e^{Rt} \cos \omega t + \frac{(R - \lambda)}{\omega} e^{Rt} \sin \omega t \right]$$

APPENDIX A

in which the parameters of  $\lambda$ ,  $R$ , and  $\omega$  for the example helicopter are determined from the roots of the cubic given by Eq. (19) as

$$\lambda = -0.627154 \quad R = +0.116236 \quad \omega = +0.365939 .$$

These numerical results give the pitching motion in response to the 5-foot-per-second gust, expressed in degrees, as

$$(29) \quad \theta = 1.19911 \left[ e^{-0.627t} - e^{+0.116t} \cos(0.366t) + 2.031 e^{+0.116t} \sin(0.366t) \right] \\ \approx 1.2e^{-0.627t} + \left[ 2\sin(0.366t) - \cos(0.366t) \right] e^{+0.116t}$$

Fig. A-1 gives you an idea of just how unstable this example helicopter is in response to the gust. In about 10 seconds, the motion would be truly frightening to a first-time student. The helicopter would (1) be pitching down at a rate of 3 degrees per second, (2) be some 75 feet from the original hovering spot, and (3) still be going backwards at about 15 feet per second. Of course the pilot, well before 10 seconds had passed, would have pushed the longitudinal cyclic stick forward as the nose came up. (The trick to flying such an unstable aircraft is to time the control input well in advance of the diverging behavior. Pilots seem, therefore, to be clairvoyant.)

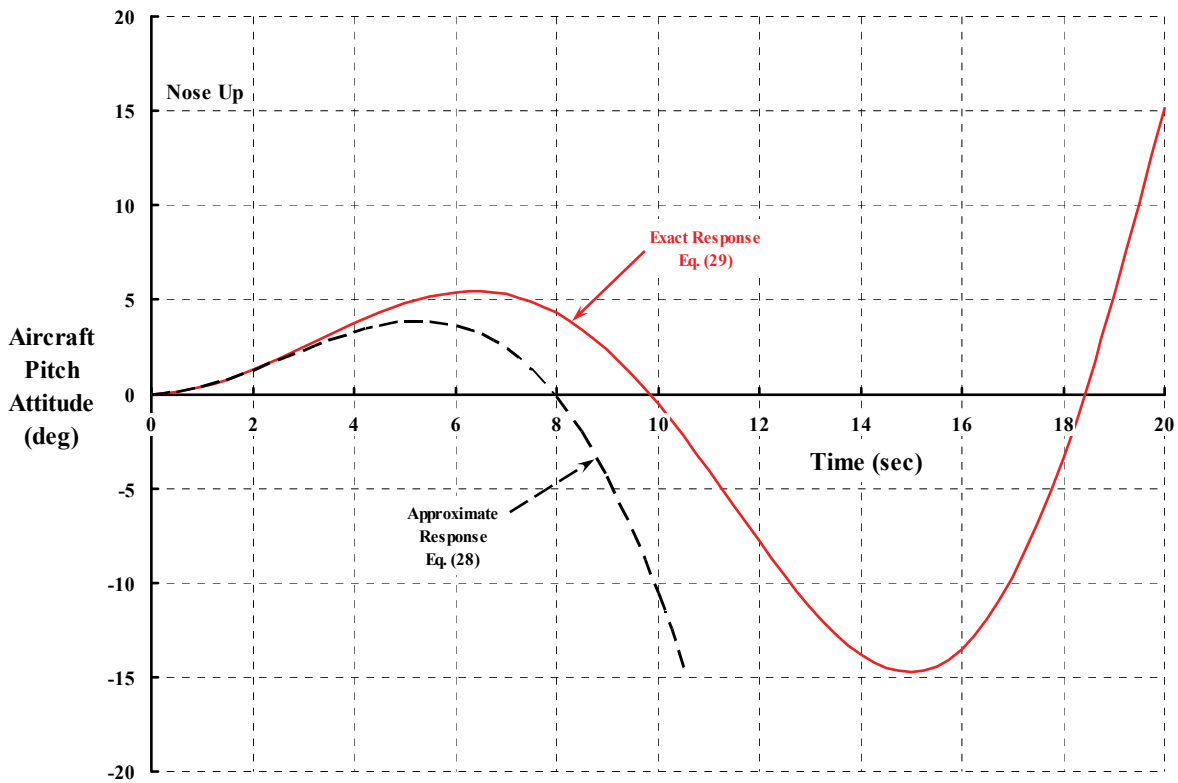


**Fig. A-1. Helicopters are inherently unstable in hover. Example helicopter response to a 5-ft/sec gust with controls fixed.**

A feeling for the level of instability can be obtained without even graphing the actual motions by using the complex roots of the cubic equation. The positive value for  $R$ —the real part of the complex roots of the cubic, defined from  $R \pm i \Omega$ —establishes the time it takes for the motion to double in amplitude. That is,

$$(30) \quad \text{Time to double amplitude} = \frac{\ln 2}{R} = \frac{0.693315}{R} \text{ in seconds.}$$

For this example helicopter, the motion doubles in amplitude every 6 seconds, which is very quick when first learning to hover. The time to complete one cycle of the oscillation is found from the imaginary part of the complex roots,  $\Omega$ , quite simply as

$$(31) \quad \text{Time for one cycle} \equiv \text{Period} = \frac{2\pi}{\Omega} \text{ in seconds.}$$

In this example, the time to complete one cycle, which is commonly referred to as the period, is about 17 seconds. This is also rather quick and does not allow one to really let go of the control stick.

The approximation to the exact solution given by Eq. (28) is also shown in Fig. A-1. The conclusion reached by both results is that helicopter hovering instability is caused by the rotor flapping—specifically, the flapping in response to the changes in speed.

### Pilot Control

Control of an unstable helicopter in hover is accomplished with well-timed, but small, stick movements. In fact, if the control could be applied at the instant a gust upset occurred, there would be no nose-up pitch motion of the helicopter. You can see this from Eq. (15) by setting  $\theta = 0$ . The stick travel needed to cancel a wind gust would then be

$$(32) \quad \delta_{\text{step}} \approx -V_{\text{gust}} \frac{(M_v + h H_v)}{(M_\delta + h H_\delta)}.$$

For the example helicopter, this amounts to less than 0.1 inch of forward longitudinal cyclic stick to counteract a 5-foot-per-second gust hitting the helicopter head-on. Of course, the longer the pilot waits to make a control input, the larger the input must be.

The question of what control movements the pilot might make to at least give the helicopter neutral stability is rather easy to answer. The pilot is, of course, sensitive to accelerations, rates, and displacements in each of the six degrees of freedom. But suppose, as a minimum, the pilot's senses are restricted to just pitch angle and pitch rate. Then the control input,  $\delta_{\text{cyclic}}$ , would be reduced to

$$(33) \quad \delta_{\text{cyclic}} = \frac{\partial \delta_{\text{cyclic}}}{\partial \dot{\theta}_{\text{cg}}} \times \dot{\theta}_{\text{cg}} + \frac{\partial \delta_{\text{cyclic}}}{\partial \theta_{\text{cg}}} \times \theta_{\text{cg}} = \delta_{\dot{\theta}} \times \dot{\theta} + \delta_{\theta} \times \theta,$$

## APPENDIX A

and the derivative of stick motion with respect to time becomes

$$(34) \quad \dot{\delta}_{\text{cyclic}} = \delta_{\dot{\theta}} \times \ddot{\theta} + \delta_{\theta} \times \dot{\theta}.$$

The basic stability and control differential equation (A-12) can now be rewritten to include the pilot input as

$$(35) \quad \begin{aligned} & \frac{WI}{g} \ddot{\theta} \\ & + \left[ \frac{W}{g} [h(M_v + hH_v) - (M_{\dot{\theta}} + hH_{\dot{\theta}})] + IH_v \right] \ddot{\theta} - \left[ \frac{W}{g} (M_{\delta} + hH_{\delta}) \delta_{\dot{\theta}} \right] \ddot{\theta} \\ & + (M_v H_{\dot{\theta}} - M_{\dot{\theta}} H_v) \dot{\theta} - \left[ \frac{W}{g} (M_{\delta} + hH_{\delta}) \delta_{\theta} + (M_{\delta} H_v - M_v H_{\delta}) \delta_{\dot{\theta}} \right] \dot{\theta} \\ & + W(M_v + hH_v) \theta - [(M_{\delta} H_v - M_v H_{\delta}) \delta_{\theta}] \theta = 0 \end{aligned}$$

To successfully stabilize the helicopter, the pilot must learn the two stick movement constants from Eqs. (33) and (34):

$$\text{inches of stick per pitch rate (rad / sec)} = \frac{\partial \delta_{\text{cyclic}}}{\partial \dot{\theta}_{\text{cg}}} = \delta_{\dot{\theta}} \quad \text{and}$$

$$\text{inches of stick per pitch angle (rad)} = \frac{\partial \delta_{\text{cyclic}}}{\partial \theta_{\text{cg}}} = \delta_{\theta}.$$

The pilot's objective is, as a minimum, to correct the inherent stability equation, Eq. (18), so that the complex roots have  $R = 0$ . In this more controlled and desirable situation, he would feel the helicopter motion improved to

$$(36) \quad \theta = V_{\text{gust}} \frac{(M_v + hH_v)}{I[\lambda^2 + \omega^2]} \left[ e^{\lambda t} - \cos \omega t - \frac{\lambda}{\omega} \sin \omega t \right],$$

which would be an initial transient motion in response to the gust, followed by a constant amplitude oscillation.

There is, in fact, a rather broad combination of  $\delta_{\dot{\theta}}$  and  $\delta_{\theta}$  that can satisfy this minimum requirement. With a little arithmetic, the combinations can be found explicitly by solving the characteristic cubic equation introduced by Eq. (19) with the restriction that  $R = 0$ . (A little shorthand is required because the cubic equation starts to become cumbersome). Suppose then that you redefine the cubic as

$$(37) \quad X^3 + AX^2 + BX + C = 0,$$

where the coefficients of A, B, and C are written in terms of the basic helicopter derivatives plus the pilot input terms. Thus,

$$\begin{aligned}
 (38) \quad A &= + \left\{ \frac{h(M_v + hH_v) - (M_{\dot{\theta}} + hH_{\dot{\theta}})}{I} + \frac{g}{W} H_v \right\} - \left[ \frac{(M_{\delta} + hH_{\delta})}{I} \right] \delta_{\dot{\theta}} \\
 B &= + \left\{ \frac{g(M_v H_{\dot{\theta}} - M_{\dot{\theta}} H_v)}{W I} \right\} - \left[ \frac{(M_{\delta} + hH_{\delta})}{I} \right] \delta_{\dot{\theta}} - \left[ \frac{g(M_{\delta} H_v - M_v H_{\delta})}{W I} \right] \delta_{\dot{\theta}} \\
 C &= + \left\{ \frac{(M_v + hH_v)}{I} \right\} - \left[ \frac{g(M_{\delta} H_v - M_v H_{\delta})}{W I} \right] \delta_{\dot{\theta}}.
 \end{aligned}$$

Note in the preceding definitions for A, B, and C that the basic helicopter stability terms have been grouped within the { } brackets while the pilot input is grouped within the [ ] brackets.

It is much easier now to continue the discussion by using some numbers. The example helicopter numerically gives the cubic coefficients as

$$\begin{aligned}
 A &= \{0.394681\} - [0.190823] \times \delta_{\dot{\theta}} \\
 B &= \{0.001626\} - [0.190823] \times \delta_{\dot{\theta}} - [0.000121962] \times \delta_{\dot{\theta}} \\
 C &= \{0.092456\} - [0.000121962] \times \delta_{\dot{\theta}}.
 \end{aligned}$$

Now solve the cubic defined by Eq. (37) with the restriction that  $R = 0$ . This is not as hard as it might seem because the cubic has the following roots

$$X - \lambda = 0 \quad X^2 + \omega^2 = 0$$

so that

$$(39) \quad X^3 + A X^2 + B X + C = X^3 - \lambda X^2 + \omega^2 X - \lambda \omega^2 = 0.$$

This result shows that

$$\begin{aligned}
 -\lambda &= A \\
 +\omega^2 &= B \\
 -\lambda \omega^2 &= C \text{ and most importantly } A \times B = C.
 \end{aligned}$$

The neutral stability criteria of  $R = 0$  is reduced to the simple identity that  $A \times B = C$ . But A, B, and C only depend on the pilot inputs given a basic helicopter configuration that sets the stability derivatives. Therefore, one equation in the two pilot-stick-movement constants of  $\delta_{\dot{\theta}}$  and  $\delta_{\theta}$  is explicitly obtained. For the example helicopter, this straightforward algebra problem yields

$$(40) \quad \delta_{\dot{\theta}} = \frac{-0.0918 - 0.000358 (\delta_{\theta}) + 0.00002327 (\delta_{\theta})^2}{0.0752 - 0.0364 (\delta_{\theta})}.$$

Thus, the pilot who finds a practical combination of  $\delta_{\dot{\theta}}$  and  $\delta_{\theta}$  that satisfies Eq. (40) will bring the helicopter under control following an upset situation such as a gust of wind.

## APPENDIX A

The boundary between stable and unstable control is shown in Fig. A-2. As the pilot becomes more proficient, he is able to smooth out the control inputs. This has the effect of increasing the period and reducing the gust response. In short, the ride goes from jerky to precision hovering as the pilot stabilizes the helicopter by flying more by pitch rate and less by pitch angle. By being more responsive to pitch rate, the pilot can achieve a very comfortable hover at a much reduced workload. As a final note, if no control input is made, the very unstable response shown in Fig. A-1 would be what this example helicopter has in store for the pilot.

The electronic world of autopilots descended on the industry when helicopters got “power steering.” The ability to tailor helicopter flying qualities to any criteria, military or civil, has now become the task. The search for the inherently stable helicopter has long since stopped being even a desirable goal. Now, the only practical limit to polishing a new helicopter’s flying qualities appears to be the number of lines of software code that *must* be absolutely proven accurate before the date of first flight.

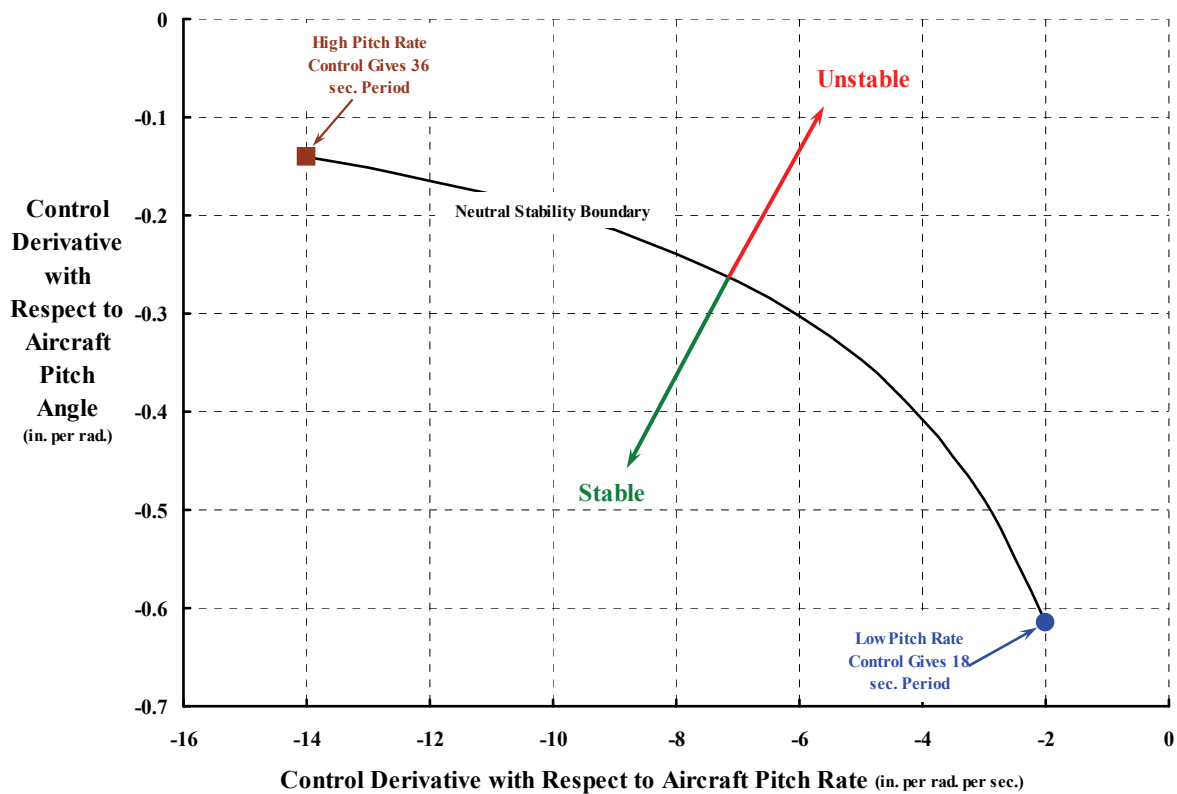


**Fig. A-2. The pilot learns to respond to aircraft pitch rate more than aircraft pitch attitude in stabilizing hover.**

## APPENDIX B

### SELF-INDUCED VELOCITY GENERATED BY A LIFTING LINE WING OR ROTOR BLADE

This appendix serves as an elementary introduction to the induced velocity created by a field of vortices that reside in the wake of a rotor blade. The approach is to build a bridge between familiar fixed-wing theory over to a rotor blade in forward flight. This bridge is built in four parts plus concluding remarks.

By way of background, rotorcraft technologists, after a nearly seven-decade effort, have finally begun to provide accurate computer-based predictions of the airloads and dynamic response of a helicopter rotor blade. The decades-long effort was capped during the last 4 years by tying airload prediction (with advanced computational fluid dynamics (CFD) methods) to completely coupled structural dynamic response (calculated with very advanced modal methods). Typical results<sup>1,2</sup> confirm the progress of what this relatively small band of engineers have achieved after some 70 years of dedicated work.

In September 1969, I presented a paper at the V/STOL Technology and Planning Conference sponsored by the Air Force Flight Dynamics Laboratory.<sup>3</sup> This paper included a figure showing the progress in removing assumptions from the original rotor performance theory developed by Juan de la Cierva in the late 1920s. The figure is reproduced here as Fig. B-1. You can see from the dashed line in Fig. B-1 that I was, in 1969, confident that by 1975 we would be done. Of course, a revision to that 1969 view reflecting history is quite in order. So, the solid line in Fig. B-1 now shows the more accurate progress in hindsight.

One of the toughest assumptions to remove was that of uniform downwash. Professor Rene Miller of Massachusetts Institute of Technology (MIT) showed the way in 1962.<sup>4</sup> Work that followed is discussed rather completely in Chapter 13 of Wayne Johnson's *Helicopter Theory*. The interaction between the rotor blades that create the induced velocity field and the effect the induced velocity feeds back on each blade was a daunting complexity that needed a computer before even rudimentary solutions became tractable.

---

<sup>1</sup> Potsdam, M.; Yeo, Hyeonsoo; and Johnson, Wayne: *Rotor Airloads Prediction Using Loose Aerodynamic/Structural Coupling*. Presented at the American Helicopter Society 60th Annual Forum, Baltimore, MD, June 7–10, 2004.

<sup>2</sup> Datta, A.; Sitaraman, J.; Chopra, I.; and Baeder, J.: *Analysis Refinements for Prediction of Rotor Vibratory Loads in High-Speed Forward Flight*. Presented at the American Helicopter Society 60th Annual Forum, Baltimore, MD, June 7–10, 2004.

<sup>3</sup> Harris, F. D.; Tarzanin, F. J.; and Fisher, R. K.: *Rotor High-Speed Performance, Theory Versus Test*. Presented at the Air Force Flight Dynamics Laboratory V/STOL Technology and Planning Conference, Sept. 1969 (also AHS Journal, vol. 15, no. 3, July 1970). This conference was held in Las Vegas, Nevada, a city—I was led to believe—that was the V/STOL technical capital of the world.

<sup>4</sup> Miller, R. H.: *Rotor Harmonic Air Loading*. Institute of the Aerospace Sciences, IAS Paper no. 62-82, Jan. 1962.

## APPENDIX B

There is some interesting knowledge to be gained, however, from disconnecting the blade loading from the induced field. That is the purpose of this appendix: to calculate the induced velocity at a blade where the blade's bound circulation is given in terms of radius and azimuth. Once specified, the blade's bound circulation and lift distribution remain unchanged despite the resulting induced velocity field. This is, of course, a comparatively simple problem compared to the real problem. Furthermore, in this appendix only a one-bladed rotor is considered and, to make the problem even simpler, only a prescribed, rigid wake is considered.

An interesting advantage of these simplifications is that it is quite easy to construct a bridge from the fixed wing to the rotary wing. To make the bridge secure, I have tried to leave nothing to the imagination concerning the sign conventions, the mathematical notations, and the steps under discussion.

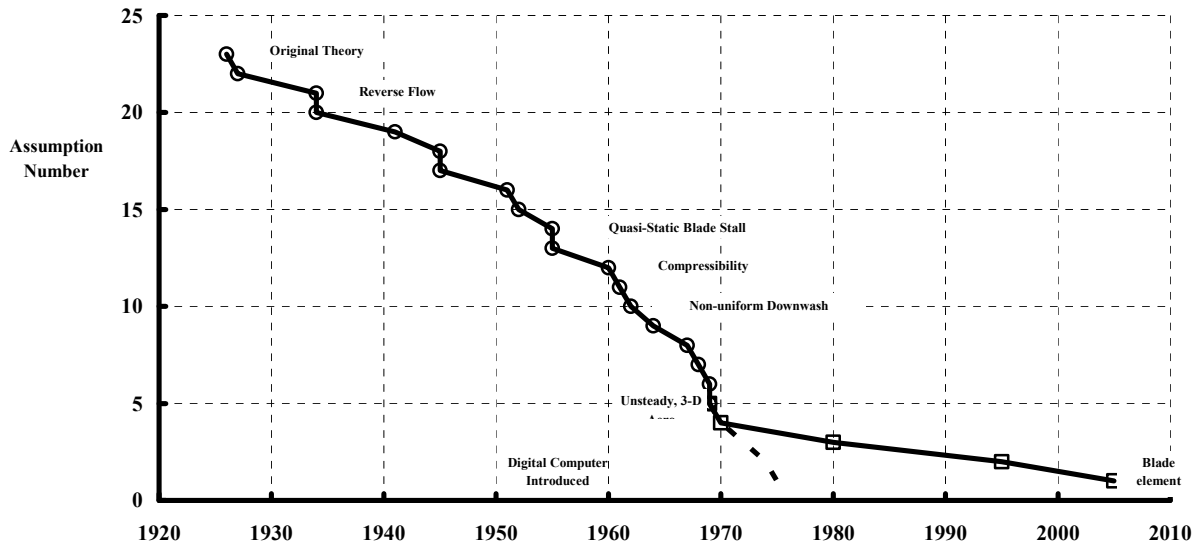


Fig. B-1

## Part I—Introduction to the Fixed Wing

### The Classical Fixed-Wing Problem

The classical fixed-wing induced velocity problem begins, as explained in most aerodynamic textbooks, by assuming a bound circulation that is elliptical. The wing is placed in straight and level flight. An array of horseshoe vortices is envisioned. The resulting induced velocity at the wing is found to be constant from the port wing tip to the starboard wing tip. In summary,

$$(1) \quad \text{if} \quad \Gamma_{xw} = \Gamma_o \sqrt{1 - \left(\frac{2xw}{b}\right)^2} \quad \text{then} \quad v_{xw} = \frac{\Gamma_o}{2b}$$

where  $\Gamma_o$  is the maximum circulation in square feet per second,  $b$  is the wingspan in feet, and  $xw$  is the span station ( $xw = -b/2$  at the port wing tip and  $xw = +b/2$  at the starboard wing tip). The induced velocity,  $v_{xw}$ , is in feet per second and is constant from tip to tip.

Now think of the wing rotating, not flying straight. It is quite helpful to approach the fundamental geometry used in the classical derivation from a different point of view. Suppose a fixed wing is East of a pylon and flying North past the pylon. Ignore, for the moment, an anticipated 180-degree U-turn around the pylon.<sup>5</sup> (The U-turn results will be discussed after reconstructing the classical problem.) The situation is illustrated with Fig. B-2.

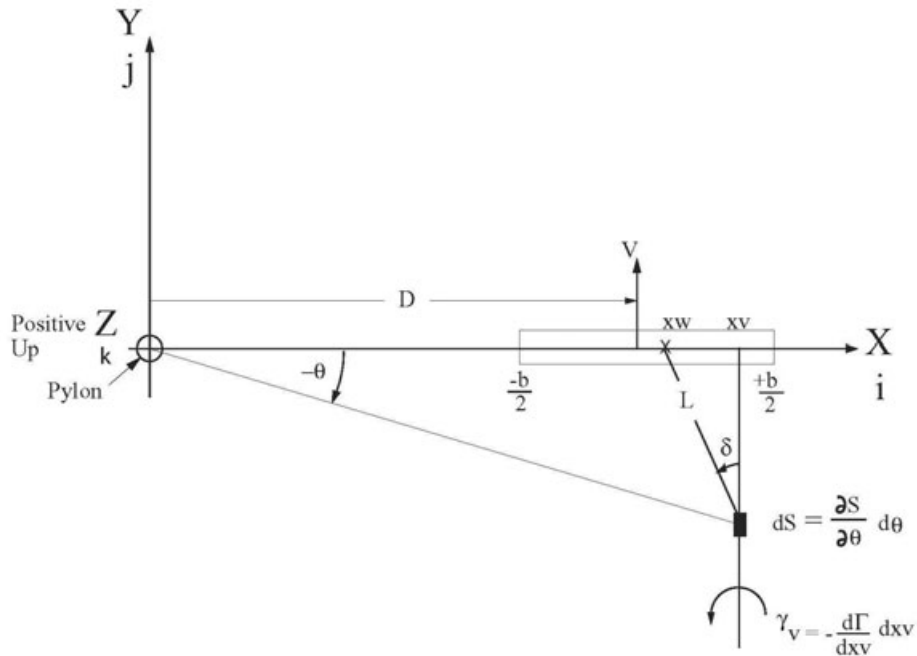


Fig. B-2

<sup>5</sup> Imagine a rotor blade at the traditional downwind, zero azimuth station, which will, after the U-turn, be at the 180-degree upwind azimuth station.

## APPENDIX B

In Fig. B-2, the right-hand axis system gives a positive Z-axis coming up out of the paper. The “pylon” is located at  $X = Y = Z = 0$ . The wing centerline is placed at a distance,  $D$ , from the pylon in the plus X direction. The wing coordinates are measured from the wing centerline. The station on the wing where induced velocity is sought is denoted by  $xw$ . A vortex trails downstream from the wing at wing station  $xv$ . A small element of the vortex,  $dS$ , is shown located at a distance  $L$  from wing station  $xw$ . The reference angle  $\theta$  is used to locate the vortex element in relation to the wing. When  $\theta$  is equal to minus  $\pi/2$ , the vortex element is at  $-\infty$ . When  $\theta$  equals zero, the vortex element is located at the wing. The calculation of induced velocity by the Biot–Savart law, as derived from vector notation, is simply

$$(2) \quad d(\mathbf{v}_{xw}) = \frac{\gamma_v}{4\pi} \left[ \frac{L_i dS_j - L_j dS_i}{L^3} \right] d\theta = \frac{1}{4\pi} \left[ - \left( \frac{d\Gamma_{xw}}{dxw} \right) dxv \right]_{xw=xv} \left[ \frac{L_i dS_j - L_j dS_i}{L^3} \right] d\theta.$$

This fundamental equation is deceptively simple because to calculate the induced velocity,  $\mathbf{v}_{xw}$ , at any station along the wing,  $xw$ , only a double integral has to be performed. That is

$$(3) \quad \mathbf{v}_{xw} = \frac{1}{4\pi} \int_{-b/2}^{+b/2} \int_{-\pi/2}^0 \left[ - \left( \frac{d\Gamma_{xw}}{dxw} \right) dxv \right]_{xw=xv} \left[ \frac{L_i dS_j - L_j dS_i}{L^3} \right] d\theta.$$

The double integration required by Eq. (3) is hampered (to put it mildly) whenever  $\frac{d\Gamma_{xw}}{dxw}$  equals either plus or minus infinity. The double integration can be an even bigger problem whenever  $L = 0$ . If the double integration is performed numerically, situations where numbers approach plus or minus  $10^{10}$  can become quite frustrating. Modern computers, using so called double precision and advanced numerical integration schemes, have helped to lower this frustration. But the fundamental basis of numerical integration is the Taylor series. The hope is that—without a breach in engineering accuracy— $d\theta$  and  $dxw$  can be replaced by  $\Delta\theta$  and  $\Delta xw$  when the integral operators are replaced by summation operators. There are, of course, a number of ingenious coordinate transformations that can completely remove an apparent integrating road block.

Here is an example of a coordinate transformation that helps lower frustrations with the fixed-wing problem. Consider the situation when a wing’s lifting line is loaded with an elliptical bound circulation defined as

$$(4) \quad \Gamma_{xw} = \Gamma_0 \sqrt{1 - \left( \frac{2xw}{b} \right)^2},$$

where  $xw = -b/2$  at the port wing tip and  $xw = +b/2$  at the starboard wing tip. The derivative that the Biot–Savart law requires is

(5)

$$\gamma_v = -\left(\frac{d\Gamma_{xw}}{dxw}\right)_{xw=xv} = -\left\{\frac{1}{2}\Gamma_o\left[1-\left(\frac{2xv}{b}\right)^2\right]^{\frac{1}{2}}\left[-2\left(\frac{2xv}{b}\right)\right]\left(\frac{2}{b}dxv\right)\right\} = +\frac{2}{b}\left[\frac{\Gamma_o}{\sqrt{1-\left(\frac{2xv}{b}\right)^2}}\right]\left(\frac{2xv}{b}\right)dxv$$

where  $xv = -b/2$  at the port wing tip and  $xv = +b/2$  at the starboard wing tip. You can immediately see that the required derivative is plus infinity at the starboard wing tip and minus infinity at the port wing tip. Now look at what happens with the coordinate transformation of

$$(6) \quad xv = -\frac{b}{2}\cos\beta \quad \text{and} \quad dxv = \frac{b}{2}\sin\beta d\beta$$

where  $\beta = 0$  is the port wing tip and  $\beta = \pi$  is the starboard wing tip. Then the bound circulation becomes

$$(7) \quad \Gamma_\beta = \Gamma_o\sqrt{1-\left(\frac{2}{b}\right)^2\left(-\frac{b}{2}\cos\beta\right)^2} = \Gamma_o\sqrt{1-\cos^2\beta} = \Gamma_o\sin\beta,$$

and the required Biot–Savart derivative becomes

$$(8) \quad \gamma_v = -\left(\frac{d\Gamma_{xw}}{dxw}\right)_{xw=xv} = \frac{2}{b}\left[\frac{\Gamma_o}{\sqrt{1-\cos^2\beta}}\right](-\cos\beta)\left(\frac{b}{2}\sin\beta d\beta\right) = -\Gamma_o\cos\beta d\beta.$$

Clearly, singularities caused by the derivative  $\frac{d\Gamma_{xw}}{dxw}$  at the wing tips have been removed.

The preceding coordinate transformation, when placed in the Biot–Savart law for this fixed-wing problem, gives

$$(9) \quad v_{xw} = \frac{1}{4\pi}\int_0^\pi\int_{-\pi/2}^0[-\Gamma_o\cos\beta d\beta]\left[\frac{L_i dS_j - L_j dS_i}{L^3}\right]d\theta.$$

The next step is to construct the second portion of the integrand required by Eq. (3), which is

$$\left[\frac{L_i dS_j - L_j dS_i}{L^3}\right]d\theta.$$

The geometric dimensions,  $L$ ,  $L_i$ ,  $L_j$ ,  $dS_i$ , and  $dS_j$  are components of vectors. When looking at Fig. B-2, there is a choice of reference systems. Since this fixed wing is flying straight and level past the pylon, there is no advantage to including the distance,  $D$ , or using the reference

## APPENDIX B

angle,  $\theta$ , in the wake geometry.<sup>6</sup> Therefore, continue using just the reference angle  $\delta$ . That means

$$\left[ \frac{L_i dS_j - L_j dS_i}{L^3} \right] d\theta \quad \text{is replaced by} \quad \left[ \frac{L_i dS_j - L_j dS_i}{L^3} \right] d\delta,$$

and  $\delta$  is positive counterclockwise. The vortex segment farthest downstream is located at  $\delta = 0$ , and a vortex segment right at the wing is located by  $\delta = +\pi/2$ .

Now, from Fig. B-2, the distance  $L$  is written as

$$\begin{aligned} L &= L_i + L_j + L_k = (X_w - X_v)i + (Y_w - Y_v)j + (Z_w - Z_v)k \\ \text{with} \quad X_w &= x_w & Y_w &= 0 & Z_w &= 0 \\ (10) \quad X_v &= x_v & Y_v &= \frac{x_v - x_w}{\tan \delta} & Z_v &= 0 \end{aligned}$$

$$\text{and} \quad L^3 = \left[ (X_w - X_v)^2 + (Y_w - Y_v)^2 + (Z_w - Z_v)^2 \right]^{3/2}.$$

Therefore, with the usual “substitute and simplify” phrase,

$$(11) \quad L^3 = \left[ \frac{(x_v - x_w)^2}{\sin^2 \delta} \right]^{3/2}.$$

In a similar manner, the vortex is describe by the vector

$$(12) \quad S = S_i + S_j + S_k = (X_v)i + (Y_v)j + (Z_v)k$$

and, therefore,

$$\begin{aligned} dS_i &= \frac{\partial S_i}{\partial \delta} d\delta = \frac{\partial X_v}{\partial \delta} d\delta = 0 \\ (13) \quad dS_j &= \frac{\partial S_j}{\partial \delta} d\delta = \frac{\partial Y_v}{\partial \delta} d\delta = \frac{(x_v - x_w)}{\sin^2 \delta} \\ dS_k &= \frac{\partial S_k}{\partial \delta} d\delta = \frac{\partial Z_v}{\partial \delta} d\delta = 0 \end{aligned}$$

Here the assumption about the trailed vortex geometry is that it extends straight aft of the wing without descending or climbing, remaining perpendicular to the wing lifting line. Again, by substitution and simplification,

$$(14) \quad \left[ \frac{L_i dS_j - L_j dS_i}{L^3} \right] d\delta = \frac{-1}{x_v - x_w} \sin \delta d\delta.$$

---

<sup>6</sup> The next part of this note addresses the U-turning wing. That problem requires, of course, some reference system that includes  $D$  and uses the reference angle as  $\theta$ .

The double integral created by the Biot–Savart law now appears, after substituting Eq. (14) into Eq. (9), as

$$(15) \quad v_{xw} = \frac{1}{4\pi} \int_0^\pi \int_0^{\pi/2} [-\Gamma_o \cos \beta d\beta] \left[ \frac{-1}{xv - xw} \sin \delta \right] d\delta.$$

A minor problem is immediately observed in Eq. (15). Formal integration really requires that  $xv$  and  $xw$  be related, in some fashion, to  $\beta$  and/or  $\delta$ . This minor problem is overcome using Eq. (6) where  $xv = -\frac{b}{2} \cos \beta$  rather than have the vortex wing station keyed by the angle  $\beta$ .

Because the wing station is keyed to  $xv$ , you can make the substitution that  $xw = -\frac{b}{2} \cos \alpha$ .

These substitutions result in

$$(16) \quad v_\alpha = \frac{1}{2b\pi} \int_0^\pi \int_0^{\pi/2} [-\Gamma_o \cos \beta d\beta] \left[ \frac{-1}{\cos \alpha - \cos \beta} \sin \delta \right] d\delta.$$

A much, much bigger problem with Eq. (15) and Eq. (16) is that any integration, whether formal or numerical, must face the possibility that  $(xv - xw)$  might be zero. Looking at Eq. (16) more closely shows that real trouble will occur if  $\beta = \alpha$ .

The integration of Eq. (16) with respect to wake age (i.e., with respect to  $\delta$ ) can be done, and the result can also be integrated with respect to  $\beta$ . That is,

$$(17) \quad v_\alpha = \frac{\Gamma_o}{2b\pi} \int_0^\pi \left[ \frac{\cos \beta}{\cos \alpha - \cos \beta} \right] d\beta = -\frac{\Gamma_o}{2b\pi} \int_0^\pi \left[ \frac{\cos \beta}{\cos \beta - \cos \alpha} \right] d\beta = -\frac{\Gamma_o}{2b}.$$

Note immediately that the preceding derivation gives a negative value for induced velocity created by a wing carrying positive lift! The reason for this outcome is the right-hand rule axis system of Fig. B-2 where the Z-axis is positive up. Therefore, the induced velocity is directed in the negative Z direction. Of course, reason prevails in all text books on the subject, so the negative induced velocity is simply called downwash, and the sign is changed to positive. This is equivalent to letting  $\gamma_v = +\Gamma_o \cos \beta d\beta$ .

Incidentally, Glauert proved the integration with respect to  $\beta$  equals  $\pi$  long ago. Also, Alan Pope, in appendix 3 of his book *Basic Wing and Airfoil Theory*, shows that

$$(18) \quad \begin{aligned} v_\alpha &= \frac{\Gamma_o}{2b\pi} \int_0^\pi \left[ \frac{\cos \beta}{\cos \beta - \cos \alpha} \right] d\beta = \frac{\Gamma_o}{2b\pi} \int_0^\pi \left[ 1 + \frac{\cos \alpha}{\cos \beta - \cos \alpha} \right] d\beta \\ &= \frac{\Gamma_o}{2b\pi} \int_0^\pi d\beta + \frac{\Gamma_o}{2b\pi} \cos \alpha \int_0^\pi \left[ \frac{1}{\cos \beta - \cos \alpha} \right] d\beta = \frac{\Gamma_o}{2b\pi} [\pi] + \frac{\Gamma_o}{2b\pi} \cos \alpha [0] \end{aligned}$$

## APPENDIX B

But now suppose numerical integration (rather than formal, closed form integration) of Eq. (16) is the solution approach. I took an approach with the MathSoft, Inc. product called MathCad Plus 6.0 that goes like this:

$$\begin{aligned}
 \Gamma_o &= 2 & b &= 1 \\
 s &= 0, 1, \dots, 179 \\
 \alpha_s &= (s + 1/2) \frac{\pi}{180} \\
 d\text{vd}\beta d\delta_{n,m} &= \frac{\Gamma_o}{2b\pi} \left\{ \frac{\cos \beta_m}{\cos \beta_m - \cos \alpha_s} \right\} \sin \delta_n \\
 n &= 0, 1, \dots, 90 & \delta_n &= \frac{\pi}{180} n \\
 m &= 0, 1, \dots, 180 & \beta_m &= \frac{\pi}{180} m \\
 d\text{vd}\beta_m &= \frac{\pi}{180} \sum_{n=0}^{89} \frac{d\text{vd}\beta d\delta_{n,m} + d\text{vd}\beta d\delta_{n+1,m}}{2} \\
 v_s &= \frac{\pi}{180} \sum_{n=0}^{179} \frac{d\text{vd}\beta_m + d\text{vd}\beta_{m+1}}{2} \\
 xw_s &= -\frac{b}{2} \cos \alpha_s
 \end{aligned}$$

This numerical solution “programmed” in MathCad gave +0.9999746151 accuracy nearly within a blink of an eye, using a Dell Optiplex high-end computer bought in 2001. The answer from Eq. (17) is exactly unity (when you ignore the minus sign). As a reminder, the fixed wing represented by a lifting line and an elliptical bound circulation produces a lift calculated from

$$\begin{aligned}
 (19) \quad L &= \rho V \Gamma_o \int_{-b/2}^{+b/2} \sqrt{1 - \left(\frac{2xw}{b}\right)^2} dxw = \rho V \Gamma_o \int_{-\pi/2}^{+\pi/2} \sqrt{1 - \sin^2 \theta} \left(\frac{b}{2} \cos \theta d\theta\right) \\
 &= \rho V \Gamma_o \frac{b}{2} \int_{-\pi/2}^{+\pi/2} \cos^2 \theta d\theta = \rho V \Gamma_o \frac{b}{2} \left(\frac{\pi}{2}\right) = \frac{\pi}{4} \rho b V \Gamma_o \quad \text{so} \quad \Gamma_o = \frac{4L}{\pi \rho b V}.
 \end{aligned}$$

The wing incurs an induced drag to carry this lift that is

$$(20) \quad \text{Induced drag} = L \frac{v_{xw}}{V} = \left(\frac{\pi}{4} \rho b V \Gamma_o\right) \left(\frac{\Gamma_o}{2bV}\right) = \frac{\pi}{8} \rho \Gamma_o^2 = \frac{L^2}{(\rho/2) V^2 \pi b^2}.$$

This drag can be used to calculate a horsepower required by multiplying both sides of the equation by velocity,  $V$ , and dividing by 550. Thus,

$$(21) \quad \text{Induced Horsepower} \equiv \text{HP}_i = \frac{V}{550} \left[ \frac{L^2}{(\rho/2) V^2 \pi b^2} \right] = \frac{Vq}{550\pi} \left(\frac{L}{qb^2}\right)^2 \quad \text{with } q = (\rho/2) V^2.$$

A numerical example calculated here will be a useful result to compare later to rotating wing calculations. Suppose both a wing and a rotor have an equal span, say, 44 feet. In rotor notation, the rotor radius is 22 feet. Assume, for example, that each lifting device carries a lift of 2,712 pounds, each is flying at sea level ( $\rho = 0.002378$  slug/ft<sup>3</sup>), and each is flying at  $V = 301.8$  ft/sec or 178 knots. Then, using Eq. (21), the induced horsepower required by the wing is 6.13 horsepower.

Keep in mind that the elliptical bound circulation distribution used in the preceding discussion is the first term of the more general distribution used in fixed-wing analyses. Recall that the general distribution is seen in the form

$$(22) \quad \Gamma = 2bV \sum_1^{\infty} A_n \sin n\beta.$$

*Everything read in this appendix, including the rotor analyses, could be extended by this fixed-wing logic of Eq. (22).*

And there you have the fixed wing flying North past the pylon located off its port wing tip. Now consider the situation after the fixed wing does a 180-degree U-turn.

### **The Fixed Wing After Completing a 180-Degree U-turn**

The next step in bridging the gap between a fixed wing and a rotary wing was actually taken by H. Glauert in 1923, although I doubt he had a bridge in mind when he published R&M 866. After all, in 1923 Juan de la Cierva's earliest autogyro experiments were just coming to fruition in Spain, and a practical helicopter was still 15 years away. The title of Glauert's 1923 report was *Calculation of the Rotary Derivatives Due to Yawing for a Monoplane Wing*. He was dealing with the wing rolling and yawing moments created by an induced velocity field that trailed the wing in one-half of a circle. The problem was, in fact, quite akin to a hovering one-bladed rotor where only a small part of the wake is taken into account. Glauert obtained a very simple closed-form solution by assuming that the wing made the U-turn with a large turning radius ( $D$ ) relative to the wingspan ( $b$ ) (i.e.,  $D \gg b$ ). His quite useable engineering result for the induced velocity over the wingspan was (in the notations I am using in this appendix)

$$(23) \quad v_{xw} = \frac{\Gamma_o}{2b} \left( 1 + \frac{1}{2} \frac{xw}{D} \right).$$

The purpose of this portion of the appendix is to explore this problem when the turning radius is considerably smaller than what Glauert assumed. The objective is to think of the "pylon" as a rotor hub and place the port wing tip a small distance from the hub, which gives the appearance of a "root cutout" in rotorcraft terminology. Glauert's approach is presented first, and then a numerical integrating approach is shown.

APPENDIX B

The geometry of the problem is illustrated in Fig. B-3. In contrast to Fig. B-2, the wing has now advanced 180 degrees. *Immediately note* that the X-axis is positive to the left, but the Y-axis is left in its commonly found, ordinate position. By the right-hand rule then, the positive Z-axis now points down, which is into the paper. The wing is doing a U-turn of distance D, which is measured from the “pylon” to the wing mid-span point. The wing is represented by a lifting line vortex having an elliptical bound circulation, just as with the classical fixed-wing problem. The Biot–Savart law is again invoked so

$$(24) \quad d(dv_{xw}) = \frac{\gamma_v}{4\pi} \left[ \frac{L_i dS_j - L_j dS_i}{L^3} \right] d\theta,$$

and the dimensions are expressed as vectors. However, the basic vortex geometry has changed going from Fig. B-2 to Fig. B-3. Now

(25)

$$L = L_i + L_j + L_k = (Xw - Xv)i + (Yw - Yv)j + (Zw - Zv)k$$

where $Xw = D + xw$	$Yw = 0$	$Zw = 0$
$Xv = (D + xv) \cos \theta$	$Yv = -(D + xv) \sin \theta$	$Zv = 0$

and  $L^3 = [(Xw - Xv)^2 + (Yw - Yv)^2 + (Zw - Zv)^2]^{3/2}$ .

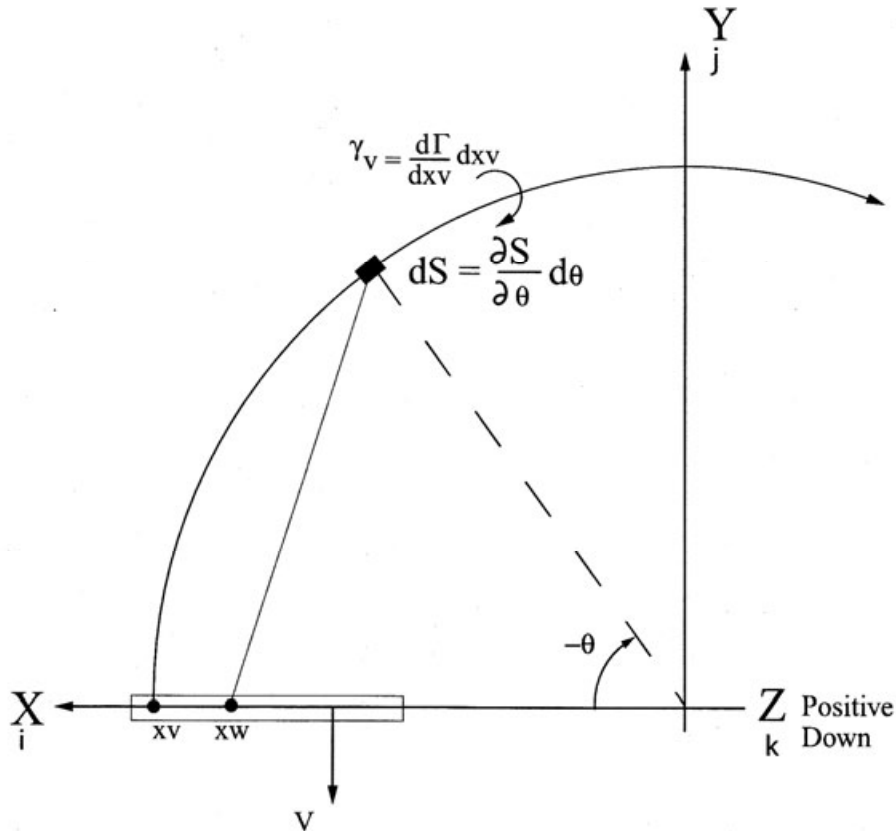


Fig. B-3

The reference angle,  $\theta$ , is taken positive counterclockwise in Fig. B-3. In a similar manner, the vortex is describe by

$$(26) \quad S = S_i + S_j + S_k = (Xv)i + (Yv)j + (Zv)k,$$

but with changed vortex geometry reflecting the one-half circle wake, the vortex element geometry is

$$(27) \quad \begin{aligned} dS_i &= \frac{\partial S_i}{\partial \theta} d\theta = \frac{\partial Xv}{\partial \theta} d\theta = \frac{\partial (D + xv) \cos \theta}{\partial \theta} d\theta = -(D + xv) \sin \theta \\ dS_j &= \frac{\partial S_j}{\partial \theta} d\theta = \frac{\partial Yv}{\partial \theta} d\theta = \frac{\partial [-(D + xv)] \sin \theta}{\partial \theta} d\theta = -(D + xv) \cos \theta . \\ dS_k &= \frac{\partial S_k}{\partial \theta} d\theta = \frac{\partial Zv}{\partial \theta} d\theta = 0 \end{aligned}$$

Here the assumption about the trailed vortex geometry is that it extends in a circular arc aft of the wing for 180 degrees without descending or climbing. Furthermore, any given vortex has constant circulation,  $\gamma_v$ , from when it leaves the wing all the way back to when the turn began (i.e.,  $\theta = 0$  back to  $\theta = -\pi$ ).

The substitution of this U-turn geometry into the Biot–Savart law gives, with simplification

$$(28) \quad d(dv_{xw}) = \frac{\gamma_v}{4\pi} \left\{ \frac{(D + xv)(D + xw) \cos \theta - (D + xv)^2}{\left[ (D + xv)^2 + (D + xw)^2 - 2(D + xv)(D + xw) \cos \theta \right]^{3/2}} \right\} d\theta .$$

The wake-age integral problem is immediately seen as requiring elliptical integrals—even if the wing's bound vortex circulation varies with wake age. For this example, assume, as Glauert did, that  $\gamma_v$  does not vary with  $\theta$ . Now, at the risk of boring you, the transformation to complete elliptical integrals (i.e., E and K) begins by letting  $\theta = \pi - 2\phi$  and  $d\theta = -2 d\phi$ . You also need to recall that

$$\cos \theta = \cos(\pi - 2\phi) = -\cos(2\phi) = 2 \sin^2 \phi - 1.$$

Then, a couple of substitutions and rearrangements immediately show that

$$(29) \quad \begin{aligned} d(dv_{xw}) &= \frac{\gamma_v}{4\pi} \frac{2(D + xv)(2D + xw + xv)}{(2D + xw + xv)^{3/2}} \left\{ \frac{1}{\left[ 1 - k^2 \sin^2 \phi \right]^{3/2}} \right\} d\phi - \\ &\quad - \frac{\gamma_v}{4\pi} \frac{4(D + xv)(D + xw)}{(2D + xw + xv)^{3/2}} \left\{ \frac{\sin^2 \phi}{\left[ 1 - k^2 \sin^2 \phi \right]^{3/2}} \right\} d\phi \end{aligned}$$

APPENDIX B

where

$$(30) \quad k^2 = \frac{4(D+xw)(D+xv)}{(2D+xv+xw)^2}.$$

This substitution changes the wake-age integrating limits from  $\theta = -\pi$  to  $\theta = 0$  over to  $\phi = 0$  to  $\phi = +\pi/2$ . The two budding integrals can be found, for example, in the translated Russian handbook written by I. S. Gradshteyn and I. M. Ryzhik, and edited by Alan Jeffrey, titled *Tables of Integrals, Series, and Products*. Thus,

$$(31) \quad \int_0^{\pi/2} \frac{1}{[1-k^2 \sin^2 \phi]^{3/2}} d\phi = \frac{1}{1-k^2} E$$

$$\int_0^{\pi/2} \frac{\sin^2 \phi}{[1-k^2 \sin^2 \phi]^{3/2}} d\phi = \int_0^{\pi/2} \frac{1}{[1-k^2 \sin^2 \phi]^{3/2}} d\phi - \int_0^{\pi/2} \frac{\cos^2 \phi}{[1-k^2 \sin^2 \phi]^{3/2}} d\phi$$

$$= \frac{1}{1-k^2} E - \left( \frac{1}{k^2} K - \frac{1}{k^2} E \right)$$

where the complete elliptical integrals, E and K, are computed as

$$(32) \quad E = \int_0^{\pi/2} \sqrt{1-k^2 \sin^2 \phi} d\phi \quad K = \int_0^{\pi/2} \frac{1}{\sqrt{1-k^2 \sin^2 \phi}} d\phi,$$

and their values depend on the modulus,  $k^2$ , which for this U-turning wing problem is given by Eq. (30). Note that when  $xv = xw$ ,  $k^2 = 1.0$ ,  $E = 1.0$ , and  $K = +\infty$ .

In this way

$$(33) \quad dv_{xw} = \frac{\gamma_v}{4\pi} \int_{-\pi}^0 \left\{ \frac{(D+xv)(D+xw) \cos \theta - (D+xv)^2}{[(D+xv)^2 + (D+xw)^2 - 2(D+xv)(D+xw) \cos \theta]^{3/2}} \right\} d\theta$$

is converted into

$$(34) \quad dv_{xw} = \frac{\gamma_v}{4\pi} \frac{2(D+xv)(2D+xw+xv)}{(2D+xw+xv)^{3/2}} \int_0^{\pi/2} \left\{ \frac{1}{[1-k^2 \sin^2 \phi]^{3/2}} \right\} d\phi -$$

$$- \frac{\gamma_v}{4\pi} \frac{4(D+xv)(D+xw)}{(2D+xw+xv)^{3/2}} \int_0^{\pi/2} \left\{ \frac{\sin^2 \phi}{[1-k^2 \sin^2 \phi]^{3/2}} \right\} d\phi$$

which, upon simplification, reduces to

$$(35) \quad dv_{xw} = \frac{\gamma_v}{4\pi} \left[ \frac{E}{xv - xw} + \frac{K}{2D + xv + xw} \right].$$

The wake integration being complete, the problem is reduced to the spanwise collection of all vortices trailed from the wing.

The insightful step Glauert took next was to make use of the approximations for  $E$  and  $K$ , when  $k^2$  was closer to 1.0 than to 0, rather than calculate them using Eq. (32). These approximations are

$$(36) \quad \begin{aligned} E &\approx 1 + \frac{1}{4} \left( \ln \left( \frac{16}{1-k^2} \right) - \frac{1}{2} \right) (1-k^2) \\ K &\approx \frac{1}{2} \ln \left( \frac{16}{1-k^2} \right) + \frac{1}{8} \left( \ln \left( \frac{16}{1-k^2} \right) - 1 \right) (1-k^2) \end{aligned}$$

*The fact that the approximation for  $E$  begins with one (1) is enormously important*, as shown when these approximations are substituted into Eq. (35). Of course, a lengthy integration problem results, which is

$$(37) \quad \begin{aligned} v_{xw} &= \int_{-b/2}^{+b/2} \frac{\gamma_v}{4\pi} \left( \frac{1}{xv - xw} \right) \\ &+ \int_{-b/2}^{+b/2} \frac{\gamma_v}{4\pi} \left( \frac{1}{xv - xw} \right) \left[ \frac{1}{4} \left( \ln \left( \frac{16}{1-k^2} \right) - \frac{1}{2} \right) (1-k^2) \right] \\ &+ \int_{-b/2}^{+b/2} \frac{\gamma_v}{4\pi} \left( \frac{1}{2D + xv + xw} \right) \left[ \frac{1}{2} \ln \left( \frac{16}{1-k^2} \right) \right] \\ &+ \int_{-b/2}^{+b/2} \frac{\gamma_v}{4\pi} \left( \frac{1}{2D + xv + xw} \right) \left[ \frac{1}{8} \left( \ln \left( \frac{16}{1-k^2} \right) - 1 \right) (1-k^2) \right] \end{aligned}$$

But now look very closely at the first integral obtained in Eq. (37). Recognize that

$$v_{xw} = \int_{-b/2}^{+b/2} \frac{\gamma_v}{4\pi} \left( \frac{1}{xv - xw} \right)$$

is nothing more than the classical fixed-wing problem presented in Part I of this appendix.

This is a key result that Glauert provided in his 1923 report because it says that the so-called “near wake” of a U-turning fixed wing (i.e., think of a rotor blade’s near wake) is a no tougher problem than the straight-flying wing with the added influence of a curved “far wake.” For the elliptical bound circulation used as the example in this appendix, the spanwise integration becomes

APPENDIX B

$$\begin{aligned}
 v_x = & \frac{\Gamma_o}{2b} \\
 & + \int_{-b/2}^{+b/2} \frac{\gamma_v}{4\pi} \left( \frac{1}{xv - xw} \right) \left[ \frac{1}{4} \left( \ln \left( \frac{16}{1-k^2} \right) - \frac{1}{2} \right) (1-k^2) \right] \\
 & + \int_{-b/2}^{+b/2} \frac{\gamma_v}{4\pi} \left( \frac{1}{2D + xv + xw} \right) \left[ \frac{1}{2} \ln \left( \frac{16}{1-k^2} \right) \right] \\
 & + \int_{-b/2}^{+b/2} \frac{\gamma_v}{4\pi} \left( \frac{1}{2D + xv + xw} \right) \left[ \frac{1}{8} \left( \ln \left( \frac{16}{1-k^2} \right) - 1 \right) (1-k^2) \right]
 \end{aligned}
 \tag{38}$$

The additional three integrals can be grouped into one integral. But first, the vortex circulation strength, assuming an elliptical bound circulation for the wing lifting line, Eq. (8), is substituted into Eq. (38). Next the elliptic integral modulus,  $k^2$ , from Eq. (30), is substituted into Eq. (38).<sup>7</sup> Then a selection of wingspan stations,  $xw$ , is made (say 50) and, in short order, MathCad calculated the induced velocity distributions at any turning distance,  $D$ .

Despite the appearance of possible singularities in Eq. (38), MathCad actually experienced no numerical integration problems. I *did not* let MathCad try to simplify the integrand. The temptation is to fiddle with  $1-k^2$ , which MathCad or I fouled up. It was a very unproductive effort given MathCad’s speed on my Dell computer.

Glauert, in R&M 866, assumed that the turning radius was considerably greater than the wingspan, which allowed simple integration of Eq. (38), the result being Eq. (23). But consider the results as the wing makes tighter and tighter U-turns. A nondimensional measure of the semicircle tightness is wingspan ( $b$ ) divided by the distance from the “pylon” ( $D$ ). The tightest turn would be when the port wing tip is touching the “pylon,” in which case  $D = b/2$  or  $b/D = 2.0$ . This corresponds to a rotor blade with zero root cutout. A turning ratio of  $b/D = 1$  corresponds to a 0.33 root cutout. The extreme in the other direction would be, of course, not turning at all, and so  $D = \infty$  and  $b/D = 0$ .

For simple illustration purposes, let the wingspan be unity (i.e.,  $b = 1.0$  foot) and let the maximum elliptical bound circulation, which occurs at the wing mid-span, be two (i.e.,  $\Gamma_o = 2.0$  square feet per second). Thus, for the following examination,  $\Gamma_o / 2b = 1.0$  foot per second. Two results shown in Table B-1 are immediately known from the preceding discussion.

**Table B-1**

Turn Parameter, $b/D$	Spanwise Induced Velocity, $v_x$	Source
Not Turning	$v_x = \Gamma_o / 2b = 1.0$	Eq. (1)
Wide Turn	$v_x = (1+xw)/2D$	Eq. (23)

<sup>7</sup> I would have included the results of these substitutions, but the resulting expression is way too long.

The results for several tighter and tighter turns are shown in Figs. B-4 through B-7. For a turn distance,  $D$ , that is 10 times the wingspan, Glauert's approximation is very useful as Fig. B-4 shows. When the turn distance is equal to the wingspan (equivalent to a rotor blade root cutout of 1/3), the distortion in induced velocity across the wingspan is significant as shown in Fig. B-5. This distortion grows more pronounced as the turn distance shrinks, which is illustrated in Figs. B-6 and B-7. These two figures correspond to a rotor blade root cutout of 0.1667 and 0.0476, respectively.

Now consider the numerical double integration involved in this U-turning wing problem. Fig. B-6 offers a virtually exact example to which numerical integration can be compared. The integration problem at hand is

$$(39) v_{xw} = \int_{-b/2}^{+b/2} \int_{-\pi}^0 \frac{\gamma_v}{4\pi} \left\{ \frac{(D+xv)(D+xw)\cos\theta - (D+xv)^2}{\left[ (D+xv)^2 + (D+xw)^2 - 2(D+xv)(D+xw)\cos\theta \right]^{3/2}} \right\} d\theta dxv .$$

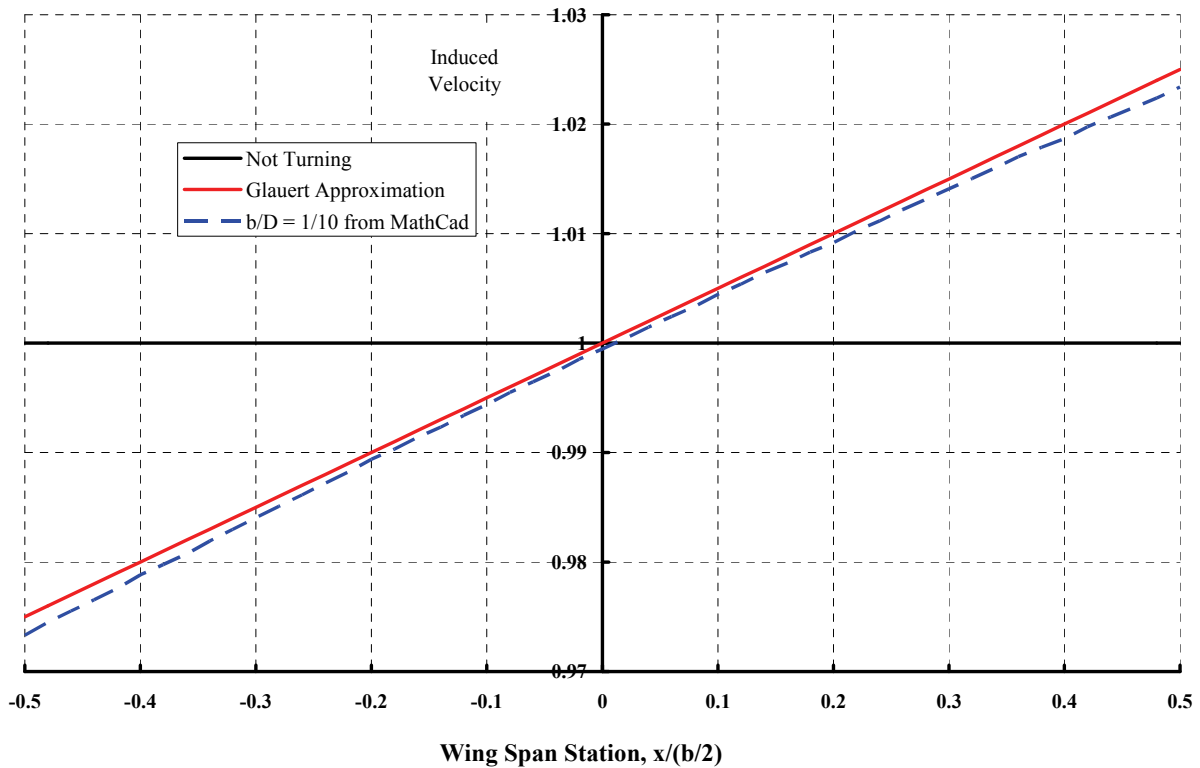


Fig. B-4

APPENDIX B

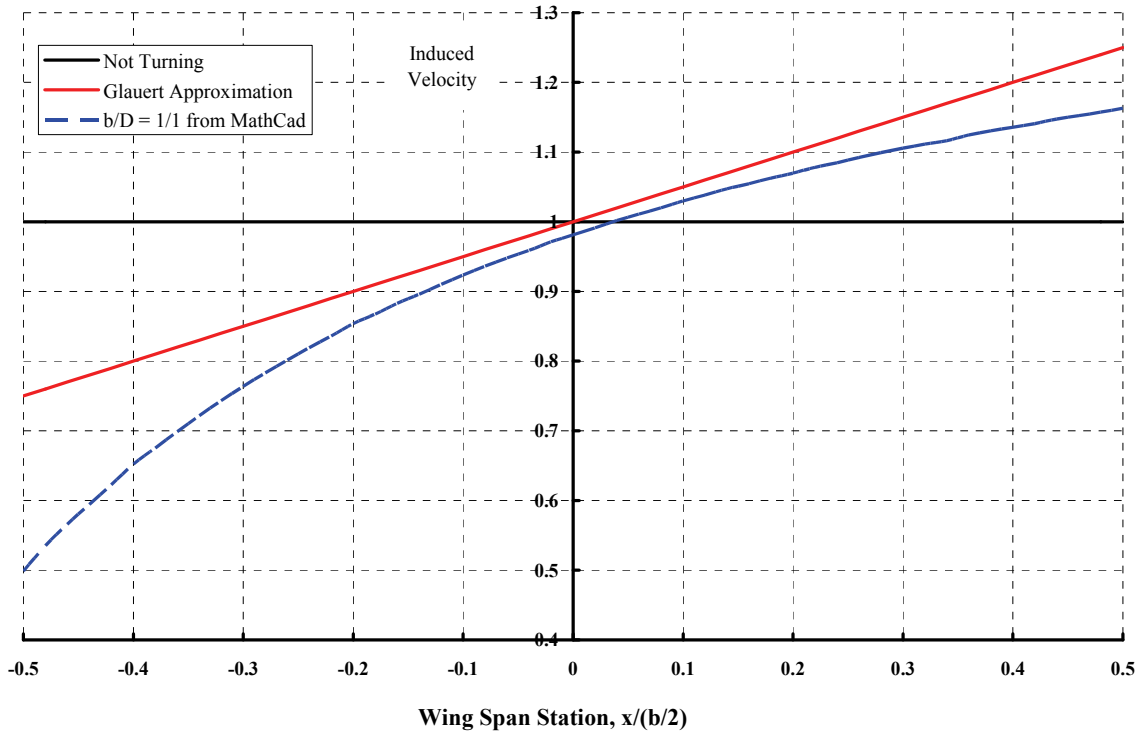


Fig. B-5

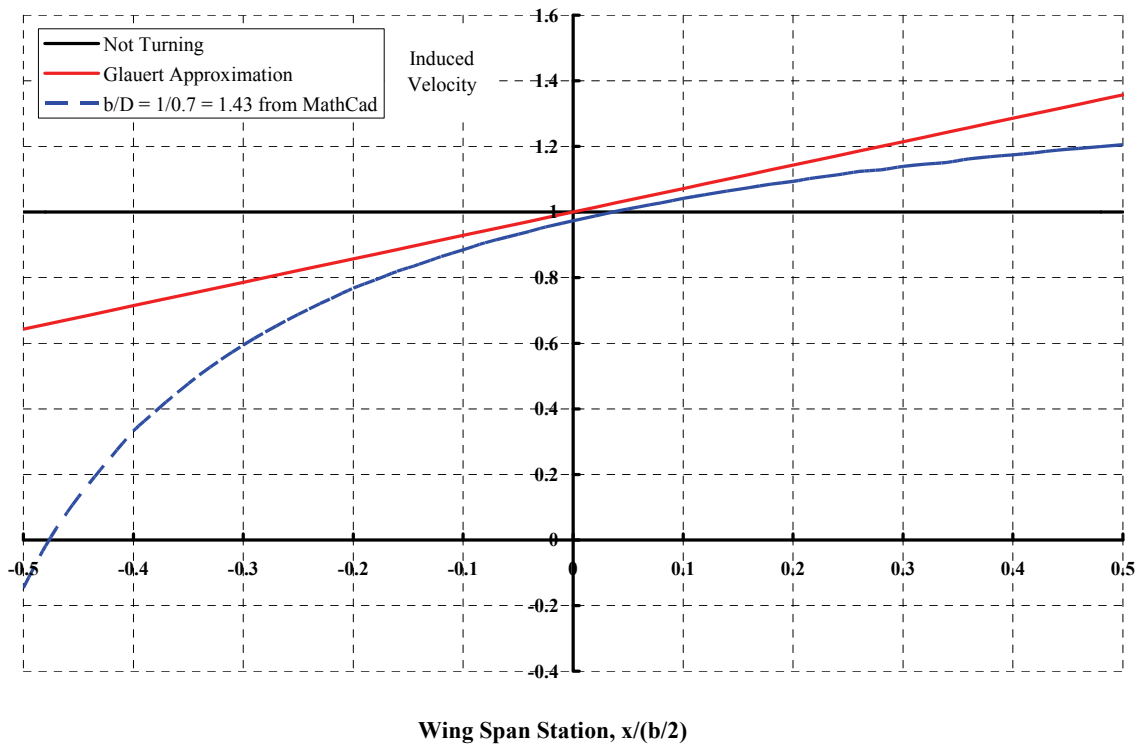


Fig. B-6

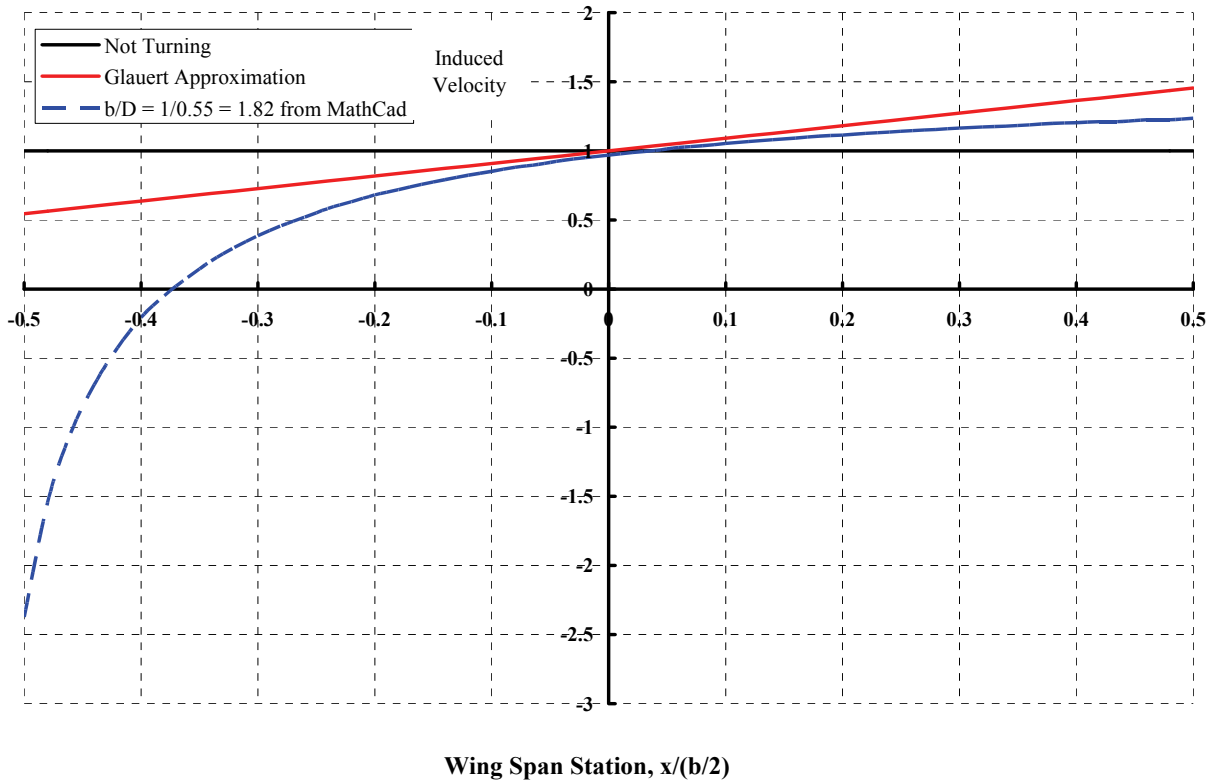


Fig. B-7

Philosophically, Glauert found the fixed-wing induced velocity equation is buried obscurely within the U-turning wing problem posed by Eq. (39). Therefore, the MathCad-provided integration scheme encounters all of the fixed-wing problems at the wing tips. (MathCad returns the notice “will not converge,” which makes for frustration.) A second thing you know is that the denominator of the integrand can get very, very small, or even be zero when  $\theta = 0$ . Both of these probable problems suggest using the fixed-wing coordinate transformations, which to repeat, are

$$(40) \quad xv = -\frac{b}{2} \cos \beta \quad dxv = \frac{b}{2} \sin \beta \quad xw = -\frac{b}{2} \cos \alpha$$

and assume an elliptical bound circulation along the wing’s lifting line so that

$$(41) \quad \gamma_v = -\Gamma_o \cos \beta d\beta.$$

With the preceding thoughts in mind, a “brute force” numerical integration scheme goes like this:

## APPENDIX B

$$\Gamma_o = 2 \quad b = 1 \quad D = 0.7$$

Dimension integration.

Number of radial stations at which vortices leave wing,  $M = 90$

Number of azimuthal stations between 0 and 180 degrees,  $N = 18,000$

Range of radial stations where induced velocity is calculated,  $s = 0, 1, \dots, M-1$

Then proceed with these calculations

$$\alpha_s = \frac{\pi}{M} \left( s + \frac{1}{2} \right)$$

$$n = 0, 1, \dots, N \quad \theta_n = \left( -\frac{\pi}{N} \right) n$$

$$m = 0, 1, \dots, M \quad \beta_m = \left( \frac{\pi}{M} \right) m$$

$$dvd\beta d\theta_{n,m} = \frac{\Gamma_o}{4\pi} \cos\beta_m \left\{ \frac{\left( D - \frac{b}{2} \cos\beta_m \right) \left( D - \frac{b}{2} \cos\alpha_s \right) \cos\theta_n - \left( D - \frac{b}{2} \cos\beta_m \right)^2}{\left[ \left( D - \frac{b}{2} \cos\beta_m \right)^2 + \left( D - \frac{b}{2} \cos\alpha_s \right)^2 - 2 \left( D - \frac{b}{2} \cos\beta_m \right) \left( D - \frac{b}{2} \cos\alpha_s \right) \cos\theta_n \right]^{3/2}} \right\}$$

$$dvd\beta_m = \frac{\pi}{N} \sum_{n=0}^{N-1} \frac{dvd\beta d\theta_{n,m} + dvd\beta d\theta_{n+1,m}}{2}$$

$$v_s = \frac{\pi}{M} \sum_{m=0}^{M-1} \frac{dvd\beta_m + dvd\beta_{m+1}}{2}$$

$$xw_s = -\frac{b}{2} \cos\alpha_s$$

The brute force aspects of the above scheme are obvious. The wake age from  $\theta = 0$  to 180 degrees is divided into 18,000 segments, or 0.01 of a degree. The spanwise segmentation is a little more rational. Ninety vortices are trailed, and induced velocity at the wing is calculated in between each pair of trailed vortices. This density is far from practical for the real problems rotorcraft engineers are solving everyday with computers. Calculating area as the sum of rectangular slivers is hardly advanced. Despite the obvious improvements that might be made, the scheme works.

The first numerical integration result, compared to the virtually exact solution obtained by following Glauert, is shown in Fig. B-8. The agreement over 99.9 percent of the wingspan is more than acceptable for engineering purposes. The only problem that occurred was calculation of induced velocity at the most outboard span station (i.e.,  $s + 1/2 = 89.5$  or  $xw = 0.4999238476$ ). This span station is halfway between the vortex trailed from the tip (i.e.,  $m = 90$ ) and the next vortex inboard at  $m = 89$ . The numerical solution gave  $v = 19.65$  feet/second versus the virtually exact 1.206 feet/second. In contrast, the port wing tip encountered no such problems. Other than this one ridiculous answer at the starboard wing tip (plus being rather slow), the numerical integration scheme functioned in a satisfactory manner.

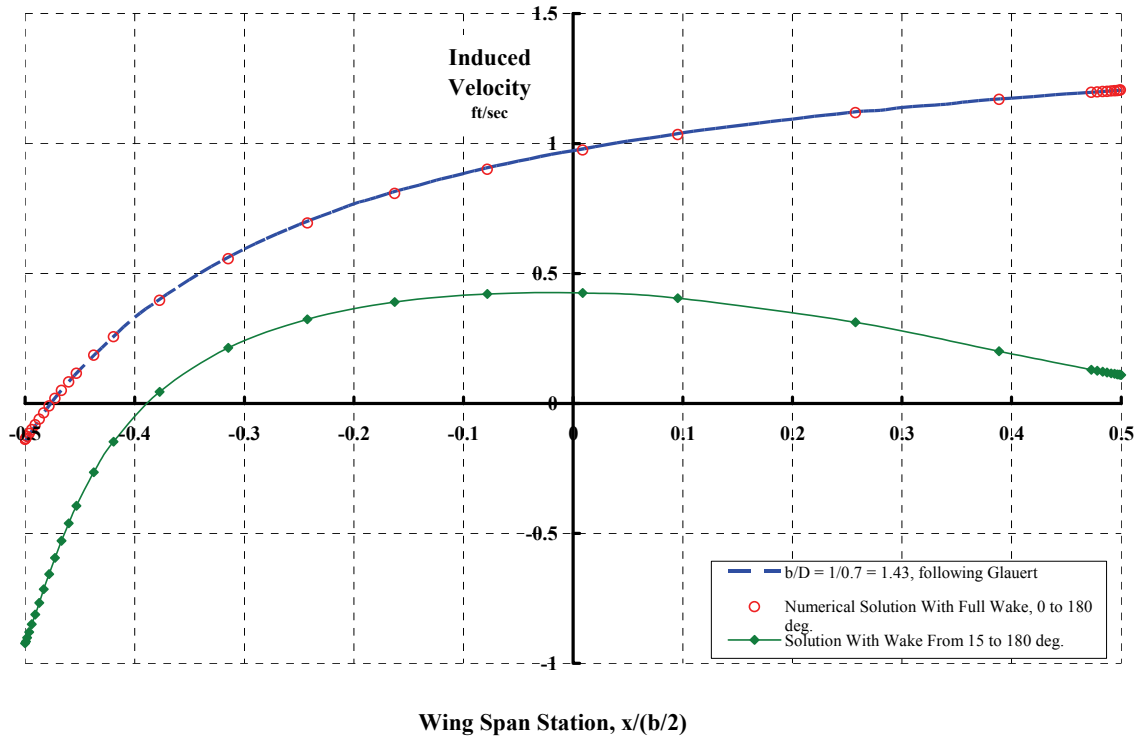


Fig. B-8

There are several interesting features to this U-turning wing problem. For example, the numerical integration proceeded from port to starboard wing tip with the numerous trailed vortices in between. Fig. B-9 illustrates what the induced velocity wake-age summation appears like for the calculation point next to the wing mid-span. The span station of interest is  $s + \frac{1}{2}$  ( $\alpha_s = 90.5$  degrees,  $x_w = 0.0087$ ). Fig. B-9 shows that  $dv/d\beta$  sees the impending discontinuity at the span station point, but the summation averages the calculation to the left of the point with the calculation to the right of the point. Therefore, the induced velocity is the integral found from

$$\text{induced velocity, } v = \text{area under } \frac{dv}{d\beta} \text{ versus } \beta$$

and is obtained with quite reasonable results.

Another interesting behavior of this U-turning wing problem is shown in Fig. B-10. This figure looks at the wake-age integration involved with

$$\frac{dv}{d\beta} d\beta = \text{area under } \frac{d\left(\frac{dv}{d\beta} d\beta\right)}{d\theta} \text{ versus } \theta.$$

The summation is illustrated at the two vortex trailed wing stations of  $\beta = 160$  and  $\beta = 162$  degrees (i.e.,  $m = 80$  and  $m = 81$ ). The station at which induced velocity is sought is  $\alpha_s = 161$  degrees. The fascinating point made here is that the two vortices appear to make enormous contributions to induced velocity within the first 2 degrees of wake age. This

APPENDIX B

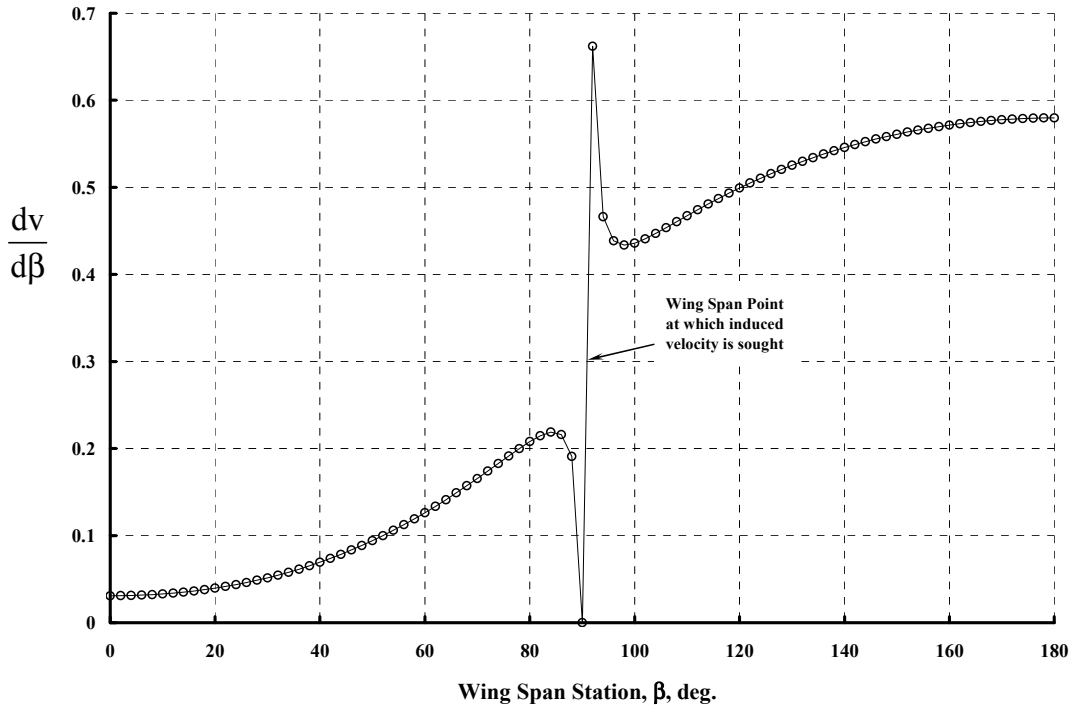


Fig. B-9

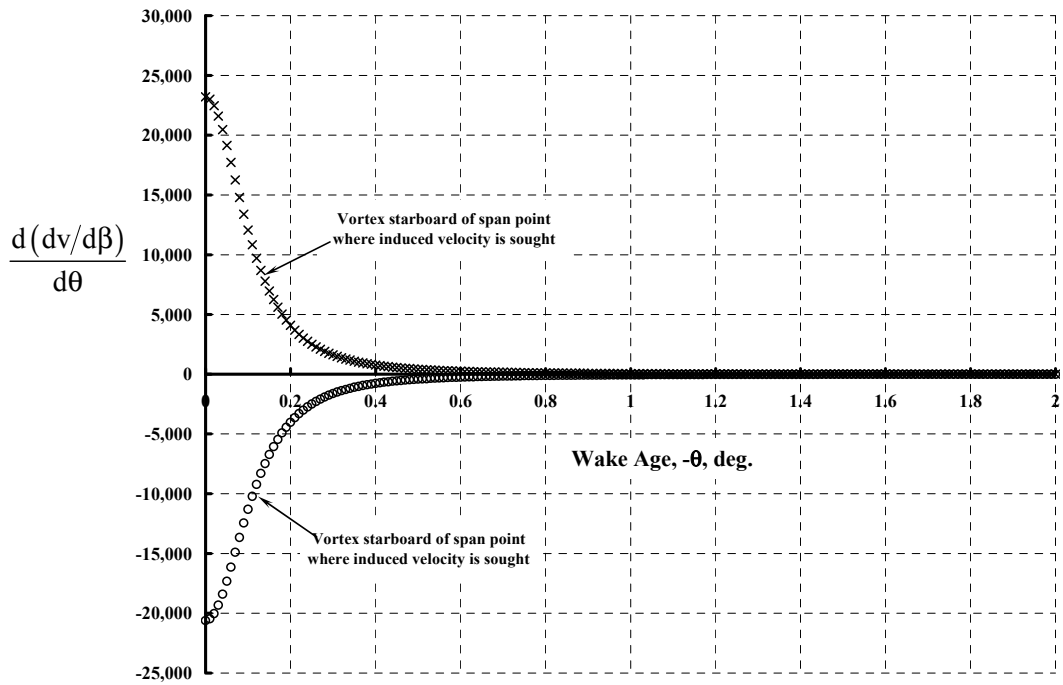


Fig. B-10

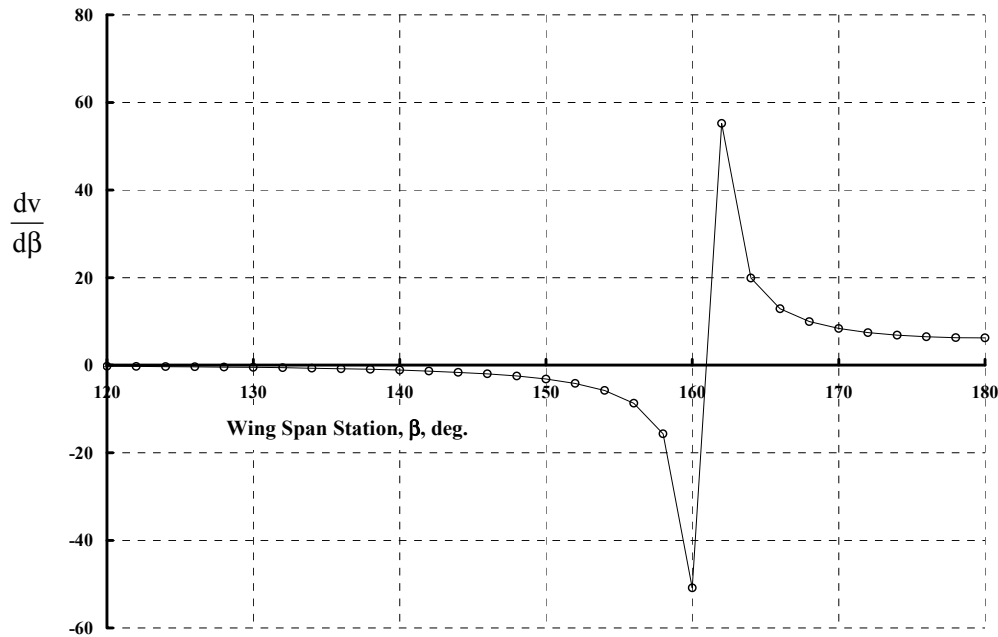


Fig. B-11

is one of the reasons such small increments in wake age (i.e., 180 degrees of wake divided into 18,000 segments) are required for the rudimentary rectangular area summation scheme. The spanwise distribution of  $dv/d\beta$ , provided with Fig. B-11, shows just how large the numbers are that, when summed, however, come out  $v = 1.1968318858$ .

The situation near the port wing tip, which is closest to the pylon, is quite similar to that near the starboard wing tip. The conclusion is that the first 15 degrees of wake age must be very densely populated with points if a rudimentary numerical integration is used. Fortunately, advanced methods currently used in the rotorcraft industry accomplish the numerical integration much more efficiently.

Rotorcraft engineers have improved their nonuniform induced velocity calculating methods by dividing the wake into a near wake and a far wake. Thus, Fig. B-8 shows that the near wake (i.e.,  $\theta = 0$  to  $-15$  degrees in this case) is the most troublesome for numerical integration, particularly at the wing tips. The far wake (i.e.,  $\theta$  from  $-15$  to  $\theta = -180$  degrees in this case) responds to numerical integration with virtually no problems. In fact, the wake age can be divided into 1-degree segments versus 0.01-degree segments, and virtually the same contribution of the far wake to the induced velocity at the wing will be obtained.

The U-turning wing problem can be divided into a near wake and a far wake with relative ease. The induced velocity at the wing due to 180 degrees of circular arc wake in elliptic integral form is

APPENDIX B

$$(42) \quad v_{xw} = \int_{-b/2}^{+b/2} \left[ \frac{-\frac{\partial \Gamma}{\partial xv}}{4\pi} \left[ \frac{\int_0^{\pi/2} \sqrt{1-k^2 \sin^2 \phi} d\phi}{xv - xw} + \frac{\int_0^{\pi/2} \frac{1}{\sqrt{1-k^2 \sin^2 \phi}} d\phi}{2D + xv + xw} \right] \right] dxv.$$

Keep in mind that  $\phi = \pi/2$  is closest to the wing. Conversely,  $\phi = 0$  corresponds to the end of the wake, or where the wing was *before* it started the U-turn. Therefore, the wake integration amounts to integrating from zero up to the start of the near wake, say  $\phi_{NW}$ , and then adding the near-wake contribution, which extends from  $\phi = \phi_{NW}$  to  $\phi = \pi/2$ . It is, however, much more direct in this case to subtract the wake behind the near wake (i.e.,  $\int_0^{\phi_{NW}} f(\phi)d\phi$ ) from the total wake (i.e.,  $\int_0^{\pi/2} f(\phi)d\phi$ ). Thus, the two elliptic integrals are rearranged as follow:

$$(43) \quad \begin{aligned} \text{Near wake} &= \int_0^{\pi/2} \sqrt{1-k^2 \sin^2 \phi} d\phi - \int_0^{\phi_{NW}} \sqrt{1-k^2 \sin^2 \phi} d\phi = \int_0^{\chi} \sqrt{1-k^2 \sin^2 \phi} d\phi - k^2 \sin \phi_{NM} \sin \chi \\ \text{Near wake} &= \int_0^{\pi/2} \frac{1}{\sqrt{1-k^2 \sin^2 \phi}} d\phi - \int_0^{\phi_{NW}} \frac{1}{\sqrt{1-k^2 \sin^2 \phi}} d\phi = \int_0^{\chi} \frac{1}{\sqrt{1-k^2 \sin^2 \phi}} d\phi \end{aligned}$$

where the angle,  $\chi$ , a new upper limit of integration, is given as

$$(44) \quad \chi = 2 \arctan \left( \frac{\sqrt{1-k^2 \sin^2 \phi_{NW}} - \sin \phi_{NW} \sqrt{1-k^2}}{\cos \phi_{NW}} \right).$$

Then, in elliptic integral shorthand, the near-wake contribution to induced velocity at the wing is simply

$$(45) \quad (v_{xw})_{\text{Near Wake}} = \int_{-b/2}^{+b/2} \frac{-\frac{\partial \Gamma}{\partial xv}}{4\pi} \left[ \frac{E(\chi, k) - k^2 \sin \phi_{NM} \sin \chi}{xv - xw} + \frac{F(\chi, k)}{2D + xv + xw} \right] dxv$$

where

$$(46) \quad \begin{aligned} E(\chi, k) &= \int_0^{\chi} \sqrt{1-k^2 \sin^2 \phi} d\phi \\ F(\chi, k) &= \int_0^{\chi} \frac{1}{\sqrt{1-k^2 \sin^2 \phi}} d\phi \end{aligned}$$

In like manner, the induced velocity at the wing due to the far wake becomes

$$(47) \quad (v_{xw})_{\text{Far Wake}} = \int_{-b/2}^{+b/2} \left[ \frac{-\frac{\partial \Gamma}{\partial xv}}{4\pi} \left[ \frac{\int_0^{\phi_{NW}} \sqrt{1-k^2 \sin^2 \phi} d\phi}{xv-xw} + \frac{\int_0^{\phi_{NW}} \frac{1}{\sqrt{1-k^2 \sin^2 \phi}} d\phi}{2D+xv+xw} \right] \right] dxv$$

where, to repeat,  $k^2 = \frac{4(D+xw)(D+xv)}{(2D+xv+xw)^2}$ .

This completes the discussion of the U-turning wing problem. Two points have been made:

- (1) A virtually exact calculation of induced velocity without numerical integration questions has been provided. Figure B-6 gives an example to which any numerical integration result may be compared.
- (2) The so-called near wake is built upon the fundamental integral solved by the fixed-wing community, which is

$$(48) \quad \text{Fixed Wing } (v_{xw}) = \int_{-b/2}^{+b/2} \frac{-\frac{\partial \Gamma}{\partial xv}}{4\pi} \left[ \frac{1}{xv-xw} \right] dxv.$$

### Part II—The Rotating Wing Done With Rotor Notation

The next step along the bridge from the fixed-wing world to the rotary wing world is rotor blade geometry and notations. This geometry is provided in Fig. B-12. The intent here is to think of a one-bladed rotor in hovering flight. (The case of forward flight is addressed in Part III of this appendix.) The rotating wing is again represented as a lifting line having an elliptical bound circulation. The trailing vortex wake structure resembles a lock washer or, perhaps more descriptively, a “slinky” spring-like toy. That is, each vortex has a circular path just like the U-turning wing problem. The addition is that each trailing vortex spirals downward at a constant rate, and the wake age can extend back to the beginning of time. In short, the wake of this rotating wing or, better yet, a one-bladed hovering rotor, need not stop at minus 180 degrees as was the case with the U-turning wing.

Now study the geometry of Fig. B-12 quite closely. The rotor blade is shown rotating around the Z-axis, which is positive down. The blade rotates in the X–Y plane where X is taken positive “forward,” although what forward means in this case of no forward speed is not really meaningful. The Y-axis is normal to the X–Z plane. This X-, Y-, Z-axis system does not rotate with the blade, nor does it move with time.

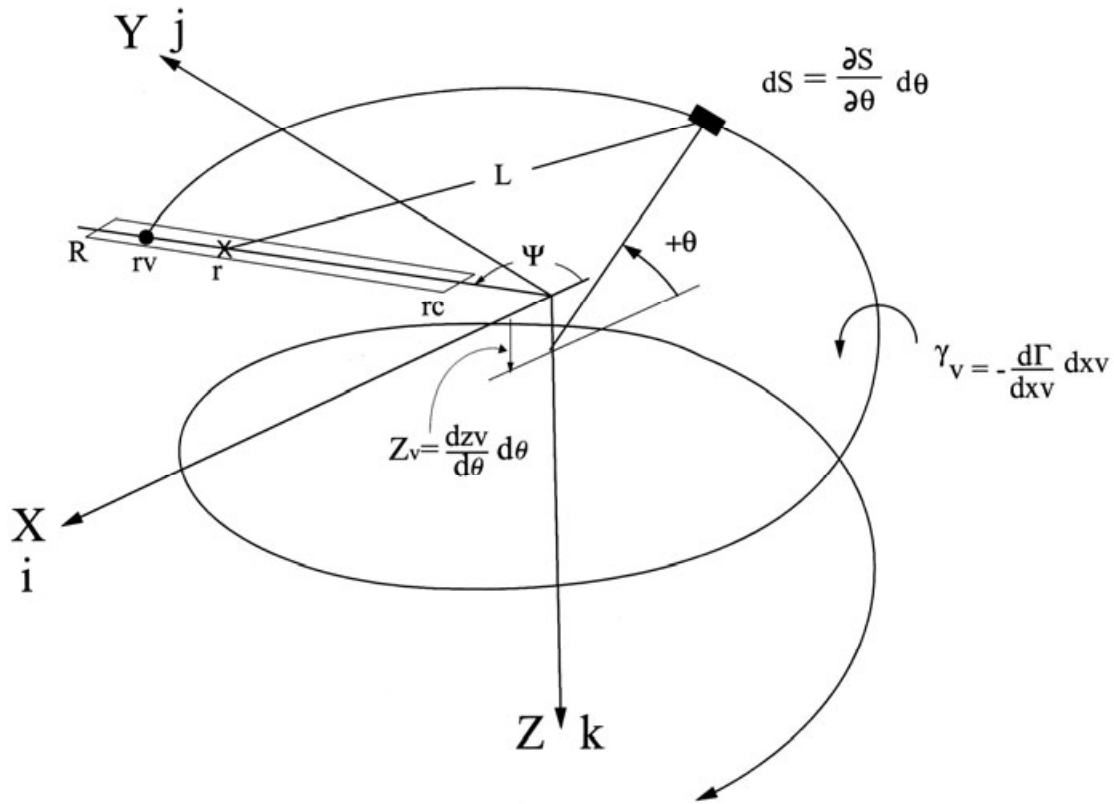


Fig. B-12

The blade itself has a radius,  $R$ , measured from the  $Z$ -axis. The blade is shown in Fig. B-12 with a root cutout,  $r_c$ . Thus, the blade's span (thinking in terms of a wing) is simply  $R - r_c$ . Any radial station measured positive outward from the  $Z$ -axis and along the lifting line is denoted by  $(r)$ .

The rotation angle of the blade is measured by the azimuth angle ( $\psi$ ), which, for convenience, equals zero when the blade lies along the negative  $X$ -axis. The azimuth angle increases with time, simply as the rotational speed ( $\Omega$ ) in radians per second times time in seconds. Obviously, Fig. B-12 is a snapshot at any given time you care to start the watch. The blade is simply going round and round, and the trailed vortex structure is left in space to descend at a prescribed rate ( $dZ/dt$ ) in feet per second. Fig. B-12 is drawn to imply that the blade has been rotating for the time it takes to complete about two revolutions. However, the arrowhead shown at the end of the one trailed vortex implies that time has been going on forever and, with a longer piece of paper, the spiral would extend down and around the  $Z$ -axis to infinity.

As with the preceding fixed-wing examples, the Biot–Savart law requires a very careful mathematical definition for the blade and vortex wake dimensions. This is especially true when tackling the rotor blade problem. Using Fig. B-12 as the geometric model of a single bladed rotor, the radius station ( $r$ ) at which the induced velocity is sought is set relative to the  $X - Y - Z$  axis by

$$(49) \quad X_r = -r \cos \psi \quad Y_r = +r \sin \psi \quad Z_r = 0.$$

A vortex trails aft from the blade from radius station  $r_v$ . Any segment of this long, spiraling vortex is therefore deposited at a point behind the blade and below the  $X$ - $Y$  plane. This vortex segment,  $dS$ , is located at the coordinates

$$(50) \quad X_v = -r_v \cos \theta \quad Y_v = +r_v \sin \theta \quad Z_v = + \frac{dZ_v}{dt} \Delta t.$$

Eq. (50) introduces the possibility that the wake trailing behind the rotor blade does not stay in the  $X$ - $Y$  plane in which the rotor blade turns. This is quite different from classical fixed-wing wake geometry assumptions. The rotor blade wake descends with some velocity ( $dZ_v/dt$ ), and this velocity need not be constant. In fact, in the more complete analyses of rotor systems, freedom is given for any given vortex segment to wander throughout the  $X - Y - Z$  axis system. For elementary discussion purposes, just assume a constant diameter spiral (i.e., neither  $r_v$  nor  $dZ_v/dt$  are influenced by time). Furthermore, it is not necessary at this point in the discussion to be more specific about the descent velocity of the vortex segment.

Now consider the matter of time introduced by Eq. (50). For the rotor blade, the time increment ( $\Delta t$ ) represents the time ( $t$ ) it takes to travel back from the blade, which is at the snapshot azimuth angle ( $\psi$ ) (at time,  $t_0$ ) to the vortex segment,  $dS$ , which is located at  $\theta$  (at time,  $t$ ). That is,

$$(51) \quad \Delta t = t - t_0.$$

Because the blade's angular rotation speed is  $\Omega$ , it follows that

APPENDIX B

$$(52) \quad \Delta t = t - t_0 = \frac{\theta - \psi}{\Omega},$$

which immediately says that

$$(53) \quad Z_v = + \frac{dz_v}{dt} \Delta t = \frac{dz_v}{dt} \left( \frac{\theta - \psi}{\Omega} \right) = \frac{dz_v}{\Omega dt} \theta = \frac{dz_v}{d\theta} \theta.$$

In many propeller studies,  $dZ_v/d\theta$  is a measure of helix angle or sometimes propeller pitch.

Now, quite methodically, begin with the Biot–Savart law as previous stated:

$$(54) \quad d(dv_x / dx_v) = \frac{\gamma_v}{4\pi} \left[ \frac{L_i dS_j - L_j dS_i}{L^3} \right] d\theta$$

where the dimensions are expressed as vectors. The distance ( $L$ ) between the vortex segment and the radius station ( $r$ ) at which the induced velocity is sought, is determined by

$$(55) \quad \begin{aligned} L &= L_i + L_j + L_k = (X_r - X_v)i + (Y_r - Y_v)j + (Z_r - Z_v)k \\ \text{where } X_r &= -r \cos \psi & Y_r &= +r \sin \psi & Z_r &= 0 \\ X_v &= -rv \cos \theta & Y_v &= +rv \sin \theta & Z_v &= + \frac{dz_v}{d\theta} \theta \end{aligned}$$

$$\text{and } L^3 = \left[ (X_r - X_v)^2 + (Y_r - Y_v)^2 + (Z_r - Z_v)^2 \right]^{3/2}.$$

In a similar manner, the vortex is describe by

$$(56) \quad S = S_i + S_j + S_k = (X_v)i + (Y_v)j + (Z_v)k$$

but with rotor blade vortex geometry,

$$(57) \quad \begin{aligned} dS_i &= \frac{\partial S_i}{\partial \theta} d\theta = \frac{\partial X_v}{\partial \theta} d\theta = (rv \sin \theta) d\theta \\ dS_j &= \frac{\partial S_j}{\partial \theta} d\theta = \frac{\partial Y_v}{\partial \theta} d\theta = (rv \cos \theta) d\theta \\ dS_k &= \frac{\partial S_k}{\partial \theta} d\theta = \frac{\partial Z_v}{\partial \theta} d\theta. \end{aligned}$$

The substitution of this rotor blade geometry into the Biot–Savart law gives, with simplification

$$(58) \quad d(dv_r / dr_v) = \frac{\gamma_v}{4\pi} \left\{ \frac{rv^2 - r(rv) \cos(\psi - \theta)}{\left[ rv^2 + r^2 - 2r(rv) \cos(\psi - \theta) + \left( \frac{dz_v}{d\theta} \right)^2 \theta^2 \right]^{3/2}} \right\} d\theta.$$

Because this is a single bladed rotor in hover, there is an opportunity to chose the blade azimuth position at any value that is convenient. This is because the hover problem is completely symmetrical around the Z-axis and “forward” has no meaning. (This is not possible in the forward flight case as you will see in Part III of this appendix.) Given this latitude, choose  $\psi = 0$ . This reduces Eq. (58) to

$$(59) \quad d(dv_r / drv) = \frac{\gamma_v}{4\pi} \left\{ \frac{rv^2 - r(rv)\cos\theta}{\left[ rv^2 + r^2 - 2r(rv)\cos\theta + \left( \frac{dzv}{d\theta} \right)^2 \theta^2 \right]^{3/2}} \right\} d\theta,$$

which is a variation on Eq. (28) arrived at for the fixed wing after a U-turn. The variation is, of course, the addition of the term

$$\left( \frac{dzv}{d\theta} \right)^2 \theta^2.$$

Now let me address the wake-age parameter ( $\theta$ ). The vortex wake leaves the blade lifting line referenced to  $\psi = 0$ . Therefore, the smallest that  $\theta$  can be is  $\theta = \psi = 0$ . The vortex spirals backwards (round and round and down) to  $\theta = -\infty$ . While it is not practical to go all the way back to  $\theta = -\infty$ , the intent is to go as far back as possible to avoid missing any influence of what many refer to as the far wake. Nevertheless, the integration over the wake age becomes

$$(60) \quad dv_r / drv = \int_{-\infty}^0 \left\{ \frac{\gamma_v}{4\pi} \left[ \frac{rv^2 - r(rv)\cos\theta}{rv^2 + r^2 - 2r(rv)\cos\theta + \left( \frac{dzv}{d\theta} \right)^2 \theta^2} \right]^{3/2} \right\} d\theta.$$

The immediate objective is to perform the integration required by Eq. (60). Suppose the vortex circulation,  $\gamma_v$ , does not vary with wake age, and suppose the vortex descent measure,  $dzv/d\theta$ , is constant. The only immediate numerical problem that is apparent in Eq. (60) is when the integrand’s denominator is identically zero, or so close to zero that numerical integration built into MathCad flounders. This situation will *only* occur when  $\theta$  is actually zero *and* when  $r = rv$ .

To illustrate the results of integrating Eq. (60) over the wake age using MathCad’s built-in scheme, choose some rational values for a single bladed rotor (Table B-2). For this example, MathCad was quite happy to whip out the answer so long as the input was chosen

**Table B-2**

Parameter	Value
Rotor radius, R, feet	30.0
Root cutout, r <sub>c</sub> , feet	3.0
Trail vortex from radius, r <sub>v</sub> , feet	27.0
Calculate induced velocity at radius, r, feet	16.5
Trailed vortex strength, γ <sub>v</sub> , ft <sup>2</sup> per second	1,265.0
Vortex descent measure, dzv/dθ, feet per radian	2.0
Wake age, θ <sub>end</sub> , radians	-157.0
Number of 360 degree spirals	25
Distance from rotor down to last spiral, z <sub>v</sub> , feet	314

that avoids  $r = r_v$  by a considerable margin. (Just imagine the wake-age integral in summation form with wake-age segments of 0.01 degrees! It would take forever.) In the blink of an eye MathCad produced Fig. B-13. Fig. B-13 shows that induced velocity accumulates very quickly with the increasing number of spirals included in the integration. Closer inspection of Fig. B-14, an enlargement of Fig. B-13, shows that the vortex segments included in the first-half spiral contribute in a rather linear fashion to the induced velocity at blade radius station,  $r$ . But as the spiral continues around, it comes back underneath the blade (see Fig. B-12), and the close proximity allows the vortex to become very influential. In short, the denominator in Eq. (60) with  $\theta$  around  $-360$  degrees is very influenced by the vortex descent measure,  $dzv/d\theta$ .

In advanced, modern numerical integration of the real rotor system problem, wandering vortices do come close and, indeed, even intersect the lifting line or lifting surface of the blade that trailed the vortices. This is to say that the denominator of Eq. (60) finds some way to go to zero in the real problem. Furthermore, when there are more blades to consider, the ensuing possibilities of this denominator going to zero have been a major source of frustration in achieving accurate solutions for the rotor hovering and forward-flight problems. The current crutch most widely used has been to add what is called a vortex core to the denominator of Eq. (60) so zero can never occur. The fact that a vortex does have a real physical core of measurable diameter makes the core's inclusion in Eq. (60) reasonable. This concept of a vortex core diameter (VCD) means that Eq. (60) can be written as

$$(61) \quad dv_r / drv = \int_{-\infty}^0 \frac{\gamma_v}{4\pi} \left\{ \frac{rv^2 - r(rv)\cos\theta}{\left[ rv^2 + r^2 - 2r(rv)\cos\theta + \left( \frac{dzv}{d\theta} \right)^2 \theta^2 + VCD^2 \right]^{3/2}} \right\} d\theta.$$

To make progress over recent years, technologists have achieved considerable numerical stability even when tackling the hardest problems using this concept of a vortex core. For this part of the appendix, let me completely dismiss the whole VCD issue.

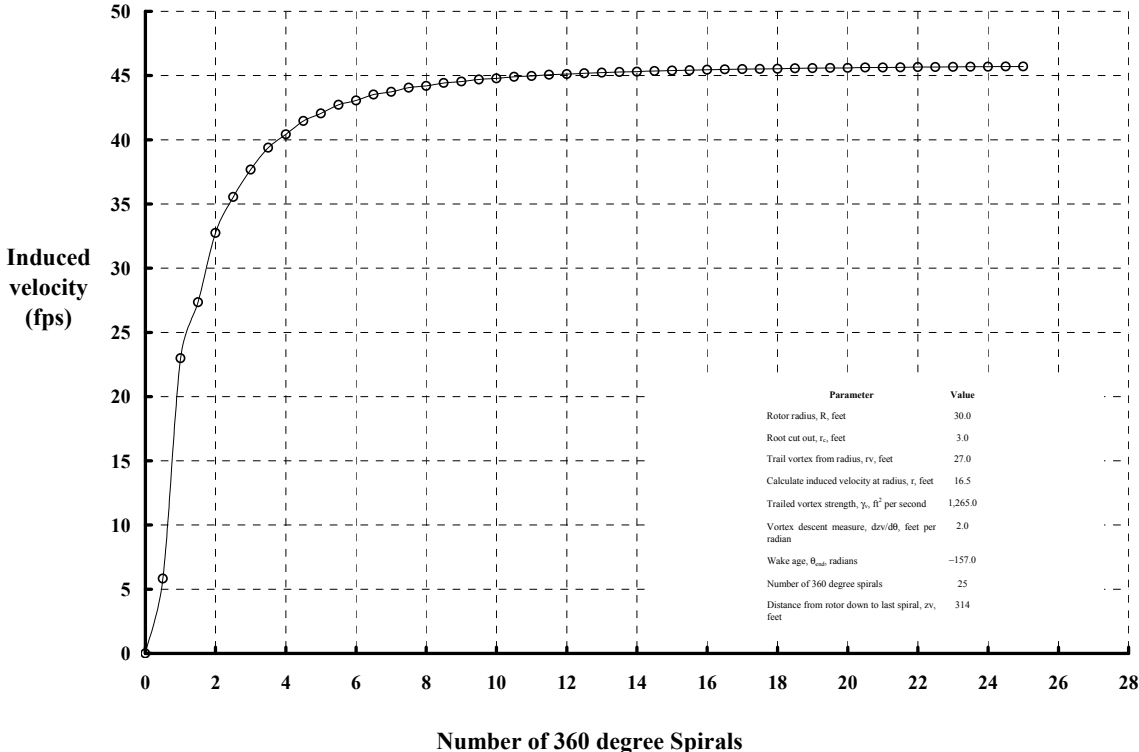


Fig. B-13

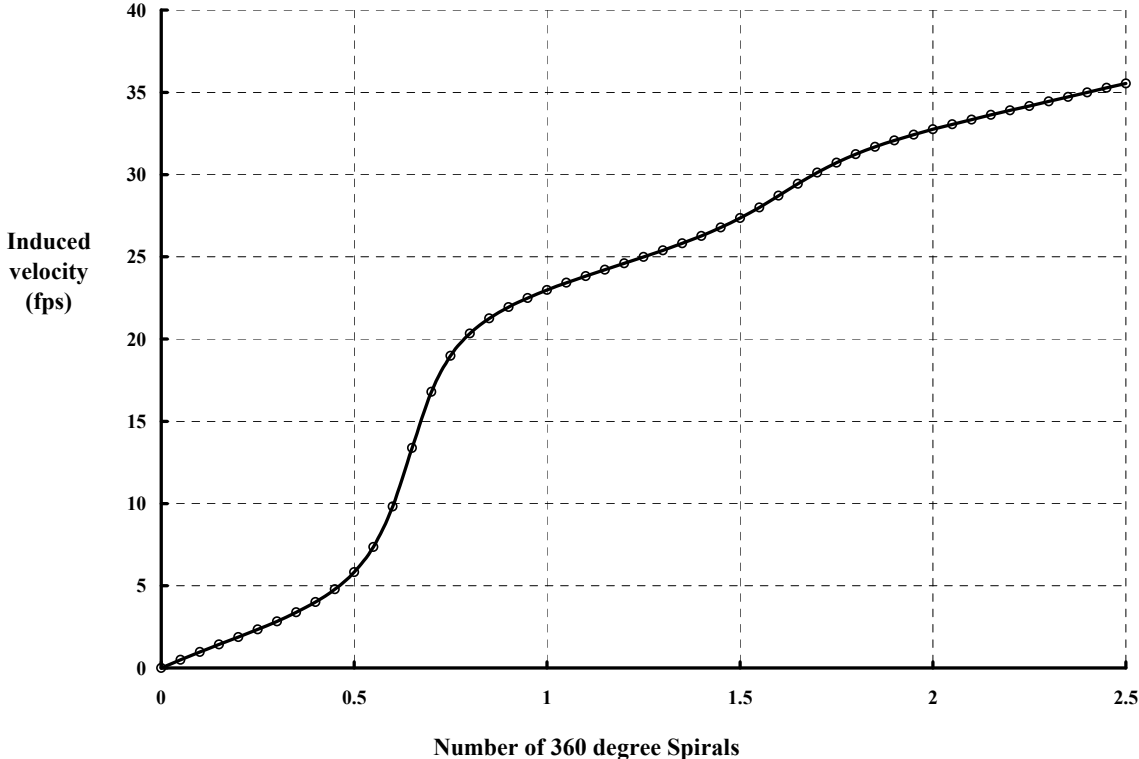


Fig. B-14

APPENDIX B

Proceeding then, consider the collection of all the trailed vortices by performing the radial integration over the blade span from the root cutout ( $r_c$ ) to the blade tip,  $r = R$ . This step begins by assuming a bound circulation distribution carried on the lifting line. Assume the bound circulation has an elliptical distribution<sup>8</sup> described by

$$(62) \quad \Gamma_r = \Gamma_o \sqrt{1 - \frac{(2r - r_c - R)^2}{(R - r_c)^2}},$$

which gives the circulation strength of a vortex trailing from radius station,  $rv$ , as

$$(63) \quad \gamma_v = -1 \left\{ \frac{-2R\Gamma_o}{\sqrt{1 - \frac{(2rv - r_c - R)^2}{(R - r_c)^2}}} \left[ \frac{2rv - r_c - R}{(R - r_c)^2} \right] \right\} drv.$$

The induced velocity along the blade's radius collecting all vortices is then

$$(64) \quad v_r = \int_{r_c}^R \int_{-\infty}^0 \frac{1}{4\pi} \frac{2\Gamma_o}{\sqrt{1 - \frac{(2rv - r_c - R)^2}{(R - r_c)^2}}} \left[ \frac{2rv - r_c - R}{(R - r_c)^2} \right] \left\{ \frac{rv^2 - r(rv) \cos \theta}{\left[ rv^2 + r^2 - 2r(rv) \cos \theta + \left( \frac{dzv}{d\theta} \right)^2 \theta^2 \right]^{3/2}} \right\} d\theta drv.$$

Now, let me illustrate a completely numerical solution for this double integral. From Parts I and II of this appendix, the numerical integration of Eq. (64) does not converge to a solution because of any number of singular points. MathCad's built-in integration scheme flounders even if a close proximity situation occurs. You also know that the induced velocity—given an elliptical bound circulation along the lifting line—must contain the solution for a fixed wing. That is, at the very least

$$v_r = \frac{\Gamma_o}{2(R - r_c)}.$$

The approach, therefore, is to first borrow the fixed-wing solution technique of letting

$$(65) \quad \begin{aligned} r &= \left( \frac{R + r_c}{2} \right) - \left( \frac{R - r_c}{2} \right) \cos \alpha = a - b \cos \alpha \\ rv &= \left( \frac{R + r_c}{2} \right) - \left( \frac{R - r_c}{2} \right) \cos \beta = a - b \cos \beta \\ drv &= \left( \frac{R - r_c}{2} \right) \sin \beta d\beta = b \sin \beta d\beta \end{aligned}$$

---

<sup>8</sup> Keep in mind that the more general distribution used by fixed-wing engineers, Eq. (22), could be used to extend the results beyond an elliptical distribution.

where  $\beta$  goes from 0 to  $\pi$ . This coordinate system change at least transforms the vortex circulation strength,  $\gamma_v$ , of Eq. (63) to the much simpler

$$(66) \quad \gamma_v = -\Gamma_o \cos\beta d\beta.$$

The completed substitution of Eqs. (65) and (66) into Eq. (64) restates the induced velocity double integral problem as

$$(67) \quad v_r = \int_0^\pi \int_{-\infty}^0 \frac{-\Gamma_o \cos\beta}{4\pi} \left\{ \frac{(a-b\cos\alpha)(a-b\cos\beta)\cos\theta - (a-b\cos\beta)^2}{\left[ (a-b\cos\beta)^2 + (a-b\cos\alpha)^2 - 2(a-b\cos\alpha)(a-b\cos\beta)\cos\theta + \left(\frac{dzv}{d\theta}\right)^2 \theta^2 \right]^{3/2}} \right\} d\theta d\beta.$$

So now, let me numerically integrate Eq. (67). The scheme allows MathCad to perform the wake-age integral, *but* the spanwise integration is performed with a summation. This takes advantage of MathCad's very, very fast integration over wake age. Thus, a useable numerical integration scheme reads like this:

INPUT

$$\Gamma_o = 2 \quad R = 1.2 \quad r_c = 0.2 \quad \frac{dzv}{d\theta} = 0$$

Dimension integration.

Extent of wake age, WA =  $-\pi$

Number of radial stations at which vortices leave rotor blade, M = 90

Range of radial stations where induced velocity is calculated, s = 0, 1, ..... M - 1

Then proceed with these calculations

$$a = \frac{R - r_c}{2} \quad b = \frac{R + r_c}{2}$$

$$\alpha_s = \frac{\pi}{M} \left( s + \frac{1}{2} \right)$$

$$m = 0, 1, \dots, M \quad \beta_m = \left( \frac{\pi}{M} \right) m$$

$$dvd\beta_m = \int_{WA}^0 \frac{-\Gamma_o \cos\beta}{4\pi} \left\{ \frac{(a-b\cos\alpha)(a-b\cos\beta)\cos\theta - (a-b\cos\beta)^2}{\left[ (a-b\cos\beta)^2 + (a-b\cos\alpha)^2 - 2(a-b\cos\alpha)(a-b\cos\beta)\cos\theta + \left(\frac{dzv}{d\theta}\right)^2 \theta^2 \right]^{3/2}} \right\} d\theta$$

$$v_s = \frac{\pi}{M} \sum_{m=0}^{M-1} \frac{dvd\beta_m + dvd\beta_{m+1}}{2}$$

$$r_s = a - b \cos \alpha_s$$

## APPENDIX B

Notice that this sample input corresponds to the U-turning wing problem of  $D = 0.7$ ,  $b = 1$ ,  $\Gamma_o = 2$ , which gives the induced velocity distribution shown in Fig. B-8. This check case did check. MathCad was faster and more accurate with the wake-age integral broken into several ranges. The following seemed best

$$\int_{WA}^0 f(\alpha, \beta) d\theta = \int_{-\frac{\pi}{180}^5}^0 f(\alpha, \beta) d\theta + \int_{-\pi}^{-\frac{\pi}{180}^5} f(\alpha, \beta) d\theta + \int_{-3\pi}^{-\pi} f(\alpha, \beta) d\theta + \int_{WA}^{-3\pi} f(\alpha, \beta) d\theta.$$

Now consider a practical case of a four-bladed, 44-foot-diameter rotor lifting about 10,800 pounds while operating at a tip speed of  $V_t = \Omega R = 600$  ft/sec. The preceding input requires an estimate for maximum bound circulation,  $\Gamma_o$ , and the vortex segment descent rate,  $dzv/d\theta$ . Rational estimates for both parameters can be obtained. To begin with, assume each blade has a root cutout of  $r_c = R/6$ , and each blade has an elliptical bound circulation over its span. The maximum of the bound circulation is  $\Gamma_o = 225$  ft<sup>2</sup>/sec, which is calculated from

$$(68) \quad \text{Lift per blade} = \frac{\pi}{8} \rho R V_t \Gamma_o \left[ 1 - \left( \frac{rc}{R} \right)^2 \right] \quad \text{so} \quad \Gamma_o = \frac{8L}{\pi \rho R V_t \left[ 1 - (rc/R)^2 \right]}.$$

Next, assume a vortex segment,  $dS$ , is carried downward with the downwash velocity. From simple momentum theory, this downwash or induced velocity is 19.3 feet/second when calculated with

$$(69) \quad \text{Momentum induced velocity} \equiv v_i = \sqrt{\frac{L}{2\rho\pi R^2}}.$$

Then, in one second, a segment descends 19.3 feet. But in one second, the rotor blade moves through a wake age angle of  $\theta = \Omega$  times one second. Therefore, the vortex segment descent rate is simply

$$(70) \quad \frac{dzv}{d\theta} = \frac{v_i \text{ times 1 second}}{\Omega \text{ times 1 second}} = \frac{v_i}{V_t/R} = R \frac{v_i}{V_t},$$

which is roughly 0.7 feet per radian for this representative example. This means that in one complete spiral revolution, the vertical distance will be  $0.7(2\pi)$  feet, or roughly 4.4 feet for every revolution. This is a measure of the spiral spacing or pitch of Fig. B-12.

To summarize this typical operating situation of a one-bladed rotor, the representative calculations that follow were based on

INPUT

$$\Gamma_o = 225 \text{ ft}^2/\text{sec} \quad R = 22 \text{ ft} \quad r_c = R/6 \quad \frac{dzv}{d\theta} = 0.7 \text{ ft/rad}$$

Dimension integration.

Extent of wake age, WA = variable for this example

Number of radial stations at which vortices leave rotor blade,  $M = 90$

Range of radial stations where induced velocity is calculated,  $s = 0, 1, \dots, M-1$

An immediate question is, “How many spirals does it take to accurately approximate an infinite wake?” As seen from Fig. B-15, perhaps about 100 360-degree spirals capture the problem in a promising way. This amounts to 440 feet of wake or about 10 rotor diameters.

A more quantitative measure of a practical engineering solution is induced horsepower,  $HP_i$ . This major contributor to total power is calculated as

$$(71) \quad HP_i = \frac{1}{550} \int_{rc}^R v_r dL_r = \frac{1}{550} \int_{rc}^R v_r (\rho V_r \Gamma_r) dr .$$

The calculation was made using the summation of 90 rectangular slivers. The results, tabulated in Table B-3, indicate that even 20 spirals will neglect about 2 to 3 horsepower, which is on the order of 2 to 3 percent missing horsepower because the wake age was not extended to infinity. The ratio of calculated induced horsepower to ideal momentum horsepower (i.e.,  $Lv_i/550 = 95.524$  horsepower) is the fourth column in Table B-3. The reciprocal of this ratio, known as Figure of Merit, is provided by the sixth column. A Figure of Merit above 1.0 is not possible, and thus at least 10.5 spirals are required before a rational answer starts to become apparent. Clearly, an elliptical bound circulation, which is ideal for a fixed wing (i.e., the equivalent of  $FM = 1$  for a rotating wing), is far from ideal for a rotating wing.

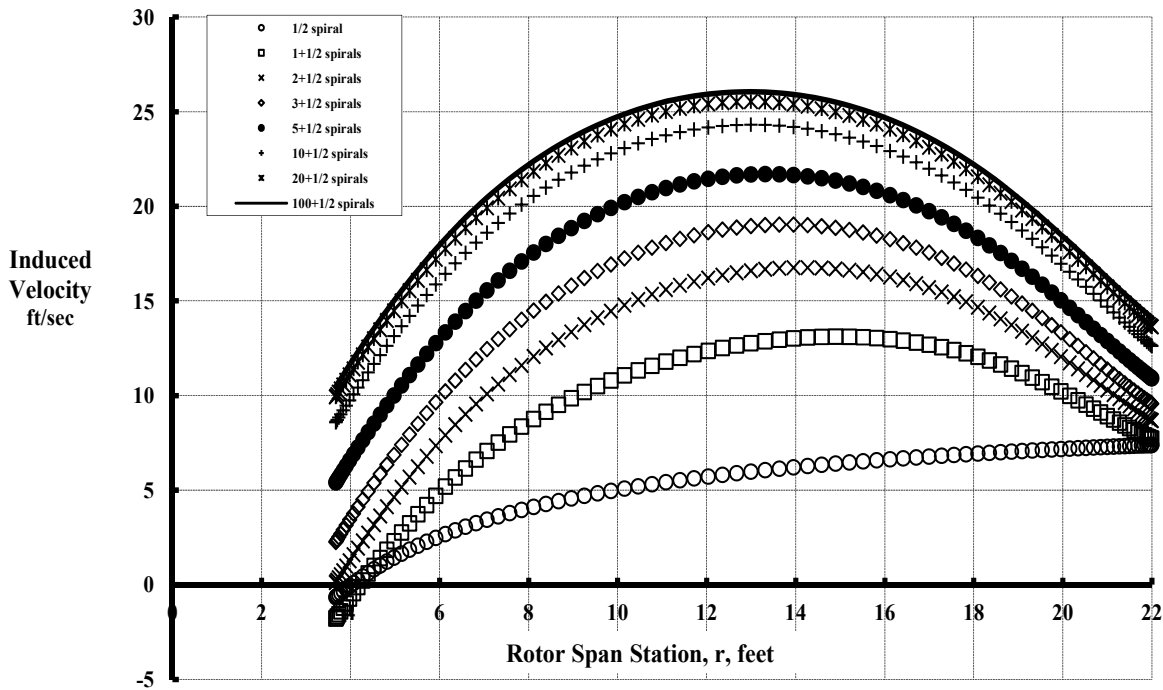


Fig. B-15

**Table B-3**

Number of Spirals	Blade Lift	Calculated Induced HP	Ideal Induced HP	Calculated HP/HP <sub>ideal</sub>	Figure of Merit
0.5	2712.52	29.57	95.52	0.31	3.23
1.5		55.31		0.58	1.73
2.5		70.41		0.74	1.36
3.5		80.32		0.8408	1.189
5.5		92.33		0.9666	1.0346
10.5		104.44		1.0934	0.9146
20.5		110.25		1.1541	0.8665
100.5		112.79		1.1808	0.8469
200.5	↓	112.84	↓	1.1813	0.8465

Do not assume that this example provides anything more than a crude estimate for the actual performance of a single bladed rotor. The prescribed wake geometry used is very, very far from the wake visually observed in any number of experiments. The example would surely come out differently—and more accurately compared to experiment—if (or when) this sample problem is calculated with advanced methods in use today. For the sake of completeness, Fig. B-16 gives the running lift ( $\Delta L_r$ ) and running horsepower ( $\Delta HP_r$ ) versus radius station. This data is for 100.5 spirals.

This concludes Part I and Part II of this appendix. The next step is to apply this background to the single bladed rotor in forward flight.

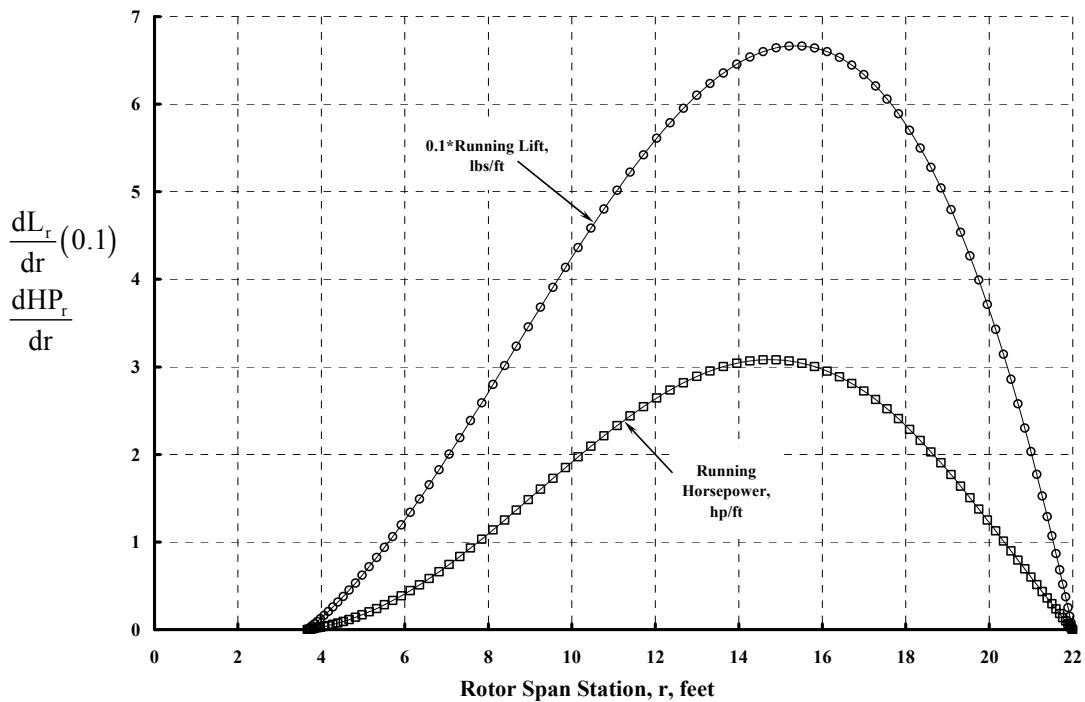


**Fig. B-16**

### Part III—A Rotating Blade in Forward Flight

The next step in the bridge between a fixed and rotating wing is examined in this portion of the appendix. The rotating wing in forward flight deposits a rather complicated vortex wake in space as it flies away. A hint of the wake's complexity is shown below in Fig. B-17.

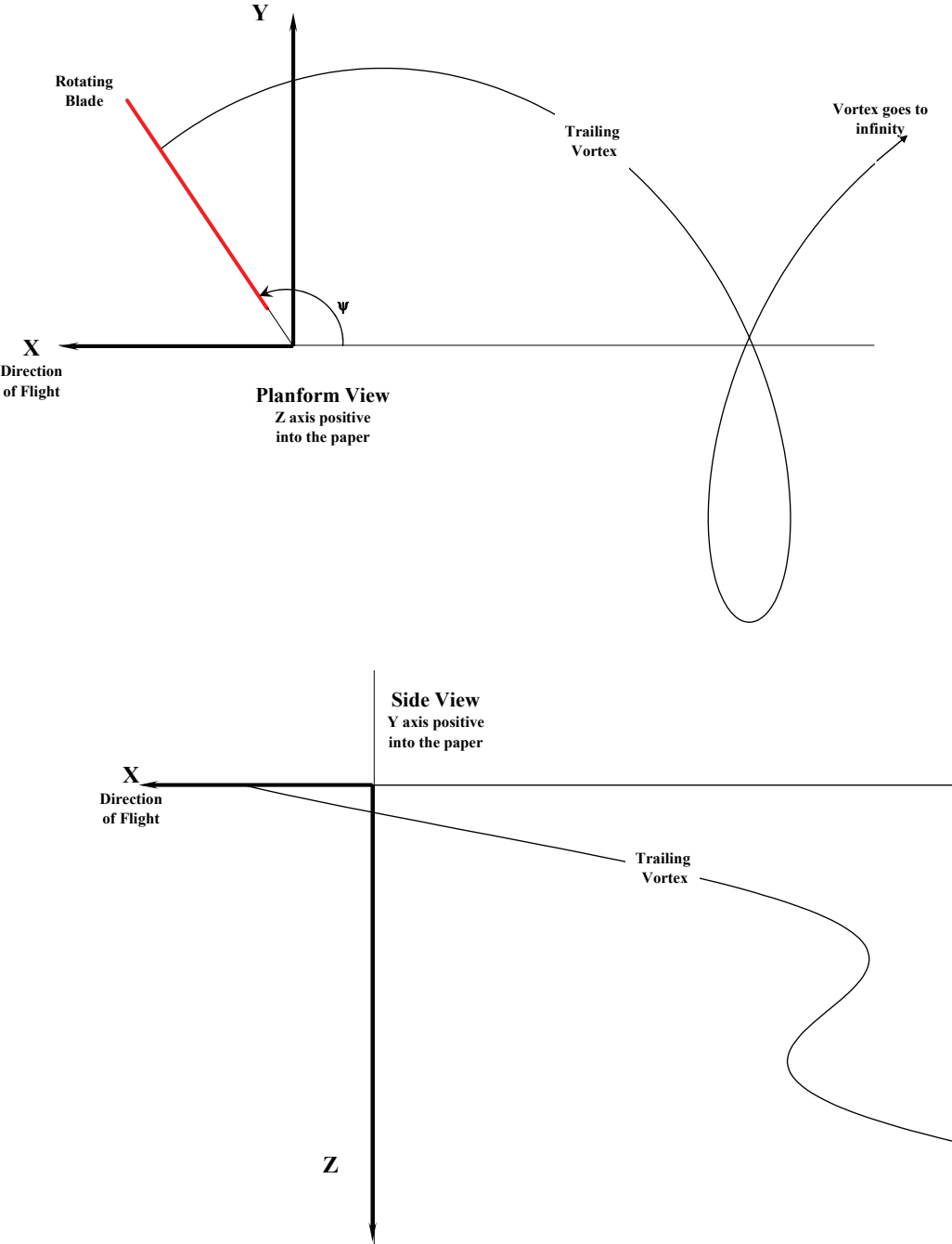
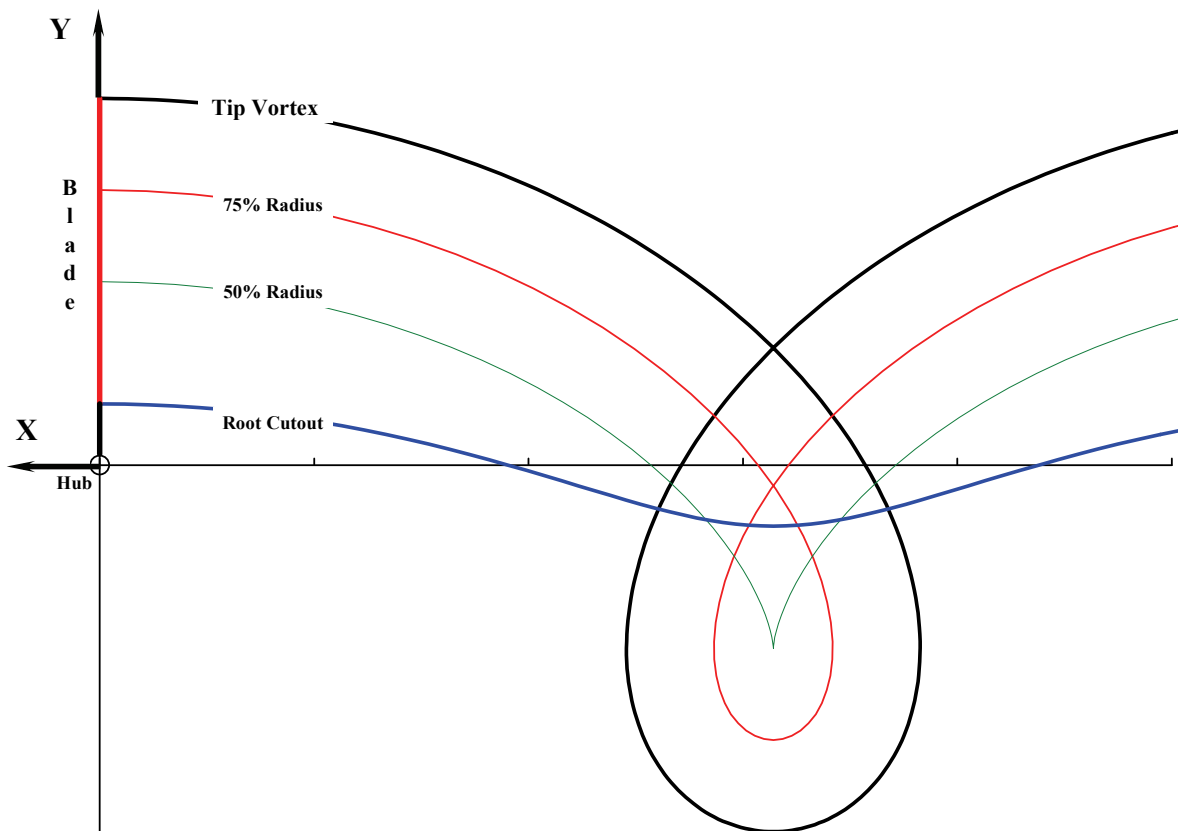


Fig. B-17

## APPENDIX B

In the preceding sketch, the rotating wing, the single bladed rotor, is rotating about the Z-axis in the X–Y plane at angular velocity ( $\Omega$ ) in radians per second. The blade is attached to a hub. The hub is located at  $X = Y = Z = 0$ . The X – Y – Z axis system moves through space straight along the plus X direction with forward velocity (V) in feet per second. The axis system neither pitches nor rolls, and it does not climb or descend. The rotor blade has a radius (R) in feet and a root cutout ( $r_c$ ) in feet. The tip speed of the rotor is  $V_t = \Omega R$  in feet per second. The one vortex shown illustrates the drifting, down spiraling path typical of all vortices.

A more complete picture of the wake complexity is provided with Figs. B-18 through B-21. These figures have been drawn for an advance ratio,  $\mu = V/V_t = 0.5$ , and show the planform view. Start with Fig. B-18 where the blade is at the azimuth angle ( $\psi$ ) of 90 degrees. This azimuth is generally referred to as the advancing side of the rotor disc. In the fixed-wing problem, all vortices trail straight back, parallel to the X-axis. Obviously, this is not true for a rotor blade. The tip vortex traces out a prolate cycloid, while the root cutout vortex follows a curtate cycloid.



**Fig. B-18**

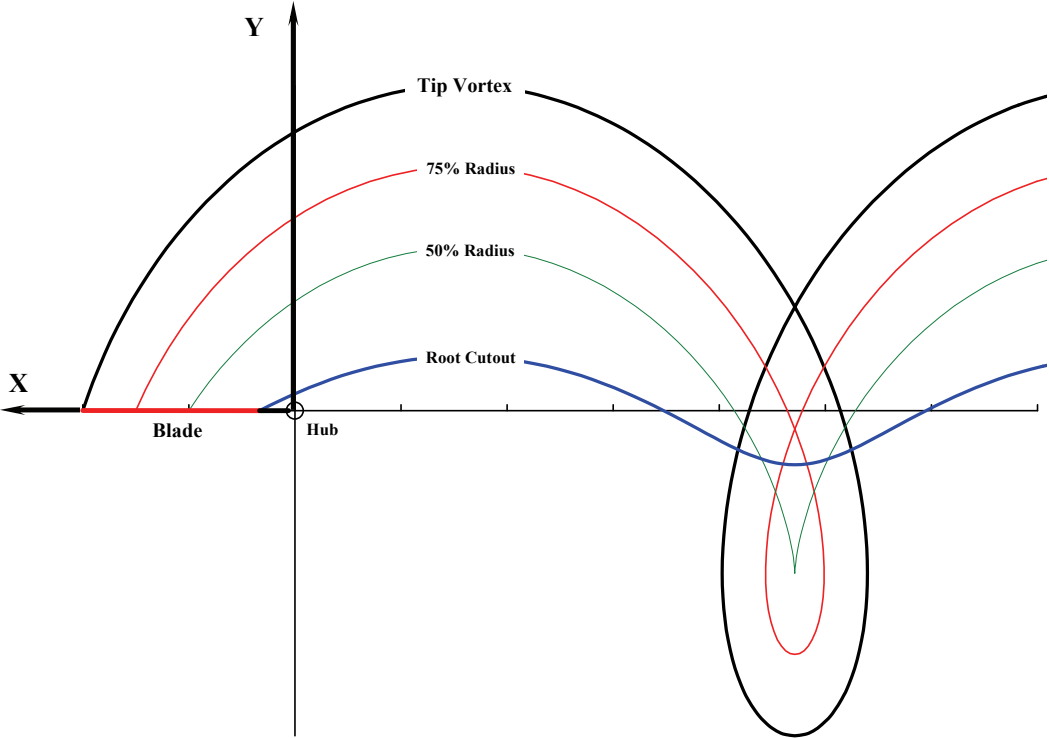


Fig. B-19

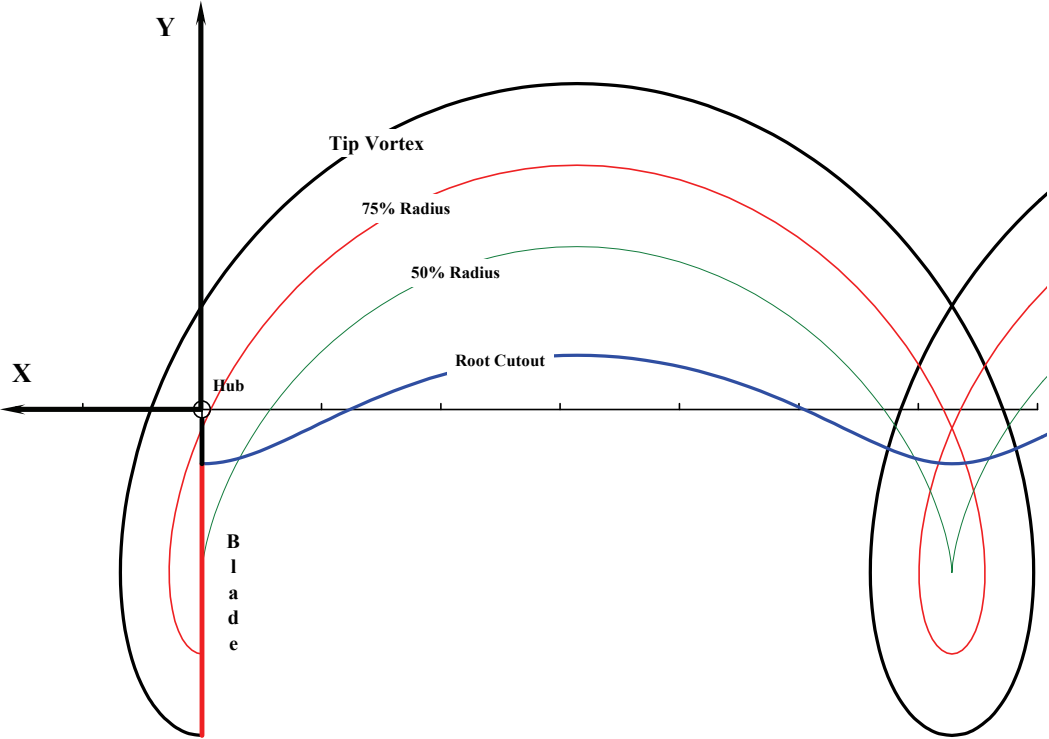


Fig. B-20

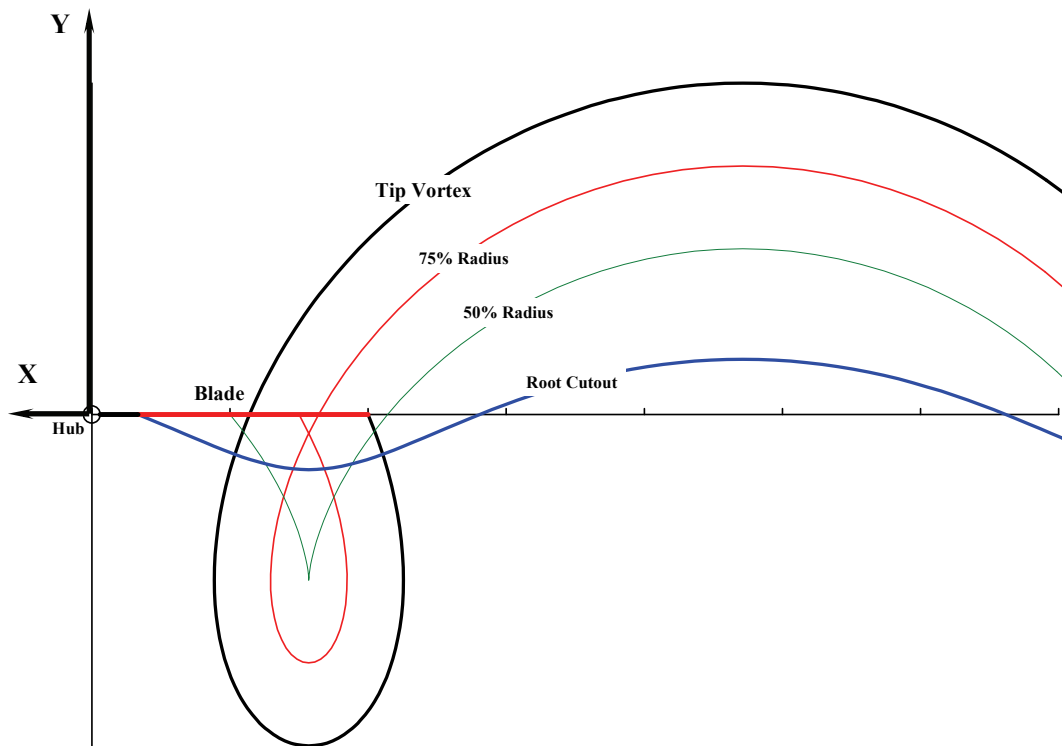


Fig. B-21

Fig. B-19 shows the planform view with the blade at the 180-degree azimuth position. Fig. B-20 places the blade at  $\psi = 270$  degrees, which is the retreating side of the rotor disc. Notice with the blade at  $\psi = 270$  degrees that the two outboard vortices trailed from the blade sharply turn nearly back on the blade itself. Finally, Fig. B-21 shows the blade at its most downwind position of  $\psi = 360$ , or zero degrees. Here the trailed vortices really attack the blade. The possibilities of any given vortex directly intersecting the generating lifting line are quite real in the practical problem.

Before bringing the Biot–Savart law to bear on this problem, there are a few aspects of the notations to observe. To begin with, rather than deal with the geometry dimensionally, use the conventional rotor nondimensional notations of

$$\begin{aligned}
(72) \quad x &= \frac{r}{R} \quad \text{radius station where induced velocity is sought} \\
xv &= \frac{r_v}{R} \quad \text{radius station where vortex is trailed} \\
\alpha_{\text{tpp}} &\equiv \quad \text{angle of attack of the tip path plane, positive nose up} \\
\mu &= \frac{V}{V_t} \cos \alpha_{\text{tpp}} \quad \text{advance ratio} \\
v_i &\equiv \quad \text{induced velocity calculated by momentum theory} \\
\lambda_{\text{tpp}} &= \frac{V \sin \alpha_{\text{tpp}} - v_i}{V_t} \quad \text{inflow ratio.}
\end{aligned}$$

Now, using Fig. B-22 as the reference, methodically begin with the Biot–Savart law as previous stated:

$$(73) \quad d(dv_x / dxv) = \frac{\gamma_v}{4\pi} \left[ \frac{L_i dS_j - L_j dS_i}{L^3} \right] d\theta$$

where the dimensions are expressed as vectors as displayed in Fig. B-22. For the distance ( $L$ ) between the vortex segment ( $dS$ ) to the radius station ( $x$ ) at which the induced velocity is sought, you have

$$\begin{aligned}
(74) \quad L &= L_i + L_j + L_k = (Xr - Xv)i + (Yr - Yv)j + (Zr - Zv)k \\
\text{where } Xr &= -R [x \cos \psi] & Yr &= +R [x \sin \psi] & Zr &= 0 \\
Xv &= -R [xv \cos \theta + \mu (\psi - \theta)] & Yv &= +R [xv \sin \theta] & Zv &= -R \lambda_{\text{tpp}} (\psi - \theta) \\
\text{and } L^3 &= [(Xr - Xv)^2 + (Yr - Yv)^2 + (Zr - Zv)^2]^{3/2}.
\end{aligned}$$

In a similar manner, the vortex is describe by

$$(75) \quad S = S_i + S_j + S_k = (Xv)i + (Yv)j + (Zv)k$$

but with rotor blade vortex geometry, you have

$$\begin{aligned}
(76) \quad dS_i &= \frac{\partial S_i}{\partial \theta} d\theta = \frac{\partial Xv}{\partial \theta} d\theta = +R (xv \sin \theta + \mu \theta) d\theta \\
dS_j &= \frac{\partial S_j}{\partial \theta} d\theta = \frac{\partial Yv}{\partial \theta} d\theta = +R (xv \cos \theta) d\theta \\
dS_k &= \frac{\partial S_k}{\partial \theta} d\theta = +R \lambda_{\text{tpp}} \theta.
\end{aligned}$$

The substitution of this rotor blade and wake geometry into the Biot–Savart law gives, with simplification

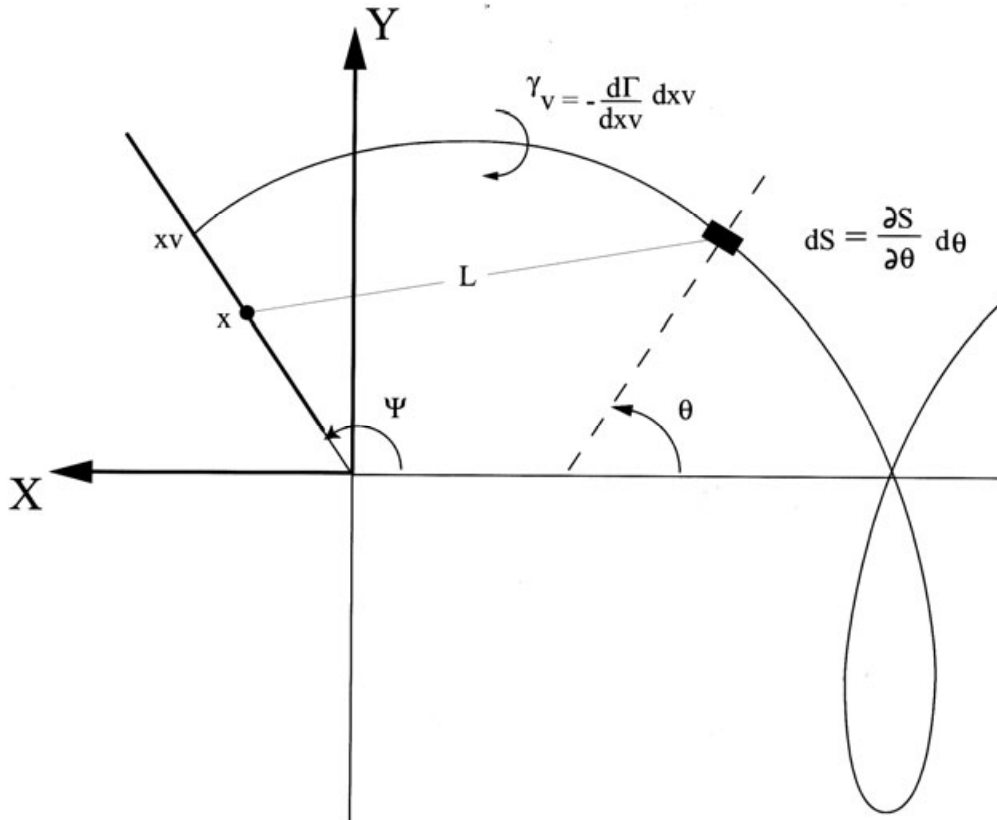


Fig. B-22

$$(77) \quad \left[ \frac{L_i dS_j - L_j dS_i}{L^3} \right] = \frac{xv^2 - x(xv) \cos(\psi - \theta) + \mu [xv \sin \theta - x \sin \psi + xv(\psi - \theta) \cos \theta]}{R \left\{ [xv^2 + x^2 - 2x(xv) \cos(\psi - \theta)] + 2\mu(xv \cos \theta - x \cos \psi)(\psi - \theta) + (\psi - \theta)^2 (\mu^2 + \lambda_{ipp}^2) \right\}^{\frac{3}{2}}}$$

As an intermediate step, I integrated the Biot-Savart law with respect to wake age assuming the vortex circulation is simply a constant. That is, I tackled

$$(78) \quad (dv_x / dxv)_{\psi} = \frac{\gamma_v}{4\pi} \int_{-\infty}^{\psi} \left[ \frac{L_i dS_j - L_j dS_i}{L^3} \right] d\theta.$$

The purpose of this step was to test MathCad's built-in integrator and be sure it did not flounder at any azimuth ( $\psi$ ) or radius station ( $x$ ) with the provision that  $x \neq xv$ . To perform this test, I set  $\gamma_v = 4\pi$  and  $R = 1$ . I found that the near wake needed integration in several parts and finally selected integration as follows:

$$(79) \quad \int_{-\infty}^{\psi} \left[ \frac{L_i dS_j - L_j dS_i}{L^3} \right] d\theta = \int_{\psi - \frac{\pi}{180}}^{\psi} + \int_{\psi - \frac{\pi}{180} - 1}^{\psi - \frac{\pi}{180}} + \int_{\psi - \frac{\pi}{180} - 2}^{\psi - \frac{\pi}{180} - 1} + \int_{\psi - \frac{\pi}{180} - 5}^{\psi - \frac{\pi}{180} - 2} + \int_{\psi - \frac{\pi}{180} - 15}^{\psi - \frac{\pi}{180} - 5} + \int_{\psi - \frac{\pi}{180} - 90}^{\psi - \frac{\pi}{180} - 15} + \int_{\psi - \frac{\pi}{180} - 180}^{\psi - \frac{\pi}{180} - 90} + \int_{-5\pi}^{\psi - \pi} + \int_{-20\pi}^{-5\pi} .$$

MathCad's built-in integrator struggled with the calculation at and near the blade's root end (i.e., around the root cutout region) in the azimuth region from  $\psi = 330$  to  $360$  degrees. The reason for this struggle is, of course, the near-zero value of the distance ( $L$ ) as Fig. B-21 clearly shows. Adding a vortex core diameter would obviate the problem in regions where the vortices are so closely packed.

The next step requires picking a bound circulation for the blade lifting line. Suppose the elliptical distribution is chosen *and this distribution does not vary with azimuth*. This means there will only be trailed vortices and no shed vortices to add to the problem for this example. (The case of a shed wake will be addressed shortly.) Thus,

$$(80) \quad \Gamma_{x,\psi} = \Gamma_o \sqrt{1 - \frac{(2x - x_c - 1)^2}{(1 - x_c)^2}} \quad \text{does not vary with azimuth, } \psi .$$

Then, borrowing from the fixed-wing solution technique, let

$$(81) \quad \begin{aligned} x &= \frac{r}{R} = \left( \frac{1 + x_c}{2} \right) - \left( \frac{1 - x_c}{2} \right) \cos \alpha = a - b \cos \alpha \\ xv &= \frac{r_v}{R} = \left( \frac{1 + x_c}{2} \right) - \left( \frac{1 - x_c}{2} \right) \cos \beta = a - b \cos \beta \\ dxv &= \left( \frac{1 - x_c}{2} \right) \sin \beta d\beta = b \sin \beta d\beta \end{aligned}$$

where  $\beta$  goes from  $0$  to  $\pi$ . This coordinate system change at least transforms the trailed vortex circulation strength,  $\gamma_v$ , to the very much simpler

$$(82) \quad \gamma_v = -\Gamma_o \cos \beta d\beta ,$$

and thus the induced velocity double integral problem for an elliptical bound circulation that does not vary with azimuth is restated as

$$(83) \quad v_r = \int_0^\pi \int_{-\infty}^\psi \frac{-\Gamma_o \cos \beta}{4\pi R} \left\{ \frac{xv^2 - x(xv) \cos(\psi - \theta) + \mu [xv \sin \theta - x \sin \psi + xv(\psi - \theta) \cos \theta]}{\left\{ [xv^2 + x^2 - 2x(xv) \cos(\psi - \theta)] + 2\mu(xv \cos \theta - x \cos \psi)(\psi - \theta) + (\psi - \theta)^2 (\mu^2 + \lambda_{\text{tip}}^2) \right\}^{\frac{3}{2}}} \right\} d\theta d\beta .$$

## APPENDIX B

The question now arises as to what value of the maximum bound circulation ( $\Gamma_o$ ) is representative for this example. The calculation of the *average* or *steady* lift of this single bladed rotor follows as:

$$\begin{aligned}
 dL_{r,\psi} &= \rho(\vec{V}_{r,\psi} \times \vec{\Gamma}_{r,\psi}) dr && \text{both } V \text{ and } \Gamma \text{ are vectors} \\
 dL_{x,\psi} &= \rho V_{x,\psi} \Gamma_{x,\psi} R dx = \rho [V_t (x + \mu \sin \psi)] \left[ \Gamma_o \sqrt{1 - \frac{(2x - x_c - 1)^2}{(1 - x_c)^2}} \right] R dx \\
 L_\psi &= \int_{x_c}^1 dL_{x,\psi} = \int_{x_c}^1 \rho [V_t (x + \mu \sin \psi)] \left[ \Gamma_o \sqrt{1 - \frac{(2x - x_c - 1)^2}{(1 - x_c)^2}} \right] R dx \\
 (84) \quad L_\psi &= \frac{\pi}{8} \rho R V_t \Gamma_o (1 - x_c) (1 + 2\mu \sin \psi + x_c) \\
 L_{\text{steady}} &= \frac{1}{2\pi} \int_0^{2\pi} L_\psi d\psi = \frac{1}{2\pi} \int_0^{2\pi} \frac{\pi}{8} \rho R V_t \Gamma_o (1 - x_c) (1 + 2\mu \sin \psi + x_c) d\psi \\
 \text{Steady lift per blade} &= \frac{\pi}{8} \rho R V_t \Gamma_o [1 - x_c^2] \quad \text{so} \quad \Gamma_o = \frac{8L_{\text{Steady}}}{\pi \rho R V_t [1 - x_c^2]}.
 \end{aligned}$$

On this basis, chose the blade geometry from Part II

$$\begin{aligned}
 R &= 22 \text{ feet} \\
 x_c &= 1/6 \text{ nondimensional}
 \end{aligned}$$

and the forward flight conditions for this Part III problem are:

$$\begin{aligned}
 \rho &= 0.002378 \text{ slugs per cubic feet} \\
 V_t &= 603.605 \text{ feet per second} \\
 \mu &= 0.5 \text{ nondimensional} \\
 \lambda_{\text{pp}} &= -0.03 \text{ nondimensional} \\
 \Gamma_o &= 225 \text{ square feet per second}
 \end{aligned}$$

in which case the steady lift per blade is 2,712 pounds at 178 knots.

With this information as input, MathCad and its built-in integrator is used to calculate Eq. (83) as follows:

INPUT

$$\mu = 0.5 \quad \Gamma_o = 225 \quad R = 22 \quad x_c = 1/6 \quad \lambda_{ipp} = -0.03$$

Dimension integration.

Select azimuth station,  $\psi$  = variable for this problem

Extent of wake age,  $WA = -20\pi$

Number of radial stations at which vortices leave rotor blade,  $M = 90$

Range of radial stations where induced velocity is calculated,  $s = 0, 1, \dots, M-1$

Then proceed with these calculations

$$a = \frac{1-x_c}{2} \quad b = \frac{1+x_c}{2}$$

$$\alpha_s = \frac{\pi}{M} \left( s + \frac{1}{2} \right)$$

$$x_s = \frac{r}{R} = \left( \frac{1+x_c}{2} \right) - \left( \frac{1-x_c}{2} \right) \cos \alpha_s = a - b \cos \alpha_s$$

$$m = 0, 1, \dots, M \quad \beta_m = \left( \frac{\pi}{M} \right) m$$

$$xv_m = \frac{r_v}{R} = \left( \frac{1+x_c}{2} \right) - \left( \frac{1-x_c}{2} \right) \cos \beta_m = a - b \cos \beta_m$$

$$dvd\beta_{s,m} = \int_{WA}^{\psi} \frac{-\Gamma_o \cos \beta}{4\pi R} \left\{ \frac{xv^2 - x(xv) \cos(\psi - \theta) + \mu [xv \sin \theta - x \sin \psi + xv(\psi - \theta) \cos \theta]}{\left[ [xv^2 + x^2 - 2x(xv) \cos(\psi - \theta)] + 2\mu(xv \cos \theta - x \cos \psi)(\psi - \theta) + (\psi - \theta)^2 (\mu^2 + \lambda_{ipp}^2) \right]^{\frac{3}{2}}} \right\} d\theta$$

$$v_{s,\psi} = \frac{\pi}{M} \sum_{m=0}^{M-1} \frac{dvd\beta_{s,m} + dvd\beta_{s,m+1}}{2}$$

$$x_s = a - b \cos \alpha_s$$

The calculation of induced velocity at the lifting line—as created by the trailed vortices from the lifting line—now follows from the above scheme. Additionally, lift and horsepower distributions are calculated from

$$\Delta L_{s,\psi} = [\rho V_t (x_s + \mu \sin \psi) R] \left\{ \Gamma_o \sqrt{1 - \frac{(2x_s - x_c - 1)^2}{(1-x_c)^2}} \right\} \Delta_s \Rightarrow \text{Running lift}$$

$$L_\psi = \sum_{s=0}^{M-1} \Delta L_{s,\psi} \Rightarrow \text{Single blade lift at input azimuth}$$

$$(85) \quad \Delta HP_{s,\psi} = \frac{1}{550} v_{s,\psi} \Delta L_{s,\psi} \Rightarrow \text{Running horsepower}$$

$$HP_\psi = \sum_{s=0}^{M-1} \Delta HP_{s,\psi} \Rightarrow \text{Single blade horsepower at input azimuth}$$

$$\text{where } \Delta_s = \left( \frac{1+x_c}{2} \right) \left[ \cos \left( \frac{\pi}{M} s \right) - \cos \left( \frac{\pi}{M} (s+1) \right) \right]$$

## APPENDIX B

A representative illustration of azimuth-varying induced velocity at several radial stations is shown in Figs. B-23 and B-24. Remember that this result is for a single-bladed rotor lifting 2,712 pounds at 0.5 advance ratio (i.e.,  $V = 178$  knots at  $V_t = 603.6$  fps). Even more interesting is the azimuthal variation of the blade's total lift and induced horsepower shown in Fig. B-25. The average or steady induced horsepower is obtained by

$$(86) \quad \text{Steady Induced Horsepower} \equiv \text{HP}_i = \frac{1}{2\pi} \int_0^{2\pi} \text{HP}_\psi \cdot d\psi$$

The result is  $\text{HP}_i = 50.1$  hp. This induced horsepower, calculated with the prescribed wake, compares to the ideal induced horsepower calculated in Part I as

$$(87) \quad \text{Ideal Induced Horsepower} \equiv \text{Ideal HP}_i \approx \frac{1}{550} (\text{Lift}) \left( \frac{\text{Lift}}{2\rho\pi R^2 V} \right) \text{ for } \mu > 0.2,$$

which yields ideal  $\text{HP}_i = 6.13$  hp. This means that the elliptically loaded, single-bladed rotor requires about eight times the power calculated by simple momentum theory!

An additional point made by Fig. B-25 is that the highest lift is carried primarily on the advancing side of the rotor disc. As such, the rotor is out of trim because of the rolling moment inferred by Fig. B-25.

This leads to the question, "If the rotor has an elliptical bound circulation that varies with azimuth so that the rolling moment is zero, what is the induced power?" And this leads to the fourth and final part of this appendix.

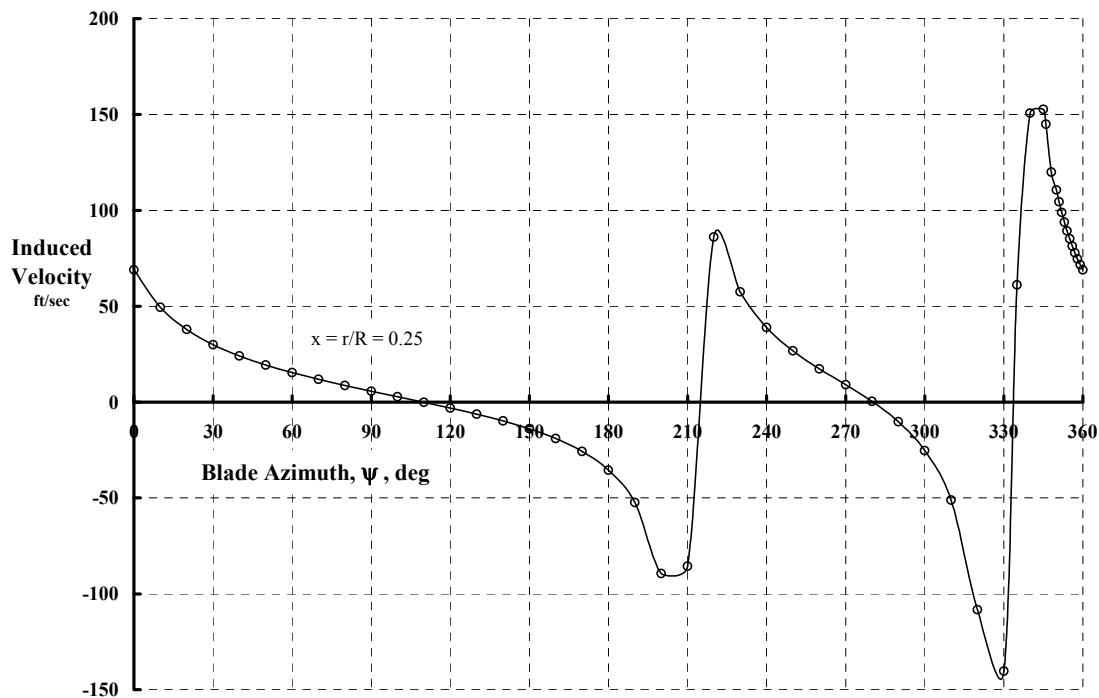


Fig. B-23

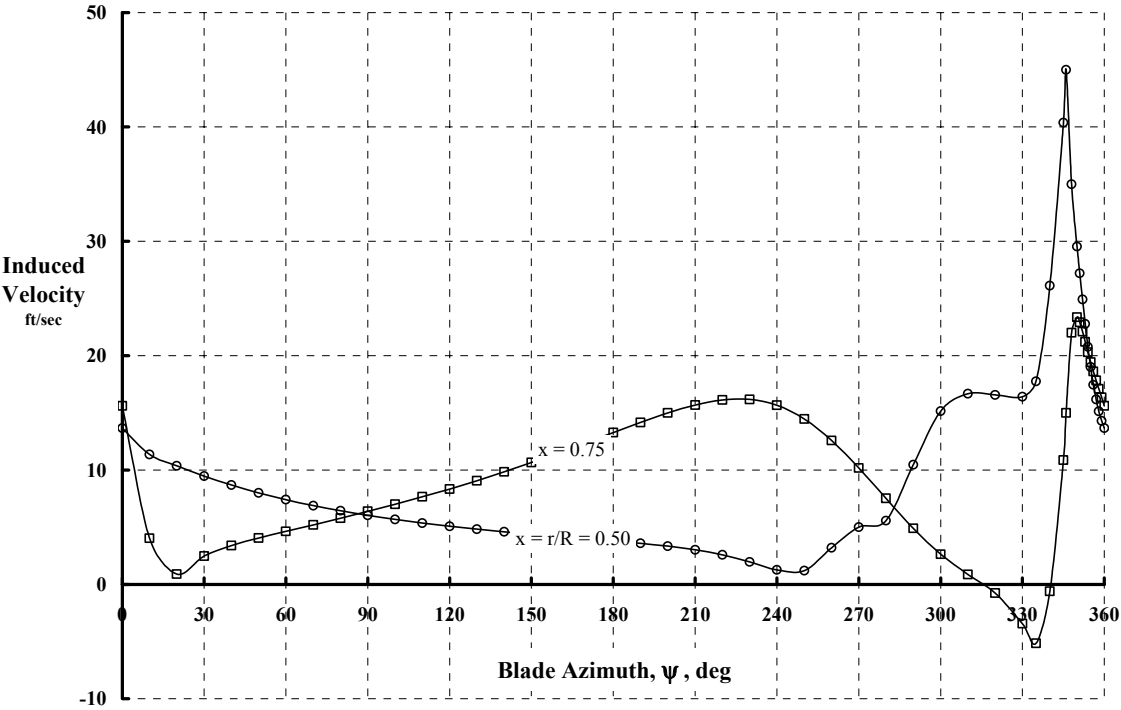


Fig. B-24

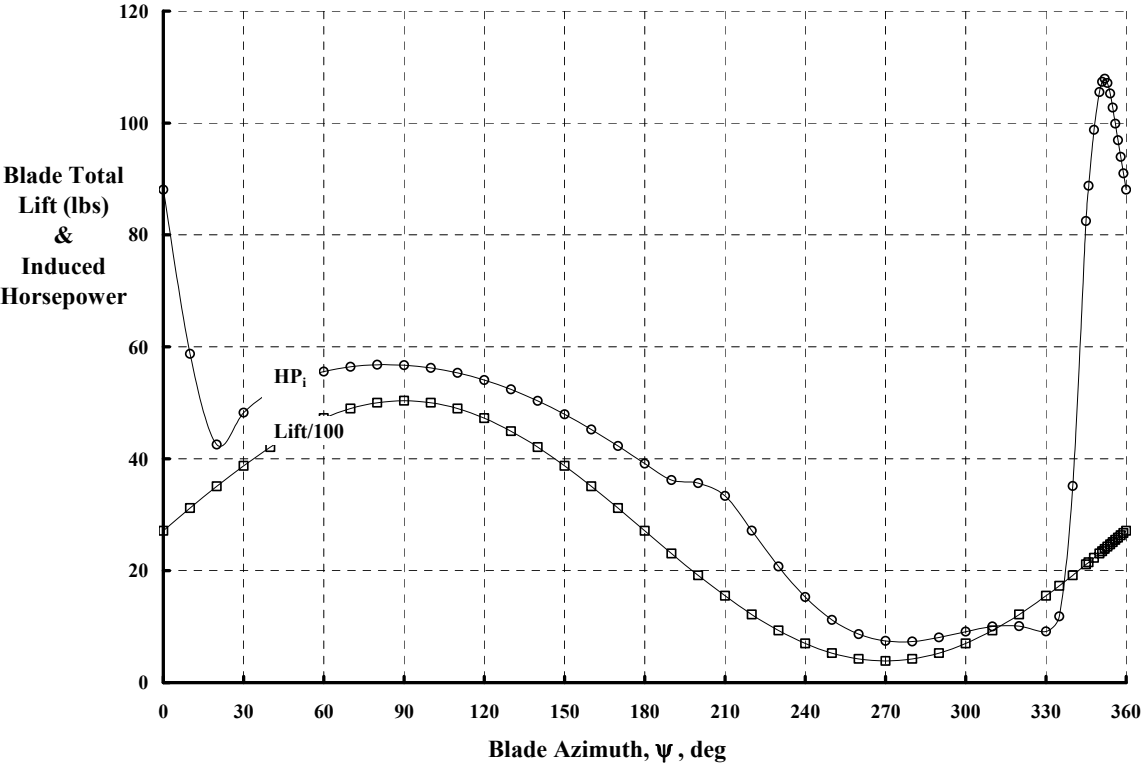


Fig. B-25

### Part IV—A Rotating Blade in Forward Flight With Zero Rolling Moment

The last step in the bridge between a fixed and rotating wing is addressed in this portion of the appendix. A fixed wing generally flies with zero rolling moment, RM. This same criterion can be applied to a rotating wing. (I refer to a rotating wing with  $RM = 0$  as a “balanced” rotor.) Suppose the bound circulation of the single-bladed rotor is describe by

$$(88) \quad \Gamma_{x,\psi} = (\Gamma_o + \Gamma_1 \sin \psi) \sqrt{1 - \frac{(2x - x_c - 1)^2}{(1 - x_c)^2}}.$$

In this case, the lift and rolling moment are found as

$$(89) \quad \begin{aligned} L_{\text{Steady}} &= \frac{\pi}{8} \rho R V_t \Gamma_o [1 - x_c] [(1 + x_c) \Gamma_o + \mu \Gamma_1] \\ RM_{\text{Steady}} &= -\frac{\pi}{128} \rho R^2 V_t \Gamma_o [1 - x_c] [8\mu(1 + x_c) \Gamma_o + (5 + 6x_c + 5x_c^2) \Gamma_1]^2 \end{aligned}$$

and if the rolling moment is set to zero

$$(90) \quad \begin{aligned} \Gamma_1 &= -\frac{8\mu(1 + x_c) \Gamma_o}{(5 + 6x_c + 5x_c^2)} \\ L_{\text{Steady}} &= \frac{\pi}{8} \rho R V_t \Gamma_o [1 - x_c^2] \left[ 1 - \frac{8\mu^2}{(5 + 6x_c + 5x_c^2)} \right] \Gamma_o. \end{aligned}$$

The Biot–Savart law of Eq. (83) now must include the trailed vortex circulation,  $\gamma_v$ , which is azimuth varying according to Eq. (88). Therefore, for this Part IV

$$(91) \quad v_{x,\psi} = \int_0^\pi \int_{-\infty}^{\psi} \frac{-(\Gamma_o + \Gamma_1 \sin \psi) \cos \beta}{4\pi R} \left\{ \frac{xv^2 - x(xv) \cos(\psi - \theta) + \mu [xv \sin \theta - x \sin \psi + xv(\psi - \theta) \cos \theta]}{\left\{ [xv^2 + x^2 - 2x(xv) \cos(\psi - \theta)] + 2\mu(xv \cos \theta - x \cos \psi)(\psi - \theta) + (\psi - \theta)^2 (\mu^2 + \lambda_{\text{tip}}^2) \right\}^{\frac{3}{2}}} \right\} d\theta d\beta.$$

The numerical integration of this slightly different equation (i.e., with azimuth-varying circulation) follows exactly that given in Part III of this appendix.

The contribution of *trailed vorticity* to induced velocity at the lifting line of this “balanced” rotor is show in Figs. B-26 and B-27. The total blade lift and induced power is given in Fig. B-28. These results are for the balanced rotor producing 2,712 pounds of lift at 178 knots and can be compared to Fig. B-25, which is for the “unbalanced” rotor. Only trailed vortices are contributing to the induced power at this point. The additional induced velocity and horsepower due to the *shed wake* still need to be included.

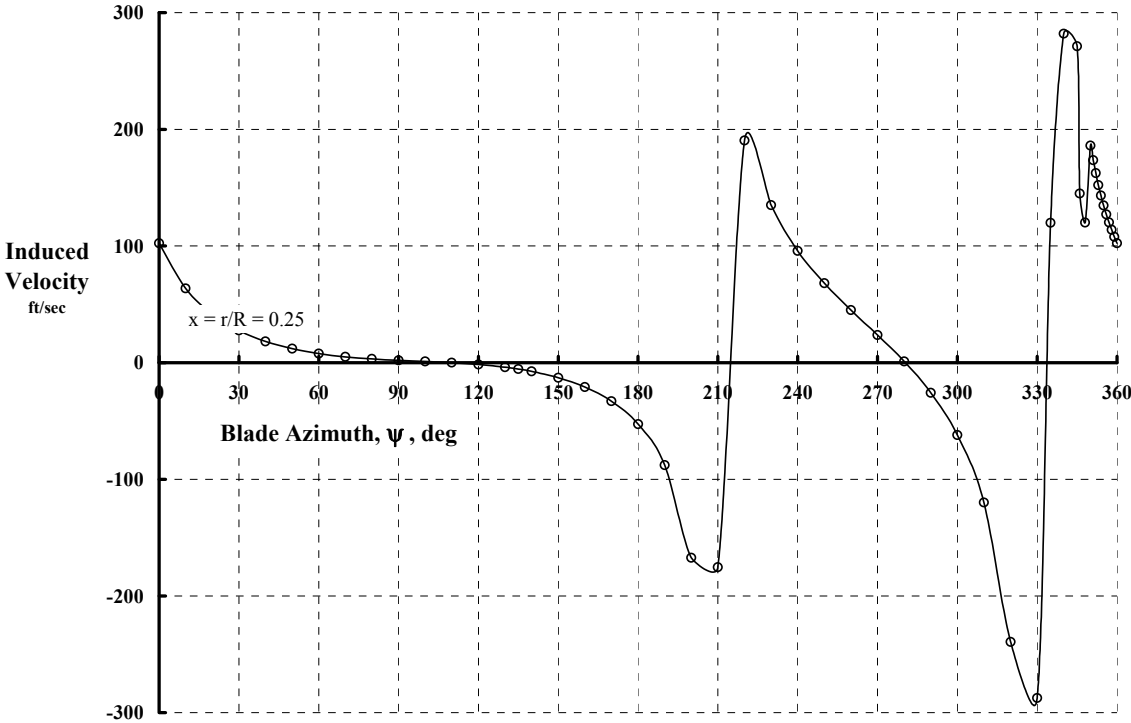


Fig. B-26

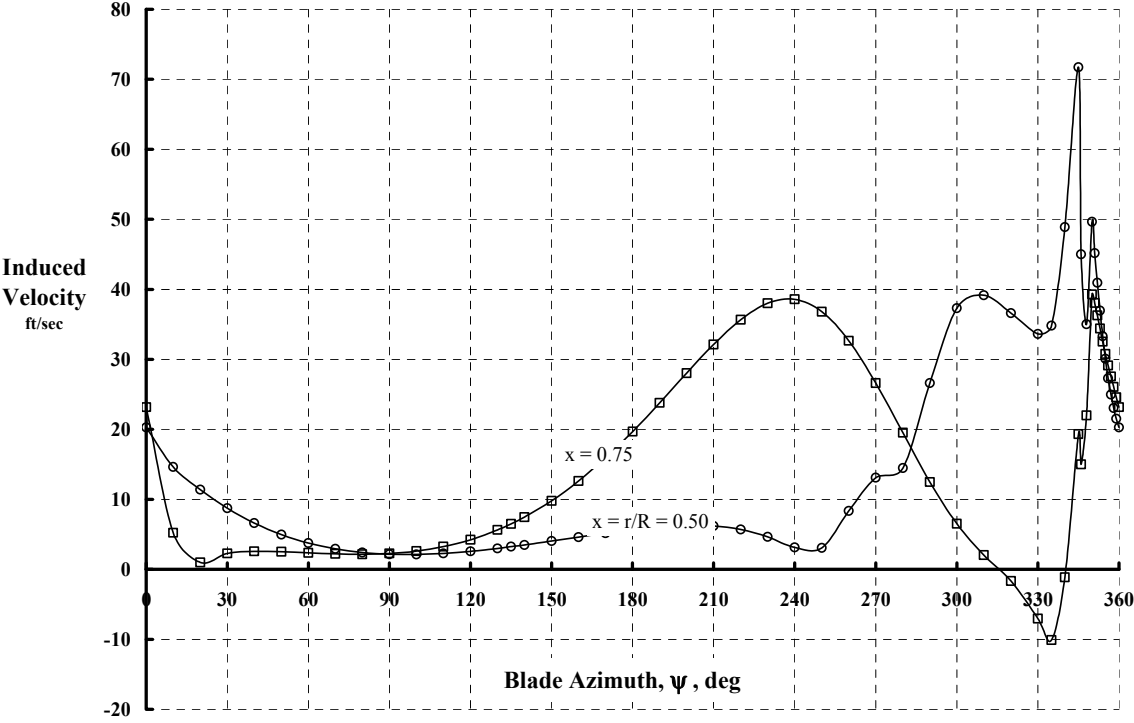


Fig. B-27

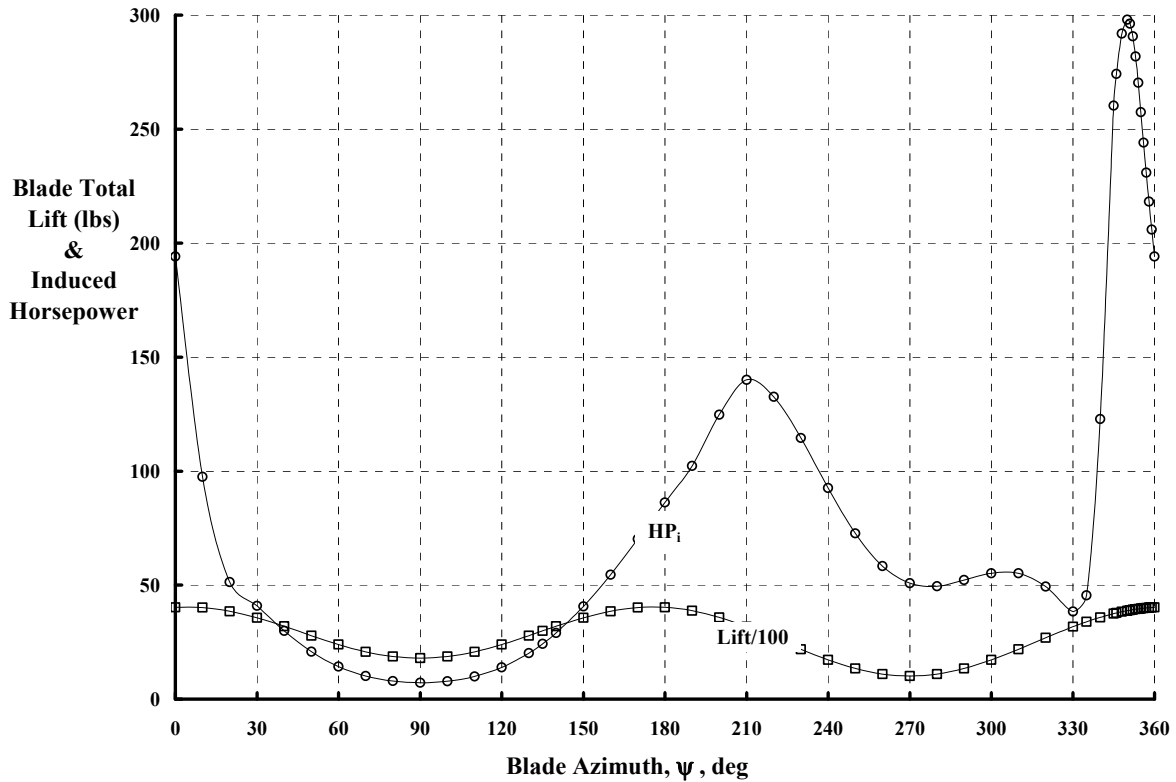


Fig. B-28

A numerical solution scheme for the *shed wake* is relatively simple compared to the trailed wake. In the shed wake problem, the vortex left behind the blade has a radial geometry and circulation just like the blade's when the blade was at that azimuth, however, the vortex circulation is the negative of the blade's bound circulation at azimuth. The geometry of this shed wake problem is shown in Fig. B-29. Again, the conventional rotor nondimensional notations are:

$$\begin{aligned}
 (92) \quad x &= \frac{r}{R} && \text{radius station where induced velocity is sought} \\
 xv &= \frac{r_v}{R} && \text{radius station where vortex is trailed} \\
 \alpha_{\text{tp}} &\equiv && \text{angle of attack of the tip path plane, positive nose up} \\
 \mu &= \frac{V}{V_t} \cos \alpha_{\text{tp}} && \text{advance ratio} \\
 v_i &\equiv && \text{induced velocity calculated by momentum theory} \\
 \lambda_{\text{tp}} &= \frac{V \sin \alpha_{\text{tp}} - v_i}{V_t} && \text{inflow ratio.}
 \end{aligned}$$

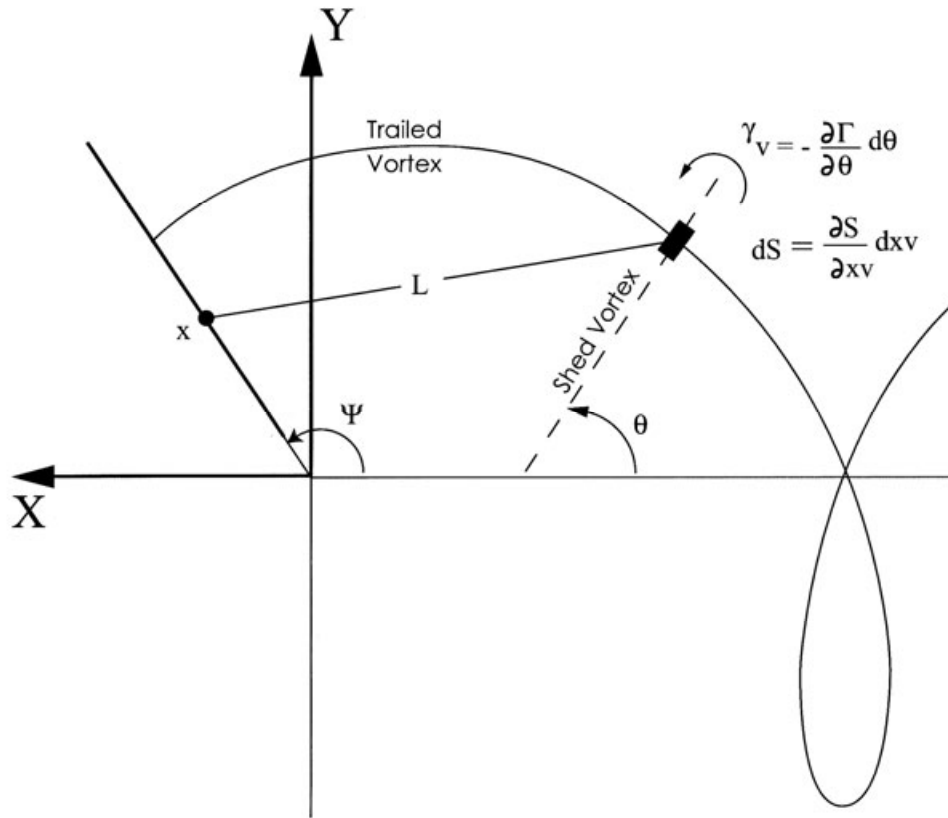


Fig. B-29

Now, using Fig. B-29 as the reference, begin with the Biot-Savart law

$$(93) \quad d(dv_x / dxv) = \frac{\gamma_v}{4\pi} \left[ \frac{L_i dS_j - L_j dS_i}{L^3} \right] d\theta,$$

where the dimensions are expressed as vectors. The distance,  $L$ , between the shed vortex segment,  $dS$ , to the radius station,  $x$ , at which the induced velocity is sought, is

(94)

$$L = L_i + L_j + L_k = (Xr - Xv)i + (Yr - Yv)j + (Zr - Zv)k$$

$$\text{where } Xr = -R[x \cos \psi] \quad Yr = +R[x \sin \psi] \quad Zr = 0$$

$$Xv = -R[xv \cos \theta + \mu(\psi - \theta)] \quad Yv = +R[xv \sin \theta] \quad Zv = -R\lambda_{tp}(\psi - \theta)$$

$$\text{and } L^3 = [(Xr - Xv)^2 + (Yr - Yv)^2 + (Zr - Zv)^2]^{3/2}$$

$$\text{so } L^3 = R \left\{ [xv^2 + x^2 - 2x(xv) \cos(\psi - \theta)] + 2\mu(xv \cos \theta - x \cos \psi)(\psi - \theta) + (\psi - \theta)^2 (\mu^2 + \lambda_{tp}^2) \right\}^{3/2}.$$

APPENDIX B

Notice that the length ( $L$ ) is the same for the shed wake as for the trailed wake. To continue then, the vortex element is describe by

$$(95) \quad S = S_i + S_j + S_k = (Xv)i + (Yv)j + (Zv)k,$$

but with rotor blade shed vortex geometry, the vortex extends radially so the partial derivatives of  $S$  are with respect to  $xv$ . Thus

$$(96) \quad \begin{aligned} dS_i &= \frac{\partial S_i}{\partial xv} dxv = \frac{\partial Xv}{\partial xv} dxv = -R \cos \theta dxv \\ dS_j &= \frac{\partial S_j}{\partial xv} dxv = \frac{\partial Yv}{\partial xv} dxv = +R \sin \theta dxv \\ dS_k &= \frac{\partial S_k}{\partial xv} dxv = \frac{\partial Zv}{\partial xv} dxv = 0. \end{aligned}$$

With this information, the geometric part of the Biot–Savart law becomes

$$(97) \quad \left[ \frac{L_i dS_j - L_j dS_i}{L^3} \right] = \left\{ -\frac{x \sin(\psi - \theta) + \mu(\psi - \theta) \sin \theta}{L^3} \right\} dxv.$$

The Biot–Savart also needs the shed vortex circulation as it varies with wake age. Thus,

$$(98) \quad \text{Shed } \gamma_v = - \left( \frac{d\Gamma_{x,\psi}}{d\psi} \right)_{\substack{\text{at } \psi=\theta \\ \text{and} \\ x=xv}} d\theta = -(\Gamma_1 \cos \theta) \sqrt{1 - \frac{(2xv - x_c - 1)^2}{(1 - x_c)^2}} d\theta,$$

and the double integral giving induced velocity at any radius station,  $x$ , and azimuth,  $\psi$ , using Eqs. (97) and (98) is

$$(99) \quad v_{x,\psi} = \int_{x_c}^1 \int_{-\infty}^{\psi} \left[ (\Gamma_1 \cos \theta) \sqrt{1 - \frac{(2xv - x_c - 1)^2}{(1 - x_c)^2}} \right] \left[ \frac{x \sin(\psi - \theta) + \mu(\psi - \theta) \sin \theta}{L^3} \right] d\theta dxv.$$

It is particularly important to study the integration with respect to wake age,  $\theta$ , before discussing a complete integration of Eq. (99). The reason is that this portion of the integration has a definite possibility of “blowing up.” Therefore, reverse the integration order of Eq. (99) to read as

$$(100)$$

$$v_{x,\psi} = \int_{-\infty}^{\psi} \left\{ \int_{x_c}^1 \left[ (\Gamma_1 \cos \theta) \sqrt{1 - \frac{(2xv - x_c - 1)^2}{(1 - x_c)^2}} \right] \left[ \frac{x \sin(\psi - \theta) + \mu(\psi - \theta) \sin \theta}{L^3} \right] dxv \right\} d\theta.$$

In the first place, the integration *is not* a problem when  $\theta = \psi$  because the numerator of the integrand is zero (i.e.,  $\psi - \theta = 0$ ). Furthermore, from Eq. (94), the distance,  $L$ , between the vortex segment and the point on the blade where induced velocity is sought, reduces to

$$L^3 = R \left\{ \left[ xv^2 + x^2 - 2x(xv)\cos(0) \right] \right\}^{\frac{3}{2}} = R \left\{ (xv - x)^2 \right\}^{\frac{3}{2}},$$

which is only zero when  $x = xv$ . The physical meaning of this situation when  $\theta = \psi$  is that the only vortex that exists is the blade's bound circulation, and this straight line vortex cannot induce a velocity on itself.

Now look at the solution when a shed vortex is in the region  $\psi = -\theta$  to 0 or, if you prefer, in the near wake. Suppose, for example, that the blade is at the 135-degree azimuth and  $\theta$  is in the range 135 degrees backwards to 132 degrees in 1/30-of-a-degree increments. This represents 3 degrees of near wake. Assume the induced velocity is sought at the blade station,  $x = 0.5$ , and place the blade at azimuth  $\psi = 135$  degrees. The accumulation of the shed wake influence is

$$\text{area under } \frac{dv_{x,\psi}}{d\theta} \text{ versus } \theta.$$

The curve of  $dv_{x,\psi}/d\theta$  versus wake age is illustrated in Fig. B-30. This figure suggests an impending singularity as computations are made very close to the blade's lifting line. In fact, the velocity induced at the blade station,  $x = 0.5$ , of the lifting line becomes so large that a semi-log scale for the ordinate in Fig. B-30 is helpful in capturing how rapidly the shed wake's influence drops off as the blade moves away from the deposited shed wake.

An empirical solution to the situation illustrated by Fig. B-30 is to add a vortex core diameter (VCD) nondimensionalized by rotor radius ( $R$ ) to the  $L$  dimension of the shed wake problem [refer back to the discussion surrounding Eq. (61)].<sup>9</sup> This solution is effective as Fig. B-31 shows. Of course, it is the integrated value

$$v_{x=0.5} = \int_{\frac{\pi}{180}^{132}}^{\frac{\pi}{180}^{135}} \frac{dv_{x,\psi}}{d\theta} d\theta$$

that is more important, and this integrated result is shown versus VCD ratioed to radius in Fig. B-32 for  $x = 0.5$  and  $\psi = 135$  degrees. And even more important is the integrated value of induced velocity considering the wake extending all the way back to, say,  $\theta = -20\pi$ . The induced velocity at  $x = 0.5$  (and with  $\psi = 135$  degrees) including this far wake is also shown in Fig. B-32.

---

<sup>9</sup> The correct approach is to changed from a lifting line to a lifting surface representation of the rotor blade.

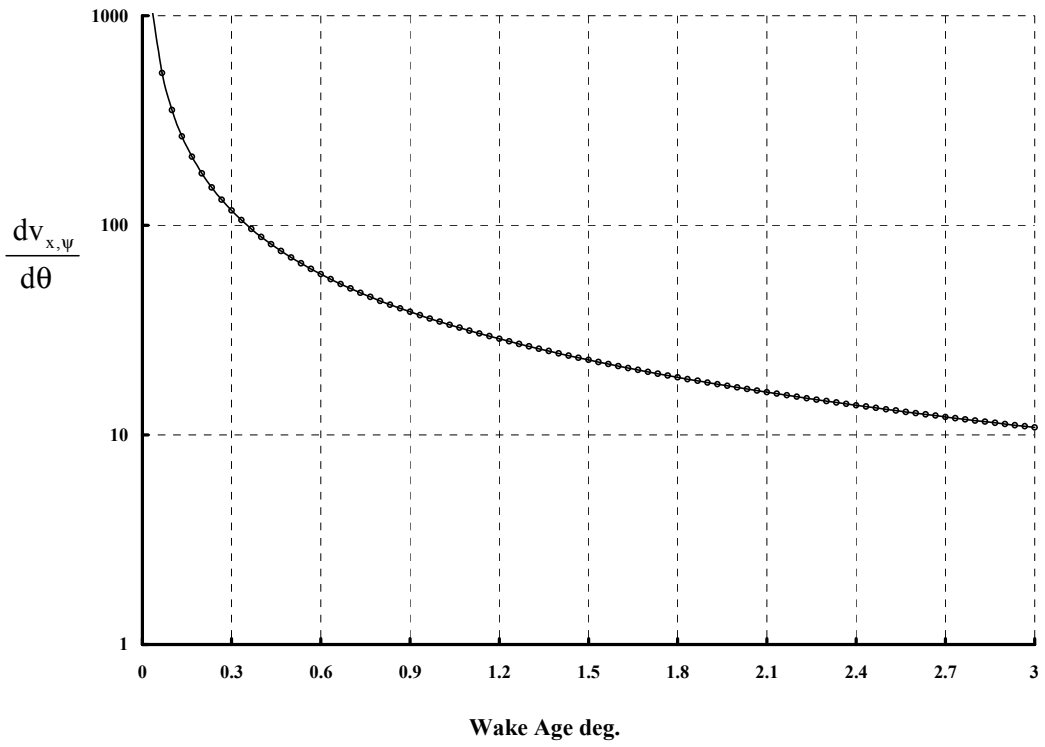


Fig. B-30

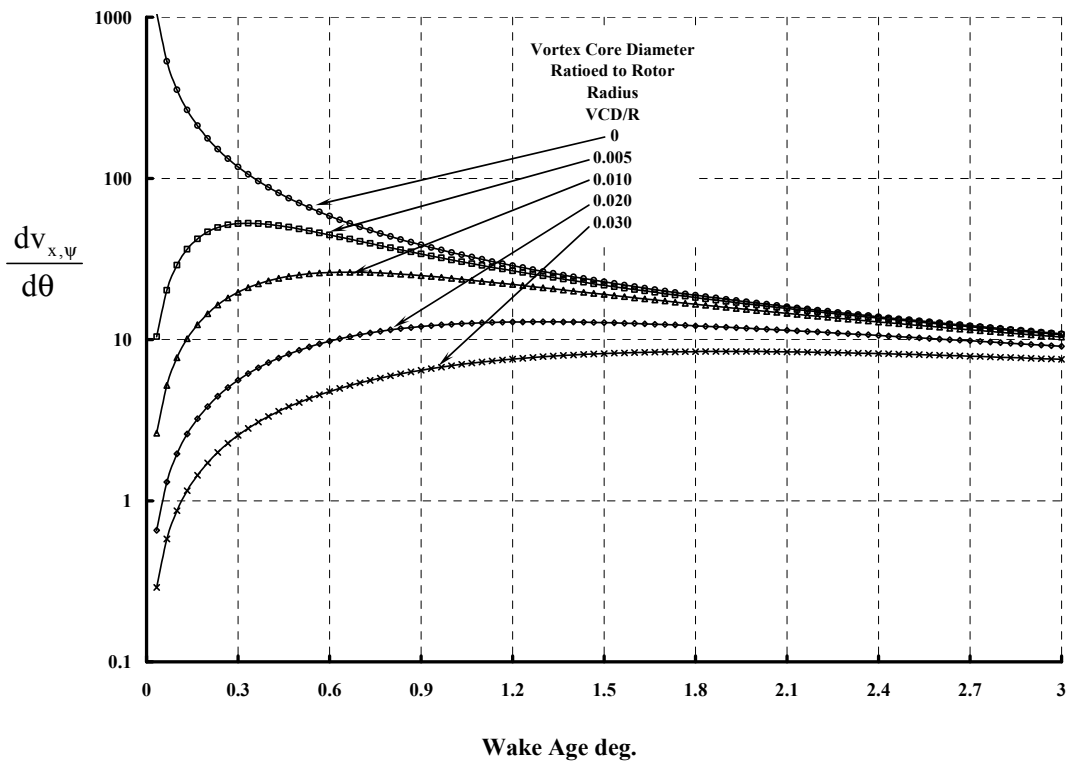


Fig. 31

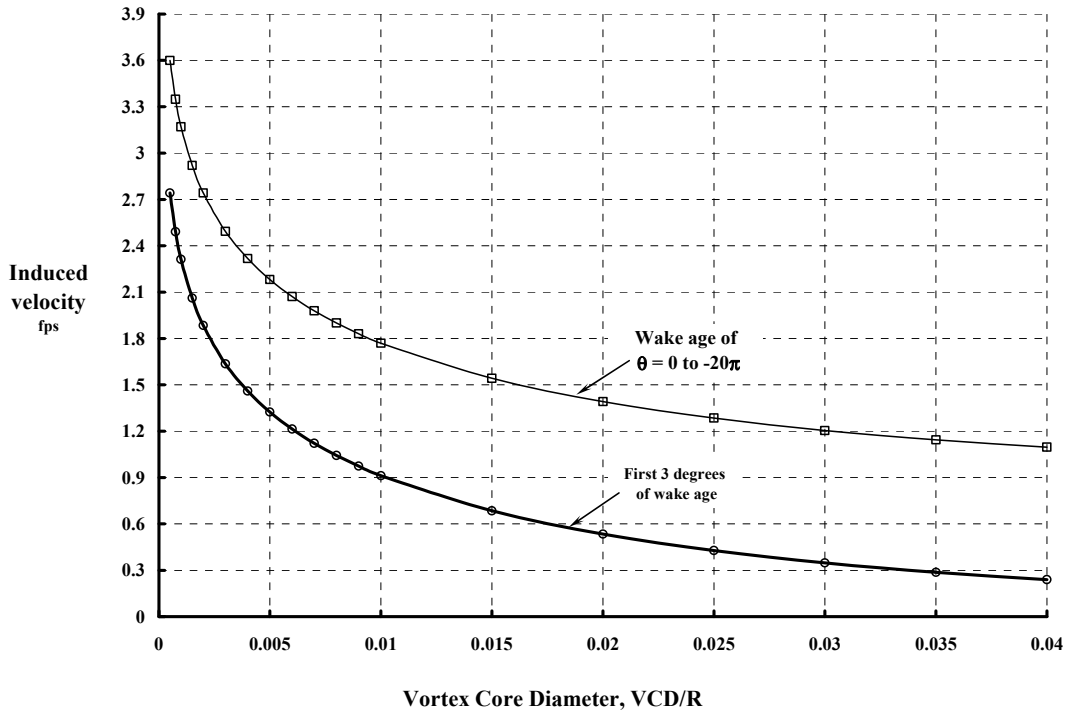


Fig. B-32

To examine the influence of the shed wake further, select, somewhat arbitrarily, the ratio of VCD to rotor radius equal to 0.015. Now the distance,  $L$ , between the vortex segment and rotor blade station where induced velocity is sought,  $x$ , is rewritten as

$$(101) \quad L^3 = R \left\{ \begin{array}{l} \left[ xv^2 + x^2 - 2x(xv) \cos(\psi - \theta) \right]^{\frac{3}{2}} \\ + 2\mu(xv \cos \theta - x \cos \psi)(\psi - \theta) \\ + (\psi - \theta)^2 (\mu^2 + \lambda_{pp}^2) + \left( \frac{VCD}{R} \right)^2 \end{array} \right\} .$$

MathCad's built-in numerical integrator had absolutely no problem calculating the induced velocity at all radius stations and any azimuth:

$$(102) \quad v_{x,\psi} = \int_{x_c}^1 \int_{-\infty}^{\psi} \left[ (\Gamma_1 \cos \theta) \sqrt{1 - \frac{(2xv - x_c - 1)^2}{(1 - x_c)^2}} \right] \left[ \frac{x \sin(\psi - \theta) + \mu(\psi - \theta) \sin \theta}{L^3} \right] d\theta dxv .$$

The calculation could be performed even at  $x = xv$  because the distance,  $L$ , can never be smaller than  $VCD/R$ . Furthermore, because the shed wake's circulation goes smoothly to zero at both the blade root and tip, there is no need to perform a fixed-wing coordinate transformation, as was helpful for the trailed wake integration of both fixed and rotary wings.

## APPENDIX B

The next objective is to calculate the induced velocity for the geometry and operating condition of the sample problem. To begin the numerical integration, however, additional input is required. The additional input that satisfies rotor lift = 2,712 pounds at an advance ratio of 0.5 is that  $\Gamma_0 = 334$  and  $\Gamma_1 = -253.9$ . For convenience, the complete input for the shed wake numerical integration is:

$$\begin{aligned} R &= 22 \text{ feet} \\ x_c &= 1/6 \text{ nondimensional} \\ \rho &= 0.002378 \text{ slugs per cubic foot} \\ \text{VCD}/R &= 0.015 \text{ nondimensional} \\ V_t &= 603.605 \text{ feet per second} \\ \mu &= 0.5 \text{ nondimensional} \\ \lambda_{\text{tp}} &= -0.03 \text{ nondimensional} \\ \Gamma_0 &= 334 \text{ square feet per second} \\ \Gamma_1 &= -253.9 \text{ square feet per second.} \end{aligned}$$

With this information as input, put MathCad and it's built-in integrator to work calculating Eq. (102) as follows:

INPUT

$$\mu = 0.5 \quad \Gamma_0 = 334 \quad \Gamma_1 = -253.9 \quad R = 22 \quad x_c = 1/6 \quad \lambda_{\text{tp}} = -0.03 \quad \text{VCD}/R = 0.015$$

Dimension integration.

Select azimuth station,  $\psi$  = variable for this problem

Extent of wake age,  $\text{WA} = -20\pi$

Maximum number of radial stations,  $M = 90$

Range of radial stations where induced velocity is calculated,  $s = 0, 1, \dots, M - 1$

Then proceed with these calculations

$$a = \frac{1 - x_c}{2} \quad b = \frac{1 + x_c}{2}$$

$$\alpha_s = \frac{\pi}{M} \left( s + \frac{1}{2} \right) \Rightarrow \text{To correspond to radius stations used in trailed wake problem}$$

$$x_s = \frac{r}{R} = \left( \frac{1 + x_c}{2} \right) - \left( \frac{1 - x_c}{2} \right) \cos \alpha_s = a - b \cos \alpha_s$$

$$v_{s,\psi} = \int_{x_c}^1 \int_{-\infty}^{\psi} \left[ (\Gamma_1 \cos \theta) \sqrt{1 - \frac{(2xv - x_c - 1)^2}{(1 - x_c)^2}} \right] \left[ \frac{x \sin(\psi - \theta) + \mu(\psi - \theta) \sin \theta}{R \left\{ \left[ xv^2 + x^2 - 2x(xv) \cos(\psi - \theta) \right]^{\frac{3}{2}} + 2\mu(xv \cos \theta - x \cos \psi)(\psi - \theta) + (\psi - \theta)^2 (\mu^2 + \lambda_{\text{tp}}^2) + \left( \frac{\text{VCD}}{R} \right)^2 \right\}} \right] d\theta dxv$$

$$x_s = a - b \cos \alpha_s$$

The calculation of induced velocity at the lifting line—as created by the shed vortices from the lifting line—follows from the preceding scheme. Additionally, lift and horsepower distributions are calculated from

$$\begin{aligned}
 \Delta L_{s,\psi} &= [\rho V_t (x_s + \mu \sin \psi) R] \left\{ (\Gamma_o + \Gamma_1 \sin \psi) \sqrt{1 - \frac{(2x_s - x_c - 1)^2}{(1 - x_c)^2}} \right\} \Delta_s \Rightarrow \text{Running Lift} \\
 L_\psi &= \sum_{s=0}^{M-1} \Delta L_{s,\psi} \Rightarrow \text{Single-blade lift at input azimuth} \\
 \Delta HP_{s,\psi} &= \frac{1}{550} v_{s,\psi} \Delta L_{s,\psi} \Rightarrow \text{Running horsepower} \\
 HP_\psi &= \sum_{s=0}^{M-1} \Delta HP_{s,\psi} \Rightarrow \text{Single-blade horsepower at input azimuth} \\
 \text{where } \Delta_s &= \left( \frac{1 + x_c}{2} \right) \left[ \cos \left( \frac{\pi}{M} s \right) - \cos \left( \frac{\pi}{M} (s+1) \right) \right].
 \end{aligned}
 \tag{103}$$

The shed wake significantly contributes to the total induced velocity that the rotor blade sees, primarily over the mid-span portion of the blade. For example, the azimuthal variation in induced velocity at the three radius stations under examination (i.e.,  $x = 0.25$ ,  $0.50$ , and  $0.75$ ) is provided by Figs. B-33, B-34, and B-35, respectively. It is at the mid-span that the shed wake's additional induced velocity is the greatest.

The blade's azimuthally varying lift for the balanced rotor is illustrated in Fig. B-36. Note, in contrast to the unbalanced rotor shown in Fig. B-25, the balanced rotor carries lift in the fore and aft quadrants of the revolution. This gives, in effect, a short wingspan or low aspect ratio characteristic to the balanced rotor. As Fig. B-37 shows, this concentration of balanced rotor lift in the fore and aft direction is accompanied by excessive induced horsepower when compared to the unbalanced rotor in Fig. B-25. The average or steady induced horsepower for the balanced rotor is  $HP_i = 76.4$  hp versus  $50.1$  hp for the unbalance rotor and versus  $6.13$  hp for the ideal fixed wing.

The requirement for a rotor to have zero rolling moment is clearly adverse to the induced power required to produce lift. The ratio of balanced rotor-induced horsepower to ideal fixed-wing-induced horsepower is  $76.4/6.13 = 12.4$ . But, keep in mind that while an elliptical bound circulation is ideal for a fixed wing, it is not *obviously* true for a rotary wing.

APPENDIX B

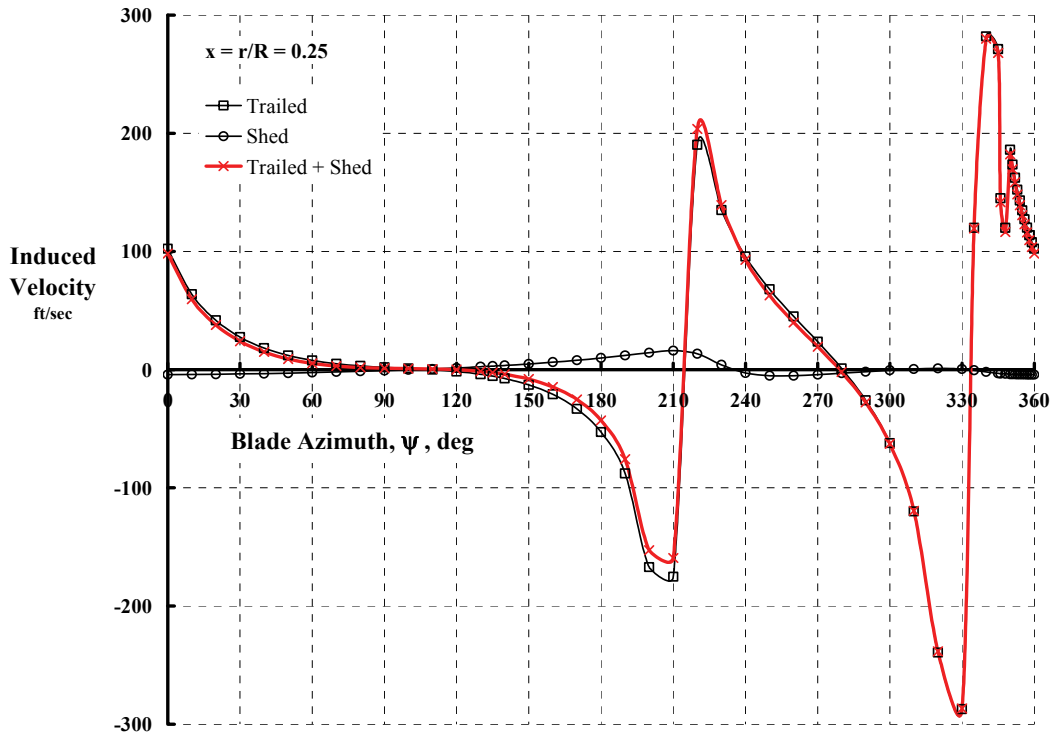


Fig. B-33

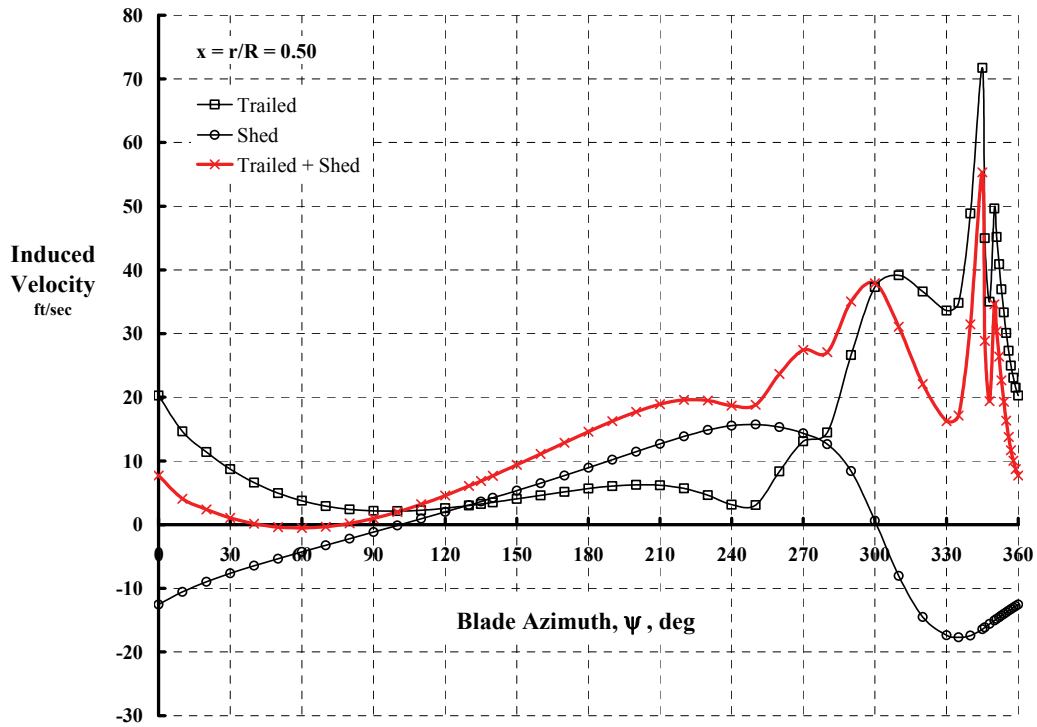


Fig. B-34

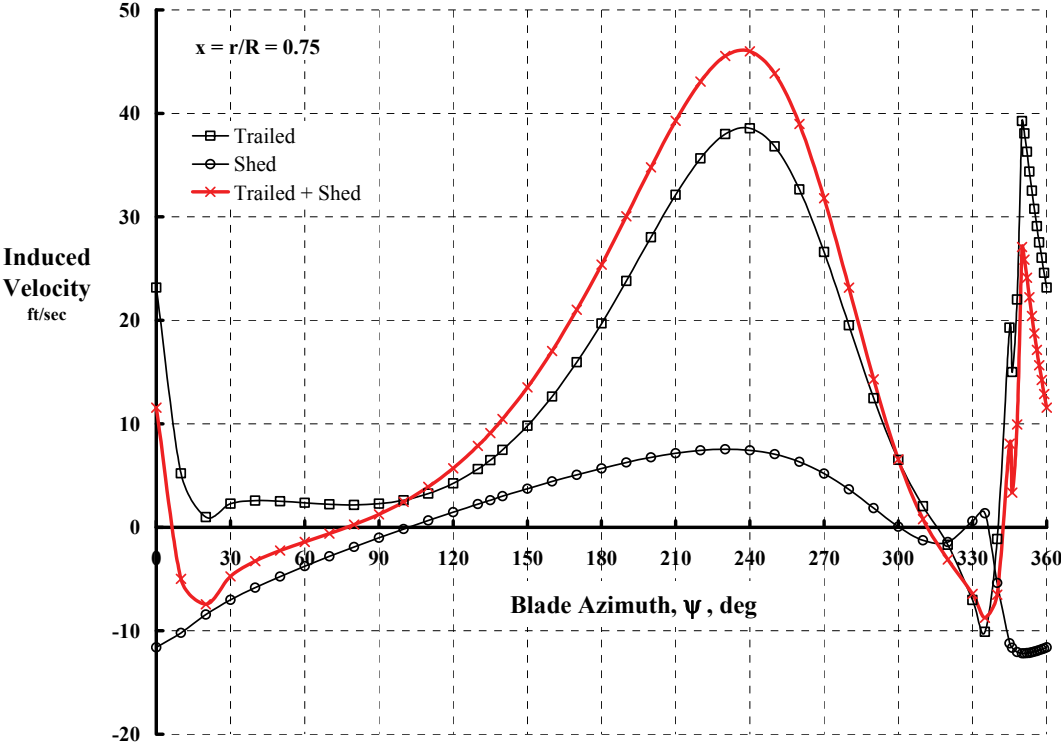


Fig. B-35

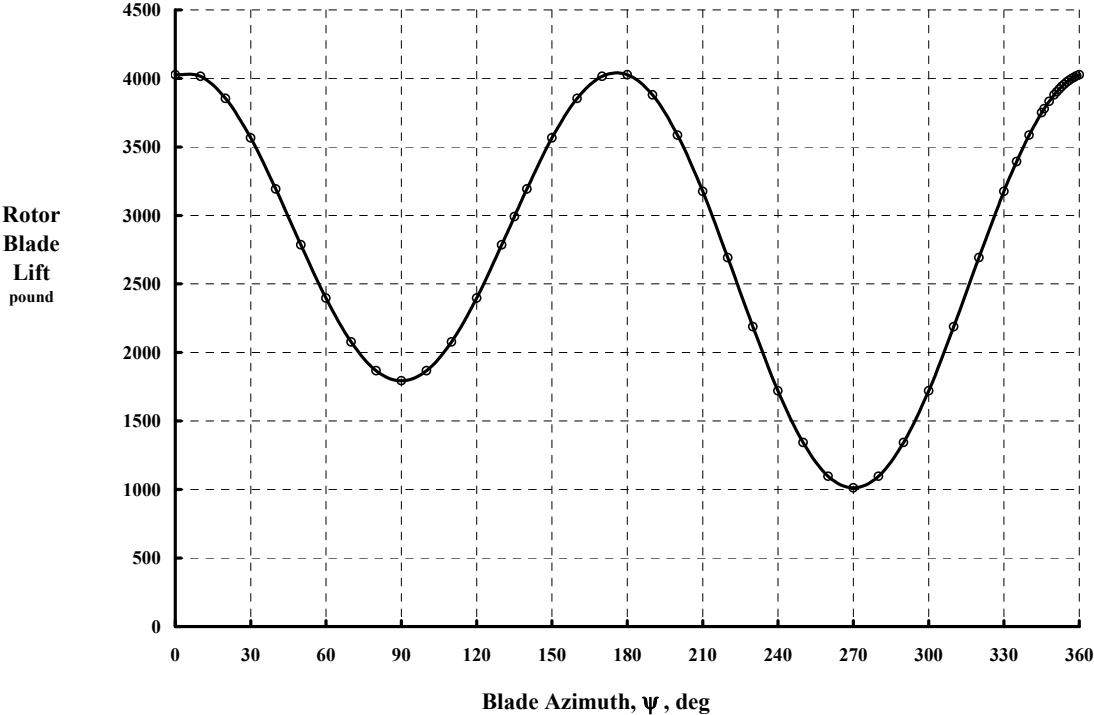


Fig. B-36

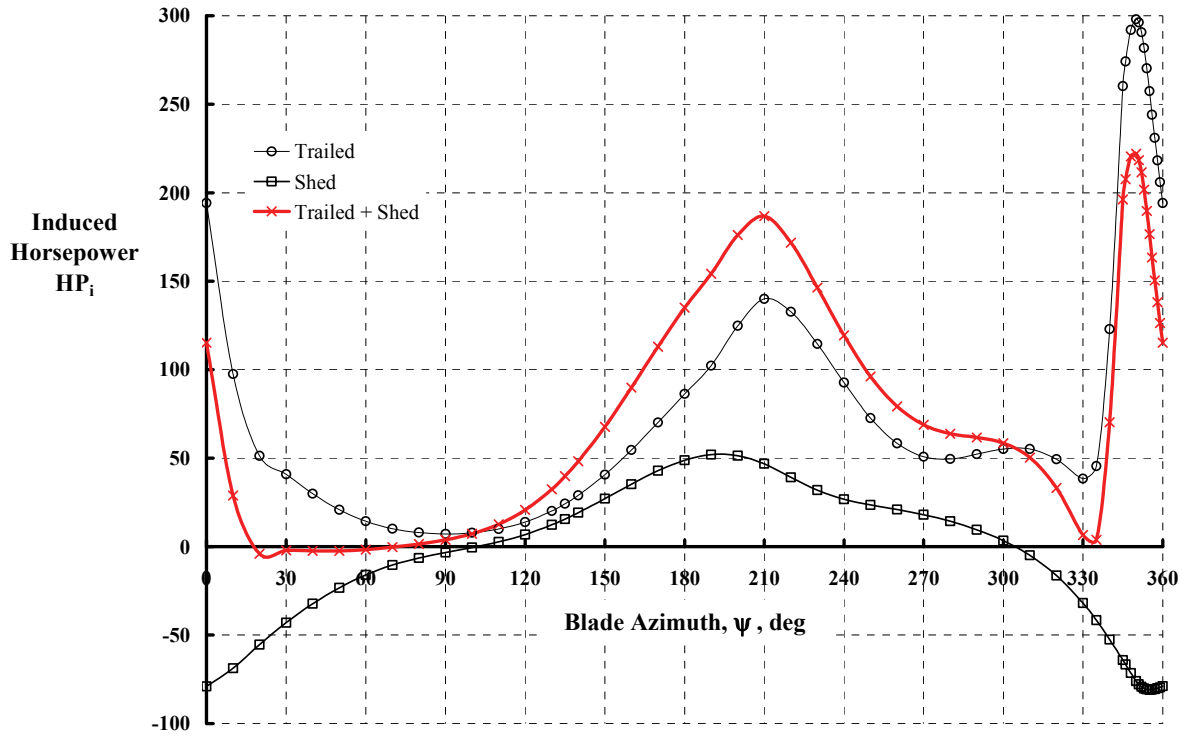


Fig. B-37

### Part V—Closing Remarks

This elementary introduction to induced velocity has been presented assuming an elliptical bound circulation distributed along a lifting line to represent both the wing and the rotor. The assumption has been that

$$\Gamma \propto \sum_1^{\infty} A_n \sin n\beta,$$

and that  $A_1 = 1$  while  $A_2$  through  $A_{\infty} = 0$ . An extension of the fundamental equations provided by this appendix could easily be made using a full set of the Fourier series. This extension, if made, would completely generalize the lift distribution for the rotor just as in the case of fixed-wing theory.

The spiraling vortex wake structure of the lifting rotor leads to very high induced power when compared to the ideal wing. For an advance ratio of 0.50, interference created by the spiraling rotor wake leads—just for a single blade—to induced power on the order of 10 times that of the wing when the comparison is made at wingspan equals rotor diameter and equal lift. While an elliptical bound circulation is known to be ideal for the fixed wing, it is not ideal for the rotary wing in high-speed forward flight.

A single-bladed rotor and prescribed wake geometry have been selected for this rotary wing introduction. This has been useful for an elementary discussion. However, the practical problem includes any number of blades, and a vortex wake structure that is free to deform based on fundamental principles. Furthermore, representing the rotor blade by a lifting line is quite unsatisfactory when the rotor lift distribution varies with time. Fortunately, advanced analyses, coupled with powerful digital computers, give today's rotorcraft engineers insight and practical answers to the effect of a rotor system's wake on the lifting surfaces that created the wake.

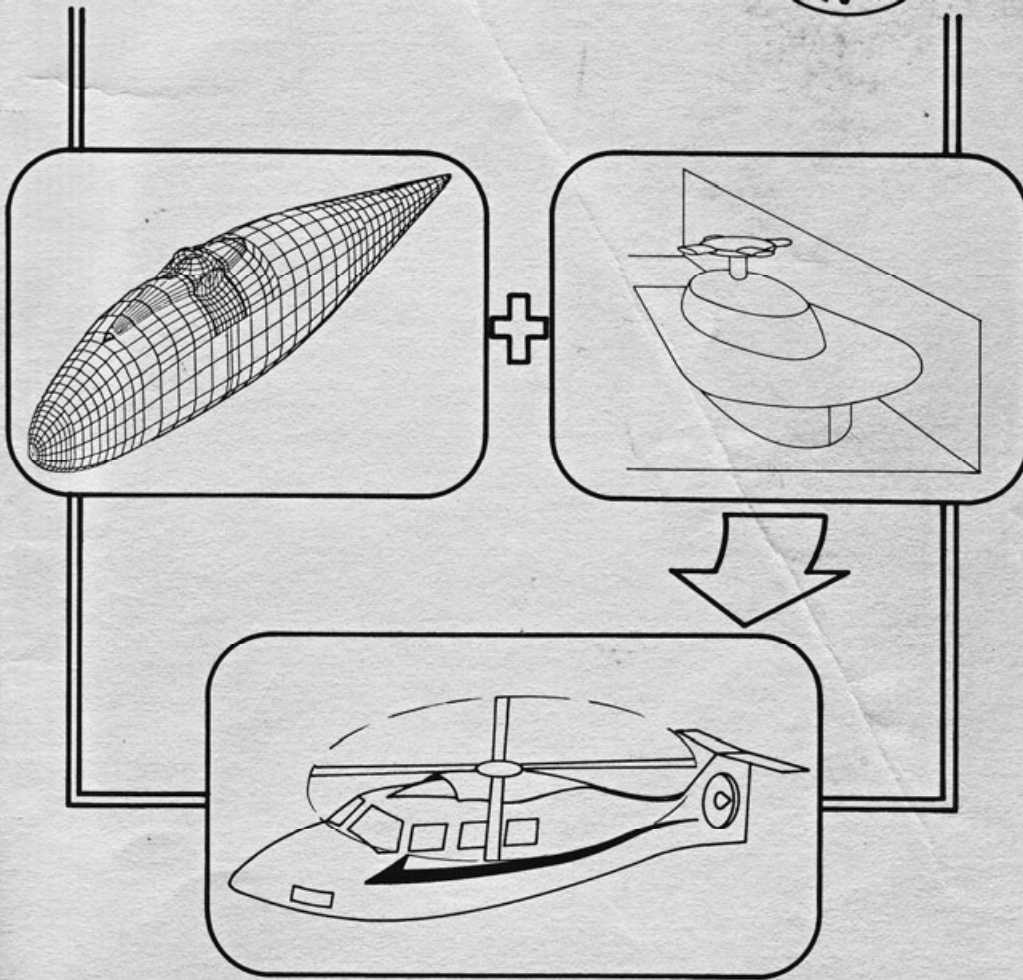


APPENDIX C

RETURN TO W. WIESNER

484

**ROTORCRAFT PARASITE DRAG**



SPECIAL REPORT PRESENTED TO THE 31ST ANNUAL NATIONAL FORUM  
BY THE AD HOC COMMITTEE ON ROTORCRAFT DRAG  
WASHINGTON, D. C. MAY 14-15, 1975

## APPENDIX C

### AMERICAN HELICOPTER SOCIETY AD HOC COMMITTEE ON ROTORCRAFT PARASITE DRAG

#### INTRODUCTION

This document is the product of the combined efforts of technical representatives from government and industry. The committee was created in May 1974, for a 1-year period, for the express purpose of examining the overall area of rotorcraft parasite drag. In this regard, it was intended that the committee's work should be as comprehensive as possible and should encompass four major aspects of the problem. These areas are:

- I. Methods for the Reduction of Parasite Drag
- II. Possible Design Penalties (Tradeoffs) Associated with Drag Reduction
- III. Potential Payoffs Associated with Drag Reduction
- IV. Measurement, Prediction and Analysis of Rotorcraft Drag

The four categories were selected because they provide a reasonable balance of the many different elements which must be considered in such an undertaking. It will be apparent to the reader of this report that it represents, in fact, a systematic approach containing a most interesting mix of studies ranging over the spectrum of theory, experiment, and many of the factors involved with design.

The approach followed in assembling this document was to incorporate separately authored papers representing the individual views of the respective members. Each paper develops one aspect of the drag issue, by use of examples and quantitative calculation where possible. The authors have included conclusions and recommendations as they deemed appropriate. The committee's recommendations are listed separately after this introduction. These recommendations are basically a condensation of the individual author's work, grouped under the four major categories listed above. The committee has stopped short of laying out an actual program, feeling that the recommendations themselves would be the primary technical elements of any program.

One of the key factors contributing to the success of the committee was the participation of highly qualified and experienced people. The individual papers may be seen to require a knowledge of not only the aerodynamics of drag reduction but also the implications for design - design-to-cost, design for increased operation effectiveness, practical design limitations, etc. A great deal of this practical experience and knowledge was evident throughout the effort, and the eventual findings of the committee can be seen to reflect this. The experience base was further enhanced by the respective position of the members. For example, government participants represented the user's requirements side, while industry members offered the manufacturer's viewpoint. The three working sessions held during the year permitted numerous exchanges on the designer's problem of reducing drag while maintaining operational effectiveness, cost objectives, weight constraints, etc. Here again the wealth of experience contained in the committee was manifest.

This document does not claim to be the final authority on the drag issue. Most of the studies presented were not funded under any ongoing drag program and are of necessity only initial investigations. Their purpose was served in that they helped to further illuminate the many implications of a substantial drag reduction. If this report has any outstanding or lasting significance, it is simply that here for the first time is a unified effort by the entire profession to place emphasis on the importance of reducing rotorcraft parasite drag. Our recommendations contain within them the major ingredients of a methodical R&D program. It is our hope that we have provided the impetus and rationale for such a program.

The Committee  
Robert M. Williams, Chairman  
May 14, 1975

## COMMITTEE CONCLUSIONS AND RECOMMENDATIONS

The following material summarizes the key findings of each of the four subgroups. For additional information, the reader is referred to the actual papers contained within the respective category.

GROUP I - Drag Reduction Goals and Methods

Current helicopters possess parasitic drag levels far in excess of fixed wing aircraft. For example, a 20,000 lb. helicopter would have approximately ten times the parasite drag of a turboprop airplane with the same gross weight. At a speed of 150 knots this drag accounts for 45 percent of the total power required. The major unsolved problem area is the rotor hub, shaft, blade shanks and control system drag which may amount to as much as forty percent of total drag on a retractible gear design. The origin of this drag is bluff body flow separation which is aggravated by the high interference of the fuselage/pylon. A detailed examination of some present configurations indicates that, with the exception of the hub region, marked drag reductions are possible using design knowledge presently contained in industry and government. Furthermore with the application of available experimental and analytical methods the potential exists for eventual parasite drag reductions on the order of 70 percent. Specific recommendations are listed below which will aid in the timely realization of this goal.

1. Develop a handbook for use by designers and engineers which contains guidelines for use in designing low drag rotary wing aircraft
2. Undertake studies to understand the mechanism of flow separation on bluff bodies and develop means to avoid separation
3. Implement the specific theoretical and experimental recommendations of Group IV
4. Assess the download "drag" problem and determine the implication for design
5. Conduct industry wide aircraft design studies to determine accurately the drag savings achievable with current knowledge of the proper design of components
6. Design, fabricate and flight test a "low drag helicopter" configuration to demonstrate the practicality and feasibility of low drag design

GROUP II - Possible Design Tradeoffs Associated with Drag Reduction

The full impact of a substantial reduction in parasite drag must be assessed from the point of view of the entire aircraft system. The potential benefits are strongly dependent on the particular helicopter mission. For example, each of the five primary "performance missions" - range, payload, speed, endurance and hover have somewhat separate implications for drag. In a hover mission the download is most important so that the fuselage cross section should produce the minimum practical "vertical drag". On the other hand, at high speeds, the streamwise fineness ratio and hub/fuselage interference effects are dominant. An endurance mission might imply a compromise of both extremes. An attack helicopter, while concerned chiefly with payload might well improve its survivability with increased speed capability. For this mission increased speed could result by efficient streamwise aerodynamic design of the basic aircraft and also by the design of low drag disposable stores and weapons - perhaps conformal stores with the basic aircraft.

In addition to the performance aspects there are numerous operational requirements which should also be assessed in terms of drag. The most outstanding example is probably the retractable landing gear argument where it is necessary to tradeoff the potential performance improvements (say speed or payload/range) versus increased complexity and reduced reliability/maintainability. There are numerous other specific operational requirements which result in large increments of parasite drag - from flat glass windshields to radar reflective paint. Each of these are amenable to design compromise so that the aerodynamic drag can be minimized while still permitting maximum operational effectiveness.

## APPENDIX C

These examples illustrate some of the considerations which affect the implementation of low drag design. Another critically important factor is the cost tradeoff - design/development/production/maintenance and operational costs (the latter should include both direct fuel costs and fuel logistics costs). It can be demonstrated that, for many missions, it is entirely possible to develop smaller, lighter, cheaper aircraft by designing for low drag. This is true, however, only if a low drag philosophy is implemented in the initial design stage. The recommendations listed below address some specific objectives leading toward this low drag concept:

1. Determine the potential performance benefits attainable for various missions by substantial reduction of parasite drag
2. Assess the various specific operational requirements which adversely impact drag and study new (component) designs that may alleviate the problem
3. Study the design of disposable stores for reduced drag
4. Study the mechanical redesign of the rotor hub and controls
5. Assess the improvement in tail surface effectiveness associated with reduced rotor hub drag (i.e. increased dynamic pressure at the tail) and determine the potential improvements in size, weight, C.G. travel and drag
6. Study the design of combined fuselages and tails for reduced drag while maintaining adequate stability
7. Using the above technology developments and also those of Groups I and IV, conduct complete vehicle preliminary design studies for specific missions and operational requirements. Analyze cost, weight, maintainance and other tradeoffs
8. Conduct wind tunnel verification studies of these designs
9. Conduct a detailed design of a low drag operational vehicle

### GROUP III - Potential Payoffs Associated With Drag Reduction

The potential improvement in helicopter capability due to a decrease in drag and a commensurate increase in efficiency appears to be very substantial. In addition to the more obvious aspects of increased range, payload, and maximum speed, there are several additional payoffs which are not as apparent. One of these is the reduction in aircraft size and gross weight needed to perform a given one mission. An increase in efficiency due to a reduction in drag produces an associated reduction in power required which in turn reduces engine/drive system size and results in reduced weight. The reduced size and weight further reduces power required, and so on until the design process converges. This multiplicative effect is only possible if a drag reduction is introduced in the early design stages - before the aircraft configuration is frozen. Although a similar argument can also be made for improvements in rotor airfoil efficiency, it appears that the relative benefits for parasite drag reduction are currently an order of magnitude greater and should therefore receive relatively greater emphasis.

Another more subtle payoff from drag reduction is the potential reduction in blade loads and moments and the associated transmitted vibrations. A quantitative assessment of this area indicates that large benefits in both loads and performance may be realized if the blades are properly designed for the low drag condition (usually this implies changing the twist).

One major impetus for concerted work on the drag problem is the potential for very substantial savings in fuel cost. A relatively conservative estimate (based on current prices) indicates that the recurring fuel costs of the projected 1980 helicopter fleet greatly outweighs the costs of even a large drag program. Such a program would include not only aerodynamics but also the needed emphasis on design integration so that such areas as reliability and maintainability would be given sufficient attention. Other specific recommendations for such a program include the following:

1. Assess the impact of various levels of drag reductions on aircraft performance and also size and weight to perform given missions.
2. Conduct detailed studies which evaluate the effect of reduced drag on blade loads and vibrations of new helicopter designs.
3. Design and evaluate low drag components which provide acceptable reliability and maintainability characteristics.
4. Apply the above technology developments to the detailed design of a low drag operational vehicle.

GROUP IV - Measurement, Prediction and Analysis of Rotorcraft Drag

The problem of determining the drag of helicopter fuselages and appendages is largely one of bluff body aerodynamics. In the case of experimental data, tunnel blockage and Reynolds number effects contribute to uncertainties in the data. Present theoretical methods are inadequate because they do not model separation effects, viscous effects and the interaction of the rotor wake with the fuselage pressure field. In order to overcome these experimental and analytical deficiencies, the following recommendations are made.

A. Experimental Data

1. New test techniques are required to remove uncertainties in experimental results due to interference effects
2. A calibration model is needed for testing in several wind tunnels
3. Full scale tests are required to avoid Reynolds number effects when separation is present
4. A full scale wind tunnel/flight test program is needed for correlation and comparison with theoretical models.

B. Theoretical Methods

1. A general analysis method applied to helicopters is needed. This method will need to consider the following:
  - a. Modeling of separation including the prediction of the base pressure
  - b. Inclusion of boundary layer (viscous) effects in the potential flow
  - c. Inclusion of rotor wake effects in cruise
  - d. Inclusion of rotor wake effects in hover considering such things as ground effect.

# APPENDIX C

## FINAL REPORT OF THE AHS AD HOC COMMITTEE ON ROTORCRAFT PARASITE DRAG

### TABLE OF CONTENTS

	Paper Number
GROUP I - Drag Reduction Goals and Methods	
A Comprehensive Plan for Helicopter Drag Reduction Robert Williams <sup>1</sup> and Peter Montana <sup>2</sup> , NSRDC . . . . .	1
A General Review of Helicopter Rotor Hub Drag Data Thomas Sheehy and Dr. David Clark, Sikorsky Aircraft . . . . .	2
Guidelines for Reducing Helicopter Parasite Drag Charles Keys and Robert Wiesner <sup>3</sup> , Boeing-Vertol . . . . .	3
Rotorcraft Low Flight Speed Download Drag and Its Reduction John Wilson, NASA-Langley . . . . .	4
GROUP II - Possible Design Tradeoffs Associated with Drag Reduction	
Cost-Benefit Evaluation of Helicopter Parasite Drag Reductions John Duhon <sup>3</sup> , Bell Helicopter . . . . .	5
Cost Effectiveness of Drag Reduction Bill Barlowe, Hughes Helicopters . . . . .	*
Some Important Practical Design Constraints Affecting Drag Reduction Ron Gormont, Army AVSCOM, St. Louis . . . . .	7
The Relationship Between Rotorcraft Drag and Stability and Control John Hoffman, Paragon Pacific, Inc. . . . .	8
GROUP III - Potential Payoffs Associated with Drag Reduction	
Wasted Fuel - Another Reason for Drag Reduction John P. Rabbot, Jr. <sup>3</sup> and Robert Stroub, NASA-Ames . . . . .	9
Effect of Drag Reduction on Rotor Dynamic Loads and Blade Lift Andrew Kerr, Lockheed California Company . . . . .	10
Effect of Parasite Drag on Rotor Performance and Dynamic Response Helicopter Vibratory Loading Arthur Smith, Kaman Aircraft . . . . .	11
GROUP IV - Measurement, Prediction, and Analysis of Rotorcraft Drag	
Prediction of Rotorcraft Drag Robert Tracy, NASC . . . . .	13
Aerodynamic Analysis of Helicopter Configurations Dr. Frank Dvorak <sup>3</sup> , Flow Research, Inc. . . . .	14
Application of Potential Flow Methods to Design Don Vann, USAAMRDL, Ft. Eustis . . . . .	*
A Method for Correlating Wind Tunnel Experiments with Potential Flow Theory Peter Montana, NSRDC . . . . .	16
SUPPLEMENT - Rotorcraft Drag Bibliography . . . . .	17

\*Title Denotes the Speciality Area of Committee Members; No Written Paper Submitted.

<sup>1</sup>Chairman.

## HELICOPTER PARASITE DRAG BIBLIOGRAPHY

Robert M. Williams  
 Naval Ship Research and Development Center  
 Bethesda, Maryland 20884

With the exception of the present committee report, specific studies of helicopter drag are relatively rare in the literature.\* Unlike the fixed wing field of the 1940's which essentially standardized on the low wing semi-monocoque design, the helicopter has yet to crystalize on a basic or reference type. Consequently, there have been no systematic tests which vary a single parameter at a time to determine its influence on the configuration as a whole. On the other hand, many of the early fixed wing component studies are applicable to rotorcraft designs--if properly interpreted and applied. The standard reference in rotary wing as well as fixed wing circles for many years, has been Sigmund Hoerner's famous "Fluid Dynamic Drag" (Library of Congress Catalog Card Number 64-19666). This text has formed the basis for numerous "cookbook" methods of drag prediction which work quite well so long as they are used within their applicable range of empiricism. However, extrapolation of these methods has often resulted in disastrous results. This is particularly the case with helicopter pylon/hub drag prediction. The specialized interference and flow separation problems of this region preclude the use of existing methods.

The references cited herein are chosen to cover primarily three areas: any known helicopter drag studies in the open (or accessible) literature; theoretical studies; certain selected studies from the fixed wing field related to the special helicopter drag problems of strong component interference between bluff shapes. In addition, supplemental material is included on some promising means of boundary layer control. It should be noted that much of the latter literature is only introductory so that further search may yield detailed information in any one particular BLC area.

The material is organized according to the following outline.

<u>Section</u>	<u>Classification</u>
A	General Experimental and Design Studies of Helicopter Parasite Drag
B	Experimental Studies of Rotor Hub Drag
C	Theoretical and Experimental Studies of Bodies of Revolution
D	Potential Flow Theory
E	Three-Dimensional Boundary Layer Theory
F	Bluff Body Aerodynamics
G	Fixed Wing Aircraft Drag Studies
H	Experimental Studies of Aerodynamic Interference
I	Cowling and Intake System
J	Low-Drag Anti-Torque Systems
K	Boundary Layer Control Studies
L	Theory of Tangential Blowing BLC About Rounded Shapes (Coanda Blowing)
M	Flow Visualization

---

\* Report of the American Helicopter Society Ad Hoc Committee on Rotorcraft Parasite Drag to the 31st Annual National Forum, 14-15 May 1975, Washington, D.C.

## APPENDIX C

- A. General Experimental and Design Studies of Helicopter Parasite Drag
1. Linville, James C., "An Experimental Investigation of High-Speed Rotorcraft Drag," USAAMRDL Technical Report 71-46 (Feb 1972).
  2. "Aerodynamic Tests of an Operational OH-6A Helicopter in the Ames 40' x 80' Wind Tunnel," prepared under contract NOW66-0657-f for Naval Air Systems Command, HTC-AD Report 369-A-8020 (May 1970).
  3. Gillespie, James, Jr., "An Investigation of the Flow Field and Drag of Helicopter Fuselage Configurations," presented at the 29th Annual National Forum of the American Helicopter Society, Washington, D.C. (May 1973).
  4. Sweet, George E. and Julian L. Jenkins, Jr., "Wind Tunnel Investigation of the Drag and Static Stability Characteristics of Four Helicopter Fuselage Models," NASA Technical Note D-1363 (Jul 1962).
  5. Biggers, James, John L. McCloud, III, and Pete Patterakis, "Wind Tunnel Tests of Two Full-Scale Helicopter Fuselages," NASA Technical Note D-1548, Washington, D.C. (Oct 1962).
  6. Hickey, David H., "Full-Scale Wind-Tunnel Tests of the Longitudinal Stability and Control Characteristics of the XV-1 Convertiplane in the Autorotating Flight Range," National Advisory Committee for Aeronautics, NACA RM A55K21a, Moffett Field, California (May 1956).
  7. Moser, Herbert H., "Full Scale Wind Tunnel Investigation of Helicopter Drag," Journal of the American Helicopter Society, Vol. 6, No. 1, pp. 27-33 (Jan 1961).
  8. Harrington, Robert D., "Reduction of Helicopter Parasite Drag," National Advisory Committee for Aeronautics, Technical Note 3234, Washington, D.C. (Aug 1954).
  9. Fradenburgh, Evan A., "Aerodynamic Efficiency Potentials of Rotary Wing Aircraft," Proceedings of the 16th Annual National Forum of the American Helicopter Society (May 1960).
  10. "High Performance Single Rotor Helicopter Study," U.S. Army Transportation Research Command, TREC Technical Report 61-44, Ft. Eustis, Virginia (Apr 1961).
  11. Rabbott, John P., Jr., "A Study of the Optimum Rotor Geometry for a High Speed Helicopter," U.S. Army Transportation Research Command, TRECOM Technical Report 62-53, Ft. Eustis, Virginia (May 1962).
  12. Mouille, Rene, "The World Speed Records of the SA.341 Gazelle," presented at the 28th Annual National Forum of the American Helicopter Society, Preprint 651, Washington, D.C. (May 1972).
  13. Jenkins, Julian L., Jr., Matthew M. Winston, and George E. Sweet, "A Wind Tunnel Investigation of the Longitudinal Aerodynamic Characteristics of Two Full-Scale Helicopter Fuselage Models with Appendages," National Aeronautics and Space Administration, Technical Note D-1364, Washington, D.C. (Jul 1962).
  14. McCloud, John L., III, James C. Biggers, and Ralph L. Maki, "Full-Scale Wind-Tunnel Tests of a Medium-Weight Utility Helicopter at Forward Speeds," National Aeronautics and Space Administration, Technical Note D-1887, Washington, D.C. (May 1963).
  15. Scallion, William, I., "Full-Scale Wind-Tunnel Investigation of the Drag Characteristics of an HU2K Helicopter Fuselage," National Aeronautics and Space Administration Technical Memo SX-848.
  16. Fabre, Paul, "Drag Problems on Rotary Wing Aircraft," Advisory Group for Aerospace Research and Development, AGARD Lecture Series 63, Helicopter Aerodynamics and Dynamics, Brussels (Apr 1973).
  17. Bosco, Dott. Ing. Angelo, "Aerodynamics of Helicopter Components Other Than Rotors," Meeting of Advisory Group for Aerospace R&D (Aerodynamics of Rotary Wings), Marseilles, France (13-15 Sep 1972); in AGARD-CPP-111.
  18. Dingeldein, R. C., "Considerations of Methods of Improving Helicopter Efficiency," NASA Technical Note D-734 (1961).
  19. Keys, C. N. and R. Wiesner, "Guidelines for Reducing Helicopter Parasite Drag," Journal of the American Helicopter Society, Vol. 20, No. 1 (Jan 1975).
  20. Montana, P. S., "Helicopter Drag Technology Program Fiscal 1973 Progress Report," Naval Ship Research and Development Center, ASED Tech Note AL-310, Bethesda, Maryland (Sep 1973).

21. Wagner, S. N., "Problems of Estimating the Drag of a Helicopter," Meeting of Advisory Group for Aerospace R&D (Aerodynamic Drag), Ismir, Turkey (10-13 Apr 1973); in AGARD-CP-124.
  22. Williams, R. M., "Recent Developments in Circulation Control Rotor Technology," Meeting of Advisory Group for Aerospace R&D (Aerodynamics of Rotary Wings), Marseilles, France (13-15 Sep 1972); in AGARD-CPP-111.
- B. Experimental Studies of Rotor Hub Drag
1. Ware, George M., "Static Stability and Control Characteristics at Low-Subsonic Speeds of a Lenticular Reentry Configuration," National Aeronautics and Space Administration, Technical Memo X-431, Washington, D.C. (Dec 1960).
  2. Demele, Fred A. and Jack J. Brownson, "Subsonic Longitudinal Aerodynamic Characteristics of Disks with Elliptic Cross Sections and Thickness-Diameter Ratios from 0.225 to 0.425," National Aeronautics and Space Administration, Technical Note D-788, Washington, D.C. (Apr 1961).
  3. Boatwright, Donald W., "In Flight Drag Measurements and Flow Studies of an 'Intermediate' Size Pylon, Paired Swashplate Assembly, and Full-Scale Hub Mockup Configuration 3," Mississippi State University, Final Report Task Order 750-G-79844 (Mar 1965).
  4. "Full-Scale Investigation of Rotor Hub Fairing for a Sikorsky H-5 Rotor Hub," Report 55McC103R.
  5. "Results of Rotor Hub Fairing Analytical Study," The Boeing Company Vertol Division, R-356, Morton, Pennsylvania (Sep 1964).
  6. "Smoke Tunnel Test of Paired Rotor Hubs on the 1/8-Scale HC-1B Model," The Boeing Company Vertol Division, R-359, Morton, Pennsylvania (Sep 1963).
  7. Foster, John J., "Wind-Tunnel Tests of a Full-Scale Piasecki H-21 Helicopter Rotor Hub," Naval Ship Research and Development Center, Report 866, Aero Data 8, Bethesda, Maryland (Aug 1953).
  8. Linville, James C., "An Experimental Investigation of the Effects of Rotor Head Configuration and Fuselage Yaw on the Wake Characteristics and Rotor Performance of a 1/8th-Scale Helicopter," U.S. Army Aviation Materiel Laboratories Technical Report 69-94, Ft. Eustis, Virginia (Feb 1970).
  9. Mugler, John P., Jr. and Walter B. Olstad, "Static Longitudinal Aerodynamic Characteristics at Transonic Speeds of a Lenticular-Shaped Reentry-Vehicle," National Aeronautics and Space Administration, Technical Memo X-423, Langley Field, Virginia (Dec 1960).
  10. Churchill, Gary B. and Robert D. Harrington, "Parasite-Drag Measurements of Five Helicopter Rotor Hubs," National Aeronautics and Space Administration, Memorandum 1-31-59L, Washington, D.C. (Feb 1959).
  11. Barlow, W. H. and F. Okamoto, "Aerodynamic Tests of a 1/3 Scale Model HO-6 Helicopter at Hughes Tool Company and NorAir Wind Tunnel Test Series No. 8 - August 1962," HTC Report 369-A-8007 (Aug 1962).
  12. Barlow, W. H. and F. S. Okamoto, "Aerodynamic Tests of a 1/3 Scale Model HO-6 Helicopter at Hughes Tool Company and NorAir Wind Tunnel Test Series No. 6 - January 1962," HTC Report 369-A-8003, (Jan 1962).
  13. "Results of the 1/2 Scale HU-1 and High Speed Helicopter Pylon and Hub Model Wind Tunnel Investigation," Bell Helicopter Company Report 8025-099-012, Ft. Worth, Texas (Jun 1961).
  14. Reader, K. R., "Wind-Tunnel Tests, at High Advance Ratios, of the Hughes Rotor/Wing Aircraft Model (Series X) with Wing Flaps," Naval Ship Research and Development Center, Test Report AL-65, Bethesda, Maryland (Dec 1969).
  15. Montana, P. S., "Experimental Investigation of Three Rotor Hub Fairing Shapes," Naval Ship Research and Development Center, Report ASED 333, Bethesda, Maryland (to be published).
- C. Theoretical and Experimental Studies of Bodies of Revolution
1. Neumark, S., "Velocity Distribution on Thin Bodies of Revolution at Zero Incidence in Incompressible Flow," Ministry of Supply, Aeronautical Research Council, R&M 2814, London (1954).

## APPENDIX C

2. Cole, Richard I., "Pressure Distributions on Bodies of Revolution at Subsonic and Transonic Speeds," National Advisory Committee for Aeronautics Research, Memorandum L52D30, Washington, D.C. (Jul 1952).
3. Jones, R., "The Distribution of Normal Pressures on a Prolate Spheroid," Aeronautical Research Council, R&M 1061, London (1925).
4. Freeman, Hugh B., "Pressure-Distribution Measurements on the Hull and Fins of a 1/40-Scale Model of the U.S. Airship 'Akron'," National Advisory Committee for Aeronautics, Report 443, Washington, D.C. (1932).
5. Gertler, Morton, "Resistance Experiments on a Systematic Series of Streamlined Bodies of Revolution-For Application to the Design of High-Speed Submarines," Naval Ship Research and Development Center, DTMB Report C-297, Washington, D.C. (Apr 1950).
6. Beveridge, John L., "Effect of Axial Position of Propeller on the Propulsion Characteristics of a Submerged Body of Revolution," Naval Ship Research and Development Center, DTMB Report 1456, Washington, D.C. (Mar 1963).
7. Matthews, Clarence W., "A Comparison of the Experimental Subsonic Pressure Distributions about Several Bodies of Revolution with Pressure Distributions Computed by Means of the Linearized Theory," National Advisory Committee for Aeronautics, Report 1155, Washington, D.C. (1953).
8. Bates, William R., "Static Stability of Fuselages Having a Relatively Flat Cross Section," National Advisory Committee for Aeronautics, Technical Note 3429, Washington, D.C. (Mar 1955).
9. Fox, Charles, H., Jr., "Experimental Surface Pressure Distributions for a Family of Axisymmetric Bodies at Subsonic Speeds," National Aeronautics and Space Administration, Technical Memorandum X-2439, Washington, D.C. (Dec 1971).
10. Thompson, Jim Rogers, "Measurements of the Drag and Pressure Distribution on a Body of Revolution Throughout Transition from Subsonic to Supersonic Speeds," National Advisory Committee for Aeronautics, Research Memorandum L9127, Washington, D. C. (Jan 1950).
11. Beveridge, John L., "Pressure Distribution on Towed and Propelled Streamline Bodies of Revolution at Deep Submergence," Naval Ship Research and Development Center, DTMB Report 1665, Washington, D.C. (Jun 1966).
12. Abbott, Ira H., "Airship Model Tests in the Variable Density Wind Tunnel," National Advisory Committee for Aeronautics, Report 394, Washington, D.C. (1931).

### D. Potential Flow Theory

1. Hess, J. L. and A.M.O. Smith, "Calculation of Potential Flow About Arbitrary Bodies," Progress in Aeronautical Sciences, Vol. 8, The Pergamon Press, (1967).
2. Hess, J. L. and A.M.O. Smith, "Calculation of Non-Lifting Potential Flow About Arbitrary Three-Dimensional Bodies," Journal of Ship Research, Vol. 8, No. 2 (1964).
3. Rubbert, P. E., G. R. Saaris et al., "A General Method for Determining the Aerodynamic Characteristics of Fan-In-Wing Configurations," USAAVLABS Technical Report 67-61A, Vol. 1, U.S. Army Aviation Material Laboratories, Ft. Eustis, Virginia (Dec 1967).
4. Hurwitz, Shirley M. and Mery C. Leonhart, "Preliminary Description of Graphic Pac Subroutines for the CDC 6000 Series," Naval Ship Research and Development Center, Washington, D.C. (Aug 1971).
5. Dawson, Charles W. and Janet S. Dean, "The XYZ Potential Flow Program," Naval Ship Research and Development Center, Report 3892, Bethesda, Maryland (Jun 1972).
6. Gillespie, James, Jr., and R. I. Windsor, "An Experimental and Analytical Investigation of the Potential Flow Field, Boundary Layer, and Drag of Various Helicopter Fuselage Configurations," USAAMRDL Tech Note 13, Ft. Eustis, Virginia (Jan 1974).
7. Gillespie, James, Jr., "Streamline Calculations Using the XYZ Potential Flow Program," USAAMRDL Tech Note 16, Ft. Eustis, Virginia (May 1974).
8. Kraus, W. and P. Sacher, "Das MBB-Unterschall Panel Verfahren: Dreidimensionale Potentialtheorie bei

beliebig Vorgegebener Mehr Korperanordnung," MBB Report UFE-672-70(0) (Dec 1970).

9. Rubbert, P. E., G. R. Saaris et al., "A General Method for Determining the Aerodynamic Characteristics of Fan-In-Wing Configurations," Vol. I - Theory and Applications, The Boeing Company, USAAVLABS TR 67-61A, AD667980 (Dec 1967).
10. Woodward, F. A., F. A. Dvorak and E. W. Geller, "A Computer Program for Three-Dimensional Lifting Bodies in Subsonic Inviscid Flow," USAAMRDL-TR-74-18, Ft. Eustis, Virginia (Apr 1974).
11. Klepinger, R. H. and R. Weissman, "Potential Payoff of New Aerodynamic Prediction Methods," Meeting of Advisory Group for Aerospace R&D (Aircraft Design Integration and Optimization), Florence, Italy (1-4 Oct 1973); in AGARD-CP-147.

#### E. Three-Dimensional Boundary Layer Theory

1. Cebeci, T., G. J. Mosinskis, and K. Kaups, "A General Method for Calculating Three-Dimensional Incompressible Laminar and Turbulent Boundary Layers I. Swept Infinite Cylinders and Small Cross Flow," Douglas Aircraft Company, Report MDC J5694, Long Beach, California (Nov 1972).
2. Hahn, M., P. E. Rubbert, and A. Mahal, "Evaluation of Separation Criteria and Their Application to Separated Flow Analysis," Air Force Flight Dynamics Laboratory, Technical Report AFFDL-TR-72-145, Wright-Patterson AFB, Ohio (Jan 1973).
3. "Progress in Aeronautical Sciences, Vol. 2, Boundary Layer Problems," edited by Antonio Ferri, D. Kuchemann, L.H.G. Sterne, Pergamon Press, New York (1962).
4. Allen, H. J. and E. W. Perkins, "A Study of Effects of Viscosity on Flow over Slender Inclined Bodies of Revolution," National Advisory Committee for Aeronautics, Report 1048, Washington, D.C. (1951).
5. Granville, Paul S., "A Calculation of the Viscous Drag of Bodies of Revolution," Naval Ship Research and Development Center, DTMB Report 849, Washington, D.C. (Jul 1953).
6. von Kerczek, C., "Calculation of the Turbulent Boundary Layer on a Ship Hull at Zero Froude Number," Naval Ship Research and Development Center, Ship Performance Department Tech Note 235, Washington, D.C. (Aug 1972).
7. Price, Joseph M. and Julius E. Harris, "Computer Program for Solving Compressible Nonsimilar-Boundary-Layer Equations for Laminar, Transitional, or Turbulent Flows of a Perfect Gas," National Aeronautics and Space Administration, Technical Memo X-2458, Washington, D.C. (Apr 1972).
8. Myring, D. F., "The Effects of Normal Pressure Gradients on the Boundary Layer," Royal Aircraft Establishment, Report AD 846 516, Farnborough, England (Aug 1968).
9. Presz, W. M., Jr. and E. T. Pitkin, "Flow Separation over Axisymmetric Afterbody Models," presented as AIAA Paper 74-17 at 12th Aerospace Sciences Meeting, Washington, D.C. (Feb 1974).
10. Cebeci, T. and G. J. Mosinskis, "Calculation of Viscous Drag and Turbulent Boundary-Layer Separation of Two-Dimensional and Axisymmetric Bodies in Incompressible Flows," McDonnell-Douglas Corporation, Report MDC J0973-01, Long Beach, California (Nov 1970).
11. East, L. F. and R. P. Hoxey, "Low-Speed Three-Dimensional Turbulent Boundary Layer Data: Part I," Royal Aircraft Establishment, Report RAE-TR-69041, Farnborough, England (Mar 1969).
12. East, L. F. and R. P. Hoxey, "Boundary Layer Effects in an Idealized Wing-Body Junction at Low Speed," Royal Aircraft Establishment, Report FLD/GP 20/4, Farnborough, England (Jul 1968).
13. Cumpsty, N. A. and M. R. Head, "The Calculation of Three-Dimensional Turbulent Boundary Layers: Part II - Attachment-Line Flow on an Infinite Swept Wing," The Aeronautical Quarterly (May 1967).
14. Gaster, M., "On the Flow Along Swept Leading Edges," The Aeronautical Quarterly (May 1967).
15. Maskell, E. C., "Flow Separation in Three Dimensions," Royal Aircraft Establishment, Report Aero 2565, Farnborough, England (Nov 1955).
16. Peake, D. J., "Three-Dimensional Flow Separations on Upswept Rear Fuselages," National Research Council, Canada (1969).

## APPENDIX C

### F. Bluff Body Aerodynamics

1. Hansen, S. Gordon, "Aerodynamics of Bluff Bodies," Lockheed California Company, Report 21947 (Nov 1968).
2. Roshko, Anatol, "On the Wake and Drag of Bluff Bodies," 22nd Annual Meeting of the Institute of Aeronautical Sciences, New York (Jan 1954).
3. Wood, C. J., "The Effect of Base Bleed on a Periodic Wake," Journal of the Royal Aeronautical Society, London (Jul 1964).
4. Nash, J. F., "A Review of Research on Two-Dimensional Base Flow," Aeronautical Research Council, R&M 3323, London (1963).
5. Theodorsen, Theodore and Arthur Regier, "Experiments on Drag of Revolving Disks, Cylinders, and Streamline Rods at High Speeds," National Advisory Committee for Aeronautics, Report 793, Washington, D.C. (1944).
6. Polhamus, Edward C., Edward W. Geller, and Kalman J. Grunwald, "Pressure and Force Characteristics of Noncircular Cylinders as Affected by Reynolds Number with a Method Included for Determining the Potential Flow About Arbitrary Shapes," National Aeronautics and Space Administration, Technical Report R-46, Washington, D.C. (1959).
7. Polhamus, Edward C., "Effect of Flow Incidence and Reynolds Number on Low Speed Aerodynamic Characteristics of Several Noncircular Cylinders with Applications to Directional Stability and Spinning," National Aeronautics and Space Administration, Technical Report R-29, Washington, D.C. (1959).
8. "Wind Forces on Aeroplane Struts and Wires," Advisory Committee for Aeronautics, R&M 256, London (1916).

### G. Fixed Wing Aircraft Drag Studies

1. Jones, B. Melville, "The Streamline Aeroplane," Proceedings First Meeting, Second Half, 64th Session, The Journal of "The Royal Aeronautical Society" (May 1929).
2. Dryden, Hugh L., "The 37th Wilbur Wright Memorial Lecture - The Aeronautical Research Scene - Goals, Methods, and Accomplishments," Journal of the Royal Aeronautical Society (Jul 1949).
3. Lange, Roy H., "A Summary of Drag Results from Recent Langley Full-Scale Tunnel Tests of Army and Navy Airplanes," National Advisory Committee for Aeronautics Wartime Report, Advance Confidential Report L5A30, Washington, D.C. (Feb 1945).
4. Burgan, Elmer T. and John T. Matthews, "Longitudinal Characteristics of the Current Configuration of a 1/11-Scale Model W2F Airplane," Naval Ship Research and Development Center, DTMB Aero Report 3261, Washington, D.C. (Aug 1961).
5. Dearborn, C. H. and A. Silverstein, "Drag Analysis of Single-Engine Military Airplanes Tested in the NACA Full-Scale Wind Tunnel," National Advisory Committee for Aeronautics Wartime Report, Advance Confidential Report, Washington, D.C. (Oct 1940).
6. Johnson, Clarence L., "Development of the Lockheed P-80A Jet Fighter Airplane," Journal of the Aeronautical Sciences, Vol. 14, No. 12 (Dec 1947).

### H. Experimental Studies of Aerodynamic Interference

1. NACA Studies on Aerodynamic Interference: Reports 451 (1932), 540 (1935), 575 (1936), 678 (1939); Tech Notes 641 (1938), 1272 (1947); Tech Memos 400 (1927), 517 (1929).
2. Kuchemann, D. and J. Weber, "The Subsonic Flow Past Swept Wings at Zero Lift Without and With Body," Aeronautical Research Council, R&M, London (1956).
3. Willmer, M.A.P., "Effect of Flow Curvature Due to the Fuselage on the Flapping Motion of a Helicopter Rotor," Royal Aircraft Establishment, Technical Note NAVAL 61, Ministry of Aviation, London (1963).

4. Crimi, Peter, "Theoretical Prediction of the Flow in the Wake of a Helicopter Rotor Addendum - Effects Due to a Fuselage in a Constant Nonuniform Flow," BB-1994-S-3, Cornell University, Buffalo, New York (Aug 1966).
5. Ower, E., "Some Aspects of the Mutual Interference Between Parts of Aircraft," Aeronautical Research Committee, R&M Report 1480, London (Jun 1932).
6. "Airframe/Engine Integration" Advisory Group for Aerospace Research and Development, AGARD Lecture Series No. 53.
7. Bain, Lawrence J., "Investigation of Compound Helicopter Aerodynamic Interference Effects," United Aircraft Corporation, Report AD 665427, Stratford, Conn. (Nov 1967).
8. Chaplin, Harvey R., "Wind Tunnel Tests of a 1/48-Scale Model of the XZS2G-1 Airship with Various Tail Configurations Part III - Static Pressure Measurements on the Car and Radome," Naval Ship Research and Development Center, DTMB AD-3110, Washington, D.C. (May 1955).
9. Robinson, Russell G. and James B. Delano, "An Investigation of the Drag of Windshields in the 8-Foot High-Speed Wind Tunnel," National Advisory Committee for Aeronautics, Report 730, Washington, D.C. (1942).
10. Chaplin, Harvey R., "Wind Tunnel Tests of the XZS2G-1 Airship Part III - Effect Upon Stability and Drag on an Envelope-Mounted Search-Height Radome and Pressure Measurements on a Car-Mounted Elliptical Radome," Naval Ship Research and Development Center, DTMB Report AD-3168, Washington, D.C. (Feb 1955).
11. Prandtl, L., "Effects of Varying the Relative Vertical Position of Wing and Fuselage," National Advisory Committee for Aeronautics, Technical Note 75, Washington, D.C. (1921).

#### I. Cowling and Intake System

1. Rogallo, R. M., "Internal-Flow Systems for Aircraft," National Advisory Committee for Aeronautics, Report 713, Washington, D.C. (1941).
2. Christiani, R. Duane and Lauros M. Randall, "A Preliminary Experimental Investigation of a Submerged Cascade Inlet," National Advisory Committee for Aeronautics, Research Memorandum A9A24, Washington, D.C. (Mar 1949).
3. Czarnecki, K. R. and W. J. Nelson, "Wind-Tunnel Investigation of Rear Underslung Fuselage Ducts," National Advisory Committee for Aeronautics, Advance Restricted Report 3121, Wartime Report, Washington, D.C. (Sep 1943).
4. Mossman, Emmet A. and Lauros M. Randall, "An Experimental Investigation of the Design Variables for NACA Submerged Duct Entrances," National Advisory Committee for Aeronautics, Research Memorandum A7130, Washington, D.C. (Jan 1948).
5. Pinkel, Benjamin, Richard Turner, and Fred Voss, "Design of Nozzles for the Individual Cylinder Exhaust Jet Propulsion System," National Advisory Committee for Aeronautics, Wartime Report, Advance Confidential Report, Washington, D.C. (Apr 1941).
6. Nelson, W. J. and K. R. Czarnecki, "Wind-Tunnel Investigation of Wing Ducts on a Single-Engine Pursuit Airplane," National Advisory Committee for Aeronautics, Wartime Report, Advance Restricted Report 3J13, Washington, D.C. (Oct 1943).
7. Pinkel, Benjamin and L. Richard Turner, "Flight Tests of Exhaust-Gas Jet Propulsion," National Advisory Committee for Aeronautics, Wartime Report, Advance Confidential Report, Washington, D.C. (Nov 1940).
8. Pinkel, Benjamin et al., "Exhaust-Stack Nozzle Area and Shape for Individual Cylinder Exhaust-Gas Jet-Propulsion System," National Advisory Committee for Aeronautics, Report 765, Washington, D.C. (1943).
9. Silverstein, Abe and Eugene R. Guryansky, "Development of Cowling for Long-Nose Air-Cooled Engine in the NACA Full-Scale Wind Tunnel," National Advisory Committee for Aeronautics, Wartime Report, Advance Restricted Report, Washington, D.C. (Oct 1941).

## APPENDIX C

10. Theodorsen, Theodore, M. J. Brevoort, and George W. Stickle, "Full-Scale Tests of N.A.C.A. Cowlings, National Advisory Committee for Aeronautics, Report 592, Washington, D.C. (1937).
- J. Low Drag Anti-Torque Systems
1. Velazquez, J. L., "Advanced Anti-Torque Concepts Study," U.S. Army Air Mobility Research and Development Laboratory, Technical Report 71-44, Ft. Eustis, Virginia (Aug 1971).
  2. Grumm, Arthur W. and Groves E. Herrick, "Advanced Antitorque Concepts Study," U.S. Army Air Mobility Research and Development Laboratory, Technical Report 71-23, Ft. Eustis, Virginia (Jul 1971).
  3. Gallot, Jacques, "The Fenestron, A New Concept of Tail Rotor," presented at the 39th AGARD Flight Mechanics Panel Meeting on Advanced Rotorcraft, NASA Langley, Virginia (20-23 Sep 1971).
  4. Sowyrda, A., "On the Feasibility of Replacing a Helicopter Tail Rotor," Cornell Aeronautical Laboratory, Inc., Cal No. BB-2584-S-1, Buffalo, New York (Jul 1968).
  5. Amer, Kenneth B. and Alfred Gessow, "Charts for Estimating Tail-Rotor Contribution to Helicopter Directional Stability and Control in Low-Speed Flight," National Advisory Committee for Aeronautics, Report 1216, Washington, D.C. (1955).
  6. Gustafson, Frederic B., "History of NACA/NASA Rotating-Wing Aircraft Research, 1915-1970," VertiFlite, Vol. 16, No. 10, p. 14 (Oct 1970).
  7. Lehman, August F., "Model Studies of Helicopter Tail Rotor Flow Patterns in and out of Ground Effect U.S. Army Mobility Research and Development Laboratory, Technical Report 71-72, Ft. Eustis, Virginia (Apr 1971).
- K. Boundary Layer Control Studies
1. Richards, E. J., W. S. Walker and C. R. Taylor, "Wind-Tunnel Tests on a 30-Percent Suction Wing," Aeronautical Research Council, R&M Report, London (1948).
  2. Gregory, N. and W. S. Walker, "Wind-Tunnel Tests on the Use of Distributed Suction for Maintaining Laminar Flow on a Body of Revolution," Ministry of Aviation, R&M 314, London (1960).
  3. Smith, F. and D. J. Highton, "Flight Tests on 'King Cobra' FS.440 to Investigate the Practical Requirements for the Achievement of Low Profile Drag Coefficients on a 'Low Drag' Aerofoil," Ministry of Supply, R&M 2375, London (1950).
  4. Richards, E. J., W. S. Walker, and J. R. Greening, "Tests of a Griffith Aerofoil in the 13 ft. x 9 ft. Wind Tunnel," Ministry of Supply, R&M 2148, London.
  5. Wallis, R. A., "The Use of Air Jets for Boundary Layer Control," Commonwealth of Australia, Department of Supply, Aeronautical Research Laboratories, Aerodynamics Note 110, Melbourne (Jun 1952).
  6. Schubauer, G. B. and W. G. Spangenberg, "Forced Mixing in Boundary Layers," Journal of Fluid Mechanics, Vol. 8, Part I, pp 10-32 (1960).
  7. McCullough, George B., Gerald E. Nitzberg, and John A. Kelly, "Preliminary Investigation of the Delay of Turbulent Flow Separation by Means of Wedge-Shaped Bodies," National Advisory Committee for Aeronautics, Research Memorandum A50L12, Washington, D.C. (1951).
  8. Young, Maurice and Jaan Liiva, "Performance Potential of Rotor Blade Inboard Aerodynamic Devices," Aerodynamic Problems Associated with V/STOL Aircraft, CAL/USAAVLABS, Symposium Proceedings, Vol. I (Jun 1966).
  9. Lachmann, G. V., editor, "Boundary Layer and Flow Control, Its Principles and Application," Vols. I and 2, Pergamon Press, New York (1961).
  10. Head, M. R., "History of Research on Boundary Layer Control for Low Drag in U.K.," Part I. History of Boundary Layer and Flow Control Research in Various Countries (Vol. I of reference 9).

11. Cooke, J. C. and G. G. Brebner, "The Nature of Separation and Its Prevention by Geometric Design in a Wholly Subsonic Flow," Part I. History of Boundary Layer and Flow Control Research in Various Countries (Vol. I of reference 9).
  12. Wuest, W., "Theory of Boundary Layer Suction to Prevent Separation," Part I. History of Boundary Layer and Flow Control Research in Various Countries (Vol. I of reference 9).
  13. Carriere, P. and E. A. Eichelbrenner, "Theory of Flow Reattachment by a Tangential Jet Discharging Against a Strong Adverse Pressure Gradient," Part I. History of Boundary Layer and Flow Control Research in Various Countries (Vol. I of reference 9).
  14. Wortmann, F. X., "Progress in the Design of Low Drag Aerofoils," Part III. Boundary Layer Control for Low Drag (Vol. 2 of reference 9).
  15. Gregory, N., "Research on Suction Surfaces for Laminar Flow," Part III. Boundary Layer Control for Low Drag (Vol. 2 of reference 9).
  16. Ringleb, F. O., "Separation Control by Trapped Vortices," Part III. Boundary Layer Control for Low Drag (Vol. 2 of reference 9).
  17. Chaplin, Harvey R., "Sink Effect of an Incompressible Turbulent Jet Flowing over a Flat Plate," Naval Ship Research and Development Center, DTMB Aero Memorandum 24, Washington, D.C. (Nov 1954).
  18. Beveridge, John L., "Bow-Thruster Jet Flow," Journal of Ship Research, Vol. 15, No. 3, pp 177-195 (Sep 1971).
  19. Ousterbout, Donald S., "An Experimental Investigation of a Cold Jet Emitting from a Body of Revolution into a Subsonic Free Stream," NASA Contractor Report, NASA CR-2089, Washington, D.C. (Aug 1972).
  20. Williams, Robert M., "Some Research on Rotor Circulation Control," in CAL/AVLABS Symposium: Aerodynamics of Rotary Wing and V/STOL Aircraft, 3rd Proceedings, Vol. 2, Buffalo, New York (Jan 1969).
  21. Williams, Robert M. and Harvey J. Howe, "Two-Dimensional Subsonic Wind Tunnel Tests on a 20-Percent Thick, 5-Percent Cambered Circulation Control Airfoil," Naval Ship Research and Development Center, Tech Note AL-176, AD 877-764.
  22. Englar, Robert J. and Robert M. Williams, "Design of a Circulation Control Stern Plane for Submarine Applications," Naval Ship Research and Development Center, Tech Note AL-201 (May 1972).
  23. Williams, R. M. and E. O. Rogers, "Design Considerations of Circulation Control Rotors," presented at 28th Annual National Forum of American Helicopter Society, Paper 603, Washington, D.C. (May 1972).
  24. Englar, R. J., "Two-Dimensional Subsonic Wind-Tunnel Tests of Two 15-Percent Thick Circulation Control Airfoils," Naval Ship Research and Development Center, Tech Note AL-211, AD 900-210L, Bethesda, Maryland (Aug 1971).
  25. Ottensoser, J., "Two-Dimensional Subsonic Evaluation of a 15-Percent Thick Circulation Control Airfoil with Slots at Both Leading and Trailing Edges," Naval Ship Research and Development Center, Report 4456, Bethesda, Maryland (Jul 1974).
- L. Theory of Tangential Blowing BLC About Rounded Shapes (Coanda Blowing)
1. Dunham, J., "A Tentative Theory of Circulation Control Applied to a Circular Cylinder," N.G.T.E. Note NT 567 (unpublished, 1965).
  2. Dunham, J., "A Theory of Circulation Control by Slot-Blowing Applied to a Circular Cylinder," Journal of Fluid Mechanics, Vol. 33, Part 3 (Sep 1968).
  3. Kind, R. J., "A Calculation Method for Circulation Control By Tangential Blowing Around a Bluff Trailing Edge," Aeronautical Quarterly, Vol. XIX, pp 205-223 (Aug 1968).
  4. Kind, R. J. and D. J. Maull, "An Experimental Investigation of a Low-Speed Circulation-Controlled Aerofoil," Aeronautical Quarterly, Vol. XIX, pp. 170-182 (May 1968).

## APPENDIX C

5. Kind, R. J., "A Proposed Method of Circulation Control," Ph.D. Dissertation, University of Cambridge (1967).
6. Jones, D. G., "Measurements of Wall Jet Development on a Circulation Controlled Aerofoil," University of California, Davis, Mechanical Engineering Department (Jan 1971).
7. Jones, D. G., "The Performance of Circulation-Controlled Airfoils," Ph.D. Dissertation, University of Cambridge, Churchill College (Jul 1970).
8. Gartshore, I. S. and B. G. Newman, "The Turbulent Wall Jet in an Arbitrary Pressure Gradient," *The Aeronautical Quarterly*, pp 25-56 (Feb 1969).
9. Kind, R. J., "Calculation of the Normal-Stress Distribution in a Curved Wall Jet," West Virginia University, Department of Aerospace Engineering, TR-18 (Aug 1969).
10. Ambrosiani, J. P. and N. Ness, "Analysis of Circulation Controlled Elliptical Airfoil," West Virginia University, College of Engineering, TR-30 (Apr 1971).
11. Levinsky, E. S. and T. T. Yeh, "Analytical and Experimental Investigation of Circulation Control by Means of a Turbulent Coanda Jet," NASA CR-2114 (Sep 1972).
12. Kind, R. J., "A Calculation Method for Boundary Layer Control by Tangential Blowing," *CASI Transactions*, Vol. 4, No. 2 (Sep 1971).
13. Wagnansky, I. and B. G. Newman, "The Effect of Jet Entrainment on Lift and Moment for a Thin Airfoil with Blowing," *Aeronautical Quarterly*, Vol. XV, Part 2 (May 1964).
14. Dvorak, F. A., "Calculation of Turbulent Boundary Layers and Wall Jets over Curved Surfaces," *AIAA Journal*, Vol. 11, No. 4 (Apr 1973).
15. Dvorak, F. A., "A Viscous/Potential Flow Interaction Analysis for Circulation Control Airfoils," Analytical Methods Report 75-01, Bellevue, Washington (May 1975).

### M. Flow Visualization

1. Maltby, R. L. and R. F. A. Keating, "Flow Visualization in Low-Speed Wind Tunnels: Current British Practice," Royal Aircraft Establishment, Technical Note Aero 2715, Bedford, England (Aug 1960).
2. Stalker, R. J., "A Study of the China-Film Technique for Flow Indication," Commonwealth of Australia, Department of Supply, Research and Development Branch, Aeronautical Research Laboratories, Report A.R.L./A.96 (Oct 1955).
3. Griswold, Roger W., II., "Visualized Aerodynamic Research," *Society of Automotive Engineers Journal (Transactions)*, Vol. 48, No. 5, pp 180-187.
4. Preston, J. H., "Visualization of Boundary Layer Flow," Ministry of Supply, Aeronautical Research Council, R&M 2267 (Nov 1946).
5. Stanbrook, A., "Experimental Observation of Vortices in Wing-Body Junctions," Ministry of Supply, Aeronautical Research Council, R&M 3114 (1959).
6. Bird, John D. and Donald R. Riley, "Some Experiments on Visualization of Flow Fields Behind Low-Aspect-Ratio Wings by Means of a Tuft Grid," National Advisory Committee for Aeronautics, Technical Note 2674 (May 1952).
7. Compiled by Maltby, R. L., "Flow Visualization in Wind Tunnels Using Indicators," North Atlantic Treaty Organization, Advisory Group for Aeronautical Research and Development, AGARDograph 70 (Apr 1962).
8. Murphy, J. S. and Ralph E. Phinney, "Visualization of Boundary-Layer Flow," *Journal of the Aeronautical Sciences*, pp 771-772 (Nov 1951).
9. Richards, E. J. and F. H. Burstall, "The 'China Clay' Method of Indicating Transition," Ministry of Supply, Aeronautical Research Council, R&M 2126 (Aug 1945).

10. Loving, Donald L. and S. Katzoff, "Fluorescent-Oil Film Method and Other Techniques for Boundary-Layer Flow Visualization," National Aeronautics and Space Administration Memorandum 3-17-59L (Mar 1959).
11. Ogle, John S., "Memorandum on the Fluorescent Oil Flow Visualization System," Southern California Cooperative Wind Tunnel Project No. K323, California Institute of Technology, Pasadena (Mar 1958).



## APPENDIX D

### ROTOR HUBS

The following drawings of hubs came from four sources, namely

- a. Bill Bousman's collection.<sup>1</sup> Bill collected photos of many hubs from several manufacturers. Then he had the NASA Ames Research Center graphic arts department create line drawings on vellum. He had the drawings framed. They were mounted on the second floor wall in Building 215 at Ames Research Center.
- b. Schindler's and Pfisterer's AGARD paper,<sup>2</sup> which I consider an exceptionally thorough piece of work.
- c. Tom Hanson's small book titled *A Designers Friendly Handbook of Helicopter Rotor Hubs*, which he publishes himself and is extremely valuable.<sup>3</sup>
- d. A few out of my own files.

The aircraft and/or hubs shown are:

1. Eurocopter AS-365, AS-360, SA-342, SA-330, AS-332, Triflex
2. Agusta/Westland EH-101
3. Bell Model 47, Model 206, Model 222, Model 412, Model 407/OH-58D, Model 680
4. Boeing Vertol BMR, CH-46, CH-47
5. Doman LZ-5
6. Cessna CH-1
7. Hiller Model 360/UH-12
8. Hughes AH-64, OH-6, HARP
9. Lockheed AH-56, CL-475, XH-51
10. Messerschmitt-Bölkow-Blohm (MBB), BMR, BO-105, PAH-2
11. McDonnell XV-1
12. Mil Mi-26
13. Robinson R-22
14. Sikorsky H-34, S-61, S-76, UH-60
15. Westland Lynx

Lastly, you will find Ray Prouty's article in the January 1983 issue of *Rotor & Wing International* magazine (pages 26–28) very, very helpful. His article is at the end of this appendix.

---

<sup>1</sup> Bousman, W. G.; Ormiston, R. A.; and Mirick, P. H.: *Design Considerations for Bearingless Rotor Hubs*. Paper No. A-83-39-62-1000, Proc. 39th Annual Forum of the American Helicopter Society, St. Louis, Mo., May 9–11, 1983.

<sup>2</sup> Schindler, R. and Pfisterer, E.: *Impacts of Rotor Hub Design Criteria on the Operational Capabilities of Rotorcraft Systems*. AGARD CP-423, Rotorcraft Design for Operations Symposium, Amsterdam, The Netherlands, Oct. 13–16, 1986.

<sup>3</sup> Hanson, T. F.: *A Designer Friendly Handbook of Helicopter Rotor Hubs*. Newhall, Calif.: Author Published, 2005.

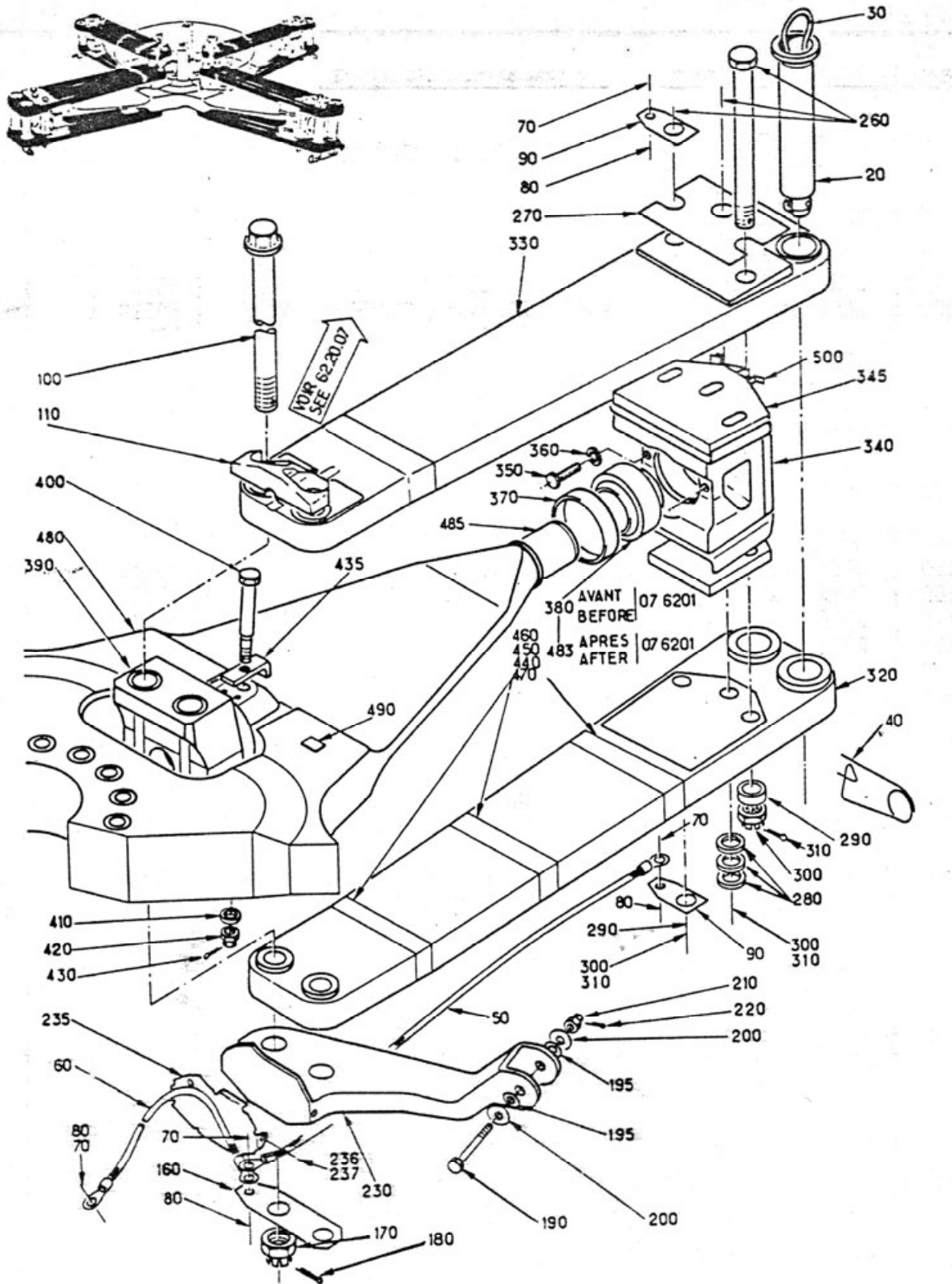


Fig. D-1. Eurocopter AS-365 (author's collection).

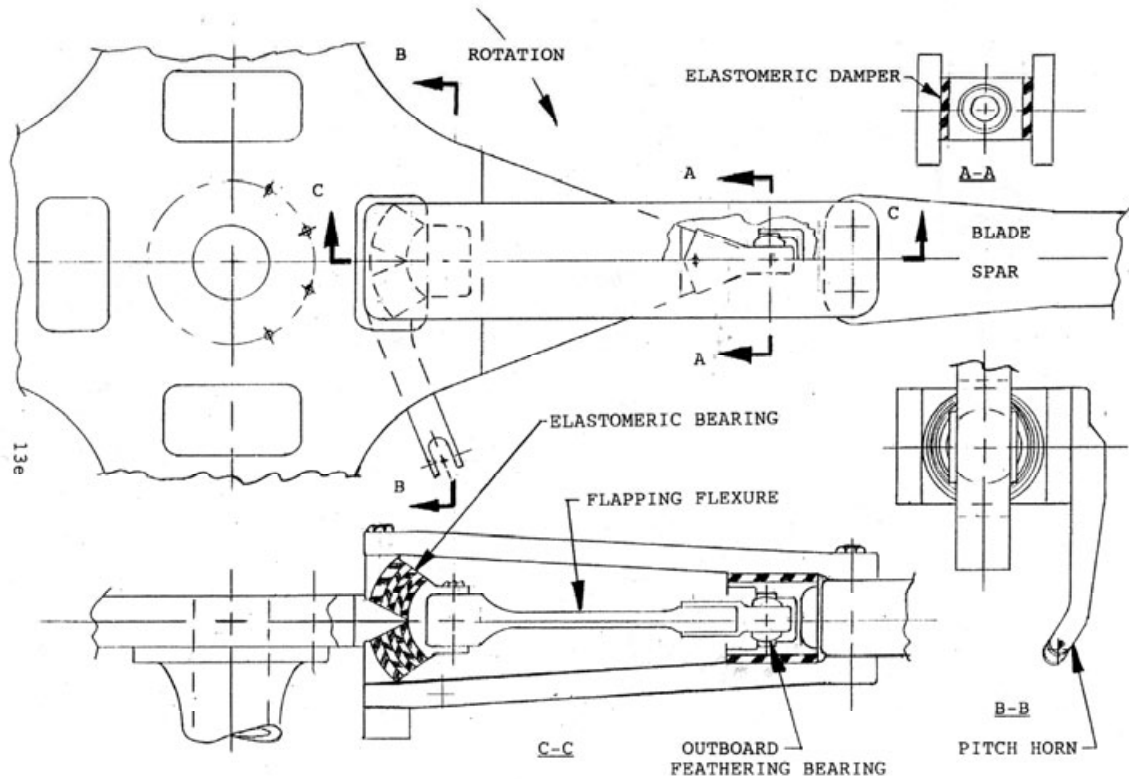


FIG. # I-26 EUROCOPTER AS-365

Fig. D-2. Eurocopter AS-365 (courtesy of Tom Hanson).

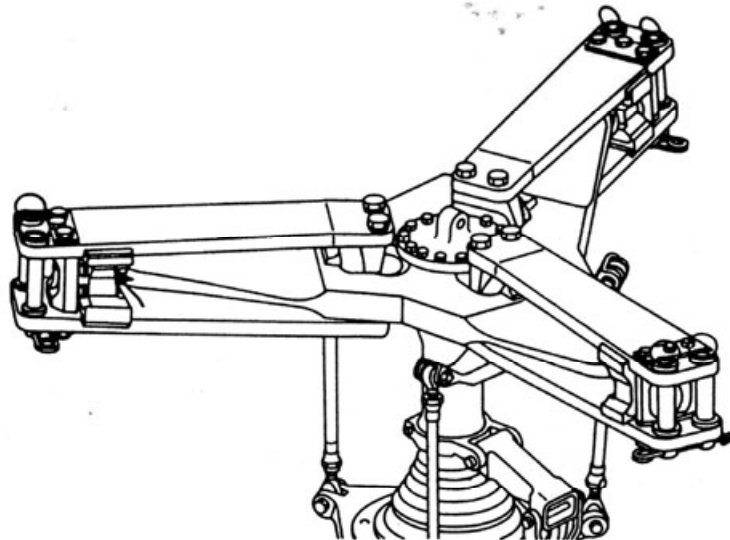
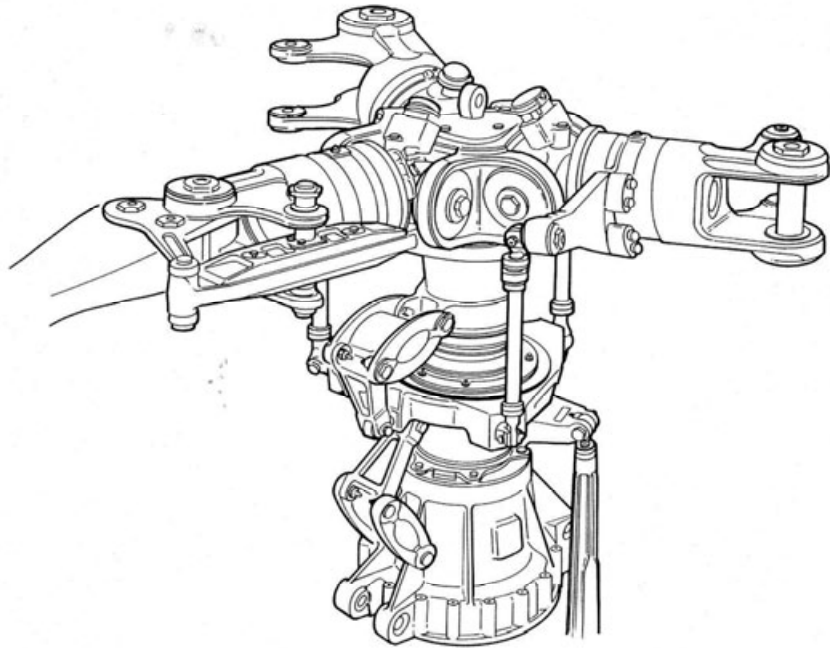


FIG : 10 STARFLEX ROTOR HEAD OF AEROSPATIALE AS 350/355 ECUREUIL

Fig. D-3. Eurocopter AS-360 (Schindler/Pfisterer AGARD paper).

AEROSPATIALE SA 342  
FIRST FLIGHT-APRIL 1967



**Fig. D-4. Aerospatiale SA 342 (courtesy of Bill Bousman).**

AEROSPATIALE SA 330  
FIRST FLIGHT-APRIL 1965

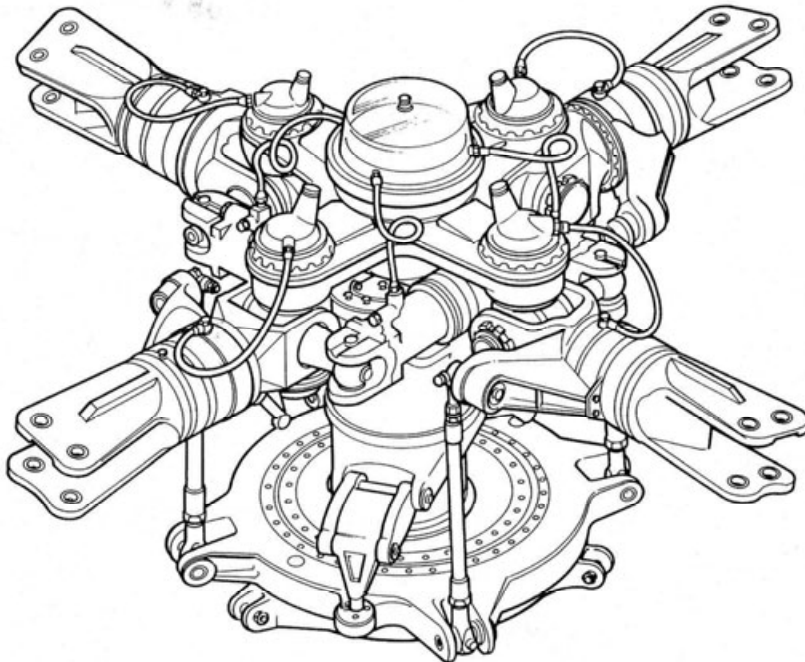


**Fig. D-5. Aerospatiale SA 330 (courtesy of Bill Bousman).**

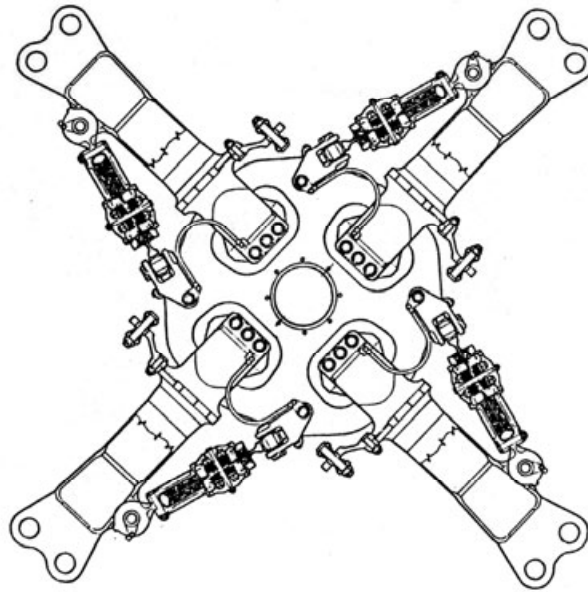


FIG.: 11 SPHERIFLEX ROTOR HEAD OF AEROSPATIALE AS 332

Fig. D-6. Eurocopter AS-332 (Schindler/Pfisterer AGARD paper).

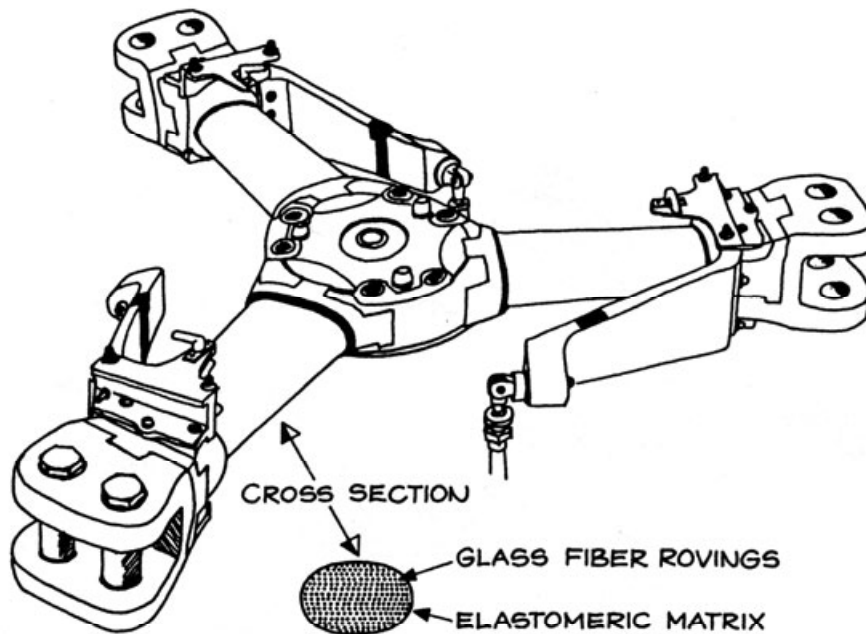


FIG.: 16 TRIFLEX ROTOR HEAD OF AEROSPATIALE

Fig. D-7. Aerospatiale Triflex (Schindler/Pfisterer AGARD paper).

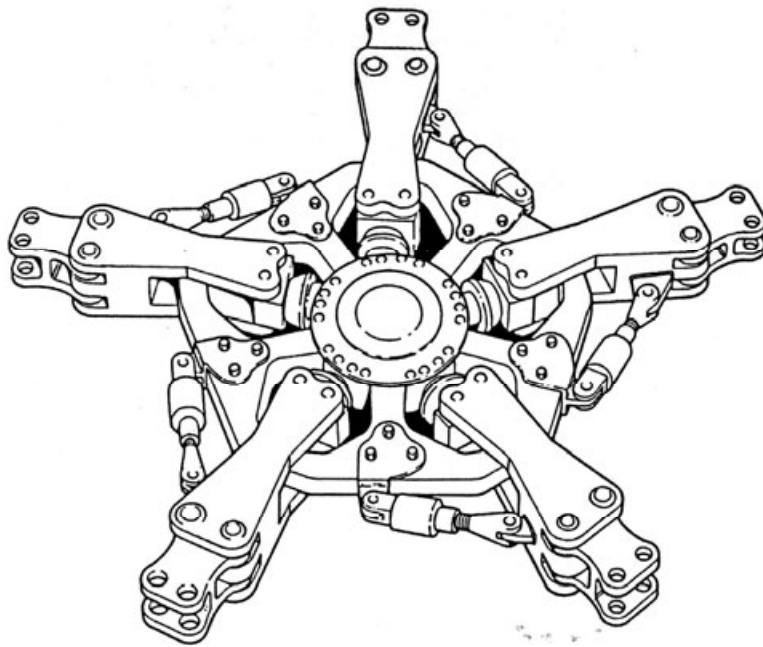


FIG. 12 ROTOR HEAD OF AGUSTA AND WESTLAND EH-101

Fig. D-8. Agusta/Westland EH-101 (Schindler/Pfisterer AGARD paper).

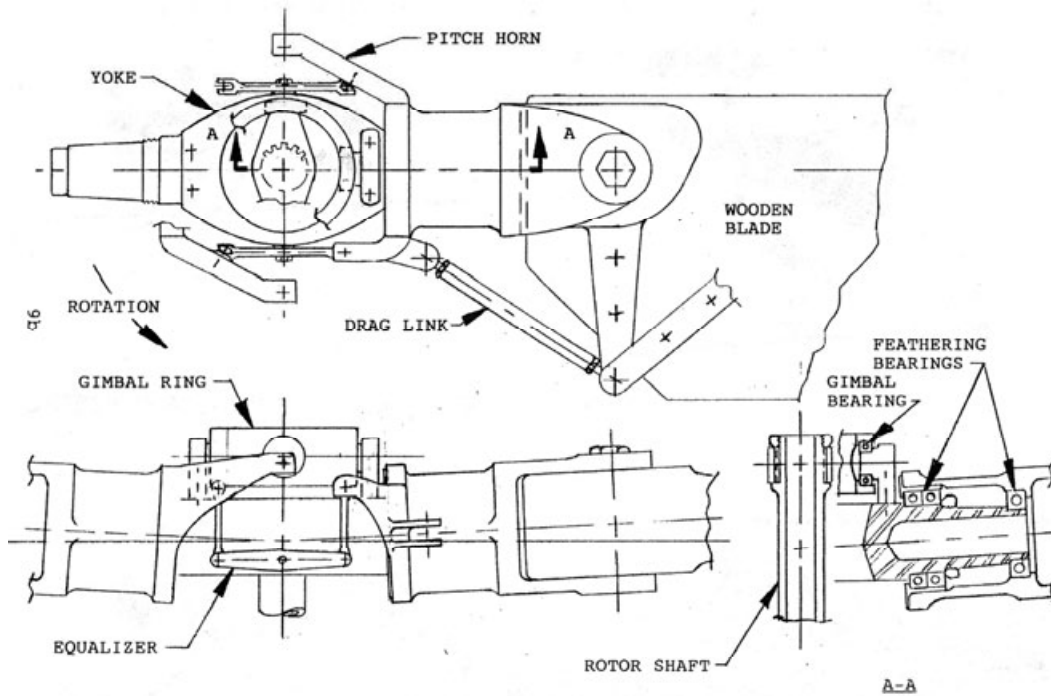


FIG. # I-12 BELL Model 47

Fig. D-9. Bell Model 47 (courtesy of Tom Hanson).

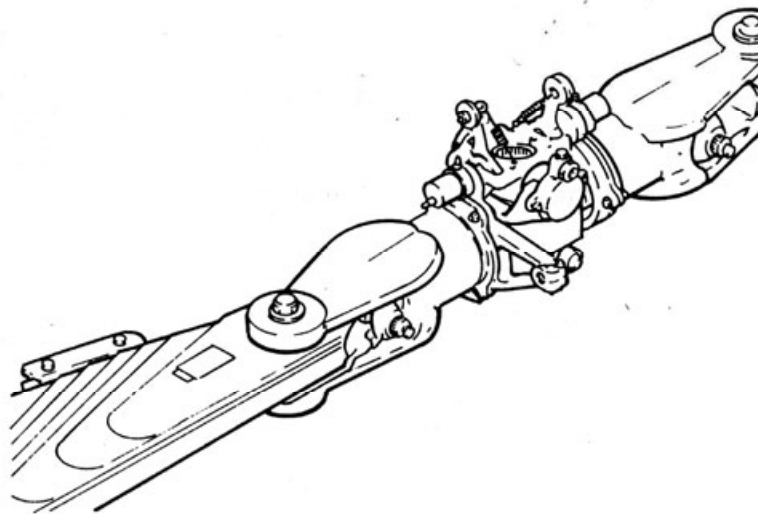


FIG.: 3 ROTOR HEAD OF BELL 206

Fig. D-10. Bell Model 206 (Schindler/Pfisterer AGARD paper).

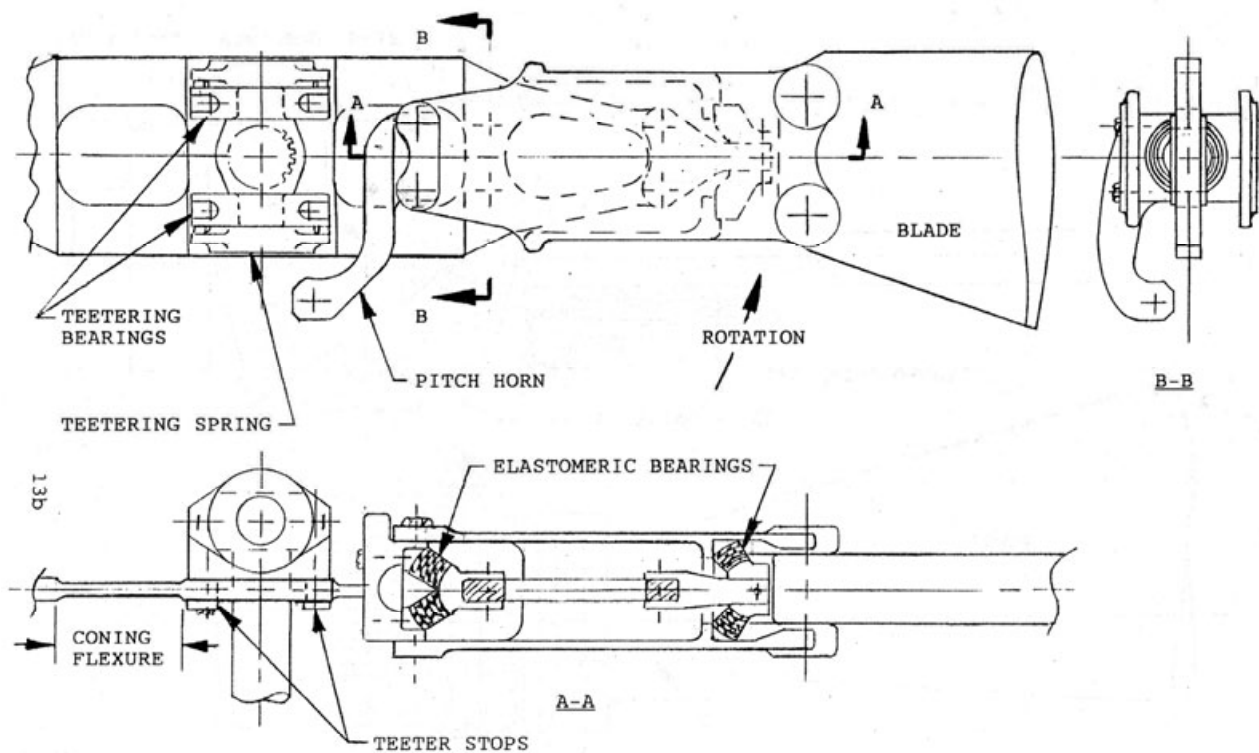
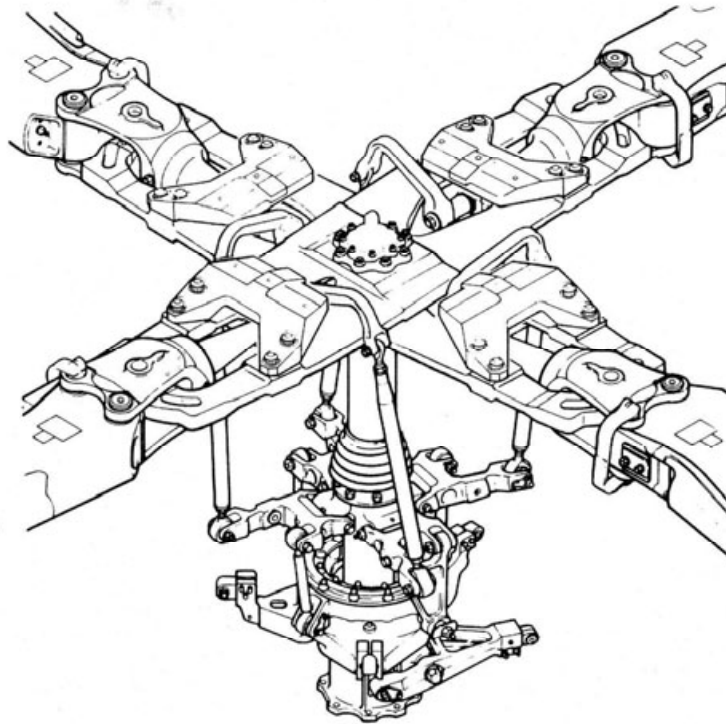


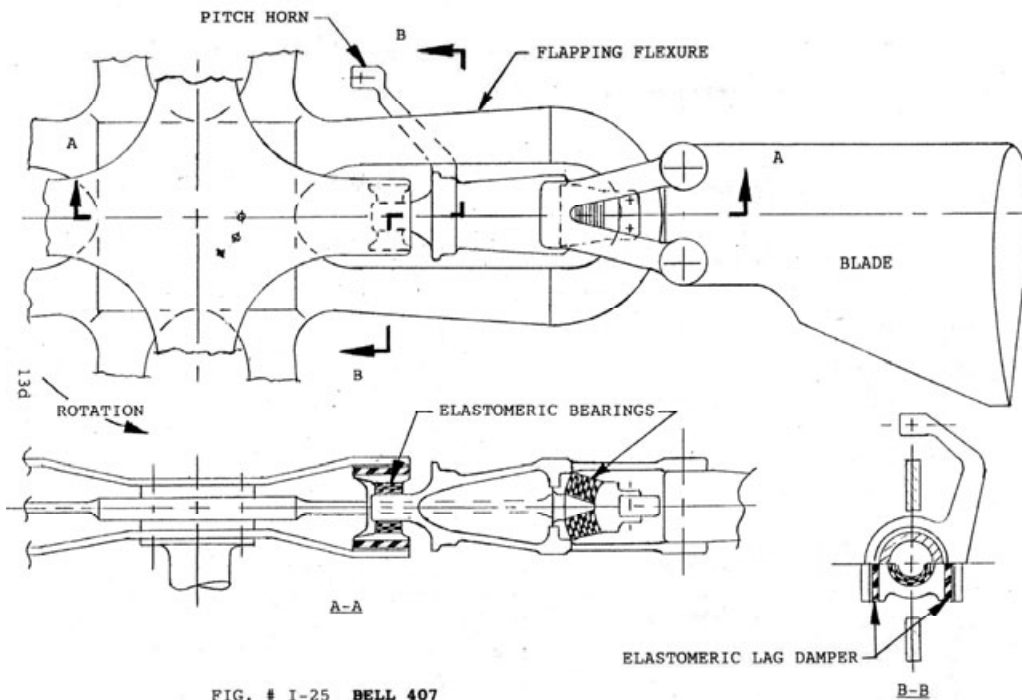
FIG. # I-23 BELL 222

Fig. D-11. Bell Model 222 (courtesy of Tom Hanson).

**BELL MODEL 412  
FIRST FLIGHT — AUGUST 1979**



**Fig. D-12. Bell Model 412 (courtesy of Bill Bousman).**



**Fig. D-13. Bell Model 407/OH-58D (courtesy of Tom Hanson).**

**BELL AHIP  
FIRST FLIGHT—SEPTEMBER 1983**

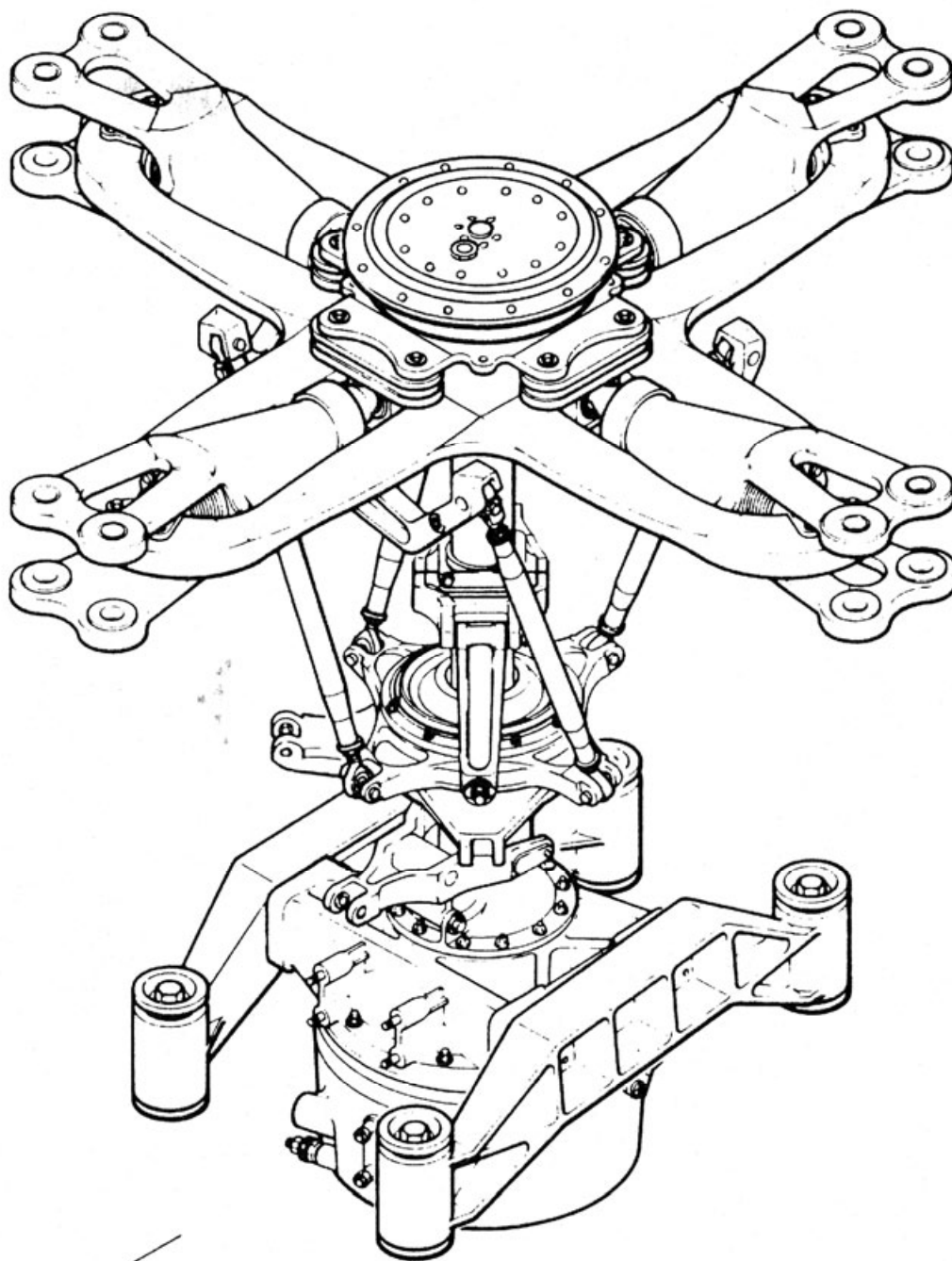


**Fig. D-14. Bell OH-58D (courtesy of Bill Bousman).**

**BELL MODEL 680  
FIRST FLIGHT — MAY 1982**

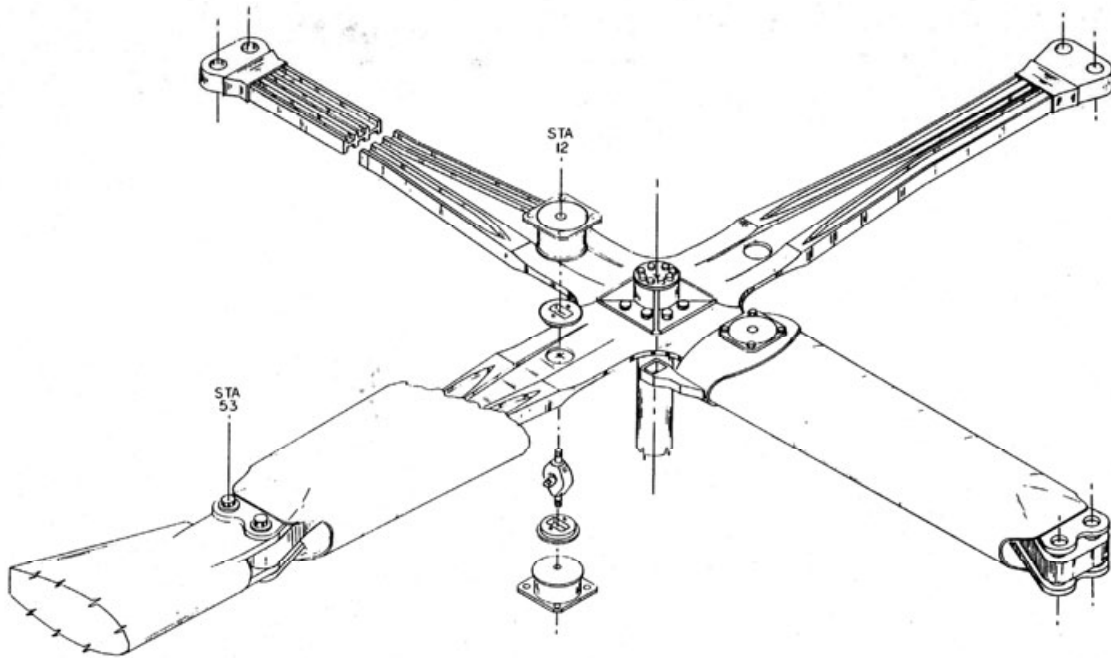


**Fig. D-15. Bell Model 680 (courtesy of Bill Bousman).**

**BOEING VERTOL BEARINGLESS MAIN ROTOR (BMR)  
FIRST FLIGHT — OCTOBER 1978**

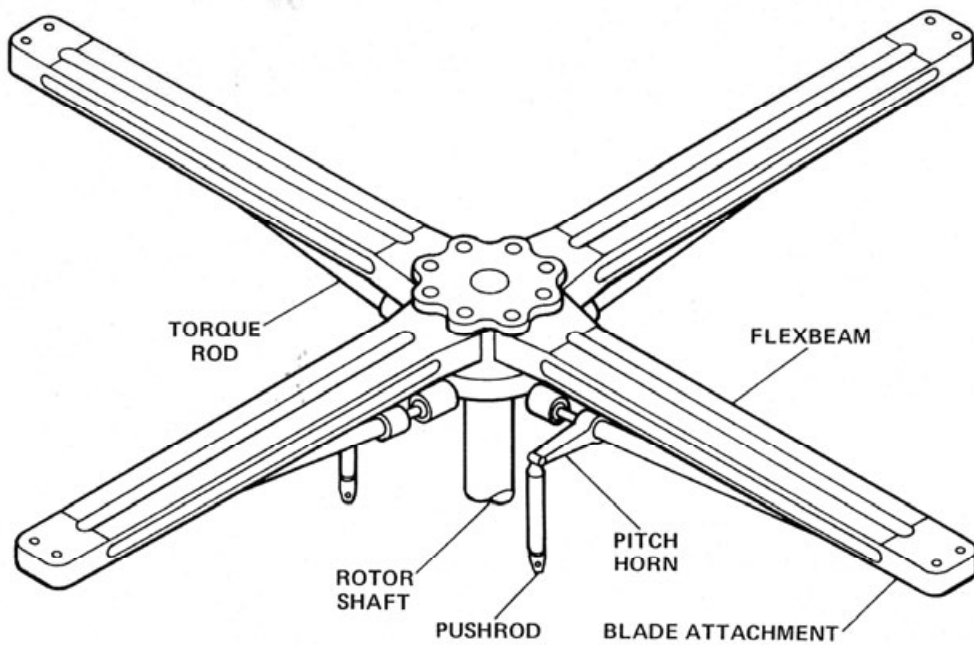


**Fig. D-16. Boeing Vertol BMR (courtesy of Bill Bousman).**

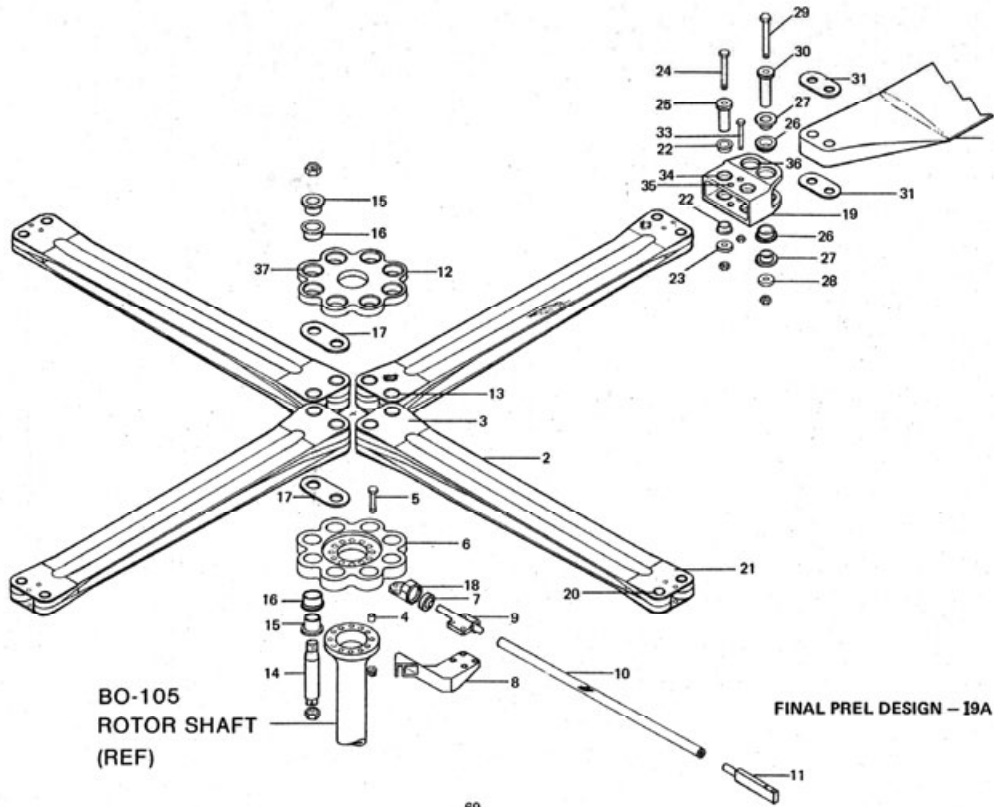
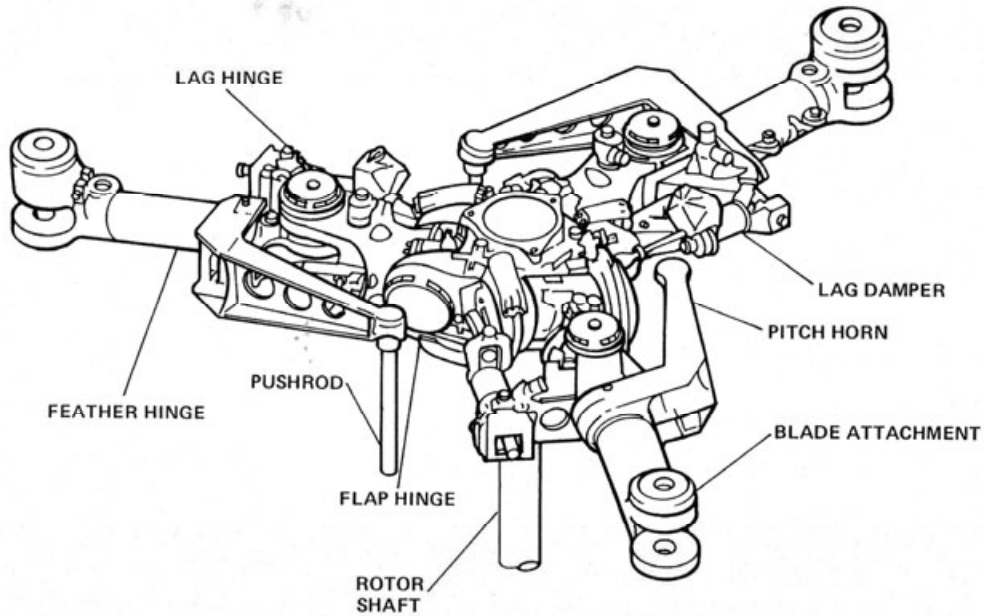


Fig. D-17. Boeing Vertol BMR (author's collection).

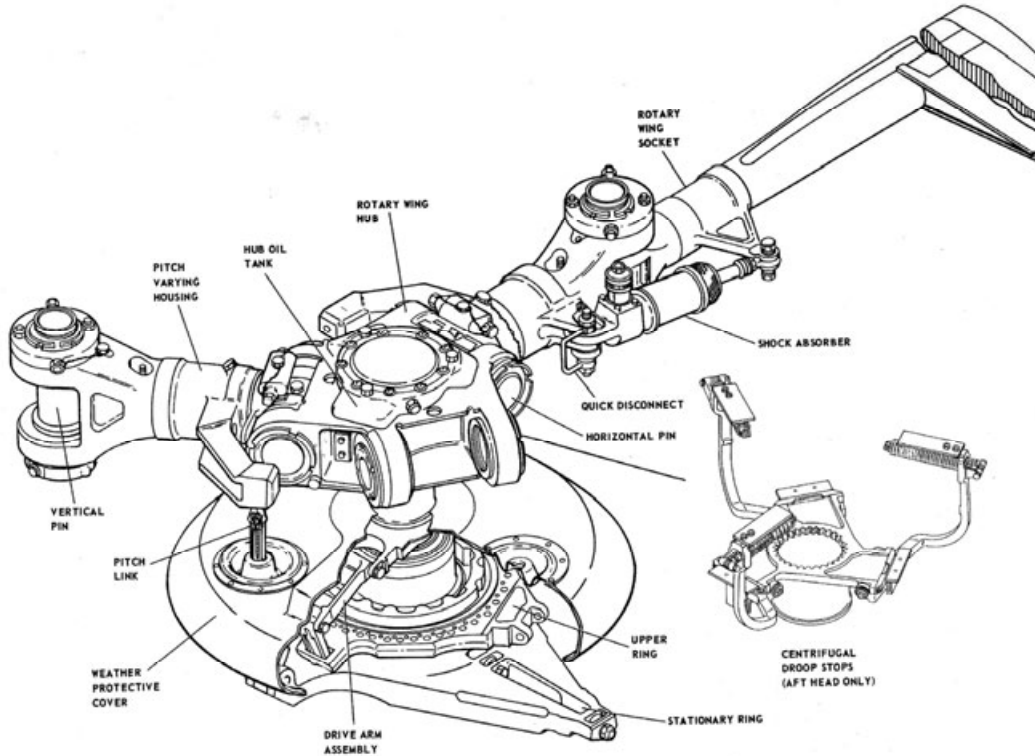
QTY. REQ.	PART NUMBER	DESCRIPTION	MATERIAL	WEIGHT EACH IN POUNDS
	-1	HUB/BLADE INSTL		
4	-2	C-BEAM ASSY	1002-SFI LAYUP	14.77
8	-3	PLATE, SHEAR TIE	1002-SFI LAYUP	.25
12	-4	BUSHING, SHEAR	STL	.04
12	-5	BOLT, INTERFACE	STL (STANDARD)	.22
1	-6	HUB PLATE, LOWER	STL	20.03
4	-7	SPHERICAL BEARING	LEAR SIEGLER	.75
4	-8	PITCH ARM	AL	1.38
4	-9	TORQUE TUBE FITTING, INBD	STL	1.07
4	-10	TORQUE TUBE	HMS GRAPHITE	2.06
4	-11	TORQUE TUBE FITTING, OUTBD	STL	2.35
1	-12	HUB PLATE, UPPER	STL	14.35
8	-13	BUSHING, C-BEAM	STL	.64
8	-14	PIN, HUB	STL	2.80
16	-15	BUSHING, PRECONE	STL	.58
16	-16	BUSHING, ECCENTRIC	STL	.46
8	-17	PLATE, PRECONE	STL	.88
4	-18	BRACKET, SPHERICAL	AL	.31
4	-19	HUB/BLADE CLEVIS	AL	3.74
8	-20	BUSHING, C-BEAM	STL	.22
8	-21	PLATE, SHEAR TIE	1002-SFI LAYUP	.24
16	-22	BUSHING, ECCENTRIC	STL	.10
8	-23	WASHER	STL	.07
8	-24	BOLT	STL (STANDARD)	.27
8	-25	PIN, C-BEAM	STL	.69
16	-26	BUSHING, BLADE SWEEP	STL	.19
16	-27	BUSHING, BLADE PRECONE	STL	.28
8	-28	WASHER	STL	.11
8	-29	BOLT	STL (STANDARD)	1.16
8	-30	PIN, BLADE	STL	1.15
8	-31	PLATE, BLADE PRECONE	STL	.77
4	-32	BLADE		51.20
8	-33	BOLT	STL (STANDARD)	.15
16	-34	BUSHING, CLEVIS	STL	.04
16	-35	BUSHING, CLEVIS	STL	.01
16	-36	BUSHING, CLEVIS	STL	.06
8	-37	BUSHING, HUB PLATE	STL	.09
274 NON STANDARD PARTS				
+36 STANDARD PARTS				
310 TOTAL PARTS				
			TOTAL SYSTEM	451.44

Fig. D-18. Boeing Vertol BMR (author's collection).

**BOEING VERTOL CH-46  
FIRST FLIGHT — APRIL 1958  
(BLADE FOLD HARDWARE REMOVED)**



**Fig. D-19. Boeing Vertol CH-46. Hinge sequence flap-lag-pitch (courtesy of Bill Bousman).**



**Fig. D-20. Boeing Vertol CH-47. Hinge sequence flap-pitch-lag (author's collection).**

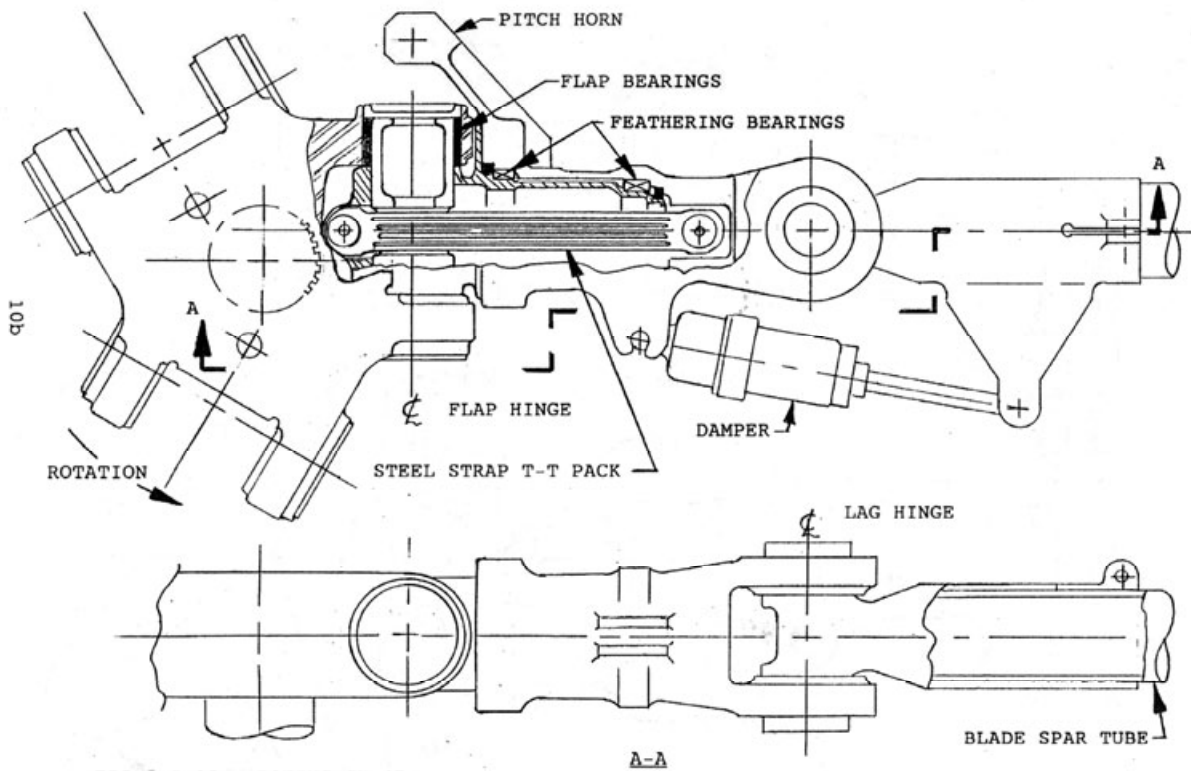


FIG.# I-15 BOEING CH-47

Fig. D-21. Boeing Vertol CH-47 (courtesy of Tom Hanson).

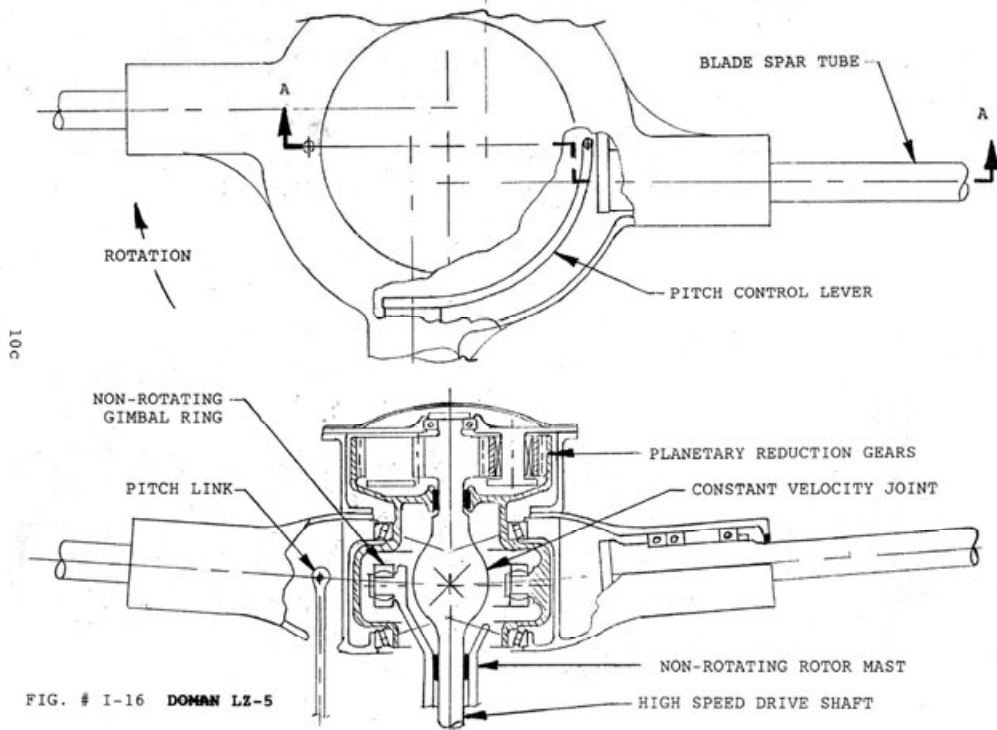
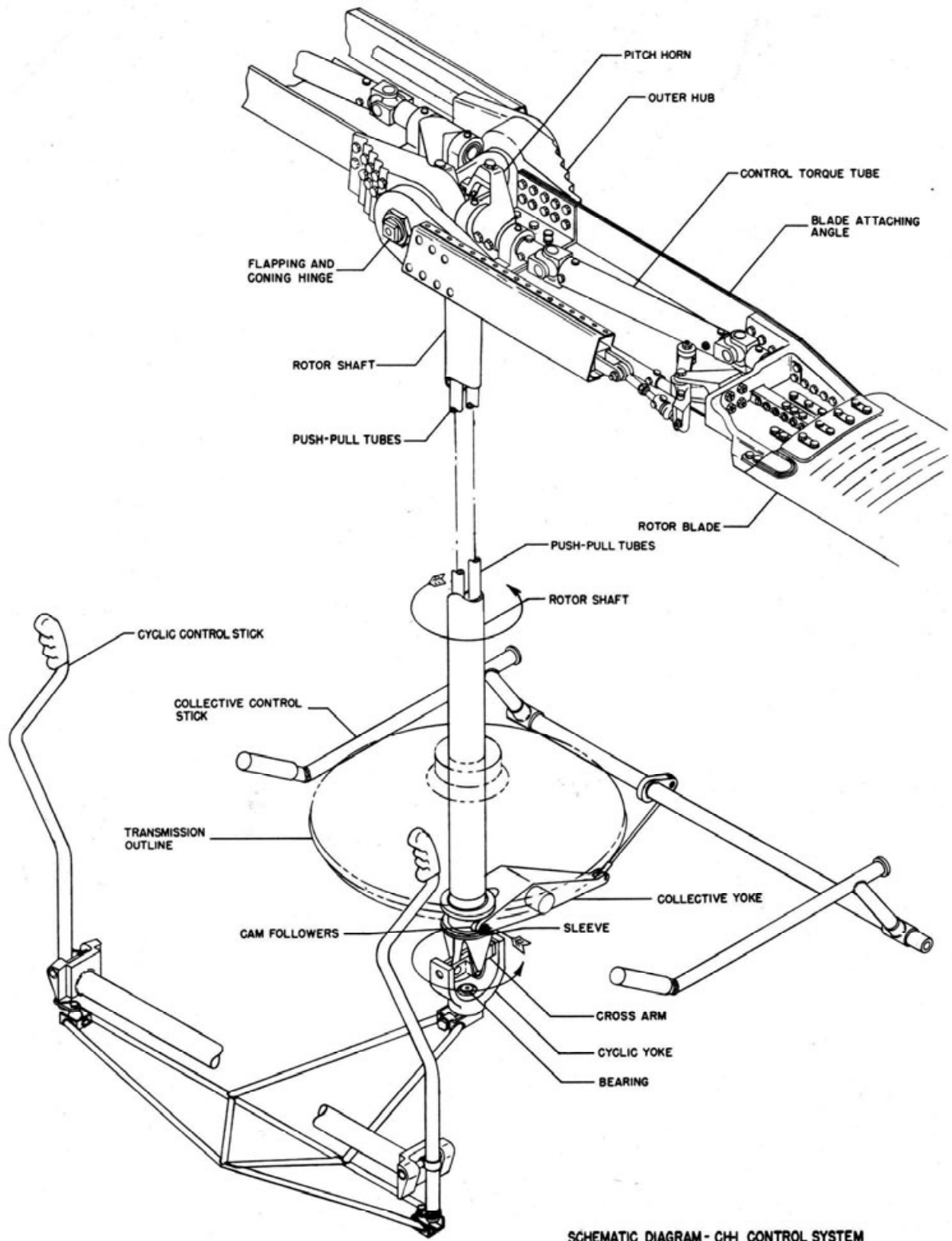


FIG. # I-16 DOMAN LZ-5

Fig. D-22. Doman LZ-5 (courtesy of Tom Hanson).



SCHEMATIC DIAGRAM - CH-1 CONTROL SYSTEM

Fig. D-23. Cessna CH-1 (author's collection).

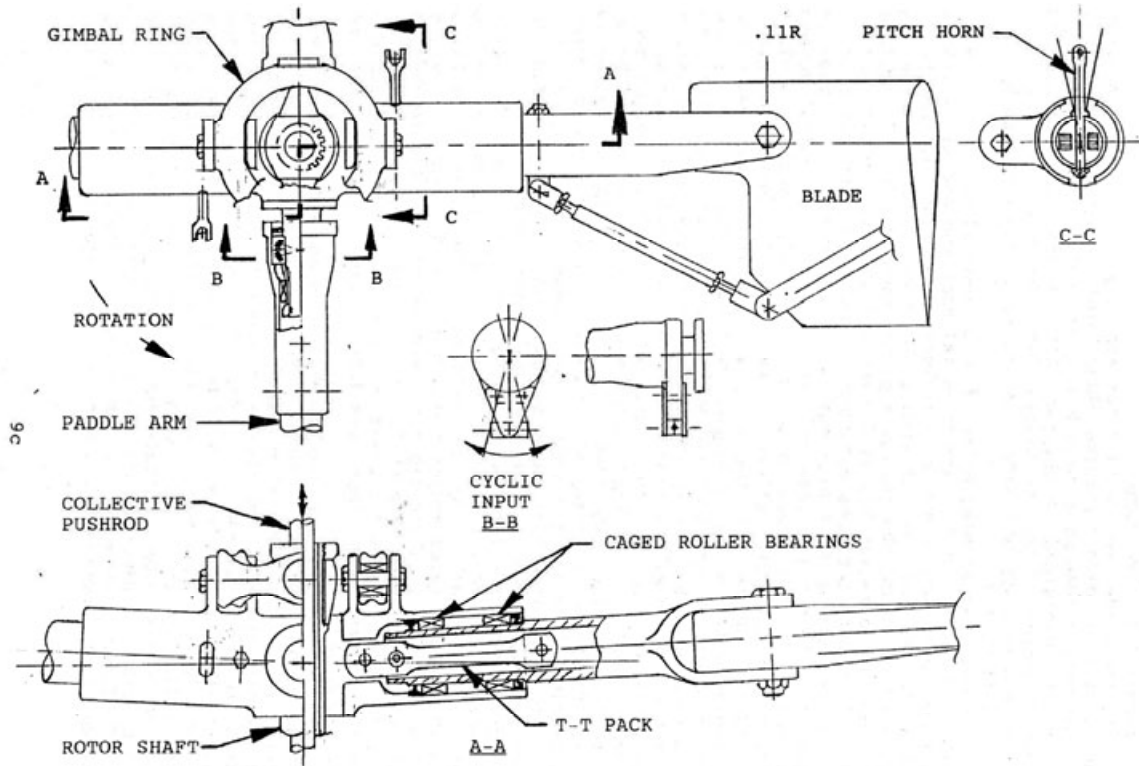


Fig. D-24. Hiller Model 360 (courtesy of Tom Hanson).

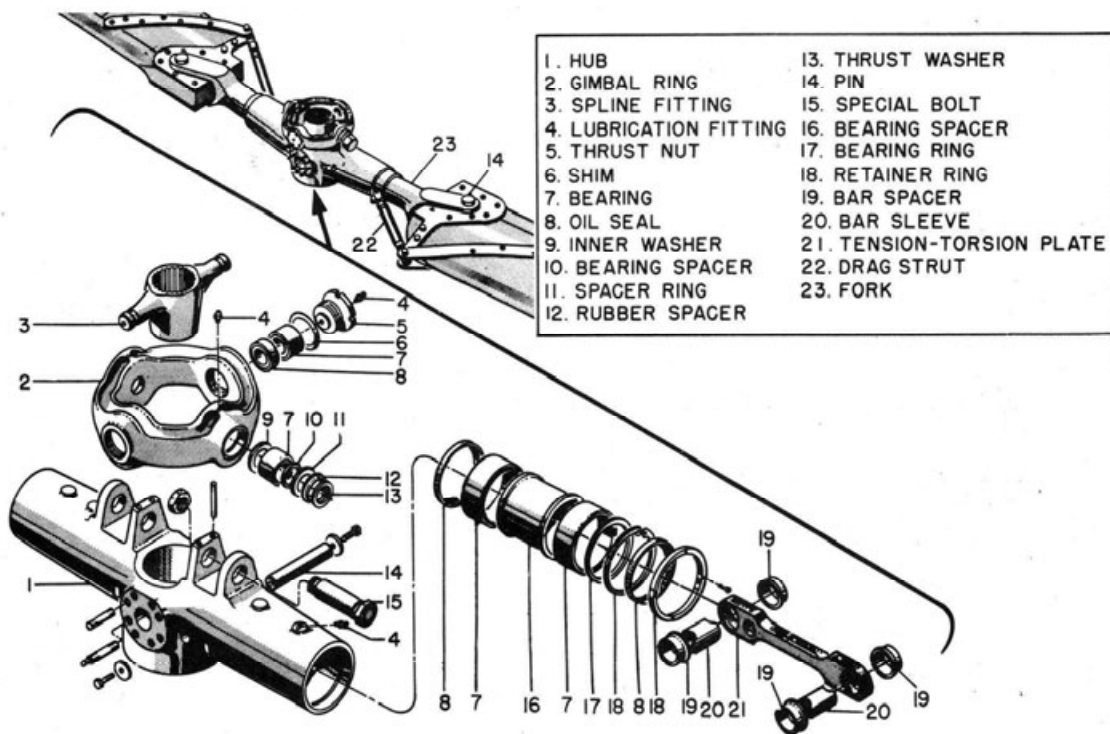


Fig. D-25. Hiller Model 360 (author's collection).

HUGHES AH-64A  
FIRST FLIGHT—SEPTEMBER 1975

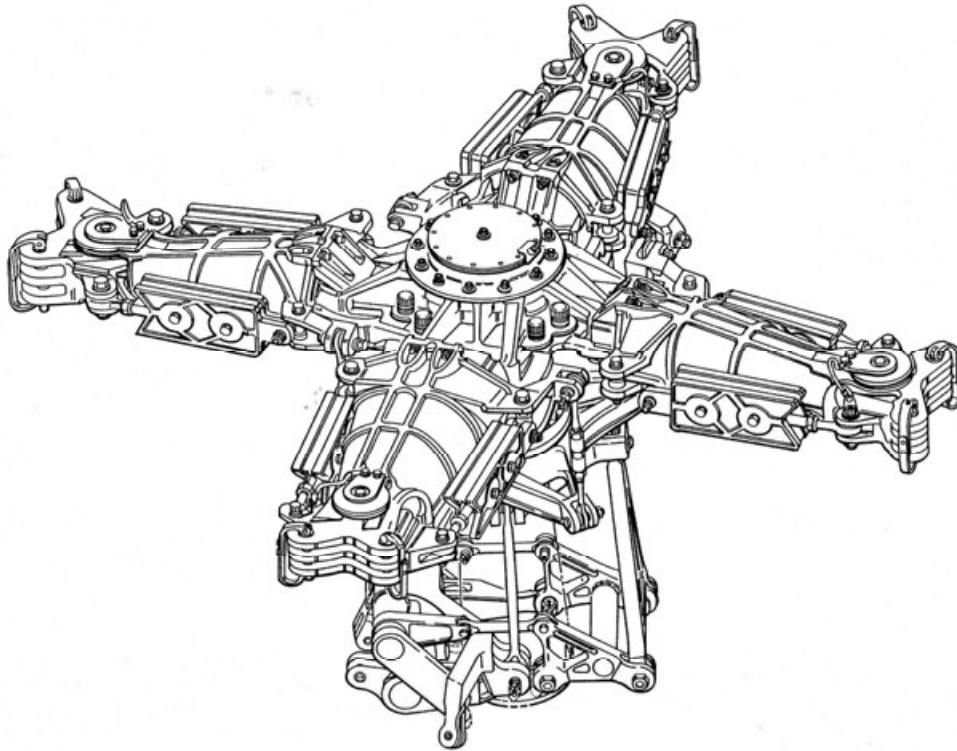


Fig. D-26. Hughes AH-64 (courtesy of Bill Bousman).

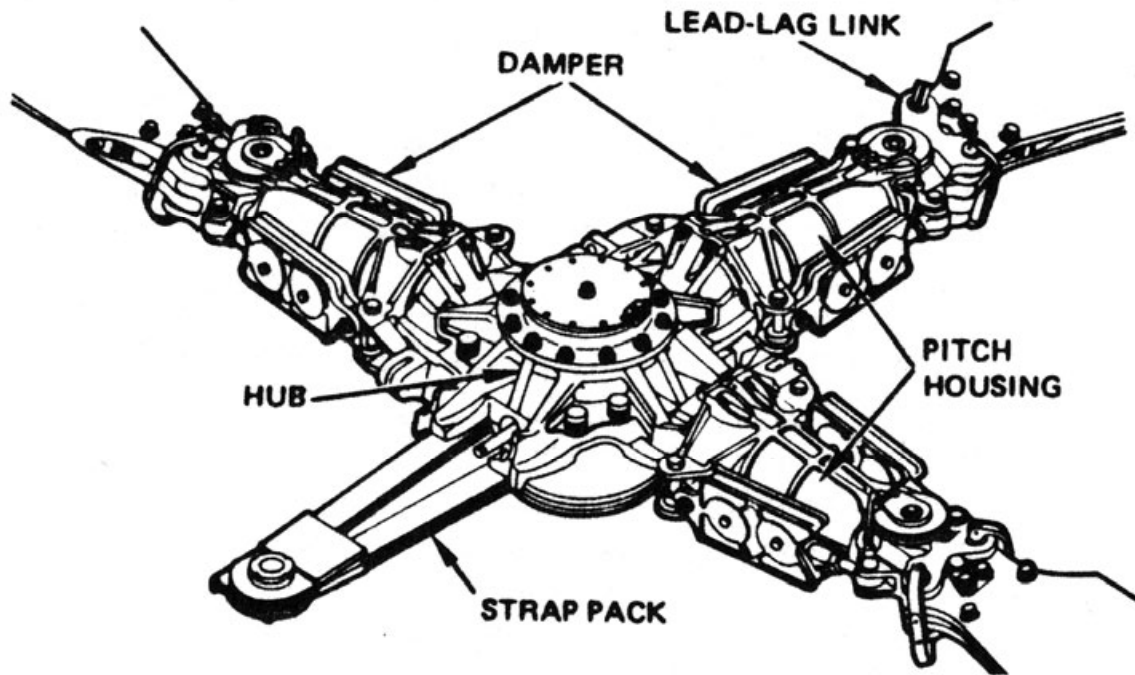


Fig. D-27. Hughes AH-64 (courtesy of Bill Bousman).

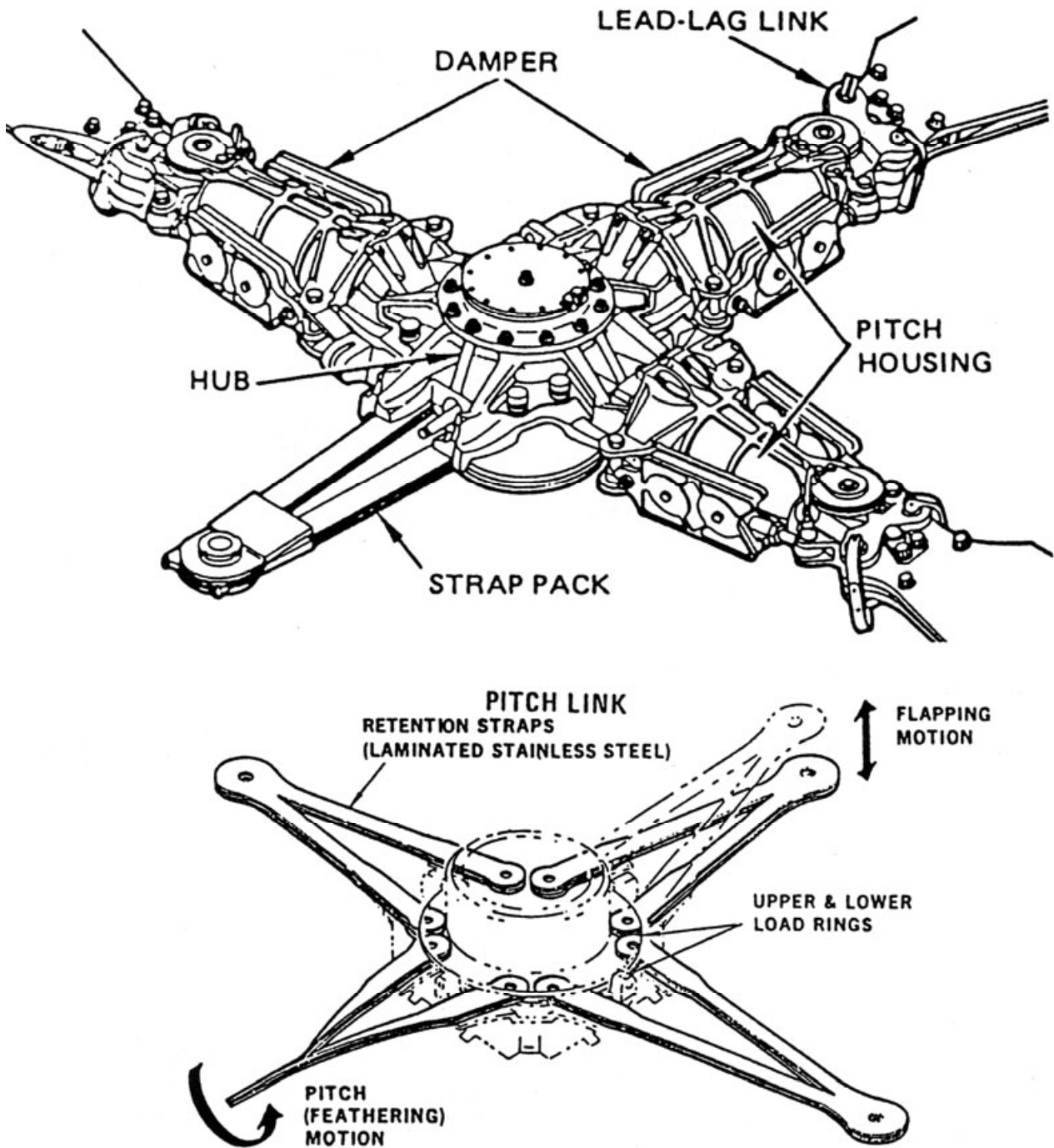


FIG.: 9 ROTOR HEAD OF HUGHES AH-64

Fig. D-28. Hughes AH-64 (Schindler/Pfisterer AGARD paper).

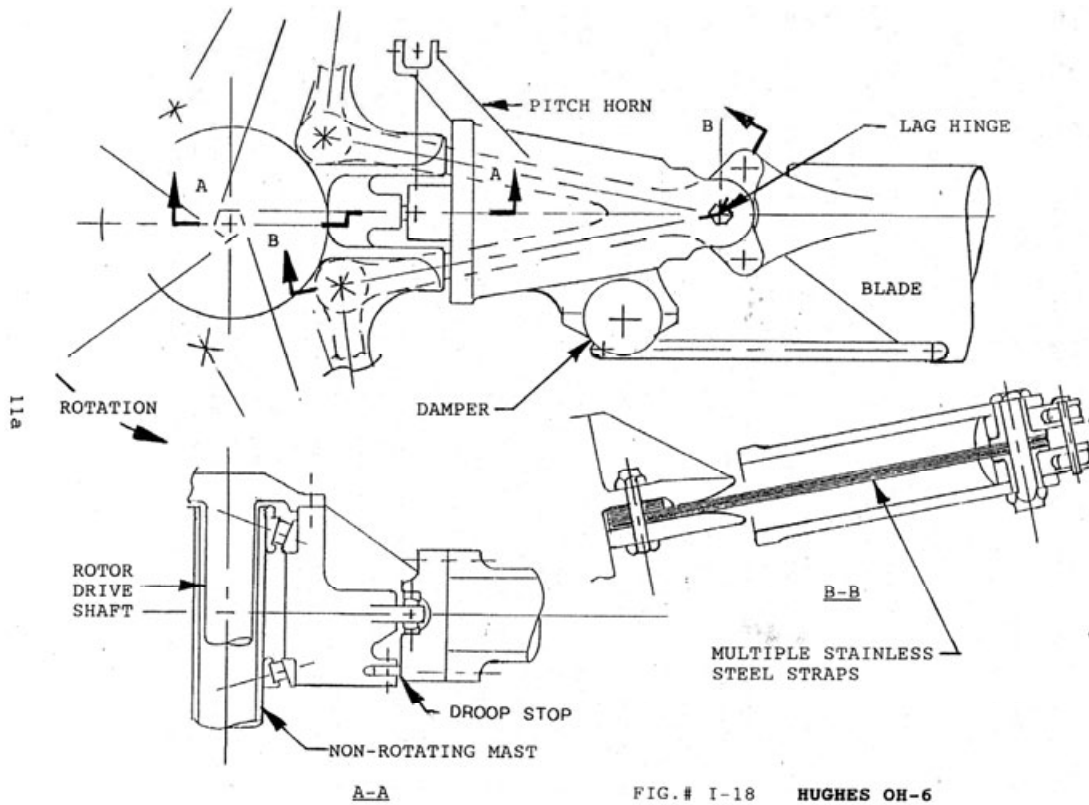


Fig. D-29. Hughes OH-6 (courtesy of Tom Hanson).

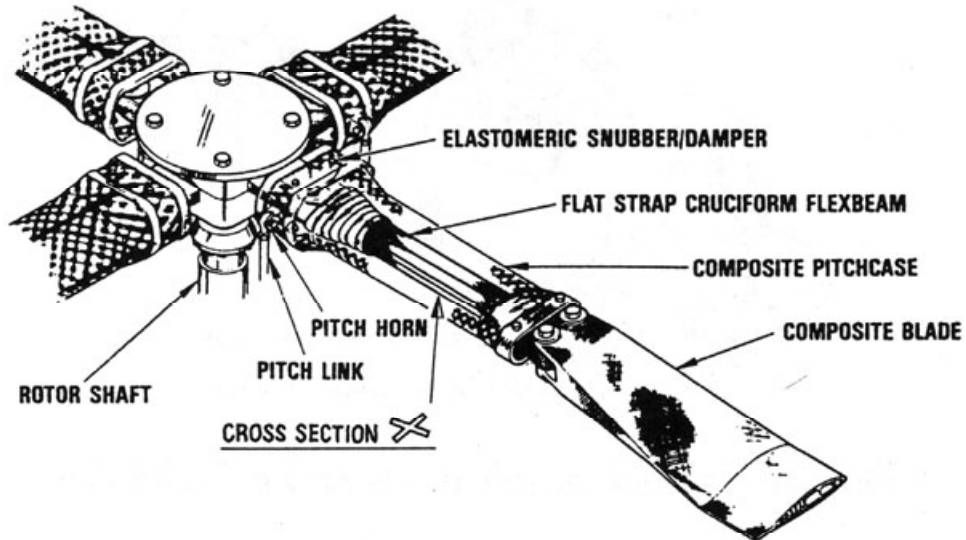


FIG.: 19 BEARINGLESS ROTOR HEAD OF HUGHES HARP

Fig. D-30. Hughes HARP (Schindler/Pfisterer AGARD paper).

LOCKHEED AH-56A  
FIRST FLIGHT—SEPTEMBER 1967

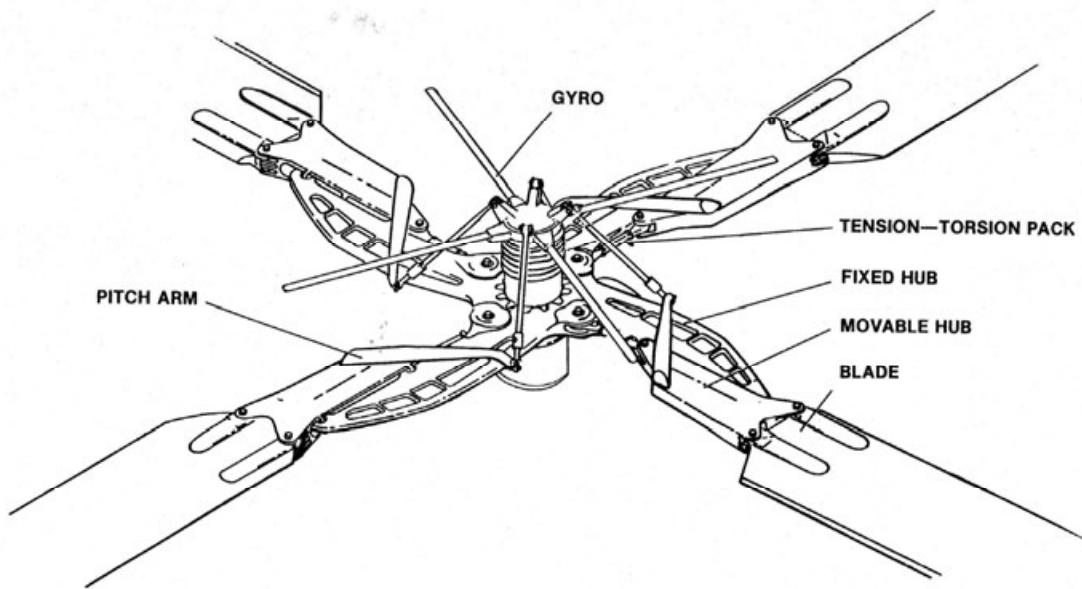


Fig. D-31. Lockheed AH-56 (courtesy of Bill Bousman).

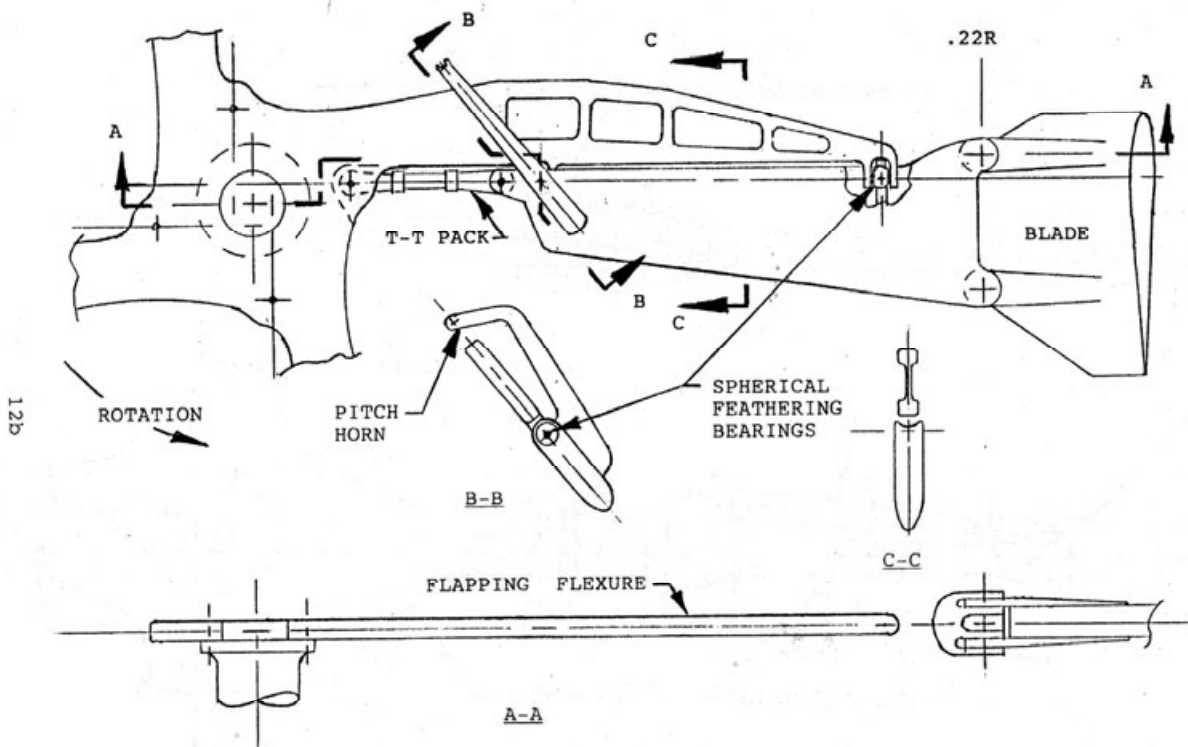


FIG. # I-20 LOCKHEED AH-56

Fig. D-32. Lockheed AH-56 (courtesy of Tom Hanson).

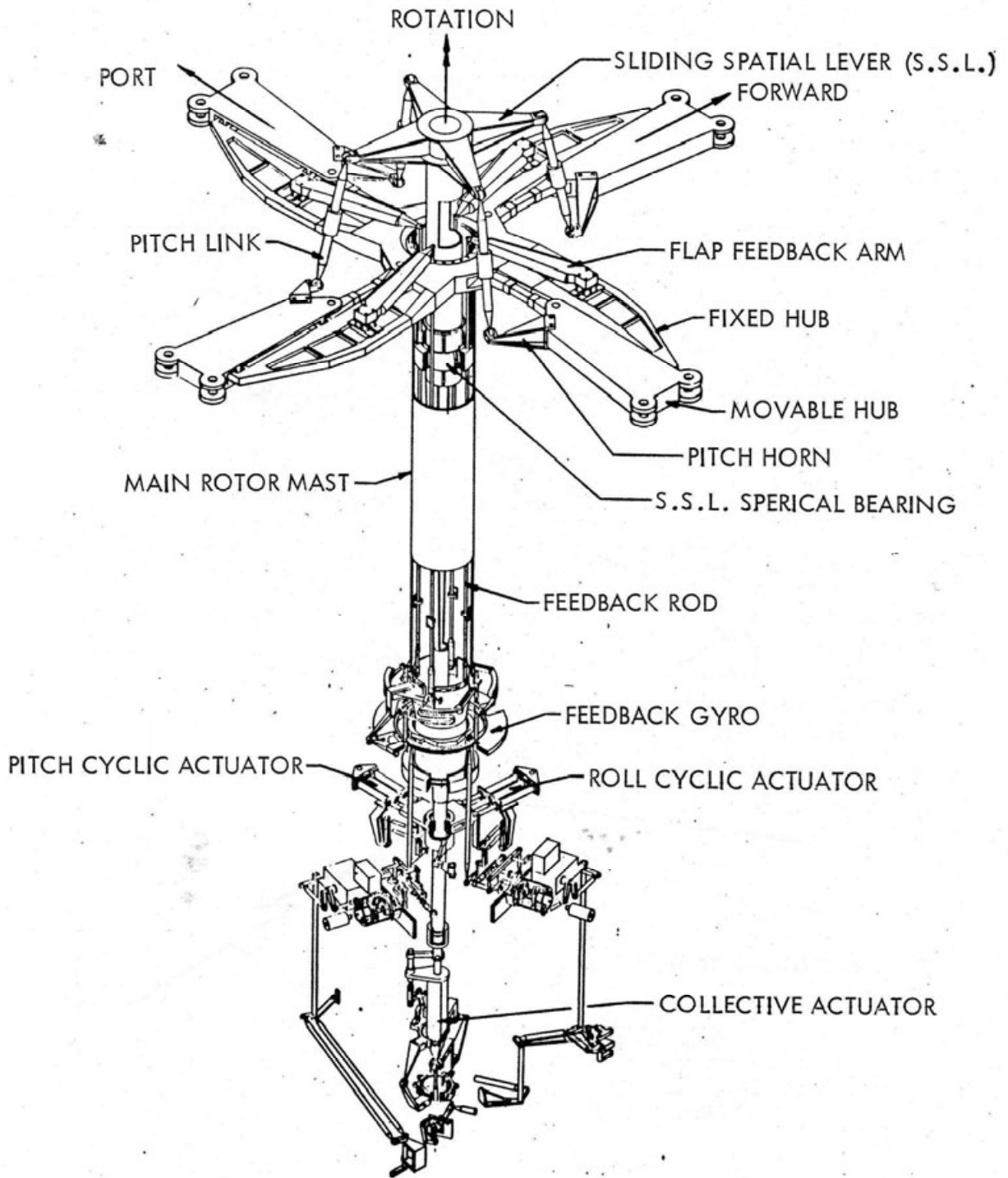


Fig. D-33. Lockheed AH-56 (author's collection).

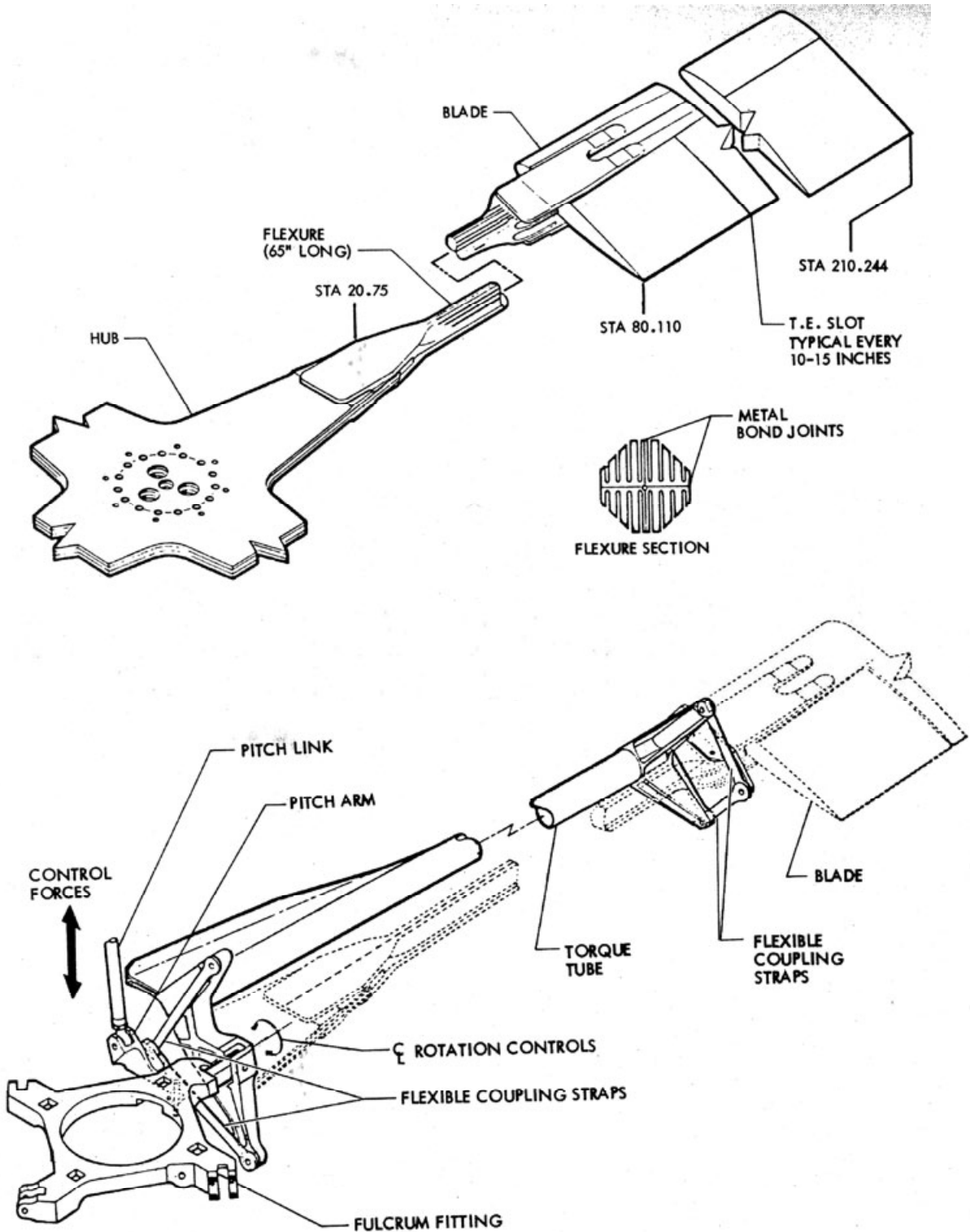


Fig. D-34. Lockheed CL-475 (author's collection).

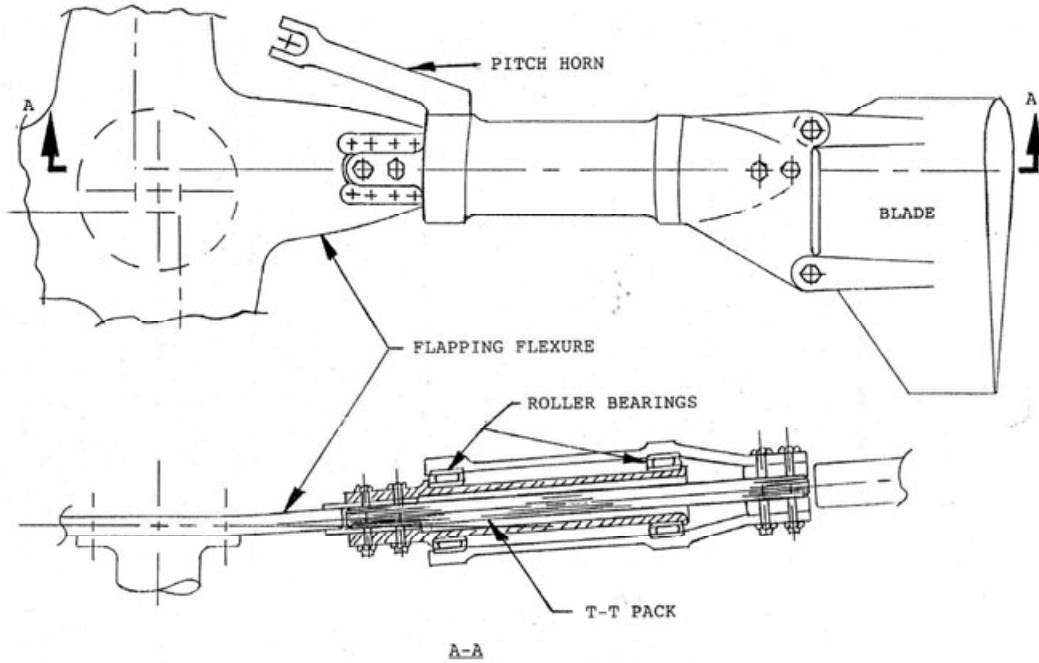


FIG. # I-19 LOCKHEED XH-51A

Fig. D-35. Lockheed XH-51 (courtesy of Tom Hanson).

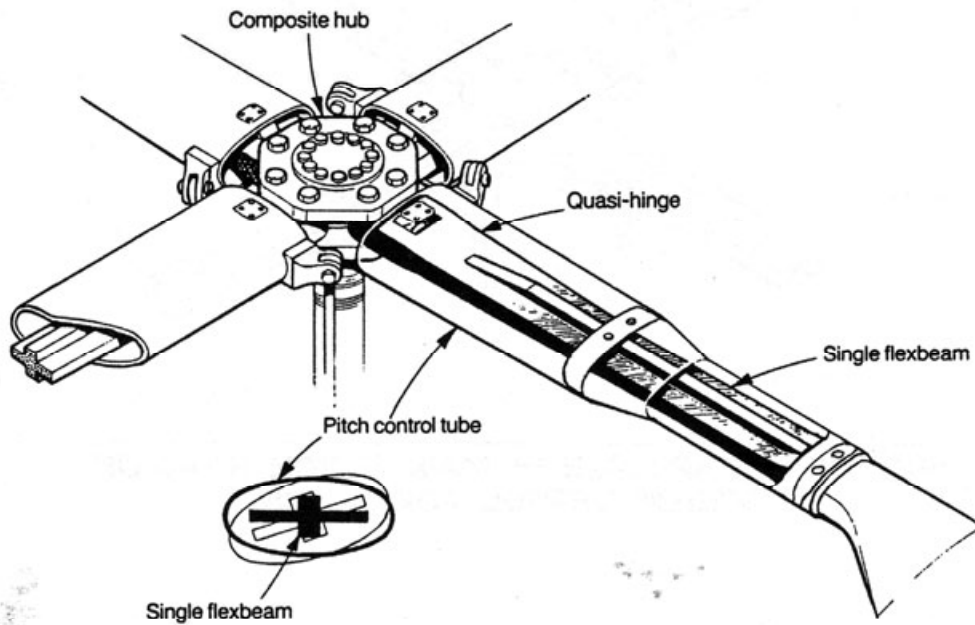


FIG.: 18 BEARINGLESS ROTOR HEAD OF MBB

Fig. D-36. MBB Bearingless Main Rotor (Schindler/Pfisterer AGARD paper).

MBB BO 105  
FIRST FLIGHT—FEBRUARY 1967

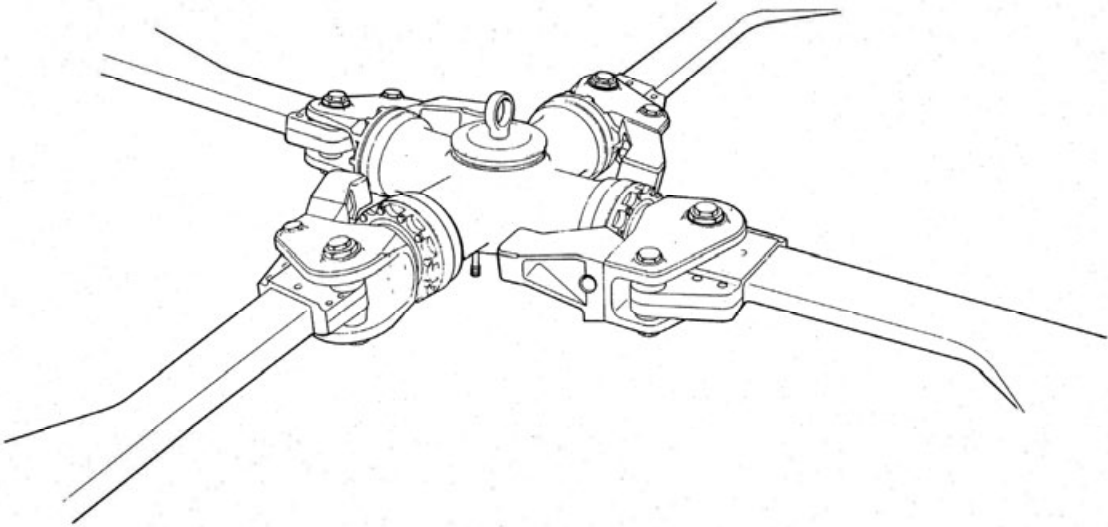


Fig. D-37. MBB BO-105 (courtesy of Bill Bousman).

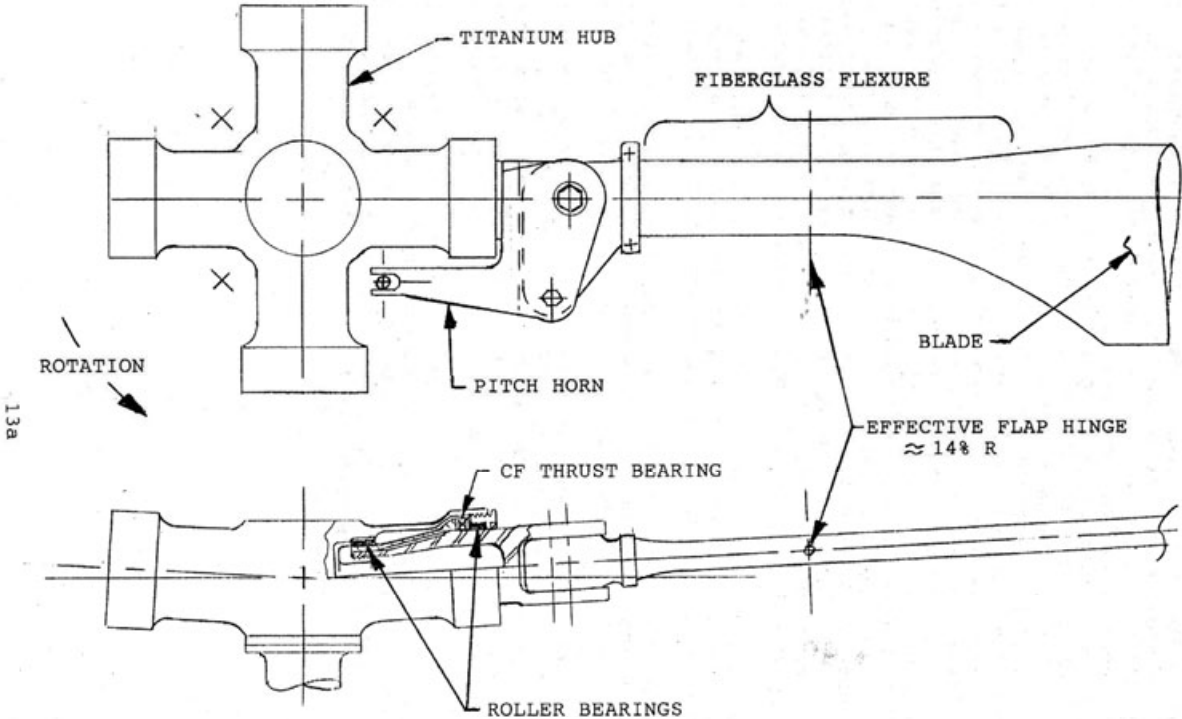


FIG. # I-22 MBB Bo-105

Fig. D-38. MBB BO-105 (courtesy of Tom Hanson).



FIG./ REF NO.	NOMENCLATURE	QTY PER UNIT
-1	ROTOR STAR . . . . .	1
-2	BOLT . . . . .	1
-6	WINDOW . . . . .	1
-8	COVER . . . . .	1
-9	LOCKING NUT (SPECIAL) . . . . .	1
-10	RING NUT (SPECIAL) . . . . .	1
-12	BLEED SCREW (SPECIAL) . . . . .	2
-15	SCALE . . . . .	4
-17	QUADRUPLE NUT, TOP . . . . .	1
-18	QUADRUPLE NUT, BOTTOM . . . . .	1
-19	BUSHING . . . . .	1
-20	WASHER (SPECIAL) . . . . .	2
-21	PIN . . . . .	4
-22	NUT (SPECIAL) . . . . .	1
-23	STUD . . . . .	12
-24	WASHER (SPECIAL) . . . . .	4
-25	SIMMER GASKET . . . . .	4
-26	NEEDLE BEARING - OUTER RING . . . . .	4
-27	SPACER-OUTER . . . . .	4
-28	NEEDLE BEARING OUTER RING . . . . .	4
-30	SPACER . . . . .	4
-31	SIMMER GASKET . . . . .	4
-32	SIMMER GASKET RETAINER . . . . .	4
-35	INNER SLEEVE . . . . .	4
-36	NEEDLE BEARING INNER-RING . . . . .	4
-38	SPACER-INNER . . . . .	4
-39	NEEDLE BEARING INNER-RING . . . . .	4
-41	RING . . . . .	4
-43	FLANGE BUSHING . . . . .	8
-44	FLANGE BUSHING . . . . .	8
-45	STRAP . . . . .	4
-46	FITTED SCREW . . . . .	8
-50	CONTROL LEVER . . . . .	4
-51	FLANGE BUSHING . . . . .	4
-52	HEX BOLT (SPECIAL) . . . . .	16
-54	POINTER . . . . .	4
-62	SECONDARY BOLT (SPECIAL) . . . . .	4
-66	TORSION FLEXIBLE TENSION ELEMENT . . . . .	4
-67	NUT (SPECIAL) . . . . .	4
-68	LOCKPLATE . . . . .	4
-70	PIN . . . . .	4
	<b>TOTAL</b>	<b>162</b>
<b>BO-105 BLADE ATTACHMENT FITTING</b>		
-14	BLADE FITTING, UPPER . . . . .	4
-15	BLADE FITTING, LOWER . . . . .	4
-16	ELASTIC BUSHING (SECONDARY BOLT) . . . . .	4
-17	BUSHING (SECONDARY BOLT) . . . . .	4
	<b>TOTAL</b>	<b>16</b>
<b>TOTAL NUMBER OF PARTS IN HUB AND BLADE ATTACHMENT FITTING (OTHER THAN MAIN BOLT AND STD HARDWARE):</b>		<b>178</b>

Fig. D-40. MBB BO-105 (author's collection).

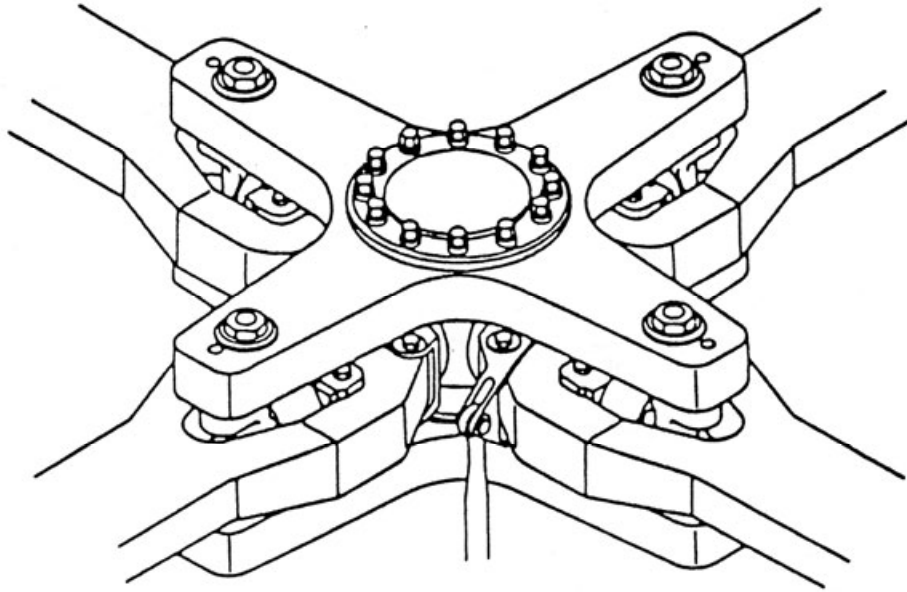


FIG. : 14 FEL ROTOR HEAD OF MBB PAH-2/HAP/HAC

Fig. D-41. MBB PAH-2 (Schindler/Pfisterer AGARD paper).



Fig. D-42. McDonnell XV-1 (author's collection).

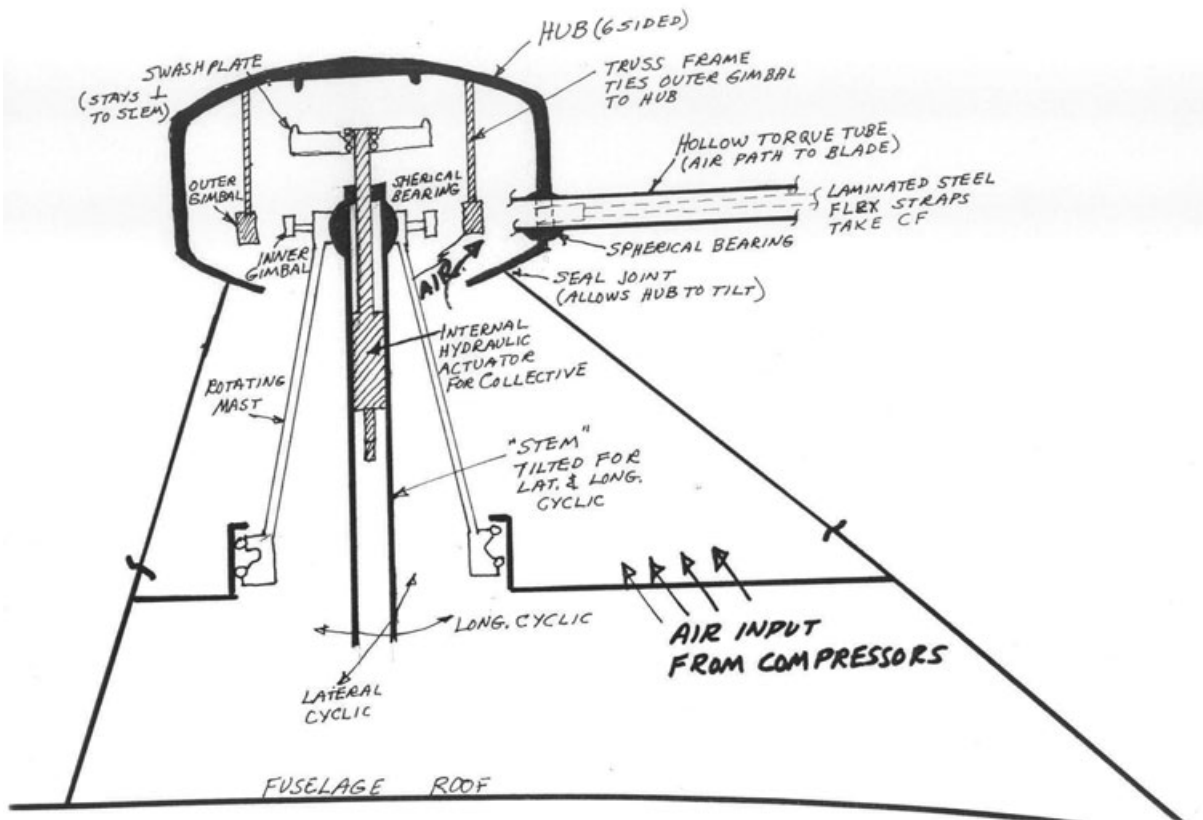


Fig. D-43. McDonnell XV-1 (author's collection).

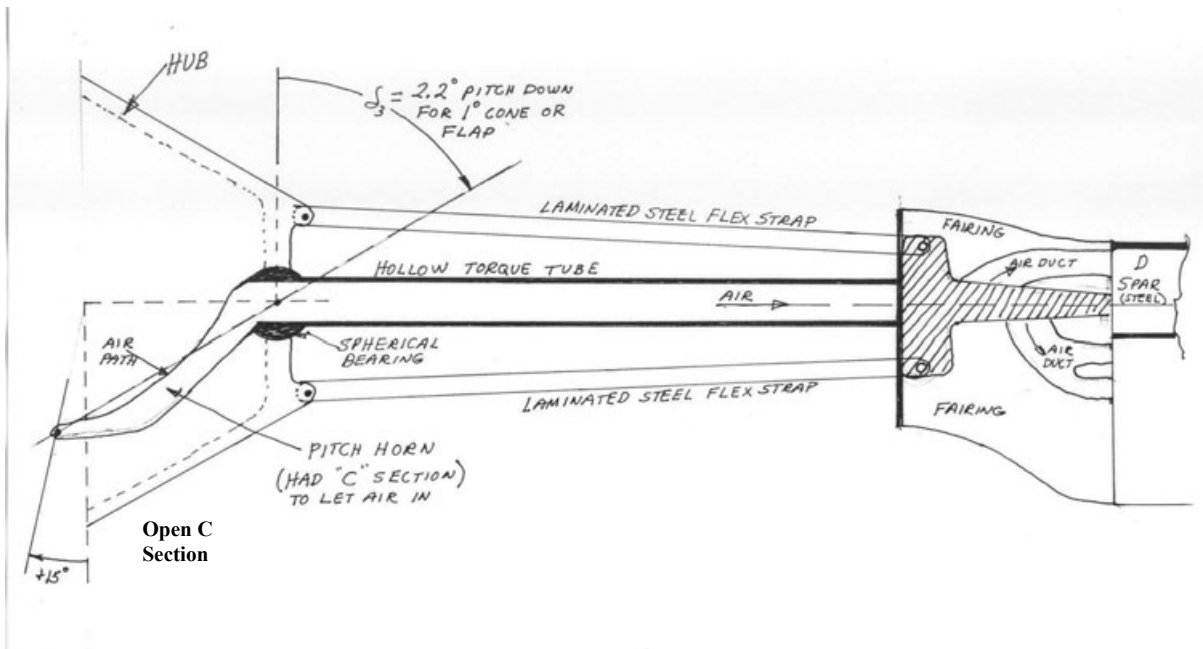


Fig. D-44. McDonnell XV-1 (author's collection).

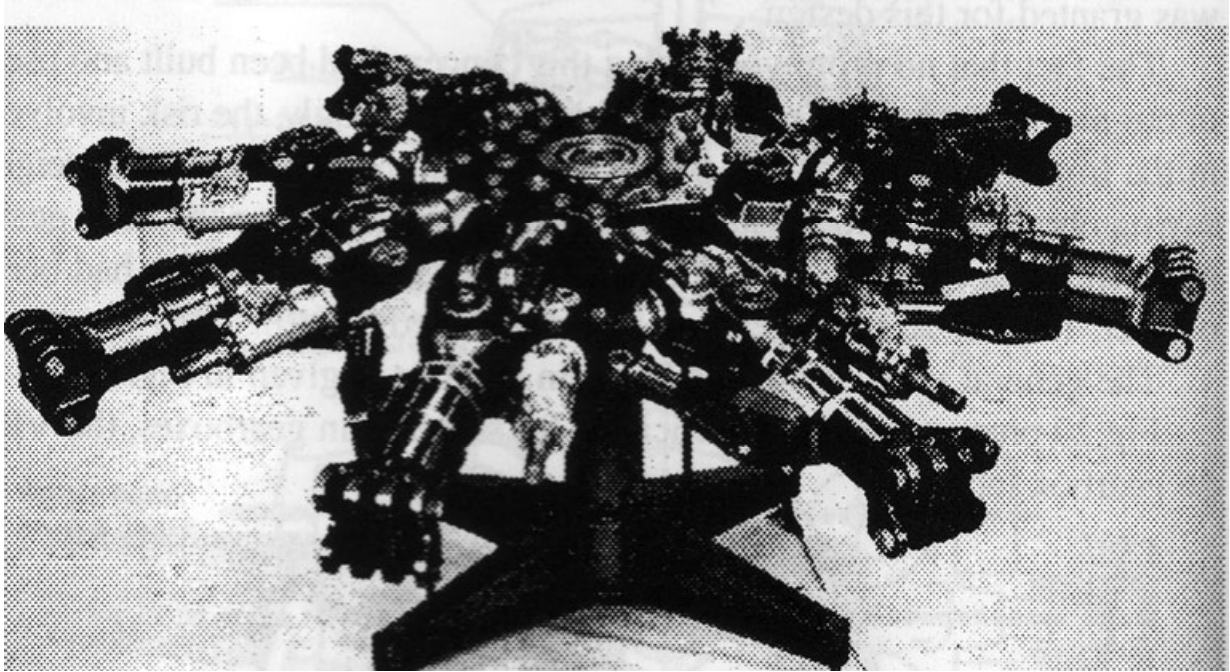


Fig. D-45. Mil Mi-26 (author's collection).

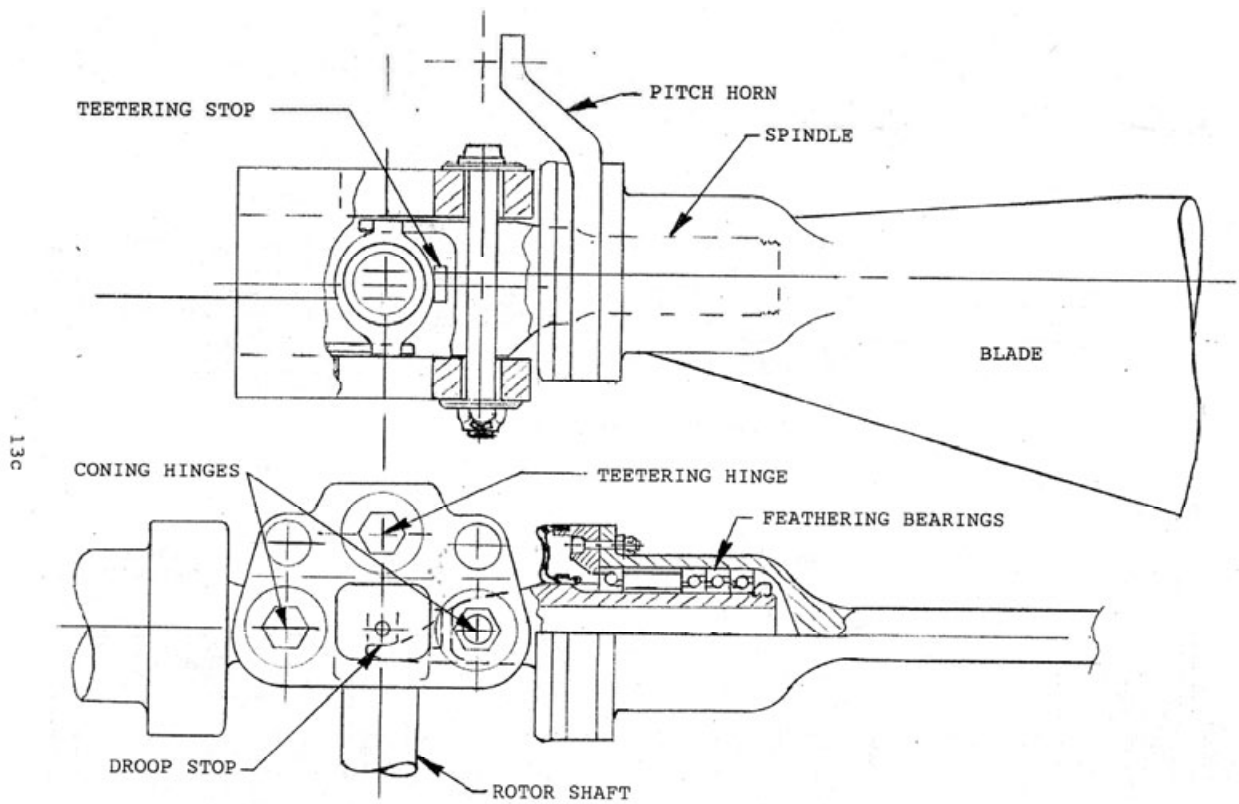
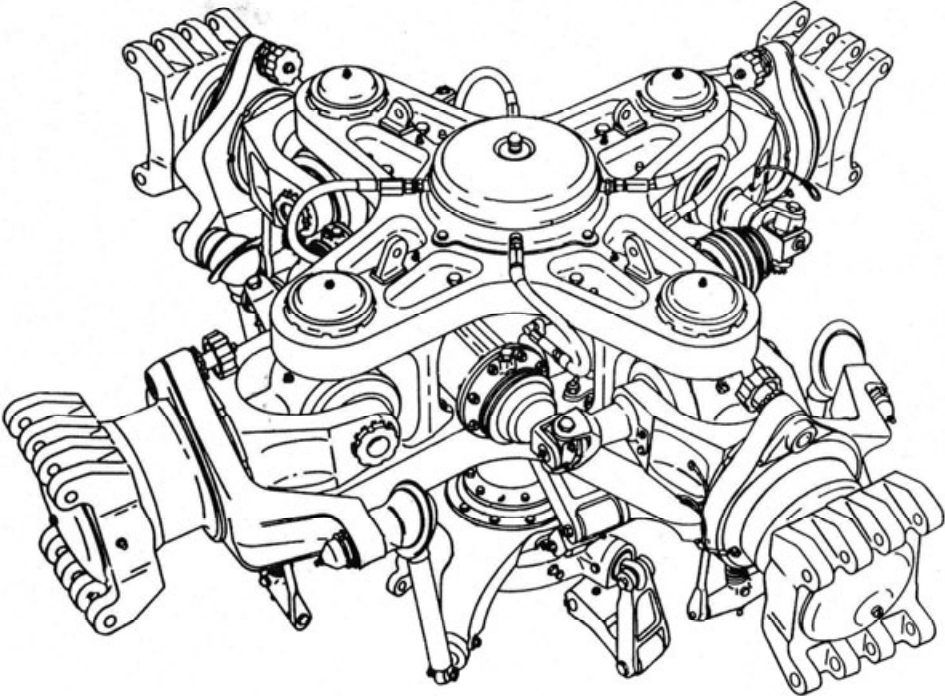


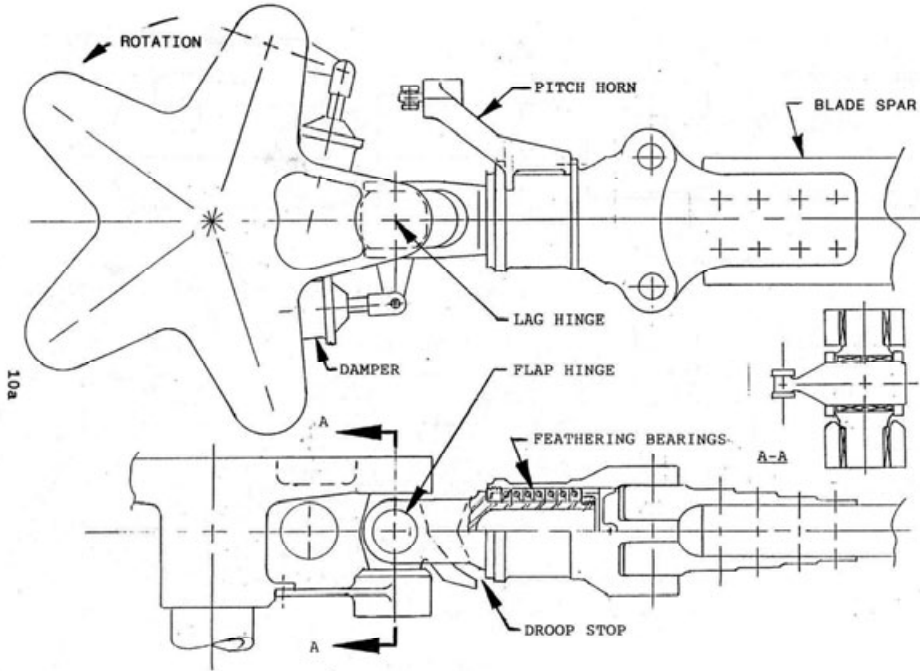
FIG.# I-24 ROBINSON R-22

Fig. D-46. Robinson R-22 (courtesy of Tom Hanson).

**SIKORSKY H-34  
FIRST FLIGHT — MARCH 1954**



**Fig. D-47. Sikorsky H-34 (courtesy of Bill Bousman).**



**FIG. # I-14 SIKORSKY S-61**

**Fig. D-48. Sikorsky S-61 (courtesy of Tom Hanson).**

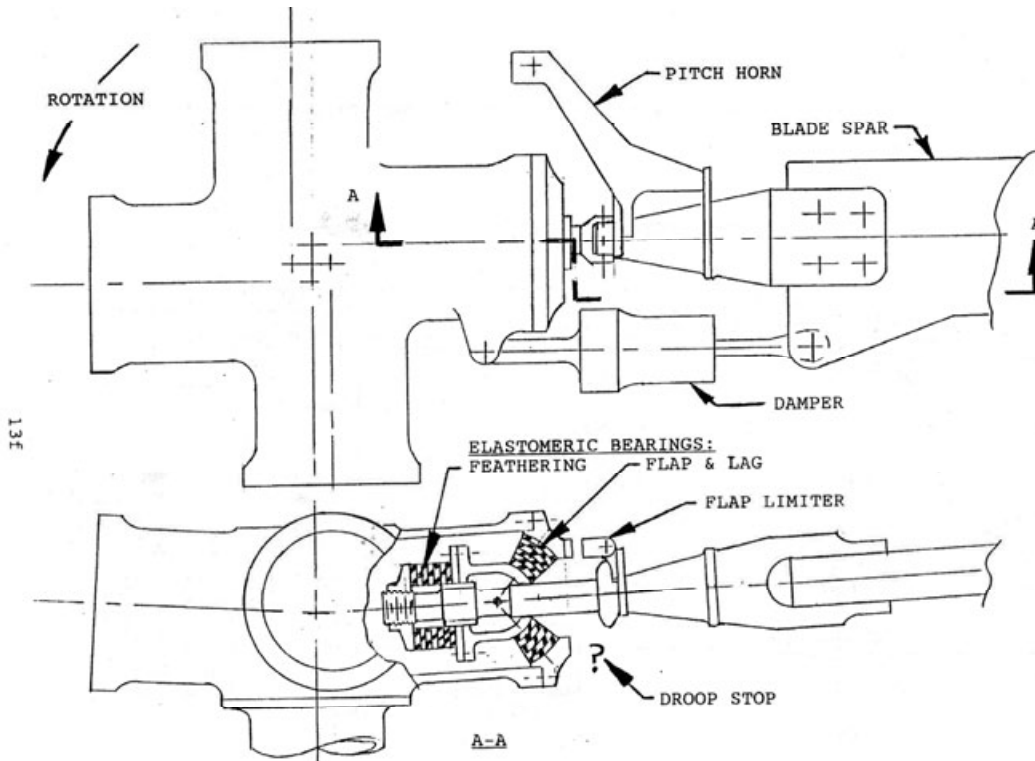


FIG. # I-27 SIKORSKY S-76

Fig. D-49. Sikorsky S-76 (courtesy of Tom Hanson).

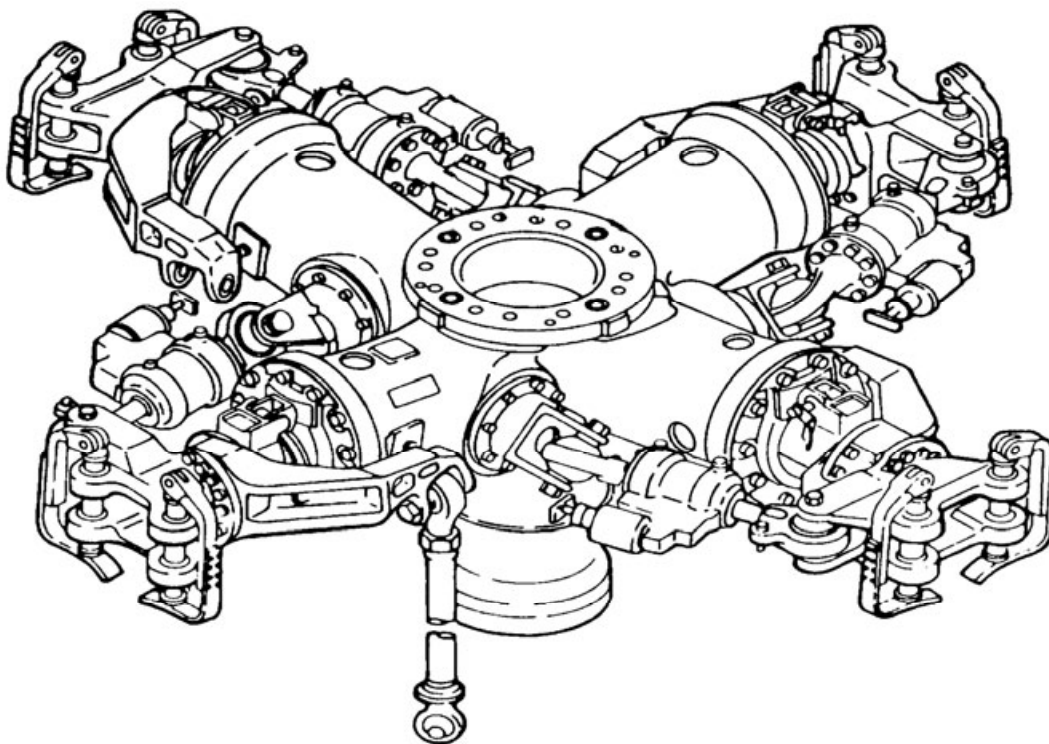


Fig. D-50. Sikorsky UH-60 (courtesy of Bill Bousman).

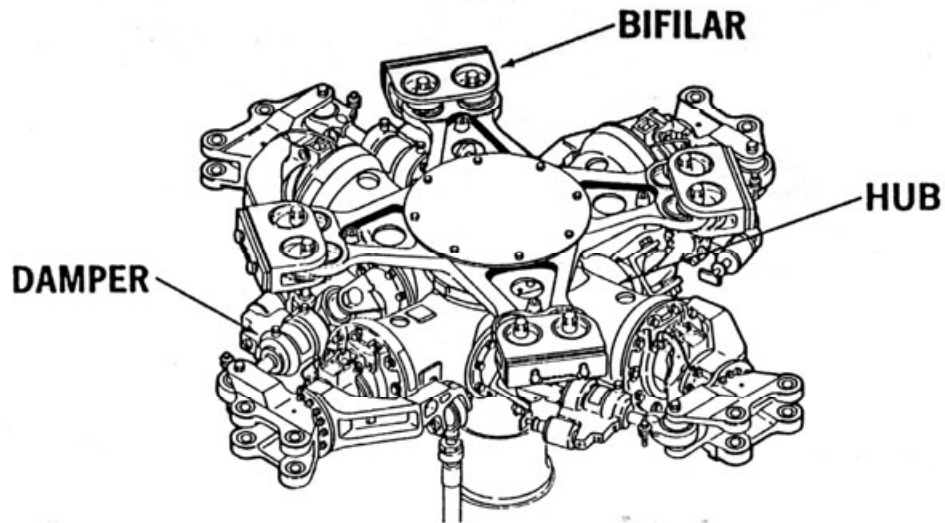


FIG.: 7 ROTOR HEAD OF SIKORSKY UH-60A

Fig. D-51. Sikorsky UH-60 (Schindler/Pfisterer AGARD paper).

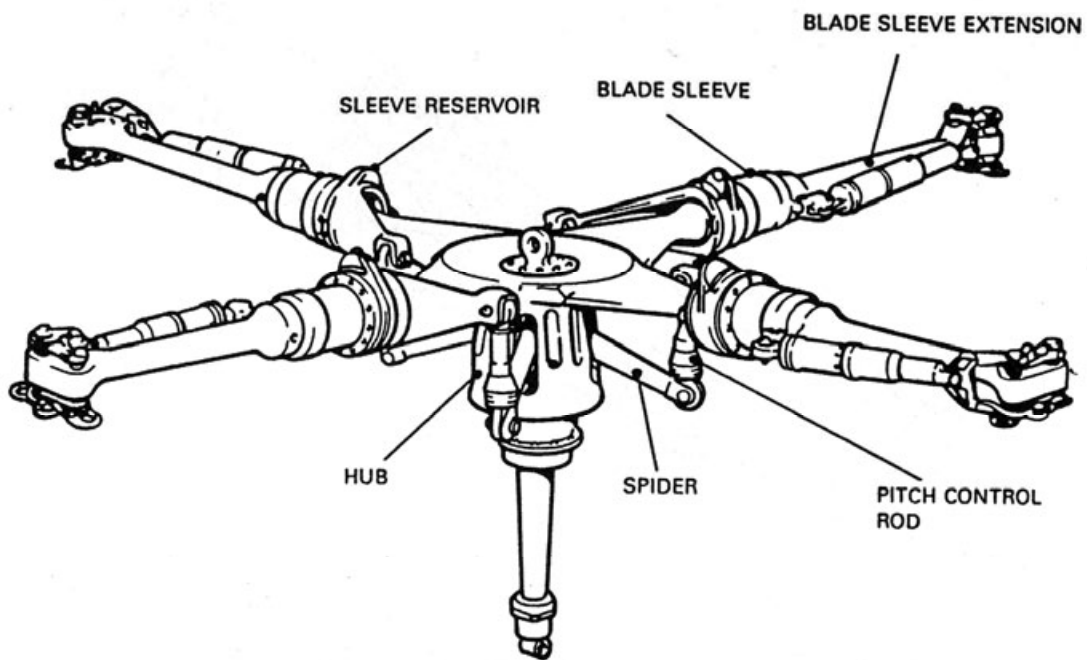


FIG.: 6 ROTOR HEAD OF WESTLAND LYNX

Fig. D-52. Westland Lynx (Schindler/Pfisterer AGARD paper).

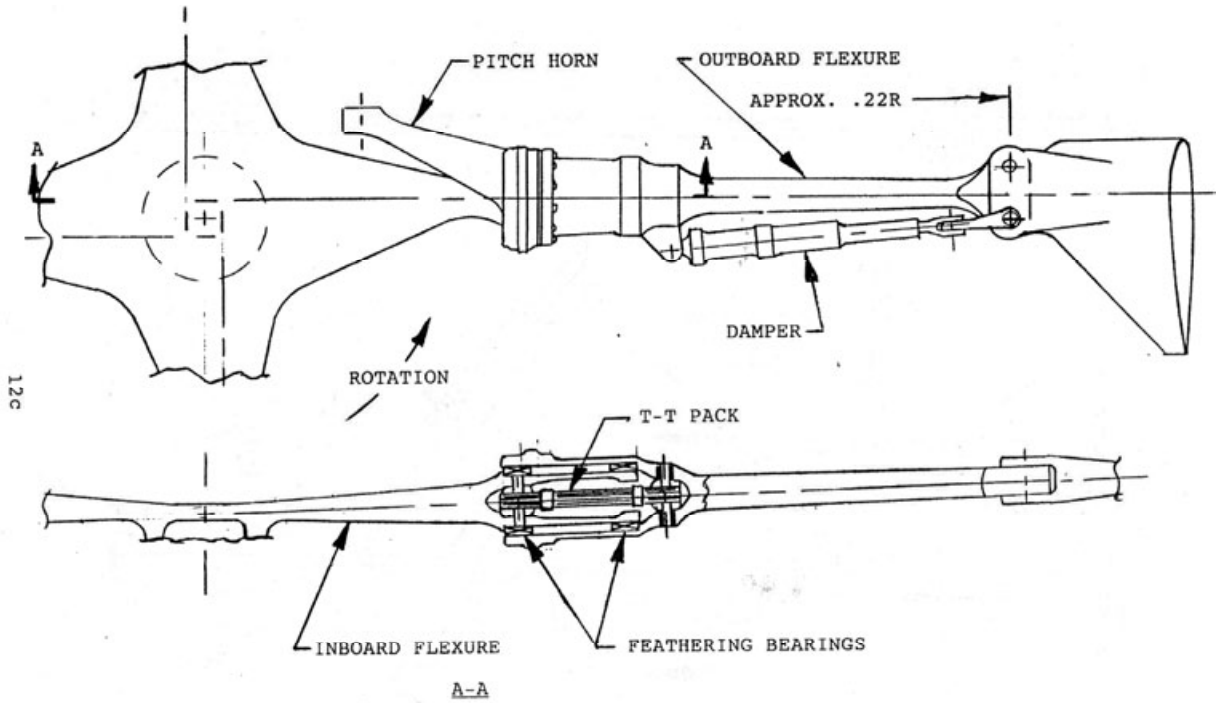


FIG. # I-21 GKN WESTLAND LYNX

Fig. D-53. Westland Lynx (courtesy of Tom Hanson).

WESTLANDS W.G. 13  
FIRST FLIGHT - MARCH 1971

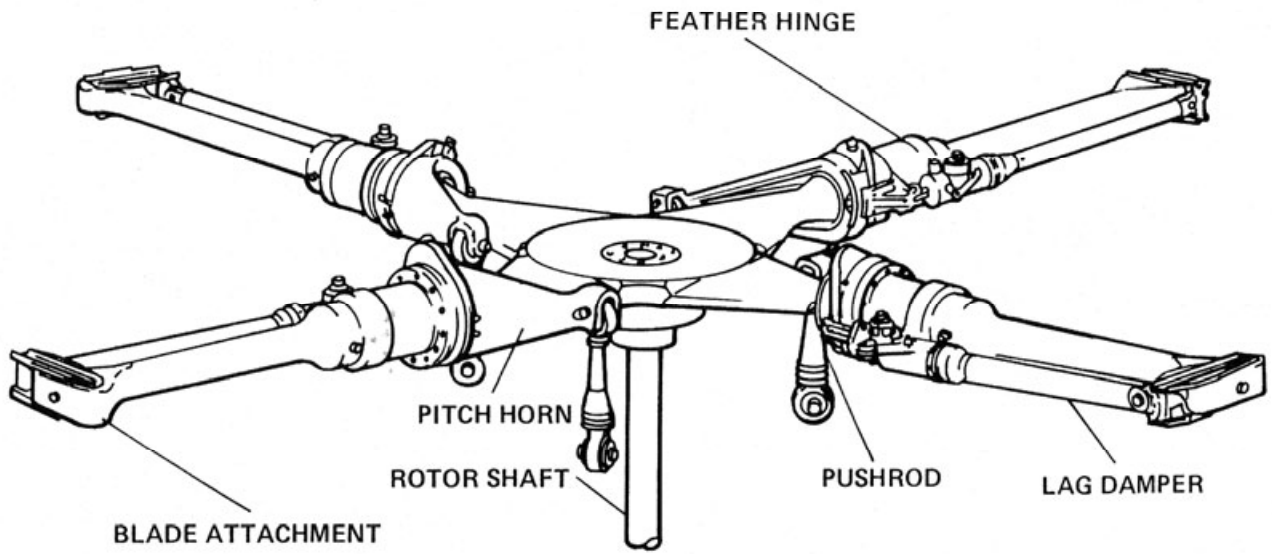


Fig. D-54. Westland W.G.-13 (courtesy of Bill Bousman).

# Is the Ideal Rotor-Hub Design Close at Hand?

A stroll through a gallery of main-rotor hub designs traces the origins of the current state of the art. It also reveals that the ultimate masterpiece has yet to be created.

By R. W. Prouty

SINCE ROTARY-WING flight began, the design of rotor hubs has been one of the greatest challenges. Today, the art remains in a state of flux. Many different configurations are used on production and experimental aircraft because the designers of helicopter dynamics have yet to combine features to satisfy every user's needs in one rotor hub. Among those desired features are: low weight, low drag, low cost, long life, easy maintenance, low part count, freedom from dynamic problems, adequate control power and, for military helicopters, ballistic tolerance.

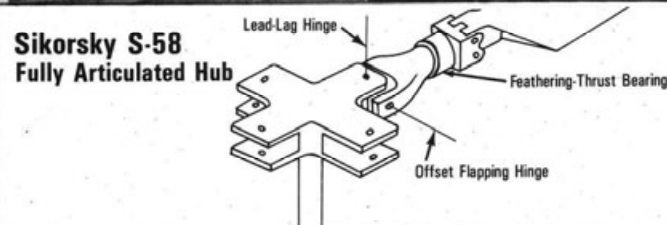
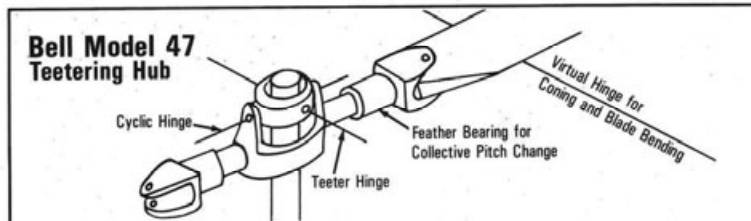
Designers of rotor hubs are aware that improvements must be made but many design teams are constrained and often guided by the principle, "Don't fiddle with success". Of course, this premise is based on how much time and effort has been invested in getting the bugs out of previous designs.

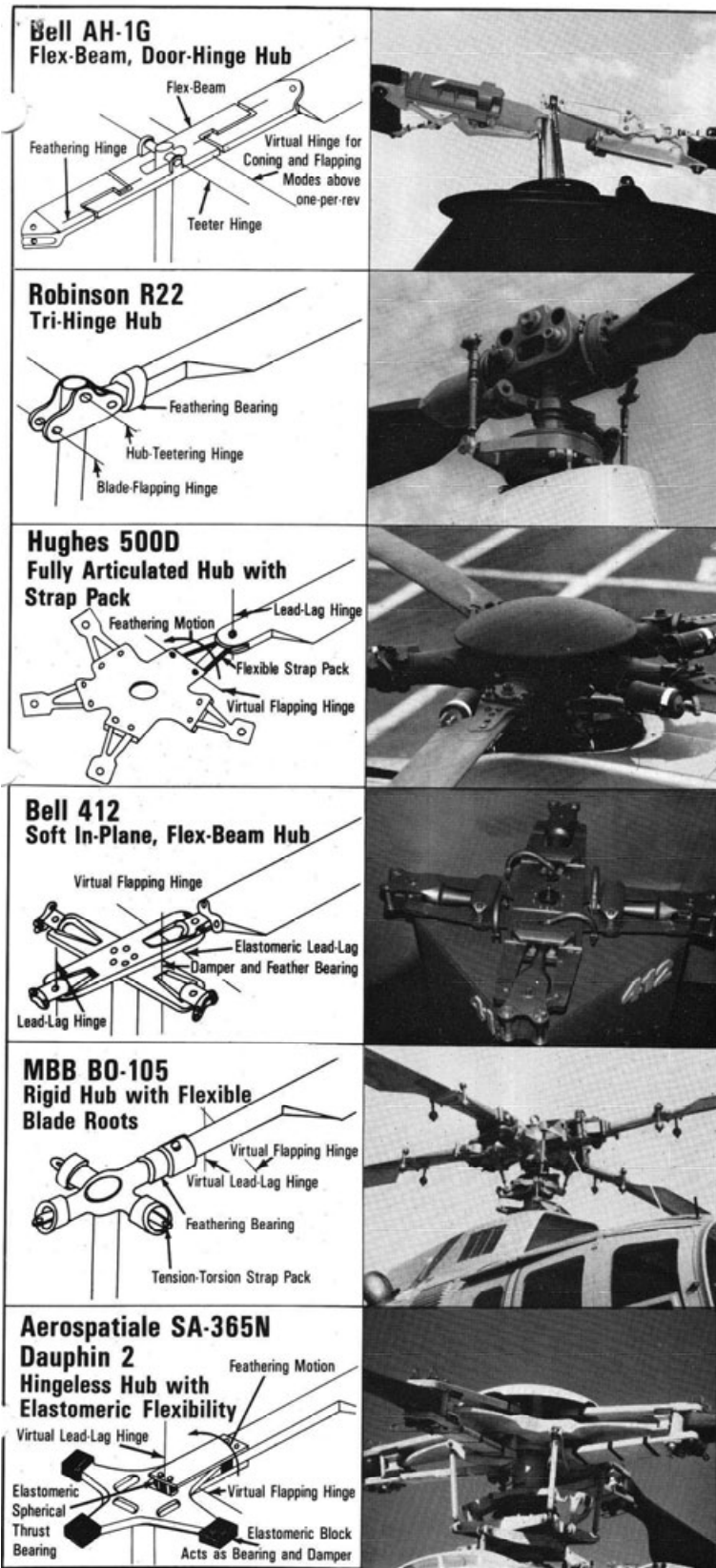
Assuming a rotor-hub designer is without the guidance of previous designs, his primary decision would be to determine how to handle the flapping, lead-lag and feathering motions. The choices in design can vary from a very loose blade attachment with rotary feathering bearings and mechanical hinges for flapping and lead-lag, to a rotor with no hinges or bearings at all.

## Old designs

Until about 1970, the two most familiar hub designs were the two-bladed teetering hub used on the Bell Model 47 and the fully articulated hub with offset flapping hinges as used on the Sikorsky S-58.

The Bell hub was simple, had relatively low drag and, being stiff in-plane, needed no dampers to prevent ground resonance. It did, however, have low control moment capability and was inherently limited to two blades. While this makes the helicopter easy to hangar, it does result in a two-per-rev bounce at high forward speed since most of the rotor thrust is produced by the blades over the nose and tail.





The Sikorsky hub provided high control power and allowed for almost any number of blades but had many parts, high drag, needed lead-lag dampers and had many mechanical bearings to maintain.

Designers of the two-bladed rotors do not use lead-lag hinges for two reasons: First, these hinges are not as necessary to relieve chordwise blade stresses as on multibladed rotors and, second, they are more dangerous because they're susceptible to ground resonance. (Ground resonance is defined as a destructive coupling of blade lead-lag motion with the aircraft rocking on its landing gear.) The first reason can be explained by the fact that most of the in-plane (back-and-forth) motion of the blades is caused by the flapping (up-and-down) motion due to a law of physics called "conservation of momentum".

You can observe an example of this law at an ice show. A skater will start spinning with arms outstretched and then, as he spins faster and faster, he pulls his hands close to his body. The same thing happens when a blade flaps either up or down, its center of gravity moves in toward the center of rotation and it wants to speed up. Blade flapping takes place on a regular basis—once every revolution—and so the blade tries to speed up twice every revolution: once when it is flapping up and again when it is flapping down.

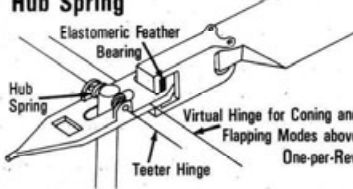
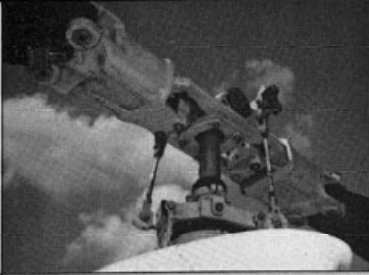
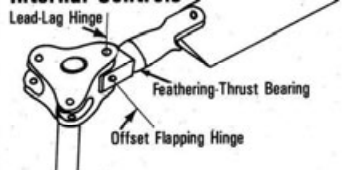
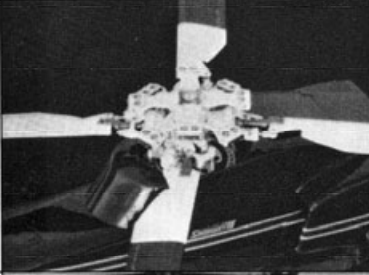
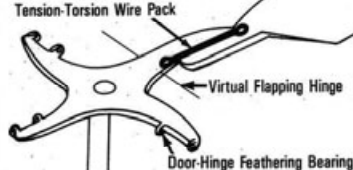
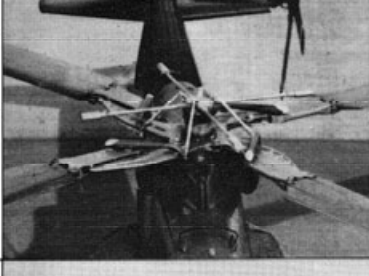
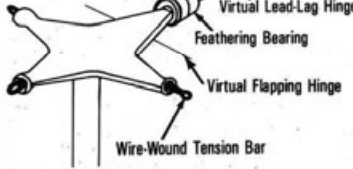
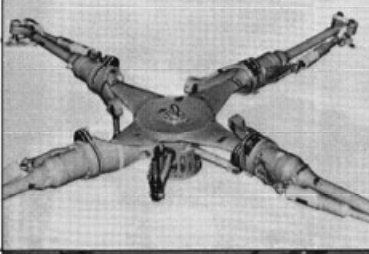
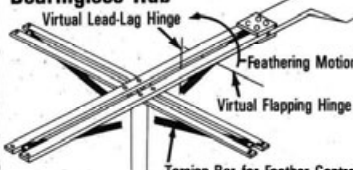
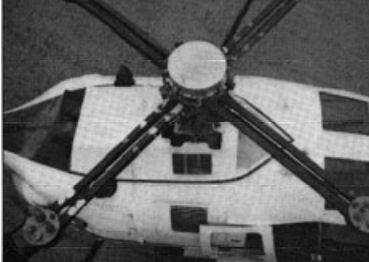
On a two-bladed rotor, this means the two blades are doing the same thing at the same time and the only restraint is from the inertia of the engine softened by the torsional flexibility of the drive system. This restraint is soft enough that the chordwise bending moments can be successfully handled by using a moderate amount of stiffening in the root of the blade.

In a multibladed rotor, the blades are not simultaneously doing the same in-plane dance, so some blades are resisting the motion of other blades. This problem was solved by Juan de la Cierva, the Spanish inventor of the autogyro, when he eliminated the restraint with lead-lag hinges. Modern designers either use his idea or a flexible structure that acts like a mechanical hinge, or they put enough material in the rotor to accommodate the high chordwise bending moments with acceptable low stress levels. These latter rotors are called "stiff in plane".

The other reason for not using lead-lag hinges on a two-bladed hub is that such a rotor would have a wide range of rotor speeds that could cause unstable ground resonance. (See Oct. '81, page 26, for a discussion of this accident waiting to happen.) On the other hand, rotors with three or more hinged blades are only susceptible to ground resonance over a very narrow range of rotor speeds. With suitable dampers around the lead-lag hinges and in the landing gear, they can safely get through this dangerous range.

**Evolutionary designs**

Designers have been gradually making changes on the baseline hubs for many years. Bell Helicopter Textron went to a "flex-beam, door-hinge hub", on later UH-1s and AH-1s. This design locates a bit of hub flexibility and uses it to reduce the two-per-rev bounce by applying the blade's own inertia as a vibration absorber. The door-hinge design also reduces drag by making the hub significantly thinner. Unlike the earlier Bell

<p><b>Bell 222</b> Flex-Beam, Teetering Hub with Hub Spring</p>  <p>Elastomeric Feather Bearing Hub Spring Virtual Hinge for Coning and Flapping Modes above One-per-Rev Teeter Hinge</p>	
<p><b>Enstrom</b> Fully Articulated Hub with Internal Controls</p>  <p>Lead-Lag Hinge Feathering-Thrust Bearing Offset Flapping Hinge</p>	
<p><b>Sikorsky S-76</b> Fully Articulated with Elastomeric Bearings</p>  <p>Elastomeric Bearings for Feathering, Flapping and Lead-Lag Motion</p>	
<p><b>Lockheed AH-56</b> Stiff In-Plane, Flex-Beam Hub</p>  <p>Tension-Torsion Wire Pack Virtual Flapping Hinge Door-Hinge Feathering Bearing</p>	
<p><b>Westland Lynx</b> Hingeless Hub</p>  <p>Virtual Lead-Lag Hinge Feathering Bearing Virtual Flapping Hinge Wire-Wound Tension Bar</p>	
<p><b>MBB/Boeing Vertol</b> Experimental Design Bearingless Hub</p>  <p>Virtual Lead-Lag Hinge Feathering Motion Virtual Flapping Hinge Torsion Bar for Feather Control</p>	

hubs in which cyclic and collective feathering motions were done with separate bearings, both motions are done about the door hinges on the flex-beam hub.

The hub for the Bell Model 222 is also a flex-beam design but feathering is done with elastomeric bearings. In addition, hub springs are installed to increase control moments, especially during low load-factor maneuvers.

On his R22, Frank Robinson has installed separate blade-flapping hinges in addition to the hub teetering hinge. This achieves the same result as the Bell flex-beam while reducing blade-root bending moments and the oscillating forces fed down to the control stick.

Variations on the fully articulated hub are on many current helicopters. The Enstrom hub is similar to the basic Sikorsky configuration, except that the controls go up the inside of the rotor shaft, not outside. Hughes has eliminated the mechanical flapping and feathering bearings by using straps that bend and twist to produce these motions.

Sikorsky, in their Black Hawk and S-76, have replaced all three mechanical hinges with a pair of bearings made of shaped layers of a rubber-like elastomeric material. These bearings deflect to allow flapping, lead-lag and feathering motions.

Bell, in its four-bladed Model 412, has also used elastomeric bearings although flapping is done with a flex-beam. This rotor has lead-lag hinges and the required damping is achieved with elastomeric dampers.

**Revolutionary designs**

In 1959, Lockheed initiated the current trend to hingeless rotors (although a hingeless autogyro had been flown during the '30s and Bell had started its experimental efforts along this line in 1957). Called "rigid rotors" in the early days, they actually had considerable flexibility, thus the term is misleading and should only be applied to such rotors as the two very rigid ones on the Sikorsky Advancing Blade Concept (ABC) coaxial aircraft. The key to hingeless rotors is that cyclic pitch can be used to trim out almost all of the flapping, leaving flexibility to do the rest.

On the Lockheed Cheyenne AH-56, a thin portion of the hub was used for flapping flexibility but was stiff in the lead-lag direction. The door-hinge feathering bearing made the basic hub relatively streamlined.

Hingeless hubs are currently produced and used on the MBB BO-105, the Westland Lynx and the Aerospatiale SA-365N Dauphin 2. The difference in configuration depends primarily on where the designer chose to introduce flexibility. All of these hubs use some sort of bearing—either mechanical or elastomeric—for feathering.

The in-plane stiffness of the Lynx and Dauphin hubs is low enough to require dampers for preventing ground resonance but the MBB BO-105 is stiff enough that it does not.

A hub that can truly be called bearingless was built as an experiment by Boeing Vertol Co. and installed on a BO-105. It relies on structural flexibility for all of its articulation. When fully developed, it should come about as close as possible to achieving those desired goals of low weight, low drag, low cost, easy maintenance, long life, low part count, freedom from dynamic problems, adequate control power and ballistic tolerance. ■



## APPENDIX E

You're treading dangerous ground if you use S-N curves as though they represented immutable physical constants. They're only statistical averages, and for every specimen that exceeds the average, one falls short. To avoid unpleasant surprises, you must view fatigue properties within a statistical framework.

# A New Look at Metal Fatigue

JOHN A. STROMMEN  
*Consultant*  
*West Allis, Wis.*

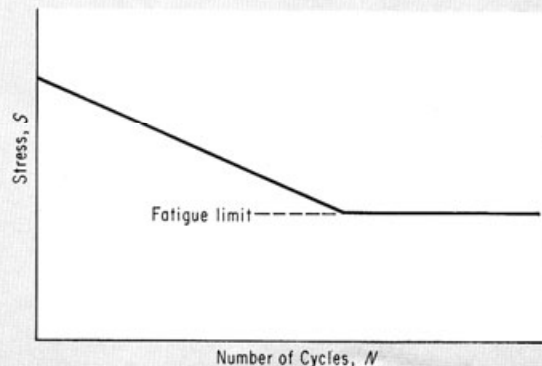
NO MECHANICAL PROPERTY is a physical constant. The results of strength tests always show some scatter. Even in a series of simple tensile tests, identical specimens usually fracture at loads varying by 10% or more.

But this scatter doesn't trouble us. We select some appropriate value (usually the average) as being representative of strength. Then by conservative design, liberal safety factors—or whatever—we rarely have to answer for the statistical sample that inevitably falls below the representative value.

The same type of simplification provides the familiar S-N curves developed from fatigue tests.

### 1 — The S-N Curve

The fatigue life of a mechanical part varies with the load applied to it. The greater the load, the fewer cycles which can be tolerated before the part fails. A plot showing this relationship is called an S-N curve, where stress is plotted against the number of stress cycles before failure. Logarithmic scales are almost always used on the  $N$  axis, and are often used on the  $S$  axis—in which case the curve typically assumes the straight-line character shown here. For ferrous materials, below some  $S$  value the  $N$  value becomes so large that it is assumed to be infinite. This point, the maximum stress providing "infinite" life, is often called the fatigue limit. This limit is often indicated on S-N curves published prior to about 1950. More recently, with the increased use of nonferrous materials (which do not exhibit a fatigue limit), this term is rarely employed. Also, older publications often ignored the  $N$  region below about  $10^4$  cycles, an area that is now quite important in fatigue analysis.



Specimens are tested at specific load levels, and a record is made of the number of cycles endured before failure.

Scatter in this type of test is atrocious. Nevertheless, we pick an average strength for each endurance life, and the resulting plot suggests a curve that can be drawn through these values. Obviously, any such curve represents a coarse fit of the scattered data.

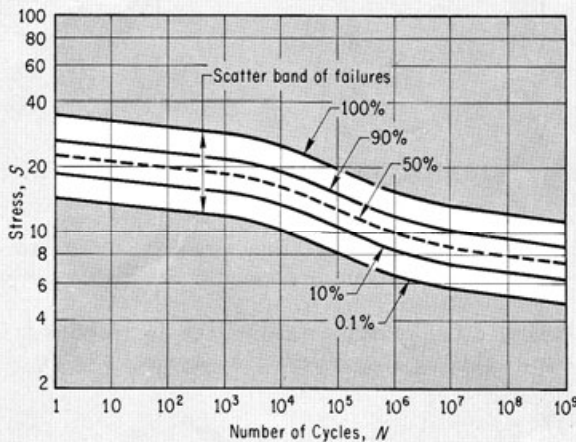
Because so much approximation is involved, a simple *S-N* curve is not the best type of benchmark to use for design. There are better ways to express fatigue data, and these methods use a statistical framework. In this way, strength and failure rate

can be expressed in terms of probability, which gives a more realistic cast to what the numbers actually represent.

The following curves show the many ways in which fatigue properties can be expressed. Properties published in handbooks and the technical literature are usually in forms illustrated by Fig. 1, 2, 3, 7, 8, 9, and 10. Fig. 11 is not used in design but merely demonstrates the statistical relationship between load, strength, and failure. Likewise, Fig. 4, 5, 6, and 12 are not normally used for design analysis but instead reveal the statistical mechanisms at work determining that all important factor—reliability.

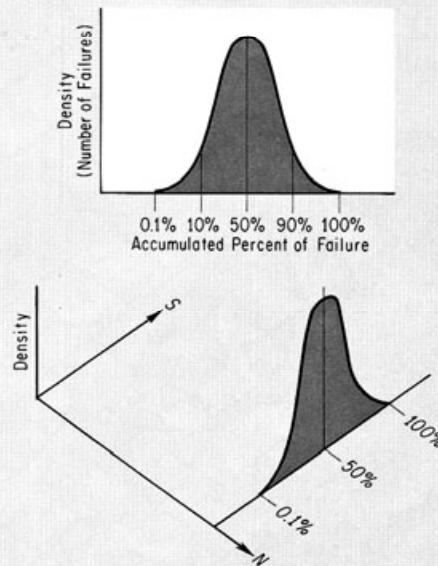
### 2 — An S-N Curve that Tells More

Increasingly over the past 20 years, the basic *S-N* curve has been expanded to show the proportion (and thus probability) of failures encountered at specific *S-N* values. Also, the region below  $10^4$  cycles is included. The 50% failure curve is the plot used on the simpler *S-N* plot. The more expanded *N* scale reveals that the basic shape of the curve is quite different from that suggested by the older, limited scale.



### 3 — The Statistical Distribution

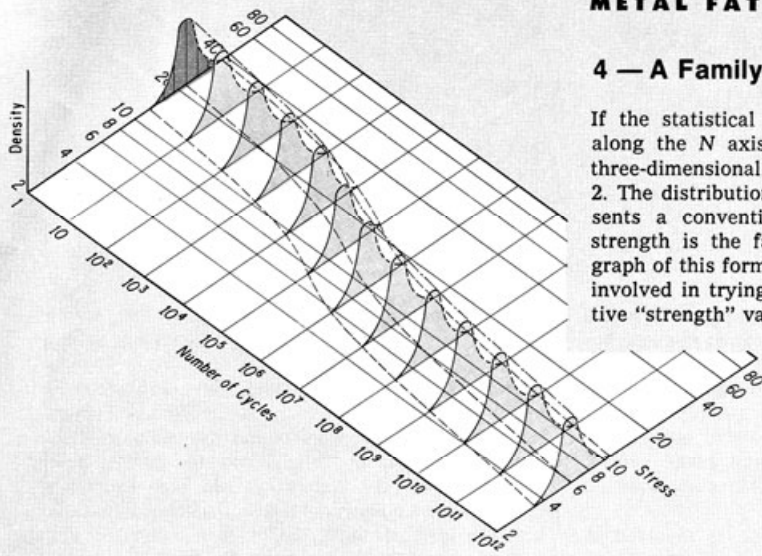
At some given fatigue life—say  $10^4$  cycles, for example—a specific percentage of test samples has failed at each stress level. Therefore, there is no specific “fatigue strength” at that life, but rather a statistical distribution showing probability of failure.



**METAL FATIGUE**

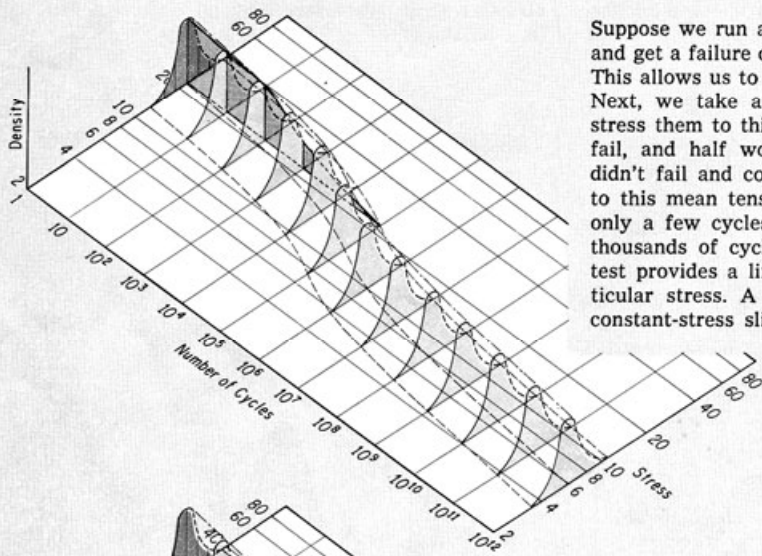
**4 — A Family of Distributions**

If the statistical distribution of Fig. 3 is plotted along the  $N$  axis, we get an  $S-N$  envelope or a three-dimensional form of the graph shown in Fig. 2. The distribution at one cycle of  $N$  merely represents a conventional static test, and the mean strength is the familiar mean tensile strength. A graph of this form emphasizes the basic uncertainty involved in trying to reduce fatigue data to definitive "strength" values.



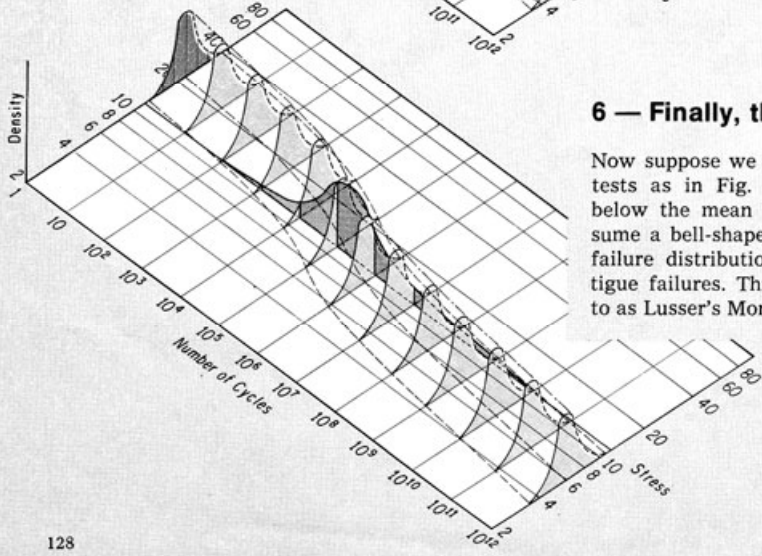
**5 — A New View of the S-N Envelope**

Suppose we run a series of static tensile strengths and get a failure distribution at one cycle ( $N = 1$ ). This allows us to establish a mean tensile strength. Next, we take a new collection of samples and stress them to this value. About half of them will fail, and half won't. We take the samples that didn't fail and continue to stress them repeatedly to this mean tensile strength. Some will fail after only a few cycles, while some will last for many thousands of cycles. The data collected from this test provides a life-distribution curve for this particular stress. A curve of this type is merely a constant-stress slice through the  $S-N$  envelope.



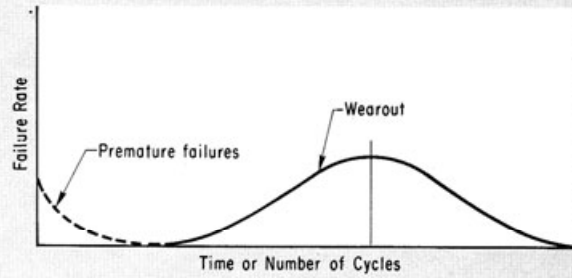
**6 — Finally, the Failure Distribution**

Now suppose we run additional constant-stress life tests as in Fig. 5, but they are run at stresses below the mean tensile strength. The failures assume a bell-shaped distribution that represents the failure distributions normally seen in real-life fatigue failures. This distribution is usually referred to as Lusser's Mortality Curve.



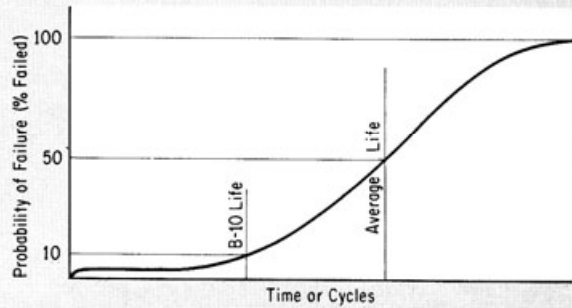
### 7 — The Mortality Curve

Here is the form in which Lusser's Mortality Curve is usually presented. Actually, a number of parts will fail prematurely from poor workmanship or other reasons outside the province of fatigue phenomena. These failures are regarded as "infant mortality." The wearout region is the portion usually associated with reliability studies, and it is the distribution illustrated in Fig. 6.



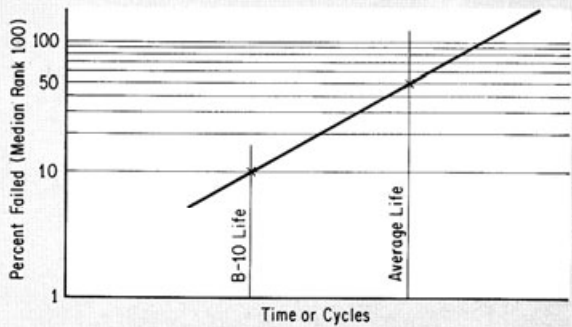
### 8 — Another Mortality Curve

Another way of expressing mortality is by accumulated percent of failure, which also represents probability of failure. This curve is the integral of the Lusser Mortality Curve. Two points of interest on this curve are those representing 10% accumulated failure—which designates the B-10 life in ASTM standards—and 50% accumulated failure—which represents average life.



### 9 — The Weibull Plot

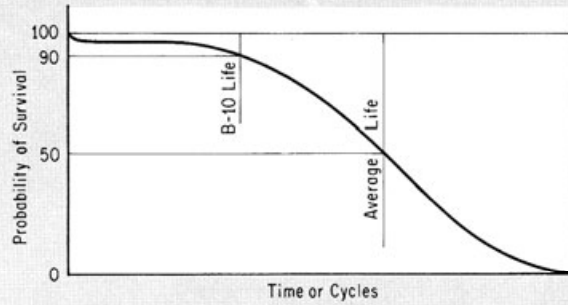
If the probability or accumulated percentage of failure is plotted on a logarithmic scale, the resulting curve is a straight line commonly referred to as a Weibull plot. This curve is widely used to predict service lives for bearings and automotive parts. The chief value of this plot is that it translates the complex phenomena of fatigue into something that can be expressed very simply. For example, one point on the curve and the slope of the line defines all significant information about life expectancy. Weibull curves are useful for extrapolating fatigue data because samples need be tested only over a portion of the  $N$  axis, and then a straight line can be drawn to imply life characteristics in other regions. Lusser's Mortality Curve can then be estimated from limited tests. An ideal Weibull plot is one approaching a vertical line at the far right of the curve. Such a plot would indicate that all parts fail at once after a long service life. Bearing manufacturers, for example, are using vacuum-melted steels and improved grinding techniques to increase the slope of the Weibull plot to reduce life variations. At the same time, they are trying to increase the number of cycles for 50% failure so that average life is increased.



(continued)

### 10 — A Measure of Survival

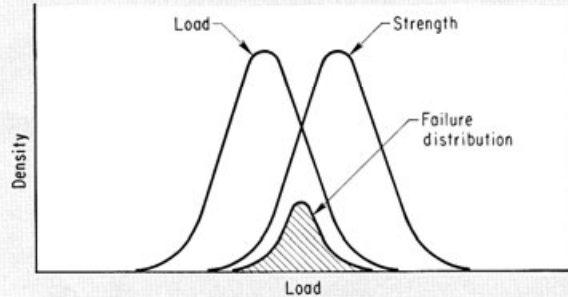
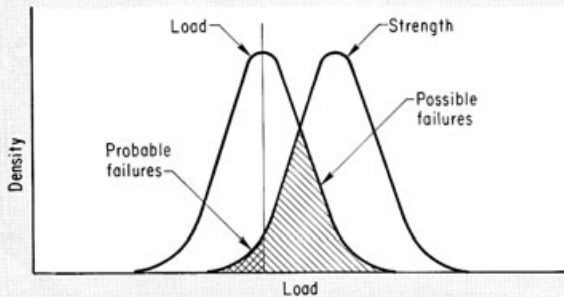
Another way of expressing fatigue characteristics is by the number of parts that survive (rather than by the number that fail). This plot, Probability of Survival showing the samples remaining after various service lives, is an expression of reliability. For example, at the B-10 life, a part is 90% reliable. At average life it is 50% reliable. Obviously, a component becomes quite unreliable as it approaches its average life.



### 11 — How Loads Vary

Now, for an added complication. For any given load, different specimens fracture at different lives. But whether we are talking about the test lab or actual field service, loads also vary. (The variation, of course, is smaller in the lab than in the field; nevertheless, a variation always exists.) The variations come from errors in measurement, variations in the specimen, or simple errors in recording data.

Therefore, we have not only a strength distribution, but also a statistical load distribution. These two distributions intersect and enclose an area indicating the degree of failure expected. "Possible Failures" indicates a region in which load may exceed strength. "Probable Failures" indicates a region in which load probably exceeds strength. (Average load exceeds some expected strengths.) The failures actually experienced will be distributed as shown in the second graph.



### 12 — The Complete Picture

In any fatigue test, there is an attempt to keep loads constant. Nevertheless, they will vary and produce a distribution that does not change (theoretically speaking) with variation in number of cycles. Thus, we get an envelope of applied load. (Upper graph.) Next, we superimpose the S-N envelope—representing strength—from Fig. 4. (Middle graph.) The load and strength distributions interact—as they did in Fig. 11—to produce failure distributions for every value of imposed stress. (Lower graph.) This last graph is quite complicated and need not be developed in practical design, but it does drive home the fact that fatigue life involves quite a bit more than a simple curve drawn across a two-dimensional grid.

velope—representing strength—from Fig. 4. (Middle graph.) The load and strength distributions interact—as they did in Fig. 11—to produce failure distributions for every value of imposed stress. (Lower graph.) This last graph is quite complicated and need not be developed in practical design, but it does drive home the fact that fatigue life involves quite a bit more than a simple curve drawn across a two-dimensional grid.



## APPENDIX F

### DYNAMICS OF A FREE-FREE UNIFORM BEAM

When a helicopter airframe is subjected to hub forces and moments, there can be serious airframe responses that impact all components and occupants of the aircraft. This appendix illustrates the dynamics of the situation with the simplest example I could think of—a beam shaken in the middle of its span by either a vertical force or a moment. To create this example, I imagined an empty Sikorsky UH-60, Fig. F-1, with the main- and tail-rotor blades removed. Then I melted it down and made a 50-foot-long rod out of the materials, which are mostly aluminum and steel. This rod, Fig. F-2, is a 50-foot-long, solid aluminum rod, 14.25 inches in diameter. This amounts to a volume of 95,690 cubic inches. Given that aluminum weighs about 0.1 pounds per cubic inch, this beam weights slightly more than 9,569 pounds. Thus, the mass per unit length ( $m$ ) is  $9,569/32.174/50$ , which gives  $m = 5.948$  slugs per foot. The moment of inertia ( $I$ ) of the beam's cross-section<sup>1</sup> is  $\pi R^4/4$  or 2,024 inches cubed. Because the modulus of elasticity ( $E$ ) of aluminum is  $10 \times 10^6$  pounds per square inch, the beam's stiffness is  $EI = 20,240 \times 10^6$  pounds-inch squared or  $140.6 \times 10^6$  pounds-feet squared. Therefore, the beam parameter of  $EI/mL^4$  equals 3.766 per second squared.

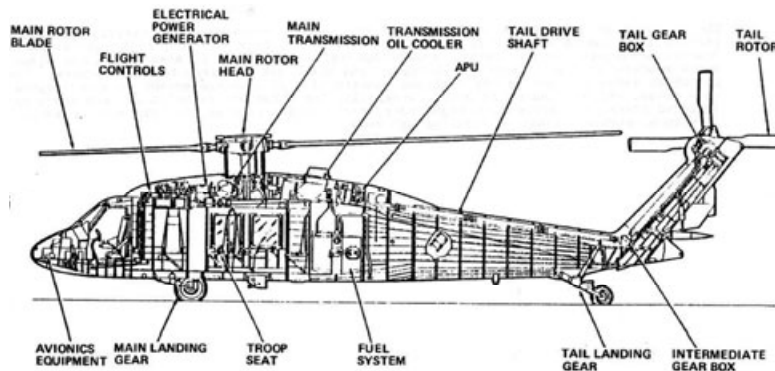


**Fig. F-1. The general arrangement of the Sikorsky UH-60.**

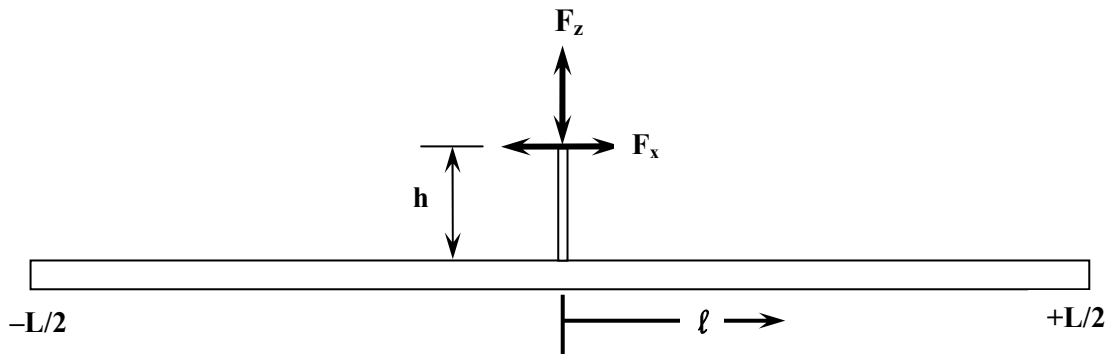


**Fig. F-2. Elementary beam model.**

<sup>1</sup> Roark, R. J. and Young, W. C.: *Roark's Formulas for Stress and Strain*, 5th Edition, McGraw-Hill Book Co., New York, N.Y., 1965.

## APPENDIX F

My elementary beam has a constant stiffness ( $EI$ ) in pounds-feet squared and a mass per unit length ( $m$ ) in slugs per foot from one end to the other. Admittedly, this is a poor assumption about a helicopter airframe that has many portions filled with engines, fuel, gear boxes, shafts, electronic boxes, cargo, and humans. This makes the assumption that the mass per foot is constant over the whole beam length hardly reasonable. Certainly the assumption that the beam has constant stiffness is unreasonable because a fuselage has “holes” such as doors, windows, and joints. Still, this example introduces you to the mathematics of the basic helicopter dynamics problem.

Now let me first calculate this elementary beam’s response to a hub vertical vibratory force ( $Fz$ ), and second, calculate the response to a horizontal vibratory force ( $Fx$ ), which acts at a height ( $h$ ) above the beam’s center of gravity (c.g.) and, therefore, really creates a moment. Thirdly, I want to convey the possible responses when the two forces act simultaneously.

### Beam Response to a Vertical Vibratory Force

The elementary beam I have assumed is shaken in the middle as Fig. F-2 shows. No forces or moments are applied at the ends of the beam, which is what free-free means. Because I have placed the shaking force dead center in the middle of the beam, the mathematics can be developed using just one-half of the beam. That is, whatever shape the right-hand side takes, the left-hand side is the mirror image. Notice that I have denoted any station from the beam’s center along the beam to the right by the script letter ( $\ell$ ) measured in feet. Vertical deflection of the beam is denoted by ( $z$ ), which is also in feet. The right-hand end of the beam is reached when  $\ell = L/2$ , where  $L$  is the total length of the beam in feet. This type of vibration problem is studied in several textbooks, but my favorite reference has always been Timoshenko’s third edition.<sup>2</sup>

The vibrating beam problem is approached by equating the moments at some station ( $\bar{\ell}$ ). That is, a moment at ( $\bar{\ell}$ ) is created by each beam element inertia force ( $ma$ ) times its distance to the station of interest ( $\ell - \bar{\ell}$ ). This moment due to inertia is resisted by the beam’s structural moment, which leads to the equation

$$(1) \quad EI \frac{\partial^2 z_{\ell,t}}{\partial \ell^2} = M_{\ell,t} = -m \int_{\bar{\ell}}^{L/2} \frac{\partial^2 z_{\ell,t}}{\partial t^2} (\ell - \bar{\ell}) d\ell.$$

The integral form of the beam equation is put in the fourth-order partial differential equation classical form by taking the second derivative of Eq. (1) with respect to beam length, which leads to

$$(2) \quad EI \frac{\partial^4 z_{\ell,t}}{\partial \ell^4} = -m \frac{\partial^2 z_{\ell,t}}{\partial t^2}.$$

---

<sup>2</sup> Timoshenko, S. and Young, D. H.: *Vibration Problems in Engineering*, D. Van Nostrand Company, Inc., Princeton, New Jersey, Jan. 1955.

The solution process is to assume an analytical equation that satisfies Eq. (2). Based on some experience, I chose

$$(3) \quad z_{\ell,t} = [A \cosh(k\ell) + B \sinh(k\ell) + C \cos(k\ell) + D \sin(k\ell)] F_z$$

where the vertical vibratory force ( $F_z$ ) in pounds is defined as

$$(4) \quad F_z = F_{z\sin} \sin(\omega_h t) + F_{z\cos} \cos(\omega_h t) = \sqrt{F_{z\sin}^2 + F_{z\cos}^2} \sin \left[ \omega_h t + \arctan \left( \frac{F_{z\cos}}{F_{z\sin}} \right) \right].$$

Note that this forcing equation contains both a sine and a cosine component, and that the shaking frequency ( $\omega_h$ ) is in radians per second.

Now the first step towards a solution of this partial differential equation problem is to establish the value of the constant ( $k$ ) required by Eq. (3). First, you take the fourth derivative of deflection with respect to the beam station ( $\ell$ ), which, it turns out, is simply

$$(5) \quad \frac{\partial^4 z_{\ell,t}}{\partial \ell^4} = k^4 z_{\ell,t},$$

and then you take the second derivative of deflection with respect to time ( $t$ ), which also turns out to be simply

$$(6) \quad \frac{\partial^2 z_{\ell,t}}{\partial t^2} = -\omega_H^2 z_{\ell,t}.$$

Inserting these two derivatives into Eq. (2) gives

$$(7) \quad EI(k^4 z_{\ell,t}) = -m(-\omega_H^2 z_{\ell,t}),$$

and this leads to the constant ( $k$ ) being defined as

$$(8) \quad k = \left( \frac{m\omega_H^2}{EI} \right)^{1/4}.$$

The question now becomes one of finding out what A, B, C, and D equal. These constants are found from the boundary conditions, which are values associated with the center of the beam and the free end of the beam. At the free end of the beam, where  $\ell = L/2$ , no forces or moments are applied. Therefore, the moment (i.e., the second derivative of Eq. 3) and the shear (i.e., the third derivative Eq. 3) must be zero. At the center of the beam ( $\ell = 0$ ) where the vibratory force is applied, the beam shear must equal one-half of the applied vibratory force (i.e.,  $F_z/2$ ). Lastly, because the left-hand side of the beam must mirror the right-hand side, the beam slope (i.e., the first derivative) must be zero. These boundary conditions lead to four equations in the four unknowns (A, B, C, and D) and appear mathematically as

APPENDIX F

$$\begin{aligned}
 (9) \quad EI \frac{\partial^2 z_{\ell=L/2,t}}{\partial \ell^2} &= (EI)k^2 [A \cosh(k\ell) + B \sinh(k\ell) - C \cos(k\ell) - D \sin(k\ell)] F_z = 0 && \text{moment} \\
 EI \frac{\partial^3 z_{\ell=L/2,t}}{\partial \ell^3} &= (EI)k^3 [A \sinh(k\ell) + B \cosh(k\ell) + C \sin(k\ell) - D \cos(k\ell)] F_z = 0 && \text{shear} \\
 EI \frac{\partial^3 z_{\ell=0,t}}{\partial \ell^3} &= (EI)k^3 [A \sinh(k\ell) + B \cosh(k\ell) + C \sin(k\ell) - D \cos(k\ell)] F_z = F_z/2 && \text{shear} \\
 \frac{\partial z_{\ell=0,t}}{\partial \ell} &= k [A \sinh(k\ell) + B \cosh(k\ell) - C \sin(k\ell) + D \cos(k\ell)] F_z = 0 && \text{slope.}
 \end{aligned}$$

When these four equations are evaluated at the correct boundary condition stations, things simplify to

$$\begin{aligned}
 (10) \quad (EI)k^2 [A \cosh(kL/2) + B \sinh(kL/2) - C \cos(kL/2) - D \sin(kL/2)] F_z &= 0 && \text{moment} \\
 (EI)k^3 [A \sinh(kL/2) + B \cosh(kL/2) + C \sin(kL/2) - D \cos(kL/2)] F_z &= 0 && \text{shear} \\
 (EI)k^3 [B - D] F_z &= F_z/2 && \text{shear} \\
 k [B + D] F_z &= 0 && \text{slope.}
 \end{aligned}$$

From these four equations, it is immediately clear that  $D = -B$  and that  $B = \frac{1}{4k^3 (EI)}$ .

With values for  $B$  and  $D$ , you have reduced the problem to two equations in two unknowns ( $A$  and  $C$ ). Admittedly, the expressions for  $A$  and  $C$  are a little messy, but nevertheless

$$\begin{aligned}
 (11) \quad A &= \frac{-1}{4k^3 (EI)} \left[ \frac{\cosh(kL/2) \cos(kL/2) + \sinh(kL/2) \sin(kL/2) + 1}{\sinh(kL/2) \cos(kL/2) + \cosh(kL/2) \sin(kL/2)} \right] \\
 C &= \frac{-1}{4k^3 (EI)} \left[ \frac{1 + \cosh(kL/2) \cos(kL/2) - \sinh(kL/2) \sin(kL/2)}{\sinh(kL/2) \cos(kL/2) + \cosh(kL/2) \sin(kL/2)} \right]
 \end{aligned}$$

Remember that  $k$  was obtained at Eq. (8), which is, to repeat,  $k = \left( \frac{m\omega_H^2}{EI} \right)^{1/4}$ .

The equations for  $A$  and  $C$  both contain a denominator that has the potential to go to zero given certain values of the product of  $k$  and  $L/2$ . The denominator goes to zero at several values of  $(kL/2)$ . To see this, consider the following equation:

$$\sinh(kL/2) \cos(kL/2) + \cosh(kL/2) \sin(kL/2) = 0.$$

In mathematics, this equation is called a transcendental equation because the values of  $(kL/2)$  that make the equation zero must be found numerically. One simple way to attack this problem is to reform the equation by dividing through by  $\cosh(kL/2)$ , and then by  $\cos(kL/2)$ , to obtain

$$(12) \quad \tanh(kL/2) + \tan(kL/2) = 0,$$

and then graph this sum versus  $kL = (m\omega_H^2 L^4 / EI)^{1/4}$ . I have done this as you can see in Fig. F-3. The roots of Eq. (12) are shown in Table F-1.

Because the hyperbolic tangent of large numbers becomes virtually 1.0, the roots at 4 and beyond are found with adequate engineering precision from

$$(13) \quad kL = (m\omega_H^2 L^4 / EI)^{1/4} = \frac{\pi}{2} [4(\text{Root No.}) - 1].$$

The importance of Eq. (13) cannot be overstated because it defines the frequency ( $\omega_H$ ) in radians per second at which response (say deflections or accelerations) of this uniform beam will be extreme. Of course, this does not happen in practice because there is always some structural damping, which I have not considered in this example.

With the preceding background, consider a shake test of a uniform beam. The beam is hanging from a rigid ceiling by the softest of springs so that the beam response is not influenced by the support system. In the middle of the beam is a *weightless* shaker that can apply a vibratory force in pounds of

$$(14) \quad F_z = 100 \sin(\omega_h t).$$

The shaker is turned on and the frequency ( $\omega_H$ ) is increased from zero while you are watching the beam's response. You know in advance that certain frequencies must be avoided because the beam will go into resonance. These critical frequencies—*converted to cycles per second* or hertz (Hz)—are calculated using ( $kL$ ) from Table F-1 and Eq. (13) as

$$(14) \quad f = \frac{1}{2\pi} \sqrt{(kL)^4 \frac{EI}{mL^4}} \quad \text{in cycles/sec or Hz}$$

and this means to take care as the frequency approaches 6.91 Hz, and then again as the frequency approaches 37.3 Hz, the first two resonance frequencies of the beam when shaken with a vertical force.

**Table F-1.  $kL$  Values to Be Avoided**

Root Number	Value of $kL$
1	4.7300407449
2	10.9956078380
3	17.2787596574
4	23.5619449023

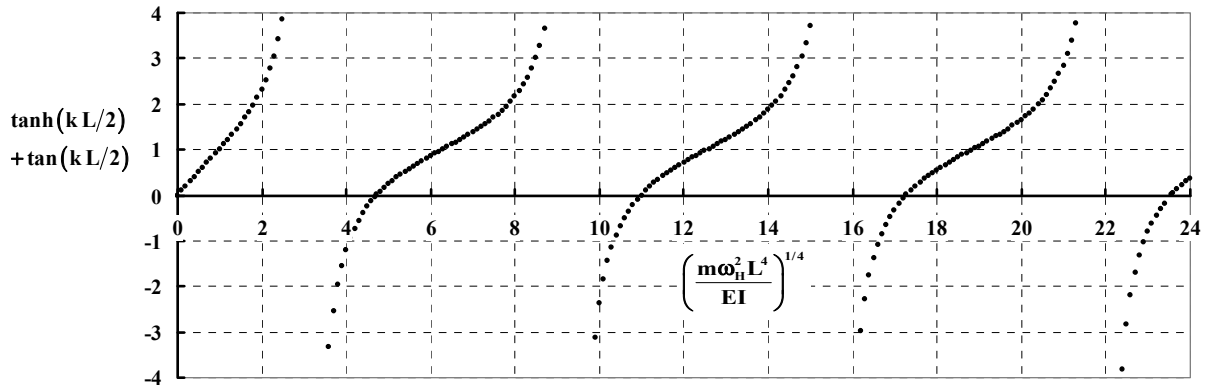


**Fig. F-3. Roots of Eq. (12) found graphically.**

Now think about the recording equipment you would use for this relatively simple test. A high-speed motion picture camera would be nice so the deflected shape of the beam could be seen and deflection measured, and an array of accelerometers attached to the beam all along its length would give you a measurement of beam vertical accelerations from beam nose (+L/2) to tail (-L/2).

First, imagine what you could learn from just one frame recorded by the high-speed camera at shaker frequencies of 6 and 36 cycles per second. You could, for example, select a frame from each input frequency and compare theory to test. Based on what you have learned above, the theory would be computed as

$$(15) \quad z_{\ell,t} = [A \cosh(k\ell) + B \sinh(k\ell) + C \cos(k\ell) + D \sin(k\ell)] F_z \sin(\omega_H t).$$

Notice that the maximum deflection occurs when  $\sin(\omega_H t)$  equals  $\pm 1.0$ , so pick those frames where the deflection is maximum. What you would see is shown in Figs. F-4 and F-5. In each figure the solid lines go with  $\sin(\omega_H t) = +1.0$  and the dash lines go with  $\sin(\omega_H t) = -1.0$ . The applied force is 100 pounds in both cases. Keep in mind that the deflection is directly proportional to the applied force, so the shapes shown in Figs. F-4 and F-5 can be scaled to any other applied force.

Fig. F-5 makes an important point. If a six-bladed rotor were applying the vibratory force and its once-per-revolution frequency was 6 Hz, then its next higher frequency input would be at six per revolution, which is 36 Hz. It would be nice if the pilot's and copilot's seats were near the nose and specifically at beam station +20 feet. That station is a beam node as Fig. F-5 shows. At the node there is no deflection. Furthermore, a few passengers could be located near beam station +7 feet to enjoy a better ride.

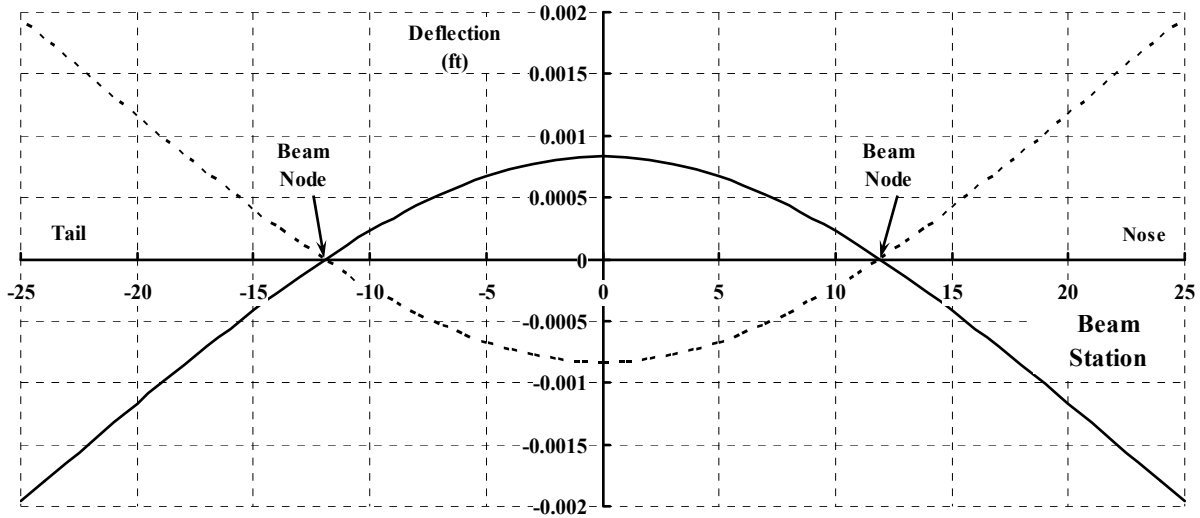


**Fig. F-4. Beam vibratory maximum deflection extremes. Forcing frequency of 6 Hz, force of  $Fz = 100 \sin(\omega_H t)$ .**

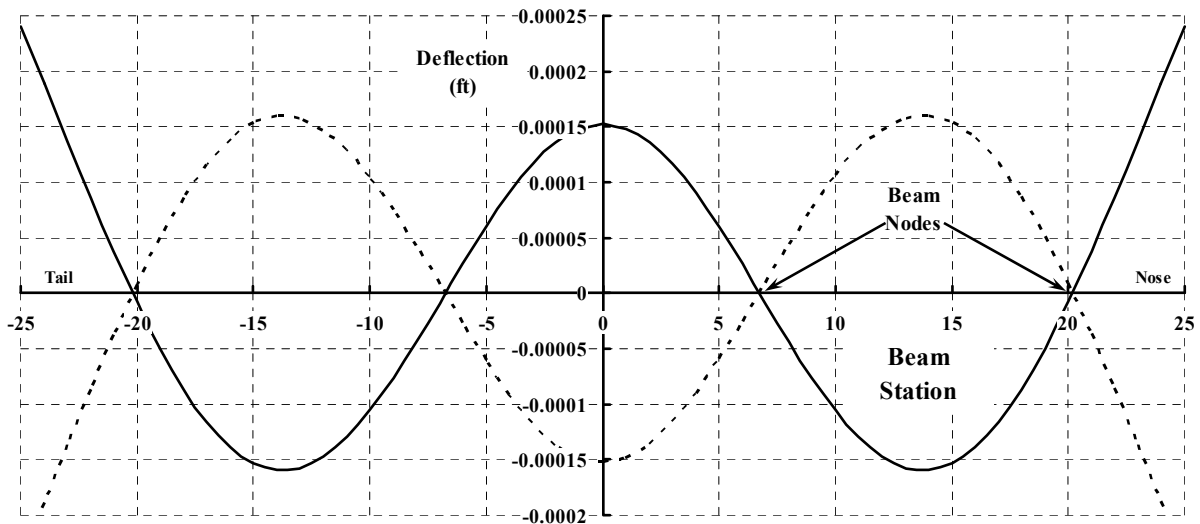


**Fig. F-5. Beam vibratory maximum deflection extremes. Forcing frequency of 36 Hz, force of  $Fz = 100 \sin(\omega_H t)$ .**

## APPENDIX F

The important factor for the human occupants and the aircraft structure is the beam's acceleration from nose to tail. This acceleration is, from Eq. (6),

$$(16) \quad \frac{\partial^2 z_{\ell,t}}{\partial t^2} = -\omega_H^2 z_{\ell,t} = -\omega_H^2 \left[ A \cosh(k\ell) + B \sinh(k\ell) + C \cos(k\ell) + D \sin(k\ell) \right] F_z$$

where, to repeat, the vertical vibratory force ( $F_z$ ) is defined as

$$(4) \quad F_z = F_{z\sin} \sin(\omega_h t) + F_{z\cos} \cos(\omega_h t) = \sqrt{F_{z\sin}^2 + F_{z\cos}^2} \sin \left[ \omega_h t + \arctan \left( \frac{F_{z\cos}}{F_{z\sin}} \right) \right].$$

The accelerometers installed along the beam mentioned earlier are the most important sensors. Suppose an oscillograph or digital recording of the accelerometer placed at the beam's nose is chosen as the key sensor to watch during a sweep of vibratory frequency from 3 to 45 hertz. This sensor would be at beam station  $\ell = L/2$ . An accelerometer at this nose location simplifies the calculation of Eq. (16) to

$$(17) \quad \frac{\partial^2 z_{\ell=L/2,t}}{\partial t^2} = -\omega_H^2 z_{\ell,t} = \omega_H^2 \left[ \frac{\cosh(\frac{1}{2}kL) + \cos(\frac{1}{2}kL)}{\sinh(\frac{1}{2}kL) \cos(\frac{1}{2}kL) + \cosh(\frac{1}{2}kL) \sin(\frac{1}{2}kL)} \right] \left( \frac{F_z}{2k^3 EI} \right).$$

Notice again that the acceleration is proportional to the vertical vibratory force so the acceleration can be scaled on the basis of a pound of  $F_z$ . Expressing the acceleration in units of gravity is also quite common. Following this practice yields

$$(18) \quad \left( \frac{1}{\sqrt{F_{\sin}^2 + F_{\cos}^2}} \right) \frac{\partial^2 z_{\ell=L/2,t}}{\partial t^2} = \left( \frac{\omega_H^2}{2gk^3 EI} \right) \left[ \frac{\cosh(\frac{1}{2}kL) + \cos(\frac{1}{2}kL)}{\sinh(\frac{1}{2}kL) \cos(\frac{1}{2}kL) + \cosh(\frac{1}{2}kL) \sin(\frac{1}{2}kL)} \right] \sin \left[ \omega_h t + \arctan \left( \frac{F_{\cos}}{F_{\sin}} \right) \right].$$

Now, by picking time ( $t$ ) where the sine term in Eq. (18) is  $\pm 1.0$ , the maximum acceleration will be immediately clear, because

$$(19) \quad \left[ \left( \frac{1}{\sqrt{F_{\sin}^2 + F_{\cos}^2}} \right) \frac{\partial^2 z_{\ell=L/2,t}}{\partial t^2} \right]_{\text{MAX}} = \pm \left( \frac{\omega_H^2}{2gk^3 EI} \right) \left[ \frac{\cosh(\frac{1}{2}kL) + \cos(\frac{1}{2}kL)}{\sinh(\frac{1}{2}kL) \cos(\frac{1}{2}kL) + \cosh(\frac{1}{2}kL) \sin(\frac{1}{2}kL)} \right].$$

Throughout the preceding discussion you must keep in mind that the denominator in Eqs. (17), (18), and (19) can go to zero. That situation means the beam will be in resonance, and the acceleration in g's and a per-pound basis can get very large.

Now let me do a frequency sweep from 3 to 45 Hz with the example beam. Figure F-6 shows the maximum vibratory acceleration in g's per pound of  $\sqrt{F_{\sin}^2 + F_{\cos}^2}$  versus frequency in cycles per second (i.e., hertz). Because I have not included structural damping in the discussion, you can see that the maximum acceleration can be extremely large around frequencies of 7 and 37 Hz. In fact, this simple mathematical analysis gives an infinite acceleration, but I limited my choice of frequencies to graph in order to emphasize the danger of resonance. At a vibratory frequency of 6 Hz (recall Fig. F-4), a resultant force (i.e.,  $\sqrt{F_{z\sin}^2 + F_{z\cos}^2}$ ) of 1,000 pounds will produce  $\pm 0.8632$  g acceleration at the beam's nose.

Because I used this elementary beam as a model for the full-scale Sikorsky UH-60, it is worth a moment to calculate the response for the UH-60's four-bladed rotor. This rotor's normal speed is 258 rpm, which is 4.3 Hz. At that speed, the rotor might create vertical vibration at once per revolution (i.e., 4.3 Hz), four per rev (17.2 Hz), and probably eight per rev (34.4 Hz). Figure F-6 notes these frequencies with large, solid black symbols. Now let me guess that the vertical vibratory forces at each of these frequencies is  $\pm 100$  pounds,  $\pm 1,000$  pounds, and  $\pm 500$  pounds, respectively. Then, the acceleration at the nose would be as shown in Table F-2.

Of course, the example beam can be vibrated by forces other than vertical. Now consider a horizontal force acting above the beam's center of gravity (c.g.), which is at the half span of the beam.

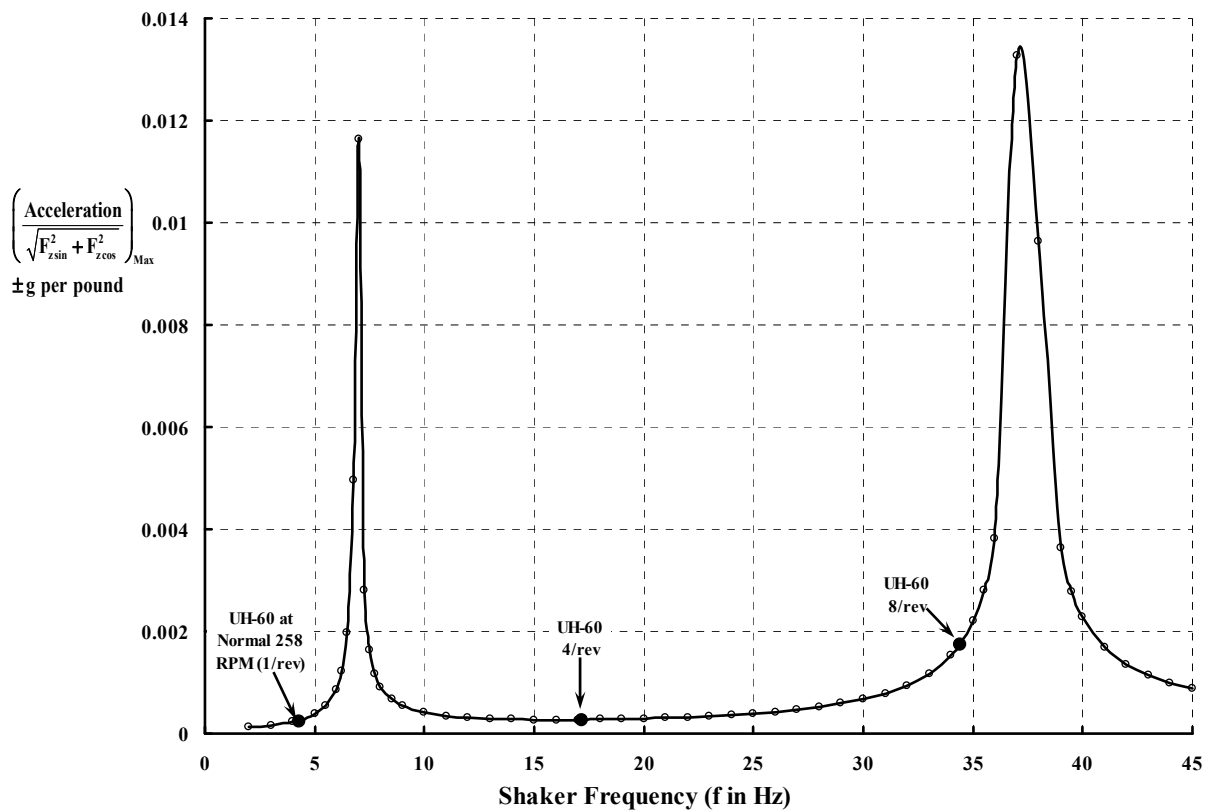


Fig. F-6. Nose maximum acceleration response to vertical vibratory response of the example beam.

Table F-2. Vertical Force Response

UH-60 Rotor	Vertical Force (lbs) and Frequency (Hz)	Nose Acceleration Per Fig. F-6	Nose Acceleration (g)
1/rev	100 at 4.3	0.000229	0.023
4/rev	1,000 at 17.2	0.000270	0.270
8/rev	500 at 34.4	0.001746	0.873

**Beam Response to a Horizontal Vibratory Force Acting Above the Beam's c.g.**

When a horizontal force ( $F_x$ ) is applied at some distance ( $h$ ) above the example beam's c.g., say at a height of 5 feet, the beam has a vibratory moment acting on it. Figure F-2 illustrates the geometry. The mathematics of this example parallels the preceding discussion. In fact, the starting point (the beam equation) is Eq. (2), which is repeated here for convenience

$$(2) \quad EI \frac{\partial^4 z_{\ell,t}}{\partial \ell^4} = -m \frac{\partial^2 z_{\ell,t}}{\partial t^2}.$$

The same assumed solution works again, but with the horizontal force being applied at a distance ( $h$ ) so

$$(20) \quad z_{\ell,t} = [\bar{A} \cosh(k\ell) + \bar{B} \sinh(k\ell) + \bar{C} \cos(k\ell) + \bar{D} \sin(k\ell)](hF_x),$$

and the horizontal vibratory force ( $F_x$ ) in pounds is defined as

$$(21) \quad F_x = F_{x\sin} \sin(\omega_h t) + F_{x\cos} \cos(\omega_h t) = \sqrt{F_{x\sin}^2 + F_{x\cos}^2} \sin \left[ \omega_h t + \arctan \left( \frac{F_{x\cos}}{F_{x\sin}} \right) \right].$$

Furthermore, the beam constant ( $k$ ) that was obtained with Eq. (8) is valid, so keep in mind that  $k = \left( \frac{m\omega_h^2}{EI} \right)^{1/4}$ , and remember that the shaking frequency ( $\omega_h$ ) is in radians per second.

The question again becomes one of finding out what  $\bar{A}$ ,  $\bar{B}$ ,  $\bar{C}$ , and  $\bar{D}$  equal. These constants are found from the boundary conditions, which are values associated with the center of the beam and the free end of the beam. At the free end of the beam where  $\ell = L/2$ , no forces or moments are applied. These are the same conditions applied with the vertical force vibration studied above. At the center of the beam ( $\ell = 0$ ), the boundary conditions are different because a moment equal to  $hF_x/2$  is applied. In this moment case, the loading is zero at the beam center, which means the deflection is also zero. Therefore, you have four equations in the four unknowns ( $\bar{A}$ ,  $\bar{B}$ ,  $\bar{C}$ , and  $\bar{D}$ ) appearing as

$$(22) \quad \begin{aligned} (EI)k^2 [\bar{A} \cosh(kL/2) + \bar{B} \sinh(kL/2) - \bar{C} \cos(kL/2) - \bar{D} \sin(kL/2)](hF_x) &= 0 \quad \text{moment} \\ (EI)k^3 [\bar{A} \sinh(kL/2) + \bar{B} \cosh(kL/2) + \bar{C} \sin(kL/2) - \bar{D} \cos(kL/2)](hF_x) &= 0 \quad \text{shear} \\ (EI)k^2 [\bar{A} - \bar{C}](hF_x) &= hF_x/2 \quad \text{moment} \\ [\bar{A} + \bar{C}](hF_x) &= 0 \quad \text{deflection} \end{aligned}$$

From these four equations, it is immediately clear that  $\bar{C} = -\bar{A}$  and that  $\bar{A} = \frac{1}{4k^2(EI)}$ .

With values for  $\bar{A}$  and  $\bar{C}$ , you have reduced the problem to two equations in two unknowns ( $\bar{B}$  and  $\bar{D}$ ), and these constants are found as

$$\bar{B} = \frac{1}{4k^2 (EI)} \left[ \frac{\cosh(kL/2)\cos(kL/2) - \sinh(kL/2)\sin(kL/2) + 1}{\cosh(kL/2)\sin(kL/2) - \sinh(kL/2)\cos(kL/2)} \right] \tag{23}$$

$$\bar{D} = \frac{-1}{4k^2 (EI)} \left[ \frac{1 + \cosh(kL/2)\cos(kL/2) + \sinh(kL/2)\sin(kL/2)}{\cosh(kL/2)\sin(kL/2) - \sinh(kL/2)\cos(kL/2)} \right]$$

The equations for ( $\bar{B}$  and  $\bar{D}$ ) both contain a denominator that has the potential to go to zero given certain values of the product of  $k$  and  $L/2$ . However the transcendental equation from which the critical roots are found in the applied vibratory moment case is noticeably different— it is the difference between the hyperbolic tangent and the tangent. That is,

$$\tanh(kL/2) - \tan(kL/2) = 0. \tag{24}$$

A graph of this difference versus  $kL = (\frac{m\omega_H^2 L^4}{EI})^{1/4}$  is shown in Fig. F-7. The roots of Eq. (24) are shown in Table F-3.

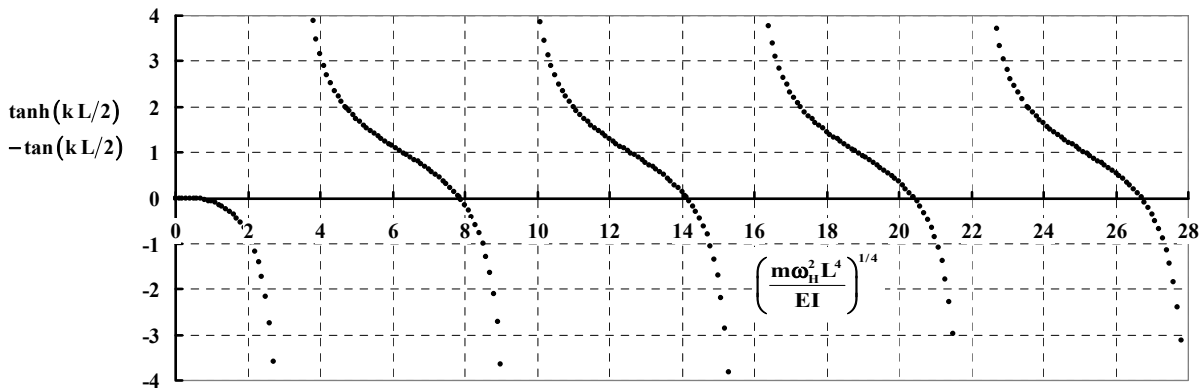


Fig. F-7. Roots of Eq. (24) found graphically.

Table F-3.  $kL$  Values to Be Avoided

Root Number	Value of $kL$
1	7.853204624096
2	14.13716549125
3	20.42035224561
4	26.70353755551

APPENDIX F

Because the hyperbolic tangent of large numbers becomes virtually 1.0, the roots at 4 and beyond are found, with adequate engineering precision, from

$$(25) \quad kL = (m\omega_H^2 L^4 / EI)^{1/4} = \frac{\pi}{2} [4(\text{Root No.}) + 1].$$

The importance of Eq. (24) cannot be overstated because it defines the frequency ( $\omega_H$ ) at which response (say deflections or accelerations) of this uniform beam will be extreme. Of course, this does not happen in practice because there is always some structural damping, which I have not considered in this example.

Now let me shake this example beam with an applied moment ( $hF_x$ ) of 500 foot-pounds. I will select a shaker frequency of 18 cycles per second because this value is close to resonance for the example beam. The beam's response is calculated as

$$(26) \quad z_{\ell,t} = [\bar{A} \cosh(k\ell) + \bar{B} \sinh(k\ell) + \bar{C} \cos(k\ell) + \bar{D} \sin(k\ell)] (hF_x) \sin(\omega_H t),$$

and the maximum deflection will occur when  $\sin(\omega_H t)$  equals  $\pm 1.0$ . The beam's response for this shaker frequency is shown in Fig. F-8. In this figure, the solid lines goes with  $\sin(\omega_H t) = +1.0$  and the dash lines go with  $\sin(\omega_H t) = -1.0$ . The applied moment is 500 pounds. Keep in mind that the deflection is directly proportional to the applied moment, so the shape shown in Fig. F-8 can be scaled to any other applied moment.

Now let me again perform a frequency sweep from 3 to 45 Hz with the example beam. For the sake of contrast, I will add the maximum acceleration due to a vibratory horizontal force (really a moment caused by this force acting above the beam's c.g.) calculated by Eq. (28) to Fig. F-6, which showed the maximum vibratory acceleration in g's per pound of vertical force versus frequency in cycles per second. The composite result is shown in Fig. F-9.

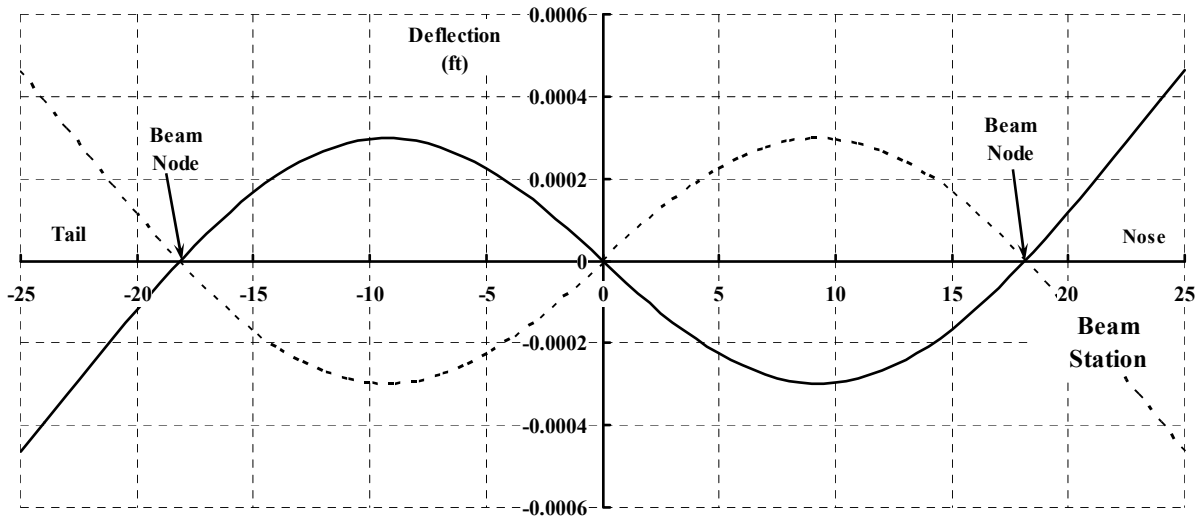


**Fig. F-8. Beam vibratory maximum deflection extremes. Forcing frequency of 18 Hz, moment of  $hF_x = 500 \sin(\omega_H t)$ .**

$$(27) \left[ \left( \frac{1}{\sqrt{F_{x\sin}^2 + F_{x\cos}^2}} \right) \frac{\partial^2 z_{(t=L/2,t)}}{\partial t^2} \right]_{MAX} = \pm h \left( \frac{\omega_H^2}{2gk^3EI} \right) \left[ \frac{\sinh(\frac{1}{2}kL) + \sin(\frac{1}{2}kL)}{\sinh(\frac{1}{2}kL)\cos(\frac{1}{2}kL) - \cosh(\frac{1}{2}kL)\sin(\frac{1}{2}kL)} \right].$$

Suppose the horizontal force is created by the Sikorsky UH-60, four-blade rotor system. And suppose the horizontal forces at once per revolution (i.e., 4.3 Hz), four per rev (17.2 Hz), and eight per rev (34.4 Hz) are ±100 pounds, ±1,000 pounds, and ±500 pounds, respectively. Then, the acceleration at the nose would be as shown in Table F-4. This result may be directly compared to the response to the same vertical vibratory forces given in Table F-2.

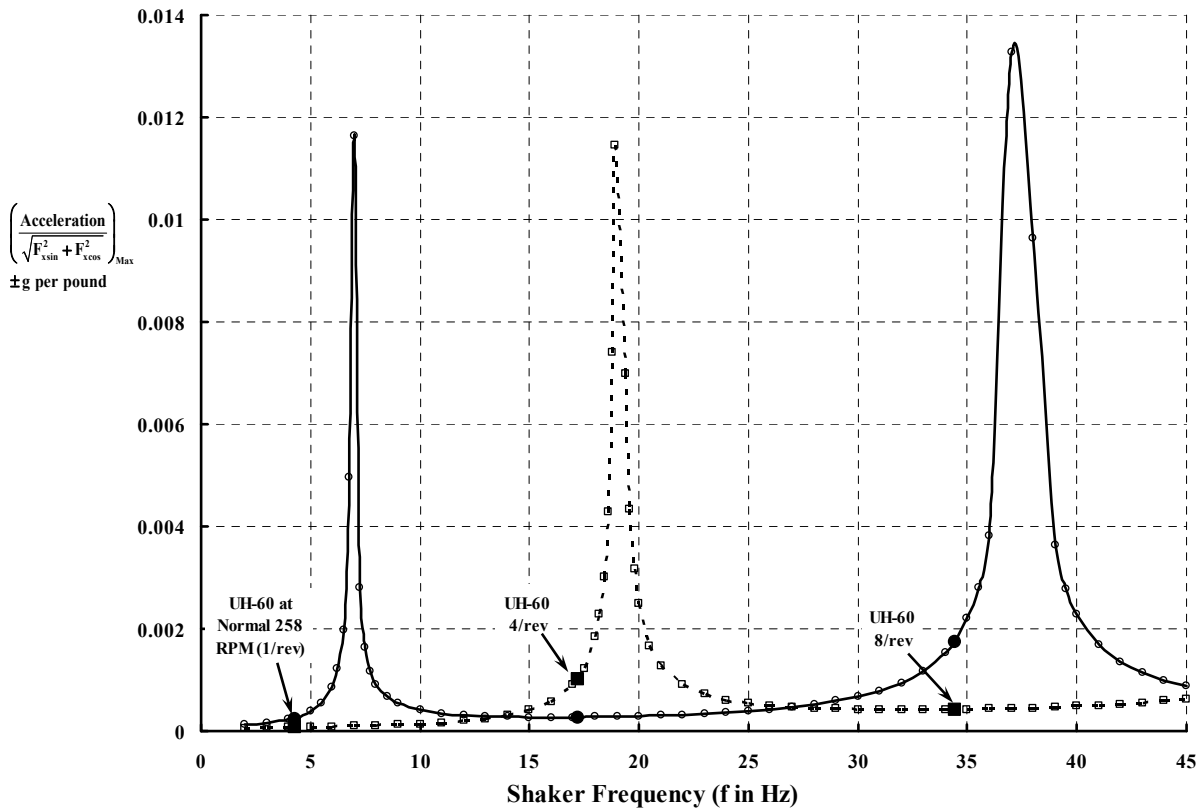


**Fig. F-9.** Nose maximum acceleration responses of the example beam to vertical vibratory force (solid line) and horizontal vibratory force (dashed line), which creates a vibratory moment. Horizontal force acts 5 feet above the beam’s c.g.

**Table F-4.** Response to Horizontal Force Acting 5 Feet Above the Beam’s c.g.

UH-60 Rotor	Horizontal Force (lbs) and Frequency (Hz)	Nose Acceleration Per Fig. F-6	Nose Acceleration (g)
1/rev	100 at 4.3	0.000073213	0.007
4/rev	1,000 at 17.2	0.001011340	1.011
8/rev	500 at 34.4	0.000417755	0.209

**Simultaneous Application of Rotor Hub Forces and Moments**

It should now become clearer that a rotor shaking an airframe has more than a few factors influencing just what the structural and human response might be. To help in this understanding, recognize that the rotor hub can shake with three forces (vertical, horizontal, and lateral) and the corresponding three moments. This makes a total of six loads to consider. But then each load can have, at a minimum, sine and cosine components. For a four-bladed rotor such as the Sikorsky UH-60, this means sine and cosine values at 1 per rev, 4 per rev, and probably 8 per rev. The amount of required numbers is growing rapidly before an accurate calculation of even my simple beam’s response can be obtained.

Perhaps Table F-5 puts the problem in the proper perspective. There are 36 values to be accurately obtained. If you consider that there are no perfectly matched blade sets, then the Sikorsky UH-60 would need contributions to hub forces and moments from each blade individually, which becomes a daunting task—to put it mildly.

Of course, having the hub loads is only half the battle. How a complicated beam such as a real helicopter is going to respond—even to perfectly calculated hub loads—is pure conjecture. As I write this during April 2012, neither half of the problem has been solved by any member of the rotorcraft community. There is, however, no doubt in my mind that it will be done.

**Table F-5. A Bare Minimum of 36 Hub Force and Moment Components Must Be Accurately Obtained Before a Prediction of Helicopter Vibration Is Possible**

<b>Parameter</b>	<b>Vertical Force</b>	<b>Horizontal Force</b>	<b>Lateral Force</b>	<b>Yawing Moment</b>	<b>Rolling Moment</b>	<b>Pitching Moment</b>
1/rev Sin						
1/rev Cos						
4/rev Sin						
4/rev Cos						
8/rev Sin						
8/rev Cos						

## APPENDIX G

This appendix contains my conversion of the original report from double-row spacing to single-row spacing to reduce the page count in Volume II. I have a PDF of the original or you may be able to find it on the internet.

ECONOMIC REPORT

# PROJECT HUMMINGBIRD

## THE HELICOPTER AND OTHER V/STOL AIRCRAFT IN COMMERCIAL TRANSPORT SERVICE

Growth to Date  
and Forecasted Growth  
to 1965 and 1970



**FEDERAL AVIATION AGENCY**

FEDERAL AVIATION AGENCY

THE HELICOPTER AND OTHER V/STOL AIRCRAFT  
IN COMMERCIAL TRANSPORT SERVICE

Growth to Date  
And Forecasted Growth  
to 1965 and 1970

Prepared by  
Economics Branch Office of Plans  
November 1960

## FOREWORD

Taking note of an advancing technology resulting in large part from research and development sponsored by the military services, and noting also the continuing active interest by the aviation community as a whole in steep-gradient aircraft, the Federal Aviation Agency has established a program bearing the name "Project Hummingbird" to investigate this field. The purpose of this effort is to provide FAA and the aviation community with planning guidance regarding the future role and utilization of steep-gradient aircraft in civil aviation.

The focus of this report, which is the first to be published under "Project Hummingbird," is on the uses of the helicopter and other vertical take-off and landing aircraft in short-haul commercial air transportation during the next ten years. Its basic objective is to develop forecasts both of the number of these aircraft which will be in airline service in 1965 and 1970 in the United States and of the number of passengers they will carry. The impending conversion of the helicopter airlines to multi-engine turbine powered equipment make a comprehensive evaluation of the role that steep-gradient aircraft will play in commercial air transportation during the next decade particularly timely. While small size helicopters have achieved a considerable use in patrol and survey work, aerial application and in business flying, such activity is more appropriately considered in the context of the overall general aviation uses of aircraft in business and industry.

The preparation of this report was materially aided by many individuals in industry and government. Members of the staffs of aircraft manufacturers, certificated airlines, the Civil Aeronautics Board, the Port of New York Authority, the National Aeronautics and Space Administration, and a number of experts privately employed contributed special background information and statistics for use herein. Industry replies to an FAA questionnaire also provided new information on V/STOL aircraft development and markets. Chicago Helicopter Airways, New York Airways and Los Angeles Airways each provided members of the FAA staff with an opportunity to observe scheduled helicopter operations at first hand. For this assistance and cooperation the FAA staff expresses its appreciation. It should be stated, however, that the responsibility for the forecasts and opinions presented herein, and for the particular analytical use made of the information which was made available by industry and Government sources, belongs solely with the FAA staff.

## TABLE OF CONTENTS

I. SUMMARY AND CONCLUSIONS	893
II. POTENTIAL SHORT-HAUL MARKETS FOR THE HELICOPTER AND V/STOL TRANSPORT AIRCRAFT	
Background	895
Nature of V/STOL Transport Aircraft	895
Extent of Federal Government Regulation	897
Identity of Types of Markets	897
General Aviation Uses	898
III. THE GROWTH OF COMMERCIAL TRANSPORT OPERATIONS TO 1960	
The Beginnings of Certificated Helicopter Services	899
Passenger Traffic Trends	900
Mail and Cargo	901
Passenger Traffic Pattern	902
Helicopter Passenger Trip Length	903
Passenger Load Factors	903
Operational Trends	904
Performance Factors	905
The Helicopter Fleet	906
Economic Trends	907
Unit Costs	907
Helicopter Direct Operating Costs	908
Summary of Record to Data	909
IV. THE METROPOLITAN MARKET, 1965–1970	
New Transport Aircraft	912
Unit Costs and Fares	914
Attitude of the Civil Aeronautics Board	915
Other Growth Factors	917
1965–1970 Passenger Traffic and Aircraft Fleet Forecasts	918
Air Taxi Operations	919
New Metropolitan Area Services	920
V. THE INTERCITY AND COMMUTER MARKETS, 1965–1970	
Short-Haul Intercity Travel	925
The Problem of Speed	927
The Cost Problem	929
The Commuter Market	931

## I. SUMMARY AND CONCLUSIONS

1. The unique characteristic possessed by the helicopter and V/STOL aircraft which distinguishes them from conventional aircraft and makes them ideally suited technically for the short-haul passenger markets is their ability to operate from small landing areas with steep approach and departure paths. Three types of short-haul passenger markets have generally been regarded as susceptible to development by the helicopter and V/STOL transport aircraft. They are: (1) the airport-metropolitan area market; (2) the short-haul intercity market. and (3) the commuter or intra-city market.
2. The transport helicopter is presently being used for scheduled, certificated airline service in the metropolitan areas of New York, Chicago and Los Angeles. Passenger traffic carried by the three helicopter airlines has grown rapidly, amounting to 366,000 passengers in calendar year 1959. However, operations are considered experimental as yet and all three helicopter airlines are dependent for their continued existence on Federal Government subsidy which provided 63 percent of total revenues in 1959.
3. The transport helicopter has achieved its greatest success in airline service as a special purpose vehicle transferring fixed-wing air passengers between airports in the Chicago and New York areas. There has been limited development of helicopter traffic between the airports and the downtown city centers and between the airports and suburban points in these two areas. In the Los Angeles area where there is only one major airline airport, helicopter traffic flow is between the airport and suburban communities but this market has grown at a slower rate than the airport shuttle services provided in New York and Chicago.
4. The high operating costs of the relatively small, single-engine, piston-powered helicopters currently in use have been the major problem confronting the helicopter airlines. The lowest direct operating cost achieved so far has been approximately 20 cents per available seat mile.
5. The impending re-equipment of the helicopter airlines with turbine-powered helicopters is expected to provide new impetus to traffic growth. There are now 21 multi-engine, turbine-powered helicopters on order or on option by the three operators with deliveries scheduled to begin in 1961.
6. Equipment purchase plans of the three helicopter airlines beyond 1964–1965 are not known at this time, but appear to depend on traffic growth and the availability of improved versions of the multi-engine, turbine-powered types of helicopters. Some interest has been reported in the compounded helicopter which may become available by 1965, but this aircraft still has cost and serious noise problems to overcome.
7. Direct operating costs of the new turbine-powered helicopters are estimated at 10 to 16 cents per available seat mile. However, even with these projected lower unit costs the helicopter airlines will be unable to achieve a self-sufficient operation. A continuing

## APPENDIX G

requirement for Federal subsidy appears in prospect at least until more economic helicopter types are forthcoming.

8. In addition to the stimulus provided by new equipment, passenger traffic of the helicopter airlines is expected to grow rapidly during the 1960–1970 period as a result of increasing fixed-wing traffic, greater penetration of the available market, and improved dependability of service. Airport shuttle service is expected to remain the mainstay of operations. It appears unlikely that helicopter fares will be reduced.
9. Traffic of the three helicopter airlines is forecast to increase from 366,000 passengers in 1959 to an estimated 1.2 million passengers by 1965 and to 2.0 million passengers by 1970. The number of helicopters in service with these airlines is forecast to increase from 24 at the close of 1959 to 30–32 by 1965, and to 40–45 by 1970.
10. Washington, D.C. and San Francisco/Oakland are the most likely metropolitan areas for new scheduled helicopter services. Other metropolitan areas which appear to have a potential requirement for scheduled helicopter services are Miami, Dallas/Fort Worth, Boston, Detroit, Atlanta, Cleveland, Pittsburgh, Philadelphia and St. Louis. However, the Civil Aeronautics Board, noting the increasing subsidy requirements of the presently certificated helicopter airline, is on record that it has no current intention to certificate additional helicopter airlines.
11. Penetration of the short-haul intercity passenger market by V/STOL aircraft operating between city centers depends on the availability of suitable aircraft and the necessary ground facilities. Such aircraft are still in a very early stage of development but might be available toward the close of the forecast period. While V/STOL city center operations can provide impressive time savings for many travelers, costs now projected for these aircraft appear to preclude fares which would be reasonably competitive with other means of transport.
12. Commuter travel by helicopter between suburban points and city centers seems likely to develop only to a very limited extent for the foreseeable future and then merely as an extension of service by existing metropolitan area helicopter operators.

## II. POTENTIAL SHORT-HAUL MARKETS FOR THE HELICOPTER AND V/STOL TRANSPORT AIRCRAFT

### Background

The continued domination of the short-haul passenger markets in the United States by surface means of transport is regarded by many as commercial aviation's greatest challenge. Although these markets have never been surveyed in their entirety, sample data have shown that the traffic carried by the airlines remains insignificant in comparison to the sum of the traffic carried by the railroads, bus lines and the private automobile. The efforts of the airlines since the end of World War II to penetrate these markets have not been without success, it should be noted. But the fact that the overwhelming majority of short-haul passengers today still travel by surface means of transport establishes the air traffic growth which has occurred to date as one of the few disappointments in the record of commercial aviation in the United States.

It has long been recognized that the key to successful entry into any of the short-haul passenger markets is a suitable transport vehicle. The challenge of the short-haul passenger markets is, therefore, a challenge primarily to the aircraft manufacturing industry. The potential for spectacular air traffic growth which exists in these markets has not been overlooked by the aircraft manufacturers. From their market and engineering research and from their experience in producing a variety of both military and civil short-range aircraft since the end of World War II, and particularly since the end of the Korean hostilities, there has evolved a conviction that the greatest promise of success in capturing significant shares of the short-haul passenger markets for air transportation lies in the development of helicopters and other V/STOL aircraft.

During the past two years market and engineering research directed towards the design and production of economically competitive types of these newer aircraft has become both more intense and more widespread within the aircraft manufacturing industry. The great spur to this increased activity has been the likelihood of large amounts of unused plant capacity and productive capability in the industry in the 1960's as requirements diminish for manned aircraft by the military services and for jet transports by the larger airlines of the world. Additionally, this activity has been spurred by a new promise of success—the availability of turbine-powered engine designs which are largely the outgrowth of military development and production.

### Nature of V/STOL Transport Aircraft

It is, of course, the flight characteristics of transport aircraft which determine the kind of markets in which they can operate. The unique characteristics possessed by the helicopter and other V/STOL aircraft which distinguish them from conventional aircraft and make them ideally suited technically for the short-haul passenger markets are their vertical or near vertical lift capability, and the attendant slow flight maneuver-ability and hovering ability. Because of these attributes helicopters and other V/STOL aircraft need no long runways to

## APPENDIX G

take off and land and can be operated from relatively small areas. These areas obviously can be located with far greater freedom than the large airports required by conventional aircraft—in city centers, for example, or at other locations close to the true origin and destination of travelers. V/STOL aircraft are singularly capable, therefore, in theory at least, of freeing air travel from one of its most serious handicaps—the requirement it places on the traveler to make time consuming trips to and from an airport. This requirement is most onerous to the travelers making short trips.

In actual commercial transportation, it should be noted, the vertical lift capability of helicopters is not used to ascend to and descend from cruising altitudes. Although the helicopter is capable with limitations of vertical ascent to, and descent from, any desired height, and can hover in a stationary position before commencing horizontal motion, the factors of safety, load capacity and economy of operation dictate an angular ascent and descent. Thus, in takeoffs, for example, a vertical rise of only three to ten feet is generally made, after which horizontal acceleration is begun. The forward speed then provides additional lift. Multi-engine helicopters, however, will have the safe capability to increase the vertical portion of their takeoff and landing and this ability may be utilized in clearing obstacles and in making landings and takeoffs under zero-zero visibility conditions.

It may be assumed that other V/STOL aircraft, when operational in commercial transport service, will also ascend and descend angularly. But it is in no way required that the angle be comparable to that required for conventional aircraft. The result is that the area required for takeoff and landing for steep-gradient aircraft will always be small compared to the area required for takeoff and landing of conventional aircraft.

It is the hope of the aviation industry that the new turbine-powered engines now becoming available will enable helicopters and other V/STOL aircraft to compete economically in the short-haul passenger markets to support the technical advantage provided by their vertical lift capability. However, a difficult problem in achieving profitable commercial operations exists for these aircraft because of the price paid for this lift capability. At their present stage of development helicopters are small, slow, and complex. But more importantly, they are expensive to purchase and to operate. It may be expected that the handicap of complexity will always exist for the helicopter, and for the newer V/STOL aircraft, but that this will not be a crippling handicap. It may also be expected that engineering developments will overcome the problems of small size and slowness. The degree of success helicopters and other V/STOL aircraft achieve in commercial transport will depend, therefore, largely on the extent to which advances in engine design eliminate the handicaps of high initial and high operating costs. The requirement is not necessarily that these costs be reduced to a level below that of competing vehicles, but rather to a level which will enable them to compete on the basis of service.

## **Extent of Federal Government Regulation**

A factor important to the commercial transport use, of helicopters and other V/STOL aircraft is that of Federal Government regulation. The method of this regulation is the same as that which applies to fixed-wing aircraft. In order to offer scheduled V/STOL air transport service in interstate commerce,<sup>1</sup> the applicant operator must obtain from the Civil Aeronautics Board a certificate of public convenience and necessity. The authority to grant such certificates is given the Board under Section 401 of the Federal Aviation Act of 1958. The aircraft operator, or the airline, which receives a certificate of public convenience and necessity is then subject to the Board's authority over almost all phases of its operation—routes served, schedules operated, fares charged, agreements entered into, etc. It is required to submit traffic and financial reports periodically. The certificate which is granted by the Board specifically authorizes the carriage of passengers or cargo or United States mail, or some combination of the three, and may or may not provide for eligibility to receive Federal Government subsidy upon establishment of need under honest, efficient and economical airline management. At the present time only three airlines have been awarded certificates providing subsidy eligibility for scheduled helicopter passenger, mail and cargo operations in the United States. Approximately 75 additional applications for certificates are on file with the Civil Aeronautics Board.

Any operator or airline proposing to provide scheduled or charter transport service solely with aircraft having a certificated take-off weight of 12,500 pounds or less is not required to obtain a certificate of public convenience and necessity from the Civil Aeronautics Board. Part 298 of the Board's economic regulations exempts the operators of these aircraft in commercial transport service from the requirements of Section 401 of the Federal Aviation Act of 1958. The Board does not require any traffic or financial reports of these operators, and allows them to operate generally without restrictions except for routes. They are not authorized to carry United States mail and are not eligible for Federal Government subsidy. However, such operators must obtain an air taxi operating certificate from the Federal Aviation Agency. This certificate is granted only after FAA inspects the operator's aircraft and facilities and determines that they meet the safety requirements of the Civil Air Regulations. At the end of 1959 there were in the United States about 2,300 air taxi operators, of which 71 were utilizing helicopters.

## **Identity of Types of Markets**

It is the consensus of opinion in the aviation industry that three types of short-haul passenger markets are susceptible to development by steep-gradient aircraft because of their ability to operate from small areas. These markets are:

1. The aerobus market; sometimes referred to as the aerocab or aerolimousine market; it consists of travel between a Community airport and its business or commercial

---

<sup>1</sup> It should be noted that the service may physically be intrastate but if it links interstate commerce, it is legally defined as interstate commerce.

## APPENDIX G

centers, and of travel between airports of those larger communities having more than one air commerce airport.

2. The intercity market; it consists of travel of less than 250 miles between city centers, and of feeder travel into and out of large community airports.
3. The commuter market; sometimes referred to as the suburban market; it consists of travel of some 15 to 50 miles between the downtown areas of a community and its surrounding or adjacent suburbs.

It is apparent that in terms of distances these markets overlap. But their classification is based on the function of the travel rather than the travel distance. The distances are not regarded as rigidly defined. For example, the intercity market is sometimes defined to include travel of less than 200 miles to fit an aircraft type under consideration, and sometimes, for other aircraft types being considered, to include travel of 300 to 400 miles. The commuter market, too, is sometimes defined to include travel of not only from 15 to 50 miles but also from 5 to 75 miles.

### **General Aviation Uses**

Although the focus of this report is on the usage of helicopters and V/STOL aircraft in commercial transport service, it should be noted that the helicopter has played a modest but increasing role in general aviation in the last several year. As of January 1, 1960, there were 525 active helicopters in a total general aviation fleet of 68,727 aircraft. This number compares with 237 helicopters four years earlier.

The more important general aviation uses of the helicopter include patrol and survey work, petroleum and mineral prospecting, detailed mapping in rugged terrain, police traffic control and search and rescue. A number of helicopters are also being used by corporations for the movement of personnel between offices and plants in congested metropolitan areas and by petroleum companies for transportation to off-shore drilling stations as well as for other corporate purposes. Other uses include the aerial treatment of crops and land and passenger and cargo transportation for hire in many varied activities. Use of the helicopter in air taxi services is discussed in greater detail in a later section of the report.

It is generally anticipated that because of its unique operating characteristics and its ability to do special tasks which cannot be performed by conventional aircraft, usage of the helicopter in general aviation will expand significantly. Despite this growth their wide geographic dispersion and the nature of their use, much of which is in thinly populated areas, would appear to limit their potential impact on the air traffic control and navigation system except insofar as air taxi operations and corporate usage in metropolitan areas increase. However, the certification of engines and airframes and the development of appropriate operational rules and regulations will represent a sizeable workload.

### III. THE GROWTH OF COMMERCIAL TRANSPORT OPERATIONS TO 1960

#### The Beginnings of Certificated Helicopter Services

Only the helicopter has operated as a V/STOL aircraft in commercial transport service in the United States to date. Other transport V/STOL aircraft—the compounded helicopter and the convertiplane, for example, have at present advanced no farther than the prototype stage.

All transport helicopters now in commercial use are an outgrowth of military development and production. The first practical helicopter, as it is known today, was flown experimentally in the United States by its designer, Igor Sikorsky, in 1939—21 years ago. It won the immediate interest of the United States Army and, in the form of subsequent models, was used to a minor extent during World War II. The first transport helicopter was flown in 1945 but it was not until the Korean War that the helicopter won widespread notice as an important transport vehicle. Its success on missions of supply, reconnaissance and mercy over difficult terrain spurred its development and established the Army as the largest single purchaser of helicopters, a position it holds to this day.

Commercial transport use of the helicopter followed on the heels of military use. The Civil Aeronautics Board scheduled its first prehearing conference on a helicopter application for a certificate of convenience and necessity to operate scheduled service as long ago as 1944. The hearing was postponed because the war was still in progress and no helicopters for civilian use were available. But the applicant in that case, Los Angeles Airways, was awarded a certificate by the Board in 1947 to operate scheduled helicopter mail and property service. Since that first award the Board has granted certificates to Chicago Helicopter Airways and to New York Airways to conduct scheduled helicopter service for passengers as well as for property and mail, and has amended the certificate of Los Angeles Airways to allow the carriage of passengers.

TABLE 1.  
DATES OF CERTIFICATION AND INAUGURATION OF SERVICE,  
CERTIFICATED HELICOPTER AIRLINES

Item	Los Angeles Airways	Chicago Helicopter Airways	New York Airways
<u>Effective Date of Certificate for:</u>			
Mail and property	Oct. 1947	July 1949	March 1952
Passengers	Oct. 1951	August 1956	March 1952
<u>Date Scheduled Service Began for:</u>			
Mail and property	Oct. 1947	Sept. 1949	Oct. 1952
Passengers	Nov. 1954	Nov. 1956	July 1953

## APPENDIX G

Each of the certificates awarded these three airlines provided for subsidy payments. In 1947 the Board also certificated the Yellow Cab Company of Cleveland, Ohio to carry passengers and property, but not mail, between the city airport and its downtown area. No operations were ever conducted, however, apparently because the non-mail certificate meant no subsidy, and the certificate expired. Only two airlines in the United States have offered scheduled passenger service in helicopters without specific subsidy support from the Civil Aeronautics Board. National Airlines, a trunk airline, operated an experimental helicopter service in Florida in 1954 as an adjunct to its regular scheduled passenger operations. In the same year Mohawk Airlines, a local service airline, operated a scheduled passenger helicopter service over one of its routes originating at Newark Airport. Both these airlines abandoned their helicopter operations.

Because Federal Government regulation requires periodic and detailed traffic and financial reporting from the certificated airlines, a substantial body of data on commercial helicopter operations is available for the three helicopter airlines now offering scheduled transport service in the metropolitan areas of Los Angeles, Chicago and New York. The experience accumulated by these airlines since 1947 provides a valuable insight into the future of the commercial transport helicopter and to a lesser extent other V/STOL aircraft; accordingly a comprehensive examination of this record follows.

### **Passenger Traffic Trends**

In general, the three certificated helicopter airlines have been authorized to provide service within a 50 to 60 mile radius of the metropolitan areas in which they operate. Within these areas they offer service from airport to airport and between airports and business centers. In addition, service is provided to suburban communities which fall within their authorized area of operations. In total the three airlines provided service to about 60 locations in 1959.

Although scheduled helicopter service was initially established for the purpose of carrying mail and property, the carriage of passengers, subsequently authorized, quickly became the most important form of traffic. Since its beginning, passenger traffic has shown a sharply rising growth trend; in calendar year 1959 366,000 passengers were flown 7.5 million passenger miles. This volume is small compared to the domestic trunk line volume (44.5 million passengers) and to the local service volume (5.2 million passengers), but for the three helicopter airlines it represented an increase of 60 percent over the number of passengers carried in calendar year 1958.

Measured by passenger traffic, Chicago Helicopter Airways is by far the largest of the three helicopter airlines, with New York Airways the next largest and Los Angeles Airways the smallest. CHA's passenger traffic between Midway and O'Hare airports boomed with the inauguration of jet flights at O'Hare, and total passenger traffic in 1959 was nearly four times the 1957 level. During the same period helicopter passenger traffic increased 76 percent in New York and 40 percent in Los Angeles. Passengers now account for 84 percent of the total revenue ton miles flown by the three helicopter airlines. Table 3 shows the passengers carried by each of the airlines during the past three years.

**TABLE 2.**  
**DOMESTIC SCHEDULED AIRLINE PASSENGER TRAFFIC, 1959**

Airline Group	Revenue Passengers (Originations) (000)	Revenue Passenger Miles (000,000)
Trunk	44,489	28,127.2
Local Service	5,213	1,023.5
Helicopter	366	7.5
TOTAL	50,068	29,158.2

**TABLE 3.**  
**REVENUE PASSENGERS CARRIED BY CERTIFICATED HELICOPTER AIRLINES, 1957-1959**  
**(000 omitted)**

Year	Total	Chicago	Los Angeles	New York
1957	153	55	30	68
1958	229	108	31	90
1959	366	204	42	120

### Mail and Cargo

While the passenger traffic has been rising, the volume of U. S. mail has been declining fairly steadily. In 1959 some 87,000 ton miles of mail were flown or 30 percent less than in 1953. The decrease appears partly due to the greater concentration of the carriers on their growing passenger traffic and the fact that they are scheduling their operations more to meet the needs of the passengers than the mail service. During periods of peak mail loads, the helicopter carriers have been unable to handle all of the traffic offered and the Post Office has been forced to divert mail traffic to trucks. Additionally, the helicopter carriers have cut back mail routes. Chicago Airways discontinued service between the airport and the downtown Chicago Post Office while New York Airways is no longer providing service to a considerable number of outlying communities it formerly served.

Freight and express are a relatively minor part of the helicopter airline traffic, constituting less than 7 percent of total revenue ton miles flown. In 1959 traffic totaled 48,000 ton miles, an increase of one-third since 1955. Chicago Airways does not carry either freight or express and Los Angeles does not handle freight.

Table 4 shows traffic trends of the three certificated helicopter air carriers since 1953.

**TABLE 4.**  
**TOTAL TRAFFIC CARRIED BY CERTIFICATED HELICOPTER AIRLINES,**  
**1953–1959**

<b>Year</b>	<b>Revenue Passengers (000)</b>	<b>Revenue Passenger Miles (000)</b>	<b>Mail Ton Miles (000)</b>	<b>Freight and Express Ton Miles (000)</b>	<b>Total Revenue Ton Miles (000)</b>
1953	1	26	123	1	
1954	8	183	115	16	150
1955	28	628	97	36	194
1956	63	1,585	90	42	282
1957	153	3,275	92	40	449
1958	229	4,885	83	38	594
1959	366	7,477	87	48	857

### **Passenger Traffic Pattern**

Although origin and destination data on helicopter passenger traffic are not available, an analysis of passenger originations provides a reasonably good indication of the passenger traffic pattern of the three helicopter airlines. Approximately 85 percent of the passengers carried in 1959 originated at major scheduled airline airports. Only 6.5 percent of the passengers carried originated in the downtown city centers, and the remaining 8.2 percent originated at other points within the metropolitan areas served.

The distributions of passenger traffic by origin points indicate that in Chicago and New York most of the helicopter passenger traffic is between terminal airports—between Midway and O’Hare airports in Chicago and between Idlewild, LaGuardia and Newark airports in New York. A relatively small portion of the traffic moves between the city centers (West 30th Street in New York and Meigs Field in the Chicago Loop) and the major airports, and between other locations in the New York and Chicago metropolitan areas and the airports or downtown.

The traffic pattern in Los Angeles is somewhat different because of the widely dispersed business and residential areas and the fact that the metropolitan area has only one major airline airport. There the traffic is between Los Angeles International Airport and approximately 15 communities in the metropolitan area, the largest of which in terms of originated passengers is Anaheim. No passenger service between the airport and downtown Los Angeles is provided by Los Angeles Airways.

Table 5 shows the concentration of helicopter passenger originations at the major terminal airports, and the limited development of traffic at the downtown city centers and at other communities in the metropolitan areas served.

**TABLE 5.**  
**HELICOPTER PASSENGER ORIGINATIONS IN 1959,**  
**CERTIFICATED HELICOPTER AIRLINES**

Originating Point	Total		Los Angeles		Chicago		New York	
	Number	Percent	Number	Percent	Number	Percent	Number	Percent
Terminal Airport	312,640	85.3	20,252	48.5	177,449	86.8	114,939	95.6
Downtown City Center <sup>(1)</sup>	23,750	6.5	–	–	20,903	10.2	2,847	2.4
Other Area Communities	29,925	8.2	21,484	51.5	6,037	3.0	2,404	2.0
Total	366,315	100.0	41,736	100.0	204,389	100.0	120,190	100.0

1. Includes Meigs Field, Chicago.

### Helicopter Passenger Trip Length

As is to be expected, distances traveled by passengers over helicopter routes are extremely short. The average helicopter passenger trip in 1959 was 20.4 miles. As is shown in the table below, however, Los Angeles Airways with an average passenger trip length of 35.4 miles was significantly higher than the average. Available information reveals that there has been little change in recent years in the length of the average passenger trip of each of the helicopter carriers.

**TABLE 6.**  
**AVERAGE LENGTH OF HELICOPTER PASSENGER TRIP (MILES)**  
**1958–1959**

Airline	1959	1958
Chicago	17.9	18.4
Los Angeles	35.4	37.7
New York	19.4	19.2
3-Airline Average	20.4	21.3

### Passenger Load Factors

The increase in passenger traffic has been accompanied by a steady improvement in the revenue passenger load factor. Load factors for the three operators averaged 51.5 percent in 1959 compared with 40.3 percent in 1957 and 25.6 percent in 1954. Los Angeles Airways which had a 56.4 percent load factor in 1959 has consistently recorded the highest load factor of the three carriers largely because of the limited capacity it has offered and the small size helicopters it has been operating.

The 1959 load factors of the helicopter operators were substantially higher than the 44.3 percent average of the local service airlines but were still well below the trunk line average of 61.4 percent. As traffic and the capacity of equipment utilized increased, the average passenger load per aircraft also rose.

**TABLE 7.**  
**REVENUE PASSENGER LOAD FACTOR LOAD AND PASSENGER**  
**LOAD PER AIRCRAFT, CERTIFICATED HELICOPTER AIRLINES**  
**1953-1959**

Year	Revenue Passenger Load Factor	Passenger Load Per Aircraft
1953	13.67%	0.38
1954	25.6	1.03
1955	36.8	1.44
1956	44.5	2.26
1957	40.3	3.05
1958	42.8	3.93
1959	51.5	5.00

### Operational Trends

Both the aircraft miles flown and the number of aircraft departures made by the helicopter carriers have registered substantial increases since 1953. However, their rate of growth has been appreciably less than that of traffic carried because of steady increases in the size of helicopter utilized and in the passenger load factor. In 1959 a total of 1,899,000 revenue aircraft miles were flown, up 89 percent from 1953, while aircraft departures totaled 138,000 or 53 percent more than in 1953. Comparatively, revenue ton miles flown rose by 564 percent during the same period.

Because of the nature of the route patterns being operated, the average flight stage of the helicopter operators is very short. In 1959 the average hop was 13.7 miles with Los Angeles Airways' average flight somewhat longer than either New York's or Chicago's. The short stages being flown, of course, contribute significantly to the high cost of current helicopter operations.

Although aircraft operations by the helicopter operators represent only a minute fraction of the total aircraft operations handled by FAA airport traffic control towers, they represent a fairly sizeable proportion of the landings and take-offs at the major airports in New York, Chicago and Los Angeles. At these high density airline terminals helicopter aircraft operations constitute 5 to 13 percent of the total aircraft operations. At Meigs Field, which is a leading helicopter traffic point but is not served by any domestic trunk or local service airline, helicopter aircraft operations account for 18 percent of all operations handled.

**TABLE 8.**  
**REVENUE AIRCRAFT MILES FLOWN, AIRCRAFT DEPARTURES, AND**  
**AVERAGE FLIGHT STAGE, CERTIFICATED HELICOPTER AIRLINES**  
**1953-1959**

<b>Year</b>	<b>Revenue Aircraft Miles Flown (000)</b>	<b>Aircraft Departures (000)</b>	<b>Average Flight Stage (miles)</b>
1953	1,006	90	11.2
1954	1,071	90	12.0
1955	1,152	94	12.3
1956	1,317	104	12.7
1957	1,603	126	12.7
1958	1,675	127	13.3
1959	1,899	138	13.7

**TABLE 9.**  
**SCHEDULED AIRLINE HELICOPTER AIRCRAFT OPERATIONS AS A PERCENT**  
**OF TOTAL AIRCRAFT OPERATIONS AT MAJOR AIRPORTS IN 1959**

<b>Airport</b>	<b>Total Aircraft Operations</b>	<b>Helicopter Aircraft Operations<sup>(1)</sup></b>	<b>Percent Scheduled Helicopter</b>
La Guardia	274,732	27,610	10.0
Newark	187,099	13,938	7.4
New York International	239,836	13,132	5.5
Meigs	106,791	19,384	18.2
Midway	431,600	34,788	8.1
O'Hare	234,983	30,164-	12.8
Los Angeles International	316,068	22,708	7.2

1. Estimated by multiplying departures by two.

### **Performance Factors**

The growth of helicopter traffic appears to have been adversely affected by the relatively poor schedule reliability maintained. The best available measure of dependability of operations is the performance factor which is the ratio of scheduled aircraft miles completed to aircraft miles scheduled. During the past three years the performance factor of the helicopter operators averaged 88 percent. Comparatively the domestic trunk lines and local service carriers averaged over 97 percent during the same period.

**TABLE 10.**  
**COMPARISON OF PERFORMANCE FACTORS, CERTIFICATE HELICOPTER,**  
**TRUNK AND LOCAL SERVICE AIRLINES**  
**1955-1959**

Year	Helicopter Airlines	Trunk Airlines	Local Service Airlines
1955	85.9%	97.8%	97.5%
1956	85.9	96.4	96.7
1957	88.0	97.5	96.7
1958	88.5	96.6	97.5
1959	88.0	97.4	97.2

The performance factors of the three helicopter carriers has varied widely. Chicago has consistently had the highest percentage of completions with 96.4 percent in 1958 and 93.6 percent in 1959, thus comparing favorably with the fixed-wing operators. Los Angeles completed 89.7 percent of its scheduled mileage in 1959. New York has regularly made the poorest showing in this area with a performance factor of only 76.5 percent in 1959. The primary cause of this relatively unfavorable record appears to have been the inability to fly during bad weather conditions. Maintenance problems appear to have been a contributing although less significant factor.

**TABLE 11.**  
**PERFORMANCE FACTORS, CERTIFICATED HELICOPTER AIRLINES**  
**1955-1959**

Year	Chicago	Los Angeles	New York
1955	97.1%	89.4%	82.1%
1956	94.2	89.0	77.2
1957	92.9	90.9	79.8
1958	96.4	87.2	78.6
1959	93.6	89.7	76.4

### **The Helicopter Fleet**

At the end of 1959 the fleet of the three helicopter airlines consisted of 24 piston-powered helicopters, an increase of five aircraft since 1955. The period was marked by the introduction into service of the 12 passenger S-58 in 1956 and by the 15 passenger Vertol 44-B in 1958. The smaller Bell 47's continued in operation. Although both Chicago and New York Airways made changes in the composition of their fleets during the period, Los Angeles Airways made no change either in the number or type of helicopters operated (2 S-51's and 5 S-55's). The tabulation shows trends in the structure of the helicopter airline fleet since 1955.

**TABLE 12.**  
**AIRCRAFT FLEET OF THE CERTIFICATED HELICOPTER AIRLINES**  
**1955-1959**

As of Dec. 31	Total	B-47	S-58	S-55	S-51	V-44B
1955	19	7	—	10	2	—
1956	20	7	3	8	2	—
1957	26	6	6	12	2	—
1958	22	4	5	6	2	5
1959	24	6	6	5	2	5

### Economic Trends

Financially the helicopter airlines have made steady progress. Commercial revenues have increased sharply with the growth of traffic and net income has improved steadily. Despite these gains subsidy requirements have continued to rise although at a considerably lesser rate than commercial revenues. Each of the three airlines is still dependent on Federal subsidy for its continued existence.

Table 13 shows trends since 1955 in revenues and subsidy. In 1959 Federal subsidy represented over 63 percent of total operating revenue with subsidy needs amounting to \$4.9 million compared to total passenger revenues of \$2.3 million. This has meant that while the average passenger fare was \$6.31, the average subsidy per passenger was \$13.43.

**TABLE 13.**  
**REVENUES AND FEDERAL SUBSIDY, CERTIFICATED HELICOPTER AIRLINES**  
**1955-1959**

Year	Passenger Revenues (000)	Federal Subsidy (000)	Total Operating Revenues (000)	Percent, Subsidy of Total Operating Revenues
1955	\$208	\$2,710	\$3,355	80.87
1956	438	2,834	3,711	76.4
195	968	4,173	5,032	82.9
1958	1,459	4,616	6,289	73.4
1959	2,309	4,914	7,760	63.3

### Unit Costs

High operating costs have been the major economic problem encountered by the helicopter operators. In 1959 it cost these carriers an average of \$4.05 per available ton mile and \$8.29 to carry one ton mile of revenue pay load.

To provide some perspective on these costs it is of interest to compare them with the unit costs experienced by the domestic trunk line and the local service air carriers.

**TABLE 14.**  
**COMPARISON OF TOTAL OPERATING COSTS IN 1959**

<b>Airline Group</b>	<b>Per Available Ton Mile</b>	<b>Per Revenue Ton Mile</b>
Helicopter	\$4.05	\$8.29
Domestic Trunk	0.28	0.53
Local Service	0.51	1.12

While helicopter unit operating costs are thus still extremely high, it is encouraging to note that they have shown a marked improvement; in 1959 they averaged approximately 40 percent below the level of 1955. This decline appears largely due to the increasing efficiency of the newer helicopters which have been put into service and the expansion in volume of traffic. However, it should be noted that the cost problem of the helicopter carriers is not merely one of high direct operating costs. Indirect costs are also extremely high as is indicated in the following table. Moreover, there are wide differences in indirect unit costs among the three carriers with Chicago averaging \$0.95, Los Angeles \$1.61 and New York \$2.30 per available ton mile.

**TABLE 15.**  
**DIRECT AND INDIRECT OPERATING COSTS, CERTIFICATED**  
**HELICOPTER AIRLINES, 1955-1959**

<b>Year</b>	<b>Dollars Per Available Ton Mile</b>			<b>Dollars Per Revenue Ton Mile</b>		
	<b>Total</b>	<b>Direct</b>	<b>Indirect</b>	<b>Total</b>	<b>Direct</b>	<b>Indirect</b>
1955	\$6.75	\$3.62	\$3.13	\$15.22	\$8.16	\$7.06
1956	6.37	3.22	3.15	12.96	6.55	6.41
1957	4.82	2.93	1.89	11.50	6.99	4.51
1958	3.98	2.47	1.51	10.04	6.22	3.82
1959	4.05	2.54	1.51	8.29	5.20	3.09

### **Helicopter Direct Operating Costs**

To focus more closely on the problem of helicopter costs, an analysis has been made of the direct operating costs of the various helicopter types now being flown by the certificated helicopter airlines. The results of this analysis are almost startling to those who have been accustomed to think in terms of fixed-wing aircraft costs. In its most efficient usage, the S-58, the most economical helicopter now in service, has a direct operating cost of approximately 20 cents per available seat mile. Comparatively, fixed-wing aircraft have direct operating costs of about two to three cents per available seat mile.

The table which follows compares the direct costs of the various helicopters now in service. The table shows a range for each type because of the wide differences in costs among the three operators. Additionally, a direct comparison between the S-58 and V-44B is difficult since these two aircraft are not now being flown by any one operator. However, New York Airways has flown both types, and its experience appears to indicate that while direct costs per hour are relatively comparable, ton mile and seat mile costs on the S-58 are slightly lower than on the V-44B.

**TABLE 16.**  
**DIRECT OPERATING COSTS OF HELICOPTERS IN CERTIFICATED AIRLINE**  
**SERVICE 1958-1959<sup>(1)</sup>**

Helicopter Type	Year Entered Service	Per Hour Flown	Per Available Ton Mile	Per Available Seat Mile
Sikorsky S-51 <sup>(2)</sup>	1947	–	–	–
Bell B-47	1949	\$54.37–54.75	\$4.95–5.33	–
Sikorsky S-55	1952	77.97–142.10	2.38–7.35	\$0.28–0.35
Sikorsky S-58	1956	208.05–260.92	1.67–3.02	0.20–0.33
Vertol V-44B	1958	256.28–260.35	3.35–3.47	0.36–0.40

1. For years ended June 30, 1958 and September 30, 1959. Cost experience is shown only where there was substantial utilization of the particular helicopter type.
2. The S-51 was flown too few hours for any meaningful cost experience.

### Summary of Record to Date

The foregoing data on the record to date of the three certificated helicopter airlines reveal two significant developments:

1. The helicopter has achieved its greatest success in commercial transport services as a special purpose vehicle transferring fixed-wing air passengers between airports in the Chicago and New York metropolitan areas; and
2. despite the achievement of a sizeable growth in passenger traffic and improved operating efficiency, the three helicopter airlines have been unable to reduce their aggregate subsidy requirements with the single-engine, piston-powered helicopters which have been available for purchase.

The inability of the helicopter airlines to achieve any significant progress toward economic self-sufficiency utilizing their relatively small, high unit cost helicopters has not been entirely unexpected. The Civil Aeronautics Board has indicated several times in certificate renewal and mail rate decisions that no final judgment of the helicopter experiment would be made until larger aircraft had become available and had been placed in service. For example, in the Los Angeles Airways Renewal Case (Docket No. 8178) decided July 28, 1958 the Board stated:

“Until a larger commercial helicopter is in operation and has been shown to be economically feasible, operations by rotary wing carriers must still be considered as developmental in nature and as requiring a further period of experimentation.”

This statement was repeated in the New York Renewal Case (Docket No. 8569) decided March 17, 1960.

## APPENDIX G

The emergence of inter-airport transfers as the mainstay of helicopter traffic has undoubtedly been the outstanding market development in helicopter airline operations to date. To a considerable extent it may be noted this has been an unexpected turn of events. Although there was early recognition of airport shuttle service as an important helicopter market, proponents of the helicopter generally have emphasized its potential use in city center operations and the community service that such operations would provide. However, as the record shows there has been only limited development of the airport-city center and suburban markets so far.

The use of the helicopter as an airport shuttle vehicle has developed most notably in the Chicago metropolitan area. Although Chicago Helicopter Airways was the last of the three helicopter airlines to offer scheduled passenger service, it has by far the largest passenger traffic volume. This achievement appears due almost entirely to the heavy air passenger movement between O'Hare International Airport, which handles all jet aircraft flights to and from Chicago, and Midway Airport, which has more passenger traffic than any other airport in the world. Chicago's Department of Aviation has estimated that perhaps 60 percent or more of Chicago's air passengers make transfers from one plane to another.

On the other hand, Los Angeles Airways which operates in an area with only one large air commerce airport is the smallest of the three helicopter airlines. Although New York Airways operates in an area with three large airports and has been providing passenger service three years longer than Chicago, its traffic is now less than half that of Chicago. This appears due to the lesser requirement for plane transfers generated in New York. According to a Port of New York Authority survey, about one-fifth of New York's outbound domestic passengers transfer from one airport to another. This proportion, however, has probably increased somewhat with the concentration of jet service at New York International Airport.

The fact that helicopter traffic so far is confined largely to airport shuttle service (and the steady increase in aggregate subsidy requirements) point up the developmental nature of current commercial helicopter operations. In attempting to forecast the 1965 and 1970 passenger traffic and aircraft fleet size of the three certificated helicopter airlines therefore, the two traditional methods of projection (trend analysis and correlation analysis) are of little value. Both methods appear unsuitable because the scheduled arrival early in 1961 of turbine-powered helicopters will bring down the curtain on the piston-engine era. The data applicable to that era will manifestly be inadequate, when used solely mathematically, to describe the new era. What remains then, is the method of subjective evaluation of the factors which have had an impact on traffic in the past and of the new factors which will have an impact on traffic in the future.

Before listing these factors and then proceeding to the forecast data, two pertinent assumptions should be noted. The first is in regard to the duration of the operating authority of the three currently certificated helicopter airlines. All three airlines have only temporary certificates; the Civil Aeronautics Board has refused in the renewal applications of each airline to grant permanent certificates. The Board stated its position in this regard as recently as March 1960 in the New York Airways Renewal Case (Docket No. 8569):

“We agree ... that continuation of New York Airways’ operating authority is required by the public convenience and necessity. But we do not find that renewal of the carrier’s certificate on a permanent basis is warranted at this time in view of the substantial Government support that is still required. We recognize that the inter-airport shuttle service and the suburban airport - feeder service offered by New York Airways in the New York metropolitan area provides substantial public benefits and that probable improvement in the carriers’ total subsidy position may occur if the large capacity direct lift equipment presently in the developmental stage proves feasible in commercial use. Yet we cannot overlook the high price the Government is presently paying for the amount of benefits being provided and the probability that the carrier will continue to need substantial amounts of subsidy for some time to come ... The Board recently denied permanent certification to Los Angeles Airways even though that carrier has been a certificated carrier longer than New York Airways and also provides a unique and valuable service in the sprawling and densely populated Los Angeles area. We find the factors which led the Board to deny permanent certification to Los Angeles Airways are equally applicable to New York Airways’ request for a certificate of unlimited duration in this proceeding.”

New York Airways’ operating authority now extends through March 16, 1967; that of Los Angeles through December 31, 1964; and that of Chicago Helicopter Airways through April 6, 1963. Whether or not the Board will grant permanent certificates upon expiration of the current certificates, or whether the Board will or will not renew the present certificates for even a temporary period, are not properly subjects for forecasting. An assumption has been made here, therefore, that the three currently certificated helicopter airlines will retain at least temporary certificates, authorizing service over the routes now being served, through 1970. (The question of whether additional carriers will be certificated for helicopter operations in cities other than New York, Chicago and Los Angeles is discussed in a subsequent part of this report.)

The second assumption made for purposes of this report is that passenger traffic, rather than freight, express or mail traffic will determine the size of the helicopter operations and the helicopter aircraft fleet during the next ten years in New York, Chicago and Los Angeles. As noted in the previous section, cargo ton miles were only six percent of the three airlines’ total revenue ton miles in 1959. Mail traffic was a somewhat more important source of traffic (about ten percent of the total revenue ton miles in 1959) but in absolute volume it has declined almost steadily since 1953. Passenger traffic is the most important part of the operations of the helicopter airlines and it appears certain to remain so during the forecast period.

#### IV. THE METROPOLITAN AREA MARKET, 1965–1970

The prospects for further development and growth of helicopter and V/STOL airline operations can be analyzed most meaningfully in terms of the different markets in which these aircraft may be utilized. In this section the outlook during the next decade for the metropolitan area operators in New York, Chicago and Los Angeles will be examined. In the following sections, the V/STOL potential in other segments of the short-haul travel market will be analyzed.

##### **New Transport Aircraft**

Undoubtedly the most important single operational factor affecting the future growth of scheduled helicopter service in the three metropolitan areas of New York, Los Angeles and Chicago is the one of new turbine-powered transport aircraft. The helicopter industry may be said to have entered the turbine-powered era in September 1960, with the delivery to Los Angeles Airways of a Sikorsky S-62—a single turbine-engine helicopter with a capacity for nine to twelve passengers and a cruising speed of about 100 mph. However, this one new helicopter is being leased by Los Angeles Airways only as an interim aircraft to gain turbine experience pending delivery of the five larger turbine-powered helicopters it has on order.

Early in 1961, a long-awaited, large-scale fleet modernization program will get under way with the introduction into service by the helicopter airlines of the first twin-turbine transport helicopters. These new aircraft will have appreciably greater capacities and cruising speeds than the piston-powered helicopters now in operation. The airlines are hopeful that the improved performance, greater comfort and all-weather capability of these aircraft will provide the basis for substantial traffic growth.

As of September 1960, the three airlines had 21 twin-turbine helicopters on order and on option. Both Los Angeles Airways and Chicago Helicopter Airways have ordered S-61's, a 25-28 passenger turbine transport with a cruising speed of 140 mph. Los Angeles Airways has ordered five S-61's for delivery beginning in April 1961, and Chicago Helicopter Airways has ordered six S-61's for delivery beginning in June 1961. It is expected that when the S-61's are received, the piston-engine helicopters now being used will gradually be phased out of service. Whether Los Angeles Airways will retain or return to Sikorsky, after delivery of its S-61's, the one S-62-it leased in September 1960, is not known at present; a decision will apparently await actual delivery of the S-61's.

New York Airways has contracted to purchase five Vertol 107's, a 25-passenger, 158 mph twin-turbine engine helicopter for 1961 delivery and has an option on five more, with delivery dates to be determined by traffic requirements. It has been reported that the New York Airways purchase contract provides for trading in the five Vertol 44B's they are now operating.

Because of their larger capacities and higher cruising speeds, the annual productivity of the new helicopters will be appreciably greater than that of the smaller piston-engine helicopters currently in service. Thus, the new helicopters are expected to be of particular value to the airlines during peak travel times. Both Chicago Helicopter Airways and New York Airways, for example, have reported losing passengers in their airport-to-airport shuttle service because of a lack of available seats during their busiest hours of the day.

The turbine-powered helicopters are also expected to attract new passengers because of their greater appeal in terms of size, speed and comfort. The aircraft will look more substantial, and more like the larger fixed-wing aircraft to which the air traveler is accustomed. The twin-turbine engines will provide a smoother ride than do the single piston engines on present helicopters. And although the greater speed of the new aircraft will not bring about large aggregate time savings to air travelers because of the shortness of helicopter trips, the flying public is expected to be increasingly receptive to any possible time savings because of the impact of jet airlines in reducing flight times on intercity routes. The air traveler who saves travel time by flying a jet airliner will not wish to lose that time getting to, from or between airports.

The newer helicopters are also expected to aid traffic growth by providing all-weather capability and improving schedule reliability significantly. Lack of instrument flying has adversely affected helicopter traffic growth at each of the three metropolitan areas that now have scheduled helicopter service. New York Airways has estimated, for example, that bad weather forced cancellation of approximately 20 percent of its scheduled flights.

Equipment purchase plans of the three metropolitan area operators beyond 1964–1965 are unknown at this time and appear to depend both on the rate at which traffic grows in the next three to four years, and on the availability of more efficient helicopters. Past experience indicates that there will be a continuing improvement in the state of the art, which should result in more comfortable, more efficient helicopters, with seating capacities fitted to specific market requirements. Improved versions of the S-61 and V-107 types of helicopters may therefore reasonably be expected to be available to the helicopter airlines in the 1965–1970 period.

Additionally, there is the possibility that compounded helicopters may become available in the 1965–1970 time period for use in metropolitan area service or short-haul intercity service. The British manufactured Rotodyne is most often reported in this respect. New York Airways has expressed its interest in acquiring five Rotodynes in 1964 or thereafter. However, a number of problems are attached to this aircraft. One is noise, which at present appears to be unacceptably high for close-in operations. Another is high unit costs for very short haul, i.e., 10 to 50 miles, stage lengths. The Rotodyne is a 55-64 passenger aircraft which appears designed for the 150–250 mile intercity passenger markets rather than for the airport-metropolitan area markets now served by New York Airways and the other two helicopter airlines. Efficient utilization of this aircraft would probably be limited, therefore, to a few longer route segments, such as La Guardia Airport–New Haven unless the Civil Aeronautics Board extended the airline's present route authorization. However, the Board is

on record as opposing extensions of service into areas already served by fixed-wing airlines. In the New York Airways Renewal Case, referred to earlier, the Board stated:

“In renewing New York Airways’ authority without the customary rotary-wing limitations, it should be emphasized, however, that in doing so we have no intention of permitting the carrier to duplicate the short-haul services now being provided by the local service carriers. We fully expect that New York Airways will continue to provide service complementary to and not competitive with fixed-wing operators.”

### **Unit Costs and Fares**

In addition to greatly improved performance characteristics, the new twin-turbine helicopters ordered by the three certificated operators are also expected to provide important reductions in unit costs. Actual operating experience with the new turbocopters is lacking, of course, but available estimates show a range of about 10 cents to 16 cents for direct operating costs per available seat mile. Comparatively, direct operating costs of the piston-powered S-58 are 20 cents per seat mile.

If these unit cost estimates are realized, they will therefore represent a substantial improvement over current levels which suggest the possibility of lower fares as a factor which will promote traffic growth. The fact is, however, that the passenger fares currently charged by the helicopter airlines are largely unrelated to costs. In 1959 the total direct, indirect and capital costs of providing helicopter service to the average passenger was \$19.74. The fare charged the average passenger was only \$6.31, however—the difference being made up by subsidy payments. As a practical matter, the fares charged by the helicopter airlines appear to be set at levels which in the judgment of airline management produce the maximum gross revenues while meeting requirements to be competitive with limousine and cab fares and to contribute to traffic development. Because current helicopter fares are developmental, it appears unlikely, therefore, that they will be lowered upon the showing of an improvement in direct operating costs.

There is the question, too, whether any small or nominal reduction in fares, based on an improvement in direct operating costs, would bring about an increase in passenger traffic. No analytical data on the elasticity of demand for helicopter travel are available, but the airlines have made surveys which indicate that business, expense-account travelers account for most of the passenger traffic. A six-week survey in 1957 conducted by the Port of New York Authority in collaboration with New York Airways reported, for example:

“The business traveler accounts for three-fourths of all helicopter passengers, and two-thirds of the people connecting planes. Of those linking air and ground transportation, four-fifths are on business trips. The proportion of helicopter passengers on business trips is considerably higher than that of airplane passengers.”

This composition of helicopter passenger traffic may be attributable in part to the relatively high level of helicopter fares. They range from 15 to 20 cents per passenger mile on airport-suburban routes to 50 to 60 cents on inter-airport, high density routes and average about 30 cents per passenger mile on all routes. On the other hand, air travel by fixed-wing aircraft costs, in most instances, between five and eight cents per passenger mile. Although by

no means conclusive, the evidence is that the demand for helicopter travel is relatively inelastic. In these circumstances the possibility cannot be ignored that helicopter fares might well be increased in order to lessen subsidy requirements.

One promotional factor in the matter of helicopter fares has been the development of joint fare agreements with connecting fixed-wing airlines which provide for much of the costs of the helicopter fare to be included in the regular fixed-wing fare. Such agreements have meant in Los Angeles, for example, that fixed-wing air travelers destined for eastern points can fly from any local heliport to Los Angeles International Airport via Los Angeles Airways for just two dollars more than the regular air fare from the airport.

### **Attitude of the Civil Aeronautics Board**

Because of the dependence of certificated helicopter operations on Federal subsidy and the probability of a continuing subsidy requirement until more economical helicopters become available, the attitude of the Civil Aeronautics Board will be a decisive factor in determining the future scope of airline helicopter operations. The Board occupies this position of control by virtue of its statutory authority to grant or withhold certificates of public convenience and necessity and subsidy eligibility, and to determine the duration and amount of subsidy which will be paid to eligible airlines.

Current CAB policy is to maintain the certificated helicopter experiment in approximately its present framework until such time as a more economical helicopter type can be produced. On the question of subsidy, the Board has taken the position that there is a limit to the subsidy support it can reasonably provide for the helicopter experiment. Statements from Board decisions involving the helicopter airlines and quoted in part in prior sections of this report indicate the Board's intention to try to hold subsidy costs to the Government at approximately their current level. In furtherance of this Objective, the Board has consistently refused to award unlimited or permanent certificates to the helicopter airlines so that it might maintain control over the duration of subsidy payments. In the Los Angeles Airways Renewal Case (Docket No. 8178) decided July 28, 1958, the Board stated, for example:

“The Examiner concluded that, in view of the sizeable amount of subsidy LAA is presently receiving and the fact that the Government's obligation to support helicopter operations with substantial sums of subsidy mail pay will continue for some time to come, renewing LAA's certificate on a permanent basis, as requested by the applicant, is not warranted at this time. We concur with his finding in this regard. We find that LAA's certificate should be renewed for a temporary period of approximately seven years, or until December 31, 1964, as recommended by the Examiner. In that way, the Board will have an opportunity to review the results of the carrier's operations for a reasonable period after the introduction of the S-61's and will be in a better position to evaluate the benefits of the service in relation to the cost to the Government.”

The Board has also limited the amount of routes to be served by helicopter in order to hold down subsidy payments. In the Chicago Area Service Case (Docket No. 6600 et al.) decided June 7, 1956, the Board stated:

## APPENDIX G

“....None of the foregoing arguments have convinced us that we should expand the certificate authority of CHA beyond that recommended by the Examiner. In view of the experimental nature of the proposed passenger operations, the fluid character of the service to be rendered, the prospective cost to the Government, and the need of the carrier for maximum operational flexibility, we believe it is necessary to limit CHA’s certificated operations to the inner triangle route. Although the record contains no reliable estimate of the total cost of establishing and maintaining a combined passenger and mail service to the outlying cities, we are convinced that the annual cost to the Government in the form of subsidy pay would be substantial.”

Thus the Board has moved cautiously in granting certificate authority to serve additional points requested by the helicopter airlines and has limited their operations to metropolitan area service.

In view of the Board’s position, the basic question to be answered is whether during the next ten years scheduled helicopter service will become profitable to the extent that Government subsidy would not be required. If subsidy is not required, then obviously the Civil Aeronautics Board would not be bound in its certificate award and renewal decisions by concern of costs to the Government, and the restraining influence of subsidy requirements would not exist to limit helicopter operations.

An evaluation of available data, particularly that presented by the helicopter airlines to the Board in recent certificate renewal and mail pay cases, indicates no likelihood of helicopter subsidy requirements being eliminated during the next five years. In fact, the Board anticipates that the subsidy needs of the three operators may increase initially when the new turbine-powered helicopters are placed in service. The picture beyond 1965 is much less clear in this regard, but the magnitude of the subsidy requirements forecast by the helicopter airlines and the Board’s staff for initial turbine powered operations, together with evidence that periods of three to five years are needed to develop and place into service newer and more economical aircraft, point to the continuance of subsidy requirements in the 1965–1970 period also.

As noted previously, the direct operating costs per available seat mile for the new helicopters which the three helicopter airlines will put into service in 1961 are estimated at 10 to 16 cents—about 20 to 50 percent lower than the seat mile costs for the piston-engined S-58 helicopter. However, it appears unlikely that even with these projected cost reductions, the helicopter airlines will be able to achieve a self-sufficient operation by 1965. Assuming that direct costs would actually average about 12 to 13 cents per seat mile for the new helicopters and that indirect costs would average about 10 to 14 cents per seat mile, total costs would be approximately 22 to 27 cents per seat mile. With an average passenger load factor of 50 to 55 percent those seat mile costs become 40 to 54 cents per passenger mile. The current average yield of the helicopter operators is about 30 cents per passenger mile. Thus, if current fare levels are maintained, about 10 to 24 cents of the total direct and indirect cost, or 25 to 40 percent would have to be made up by subsidy payments.

Under such circumstances it appears unlikely that any significant changes in the scope of the present helicopter experiment can be expected for the next five years at least and possibly for the next ten years. Obviously however, in view of the evolving helicopter technology, no final judgment on this point can be made at this stage, particularly for the latter part of the 1960s.

### **Other Growth Factors**

New York, Los Angeles, and Chicago are the largest and most congested metropolitan areas in the United States. As such they provide the most promising markets for utilization of the unique capabilities of the helicopter. The size and population concentrations of these communities have created serious surface transport problems. Distances between airports, and between airports, city centers and other important commercial or residential areas are generally long, and surface travel is inconvenient and time consuming. These three communities, more than any others, therefore, present the helicopter airlines with a great potential for traffic growth.

These three communities are also the busiest fixed-wing air traffic hubs in the United States. Together they account for approximately 27 percent of the total national air passenger market. Surveys taken by the three helicopter airlines show that almost all of their passengers are fixed-wing aircraft passengers who use the helicopter to transfer from one airport to another in a metropolitan area, or to begin or end an intercity air journey. In 1959, more than 33 million passengers arrived at or departed from these three metropolitan areas. The 366,000 helicopter passengers in 1959 represent only slightly more than one percent of this total.

The continuing growth in total fixed-wing air passenger traffic provides an additional potential for helicopter service. The Los Angeles Airport Commission estimates that passengers at Los Angeles International Airport will total 9 million by 1965 and 13 million by 1970, increases of 53 and 120 percent respectively over the 1959 total. The Port of New York Authority expects New York's air passengers to grow to 24.7 million by 1965 and to 45 million by 1975—increases of 58 and 189 percent over the 1959 total. As air traffic grows it is likely that the helicopter operators will establish additional gate positions at the major airports in New York, Chicago and Los Angeles, thereby improving the convenience and accessibility of their services, which in turn should lead to greater penetration of the available market.

No major changes in the traffic flow pattern of the helicopter airlines appear likely during the next ten years. Thus, in the New York and Chicago areas the major portion of the passenger traffic is expected to consist, as it does now, of travel between terminal airports. The possible construction of another major airport in both New York and Los Angeles during the latter part of the 1960's would substantially expand the available market. The Los Angeles helicopter operation in particular should grow with the opening of an additional large air commerce airport and the establishment of an airport shuttle route which now does not exist.

## APPENDIX G

Growth in city center airport traffic which now constitutes a relatively small proportion of total helicopter traffic appears to depend largely on the availability of additional and more conveniently located heliports. The FAA National Airport Plan contains recommendations for a sizable program of heliport development. It appears likely that this program will move forward as air traffic grows. In New York the planned opening late in 1960 of another heliport in Manhattan in an area close to the financial district should develop more downtown traffic. It should be recognized, however, that while the helicopter can provide time savings over surface transport between many downtown areas and the airports, this is dependent on the nearness of the heliport to the traveler; there will also be many air passengers who will begin or end their trips at downtown or near downtown points from which time savings by helicopter to and from the airports will be marginal or nonexistent.

Traffic between suburban points and the airports may also be expected to increase with more frequent flights and with the inauguration of service at additional heliports. However, so far there is no evidence of any real development of traffic between the city centers and suburban points. Thus the suburban routes appear likely to remain the weakest part of the New York and Chicago helicopter operations. Only in the faster growing, more widely dispersed Los Angeles area does it appear that the suburban routes will account for a significant share of the total helicopter passenger traffic.

While past growth trends cannot be used mathematically for forecasting purposes, as previously noted, the growth the three helicopter airlines have achieved since their beginnings has meaning which cannot be ignored. Passenger traffic has maintained a consistent and sharp upward trend. Passengers carried in 1959 were almost six times the number carried in 1956. Data for the first six months of 1960 reveal a further marked advance with traffic up 63 percent over the corresponding months of 1959. Such a remarkable rate of growth indicates a growing acceptance and popularity of helicopter service which augurs well for the three helicopter airlines.

### **1965–1970 Passenger Traffic and Aircraft Fleet Forecasts**

An evaluation of the factors discussed in the preceding sections indicates the three helicopter airlines in New York, Chicago and Los Angeles will carry approximately 1.2 million passengers in 1965 and 2.0-million passengers in 1970. This traffic will require a fleet of 30 to 32 helicopters in 1965 and of 40 to 45 helicopters in 1970. It will generate an estimated 210,000 aircraft departures in 1965 and 290,000 aircraft departures in 1970.

These forecasts are limited to the operations at the three metropolitan areas now served by the helicopter airlines, it should be noted, and must be regarded as subject to a sizeable margin of error due to the developmental nature of helicopter operations to date, and to the circumstance of the major change in the type of flight equipment scheduled for the near future. The 1.2 million passengers forecasted for 1965 is presented, therefore, as the midpoint in a forecast ranging from a low of 1.0 million passengers to a high of 1.4 million passengers. Similarly, the 1970 forecasts of 2.0 million passengers is presented as the midpoint of a forecast ranging from a low of 1.7 million passengers to a high of 2.3 million passengers.

The low estimates of 1.0 million for 1965 and 1.7 million for 1970 will allow for growth in passenger traffic at approximately the same aggregate annual increments as was experienced by the three helicopter airlines in the three year 1958-1960 period. The high estimates at 1.4 million for 1965 and 2.3 million for 1970 call for a more rapid traffic build-up and larger aggregate annual traffic increments, with a substantial traffic bulge following the introduction of the new turbine-powered helicopters.

In Table 17 forecasts of passenger-miles and aircraft operations are also presented. The passenger-mile forecasts provide for approximately the same growth rate as the passenger forecasts, and assume no significant change in the average passenger trip during the next ten years.

**TABLE 17.**  
**SCHEDULED HELICOPTER OPERATIONS IN THE METROPOLITA AREAS OF NEW YORK,**  
**CHICAGO AND LOS ANGELES: REPORTED FOR 1959 AND FORECASTED FOR**  
**1965 AND 1970**

Item	Calendar Year		
	1959	1965	1970
Revenue Passengers (000)	366	—	—
Low	—	1,000	1,700
Intermediate	—	1,200	2,000
High	—	1,400	2,300
Revenue Passenger Miles (000)	7,477	—	—
Low	—	23,000	41,000
Intermediate	—	25,000	44,000
High	—	27,000	47,000
Aircraft Departures	138,374	—	—
Low	—	190,000	260,000
Intermediate	—	210,000	290,000
High <sup>(1)</sup>	—	230,000	320,000
Aircraft Operations	276,748	—	—
Low	—	380,000	520,000
Intermediate	—	420,000	580,000
High	—	460,000	640,000
Number of Helicopters in Service	24	30-32	40-45

1. Aircraft operations have been estimated by multiplying departures forecast totals by two.

### Air Taxi Operations

In addition to the certificated helicopter airlines, there are a number of air taxi operators who use helicopters for the commercial transportation of passengers and cargo. In general, these air taxi operators are authorized by the Civil Aeronautics Board to engage in air transportation utilizing aircraft up to 12,500 pounds maximum certificated take-off weight, without restrictions as to frequency or regularity of service. However, they are expressly prohibited from offering any service by helicopter, or regular service by fixed-wing aircraft,

## APPENDIX G

between any two points which already have scheduled helicopter service provided by the holder of a certificate of public convenience and necessity issued by the Board. The air taxi operators have been denied permission by the Board to compete directly with the certificated helicopter airlines because of the likelihood that competition would bring about increased subsidy requirements for the certificated helicopter airlines.

Because the air taxi operators are not required to report traffic and financial data to the Civil Aeronautics Board, data on the extent and size of their operations are sketchy. However, registration and maintenance records on file with FAA reveal that at the end of 1959, there were approximately 2,300 air taxi operators, of which 71, or about 3 percent, were using helicopters. These 71 operators were estimated to be flying about 90 to 100 helicopters, of which over 90 percent were small Bell 47's. Additionally, of course, many of these 71 operators use small fixed-wing aircraft.

FAA records show further that in 1959 these air taxi helicopters flew about 36,000 hours compared to about 26,000 hours in 1957, an increase of about 5,000 hours annually. Services provided by helicopters used by the air taxi operators are by no means limited to metropolitan area services, it should be noted. Such services include not only the movement of executives between airports, plants and offices in metropolitan areas, but also movements of a more specialized nature, such as the carriage of workers to and from off-shore oil drilling platforms, and the provision of ambulance service for such platforms.

Continued but unspectacular growth appears in prospect for this category of helicopter flying. It appears likely that it will remain a relatively small part of the total air taxi industry; that is, subordinate in volume to fixed-wing aircraft flying, because charges are necessarily high—averaging \$1.00 to \$1.25 per mile or about \$85 per hour on the Bell 47's. Such charges tend to limit the use of the air taxi helicopters to busy executives, and to special temporary tasks and odd jobs that cannot be more easily performed by small fixed-wing aircraft.

However, in some metropolitan areas, fairly sizeable air taxi helicopter operations may develop. Two new scheduled services have recently been reported – one in St. Louis with 40 flights daily and another in Atlanta with 30 flights daily. Both of these air taxi operators are flying Bell 47's on airport-downtown routes. Pilgrim Helicopter Services of Washington, D.C., an air taxi operator, has announced that it will inaugurate turbine-powered helicopter service between downtown Washington and Baltimore's Friendship Airport before the end of 1960, using a 10-passenger Sikorsky S-62. When Dulles International Airport opens in the Washington, D. C. metropolitan area in 1961, there undoubtedly will be a requirement, in the absence of operations by a certificated, subsidized helicopter airline, for air taxi service between the new and the old airports.

### **New Metropolitan Area Services**

Assuming advances in helicopter technology with concomitant improvements in the economics of helicopter operations, the next important development in the commercial use of transport helicopters beyond the extension of air taxi service would appear to be inauguration

of scheduled helicopter services by newly certificated airlines in additional metropolitan areas. Such services would logically be essentially similar to those now available in the New York, Chicago and Los Angeles metropolitan areas.

It is readily apparent, however, that such advances in technology and improvements in the economics of operations will not occur suddenly in the next two or three years. At the present time, there are about 75 applications on file with the Civil Aeronautics Board for proposed helicopter services in various locations throughout the United States. To date no action has been taken with respect to these applications. In view of the continuing large subsidy requirements of the three presently certificated helicopter airlines, it appears unlikely that new certificated operations carrying subsidy eligibility will be authorized by the Board within the next five years unless the applicants can show a pressing public need for the proposed services. However, should model improvements and hoped for advances in the state of the art improve the helicopter operators' prospects for self-sufficiency, the 1965-1970 period could see the inauguration of a number of additional metropolitan area helicopter services.

There are a number of objective criteria which provide an indication of the specific metropolitan areas which are likely to have a requirement for scheduled helicopter services of the type now provided in New York, Chicago and Los Angeles.

1. The current helicopter experiment has revealed that the principal public need to be served is the movement of fixed-wing air passengers in the metropolitan area either (a) from airport to airport or, (b) between the airports and other points in the metropolitan area. Thus a basic guide to the potential for an airport type helicopter operation is the number of fixed-wing air passengers arriving in or departing from a community.
2. Since the busiest helicopter routes by far are those between airports in a given metropolitan area, the number of major air commerce airports in a community provides another important yardstick for measuring the need for helicopter services. Helicopter traffic volume on these routes can be expected to be closely related to the distance between the airports and the time that can be saved by air over ground travel. The number of passengers transferring between airports also would provide a good measure of the total inter-airport markets. However, such data are not available for study.
3. The population and area of a community provide a broad indication of the public need for helicopter services. As population density and the size of the metropolitan area increases, ground travel times between the city centers and the airport and between other points and the airport become even greater. In all but a few of the larger cities, air commerce airports are located relatively far from the city centers. The newer airports are generally located the farthest out.

Table 18 shows the 20 metropolitan areas which, on the basis of these criteria, can be considered the leading candidates for scheduled airport type helicopter services.

**TABLE 18.**  
**SELECTED DATA INDICATING POTENTIAL FOR CERTIFICATED HELICOPTER SERVICES IN MAJOR METROPOLITAN AREAS**  
**(In Rank Order of Airline Passengers Generated in 1959)**

Metropolitan Area	Fixed-Wing Air Passengers Enplaned 1959	Population 1960 <sup>(1)</sup>	Number of Major Air Commerce Airports	Land Area (Sq. Miles)	Distance of Airports From City Center (Miles)	Ground Travel Time, Airports to City Center (Minutes)	Number of Airports Planned for 1970 Time Period
New York	6,553,616	10,604,300	3	3,939	8; 12; 15	30–60	4
Chicago	4,573,770	6,172,127	2	3,617	10; 23	40–65	2
Los Angeles	2,797,189	6,683,563	1	4,853	14	60	3
Washington, D. C.	2,230,866	1,968,562	1	1,488	4; 24	15–50	2
San Francisco/Oakland	1,936,400	2,721,045	1	3,314	9; 16	25–60	2
Miami	1,889,785	917,851	1	2,054	7	15–30	2
Dallas/Fort Worth	1,378,500	1,642,057	2	1,770	7	25–30	2
Boston	1,366,667	2,566,872	1	770	3	20–30	1
Detroit	1,294,694	3,744,544	2	1,965	17; 30	25–60	2
Atlanta	1,082,048	1,014,349	1	1,287	9	15	1
Cleveland	1,000,344	1,780,263	1	688	14	35	1
Pittsburgh	978,286	2,395,249	1	3,053	16	25	1
Philadelphia	901,451	4,289,194	1	3,550	6	15–25	1
St. Louis	874,989	2,040,188	1	2,520	15	35–50	1
Denver	789,319	923,161	1	2,918	7	15	1
Seattle	786,652	1,096,778	1	2,134	12	30–50	2
Minneapolis–St. Paul	762,448	1,477,080	1	1,721	9	25–30	1
Kansas City	699,146	1,027,562	1	1,643	2	5 <sup>(2)</sup>	2
New Orleans	665,617	860,205	1	1,118	13	40	1
Houston	637,806	1,234,868	1	1,730	10	20–30	2

1. Source: Bureau of the Census preliminary reports, PC(P2)'s, 1960 Census of Population.

2. Mid-continent airport is in the planning stage and will be 16 miles from city center; ground travel time is unknown.

The communities are listed in rank order of the number of airline passengers enplaned. (Enplaned passengers have been used in the absence of data covering both arrivals and departures. It is reasonable to assume, however, that in most cases deplaned passengers will approximately equal enplaned passengers.) The New York, Chicago and Los Angeles metropolitan areas are included in the table for comparative purposes.

Washington, D. C. and San Francisco/Oakland show up as the most promising metropolitan areas for new scheduled helicopter services on the basis of the criteria shown. Traffic development at the new Dulles International Airport which is being constructed at a relatively remote location at the outer edge of the metropolitan area should provide the basis for a strong triangular route system between Dulles, Washington National Airport and downtown Washington. The inclusion of Baltimore Friendship Airport in this route system would also be a distinct possibility. In the San Francisco Bay Area, growth in passenger traffic between the two international airports plus the long ground travel times between the airports and the outer counties of Marin, Sonoma and Contra Costa are indicative of a sizeable potential market for helicopter operations. The metropolitan area of San Francisco has shown a high degree of interest in obtaining scheduled helicopter service as evidenced by the work of the San Francisco Bay Area Council.

Whether certificated helicopter services will actually be inaugurated in Washington and San Francisco cannot now be foretold. It is significant, however, that the CAB has received eight applications for service in San Francisco and seven proposals for service in Washington, a larger number than for any other cities in the country. Moreover, the Washington metropolitan area already has a small charter helicopter operation and one is expected to begin soon in the San Francisco metropolitan area. The ability of these operators to develop their markets should help pave the way for larger scheduled operations at a later date.

Other metropolitan areas which appear to have a public need for helicopter services include Miami, Dallas/Fort Worth, Boston, Detroit, Atlanta, Cleveland, Pittsburgh, Philadelphia and St. Louis. Applications proposing scheduled helicopter services in all of these communities are on file with the Civil Aeronautics Board. However, it will be noted from the table that as one moves down this list of communities, the potential market declines very rapidly. Pittsburgh, Philadelphia and St. Louis, for example, generate only about one-third of the fixed-wing air traffic of Los Angeles, which now has the smallest scheduled helicopter operation. Only three of these cities will have more than one major air commerce airport in the next ten years with a resulting need for inter-airport shuttle service. Moreover, with the exception of Detroit and St. Louis, the airports in these communities are considerably closer to the city centers in terms of ground travel time than in the largest metropolitan areas.

It would appear likely, therefore, that if certificated helicopter services were inaugurated in any of this group of cities, it would be on a considerably smaller scale than in New York, Chicago or Los Angeles. Initially operations would probably require no more than three to five helicopters. In this connection, the findings of a recent report titled, "Helicopter Service Requirements of Pennsylvania," prepared for the Pennsylvania Aeronautics

## APPENDIX G

Commission in 1957, are pertinent. The report found “a limited need” for scheduled helicopter service “on a modest scale” in Philadelphia and Pittsburgh. Recognizing that subsidy would be required, it recommended an operation utilizing three passenger helicopters over a minimum route pattern in each community, linking the downtown area and the airport, with two or three spurs to outlying points.

## V. THE INTERCITY AND COMMUTER MARKETS, 1965–1970

The utilization of the helicopter in airport shuttle service within metropolitan areas and in air taxi service is regarded by steep-gradient aircraft enthusiasts as prologue. The greatest success of the transport helicopter and of the more sophisticated transport V/STOL aircraft now being designed and developed lies ahead, these advocates believe. They see two vast markets awaiting these transports – the short-haul intercity and the commuter travel markets.

There can be little doubt that if helicopters and V/STOL aircraft are to realize their full potentiality as important means of passenger transport, rather than as special purpose and odd-job vehicles, they will have to succeed in either or both of these two markets. It is the consensus of expert opinion that if success is achieved it will be in the intercity short-haul travel market first and later, perhaps, in the commuter travel market.

### Short-Haul Intercity Travel

To date air transportation has played a very limited role with fixed-wing aircraft in the short haul intercity travel Market. The market is dominated by the private automobile, but substantial volumes of passenger traffic are also carried by the railroads and motor buses. No recent data on the total size of this market are available, but an analysis of the common carrier data indicates the great majority of the 301.2 million passengers moving by rail and bus in 1959 travelled less than 250 miles. The average passenger journey by rail was about 125 miles and by bus about 80 miles. Comparatively, the average air passenger trip in 1959 in the United States was in excess of 500 miles, and only one-fourth of the total air passengers travelled less than 250 miles.

TABLE 19.

#### DISTRIBUTION OF DOMESTIC COMMON CARRIER INTERCITY PASSENGERS (Total Revenue Passengers in Thousands)

Calendar	Air	Rail <sup>(1)</sup>	Bus <sup>(2)</sup>	Percent Air of Total
1950	17,345	209,094	322,802	3.2
1954	32,343	189,580	241,612	7.0
1956	41,738	181,460	208,047	9.7
1958	48,128	140,147	173,720	13.3
1959	54,768	130,905	170,305	15.4

1. For Class I Mine-Haul Railways; includes parlor and sleeping car traffic, but excludes commutation traffic.
2. For Class I Motor Carriers; the relatively small amount of passengers carried by Class II and III Motor Carriers is not available. Excludes local, suburban and charter service.

Source: Interstate Commerce Commission for rail and bus statistics; FAA Statistical Handbook of Aviation for Air Statistics.

## APPENDIX G

The inability of air transport to capture a major share of the short-haul intercity travel market appears largely due to two factors: (1) the failure of fixed-wing airport-to-airport transport to provide appreciable overall time savings over surface transport on short distances; and (2) the substantially lower costs of travel by private automobile, rail coach and motor bus for short distance travel. Helicopters and V/STOL aircraft, with their ability to operate directly from city center to city center, provide the means for greatly reduced air travel time on short intercity routes. However, whether these aircraft in the foreseeable future can overcome the economic problem which has plagued the helicopter to date, and provide short-haul transportation at reasonably competitive rates appears doubtful at this time.

While the pure helicopter appears to be the logical vehicle for the metropolitan area and commuter markets, the compounded helicopter or V/STOL aircraft is generally considered as more appropriate for the intercity market for distances up to about 250–400 miles. No such vehicle is currently available. However, a compounded helicopter such as the Rotodyne in which New York Airways has expressed an interest may be commercially available by about 1965.

In the United States, considerable design work is being conducted with tilt-wing, tilt-rotor, tilt-engine types of steep-gradient aircraft for the military services. Recently the Department of Defense established a joint tri-service program directed toward developing a prototype of an operational V/STOL transport aircraft for operational suitability testing. In announcing the program, the Department stated that while the technical feasibility of various approaches to V/STOL aircraft have been thoroughly explored, operational problems associated with these aircraft remain highly speculative. It went on to say that these operational questions must be answered before the military services can make realistic plans and prepare detailed requirements for advance types of V/STOL aircraft.

Studies of the National Aeronautics and Space Administration indicate that a tilt-wing, turbo-prop V/STOL transport of 40,000 to 80,000 pounds gross weight shows more ultimate promise for use as a short-haul transport aircraft than the compounded helicopter. However, such an aircraft is some three to four years behind the compounded helicopter in the development cycle because of the lack of flight research. NASA estimates that the V/STOL transport would not be available for military or commercial service before the 1970–1975 time period.

In addition to uncertainties surrounding the actual availability of V/STOL transport aircraft for commercial airline use during the next ten years, there are a number of operational and economic factors which must be considered in evaluating their potential commercial acceptance and utilization. The most significant of these factors appear to be: (1) the actual speed differential between V/STOL transports and fixed-wing aircraft; and (2) their economic feasibility and ability to operate at rates which are reasonably competitive with fixed-wing aircraft and with surface means of transport. In the discussion which follows, a city-center-to-city-center type of operation is assumed in order to take full advantage of the inherent capabilities of the V/STOL vehicle. Such usage is, of course, dependent on the availability of close-in conveniently located heliports of a size suitable for high density intercity operations.

However, it may be that initially V/STOL techniques may be utilized in an airport-to-airport type of operation. This more evolutionary course of development is considered a possibility by NASA because of the capability of V/STOL aircraft of using airspace and landing facilities unused by conventional airplanes in terminal areas, thereby permitting a reduction in flight delays.

### **The Problem of Speed**

Past studies of the potential traffic available for V/STOL aircraft generally agree that such aircraft would probably be most suitable for high density intercity routes for distances up to about 250 miles. Examples of such routes might include Boston–New York; Philadelphia–New York and Washington–New York. It also has been thought that V/STOL aircraft would generally be suitable for local service airline routes.

The basic advantage cited for the V/STOL airliner is that it can operate from city-center-to-city-center, rather than from airport-to-airport, with resultant savings in total journey time. A typical example might be the Boston-New York route, with an airport-to-airport distance of 185 miles. On this route total travel time via a 200 mile per hour V/STOL airliner would be approximately one hour less from city-center-to-city-center than fixed-wing flight time plus ground travel time to and from the airports.

Such examples of possible time savings are, of course, impressive, and indicate that V/STOL flight would provide important travel benefits to those travelers whose ultimate point of origin or destination is in the city center and is within walking distance or reasonably close to the heliport from which the V/STOL airliner operates. Available statistics show that the city centers are the most important points of origin or destination of an airline trip. A conveniently located city center heliport would thus give the V/STOL aircraft access to a major segment of the potential short-haul intercity travel market.

Nevertheless, it must be recognized that for many travelers time savings by V/STOL aircraft will be marginal. Because of the size of the central business districts of major metropolitan areas, it is likely that there will be many points at which passengers will start, or end, their journeys that will be nearly as close or closer to the airport as to the heliport. Moreover, the city centers are by no means the only points between which air travelers move. They originate and terminate their journeys in all parts of the metropolitan area and in many cases have no need or desire to go to the city center. In this connection the conclusions of a recent study of the points of origin and destination of airline passengers in and around a community are enlightening:

“Trips of people traveling for such personal reasons as family visits, recreation, sightseeing, etc., most probably originate at their home which may be located anywhere within the community. Only a small number will be living in or close to the central business district or have a desire to pass through there on the way to the airport. At the destination city the personal travelers may go to a home in any part of the community, or to a nearby recreation area, and only in some cases to a hotel in the central business district.

## APPENDIX G

Business travelers at the origin city may proceed to the airport either directly from their home or else from their office, which may be in the central business district or otherwise, with a steady suburbanization of industry, somewhere else in the community. At the destination city they will go to a place of business either in the central business district or perhaps in a decentralized location. Upon return to their city of origin they may go to their office, but frequently such return will be after business hours and they will proceed directly home.”<sup>2</sup>

The following table provides a distribution of the originating points of the journeys of airline passengers in a number of metropolitan areas. The usefulness of the data as an indicator of potential for V/STOL operation is limited, however, by the fact that the percentages shown for the city centers include all origins in the central county of the metropolitan areas.

**TABLE 20.**  
**ORIGINS OF ENPLANING PASSENGERS AT REPRESENTATIVE AIRPORTS<sup>2</sup>**

Airport of Departure	Passenger Origins	
	City Center (County)	Other Points
New York–International	47%	53%
New York–LaGuardia	53	47
New York–Newark	38	62
San Francisco International	56	44
Minneapolis/St Paul–Wold–Chamberlain	46	54
Cleveland–Hopkins	39	61

City center to city center V/STOL operations also would present some problems to local service airlines from the operational point of view. According to reports filed with the Civil Aeronautics Board, 45 percent of the passengers carried by the local service airlines are connecting passengers who continue their journeys on major air carriers. This is in accord with the concepts under which these airlines were originally established. The proportion varies by airline but represents a substantial proportion of the total traffic for each. Connecting passengers obviously would not want to go to the city center on at least one end of their local service flight.

---

<sup>2</sup> Source: V. J. Roggeveen and L. V. Hammell, Journal of the Air Transport Div., Proceedings of the American Society of Civil Engineers, July 1959, p. 41.

TABLE 21.

**LOCAL SERVICE AIR CARRIERS—LOCAL AND CONNECTING PASSENGERS CARRIED  
(September 17–30, 1958)**

Carrier	Number of Passengers			Percent of Passengers Connecting
	Total	(One Carrier)	Connecting	
Allegheny	19,598	11,990	7,608	38.8 %
Bonanza	6,209	3,846	2,363	59.2
Central	5,749	2,344	3,405	59.2
Frontier	8,130	5,152	2,978	36.6
Lake Central	7,309	3,964	3,345	34.8
Mohawk	18,604	14,149	4,455	-23.9
North Central	30,400	11,543	18,857	62.0
Ozark	17,453	8,156	9,297	53.3
Pacific	12,957	9,319	3,638	28.1
Piedmont	16,719	8,253	8,466	50.6
Southern	8,220	3,477	4,743	57.7
Trans-Texas	8,561	4,429	4,132	48.2
West Coast	9,107	6,661	2,446	26.9
TOTAL	169,016	93,283	75,733	44.8

Source: Civil Aeronautics Board; "Competition Among Domestic Air Carriers," September 17–30, 1958.

### The Cost Problem

The major problem to be overcome by the V/STOL aircraft is that of high operating costs. If there is to be commercial acceptance and utilization, the V/STOL airliner must be able to operate at rates which are reasonably competitive with those of other means of transport. In the following discussion a range of V/STOL fares that might be considered competitive under varying assumptions in regard to the market are shown, using the 185-mile Boston-New York market as a specific example. Passenger fares of fixed-wing air travel, which is currently the fastest means of transport between Boston and New York, have been used as the basis for comparison. The first class fare for this trip (excluding Federal excise tax) is \$15.00. Ground transportation between the city centers and the airports is \$2.50.

1. The first class fixed-wing air fare is 8.1 cents per mile. V/STOL aircraft would probably have to meet this fare level to attract those travelers for whom a V/STOL flight would provide no time savings over a fixed-wing flight. In this segment of the market would be those passengers whose journey origins and destinations are as close to the airports as they are to the city center heliport from which the V/STOL airliner presumably would be operating.

To break even at a 8.1 cents per mile fare would require V/STOL airliner direct operating costs of 2.4 cents per seat mile at a 60 percent load factor and with 100 percent indirect cost.

2. For those travelers whose journey origins and destinations are from city center to city center a competitive V/STOL airliner passenger fare would be of the order of \$17.50 (the cost of fixed-wing transportation plus ground transport between city center and airport) or approximately 9.5 cents per passenger mile in those cases where the traveler places no additional value on the time saved by V/STOL flight, or where—because of the location of the journey origin and destination in the city center—the V/STOL flight provides little or no time savings over fixed-wing journey time.

To break even at a 9.5 cent per mile fare would require V/STOL direct operating costs of about 2.9 cents per seat mile at a 60 percent factor and with 100 percent indirect costs.

3. If it is assumed that a passenger values his time at \$5 per hour and that a 200 mile per hour V/STOL airliner would provide time savings of approximately one hour over fixed-wing travel on a city-center-to-city center journey, a competitive V/STOL fare might be on the order of \$22.50 for this segment of the market or about 12.2 cents per passenger mile.

A break-even V/STOL operation would then require direct operating costs of 3.7 cents per seat mile at a 60 percent load factor and with 100 percent indirect costs.

4. The preceding discussion applies only to first class air travel. The coach fare between Boston–New York is \$13.10 or 7.1 cents per passenger mile from airport-to-airport and 8.4 cents from city-center-to-city-center. To be attractive to this segment of the air travel market, a breakeven V/STOL operation would require direct operating costs ranging from about 2.1 cents to 3.3 cents per seat mile under the same assumptions as were used above.

Insofar as can be determined at this time, no V/STOL aircraft which would be designed for speeds under approximately 300 knots appears capable of operating within the range of fares and seat mile costs shown above. Information on costs are very speculative at this stage. United States manufacturers place the prospective direct costs of V/STOL aircraft types in the neighborhood of 6 cents per seat mile. Available cost estimates on the compounded helicopter fall at approximately the same level, varying from over 4 cents to about 7 cents per se mile. In contrast the Fairchild F-27 had direct operating costs in local service airline operations in 1959 of 2.9 cents per seat mile.

The prospects that V/STOL aircraft will be able to support fares which would be attractive to travelers moving by surface carriers appear even more remote. Passenger fares by surface carriers are lower than first class air fares on a city-center-to-city-center basis, with the great majority of the short haul common carrier traffic moving by rail coach and motor bus at fares of about three to five cents per passenger mile. Although clearly a V/STOL operation from city center to city center could provide these travelers with substantial time

savings, attainable costs with projected V/STOL aircraft appear for the foreseeable future to preclude passenger fares which would be attractive to any but a minute fraction of this travel market.

### **The Commuter Market**

There has been no more exciting use suggested for the helicopter than that of an air bus in the daily commuter market. This intra-city market is potentially even greater in terms of the number of people transported than the short-haul intercity market. In 1959, for example, more than seven billion passengers were carried by intra-city buses, trolleys, and electric railways of one kind or another. Not all these passengers are commuters, of course, but on the other hand this total does not include the many millions of automobile riders who are commuters.

Like the airport metropolitan area and short-haul intercity passenger market, the suburban commuter market is not rigidly defined. It is generally considered to include that travel to and from work by residents of a metropolitan area which involves getting into the city center in the morning and back to the suburbs in the evening. Because metropolitan areas vary in size in the United States the travel distances in this market may range from some 15 to 50 miles. In many respects a helicopter commuter operation might be considered a natural extension of metropolitan area helicopter services as they are presently known. And at its outer boundaries the commuter service would to a limited extent overlap the very short-haul portion of the intercity market discussed in the previous section.

It is not great size alone that characterizes the suburban commuter market and attracts the helicopter enthusiasts. This is the travel market most sorely troubled by the inadequacies and complexities of surface transportation – the market in which millions of daily commuters could be helped if some way were found to rescue them from the acute traffic congestion, and all its attendant inconveniences, which plague our larger metropolitan areas during the morning and evening “rush hours.”

Enthusiasm for the helicopter as the ultimate solution to the metropolitan area mass transportation problem probably was highest during the period immediately after the Korean War had ended. The new aircraft, it was predicted by some market analysts, would revolutionize intra-city mass transportation within 15 years. However, developments since then have convinced most observers that this time table was unduly optimistic and that the helicopter will not play a significant role in this short-haul market for the foreseeable future. For the most part, the helicopter is no longer looked upon as the vehicle for low cost mass transportation commuting service; it is seen, rather, as a medium for premium rate service designed to meet special needs of the community.

## APPENDIX G

The reasons for assigning the helicopter this less ambitious role in the commuter market are to be found in the speed and operating costs of the aircraft. In general it seems clear that air commuting would provide time savings on suburban routes in major metropolitan areas such as New York, Chicago and Los Angeles. Estimates made for the New York area show, for example, that if non-stop helicopter service were provided, travel time between typical outlying suburban points and Manhattan would be reduced from 50–75 percent over rail time. However, as the distance between stops is reduced so as to permit a more widespread penetration of the market, this speed advantage diminishes. Thus, with an average flight stage of 5 miles, a helicopter with a cruising speed of about 150 miles per hour would have a block speed of about 65 miles per hour.

The bigger problem for the helicopter is one of costs and fares, however. Rail commuter fares are relatively low, averaging 2.57 cents per passenger mile for a total cost of 51 cents for the average 20 mile trip. In contrast, helicopter fares on suburban-airport routes average about 15–20 cents per passenger mile and at this level require heavy subsidy support; a break-even operation with the new turbine-powered helicopters, as shown previously, would probably require fares of about 40–54 cents per passenger mile. Such fare levels would obviously not be feasible for the average commuter who would have to pay them from his own funds rather than charging them off as a business expense. Only the business traveler would be willing to pay these premium fares if the service were available.

In this connection it is of interest to note that the subsidy supported 15–20 cent per passenger mile fare level on helicopter suburban-airport routes has generated relatively little traffic in New York and Chicago despite the time saving provided by these flights for trunk line connections. In 1959 Gary and Winnetka, the two suburban points served by Chicago Helicopter Airways, provided only 3.4 passengers per flight while New York suburban points provided only 1.2 passengers per flight. And in the sprawling Los Angeles area, suburban points have provided an average of less than one passenger per flight.

Commuter air travel can also be expected to face a number of additional problems. Commuter travel is inherently highly directional and peaked. There is a heavy flow in the morning for about two hours into the city. In the late afternoon the reverse is true. Relatively little traffic moves during midday or in the evening. This situation has plagued the commuter railroads and would, of course, have an adverse impact on helicopter utilization and load factors, with a resultant effect on unit costs. While there has been some speculation that the flying crane might, because of its versatility, solve some of these problems, no information is available which would indicate that the crane would be economically feasible in such service.

Because of these problems it seems likely that commuter travel by air will develop only to a very limited extent during the next ten years and then merely as an extension of existing metropolitan area helicopter services at premium rates. It is only beyond 1970 that more widespread use of the helicopter and possibly the V/STOL transport in the commuter market may appear. Any numerical forecast of traffic to be carried, however, is obviously premature.

# AIRPLANES, ENGINES, AND HELICOPTERS

## AIRPLANES

Aeronca L-16, 208  
Boeing Clipper, 121  
Boeing Model 40, 586, 587, 588  
Boeing Model 247, 214, 251, 292, 587, 588, 669  
Boeing 307, 586  
Boeing B-29, 559, 560  
Boeing 737, 687  
Boeing 707, 555, 561, 562, 590  
Boeing 777, 687  
Cessna L-19, 208, 209, 237, 238  
Cessna TL-19D, 213, 214, 226, 227, 228, 229, 238  
Chance Vought VE-7, 214, 216, 217, 218  
Douglas DC-1, 214, 251, 261, 292  
Douglas DC-3, 251, 263, 350, 447, 548, 550, 553, 579, 581, 582, 584, 585, 586, 587, 588, 590, 596, 601, 661, 669, 687  
Douglas DC-3A, 584, 585, 588, 592, 593  
Ford Tri-Motor, 251, 550, 579, 580, 582, 584, 585, 586, 587, 588, 590, 592, 593, 601, 668  
Grumman OV-1C, 519, 521  
Lockheed C-130, 356, 357, 568  
Lockheed Electra, 548  
Lockheed YO-3, 516, 526  
McDonnell XF-88B, 447  
Piper L-4, 96, 207, 208  
Spirit of St. Louis, 273, 275  
Stinson L-5, 207, 208, 455, 508  
Wright Flyer, 548

## ENGINES

Allison 250-C18, 632  
Allison 250-C18B, 86  
Allison 250-C30, 631  
Allison 250-C40, 631  
Allison T-63, 77, 82, 287, 504  
Allison, 77, 78, 81, 82, 86, 100, 102, 275, 287, 446, 457, 504, 506, 541, 569, 631, 632  
Boeing 505, 75, 238  
Continental R-975-34, 182  
Continental, A65-8  
Continental, O-470-11-C1  
Continental, R-975-34  
General Electric CT7, 632  
General Electric T-64-GE-416, 252  
General Electric YT-700-GE-700, 78, 79  
Hirth 2703, 84  
Light Helicopter Turbine Engine Co. LHTEC T-800, 81, 82  
Lycoming, YT-53-L-1, 76  
Lycoming, LTS 101, 151, 152, 630, 631  
Lycoming, O-360-A1D, 84  
Lycoming, O-360-C2B, 62, 271  
Lycoming, O-360-J2A, 638

Lycoming, T-53, 77, 81, 238, 240  
Lycoming, VO-435, 83, 100  
Pratt & Whitney, 251, 579, 584, 593, 612, 632  
Rolls Royce RR300, 632, 633  
Rotax 503, 84  
RTM 322-01/8, 252  
Turbomecca ARRIEL 1C1, 152  
Wright J-5-C, 275  
Wright R-1820, 60, 82, 240

## HELICOPTERS

American Sportscopter Ultraspot 254, 84  
Armed Attack Helicopter (AAH), 138, 141, 142, 143, 144, 145, 200, 202, 328, 576  
Augusta-Westland AW 139, 636  
Augusta-Westland EH 101, 214, 217, 236, 252, 292, 294, 295, 377, 401, 405, 636, 640, 648, 686  
Bell 206B III, 541  
Bell 206B, 540, 541, 544, 587, 637, 646, 652  
Bell 206B-II, 540  
Bell AH-1G, 354, 372, 373, 377, 378, 379, 380, 383, 385  
Bell AH-1S, 524, 525, 526  
Bell AH-1Z, 304  
Bell AHIP/OH-58D, 96, 97, 99, 100, 104, 105, 128, 208, 552, 566, 571, 573, 574, 575, 576, 577, 624, 625, 630  
Bell H-13, 96, 208, 209, 230, 231, 233, 235, 236, 237, 238, 284, 343  
Bell H-13H, 209, 210, 211, 230, 232, 235, 252, 344  
Bell Huey, 76, 78, 88, 89, 124, 291, 310, 350, 354, 356, 553, 555, 561, 563, 567, 568  
Bell Model 206, 77, 205, 541, 544, 693  
Bell Model 206B, 78, 86, 540, 542, 543, 544, 637, 646  
Bell Model 212, 636  
Bell Model 214ST, 205  
Bell Model 222, 149, 151, 152, 290, 291, 308, 630, 631, 634  
Bell Model 30, 33, 34, 50  
Bell Model 412, 295, 296, 309, 329, 646  
Bell Model 430, 304, 307, 308, 631  
Bell Model 47, 9, 14, 15, 33, 50, 231, 343, 597, 659, 669, 693  
Bell Model 680, 304, 308  
Bell OH-13, 284  
Bell OH-4A, 77, 78, 96  
Bell OH-58A, 78, 96, 354, 540, 541  
Bell OH-58C, 96, 97, 99, 100, 541  
Bell UH-1A, 89, 470  
Bell UH-1D, 89, 562  
Bell UH-1Y, 304  
Bell XH-40, 76, 88, 89, 285, 350, 351, 352, 353, 354, 555  
Bell YAH-1G, 555  
Bell YAH-63, 78, 79, 200

## AIRPLANES, ENGINES, AND HELICOPTERS

- Bell YUH-1D, 89, 457, 460, 461, 462, 484, 488, 489, 555  
Boeing (HLH) YCH-62A, 90  
Boeing CH-146, 329  
Boeing CH-46, 179, 185, 250, 255, 265  
Boeing CH-47, 91, 179, 185, 247, 250, 297, 298, 300, 571  
Boeing CH-47C, 354  
Boeing CH-47D, 91, 349, 371  
Boeing Model 107, 179, 236, 255, 256, 257, 258, 259, 261, 263, 265, 333, 368, 503, 526, 591, 596, 600, 602, 611, 614  
Boeing Model 234 LR, 259  
Boeing Model 360, 18, 50, 343, 669  
Boeing YUH-61A, 78, 79, 125, 143, 144, 200, 356, 357  
Boeing/Vertol HC-1B, 297  
Boeing/Vertol Model 107-II, 256, 258, 265  
Boeing/Vertol Model 44, 60, 597  
Boeing/Vertol YHC-1B, 91  
Bréguet G-11E, 120  
Bréguet Type 314, 120, 121  
Eurocopter AS 355F, 259  
Eurocopter EC 225, 636  
Eurocopter/Aerospatiale Alouette II, 75, 465  
Eurocopter/Aerospatiale AS 332, 496, 562, 636, 673  
Eurocopter/Aerospatiale AS 332C, 259  
Eurocopter/Aerospatiale SA 365 N-1 Dauphin 2, 146, 151  
Flettner FL 265, 3  
Flettner Fl-265, 281  
Focke Achgelis Fa 223, 2, 141  
Focke Achgelis Fa-284, 91  
Focke F. 61, 2, 8, 40, 43, 91, 94, 108, 141, 270  
Hiller FH-1100, 77, 86  
Hiller H-23, 96, 208, 209, 284, 343  
Hiller OH-23, 284  
Hiller OH-5A, 77, 96  
Hiller UH-12, 18, 343, 669, 670, 693  
Hiller UH-12E, 210  
Hiller UH-4, 17  
Hiller XH-32, 456  
Hiller YH-32, 484  
Hughes Model 269, 344, 345  
Hughes Model 269A, 62, 83  
Hughes 500P (The Quiet One), 499, 501-504, 547, 508, 550, 551, 552, 533, 554, 558, 592  
Hughes OH-6A, 77, 78, 96, 97, 99, 100, 102, 289, 354, 456, 457, 459, 484, 488, 489, 498, 499, 500, 501, 502, 503, 504, 505, 506, 507, 508, 509  
Hughes T-55 Osage, 344, 345, 346, 347  
Hughes YHO-2HU, 62, 271, 344, 345, 457, 458, 475, 476, 477, 478, 479, 480, 483, 490, 491  
Hughes YOH-6A, 102, 274, 275, 276  
Kaman H-43, 75, 178, 179, 180, 191, 192, 196, 238, 239, 241  
Kaman HH-43B, 498  
Kaman K-125, 50  
Kamov Ka-22, 90  
Kellett XR-8, 280, 281, 282  
Kellett XR-10, 280  
Light Helicopter Experimental (LHX), 469, 552, 566, 567, 569, 571, 572, 575, 701  
Light Observation Helicopter (LOH), 48, 77, 284, 285, 286, 287, 288, 289, 502, 503, 540, 541, 632  
Lockheed AH-56, 311, 312, 313, 571, 701  
Lockheed CL-475, 296, 297, 302  
Lockheed XH-51, 292, 293, 297, 302  
MBB BO-105, 50, 259, 302, 305, 306, 528, 529, 534  
McDonnell Douglas MD Explorer, 147  
McDonnell XV-1, 296, 302, 304, 465  
McDonnell Douglas/Hughes 500 D, 503, 553  
McDonnell Douglas/Hughes 500E, 304  
McDonnell Douglas/Hughes Model 500, 77, 86, 503  
McDonnell Douglas/Hughes YAH-64, 78, 79, 200  
Mil Mi-6, 90  
Mil Mi-10, 90  
Mil Mi-12, 90  
Mil Mi-26, 90, 688, 701  
NH Industries NH 90, 292  
Nord 1700, 146  
Nord NC-2001, 120  
Piasecki XHJP-1, 20, 180, 182, 185  
Piasecki/Vertol H-21, 60, 178, 179, 180, 238, 239, 241, 246, 247, 248, 249, 250, 251, 252, 253, 285, 305, 347, 348  
Piasecki/Vertol H-21B, 239, 240, 241, 247, 249, 250, 252, 255, 347, 348, 368  
Piasecki/Vertol H-25, 178, 179  
Piasecki/Vertol HUP, 20, 178, 179, 180, 182, 183, 185, 239, 349, 363, 365  
Piasecki/Vertol HUP-1, 20  
Platt-LePage XR-1, 43, 94  
Robinson R22 Beta II, 638, 639, 642, 658, 659  
Robinson R22, 637, 646, 694  
Robinson R-22, 83, 84, 540, 587  
Robinson R-44, 83, 540  
Robinson R-66, 504, 540, 632, 633, 659  
Schweizer/Hughes Model 300, 344, 345  
Sikorsky Advancing Blade Concept (ABC) XH-59A, 180, 195, 196, 197  
Sikorsky CH-3, 255  
Sikorsky CH-37, 252  
Sikorsky CH-3C, 257, 261  
Sikorsky CH-53, 91, 252  
Sikorsky CH-53E, 91  
Sikorsky CH-54, 252  
Sikorsky H-19, 14, 20, 60, 285  
Sikorsky H-34, 60, 238, 239, 241, 249, 251, 252, 253, 285, 348, 366  
Sikorsky H-37, 285, 418  
Sikorsky HSS-2, 255  
Sikorsky R-4, 1, 2, 3, 43, 96, 101, 108, 315, 343, 559, 669, 670  
Sikorsky R-4B, 97, 99, 100, 252, 285  
Sikorsky R-5, 3, 96, 180, 343, 559, 669  
Sikorsky R-6, 3, 96, 97, 99, 100, 101, 102, 343, 559, 560, 669, 670  
Sikorsky S-51, 96, 180, 296, 341, 343, 550, 597, 600, 602, 603, 669, 670  
Sikorsky S-55, 60, 239, 597, 600, 602, 604, 605, 606, 607, 608, 610, 611, 612, 614, 615, 670  
Sikorsky S-56, 252

## AIRPLANES, ENGINES, AND HELICOPTERS

- Sikorsky S-58, 60, 238, 239, 366, 597, 600, 601, 670  
Sikorsky S-61, 255, 256, 257, 259, 261, 262, 263, 307,  
309, 600, 601, 602, 603, 606, 607, 608, 610, 611,  
612, 614, 615, 616, 617, 618, 621, 622, 623, 635  
Sikorsky S-61N, 596, 608, 616  
Sikorsky S-62, 256, 257, 596  
Sikorsky S-62A, 457, 463, 464, 484, 489  
Sikorsky S-64, 252  
Sikorsky S-67, 307, 309  
Sikorsky S-70, 329  
Sikorsky S-76, 231, 232, 291, 292, 293, 302, 526, 527,  
529, 548, 633, 646, 701  
Sikorsky S-76D, 634  
Sikorsky S-92, 292, 294, 360, 570, 571, 628, 636  
Sikorsky SH-3A, 457, 459, 465, 485, 486, 487, 489, 498  
Sikorsky UH-60, 124, 125, 126, 130, 202, 291, 306, 328,  
329, 332, 360, 361, 369, 373, 402, 403, 405, 406,  
417, 418, 489, 490, 491, 492, 493, 494, 495, 496,  
497, 553, 571, 573  
Sikorsky UH-60A, 124, 125, 126, 127, 128, 130, 131,  
132, 133, 134, 135, 136, 205, 247, 277, 278, 279,  
356, 357, 358, 359, 360, 361, 369, 370, 371, 373,  
374, 375, 376, 385, 386, 387, 388, 389, 390, 391,  
392, 393, 394, 396, 397, 400, 401, 405, 408, 410,  
415, 418, 42  
Sikorsky UH-60M, 360  
Sikorsky VS 300, 3  
Sikorsky VS-300A, 44  
Sikorsky XR-4, 3, 14, 23, 24, 25, 27, 28, 29, 30, 32, 35,  
40, 42, 44, 46, 94, 95, 101, 102  
Sikorsky YR-4, 23  
Sikorsky YR-4B, 46, 47, 95, 202, 203, 204, 205, 280,  
281, 282  
Sikorsky YUH-60A, 78, 79, 80, 124, 125, 126, 127, 130,  
131, 132, 133, 134, 135, 138, 143, 144, 199, 200,  
201, 357  
Sikorsky/Boeing RAH-66, 81, 105, 304, 552, 567, 568,  
569, 571, 572, 575  
Sud Quest S.O. 1221 (Djinn), 457, 466, 484  
Utility Tactical Transport Aircraft System (UTTAS),  
138, 141, 142, 143, 144, 145, 200, 202, 328, 357, 576  
Vertol/Boeing YHC-1A, 255, 257, 261, 265



## INDIVIDUALS

**These men and women, with their thoughts, words, and deeds, helped crystallize my views about helicopters.**

- Alex, Ralph, 23, 44, 49, 50, 101, 102  
Allard, Sylvain, 673  
Alldridge, Phil, 300  
Allen, William, 566  
Ambrose, James, 566, 567  
Amer, Ken, 145, 311  
Anderson, Seth, 696, 703, 733, 734, 737  
Atkins, Jim, 561, 630  
Augustine, Norm, 539, 540, 550, 551, 565, 568, 574  
Baeder, Jim, 533  
Balzar, Stephen, 55  
Barlow, William, 498, 499, 502, 503, 506, 508  
Bell, Alexander Graham, 438  
Bell, Lawrence, 14, 33, 35, 50, 553  
Betz, Albert, 5, 7  
Bousman, Bill, 205, 247, 300, 313, 386, 397  
Boxwell, Don, 516, 517, 522, 528  
Bréguet, Louis, 2, 4, 51, 119, 120, 121, 122, 271, 273, 274  
Brentner, Ken, 469, 497, 516, 533  
Brooks, George, 362, 365, 366, 367, 368, 369  
Brooks, Peter, 1, 8, 579  
Brooks, Thomas, 534  
Bruel, Andre, 146  
Burkam, John, 20, 21  
Burley, Casey, 537  
Caradonna, Frank, 400  
Carlson, Dick, 84, 687  
Carlson, Floyd, 33, 34, 35, 84, 687  
Carter, Ted, 316  
Cayley, George, 4  
Chanute, 663  
Chopra, Inder, 385, 570  
Churchhill, Gary, 305  
Cierva, Juan de la, 1, 8, 35, 36, 38, 40, 50, 114, 121, 211, 278, 280, 310, 315, 336, 337, 339, 371, 379, 434, 595, 637, 642, 648, 697, 702  
Claisse, Maurice, 119, 120, 121  
Cline, John, 371  
Cole, Jeffrey, 265  
Conner, David, 537  
Cox, Charlie, 470  
Craddock, Perry, 208  
Crawford, Charlie, 125, 202  
Crews, Sam, 328, 329, 354  
Crim, Al, 379  
Crimi, Peter, 244, 245  
Cronkhite, Jim, 371, 372, 378  
Culver, Irv, 102, 274, 296, 302  
Daimler, Gottlieb, 54  
Davies, R.E.G., 579, 595, 596, 665  
De Bothezat, George, 4, 94  
de Decker, Bill, 616, 650  
de Rochas, Beau, 53  
Delamer, Kevin, 693  
Deming, Arthur, 468  
Desfor, Sharon, 606  
Desopper, Andre, 400  
Diamond, Jack, 285, 286  
Dingeldein, Dick, 192, 204, 281, 283  
Doblhoff, Fred, 50, 302  
Domka, Bob, 372, 373  
Dorand, Rene, 4, 51, 119, 120, 121, 122  
Douglas, Donald, 251, 566, 596  
Drees, Jan, 7, 310  
Drzewiecki, M. Stefan, 7  
Dugan, Dan, 693, 736  
Durno, Jason, 373, 375, 390  
DuWaldt, Frank, 243, 244  
Ellis, Chuck, 356  
Farassat, Feri, 469, 516, 533  
Ferry, Bob, 102, 274, 276, 350, 351, 353  
Flax, Al, 84  
Fletcher, Harvey, 438, 440, 441  
Flettner, Anton, 1, 3, 5, 36, 43, 50, 108, 120, 141, 179, 281  
Florine, Nicolas, 4  
Floyd, Jack, 574  
Focke, Henrich, 1, 2, 19, 23, 36, 40, 43, 50, 91, 94, 108, 120, 141, 178, 179, 270, 697, 702  
Forster, William (Bud), 576, 577  
Fradenburgh, Evan, 231, 302, 307, 548  
Frederich, Lucretia, 594  
Fries, Gordon, 280, 283  
Froude, William, 5  
Gabel, Dick, 316, 317, 328, 329, 360, 368, 371, 418, 435  
Gabriel, Ed, 297  
Gallagher Jr., Jack, 602  
Gallagher, John (Jack), 602, 605, 606, 607, 608, 609, 610, 611, 612, 614, 615, 616  
Gessow, Al, 45, 145, 155, 166, 202, 204, 205, 219, 379, 473, 570  
Gibbs-Smith, Charles, 1, 537  
Glauert, Hermann, 7, 37, 38, 114, 115, 121, 237, 242, 243, 265, 277  
Gopalan, Gaurav, 469, 471, 472, 473, 474, 475, 480, 481, 483, 489, 493, 494, 495  
Gray, Harry, 435  
Gregory, Frank, 9, 10, 11, 12, 13, 14, 24, 25, 27, 28, 45, 94, 101, 102  
Grina, Ken, 356  
Gustafson, Fred, 202, 204, 205, 281, 283  
Gutin, L. Ya, 448, 468  
Hall, Kenneth, 265

## INDIVIDUALS

Hall, Steven, 265  
Hansford, Bob, 318  
Hanson, Tom, 300, 302, 313, 455  
Harper, Bill, 552, 571  
Harrington, Robert, 283, 284, 305, 306  
Hawkings, D. L., 469, 471, 516, 533  
Hayden, Jim, 198, 199, 201, 348  
Hayson, Harry, 246, 247, 248  
Hefner, Ralph, 153-168, 170, 174, 175, 176, 187, 192, 193  
Heinemann, Ed, 566  
Heyson, Harry, 32, 242, 243, 244, 245, 246, 247, 248  
Hiller, Stanley, 17, 18, 19, 20, 36, 50, 693, 702  
Hoerner, Jack, 561  
Hoffman, Teddy, 128, 576  
Hohenemser, Kurt, 9, 19, 302, 304  
Houbolt, John, 362, 365, 366, 368  
Howland, Guy, 373, 375, 390  
Hubbard, Harvey, 469, 470, 485, 488, 516, 528  
Huber, Helmut, 304  
Huesca, Dan, 650  
Hunt, Bill, 269  
Huston, Bob, 246, 247, 371  
Iseler, Laura, 680  
Jellinek, Emil, 54  
Jellinek, Mercedes, 54  
Johnson, Kelly, 566, 702  
Johnson, Wayne, 186, 244, 368, 398, 399, 400, 430, 495, 536, 537, 566, 571, 578  
Joiner, Webb, 561  
Kasper, Gene, 680, 684, 736  
Kawa, Mike, 574  
Kelley, Bart, 6, 15, 33, 50  
Keys, Chuck, 185, 305  
Kidd, Dave, 328  
Klemin, Alexander, 14, 18, 45, 49, 118, 216  
Knight, Montgomery, 153-168, 170, 174, 175, 176, 187, 192, 193  
Kocurek, Dave, 172, 205  
Kryter, Karl, 444  
Kufeld, Bob, 386  
Kurbjun, Max, 447, 448, 450, 452  
Kvaternik, Ray, 371, 376, 384  
Laing, Emmett, 354, 356  
Lakinsmith, Barry, 312  
Landgrebe, Jack, 156, 168  
Launoy, Claude Jean Veau de and Bienvenue, Francois, 2  
Leoni, Ray, 124, 356, 357, 360, 553  
LePage, Laurence, 43, 44  
Leverson, John, 470  
Lewis, Dick, 136, 214, 455, 516  
Liberatore, Gene, 1, 315  
Lilienthal, Otto, 663  
Lindbergh, Charles, 251, 273, 663  
Lindenbaum, Bernie, 94  
Loewy, Bob, 316, 368  
Lynn, Bob, 310  
Mallen, Joe, 238  
Manly, Charles, 55  
Mashman, Joe, 33, 34, 35, 36  
McClarren, Ralph, 45  
McCroskey, Jim, 244  
McGuire, Frank, 51  
Metzger, Bob, 310, 311  
Mil, Mikhail, 570  
Miller, Rene, 19  
Miller, Ronald, 589  
Miner, Milton, 338, 339  
Morris, Charles, 14, 23, 24, 25, 27, 28, 29, 30, 32, 33, 35, 101, 550, 567  
Morse, Andy, 530  
Moser, Herb, 286, 287, 288  
Munson, Wilden, 438, 440, 441  
Myers, Garry, 204  
Naumann, Gene, 371  
Nichols, Erickson, 45, 66, 564  
Nichols, John, 66  
Nikolsky, Alexander, 706  
Norman, Tom, 393, 401, 420, 423  
O'Bryan, Tom, 454  
Oehmichen, Etienne, 2, 4  
Ormiston, Bob, 300, 316, 368, 397, 404, 405  
Oswald, W. Bailey (Ozzy), 212, 213, 230, 233, 265  
Otto, Nikolaus, 53  
Parker, Don, 577  
Parkinson, Harry, 84  
Patnode, Clarence (Bud), 576  
Penaud, Alphonse, 4  
Pescara, Raul Pateras, 4  
Peterson, Randy, 423  
Piasecki, Frank, 19, 36, 50, 178, 180, 182, 239, 347, 349, 702  
Pitcairn, Harold, 8, 36, 38, 43, 94, 211, 697, 702  
Piziali, Ray, 243, 244  
Platt, Haviland, 43, 44, 94, 95, 120  
Prandtl, Ludwig, 5, 8, 155, 166, 265  
Prouty, Ray, 233, 311, 328  
Pruyn, Dick, 247  
Putnam, Keith, 213, 350, 351, 353  
Raborg, William, 559, 564  
Rankine, William John Macquom, 5, 64, 168  
Reed, Albert, 336  
Reichert, Gunter, 50, 302, 304  
Richey, Mike, 552, 571  
Robinson, Frank, 83, 503, 504, 508, 632, 633, 659, 693  
Rohlf, Ewald, 23, 40  
Romander, Ethan, 386, 393, 396, 400, 406, 424, 432  
Rosenstein, Hal, 305  
Russell, Carl, 533  
Rutkowski, Mike, 369  
Sawers, David, 589  
Schlegel, Ron, 470  
Schmitz, Fred, 469, 470, 471, 516, 517, 520, 522, 524, 530  
Schrage, Dan, 328  
Scott, Mark, 687, 688  
Scully, Mike, 71, 368, 539, 545, 546, 548, 570  
Selfridge, Thomas, 663  
Sheehy, Tom, 306  
Shinoda, Rick, 401  
Shute, Nevil, 550, 567, 698

## INDIVIDUALS

Sikorsky, Igor, 1, 2, 3, 9, 13, 14, 19, 20, 23, 30, 36, 44, 53, 108, 120, 239, 269, 270, 271, 343, 702  
Sissingh, Gerhard, 19, 20, 155  
Smith, Chuck, 537  
Spencer, Bob, 528  
Statler, Irv, 516, 530  
Stepniewski, Wieslaw (Steppy), 156, 182, 183, 184, 185, 187, 188, 189, 192, 197, 241, 245, 246  
Sternfeld, Harry, 470  
Stoessel, Bob, 602, 605, 606, 607, 608, 609, 610, 611, 612, 614, 615, 616  
Stroub, Bob, 307  
Stuart, Joe, 17, 18  
Studebaker (Fletcher), Karen, 361, 386, 387, 394  
Suggs, Mrs. Carroll, 673  
Sweet, George, 168, 192, 193, 194  
Tishchenko, Marat, 570  
Toossi, Mostafa, 371  
Tung, Chee, 400  
Turner, Leo, 576, 577  
Twomey, Bill, 371, 373, 375, 390  
Ulisnik, Harold, 12, 13, 108  
Wagner, Bob, 315, 470, 577  
Walton, Bill, 371  
Ward, John, 204, 371  
Warmbrodt, Bill, 289, 290, 386, 423, 500, 501, 591  
Warner, Edward, 582, 585, 586, 587, 588, 589, 592, 593, 594  
Watt, Mike, 516, 536  
Weichsel, Hans, 341  
Weick, Fred, 216, 218, 219, 221, 222, 225, 226, 227  
Wheatley, John, 37, 38  
Whittle, Frank, 63  
Williams, Bob, 291  
Williams, J. E. Ffowcs, 469, 471, 516, 533, 576  
Wood, Edgar, 46  
Wood, Tom, 46, 260, 687, 688, 697  
Wright, Theodore (T. P.), 556, 557, 558, 559, 560, 561, 564, 565  
Yamauchi, Gloria, 516, 536  
Yeates, John, 362, 365, 366, 368  
Yeo, Hyeonsoo, 385  
Young, Art, 14, 15, 16, 17, 19, 20, 33, 34, 36, 50  
Young, Larry, 307, 308, 516, 536, 693, 702  
Yu, Yung, 516, 524, 529, 530  
Yudin, E. Ya, 468  
Zinner, Russ, 528



# INDEX

- accident
    - accident bubble, 676
    - accident rate, 663, 665, 673, 674, 675, 696
    - accidents per 100,000 flight hours, 673
    - by amateurs, 669, 681, 684, 691, 697
    - classification, 666, 668, 679, 680
    - crop dusting, 689
    - crosswinds, 692, 693
    - dead man's curve, 697
    - directional control, 13, 136, 141, 145, 691, 699
    - engine structural failure, 685, 697
    - failure or malfunction of the airframe, 681, 683, 694, 695
    - fatigue, 576, 646, 689, 695
    - fuel exhaustion, 685
    - fuel/air mixture, 685, 687, 697
    - in-flight collision with objects, 681, 684, 689
    - loss of control, 683, 684, 691, 693
    - loss of engine power, 684, 685, 687, 688, 690, 691, 694
    - loss of tail rotor effectiveness, 693
    - main-rotor strikes, 689, 690
    - multi-engine helicopter safety, 687
    - power-off landing proficiency, 685
    - situational awareness of objects, 690
    - tail-rotor strikes, 689, 690
    - wires, wires/poles, and trees, 689
  - Advanced Technology Demonstrator Engine, 81
  - Advanced Vibration Development (AVID), 368, 386
  - Aeronautical Design Standard, ADS-27A-SP, 329
  - aeroscout, 99, 102, 103, 104, 105, 106, 107, 109
  - Aerospatiale, 51, 146, 149, 151, 259, 636
  - airspeed, 212
    - indicated (IAS), 212
    - true (TAS), 212
  - Air Transport Association (ATA), 602, 609, 610, 616, 623
  - Air Transport Association's Specification 100, 609
  - air transportability, 356, 357, 568
  - Aircraft Cost Evaluator (ACE), 616, 617, 619, 620, 621, 622, 623, 624, 625, 626, 627, 630, 631, 632, 634, 635, 650, 657, 658, 659
  - airfoil, 7
    - drag coefficient, 183, 184, 214, 217, 227, 233, 234, 235, 236, 260, 264, 300, 463
    - drag, 7, 8, 137, 138, 161, 162, 164, 184, 217, 220, 222, 230, 259, 299
    - lift coefficient, 138, 157, 210, 311, 312, 326, 463
    - lift, 184, 230, 259, 312
    - lift-to-drag ratio, 183, 227
    - pitching moment, 172, 399, 420, 424, 425, 426, 427, 428, 429
    - thickness, 490, 518, 540
  - airlines, 49,
    - helicopter, 251, 254, 255, 256, 258, 264, 265, 579, 595, 596, 597, 598, 599, 600, 601, 602, 606, 607, 609, 611, 612, 615, 635, 660, 661, 687
    - airplane, 444, 455, 550, 579, 582, 586, 589, 590, 591, 594, 595, 601, 602, 616, 623, 629, 660, 663, 664, 673, 675, 687, 700
    - short-haul, 597, 600, 608, 613, 660, 700
    - trunk-line, 597
  - Airworthiness Limitations, 646, 648
  - airworthiness, 339, 340, 357, 359, 362, 509, 576, 646, 647, 670
  - American Helicopter Society (AHS), 19, 45, 46, 49, 94, 118, 202, 204, 233, 238, 265, 286, 288, 291, 305, 315, 338, 354, 386, 399, 534, 537, 675
  - Army Aerodynamic and Acoustic Testing of Model Rotors (AATMR), 528, 529
  - Army Helicopter Improvement Program (AHIP), 104, 552
  - Augusta Helicopter Company, 50, 252, 636
  - autogyros, 8,
    - Cierva C.30, 1, 278, 280, 337, 379
    - Cierva C-30 parts count, 637
    - Kellett XR-2/XR-3, 94
    - Kellett YG-1B, 94, 97, 99, 100, 280, 282
    - Kellett YO-60, 46, 47, 94, 97, 99, 100
    - Pitcairn PCA-2, 33, 38
    - Umbaugh Model 18-A, 84
    - Groen Hawk, 84
  - transition to helicopters, 43, 44, 45, 94, 95, 280, 281, 339, 343, 434, 699
  - versus airplane, 45, 207, 211
  - versus helicopter, 23, 29, 31, 46, 47, 48, 619, 642, 686, 697
- automatic flight control system, 20
  - Avgas, 607
  - Bell Aircraft Corporation, 14, 50, 670
  - Bell Helicopter Company, 76, 77, 78, 553, 669
  - Bell Helicopter Textron, 16, 35, 81, 149, 152, 176, 205, 290, 291, 300, 307, 310, 328, 332, 343, 377, 434, 498, 510, 540, 541, 542, 544, 552, 555, 561, 563, 567, 568, 602, 627, 628, 631, 658, 693, 699
  - blade element airloads, 398, 400
  - blade element drag, 495, 496, 497
  - blade element thrust, 154, 496
  - blade elemental thrust integral, 422
  - Boeing Bearingless Main Rotor (BMR), 302, 304
  - Boeing Company, 552, 566
  - Boeing Helicopters, 56, 75, 90, 125, 146, 179, 241, 377, 528
  - Boeing Vertol, 241, 285, 297, 300, 302, 304, 305, 328, 348, 356, 368, 418, 470, 660
  - Boeing Vertol V/STOL Wind Tunnel, 56
  - C-60, 378, 380
  - C-81, 369, 378, 434
  - CAMRAD II + Overflow 2, 400, 420, 422, 424, 425, 426, 430, 432, 435
  - CHC Helicopters, Inc., 673
  - Chicago Helicopter Airways, 254, 596, 615

## INDEX

- computational fluid dynamics (CFD), 172, 237, 244, 314, 316, 318, 386, 393, 396, 399, 400, 401, 406, 410, 415, 420, 424, 426, 430, 431, 435, 530, 533, 534
- computational structural dynamics (CSD), 393, 396, 399, 400, 401, 406, 415, 424, 426, 431, 435
- Conklin & de Decker, 578, 616, 617, 618, 621, 623, 624, 626, 627, 628, 631, 632, 634, 635, 650, 651, 652, 657, 659
- cost, 19
  - accounting, 97, 186, 193, 307, 471, 575, 582, 585, 586, 594, 602, 619, 623, 624, 646, 653, 654
  - Aircraft Cost Evaluator (ACE), xiv, 616, 617, 619, 620, 621, 622, 623, 624, 625, 626, 627, 630, 631, 632, 634, 635, 650, 657, 658, 659
  - airframe maintenance costs, 609
  - cost categories, 585
  - cost-plus-fee contract, 552
  - crew cost, 585
  - depreciation cost, 587
  - depreciation of flight equipment, 614
  - Design to Unit Production Cost (DTUPC), 577
  - Direct Operating Cost (DOC), viii, 582, 588, 589, 590, 592, 593, 600, 602, 605, 606, 611, 612, 615, 616, 617, 618, 619, 620, 622, 623, 624, 626, 630, 631, 632, 633, 634, 635, 636, 657 (definition)
  - dollars per available seat-mile, 620
  - dollars per flight hour, 620, 623, 635
  - economic operating cost model, 594
  - engine maintenance costs, 611
  - engine overhaul costs per flight hour, 632
  - fatigue life-limited parts, 646
  - fixed cost, 653, 658
  - flight crew cost, 606
  - flight hours flown per year, 657
  - flight profile, 511, 512, 605, 606, 607, 610, 615, 619
  - flying operations, 592, 616, 617
  - fuel and oil costs, 584, 607, 620
  - ground-air-ground cycle, 336
  - HAI Guide for the Presentation of Helicopter Operating Cost Estimates, 623, 624, 654, 655, 657
  - Indirect Operating Costs, 592, 601, 657 (definition)
  - inflation, 543, 544, 545, 546, 563, 567, 570, 571, 589, 590, 616, 636, 643, 646, 679
  - insurance and reserve cost, 588, 608, 661, 665
  - insurance, 585, 587, 593, 602, 606, 608, 661, 665
  - labor rates, 610, 626
  - Maintenance DOC Near-Term Goal, 635
  - maintenance man-hours per flight hour (MMH/FH), 610, 614, 624, 627, 636, 637, 650, 651, 652, 653, 659
  - major design-to-cost factors, 567
  - man-hours, 559, 560, 574, 608, 610, 612, 613, 614, 623, 628, 634, 635, 637, 649
  - operating cost, 579, 582, 592, 653, 654
  - overhaul, 101, 102, 132, 302, 586, 623, 631, 632, 649, 650, 653, 659, 700
  - price of fuel, 617
  - refurbishing, 634, 635
  - Robinson R22 Factory Overhaul, 646
  - scheduled maintenance, 339, 498, 551, 552, 565, 574, 577, 602, 606, 648, 649
  - spare, 122, 636, 638, 639, 641, 642, 671
  - time between overhaul (TBO), 102, 113, 541, 631, 632, 636, 700
  - TOC per flight hour, 657, 658
  - total aircraft operating expenses, 594
  - total of direct maintenance costs, 612
  - total operating costs, 579, 592, 594, 599, 600, 616, 653, 657, 658, 659, 660, 664
  - unscheduled maintenance, 593, 606, 650, 651, 652
  - variable costs, 579, 623, 653, 655, 657
- cyclic, 9, 10, 11, 12, 13, 14, 18, 19, 25, 33, 250, 262, 263, 315, 380, 381, 382, 609
- cyclic control angles, 380
- Daimler, 54
- Design Analysis Methods for Vibrations (DAMVIBS), 368, 371, 372, 373, 374, 376, 377, 378, 379, 382, 383, 384, 385, 386, 390, 391, 392
- Data Base Products, 594
- Deutsch–Niederländischer Windkanal (DNW), 524, 528, 529
- Douglas Aircraft Company, 338, 589, 593
- endurance limit, 333, 334, 338, 339, 340
- engine failure, 259, 262
- Eurocopter, 51, 146, 304, 636
- Fast Fourier Transform, 389
- fatigue, 231, 331, 332, 333, 334, 336, 338, 339, 340, 342, 426, 576, 646, 689, 695
- Fenestron, 146, 147, 148, 149, 150, 151, 152
- Figure of Merit, 137, 180, 181, 182, 267, 271, 701
- fixed turbine, 63
- flapping, 10, 11, 13, 19, 34, 35, 89, 121, 364, 380, 382, 392, 396
- free turbine, 63
- gas turbine engine, 48, 53, 59, 60, 63, 64, 66, 67, 70, 71, 72, 74, 75, 77, 79, 81, 82, 83, 84, 86, 94, 100, 107, 112, 114, 119, 121, 541, 546, 550, 566, 577, 618, 632, 686
- General Aviation, 623, 672, 673, 679, 699
- General Electric, 78, 80, 82, 125, 130, 252, 265, 632, 660
- ground resonance, 8, 17, 19, 362
- Helicopter Association of Great Britain, 338
- Helicopter Association International, 509, 510, 512, 514, 515, 623, 624, 629, 630, 653, 654, 675, 678
- Helicopter Association International *Fly Neighborly Guide*, 509, 510, 512, 513, 514, 515
- Helicopter Association International *Helicopter Annual*, 629
- Helicopter Association International Safety Committee, 678
- HeliValue\$, 84, 539, 543, 608, 646, 653
- high-speed rail, 595
- Hiller Aircraft Corporation, 18, 20, 77, 210, 285, 315, 457, 540, 564, 670
- Hiller Servo Paddle, 18, 20
- Hindenburg, 663

- hub, xi,
  - drag, 231, 292, 295, 296, 302, 304, 305, 306, 307, 308, 310, 314
  - fairing, 297, 307, 308, 309
  - plane, 7, 35, 198, 237
  - pitching moment, 10, 11
  - teetering angle, 379, 380, 382
  - types, (see Appendix D)
  - vibratory loads, 318, 329, 343, 349, 351, 362, 364, 368, 369, 373, 375, 376, 377, 385, 386, 390, 393-397, 400, 403, 410, 418
- Hughes Tool Company, 62, 78, 102, 138, 285, 289, 302, 304, 328, 344, 500, 501, 503, 504, 508, 509, 533, 540, 700
- human, 318-331, 336, 354, 437, 438, 439, 441, 443, 470, 504, 566, 590, 663, 675, 680, 698
- Integrated Product Teams (IPT), 572, 575
- International Civil Aviation Organization (ICAO), 509, 510, 528
- International Helicopter Safety Team (IHST), 675, 698
- International Organization for Standardization (ISO), 71, 326, 331, 329, 343, 344, 346, 375, 439, 441, 442, 509, 510, 528
- ISO 2631 *Guide for the Evaluation of Human Exposure to Whole-Body Vibration*, 326, 331
- Jet A, 72, 607, 617, 618, 619, 621
- Kamov Design Bureau, 51, 90, 178, 179, 180, 195
- Kaman Aircraft, 36, 50, 75, 178, 179, 191, 196, 238, 239, 240, 498, 504, 702
- Kellett Autogiro Corporation, 8, 36, 43, 46, 47, 94, 280, 281, 282, 285, 697, 702
- LHX/RAH-66 program, 552, 571
- life, 332
  - blade, 643, 646, 653
  - cycle, 547, 551, 565, 566, 578
  - drive train, 694
  - engine, 584, 587, 593
  - equipment, 587, 642, 654
  - fatigue, 332, 334, 336, 339, 342, 426, 646
  - limited, 637, 642
  - on condition, 631, 632, 646, 700
  - production, 541, 543, 544
  - service, 336, 337, 339
- Lockheed Aircraft Company, 292, 293, 296, 297, 302, 304, 310, 311, 313, 447, 539, 548, 586, 587
- Lockheed stiff inplane, hingeless rotor, 313
- Lord Manufacturing Company, 300
- Los Angeles Airways, 254, 256, 595, 596, 615
- materials
  - aluminum, 54, 336, 337, 338
  - duralumin, 336
  - MIL-HDBK-5J, 333, 334, 339
  - steel, 56, 332, 333, 334, 336, 337, 338, 339, 356, 392
  - titanium, 340
  - wood, 208, 336, 338, 341, 349, 369
- McDonnell Douglas Helicopter, 81, 146, 302, 371, 377, 378, 384, 447, 529
- Messerschmitt-Bölkow-Blohm (MBB), 50, 146, 259, 304, 305, 528
- Mil Moscow Helicopter Plant, 51, 90, 252, 570, 688
- Milestone Done-Done (MD<sup>2</sup>) method, 573, 574, 575
- MIL-H-8501A, 328, 329, 345, 356, 368
- MIL-HDBK-5J, 333, 334, 339
- MIL-STD-1374A, 93
- MIL-STD-811C, 566
- MIL-W-25140, 93
- N number, 671
- NASA In-Flight Rotor Acoustic Program, 526
- Nash-Kelvinator, 560
- NASA Structural Analysis (NASTRAN), 369, 370, 371, 372, 373, 376, 377, 384, 385, 386, 393, 701
- New York Airways, 254, 256, 595, 596, 602, 606, 609, 611, 612, 615, 617, 635
- New York Yankee baseball team, 669
- Nikolsky Lecture, 202, 204, 307, 316, 386, 399, 548, 681
- noise, 437 (definition)
  - A-, B-, and C-weightings, 443
  - abatement, 510
  - add thickness, thrust, and torque sound pressures, 478
  - addition of pressures, 474
  - aircraft noise standards, 510
  - Anechoic Hover Chamber, 530, 531
  - Army Aerodynamic and Acoustic Testing of Model Rotors (AATMR), 528, 529
  - aural detection distance, 508
  - blade vortex interaction (BVI), 512, 513, 514, 528, 529, 530, 533
  - Blade-Vortex Impulsive, 510
  - broadband, 516, 529, 533
  - decibel, 441, 450, 516, 525
  - Doppler effect, 474, 475, 495
  - drive train, 506
  - ear, 309, 437, 438, 467
  - Effective Perceived Noise (EPN), 536
  - engine-alone, 506
  - far field, 471
  - HART II, 529, 534
  - Helicopter Association International Fly Neighborly Guide, 509, 510, 512, 513, 514, 515
  - high-speed impulsive, 510
  - impulsive noise, 510, 512, 513, 516, 519, 524, 525, 526, 529, 530, 532, 533, 534
  - International Civil Aviation Organization (ICAO), 509, 510, 528
  - loudness curves, 441, 442, 443, 444
  - loudness scale, 441
  - Mach number, 444, 447, 448, 449, 450, 451, 455, 472, 474, 475, 476, 483, 484, 489, 490, 492, 493, 497, 510, 520, 524, 526, 530, 532, 533, 534
  - main-rotor-alone, 507
  - mosquito, 439
  - NASA In-Flight Rotor Acoustic Program, 526
  - Noise Sensitivity Trade Study, 489
  - observer distance, 491
  - observer distance to radius ratio (S/R), 484, 485, 490, 491, 521
  - observer time, 474, 475
  - observer, 96, 207, 208, 471, 472, 474, 475, 476, 477, 479, 480, 481, 483, 484, 490, 491, 495, 497, 510, 522

# INDEX

- overall sound pressure level (OSPL), 468, 469, 470, 471, 478, 479, 480, 484, 488, 489, 491, 492, 496, 497, 500, 502, 504, 505, 506, 507, 520, 521, 522
- pascals, 438, 441, 470, 472, 476, 480, 495, 516, 520, 521, 534
- phon, 440, 443
- PSU-WOPWOP, 469
- Quiet Helicopter Program, 484, 485, 488, 498, 499, 502, 508, 509
- reduction, 490, 493, 497, 498, 508
- reference hearing level, 441
- reflection, 485, 488
- root mean square, 438, 441
- rotational noise, 469, 488, 490, 493
- sound pressure level (SPL), 440, 441, 443, 453, 468, 470, 471, 475, 476, 477, 478, 479, 480, 482, 483, 484, 485, 488, 491, 492, 497, 498, 504, 507, 520, 521, 522, 524, 526
- sound pressure time history, 470
- sound pressure waveforms, 475, 477, 518, 519, 520, 521
- sound source, 467, 474
- tail-rotor-alone noise, 507
- The Quiet One, 499, 501, 502, 503, 504, 508, 533
- thickness sound pressure, 476, 497
- three weighting curves, 442, 444
- threshold, 438, 441
- tone, 438, 440, 441, 443, 444, 470, 474, 524
- WOPWOP, 469, 533, 534
- Outlook for Vertical-Lift Aircraft in Scheduled Commercial Transportation*, 660
- part, 332(definition)
- parts count, 300, 301, 302, 309, 637, 638, 642
- performance, 119
  - Army hover design requirement, 122
  - autorotation, 24, 25, 28, 33, 34, 120, 679, 686, 687
  - autorotational, 103, 686, 688, 697
  - blade shank fairing, 298
  - blade stall, 156, 157, 345, 350, 351, 352, 353, 424, 426, 429, 491
  - brake horsepower, 55, 56, 204, 213, 227, 228, 230, 232, 235, 275
  - flat plate, 213, 232, 233, 235, 278
  - fuel efficiency, 267, 271, 619, 620
  - fuel flow, 60, 62, 67, 69, 70, 71, 72, 76, 77, 79, 80, 82, 83, 84, 251, 271, 273, 274, 618, 619, 620
  - ground effect, 6, 7, 32, 112, 120, 124, 128, 142, 144, 175, 176, 189, 198, 201, 202, 253, 270, 271, 456, 467, 485, 489, 490
  - height-velocity, 28, 32, 33, 37, 697, 699
  - hover ceiling, 124, 130, 134, 200
  - hover in ground effect (HIGE), 124, 144, 198, 199, 200, 201
  - hover out of ground effect (HOGE), 5, 6, 7, 39, 120, 121, 122, 124, 126, 127, 130, 141, 142, 144, 145, 198, 199, 200, 201, 202
  - hover power required, 5, 8, 126, 128, 130, 134, 139, 160, 172, 197, 251, 267
  - hovering performance, 119, 124, 125, 126, 133, 134, 178, 188, 192, 195, 204, 280, 283, 701
  - hub drag, 305, 306, 314
  - ideal horsepower required, 5, 120, 147
  - induced drag, 233, 237, 238, 265
  - induced power, 128, 162, 165, 168, 169, 170, 171, 173, 174, 177, 182, 185, 188, 190, 219, 224, 227, 228, 232, 233, 234, 235, 237, 238, 244, 249, 265, 266, 314
  - installed horsepower, 6, 114, 130, 252, 584
  - intermediate rated power, 130, 200
  - lift-to-drag ratio (L/D), 33, 115, 116, 137, 138, 170, 171, 230, 272, 274, 275, 276, 277, 278, 279, 314
  - Mach number, 168, 226, 227
  - nautical mile per pound, 621
  - NOTAR, 146, 147, 148, 151
  - one-engine-inoperative (OEI), 252, 253, 254, 257, 261, 262, 263, 265
  - overlap correction factor, 185
  - parasite drag, 227, 233, 235, 237, 245, 277, 278, 280, 281, 283, 284, 285, 286, 287, 288, 289, 291, 292, 293, 295, 296, 297, 300, 304, 306, 309, 314, 619, 701
  - power coefficient, 8, 142, 143, 149, 164, 188, 193, 198, 225, 252, 253
  - power margin, 119, 120, 122, 130, 182, 200, 231
  - power-off landing, 23
  - profile power, 8, 160, 162, 164, 165, 166, 168, 169, 170, 171, 185, 188, 190, 219, 223, 227, 232, 233, 234, 235, 238, 246, 314
  - propeller Activity Factor, 218, 219, 222, 226
  - propeller, 7, 46, 211-234, 238, 272, 275, 278, 312, 444-456, 470, 472, 491, 516, 523, 553
  - propeller history, 336, 337
  - propulsive efficiency, 455
  - referred power, 69, 215
  - rotor thrust, 5, 10, 29, 30, 88, 134, 138, 141, 142, 143, 144, 168, 169, 173, 174, 187, 191, 196, 222, 226, 234, 235, 237, 403, 405, 410, 415, 472, 489, 491, 492, 493, 496, 503, 504, 526, 533
  - shank drag, 300
  - solidity, 8
  - specific fuel consumption (SFC), 60, 62, 70, 71, 72, 79, 80, 84, 111, 112, 267, 268, 269, 271, 272, 275, 276SFC, , 112, 267, 268, 269, 271, 272, 273, 274, 275, 276, 277, 584
  - specific range, 275, 276, 617, 620, 621
  - tail rotor, 14, 17, 140-151, 172-178, 204, 205, 234, 235, 302, 329, 444, 465, 466, 487, 494, 489, 498, 500, 501, 503, 504, 507, 541, 640, 646, 648, 690, 693
  - takeoff gross weight, 84, 88, 90, 91, 92, 93, 94, 105, 113, 124, 252, 256, 269, 272, 275, 503, 548, 701
  - tandem-rotor induced velocity interference, 247
  - thrust coefficient, 8, 143, 149, 155, 158, 164, 166, 222, 226, 228, 455
  - variable-pitch propeller, 214, 218
  - wake skew angle, 242, 243, 247, 248
- Petroleum Helicopters, Inc., 673
- Piasecki Helicopter Corporation, 19, 60, 179, 180, 182, 239, 241, 285
- piston engine, 53

- Premier Congr s International de la Navigation A rienne, 663
- price
- average unit cost, 554, 555, 566
  - Avgas, 607
  - avionics, 546
  - Bell Model 206,
  - Consumer Price Index, 563, 571
  - cost plus fixed fee contract, 552
  - Douglas DC-3, 582, 584
  - engine, 86
  - Ford Tri-motor, 585, 584
  - fixed price contract, 552, 576
  - Joint Design-to-Cost Guide, Life Cycle Cost as a Design Parameter, 565
  - Huey, 567, 568
  - LHX/RAH-66, 567, 568
  - list price, 539, 540, 542, 545, 546, 547, 548, 578, 611, 617, 642, 657
  - Learning Curve Factor, 557, 558, 560, 563, 567
  - learning curve, 542, 555, 556, 557, 559, 560, 563, 564, 565
  - military, 546, 551, 578
  - price of fuel, 617, 618
  - price-estimating relationship, 546
  - program, 569
  - purchase price, 114, 116, 539, 542, 545, 546, 570, 578, 630, 700
  - Robinson R22, 638
  - selling price, 87, 492, 503, 533, 539, 540, 542, 545, 565, 636
  - Sikorsky S-61, 617
  - Sikorsky S-92, 570
  - spares, 122, 636, 638, 639, 641, 642, 671
  - Tishchenko view, 570
  - The Official Helicopter Blue Book<sup>®</sup>, 539, 542, 543, 544, 630, 646, 653
- productivity, 87, 115, 116, 118, 170, 547, 548, 549, 550
- Project Hummingbird, 254, 596, 599, 600, 601, 615, 660
- PSU-WOPWOP, 469
- Quiet Helicopter Program, 484, 485, 488, 498, 499, 502, 508, 509
- rotor types (see Appendix D)
- bearingless rotor, 145, 297, 302, 304, 306, 307, 308, 309, 529
  - doorhinge rotor, 309, 310, 311, 314, 701
  - hingeless rotor, 50, 302, 305, 306, 309, 311, 313, 634
- Rotor Airframe Comprehensive Aeroelastic Program (RACAP), 378
- Rotorcraft Dynamics Analysis (RDYNE), 378
- referred power, 69, 215
- Robinson Helicopter Company, 504, 540, 632, 637, 642, 646, 649, 650, 658, 659, 694
- Rolls Royce, 252, 541, 631, 632, 633
- Rotor Breeze, 627
- rotorcraft
- inactive rotorcraft, 66 (FAA definition), 392, 670, 671
  - active rotorcraft, 66 (FAA definition), 128, 331, 360, 564, 670, 671, 672, 673
  - rotor inertia, 29, 33, 34, 35, 36, 37, 103, 686, 687, 697, 699
  - Bell RotorBreeze, 627, 628, 693
  - San Francisco and Oakland Helicopter Airlines, 256, 595
  - stability augmentation system (SAS), 699
  - Hiller servo paddle control system, 17
  - Sikorsky Aircraft, 34, 43, 46, 50, 96, 101, 108, 125, 130, 141, 176, 182, 231, 238, 252, 256, 291, 296, 305, 328, 341, 356, 357, 360, 370, 377, 559, 570, 571, 628, 670, 687,
  - Sikorsky Commercial Links, 628
  - single turbine-powered helicopters, 676, 677, 684, 689, 691, 695
  - sound, 437 (definition)
    - Spirit of St. Louis, 273, 275
  - stabilizer bar, 14, 15, 19
  - stress, 331, 332, 333, 334, 338, 339, 340, 701
  - subsidy, 120, 254, 255, 265, 595, 596, 598, 600, 615, 660, 661
  - Sud-Aviation Company, 75
  - supercharged engine, 57, 58
  - synchropter, 3, 5, 75, 108, 111, 120, 141, 178, 179, 180, 191, 195, 238, 268, 280, 281
  - system engineering, 572, 573, 575, 638
  - time between overhaul (TBO), 102, 113, 541, 631, 632, 636, 700
  - The Official Helicopter Blue Book<sup>®</sup>, 539, 542, 543, 544, 630, 646, 653
  - thermodynamic energy equation, 64
  - tiltrotor, 214, 455, 544, 575, 661
  - turbine inlet temperature (TIT), 70, 71, 72, 73, 74, 113, 131
  - transmission, 5
    - belt drive, 5
    - efficiency, 138, 142, 175, 176, 190, 192, 196, 197, 204, 235, 236, 247, 249, 278
    - limits, 122, 127, 131, 132, 133, 240, 257, 262
    - Augusta/Westland EH 101, 252
    - Bell H-13, 231
    - Bell AH-1G, 385
    - Boeing Model 107-II, 265
    - cost to maintain, 609
    - main rotor, 99
    - oil temperature, 101
    - overheating, 101, 102
    - overhaul, 636
    - gear reduction, 119
    - Sikorsky YR-4B, 204
    - Sikorsky YUH-60A, 132
    - torque limits, 133
    - Vertol YHC-1A, 257
  - trim, 144, 212, 234, 245, 250, 378, 379, 380, 382, 385, 415, 424, 528, 534
  - turboshaft engine, 63, 70, 72, 75, 81, 82, 83, 84, 86, 252, 287, 289, 602, 612, 615
  - United States, 9
    - Air Force Flight Test Center at Edwards Air Force Base Edwards, 60, 76, 77, 78, 124, 136, 213, 239, 285, 343, 350, 354, 516, 524, 595
    - Army Aviation Systems Test Activity, 77, 136, 216
    - Civil Aeronautics Act of 1938, 696

# INDEX

- Census of U.S. Civil Aircraft, 672
- Civil Aeronautics Administration (CAA), 9, 14, 231, 343, 666, 668, 669, 670, 672
- Civil Aeronautics Board (CAB), 256, 259, 261, 582, 589, 594, 595, 598, 600, 601, 668
- Defense Advanced Research Projects Agency (DARPA), 498
- Department of Defense (DoD), 71, 311, 332, 539, 550, 552, 555, 565, 566, 572, 577, 578, 699
- Department of Transportation (DOT), 661, 696, 735
- U. S. Federal Aviation Administration (FAA), 9, 77, 84, 102, 231, 254, 255, 259, 260, 261, 262, 263, 265, 503, 504, 509, 510, 511, 512, 514, 515, 536, 537, 541, 566, 594, 596, 597, 598, 601, 619, 623, 646, 647, 648, 666, 671, 672, 673, 674, 675, 676, 679, 680, 685, 687, 688, 696, 697, 699
- FAA Category A, 231, 256, 257
- FAA Master List, 671
- FAA Mike Monroney Aeronautical Center, 671
- FAA Notice of Proposed Rulemaking, 509
- FAA Registry, 671, 675, 676, 699
- FAA Statistics and Forecast Branch, 672
- National Transportation Safety Board (NTSB), 663, 666, 668, 671, 672, 673, 674, 675, 679, 680, 681, 684, 685, 687, 689, 690, 694, 695, 696, 697, 698
- National Transportation Safety Board (NTSB), Report CHI82DA034, 685
- National Transportation Safety Board (NTSB), Report ERA11CA166, 680
- Statistical Handbook of Civil Aviation, 666
- UH-1 Program, 553
- UH-60A Airloads Program, 361, 373, 386, 390, 391, 392, 393, 394, 396, 400, 435
- United Research Inc., 660
- USAAMRDL, 498
- Vertol Aircraft Corporation, 241, 255, 597, 600
- vibration, 40, 315
  - 1/rev, 329, 330, 331, 337, 343, 344, 345, 348, 393, 394, 415
  - acceleration, 320, 321, 322, 323, 325, 326, 354, 356, 359, 365, 375, 376
  - Advanced Vibration Development (AVID) Program, 368, 386
  - Aeronautical Design Standard, ADS-27A-SP, 329
  - amplification factor, 323
  - blade elastic twisting, 399, 422
  - coupled rotor-fuselage, 126, 245, 349, 362, 364, 365, 366, 367, 369, 396, 399, 434
  - damping, 13, 304, 322, 323, 384, 408
  - frequencies, 320, 325, 328, 330, 331, 340, 342, 356, 360, 362, 366, 367, 369, 372, 373, 376, 384, 390, 392, 440, 470, 500
  - fuselage pitch attitude, 380
  - fuselage-rotor coupled, 375
  - hertz, 320, 331, 438, 439, 440, 441, 442, 443, 506
  - inertia integral, 423
  - inertia term, 410, 422, 423
  - inplane bending, 399
  - inplane shear loads, 397
  - lateral vibration, 346
  - mean stress, 333, 334
  - natural frequency, 304, 320, 322, 323, 324, 362, 365, 373
  - out-of-plane bending, 398
  - pitch link load, 396, 397, 398, 399, 410, 416, 423, 424, 425, 426
  - rotating blade root shears, 397
  - shake tests, 343, 362, 363, 364, 370, 371
  - steady loads, 410
  - time history, 40, 323, 469, 470, 516, 520, 524
  - trim, 144, 212, 234, 245, 250, 378, 379, 380, 382, 385, 415, 424, 528, 534
- UH-60A Airloads Program, 361, 373, 386, 390, 391, 392, 393, 394, 396, 400, 435
- vertical shear load, 397
- vertical vibration, 326, 345, 348, 350, 351, 359, 361, 386
- vibrating beam, 340, 343
- vibration limits, 326
- Vibration Rating Scale (VRS), 349, 359
- vibration rating scale, 349
- vibratory loads, 318, 343, 368, 369, 373, 377, 379, 385, 386, 393, 396, 418, 701
- vibratory pressure, 438, 441
- vibratory response, 319, 360
- whole body response, 320, 331
- VTOL, 94, 254, 328, 596, 602, 608, 609, 610, 611, 613, 614, 660, 661, 687, 688, 700, 701
- Work Breakdown Structure (WBS), 565, 566, 573, 574, 575
- weight, 5, 10, 26, 27, 28, 30, 31, 43, 51, 56, 72, 75, 77, 81, 82, 84, 87
  - GW-c.g. envelope, 348
  - All Other Groups, 99, 103, 104, 105, 106, 108, 109, 111, 112, 118
  - design loads, 87, 88, 89, 90
  - design weight, 87, 88, 89, 90
  - empty weight, 87, 92
  - load factors, 87, 88, 89, 90, 92, 660
  - MIL-STD-1374A, 93
  - MIL-STD-811C, 566
  - MIL-W-25140, 93
  - mission equipment package (MEP), 96, 207, 568, 575
  - primary mission, 92, 94, 102, 103, 126, 128, 130, 200, 359, 503
  - Propulsion Group, 97, 99, 100, 102, 107, 108, 111, 112, 114, 118
  - Structural Groups, 97, 99, 102, 103, 107, 108, 111, 112, 113, 114, 118
  - takeoff gross weight, 84, 88, 90, 91, 92, 93, 94, 105, 113, 124, 252, 256, 269, 272, 275, 503, 548, 701
  - useful load, 49, 87, 88, 91, 92, 93, 94, 96, 97, 98, 105, 109, 114, 115, 117, 118, 122, 130, 134, 136, 200, 252, 253, 503, 533, 548, 550, 699, 700, 701
  - weight empty, 87, 88, 92, 94, 97, 102, 103, 105, 112, 114, 503, 545, 547, 610, 613, 626
- Westland Helicopter, 50, 149, 150, 179, 252, 292, 294, 318, 636
- WOPWOP, 469, 533, 534
- Young Stabilizer Bar, 15, 16, 20



National Aeronautics and  
Space Administration

**Ames Research Center**  
Moffett Field, California 94035-1000

Prepared for Monterey Technology, Inc.  
under NASA Contract NNA07BB01G

Task Order 01G-38

ISBN 978-0-615-71562-9



9 780615 715629